Modeling and Simulation in Science, Engineering and Technology

Molecular Gas Dynamics

Theory, Techniques, and Applications

Yoshio Sone

BIRKHÄUSER

Modeling and Simulation in Science, Engineering and Technology

Yoshio Sone

Molecular Gas Dynamics

Theory, Techniques, and Applications

Birkhäuser
Boston • Basel • Berlin

Yoshio Sone
Professor Emeritus
Kyoto University
230-133 Iwakura-Nagatani-cho
Sakyo-ku Kyoto 606-0026
Japan

Mathematics Subject Classification: 35Q30, 35Q35, 76A02, 76N15, 76P05, 82B40, 82C40, 82C70

Library of Congress Control Number: 2006936547

ISBN-10: 0-8176-4345-1 e-ISBN-10: 0-8176-4573-X
ISBN-13: 978-0-8176-4345-4 e-ISBN-13: 978-0-8176-4573-1

Printed on acid-free paper.

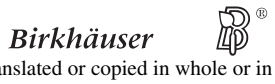

9 8 7 6 5 4 3 2 1

www.birkhauser.com (EB)

Contents

Preface

Molecular Gas Dynamics originates from lectures and seminars delivered by the author at various universities and institutions worldwide. These materials are supplemented and arranged in a form appropriate to a graduate textbook on molecular gas dynamics, or gas dynamics on the basis of kinetic theory. The book provides an up-to-date description of the basic theory of molecular gas dynamics and its various applications giving interesting and important gas dynamic phenomena. The progress of molecular gas dynamics in the last forty years has greatly enhanced the contents of the basic theory and provided information on various interesting and important gas dynamic problems. This has made it possible to compile a new graduate textbook on molecular gas dynamics. The present book reflects these developments providing working knowledge: theory, techniques, and typical phenomena in a rarefied gas (low-density and micro flows), for future theoretical development and applications.

The book begins with a brief presentation of the fundamental properties of the Boltzmann equation and a summary of notation used globally in subsequent chapters of the book. A full explanation of the fundamental properties is given in Appendix A. The author hopes that readers of various backgrounds can proceed quickly to the main subject, with reference to Appendix A if necessary. As is apparent from the table of contents, after presenting general theories for highly and slightly rarefied gases and various simple flows, such as unidirectional or quasi-unidirectional flows, and flows around a sphere, the author discusses various subjects: flows induced by temperature fields, which are typical in a rarefied gas; flows with evaporation and condensation; bifurcation of flows in a rarefied gas; and ghost effects in a gas in the continuum limit. In Appendix B, where methods of solution are described, the theoretical background of the direct simulation Monte Carlo method (DSMC method) is explained in a way that can be read by nonmathematicians.

The existence of ghost effects in a gas in the continuum limit makes molecular gas dynamics indispensable to the study of a gas in the continuum limit, which is traditionally discussed by classical fluid dynamics. Ghost and non-Navier–Stokes effects present themselves in well-known classical fluid dynamic problems, such as the Bénard and Taylor–Couette problems; they are discussed in Chapter 8. Another type of ghost effect, the recently proposed infinitesimal curvature effect, is discussed in Chapter 9, where bifurcation of the plane Couette flow, a long-standing problem, is worked out as an example. The discussion on ghost

effects will be essential to a modern treatment of traditional fluid dynamics.

Basic theory is developed in a systematic way and presented in a form easily applicable to practical use. Fundamental examples showing kinetic effects and various interesting physical phenomena are discussed analytically, numerically, or experimentally. Mathematical discussion is on the level of classical advanced calculus; definitions, assumptions, and formulations are stated explicitly. Thus, engineers can apply theoretical works to practical problems, and mathematicians will have access to physically interesting mathematical problems without much difficulty. Readers should be aware of the relationship of the present book to the author's previous one, *Kinetic Theory and Fluid Dynamics* (Birkhäuser, 2002). The latter is a monograph mainly discussing the time-independent problems in Chapter 3 of the present book in more detail. Some supplementary discussions on the subject, including a brief but systematic discussion of its time-dependent problems, are naturally made in the present book. Thus, the two books are complementary. Misprints that are found in the two above-mentioned books will be posted at http://fd.kuaero.kyoto-u.ac.jp/members/sone.

The author owes a great deal to many people. He was influenced by fruitful discussion with the late Harold Grad, who offered the author a chance to work with him at the Courant Institute for two years. Collaboration with French mathematicians, especially C. Bardos and F. Golse, was initiated by H. Cabannes's invitation of the author to be a visiting professor at the Université Pierre et Marie Curie. The author enjoyed very fruitful discussions with Tai-Ping Liu and Shih-Hsien Yu, who offered the author their unpublished works. He also enjoyed discussions with L. Arkeryd in the comfortable climate of several Swedish summers. The conversations and correspondences with J. B. Keller and A. Acrivos were instructive. The discussions and collaboration enhanced the content of the book. G. Bird and W. Wagner read Section B.1 on the DSMC method and gave the author useful comments. T. Yano, M. Hasegawa, T. Doi, H. Sugimoto, S. Takata, T. Kataoka, and M. Handa, each kindly examined considerable parts of the draft manuscript carefully, providing helpful suggestions and improvements; Kataoka read more than ninety percent of the manuscript in detail, and Doi examined the whole manuscript with a particular emphasis on typographical errors. T. Doi, H. Sugimoto, S. Takata, T. Kataoka, K. Sawada, and M. Handa helped the author to prepare figures; Sugimoto also worked to modify all of the figure files to the publisher's standard. Tom Grasso's editorial group at Birkhäuser processed the manuscript carefully and efficiently. The author would like to express his thanks for the various courtesies provided and contributions made. After retirement from Kyoto University in 2000, the author has spent most of his time at home writing contributed papers on molecular gas dynamics and two books, the above-mentioned book and the present one. His life during this period was regulated by the regular request of his family dog, Mill, to go out for walks, which must be considered a nonnegligible contribution.

Yoshio Sone
Kyoto, 2006

Molecular Gas Dynamics

Chapter 1

Boltzmann Equation

In this chapter we summarize the preliminary information on the Boltzmann equation (the definitions, notations, formulas, etc.) for the convenience of the discussions in the following chapters. With this preliminary summary, the readers will proceed faster to the discussion of gas-dynamic problems treated in those chapters. Its detailed or supplementary explanation is given in Appendix A. Related information is found in Boltzmann [1896, 1898], Grad [1958], Vincenti & Kruger [1965], Kogan [1969], Cercignani [1988], Sone & Aoki [1994], and Sone [2002].

1.1 Velocity distribution function and macroscopic variables

Consider a gas consisting of identical molecules whose intermolecular potential is spherically symmetric. The gas is assumed not to be dense. That is, in a volume of the gas, the volume of the molecules there packed together, or the total volume of the ranges where their intermolecular forces are effective, is negligibly small compared with the volume of the gas.[1] Let X_i (or $\boldsymbol{X}$) be the Cartesian (or rectangular) coordinates of our physical space, and ξ_i (or $\boldsymbol{\xi}$) the molecular velocity.[2] Let the number $\mathrm{d}N$ of molecules in the six-dimensional

[1] This is called the *perfect-gas condition*. In statistical physics, the gas is sometimes called rarefied gas. However, in gas dynamics, the term *rarefied gas* is used for a gas where the length of the mean free path (Section 1.5) is not negligible.

[2] In this book, the Cartesian-tensor notation (Jeffreys [1965]) is mainly used. However, the vector notation is sometimes convenient, for example, to express the arguments of a function. The subscripts of these variables are cumbersome and confusing with subscripts used in real operations. Thus, we introduce the vector notation without notice. What should be noted in the Cartesian-tensor notation is the summation convention: that is, double indices mean the summation without the $\sum$ sign (e.g., $a_i b_i = a_1 b_1 + a_2 b_2 + a_3 b_3$, $a_{ii} = a_{11} + a_{22} + a_{33}$). Note that the expression $\partial^2/\partial X_i^2$ means the Laplacian, i.e., $\partial^2/\partial X_1^2 + \partial^2/\partial X_2^2 + \partial^2/\partial X_3^2$. Here, Cartesian coordinates are used in their narrower definition, i.e., rectangular ones.

volume element $\mathrm{d}X_1\mathrm{d}X_2\mathrm{d}X_3\mathrm{d}\xi_1\mathrm{d}\xi_2\mathrm{d}\xi_3$ ($\mathbf{d}\boldsymbol{X}\mathbf{d}\boldsymbol{\xi}$, for short) be expressed as

$$\mathrm{d}N = \frac{1}{m} f(\boldsymbol{X}, \boldsymbol{\xi}, t)\mathbf{d}\boldsymbol{X}\mathbf{d}\boldsymbol{\xi}, \tag{1.1}$$

where m is the mass of a molecule and t is the time. Then, f or f/m, which is a function of the seven variables $\boldsymbol{X}$, $\boldsymbol{\xi}$, and t, is called the *velocity distribution function* of the gas molecules.

The macroscopic variables—the *density* ρ of the gas, the *flow velocity* v_i, the *temperature* T, the *pressure* p, the *specific internal energy* e, the *stress tensor* p_{ij}, and the *heat-flow vector* q_i at position $\boldsymbol{X}$ and at time t—are defined by the following moments of f:

$$\rho = \int f(\boldsymbol{X}, \boldsymbol{\xi}, t)\mathbf{d}\boldsymbol{\xi}, \tag{1.2a}$$

$$v_i = \frac{1}{\rho}\int \xi_i f(\boldsymbol{X}, \boldsymbol{\xi}, t)\mathbf{d}\boldsymbol{\xi}, \tag{1.2b}$$

$$3RT = \frac{1}{\rho}\int (\xi_i - v_i)^2 f(\boldsymbol{X}, \boldsymbol{\xi}, t)\mathbf{d}\boldsymbol{\xi}, \tag{1.2c}$$

$$p = \frac{1}{3}\int (\xi_i - v_i)^2 f(\boldsymbol{X}, \boldsymbol{\xi}, t)\mathbf{d}\boldsymbol{\xi} = R\rho T, \tag{1.2d}$$

$$e = \frac{1}{\rho}\int \frac{1}{2}(\xi_i - v_i)^2 f(\boldsymbol{X}, \boldsymbol{\xi}, t)\mathbf{d}\boldsymbol{\xi} = \frac{3}{2}RT, \tag{1.2e}$$

$$p_{ij} = \int (\xi_i - v_i)(\xi_j - v_j) f(\boldsymbol{X}, \boldsymbol{\xi}, t)\mathbf{d}\boldsymbol{\xi}, \tag{1.2f}$$

$$q_i = \int \frac{1}{2}(\xi_i - v_i)(\xi_j - v_j)^2 f(\boldsymbol{X}, \boldsymbol{\xi}, t)\mathbf{d}\boldsymbol{\xi}, \tag{1.2g}$$

where R is the specific gas constant [the Boltzmann constant k_B ($= 1.3806505 \times 10^{-23}\mathrm{J{\cdot}K^{-1}}$) divided by m] and the three-dimensional integration with respect to $\boldsymbol{\xi}$ is, hereafter, carried out over the whole space of $\boldsymbol{\xi}$ unless otherwise stated. These definitions are compatible with those in the classical fluid dynamics.

According to the explanation in Fig. 1.1, the mass $-m_f$, momentum $-p_i$, and energy $-e_f$ transferred from the gas to its (real or imaginary) boundary, at a point $\boldsymbol{X}$, per its unit area and per unit time are given by[3]

$$\begin{aligned} m_f &= \int (\xi_j - v_{wj}) n_j f(\boldsymbol{X}, \boldsymbol{\xi}, t)\mathbf{d}\boldsymbol{\xi} \\ &= n_j \rho (v_j - v_{wj}), \end{aligned} \tag{1.3a}$$

$$\begin{aligned} p_i &= \int \xi_i (\xi_j - v_{wj}) n_j f(\boldsymbol{X}, \boldsymbol{\xi}, t)\mathbf{d}\boldsymbol{\xi} \\ &= n_j [p_{ij} + \rho v_i (v_j - v_{wj})], \end{aligned} \tag{1.3b}$$

[3]Quantities or variables expressing flows per unit area and per unit time will be called fluxes. The heat-flow vector q_i in Eq. (1.2g) may be better called a heat-flux vector, but we follow the convention.

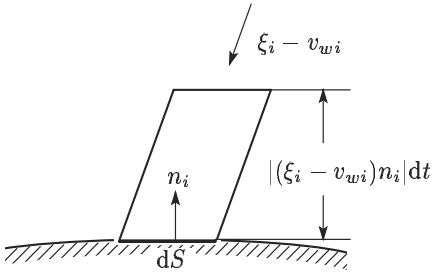

Figure 1.1. Explanatory figure for the formulas (1.3a)–(1.3c). The molecules with velocity $\boldsymbol{\xi}$ in the cylinder with its generatrices parallel to the relative velocity $\xi_i - v_{wi}$, its base given by the surface element $\mathrm{d}S$, and its height given by $|(\xi_i - v_{wi})n_i|\mathrm{d}t$ will reach the surface element $\mathrm{d}S$ within time $\mathrm{d}t$ when $(\xi_i - v_{wi})n_i < 0$ and have left $\mathrm{d}S$ within time $\mathrm{d}t$ in the past when $(\xi_i - v_{wi})n_i > 0$. Thus, total mass, momentum, and energy transferred by the molecules with their velocities in $\mathbf{d}\boldsymbol{\xi}$ at $\boldsymbol{\xi}$ to the surface element $\mathrm{d}S$ in time $\mathrm{d}t$ are, respectively given by $-f(\boldsymbol{X}, \boldsymbol{\xi}, t)\mathbf{d}\boldsymbol{\xi}(\xi_j - v_{wj})n_j \mathrm{d}S\mathrm{d}t$, $-\xi_i f(\boldsymbol{X}, \boldsymbol{\xi}, t)\mathbf{d}\boldsymbol{\xi}(\xi_j - v_{wj})n_j \mathrm{d}S\mathrm{d}t$, and $-\frac{1}{2}\xi_i^2 f(\boldsymbol{X}, \boldsymbol{\xi}, t)\mathbf{d}\boldsymbol{\xi}(\xi_j - v_{wj})n_j \mathrm{d}S\mathrm{d}t$. Summing up for all molecular velocities, we obtain the formulas (1.3a)–(1.3c).

$$
\begin{aligned}
e_f &= \int \frac{1}{2}\xi_i^2(\xi_j - v_{wj})n_j f(\boldsymbol{X}, \boldsymbol{\xi}, t)\mathbf{d}\boldsymbol{\xi} \\
&= n_j \left[q_j + p_{ij}v_i + \rho\left(e + \frac{1}{2}v_i^2\right)(v_j - v_{wj}) \right], \qquad (1.3c)
\end{aligned}
$$

where v_{wi} is the velocity of the boundary and n_i is the unit normal vector to the boundary, pointed to the gas. When there is no mass flux ($m_f = 0$) through a boundary,

$$
p_i = n_j p_{ij}, \qquad e_f = n_j(q_j + p_{ij}v_i). \qquad (1.4)
$$

1.2 Boltzmann equation

The behavior of the velocity distribution function f is determined by the *Boltzmann equation*

$$
\frac{\partial f}{\partial t} + \xi_i \frac{\partial f}{\partial X_i} + \frac{\partial F_i f}{\partial \xi_i} = J(f, f), \qquad (1.5)
$$

where

$$
J(f, f) = \frac{1}{m}\int_{\text{all } \alpha_i,\ \text{all } \xi_{i*}} (f'f'_* - ff_*)B\mathrm{d}\Omega(\boldsymbol{\alpha})\mathbf{d}\boldsymbol{\xi}_*, \qquad (1.6)
$$

$$
\left.
\begin{aligned}
&f = f(X_i, \xi_i, t), \qquad f_* = f(X_i, \xi_{i*}, t), \\
&f' = f(X_i, \xi'_i, t), \qquad f'_* = f(X_i, \xi'_{i*}, t), \\
&\xi'_i = \xi_i + \alpha_i\alpha_j(\xi_{j*} - \xi_j), \qquad \xi'_{i*} = \xi_{i*} - \alpha_i\alpha_j(\xi_{j*} - \xi_j), \\
&B = B(|\alpha_i(\xi_{i*} - \xi_i)|/|\xi_{j*} - \xi_j|, |\xi_{j*} - \xi_j|), \\
&|\xi_{j*} - \xi_j| = [(\xi_{j*} - \xi_j)^2]^{1/2},
\end{aligned}
\right\} \qquad (1.7)
$$

and mF_i is the external force on a molecule;[4] α_i (or $\boldsymbol{\alpha}$) is a unit vector, expressing the variation of the direction of the molecular velocity owing to a molecular collision; $\mathrm{d}\Omega(\boldsymbol{\alpha})$ is the solid-angle element in the direction of α_i; and B is a function of $|\alpha_i(\xi_{i*} - \xi_i)|/|\xi_{j*} - \xi_j|$ and $|\xi_{j*} - \xi_j|$, positive almost everywhere[5] in the space $(\boldsymbol{\xi}, \boldsymbol{\alpha})$, and its functional form is determined by the intermolecular force [e.g., $B = d_m^2|(\xi_{i*} - \xi_i)\alpha_i|/2$ for a gas consisting of hard-sphere molecules with diameter d_m].[6] The definition of B is given in Eq. (A.20), and its relation to the intermolecular potential is discussed in Section A.2.4. The integrations with respect to ξ_{i*} and α_i are carried out over the whole space of ξ_{i*} and over the whole direction of α_i (the whole spherical surface), respectively. The integral $J(f, f)$ is called the *collision integral* or the *collision term* of the Boltzmann equation (1.5). Its first part $m^{-1}\int f'f'_*B\mathrm{d}\Omega\mathbf{d}\boldsymbol{\xi}_*$ is called the *gain term* (denoted by J_G for short), and the second $m^{-1}\int ff_*B\mathrm{d}\Omega\mathbf{d}\boldsymbol{\xi}_*$ the *loss term* (denoted by J_L). Then,

$$J = J_G - J_L = J_G - \nu_c f, \tag{1.8}$$

where ν_c is the collision frequency to be defined by Eq. (1.18).

The Boltzmann equation (1.5) expresses the variation of the velocity distribution function f along a molecular path under the external force F_i owing to intermolecular collisions. If the intermolecular collision is absent, $f\mathbf{d}\boldsymbol{X}\mathbf{d}\boldsymbol{\xi}$ is invariant along a molecular path, where $\mathbf{d}\boldsymbol{X}\mathbf{d}\boldsymbol{\xi}$ is taken to move along the path, i.e.,

$$\frac{\partial f}{\partial t} + \xi_i\frac{\partial f}{\partial X_i} + \frac{\partial F_i f}{\partial \xi_i} = 0,$$

in view of the variation of the volume $\mathbf{d}\boldsymbol{X}\mathbf{d}\boldsymbol{\xi}$ along the path determined by the law of dynamics.[7] According to Boltzmann [1896, 1898], the $(J_L/m)\mathbf{d}\boldsymbol{X}\mathbf{d}\boldsymbol{\xi}\mathrm{d}t$ is the number of the molecules in $\mathbf{d}\boldsymbol{X}\mathbf{d}\boldsymbol{\xi}$ that will make intermolecular collision in time $\mathrm{d}t$ or the number of the molecules that leave $\mathbf{d}\boldsymbol{X}\mathbf{d}\boldsymbol{\xi}$ in $\mathrm{d}t$ owing to intermolecular collision; $(J_G/m)\mathbf{d}\boldsymbol{X}\mathbf{d}\boldsymbol{\xi}\mathrm{d}t$ is the number of the molecules in $\mathbf{d}\boldsymbol{X}\mathbf{d}\boldsymbol{\xi}$ that have made intermolecular collision in the past $\mathrm{d}t$ or the number of the molecules that have entered $\mathbf{d}\boldsymbol{X}\mathbf{d}\boldsymbol{\xi}$ in the past $\mathrm{d}t$ owing to intermolecular collision (see also, e.g., Sommerfeld [1964], Sone & Aoki [1994]). Thus, the variation of f is given by Eq. (1.5).

The Boltzmann equation is derived from the Liouville equation in Section A.1 for a gas consisting of molecules with *their intermolecular force extending*

[4] The external force F_i does not appear in the following chapters except in Sections 3.3, 5.1.3, 8.1, 8.2, A.3, and B.1. In some places, it is absent, i.e., $F_i = 0$, and in the others, the discussion is independent of F_i. Their difference may be obvious. When the external force is absent, the symbol F_i is sometimes used for other kinds of forces; they are defined in each place, and no confusion will happen.

[5] The term *almost everywhere* is used to state that the fact in question holds everywhere except at the points of a set of *measure zero*, which is defined by a set of points that can be covered by a finite number or by a denumerable sequence of rectangular parallelepipeds whose total volume (i.e., the sum of the individual volumes) is arbitrarily small (see, e.g., Jeffreys & Jeffreys [1946], Riesz & Sz.-Nagy [1990]).

[6] (i) The gravity between molecules is not considered in the study of this book.
(ii) A gas consisting of identical hard-sphere molecules is called a *hard-sphere gas*.

[7] It is invariant when $F_i = 0$ or generally $\partial F_i/\partial\xi_i = 0$ (see, e.g., Reif [1965], Diu, Guthmann, Lederer & Roulet [1989], Sone & Aoki [1994]).

only within a finite distance (say d_m). That is, take a system consisting of N particles (or molecules) with a spherically symmetric intermolecular potential with finite range d_m and investigate the limiting behavior where the characteristic number density n_0 of the particles as well as N increases indefinitely ($n_0 \to \infty$, $N \to \infty$) and $d_m \to 0$ with $n_0 d_m^2$ fixed.[8] In the derivation, in addition to the molecular chaos assumption for molecules before collision (Section A.1), the velocity distribution function f is assumed to be invariant over the distance of the molecular size or d_m and over the time to proceed the distance by a characteristic molecular speed or d_m divided by a characteristic molecular speed (slowly varying assumption). Thus, the Boltzmann equation cannot describe the behavior of the molecular scale. For an intermolecular force extending to infinity ($d_m = \infty$), the formula for B, obtained by the discussion of a binary molecular collision, is substituted in the equation for a finite d_m (Section A.2.4). For $d_m = \infty$, each of the gain and loss terms diverges though $J(f, f)$ converges for the potential decaying fast enough.

The generalized form $J(f, g)$ of the collision integral $J(f, f)$,

$$J(f,g) = \frac{1}{2m} \int_{\text{all } \alpha_i,\, \text{all } \xi_{i*}} (f'g'_* + f'_*g' - fg_* - f_*g) B \mathrm{d}\Omega(\boldsymbol{\alpha}) \mathbf{d}\boldsymbol{\xi}_*, \tag{1.9}$$

is often used in the following chapters. The rule (1.7) is, hereafter, applied to the other functions (e.g., g, φ) of ξ_i. The following properties of the integral $J(f, g)$ are also frequently used in the analysis of the Boltzmann equation. The moment $\int \varphi(\boldsymbol{\xi}) J(f, g) \mathbf{d}\boldsymbol{\xi}$, where φ is an arbitrary function of $\boldsymbol{\xi}$, satisfies the *symmetry relation*

$$\begin{aligned}
&\int \varphi(\boldsymbol{\xi}) J(f,g) \mathbf{d}\boldsymbol{\xi} \\
&= \frac{1}{8m} \int (\varphi + \varphi_* - \varphi' - \varphi'_*)(f'g'_* + f'_*g' - fg_* - f_*g) B \mathrm{d}\Omega(\boldsymbol{\alpha}) \mathbf{d}\boldsymbol{\xi}_* \mathbf{d}\boldsymbol{\xi} \\
&= \frac{1}{4m} \int (\varphi' + \varphi'_* - \varphi - \varphi_*)(fg_* + f_*g) B \mathrm{d}\Omega(\boldsymbol{\alpha}) \mathbf{d}\boldsymbol{\xi}_* \mathbf{d}\boldsymbol{\xi},
\end{aligned} \tag{1.10}$$

where the integration is carried out over the whole spaces of $\boldsymbol{\xi}$, $\boldsymbol{\xi}_*$, and $\boldsymbol{\alpha}$ (see Section A.2.2). By choosing 1, ξ_i, or ξ_i^2 for φ, it is easily seen that

$$\int \begin{pmatrix} 1 \\ \xi_i \\ \xi_i^2 \end{pmatrix} J(f,g) \mathbf{d}\boldsymbol{\xi} = 0, \tag{1.11}$$

because $\xi_i + \xi_{i*} = \xi'_i + \xi'_{i*}$ and $\xi_i^2 + \xi_{i*}^2 = \xi_i'^2 + \xi_{i*}'^2$.

[8] (i) It is implicitly assumed that the mass m of a molecule vanishes ($m \to 0$) as $n_0 \to \infty$ with mn_0 (a characteristic density of the gas) fixed. Thus, f is finite, but f/m, which is also used as the velocity distribution function in many literatures, is infinite. In the latter case, some relative number of molecules should be considered.

(ii) The inverse of $n_0 d_m^2$ is of the order of the characteristic mean free path (Section 1.5).

(iii) In this limit, $n_0 d_m^3 \to 0$ automatically, that is, the perfect gas condition is satisfied.

1.3 Conservation equations

Multiplying the Boltzmann equation (1.5) by 1, ξ_i, or ξ_i^2, and integrating the result over the whole space of ξ_i,[9] we obtain the following conservation equations:

$$\frac{\partial \rho}{\partial t} + \frac{\partial}{\partial X_i}(\rho v_i) = 0, \tag{1.12}$$

$$\frac{\partial}{\partial t}(\rho v_i) + \frac{\partial}{\partial X_j}(\rho v_i v_j + p_{ij}) = \rho F_i, \tag{1.13}$$

$$\frac{\partial}{\partial t}\left[\rho\left(e + \frac{1}{2}v_i^2\right)\right] + \frac{\partial}{\partial X_j}\left[\rho v_j\left(e + \frac{1}{2}v_i^2\right) + v_i p_{ji} + q_j\right] = \rho v_j F_j, \tag{1.14}$$

where the force F_i is assumed to be independent of the molecular velocity ξ_i. The collision term vanishes on integration [see Eq. (1.11)]. Equations (1.12), (1.13), and (1.14) are, respectively, called the *conservation equations of mass, momentum, and energy*. In the classical fluid dynamics, p_{ij} and q_i are assumed to be in appropriate forms to close the system (1.12)–(1.14). For example,

$$p_{ij} = p\delta_{ij}, \quad q_i = 0, \tag{1.15}$$

or

$$p_{ij} = p\delta_{ij} - \mu\left(\frac{\partial v_i}{\partial X_j} + \frac{\partial v_j}{\partial X_i} - \frac{2}{3}\frac{\partial v_k}{\partial X_k}\delta_{ij}\right) - \mu_B \frac{\partial v_k}{\partial X_k}\delta_{ij}, \quad q_i = -\lambda\frac{\partial T}{\partial X_i}, \tag{1.16}$$

where δ_{ij} is Kronecker's delta (i.e., $\delta_{ij} = 1$ for $i = j$, $\delta_{ij} = 0$ for $i \neq j$), and μ, μ_B, and λ, called the *viscosity*, *bulk viscosity*, and *thermal conductivity* of the gas respectively, are functions of temperature. The set of equations with the former stress and heat flow is called the *Euler set*, and the set with the latter the *Navier–Stokes set*. The relations for p_{ij} and q_i given in Eq. (1.16) are, respectively, called Newton's law and Fourier's law.

1.4 Maxwell distribution (Equilibrium distribution)

The solution f_E of the Boltzmann equation (1.5) with $F_i = 0$ for an equilibrium state ($\partial f/\partial t = \partial f/\partial X_i = 0$) is given by the following *Maxwell distribution* (or *Maxwellian*) with constant parameters ρ, v_i, and T (see Section A.7.1):

$$f_E = \frac{\rho}{(2\pi RT)^{3/2}} \exp\left(-\frac{(\xi_i - v_i)^2}{2RT}\right). \tag{1.17}$$

[9] As to be explained in Section 3.1.6, the velocity distribution function generally has discontinuities along the characteristic of the Boltzmann equation, though the macroscopic variables are continuous. Thus, interchanging the order of differentiation and integration in the process should be done carefully.

The same form of the velocity distribution function f_e where ρ, v_i, and T depend on X_i or t does not satisfy Eq. (1.5) with $F_i = 0$ except for some special cases. The distribution f_e is called *local Maxwell distribution* (or *local Maxwellian*). The local Maxwellian that satisfies the Boltzmann equation is discussed in Section A.7.2.

1.5 Mean free path

The *collision frequency* $\nu_c(\boldsymbol{\xi})$ of a molecule with velocity $\boldsymbol{\xi}$ (per unit time) is[10]

$$\nu_c = \frac{1}{m} \int f(\boldsymbol{\xi}_*) B \mathrm{d}\Omega(\boldsymbol{\alpha}) \mathbf{d}\boldsymbol{\xi}_*. \tag{1.18}$$

Its average over all the molecules (the *mean collision frequency* $\bar{\nu}_c$) is

$$\bar{\nu}_c = \frac{1}{\rho m} \int f(\boldsymbol{\xi}) f(\boldsymbol{\xi}_*) B \mathrm{d}\Omega \mathbf{d}\boldsymbol{\xi}_* \mathbf{d}\boldsymbol{\xi}. \tag{1.19}$$

The inverse of $\nu_c(\boldsymbol{\xi})$ is called the *free time* $\tau_c(\boldsymbol{\xi})$ $[= 1/\nu_c(\boldsymbol{\xi})]$ of a molecule with velocity $\boldsymbol{\xi}$, and the inverse of $\bar{\nu}_c$ is called the *mean free time* $\bar{\tau}_c$ of the gas molecules. The mean free time multiplied by the average speed $\overline{\xi}$ $[= \rho^{-1} \int \xi f \mathbf{d}\boldsymbol{\xi}$; $\xi = |\xi_i| = (\xi_i)^{1/2}]$ of the gas molecules is called their *mean free path* ℓ:[11]

$$\ell = \overline{\xi} \bar{\tau}_c. \tag{1.20}$$

If the velocity distribution function is a Maxwellian, the mean collision frequency is given by (see Section A.8)

$$\bar{\nu}_c = 2\sqrt{2}\pi^{1/2} d_m^2 (2RT)^{1/2} (\rho/m), \tag{1.21}$$

and for a Maxwellian with $v_i = 0$, the mean free path ℓ is given by

$$\ell = [\sqrt{2}\pi d_m^2 (\rho/m)]^{-1}, \tag{1.22}$$

where d_m is the radius of the influence range of the intermolecular force. (For a hard-sphere molecule, d_m is the diameter of a molecule.)

The above definitions of the collision frequency, the mean collision frequency, the mean free time, and the mean free path are not useful when the intermolecular force extends to infinity, for the first and second ones are infinite for any such potential, however fast it decays. In such a case its effective value, as a quantitative symbol of the collision effect, is defined. For example, the range of integral in Eq. (1.19) is limited in a domain where a range $|\alpha_i(\xi_{i*} - \xi_i)|/|\xi_{j*} - \xi_j| \ll 1$ is excluded (or the intermolecular interactions that induce only small velocity changes are not counted as collision); the mean free time $\bar{\tau}_c$ and the mean free path ℓ are defined on the basis of this $\bar{\nu}_c$ by the relations shown above.

[10] (i) The expression for ν_c can be understood by the discussion in the paragraph next to that containing Eq. (1.8).

(ii) The argument or arguments of a function are not always shown when no fear of confusion or misunderstanding is expected. This rule is applied to a special argument or arguments. That is, $\nu_c(\boldsymbol{\xi})$ and $f(\boldsymbol{\xi})$ instead of $\nu_c(\boldsymbol{X}, \boldsymbol{\xi}, t)$ and $f(\boldsymbol{X}, \boldsymbol{\xi}, t)$.

[11] There are variations of the choice of the reference speed in the definition of the mean free path. The *free path* of a molecule of velocity $\boldsymbol{\xi}$ is defined on the basis of τ_c.

1.6 Kinetic boundary condition

1.6.1 Simple boundary

On a boundary or wall where there is no mass flux across it [or $m_f = 0$; see Eq. (1.3a)], which will be called a *simple boundary*, the following condition (the *Maxwell-type condition*) is widely used:

$$f(X_i,\xi_i,t) = (1-\alpha)f(X_i,\xi_i - 2(\xi_j - v_{wj})n_j n_i, t) + \frac{\alpha\sigma_w}{(2\pi RT_w)^{3/2}}\exp\left(-\frac{(\xi_j - v_{wj})^2}{2RT_w}\right) \quad [(\xi_j - v_{wj})n_j > 0], \tag{1.23a}$$

$$\sigma_w = -\left(\frac{2\pi}{RT_w}\right)^{1/2}\int_{(\xi_i - v_{wi})n_i<0}(\xi_j - v_{wj})n_j f(\boldsymbol{X},\boldsymbol{\xi},t)\mathbf{d}\boldsymbol{\xi}, \tag{1.23b}$$

where T_w and v_{wi} are, respectively, the temperature and velocity of the boundary, n_i is the unit normal vector to the boundary, pointed to the gas, and α ($0 \le \alpha \le 1$) is the *accommodation coefficient*.[12] These quantities depend on the position of the boundary. The case $\alpha = 1$ is called the *diffuse-reflection condition*, and $\alpha = 0$ the *specular-reflection condition*. That is, the diffuse-reflection condition is

$$f(\boldsymbol{X},\boldsymbol{\xi},t) = \frac{\sigma_w}{(2\pi RT_w)^{3/2}}\exp\left(-\frac{(\xi_j - v_{wj})^2}{2RT_w}\right) \quad [(\xi_j - v_{wj})n_j > 0], \tag{1.24a}$$

$$\sigma_w = -\left(\frac{2\pi}{RT_w}\right)^{1/2}\int_{(\xi_i - v_{wi})n_i<0}(\xi_j - v_{wj})n_j f(\boldsymbol{X},\boldsymbol{\xi},t)\mathbf{d}\boldsymbol{\xi}, \tag{1.24b}$$

and the specular-reflection condition is

$$f(X_i,\xi_i,t) = f(X_i,\xi_i - 2(\xi_j - v_{wj})n_j n_i, t) \quad [(\xi_j - v_{wj})n_j > 0]. \tag{1.25}$$

More generally, the boundary condition is expressed in terms of a *scattering kernel* $K_B(\boldsymbol{\xi},\boldsymbol{\xi}_*,\boldsymbol{X},t)$ as

$$f(\boldsymbol{X},\boldsymbol{\xi},t) = \int_{(\xi_{i*} - v_{wi})n_i<0} K_B(\boldsymbol{\xi},\boldsymbol{\xi}_*,\boldsymbol{X},t)f(\boldsymbol{X},\boldsymbol{\xi}_*,t)\mathbf{d}\boldsymbol{\xi}_* \quad [(\xi_i - v_{wi})n_i > 0]. \tag{1.26}$$

The kernel $K_B(\boldsymbol{\xi},\boldsymbol{\xi}_*,\boldsymbol{X},t)$ is required to satisfy the following conditions (i)–(iii):

(i) $K_B(\boldsymbol{\xi},\boldsymbol{\xi}_*) \ge 0 \quad [(\xi_i - v_{wi})n_i > 0,\ (\xi_{i*} - v_{wi})n_i < 0]$. (1.27a)

(ii) $$-\int_{(\xi_i - v_{wi})n_i>0}\frac{(\xi_k - v_{wk})n_k}{(\xi_{j*} - v_{wj})n_j}K_B(\boldsymbol{\xi},\boldsymbol{\xi}_*)\mathbf{d}\boldsymbol{\xi} = 1 \quad [(\xi_{i*} - v_{wi})n_i < 0], \tag{1.27b}$$

[12] When the condition of the boundary is specified, it is generally rather loosely mentioned that the temperature or velocity of the body or the condensed phase under consideration is so and so. This means that the surface temperature or velocity of the body or the condensed phase is so and so; then the temperature or velocity inside it is not important. Hereafter we do not repeat this type of note.

which corresponds to the condition of a simple boundary (or $m_f = 0$).[13]
(iii) When the kernel K_B is determined by the local condition of the boundary,[14]

$$f_B(\boldsymbol{\xi}) = \int_{(\xi_{i*}-v_{wi})n_i<0} K_B(\boldsymbol{\xi},\boldsymbol{\xi}_*) f_B(\boldsymbol{\xi}_*)\mathbf{d}\boldsymbol{\xi}_* \quad [(\xi_i - v_{wi})n_i > 0], \tag{1.27c}$$

where

$$f_B(\boldsymbol{\xi}) = \frac{\rho}{(2\pi RT_w)^{3/2}} \exp\left(-\frac{(\xi_i - v_{wi})^2}{2RT_w}\right),$$

with ρ being arbitrary, and the other Maxwellians do not satisfy the relation (1.27c). This uniqueness condition excludes the specular condition. The condition (1.27c) is the result of the local property of the kernel K_B and the natural requirement that the equilibrium state at temperature $\bar{T}_w$ and velocity $\bar{v}_{wi}$ is established in a box with a uniform temperature $\bar{T}_w$ and moving with a uniform velocity $\bar{v}_{wi}$.

For the Maxwell-type condition (1.23a) with (1.23b), the scattering kernel K_B is given by

$$\begin{aligned} K_B(\boldsymbol{\xi},\boldsymbol{\xi}_*) &= K_{BM}(\boldsymbol{\xi},\boldsymbol{\xi}_*) \\ &= \frac{-\alpha}{2\pi(RT_w)^2}(\xi_{j*} - v_{wj})n_j \exp\left(-\frac{(\xi_k - v_{wk})^2}{2RT_w}\right) \\ &\quad + (1-\alpha)\delta(\xi_{i*} - [\xi_i - 2(\xi_j - v_{wj})n_j n_i]), \end{aligned}$$

where $\delta(\xi_i)$ is the Dirac delta function.

1.6.2 Interface

On the interface of a gas and its condensed phase, the following mixed-type condition is often mentioned:

$$\begin{aligned} f(X_i,\xi_i,t) = {} & \frac{\alpha_c\rho_w}{(2\pi RT_w)^{3/2}} \exp\left(-\frac{(\xi_j - v_{wj})^2}{2RT_w}\right) \\ & + (1-\alpha_c)\Bigg[(1-\alpha) f(X_i, \xi_i - 2(\xi_j - v_{wj})n_j n_i, t) \\ & \quad + \frac{\alpha\sigma_w}{(2\pi RT_w)^{3/2}} \exp\left(-\frac{(\xi_j - v_{wj})^2}{2RT_w}\right)\Bigg] \quad [(\xi_j - v_{wj})n_j > 0], \end{aligned} \tag{1.28a}$$

[13]Consider the case where $f(\boldsymbol{X},\boldsymbol{\xi},t) = c_0\delta(\boldsymbol{\xi} - \boldsymbol{\xi}_\dagger)$ for $(\xi_j - v_{wj})n_j < 0$, where c_0 is a constant. Compute the integral

$$\int_{(\xi_j - v_{wj})n_j>0} (\xi_j - v_{wj})n_j f(\boldsymbol{X},\boldsymbol{\xi},t)\mathbf{d}\boldsymbol{\xi}$$

by two equations, one by the condition $m_f = 0$ of a simple boundary [see Eq. (1.3a)] and the other by the boundary condition (1.26). Then, equating the two expressions of the integral, we obtain Eq. (1.27b).

[14]The kernel is determined by the velocity v_{wi}, the temperature T_w, and the other properties of the boundary at the position $\boldsymbol{X}$ and the time t under consideration and is independent of their derivatives.

$$\sigma_w = -\left(\frac{2\pi}{RT_w}\right)^{1/2} \int_{(\xi_i - v_{wi})n_i < 0} (\xi_j - v_{wj}) n_j f(\boldsymbol{X}, \boldsymbol{\xi}, t) \mathbf{d}\boldsymbol{\xi}, \tag{1.28b}$$

where ρ_w is the saturated gas density at temperature T_w, α_c $(0 < \alpha_c \leq 1)$ is the *condensation coefficient*, and α $(0 \leq \alpha \leq 1)$ is the accommodation coefficient. Especially the case $\alpha_c = 1$ (the *complete-condensation* condition) is widely used. The complete-condensation condition is expressed as

$$f(\boldsymbol{X}, \boldsymbol{\xi}, t) = \frac{\rho_w}{(2\pi R T_w)^{3/2}} \exp\left(-\frac{(\xi_j - v_{wj})^2}{2RT_w}\right) \qquad [(\xi_j - v_{wj}) n_j > 0]. \tag{1.29}$$

The experimental discussion is found in Takens, Mischke, Korving & Beenakker [1984]. The saturated gas pressure p_w $(= R\rho_w T_w)$ at temperature T_w is more often used instead of ρ_w. The saturated gas pressure p_w is an increasing function of the temperature of the condensed phase (e.g., see Table C.2). Their relation is determined by the Clausius–Clapeyron relation (see, e.g., Feynman, Leighton & Sands [1963], Reif [1965], Landau & Lifshitz [1963]).

More generally, the condition is expressed in terms of a *scattering kernel* $K_I(\boldsymbol{\xi}, \boldsymbol{\xi}_*, \boldsymbol{X}, t)$ as

$$f(\boldsymbol{X}, \boldsymbol{\xi}, t) = g_I(\boldsymbol{X}, \boldsymbol{\xi}, t) + \int_{(\xi_{i*} - v_{wi})n_i < 0} K_I(\boldsymbol{\xi}, \boldsymbol{\xi}_*, \boldsymbol{X}, t) f(\boldsymbol{X}, \boldsymbol{\xi}_*, t) \mathbf{d}\boldsymbol{\xi}_* \qquad [(\xi_i - v_{wi}) n_i > 0], \tag{1.30}$$

where g_I, independent of f, corresponds to the term containing ρ_w in Eq. (1.28a).[15] The g_I and $K_I(\boldsymbol{\xi}, \boldsymbol{\xi}_*, \boldsymbol{X}, t)$ are required to satisfy the following conditions (i)–(iii):

(i) $g_I(\boldsymbol{X}, \boldsymbol{\xi}, t) \geq 0 \qquad [(\xi_i - v_{wi}) n_i > 0].$ (1.31a)

(ii) $K_I(\boldsymbol{\xi}, \boldsymbol{\xi}_*) \geq 0 \qquad [(\xi_i - v_{wi}) n_i > 0,\ (\xi_{i*} - v_{wi}) n_i < 0].$ (1.31b)

(iii) When the kernel K_I is determined by the local condition of the boundary,[16]

$$f_w(\boldsymbol{\xi}) = g_I(\boldsymbol{X}, \boldsymbol{\xi}, t) + \int_{(\xi_{i*} - v_{wi})n_i < 0} K_I(\boldsymbol{\xi}, \boldsymbol{\xi}_*) f_w(\boldsymbol{\xi}_*) \mathbf{d}\boldsymbol{\xi}_* \quad [(\xi_i - v_{wi}) n_i > 0], \tag{1.31c}$$

where

$$f_w(\boldsymbol{\xi}) = \frac{\rho_w}{(2\pi R T_w)^{3/2}} \exp\left(-\frac{(\xi_i - v_{wi})^2}{2RT_w}\right),$$

and the other Maxwellians do not satisfy the relation (1.31c). The condition (1.31c) is the result of the local property of the kernel K_I and the natural requirement that the equilibrium state at temperature $\bar{T}_w$, density $\bar{\rho}_w$ (the saturated gas density at temperature $\bar{T}_w$), and velocity $\bar{v}_{wi}$ is established in a box, with a uniform temperature $\bar{T}_w$ and moving with a uniform velocity $\bar{v}_{wi}$, made of the condensed phase of the gas.

[15] In Sone [2002], g_B is used for g_I here.
[16] See Footnote 14 in Section 1.6.1.

For the condition (1.28a) with (1.28b), g_I and K_I are given by

$$g_I(\boldsymbol{\xi}) = \frac{\alpha_c \rho_w}{(2\pi R T_w)^{3/2}} \exp\left(-\frac{(\xi_j - v_{wj})^2}{2RT_w}\right),$$
$$K_I(\boldsymbol{\xi}, \boldsymbol{\xi}_*) = (1-\alpha_c) K_{BM}(\boldsymbol{\xi}, \boldsymbol{\xi}_*).$$

1.7 H theorem

Consider the following functional, called the *H function*, of the velocity distribution function f :

$$H(X_i, t) = \int f \ln(f/c_0) \mathbf{d}\boldsymbol{\xi}, \tag{1.32}$$

where c_0 is a constant to make f/c_0 dimensionless. Multiplying the Boltzmann equation (1.5) with $F_i = 0$ by $1 + \ln(f/c_0)$, and integrating the result over the whole space of $\boldsymbol{\xi}$, we obtain the equation

$$\frac{\partial H}{\partial t} + \frac{\partial H_i}{\partial X_i} = G, \tag{1.33}$$

where

$$H_i = \int \xi_i f \ln(f/c_0) \mathbf{d}\boldsymbol{\xi}, \tag{1.34a}$$

$$G = \int [1 + \ln(f/c_0)] J(f,f) \mathbf{d}\boldsymbol{\xi}$$
$$= -\frac{1}{4m} \int (f' f'_* - f f_*) \ln\left(\frac{f' f'_*}{f f_*}\right) B \mathrm{d}\Omega \mathbf{d}\boldsymbol{\xi}_* \mathbf{d}\boldsymbol{\xi} \le 0. \tag{1.34b}$$

The equality in the last relation holds when and only when f is a (local) Maxwellian.[17] Incidentally, for a Maxwellian, i.e., $f = \rho(2\pi RT)^{-3/2} \exp[-(\xi_j - v_j)^2/2RT]$,

$$\frac{H}{\rho} = \ln \frac{\rho}{c_0 (2\pi RT)^{3/2}} - \frac{3}{2}, \quad H_i = H v_i, \tag{1.35}$$

where $-RH/\rho$ corresponds to the entropy per unit mass in thermodynamics. The time variation of the integral $\overline{H}$ of H over a domain D bounded by ∂D, which may be a moving boundary, is given by[18]

$$\frac{\mathrm{d}\overline{H}}{\mathrm{d}t} - \int_{\partial D} (H_i - H v_{wi}) n_i \mathrm{d}S = \int_D G \mathbf{d}\boldsymbol{X} \le 0, \tag{1.36}$$

where

$$\overline{H} = \int_D H \mathbf{d}\boldsymbol{X}, \tag{1.37}$$

[17] See the process of derivation of the Maxwell distribution in Section A.7.1.
[18] See Lemma in Section A.1.

and v_{wi} is the velocity of the boundary and n_i is the unit normal vector to the boundary, pointed to the gas.

From these equations, we have
(i) If the state, or f, is spatially uniform, then H never increases.
(ii) If $(H_i - Hv_{wi})n_i = 0$ on the boundary ∂D, then $\overline{H}$ never increases.
In both cases, H or $\overline{H}$ remains constant only when f is a (local) Maxwellian. These are the *Boltzmann H theorem*, which shows that the time evolution of a solution of the Boltzmann equation has a direction.

When the boundary is a simple boundary, the statement (ii) is made more explicit with the aid of the inequality (A.262) derived by Darrozes & Guiraud [1966]. The boundary term of Eq. (1.36) is estimated as Eq. (A.268) or

$$\int_{\partial D} (H_i - Hv_{wi})n_i \mathrm{d}S \leq -\int_{\partial D} \frac{n_i[q_i + p_{ij}(v_j - v_{wj})]}{RT_w}\mathrm{d}S, \tag{1.38}$$

where T_w is the temperature of the boundary. The equality in Eq. (1.38) holds when and only when f is the Maxwellian that satisfies the boundary condition (1.26) (or a Maxwellian with $v_i = v_{wi}$ and $T = T_w$); in this case its right-hand side vanishes. From Eqs. (1.36) and (1.38), we have

$$\frac{\mathrm{d}\overline{H}}{\mathrm{d}t} \leq -\int_{\partial D} \frac{n_i[q_i + p_{ij}(v_j - v_{wj})]}{RT_w}\mathrm{d}S. \tag{1.39}$$

From this relation, we have
(ii´) If there is no heat flow that flows into the boundary on each point of a simple boundary,[19] then $\overline{H}$ never increases.

1.8 Model equation

The following model equation, called the *Boltzmann–Krook–Welander, BKW,* or *BGK equation* (Bhatnagar, Gross & Krook [1954], Welander [1954], Kogan [1958], Sone & Aoki [1994]), where the collision term in Eq. (1.5) is simplified, is widely used in analyses of rarefied gas flows:[20]

$$\frac{\partial f}{\partial t} + \xi_i \frac{\partial f}{\partial X_i} + \frac{\partial F_i f}{\partial \xi_i} = A_c \rho (f_e - f), \tag{1.40a}$$

$$f_e = \frac{\rho}{(2\pi RT)^{3/2}} \exp\left(-\frac{(\xi_i - v_i)^2}{2RT}\right), \tag{1.40b}$$

where A_c is a constant, and f_e is the local Maxwellian whose parameters ρ, v_i, and T are defined with f by Eqs. (1.2a)–(1.2c).

[19] On a simple boundary, the energy transferred to the boundary per unit area and unit time from the gas is $-n_i(q_i + p_{ij}v_j)$ [Eq. (1.3c)], and the work done on the boundary per unit area and unit time by the gas is $-n_i p_{ij} v_{wj}$. Thus, their difference $-n_i[q_i + p_{ij}(v_j - v_{wj})]$ is the heat flow into the boundary.

[20] Some unreasonably undervalue this model equation. However, many fundamental and important results for the standard Boltzmann equation have been obtained with the studies of the BKW equation as precursors.

In the BKW equation, the loss term J_L of the collision integral is put in the form $A_c\rho f$, which is equivalent to that of the pseudo Maxwell molecule (Section A.2.4), but the gain term J_G is put in the form $A_c\rho f_e$, which is just a crude assumption. Identification of the $A_c\rho f$ term in Eq. (1.40a) as the loss term gives the physical meaning of A_c, i.e., $A_c\rho$ is the collision frequency, which is independent of $\boldsymbol{\xi}$ in accordance with the pseudo Maxwell molecule. Thus, the mean free path ℓ of the gas in the equilibrium state at rest with density ρ and temperature T is related to A_c as

$$\ell = \frac{(8RT/\pi)^{1/2}}{A_c\rho}. \tag{1.41}$$

The crude assumption in the BKW model is that the molecules just collided are distributed in Maxwellian with local flow velocity and temperature. This does not mean that the velocity distribution function f itself of the gas is to be close to a Maxwellian. If $|J_G^{pM}(f,f) - A_c\rho f_e|$ is much smaller than $A_c\rho|f_e - f|$, where $J_G^{pM}(f,f)$ is the gain term for the pseudo Maxwell molecule, the BKW equation approximates the Boltzmann equation for the pseudo Maxwell molecule well; f may differ considerably from f_e. The above criterion can be examined from the solution of the BKW equation for each problem.

For the BKW equation, the same conservation equations as in Section 1.3, where the collision term has vanished on integration (this is an important property of the collision term), are derived, and the H theorem (Section 1.7), an important property of the Boltzmann equation, holds.

1.9 Nondimensional expressions I

The nondimensional variables and equations, which are used in the following chapters, are listed here.

Let L, p_0, T_0, and t_0 be, respectively, the reference length, pressure, temperature, and time, and put

$$\rho_0 = p_0/RT_0. \tag{1.42}$$

Then, the nondimensional variables are defined as follows:

$$\left.\begin{array}{lll}
x_i = X_i/L, & \hat{t} = t/t_0, & \zeta_i = \xi_i/(2RT_0)^{1/2}, \\
\hat{f} = f/[\rho_0(2RT_0)^{-3/2}], & \hat{F}_i = F_i/(2RT_0/L), & \\
\hat{\rho} = \rho/\rho_0, & \hat{v}_i = v_i/(2RT_0)^{1/2}, & \hat{T} = T/T_0, \\
\hat{p} = p/p_0, & \hat{p}_{ij} = p_{ij}/p_0, & \hat{q}_i = q_i/p_0(2RT_0)^{1/2}, \\
\hat{H} = H/\rho_0, & \hat{H}_i = H_i/\rho_0(2RT_0)^{1/2}, & \hat{G} = G/(\rho_0^2 B_0/m), \\
\hat{v}_{wi} = v_{wi}/(2RT_0)^{1/2}, & \hat{T}_w = T_w/T_0, & \hat{\rho}_w = \rho_w/\rho_0, \\
\hat{p}_w = p_w/p_0, & (\hat{p}_w = \hat{\rho}_w\hat{T}_w), &
\end{array}\right\} \tag{1.43}$$

where $(2RT_0)^{1/2}$ and $p_0(2RT_0)^{1/2}$ are, respectively, chosen as the reference magnitudes of velocity and heat-flow vector. With the notation $E(\zeta)$

$$E(\zeta) = \frac{1}{\pi^{3/2}} \exp(-\zeta^2), \quad \zeta = |\zeta_i| = (\zeta_i^2)^{1/2} = |\boldsymbol{\zeta}|, \tag{1.44}$$

the Maxwell distribution f_0 with $v_i = 0$, $p = p_0$, and $T = T_0$, i.e.,

$$f_0 = \frac{\rho_0}{(2\pi RT_0)^{3/2}} \exp\left(-\frac{\xi_i^2}{2RT_0}\right), \tag{1.45}$$

is expressed in the form

$$f_0 = \frac{\rho_0}{(2RT_0)^{3/2}} E(\zeta). \tag{1.46}$$

The nondimensional form of the Boltzmann equation for $\hat{f}$ is

$$\mathrm{Sh}\frac{\partial \hat{f}}{\partial \hat{t}} + \zeta_i \frac{\partial \hat{f}}{\partial x_i} + \frac{\partial \hat{F}_i \hat{f}}{\partial \zeta_i} = \frac{1}{k} \hat{J}(\hat{f}, \hat{f}), \tag{1.47a}$$

$$\hat{J}(\hat{f}, \hat{g}) = \frac{1}{2} \int (\hat{f}' \hat{g}'_* + \hat{f}'_* \hat{g}' - \hat{f}\hat{g}_* - \hat{f}_* \hat{g}) \widehat{B} \, \mathrm{d}\Omega(\boldsymbol{\alpha}) \, \mathbf{d}\boldsymbol{\zeta}_*, \tag{1.47b}$$

where

$$\mathrm{Sh} = \frac{L}{t_0(2RT_0)^{1/2}}, \tag{1.48a}$$

$$k = \frac{(2RT_0)^{1/2}}{(\rho_0/m)B_0 L} = \frac{\sqrt{\pi}\ell_0}{2L} = \frac{\sqrt{\pi}}{2}\mathrm{Kn}, \tag{1.48b}$$

$$\begin{aligned} \widehat{B} &= \widehat{B}\left(|\boldsymbol{\alpha} \cdot (\boldsymbol{\zeta}_* - \boldsymbol{\zeta})|/|\boldsymbol{\zeta}_* - \boldsymbol{\zeta}|, |\boldsymbol{\zeta}_* - \boldsymbol{\zeta}|\right) \\ &= \frac{B(|\boldsymbol{\alpha} \cdot (\boldsymbol{\xi}_* - \boldsymbol{\xi})|/|\boldsymbol{\xi}_* - \boldsymbol{\xi}|, |\boldsymbol{\xi}_* - \boldsymbol{\xi}|)}{B_0}, \end{aligned} \tag{1.48c}$$

$$\begin{aligned} B_0 &= \frac{1}{\rho_0^2} \int f_0 f_{0*} B(|\boldsymbol{\alpha} \cdot (\boldsymbol{\xi}_* - \boldsymbol{\xi})|/|\boldsymbol{\xi}_* - \boldsymbol{\xi}|, |\boldsymbol{\xi}_* - \boldsymbol{\xi}|) \mathrm{d}\Omega(\boldsymbol{\alpha}) \, \mathbf{d}\boldsymbol{\xi} \mathbf{d}\boldsymbol{\xi}_* \\ &= \int E E_* B(|\boldsymbol{\alpha} \cdot (\boldsymbol{\zeta}_* - \boldsymbol{\zeta})|/|\boldsymbol{\zeta}_* - \boldsymbol{\zeta}|, (2RT_0)^{1/2}|\boldsymbol{\zeta}_* - \boldsymbol{\zeta}|) \mathrm{d}\Omega(\boldsymbol{\alpha}) \, \mathbf{d}\boldsymbol{\zeta} \mathbf{d}\boldsymbol{\zeta}_* \\ &= 4\sqrt{\pi} d_m^2 (RT_0)^{1/2}, \end{aligned} \tag{1.48d}$$

$$\mathbf{d}\boldsymbol{\zeta} = \mathrm{d}\zeta_1 \mathrm{d}\zeta_2 \mathrm{d}\zeta_3, \quad \mathbf{d}\boldsymbol{\zeta}_* = \mathrm{d}\zeta_{1*} \mathrm{d}\zeta_{2*} \mathrm{d}\zeta_{3*}, \tag{1.48e}$$

$$\left.\begin{aligned} &\hat{f} = \hat{f}(\zeta_i), \quad \hat{f}_* = \hat{f}(\zeta_{i*}), \quad \hat{f}' = \hat{f}(\zeta'_i), \quad \hat{f}'_* = \hat{f}(\zeta'_{i*}), \\ &\zeta'_i = \zeta_i + \alpha_i \alpha_j (\zeta_{j*} - \zeta_j), \qquad \zeta'_{i*} = \zeta_{i*} - \alpha_i \alpha_j (\zeta_{j*} - \zeta_j), \end{aligned}\right\} \tag{1.48f}$$

and Eq. (1.48f) is applied also to the function $\hat{g}$ of ζ_i, and the dot $\cdot$ between bold

letters indicates their scalar product.[21] It is noted that the nondimensionalized form $\widehat{B}$ of B, a function of $|\alpha_i(\zeta_{i*}-\zeta_i)|/|\zeta_{k*}-\zeta_k|$ and $|\zeta_{i*}-\zeta_i|$, generally depends on T_0 as well as the intermolecular potential.[22] For a hard-sphere gas,

$$\widehat{B} = \frac{|\alpha_i(\zeta_{i*} - \zeta_i)|}{4(2\pi)^{1/2}}, \tag{1.49}$$

which is exceptionally independent of T_0. According to the definitions given in Section 1.5, $\rho_0 B_0 m^{-1}$ is the mean collision frequency of the gas in the equilibrium state at rest with pressure p_0 and temperature T_0 [or the state given by Eq. (1.45)], and ℓ_0 [$= (8RT_0/\pi)^{1/2}/(\rho_0/m)B_0$] is the mean free path of the gas in the equilibrium state. The Sh is called the *Strouhal number*, and Kn the *Knudsen number*. The product ShKn [$= 2/\sqrt{\pi}(\rho_0/m)B_0 t_0$] is $2/\sqrt{\pi}$ times the ratio of the mean free time $[(\rho_0/m)B_0]^{-1}$ to the reference time t_0. The nondimensional collision term $\hat{J}$ is split into the gain and loss terms as

$$\hat{J} = \hat{J}_G - \hat{J}_L = \hat{J}_G - \hat{\nu}_c \hat{f}, \tag{1.50}$$

where

$$\hat{J}_G = \int \hat{f}' \hat{f}'_* \widehat{B} \, \mathrm{d}\Omega(\boldsymbol{\alpha}) \, \mathbf{d}\boldsymbol{\zeta}_*, \tag{1.51a}$$

$$\hat{\nu}_c = \int \hat{f}_* \widehat{B} \, \mathrm{d}\Omega(\boldsymbol{\alpha}) \, \mathbf{d}\boldsymbol{\zeta}_*. \tag{1.51b}$$

The Knudsen number Kn and the product ShKn are the nondimensional parameters that characterize the effect of molecular collisions. They are, respectively, the weight of the space-derivative terms and that of the time-derivative term relative to the collision term in the Boltzmann equation (1.5). According to Footnote 22 in this section (or the more detailed discussion in Section A.2.4), another nondimensional parameter $U_0/k_B T_0$ is contained in the Boltzmann equation (1.47a), in addition to Kn and ShKn. These three parameters are the similarity parameters in the Boltzmann equation.

---

[21] When the intermolecular potential extends up to infinity ($d_m \to \infty$), B_0 is infinite and therefore the above-defined nondimensionalization is useless. In such a case, the range of integral of the definition of B_0 is limited, for example, to a domain where the range $|\alpha_i(\zeta_{i*} - \zeta_i)|/|\zeta_{k*} - \zeta_k| \ll 1$ is excluded. The other quantities, i.e., ℓ_0, k, Kn, and $\widehat{B}$, are defined on the basis of this B_0 by the relations shown above (see also Sections 1.2, 1.5, and A.2.4).

[22] When the intermolecular potential of the finite range d_m is given, for example, by $U_0 U(r/d_m)$, where r is the intermolecular distance, the function $\widehat{B}$ is a function of $|\alpha_i(\zeta_{i*} - \zeta_i)|/|\zeta_{k*} - \zeta_k|$, $|\zeta_{i*} - \zeta_i|$, and $U_0/k_B T_0$, i.e., $\widehat{B}(|\alpha_i(\zeta_{i*} - \zeta_i)|/|\zeta_{k*} - \zeta_k|, |\zeta_{i*} - \zeta_i|, U_0/k_B T_0)$ and its functional form depends on U (see Section A.2.4). Thus, the nondimensional Boltzmann equation contains the parameter $U_0/k_B T_0$ in addition to the Strouhal and Knudsen numbers Sh and Kn (and external force). The Boltzmann equation for a hard-sphere gas and the BKW equation are exceptional cases, where this parameter is absent in their nondimensional forms [see Eqs. (1.49) and (1.60a)]. This fact is not widely mentioned, but it should be noted that the solution of the nondimensional Boltzmann equation depends on this parameter as well as Sh and Kn.

The generalized collision integral $\hat{J}(\hat{f},\hat{g})$ satisfies the following symmetry relation corresponding to Eq. (1.10): For any $\varphi(\boldsymbol{\zeta})$, $\hat{f}(\boldsymbol{\zeta})$, and $\hat{g}(\boldsymbol{\zeta})$,

$$\int \varphi(\boldsymbol{\zeta})\hat{J}(\hat{f},\hat{g})\mathbf{d}\boldsymbol{\zeta} = \frac{1}{8}\int(\varphi+\varphi_*-\varphi'-\varphi'_*)(\hat{f}'\hat{g}'_*+\hat{f}'_*\hat{g}'-\hat{f}\hat{g}_*-\hat{f}_*\hat{g})\widehat{B}\mathrm{d}\Omega\mathbf{d}\boldsymbol{\zeta}_*\mathbf{d}\boldsymbol{\zeta}, \tag{1.52}$$

from which

$$\int \begin{pmatrix} 1 \\ \zeta_i \\ \zeta_i^2 \end{pmatrix} \hat{J}(\hat{f},\hat{g})\mathbf{d}\boldsymbol{\zeta} = 0. \tag{1.53}$$

The relations between the nondimensional macroscopic variables $\hat{\rho}, \hat{v}_i, \hat{T}$, etc. and the nondimensional velocity distribution function $\hat{f}$ are

$$\hat{\rho} = \int \hat{f}\mathbf{d}\boldsymbol{\zeta}, \tag{1.54a}$$

$$\hat{\rho}\hat{v}_i = \int \zeta_i \hat{f}\mathbf{d}\boldsymbol{\zeta}, \tag{1.54b}$$

$$\frac{3}{2}\hat{\rho}\hat{T} = \int (\zeta_i-\hat{v}_i)^2\hat{f}\mathbf{d}\boldsymbol{\zeta}, \tag{1.54c}$$

$$\hat{p} = \hat{\rho}\hat{T}, \tag{1.54d}$$

$$\hat{p}_{ij} = 2\int(\zeta_i-\hat{v}_i)(\zeta_j-\hat{v}_j)\hat{f}\mathbf{d}\boldsymbol{\zeta}, \tag{1.54e}$$

$$\hat{q}_i = \int(\zeta_i-\hat{v}_i)(\zeta_j-\hat{v}_j)^2\hat{f}\mathbf{d}\boldsymbol{\zeta}. \tag{1.54f}$$

The local Maxwellian $\hat{f}_e$ in the present nondimensional expression is given by

$$\hat{f}_e = \frac{\hat{\rho}}{(\pi\hat{T})^{3/2}}\exp\left(-\frac{(\zeta_i-\hat{v}_i)^2}{\hat{T}}\right), \tag{1.55}$$

for which

$$\hat{J}(\hat{f}_e,\hat{f}_e) = 0. \tag{1.56}$$

The nondimensional forms of the conservation equations (1.12)–(1.14) are

$$\mathrm{Sh}\frac{\partial\hat{\rho}}{\partial\hat{t}} + \frac{\partial\hat{\rho}\hat{v}_i}{\partial x_i} = 0, \tag{1.57}$$

$$\mathrm{Sh}\frac{\partial\hat{\rho}\hat{v}_i}{\partial\hat{t}} + \frac{\partial}{\partial x_j}\left(\hat{\rho}\hat{v}_i\hat{v}_j + \frac{1}{2}\hat{p}_{ij}\right) = \hat{\rho}\hat{F}_i, \tag{1.58}$$

$$\mathrm{Sh}\frac{\partial}{\partial\hat{t}}\left[\hat{\rho}\left(\hat{v}_i^2+\frac{3}{2}\hat{T}\right)\right] + \frac{\partial}{\partial x_j}\left[\hat{\rho}\hat{v}_j\left(\hat{v}_i^2+\frac{3}{2}\hat{T}\right)+\hat{p}_{ij}\hat{v}_i+\hat{q}_j\right] = 2\hat{\rho}\hat{v}_j\hat{F}_j, \tag{1.59}$$

where $\hat{F}_i$ is assumed to be independent of $\boldsymbol{\zeta}$.

For the BKW equation the collision integral $\hat{J}(\hat{f},\hat{f})$ and k are given by[23]

$$\hat{J}(\hat{f},\hat{f}) = \hat{\rho}(\hat{f}_e - \hat{f}), \tag{1.60a}$$

$$k = \frac{\sqrt{\pi}\ell_0}{2L} = \frac{(2RT_0)^{1/2}}{A_c\rho_0 L}. \tag{1.60b}$$

That is, the nondimensional form of the BKW equation is given by

$$\mathrm{Sh}\frac{\partial \hat{f}}{\partial \hat{t}} + \zeta_i \frac{\partial \hat{f}}{\partial x_i} + \frac{\partial \hat{F}_i \hat{f}}{\partial \zeta_i} = \frac{1}{k}\hat{\rho}(\hat{f}_e - \hat{f}). \tag{1.61}$$

The Maxwell-type boundary condition on a simple boundary is expressed as

$$\hat{f}(x_i,\zeta_i,\hat{t}) = (1-\alpha)\hat{f}(x_i,\zeta_i - 2(\zeta_j - \hat{v}_{wj})n_j n_i,\hat{t}) + \frac{\alpha\hat{\sigma}_w}{(\pi\hat{T}_w)^{3/2}}\exp\left(-\frac{(\zeta_i-\hat{v}_{wi})^2}{\hat{T}_w}\right) \quad [(\zeta_j-\hat{v}_{wj})n_j > 0], \tag{1.62a}$$

$$\hat{\sigma}_w = -2\left(\frac{\pi}{\hat{T}_w}\right)^{1/2}\int_{(\zeta_j-\hat{v}_{wj})n_j<0}(\zeta_j-\hat{v}_{wj})n_j\hat{f}(x_i,\zeta_i,\hat{t})\mathbf{d}\boldsymbol{\zeta}. \tag{1.62b}$$

The diffuse-reflection condition is given by putting $\alpha = 1$ in Eq. (1.62a), i.e.,

$$\hat{f}(x_i,\zeta_i,\hat{t}) = \frac{\hat{\sigma}_w}{(\pi\hat{T}_w)^{3/2}}\exp\left(-\frac{(\zeta_i-\hat{v}_{wi})^2}{\hat{T}_w}\right) \quad [(\zeta_j-\hat{v}_{wj})n_j > 0], \tag{1.63a}$$

$$\hat{\sigma}_w = -2\left(\frac{\pi}{\hat{T}_w}\right)^{1/2}\int_{(\zeta_j-\hat{v}_{wj})n_j<0}(\zeta_j-\hat{v}_{wj})n_j\hat{f}(x_i,\zeta_i,\hat{t})\mathbf{d}\boldsymbol{\zeta}, \tag{1.63b}$$

and the specular-reflection condition is given by putting $\alpha = 0$ in Eq. (1.62a), i.e.,

$$\hat{f}(x_i,\zeta_i,\hat{t}) = \hat{f}(x_i,\zeta_i - 2(\zeta_j-\hat{v}_{wj})n_j n_i,\hat{t}) \quad [(\zeta_j-\hat{v}_{wj})n_j > 0].$$

The nondimensional form of the boundary condition (1.26) expressed by the scattering kernel is

$$\hat{f}(\boldsymbol{x},\boldsymbol{\zeta},\hat{t}) = \int_{(\zeta_{i*}-\hat{v}_{wi})n_i<0}\hat{K}_B(\boldsymbol{\zeta},\boldsymbol{\zeta}_*,\boldsymbol{x},\hat{t})\hat{f}(\boldsymbol{x},\boldsymbol{\zeta}_*,\hat{t})\mathbf{d}\boldsymbol{\zeta}_* \quad [(\zeta_i-\hat{v}_{wi})n_i > 0], \tag{1.64}$$

where

$$\hat{K}_B(\boldsymbol{\zeta},\boldsymbol{\zeta}_*,\boldsymbol{x},\hat{t}) = K_B(\boldsymbol{\xi},\boldsymbol{\xi}_*,\boldsymbol{X},t)(2RT_0)^{3/2}. \tag{1.65}$$

[23]For the BKW equation, the expression $\hat{J}(\hat{f},\hat{g})$ is not defined unless $\hat{g} = \hat{f}$, and $\hat{J}(\hat{f},\hat{f})$ is taken as the collision integral as a whole. Various expressions obtained by the use of the bilinear character of $\hat{J}(\hat{f},\hat{g})$ in the following chapters are not applied to the BKW equation, including the case where the same arguments happen to appear. Some $\hat{J}(\hat{f},\hat{g})$ expressions in equations correspond to linearized collision integrals linearized around some Maxwell distributions (see Section A.2.8) and play an important role there.

Corresponding to the conditions (i), (ii), and (iii) just after Eq. (1.26), the kernel $\hat{K}_B(\boldsymbol{\zeta}, \boldsymbol{\zeta}_*)$ satisfies the following conditions:

$$\text{(i)} \quad \hat{K}_B(\boldsymbol{\zeta}, \boldsymbol{\zeta}_*) \geq 0 \qquad [(\zeta_i - \hat{v}_{wi})n_i > 0,\ (\zeta_{i*} - \hat{v}_{wi})n_i < 0]. \tag{1.66a}$$

$$\text{(ii)} \quad -\int_{(\zeta_i - \hat{v}_{wi})n_i > 0} \frac{(\zeta_k - \hat{v}_{wk})n_k}{(\zeta_{j*} - \hat{v}_{wj})n_j} \hat{K}_B(\boldsymbol{\zeta}, \boldsymbol{\zeta}_*) \mathbf{d}\boldsymbol{\zeta} = 1 \qquad [(\zeta_{i*} - \hat{v}_{wi})n_i < 0]. \tag{1.66b}$$

$$\text{(iii)} \quad \hat{f}_B(\boldsymbol{\zeta}) = \int_{(\zeta_{i*} - \hat{v}_{wi})n_i < 0} \hat{K}_B(\boldsymbol{\zeta}, \boldsymbol{\zeta}_*) \hat{f}_B(\boldsymbol{\zeta}_*) \mathbf{d}\boldsymbol{\zeta}_* \quad [(\zeta_i - \hat{v}_{wi})n_i > 0], \tag{1.66c}$$

where

$$\hat{f}_B(\boldsymbol{\zeta}) = \frac{\hat{\rho}}{(\pi \hat{T}_w)^{3/2}} \exp\left(-\frac{(\zeta_i - \hat{v}_{wi})^2}{\hat{T}_w} \right),$$

with arbitrary $\hat{\rho}$, and any other Maxwellian does not satisfy Eq. (1.66c).

The mixed-type condition (1.28a) with (1.28b) on the interface is reduced to the following form:

$$\begin{aligned} \hat{f}(x_i, \zeta_i, \hat{t}) = {} & \frac{\alpha_c \hat{\rho}_w}{(\pi \hat{T}_w)^{3/2}} \exp\left(-\frac{(\zeta_i - \hat{v}_{wi})^2}{\hat{T}_w} \right) \\ & + (1 - \alpha_c) \Bigg[(1 - \alpha) \hat{f}(x_i, \zeta_i - 2(\zeta_j - \hat{v}_{wj}) n_j n_i, \hat{t}) \\ & \qquad + \frac{\alpha \hat{\sigma}_w}{(\pi \hat{T}_w)^{3/2}} \exp\left(-\frac{(\zeta_i - \hat{v}_{wi})^2}{\hat{T}_w} \right) \Bigg] \quad [(\zeta_j - \hat{v}_{wj}) n_j > 0], \end{aligned} \tag{1.67a}$$

$$\hat{\sigma}_w = -2 \left(\frac{\pi}{\hat{T}_w} \right)^{1/2} \int_{(\zeta_j - \hat{v}_{wj}) n_j < 0} (\zeta_j - \hat{v}_{wj}) n_j \hat{f}(x_i, \zeta_i, \hat{t}) \mathbf{d}\boldsymbol{\zeta}. \tag{1.67b}$$

The complete-condensation condition is given by putting $\alpha_c = 1$ in Eq. (1.67a), i.e.,

$$\hat{f}(x_i, \zeta_i, \hat{t}) = \frac{\hat{\rho}_w}{(\pi \hat{T}_w)^{3/2}} \exp\left(-\frac{(\zeta_i - \hat{v}_{wi})^2}{\hat{T}_w} \right) \qquad [(\zeta_j - \hat{v}_{wj}) n_j > 0]. \tag{1.68}$$

The nondimensional form of the boundary condition (1.30) expressed by the scattering kernel is

$$\hat{f}(\boldsymbol{x}, \boldsymbol{\zeta}, \hat{t}) = \hat{g}_I(\boldsymbol{x}, \boldsymbol{\zeta}, \hat{t}) + \int_{(\zeta_{i*} - \hat{v}_{wi}) n_i < 0} \hat{K}_I(\boldsymbol{\zeta}, \boldsymbol{\zeta}_*, \boldsymbol{x}, \hat{t}) \hat{f}(\boldsymbol{x}, \boldsymbol{\zeta}_*, \hat{t}) \mathbf{d}\boldsymbol{\zeta}_* \qquad [(\zeta_i - \hat{v}_{wi}) n_i > 0], \tag{1.69}$$

where

$$\hat{K}_I(\boldsymbol{\zeta}, \boldsymbol{\zeta}_*, \boldsymbol{x}, \hat{t}) = K_I(\boldsymbol{\xi}, \boldsymbol{\xi}_*, \boldsymbol{X}, t)(2RT_0)^{3/2}, \tag{1.70a}$$

$$\hat{g}_I(\boldsymbol{x}, \boldsymbol{\zeta}, \hat{t}) = g_I(\boldsymbol{X}, \boldsymbol{\xi}, t)/[\rho_0 (2RT_0)^{-3/2}]. \tag{1.70b}$$

Corresponding to the conditions (i), (ii), and (iii) just after Eq. (1.30), $\hat{g}_I$ and $\hat{K}_I$ satisfy the following conditions:

(i) $\hat{g}_I(\boldsymbol{x}, \boldsymbol{\zeta}, \hat{t}) \geq 0 \qquad [(\zeta_i - \hat{v}_{wi})n_i > 0].$ (1.71a)

(ii) $\hat{K}_I(\boldsymbol{\zeta}, \boldsymbol{\zeta}_*) \geq 0 \qquad [(\zeta_i - \hat{v}_{wi})n_i > 0,\ (\zeta_{i*} - \hat{v}_{wi})n_i < 0].$ (1.71b)

(iii) $$\hat{f}_w(\boldsymbol{\zeta}) = \hat{g}_I(\boldsymbol{x}, \boldsymbol{\zeta}, \hat{t}) + \int_{(\zeta_{i*} - \hat{v}_{wi})n_i < 0} \hat{K}_I(\boldsymbol{\zeta}, \boldsymbol{\zeta}_*)\hat{f}_w(\boldsymbol{\zeta}_*)\mathbf{d}\boldsymbol{\zeta}_* \quad [(\zeta_i - \hat{v}_{wi})n_i > 0], \tag{1.71c}$$

where

$$\hat{f}_w(\boldsymbol{\zeta}) = \frac{\hat{\rho}_w}{(\pi\hat{T}_w)^{3/2}} \exp\left(-\frac{(\zeta_i - \hat{v}_{wi})^2}{\hat{T}_w}\right),$$

and any other Maxwellian does not satisfy Eq. (1.71c).

The nondimensional form of the equation for H [Eq. (1.33)] is

$$\mathrm{Sh}\frac{\partial \hat{H}}{\partial \hat{t}} + \frac{\partial \hat{H}_i}{\partial x_i} = \frac{1}{k}\hat{G}, \tag{1.72}$$

where

$$\left.\begin{aligned} &\hat{H}(x_i, \hat{t}) = \int \hat{f}\ln(\hat{f}/\hat{c}_0)\mathbf{d}\boldsymbol{\zeta}, \quad \hat{H}_i(x_i, \hat{t}) = \int \zeta_i \hat{f}\ln(\hat{f}/\hat{c}_0)\mathbf{d}\boldsymbol{\zeta}, \\ &\hat{G} = -\frac{1}{4}\int (\hat{f}'\hat{f}'_* - \hat{f}\hat{f}_*)\ln\left(\frac{\hat{f}'\hat{f}'_*}{\hat{f}\hat{f}_*}\right)\widehat{B}\mathrm{d}\Omega\mathbf{d}\boldsymbol{\zeta}_*\mathbf{d}\boldsymbol{\zeta} \leq 0, \end{aligned}\right\} \tag{1.73}$$

with $\hat{c}_0 = c_0(2RT_0)^{3/2}/\rho_0$.

1.10 Nondimensional expressions II

When we consider the case where the state of a gas is not much different from an equilibrium state at rest in a system with $F_i = 0$, it is convenient to choose the variables expressing the perturbation from this state. The Maxwell distribution f_0 given by Eq. (1.45) is taken as the reference state. The nondimensional perturbed variables are chosen as follows:

$$\left.\begin{aligned} &\phi = f/f_0 - 1 && \omega = \rho/\rho_0 - 1 && u_i = v_i/(2RT_0)^{1/2} \\ &\quad = \hat{f}/E - 1, && \quad = \hat{\rho} - 1, && \quad = \hat{v}_i, \\ &\tau = T/T_0 - 1 && P = p/p_0 - 1 && P_{ij} = p_{ij}/p_0 - \delta_{ij} \\ &\quad = \hat{T} - 1, && \quad = \hat{p} - 1, && \quad = \hat{p}_{ij} - \delta_{ij}, \\ &Q_i = q_i/p_0(2RT_0)^{1/2} && u_{wi} = v_{wi}/(2RT_0)^{1/2} && \tau_w = T_w/T_0 - 1 \\ &\quad = \hat{q}_i, && \quad = \hat{v}_{wi}, && \quad = \hat{T}_w - 1, \\ &\omega_w = \rho_w/\rho_0 - 1 && P_w = p_w/p_0 - 1 && (P_w = \omega_w + \tau_w + \omega_w\tau_w). \\ &\quad = \hat{\rho}_w - 1, && \quad = \hat{p}_w - 1, && \end{aligned}\right\} \tag{1.74}$$

This system of notation is suitable to perturbation analyses.

The nondimensional form of the Boltzmann equation with $F_i = 0$ is given as

$$\mathrm{Sh}\frac{\partial \phi}{\partial \hat{t}} + \zeta_i \frac{\partial \phi}{\partial x_i} = \frac{1}{k}[\mathcal{L}(\phi) + \mathcal{J}(\phi, \phi)], \tag{1.75a}$$

$$\mathcal{L}(\phi) = \int E_*(\phi' + \phi'_* - \phi - \phi_*)\widehat{B}\,\mathrm{d}\Omega(\boldsymbol{\alpha})\,\mathbf{d}\boldsymbol{\zeta}_*, \tag{1.75b}$$

$$\mathcal{J}(\phi, \psi) = \frac{1}{2}\int E_*(\phi'\psi'_* + \phi'_*\psi' - \phi\psi_* - \phi_*\psi)\widehat{B}\,\mathrm{d}\Omega(\boldsymbol{\alpha})\,\mathbf{d}\boldsymbol{\zeta}_*, \tag{1.75c}$$

where

$$\phi = \phi(\zeta_i), \quad \phi_* = \phi(\zeta_{i*}), \quad \phi' = \phi(\zeta'_i), \quad \phi'_* = \phi(\zeta'_{i*}), \tag{1.76a}$$

$$\zeta'_i = \zeta_i + \alpha_i\alpha_j(\zeta_{j*} - \zeta_j), \qquad \zeta'_{i*} = \zeta_{i*} - \alpha_i\alpha_j(\zeta_{j*} - \zeta_j). \tag{1.76b}$$

The rule (1.76a) is applied to the function ψ of ζ_i. The operator $\mathcal{J}$ is related to $\mathcal{L}$ and $\hat{J}$ [Eq. (1.47b)] in the following way:

$$2\mathcal{J}(1, \phi) = \mathcal{L}(\phi), \tag{1.77a}$$

$$E\mathcal{J}(\phi, \psi) = \hat{J}(E\phi, E\psi). \tag{1.77b}$$

The relations between the nondimensional macroscopic variables and the nondimensional velocity distribution function ϕ are

$$\omega = \int \phi E\mathbf{d}\boldsymbol{\zeta}, \tag{1.78a}$$

$$(1 + \omega)u_i = \int \zeta_i \phi E\mathbf{d}\boldsymbol{\zeta}, \tag{1.78b}$$

$$\frac{3}{2}(1 + \omega)\tau = \int \left(\zeta_i^2 - \frac{3}{2}\right)\phi E\mathbf{d}\boldsymbol{\zeta} \; - (1 + \omega)u_i^2, \tag{1.78c}$$

$$P = \omega + \tau + \omega\tau, \tag{1.78d}$$

$$P_{ij} = 2\int \zeta_i\zeta_j\phi E\mathbf{d}\boldsymbol{\zeta} - 2(1 + \omega)u_iu_j, \tag{1.78e}$$

$$Q_i = \int \zeta_i\zeta_j^2\phi E\mathbf{d}\boldsymbol{\zeta} - \frac{5}{2}u_i - u_jP_{ij} - \frac{3}{2}u_iP - (1 + \omega)u_iu_j^2. \tag{1.78f}$$

The linear part $\mathcal{L}(\phi)$ of the collision integral, called the *linearized collision integral*, satisfies the following relations (see Section A.2.2):
The symmetry relation, corresponding to Eq. (1.52), is

$$\int \psi(\boldsymbol{\zeta})\mathcal{L}(\phi)E\mathbf{d}\boldsymbol{\zeta} = \frac{1}{4}\int EE_*(\psi + \psi_* - \psi' - \psi'_*)(\phi' + \phi'_* - \phi - \phi_*)\widehat{B}\mathrm{d}\Omega\mathbf{d}\boldsymbol{\zeta}_*\mathbf{d}\boldsymbol{\zeta}$$
$$\text{for any } \phi \text{ and } \psi. \tag{1.79}$$

With $\psi = \phi$ in Eq. (1.79),

$$\int \phi \mathcal{L}(\phi) E \mathbf{d}\boldsymbol{\zeta} \leq 0, \tag{1.80}$$

where the equality sign holds when and only when ϕ is a summational invariant, i.e., a linear combination of 1, ζ_i, and ζ_i^2 (see Section A.2.3). Also from Eq. (1.79), the operator $\mathcal{L}(*)$ is found to be *self-adjoint*, i.e.,

$$\int \psi \mathcal{L}(\phi) E \mathbf{d}\boldsymbol{\zeta} = \int \phi \mathcal{L}(\psi) E \mathbf{d}\boldsymbol{\zeta} \quad \text{for any } \phi \text{ and } \psi. \tag{1.81}$$

Each of the following two relations holds when and only when φ is a linear combination of 1, ζ_i, and ζ_i^2 :[24] the equation

$$\mathcal{L}(\varphi) = 0, \tag{1.82}$$

and the relation

$$\int \varphi \mathcal{L}(\phi) E \mathbf{d}\boldsymbol{\zeta} = 0 \quad \text{for any } \phi. \tag{1.83}$$

Corresponding to Eq. (1.53), in view of the relation (1.77b),

$$\int \begin{pmatrix} 1 \\ \zeta_i \\ \zeta_i^2 \end{pmatrix} \mathcal{J}(\phi, \psi) E \mathbf{d}\boldsymbol{\zeta} = 0 \quad \text{for any } \phi \text{ and } \psi. \tag{1.84}$$

The (local) Maxwell distribution ϕ_e in the present nondimensional perturbed expression is

$$E\phi_e = \frac{1+\omega}{\pi^{3/2}(1+\tau)^{3/2}} \exp\left(-\frac{(\zeta_i - u_i)^2}{1+\tau}\right) - E. \tag{1.85}$$

Sometimes, its parameters ω, u_i, and τ are explicitly shown as $\phi_e(\omega, u_i, \tau)$. Corresponding to Eq. (1.56),

$$\mathcal{L}(\phi_e) + \mathcal{J}(\phi_e, \phi_e) = 0. \tag{1.86}$$

The conservation equations are expressed as

$$\mathrm{Sh}\frac{\partial \omega}{\partial \hat{t}} + \frac{\partial (1+\omega) u_i}{\partial x_i} = 0, \tag{1.87}$$

$$\mathrm{Sh}\frac{\partial (1+\omega) u_i}{\partial \hat{t}} + \frac{\partial}{\partial x_j}\left((1+\omega) u_i u_j + \frac{1}{2} P_{ij}\right) = 0, \tag{1.88}$$

$$\mathrm{Sh}\frac{\partial}{\partial \hat{t}}\left((1+\omega) u_i^2 + \frac{3}{2} P\right) + \frac{\partial}{\partial x_j}\left(\frac{5}{2} u_j + u_i P_{ij} + \frac{3}{2} P u_j + (1+\omega) u_j u_i^2 + Q_j\right) = 0. \tag{1.89}$$

[24] Each relation is obviously satisfied by the linear combination. It is seen from the above-mentioned results, including the self-adjoint property of $\mathcal{L}(*)$, that φ is limited to the linear combination.

The BKW equation is

$$\mathrm{Sh}\frac{\partial \phi}{\partial \hat{t}} + \zeta_i \frac{\partial \phi}{\partial x_i} = \frac{1}{k}(1+\omega)(\phi_e - \phi), \tag{1.90}$$

where

$$k = (2RT_0)^{1/2}(\rho_0 A_c L)^{-1} [= (\sqrt{\pi}/2)\ell_0 L^{-1}]. \tag{1.91}$$

The Maxwell-type boundary condition in a general case is just a transcription of the formula (1.62a) with (1.62b) by Eq. (1.74) and not a simple form, because the Maxwellian $E(\zeta)$ with ζ_i replaced by $\zeta_i - 2(\zeta_j - \hat{v}_{wj})n_j n_i$ [or $\zeta_i - 2(\zeta_j - u_{wj})n_j n_i$] is not a simple form unless $\hat{v}_{wi} n_i = 0$ (or $u_{wi} n_i = 0$), i.e.,

$$E(\zeta)[1+\phi(x_i,\zeta_i,\hat{t})] = (1-\alpha)E(\breve{\zeta})[1+\phi(x_i,\breve{\zeta}_i,\hat{t})] + \alpha E(\zeta)[1+\phi_e(\check{\sigma}_w, u_{wi}, \tau_w)] \quad [(\zeta_j - u_{wj})n_j > 0], \tag{1.92a}$$

$$\check{\sigma}_w = \hat{\sigma}_w - 1 = -2\left(\frac{\pi}{1+\tau_w}\right)^{1/2} \int_{(\zeta_j - u_{wj})n_j < 0} (\zeta_j - u_{wj}) n_j E(\zeta)[1+\phi(x_i,\zeta_i,\hat{t})]\mathbf{d\zeta} - 1, \tag{1.92b}$$

$$\breve{\zeta}_i = \zeta_i - 2(\zeta_j - u_{wj})n_j n_i, \quad \breve{\zeta} = (\breve{\zeta}_i^2)^{1/2}. \tag{1.92c}$$

When $u_{wi} n_i = 0$, the variable $\breve{\zeta}$ is reduced to ζ, and the formula is a little simplified as

$$\phi(x_i,\zeta_i,\hat{t}) = (1-\alpha)\phi(x_i,\breve{\zeta}_i,\hat{t}) + \alpha\phi_e(\check{\sigma}_w, u_{wi}, \tau_w) \quad (\zeta_j n_j > 0), \tag{1.93a}$$

$$\check{\sigma}_w = -2\left(\frac{\pi}{1+\tau_w}\right)^{1/2} \int_{\zeta_j n_j < 0} \zeta_j n_j E(\zeta)\phi(x_i,\zeta_i,\hat{t})\mathbf{d\zeta} + \left(\frac{1}{1+\tau_w}\right)^{1/2} - 1, \tag{1.93b}$$

$$\breve{\zeta}_i = \zeta_i - 2\zeta_j n_j n_i. \tag{1.93c}$$

The nondimensional mixed-type condition in the perturbed variables corresponding to Eq. (1.67a) on the interface of a gas and its condensed phase is

$$E(\zeta)[1+\phi(x_i,\zeta_i,\hat{t})] = \alpha_c E(\zeta)[1+\phi_e(\omega_w, u_{wi}, \tau_w)] + (1-\alpha_c)\big\{(1-\alpha)E(\breve{\zeta})[1+\phi(x_i,\breve{\zeta}_i,\hat{t})] + \alpha E(\zeta)[1+\phi_e(\check{\sigma}_w, u_{wi}, \tau_w)]\big\} \quad [(\zeta_j - u_{wj})n_j > 0], \tag{1.94}$$

where $\check{\sigma}_w$ and $\breve{\zeta}_i$ are given by the same expressions as Eqs. (1.92b) and (1.92c). When $u_{wi} n_i = 0$, similarly to Eq. (1.93a), this formula is reduced to

$$\phi(x_i,\zeta_i,\hat{t}) = \alpha_c\phi_e(\omega_w, u_{wi}, \tau_w) + (1-\alpha_c)[(1-\alpha)\phi(x_i,\breve{\zeta}_i,\hat{t}) + \alpha\phi_e(\check{\sigma}_w, u_{wi}, \tau_w)] \quad (\zeta_j n_j > 0), \tag{1.95}$$

where $\breve{\sigma}_w$ and $\breve{\zeta}_i$ are given by the same simplified expressions as Eqs. (1.93b) and (1.93c).

Here some notes may be in order.

(i) The formulas (equations, boundary conditions, etc.) in this section are expressed in the perturbed quantities defined by Eq. (1.74), and are conveniently used in analyzing problems where the state of a gas is close to an equilibrium state at rest. The expressions are the simple transformations of the corresponding formulas in the dimensional variables in Sections 1.1–1.8 or in the nondimensional variables in Section 1.9, and no approximation is introduced.

(ii) In a problem consisting of a gas and its condensed phase, the density of the gas in an equilibrium state at rest is given by the saturated gas density at its temperature. The choice of the reference Maxwellian [or f_0 in Eq. (1.74) given by Eq. (1.45)] in perturbation analyses is not unique. The variables ρ_0 and T_0 may be chosen at any values such that the perturbed velocity distribution function ϕ is small, and ρ_0 may not necessarily be the saturated gas density at temperature T_0.

1.11 Linearized Boltzmann equation

In analyzing the behavior of a gas that deviates only slightly from an equilibrium state at rest in a system with $F_i = 0$, the *linearized Boltzmann equation*, which is obtained by neglecting the nonlinear terms of ϕ in Eq. (1.75a), is widely used.[25] It is given as

$$\mathrm{Sh}\frac{\partial \phi}{\partial \hat{t}} + \zeta_i \frac{\partial \phi}{\partial x_i} = \frac{1}{k}\mathcal{L}(\phi). \tag{1.96}$$

The linearized version of Eqs. (1.78a)–(1.78f) is

$$\omega = \int \phi E \mathbf{d}\boldsymbol{\zeta}, \tag{1.97a}$$

$$u_i = \int \zeta_i \phi E \mathbf{d}\boldsymbol{\zeta}, \tag{1.97b}$$

$$\frac{3}{2}\tau = \int \left(\zeta_i^2 - \frac{3}{2}\right) \phi E \mathbf{d}\boldsymbol{\zeta}, \tag{1.97c}$$

$$P = \omega + \tau, \tag{1.97d}$$

$$P_{ij} = 2\int \zeta_i \zeta_j \phi E \mathbf{d}\boldsymbol{\zeta}, \tag{1.97e}$$

$$Q_i = \int \zeta_i \zeta_j^2 \phi E \mathbf{d}\boldsymbol{\zeta} - \frac{5}{2} u_i. \tag{1.97f}$$

[25] The Boltzmann equation linearized around a Maxwellian with flow velocity is also called the linearized Boltzmann equation. In this book, the linearized Boltzmann equation given by Eq. (1.96), the Boltzmann equation linearized around a Maxwellian at rest, is used without a special notice. When we refer to the former linearized equation, we mention it explicitly.

The linearized expression for the perturbed (local) Maxwellian ϕ_e is

$$\phi_e = \omega + 2\zeta_i u_i + \left(\zeta_i^2 - \frac{3}{2}\right)\tau. \tag{1.98}$$

The linearized form of the conservation equations is

$$\mathrm{Sh}\frac{\partial \omega}{\partial \hat{t}} + \frac{\partial u_i}{\partial x_i} = 0, \tag{1.99}$$

$$\mathrm{Sh}\frac{\partial u_i}{\partial \hat{t}} + \frac{1}{2}\frac{\partial P_{ij}}{\partial x_j} = 0, \tag{1.100}$$

$$\frac{3}{2}\mathrm{Sh}\frac{\partial P}{\partial \hat{t}} + \frac{\partial}{\partial x_i}\left(\frac{5}{2}u_i + Q_i\right) = 0. \tag{1.101}$$

The linearized BKW equation is

$$\mathrm{Sh}\frac{\partial \phi}{\partial \hat{t}} + \zeta_i \frac{\partial \phi}{\partial x_i} = \frac{1}{k}\left[-\phi + \omega + 2\zeta_i u_i + \left(\zeta_i^2 - \frac{3}{2}\right)\tau\right]. \tag{1.102}$$

With the same notation $\mathcal{L}(\phi)$ as the standard Boltzmann equation for the expression in the brackets,

$$\mathcal{L}(\phi) = \int \left[1 + 2\zeta_i\zeta_{i*} + \frac{2}{3}\left(\zeta_i^2 - \frac{3}{2}\right)\left(\zeta_{j*}^2 - \frac{3}{2}\right)\right]\phi(\boldsymbol{\zeta}_*)E(\zeta_*)\mathbf{d}\boldsymbol{\zeta}_* - \phi. \tag{1.103}$$

The linearized form of the kinetic boundary conditions on a simple boundary is summarized as follows:
The Maxwell-type condition (1.92a) with (1.92b) on a simple boundary is

$$\begin{aligned}\phi(x_i, \zeta_i, \hat{t}) = (1-\alpha)&\Big(\phi(x_i, \zeta_i - 2(\zeta_j - u_{wj})n_j n_i, \hat{t}) + 4\zeta_j u_{wk} n_j n_k\Big) \\ &+ \alpha\left[\check{\sigma}_w + 2\zeta_j u_{wj} + \left(\zeta_j^2 - \frac{3}{2}\right)\tau_w\right] \qquad [(\zeta_j - u_{wj})n_j > 0],\end{aligned} \tag{1.104a}$$

$$\check{\sigma}_w = \sqrt{\pi}u_{wj}n_j - \frac{1}{2}\tau_w - 2\sqrt{\pi}\int_{(\zeta_k - u_{wk})n_k < 0} \zeta_j n_j \phi E \mathbf{d}\boldsymbol{\zeta}. \tag{1.104b}$$

The diffuse-reflection condition is given by putting $\alpha = 1$ in Eq. (1.104a), i.e.,

$$\phi(x_i, \zeta_i, \hat{t}) = \check{\sigma}_w + 2\zeta_j u_{wj} + \left(\zeta_j^2 - \frac{3}{2}\right)\tau_w \qquad [(\zeta_j - u_{wj})n_j > 0], \tag{1.105a}$$

$$\check{\sigma}_w = \sqrt{\pi}u_{wj}n_j - \frac{1}{2}\tau_w - 2\sqrt{\pi}\int_{(\zeta_k - u_{wk})n_k < 0} \zeta_j n_j \phi E \mathbf{d}\boldsymbol{\zeta}, \tag{1.105b}$$

and the specular-reflection condition is given by putting $\alpha = 0$ in Eq. (1.104a), i.e.,

$$\phi(x_i, \zeta_i, \hat{t}) = \phi(x_i, \zeta_i - 2(\zeta_j - u_{wj})n_j n_i, \hat{t}) + 4\zeta_j u_{wk} n_j n_k. \tag{1.106}$$

The boundary condition (1.64) expressed in a scattering kernel is reduced to (see Section A.9)

$$\begin{aligned} E(\zeta)\phi(\boldsymbol{\zeta}) = &\left[2\zeta_i u_{wi} + \left(\zeta_i^2 - \frac{3}{2}\right)\tau_w\right] E(\zeta) \\ &- \int_{(\zeta_{i*}-u_{wi})n_i<0} \hat{K}_{B0}(\boldsymbol{\zeta},\boldsymbol{\zeta}_*)\left[2\zeta_{i*}u_{wi} + \left(\zeta_{i*}^2 - \frac{3}{2}\right)\tau_w\right]E(\zeta_*)\mathbf{d}\boldsymbol{\zeta}_* \\ &+ \int_{(\zeta_{i*}-u_{wi})n_i<0} \hat{K}_{B0}(\boldsymbol{\zeta},\boldsymbol{\zeta}_*)\phi(\boldsymbol{\zeta}_*)E(\zeta_*)\mathbf{d}\boldsymbol{\zeta}_* \quad [(\zeta_i - u_{wi})n_i > 0], \end{aligned} \tag{1.107}$$

where $\hat{K}_{B0}$ is the kernel $\hat{K}_B$ in Eq. (1.64) on a simple boundary in the reference state. The conditions on $\hat{K}_{B0}$ corresponding to the conditions (i)–(iii) on $\hat{K}_B$ after Eq. (1.64) are given as

$$\text{(i)} \quad \hat{K}_{B0}(\boldsymbol{\zeta},\boldsymbol{\zeta}_*) \geq 0 \quad (\zeta_i n_i > 0,\ \zeta_{i*}n_i < 0). \tag{1.108a}$$

$$\text{(ii)} \quad -\int_{\zeta_i n_i>0} \frac{\zeta_k n_k}{\zeta_{j*}n_j}\hat{K}_{B0}(\boldsymbol{\zeta},\boldsymbol{\zeta}_*)\mathbf{d}\boldsymbol{\zeta} = 1 \quad (\zeta_{i*}n_i < 0). \tag{1.108b}$$

(iii) Let φ be $\varphi = c_0 + c_i\zeta_i + c_4\zeta_i^2$, where c_0, c_i, and c_4 are constants. Among this φ, only $\varphi = c_0$ satisfies the relation

$$E(\zeta)\varphi(\boldsymbol{\zeta}) = \int_{\zeta_{i*}n_i<0} \hat{K}_{B0}(\boldsymbol{\zeta},\boldsymbol{\zeta}_*)\varphi(\boldsymbol{\zeta}_*)E(\zeta_*)\mathbf{d}\boldsymbol{\zeta}_* \quad (\zeta_i n_i > 0). \tag{1.108c}$$

The linearized form of the kinetic boundary conditions on an interface is summarized as follows:
The mixed-type boundary condition (1.94) on an interface of a gas and its condensed phase is

$$\begin{aligned} \phi(x_i,\zeta_i,\hat{t}) = \alpha_c &\left[\omega_w + 2\zeta_j u_{wj} + \left(\zeta_j^2 - \frac{3}{2}\right)\tau_w\right] \\ &+ (1-\alpha_c)\Bigg\{(1-\alpha)\left(\phi(x_i,\zeta_i - 2(\zeta_j - u_{wj})n_j n_i,\hat{t}) + 4\zeta_j u_{wk}n_j n_k\right) \\ &\qquad + \alpha\left[\check{\sigma}_w + 2\zeta_j u_{wj} + \left(\zeta_j^2 - \frac{3}{2}\right)\tau_w\right]\Bigg\} \quad [(\zeta_j - u_{wj})n_j > 0], \end{aligned} \tag{1.110}$$

where $\check{\sigma}_w$ is given by the same expression as Eq. (1.104b).
The linearized complete-condensation condition is given by putting $\alpha_c = 1$ in Eq. (1.110), i.e.,

$$\phi(x_i,\zeta_i,\hat{t}) = \omega_w + 2\zeta_j u_{wj} + \left(\zeta_j^2 - \frac{3}{2}\right)\tau_w \quad [(\zeta_j - u_{wj})n_j > 0]. \tag{1.111}$$

The boundary condition (1.69) expressed in a scattering kernel is reduced to (see Section A.9)

$$E(\zeta)\phi(\boldsymbol{\zeta}) = \left[\omega_w + 2\zeta_i u_{wi} + \left(\zeta_i^2 - \frac{3}{2}\right)\tau_w\right] E(\zeta) - \int_{(\zeta_{i*}-u_{wi})n_i<0} \hat{K}_{I0}(\boldsymbol{\zeta},\boldsymbol{\zeta}_*)\left[\omega_w + 2\zeta_{i*}u_{wi} + \left(\zeta_{i*}^2 - \frac{3}{2}\right)\tau_w\right]E(\zeta_*)\mathbf{d}\boldsymbol{\zeta}_* + \int_{(\zeta_{i*}-u_{wi})n_i<0} \hat{K}_{I0}(\boldsymbol{\zeta},\boldsymbol{\zeta}_*)\phi(\boldsymbol{\zeta}_*)E(\zeta_*)\mathbf{d}\boldsymbol{\zeta}_* \quad [(\zeta_i - u_{wi})n_i > 0], \tag{1.112}$$

where $\hat{K}_{I0}$ is the kernel $\hat{K}_I$ in Eq. (1.69) on an interface in the reference state. The conditions on $\hat{K}_{I0}$ corresponding to the conditions on $\hat{K}_I$ after Eq. (1.69) are given as

(i) $\hat{K}_{I0}(\boldsymbol{\zeta},\boldsymbol{\zeta}_*) \geq 0 \qquad (\zeta_i n_i > 0,\ \zeta_{i*}n_i < 0).$ (1.113a)

(ii-a) $E = \hat{g}_{I0} + \displaystyle\int_{\zeta_{i*}n_i<0} \hat{K}_{I0}(\boldsymbol{\zeta},\boldsymbol{\zeta}_*)E_*\mathbf{d}\boldsymbol{\zeta}_* \quad (\zeta_i n_i > 0),$ (1.113b)

where $\hat{g}_{I0}$ is $\hat{g}_I$ at the reference state;

(ii-b) Let φ be $\varphi = c_0 + c_i\zeta_i + c_4\zeta_i^2$, where c_0, c_i, and c_4 are constants. Among this φ, only $\varphi = 0$ satisfies the relation

$$E(\zeta)\varphi(\boldsymbol{\zeta}) = \int_{\zeta_{i*}n_i<0} \hat{K}_{I0}(\boldsymbol{\zeta},\boldsymbol{\zeta}_*)\varphi(\boldsymbol{\zeta}_*)E(\zeta_*)\mathbf{d}\boldsymbol{\zeta}_* \quad (\zeta_i n_i > 0). \tag{1.113c}$$

Here some notes may be in order.

(i) The formulas given in this section are the simplified version of those in Section 1.10 obtained by neglecting the second and higher-order terms of the perturbed quantities introduced in Eq. (1.74).

(ii) The choice of the reference Maxwellian [or f_0 in Eq. (1.74) given by Eq. (1.45)] in perturbation analyses is not unique, and it can be chosen freely as far as the perturbed velocity distribution function ϕ is so small that its nonlinear terms can be neglected [see also the note (ii) in the last paragraph of Section 1.10].

(iii) The term $4\zeta_j u_{wk} n_j n_k$ in Eqs. (1.104a), (1.106), and (1.110) and the term $\sqrt{\pi}u_{wj}n_j$ in Eqs. (1.104b) and (1.105b) come from the leading term E of the velocity distribution function $E(1+\phi)$ owing to the normal velocity $u_{wk}n_k n_i$ of the boundary. The first one arises because the Maxwellian E is not symmetric with respect to $(\zeta_i - u_{wi})n_i = 0$, and the second arises because the mass fluxes of the Maxwellian E for $(\zeta_i - u_{wi})n_i < 0$ and $(\zeta_i - u_{wi})n_i > 0$ do not cancel out.

(iv) Refer to Section A.9, especially the discussion in its last two paragraphs on the range $(\zeta_{i*} - u_{wi})n_i < 0$ of integration and the small shift $u_{wj}n_j$ of the variable ζ_i in $\phi(x_i, \zeta_i - 2(\zeta_j - u_{wj})n_j n_i, \hat{t})$.

(v) In Eqs. (1.107) and (1.112), the kernels $\hat{K}_{B0}$ and $\hat{K}_{I0}$ have to be extended outside the original range of definition (see Section A.9).

Corresponding to Eq. (1.33) for the H function, which is related to the direction of variation of the solution of the Boltzmann equation, the following equation [the linearized-Boltzmann-equation version of Eq. (1.33)] is obtained for the linearized Boltzmann equation (1.96):

$$\mathrm{Sh}\frac{\partial}{\partial \hat{t}}\int \phi^2 E\mathbf{d\zeta} + \frac{\partial}{\partial x_i}\int \zeta_i \phi^2 E\mathbf{d\zeta} = \frac{1}{k}LG, \tag{1.115}$$

where

$$LG = -\frac{1}{2}\int EE_*(\phi' + \phi'_* - \phi - \phi_*)^2 \widehat{B}\mathrm{d}\Omega\mathbf{d\zeta}_*\mathbf{d\zeta} \leq 0. \tag{1.116}$$

Equation (1.115) is obtained simply by multiplying Eq. (1.96) by ϕE, integrating over the whole space of $\boldsymbol{\zeta}$, and using the symmetry relation (1.79).[26] The equality in the last relation of LG holds when and only when ϕ is a local Maxwellian, i.e., a linear combination of 1, ζ_i, and ζ_j^2. The H theorem for the linearized Boltzmann equation is similarly expressed in terms of $\int \phi^2 E\mathbf{d\zeta}$ and $\int \zeta_i \phi^2 E\mathbf{d\zeta}$.

Finally, it may be noted that the linearization is carried out by neglecting the second and higher-order terms of the perturbations formally, and that it is not a rigorous mathematical process to assure that the linearized system really approximates the original system when the parameter of the basis of linearization is small (see the discussion in the last part of Section A.9). Thus, the linearized system should be taken as an independent system and be clearly posed when one poses the system.

[26] Equation (1.115) is not the linearized form of Eq. (1.33). It is the second-order terms of the perturbation ϕ in Eq. (1.33). That is, noting that $\hat{f} = E(1+\phi)$ and examining Eq. (1.72) for small ϕ, we find that the terms of the order of ϕ are reduced to Eq. (1.99) and that the second-order terms correspond to Eq. (1.115). The functions $\int \phi^2 E\mathbf{d\zeta}$, $\int \zeta_i \phi^2 E\mathbf{d\zeta}$, and LG are, respectively, the second-order terms in ϕ of H (the H function), H_i, and G in Section 1.7 (or $\hat{H}$, $\hat{H}_i$, and $\hat{G}$ in Section 1.9) except for a common constant factor.

Chapter 2

Highly Rarefied Gas: Free Molecular Gas and Its Correction

With an increase of the Knudsen number of the system, the effect of intermolecular collisions becomes less important. When their effect can be neglected, the gas (its state) is called a *free molecular gas* (*free molecular flow*). In this chapter, we discuss the free molecular flow and its correction by molecular collisions when external force is absent.

2.1 General solution of a free molecular flow

In a free molecular flow, where the intermolecular collisions are absent, the Boltzmann equation (1.5) reduces to the simple form without the collision term

$$\frac{\partial f}{\partial t} + \xi_i \frac{\partial f}{\partial X_i} = 0. \tag{2.1}$$

The velocity distribution function f at time t is related to that at time t_0 as

$$f(X_i, \xi_i, t) = f(X_i - \xi_i(t - t_0), \xi_i, t_0). \tag{2.2}$$

In a time-independent case ($\partial/\partial t = 0$), the above relation is reduced to

$$f(X_i, \xi_i) = f(X_i - \xi_i t, \xi_i), \tag{2.3}$$

where t is just a parameter.

Owing to the absence of the collision term, the solution of Eq. (2.1) shows a decisively different feature from that of the Boltzmann equation (1.5) with $F_i = 0$. An arbitrary time-independent and spatially uniform state, i.e., an arbitrary function of ξ_i that is independent of X_i and t is a solution of Eq. (2.1)

in contrast to the case of the Boltzmann equation, where a time-independent and spatially uniform solution is given by a Maxwellian (Section A.7.1). This difference should be kept in mind when the boundary-value problem for a free molecular gas in an infinite domain is considered. Even if the state at infinity is uniform, the velocity distribution function is not necessarily Maxwellian. For economy of expression, when we often mention, for example, that the state at infinity is in the equilibrium state at rest with density ρ_∞ and temperature T_∞ in the examples in this chapter, it means that the velocity distribution function of the molecules *leaving* the infinity is given by

$$f = \frac{\rho_\infty}{(2\pi R T_\infty)^{3/2}} \exp\left(-\frac{{\xi_i}^2}{2RT_\infty}\right).$$

The distribution for the other molecular velocities is not mentioned. Whether the state at infinity is really given by the Maxwellian (for all the molecular velocities) or not depends on the problem considered.[1] In the latter case, the density, temperature, or velocity at infinity is not necessarily ρ_∞, T_∞, or zero respectively.[2]

2.2 Initial-value problem

Consider a gas in an infinite domain without any boundary (body) in the domain. The state (the velocity distribution function) of the gas at time $t = t_0$ is given as

$$f(X_i, \xi_i, t_0) = g(X_i, \xi_i), \tag{2.4}$$

where $g(X_i, \xi_i)$ is a given function. Then the behavior of the gas in the later time t is given as follows:

$$f(X_i, \xi_i, t) = g(X_i - \xi_i(t - t_0), \xi_i). \tag{2.5}$$

By substitution of the solution (2.5) into Eqs. (1.2a)–(1.2g), the macroscopic variables, such as density, flow velocity, and temperature, are obtained.

2.3 Boundary-value problem

2.3.1 Preparation

Consider the boundary-value problem in a time-independent (or steady) state. Let the boundary conditions (1.26) and (1.30) be written in a common form as

[1] If the bodies are confined in a finite domain, the state is the corresponding (full) Maxwellian.

[2] Examine the uniform state

$$f = \begin{cases} \rho_{-\infty}(2\pi R T_{-\infty})^{-3/2} \exp(-{\xi_i}^2/2RT_{-\infty}) & (\xi_1 > 0), \\ \rho_\infty (2\pi R T_\infty)^{-3/2} \exp(-{\xi_i}^2/2RT_\infty) & (\xi_1 < 0), \end{cases}$$

which is a solution of Eq. (2.1). Here, $\rho_{-\infty}$ and $T_{-\infty}$ as well as ρ_∞ and T_∞ are constants.

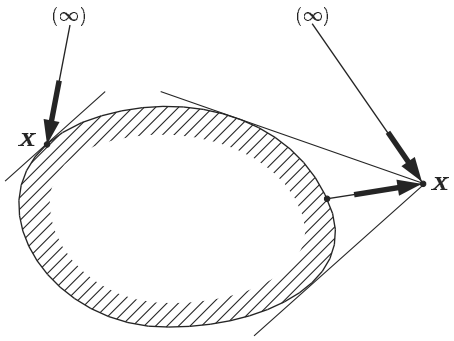

Figure 2.1. Free molecular gas around a convex body.

follows:

$$f(\boldsymbol{X},\boldsymbol{\xi}) = g(\boldsymbol{X},\boldsymbol{\xi}) + \int_{\xi_{j*}n_j<0} K(\boldsymbol{\xi},\boldsymbol{\xi}_*,\boldsymbol{X}) f(\boldsymbol{X},\boldsymbol{\xi}_*)\mathbf{d}\boldsymbol{\xi}_* \quad [\xi_j n_j(\boldsymbol{X}) > 0], \quad (2.6)$$

where $(g,K) = (0,K_B)$ for a simple boundary and $(g,K) = (g_I,K_I)$ for an interface of the gas and its condensed phase (see Section 1.6) and the $v_{wi}n_i$ terms in (1.26) and (1.30) have dropped off, because the velocity v_{wi} of the boundary must satisfy the condition $v_{wi}n_i = 0$ for the system to be time-independent. According to the general solution (2.3), the velocity distribution function at an arbitrary point in the gas can be expressed by the boundary data of the velocity distribution function. That is, let $X_{Bi}(\boldsymbol{X},\boldsymbol{\xi}/\xi)$ $[\xi = (\xi_i^2)^{1/2}]$ be the point on the boundary or infinity encountered for the first time when we trace back the path of a molecule with velocity ξ_i (or trace in the $-\xi_i$ direction) from X_i, i.e.,

$$X_{Bi}(\boldsymbol{X},\boldsymbol{\xi}/\xi) = X_i - s_B\xi_i/\xi, \quad (2.7)$$

where s_B is the distance from $\boldsymbol{X}$ to the nearest boundary point in the $-\xi_i$ direction. Then,

$$f(\boldsymbol{X},\boldsymbol{\xi}) = f(\boldsymbol{X}_B(\boldsymbol{X},\boldsymbol{\xi}/\xi),\boldsymbol{\xi}), \quad (2.8)$$

where $\xi_j n_j(\boldsymbol{X}_B) > 0$ with $n_i(\boldsymbol{X}_B)$ being the unit normal vector to the boundary at X_{Bi}, pointed to the gas domain. Thus, the problem is reduced to obtaining the velocity distribution function of the molecules leaving the boundary.

2.3.2 Free molecular gas around a convex body

Consider the case where a convex body lies solely in an infinite expanse of a gas (Fig. 2.1). All the molecules impinging on a point X_i of the body [those with $\xi_j n_j(\boldsymbol{X}) < 0$] come from infinity ($\boldsymbol{X}_B$ is at infinity). The velocity distribution function for these molecules is determined by the condition at infinity, i.e.,

$$f(\boldsymbol{X},\boldsymbol{\xi}) = f(\infty(\boldsymbol{X},\boldsymbol{\xi}/\xi),\boldsymbol{\xi}) \qquad [\xi_j n_j(\boldsymbol{X}) < 0], \quad (2.9)$$

where the arguments of ∞ are shown for discrimination because the condition at infinity may not be uniform. With Eq. (2.9) in the boundary condition (2.6), the velocity distribution function of the molecules leaving a point X_i on the boundary is given by

$$\begin{aligned} f(\boldsymbol{X},\boldsymbol{\xi}) &= f_w(\boldsymbol{X},\boldsymbol{\xi}) \\ &= g(\boldsymbol{X},\boldsymbol{\xi}) + \int_{\xi_{j*}n_j(\boldsymbol{X})<0} K(\boldsymbol{\xi},\boldsymbol{\xi}_*,\boldsymbol{X}) f(\infty(\boldsymbol{X},\boldsymbol{\xi}_*/\xi_*),\boldsymbol{\xi}_*)\mathbf{d}\boldsymbol{\xi}_* \\ &\qquad\qquad [\xi_j n_j(\boldsymbol{X}) > 0]. \end{aligned} \tag{2.10}$$

The condition at infinity being given, the velocity distribution function f of the gas at an arbitrary point in the gas is obtained with the aid of Eqs. (2.8) and (2.10). That is, let X_i be an arbitrary point and let s_B be the distance from X_i to the nearest boundary point in the direction $-\xi_i$. Then, the velocity distribution function $f(\boldsymbol{X},\boldsymbol{\xi})$ of a gas around a convex body is given by

$$\begin{aligned} f(\boldsymbol{X},\boldsymbol{\xi}) &= f_w(\boldsymbol{X}-s_B\boldsymbol{\xi}/\xi,\boldsymbol{\xi}) \\ &= g(\boldsymbol{X}-s_B\boldsymbol{\xi}/\xi,\boldsymbol{\xi}) \\ &\quad + \int_{\xi_{j*}n_j(\boldsymbol{X}-s_B\boldsymbol{\xi}/\xi)<0} K(\boldsymbol{\xi},\boldsymbol{\xi}_*,\boldsymbol{X}-s_B\boldsymbol{\xi}/\xi) f(\infty(\boldsymbol{X}-s_B\boldsymbol{\xi}/\xi,\boldsymbol{\xi}_*/\xi_*),\boldsymbol{\xi}_*)\mathbf{d}\boldsymbol{\xi}_*, \end{aligned} \tag{2.11a}$$

if s_B is finite, and by

$$f(\boldsymbol{X},\boldsymbol{\xi}) = f(\infty(\boldsymbol{X},\boldsymbol{\xi}/\xi),\boldsymbol{\xi}), \tag{2.11b}$$

if s_B is infinite.

We will give some applications of the general formulas.

Example. A flat plate with temperature T_0 lies in a uniform gas with flow velocity $(U,0,0)$, density ρ_0, and temperature T_0, with its surface parallel to the flow. The plate is of width L and length infinite and the edge of infinite length is placed normal to the flow. The gas molecules make the diffuse reflection (1.24a) on the plate.

Let the plate be on the plane $X_2 = 0$. The velocity distribution function f of the molecules impinging on the $X_2 > 0$ side of the plate is

$$f = \frac{\rho_0}{(2\pi RT_0)^{3/2}} \exp\left(-\frac{(\xi_i - U\delta_{1i})^2}{2RT_0}\right) \qquad (\xi_2 < 0),$$

from which the velocity distribution of the molecules leaving there is obtained, with the aid of the diffuse-reflection condition, as

$$f = \frac{\rho_0}{(2\pi RT_0)^{3/2}} \exp\left(-\frac{{\xi_i}^2}{2RT_0}\right) \qquad (\xi_2 > 0).$$

Thus, the state is uniform on the plate. In view of the symmetry, the plate is, per unit length, subject to the force $2p_0LU/(2\pi RT_0)^{1/2}$ in the direction of the flow, where $p_0\,(= R\rho_0T_0)$ is the pressure at infinity. ■

Example. A convex body B with a uniform temperature T_1 and surface area S lies in a gas in the equilibrium state at rest with temperature T_0 and density ρ_0. The gas molecules make the diffuse reflection on the body.

The gas molecules ($\xi_i n_i < 0$) impinging on the body B all come from infinity, and therefore its velocity distribution is given by that at infinity, i.e.,

$$f = \frac{\rho_0}{(2\pi RT_0)^{3/2}} \exp\left(-\frac{\xi_i^2}{2RT_0}\right). \tag{2.12}$$

Then, with the aid of the diffuse-reflection condition, the velocity distribution of the molecules leaving the body is given by

$$f = \frac{\rho_w}{(2\pi RT_1)^{3/2}} \exp\left(-\frac{\xi_i^2}{2RT_1}\right) \qquad (\xi_i n_i > 0), \tag{2.13a}$$

$$\begin{aligned}\rho_w &= -\left(\frac{2\pi}{RT_1}\right)^{1/2} \int_{\xi_i n_i<0} \xi_j n_j \frac{\rho_0}{(2\pi RT_0)^{3/2}} \exp\left(-\frac{\xi_i^2}{2RT_0}\right) \mathbf{d}\boldsymbol{\xi} \\ &= \rho_0 \left(\frac{T_0}{T_1}\right)^{1/2}. \end{aligned} \tag{2.13b}$$

The velocity distribution function at a point in the gas is obtained by Eqs. (2.11a) and (2.11b) with the data given by Eqs. (2.12), (2.13a) and (2.13b).

By simple manipulation, we find that the flow velocity of the gas vanishes and that the temperature in the gas is expressed as

$$T = \frac{1 + \dfrac{1}{4\pi}\left[\left(\dfrac{T_1}{T_0}\right)^{1/2} - 1\right]\Omega(\boldsymbol{X}, B)}{1 + \dfrac{1}{4\pi}\left[\left(\dfrac{T_0}{T_1}\right)^{1/2} - 1\right]\Omega(\boldsymbol{X}, B)} T_0,$$

where $\Omega(\boldsymbol{X}, B)$ is the solid angle viewing the body B from the point $\boldsymbol{X}$. The energy ET transferred per unit time from the body to the gas is

$$ET = \frac{\rho_0(2RT_0)^{3/2}}{2\sqrt{\pi}} \left(\frac{T_1}{T_0} - 1\right) S. \qquad ■$$

Example. Two equilibrium states of a gas at rest, one at pressure p_1 and temperature T_1 in $X_1 < 0$ and the other at pressure p_2 and temperature T_2 in $X_1 > 0$, are separated by a thin flat plate at $X_1 = 0$ with a small hole (area S) connecting the two regions (or two reservoirs).[3]

[3]The states at infinities are the corresponding (full) Maxwellians if the temperatures of the walls are T_1 on the $X_1 < 0$ side and T_2 on the $X_1 > 0$ side (see the discussion in the last paragraph of Section 2.1).

The plate with a hole is not a convex body, but the velocity distribution function of the gas molecules on the hole is known because all the molecules come from $X_1 = \infty$ or $X_1 = -\infty$. That is, the velocity distribution function f on the hole is uniformly given by

$$f = \frac{2\pi p_1}{(2\pi RT_1)^{5/2}} \exp\left(-\frac{\xi_i^2}{2RT_1}\right) \quad (\xi_1 > 0),$$
$$f = \frac{2\pi p_2}{(2\pi RT_2)^{5/2}} \exp\left(-\frac{\xi_i^2}{2RT_2}\right) \quad (\xi_1 < 0),$$

where the gas with pressure p_1 is taken to be in the region $X_1 < 0$. Thus, the state is uniform on the hole, and the mass flow M per unit time through the hole from $X_1 < 0$ to $X_1 > 0$ is given by

$$M = S \int \xi_1 f \mathbf{d}\boldsymbol{\xi}$$
$$= \left(\frac{p_1}{(2\pi RT_1)^{1/2}} - \frac{p_2}{(2\pi RT_2)^{1/2}}\right) S.$$

When there is a temperature difference ($T_1 \neq T_2$), a flow is induced even if there is no pressure difference. The condition that no flow is induced is

$$p_1/\sqrt{T_1} = p_2/\sqrt{T_2}.$$

This condition is proved to be true for a general situation in Sone [1984a, 1985] (see Section 2.5.6). ■

2.3.3 Arbitrary body shape and arrangement

General boundary condition

Consider a system where a nonconvex body or several convex or nonconvex bodies lie in a gas, bounded or unbounded (Fig. 2.2). Expressing the velocity distribution function f of the impinging molecules under the integral sign in the boundary condition (2.6) by that of the molecules reflected on other parts of the boundary and those coming from infinity, we obtain an integral equation of the velocity distribution function for the reflected molecules on the boundary, i.e.,

$$f(\boldsymbol{X}, \boldsymbol{\xi}) = g(\boldsymbol{X}, \boldsymbol{\xi}) + \int_{\xi_{j*} n_j < 0} K(\boldsymbol{\xi}, \boldsymbol{\xi}_*, \boldsymbol{X}) f(\boldsymbol{X}_B(\boldsymbol{X}, \boldsymbol{\xi}_*/\xi_*), \boldsymbol{\xi}_*) \mathbf{d}\boldsymbol{\xi}_*$$
$$[\xi_j n_j(\boldsymbol{X}) > 0]. \tag{2.14}$$

It is noted that $\boldsymbol{X}$ in this equation runs only on the boundary.

Diffuse reflection I

In the case of the diffuse-reflection boundary condition, we can eliminate the molecular velocity $\boldsymbol{\xi}$ from the above integral equation (2.14). This is done

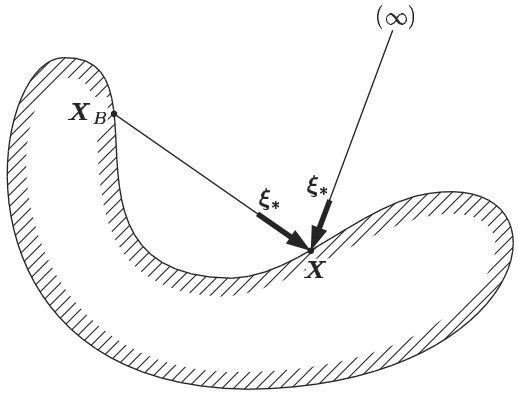

Figure 2.2. Free molecular gas around a nonconvex body.

directly from the diffuse-reflection condition as follows. Let $\boldsymbol{X}$ be a point on the boundary. The diffuse-reflection condition (1.24a) with (1.24b) is

$$f(\boldsymbol{X},\boldsymbol{\xi}) = \frac{\sigma_w(\boldsymbol{X})}{[2\pi RT_w(\boldsymbol{X})]^{3/2}} \exp\left(-\frac{[\xi_j - v_{wj}(\boldsymbol{X})]^2}{2RT_w(\boldsymbol{X})}\right) \qquad (\xi_j n_j > 0), \quad (2.15a)$$

$$\sigma_w(\boldsymbol{X}) = -\left(\frac{2\pi}{RT_w(\boldsymbol{X})}\right)^{1/2} \int_{\xi_{i*}n_i<0} \xi_{j*} n_j(\boldsymbol{X}) f(\boldsymbol{X},\boldsymbol{\xi}_*) \mathbf{d}\boldsymbol{\xi}_*. \quad (2.15b)$$

The distribution function f of the impinging molecules on $\boldsymbol{X}$ in the integrand of Eq. (2.15b) is replaced by that of the molecules leaving other points on the boundary or infinity with the aid of the relation (2.8), i.e.,

$$\sigma_w(\boldsymbol{X}) = -\left(\frac{2\pi}{RT_w(\boldsymbol{X})}\right)^{1/2} \int_{\xi_{i*}n_i<0} \xi_{j*} n_j(\boldsymbol{X}) f(\boldsymbol{X}_B(\boldsymbol{X},\boldsymbol{\xi}_*/\xi_*),\boldsymbol{\xi}_*) \mathbf{d}\boldsymbol{\xi}_*. \quad (2.16)$$

Here, if $\boldsymbol{X}_B(\boldsymbol{X},\boldsymbol{\xi}_*/\xi_*)$ is on the boundary, $f(\boldsymbol{X}_B(\boldsymbol{X},\boldsymbol{\xi}_*/\xi_*),\boldsymbol{\xi}_*)$ is expressed in terms of $\sigma_w(\boldsymbol{X}_B)$ with the aid of the diffuse-reflection condition (2.15a), i.e.,

$$f(\boldsymbol{X}_B,\boldsymbol{\xi}_*) = \frac{\sigma_w(\boldsymbol{X}_B)}{[2\pi RT_w(\boldsymbol{X}_B)]^{3/2}} \exp\left(-\frac{[\xi_{j*} - v_{wj}(\boldsymbol{X}_B)]^2}{2RT_w(\boldsymbol{X}_B)}\right), \quad (2.17)$$

and if $\boldsymbol{X}_B(\boldsymbol{X},\boldsymbol{\xi}_*/\xi_*)$ is at infinity, $f(\boldsymbol{X}_B(\boldsymbol{X},\boldsymbol{\xi}_*/\xi_*),\boldsymbol{\xi}_*)$ is given by the condition at infinity, i.e.,

$$f(\boldsymbol{X}_B(\boldsymbol{X},\boldsymbol{\xi}_*/\xi_*),\boldsymbol{\xi}_*) = f_\infty, \quad (2.18)$$

where f_∞ is the velocity distribution function of the molecules starting at infinity. Substituting Eqs. (2.17) and (2.18) into Eq. (2.16), we obtain the integral equation for $\sigma_w(\boldsymbol{X})$, which is independent of $\boldsymbol{\xi}$. This is much simpler than the integral equation (2.14) of $f(\boldsymbol{X},\boldsymbol{\xi})$ for $\xi_j n_j(\boldsymbol{X}) > 0$, although three-dimensional integral with respect to $\boldsymbol{\xi}_*$ has still to be carried out.

Diffuse reflection II

In the integral equation for $\sigma_w(\boldsymbol{X})$, Eq. (2.16) with Eqs. (2.17) and (2.18) substituted for $f(\boldsymbol{X}_B(\boldsymbol{X}, \boldsymbol{\xi}_*/\xi_*), \boldsymbol{\xi}_*)$, the three-dimensional integration with respect to $\boldsymbol{\xi}_*$, which is also contained in $\sigma_w(\boldsymbol{X}_B)$, $v_{wj}(\boldsymbol{X}_B)$, and $T_w(\boldsymbol{X}_B)$ through $\boldsymbol{X}_B$, has to be carried out. When the boundary except the infinity is at rest ($v_{wi} = 0$), this integral is reduced to two-dimensional one as shown below. We introduce new quantities $j(\boldsymbol{X})$ and $j_\infty(\boldsymbol{X})$ defined on the boundary by

$$\begin{aligned} j(\boldsymbol{X}) &= -\int_{\xi_{i*} n_i(\boldsymbol{X})<0} \xi_{j*} n_j(\boldsymbol{X}) f(\boldsymbol{X}_B(\boldsymbol{X}, \boldsymbol{\xi}_*/\xi_*), \boldsymbol{\xi}_*) \mathrm{d}\boldsymbol{\xi}_* \\ &= \left(\frac{RT_w(\boldsymbol{X})}{2\pi}\right)^{1/2} \sigma_w(\boldsymbol{X}), \end{aligned} \tag{2.19}$$

$$j_\infty(\boldsymbol{X}) = -\int_{\substack{\xi_{i*} n_i(\boldsymbol{X})<0 \\ |\boldsymbol{X}_B|=\infty}} \xi_{j*} n_j(\boldsymbol{X}) f(\boldsymbol{X}_B(\boldsymbol{X}, \boldsymbol{\xi}_*/\xi_*), \boldsymbol{\xi}_*) \mathrm{d}\boldsymbol{\xi}_*. \tag{2.20}$$

The function $j(\boldsymbol{X})$ is the mass flux of the molecules impinging on the boundary element at $\boldsymbol{X}$ (per unit area and per unit time), which is also the same as the flux of the molecules leaving the element; $j_\infty(\boldsymbol{X})$ is the mass flux of the molecules impinging on the boundary element at $\boldsymbol{X}$ from infinity directly and therefore is a known function of $\boldsymbol{X}$ determined by f_∞. The integral in Eq. (2.19) is split into two parts

$$j(\boldsymbol{X}) = -\int_{\substack{\xi_{i*} n_i(\boldsymbol{X})<0 \\ |\boldsymbol{X}_B|<\infty}} - \int_{\substack{\xi_{i*} n_i(\boldsymbol{X})<0 \\ |\boldsymbol{X}_B|=\infty}} = -\int_{\substack{\xi_{i*} n_i(\boldsymbol{X})<0 \\ |\boldsymbol{X}_B|<\infty}} + j_\infty(\boldsymbol{X}). \tag{2.21}$$

With the aid of Eqs. (2.17) with $v_{wi} = 0$ and (2.19), $f(\boldsymbol{X}_B(\boldsymbol{X}, \boldsymbol{\xi}_*/\xi_*), \boldsymbol{\xi}_*)$ in the first integral is expressed as

$$\begin{aligned} f(\boldsymbol{X}_B(\boldsymbol{X}, \boldsymbol{\xi}_*/\xi_*), \boldsymbol{\xi}_*) &= \frac{\sigma_w(\boldsymbol{X}_B)}{[2\pi RT_w(\boldsymbol{X}_B)]^{3/2}} \exp\left(-\frac{\xi_{j*}^2}{2RT_w(\boldsymbol{X}_B)}\right) \\ &= \frac{2j(\boldsymbol{X}_B)}{\pi[2RT_w(\boldsymbol{X}_B)]^2} \exp\left(-\frac{\xi_{j*}^2}{2RT_w(\boldsymbol{X}_B)}\right). \end{aligned}$$

With this expression in Eq. (2.21), we have the integral equation for $j(\boldsymbol{X})$

$$j(\boldsymbol{X}) = -\int_{\substack{\xi_{i*} n_i(\boldsymbol{X})<0 \\ |\boldsymbol{X}_B|<\infty}} \frac{2j(\boldsymbol{X}_B)\xi_{j*} n_j(\boldsymbol{X})}{\pi[2RT_w(\boldsymbol{X}_B)]^2} \exp\left(-\frac{\xi_{i*}^2}{2RT_w(\boldsymbol{X}_B)}\right) \mathbf{d}\boldsymbol{\xi}_* + j_\infty. \tag{2.22}$$

Here, we change the variable $\boldsymbol{\xi}_*$ of integration to ξ_* and $\bar{l}_{i*}$ ($= -\xi_{i*}/\xi_*$). Noting the relations[4]

$$\mathbf{d}\boldsymbol{\xi}_* = \xi_*^2 \mathrm{d}\xi_* \mathrm{d}\Omega(\bar{\boldsymbol{l}}_*), \quad \bar{l}_{i*} = \frac{X_{Bi} - X_i}{|\boldsymbol{X}_B - \boldsymbol{X}|}, \quad \xi_{i*} n_i(\boldsymbol{X}) = -\xi_* \bar{l}_{i*} n_i(\boldsymbol{X}), \tag{2.23}$$

[4]In the second relation, the range $\xi_{i*} n_i(\boldsymbol{X}) < 0$ of integration is taken into account.

where $\mathrm{d}\Omega(\bar{\boldsymbol{l}}_*)$ is the solid-angle element in the direction $\bar{\boldsymbol{l}}_*$, we can carry out the integration with respect to ξ_* irrespectively of the shape and temperature distribution of the boundary as

$$j(\boldsymbol{X}) = \frac{1}{\pi}\int_{\Omega_*} \bar{l}_{i*} n_i(\boldsymbol{X}) j(\boldsymbol{X}_B)\mathrm{d}\Omega(\bar{\boldsymbol{l}}_*) + j_\infty(\boldsymbol{X}), \tag{2.24}$$

where Ω_* is the range of $\bar{\boldsymbol{l}}_*$ in which direction the boundary can be seen from the point $\boldsymbol{X}$, and the relation between $\boldsymbol{X}_B$ and $\bar{\boldsymbol{l}}_*$ is determined by the geometry of the system. Further, changing the variable of integration from $\bar{\boldsymbol{l}}_*$ to $\boldsymbol{X}_B$, and noting the relation

$$|\boldsymbol{X}_B - \boldsymbol{X}|^2 \mathrm{d}\Omega(\bar{\boldsymbol{l}}_*) = \frac{(X_i - X_{iB}) n_i(\boldsymbol{X}_B)}{|\boldsymbol{X} - \boldsymbol{X}_B|}\mathrm{d}S(\boldsymbol{X}_B),$$

where $\mathrm{d}S(\boldsymbol{X}_B)$ is the surface element of the boundary at $\boldsymbol{X}_B$, we have

$$j(\boldsymbol{X}) = -\frac{1}{\pi}\int_{S_*} \frac{n_i(\boldsymbol{X})(X_{i*} - X_i) n_j(\boldsymbol{X}_*)(X_{j*} - X_j)}{|\boldsymbol{X}_* - \boldsymbol{X}|^4} j(\boldsymbol{X}_*)\mathrm{d}S(\boldsymbol{X}_*) + j_\infty(\boldsymbol{X}), \tag{2.25}$$

where $\boldsymbol{X}$ is a point on the boundary and the integration is carried out over the boundary S_* that can be seen from the point $\boldsymbol{X}$. It may be noted that the homogeneous part of Eq. (2.25) is independent of the temperature distribution on the boundary and is determined by the geometrical configuration of the system. Physical variables enter only through j_∞. When the domain is bounded, the inhomogeneous term j_∞ disappears and $j(\boldsymbol{X}) = \text{const}$ is a solution of Eq. (2.25).[5] The problem is studied under a more general boundary condition and the solution and its uniqueness are given in Sone [1985]. The theory and its applications are given in Section 2.5.

Take a system that is joined with N reservoirs extending to infinities in the equilibrium states at rest with pressure p_m and temperature T_m ($m = 1, 2, \ldots, N$), as shown in Fig. 2.3. The expression (2.20) is transformed by changing the variable $\boldsymbol{\xi}_*$ of integration to ξ_* and $\bar{l}_{i*}$ in the following form:

$$j_\infty = \sum_{m=1}^{N} \frac{p_m}{(2\pi R T_m)^{1/2}} j_{\infty m}, \tag{2.26}$$

where

$$j_{\infty m}(\boldsymbol{X}) = \frac{1}{\pi}\int_{\Omega_{\infty m}} \bar{l}_{i*} n_i(\boldsymbol{X})\mathrm{d}\Omega(\bar{\boldsymbol{l}}_*). \tag{2.27}$$

Here, the domain $\Omega_{\infty m}$ of integration is the region of $\bar{l}_{i*}$ in which direction the infinity with pressure p_m and temperature T_m can be seen from the point $\boldsymbol{X}$.[6]

[5] For this case, Eq. (2.24) or (2.25) is reduced to

$$j(\boldsymbol{X}) = \frac{1}{\pi}\int_{\bar{l}_{i*} n_i(\boldsymbol{X}) > 0} \bar{l}_{i*} n_i(\boldsymbol{X}) j(\boldsymbol{X}_*)\mathrm{d}\Omega(\bar{\boldsymbol{l}}_*).$$

It is easily seen that $j(\boldsymbol{X}) = \text{const}$ is a solution, because $\int_{\bar{l}_{i*} n_i(\boldsymbol{X}) > 0} \bar{l}_{i*} n_i(\boldsymbol{X})\mathrm{d}\Omega(\bar{\boldsymbol{l}}_*) = \pi$.

[6] The expression of $j_{\infty m}$ is derived in the same way as Eq. (2.24).

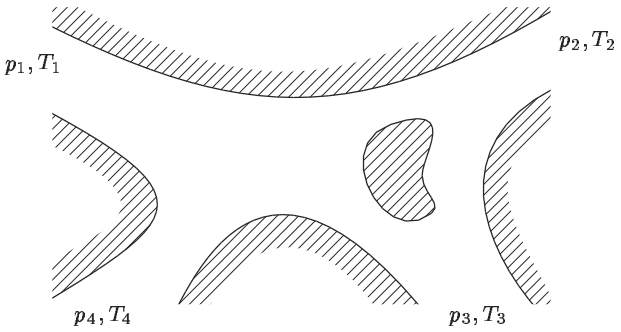

Figure 2.3. A system connected with various states $[(p_1, T_1),\ (p_2, T_2),\ (p_3, T_3),\ (p_4, T_4)]$ at infinities.

Let j_n be the solution j of Eq. (2.25) with $p_m/(2\pi RT_m)^{1/2} = \delta_{mn}$ ($\delta_{mn} = 1$ for $m = n$ and $\delta_{mn} = 0$ for $m \neq n$; $m,\ n = 1, 2, \ldots, N$).[7] The solution j of the original problem is expressed by the linear combination of j_n

$$j = \sum_{m=1}^{N} \frac{p_m}{(2\pi RT_m)^{1/2}} j_m, \tag{2.28}$$

because the corresponding homogeneous equation has no nontrivial solution.[8] The solution j_m is determined by the geometrical configuration and is independent of physical variables. Thus, the temperature distribution of the boundary walls in a finite region does not contribute to the solution j of the original problem.

Applications and comments

Several examples and comments are given here.

Example. There is a highly rarefied gas between two parallel plane walls: one is at rest at $X_2 = 0$ and the other is moving with a uniform velocity U in the X_1 direction at $X_2 = D$ (the plane-Couette-flow problem). The temperatures

[7] Strictly, the j_n is the solution with the nondimensional δ_{mn} being substituted instead of $p_m/(2\pi RT_m)^{1/2}$ that has dimension.

[8] This is intuitively clear because the homogeneous equation corresponds to the system with uniform wall temperature to which no gas enters through the exits, and thus all the gas escapes from the system. The difference from the homogeneous equation for the bounded domain problem in Footnote 5 in this subsection is that the direction of the exits is excluded from the range of integration with respect to $\bar{l}_{i*}$. Thus, $\int_{\Omega_*} \bar{l}_{i*} n_i(\boldsymbol{X}) \mathrm{d}\Omega(\bar{\boldsymbol{l}}_*) = \pi$ or $< \pi$, depending on whether the infinity cannot or can be seen from $\boldsymbol{X}$. Let the maximum of $j(\boldsymbol{X})$ be j_M at $\boldsymbol{X}_M$. Then, from the above inequality and Eq. (2.24) with $\boldsymbol{X} = \boldsymbol{X}_M$, $\boldsymbol{X}_B = \boldsymbol{X}$, and $j_\infty = 0$, it is found that $j(\boldsymbol{X}) = j_M$ or $j(\boldsymbol{X}) = j_M = 0$ for all the points $\boldsymbol{X}$ on the boundary that can be seen from $\boldsymbol{X}_M$ depending on whether the infinity cannot or can be seen from $\boldsymbol{X}_M$. Here, we consider the system where any two points on the boundary of the system can be connected by a broken line inside the gas with the broken points on the boundary. Then, repeating the above process, we find that $j(\boldsymbol{X}) = 0$ everywhere.

of the walls are at the same uniform temperature T_0. The gas molecules make the diffuse reflection on the walls.

The state of the gas or the velocity distribution function f can be considered to be uniform with respect to X_1 and X_3. Then, from Eq. (2.1) or (2.8), it is also independent of X_2. From Eq. (2.15b),

$$\sigma_w(D) = \left(\frac{2\pi}{RT_0}\right)^{1/2} \int_{\xi_2>0} \xi_2 f(D, \boldsymbol{\xi}) \mathbf{d}\boldsymbol{\xi}.$$

By successive application of Eqs. (2.8) and (2.15a), we have

$$\begin{aligned}\sigma_w(D) &= \left(\frac{2\pi}{RT_0}\right)^{1/2} \int_{\xi_2>0} \xi_2 f(D, \boldsymbol{\xi}) \mathbf{d}\boldsymbol{\xi} = \left(\frac{2\pi}{RT_0}\right)^{1/2} \int_{\xi_2>0} \xi_2 f(0, \boldsymbol{\xi}) \mathbf{d}\boldsymbol{\xi} \\ &= \frac{2\sigma_w(0)}{\pi(2RT_0)^2} \int_{\xi_2>0} \xi_2 \exp\left(-\frac{\xi_i^2}{2RT_0}\right) \mathbf{d}\boldsymbol{\xi} = \sigma_w(0).\end{aligned}$$

Thus, from Eqs. (2.15a) and (2.8) with the one-dimensional character of the problem, the distribution function in the gas is given by

$$\begin{aligned} f(X_2, \boldsymbol{\xi}) &= \frac{\sigma_w(0)}{(2\pi RT_0)^{3/2}} \exp\left(-\frac{\xi_i^2}{2RT_0}\right) \qquad (\xi_2 > 0), \\ f(X_2, \boldsymbol{\xi}) &= \frac{\sigma_w(0)}{(2\pi RT_0)^{3/2}} \exp\left(-\frac{(\xi_i - U\delta_{1i})^2}{2RT_0}\right) \qquad (\xi_2 < 0). \end{aligned}$$

The density, flow velocity, and temperature of the gas are

$$\rho = \sigma_w(0), \quad v_1 = \frac{U}{2}, \quad v_2 = v_3 = 0, \quad T = T_0 + \frac{U^2}{12R}.$$

The density ρ is what we have to specify as is in a general finite domain problem. The force f_i acting on the wall at $X_2 = 0$ per unit area is

$$f_1 = \frac{1}{2\sqrt{\pi}} \rho U (2RT_0)^{1/2}, \quad f_2 = -R\rho T_0, \quad f_3 = 0. \qquad \blacksquare$$

Example. There is a highly rarefied gas between two parallel plane walls at rest: one with temperature T_0 is at $X_2 = 0$ and the other with temperature T_1 is at $X_2 = D$ (the heat-transfer problem). The gas molecules make the diffuse reflection on the walls.

The state of the gas or the velocity distribution function f can be considered to be uniform with respect to X_1 and X_3. Then, from Eq. (2.8), it is also independent of X_2. By successive application of Eqs. (2.8) and (2.15a) to Eq. (2.15b) at $X_2 = D$, we have

$$\begin{aligned}\sigma_w(D) &= \left(\frac{2\pi}{RT_1}\right)^{1/2} \int_{\xi_2>0} \xi_2 f(D, \boldsymbol{\xi}) \mathbf{d}\boldsymbol{\xi} = \left(\frac{2\pi}{RT_1}\right)^{1/2} \int_{\xi_2>0} \xi_2 f(0, \boldsymbol{\xi}) \mathbf{d}\boldsymbol{\xi} \\ &= \left(\frac{2\pi}{RT_1}\right)^{1/2} \frac{\sigma_w(0)}{(2\pi RT_0)^{3/2}} \int_{\xi_2>0} \xi_2 \exp\left(-\frac{\xi_i^2}{2RT_0}\right) \mathbf{d}\boldsymbol{\xi} = \sigma_w(0) \sqrt{\frac{T_0}{T_1}}.\end{aligned}$$

From Eqs. (2.15a) and (2.8), the velocity distribution function is

$$f(X_2,\boldsymbol{\xi}) = \frac{\sigma_w(0)}{(2\pi RT_0)^{3/2}}\exp\left(-\frac{\xi_i^2}{2RT_0}\right) \qquad (\xi_2>0),$$
$$f(X_2,\boldsymbol{\xi}) = \frac{\sigma_w(0)}{(2\pi RT_1)^{3/2}}\sqrt{\frac{T_0}{T_1}}\exp\left(-\frac{\xi_i^2}{2RT_1}\right) \qquad (\xi_2<0).$$

The density, flow velocity, and temperature of the gas are

$$\rho = \frac{\sigma_w(0)}{2}\left(1+\sqrt{\frac{T_0}{T_1}}\right), \quad v_i = 0, \quad T = \sqrt{T_0T_1},$$

where ρ is to be specified. The energy flow $e_f(1\to 0)$ from the wall with T_1 at $X_2 = D$, per unit area and per unit time, to that with T_0 at $X_2 = 0$ is

$$e_f(1\to 0) = \sqrt{\frac{8}{\pi}}R\rho T\left(\sqrt{RT_1}-\sqrt{RT_0}\right). \qquad \blacksquare$$

Example. Consider a straight circular pipe with length L and diameter D which joins two large reservoirs, one is at pressure p_1 and temperature T_1 and the other at pressure p_2 and temperature T_2. The gas molecules make the diffuse reflection on the pipe wall.

Let the axis of the pipe be on the X_1 coordinate ($X_2 = X_3 = 0$) and let the exit of the pipe to the reservoir with p_1 and T_1 be on the plane $X_1 = 0$ and the other exit to the reservoir with p_2 and T_2 be at $X_1 = L$. From the symmetry, the solution $j(\boldsymbol{X})$ of the integral equation (2.25) is a function of X_1 only, and is expressed in the form

$$j(\boldsymbol{X}) = \hat{j}(x) = \frac{p_1}{(2\pi RT_1)^{1/2}}\hat{j}_1(x) + \frac{p_2}{(2\pi RT_2)^{1/2}}\hat{j}_1(2L/D-x),$$

where $x = 2X_1/D$ and $\hat{j}_1(x)$ is the solution of Eq. (2.25) corresponding to the present geometry with $p_1/(2\pi RT_1)^{1/2} = 1$ and $p_2/(2\pi RT_2)^{1/2} = 0$.[9] The integral equation (2.25) is reduced to the following simple form for $\hat{j}_1(x)$:

$$\hat{j}_1(x) = \hat{j}_{\infty 1}(x) + \int_0^{2L/D}\hat{K}_P(|x-x_*|)\hat{j}_1(x_*)\mathrm{d}x_*, \tag{2.29}$$

where

$$\hat{K}_P(|x-x_*|) = \frac{1}{2}\left(1-\frac{6|x-x_*|+|x-x_*|^3}{(4+|x-x_*|^2)^{3/2}}\right),$$
$$\hat{j}_{\infty 1}(x) = \frac{1}{2}\left(\frac{x^2+2}{(x^2+4)^{1/2}}-x\right).$$

[9] See Footnote 7 in Section 2.3.3.

The function $\hat{j}_{\infty 1}(x)$ corresponds to $j_{\infty 1}(\boldsymbol{X})$ defined by Eq. (2.27). This integral equation is called *Clausing's equation* (Von Clausing [1932]). Let the mass-flow rate through the pipe for the case $p_1/(2\pi RT_1)^{1/2} = 1$ and $p_2/(2\pi RT_2)^{1/2} = 0$ be $\hat{M}_1$ [corresponding to $\hat{j}_1(x)$]. The mass-flow rate M through the pipe in the positive X_1 direction for the original problem is expressed with $\hat{M}_1$ in the form

$$M = \left(\frac{p_1}{(2\pi RT_1)^{1/2}} - \frac{p_2}{(2\pi RT_2)^{1/2}} \right) \hat{M}_1. \tag{2.30}$$

The mass-flow rate M vanishes when $p_1/\sqrt{T_1} = p_2/\sqrt{T_2}$ as in the case of slit (the third example in Section 2.3.2). This condition is shown to be true for a more general situation in Section 2.5.6.

The mass-flow rate $\hat{M}_1$ is the difference of the mass-flow rate $\hat{M}_{\mathrm{fr}\infty}$ of the molecules entering the exit of the pipe at $X_1 = 0$ from the infinity and the mass-flow rate $\hat{M}_{\mathrm{ret}}$ of the molecules returning to the exit from the pipe surface and is expressed as

$$\begin{aligned} \hat{M}_1 = \hat{M}_{\mathrm{fr}\infty} - \hat{M}_{\mathrm{ret}} &= \frac{\pi D^2}{4} \left(1 - \frac{2}{\pi} \int_0^{2L/D} \hat{j}_1(x) \int_{\Omega_{\infty 1}} \bar{l}_i n_i \mathrm{d}\Omega(\bar{\boldsymbol{l}}) \mathrm{d}x \right) \\ &= \frac{\pi D^2}{4} \left[1 - \int_0^{2L/D} \hat{j}_1(x) \left(-x + \frac{x^2+2}{\sqrt{x^2+4}} \right) \mathrm{d}x \right], \end{aligned}$$

where $\bar{\boldsymbol{l}}$ is a unit vector and $\Omega_{\infty 1}$ is the range of $\bar{\boldsymbol{l}}$ in the direction of which the exit at $X_1 = 0$ can be seen from a point on the pipe at x, and n_i is the unit normal to the boundary, pointed to the gas, there. This expression is further transformed into a well-known formula with the aid of Eq. (2.29)

$$\frac{\hat{M}_1}{\pi(D/2)^2} = \frac{D}{2L} \int_0^{2L/D} [x^2 + 2 - x(x^2+4)^{1/2}] \hat{j}_1(x) \mathrm{d}x. \tag{2.31}$$

The relation $\hat{M}_1/\pi(D/2)^2$ vs $2L/D$ is shown in Fig. 2.4. ■

In the first two examples, the state of gas is uniform. However, the walls are subject to a force or a heat is transferred to the walls. Thus, it is sometimes stated that the viscosity and thermal conductivity are infinite in a free molecular gas. However, this statement is easily seen to be inappropriate from the examples of a flow past a flat plate and a heat transfer from a convex body in Section 2.3.2, where the velocity or temperature field is obviously nonuniform. Local stress and heat flux in a free molecular gas are not determined by local quantities such as the velocity and temperature gradients, but the global configuration of the system plays the decisive role.

Taking the limit that $D \to \infty$ in the same two examples, we obtain the solution of the half-space problem if $\sigma_w(D)$ is replaced by ρ_1 which corresponds to ρ in the Maxwellian coming from infinity. In each case, the state at infinity is not in equilibrium (or the distribution is not Maxwellian, but is the combination of two different half-Maxwellians). As a result, the solution taking the effect of

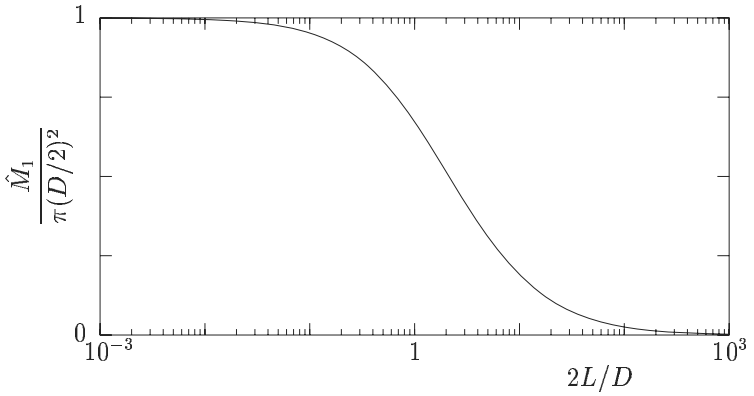

Figure 2.4. Mass-flow rate $\hat{M}_1$ of a free molecular gas through a straight circular pipe. (The numerical data are prepared by H. Sugimoto.)

molecular collisions into account cannot be obtained by a perturbation of the free molecular solution, as to be explained in Section 2.6, and the state at rest with the uniform temperature T_0 is established in both cases if the effect of molecular collisions is taken in (see Section 4.4).

The case of the complete condensation (1.29) on an interface of the gas and its condensed phase is a trivial case where the velocity distribution function of the molecules leaving the interface is known. The case of the condition (1.28a) with (1.28b) and $\alpha = 1$ can be reduced to the integral equation for σ_w as in the case of the diffuse reflection. On the basis of the integral equation of σ_w for that case, Inamuro [1989] discussed some problems related to a cryopump and vacuum vapor deposition.

2.4 Initial and boundary-value problem

The discussion on boundary-value problems for a free molecular gas in Section 2.3 is limited only to time-independent cases. We will briefly explain the initial and boundary-value problem. The initial condition is assumed to be given at time $t = 0$.

The velocity distribution function f at time t is related to that at some previous time t_0 by Eq. (2.2), i.e.,

$$f(X_i, \xi_i, t) = f(X_i - \xi_i(t - t_0), \xi_i, t_0). \tag{2.32}$$

Let $(\boldsymbol{X}, \boldsymbol{\xi}, t)$ be given. If we trace back a particle with velocity $\boldsymbol{\xi}$ from $(\boldsymbol{X}, t)$, we encounter some point on the boundary at some time $t_B(\boldsymbol{X}, \boldsymbol{\xi}, t)$ before the initial time $t = 0$, or do not encounter any point on the boundary until the initial time. We take $t_0 = t_B$ in the former case, and $t_0 = 0$ in the latter. When $t_0 = 0$ for $(\boldsymbol{X}, \boldsymbol{\xi}, t)$, then the value of the velocity distribution function f at $(\boldsymbol{X}, \boldsymbol{\xi}, t)$ is determined by the initial value, and when $t_0 = t_B$, it is determined

by its boundary value $f(X_i - \xi_i(t - t_B), \xi_i, t_B)$ for the molecules leaving the boundary. Thus the velocity distribution function is determined by the initial and boundary data. The velocity distribution function of the molecules leaving the boundary generally depends on that of the impinging molecules, which is determined by the distribution of the molecules leaving other points of the boundary in the past and that of the initial time. Expressing this process in mathematical expressions, we obtain an integral equation for the boundary data of the velocity distribution function for the molecules leaving (or impinging on) the boundary. This process is shown by simple examples.

Example. Consider a gas in the region $X_1 > 0$ bounded by a plane wall with temperature T_0 at $X_1 = 0$. The gas is in the equilibrium state at rest with density ρ_0 and temperature T_0. At time $t = 0$, the wall suddenly moves with a constant speed U in the X_1 direction. The gas molecules make the diffuse reflection on the wall. (Piston problem)

The state of the gas can be considered to be uniform with respect to X_2 and X_3. The position of the wall is given by $X_1 = Ut$, and the gas region is in $X_1 > Ut$. Let $(X_1, \boldsymbol{\xi}, t)$ be given in the gas region. When $\xi_1 < X_1/t$, the path of the particle, if we trace back the particle, is always in the gas region $[X_1 - \xi_1(t - t_0) > Ut_0$ for $t \geq t_0 \geq 0]$. Therefore, f is expressed by the initial condition, i.e.,

$$f(X_1, \boldsymbol{\xi}, t) = \frac{\rho_0}{(2\pi RT_0)^{3/2}} \exp\left(-\frac{\xi_i^2}{2RT_0}\right) \qquad (\xi_1 < \frac{X_1}{t}). \tag{2.33}$$

When $\xi_1 > X_1/t$, the path encounters the wall at $t_0 = (\xi_1 t - X_1)/(\xi_1 - U) > 0$. Therefore, f is given by the boundary condition at $X_1 = X_{10} = Ut_0$, i.e., from the diffuse-reflection boundary condition,

$$f(X_1, \boldsymbol{\xi}, t) = f(X_{10}, \boldsymbol{\xi}, t_0) = \frac{\sigma_w(t_0)}{(2\pi RT_0)^{3/2}} \exp\left(-\frac{(\xi_i - U\delta_{1i})^2}{2RT_0}\right) \qquad (\xi_1 > \frac{X_1}{t}), \tag{2.34a}$$

$$\sigma_w(t_0) = -\left(\frac{2\pi}{RT_0}\right)^{1/2} \int_{\xi_1 - U < 0} (\xi_1 - U) f(X_{10}, \boldsymbol{\xi}, t_0) \mathbf{d}\boldsymbol{\xi}, \tag{2.34b}$$

$$X_{10} = \frac{U(\xi_1 t - X_1)}{\xi_1 - U}, \qquad t_0 = \frac{\xi_1 t - X_1}{\xi_1 - U}. \tag{2.34c}$$

We can use the initial data (2.33) for $f(X_{10}, \boldsymbol{\xi}, t_0)$ $(\xi_1 - U < 0)$ in Eq. (2.34b). Thus,

$$\begin{aligned}\sigma_w(t_0) &= -\frac{\rho_0}{2\pi(RT_0)^2} \int_{\xi_1 - U < 0} (\xi_1 - U) \exp\left(-\frac{\xi_i^2}{2RT_0}\right) \mathbf{d}\boldsymbol{\xi} \\ &= \rho_0 \left[\exp\left(-\frac{U^2}{2RT_0}\right) + \frac{U}{\sqrt{2RT_0}} \left(\sqrt{\pi} + 2\int_0^{U/\sqrt{2RT_0}} \exp\left(-\zeta^2\right) \mathrm{d}\zeta\right)\right].\end{aligned}$$

With this $\sigma_w(t_0)$, the velocity distribution function is determined. This problem corresponds to the case of a gas around a convex body in Section 2.3.2. ■

Example. A gas is bounded by two parallel plane walls with the same temperature T_0, one at $X_1 = 0$ and the other at $X_1 = D$. The gas is initially in the equilibrium state at rest with density ρ_0 and temperature T_0. At time $t = 0$, the temperature of the wall at $X_1 = D$ is suddenly raised (or lowered) to T_1. The gas molecules make the diffuse reflection on the walls.

The state of the gas can be considered to be uniform with respect to X_2 and X_3. Let $(X_1, \boldsymbol{\xi}, t)$ be given in the gas region. When $-(D - X_1)/t < \xi_1 < X_1/t$, the path of the particle, if we trace back the particle, is always in the gas region $0 < X_1 < D$ for $0 \le t_0 \le t$, Therefore, f is expressed by the initial condition, i.e.,

$$f(X_1, \boldsymbol{\xi}, t) = \frac{\rho_0}{(2\pi RT_0)^{3/2}} \exp\left(-\frac{\xi_i^2}{2RT_0}\right) \qquad \left(-\frac{D - X_1}{t} < \xi_1 < \frac{X_1}{t}\right). \quad (2.35)$$

When $\xi_1 > X_1/t$, the path encounters the wall at $X_1 = 0$ at time $t_0 = t - X_1/\xi_1 > 0$. Therefore, f is given by the boundary condition at $X_1 = 0$, i.e., from the diffuse-reflection boundary condition,

$$f(X_1, \boldsymbol{\xi}, t) = \frac{\sigma_w(0, t - X_1/\xi_1)}{(2\pi RT_0)^{3/2}} \exp\left(-\frac{\xi_i^2}{2RT_0}\right) \qquad \left(\xi_1 > \frac{X_1}{t}\right), \quad (2.36)$$

where

$$\sigma_w(0, t_0) = -\left(\frac{2\pi}{RT_0}\right)^{1/2} \int_{\xi_1 < 0} \xi_1 f(0, \boldsymbol{\xi}, t_0) \mathbf{d}\boldsymbol{\xi}.$$

When $\xi_1 < -(D - X_1)/t$, the path encounters the wall at $X_1 = D$ at time $t_0 = t + (D - X_1)/\xi_1 > 0$. Therefore, f is given by the boundary condition at $X_1 = D$, that is, from the diffuse-reflection boundary condition,

$$f(X_1, \boldsymbol{\xi}, t) = \frac{\sigma_w(D, t + (D - X_1)/\xi_1)}{(2\pi RT_1)^{3/2}} \exp\left(-\frac{\xi_i^2}{2RT_1}\right) \qquad \left(\xi_1 < -\frac{D - X_1}{t}\right), \quad (2.37)$$

where

$$\sigma_w(D, t_0) = \left(\frac{2\pi}{RT_1}\right)^{1/2} \int_{\xi_1 > 0} \xi_1 f(D, \boldsymbol{\xi}, t_0) \mathbf{d}\boldsymbol{\xi}.$$

If we know $\sigma_w(0, t_0)$ and $\sigma_w(D, t_0)$ for $0 < t_0 < t$, the solution $f(X_1, \boldsymbol{\xi}, t)$ is given by Eqs. (2.35), (2.36), and (2.37).

Substituting the above form of the velocity distribution function into the definition of $\sigma_w(0, t)$ and $\sigma_w(D, t)$, we obtain the integral equations for $\sigma_w(0, t)$ and $\sigma_w(D, t)$ $(t > 0)$, i.e.,

$$\begin{aligned}
\sigma_w(0, t) &= -\left(\frac{2\pi}{RT_0}\right)^{1/2} \int_{\xi_1 < 0} \xi_1 f(0, \boldsymbol{\xi}, t) \mathbf{d}\boldsymbol{\xi} \\
&= -\left(\frac{2\pi}{RT_0}\right)^{1/2} \left[\int_{\xi_1 < -D/t} \frac{\sigma_w(D, t + D/\xi_1)}{(2\pi RT_1)^{3/2}} \xi_1 \exp\left(-\frac{\xi_i^2}{2RT_1}\right) \mathbf{d}\boldsymbol{\xi} \right. \\
&\qquad \left. + \frac{\rho_0}{(2\pi RT_0)^{3/2}} \int_{-D/t < \xi_1 < 0} \xi_1 \exp\left(-\frac{\xi_i^2}{2RT_0}\right) \mathbf{d}\boldsymbol{\xi} \right],
\end{aligned}$$

$$\sigma_w(D,t) = \left(\frac{2\pi}{RT_1}\right)^{1/2} \int_{\xi_1>0} \xi_1 f(D,\boldsymbol{\xi},t)\mathbf{d}\boldsymbol{\xi}$$
$$= \left(\frac{2\pi}{RT_1}\right)^{1/2} \left[\frac{\rho_0}{(2\pi RT_0)^{3/2}} \int_{0<\xi_1<D/t} \xi_1 \exp\left(-\frac{\xi_i^2}{2RT_0}\right) \mathbf{d}\boldsymbol{\xi} \right.$$
$$\left. + \int_{\xi_1>D/t} \frac{\sigma_w(0,t-D/\xi_1)}{(2\pi RT_0)^{3/2}} \xi_1 \exp\left(-\frac{\xi_i^2}{2RT_0}\right) \mathbf{d}\boldsymbol{\xi}\right].$$

After some arrangements, the integral equations for $\sigma_w(0,t)$ and $\sigma_w(D,t)$ for $t>0$ are given in the form

$$\sigma_w(0,t) = -2\sqrt{\frac{T_1}{T_0}} \int_{-\infty}^{\frac{-D}{\sqrt{2RT_1}t}} \sigma_w\left(D, t + \frac{D}{\sqrt{2RT_1}\zeta}\right) \zeta \exp\left(-\zeta^2\right) \mathrm{d}\zeta$$
$$+ \ \rho_0 \left[1 - \exp\left(-\frac{D^2}{2RT_0t^2}\right)\right],$$

$$\sigma_w(D,t) = 2\sqrt{\frac{T_0}{T_1}} \int_{\frac{D}{\sqrt{2RT_0}t}}^{\infty} \sigma_w\left(0, t - \frac{D}{\sqrt{2RT_0}\zeta}\right) \zeta \exp\left(-\zeta^2\right) \mathrm{d}\zeta$$
$$+ \rho_0 \sqrt{\frac{T_0}{T_1}} \left[1 - \exp\left(-\frac{D^2}{2RT_0t^2}\right)\right]. \qquad \blacksquare$$

2.5 Statics of a free molecular gas: Effect of the temperature of the boundary

Consider the time-independent behavior of a free molecular gas around a group of bodies at rest. The gas region may be bounded or extend to infinity. The shape and arrangement of the boundary (bodies or outer wall) and the temperature distribution on the boundary are arbitrary. We assume that the reflected gas molecules on the boundary satisfy the Maxwell-type condition [(1.23a) and (1.23b)]. In the case where the domain extends to infinity, the condition there is reserved for a moment. A simple way to solve this problem is developed in Sone [1984a, 1985]. In the present section, we will explain the method with its applications.

2.5.1 Construction of the velocity distribution function

With the molecular speed ξ, i.e., $\xi = (\xi_i^2)^{1/2}$, and the unit vector l_i in the direction of ξ_i, i.e., $l_i = \xi_i/\xi$, Eq. (2.3) is expressed as

$$f(X_i, \xi l_i) = f(X_i - l_i s, \xi l_i), \tag{2.38}$$

where s is a parameter. The Maxwell-type boundary condition is given in the form

$$f(X_i, \xi l_i) = (1-\alpha) f(X_i, \xi(l_i - 2l_j n_j n_i)) + \alpha\sigma\beta^2 \exp(-\beta\xi^2) \qquad (l_i n_i > 0), \tag{2.39a}$$

$$\sigma = -\frac{2}{\pi} \int_{l_i n_i < 0} \xi l_j n_j f(\boldsymbol{X}, \boldsymbol{\xi}) \mathbf{d}\boldsymbol{\xi}, \tag{2.39b}$$

$$\beta = \frac{1}{2RT_w}, \tag{2.39c}$$

where T_w is the temperature of the boundary, n_i is the unit normal vector to the boundary pointed to the gas domain, α is the accommodation coefficient of the boundary, and R is the gas constant per unit mass.[10] The boundary parameters T_w, n_i, and α depend on the position on the boundary. This fact is shown like $T_w(\boldsymbol{X})$, $\alpha(\boldsymbol{X})$ when the discrimination is preferable.

Now we will construct the solution of the boundary-value problem given by Eqs. (2.38) and (2.39a). From the position X_i, we trace back the path of the molecule with velocity ξl_i that has specularly reflected on the boundary. The points that the molecule encountered the boundary are denoted by $X_i^{(m)}$ $(m = 1, 2, \ldots)$ and the direction of the molecule having impinged on the point $X_i^{(m)}$ by $l_i^{(m)}$, where m is numbered in the order from the nearest past point (Fig. 2.5). That is, let $X_i^{(0)} = X_i$ and $l_i^{(0)} = l_i$, and then the sequences $X_i^{(m)}$ and $l_i^{(m)}$ $(m = 1, 2, \ldots)$ are determined successively from $m = 1$ as follows: $X_i^{(m)}$ is the first intersection of the half-line $X_i^{(m-1)} - l_i^{(m-1)} s$ with the boundary, where s is a positive parameter, and

$$l_i^{(m)} = l_i^{(m-1)} - 2l_j^{(m-1)} n_j^{(m)} n_i^{(m)}, \tag{2.40}$$

where

$$n_i^{(m)} = n_i(\boldsymbol{X}^{(m)}).$$

If $|\boldsymbol{X}^{(m)}| = \infty$ at some m, the sequence is terminated at this stage. The sequence is uniquely determined by X_i and l_i. From the definition of $l_i^{(0)}$ and $X_i^{(1)}$, $l_i^{(0)} n_i^{(1)} > 0$. Then from Eq. (2.40),

$$|l_i^{(m)}| = 1, \qquad l_i^{(m)} n_i^{(m)} < 0, \qquad l_i^{(m)} n_i^{(m+1)} > 0. \tag{2.41}$$

From Eqs. (2.38) and (2.39a), with the notation introduced above, the velocity distribution function at $(\boldsymbol{X}, \xi\boldsymbol{l})$ is expressed as

$$\begin{aligned} f(\boldsymbol{X}, \xi\boldsymbol{l}) = {} & \alpha(\boldsymbol{X}^{(1)}) \sigma(\boldsymbol{X}^{(1)}) \beta(\boldsymbol{X}^{(1)})^2 \exp[-\beta(\boldsymbol{X}^{(1)}) \xi^2] \\ & + [1 - \alpha(\boldsymbol{X}^{(1)})] f(\boldsymbol{X}^{(1)}, \xi\boldsymbol{l}^{(1)}), \end{aligned} \tag{2.42}$$

[10] The σ introduced here is related to σ_w in Eq. (2.15b) by $\sigma = \sigma_w / \pi^{3/2} \beta^{1/2}$.

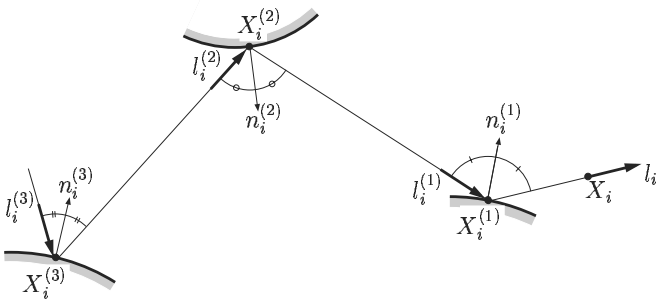

Figure 2.5. Path of a specularly reflecting molecule and $X_i^{(m)}$, $l_i^{(m)}$, and $n_i^{(m)}$.

where

$$\beta(\boldsymbol{X}^{(1)}) = \frac{1}{2RT_w(\boldsymbol{X}^{(1)})},$$

and the relation (2.40) is used. The function $f(\boldsymbol{X}^{(1)}, \xi\boldsymbol{l}^{(1)})$ in the last term on the right-hand side of Eq. (2.42) is the velocity distribution function of the molecules impinging on $\boldsymbol{X}^{(1)}$. By a similar procedure, this is replaced by $f(\boldsymbol{X}^{(2)}, \xi\boldsymbol{l}^{(1)})$ of the molecules leaving $\boldsymbol{X}^{(2)}$ and the boundary condition is applied to the result. Repeating this process, we obtain the following expression for $f(\boldsymbol{X}, \xi\boldsymbol{l})$:

$$\begin{aligned} f(\boldsymbol{X}, \xi\boldsymbol{l}) &= \alpha^{(1)}\sigma^{(1)}\mathfrak{M}^{(1)} + (1-\alpha^{(1)})\alpha^{(2)}\sigma^{(2)}\mathfrak{M}^{(2)} \\ &\quad + (1-\alpha^{(1)})(1-\alpha^{(2)})\alpha^{(3)}\sigma^{(3)}\mathfrak{M}^{(3)} + \cdots \\ &= \sum_{m=1}^{\infty}\prod_{h=1}^{m-1}(1-\alpha^{(h)})\alpha^{(m)}\sigma^{(m)}\mathfrak{M}^{(m)}, \end{aligned} \tag{2.43}$$

where

$$\left.\begin{aligned} &\mathfrak{M}^{(m)} = \beta_{(m)}^2 \exp(-\beta_{(m)}\xi^2), && \alpha^{(m)} = \alpha(\boldsymbol{X}^{(m)}), \\ &\beta_{(m)} = \beta(\boldsymbol{X}^{(m)}) = 1/2RT_w(\boldsymbol{X}^{(m)}), && \sigma^{(m)} = \sigma(\boldsymbol{X}^{(m)}), \end{aligned}\right\} \tag{2.44}$$

and the convention $\prod_{h=1}^{0}(1-\alpha^{(h)}) = 1$ is used. If $|\boldsymbol{X}^{(N)}| = \infty$, the series ends at the N-th term and the last term is given by $\prod_{h=1}^{N-1}(1-\alpha^{(h)})f(\boldsymbol{X}^{(N)}, \xi\boldsymbol{l}^{(N-1)})$, where $f(\boldsymbol{X}^{(N)}, \xi\boldsymbol{l}^{(N-1)})$ is the velocity distribution function at infinity.

The series (2.43) is constructed in such a way that it satisfies the basic equation (2.38) and the boundary condition (2.39a). However, $\sigma(\boldsymbol{X})$ in the series is, by definition, an undetermined function depending on the velocity distribution function of the molecules impinging on the boundary point $\boldsymbol{X}$. Substituting the series (2.43) into Eq. (2.39b), we obtain an integral equation for $\sigma(\boldsymbol{X})$. Now we assume that the velocity distribution function at infinity is given by

$$f(\boldsymbol{\infty}, \xi\boldsymbol{l}) = C\beta_\infty^2 \exp(-\beta_\infty \xi^2), \tag{2.45}$$

where (i) the bold $\boldsymbol{\infty}$ is used to discriminate the position at infinity, (ii) C is an arbitrary constant, (iii) β_∞ may depend on the position at infinity and $\boldsymbol{l}$, which allows the situation where many reservoirs extending to infinity are connected by pipes, and (iv) the condition (2.45) is applied only to such $\boldsymbol{l}$ that no boundary is encountered if one proceeds in the $-\boldsymbol{l}$ direction from the point under consideration. Under this assumption on the condition at infinity, we will show that

$$\sigma(\boldsymbol{X}) = C \tag{2.46}$$

is the solution of the integral equation.

Putting $\sigma^{(m)} = C$ and applying the condition (2.45) when $|\boldsymbol{X}^{(N)}| = \infty$ in the series (2.43), we have

$$\begin{aligned} f(\boldsymbol{X}, \xi\boldsymbol{l}) = C[&\alpha^{(1)}\mathfrak{M}^{(1)} + (1-\alpha^{(1)})\alpha^{(2)}\mathfrak{M}^{(2)} \\ &+ (1-\alpha^{(1)})(1-\alpha^{(2)})\alpha^{(3)}\mathfrak{M}^{(3)} + \cdots], \end{aligned} \tag{2.47}$$

where $\alpha^{(N)} = 1$ when $|\boldsymbol{X}^{(N)}| = \infty$. Substituting this expression into Eq. (2.39b), we have

$$\begin{aligned} \sigma(\boldsymbol{X}) &= -\frac{2}{\pi}\int_{\substack{l_j n_j<0 \\ 0<\xi<\infty}} l_i n_i \xi^3 f(\boldsymbol{X}, \xi\boldsymbol{l})\mathrm{d}\xi\mathrm{d}\Omega(\boldsymbol{l}) \\ &= -\frac{2C}{\pi}\int l_i n_i \xi^3[\alpha^{(1)}\mathfrak{M}^{(1)} + (1-\alpha^{(1)})\alpha^{(2)}\mathfrak{M}^{(2)} \\ &\qquad + (1-\alpha^{(1)})(1-\alpha^{(2)})\alpha^{(3)}\mathfrak{M}^{(3)} + \cdots]\mathrm{d}\xi\mathrm{d}\Omega \\ &= -\frac{C}{\pi}\int_{l_j n_j<0} l_i n_i[\alpha^{(1)} + (1-\alpha^{(1)})\alpha^{(2)} + (1-\alpha^{(1)})(1-\alpha^{(2)})\alpha^{(3)} + \cdots]\mathrm{d}\Omega \\ &= C, \end{aligned}$$

where $\mathrm{d}\Omega(\boldsymbol{l})$ is the solid angle element in the direction of $\boldsymbol{l}$, the facts that $\alpha^{(m)}$ is independent of ξ and that $\int_0^\infty \xi^3\mathfrak{M}^{(m)}\mathrm{d}\xi = \int_0^\infty \xi^3\beta_{(m)}^2\exp(-\beta_{(m)}\xi^2)\mathrm{d}\xi = 1/2$ are to be noted in the process from the second equation to the third, and the series $\alpha^{(1)} + (1-\alpha^{(1)})\alpha^{(2)} + (1-\alpha^{(1)})(1-\alpha^{(2)})\alpha^{(3)} + \cdots$ converges to unity.[11] Thus, we find that $\sigma(\boldsymbol{X}) = C$ is the solution of the integral equation.

From the preceding discussion, we find that the series

$$\begin{aligned} f(\boldsymbol{X}, \xi\boldsymbol{l}) &= C\sum_{m=1}^{\infty}\prod_{h=1}^{m-1}(1-\alpha^{(h)})\alpha^{(m)}\mathfrak{M}^{(m)}, \\ &\text{with the convention : } \ \alpha^{(N)} = 1 \text{ when } |\boldsymbol{X}^{(N)}| = \infty, \end{aligned} \tag{2.48}$$

[11] For $0 < \varepsilon \le \alpha \le 1$ (ε is a constant), all the terms of the series are non-negative and it is uniformly convergent with respect to $\boldsymbol{X}$ and $\boldsymbol{l}$. We can see that the series converges to unity from the following form of the series:

$$\alpha^{(1)} + (1-\alpha^{(1)})[1-(1-\alpha^{(2)})] + (1-\alpha^{(1)})(1-\alpha^{(2)})[1-(1-\alpha^{(3)})] + \cdots,$$

obtained by rewriting $\alpha^{(m)}$ at the m-th term as $1-(1-\alpha^{(m)})$.

is the solution of the boundary-value problem [Eqs. (2.38), (2.39a), and (2.45)]. The constant C is determined (i) by the density or pressure at infinity in an infinite domain problem [see Eq. (2.45)] or (ii) by the total mass of the system or the density or pressure at a specified point in a bounded domain problem. Here, the velocity distribution function is expressed by the temperatures and accommodation coefficients at the boundary points that are encountered when we trace back the path of the specularly reflecting molecules. The series (2.48) converges uniformly with respect to $\boldsymbol{X}$ and $\boldsymbol{l}$ when $0 < \varepsilon \le \alpha \le 1$ and $0 < \delta \le T_w$ (ε and δ are constants). The error estimate of its truncated series is easy, and the series converges rapidly when α is not too small. In the case of the diffuse reflection ($\alpha = 1$), only the first term of the series remains, i.e.,

$$f(\boldsymbol{X}, \xi\boldsymbol{l}) = C\mathfrak{M}^{(1)}. \tag{2.49}$$

This formula is applicable when only the part of the boundary that can be seen from the point $\boldsymbol{X}$ is diffusely reflecting.

2.5.2 Condition of applicability

Obviously from the derivation of the solution (2.48), it is applicable without restriction for a bounded domain problem. In an infinite domain problem, according to the assumption (2.45), the velocity distribution function of the molecules starting at infinity is required to be given by

$$f = C\beta_\infty^2 \exp(-\beta_\infty \xi^2), \tag{2.50}$$

where β_∞ may depend on $\boldsymbol{l}$ and the position at infinity.

2.5.3 Macroscopic variables

Macroscopic variables, density, flow velocity, temperature, etc., are expressed by some moments of the velocity distribution function. Three-dimensional integrations there being carried out in spherical-coordinate variables, the integration with respect to ξ can be carried out without specifying the problem explicitly as follows:

$$\begin{aligned}
&\int \xi_{i_1}\xi_{i_2}\cdots\xi_{i_h} f \mathrm{d}\boldsymbol{\xi} = \int \xi_{i_1}\xi_{i_2}\cdots\xi_{i_h} f \xi^2 \mathrm{d}\xi \mathrm{d}\Omega(\boldsymbol{l}) \\
&= CE_{h+2} \int l_{i_1} l_{i_2} \cdots l_{i_h} \Big(\alpha^{(1)} \beta_{(1)}^{(1-h)/2} + (1-\alpha^{(1)})\alpha^{(2)} \beta_{(2)}^{(1-h)/2} \\
&\qquad + (1-\alpha^{(1)})(1-\alpha^{(2)})\alpha^{(3)} \beta_{(3)}^{(1-h)/2} + \cdots \Big) \mathrm{d}\Omega,
\end{aligned} \tag{2.51}$$

where $\mathrm{d}\Omega(\boldsymbol{l})$ is the solid angle element in the direction of $\boldsymbol{l}$ and

$$\begin{aligned}
E_h &= \int_0^\infty \xi^h \exp(-\xi^2) \mathrm{d}\xi, \\
E_{2n} &= \frac{1 \cdot 3 \cdots (2n-1)}{2^{n+1}} \sqrt{\pi}, \quad E_0 = \frac{\sqrt{\pi}}{2}, \quad E_{2n+1} = \frac{n!}{2}, \quad E_1 = \frac{1}{2}.
\end{aligned}$$

2.5.4 Flow velocity

Flow velocity, which corresponds to the case $h = 1$ in Eq. (2.51), is found to be zero with the aid of the formula $\alpha^{(1)} + (1-\alpha^{(1)})\alpha^{(2)} + (1-\alpha^{(1)})(1-\alpha^{(2)})\alpha^{(3)} + \cdots = 1$.[12] Thus, no flow is induced irrespective of the distributions of temperature and accommodation coefficient on the boundary at rest (or the bodies and boundary walls) in any bounded-domain system, which is enclosed by an outer boundary, or in an unbounded-domain system where the conditions at infinities are given by Eq. (2.50), e.g., a common equilibrium state at rest. This is not an obvious matter. In a rarefied gas, it is known that various kinds of flows are induced by temperature fields, such as thermal creep flow, thermal stress flow, flow induced around the edge of a heated plate, and thermal transpiration (see Chapters 3 and 5). The above-mentioned result shows that these flows induced owing to gas rarefaction vanish in the limit of high gas rarefaction. Even in the absence of flow, as will be shown in Section 2.5.7, an interaction force generally acts between bodies with different temperatures or a propulsion force acts on a nonconvex body even if it is heated uniformly. In a gas in the continuum limit, $v_i = 0$ and $p = \text{const}$ is a solution in the situation under consideration (see Section 3.3) and no force acts on a body in the gas.[13]

2.5.5 Principle of superposition

Let the boundary (body, surrounding wall, infinity) consist of n parts B_1, B_2, $\ldots$, B_n. We try to express the effect of temperature of each boundary B_m separately. We express the solution (2.48) in a little different form

$$f = C\sum_{m=1}^{\infty}\prod_{h=1}^{m-1}(1-\alpha^{(h)})\alpha^{(m)}\mathfrak{M}^{(m)} + C\sum_{m=1}^{\infty}\prod_{h=1}^{m-1}(1-\alpha^{(h)})\alpha^{(m)}\mathfrak{M}_0 - f_0, \quad (2.52)$$

where

$$f_0 = C\mathfrak{M}_0, \quad \mathfrak{M}_0 = \beta_0^2\exp(-\beta_0\xi^2), \quad \beta_0 = \frac{1}{2RT_0}, \quad T_0 = \text{const}.$$

Here, f_0 is the solution of the problem when the boundary is at uniform temperature T_0 (i.e., the system is in the uniform equilibrium state at rest with temperature T_0). The series in the second term on the right-hand side of Eq. (2.52) is another expression of f_0.

We further transform f given by Eq. (2.52) in the following way. For a given set of $(\boldsymbol{X}, \xi\boldsymbol{l})$, let $\boldsymbol{X}^{(m_k)}$ $(k = 1, 2, \ldots)$ among $\boldsymbol{X}^{(m)}$ $(m = 1, 2, \ldots)$ be on the boundary B_1. Interchange the m_k terms in the first series and those in the second on the right-hand side of Eq. (2.52). This being performed for all the set

[12] See Footnote 11 in Section 2.5.1.

[13] The same result is derived from the Navier–Stokes set of equations.

of $(\boldsymbol{X}, \xi\boldsymbol{l})$, f in Eq. (2.52) is rewritten as

$$f = f_{(1)} + f^{(1)} - f_0, \tag{2.53a}$$

$$f_{(1)} = C \sum_{m=1}^{\infty} \prod_{h=1}^{m-1} (1-\alpha^{(h)}) \alpha^{(m)} \bar{\mathfrak{M}}_1^{(m)}, \tag{2.53b}$$

$$f^{(1)} = C \sum_{m=1}^{\infty} \prod_{h=1}^{m-1} (1-\alpha^{(h)}) \alpha^{(m)} \bar{\mathfrak{M}}_2^{(m)}, \tag{2.53c}$$

$$\bar{\mathfrak{M}}_1^{(m)} = \begin{cases} \mathfrak{M}^{(m)} & (m \neq m_k), \\ \mathfrak{M}_0 & (m = m_k), \end{cases} \quad \bar{\mathfrak{M}}_2^{(m)} = \begin{cases} \mathfrak{M}_0 & (m \neq m_k), \\ \mathfrak{M}^{(m)} & (m = m_k). \end{cases} \tag{2.53d}$$

Here, $f_{(1)}$ is the solution in the case where the temperature of B_1 is T_0 and the temperature distributions on the other boundaries B_i $(i = 2, \ldots)$ remain in their original distributions, and $f^{(1)}$ is the solution in the case where the temperature distribution on B_1 remains in the original one and the temperatures on the other boundaries B_i $(i = 2, \ldots)$ are all T_0.

The process from Eq. (2.52) to Eq. (2.53d) is applied to $f_{(1)}$ with appropriate replacements (e.g., B_1 by B_2 and therefore $\boldsymbol{X}^{(m_k)}$ is on B_2), and so on. Then, we have

$$f = f^{(1)} + f^{(2)} + \cdots + f^{(n)} - (n-1) f_0. \tag{2.54}$$

Here, $f^{(m)}$ $(m = 1, 2, \ldots, n)$ is the solution on the same geometrical problem where the temperature distribution on the boundary B_m is kept at the original one, but the temperature distributions on the other boundaries (B_1, B_2, …, B_n except B_m) are changed to a uniform temperature T_0 with the accommodation coefficient α of the boundaries kept at its original value; and f_0 is the solution of the problem where all the boundaries are set at a uniform temperature T_0. It may be noted that the common constant C in the solution $f^{(1)}$, $f^{(2)}$, etc. has a common meaning in each solution in an infinite domain problem [see Eq. (2.50)]. In a bounded domain problem, the meaning of C generally depends on $f^{(1)}$, $f^{(2)}$, etc.

Let B_s be a closed (or bounded) body. Then the force $F_i^{(s)}$acting on the body B_s is given by

$$F_i^{(s)} = F_i^{(s,1)} + F_i^{(s,2)} + \cdots + F_i^{(s,n)}, \tag{2.55}$$

where $F_i^{(s,m)}$ is the force acting on the body B_s in the situation corresponding to $f^{(m)}$. The contribution from the f_0 term vanishes because f_0 is a uniform Maxwellian.

2.5.6 Simple applications

Reservoirs joined by various pipes

Equation (2.50) is an additional condition for the series (2.48) to be the solution in the case where the domain extends to infinity, and thus it limits the

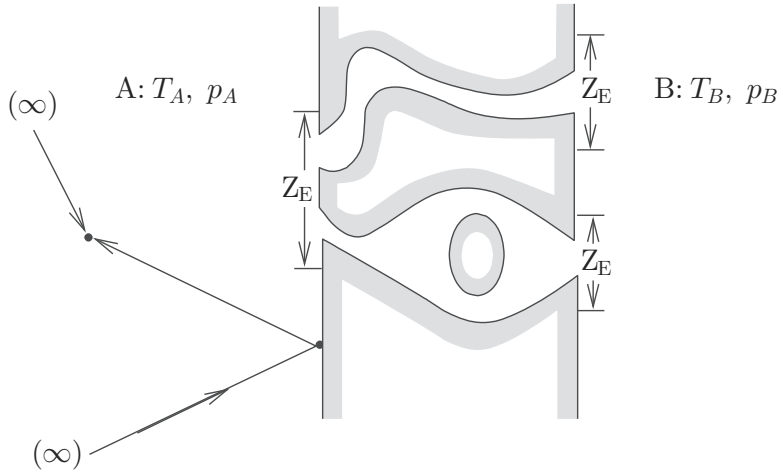

Figure 2.6. Two reservoirs joined by pipes. The reservoir A is in the equilibrium state at rest with temperature T_A and pressure p_A and the reservoir B is in the equilibrium state at rest with temperature T_B and pressure p_B. They are joined by various pipes. The temperature of the wall of reservoir A is T_A and that of the reservoir B is T_B except in a finite region Z_E in the neighborhood of the entrance of the pipes.

applicability of the solution. In return, from this restriction, we can derive the condition that keeps a gas at rest (or in a state without flow) between reservoirs with different temperatures. Two large reservoirs, one, say A, in the equilibrium state at rest with temperature T_A and pressure p_A and the other, say B, in the equilibrium state at rest with temperature T_B and pressure p_B, are joined by pipes (Fig. 2.6).[14] The temperature of the reservoir wall may differ from T_A on the side of the reservoir A or from T_B on the side of B in a finite region in the neighborhood of the entrance of the pipes. When the solution (2.48) is applicable, or the state of the gas at infinity is given by Eq. (2.50), no flow occurs in this system. In the present case, the velocity distribution function at infinity is compatible with Eq. (2.50), if $\beta_\infty = 1/2RT_A$ in A and $\beta_\infty = 1/2RT_B$ in B. Then, the pressure p_A in A and that p_B in B are given, respectively, by $\pi^{3/2}C\sqrt{RT_A/2}$ and $\pi^{3/2}C\sqrt{RT_B/2}$. Eliminating C from these relations, we obtain the condition under which no flow occurs between reservoirs A and B as follows:

$$\frac{p_A}{\sqrt{T_A}} = \frac{p_B}{\sqrt{T_B}}. \tag{2.56}$$

This relation applies irrespective of the condition of the pipes, i.e., the shape and number of the pipes or the distributions of temperature and accommodation coefficient along the pipes. The condition (2.56) is known for a long time for two

[14]The states at infinity of the reservoirs are easily seen to be the (full) Maxwellians in the case of Fig. 2.6, because the velocity distribution function of the molecules reflected on the plane wall outside Z_E region is the mirror image of that of the impinging molecules from infinity (see the discussion in the last paragraph of Section 2.1).

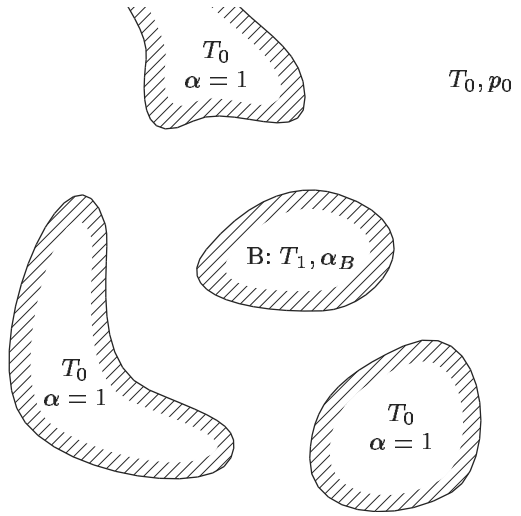

Figure 2.7. A convex body B coexisting with diffusely reflecting bodies.

special cases where the connection between the reservoirs is a slit or a straight pipe with specularly reflecting wall (see, for example, Section 2.3.2 and Kogan [1969]).

A convex body coexisting with diffusely reflecting bodies

A convex body, say, B, (temperature T_1, accommodation coefficient α_B; T_1 and α_B are constants) and several diffusely reflecting bodies (temperature T_0) lie in an infinite expanse of a uniform gas at rest with temperature T_0 and pressure p_0 (Fig. 2.7). The shapes, sizes, number, and arrangement of the bodies are arbitrary except that the body B is convex. For this situation, the solution is expressed by the series (2.48).

The velocity distribution function of the molecules leaving infinity is

$$f = C\mathfrak{M}_0, \tag{2.57a}$$

$$\mathfrak{M}_0 = \beta_0^2 \exp(-\beta_0 \xi^2), \quad \beta_0 = \frac{1}{2RT_0}, \quad C = 2\pi^{-3/2} p_0 (2RT_0)^{-1/2}. \tag{2.57b}$$

From Eq. (2.49), the velocity distribution of the molecules leaving the diffusely reflecting bodies is also given by Eq. (2.57a). Therefore, the velocity distribution of the molecules impinging on the body B is given by

$$f = C\mathfrak{M}_0 \qquad (l_i n_i < 0). \tag{2.58}$$

From Eq. (2.48), the velocity distribution function of the molecules leaving the

body B is given by

$$f = C[\alpha_B \mathfrak{M}_1 + (1-\alpha_B)\mathfrak{M}_0] \qquad (l_i n_i > 0), \tag{2.59a}$$

$$\mathfrak{M}_1 = \beta_1^2 \exp(-\beta_1 \xi^2), \qquad \beta_1 = 1/2RT_1. \tag{2.59b}$$

From Eqs. (2.58) and (2.59a), the force F_i acting on the body B and the energy ET leaving B per unit time are given as follows:

$$F_i = 0, \tag{2.60}$$

$$ET = \frac{p_0 (2RT_0)^{1/2}}{\sqrt{\pi}} \left(\frac{T_1}{T_0} - 1 \right) \alpha_B S_B, \tag{2.61}$$

where S_B is the surface area of the body B. The force (2.60) and the energy transfer (2.61) are independent of the shape of the body B and the shapes, sizes, arrangement, and number of the diffusely reflecting bodies.

2.5.7 Forces acting on heated bodies in a free molecular gas

A group of diffusely reflecting bodies

Consider a system where a group of bodies lie in an infinite expanse of a uniform stationary gas in equilibrium at temperature T_0 and pressure p_0. The gas molecules make the diffuse reflection on the bodies. Then the following propositions hold:

Proposition 2.1. *If all the bodies are heated (or cooled) at the same uniform temperature (say, T_1), neither force nor moment of force acts on the system of the bodies as a whole.*

Proof. First consider the case where the temperature of the bodies is the same as that of the gas, i.e., $T_1 = T_0$. Then, obviously, the gas is in the uniform equilibrium state at rest with temperature T_0 and pressure p_0, and neither force nor moment of force acts on each body. The force acting on a surface element $\mathrm{d}S$ of a body is

$$-p_{ij} n_j \mathrm{d}S = -p_0 n_i \mathrm{d}S,$$

which is the same as that due to static pressure. The contribution of the molecules ($\xi_k n_k < 0$) impinging on $\mathrm{d}S$ to the force is the same as that of the molecules ($\xi_k n_k > 0$) leaving $\mathrm{d}S$. That is,

$$-p_{ij} n_j (\xi_k n_k < 0)\mathrm{d}S = -\frac{1}{2} p_0 n_i \mathrm{d}S, \tag{2.62}$$

$$-p_{ij} n_j (\xi_k n_k > 0)\mathrm{d}S = -\frac{1}{2} p_0 n_i \mathrm{d}S. \tag{2.63}$$

The contribution of each of them to the force on the body as a whole, which is obtained by integrating it over the body, obviously vanishes. The same argument applies to the moment of force.

With this preparation, consider the case where the temperature T_1 of the bodies is different from that of the gas, i.e., $T_1 \neq T_0$. The velocity distribution of the molecules leaving $\mathrm{d}S$ being given by Eq. (2.49) with $C = 2\pi^{-3/2} p_0 (2RT_0)^{-1/2}$, their contribution to the force on it is given by

$$-p_{ij} n_j (\xi_k n_k > 0) \mathrm{d}S = -\frac{1}{2} p_0 n_i \left(\frac{T_1}{T_0}\right)^{1/2} \mathrm{d}S. \tag{2.64}$$

The contribution of this force to the force on the body as a whole obtained by integrating over the body also vanishes as that of Eq. (2.63). The contribution of the impinging molecules can be split into two parts, that of the molecules impinging from infinity and that from the bodies (the other part of the body and the other bodies). The former is the same as that of the case when $T_1 = T_0$. The latter contribution summed up over all the bodies is shown to vanish irrespective of the value of T_1 in the next paragraph. Therefore, the contribution of the impinging molecules is also the same as that when $T_1 = T_0$. Thus, neither force nor moment of force acts on the system.

Owing to Eq. (2.49), the contribution to the force on the surface element $\mathrm{d}S$ at X_i^B by the molecules impinging on $\mathrm{d}S$ from another surface element $\mathrm{d}S^{(1)}$ at $X_i^{(1)}$ on the bodies is given by

$$-C\left(\int_0^\infty \xi^4 \mathfrak{M}_1 \mathrm{d}\xi\right) \frac{l_i l_k n_k l_h n_h^{(1)} \mathrm{d}S^{(1)}}{(X_j^B - X_j^{(1)})^2} \mathrm{d}S = -\frac{3\sqrt{\pi} C l_i l_k n_k l_h n_h^{(1)} \beta_1^{-1/2} \mathrm{d}S^{(1)} \mathrm{d}S}{8(X_j^B - X_j^{(1)})^2}, \tag{2.65}$$

$$\mathfrak{M}_1 = \beta_1^2 \exp(-\beta_1 \xi^2), \quad \beta_1 = 1/2RT_1,$$

where l_i is the unit vector of the direction from $X_i^{(1)}$ to X_i^B, and n_i and $n_i^{(1)}$ are, respectively, unit normal vectors to $\mathrm{d}S$ and $\mathrm{d}S^{(1)}$ (Fig. 2.8); the line of force lies on the line defined by the points X_i^B and $X_i^{(1)}$. The contribution to the force on $\mathrm{d}S^{(1)}$ by the molecules impinging on $\mathrm{d}S^{(1)}$ from $\mathrm{d}S$ is, obviously from the symmetry, given by replacing l_i by $-l_i$ (see Fig. 2.8). Thus, the two contributions are equal in magnitude, opposite in direction, and on the same line of force. Summing up the contribution as the pair over all the bodies, the two contributions cancel out each other irrespective of the temperature T_1. ■

Corollary. *When the number of bodies is one, the body is subject to neither force nor moment of force.*

Corollary. *When the number of bodies is two, the force and the moment of force on a body and those on the other are equal in magnitude and opposite in direction.*

Proposition 2.2. *The temperature is uniform on each body, but it may differ depending on the bodies. Then, the force and the moment of force on a body in the system do not depend on its own temperature.*

Proof. Take a body (say, B_1), and examine the dependence of the force acting on B_1 on the temperature of B_1. The velocity distribution of the molecules leaving the surface element $\mathrm{d}S$ of B_1 is isotropic and independent of the position

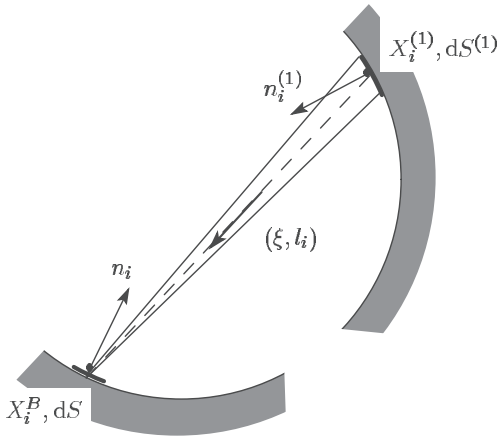

Figure 2.8. Reciprocity relation of the interaction between the surface elements $\mathrm{d}S$ and $\mathrm{d}S^{(1)}$.

on B_1. Therefore, the contributions of these molecules to the force and the moment of force on B_1 vanish, irrespective of the temperature of B_1. Among the molecules impinging on $\mathrm{d}S$ of B_1, only those that come from the other part of B_1 depend on the temperature of B_1. The contributions of those molecules to the force and the moment of force being calculated as the pair of $\mathrm{d}S$ and $\mathrm{d}S^{(1)}$ as was done in the proof in Proposition 2.1, they are found to vanish. Therefore, the force and the moment of force on B_1 are independent of the temperature of B_1. ■

Corollary. *When only one of the bodies has a temperature different from T_0, the body is subject to neither force nor moment of force.*

As examples of interaction force of a specific problem, simple formulas for two parallel cylinders and for two spheres are given here. Two parallel cylinders 1 and 2 (or spheres 1 and 2) lie in a uniform gas at rest with temperature T_0 and pressure p_0. The cylinder 1 (or sphere 1) has a uniform surface temperature T_1 and radius r_1, and the other T_2 and r_2. The distance between the axes (or centers) of the two cylinders (or spheres) is D. Then, cylinder 1 (per unit length) is subject to the force of the following magnitude F (including sign) in the direction from the axis of cylinder 2 to that of cylinder 1 and normal to the axes:

$$F = (4r_1r_2/\pi D)\, p_0(\sqrt{T_2/T_0} - 1). \tag{2.66}$$

Sphere 1 is subject to the force of the following magnitude F (including sign) in the direction from the center of sphere 2 to that of sphere 1:

$$F = (3\pi/4)(r_1r_2/D)^2 p_0(\sqrt{T_2/T_0} - 1). \tag{2.67}$$

The negative value of F in these formulas means that the direction of force is from cylinder 1 (sphere 1) to cylinder 2 (sphere 2).

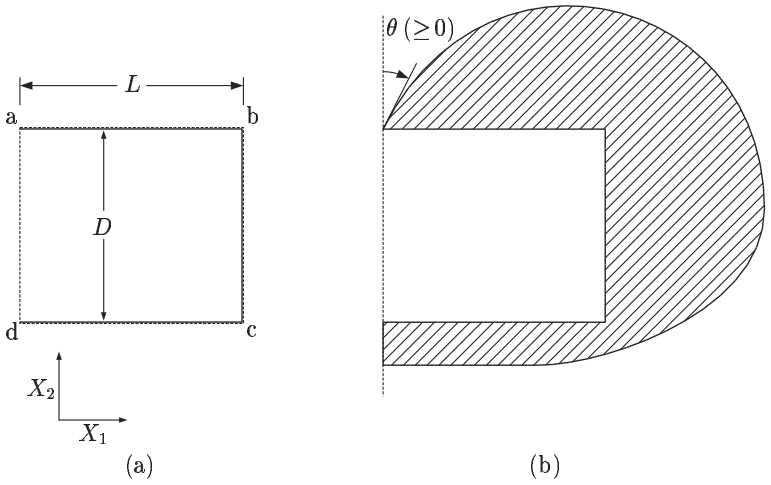

Figure 2.9. Propulsion force on a ⊔-shaped body I. (a) Heated ⊔-shaped body and (b) ⊔-shaped body with a convex outer cover. The dotted line abcda ····· in panel (a) is the control surface.

Various simple formulas are derived for the diffuse-reflection boundary condition. In the following examples, however, we will see that the forces on a body degenerate to vanish for the diffuse or specular-reflection condition. Thus, the result of a problem under the diffuse-reflection condition cannot be taken as the typical feature of the problem in a free molecular gas.

Propulsion force on a heated body

Consider a uniformly heated body with a uniform accommodation coefficient in a uniform gas at rest. If the body shape is convex, it is seen that neither force nor moment of force acts on the body (Section 2.5.6). We will show, with examples, that a uniformly heated body is subject to a force when it is not of a convex shape.

⊔-shaped body A ⊔-shaped two-dimensional body shown in Fig. 2.9 lies in a gas in the uniform equilibrium state at rest with pressure p_0 and temperature T_0. The temperature T_1 and accommodation coefficient α_1 of the body are both uniform.

The molecules impinging on the outer side of the body all come from infinity, and therefore their velocity distribution is

$$f = C\mathfrak{M}_0 \quad (l_i n_i < 0), \tag{2.68}$$
$$\mathfrak{M}_0 = \beta_0^2 \exp(-\beta_0 \xi^2), \quad \beta_0 = \frac{1}{2RT_0}, \quad C = 2\pi^{-3/2} p_0 (2RT_0)^{-1/2}.$$

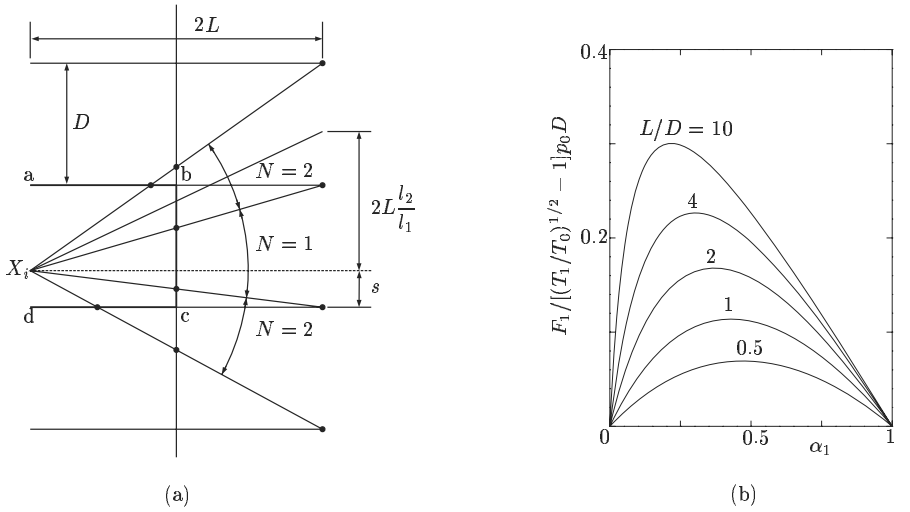

Figure 2.10. Propulsion force on ⊔-shaped body II. (a) The relation between N and l_2/l_1 and (b) the force acting on the heated ⊔-shaped body.

The velocity distribution of the molecules leaving the outer surface is

$$f = C[\alpha_1 \mathfrak{M}_1 + (1-\alpha_1)\mathfrak{M}_0] \qquad (l_i n_i > 0), \tag{2.69}$$
$$\mathfrak{M}_1 = \beta_1^2 \exp(-\beta_1 \xi^2), \qquad \beta_1 = \frac{1}{2RT_1}.$$

The molecules entering the mouth ad ($l_1 > 0$) all come from infinity. Thus,

$$f = C\mathfrak{M}_0 \quad (l_1 > 0) \quad \text{on ad.} \tag{2.70}$$

According to Eq. (2.48), the velocity distribution of the molecules going out from the mouth ad is given by

$$\begin{aligned} f &= C\{[1 + (1-\alpha_1) + \cdots + (1-\alpha_1)^{N-1}]\alpha_1 \mathfrak{M}_1 + (1-\alpha_1)^N \mathfrak{M}_0\} \\ &= C[\mathfrak{M}_1 + (1-\alpha_1)^N(\mathfrak{M}_0 - \mathfrak{M}_1)] \qquad (l_1 < 0) \quad \text{on ad,} \end{aligned} \tag{2.71}$$

where N is the positive integer that satisfies $|\boldsymbol{X}^{(N+1)}| = \infty$, that is, when we trace back the path of the specularly reflecting molecule with velocity ξl_i from the point X_i on the mouth ad, we reach infinity after N encounters on the inner wall of the body. The integer N is determined uniquely and simply by X_i and l_i with the aid of Fig. 2.10 (a). Figure 2.10 (a) shows the body abcd, its mirror images, and their successive images. The integer N is given as the number of intersection of the half-line from the point X_i in the direction of $-l_i$ with the body or the mirror images, because this line is made from the mirror images of the path of the specularly reflecting molecule. Simply from Fig. 2.10 (a), the

integer N is given by

$$\begin{aligned}(N-1)D \le 2Ll_2l_1^{-1} + s < ND \qquad & (l_2 \le 0),\\ -(N-1)D \le 2Ll_2l_1^{-1} + s < -(N-2)D \qquad & (l_2 \ge 0),\\ (N = 1, 2, 3, \ldots), & \end{aligned}$$

where s is the distance from X_i to the edge point d.

Taking the control surface abcda enclosing the body abcd, and calculating the momentum flow per unit time through it with the velocity distribution function obtained above, i.e., Eqs. (2.68)–(2.71), we obtain the force F_i acting on the ⊔-shaped body abcd per unit length in the X_3 direction as follows (Tanaka & Sone [1987]):

$$\frac{F_1}{\left[(T_1/T_0)^{1/2} - 1\right] p_0 D} = \begin{cases} \dfrac{\alpha_1^2(1-\alpha_1)}{\pi} \displaystyle\sum_{j=1}^{\infty} (1-\alpha_1)^{j-1} j \mathrm{Arctan}\left(\frac{2L}{jD}\right) \\ \qquad\qquad (\alpha_1 \ne 0), \\ 0 \qquad\qquad (\alpha_1 = 0), \end{cases}$$

$$F_2 = F_3 = 0.$$

The force F_1 vs α_1 for various L/D is shown in Fig. 2.10 (b).

The shape of the outer surface of the body is not important, if it is convex and cannot be seen from inside of the mouth ad, as shown in Fig. 2.9 (b). All the molecules impinging on the outer surface come from infinity, and their velocity distribution is given by Eq. (2.68); thus, the velocity distribution of the molecules leaving there is given by Eq. (2.69). These give a force normal to the surface element and uniform over the outer surface, and thus its integration over the outer surface is independent of its shape. For the above class of the outer surface, the molecules entering the mouth ad are not affected by the outer surface and all come from infinity as in the original ⊔-shaped body. Therefore, the force on the body is independent of its shape.

Let us consider the physical mechanism by which a propulsion force acts on a heated nonconvex body. The average of the kinetic energy of a molecule in a gas at rest is proportional to the temperature of the gas. Thus, the average speed of the molecules that have made the diffuse reflection on the heated body is faster than that of the molecules at infinity. Hereafter, for simplicity, we call them fast molecules. The molecules coming, from outside, to the control surface abcda enclosing the ⊔-shaped body are all from infinity in the uniform equilibrium state, and their momentum flow through the control surface is zero. According to the Maxwell-type boundary condition, the α_1 part of the molecules going out from the part ab, bc, and cd of the control surface are fast molecules. These are the molecules that have made the diffuse reflection on the body. The molecules that make the specular reflection keep their speed. Some of the molecules entering through the mouth ad collide with the inner surface of the body more than once before they go out through the mouth ad. When

molecules collide with the body, the fast molecules remain fast, but the α_1 part of the slow molecules become fast. Thus, the fast molecules increase at every collision. Therefore, more than the α_1 part of the molecules entering the mouth ad become fast when they go out there. Owing to the extra fast molecules, the momentum outflow through the control surface abcda by the molecules going out there has a $-X_1$ component. No momentum flow being carried by the incoming molecules, the above momentum outflow is the total momentum outflow from abcda by all the molecules passing the control surface. As its reaction, the body is subject to a force in the X_1 direction. For the specular reflection ($\alpha_1 = 0$), all the molecules are not subject to change of their speed by collision with the body, and the velocity distribution function is the uniform Maxwellian given by that at infinity; for the diffuse reflection ($\alpha_1 = 1$), all the molecules become fast by the first collision with the body, and thus there is no effect of multicollisions. Therefore, the force on the body vanishes in the two limiting cases.

Two other examples are given here.

V-shaped body Consider a uniformly heated V-shaped body with temperature T_1 and accommodation coefficient α_1 in a gas at temperature T_0 and pressure p_0 shown in Fig. 2.11 (a). The force F_i acting on the body per unit length in the X_3 direction is given as

$$\frac{F_1}{\left[(T_1/T_0)^{1/2} - 1\right] p_0 D} = \frac{\alpha_1}{4\pi} \left((2 - \alpha_1) \sum_{j=1}^{m} (1 - \alpha_1)^{j-1} (\pi - j\phi)(1 + \cos j\phi) \right.$$
$$\left. - \alpha_1 \cot \frac{\phi}{2} \sum_{j=1}^{m} (1 - \alpha_1)^{j-1} (\pi - j\phi) \sin j\phi \right),$$
$$F_2 = F_3 = 0,$$

where D and ϕ are, respectively, the width of the mouth and the opening angle of the two plates, and m is the maximum positive integer smaller than π/ϕ (Tanaka & Sone [1987]). The force F_1 vs α_1 for various ϕ is shown in Fig. 2.11 (b).

Cylindrical shell The force acting on a uniformly heated cylindrical shell [Fig. 2.12 (a)] is shown in Fig. 2.12 (b), where $F_i = (F_1, 0, 0)$ is the force on the shell per unit length in the X_3 direction, T_1, α_1, r, and θ are, respectively, the temperature, accommodation coefficient, radius, and opening angle of the cylindrical shell, and T_0 and p_0 are, respectively, the temperature and pressure of the gas at infinity (Aoki, Sone & Ohwada [1986]).

Heated body in a gas bounded by a plane wall

Consider a semi-infinite expanse of a uniform gas (pressure p_0 and temperature T_0) bounded by a plane wall W with temperature T_0 and accommodation coefficient α_w, which is also constant. A heated (or cooled) flat plate P (width L, length infinite, temperature T_1, and accommodation coefficient α_p; T_1 and α_p : constants) lies in the gas, parallel to the wall and at the distance D from the

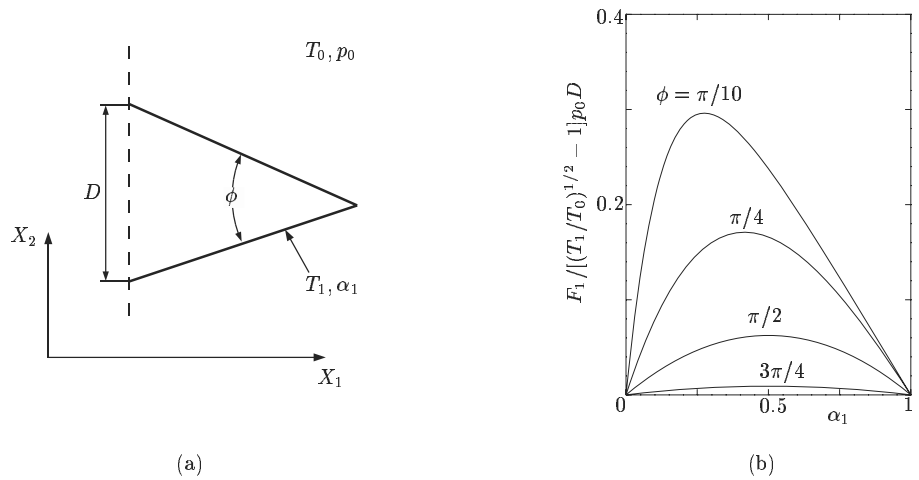

Figure 2.11. Heated V-shaped body and the force acting on it. (a) V-shaped body and (b) the force acting on it.

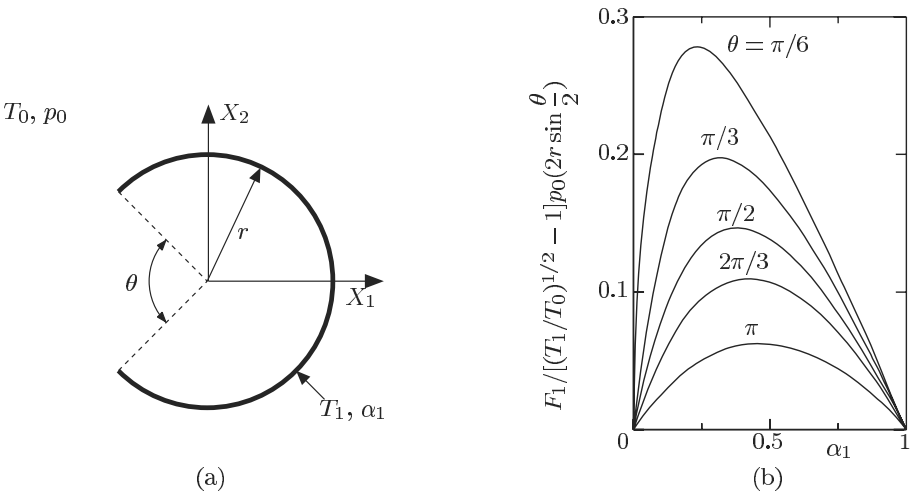

Figure 2.12. Cylindrical shell and the force acting on it. (a) Cylindrical shell and (b) the force acting on it.

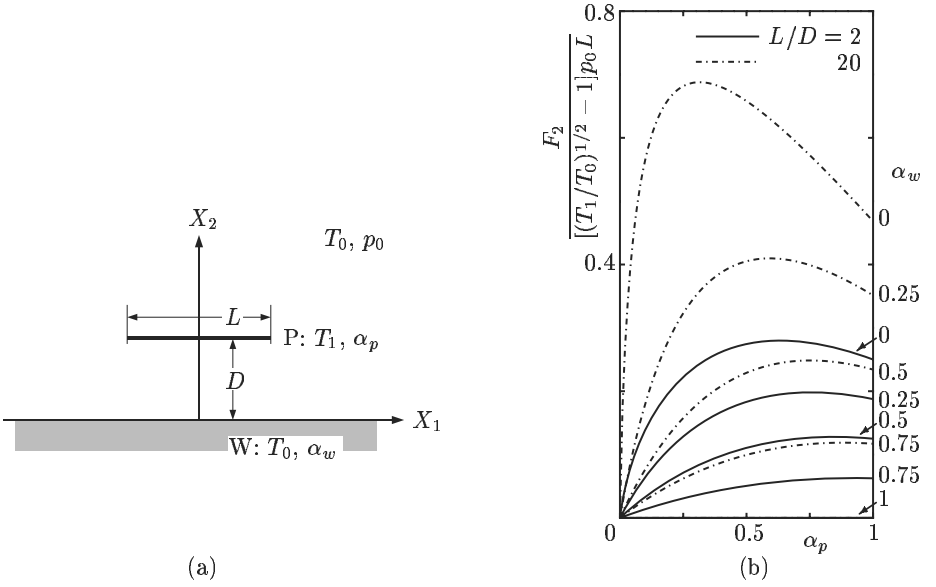

Figure 2.13. Flat plate in a gas bounded by a plane wall and the force acting on the plate. (a) A flat plate in a gas bounded by a plane wall and (b) the force acting on the plate.

wall [Fig. 2.13 (a)]. The force F_i acting on the plate per unit length in the X_3 direction is obtained analytically in the following form:

$$\frac{F_2}{\left[(T_1/T_0)^{1/2}-1\right]p_0L} = \begin{cases} \dfrac{\alpha_p(2-\alpha_p)(1-\alpha_w)}{\pi}\displaystyle\sum_{n=0}^{\infty} r^n \mathrm{Arctan}\frac{L}{2(n+1)D} \\ \qquad (\alpha_p \neq 0 \ \text{ or } \alpha_w \neq 0), \\ 0 \qquad (\alpha_p = \alpha_w = 0), \end{cases}$$

$$F_1 = F_3 = 0,$$

where

$$r = (1-\alpha_p)(1-\alpha_w),$$

and F_2 is the component normal to the plate in the direction from the wall to the plate. The force $F_2[(T_1/T_0)^{1/2}-1]^{-1}(p_0L)^{-1}$ vs α_p for $L/D = 2$ and $L/D = 20$ and for various α_w is shown in Fig. 2.13 (b).

When the plate is heated ($T_1 > T_0$), some of the fast molecules that have made diffuse reflection on the wall side of the plate P return to the plate after being reflected on the wall W. Those that have made specular reflection return with the same speed as before. These faster molecules give extra impulse to the wall side of the plate.

The analytical result when the plate is inclined is given in Sone & Tanaka [1986].

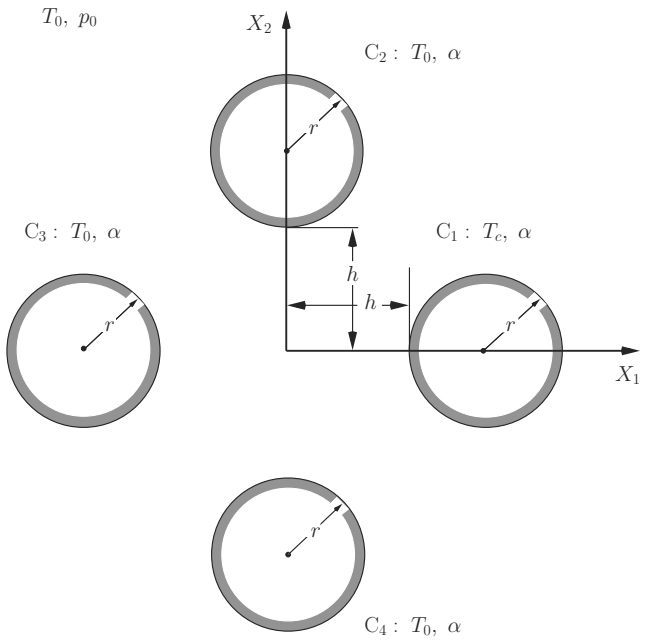

Figure 2.14. System of four cylinders.

Interaction force between heated bodies

Consider the system consisting of four cylinders shown in Fig. 2.14. The force (F_1, F_2) acting on each cylinder per its unit length is shown in Table 2.1 for the case where its temperature is shown in the figure (Aoki, Sone & Ohwada [1986]). In the table, $(\hat{F}_1, \hat{F}_2)$ is the nondimensional force defined by

$$(\hat{F}_1, \hat{F}_2) = \frac{(F_1, F_2)}{\left[(T_c/T_0)^{1/2} - 1\right] p_0 r}.$$

With the aid of the formula (2.55), the results for arbitrary combination of the temperatures of the cylinders can be obtained from the data in the table.

2.6 Effect of intermolecular collisions

Up to this point in the chapter, we have discussed the free molecular gas, where the intermolecular collisions are neglected. In this section, we will discuss the correction to the free molecular solution due to molecular collisions when the Knudsen number is large but finite.

The solution $\hat{f}$ of the Boltzmann equation (1.47a) for large Knudsen numbers (or $k \gg 1$) is looked for in a power series of k^{-1}, i.e.,

$$\hat{f} = \hat{f}_F + \frac{1}{k}\hat{f}_1 + \cdots, \tag{2.72}$$

Table 2.1. Forces acting on the four cylinders (see Fig. 2.14).

		$h/r = 0.8$		$h/r = 1.5$		$h/r = 2$	
	α	$\hat{F}_1$	$\hat{F}_2$	$\hat{F}_1$	$\hat{F}_2$	$\hat{F}_1$	$\hat{F}_2$
C_1	0.25	0.1249	0	0.0425	0	0.0257	0
	0.5	0.1215	0	0.0471	0	0.0294	0
	0.75	0.0707	0	0.0296	0	0.0190	0
	1	0	0	0	0	0	0
C_2	0.25	−0.1217	0.2141	−0.0819	0.1140	−0.0674	0.0872
	0.5	−0.2180	0.3016	−0.1513	0.1859	−0.1252	0.1473
	0.75	−0.2942	0.3404	−0.2088	0.2300	−0.1735	0.1875
	1	−0.3537	0.3537	−0.2547	0.2547	−0.2122	0.2122
C_3	0.25	−0.1955	0	−0.1089	0	−0.0842	0
	0.5	−0.2748	0	−0.1791	0	−0.1433	0
	0.75	−0.3150	0	−0.2249	0	−0.1845	0
	1	−0.3390	0	−0.2547	0	−0.2122	0

where $\hat{f}_F$ is the solution of the free molecular gas, i.e., $\partial \hat{f}_F/\partial \hat{t} + \zeta_i \partial \hat{f}_F/\partial x_i = 0$. Then, $\hat{f}_1$ is determined by the equation

$$\frac{\partial \hat{f}_1}{\partial \hat{t}} + \zeta_i \frac{\partial \hat{f}_1}{\partial x_i} = \hat{J}(\hat{f}_F, \hat{f}_F), \tag{2.73}$$

where the Strouhal number Sh is taken to be unity. Integrating along the characteristic ($x_i - \zeta_i \hat{t}$ =const) of Eq. (2.73), we have

$$\hat{f}_1(\boldsymbol{x}, \boldsymbol{\zeta}, \hat{t}) = \hat{f}_1(\boldsymbol{x} - \boldsymbol{\zeta}(\hat{t} - \hat{t}_0), \boldsymbol{\zeta}, \hat{t}_0) + \int_{\hat{t}_0}^{\hat{t}} \hat{J}(\hat{f}_F, \hat{f}_F)_{(\boldsymbol{x} - \boldsymbol{\zeta}(\hat{t}-\tau), \boldsymbol{\zeta}, \tau)} \mathrm{d}\tau, \tag{2.74}$$

where the subscript $(\boldsymbol{x} - \boldsymbol{\zeta}(\hat{t} - \tau), \boldsymbol{\zeta}, \tau)$ indicates that the standard argument $(\boldsymbol{x}, \boldsymbol{\zeta}, \tau)$ of $\hat{J}(\hat{f}_F, \hat{f}_F)$ is replaced by it, and $\hat{t}_0$ is given in the following way: Let $(\boldsymbol{x}, \boldsymbol{\zeta}, \hat{t})$ be given. If we trace back a particle with velocity $\boldsymbol{\zeta}$ from $(\boldsymbol{x}, \hat{t})$, we encounter some point on the boundary at some time $\hat{t}_B(\boldsymbol{x}, \boldsymbol{\zeta}, \hat{t})$ before the initial time $\hat{t} = 0$, or do not encounter any point on the boundary until the initial time.[15] We take $\hat{t}_0 = \hat{t}_B$ in the former case and $\hat{t}_0 = 0$ in the latter. In a time-independent case, the corresponding expression is

$$\hat{f}_1(\boldsymbol{x}, \boldsymbol{\zeta}) = \hat{f}_1(\boldsymbol{x} - s_B \boldsymbol{\zeta}/\zeta, \boldsymbol{\zeta}) + \int_0^{s_B} \frac{1}{\zeta} \hat{J}(\hat{f}_F, \hat{f}_F)_{(\boldsymbol{x} - s\boldsymbol{\zeta}/\zeta, \boldsymbol{\zeta})} \mathrm{d}s, \tag{2.75}$$

where the subscript $(\boldsymbol{x} - s\boldsymbol{\zeta}/\zeta, \boldsymbol{\zeta})$ indicates that the standard argument $(\boldsymbol{x}, \boldsymbol{\zeta})$ of $\hat{J}(\hat{f}_F, \hat{f}_F)$ is replaced by it, and s_B is the distance from $\boldsymbol{x}$ to the nearest

[15] In this process, no molecular collision is considered. That is, we trace back the characteristic of Eq. (2.73) (see, e.g., Courant & Hilbert [1961], Garabedian [1964], or Zachmanoglou & Thoe [1986] for the definition of the characteristic).

point on the boundary in the $-\boldsymbol{\zeta}$ direction. The first term on the right-hand side of Eq. (2.74) or (2.75) is the velocity distribution function in the initial or boundary condition. The integral equation for the velocity distribution function of the molecules impinging on (or the molecules leaving) the boundary is derived in the way that the corresponding equation in the free molecular gas is done (Sections 2.3.3 and 2.4); a new term determined by the free molecular solution $\hat{f}_F$ enters the equation as an inhomogeneous term.

There are some points to be discussed in this solution by simple perturbation. The integral in Eq. (2.75) obviously diverges as $\zeta \to 0$.[16] Thus, the velocity distribution function is *singular*, and therefore it deviates largely from the free molecular solution $\hat{f}_F$ for small ζ. This is because the free path for slow molecules is so small even for large Knudsen numbers that the collision effect is not negligible (the effective Knudsen number for slow molecules is not large but even small). The macroscopic variables, obtained by integrating the velocity distribution function over the molecular velocity $\boldsymbol{\zeta}$ space, are finite for s_B bounded or in bounded-domain problems, because three-dimensional integration of a function with the singularity ζ^{-1} over the space $\boldsymbol{\zeta}$ converges. The singularity in the velocity distribution function appears in the macroscopic variables as the singularity $x \ln x$ (x : the distance from the boundary) in a neighborhood of the boundary (Grad [1969], Sone [1964, 1965]).

The singular character of small effective Knudsen number for slow molecules spreads out over fast molecules in infinite-domain problems, where molecules travelling long distances have many chances of molecular collision. Consider a time-independent solution in an infinite domain. Unless the gas is in an equilibrium state [$\hat{J}(\hat{f}_F, \hat{f}_F) \neq 0$] at infinity, the integral in Eq. (2.75) diverges for $\boldsymbol{x}$ and $\boldsymbol{\zeta}$ for which $s_B = \infty$. Thus, the free molecular solution $\hat{f}_F$ is not taken as the zeroth-order solution, however large the Knudsen number may be. This situation occurs when we consider the case where the bodies in the gas extend up to infinity, for example, in a half-space problem.[17] Next, consider the case where the gas is in a uniform equilibrium state (say, $\hat{f}_{F\infty}$) at infinity and bodies are arranged in a bounded region. Then, $\hat{f}_F$ at an arbitrary point deviates from $\hat{f}_{F\infty}$ only for the molecules coming from the body region, which is only within the solid angle viewing the bodies. This solid angle vanishes with distance from the bodies as $(x_1^2 + x_2^2)^{-1/2}$ in the two-dimensional problem[18] and as $(x_1^2 + x_2^2 + x_3^2)^{-1}$ in the three-dimensional case, and therefore, the moment of the difference $\hat{f}_F - \hat{f}_{F\infty}$ with respect to $\boldsymbol{\zeta}$ decays similarly. The collision integral $\hat{J}(\hat{f}_F, \hat{f}_F)$ in the integral in Eq. (2.75) has both features of $\hat{f}_F - \hat{f}_{F\infty}$ and its moment, i.e., a finite difference within a small limited range of the

[16] When the time-independent solution is derived from Eq. (2.74), we have to trace back until the particle reaches the boundary without limiting $\hat{t}_0$ at $\hat{t}_0 = 0$. The integral diverges as $\zeta \to 0$, because $\hat{t}_0 \to -\infty$ as $\zeta \to 0$, if $\boldsymbol{x}$ is not on the boundary. Incidentally, the integral in Eq. (2.74) diverges as $\hat{t} \to \infty$. Thus, the solution is, naturally, well described by the perturbation only for a finite time.

[17] Its examples are given in the last paragraph but one of Section 2.3.3.

[18] In the two-dimensional problem, the bodies lie in a bounded region in the two-dimensional space (x_1, x_2). They extend up to infinity in the x_3 direction.

direction of $\boldsymbol{\zeta}$ and the small difference of integrated quantities.[19] The perturbations of macroscopic variables, corresponding to $\hat{f}_1$, are obtained by integrating $\hat{J}(\hat{f}_F, \hat{f}_F)$ over the whole molecular velocity space and along the characteristic. In the two-dimensional case, the integration of $\hat{J}(\hat{f}_F, \hat{f}_F)$ over the molecular velocity space vanishes as $(x_1^2 + x_2^2)^{-1/2}$ with the increase of $(x_1^2 + x_2^2)^{1/2}$, and therefore its integration along the characteristic diverges, and so do the perturbations of macroscopic variables. On the other hand, the integral converges in the three-dimensional case.

In the above discussion, the effect of molecular collisions is evaluated by the first collisions using the free molecular velocity distribution. In an infinite-domain problem, however, a molecule makes many collisions while travelling an infinite distance from a boundary point to another (i.e., from a body to infinity, from infinity to a body, and from infinity to infinity). The effect should be more carefully evaluated using the velocity distribution function affected by the previous collisions. The perturbation in the two-dimensional case may really diverge or may converge depending on situations. The divergence means that the perturbation, if it is finite, is larger than the order of k^{-1}. In fact, it is $k^{-1} \ln k$ term. We will show this under the assumption that the solution is expressed by a perturbation, i.e., $\hat{f} = \hat{f}_F + \hat{f}_1$, where $\hat{f}_1 \to 0$ as $k \to \infty$.

Take Eq. (1.47a), without $\partial/\partial\hat{t}$, that is rewritten in the form (A.166)

$$\zeta_i \frac{\partial \hat{f}}{\partial x_i} + \frac{\hat{\nu}_c}{k} \hat{f} = \frac{1}{k} \hat{J}_G, \tag{2.76}$$

where $\hat{\nu}_c$ and $\hat{J}_G$ are, respectively, the corresponding nondimensional forms of ν_c and J_G [Eqs. (1.50)–(1.51b)]. Here, we evaluate $\hat{\nu}_c$ and $\hat{J}_G$ using $\hat{f}_F$ for $\hat{f}$ and denote them by $\hat{\nu}_F$ and $\hat{J}_G^F$, respectively. The leading equation for $\hat{f}$ is given by

$$\zeta_i \frac{\partial \hat{f}}{\partial x_i} + \frac{\hat{\nu}_F}{k} \hat{f} = \frac{1}{k} \hat{J}_G^F. \tag{2.77}$$

Let $\boldsymbol{x}$ and $\boldsymbol{\zeta}$ be, respectively, the position and the molecular velocity under consideration. The velocity distribution function $\hat{f}$ at $(\boldsymbol{x}, \boldsymbol{\zeta})$ is obtained by integrating Eq. (2.77) along its characteristic $\boldsymbol{x} - s\boldsymbol{\zeta}/\zeta$. Let s_B, finite or infinite, be the distance from the point $\boldsymbol{x}$ under consideration to the nearest boundary point in the direction of $-\boldsymbol{\zeta}/\zeta$ and $\hat{f}_{sB}$ be $\hat{f}$ at that point. The velocity distribution function $\hat{f}$ is expressed in the following form depending on whether s_B is finite or infinite:

$$\hat{f}(\boldsymbol{x}, \boldsymbol{\zeta}) = \hat{f}_{sB} \exp(-t_B/k\zeta) + \frac{1}{k\zeta} \int_0^{t_B} \hat{J}_G^F(\boldsymbol{x} - s\boldsymbol{\zeta}/\zeta, \boldsymbol{\zeta}) \frac{1}{\hat{\nu}_F} \exp(-t/k\zeta) \mathrm{d}t \quad \text{for finite } s_B, \tag{2.78a}$$

$$\hat{f}(\boldsymbol{x}, \boldsymbol{\zeta}) = \frac{1}{k\zeta} \int_0^{\infty} \hat{J}_G^F(\boldsymbol{x} - s\boldsymbol{\zeta}/\zeta, \boldsymbol{\zeta}) \frac{1}{\hat{\nu}_F} \exp(-t/k\zeta) \mathrm{d}t \quad \text{for infinite } s_B, \tag{2.78b}$$

[19] The former character comes from the loss term $\hat{J}_L$. Confirmation of the moment character of the gain term $\hat{J}_G$ requires the discussion taking into account the relation between $(\boldsymbol{\zeta}, \boldsymbol{\zeta}_*)$ and $(\boldsymbol{\zeta}', \boldsymbol{\zeta}_*')$ [see Eq. (1.48f) or more detailed explanation in Section A.2.1].

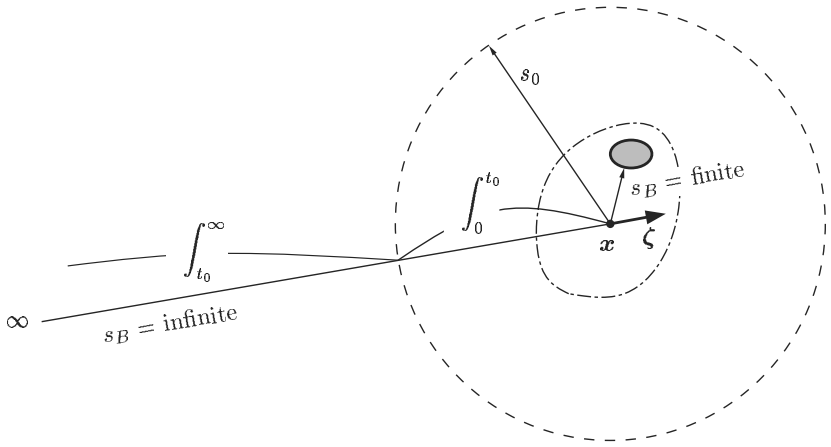

Figure 2.15. Diagram of the situation where the effect of intermolecular collisions is estimated. The point $\boldsymbol{x}$ under consideration and the bodies are confined in the bounded region surrounded by the dot-dash line. The circle of radius s_0 shown by the dashed line is taken much larger than the region surrounded by the dot-dash line. The shaded region is a body, where s_B is finite. The integrals $\int_0^{t_0}$ and $\int_{t_0}^{\infty}$ correspond, respectively, to the first and second terms after the second equality of Eq. (2.80).

where the arguments of $\hat{\nu}_F$ in the above integrals are the same as those of $\hat{J}_G^F$, that is, $\hat{\nu}_F(\boldsymbol{x} - s\boldsymbol{\zeta}/\zeta, \boldsymbol{\zeta})$, and

$$t = \int_0^s \hat{\nu}_F(\boldsymbol{x} - s\boldsymbol{\zeta}/\zeta, \boldsymbol{\zeta})\mathrm{d}s, \quad t_B = \int_0^{s_B} \hat{\nu}_F(\boldsymbol{x} - s\boldsymbol{\zeta}/\zeta, \boldsymbol{\zeta})\mathrm{d}s. \tag{2.79}$$

Now, take a point $\boldsymbol{x}$ in a finite region of the gas. All the bodies are within a finite distance from $\boldsymbol{x}$ by assumption.[20] The "finite" in the nondimensional space variable means that size of the domain in which the point $\boldsymbol{x}$ under consideration and the bodies lie is of the order of the reference length L in Eq. (1.43), on which the Knudsen number Kn or k is based. Let s_0 be such a distance from the point $\boldsymbol{x}$ under consideration that all the bodies are well inside the sphere with its center $\boldsymbol{x}$ and radius s_0. This situation is depicted in Fig. 2.15.

For $s_B = \infty$, the integral is divided into the two ranges $(0, t_0)$ and (t_0, ∞), i.e.,

$$\begin{aligned} \hat{f}(\boldsymbol{x}, \boldsymbol{\zeta}) &= \frac{1}{k\zeta} \int_0^{\infty} \hat{J}_G^F(\boldsymbol{x} - s\boldsymbol{\zeta}/\zeta, \boldsymbol{\zeta}) \frac{1}{\hat{\nu}_F} \exp(-t/k\zeta)\mathrm{d}t \\ &= \frac{1}{k\zeta} \int_0^{t_0} + \frac{1}{k\zeta} \int_{t_0}^{\infty} \qquad \text{for infinite } s_B, \end{aligned} \tag{2.80}$$

where t_0 is the value of t that corresponds to s_0, i.e., $t_0 = t(s_0)$. The first term

[20] See Footnote 18 in this section.

(say, I) in the last expression of Eq. (2.80) is bounded as

$$I = \frac{1}{k\zeta}\int_0^{t_0} = O\left(\frac{1}{k\zeta}\right).$$

For evaluation of the second term (say II), the estimate of the integrand is required. We are considering the case where $\hat{J}(\hat{f}_F, \hat{f}_F) = 0$ at infinity, and therefore,

$$\hat{J}^F_{G\infty} = \hat{\nu}_{F\infty}\hat{f}_\infty.$$

From the behavior of $\hat{f}_F$ for large s, explained in the fourth paragraph in this section, we see that $\hat{J}^F_G$, whose character is similar to the moment of $\hat{f}_F$ with respect to $\boldsymbol{\zeta}$,[21] approaches $\hat{J}^F_{G\infty}$(or $\hat{\nu}_{F\infty}\hat{f}_\infty$) with speed s^{-1} when $s \to \infty$. Thus, it is expressed as

$$\left.\begin{aligned} &\hat{J}^F_G(\boldsymbol{x} - s\boldsymbol{\zeta}/\zeta, \boldsymbol{\zeta}) = \hat{\nu}_{F\infty}\hat{f}_\infty + \frac{\hat{A}_1}{s} + \mathrm{Res}(\hat{J}^F_G), \\ &|\mathrm{Res}(\hat{J}^F_G)| < \frac{C_G}{s^m} \quad (m > 1), \end{aligned}\right\} \tag{2.81a}$$

where $\hat{A}_1$ is noted to depend on $\boldsymbol{\zeta}$ but to be independent of $\boldsymbol{x}$. Similarly,

$$\left.\begin{aligned} &\hat{\nu}_F = \hat{\nu}_{F\infty}[1 + \mathrm{Res}(\hat{\nu}_F)], \quad t = \hat{\nu}_{F\infty}s[1 + \mathrm{Res}(t)], \\ &|\mathrm{Res}(\hat{\nu}_F)| \le C_\nu s^{-1}, \quad |\mathrm{Res}(t)| \le C_t s^{-1}\ln s. \end{aligned}\right\} \tag{2.81b}$$

With this expression in the second term of Eq. (2.80),

$$\begin{aligned} II = &\int_{t_0}^\infty \hat{\nu}_{F\infty}\hat{f}_\infty \frac{\exp(-t/k\zeta)}{k\zeta\hat{\nu}_F}\mathrm{d}t \; + \int_{t_0}^\infty \frac{\hat{A}_1}{t}\frac{\exp(-t/k\zeta)}{k\zeta}\mathrm{d}t \\ &+ \int_{t_0}^\infty \left(\mathrm{Res}(\hat{J}^F_G) + \frac{\hat{\nu}_{F\infty}\hat{A}_1}{t}[\mathrm{Res}(t) - \mathrm{Res}(\hat{\nu}_F)]\right)\frac{\exp(-t/k\zeta)}{\hat{\nu}_F k\zeta}\mathrm{d}t. \end{aligned}$$

The last term II_3 of II is simply estimated as

$$|II_3| \le \frac{1}{k\zeta}\int_{t_0}^\infty \left|\mathrm{Res}(\hat{J}^F_G) + \frac{\hat{\nu}_{F\infty}\hat{A}_1}{t}[\mathrm{Res}(t) - \mathrm{Res}(\hat{\nu}_F)]\right| \frac{1}{\hat{\nu}_F}\mathrm{d}t = O\left(\frac{1}{k\zeta}\right).$$

The first term II_1 and the second term II_2 of II are evaluated as

$$\begin{aligned} II_1 &= \hat{f}_\infty[1 + O(1/k\zeta)], \\ II_2 &= \frac{1}{k\zeta}\int_{t_0/k\zeta}^\infty \frac{\hat{A}_1}{x}\exp(-x)\mathrm{d}x = \frac{\hat{A}_1}{k\zeta}\ln\frac{k\zeta}{t_0} + O\left(\frac{1}{k\zeta}\right) \\ &= \frac{\hat{A}_1}{k\zeta}\ln k\zeta + O\left(\frac{1}{k\zeta}\right). \end{aligned}$$

[21] See Footnote 19 in this section.

Combining the results for I and II, we have

$$\hat{f}(\boldsymbol{x},\boldsymbol{\zeta}) = \hat{f}_\infty + \frac{\hat{A}_1}{k\zeta}\ln k\zeta + O\left(\frac{1}{k\zeta}\right)$$
$$= \hat{f}_F(\boldsymbol{x},\boldsymbol{\zeta}) + \frac{\hat{A}_1}{k\zeta}\ln k\zeta + O\left(\frac{1}{k\zeta}\right) \qquad \text{for infinite } s_B, \tag{2.82}$$

where the last relation holds because $\hat{f}_F(\boldsymbol{x},\boldsymbol{\zeta}) = \hat{f}_\infty$ for the present direction of $\boldsymbol{\zeta}$, for which the characteristic extends to infinity. The $k^{-1}\ln k$ term is independent of the position $\boldsymbol{x}$, if it is finite. This does not mean that the velocity distribution function $\hat{f}$ is independent of $\boldsymbol{x}$, because the direction for which we can see infinity depends on $\boldsymbol{x}$.

For $\boldsymbol{\zeta}$ for which s_B is finite, each term of $\hat{f}$, given by Eq. (2.78a), is estimated as

$$\hat{f}_{sB}\exp(-t_B/k\zeta) = \hat{f}_{sB} + O(1/k\zeta),$$
$$\frac{1}{k\zeta}\int_0^{t_B} \hat{J}_G^F(\boldsymbol{x} - s\boldsymbol{\zeta}/\zeta,\boldsymbol{\zeta})\frac{1}{\hat{\nu}_F}\exp(-t/k\zeta)\mathrm{d}t = O\left(\frac{1}{k\zeta}\right).$$

In view of the estimate (2.82) of $\hat{f}$ for infinite s_B, the boundary data $\hat{f}_{sB}$ is consistently taken to be[22]

$$\hat{f}_{sB} = \hat{f}_{FsB} + O((k\zeta)^{-1}\ln k\zeta).$$

Therefore,

$$\hat{f}(\boldsymbol{x},\boldsymbol{\zeta}) = \hat{f}_{FsB} + O\left(\frac{\ln k\zeta}{k\zeta}\right) = \hat{f}_F + O\left(\frac{\ln k\zeta}{k\zeta}\right) \quad \text{for finite } s_B, \tag{2.83}$$

where $\hat{f}_{FsB}$ is the value of $\hat{f}_F$ at the point s_B, which is equal to $\hat{f}_F$ at the point under consideration.

The above estimate of $\hat{f}$ is based on Eq. (2.77) or Eqs. (2.78a) and (2.78b), where the exact $\hat{J}_G$ and $\hat{\nu}_c$ are replaced by $\hat{J}_G^F$ and $\hat{\nu}_F$ respectively. If the difference between $\hat{f}$ and $\hat{f}_F$ is of the order of $k^{-1}\ln k$, so are the differences between $\hat{J}_G$ and $\hat{J}_G^F$ and between $\hat{\nu}_c$ and $\hat{\nu}_F$. Then, the contribution of these differences when we replace $\hat{J}_G^F$ and $\hat{\nu}_F$ by $\hat{J}_G$ and $\hat{\nu}_c$ in Eqs. (2.78a) and (2.78b) does not require the correction to Eqs. (2.82) and (2.83).[23]

[22]The $\hat{f}_{sB}$ is determined by $\hat{f}$ for s_B finite and infinite. The above is an estimate by consistency. Consider the case of the diffuse-reflection condition for simplicity.

[23]Rigorously, the integral

$$\int_0^\infty \hat{J}_G^1(\boldsymbol{x} - s\boldsymbol{\zeta}/\zeta,\boldsymbol{\zeta})\frac{1}{\hat{\nu}_F}\exp(-t/k\zeta)\mathrm{d}t,$$

where $\hat{J}_G^1 = \hat{J}_G(\hat{f}_F,\hat{f}_1)$, of the correction $\hat{f}_1$ of the order of $k^{-1}\ln k$ is to be shown to be $o(\ln k)$. For this, $\hat{f}_1$ for large $|\boldsymbol{x}|$ or as $|\boldsymbol{x}| \to \infty$ is to be estimated to decay fast enough as $|\boldsymbol{x}| \to \infty$ with the aid of Eqs. (2.78a) and (2.78b).

Now we find that the leading correction to the free molecular solution $\hat{f}_F$ at a point in a finite region is of the order of $k^{-1}\ln k$ and that it is independent of s_0. The macroscopic variables, given by the moments of $\hat{f}$, have the correction term $O(k^{-1}\ln k)$. Hasegawa & Sone [1991a] considered the flow through a slit induced by the pressure difference between the two regions separated by the slit wall. On the slit, all the molecules come from infinity, and therefore the correction of the macroscopic variables of the order of $k^{-1}\ln k$ is independent of the position on the slit.[24]

Let us take simple model examples that well explain the structure of the nearly free molecular solutions for three different cases discussed above.

Model 1. Consider the following simple ordinary differential equation in the semi-infinite domain $0 < x < \infty$:

$$\frac{\mathrm{d}y}{\mathrm{d}x} - \varepsilon a y = \varepsilon, \tag{2.84}$$

where ε is a small parameter and a is a positive constant of the order of unity. We examine the solution y that tends to zero as $x \to \infty$. The inhomogeneous term does not vanish as $x \to \infty$, and the equation does not have a solution that vanishes as $x \to \infty$. ■

Model 2. Consider the equation where the inhomogeneous term of Eq. (2.84) is replaced by $\varepsilon/(1+x)$, i.e.,

$$\frac{\mathrm{d}y}{\mathrm{d}x} - \varepsilon a y = \frac{\varepsilon}{1+x}. \tag{2.85}$$

We examine the solution y that tends to zero as $x \to \infty$. The solution for $\varepsilon = 0$ is obviously $y = 0$. First try to solve the problem in terms of a simple power-series expansion in ε, i.e.,

$$y = y_0 + \varepsilon y_1 + \cdots .$$

Substituting this form into Eq. (2.85), we have

$$y_0 = 0, \qquad \frac{\mathrm{d}y_1}{\mathrm{d}x} = \frac{1}{1+x}.$$

Thus, we cannot have the solution y_1 that vanishes at infinity. The perturbation analysis fails.

On the other hand, Eq. (2.85) has the exact solution of the form

$$y = -\varepsilon \int_0^\infty \frac{\exp(-\varepsilon a s)}{1+x+s}\mathrm{d}s, \tag{2.86}$$

which vanishes as $x \to \infty$. We will examine the correction to $y_0(=0)$ for small ε on the basis of this exact solution. Split the range of integration into two parts, $0 < s \le 1+x$ and $1+x < s < \infty$:

$$\int_0^\infty \frac{\exp(-\varepsilon a s)}{1+x+s}\mathrm{d}s = \int_0^{1+x} \frac{\exp(-\varepsilon a s)}{1+x+s}\mathrm{d}s + \int_{1+x}^\infty \frac{\exp(-\varepsilon a s)}{1+x+s}\mathrm{d}s. \tag{2.87}$$

[24] See preceding Footnote 23.

Each term is estimated or transformed as

$$0 < \int_0^{1+x} \frac{\exp(-\varepsilon as)}{1+x+s}\mathrm{d}s < \int_0^{1+x} \frac{1}{1+x}\mathrm{d}s = 1, \tag{2.88}$$

and

$$\int_{1+x}^{\infty} \frac{\exp(-\varepsilon as)}{1+x+s}\mathrm{d}s = \int_{1+x}^{\infty} \frac{\exp(-\varepsilon as)}{s}\mathrm{d}s - (1+x)\int_{1+x}^{\infty} \frac{\exp(-\varepsilon as)}{(1+x+s)s}\mathrm{d}s. \tag{2.89}$$

The second term of Eq. (2.89) is bounded by unity, i.e.,

$$(1+x)\int_{1+x}^{\infty} \frac{\exp(-\varepsilon as)}{(1+x+s)s}\mathrm{d}s < (1+x)\int_{1+x}^{\infty} \frac{1}{s^2}\mathrm{d}s = 1. \tag{2.90}$$

The first term of Eq. (2.89) is transformed by putting $t = \varepsilon as$ as

$$\begin{aligned}\int_{1+x}^{\infty} \frac{\exp(-\varepsilon as)}{s}\mathrm{d}s &= \int_{\varepsilon a(1+x)}^{\infty} \frac{\exp(-t)}{t}\mathrm{d}t \\ &= -\exp[-\varepsilon a(1+x)]\ln[\varepsilon a(1+x)] + \int_{\varepsilon a(1+x)}^{\infty} \ln t \exp(-t)\mathrm{d}t.\end{aligned} \tag{2.91}$$

The second term of the last expression is bounded by a constant as

$$\left|\int_{\varepsilon a(1+x)}^{\infty} \ln t \exp(-t)\mathrm{d}t\right| < \int_0^{\infty} |\ln t \exp(-t)|\mathrm{d}t,$$

and the leading term for small ε of the first term $-\exp[-\varepsilon a(1+x)]\ln[\varepsilon a(1+x)]$ is $-\ln\varepsilon$ for a finite value of x.

With these estimates, we find that the leading correction to $y_0(=0)$ is $\varepsilon\ln\varepsilon$, which is independent of a. ■

Model 3. Consider the equation where the inhomogeneous term of Eq. (2.84) is replaced by $\varepsilon/(1+x)^2$, i.e.,

$$\frac{\mathrm{d}y}{\mathrm{d}x} - \varepsilon a y = \frac{\varepsilon}{(1+x)^2}. \tag{2.92}$$

Here the inhomogeneous term decays faster than that of Eq. (2.85) as $x \to \infty$. The solution y that tends to zero as $x \to \infty$ is given by

$$\begin{aligned} y &= -\varepsilon\int_0^{\infty} \frac{\exp(-\varepsilon as)}{(1+x+s)^2}\mathrm{d}s \\ &= \frac{-\varepsilon}{1+x} + \varepsilon^2 a\int_0^{\infty} \frac{\exp(-\varepsilon as)}{1+x+s}\mathrm{d}s, \end{aligned} \tag{2.93}$$

where the integral in the second term in the last expression is the same as that in the solution (2.86) of Eq. (2.85). Therefore, the leading correction is $-\varepsilon/(1+x)$,

and $-a\varepsilon^2 \ln \varepsilon$ appears before the ε^2-order term. The leading correction can be obtained by a simple expansion in a power series of ε, and a logarithmic term appears in the next order and depends on a. ■

The set of three simple ordinary differential equations, Eqs. (2.84), (2.85), and (2.92), whose homogeneous parts are common, has a qualitative similarity to Eq. (2.77) by the following correspondence:

$$y \Longleftrightarrow \hat{f}, \quad \frac{\mathrm{d}y}{\mathrm{d}x} \Longleftrightarrow -\frac{\zeta_i}{\zeta}\frac{\partial \hat{f}}{\partial x_i} = \frac{\partial \hat{f}}{\partial s} \text{ (i.e., } x \Longleftrightarrow s), \quad a \Longleftrightarrow \frac{\hat{\nu}_F}{\zeta},$$
$$\varepsilon \Longleftrightarrow 1/k, \quad \text{[the inhomogeneous term]} \Longleftrightarrow -\hat{J}^F_G/\zeta, \quad 0 \Longleftrightarrow \hat{f}_\infty,$$

where [the inhomogeneous term] is 1 in Model 1, $1/(1+x)$ in Model 2, and $1/(1+x)^2$ in Model 3. Model 1 corresponds to the case $\hat{J}(\hat{f}_F, \hat{f}_F) \neq 0$ at infinity, Model 2 to the two-dimensional case, and Model 3 to the three-dimensional case. From the solutions of the model equations, we can understand the behavior (or singularity) of the nearly free molecular solutions.

Chapter 3

Slightly Rarefied Gas: Asymptotic Theory of the Boltzmann System for Small Knudsen Numbers

When the mean free time and the mean free path of the gas molecules become smaller, the contribution of the collision term in the Boltzmann equation becomes larger, and the velocity distribution function will approach a local Maxwellian. Then, the behavior of the gas may be considered to admit a macroscopic description, because the distribution function is determined by the five macroscopic variables. In fact, the asymptotic theory of the Boltzmann system for small mean free time and small mean free path is developed for an initial-value problem (Grad [1963a]) and for time-independent boundary-value problems in arbitrary domains (see Sone [2002]). According to it, the overall behavior of the gas is described by fluid-dynamic-type equations with initial conditions or boundary conditions given by prescribed formulas. The corrections to the overall solution are required in a thin layer near the initial state or the boundary (or initial or Knudsen layer) and in a shock layer. The correction formulas are established.

In this chapter we first consider the time-independent boundary-value problem of the Boltzmann equation in an arbitrary domain except that the shape of the boundary is smooth, and investigate the asymptotic behavior of the solution for small Knudsen numbers. Besides the fundamental formulas mentioned above, e.g., fluid-dynamic-type equations and their associated boundary conditions where the effect of gas rarefaction is taken into account, what is specially to be mentioned here is that there are important classes of problems where the classical fluid dynamics is incomplete in describing the behavior of a gas

in the continuum limit.[1] Then we extend the asymptotic analysis to the time-dependent problem. In this chapter, except Section 3.3, we consider the case where the external force is absent. The results presented here are not complicated, but the analysis requires a lengthy manipulation, and the comprehensive discussion of the time-independent problem is given in the monograph Sone [2002]. Thus, the description of the analysis is intended not to be too complicated, and only its outline is given; the details are left to the monograph.

3.1 Linear problem

3.1.1 Problem

First, we consider the case where the behavior of the gas deviates only slightly from a uniform equilibrium state at rest, and develop the asymptotic theory on the basis of the linearized Boltzmann equation (1.96). The basic equation is

$$\zeta_i \frac{\partial \phi}{\partial x_i} = \frac{1}{k}\mathcal{L}(\phi). \tag{3.1}$$

The boundary condition [Eq. (1.107) or (1.112)] is here expressed in an abstract form

$$\phi = \phi_w \quad (\zeta_i n_i > 0), \tag{3.2}$$

on the boundary, where ϕ_w may depend on ϕ ($\zeta_i n_i < 0$) linearly.[2]

We will investigate the asymptotic behavior of ϕ for small k. The method of analysis is due to Sone [1969, 1971]. The notation defined by Eq. (1.74) is used in this section (Section 3.1). The fundamental linearized relations are listed in Section 1.11.

3.1.2 Grad–Hilbert expansion and fluid-dynamic-type equations

Putting aside the boundary condition, we look for a moderately varying solution of Eq. (3.1), whose length scale of variation is of the order of the characteristic length L of the system [or $\partial\phi/\partial x_i = O(\phi)$], in a power series of k, i.e.,

$$\phi_G = \phi_{G0} + \phi_{G1}k + \phi_{G2}k^2 + \cdots, \tag{3.3}$$

[1] The "continuum limit" means the limit that the mean free time and the mean free path both tend to zero. There is confusion in some textbooks of classical gas dynamics, where the motion of a gas in the continuum limit is discussed. They confuse the gas under their discussion with a wider class of a gas treated in kinetic theory, in which the number of molecules is so large that the macroscopic variables, such as the density, flow velocity, and temperature, can be defined as continuous functions of position and time. Thus they classify rarefied gas dynamics (or the system described by the Boltzmann equation) as a subject where the behavior of ensemble of much less number of molecules is discussed. This wrong explanation at introductory part of textbooks spreads long-lasting serious misunderstanding among fluid-dynamicists.

[2] As noted just after Eq. (2.6), the velocity u_{wi} of the boundary must satisfy the condition $u_{wi}n_i = 0$ for the state to be time-independent.

where the subscript G is attached to discriminate this class of solution.[3] The solution or expansion is called the *Grad–Hilbert solution* or *Grad–Hilbert expansion*. Corresponding to this expansion, the macroscopic variables ω, u_i, τ, etc. [Eqs. (1.97a)–(1.97f)] are also expanded in k as

$$h_G = h_{G0} + h_{G1}k + h_{G2}k^2 + \cdots , \tag{3.4}$$

where h represents ω, u_i, τ, etc. The h_{Gm} is related to ϕ_{Gm} by Eqs. (1.97a)–(1.97f) with $\phi = \phi_{Gm}$ and $h = h_{Gm}$. Substituting the series (3.3) into the linearized Boltzmann equation (3.1) and arranging the terms by the order of k, we obtain a series of integral equations for ϕ_{Gm}, i.e.,

$$\mathcal{L}(\phi_{G0}) = 0, \tag{3.5}$$

$$\mathcal{L}(\phi_{Gm}) = \zeta_i \frac{\partial \phi_{Gm-1}}{\partial x_i} \quad (m = 1, 2, 3, \ldots). \tag{3.6}$$

The homogeneous equation (3.5) has five independent solutions 1, ζ_i, and ζ_j^2 (Section A.2.2). In view of the relations (1.97a)–(1.97c) with $\phi = \phi_{G0}$, the solution ϕ_{G0} is expressed as

$$\phi_{G0} = \omega_{G0} + 2\zeta_i u_{iG0} + \left(\zeta_j^2 - \frac{3}{2}\right)\tau_{G0}. \tag{3.7}$$

From the condition for Eq. (1.83) to hold, the inhomogeneous term $\zeta_i \partial \phi_{Gm-1}/\partial x_i$ of (3.6) must satisfy the condition (solvability condition)

$$\int \varphi \zeta_i \frac{\partial \phi_{Gm-1}}{\partial x_i} E \mathbf{d}\boldsymbol{\zeta} = 0, \tag{3.8}$$

where

$$\varphi = 1,\ \zeta_j,\ \text{or}\ \zeta_k^2, \tag{3.9}$$

for the inhomogeneous equation (3.6) to have a solution. Then, in view of the relation between h_{Gm} and ϕ_{Gm}, the solution ϕ_{Gm} is given in the form

$$\phi_{Gm} = \omega_{Gm} + 2\zeta_i u_{iGm} + \left(\zeta_j^2 - \frac{3}{2}\right)\tau_{Gm} + \widehat{\phi}_{Gm}, \tag{3.10}$$

where $\widehat{\phi}_{Gm}$ is the particular solution of Eq. (3.6) orthogonal to φ, i.e.,

$$\int \widehat{\phi}_{Gm} \varphi E \mathbf{d}\boldsymbol{\zeta} = 0. \tag{3.11}$$

[3] (i) The linearized Boltzmann equation is derived under the assumption that the size δ of the perturbation ϕ is so small that its square and higher-order terms can be neglected. The solution (3.3) retains the quantities of the order of δk^n $(n = 0, 1, 2, \ldots)$. This means that the perturbation is required to be much smaller than the Knudsen number ($\delta \ll k^n$, and thus, ω, u_i, τ, etc. $\ll k^n$).

(ii) From the preceding discussion, the state in the continuum limit is a uniform state at rest. When the linearized Boltzmann equation being discussed exclusively, the term of ϕ of the order of unity in k is, sometimes, conveniently called the continuum limit, and the contribution from higher-order terms is called the effect of rarefaction of a gas for economy of words, the size of ϕ mentioned above being put aside (see also Section 3.6).

From the integral equation (3.6) up to the m-th order, together with the solutions (3.7) and (3.10) and the orthogonal relation (3.11), it is seen that $\widehat{\phi}_{Gm}$ is expressed in a linear combination of the $(m-s)$-th partial derivatives of ω_{Gs}, u_{iGs}, and τ_{Gs} with respect to x_j ($j = 1, 2$, or 3; $s = 0, 1, \ldots, m-1$), whose coefficients are functions of ζ_i. Further, from isotropic property of the collision operator $\mathcal{L}$ (Sections A.2.5 and A.2.6), these coefficient functions are polynomials of ζ_i ($i = 1, 2$, and 3), whose coefficients are functions of ζ. Substituting this form of ϕ_{Gm} (without the explicit forms of the latter coefficient functions) into the solvability condition (3.8), we obtain the following series of the *Stokes set* of partial differential equations:

$$\frac{\partial P_{G0}}{\partial x_i} = 0, \tag{3.12}$$

$$\frac{\partial u_{iGm}}{\partial x_i} = 0, \tag{3.13a}$$

$$\frac{\partial P_{Gm+1}}{\partial x_i} = \gamma_1 \frac{\partial^2 u_{iGm}}{\partial x_j^2}, \tag{3.13b}$$

$$\frac{\partial^2 \tau_{Gm}}{\partial x_j^2} = 0, \tag{3.13c}$$

$$(m = 0, 1, 2, \ldots),$$

where

$$P_{Gm} = \omega_{Gm} + \tau_{Gm}, \tag{3.14}$$

and γ_1 is a constant related to the collision integral and to be given in Eq. (3.24). The full process of derivation of the Stokes set of equations is given in Sone [2002]. Equation (3.12) corresponds to the solvability condition (3.8) with $m = 1$ for $\varphi = \zeta_i$, and the two relations of the solvability condition (3.8) with $m = 1$ for $\varphi = 1$ and ζ_i^2 degenerate into a single equation (3.13a) with $m = 0$. Equation (3.13a) for $m = n$ corresponds to the solvability condition (3.8) with $m = n+1$ for $\varphi = 1$, and Eqs. (3.13b) and (3.13c) with $m = n$ correspond, respectively, to the conditions (3.8) with $m = n+2$ for $\varphi = \zeta_i$ and ζ_i^2. Owing to the degeneracy of the solvability conditions, the staggered combination of the solvability conditions with respect to m gives the consistent sets of equations to determine ω_{Gm}, u_{iGm}, τ_{Gm}, and P_{Gm+1} successively from the lowest order. As is obvious from its derivation, the Stokes set of equations corresponds to the linearized version (1.99)–(1.101) of the conservation equations (1.12)–(1.14), i.e., Eq. (3.13a) to Eq. (1.99), Eqs. (3.12) and (3.13b) to Eq. (1.100), and Eq. (3.13c) to Eq. (1.101).

When the solvability condition is satisfied, the solution ϕ_{Gm} is given in the form

$$\phi_{G0} = \phi_{eG0}, \tag{3.15}$$

$$\phi_{G1} = \phi_{eG1} - \zeta_i \zeta_j B(\zeta) \frac{\partial u_{iG0}}{\partial x_j} - \zeta_i A(\zeta) \frac{\partial \tau_{G0}}{\partial x_i}, \tag{3.16}$$

Table 3.1. Functions $A(\zeta)$, $B(\zeta)$, etc. for a hard-sphere gas (Ohwada & Sone [1992]).

ζ	$A(\zeta)$	$B(\zeta)$	$D_1(\zeta)$	$D_2(\zeta)$	$F(\zeta)$
0.0	−6.137070	3.510384	−2.970357	5.094481	10.446110
0.2	−6.000493	3.488592	−2.929588	5.016259	10.125883
0.4	−5.601358	3.426008	−2.810643	4.796309	9.217954
0.6	−4.968023	3.330004	−2.622546	4.472115	7.857892
0.8	−4.138507	3.210186	−2.377495	4.089129	6.213220
1.0	−3.152155	3.076042	−2.088289	3.687574	4.437018
1.2	−2.044107	2.935479	−1.766585	3.296146	2.644323
1.4	−0.843026	2.794342	−1.422149	2.931792	0.909371
1.6	0.428951	2.656552	−1.062759	2.602411	−0.726525
1.8	1.755233	2.524509	−0.694443	2.310013	−2.244748
2.0	3.123547	2.399517	−0.321799	2.053253	−3.640744
2.2	4.524827	2.282139	0.051699	1.829137	−4.917909
2.4	5.952341	2.172469	0.423445	1.634051	−6.083685
2.6	7.401032	2.070310	0.791504	1.464336	−7.147220
2.8	8.867055	1.975305	1.154458	1.316567	−8.118052
3.0	10.347443	1.887008	1.511283	1.187672	−9.005409
3.2	11.839877	1.804946	1.861263	1.074970	−9.817868
3.4	13.342516	1.728639	2.203918	0.976148	−10.563225
3.6	14.853884	1.657625	2.538948	0.889234	−11.248471
3.8	16.372779	1.591466	2.866195	0.812552	−11.879827
4.0	17.898215	1.529757	3.185604	0.744679	−12.462804
4.2	19.429375	1.472124	3.497204	0.684411	−13.002275
4.4	20.965572	1.418224	3.801083	0.630726	−13.502544
4.6	22.506231	1.367745	4.097373	0.582757	−13.967417
4.8	24.050858	1.320404	4.386241	0.539765	−14.400261
5.0	25.599033	1.275944	4.667874	0.501122	−14.804060

$$\phi_{G2} = \phi_{eG2} - \zeta_i\zeta_j B(\zeta)\frac{\partial u_{iG1}}{\partial x_j} - \zeta_i A(\zeta)\frac{\partial \tau_{G1}}{\partial x_i} + \frac{1}{\gamma_1}\zeta_i D_1(\zeta)\frac{\partial P_{G1}}{\partial x_i} + \zeta_i\zeta_j\zeta_k D_2(\zeta)\frac{\partial^2 u_{iG0}}{\partial x_j \partial x_k} - \zeta_i\zeta_j F(\zeta)\frac{\partial^2 \tau_{G0}}{\partial x_i \partial x_j}, \tag{3.17}$$

where

$$\phi_{eGm} = \omega_{Gm} + 2\zeta_i u_{iGm} + \left(\zeta^2 - \frac{3}{2}\right)\tau_{Gm}, \tag{3.18}$$

and the functions $A(\zeta)$, $B(\zeta)$, $D_1(\zeta)$, $D_2(\zeta)$, and $F(\zeta)$ are related to the functions $\mathcal{A}(\zeta, a)$, $\mathcal{B}^{(0)}(\zeta, a)$, etc. defined by the integral equations in Section A.2.9 as[4]

$$\left.\begin{aligned} &A(\zeta) = \mathcal{A}(\zeta, 1), \quad B(\zeta) = \mathcal{B}^{(0)}(\zeta, 1), \quad F(\zeta) = \mathcal{B}^{(1)}(\zeta, 1), \\ &D_1(\zeta) = \mathcal{T}_1^{(0)}(\zeta, 1), \quad D_2(\zeta) = \mathcal{T}_2^{(0)}(\zeta, 1). \end{aligned}\right\} \tag{3.19}$$

The numerical data of $A(\zeta)$, $B(\zeta)$, $D_1(\zeta)$, $D_2(\zeta)$, and $F(\zeta)$ for a hard-sphere gas are tabulated in Table 3.1 (see Pekeris & Alterman [1957] for various properties of these functions). For the BKW model,

$$A(\zeta) = \zeta^2 - \tfrac{5}{2},\ B(\zeta) = 2,\ D_1(\zeta) = -1,\ D_2(\zeta) = 2,\ F(\zeta) = -\zeta^2 + \tfrac{5}{2}. \tag{3.20}$$

[4]The functions $A(\zeta), B(\zeta)$, etc. [thus, γ_1, γ_2, etc. to be defined in Eq. (3.24)] depend on the parameter U_0/k_BT_0 (Footnote 22 in Section 1.9) except for a hard-sphere molecular gas and the BKW model.

3.1.3 Stress tensor and heat-flow vector of the Grad–Hilbert solution

From ϕ_{Gm} in Eqs. (3.15)–(3.17) with the aid of the self-adjoint property (1.81), i.e., $\int[\psi\mathcal{L}(\phi)-\phi\mathcal{L}(\psi)]E\mathbf{d\zeta}=0$ with $\psi=\zeta_i A(\zeta)$ or $(\zeta_i\zeta_j-\frac{1}{3}\zeta^2\delta_{ij})B(\zeta)$, Eqs. (3.19), and (A.123)–(A.125), we obtain the stress tensor and heat-flow vector of the Grad–Hilbert solution as follows:

$$\left.\begin{aligned} P_{ijG0} &= P_{G0}\delta_{ij}, \qquad P_{ijG1} = P_{G1}\delta_{ij}+\gamma_1 S_{ijG0},\\ P_{ijG2} &= P_{G2}\delta_{ij}+\gamma_1 S_{ijG1}+\gamma_3\frac{\partial^2\tau_{G0}}{\partial x_i\partial x_j},\\ P_{ijG3} &= P_{G3}\delta_{ij}+\gamma_1 S_{ijG2}+\gamma_3\frac{\partial^2\tau_{G1}}{\partial x_i\partial x_j}-2\gamma_6\frac{\partial}{\partial x_i}\frac{\partial^2 u_{jG0}}{\partial x_k^2}\\ &= P_{G3}\delta_{ij}+\gamma_1 S_{ijG2}+\gamma_3\frac{\partial^2\tau_{G1}}{\partial x_i\partial x_j}-\frac{2\gamma_6}{\gamma_1}\frac{\partial^2 P_{G1}}{\partial x_i\partial x_j}, \end{aligned}\right\} \tag{3.21}$$

$$\left.\begin{aligned} Q_{iG0} &= 0, \qquad Q_{iG1} = \frac{5}{4}\gamma_2 G_{iG0},\\ Q_{iG2} &= \frac{5}{4}\gamma_2 G_{iG1}+\frac{\gamma_3}{2}\frac{\partial^2 u_{iG0}}{\partial x_j^2} = \frac{5}{4}\gamma_2 G_{iG1}+\frac{\gamma_3}{2\gamma_1}\frac{\partial P_{G1}}{\partial x_i},\\ Q_{iG3} &= \frac{5}{4}\gamma_2 G_{iG2}+\frac{\gamma_3}{2}\frac{\partial^2 u_{iG1}}{\partial x_j^2} = \frac{5}{4}\gamma_2 G_{iG2}+\frac{\gamma_3}{2\gamma_1}\frac{\partial P_{G2}}{\partial x_i}. \end{aligned}\right\} \tag{3.22}$$

Here,

$$S_{ijGm} = -\left(\frac{\partial u_{iGm}}{\partial x_j}+\frac{\partial u_{jGm}}{\partial x_i}\right), \qquad G_{iGm} = -\frac{\partial\tau_{Gm}}{\partial x_i}, \tag{3.23}$$

and the nondimensional transport coefficients γ_1, γ_2, γ_3, and γ_6 are defined by

$$\left.\begin{aligned} \gamma_1 &= I_6(B), \qquad \gamma_2 = 2I_6(A),\\ \gamma_3 &= I_6(AB) = 5I_6(D_1)+I_8(D_2) = -2I_6(F),\\ \gamma_6 &= \tfrac{1}{2}I_6(BD_1)+\tfrac{3}{14}I_8(BD_2), \end{aligned}\right\} \tag{3.24}$$

where $I_n(Z)$, with $Z=A,B,\ldots$, is the integral

$$I_n(Z) = \frac{8}{15\sqrt{\pi}}\int_0^\infty \zeta^n Z(\zeta)\exp(-\zeta^2)\mathrm{d}\zeta. \tag{3.25}$$

Incidentally, γ_1, γ_2, and γ_3 are related to $\Gamma_1(a)$, $\Gamma_2(a)$, and $\Gamma_3(a)$ defined in Section A.2.9 as

$$\gamma_1 = \Gamma_1(1), \quad \gamma_2 = \Gamma_2(1), \quad \gamma_3 = \Gamma_3(1). \tag{3.26}$$

For a hard-sphere gas,

$$\left.\begin{aligned} \gamma_1 &= 1.270\,042\,427, \qquad \gamma_2 = 1.922\,284\,066,\\ \gamma_3 &= 1.947\,906\,335, \qquad \gamma_6 = 1.419\,423\,836. \end{aligned}\right\} \tag{3.27}$$

For the BKW model,

$$\gamma_1 = \gamma_2 = \gamma_3 = \gamma_6 = 1. \tag{3.28}$$

It can be shown generally that γ_1 and γ_2 are positive (see Section A.2.9).

In the stress formula (3.21), the term proportional to S_{ijGm} corresponds to the viscous stress in the classical fluid dynamics, the higher-order term proportional to $\partial^2\tau_{Gm}/\partial x_i\partial x_j$ is called *thermal stress*, and the term proportional to $\partial^2 P_{G1}/\partial x_i\partial x_j$ may be called *pressure stress*. At the second and higher orders in the heat-flow formula (3.22), Q_{iGm} depends on a pressure gradient as well as a temperature gradient. A numerical example of the heat flow proportional to the pressure gradient in the Poiseuille flow is given in Section 4.2.2.

The thermal stress in Eq. (3.21) disappears in Eq. (3.13b) owing to Eq. (3.13c). This means that the thermal stress integrated over a closed surface (or a control surface) vanishes. That is, the thermal stress is balanced over the surface. This situation is violated if the part of the surface is on a simple boundary or an interface of the gas and its condensed phase, because, as we will see in Section 3.1.4, the Grad–Hilbert solution is subject to a correction in the neighborhood of these boundaries. Thus, a flow is induced owing to thermal stress, which will be discussed in Section 5.1.2.

3.1.4 Analysis of Knudsen layer

The Grad–Hilbert solution obtained in Section 3.1.2 does not have enough freedom to be fitted to the kinetic boundary condition (3.2), because each term of the expansion is of a special form in ζ_i, i.e., a polynomial of ζ_i with its coefficients of functions of ζ. Therefore, the solution of the boundary-value problem cannot be expressed only with the Grad–Hilbert solution.

The problem is resolved by introducing the Knudsen-layer correction near the boundary. That is, the asymptotic solution is obtained as the sum of two terms, the overall solution ϕ_G (Grad–Hilbert solution) and its correction ϕ_K in a neighborhood of the boundary, i.e.,

$$\phi = \phi_G + \phi_K, \tag{3.29}$$

where ϕ_K is appreciable only in a thin layer (*Knudsen layer*), with thickness of the order of the mean free path, adjacent to the boundary and makes an appreciable change in the direction normal to the boundary over the distance of the order of the mean free path [or $kn_i\partial\phi_K/\partial x_i = O(\phi_K)$]. The ϕ_G is called the *fluid-dynamic part*, and ϕ_K is the *Knudsen-layer part* (or *Knudsen-layer correction*). In the linearized problem, the equation for ϕ_K is the same as Eq. (3.1). That is,

$$\zeta_i\frac{\partial\phi_K}{\partial x_i} = \frac{1}{k}\mathcal{L}(\phi_K). \tag{3.30}$$

Here, we introduce natural variables, *Knudsen-layer variables,* (η, χ_1, χ_2) in describing the Knudsen layer, i.e.,

$$x_i = k\eta n_i(\chi_1, \chi_2) + x_{wi}(\chi_1, \chi_2), \tag{3.31}$$

where $x_i = x_{wi}(\chi_1, \chi_2)$ is the boundary surface, η is a stretched coordinate normal to the boundary, χ_1 and χ_2 are (unstretched) coordinates within a surface $\eta = \text{const}$, and the normal vector n_i is a function of χ_1 and χ_2. With these variables, Eq. (3.30) is rewritten as

$$\zeta_i n_i \frac{\partial \phi_K}{\partial \eta} = \mathcal{L}(\phi_K) - k\zeta_i \left(\frac{\partial \chi_1}{\partial x_i} \frac{\partial \phi_K}{\partial \chi_1} + \frac{\partial \chi_2}{\partial x_i} \frac{\partial \phi_K}{\partial \chi_2} \right). \tag{3.32}$$

The Knudsen-layer correction ϕ_K is also expanded in a power series of k, i.e.,

$$\phi_K = \phi_{K0} + \phi_{K1} k + \cdots . \tag{3.33}$$

Corresponding to the expansion, the Knudsen-layer corrections of the macroscopic variables are also expanded, i.e.,

$$h_K = h_{K0} + h_{K1} k + \cdots ,$$

where h represents ω, u_i, τ, etc. and $h_K = h - h_G$. The h_{Km} is related to ϕ_{Km} by Eqs. (1.97a)–(1.97f) with $\phi = \phi_{Km}$ and $h = h_{Km}$. Substituting the expansion (3.33) into Eq. (3.32) and arranging the same-order terms in k, we obtain a series of spatially one-dimensional (homogeneous or inhomogeneous) linearized Boltzmann equations for ϕ_{Km}, i.e.,

$$\zeta_i n_i \frac{\partial \phi_{K0}}{\partial \eta} = \mathcal{L}(\phi_{K0}), \tag{3.34}$$

$$\zeta_i n_i \frac{\partial \phi_{K1}}{\partial \eta} = \mathcal{L}(\phi_{K1}) - \zeta_i \left[\left(\frac{\partial \chi_1}{\partial x_i} \right)_0 \frac{\partial \phi_{K0}}{\partial \chi_1} + \left(\frac{\partial \chi_2}{\partial x_i} \right)_0 \frac{\partial \phi_{K0}}{\partial \chi_2} \right], \tag{3.35}$$

where the parentheses $(\ )_0$ with the subscript 0 indicate that the quantities in them are evaluated at $\eta = 0$.

The boundary condition for ϕ_{Km} at $\eta = 0$ is

$$\phi_{Km} = \phi_{wm} - \phi_{Gm} \qquad (\zeta_i n_i > 0), \tag{3.36}$$

where ϕ_{wm} is defined by[5]

$$\phi_w = \phi_{w0} + \phi_{w1} k + \cdots . \tag{3.37}$$

Because ϕ_K is assumed to be the correction to ϕ_G, the condition at infinity is

$$\phi_{Km} \to 0 \quad \text{as } \eta \to \infty, \tag{3.38}$$

[5]The boundary data may have some undetermined factor, which depends on the Knudsen number, e.g., the surface temperature of a particle set freely in a gas. To include the case, u_{wi}, τ_w, ω_w, and P_w are expanded in the power series of k, i.e.,

$$h_w = h_{w0} + h_{w1} k + \cdots ,$$

where h_w represents u_{wi}, τ_w, ω_w, and P_w. Even when these quantities are independent of k, ϕ_w generally depends on k, because ϕ_w depends on ϕ ($\zeta_i n_i < 0$).

where the decay is assumed to be faster than any inverse power of η.[6] This is verified in the existence and uniqueness theorem explained in the paragraph after next.

The boundary condition (3.36) contains undetermined boundary values of u_{iGm}, τ_{Gm}, and ω_{Gm}, as well as the boundary data of the $(m-s)$-th partial derivatives of u_{iGs}, τ_{Gs}, and ω_{Gs} $(s<m)$ at the previous stages of approximation, through ϕ_{Gm}.[7] On the basis of the Grad–Bardos theorem (Grad [1969], Bardos, Caflisch & Nicolaenko [1986], Coron, Golse & Sulem [1988], Golse & Poupaud [1989])[8] for the half-space problem to be explained in the next paragraph, we will show that the above undetermined boundary values must satisfy some relations for the half-space boundary-value problem for ϕ_{Km} [Eqs. (3.34) or (3.35), (3.36), and (3.38)] to have the solution for the cases of the diffuse-reflection and complete-condensation boundary conditions and give a comment for the general case. The resulting relations serve as the boundary condition for the Stokes set of equations (3.12)–(3.13c).

The existence and uniqueness theorem (the *Grad–Bardos theorem*) for the half-space problem of the linearized Boltzmann equation with or without an inhomogeneous term [Eqs. (3.34) or (3.35), (3.36), and (3.38)] is as follows. Let the boundary condition for Eq. (3.34) or (3.35) at $\eta=0$ be given by

$$\phi_{Km} = c_0 + c_i(\zeta_i - \zeta_j n_j n_i) + c_4\zeta_j^2 + f(\zeta_i) \qquad (\zeta_i n_i > 0), \tag{3.39}$$

where c_0, c_i, and c_4 are undetermined constants, which are practically four because of no contribution of $c_i n_i$ to Eq. (3.39), and $f(\zeta_i)$ is a given function. The solution vanishes as $\eta\to\infty$. Then the solution of this boundary-value problem, where exponential decay of the inhomogeneous term as $\eta\to\infty$ is assumed, exists uniquely when and only when the four undetermined constants c_0, $c_i - c_j n_j n_i$, and c_4 take a special set of values. It is also shown that the speed of decay of the solution as $\eta\to\infty$ is exponential.[9]

In Eq. (3.36) for the complete condensation, where ϕ_w is given by Eq. (1.111), the boundary data $\omega_{wm}-\omega_{Gm}-3(\tau_{wm}-\tau_{Gm})/2$, $2[u_{wim}-(u_{iGm}-u_{jGm}n_jn_i)]$, $\tau_{wm}-\tau_{Gm}$, and $-2\zeta_i u_{jGm}n_in_j-\widehat{\phi}_{Gm}$ correspond, respectively, to c_0, $c_i-c_jn_jn_i$, c_4, and $f(\zeta_i)$ in Eq. (3.39). Thus, the solution ϕ_{Km} and the boundary data $\omega_{wm}-\omega_{Gm}$, $u_{wim}-(u_{iGm}-u_{jGm}n_jn_i)$, and $\tau_{wm}-\tau_{Gm}$ are determined by $2\zeta_i u_{jGm}n_in_j+\widehat{\phi}_{Gm}$ and ϕ_{Kr} $(r<m)$ in the inhomogeneous term of Eq. (3.35)

[6] If the decay is proportional to some inverse power of η, the separation of ϕ_G and ϕ_K becomes vague. That is, if ϕ_{K0} decays as η^{-m}, it cannot be discriminated from ϕ_{Gm} term, because $\eta^{-m}=[(x_i-x_{wi})n_i]^{-m}k^m$.

[7] For simplicity, consider the case of the diffuse-reflection condition or the complete-condensation condition. In the case of specular-reflection condition or the Maxwell-type condition where the accommodation coefficient α is much smaller than the Knudsen number or k $(\alpha\ll k)$, the u_{iGm}, τ_{Gm}, and ω_{Gm} terms (or ϕ_{eGm} term) contained in ϕ_{Gm} cancel out in Eq. (3.36). Thus, the following analysis does not apply to this case, and a different analysis is required (Sone & Aoki [1977a], Aoki, Inamuro & Onishi [1979]).

[8] The form of the existence and uniqueness theorem of the solution of the half-space problem given in the next paragraph was first conjectured by Grad [1969].

[9] This guarantees the exponential decay of the inhomogeneous term in the next-order Knudsen-layer equation.

or its higher-order equations. In view of the form of $\widehat{\phi}_{Gm}$ [see Eqs. (3.10), (3.15)–(3.17)], the way that ϕ_{Km} is determined from ϕ_{Kr} $(r < m)$, and the linear property of the problem, the undetermined boundary data $\omega_{wm} - \omega_{Gm}$, $u_{wim} - (u_{iGm} - u_{jGm}n_jn_i)$, and $\tau_{wm} - \tau_{Gm}$ and the solution ϕ_{Km} are expressed by linear combinations of the boundary values of $u_{jGm}n_j$ and the $(m-r)$-th or the lower-order partial derivatives of ω_{Gr}, u_{iGr}, and τ_{Gr} $(r < m)$, where the coefficients in the expression for ϕ_{Km} are functions of η and ζ_i. The expressions for $\omega_{wm} - \omega_{Gm}$, $u_{wim} - (u_{iGm} - u_{jGm}n_jn_i)$, and $\tau_{wm} - \tau_{Gm}$ are the four relations among the five undetermined boundary values of ω_{Gm}, u_{iGm}, and τ_{Gm}. These relations serve as the boundary condition for the Stokes set of equations on an interface where the complete-condensation condition is applied.[10]

Equation (3.36) for the diffuse reflection, where ϕ_w is given by Eq. (1.105a), is of the form that ω_{wm} in Eq. (3.36) for the complete condensation is simply replaced by $\check{\sigma}_{wm}$, where $\check{\sigma}_{wm}$ is the component function of the expansion of $\check{\sigma}_w$ in k. Therefore, $\check{\sigma}_{wm} - \omega_{Gm}$, $u_{wim} - (u_{iGm} - u_{jGm}n_jn_i)$, and $\tau_{wm} - \tau_{Gm}$, as well as ϕ_{Km}, are determined by $2\zeta_i u_{jGm}n_in_j + \widehat{\phi}_{Gm}$ and ϕ_{Kr} $(r < m)$, and they are expressed by linear combinations of the boundary values of $u_{jGm}n_j$ and the $(m-r)$-th or the lower-order partial derivatives of ω_{Gr}, u_{iGr}, and τ_{Gr} $(r < m)$, where the coefficients in the expression for ϕ_{Km} are functions of η and ζ_i. In addition, $\check{\sigma}_{wm}$ is related to $\phi_{Gm} + \phi_{Km}$ $(\zeta_i n_i < 0)$ by Eq. (1.105b). That is,

$$\check{\sigma}_{wm} - \omega_{Gm} = -\frac{1}{2}(\tau_{wm} - \tau_{Gm}) - \sqrt{\pi}u_{iGm}n_i - 2\sqrt{\pi}\int_{\zeta_j n_j < 0} \zeta_i n_i (\widehat{\phi}_{Gm} + \phi_{Km}) E \mathbf{d}\boldsymbol{\zeta},$$

where the integral of ϕ_{eGm} part of ϕ_{Gm} is carried out. Eliminating $\check{\sigma}_{wm} - \omega_{Gm}$ from its two expressions, and substituting the above-explained form of $\tau_{wm} - \tau_{Gm}$, $\widehat{\phi}_{Gm}$, and ϕ_{Km} there, we obtain the expression of $u_{iGm}n_i$ that is given by the data of the previous stages of approximation. Thus, together with the expressions of $u_{wim} - (u_{iGm} - u_{jGm}n_jn_i)$ and $\tau_{wm} - \tau_{Gm}$, we find that the boundary values of $u_{iGm} - u_{wim}$ and $\tau_{Gm} - \tau_{wm}$ are determined by the $(m-r)$-th or the lower-order partial derivatives of ω_{Gr}, u_{iGr}, and τ_{Gr} $(r < m)$. These relations serve as the boundary condition for the Stokes set on a boundary where the diffuse reflection is taking place.[11]

For more general boundary conditions such as Eqs. (1.107) and (1.112), we need the Grad–Bardos theorem to be generalized so as to include the linear functional of $\phi_{Km}(\zeta_i n_i < 0)$ on the right-hand side of Eq. (3.39). On the basis of the generalized theorem, we can derive the boundary condition for the Stokes set in a way similar to that shown in the preceding two paragraphs (see Sone [2002] for more details).

[10] Hereafter, $P_{wm} - P_{Gm}$, where $P_{wm} = \omega_{wm} + \tau_{wm}$ in the linear theory, will be used instead of $\omega_{wm} - \omega_{Gm}$ in most cases.

[11] Technically, the condition on $u_{iGm}n_i$ can be obtained in a simpler way. Multiplying Eq. (3.34) or (3.35), etc. by $E(\zeta)$ and integrating over the whole space of ζ_i, we have $\partial u_{iKm}n_i/\partial\eta = F(\phi_{Kn})$ $(n \leq m-1)$. With the aid of the condition at infinity, $u_{iKm}n_i = \int_\infty^\eta F(\phi_{Kn})\mathrm{d}\eta$. From the condition $(u_i n_i = 0)$ on a simple boundary, $u_{iGm}n_i = \int_0^\infty F(\phi_{Kn})\mathrm{d}\eta$. Especially, $u_{iG0}n_i = 0$ for $m = 0$, because $F(\phi_{Kn}) = 0$. Thus, $u_{iG0} - u_{jG0}n_jn_i = u_{wi0}$, i.e., $u_{iG0} = u_{wi0}$, and $\tau_{G0} = \tau_{w0}$.

For a simple boundary (see Section 1.6.1), it is easily seen with the aid of the discussion on the linearized part in Section 4.4 that $u_{iG0} = u_{wi0}$, $\tau_{G0} = \tau_{w0}$, and $\phi_{K0} = 0$ are the unique solution for the general kinetic boundary condition (1.64), including the diffuse-reflection condition. Thus, the Knudsen-layer correction starts from ϕ_{K1} and the inhomogeneous term of Eq. (3.35) for ϕ_{K1} vanishes.[12]

3.1.5 Slip boundary condition and Knudsen-layer correction

Here we summarize the boundary condition for the Stokes set of equations on a simple boundary or on an interface of a gas and its condensed phase and the Knudsen-layer correction to its solution. The formulas apply to a locally isotropic boundary,[13] where the reflection law is expressed by Eq. (1.107) with a finite diffuse reflection part or by Eq. (1.112) with a finite complete condensation part.[14] The boundary condition is called the *slip* or *jump condition*.

On a simple solid boundary

On a simple solid boundary, the slip boundary condition and the Knudsen-layer correction are given as follows (Sone [1969, 1971, 2002]):

$$u_{iG0} - u_{wi0} = 0, \tag{3.40a}$$

$$\tau_{G0} - \tau_{w0} = 0, \tag{3.40b}$$

$$u_{iK0} = \omega_{K0} = \tau_{K0} = 0, \tag{3.40c}$$

$$\begin{bmatrix} (u_{iG1} - u_{wi1})t_i \\ u_{iK1}t_i \end{bmatrix} = S_{ijG0}n_it_j \begin{bmatrix} k_0 \\ Y_0(\eta) \end{bmatrix} + G_{iG0}t_i \begin{bmatrix} K_1 \\ \frac{1}{2}Y_1(\eta) \end{bmatrix}, \tag{3.41a}$$

$$\begin{bmatrix} u_{iG1}n_i \\ u_{iK1}n_i \end{bmatrix} = 0, \tag{3.41b}$$

$$\begin{bmatrix} \tau_{G1} - \tau_{w1} \\ \omega_{K1} \\ \tau_{K1} \end{bmatrix} = -G_{iG0}n_i \begin{bmatrix} d_1 \\ \Omega_1(\eta) \\ \Theta_1(\eta) \end{bmatrix}, \tag{3.41c}$$

[12] The equation and the boundary condition for ϕ_{K1} on a simple boundary are

$$\zeta_i n_i \partial\phi_{K1}/\partial\eta = \mathcal{L}(\phi_{K1}),\ \ \phi_{K1} = \phi_{w1} - \phi_{eG1} - \tfrac{1}{2}\zeta_i\zeta_j B(\zeta)S_{ijG0} - \zeta_i A(\zeta)G_{iG0}\ \ (\zeta_i n_i > 0).$$

The Knudsen layer and the slip condition depend linearly on S_{ijG0} and G_{iG0} on the boundary. From the preceding Footnote 11, $u_{iG1}n_i = 0$ on the boundary.

[13] The "locally isotropic boundary" means that the scattering kernel $\hat{K}_B(\boldsymbol{\zeta}, \boldsymbol{\zeta}_*, \boldsymbol{x}, \hat{t})$ or $\hat{K}_I(\boldsymbol{\zeta}, \boldsymbol{\zeta}_*, \boldsymbol{x}, \hat{t})$ and the inhomogeneous function $\hat{g}_I(\boldsymbol{x}, \boldsymbol{\zeta}, \hat{t})$ in the kinetic boundary condition (1.64) or (1.69) are invariant for the following two kinds of transformations of $\boldsymbol{\zeta} - \hat{\boldsymbol{v}}_{\boldsymbol{w}}$ and $\boldsymbol{\zeta}_* - \hat{\boldsymbol{v}}_{\boldsymbol{w}}$: a rotation around the normal vector n_i to the boundary and the reflection with respect to a plane containing the normal vector n_i. In the linearized case, $\hat{K}_{B0}$ in Eq. (1.107) or $\hat{K}_{I0}$ in Eq. (1.112) is invariant in the above two kinds of transformations of $\boldsymbol{\zeta}$ and $\boldsymbol{\zeta}_*$.

[14] This is the case where the u_{iGm}, τ_{Gm}, and ω_{Gm} terms are not canceled out and remain with finite magnitudes in Eq. (3.36). See Footnote 7 in Section 3.1.4 and Sone [2002].

$$\begin{aligned}\begin{bmatrix} (u_{iG2}-u_{wi2})t_i \\ u_{iK2}t_i \end{bmatrix} &= S_{ijG1}n_it_j\begin{bmatrix} k_0 \\ Y_0(\eta)\end{bmatrix} + \frac{\partial S_{ijG0}}{\partial x_k}n_jn_kt_i\begin{bmatrix} a_1 \\ Y_{a1}(\eta)\end{bmatrix} \\ &\quad + \bar\kappa S_{ijG0}n_it_j\begin{bmatrix} a_2 \\ Y_{a2}(\eta)\end{bmatrix} + \kappa_{ij}S_{jkG0}n_kt_i\begin{bmatrix} a_3 \\ Y_{a3}(\eta)\end{bmatrix} \\ &\quad + \frac{\partial G_{iG0}}{\partial x_j}n_jt_i\begin{bmatrix} a_4 \\ Y_{a4}(\eta)\end{bmatrix} + \bar\kappa G_{iG0}t_i\begin{bmatrix} a_5 \\ Y_{a5}(\eta)\end{bmatrix} \\ &\quad + \kappa_{ij}G_{jG0}t_i\begin{bmatrix} a_6 \\ Y_{a6}(\eta)\end{bmatrix} - \frac{\partial \tau_{w1}}{\partial x_i}t_i\begin{bmatrix} K_1 \\ \frac{1}{2}Y_1(\eta)\end{bmatrix}, \end{aligned} \tag{3.42a}$$

$$\begin{aligned}\begin{bmatrix} u_{iG2}n_i \\ u_{iK2}n_i \end{bmatrix} &= \frac{\partial S_{ijG0}}{\partial x_k}n_in_jn_k\begin{bmatrix} b_1 \\ \frac{1}{2}\displaystyle\int_\infty^\eta Y_0(\eta_0)\mathrm{d}\eta_0\end{bmatrix} \\ &\quad + \left(\frac{\partial G_{iG0}}{\partial x_j}n_in_j + 2\bar\kappa G_{iG0}n_i\right)\begin{bmatrix} b_2 \\ \frac{1}{2}\displaystyle\int_\infty^\eta Y_1(\eta_0)\mathrm{d}\eta_0\end{bmatrix}, \end{aligned} \tag{3.42b}$$

$$\begin{aligned}\begin{bmatrix} \tau_{G2}-\tau_{w2} \\ \omega_{K2} \\ \tau_{K2}\end{bmatrix} &= -G_{iG1}n_i\begin{bmatrix} d_1 \\ \Omega_1(\eta) \\ \Theta_1(\eta)\end{bmatrix} - \frac{\partial S_{ijG0}}{\partial x_k}n_in_jn_k\begin{bmatrix} d_4 \\ \Omega_4(\eta) \\ \Theta_4(\eta)\end{bmatrix} \\ &\quad - \frac{\partial G_{iG0}}{\partial x_j}n_in_j\begin{bmatrix} d_3 \\ \Omega_3(\eta) \\ \Theta_3(\eta)\end{bmatrix} - \bar\kappa G_{iG0}n_i\begin{bmatrix} d_5 \\ \Omega_5(\eta) \\ \Theta_5(\eta)\end{bmatrix}. \end{aligned} \tag{3.42c}$$

Here, the following notes (i)–(vii) are given for the above formulas:
(i) As already explained, u_{wim} and τ_{wm} are the component functions of the expansions of u_{wi} and τ_w, where $(2RT_0)^{1/2}u_{wi}$ $(u_{wi}n_i = 0)$[15] and $T_0(1+\tau_w)$ are, respectively, the velocity and temperature of the boundary,[16] i.e.,

$$u_{wi} = u_{wi0} + u_{wi1}k + \cdots, \qquad \tau_w = \tau_{w0} + \tau_{w1}k + \cdots. \tag{3.43}$$

(ii) The t_i is a unit vector tangential to the boundary.
(iii) The $\bar\kappa$ and κ_{ij} are defined by

$$\bar\kappa = \frac{1}{2}(\kappa_1+\kappa_2), \qquad \kappa_{ij} = \kappa_1 \mathsf{l}_i\mathsf{l}_j + \kappa_2 \mathsf{m}_i\mathsf{m}_j, \tag{3.44}$$

where κ_1/L and κ_2/L are the principal curvatures of the boundary, with κ_1 or κ_2 being taken negative when the corresponding center of curvature lies on the side of the gas, the l_i and m_i are the direction cosines of the principal directions corresponding to κ_1 and κ_2 respectively. The curvature tensor κ_{ij} is related to the variation of the normal vector n_i as

$$\kappa_{ij} = \left(\frac{\partial \chi_1}{\partial x_i}\right)_0\frac{\partial n_j}{\partial \chi_1} + \left(\frac{\partial \chi_2}{\partial x_i}\right)_0\frac{\partial n_j}{\partial \chi_2}. \tag{3.45}$$

[15] See Footnote 2 in Section 3.1.1.
[16] See Eq. (1.74) and Footnote 5 in Section 3.1.4.

(iv) The quantities with the subscript G are evaluated on the boundary; and S_{ijGm} and G_{iGm} are defined by Eq. (3.23).
(v) The k_0, K_1, $a_1, \ldots, a_6$, b_1 $[= \frac{1}{2}\int_0^\infty Y_0(\eta_0)\mathrm{d}\eta_0]$, b_2 $[= \frac{1}{2}\int_0^\infty Y_1(\eta_0)\mathrm{d}\eta_0]$, d_1, d_3, d_4, and d_5 are constants called *slip coefficients*, determined by the molecular model (e.g., hard-sphere, BKW) and the reflection law on the boundary (e.g., diffuse reflection); $Y_0(\eta)$, $Y_1(\eta)$, $\Omega_1(\eta)$, $\Theta_1(\eta)$, etc. are functions of η, called *Knudsen-layer functions*, whose functional forms are determined by the molecular model and the reflection law.[17]
(vi) In some literature, a temperature jump term proportional to $S_{ijG0}n_in_j$ is retained in $\tau_{G1} - \tau_{w1}$ of Eq. (3.41c). However, $S_{ijG0}n_in_j = 0$ on a simple solid boundary with the aid of Eqs. (3.13a) and (3.40a).[18]
(vii) For the specular reflection or the Maxwell-type condition with the accommodation coefficient α much smaller than the Knudsen number or k ($\alpha \ll k$), the formulas take different forms (Sone & Aoki [1977a], Aoki, Inamuro & Onishi [1979]) by the reason noted in Footnote 7 in Section 3.1.4.[19]

For a hard-sphere gas under the diffuse reflection, the first-order slip coefficients and Knudsen-layer functions and some of them of the second order are obtained as

$$\left.\begin{aligned} &k_0 = -1.2540, \quad K_1 = -0.6463, \quad d_1 = 2.4001, \\ &a_4 = 0.0330, \qquad b_1 = 0.1068, \qquad b_2 = 0.4776, \end{aligned}\right\} \tag{3.46}$$

and the corresponding Knudsen-layer functions $Y_0(\eta)$, $Y_1(\eta)$, $\Omega_1(\eta)$, $\Theta_1(\eta)$, and $Y_{a4}(\eta)$ are tabulated in Table 3.2 (Sone, Ohwada & Aoki [1989a], Ohwada, Sone & Aoki [1989a], Ohwada & Sone [1992]).[20] For the BKW model under the diffuse reflection, the slip coefficients and Knudsen-layer functions are obtained up to

[17] The slip coefficients and Knudsen-layer functions generally depend on the reference temperature T_0 (or the parameter U_0/k_BT_0) except for a hard-sphere molecular gas and the BKW model (see Footnote 22 in Section 1.9).

[18] See Footnote 13 in Section 3.4 of Sone [2002].

[19] In a special situation (Section 5.1.1), the thermal creep flow, to be mentioned in the next paragraph, appears with a different value (but of the same order) of the slip coefficient owing to degeneracy of various terms (Sone [1970]), in contrast to general situations in the above references. That is, the terms that determine the slip boundary condition degenerate, and it is determined by the terms of the order of α, which is of higher order or infinitesimal, in the special situation (the ghost effect of infinitesimal accommodation coefficient). This is an example showing that the limiting state with two or more parameters involved depends on the relative speed of the parameters that tend to the limit. This is discussed in detail in Section 3.3 and Chapter 9.

[20] (i) The corresponding results for the Maxwell-type boundary condition are given in Wakabayashi, Ohwada & Golse [1996] and Ohwada & Sone [1992] (see also Table 3.4 in Sone & Aoki [1994]).

(ii) Some works, e.g., Loyalka & Hickey [1989], are not literally for a hard-sphere gas. The Boltzmann equation for a hard-sphere gas is transformed considerably (see Wakabayashi, Ohwada & Golse [1996]), and the numerical computation is carried out for the resulting equation. Thus, the solutions there are those of model equations such as the BKW equation. In fact, the Knudsen layer in Loyalka & Hickey [1989] differs considerably from that of Ohwada, Sone & Aoki [1989a]. Its naming without notes on the difference between the two equations is misleading in those days when accurate computation was possible.

Table 3.2. Knudsen-layer functions for the Boltzmann equation for a hard-sphere gas under the diffuse-reflection condition or under the complete-condensation condition. The functions of the same symbol, i.e., Y_0, Y_1, Ω_1, and Θ_1, are common to the diffuse reflection and the complete condensation.

η	$Y_0(\eta)$	$Y_1(\eta)/2$	$\Omega_1(\eta)$	$-\Theta_1(\eta)$	$H_A(\eta)$	$H_B(\eta)$	$Y_{a4}(\eta)$	$\Omega_4^*(\eta)$	$\Theta_4^*(\eta)$
0.0000	0.34522	0.44508	0.51641	0.73783	0.13384	1.38948	0.29625	0.37815	0.05206
0.02503	0.30466	0.41870	0.46886	0.67376	0.12660	1.28950	0.28278	0.33624	0.04783
0.05011	0.28008	0.40046	0.43974	0.63360	0.12161	1.22172	0.27284	0.31065	0.04490
0.10108	0.24424	0.37107	0.39661	0.57323	0.11350	1.11477	0.25613	0.27306	0.04026
0.15138	0.21806	0.34744	0.36451	0.52766	0.10689	1.03068	0.24218	0.24538	0.03662
0.20226	0.19691	0.32686	0.33809	0.48977	0.10107	0.95884	0.22971	0.22286	0.03352
0.30081	0.16525	0.29328	0.29753	0.43097	0.09143	0.84434	0.20878	0.18886	0.02861
0.41305	0.13848	0.26186	0.26200	0.37886	0.08226	0.74030	0.18860	0.15979	0.02420
0.60049	0.10657	0.21995	0.21757	0.31303	0.06979	0.60615	0.16086	0.12468	0.01862
0.76791	0.08628	0.19014	0.18766	0.26839	0.06076	0.51404	0.14059	0.10205	0.01487
0.99185	0.06653	0.15806	0.15673	0.22204	0.05089	0.41800	0.11827	0.07973	0.01107
1.17977	0.05426	0.13621	0.13625	0.19136	0.04409	0.35452	0.10280	0.06570	0.00865
1.40407	0.04310	0.11471	0.11642	0.16171	0.03731	0.29358	0.08733	0.05279	0.00641
1.66967	0.03327	0.09416	0.09766	0.13382	0.03078	0.23688	0.07233	0.04130	0.00443
1.81952	0.02891	0.08444	0.08879	0.12072	0.02767	0.21058	0.06515	0.03615	0.00356
1.98156	0.02493	0.07517	0.08032	0.10828	0.02468	0.18585	0.05826	0.03142	0.00277
2.54689	0.01523	0.05063	0.05759	0.07538	0.01672	0.12204	0.03977	0.01974	0.00094
2.99541	0.01052	0.03733	0.04484	0.05739	0.01237	0.08856	0.02959	0.01397	0.00015
3.50590	0.00702	0.02658	0.03410	0.04257	0.00883	0.06213	0.02125	0.00960	–0.00035
4.08156	0.00453	0.01825	0.02528	0.03076	0.00607	0.04209	0.01471	0.00642	–0.00060
6.21632	0.00099	0.00472	0.00883	0.00993	0.00157	0.01057	0.00390	0.00167	–0.00054
7.97384	0.00030	0.00160	0.00385	0.00414	0.00053	0.00355	0.00135	0.00062	–0.00031
9.96662	0.00008	0.00048	0.00154	0.00159	0.00016	0.00106	0.00042	0.00022	–0.00015
15.00000	0.00000	0.00002	0.00016	0.00016	0.00001	0.00005	0.00003	0.00002	–0.00002
20.77429	0.00000	0.00000	0.00001	0.00001	0.00000	0.00000	0.00000	0.00000	–0.00000
25.39373	0.00000	0.00000	0.00000	0.00000	0.00000	0.00000	0.00000	0.00000	0.00000

the second order in Sone [1969, 1971]. The slip coefficients are

$$\left.\begin{array}{lll} k_0 = -1.01619, & K_1 = -0.38316, & d_1 = 1.30272, \\ a_1 = 0.76632, & a_2 = 0.50000, & a_3 = -0.26632, \\ a_4 = 0.27922, & a_5 = 0.26693, & a_6 = -0.76644, \\ b_1 = 0.11684, & b_2 = 0.26693, & d_3 = 0, \\ d_4 = 0.11169, & d_5 = 1.82181, & \end{array}\right\} \tag{3.47}$$

and the Knudsen-layer functions Y_{a1} etc. can be or are put in the form

$$\left.\begin{array}{lll} Y_{a1} = -Y_1, & Y_{a2} = -2\widetilde{Y}_0, & Y_{a3} = -Y_1 - k_0 Y_0, \\ Y_{a4} = 0, & Y_{a5} = Y_2 - \widetilde{Y}_1, & Y_{a6} = \tfrac{1}{2} Y_2 - (K_1 + \tfrac{1}{4}) Y_0, \\ \Omega_3 = \Theta_3 = 0, & (\Omega_4, \Theta_4) = (-\tfrac{1}{4}\Omega_4^*, -\tfrac{1}{4}\Theta_4^*), & \end{array}\right\} \tag{3.48}$$

and the functions on the right-hand sides are tabulated in Table 3.3.

The conditions (3.40a) and (3.40b) are called *nonslip condition*. The second term on the right-hand side of Eq. (3.41a) shows that a flow is induced over a wall with a temperature gradient along it. The flow is called *thermal creep flow* (Maxwell [1879], Kennard [1938], Sone [1966b, 1970], Ohwada, Sone

Table 3.3. Knudsen-layer functions for the BKW equation under the diffuse-reflection condition or under the complete-condensation condition. The functions of the same symbol, i.e., Y_0, Y_1, Ω_1, and Θ_1, are common to the diffuse reflection and the complete condensation.

η	Y_0	Y_1	Y_2	$\tilde{Y}_0$	$\tilde{Y}_1$	$\int_\eta^\infty Y_0 \mathrm{d}\eta_0$	$\int_\eta^\infty Y_1 \mathrm{d}\eta_0$
0.00	0.30908	0.54777	0.92525	0.3907	1.1922	0.23368	0.53385
0.05	0.25727	0.48117	0.83415	0.3569	1.1004	0.21974	0.50837
0.10	0.22827	0.43961	0.77446	0.3350	1.0391	0.20764	0.48539
0.20	0.18878	0.37876	0.68370	0.3017	0.9439	0.18693	0.44465
0.40	0.14003	0.29679	0.55502	0.2536	0.8032	0.15449	0.37770
0.60	0.10929	0.24081	0.46264	0.2181	0.6970	0.12976	0.32425
0.80	0.08773	0.19932	0.39151	0.1898	0.6115	0.11017	0.28042
1.00	0.07175	0.16720	0.33475	0.1666	0.5403	0.09430	0.24390
1.20	0.05948	0.14167	0.28842	0.1471	0.4800	0.08123	0.21310
1.40	0.04982	0.12096	0.25000	0.1305	0.4281	0.07033	0.18691
1.60	0.04209	0.10394	0.21777	0.1162	0.3832	0.06117	0.16447
1.80	0.03580	0.08978	0.19048	0.1038	0.3439	0.05340	0.14514
2.00	0.03063	0.07790	0.16720	0.0930	0.3093	0.04677	0.12841
2.50	0.02118	0.05551	0.12224	0.0712	0.2393	0.03399	0.09543
3.00	0.01498	0.04028	0.09068	0.0551	0.1870	0.02506	0.07172
4.00	0.00787	0.02206	0.05153	0.0338	0.1164	0.01407	0.04157
5.00	0.00434	0.01256	0.03023	0.0212	0.0740	0.00815	0.02474
10.00	0.00032	0.00104	0.00277	0.0025	0.0092	0.00071	0.00236
$(\eta \ln\eta)^*$	0.39894	0.40540	0.50519	0.2027	0.5052	0	0

η	Ω_1	$-\Theta_1$	Ω_4^*	$\Theta_4^* \times 10$	$\int_\eta^\infty (\Omega_1 + \Theta_1) \mathrm{d}\eta_0$	$\int_\eta^\infty (\Omega_4^* + \Theta_4^*) \mathrm{d}\eta_0$
0.00	0.34771	0.44920	0.36303	0.3717	−0.11609	0.23886
0.05	0.29177	0.38521	0.28722	0.3771	−0.11123	0.22106
0.10	0.26121	0.34842	0.24683	0.3639	−0.10672	0.20592
0.20	0.21987	0.29703	0.19399	0.3328	−0.09852	0.18060
0.40	0.16877	0.23114	0.13269	0.2757	−0.08466	0.14249
0.60	0.13610	0.18770	0.09669	0.2297	−0.07331	0.11479
0.80	0.11276	0.15607	0.07296	0.1927	−0.06385	0.09377
1.00	0.09507	0.13181	0.05634	0.1627	−0.05587	0.07738
1.20	0.08118	0.11258	0.04424	0.1382	−0.04908	0.06438
1.40	0.06999	0.09700	0.03519	0.1180	−0.04325	0.05392
1.60	0.06080	0.08417	0.02828	0.1012	−0.03822	0.04542
1.80	0.05315	0.07345	0.02293	0.0871	−0.03387	0.03844
2.00	0.04671	0.06440	0.01872	0.0752	−0.03007	0.03267
2.50	0.03442	0.04717	0.01156	0.0528	−0.02254	0.02210
3.00	0.02588	0.03521	0.00735	0.0376	−0.01707	0.01523
4.00	0.01524	0.02042	0.00315	0.0198	−0.01004	0.00754
5.00	0.00932	0.01231	0.00143	0.0108	−0.00606	0.00389
10.00	0.00107	0.00134	0.00004	0.0007	−0.00063	0.00021
$(\eta \ln\eta)^*$	0.46451	0.47587	0.63047	−0.5610	0	0

η	Ω_5	Θ_5	$-\Omega_6$	$-\Theta_6$	Ω_7	Θ_7
0.00	0.3516	−0.5956	0.31622	0.21690	0.5166	0.3136
0.05	0.2853	−0.4931	0.26242	0.19447	0.4441	0.2837
0.10	0.2452	−0.4292	0.23040	0.17970	0.3999	0.2640
0.20	0.1883	−0.3368	0.18563	0.15738	0.3364	0.2340
0.40	0.1153	−0.2163	0.12971	0.12619	0.2529	0.1916
0.60	0.0686	−0.1383	0.09488	0.10417	0.1976	0.1611
0.80	0.0363	−0.0838	0.07112	0.08746	0.1577	0.1375
1.00	0.0130	−0.0444	0.05413	0.07428	0.1276	0.1186
1.20	−0.0040	−0.0154	0.04161	0.06363	0.1043	0.1030
1.40	−0.0166	0.0061	0.03220	0.05487	0.0859	0.0900
1.60	−0.0260	0.0222	0.02501	0.04758	0.0712	0.0791
1.80	−0.0328	0.0341	0.01947	0.04146	0.0592	0.0697
2.00	−0.0378	0.0428	0.01515	0.03626	0.0495	0.0617
2.50	−0.0444	0.0550	0.00799	0.02632	0.0320	0.0459
3.00	−0.0460	0.0587	0.00400	0.01943	0.0209	0.0346
4.00	−0.0420	0.0545	0.00052	0.01097	0.0091	0.0203
5.00	−0.0349	0.0452	−0.00050	0.00643	0.0039	0.0122
10.00	−0.0093	0.0116	−0.00027	0.00061	−0.0001	0.0012
$(\eta \ln\eta)^*$	0.4291	−0.6043	0.34843	0.11459	0.4646	0.1528

* The Knudsen-layer functions generally have the singularity $\eta \ln\eta$ at $\eta = 0$. Its coefficient is shown in this row.

& Aoki [1989a]), whose simple experimental demonstration is given in Sone [1991b] and Sone, Sawada & Hirano [1994]. The fifth term on the right-hand side of Eq. (3.42a) shows the existence of another type of flow, called *thermal-stress slip flow* (Sone [1972]). These flows, not expected in the classical fluid dynamics and to be discussed in more detail in Section 5.1, are typical examples of flows induced by the effect of gas rarefaction[21] and they are important in the Knudsen compressor (Section 5.5) and thermophoresis[22](Section 5.3). The second term on the right-hand side of the slip condition (3.42c) is a temperature jump proportional to the normal gradient of the normal viscous stress. Thus, even in the case where the boundary temperature is uniform and the flow speed (or Mach number) is so small that its square may be neglected and the linear theory may be applicable, the temperature of the gas is nonuniform because of this jump. This phenomenon is called *thermal polarization* (Bakanov, Vysotskij, Derjaguin & Roldughin [1983], Takata, Sone & Aoki [1993]; see Section 4.5).

The Knudsen-layer corrections of the stress tensor P_{ij} and the heat-flow vector Q_i are given by

$$P_{ijK0} = 0, \tag{3.49}$$

$$P_{ijK1} = -\frac{3}{2} G_{kG0} n_k [\Omega_1(\eta) + \Theta_1(\eta)](\delta_{ij} - n_i n_j), \tag{3.50}$$

$$P_{ijK2} n_i t_j = \frac{3}{2} \left(\frac{\partial G_{iG0}}{\partial x_j} n_i t_j + G_{iG0} \kappa_{ij} t_j \right) \int_\infty^\eta [\Omega_1(\eta_0) + \Theta_1(\eta_0)] \mathrm{d}\eta_0, \tag{3.51a}$$

$$P_{ijK2} n_i n_j = -3\bar{\kappa} G_{iG0} n_i \int_\infty^\eta [\Omega_1(\eta_0) + \Theta_1(\eta_0)] \mathrm{d}\eta_0, \tag{3.51b}$$

$$Q_{iK0} = 0, \tag{3.52}$$

$$Q_{iK1} n_i = 0, \qquad Q_{iK1} t_i = -S_{ijG0} t_i n_j H_A(\eta) - G_{iG0} t_i H_B(\eta), \tag{3.53}$$

$$Q_{iK2} n_i = -\frac{1}{2} \frac{\partial S_{ijG0}}{\partial x_k} n_i n_j n_k \int_\infty^\eta H_A(\eta_0) \mathrm{d}\eta_0 - \left(\frac{\partial G_{iG0}}{\partial x_j} n_i n_j + 2\bar{\kappa} G_{iG0} n_i \right) \int_\infty^\eta H_B(\eta_0) \mathrm{d}\eta_0, \tag{3.54}$$

where the quantities with the subscript G are evaluated on the boundary, and the functions $H_A(\eta)$ and $H_B(\eta)$ for a hard-sphere gas are shown in Table 3.2. For the BKW model,

$$H_A(\eta) = \frac{1}{2} Y_0(\eta), \quad H_B(\eta) = \frac{1}{4} Y_1(\eta) + \frac{1}{\sqrt{\pi}} \int_0^\infty \exp\left(-y^2 - \frac{\eta}{y} \right) \mathrm{d}y. \tag{3.55}$$

[21] See Footnote 3 in Section 3.1.2. This use comes from the fact that the leading-order fluid-dynamic-type equations and the boundary conditions derived by the asymptotic theory is the same as those of classical fluid dynamics (see also Section 3.6).

[22] Thermophoresis is a phenomenon that a body in a rarefied gas (or a small particle in a gas) with a temperature gradient is subject to a force and drifts in the gas.

On an interface of a gas and its condensed phase with evaporation or condensation

The boundary condition for the Stokes set of equations and the Knudsen-layer correction for the macroscopic variables on an interface of a gas and its condensed phase are given as follows (Sone & Onishi [1978], Sone [2002]):

$$(u_{iG0} - u_{wi0})t_i = 0, \tag{3.56a}$$

$$u_{iK0} = 0, \tag{3.56b}$$

$$\begin{bmatrix} P_{G0} - P_{w0} \\ \tau_{G0} - \tau_{w0} \\ \omega_{K0} \\ \tau_{K0} \end{bmatrix} = u_{iG0} n_i \begin{bmatrix} C_4^* \\ d_4^* \\ \Omega_4^*(\eta) \\ \Theta_4^*(\eta) \end{bmatrix}, \tag{3.56c}$$

$$\begin{bmatrix} (u_{iG1} - u_{wi1})t_i \\ u_{iK1} t_i \end{bmatrix} = S_{ijG0} n_i t_j \begin{bmatrix} k_0 \\ Y_0(\eta) \end{bmatrix} + G_{iG0} t_i \begin{bmatrix} K_1 \\ \frac{1}{2} Y_1(\eta) \end{bmatrix} + t_j \frac{\partial}{\partial x_j}(u_{iG0} n_i) \begin{bmatrix} K_2 \\ Y_{K2}(\eta) \end{bmatrix}, \tag{3.57a}$$

$$u_{iK1} n_i = 0, \tag{3.57b}$$

$$\begin{bmatrix} P_{G1} - P_{w1} \\ \tau_{G1} - \tau_{w1} \\ \omega_{K1} \\ \tau_{K1} \end{bmatrix} = u_{iG1} n_i \begin{bmatrix} C_4^* \\ d_4^* \\ \Omega_4^*(\eta) \\ \Theta_4^*(\eta) \end{bmatrix} - G_{iG0} n_i \begin{bmatrix} C_1 \\ d_1 \\ \Omega_1(\eta) \\ \Theta_1(\eta) \end{bmatrix} - S_{ijG0} n_i n_j \begin{bmatrix} C_6 \\ d_6 \\ \Omega_6(\eta) \\ \Theta_6(\eta) \end{bmatrix} - 2\bar{\kappa} u_{iG0} n_i \begin{bmatrix} C_7 \\ d_7 \\ \Omega_7(\eta) \\ \Theta_7(\eta) \end{bmatrix}. \tag{3.57c}$$

Here, the following notes (i)–(v) are given for the above formulas:
(i) See the note (i) after Eq. (3.42c) for u_{wim} and τ_{wm}; the P_{wm} is the component function of the expansion of P_w, where $p_0(1 + P_w)$ is the saturated gas pressure at temperature $T_0(1 + \tau_w)$,[23] i.e.,

$$P_w = P_{w0} + P_{w1} k + \cdots. \tag{3.58}$$

(ii) The t_i is a unit vector tangential to the boundary.
(iii) The $\bar{\kappa}/L$ is the mean curvature of the boundary.[24]
(iv) The quantities with the subscript G are evaluated on the interface; and S_{ijGm} and G_{iGm} are defined by Eq. (3.23).
(v) The slip coefficients C_4^*, d_4^*, K_2, C_1, C_6, C_7, d_6, and d_7, as well as k_0, K_1, and d_1, are constants determined by the molecular model and the reflection

[23] See Eq. (1.74) and Footnote 5 in Section 3.1.4.
[24] See the note (iii) after Eq. (3.42c).

law on the boundary; the Knudsen-layer functions $\Omega_4^*(\eta)$, $\Theta_4^*(\eta)$, $Y_{K2}(\eta)$, $\Omega_6(\eta)$, $\Theta_6(\eta)$, $\Omega_7(\eta)$, and $\Theta_7(\eta)$, as well as $Y_0(\eta)$, $Y_1(\eta)$, $\Omega_1(\eta)$, and $\Theta_1(\eta)$, are functions of η, whose functional forms are determined by the molecular model and the reflection law. The coefficients k_0, K_1, and d_1 and the functions Y_0, Y_1, Ω_1, and Θ_1 appear commonly in the formulas on a simple boundary and those on an interface. Naturally they are not common because the reflection conditions are different. The common notation is used because the physical situation is common to these slips (or jumps) and Knudsen-layer corrections, e.g., the term proportional to $S_{ijG0}n_it_j$. However, when the condition on a simple boundary is the diffuse reflection and that on an interface is the complete condensation, they are common. That is, k_0, K_1, d_1, Y_0, Y_1, Ω_1, and Θ_1 in Eqs. (3.57a) and (3.57c) under the complete-condensation condition are the same as those in Eqs. (3.41a)–(3.42c) under the diffuse-reflection condition.

For a hard-sphere gas under the complete-condensation condition,

$$C_4^* = -2.1412, \qquad d_4^* = -0.4557, \qquad C_1 = 1.0947, \tag{3.59}$$

and the corresponding Knudsen-layer functions $\Omega_4^*(\eta)$ and $\Theta_4^*(\eta)$ are tabulated in Table 3.2 (Sone, Ohwada & Aoki [1989b]). For the BKW model under the complete-condensation condition, the slip (or jump) coefficients and Knudsen-layer functions are obtained up to the first order in Sone & Onishi [1978]. The slip coefficients are

$$\left.\begin{aligned} &C_1 = 0.55844, \quad C_4^* = -2.13204,\ C_6 = 0.82085,\ C_7 = -0.38057,\\ &K_2 = -0.79519,\ d_4^* = -0.44675,\ d_6 = 0.33034,\ d_7 = -0.13157, \end{aligned}\right\} \tag{3.60}$$

and the Knudsen-layer functions, among which Y_{K2} is given by

$$Y_{K2} = 2Y_0 + \frac{1}{2}d_4^*Y_1, \tag{3.61}$$

are tabulated in Table 3.3.

The Knudsen-layer corrections of the stress tensor P_{ij} and the heat-flow vector Q_i are given by

$$P_{ijK0} = \frac{3}{2}u_{kG0}n_k[\Omega_4^*(\eta) + \Theta_4^*(\eta)](\delta_{ij} - n_in_j), \tag{3.62}$$

$$P_{ijK1}n_in_j = 3\bar{\kappa}u_{iG0}n_i\int_\infty^\eta [\Omega_4^*(\eta_0) + \Theta_4^*(\eta_0)]\mathrm{d}\eta_0, \tag{3.63a}$$

$$P_{ijK1}n_it_j = -\frac{3}{2}\frac{\partial u_{iG0}n_i}{\partial x_j}t_j\int_\infty^\eta [\Omega_4^*(\eta_0) + \Theta_4^*(\eta_0)]\mathrm{d}\eta_0, \tag{3.63b}$$

$$Q_{iK0} = 0, \tag{3.64}$$

$$Q_{iK1}n_i = 0, \tag{3.65}$$

where the quantities with the subscript G are evaluated on the boundary.

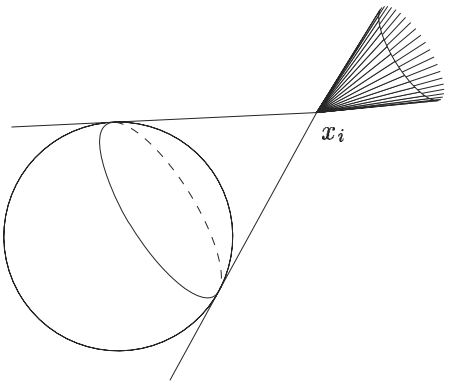

Figure 3.1. Discontinuity of the velocity distribution function in a gas around a convex boundary. At point x_i, the velocity distribution function is discontinuous on the shaded cone in ζ_i space.

3.1.6 Discontinuity of the velocity distribution function and S layer

The Boltzmann equation (3.1) determines the variation of the velocity distribution function ϕ in the ζ_i direction (or along the characteristic of the equation) in x_i space. Thus, if there is a discontinuity of ϕ at $(x_i = x_i^{(0)}, \zeta_i = \zeta_i^{(0)})$, then the discontinuity propagates from $x_i^{(0)}$ in the direction of $\zeta_i^{(0)}$.[25] This discontinuity decays owing to molecular collisions over the distance of the order of the free path of the molecules with $\zeta_i = \zeta_i^{(0)}$. From this property, we find that the velocity distribution function has discontinuities in a gas around a boundary with a convex part [e.g., around a closed (or bounded) body], irrespective of the continuity of the boundary data, by the following reason. The velocity distribution of the molecules ($\zeta_i n_i > 0$) leaving the boundary, which is determined by the boundary condition (3.2), is different in nature from that of the impinging molecules ($\zeta_i n_i < 0$), which is formed by the interaction with surrounding molecules. Thus, the velocity distribution function generally has discontinuity at the velocity ($\zeta_i n_i = 0$) tangent to the boundary. This discontinuity propagates into the gas on the convex part of the boundary (Fig. 3.1; Sugimoto & Sone [1992], Sone & Takata [1992]). On a concave part of the boundary, on the other hand, the characteristic does not enter the gas region, and therefore the discontinuity does not propagate into the gas (Sone & Takata [1992]). The discontinuity of the velocity distribution function around a convex body is an-

[25] (i) The differential operator $\zeta_i \partial/\partial x_i$ is the derivative in the direction of ζ_i. Thus, Eq. (3.1) imposes no condition on the variation of ϕ in the direction normal to ζ_i. For characteristics and propagation of discontinuity, see, e.g., Courant & Hilbert [1961], Garabedian [1964], or Zachmanoglou & Thoe [1986].

(ii) The discontinuity of the velocity distribution function is not particular to the linearized or time-independent problem. Examples of the discontinuity in flows are given in Sections 6.2–6.4 (time-independent problems) and Sections 4.8 and 6.1 (time-dependent problems).

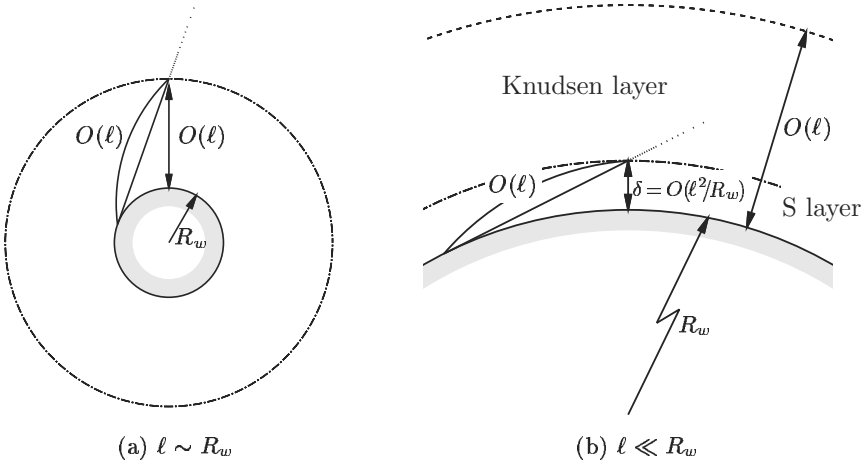

Figure 3.2. Transition region and the region where the discontinuity of the velocity distribution function is appreciable. The discontinuity is tangent to the boundary and at the velocity of the molecules leaving the boundary along this line. The discontinuity decays with distance from the boundary owing to molecular collisions; it is appreciable on the solid line with length $O(\ell)$, and negligible farther away on the vanishing dotted line. For $\ell \sim R_w$ [panel (a)], the discontinuity extends to a region, shown by the dot-dash line, of $O(\ell)$ from the boundary. For small ℓ/R_w [panel (b)], the discontinuity is in a thin layer, shown by the dot-dash line, with thickness $\delta = O(\ell^2/R_w)$; the region, bounded by the dashed line, of $O(\ell)$ from the boundary is the Knudsen layer.

alyzed by detailed numerical computation in drag and thermal force problems around a sphere and in a strong evaporation problem from a spherical or cylindrical condensed phase (Sugimoto & Sone [1992], Sone & Takata [1992], Sone & Sugimoto [1993, 1994, 1995], Takata, Sone & Aoki [1993], Sone, Takata & Wakabayashi [1994], Takata, Aoki & Sone [1994], and Takata & Sone [1995]; see Sections 6.2–6.4). Contrasting examples where the discontinuity of the velocity distribution function stays only on a plane boundary and does not exist in a gas are given in Sone, Ohwada & Aoki [1989a, 1989b, 1991] and Ohwada, Sone & Aoki [1989a, 1989b].

When the mean free path ℓ of the gas molecules is comparable to or larger than the radius R_w of the curvature of a convex body, the discontinuity is appreciable in the region where the distance from the boundary is of the order of the mean free path [Fig. 3.2 (a)].[26] This is the transition region where the gas molecules leaving the boundary are accommodated to the state of the surrounding gas by molecular collisions. That is, if ℓ/R_w (Knudsen number based on the radius of curvature) is not small, the region with the discontinuity extends in the same area as the transition region. On the other hand, if ℓ/R_w is small,

[26]Rigorously, the distance is the free path of each molecule and depends on its speed. Generally, it is longer for faster molecules, the number of which decays rapidly with their speed.

the discontinuity line is almost parallel to the boundary at the distance of the order of several mean free paths along the discontinuity, where the discontinuity has almost vanished. Thus, the discontinuity extends only in the region within $O(\ell^2/R_w)$ from the boundary [Fig. 3.2 (b)]. The discontinuity exists only at the bottom of the transition region (called Knudsen layer for small Knudsen numbers).

The discontinuity of the velocity distribution function requires corrections to the result of the asymptotic analysis.[27] That is, in a thin layer with thickness of the order of ℓ^2/R_w at the bottom of the Knudsen layer on a convex boundary, macroscopic variables are generally subject to corrections at the order next to that where the Knudsen-layer correction first appears (at the order of k^2 for the diffuse reflection or at the order of k for the complete-condensation condition). However, the corrections to the slip condition and the variables $u_i n_i$, $P_{ij} n_j$, and $Q_i n_i$ are of the higher order, and therefore their formulas given in Section 3.1.5 do not need any correction (Sone & Takata [1992]). The second boundary layer at the bottom of the Knudsen layer on a convex boundary is called *S layer*, which was found in the flow outside a circular cylinder with a temperature gradient along it by Sone [1973].[28] The numerical demonstration of the S layer is given in Sone & Takata [1992], where the correction of $u_i n_i$ is shown to be of the higher order in contrast to other variables.

Now it is clear that there is generally a discontinuity of the velocity distribution function in a gas. Thus, the proof by Arkeryd [1972] that the equality in Eq. (1.34b) holds only when the velocity distribution function is Maxwellian for a wide class of functions where discontinuous functions are included[29] is essential to the statement of the H theorem. This is an example showing that theorems apparently only of mathematical interest are very important in physical statements.

3.1.7 Force and mass and energy transfers on a closed body

Consider the total force, total moment of force, and total mass and energy transfers on a closed (or bounded) body in a gas. These global quantities can be obtained only by the knowledge of the fluid-dynamic part as follows. The body may be the condensed phase of the gas; there may be other bodies in the gas, or the domain may be enclosed by a boundary. The proof is given in Sone [1984c, 2002].

Proposition 3.1.1. *The force F_i and the moment MO_i of force (around the origin) acting on a closed body in a gas are expressed by the fluid-dynamic part*

[27] We have to take into account the discontinuity of the velocity distribution function in the analysis of the Knudsen layer.

[28] In the paper, two flows, the flow outside the cylinder and the flow inside the cylinder, are studied for small k. In the latter, where the discontinuity is absent, the result agrees with that obtained by the asymptotic theory described in Sections 3.1.2–3.1.5, but in the former, the correction is required at the order of k^2.

[29] See the fourth paragraph of Section A.7.1.

P_{ijG} of the stress tensor P_{ij} as follows:

$$F_i = -p_0 L^2 \int_S P_{ijG} \widehat{n}_j \mathrm{d}S, \tag{3.66}$$

$$MO_i = -p_0 L^3 \int_S \epsilon_{ilk} x_l P_{kjG} \widehat{n}_j \mathrm{d}S, \tag{3.67}$$

where the surface S of integration is a closed surface enclosing only the body under consideration, $\widehat{n}_i$ is the outward unit normal vector to the surface S, $\mathrm{d}S$ is the surface element (in the nondimensional x_i space) for integration, and ϵ_{ijk} is Eddington's epsilon.[30]

Proposition 3.1.2. *The mass MF and the energy ET transferred to a closed body in a gas per unit time are expressed by the fluid-dynamic parts u_{iG} and Q_{iG} of the flow velocity u_i and heat-flow vector Q_i as follows*:

$$MF = -\rho_0 (2RT_0)^{1/2} L^2 \int_S u_{iG} \widehat{n}_i \mathrm{d}S, \tag{3.68}$$

$$ET = -p_0 (2RT_0)^{1/2} L^2 \int_S (Q_{iG} + \frac{5}{2} u_{iG}) \widehat{n}_i \mathrm{d}S, \tag{3.69}$$

where the definitions of S, $\mathrm{d}S$, and $\widehat{n}_i$ are the same as in Proposition 3.1.1.

As for the contribution of the thermal stress and "pressure stress" on the force and the moment of force, we have the following proposition.

Proposition 3.1.3. *The thermal stress $\partial^2 \tau_G / \partial x_i \partial x_j$ and the "pressure stress" $\partial^2 P_G / \partial x_i \partial x_j$ in the stress tensor P_{ijG} do not contribute to the force and the moment of force acting on a closed body.*

3.1.8 Summary

Solving the Stokes set of equations (3.12)–(3.13c) under the slip boundary conditions on a simple boundary or on an interface given in Section 3.1.5 from the zeroth order, we obtain the fluid-dynamic parts of the density, flow velocity, and temperature of the gas and, on the basis of these information, their Knudsen-layer corrections from the formulas there. Further, we can obtain the stress tensor and heat-flow vector with the aid of Eqs. (3.21), (3.22), and (3.49)–(3.54) or (3.62)–(3.65). Thus the problem for the time-independent behavior of a slightly rarefied gas is reduced to solving the Stokes set of equations under the slip boundary condition. That is, a problem for a slightly rarefied gas can be treated with the same ease as the corresponding classical fluid-dynamic problem.

[30] Eddington's epsilon ϵ_{ijk} is defined by the rules

$$\epsilon_{123} = 1 \text{ and } \epsilon_{ijk} = -\epsilon_{jik} = -\epsilon_{ikj}.$$

More plainly, it is specified by the rules: (i) if any two of the i, j, k are equal, $\epsilon_{ijk} = 0$; (ii) if they are all different and occur in succession in the order 123123..., $\epsilon_{ijk} = 1$; (iii) if they are all different and occur in succession in the order 213213..., $\epsilon_{ijk} = -1$. That is, $\epsilon_{123} = \epsilon_{231} = \epsilon_{312} = 1$, $\epsilon_{213} = \epsilon_{132} = \epsilon_{321} = -1$.

In the linearized problem, which we have treated in this section, the fluid-dynamic-type equations (i.e., the Stokes set of equations) remain in the same form when we advance the degree of approximation. Thus, the effect of gas rarefaction on the density, flow velocity, temperature, and pressure enters only through the slip boundary condition. The thermal creep flow and thermal-stress slip flow, which appear, respectively, in the first and second-order slip conditions, are flows peculiar to a rarefied gas and will be discussed in more detail in Section 5.1.

The theory just developed or to be developed in this chapter is the asymptotic theory for small Knudsen numbers. That is, if the analysis is advanced up to the arbitrarily high power order of the Knudsen number or k, and the solution of a problem is obtained up to so high an order, it does not give the correct answer at a finite or infinite value of the Knudsen number [see the paragraph containing Eq. (4.16a) in Section 4.1], but it only describes the behavior for small Knudsen numbers more accurately. In the analysis, we neglected the terms smaller than any power order of k, e.g., $\exp(-1/k)$, thus $\exp[-(x_i - x_{wi})n_i/k]$ for finite $(x_i - x_{wi})n_i$. These terms are not small for a finite or infinite value of k. The second expression shows that the tail of a Knudsen layer is not small on a boundary of a finite distance from the boundary on which the Knudsen layer stands. It is neglected in the analysis. Roughly speaking, among the molecules that leave a point of the boundary, those that reach other points on the boundary of a finite distance from their origin without collision with other molecules are exponentially small for small Knudsen numbers and are neglected in the analysis, but they are finite when the Knudsen number is not small.

3.1.9 Supplement: viscosity and thermal conductivity

Up to now we have discussed the problem in nondimensional variables, and we have not given the formulas of viscosity and thermal conductivity, though we have mentioned them. They are simply obtained by rewriting the formulas for the stress tensor and heat-flow vector in the dimensional variables and by comparing them with Eq. (1.16). Then, the viscosity μ and the thermal conductivity λ are expressed in terms of the mean free path ℓ_0 of the gas molecules as follows:[31]

$$\mu = \frac{\sqrt{\pi}}{2}\gamma_1 p_0 (2RT_0)^{-1/2}\ell_0, \tag{3.70}$$

$$\lambda = \frac{5\sqrt{\pi}}{4}\gamma_2 R p_0 (2RT_0)^{-1/2}\ell_0. \tag{3.71}$$

There are two important parameters in the classical fluid dynamics, the *Reynolds number* Re and the *Mach number* Ma, which are defined by

$$\mathrm{Re} = \frac{UL}{\mu/\rho_0}, \qquad \mathrm{Ma} = \frac{U}{(\gamma RT_0)^{1/2}}, \tag{3.72}$$

[31] The relations generally hold, not limited to the time-independent linearized Boltzmann equation, if all the quantities are taken as the corresponding local values (note the analyses in Sections 3.2.2, 3.3.2, 3.4.1, 3.5.1, 3.7.1, and 3.7.2).

where U is a characteristic flow speed of the system and γ is the specific-heat ratio (5/3 for a monatomic gas).[32] Incidentally, the *Prandtl number* Pr, defined by $c_p\mu/\lambda$ (c_p : specific heat at constant pressure; $\mathrm{Pr} = 5R\mu/2\lambda$ for the present monatomic gas), is given by

$$\mathrm{Pr} = \frac{\gamma_1}{\gamma_2}. \tag{3.73}$$

With the data of γ_1 and γ_2 given in Eqs. (3.27) and (3.28), the Prandtl numbers for a hard-sphere gas and the BKW model are given by[33]

$$\mathrm{Pr} = 0.660694 \ \text{(hard sphere)}, \quad \mathrm{Pr} = 1 \ \text{(BKW)}.$$

Owing to the relation (3.70) between the viscosity and the mean free path, the three parameters, Knudsen number Kn, Reynolds number Re, and Mach number Ma, are not independent but are related as

$$\mathrm{Ma} = \left(\frac{3\pi}{40}\right)^{1/2} \gamma_1 \mathrm{ReKn}, \tag{3.74}$$

which is sometimes called the *von Karman relation* (von Karman [1963]).

In the linearized theory, we neglected the nonlinear terms of the Mach number, but retained the quantities of the order of MaKn^n.[34] This means that $\mathrm{Ma} \ll \mathrm{Kn}$ or $\mathrm{Re} \ll \mathrm{Kn}$. The Stokes set of equations in Section 3.1.2 reflects this situation.

3.2 Weakly nonlinear problem

3.2.1 Problem

According to the discussion in Section 3.1.9, the asymptotic theory of the linearized Boltzmann equation developed in the preceding section (Section 3.1) is applicable only to the case where the Reynolds number is very small. In the present section, we extend the asymptotic theory, according to Sone [1971], so as to be applicable to the case where the Reynolds number takes a finite value.

When the Reynolds number is finite, the Mach number is of the same order as the Knudsen number owing to Eq. (3.74). This fact is introduced in the analysis in the following way: the Mach number is one of the scales that indicate the deviation of the system from a uniform equilibrium state at rest, and this is extended to the velocity distribution function. That is, in this section, we

[32] The $(\gamma RT_0)^{1/2}$ is the speed of propagation of a small disturbance (or the *speed of sound* or sound wave or the *sonic speed*) in a gas at temperature T_0 governed by the Euler set of equations.

[33] For the Maxwell molecule (see Section A.2.4), Pr = 2/3 (Maxwell [1867], Boltzmann [1872, 1896–98]). The experimental data for monatomic gases are around 2/3 (see, e.g., Kennard [1938]). This is one of the reasons that some do not favor the BKW equation. However, many important theoretical results for the standard Boltzmann equation have been developed on the basis of the studies of the BKW equation.

[34] See Footnote 3 in Section 3.1.2.

consider the case where the deviation of the velocity distribution function from a uniform equilibrium state at rest is of the order of the Knudsen number. By this assumption, we extend the range of the velocity distribution function a little beyond that of the linearized theory. In terms of the macroscopic parameters, this is not only the condition on the Mach number but also the condition that the variation of the temperature, etc. is of the order of the Knudsen number. Elimination of the latter condition is discussed in Section 3.3, from which a very interesting fact will come out. In view of the above situation, we use the notation introduced in Section 1.10 in the following discussion.

Under the condition mentioned above, we investigate the asymptotic behavior for small Knudsen numbers of the time-independent boundary-value problem of the Boltzmann equation. We cannot neglect the nonlinear terms of the (perturbed) velocity distribution function ϕ [see Eq. (1.74)] when powers of k are considered, because $\phi = O(k)$ by the assumption. Thus, the basic equation is the (nonlinear) Boltzmann equation (1.75a) without $\partial/\partial\hat{t}$ term, i.e.,

$$\zeta_i \frac{\partial \phi}{\partial x_i} = \frac{1}{k}[\mathcal{L}(\phi) + \mathcal{J}(\phi, \phi)]. \tag{3.75}$$

The boundary condition [Eq. (1.64) or (1.69)] is written in an abstract form, i.e.,

$$\phi = \phi_w \quad (\zeta_i n_i > 0). \tag{3.76}$$

3.2.2 S expansion and fluid-dynamic-type equations

As in Section 3.1.2, we first look for a moderately varying solution of Eq. (3.75), whose length scale of variation is of the order of the characteristic length L of the system $[\partial\phi/\partial x_i = O(\phi)]$, in a power series of k, i.e.,

$$\phi_S = \phi_{S1}k + \phi_{S2}k^2 + \cdots, \tag{3.77}$$

where the series starts from the first-order term in k because $\phi = O(k)$, and $\phi_{Sm} = O(1)$ in contrast to ϕ_{Gm}. The subscript S is attached to discriminate this class of solution. The solution or expansion is called the *S solution* or *S expansion*. Corresponding to the expansion (3.77), the macroscopic variables ω, u_i, τ, etc. are also expanded in k, i.e.,

$$h_S = h_{S1}k + h_{S2}k^2 + \cdots, \tag{3.78}$$

where h represents ω, u_i, τ, etc. The relation between h_{Sm} and ϕ_{Sm} is obtained by expanding Eqs. (1.78a)–(1.78f) with $\phi = \phi_S$ and $h = h_S$, but their relation is a little complicated owing to the nonlinearity, in contrast to that of h_{Gm} and

ϕ_{Gm}. For example,

$$\omega_{S1} = \int \phi_{S1} E \mathbf{d}\boldsymbol{\zeta}, \tag{3.79a}$$

$$u_{iS1} = \int \zeta_i \phi_{S1} E \mathbf{d}\boldsymbol{\zeta}, \tag{3.79b}$$

$$\frac{3}{2}\tau_{S1} = \int \left(\zeta_i^2 - \frac{3}{2}\right) \phi_{S1} E \mathbf{d}\boldsymbol{\zeta}, \tag{3.79c}$$

$$P_{S1} = \omega_{S1} + \tau_{S1}, \tag{3.79d}$$

$$P_{ijS1} = 2\int \zeta_i \zeta_j \phi_{S1} E \mathbf{d}\boldsymbol{\zeta}, \tag{3.79e}$$

$$Q_{iS1} = \int \zeta_i \zeta_j^2 \phi_{S1} E \mathbf{d}\boldsymbol{\zeta} - \frac{5}{2} u_{iS1}, \tag{3.79f}$$

$$\omega_{S2} = \int \phi_{S2} E \mathbf{d}\boldsymbol{\zeta}, \tag{3.80a}$$

$$u_{iS2} = \int \zeta_i \phi_{S2} E \mathbf{d}\boldsymbol{\zeta} - \omega_{S1} u_{iS1}, \tag{3.80b}$$

$$\frac{3}{2}\tau_{S2} = \int \left(\zeta_i^2 - \frac{3}{2}\right) \phi_{S2} E \mathbf{d}\boldsymbol{\zeta} - u_{iS1}^2 - \frac{3}{2}\omega_{S1}\tau_{S1}, \tag{3.80c}$$

$$P_{S2} = \omega_{S2} + \tau_{S2} + \omega_{S1}\tau_{S1}, \tag{3.80d}$$

$$P_{ijS2} = 2\int \zeta_i \zeta_j \phi_{S2} E \mathbf{d}\boldsymbol{\zeta} - 2u_{iS1}u_{jS1}, \tag{3.80e}$$

$$Q_{iS2} = \int \zeta_i \zeta_j^2 \phi_{S2} E \mathbf{d}\boldsymbol{\zeta} - \frac{5}{2} u_{iS2} - u_{jS1} P_{ijS1} - \frac{3}{2} u_{iS1} P_{S1}. \tag{3.80f}$$

Substituting the series (3.77) into Eq. (3.75) and arranging the same-order terms in k, we obtain a series of linear integral equations for ϕ_{Sm}, i.e.,

$$\mathcal{L}(\phi_{S1}) = 0, \tag{3.81}$$

$$\mathcal{L}(\phi_{Sm}) = \zeta_i \frac{\partial \phi_{Sm-1}}{\partial x_i} - \sum_{r=1}^{m-1} \mathcal{J}(\phi_{Sm-r}, \phi_{Sr}) \quad (m = 2, 3, \ldots). \tag{3.82}$$

These are the same type of system as Eqs. (3.5) and (3.6) in the linear theory; the difference is the $\mathcal{J}$ terms in the inhomogeneous term.[35] From the last paragraph

[35]The collision term of the BKW equation is not in a bilinear form, and its expansion is more complicated than that shown here. The second term on the right-hand side is more complicated and should be taken as a symbol of the terms of expansion at this order as a whole. The linear part of the perturbation is given by Eq. (1.103). These comments apply to the whole discussion relating to expansion of the collision integral in the other parts of this book.

of Section A.2.2 and the relations (3.79a)–(3.79c), the solution ϕ_{S1} of Eq. (3.81) is given by

$$\phi_{S1} = \omega_{S1} + 2\zeta_i u_{iS1} + \left(\zeta_i^2 - \frac{3}{2}\right)\tau_{S1}. \tag{3.83}$$

From the condition for Eq. (1.83) to hold and the relation (1.84), the inhomogeneous term $\zeta_i \partial\phi_{Sm-1}/\partial x_i$ of Eq. (3.82) must satisfy the condition (solvability condition)

$$\int \varphi\zeta_i \frac{\partial\phi_{Sm-1}}{\partial x_i} E\mathbf{d\zeta} = 0 \quad (m = 2, 3, \ldots), \tag{3.84}$$

where

$$\varphi = 1,\ \zeta_j,\ \text{or}\ \zeta_k^2,$$

for the integral equation (3.82) to have a solution. Then, in view of the relation between h_{Sm} and ϕ_{Sm}, the solution of Eq. (3.82) is uniquely expressed in the following form:

$$\begin{aligned}\phi_{Sm} = \hat{\phi}_{Sm} + \omega_{Sm} + 2\zeta_i &\left(u_{iSm} + \sum_{r=1}^{m-1} \omega_{Sr} u_{iSm-r}\right) \\ &+ \left(\zeta_j^2 - \frac{3}{2}\right)\left\{\tau_{Sm} + \sum_{r=1}^{m-1}\left[\omega_{Sr}\tau_{Sm-r}\right.\right. \\ &\left.\left. + \frac{2}{3}\left(u_{iSr}u_{iSm-r} + \sum_{h=1}^{m-1-r} \omega_{Sr} u_{iSh} u_{iSm-r-h}\right)\right]\right\},\end{aligned} \tag{3.85}$$

where $\hat{\phi}_{Sm}$ is the particular solution of Eq. (3.82) orthogonal to φ, i.e.,

$$\int \varphi\hat{\phi}_{Sm} E\mathbf{d\zeta} = 0. \tag{3.86}$$

From the solvability condition (3.84), we obtain the following series of the *Navier–Stokes-type set* of equations for ω_{Sm}, u_{iSm}, τ_{Sm}, and P_{Sm}:

$$\frac{\partial P_{S1}}{\partial x_i} = 0, \tag{3.87}$$

$$\frac{\partial u_{iS1}}{\partial x_i} = 0, \tag{3.88a}$$

$$u_{jS1}\frac{\partial u_{iS1}}{\partial x_j} = -\frac{1}{2}\frac{\partial P_{S2}}{\partial x_i} + \frac{1}{2}\gamma_1 \frac{\partial^2 u_{iS1}}{\partial x_j^2}, \tag{3.88b}$$

$$u_{jS1}\frac{\partial \tau_{S1}}{\partial x_j} = \frac{1}{2}\gamma_2 \frac{\partial^2 \tau_{S1}}{\partial x_j^2}, \tag{3.88c}$$

$$\frac{\partial u_{jS2}}{\partial x_j} = -u_{jS1}\frac{\partial \omega_{S1}}{\partial x_j}, \tag{3.89a}$$

$$\begin{aligned} &u_{jS1}\frac{\partial u_{iS2}}{\partial x_j} + (\omega_{S1}u_{jS1} + u_{jS2})\frac{\partial u_{iS1}}{\partial x_j} \\ &\quad = -\frac{1}{2}\frac{\partial}{\partial x_i}\left(P_{S3} + \frac{2\gamma_3}{3}\frac{\partial^2 \tau_{S1}}{\partial x_j^2}\right) + \frac{\gamma_1}{2}\frac{\partial}{\partial x_j}\left(\frac{\partial u_{iS2}}{\partial x_j} + \frac{\partial u_{jS2}}{\partial x_i} - \frac{2}{3}\frac{\partial u_{kS2}}{\partial x_k}\delta_{ij}\right) \\ &\qquad + \frac{1}{2}\gamma_4\frac{\partial}{\partial x_j}\left[\tau_{S1}\left(\frac{\partial u_{iS1}}{\partial x_j} + \frac{\partial u_{jS1}}{\partial x_i}\right)\right], \end{aligned} \tag{3.89b}$$

$$\begin{aligned} &u_{jS1}\frac{\partial \tau_{S2}}{\partial x_j} + (\omega_{S1}u_{jS1} + u_{jS2})\frac{\partial \tau_{S1}}{\partial x_j} - \frac{2}{5}u_{jS1}\frac{\partial P_{S2}}{\partial x_j} \\ &\quad = \frac{1}{5}\gamma_1\left(\frac{\partial u_{iS1}}{\partial x_j} + \frac{\partial u_{jS1}}{\partial x_i}\right)^2 + \frac{1}{2}\frac{\partial^2}{\partial x_j^2}\left(\gamma_2\tau_{S2} + \frac{1}{2}\gamma_5{\tau_{S1}}^2\right), \end{aligned} \tag{3.89c}$$

where, from Eqs. (3.79d) and (3.80d),

$$P_{S1} = \omega_{S1} + \tau_{S1}, \quad P_{S2} = \omega_{S2} + \tau_{S2} + \omega_{S1}\tau_{S1}, \tag{3.90}$$

and the nondimensional transport coefficients γ_n's are constants related to the collision integral [γ_1, γ_2, and γ_3 are defined in Eq. (3.24); γ_4 and γ_5 will be defined in Eq. (3.98)].[36]

Equation (3.87) corresponds to the solvability condition (3.84) with $m = 2$ for $\varphi = \zeta_i$, and the two relations of the solvability condition (3.84) with $m = 2$ for $\varphi = 1$ and ζ_i^2 degenerate into a single equation (3.88a). Equations (3.88b) and (3.88c) correspond, respectively, to the conditions (3.84) with $m = 3$ for $\varphi = \zeta_i$ and ζ_i^2. Equation (3.89a) corresponds to the solvability condition (3.84) with $m = 3$ for $\varphi = 1$, and Eqs. (3.89b) and (3.89c) correspond, respectively, to the conditions (3.84) with $m = 4$ for $\varphi = \zeta_i$ and ζ_i^2. Owing to the degeneracy of the solvability conditions, the staggered combination of the solvability conditions with respect to m gives the consistent sets of equations to determine ω_{Sm}, u_{iSm}, τ_{Sm}, and P_{Sm+1} successively from the lowest order. In deriving those equations, as in the linear theory, we make use of the property that ϕ_{Sm} takes a special form in ζ_i owing to the isotropic property of the collision operators $\mathcal{L}$ and $\mathcal{J}$ (Sections A.2.5 and A.2.6). As is obvious from its derivation, the above Navier–Stokes-type set of equations corresponds to the conservation equations, i.e., Eqs. (3.88a) and (3.89a) to Eq. (1.12) or (1.87); Eqs. (3.87), (3.88b), and (3.89b) to Eq. (1.13) or (1.88); and Eqs. (3.88c) and (3.89c) to Eq. (1.14) or (1.89). The order of the above differential system remains unchanged if the level of approximation is advanced, in contrast to the Chapman–Enskog expansion (Chapman & Cowling [1952]) explained briefly in Section B.4.

The velocity distribution function ϕ_{Sm} is given in the following form:

$$\phi_{S1} = \phi_{eS1}, \tag{3.91}$$

$$\phi_{S2} = \phi_{eS2} - \zeta_i\zeta_j B(\zeta)\frac{\partial u_{iS1}}{\partial x_j} - \zeta_i A(\zeta)\frac{\partial \tau_{S1}}{\partial x_i}, \tag{3.92}$$

[36] See Footnote 4 in Section 3.1.2.

where

$$\left.\begin{aligned}
\phi_{eS1} &= \omega_{S1} + 2\zeta_i u_{iS1} + \left(\zeta_j^2 - \frac{3}{2}\right)\tau_{S1}, \\
\phi_{eS2} &= \omega_{S2} + 2\zeta_i u_{iS2} + \left(\zeta_j^2 - \frac{3}{2}\right)\tau_{S2} \\
&\quad + 2\zeta_i \omega_{S1} u_{iS1} + \left(\zeta_j^2 - \frac{3}{2}\right)\left(\frac{2}{3}u_{iS1}^2 + \omega_{S1}\tau_{S1}\right) \\
&\quad + 2\left(\zeta_i\zeta_j - \frac{1}{3}\zeta_k^2\delta_{ij}\right)u_{iS1}u_{jS1} + 2\zeta_i\left(\zeta_j^2 - \frac{5}{2}\right)u_{iS1}\tau_{S1} \\
&\quad + \left(\frac{1}{2}\zeta_i^2\zeta_j^2 - \frac{5}{2}\zeta_i^2 + \frac{15}{8}\right)\tau_{S1}^2,
\end{aligned}\right\} \tag{3.93}$$

and $A(\zeta)$ and $B(\zeta)$ are defined by Eq. (3.19) or (A.130). The ϕ_{eS1} and ϕ_{eS2} are the first two component functions of the expansion of the local Maxwellian in the power series of k, i.e.,

$$\begin{aligned}
E(1+\phi_{eS}) &= \frac{1+\omega_S}{\pi^{3/2}(1+\tau_S)^{3/2}} \exp\left(-\frac{(\zeta_i - u_{iS})^2}{1+\tau_S}\right) \\
&= E(1 + \phi_{eS1}k + \phi_{eS2}k^2 + \cdots).
\end{aligned} \tag{3.94}$$

The coefficient functions of the S expansion of the stress tensor P_{ij} and heat-flow vector Q_i are given as follows:

$$\left.\begin{aligned}
P_{ijS1} &= P_{S1}\delta_{ij}, \\
P_{ijS2} &= P_{S2}\delta_{ij} - \gamma_1\left(\frac{\partial u_{iS1}}{\partial x_j} + \frac{\partial u_{jS1}}{\partial x_i}\right), \\
P_{ijS3} &= P_{S3}\delta_{ij} - \gamma_1\left(\frac{\partial u_{iS2}}{\partial x_j} + \frac{\partial u_{jS2}}{\partial x_i} - \frac{2}{3}\frac{\partial u_{kS2}}{\partial x_k}\delta_{ij}\right) \\
&\quad -\gamma_4\tau_{S1}\left(\frac{\partial u_{iS1}}{\partial x_j} + \frac{\partial u_{jS1}}{\partial x_i}\right) + \gamma_3\left(\frac{\partial^2\tau_{S1}}{\partial x_i\partial x_j} - \frac{1}{3}\frac{\partial^2\tau_{S1}}{\partial x_k^2}\delta_{ij}\right),
\end{aligned}\right\} \tag{3.95}$$

$$\left.\begin{aligned}
Q_{iS1} &= 0, \\
Q_{iS2} &= -\frac{5}{4}\gamma_2\frac{\partial\tau_{S1}}{\partial x_i}, \\
Q_{iS3} &= -\frac{5}{4}\gamma_2\frac{\partial\tau_{S2}}{\partial x_i} - \frac{5}{4}\gamma_5\tau_{S1}\frac{\partial\tau_{S1}}{\partial x_i} + \frac{1}{2}\gamma_3\frac{\partial^2 u_{iS1}}{\partial x_j^2},
\end{aligned}\right\} \tag{3.96}$$

where γ_1, γ_2, and γ_3 are defined in Eq. (3.24), and γ_4 and γ_5 are defined as follows. Functions $C(\zeta)$, $D(\zeta)$, and $G(\zeta)$ of ζ are first defined by the equations

$$\left.\begin{aligned}
2\mathcal{J}\big(\zeta^2 - \tfrac{3}{2}, \zeta_i\zeta_j B(\zeta)\big) &= \zeta_i\zeta_j C(\zeta) + \delta_{ij}D(\zeta), \\
2\mathcal{J}\big(\zeta^2 - \tfrac{3}{2}, \zeta_i A(\zeta)\big) &= \zeta_i G(\zeta).
\end{aligned}\right\} \tag{3.97}$$

These forms of equations are compatible owing to the isotropic property of the collision operator $\mathcal{J}$. With $A(\zeta)$, $B(\zeta)$, $C(\zeta)$, and $G(\zeta)$, the nondimensional

transport coefficients γ_4 and γ_5 are defined by the equations

$$\left.\begin{aligned} \gamma_4 &= -\tfrac{5}{2}\gamma_1 + I_8(B) + \tfrac{1}{2}I_6(BC), \\ \gamma_5 &= -6\gamma_2 + 2I_8(A) + 2I_4(AG), \end{aligned}\right\} \tag{3.98}$$

where I_n is defined by Eq. (3.25). For a hard-sphere gas,[37]

$$\gamma_4 = \gamma_1/2 = 0.635021, \qquad \gamma_5 = \gamma_2/2 = 0.961142, \tag{3.99}$$

and for the BKW model,

$$\gamma_4 = \gamma_5 = 1. \tag{3.100}$$

The last term of P_{ijS3}, i.e., $\gamma_3[\partial^2\tau_{S1}/\partial x_i\partial x_j - \frac{1}{3}(\partial^2\tau_{S1}/\partial x_k^2)\delta_{ij}]$, is the *thermal stress*. The thermal stress is no longer balanced over a closed surface (or a control surface) in the gas in contrast to the case of the linearized theory (see the last paragraph of Section 3.1.3), but it can be treated by the combination with P_{S3} unless the boundary condition on P_{S3} is involved, that is, the sum $P_{S3} + \frac{2}{3}\gamma_3\partial^2\tau_{S1}/\partial x_j^2$ can be taken as a single variable (a modified pressure) [see Eq. (3.89b)]. The term $\frac{1}{2}\gamma_3\partial^2 u_{iS1}/\partial x_j^2$ in Q_{iS3} is not reduced only to the pressure gradient because of the convection term $u_{jS1}\partial u_{iS1}/\partial x_j$ in Eq. (3.88b). The terms with γ_4 and γ_5 are due to the dependence of the viscosity and thermal conductivity on the temperature of the gas.

3.2.3 Knudsen layer and slip boundary condition

The S solution ϕ_S, as the Grad–Hilbert solution ϕ_G, does not have enough freedom to be fitted to the kinetic boundary condition (3.76), because each term ϕ_{Sm} of the expansion is of a special form of ζ_i. Thus, we put the solution ϕ of the boundary-value problem (3.75) and (3.76) as the sum of two terms, the overall solution ϕ_S (S solution) and its correction ϕ_K in a neighborhood of the boundary, i.e.,

$$\phi = \phi_S + \phi_K, \tag{3.101}$$

where ϕ_K is assumed to have the behavior $[kn_i\partial\phi_K/\partial x_i = O(\phi_K)]$ similar to that of ϕ_K in Section 3.1.4, that is, ϕ_K is appreciable only in a thin layer, with thickness of the order of the mean free path, adjacent to the boundary and decays very rapidly in the layer in the direction normal to the boundary.[38] The ϕ_S is called *the fluid-dynamic part*, and ϕ_K is the *Knudsen-layer part* (or *correction*).[39] Substituting Eq. (3.101) into Eq. (3.75) and noting that ϕ_S

[37] See Footnote 10 in Section 4.3 of Sone [2002] about the relation between γ_1 and γ_4 and that between γ_2 and γ_5.

[38] The decay faster than any inverse power of η, defined in Eq. (3.103), is assumed, which is required for clear separation of ϕ_S and ϕ_K. See Footnote 6 in Section 3.1.4.

[39] The ϕ_S (and $\hat{f}_{SB}$ in Section 3.3.2, $\hat{f}_h$ and $\hat{f}_V$ in Section 3.4.1, or $\hat{f}_H$ in Section 3.5.1) is a solution of the Boltzmann equation or a closed function by itself. The corresponding macroscopic variables are related to it by Eqs. (1.78a)–(1.78f) [and by Eqs. (1.54a)–(1.54f)]. The Knudsen-layer correction ϕ_K (and $\hat{f}_K$ in Section 3.3.2, 3.4.1, or 3.5.1) is defined as the remainder. Thus, the equation for ϕ_K (and $\hat{f}_K$ in Section 3.3.2, 3.4.1, or 3.5.1) contains ϕ_S (and $\hat{f}_{SB}$, $\hat{f}_V$, or $\hat{f}_H$). Similar statements apply to the macroscopic variables.

satisfies Eq. (3.75), we obtain

$$\zeta_i n_i \frac{\partial \phi_K}{\partial \eta} = \mathcal{L}(\phi_K) + 2\mathcal{J}(\phi_S, \phi_K) + \mathcal{J}(\phi_K, \phi_K) - k\zeta_i \left(\frac{\partial \chi_1}{\partial x_i} \frac{\partial \phi_K}{\partial \chi_1} + \frac{\partial \chi_2}{\partial x_i} \frac{\partial \phi_K}{\partial \chi_2} \right). \tag{3.102}$$

Here, the Knudsen-layer variables (η, χ_1, χ_2) are introduced [Eq. (3.31) and its explanation], i.e.,

$$x_i = k\eta n_i(\chi_1, \chi_2) + x_{wi}(\chi_1, \chi_2), \tag{3.103}$$

where $x_i = x_{wi}(\chi_1, \chi_2)$ is the boundary surface.

The equation (3.102) contains the product term of ϕ_S and ϕ_K in contrast to the linear theory. In the product term, the series expansion of ϕ_S with respect to η, i.e.,

$$\begin{aligned} \phi_S &= (\phi_S)_0 + \left(\frac{\partial \phi_S}{\partial x_i} \right)_0 n_i k\eta + \cdots \\ &= (\phi_{S1})_0 k + \left[(\phi_{S2})_0 + \left(\frac{\partial \phi_{S1}}{\partial x_i} \right)_0 n_i \eta \right] k^2 + \cdots, \end{aligned} \tag{3.104}$$

where the quantities in the parentheses $(\quad)_0$ with subscript 0 are evaluated at $\eta = 0$, can be used owing to the assumption of the fast decay of ϕ_K with η. In the expansion, η always appears in the form $k\eta$ and this leads to a reshuffle of the order of k in the expansion of ϕ_S. The ϕ_K is also expanded in the power series of k, i.e.,

$$\phi_K = \phi_{K1} k + \phi_{K2} k^2 + \cdots . \tag{3.105}$$

Substituting the expansions (3.104) and (3.105) into Eq. (3.102) and arranging the same-order terms in k, we obtain a series of one-dimensional (homogeneous or inhomogeneous) linearized Boltzmann equations for ϕ_{Km}, i.e.,

$$\zeta_i n_i \frac{\partial \phi_{K1}}{\partial \eta} = \mathcal{L}(\phi_{K1}), \tag{3.106}$$

$$\zeta_i n_i \frac{\partial \phi_{K2}}{\partial \eta} = \mathcal{L}(\phi_{K2}) + 2\mathcal{J}((\phi_{S1})_0, \phi_{K1}) + \mathcal{J}(\phi_{K1}, \phi_{K1}) - \zeta_i \left[\left(\frac{\partial \chi_1}{\partial x_i} \right)_0 \frac{\partial \phi_{K1}}{\partial \chi_1} + \left(\frac{\partial \chi_2}{\partial x_i} \right)_0 \frac{\partial \phi_{K1}}{\partial \chi_2} \right]. \tag{3.107}$$

In the Knudsen-layer equations, the terms relating to ϕ_S are evaluated at $\eta = 0$, which makes the analysis simple.

Corresponding to Eq. (3.101), the Knudsen-layer corrections ω_K, u_{iK}, τ_K, etc. of the macroscopic variables ω, u_i, τ, etc. are defined as the remainders $\omega_K = \omega - \omega_S$, $u_{iK} = u_i - u_{iS}$, $\tau_K = \tau - \tau_S$, etc. The Knudsen-layer corrections h_K $(= h - h_S)$ of the macroscopic variables are also expanded, i.e.,

$$h_K = h_{K1} k + h_{K2} k^2 + \cdots , \tag{3.108}$$

where h represents ω, u_i, τ, etc. The Knudsen-layer correction h_K depends on ϕ_S as well as ϕ_K because the relations between the macroscopic variables and the velocity distribution function ϕ, i.e., Eqs. (1.78a)–(1.78f), are nonlinear.[40] For example,

$$u_{iK} = \frac{1}{1+\omega_S+\omega_K}\left(\int \zeta_i \phi_K E \mathbf{d}\boldsymbol{\zeta} - u_{iS}\omega_K\right),$$

or

$$\left.\begin{aligned} u_{iK1} &= \int \zeta_i \phi_{K1} E \mathbf{d}\boldsymbol{\zeta}, \\ u_{iK2} &= \int \zeta_i \phi_{K2} E \mathbf{d}\boldsymbol{\zeta} - (\omega_{S1})_0 u_{iK1} - (u_{iS1})_0 \omega_{K1} - \omega_{K1} u_{iK1}. \end{aligned}\right\} \tag{3.109}$$

The boundary condition for ϕ_{Km} is as follows: at $\eta = 0$,

$$\phi_{Km} = \phi_{wm} - \phi_{Sm} \qquad (\zeta_i n_i > 0), \tag{3.110}$$

where ϕ_{wm} is the expansion coefficient of ϕ_w, i.e.,

$$\phi_w = \phi_{w1}k + \phi_{w2}k^2 + \cdots, \tag{3.111}$$

and as $\eta \to \infty$,

$$\phi_{Km} \to 0, \tag{3.112}$$

where the decay is assumed to be faster than any inverse power of η. This assumption is verified in Bardos, Caflisch & Nicolaenko [1986].

From the analysis of the half-space problem of the linearized (homogeneous or inhomogeneous) Boltzmann equation [Eq. (3.106) or (3.107) and Eqs. (3.110) and (3.112)], we obtain the slip boundary condition for the Navier–Stokes-type set of equations and the Knudsen-layer correction by a process similar to that explained in the latter half part of Section 3.1.4.

Here are summarized the slip boundary condition and the Knudsen-layer correction for the macroscopic variables on a simple boundary and on an interface of a gas and its condensed phase (Sone [1971, 1991a, c], Onishi & Sone [1979], Sone [2002]). The formulas apply to a locally isotropic boundary,[41] where the reflection law is expressed by Eq. (1.64) with a finite diffuse reflection part or by Eq. (1.69) with a finite complete condensation part.[42]

On a simple solid boundary

$$u_{iS1} - u_{wi1} = 0, \tag{3.113a}$$

$$\tau_{S1} - \tau_{w1} = 0, \tag{3.113b}$$

$$u_{iK1} = \omega_{K1} = \tau_{K1} = 0, \tag{3.113c}$$

[40] See the preceding Footnote 39.
[41] See Footnote 13 in Section 3.1.5.
[42] See Footnote 14 in Section 3.1.5.

$$\begin{bmatrix} (u_{iS2}-u_{wi2})t_i \\ u_{iK2}t_i \end{bmatrix} = S_{ijS1}n_it_j \begin{bmatrix} k_0 \\ Y_0(\eta) \end{bmatrix} + G_{iS1}t_i \begin{bmatrix} K_1 \\ \frac{1}{2}Y_1(\eta) \end{bmatrix}, \quad (3.114a)$$

$$\begin{bmatrix} u_{iS2}n_i \\ u_{iK2}n_i \end{bmatrix} = 0, \quad (3.114b)$$

$$\begin{bmatrix} \tau_{S2}-\tau_{w2} \\ \omega_{K2} \\ \tau_{K2} \end{bmatrix} = -G_{iS1}n_i \begin{bmatrix} d_1 \\ \Omega_1(\eta) \\ \Theta_1(\eta) \end{bmatrix}, \quad (3.114c)$$

$$S_{ijSm} = -\left(\frac{\partial u_{iSm}}{\partial x_j} + \frac{\partial u_{jSm}}{\partial x_i}\right), \qquad G_{iSm} = -\frac{\partial \tau_{Sm}}{\partial x_i},$$

where the t_i is a unit vector tangential to the boundary, u_{wim} and τ_{wm} are the component functions of the expansions of u_{wi} ($u_{wi}n_i = 0$) and τ_w, i.e., $u_{wi} = u_{wi1}k + u_{wi2}k^2 + \cdots$ and $\tau_w = \tau_{w1}k + \tau_{w2}k^2 + \cdots$, the slip coefficients k_0, K_1, and d_1 and the Knudsen-layer functions $Y_0(\eta)$, $Y_1(\eta)$, $\Omega_1(\eta)$, and $\Theta_1(\eta)$ are the same as those in the linear theory, and the quantities with the subscript S are evaluated on the boundary.

The Knudsen-layer parts of the stress tensor P_{ij} and the heat-flow vector Q_i are

$$P_{ijK1} = 0, \quad (3.115)$$

$$P_{ijK2} = -\tfrac{3}{2}G_{kS1}n_k[\Omega_1(\eta) + \Theta_1(\eta)](\delta_{ij} - n_in_j), \quad (3.116)$$

$$Q_{iK1} = 0, \quad (3.117)$$

$$Q_{iK2}n_i = 0, \quad Q_{iK2}t_i = -S_{ijS1}t_in_jH_A(\eta) - G_{iS1}t_iH_B(\eta), \quad (3.118)$$

where $H_A(\eta)$ and $H_B(\eta)$ are the same as those in the linear theory, and the quantities with the subscript S are evaluated on the boundary.

The slip boundary condition and the Knudsen-layer correction up to the second order of k are essentially the same as those (up to the first order of k) in the linear theory.

On an interface of a gas and its condensed phase

$$(u_{iS1}-u_{wi1})t_i = 0, \quad (3.119a)$$

$$u_{iK1} = 0, \quad (3.119b)$$

$$\begin{bmatrix} P_{S1}-P_{w1} \\ \tau_{S1}-\tau_{w1} \\ \omega_{K1} \\ \tau_{K1} \end{bmatrix} = u_{iS1}n_i \begin{bmatrix} C_4^* \\ d_4^* \\ \Omega_4^*(\eta) \\ \Theta_4^*(\eta) \end{bmatrix}, \quad (3.119c)$$

$$\begin{bmatrix} (u_{iS2}-u_{wi2})t_i \\ u_{iK2}t_i \end{bmatrix} = S_{ijS1}n_it_j \begin{bmatrix} k_0 \\ Y_0(\eta) \end{bmatrix} + G_{iS1}t_i \begin{bmatrix} K_1 \\ \frac{1}{2}Y_1(\eta) \end{bmatrix} + t_j\frac{\partial}{\partial x_j}(u_{iS1}n_i) \begin{bmatrix} K_2 \\ Y_{K2}(\eta) \end{bmatrix}, \tag{3.120a}$$

$$u_{iK2}n_i = -(u_{iS1}n_i)^2\Omega_4^*(\eta), \tag{3.120b}$$

$$\begin{aligned} \begin{bmatrix} P_{S2}-P_{w2} \\ \tau_{S2}-\tau_{w2} \\ \omega_{K2} \\ \tau_{K2} \end{bmatrix} &= u_{iS2}n_i \begin{bmatrix} C_4^* \\ d_4^* \\ \Omega_4^*(\eta) \\ \Theta_4^*(\eta) \end{bmatrix} - G_{iS1}n_i \begin{bmatrix} C_1 \\ d_1 \\ \Omega_1(\eta) \\ \Theta_1(\eta) \end{bmatrix} \\ &\quad -S_{ijS1}n_in_j \begin{bmatrix} C_6 \\ d_6 \\ \Omega_6(\eta) \\ \Theta_6(\eta) \end{bmatrix} - 2\bar{\kappa}u_{iS1}n_i \begin{bmatrix} C_7 \\ d_7 \\ \Omega_7(\eta) \\ \Theta_7(\eta) \end{bmatrix} \\ &\quad +(u_{iS1}n_i)^2 \begin{bmatrix} C_8 \\ d_8 \\ \Omega_8(\eta) \\ \Theta_8(\eta) \end{bmatrix} + \tau_{w1}u_{iS1}n_i \begin{bmatrix} C_9 \\ d_9 \\ \Omega_9(\eta) \\ \Theta_9(\eta) \end{bmatrix} \\ &\quad +P_{w1}u_{iS1}n_i \begin{bmatrix} C_{10} \\ d_{10} \\ \Omega_{10}(\eta) \\ \Theta_{10}(\eta) \end{bmatrix}, \end{aligned} \tag{3.120c}$$

where P_{wm}, similarly to u_{wim} and τ_{wm}, is the component function of the expansion of P_w, i.e., $P_w = P_{w1}k + P_{w2}k^2 + \cdots$, the slip (jump) coefficients C_4^*, d_4^*, k_0, K_1, K_2, C_1, d_1, C_6, d_6, C_7, and d_7 and the Knudsen-layer functions $\Omega_4^*(\eta)$, $\Theta_4^*(\eta)$, $Y_0(\eta)$, $Y_1(\eta)$, $Y_{K2}(\eta)$, $\Omega_1(\eta)$, $\Theta_1(\eta)$, $\Omega_6(\eta)$, $\Theta_6(\eta)$, $\Omega_7(\eta)$, and $\Theta_7(\eta)$ are the same as those in the linear theory,[43] and the quantities with the subscript S are evaluated on the interface. The $\bar{\kappa}/L$ is the mean curvature of the boundary.[44] The leading terms of the slip condition and the Knudsen-layer correction are essentially the same as those in the linear theory.

For the BKW equation under the complete-condensation condition, the remaining coefficients C_8, d_8, C_9, d_9, C_{10}, and d_{10} and the Knudsen-layer functions $\Omega_8(\eta)$, $\Theta_8(\eta)$, $\Omega_9(\eta)$, $\Theta_9(\eta)$, $\Omega_{10}(\eta)$, and $\Theta_{10}(\eta)$ are obtained (Onishi & Sone [1979]).[45] The slip coefficients are

$$\left.\begin{array}{lll} C_8 = 2.320074, & C_9 = 1.066019, & C_{10} = C_4^*, \\ d_8 = -0.0028315, & d_9 = -0.223375, & d_{10} = 0. \end{array}\right\} \tag{3.121}$$

[43] See the note (v) after Eq. (3.57c).

[44] See the note (iii) after Eq. (3.42c).

[45] In Onishi & Sone [1979], $\int_0^\eta [1+\omega(\eta_0)]\mathrm{d}\eta_0$ instead of η is used as a Knudsen-layer variable. The difference affects (Ω_8, Θ_8), (Ω_9, Θ_9), and (Ω_{10}, Θ_{10}) (Footnote 18 in Chapter 4 of Sone [2002] needs correction).

The Knudsen-layer parts of the stress tensor P_{ij} and the heat-flow vector Q_i are given by

$$P_{ijK1} = \tfrac{3}{2} u_{kS1} n_k [\Omega_4^*(\eta) + \Theta_4^*(\eta)](\delta_{ij} - n_i n_j), \tag{3.122}$$

$$P_{ijK2} n_i n_j = 3\bar{\kappa} u_{iS1} n_i \int_\infty^\eta [\Omega_4^*(\eta_0) + \Theta_4^*(\eta_0)] \mathrm{d}\eta_0, \tag{3.123a}$$

$$P_{ijK2} n_i t_j = -\tfrac{3}{2} t_j \frac{\partial u_{iS1} n_i}{\partial x_j} \int_\infty^\eta [\Omega_4^*(\eta_0) + \Theta_4^*(\eta_0)] \mathrm{d}\eta_0, \tag{3.123b}$$

$$Q_{iK1} = 0, \tag{3.124}$$

$$Q_{iK2} n_i = (u_{kS1} n_k)^2 \left(\Omega_4^*(\eta) - \tfrac{3}{2} \Theta_4^*(\eta) \right), \tag{3.125}$$

where $u_{iS1} n_i$ is evaluated on the interface.

3.2.4 Rarefaction effect of a gas

The equations (3.88a)–(3.88c) are apparently the Navier–Stokes set of equations for an incompressible fluid.[46] By closer examination, Eq. (3.88c) is a little different from the energy equation in the Navier–Stokes set of equations for an incompressible fluid [$v_i \partial\rho/\partial X_i = 0$ (or $u_i \partial\omega/\partial x_i = 0$)] under the present situation with a small velocity ($u_i \ll 1$ or small Mach number), a small temperature variation ($\tau \ll 1$), and a finite Reynolds number. In the latter, the convection term $u_{jS1} \partial\tau_{S1}/\partial x_j$ in Eq. (3.88c) should be replaced by $(3/5) u_{jS1} \partial\tau_{S1}/\partial x_j$. This difference comes from the fact that the work done by pressure on a volume of the gas is of higher order in the incompressible fluid under the present situation.[47] That is, an effect of compressibility enters Eq. (3.88c). However, if we consider an incompressible fluid with the internal energy multiplied by 5/3

[46]The definition of *incompressible fluid* is that the density ρ of a given mass of fluid is invariable with change of its state. Thus, in a fluid in motion, the density is invariable along the fluid-particle path, i.e., $\partial\rho/\partial t + v_i \partial\rho/\partial X_i = 0$. It is a kind of the equation of state. Then, the conservation equation (1.12) of mass for an incompressible fluid reduces to $\partial v_i/\partial X_i = 0$ irrespective of a time-independent or time-dependent state. The Navier–Stokes set of equations for an incompressible fluid is the set of equations (1.12)–(1.14) with Eq. (1.16) supplemented by the above equation as the equation of state. Incidentally, there are sometimes found erroneous discussions where another equation of state, e.g., the equation of perfect gas $p = R\rho T$, is used in addition to the incompressibility condition.

[47]Let $-p_0 (2RT_0)^{1/2} L^2 W_p$ be the work done per unit time by the pressure on a domain V of the gas. Then, $W_p = \int_{\partial V} (1+P) u_i \hat{n}_i \mathrm{d}S = \int_V \partial(1+P) u_i / \partial x_i \mathbf{dx}$, where $\hat{n}_i$ is the outward unit normal vector to the boundary ∂V of V. In the weakly nonlinear problem, this is rewritten as $W_p = k^2 \int_V \partial u_{iS2}/\partial x_i \mathbf{dx} + \cdots$, because of the relation $(1+P) u_i = u_{iS1} k + (u_{iS2} + P_{S1} u_{iS1}) k^2 + \cdots$ and Eqs. (3.87) and (3.88a). Noting Eqs. (3.87), (3.89a), and (3.90), we find that $W_p = k^2 \int_V (u_{iS1} \partial\tau_{S1}/\partial x_i) \mathbf{dx} + \cdots$. Whereas, the work W_p is $O(|u_i|^3)$ in an incompressible fluid, because $\partial u_i/\partial x_i = 0$ and $\partial P/\partial x_i$ is $O(|u_i|^2)$ from the momentum equation. This agrees with the difference of the two equations because Eq. (3.88c) is 2/5 of the energy conservation equation (1.89). The gas under consideration, generally the gas discussed in this book, is not incompressible because the variation ω of the density is of the same order as that τ of the temperature. However, under the situation of the S expansion, the fluid-dynamic-type equations for the flow velocity at the leading order are of the same form as the equations for an incompressible fluid.

(or with the thermal conductivity multiplied by 3/5), the set (3.87)–(3.88c) is the same as the incompressible Navier–Stokes set.[48] For economy of words, we will, hereafter, call the set of equations *"the Navier–Stokes set of equations for an incompressible fluid"* or *"the incompressible Navier–Stokes set of equations"* with the quotation mark.

The next-order equations (3.89a)–(3.89c) [together with Eqs. (3.87), (3.88a)–(3.88c)] are very much like the Navier–Stokes set of equations for a slightly compressible fluid, but there is a difference. Substituting the Mach number expansion of the macroscopic variables in the Navier–Stokes set of equations for a compressible fluid[49] and transforming the Mach number expansion to the Knudsen number expansion with the aid of Eq. (3.74), then we successively obtain the equations (3.87), (3.88a)–(3.88c), and (3.89a)–(3.89c) with $\gamma_3 = 0$. The difference comes from the thermal stress in P_{ijS3} in Eq. (3.95). Introducing a new variable P^*_{S3}:

$$P^*_{S3} = P_{S3} + \frac{2\gamma_3}{3}\frac{\partial^2 \tau_{S1}}{\partial x_i^2}, \tag{3.126}$$

we can incorporate the γ_3 term in the pressure term. Thus, Eqs. (3.89a)–(3.89c) are apparently of the same form as the expansion of the Navier–Stokes set of equations. Further the slip conditions in Eqs. (3.113a)–(3.114c) or in Eqs. (3.119a)–(3.120c) do not contain P_{S3}. Thus, we have the proposition

Proposition 3.2.1. *Except for the Knudsen-layer correction, the macroscopic variables of a slightly rarefied gas are obtained correctly up to the second order of the Knudsen number (i.e., up to ω_{S2}, u_{iS2}, τ_{S2}, etc.) by solving the Navier–Stokes sets of equations for a slightly compressible fluid (giving up to the corresponding order) under the slip boundary conditions in Eqs.* (3.113a)–(3.114c) *or in Eqs.* (3.119a)–(3.120c). *The effect of rarefaction of the gas comes in only through the slip boundary conditions.*[50]

3.2.5 Force and mass and energy transfers on a closed body

We will give the extension of the propositions on the force and the moment of force or the mass and energy transfers on a closed (or bounded) body in the linear theory (Section 3.1.7) to the present weakly nonlinear case. The proof is given in Sone & Aoki [1987] and Sone [2002].

Consider the total force, total moment of force, and total mass and energy transfers on a closed (or bounded) body in a gas. These global quantities can be obtained only by the knowledge of the fluid-dynamic part as follows. The

[48] The difference is more serious in a time-dependent problem (see Section 3.7.2). It is widely said that the small Mach number limit of the compressible Navier–Stokes set of equations gives the incompressible Navier–Stokes set, but it is not exact from the above comment.

[49] The temperature variation in the gas relative to its temperature is assumed to be of the order of the Mach number in accordance with the discussion in this section (or Section 3.2).

[50] The fluid-dynamic-type system for a nontrivial state being the same as that of classical fluid dynamics, 'the effect of rarefaction of a gas' is used for the next and higher-order contribution, though the nontrivial leading-order term is of the order of k (see Section 3.6).

body may be the condensed phase of the gas; there may be other bodies in the gas, or the domain may be enclosed by a boundary.

Proposition 3.2.2. *The force F_i and the moment MO_i of force (around the origin) acting on a closed body in a gas are expressed by the fluid-dynamic part ψ_{ijS} [$= P_{ijS}+2(1+\omega_S)u_{iS}u_{jS}$] of the (nondimensional) momentum-flow tensor as follows:*

$$F_i = -p_0 L^2 \int_S \psi_{ijS}\widehat{n}_j \mathrm{d}S, \tag{3.127}$$

$$MO_i = -p_0 L^3 \int_S \epsilon_{ilk} x_l \psi_{kjS}\widehat{n}_j \mathrm{d}S, \tag{3.128}$$

where the surface S of integration is a closed surface enclosing only the body under consideration, $\widehat{n}_i$ is the outward unit normal vector to the surface S, $\mathrm{d}S$ is the surface element (in the nondimensional x_i space) for integration, and ϵ_{ijk} is Eddington's epsilon.[51]

Corollary. *On a simple boundary, F_i/p_0L^2* and *MO_i/p_0L^3 are expressed only by P_{ijS} up to the third order of k.*

Proposition 3.2.3. *The mass MF and the energy ET transferred to a closed body in a gas per unit time are expressed by the fluid-dynamic parts ψ^m_{iS} [$= (1+\omega_S)u_{iS}$] and ψ^e_{iS} [$= \int \zeta_i\zeta_j^2\phi_S E\mathbf{d\zeta}=\frac{5}{2}u_{iS}+u_{jS}P_{ijS}+\frac{3}{2}P_S u_{iS}+(1+\omega_S)u_{iS}u_{jS}^2+Q_{iS}$] of the (nondimensional) mass-flow and energy-flow vectors as follows:*

$$MF = -\rho_0(2RT_0)^{1/2}L^2 \int_S \psi^m_{iS}\widehat{n}_i \mathrm{d}S, \tag{3.129}$$

$$ET = -p_0(2RT_0)^{1/2}L^2 \int_S \psi^e_{iS}\widehat{n}_i \mathrm{d}S, \tag{3.130}$$

where the definitions of S, $\mathrm{d}S$, and $\widehat{n}_i$ are the same as in Proposition 3.2.2.

Consider the contribution of the thermal stress. First rewrite the expression of P_{ijS3} given by Eq. (3.95) using P^*_{S3} defined by Eq. (3.126) as follows:

$$\begin{aligned} P_{ijS3} = {} & P^*_{S3}\delta_{ij} - \gamma_1\left(\frac{\partial u_{iS2}}{\partial x_j}+\frac{\partial u_{jS2}}{\partial x_i}-\frac{2}{3}\frac{\partial u_{kS2}}{\partial x_k}\delta_{ij}\right) \\ & -\gamma_4\tau_{S1}\left(\frac{\partial u_{iS1}}{\partial x_j}+\frac{\partial u_{jS1}}{\partial x_i}\right)+\gamma_3\left(\frac{\partial^2\tau_{S1}}{\partial x_i\partial x_j}-\frac{\partial^2\tau_{S1}}{\partial x_k^2}\delta_{ij}\right). \end{aligned} \tag{3.131}$$

We will call this expression the stress in the P^*_{S3} system. In this system the thermal stress (non-Newtonian stress) may be taken as

$$\gamma_3\left(\frac{\partial^2\tau_{S1}}{\partial x_i\partial x_j}-\frac{\partial^2\tau_{S1}}{\partial x_k^2}\delta_{ij}\right). \tag{3.132}$$

Proposition 3.2.4. *The non-Newtonian stress in the P^*_{S3} system contributes neither to the force nor to the moment of force on a closed body in a gas.*

From Propositions 3.2.1 and 3.2.4, we have

[51] See the definition in Footnote 30 in Section 3.1.7.

Proposition 3.2.5. *Under the condition of Proposition 3.2.1, the force and the moment of force on a closed body can be obtained up to the third order of k in the expressions F_i/p_0L^2 and MO_i/p_0L^3 by the classical gas dynamic calculation where the slip condition is taken into account. Here we mean by the classical gas dynamic calculation that the force or the moment of force is calculated with the aid of the Newtonian stress from the flow velocity and pressure fields obtained by solving the Navier–Stokes set of equations under the slip boundary condition.*

3.2.6 Summary

In this section we have discussed the asymptotic behavior of a gas for small Knudsen numbers in the case where the deviation from a uniform equilibrium state at rest is of the order of the Knudsen number. The outline of derivation and the formulas (up to the second order of the Knudsen number) of the fluid-dynamic-type equations and their associated slip boundary conditions were shown. It should be noted that the fluid-dynamic-type equations that are to be used with the slip conditions (3.114a)–(3.114c) or (3.120a) and (3.120c) are not the Navier–Stokes set of equations but contain the thermal stress term. After the discussion of Sections 3.2.4 and 3.2.5, it is found that the behavior of a gas up to this order can be treated by the Navier–Stokes set with the replacement (3.126). Incidentally, in the case where the temperature variation in a gas is not small (Section 3.3), the thermal-stress term cannot be included in the pressure term. This introduces an interesting result peculiar to a rarefied gas. Moreover, a serious result about the behavior of a gas in the continuum limit (or incompleteness of the classical fluid dynamics) is derived there.

In the situation of the present section, where the Mach number is of the order of the Knudsen number, the nonlinear effect cannot be neglected for any small Mach number because "the incompressible Navier–Stokes equations" are the leading-order fluid-dynamic-type equations. This is also shown by the numerical analysis of the BKW equation in Sone, Kataoka, Ohwada, Sugimoto & Aoki [1994]. In some infinite domain problems, the variation of the velocity distribution function becomes more and more moderate in the far field or the length scale of variation becomes larger and larger there. Accordingly, the effective Knudsen number becomes smaller and smaller, and a situation where the Mach number is comparable to the effective Knudsen number takes place, however small the Mach number may be. Thus, the nonlinear effect cannot be neglected for any small Mach number, and the linearized Boltzmann equation does not give a uniformly valid solution over the whole domain (Sone [1978], Onishi & Sone [1983]; see Section 7.2).

The fluid-dynamic-type equations derived by the S expansion are a series of the Navier–Stokes-type sets of equations with "the incompressible Navier–Stokes set of equations" as their leading set, and do not have the inconvenience that the degree of differentiation increases with the progress of approximation, which is encountered in the Chapman–Enskog expansion (Chapman & Cowling [1952] and Section B.4). Further the assumption that the velocity distribution function depends on the space variables only through the five macroscopic variables and

their derivatives is unnecessary, and it comes out as a result. The difficulty of the Chapman–Enskog expansion in the boundary-value problem is discussed in Cercignani [1988]. Incidentally, an ill-posed equation is derived from this expansion (see Tamada & Sone [1966], Sone [1968, 1984b]).[52]

[52] i) An initial or boundary-value problem of a partial differential equation is called a well-posed problem if (a) a solution exists, (b) the solution is unique, and (c) the solution depends continuously on the initial or boundary data of the problem; it is called ill-posed if it is not well posed (see Garabedian [1964], Zachmanoglou & Thoe [1986]). The equation derived does not satisfy the condition (c).

ii) Owing to the character of the fluid-dynamic-type equations derived by the Chapman–Enskog expansion that the order of the differential system increases with the advance of approximation, the sizes of the terms in the equations derived by that expansion increase with the advance of the approximation for sharply varying components, sharper than the length scale of variation of the order of k, in the initial condition or in the solution; for the time-independent equations, more and more freedoms with the length scale of variation of the order of k are introduced in the solution with the advance of approximation, and their sizes in the equations remain of the same order in their higher-order terms. Thus, the analysis neglecting these contributions results in the incorrect behavior of the sharply varying components and the awkward behavior of the solution. The following equation is derived by the Chapman–Enskog expansion from the linearized Boltzmann equation for a case with a special symmetry [let ϕ in Eq. (1.96) with Sh $= 1$ spatially depend only on x_2 and be odd in ζ_1, and transcript $\hat{t} \to t$, $x_2 \to x$, and $u_1 \to u$]:

$$\partial u/\partial t = k\textstyle\sum_{n=1}^{N} c_{2n} k^{2(n-1)} \partial^{2n} u/\partial x^{2n}, \qquad (*)$$

where $c_2 = \gamma_1/2 > 0$ in general [see Eqs. (3.26) and (A.136)], and $c_4 = 0.190$ (a hard-sphere gas) and $c_4 = 1/4$ (the BKW model). When $N = 1$ (Navier–Stokes level), it is the heat-conduction equation, and when $N = 2$ (superBurnett level), it is an ill-posed equation. The above-mentioned feature of the Chapman–Enskog solution is clear in Eq. $(*)$.

We will discuss the solution of the initial-value problem of Eq. $(*)$ more explicitly. Let the initial condition be given by

$$u = \textstyle\sum_{m=0}^{\infty} U_m \cos mx. \qquad (**).$$

The solution is expressed as

$$u = \textstyle\sum_{m=0}^{\infty} U_m \cos mx \exp\left[\left(\sum_{n=1}^{N} (-1)^n c_{2n} (km)^{2n}\right)(t/k)\right]. \qquad (\#)$$

Let us evaluate the contribution to the solution from different n terms when $k \ll 1$. For $m = O(1)$, the terms in the second $\sum$ sign become smaller by the factor k^2 with advance of n by one, and the number of such terms is finite. Thus, the contribution of the terms with finite m in the solution u decays by the factor k^2 as n increases by one for $0 < t < o(1/k)$. For km being of the order of unity, all the terms in the second $\sum$ sign are of the equal order, i.e., of the order of unity, and the size of the exponent is of the order of Nt/k. Depending on its sign determined by N, the exponential function diverges or decays in a small time t (but $\gg k$; e.g., $t = k^{1/2}$). For larger m, i.e., $km \gg 1$, the last term $(-1)^N c_{2N} (km)^{2N}$ in the second $\sum$ sign is dominant, and the behavior of the exponential function is determined by the term. If $(-1)^N c_{2N} > 0$, the function grows very rapidly with respect to t. Consider the case in which U_m is of the order of $1/m^S$ with $S \geq 2N + 2$, for which the initial function $(**)$ has its smooth derivatives up to the $2N$ order of the order of unity. Even for such a moderate initial condition, the Fourier coefficients diverge exponentially even for small time t (but $t/k > k^{-1/s}; s > 1$) because it is bounded from below by $(t/k)^{-sS}(km)^{-S} \exp[(-1)^N (c_{2N}/2)(km)^{2N}(t/k)]$. Thus, the solution of the initial-value problem of Eq. $(*)$ with $(-1)^N c_{2N} > 0$ diverges in an infinitely short time even for moderately varying initial data. That is, the problem is ill-posed.

From the discussion, we see that the higher-order equation contributes to the lower-order solution and that the behavior of the solution differs drastically with N. The series of equations is not an appropriate form as that for successive approximation. Careful interpretation and applications of the expansion are required.

3.3 Nonlinear problem I: Finite temperature variations and ghost effect

3.3.1 Problem

In Section 3.2, we discussed the case where the deviation of the system from a uniform equilibrium state at rest is of the order of the Knudsen number and derived a series of fluid-dynamic-type equations with "the incompressible Navier–Stokes set of equations"[53] as the leading set of equations. In this system, the variation of temperature of the gas (compared with the average temperature of the system) as well as the flow Mach number is limited to be a small quantity of the order of the Knudsen number. In the present section, we eliminate the restriction on the temperature variation, keeping the restriction on the flow velocity. The result is not just an extension of the formulas but contains a very important fact concerning the behavior of a gas in the continuum limit. That is, the classical fluid dynamics is found to be incomplete to describe the behavior of a gas in the continuum limit, in contradiction with its purpose. This problem will be discussed in Section 3.3.4. For the later application, we consider the system subject to a weak external force independent of molecular velocity, such as weak gravity.[54] Here, we use the notation introduced in Section 1.9.

The basic equation is the Boltzmann equation (1.47a) for a time-independent state, i.e.,

$$\zeta_i \frac{\partial \hat{f}}{\partial x_i} + \hat{F}_i \frac{\partial \hat{f}}{\partial \zeta_i} = \frac{1}{k} \hat{J}(\hat{f}, \hat{f}). \tag{3.133}$$

The boundary condition is symbolically expressed as

$$\hat{f}(x_i, \zeta_i) = \hat{f}_w \quad (\zeta_j n_j > 0). \tag{3.134}$$

On a simple boundary the boundary condition is generally given by Eq. (1.64) or more simply by the diffuse-reflection condition (1.63a) with (1.63b). On an interface of the gas and its condensed phase, the condition is given by Eq. (1.69) or more simply by the complete-condensation condition (1.68).

The additional conditions on the flow velocity $\hat{v}_i$ and the external force $\hat{F}_i$, which characterize the problem discussed in this section, are specified as

$$\int \zeta_i \hat{f} \mathbf{d\zeta} = O(k), \tag{3.135a}$$

$$\hat{F}_i = O(k^2). \tag{3.135b}$$

We consider this weak external force because bifurcation in the Bénard problem (Section 8.2) takes place for this size of the gravity.

[53] See Section 3.2.4 for the meaning of the quotation mark.

[54] The external force is considered in this section for application to the Bénard problem in Section 8.2, because this gives an interesting example concerning the behavior of a gas in the continuum limit.

We will discuss the asymptotic behavior for small Knudsen numbers (or small k) of the boundary-value problem of the Boltzmann equation, i.e., Eqs. (3.133) and (3.134), under the assumptions (3.135a) and (3.135b).[55]

In the following analysis, the boundary data $\hat{T}_w$, $\hat{v}_{wi}$, $\hat{p}_w$, as well as $\hat{f}_w$, are considered to depend on k and expanded in k, i.e.,

$$\left.\begin{aligned} \hat{T}_w &= \hat{T}_{w0} + \hat{T}_{w1}k + \cdots, \\ \hat{v}_{wi} &= \hat{v}_{wi1}k + \hat{v}_{wi2}k^2 + \cdots, \\ \hat{p}_w &= \hat{p}_{w0} + \hat{p}_{w1}k + \cdots, \\ \hat{f}_w &= \hat{f}_{w0} + \hat{f}_{w1}k + \cdots, \end{aligned}\right\} \tag{3.136}$$

where $\hat{v}_{wi}$ is required to start from the term of the order of k owing to the assumption (3.135a).

3.3.2 Outline of the analysis

We will outline the analysis of the boundary-value problem described in Section 3.3.1, referring to the principal results summarized in Section 3.3.3.

The behavior of the gas is expressed as the sum of the two terms, the overall solution or the fluid-dynamic part and the Knudsen-layer correction,

$$\hat{f} = \hat{f}_{SB} + \hat{f}_K, \tag{3.137}$$

where the overall solution $\hat{f}_{SB}$ is a solution of Eq. (3.133), subject to Eqs. (3.135a) and (3.135b) but with Eq. (3.134) put aside, whose length scale of variation is the reference length of the system, i.e., $\partial\hat{f}_{SB}/\partial x_i = O(\hat{f}_{SB})$.[56] The Knudsen-layer correction $\hat{f}_K$ is appreciable only in a thin layer, with thickness of the order of the mean free path, adjacent to the boundary and decays very rapidly in the layer in the direction normal to the boundary.[57]

The solution $\hat{f}_{SB}$, to be called *SB solution*, is obtained in a power series of k, i.e.,

$$\hat{f}_{SB} = \hat{f}_{SB0} + \hat{f}_{SB1}k + \cdots, \tag{3.138}$$

where the subscript *SB* is attached to discriminate the SB solution. Corresponding to this expansion, the macroscopic variables $\hat{\rho}$, $\hat{v}_i$, $\hat{T}$, etc. are also expanded in k, i.e.,

$$\hat{h}_{SB} = \hat{h}_{SB0} + \hat{h}_{SB1}k + \cdots, \tag{3.139}$$

where $\hat{h}$ represents $\hat{\rho}$, $\hat{v}_i$, $\hat{T}$, etc. The analysis of $\hat{f}_{SBm}$ is essentially the same as in the previous sections (Sections 3.1.2 and 3.2.2). Substituting the series (3.138)

[55] This is the extension of the work by Sone & Wakabayashi [1988] for the BKW equation to that for the standard Boltzmann equation with the weak external force (see Sone [2002] and Sone & Doi [2003a] for the details of analysis).

[56] See the first two sentences of Footnote 39 in Section 3.2.3.

[57] In addition to the condition $kn_i\partial\hat{f}_K/\partial x_i = O(\hat{f}_K)$, the decay faster than any inverse power of η, defined in Eq. (3.147), is assumed, which is required for clear separation of $\hat{f}_{SB}$ and $\hat{f}_K$. See Footnote 6 in Section 3.1.4.

into the Boltzmann equation (3.133), we obtain a series of integral equations for $\hat{f}_{SBm}$,[58] i.e.,

$$\hat{J}(\hat{f}_{SB0}, \hat{f}_{SB0}) = 0, \tag{3.140}$$

$$2\hat{J}(\hat{f}_{SB0}, \hat{f}_{SBm}) = \zeta_i \frac{\partial \hat{f}_{SBm-1}}{\partial x_i} - \sum_{r=1}^{m-1} \hat{J}(\hat{f}_{SBr}, \hat{f}_{SBm-r}) + \mathcal{H}_3(m)\hat{F}_{i2}\frac{\partial \hat{f}_{SBm-3}}{\partial \zeta_i} \qquad (m \geq 1), \tag{3.141}$$

where $\hat{F}_{i2} = \hat{F}_i/k^2$, the $\sum$ term is absent when $m = 1$, and $\mathcal{H}_3(m) = 1$ for $m \geq 3$ and $\mathcal{H}_3(m) = 0$ for $m \leq 2$.

From the last paragraph of Section A.7.1, the leading distribution $\hat{f}_{SB0}$ is Maxwellian, i.e.,

$$\hat{f}_{SB0} = \frac{\hat{\rho}_{SB0}}{(\pi \hat{T}_{SB0})^{3/2}} \exp\left(-\frac{(\zeta_i - \hat{v}_{iSB0})^2}{\hat{T}_{SB0}}\right). \tag{3.142}$$

From the assumption (3.135a),

$$\hat{v}_{iSB0} = 0. \tag{3.143}$$

With this condition, we proceed with the analysis under the assumption that the parametric functions $\hat{\rho}_{SB0}$ and $\hat{T}_{SB0}$ in the Maxwellian are of the order of unity. From the condition for Eq. (1.83) to hold and the relation (1.53),[59] the inhomogeneous term of the integral equation (3.141) must satisfy the following relation (solvability condition) for Eq. (3.141) to have a solution:

$$\int \psi_r \zeta_k \frac{\partial \hat{f}_{SBm-1}}{\partial x_k} \mathbf{d\zeta} - \mathcal{H}_3(m)\mathrm{IF}_r = 0, \tag{3.144}$$

where

$$\psi_0 = 1, \quad \psi_i = \zeta_i, \quad \psi_4 = \zeta_k^2,$$

$$\mathrm{IF}_0 = 0, \quad \mathrm{IF}_i = \hat{F}_{i2}\hat{\rho}_{SBm-3}, \quad \mathrm{IF}_4 = 2\hat{F}_{j2}\sum_{n=0}^{m-4} \hat{\rho}_{SBn}\hat{v}_{jSBm-3-n}.$$

In IF_4, the convention $\sum_{n=0}^{-1} \hat{\rho}_{SBn}\hat{v}_{jSBm-3-n} = 0$ is used. Let the solvability condition (3.144) be indicated by SC_m^r. The conditions SC_1^0 and SC_1^4 reduce to identities, and from SC_1^i and SC_2^i, $\hat{p}_{SB0}$ and $\hat{p}_{SB1}$ are constants [Eqs. (3.153) and (3.154) in Section 3.3.3]. Owing to the degeneracy, staggered combination with

[58] In view of Eq. (A.116), the collision operator $\hat{J}(\hat{f}_{SB0}, *)$ [or $\hat{J}(\hat{f}_{h0}, *)$, $\hat{J}(\hat{f}_{V0}, *)$, etc.] is reduced to the linearized one $\mathcal{L}_a(\dagger)$. Thus, Eq. (3.141) is practically of the same form as Eq. (3.82). For the BKW equation, see also Footnote 35 in Section 3.2.2 and Eq. (A.113).

[59] See Footnote 58 and note that Eq. (1.83) holds when and only when $\varphi(\boldsymbol{\zeta})$ is a linear combination of 1, ζ_i, and ζ_i^2.

respect to m of the solvability conditions gives a series of sets of equations that determines the macroscopic variables consistently from the lowest order. That is, SC_2^0, SC_2^4, and SC_3^i correspond, respectively, to Eqs. (3.155), (3.157), and (3.156). Generally, the set of equations derived from the solvability conditions SC_{m+2}^0, SC_{m+2}^4, and SC_{m+3}^i contains the functions $\hat{\rho}_{SBm}$, $\hat{T}_{SBm}$, $\hat{v}_{iSBm+1}$, and $\hat{p}_{SBm+2}$ as well as functions appeared in the equations at the previous stages [or the functions $\hat{\rho}_{SBn}$, $\hat{T}_{SBn}$, $\hat{v}_{iSBn+1}$, and $\hat{p}_{SBn+2}$ $(n \le m-1)$]. Thus, with the aid of the expanded form of the equation of state $\hat{p}_{SB} = \hat{\rho}_{SB}\hat{T}_{SB}$, the staggered combination of functions $\hat{\rho}_{SBm}$, $\hat{T}_{SBm}$, $\hat{v}_{iSBm+1}$, and $\hat{p}_{SBm+2}$ is determined consistently and successively from the lowest order by the rearranged sets of equations given by the solvability condition (3.144).

Noting the condition (1.66c) or (1.71c) with the uniqueness comment for the boundary condition (1.64) or (1.69), we find that the Maxwellian (3.142) with Eq. (3.143) can be matched with the boundary condition (1.64) or (1.69), if we take

$$\hat{T}_{SB0} = \hat{T}_{w0}, \tag{3.145}$$

on a simple boundary, or if we take

$$\hat{T}_{SB0} = \hat{T}_{w0}, \quad \hat{p}_{SB0} = \hat{p}_{w0}, \tag{3.146}$$

on the interface.[60] Equations (3.145) and (3.146), respectively, give the boundary condition for $\hat{T}_{SB0}$ on the simple boundary and that for $\hat{T}_{SB0}$ and $\hat{p}_{SB0}$ on the interface. For the higher orders, we have to introduce the Knudsen-layer correction $\hat{f}_K$ to make the solution satisfy the boundary condition (3.134). The analysis is similar to that in Section 3.2.3.

Substitute Eq. (3.137) into the Boltzmann equation (3.133) and rewrite it with the Knudsen-layer variables (η, χ_1, χ_2) introduced in Eq. (3.31), i.e.,

$$x_i = k\eta n_i(\chi_1, \chi_2) + x_{wi}(\chi_1, \chi_2), \tag{3.147}$$

where $x_i = x_{wi}(\chi_1, \chi_2)$ is the boundary surface. Then, the equation for $\hat{f}_K$ is

[60] From the above discussion, this is one choice. This can be shown to be unique. That is, we introduce the Knudsen-layer correction that is introduced in the higher-order analysis at this step and apply the result in Section 4.4 (for a simple boundary) and Golse's result mentioned there (for the complete-condensation condition) to the Knudsen-layer problem. The process from introduction of the Knudsen layer to the problem in Section 4.4 is similar to that in the paragraph containing Eqs. (3.222)–(3.224b) in Section 3.5.1. Then, we find that the condition (3.145) or (3.146) must be satisfied and that the Knudsen-layer correction vanishes. The proof is not yet complete. A solution with a length scale of variation other than the Knudsen layer may be possible, as we will find the viscous boundary layer, the solution in the intermediate region between the overall region and the Knudsen layer, in Section 3.4.1. However, according to the analysis similar to that in Section 3.4.1, it is found that a solution with a shorter scale of variation than the Knudsen layer is uniform with respect to the new coordinate, which contradicts the assumption on the length scale of variation, and that a solution with a longer scale cannot be made to connect smoothly to the solution $\hat{f}_{SB}$.

given in the form

$$\zeta_i n_i \frac{\partial \hat{f}_K}{\partial \eta} = 2\hat{J}(\hat{f}_{SB}, \hat{f}_K) + \hat{J}(\hat{f}_K, \hat{f}_K) - k\hat{F}_i \frac{\partial \hat{f}_K}{\partial \zeta_i} - k\zeta_i \left(\frac{\partial \chi_1}{\partial x_i} \frac{\partial \hat{f}_K}{\partial \chi_1} + \frac{\partial \chi_2}{\partial x_i} \frac{\partial \hat{f}_K}{\partial \chi_2} \right), \tag{3.148}$$

where the terms consisting only of $\hat{f}_{SB}$ are absent because $\hat{f}_{SB}$ satisfies Eq. (3.133), and $\hat{f}_{SB}$ appears as the product with $\hat{f}_K$.[61]

The Knudsen-layer correction $\hat{f}_K$ is expanded in a power series of k starting from the first order of k, i.e.,

$$\hat{f}_K = \hat{f}_{K1}k + \cdots . \tag{3.149}$$

The series expansions of $\hat{f}_{SB}$ and $\hat{f}_K$ in k, i.e., Eqs. (3.138) and (3.149), are put into Eq. (3.148). In this process, the series expansion of the series (3.138) of $\hat{f}_{SB}$ with respect to η, i.e.,

$$\hat{f}_{SB} = (\hat{f}_{SB0})_0 + \left[(\hat{f}_{SB1})_0 + (\partial \hat{f}_{SB0}/\partial x_i)_0 n_i \eta \right] k + \cdots , \tag{3.150}$$

where the quantities in the parentheses with subscript 0 are evaluated on the boundary, is applied as in Section 3.2.3, because $\hat{f}_{SB}$ appears only as the product with the rapidly decaying $\hat{f}_K$ in Eq. (3.148). Then, we obtain the equation for $\hat{f}_{Km}$, which is a (homogeneous or inhomogeneous) linearized one-dimensional Boltzmann equation. For example,

$$\zeta_i n_i \frac{\partial \hat{f}_{K1}}{\partial \eta} = 2\hat{J}((\hat{f}_{SB0})_0, \hat{f}_{K1}). \tag{3.151}$$

The boundary condition for $\hat{f}_{K1}$ is

$$\hat{f}_{K1} = \hat{f}_{w1} - (\hat{f}_{SB1})_0 \quad (\zeta_i n_i > 0) \quad \text{at } \eta = 0, \tag{3.152a}$$

$$\hat{f}_{K1} \to 0 \quad \text{as } \eta \to \infty. \tag{3.152b}$$

The boundary-value problem (3.151)–(3.152b) is practically the same as that for ϕ_{K1} with $\phi_{K0} = 0$ discussed in Section 3.1.4 (see Section A.11). Thus, as the condition that the problem has a solution $\hat{f}_{K1}$ (the Grad–Bardos theorem), the conditions on the boundary values of $\hat{v}_{iSB1}$ and $\hat{T}_{SB1}$ on a simple boundary or those among $\hat{v}_{iSB1}$, $\hat{T}_{SB1}$, and $\hat{p}_{SB1}$ on an interface are obtained (see also Sone [2002]).

[61] See Footnote 39 in Section 3.2.3.

3.3.3 Fluid-dynamic-type equations and their boundary conditions

We summarize the result of analysis in the preceding subsection (Section 3.3.2), i.e., the fluid-dynamic-type equations and their associated boundary conditions that describe the behavior of a gas in the continuum limit.

The fluid-dynamic-type equations are

$$\hat{p}_{SB0} = \hat{p}_0, \tag{3.153}$$

$$\hat{p}_{SB1} = \hat{p}_1, \tag{3.154}$$

$$\frac{\partial \hat{\rho}_{SB0} \hat{v}_{iSB1}}{\partial x_i} = 0, \tag{3.155}$$

$$\begin{aligned}
&\hat{\rho}_{SB0} \hat{v}_{jSB1} \frac{\partial \hat{v}_{iSB1}}{\partial x_j} \\
&\quad = -\frac{1}{2} \frac{\partial \hat{p}^*_{SB2}}{\partial x_i} + \frac{1}{2} \frac{\partial}{\partial x_j} \left[\Gamma_1(\hat{T}_{SB0}) \left(\frac{\partial \hat{v}_{iSB1}}{\partial x_j} + \frac{\partial \hat{v}_{jSB1}}{\partial x_i} - \frac{2}{3} \frac{\partial \hat{v}_{kSB1}}{\partial x_k} \delta_{ij} \right) \right] \\
&\qquad + \frac{1}{2\hat{p}_0} \frac{\partial}{\partial x_j} \left\{ \Gamma_7(\hat{T}_{SB0}) \left[\frac{\partial \hat{T}_{SB0}}{\partial x_i} \frac{\partial \hat{T}_{SB0}}{\partial x_j} - \frac{1}{3} \left(\frac{\partial \hat{T}_{SB0}}{\partial x_k} \right)^2 \delta_{ij} \right] \right\} + \hat{\rho}_{SB0} \hat{F}_{i2},
\end{aligned} \tag{3.156}$$

$$\hat{\rho}_{SB0} \hat{v}_{iSB1} \frac{\partial \hat{T}_{SB0}}{\partial x_i} = \frac{1}{2} \frac{\partial}{\partial x_i} \left(\Gamma_2(\hat{T}_{SB0}) \frac{\partial \hat{T}_{SB0}}{\partial x_i} \right), \tag{3.157}$$

where $\hat{p}_0$ and $\hat{p}_1$ are constants, $\hat{\rho}_{SB0}$ and $\hat{p}^*_{SB2}$ are

$$\hat{\rho}_{SB0} = \frac{\hat{p}_0}{\hat{T}_{SB0}}, \tag{3.158a}$$

$$\hat{p}^*_{SB2} = \hat{p}_{SB2} + \frac{2}{3\hat{p}_0} \frac{\partial}{\partial x_k} \left(\Gamma_3(\hat{T}_{SB0}) \frac{\partial \hat{T}_{SB0}}{\partial x_k} \right), \tag{3.158b}$$

and the nondimensional transport coefficients $\Gamma_1(\hat{T}_{SB0})$, $\Gamma_2(\hat{T}_{SB0})$, $\Gamma_3(\hat{T}_{SB0})$, and $\Gamma_7(\hat{T}_{SB0})$ are the functions of $\hat{T}_{SB0}$ defined by Eq. (A.131) in Section A.2.9, whose functional forms are determined by the molecular model. Incidentally, for a hard-sphere gas,

$$\begin{aligned}
&\Gamma_1(a)/a^{1/2} = 1.270\,042\,427, \quad \Gamma_2(a)/a^{1/2} = 1.922\,284\,066, \\
&\Gamma_3(a)/a = 1.947\,906\,335, \qquad \Gamma_7(a) = 1.758\,705,
\end{aligned}$$

and for the BKW model,

$$\Gamma_1(a)/a = \Gamma_2(a)/a = \Gamma_3(a)/a^2 = \Gamma_7(a)/a = 1.$$

The *thermal-stress* term (or the third term on the right-hand side) in Eq. (3.156) can be reduced to the first order with the aid of Eq. (3.157). That is, with the new modified pressure $\hat{p}^\dagger_{SB2}$ defined by

$$\begin{aligned}\hat{p}^\dagger_{SB2} &= \hat{p}_{SB2} + \frac{2}{3\hat{p}_0}\frac{\partial}{\partial x_k}\left(\Gamma_3(\hat{T}_{SB0})\frac{\partial \hat{T}_{SB0}}{\partial x_k}\right) - \frac{\Gamma_7(\hat{T}_{SB0})}{6\hat{p}_0}\left(\frac{\partial \hat{T}_{SB0}}{\partial x_k}\right)^2 \\ &= \hat{p}^*_{SB2} - \frac{\Gamma_7(\hat{T}_{SB0})}{6\hat{p}_0}\left(\frac{\partial \hat{T}_{SB0}}{\partial x_k}\right)^2, \end{aligned} \tag{3.159}$$

Eq. (3.156) is rewritten in the following form with the first-order thermal-stress term:

$$\begin{aligned}&\hat{\rho}_{SB0}\hat{v}_{jSB1}\frac{\partial \hat{v}_{iSB1}}{\partial x_j} \\ &\quad = -\frac{1}{2}\frac{\partial \hat{p}^\dagger_{SB2}}{\partial x_i} + \frac{1}{2}\frac{\partial}{\partial x_j}\left[\Gamma_1\left(\frac{\partial \hat{v}_{iSB1}}{\partial x_j} + \frac{\partial \hat{v}_{jSB1}}{\partial x_i} - \frac{2}{3}\frac{\partial \hat{v}_{kSB1}}{\partial x_k}\delta_{ij}\right)\right] \\ &\qquad + \left[\frac{\Gamma_7}{\Gamma_2}\frac{\hat{v}_{jSB1}}{\hat{T}_{SB0}}\frac{\partial \hat{T}_{SB0}}{\partial x_j} + \frac{\Gamma_2^2}{4\hat{p}_0}\frac{\mathrm{d}\Gamma_7/\Gamma_2^2}{\mathrm{d}\hat{T}_{SB0}}\left(\frac{\partial \hat{T}_{SB0}}{\partial x_j}\right)^2\right]\frac{\partial \hat{T}_{SB0}}{\partial x_i} + \hat{\rho}_{SB0}\hat{F}_{i2}, \end{aligned} \tag{3.160}$$

where $\Gamma_1 = \Gamma_1(\hat{T}_{SB0})$, $\Gamma_2 = \Gamma_2(\hat{T}_{SB0})$, and $\Gamma_7 = \Gamma_7(\hat{T}_{SB0})$ for short.

The boundary conditions on a simple boundary are

$$\hat{T}_{SB0} = \hat{T}_{w0}, \tag{3.161a}$$

$$\left.\begin{aligned}&\frac{(\hat{v}_{jSB1} - \hat{v}_{wj1})(\delta_{ij} - n_j n_i)}{\hat{T}_{w0}^{1/2}} = -\frac{\hat{K}_1}{\hat{p}_0}\frac{\partial \hat{T}_{SB0}}{\partial x_j}(\delta_{ij} - n_j n_i), \\ &\hat{v}_{jSB1} n_j = 0, \end{aligned}\right\} \tag{3.161b}$$

and those on an interface are

$$\hat{T}_{SB0} = \hat{T}_{w0}, \tag{3.162a}$$

$$\hat{p}_{SB0} = \hat{p}_{w0}, \tag{3.162b}$$

$$\frac{(\hat{v}_{jSB1} - \hat{v}_{wj1})(\delta_{ij} - n_j n_i)}{\hat{T}_{w0}^{1/2}} = -\frac{\hat{K}_1}{\hat{p}_{w0}}\frac{\partial \hat{T}_{SB0}}{\partial x_j}(\delta_{ij} - n_j n_i), \tag{3.162c}$$

$$\frac{\hat{p}_{SB1} - \hat{p}_{w1}}{\hat{p}_{w0}} = \hat{C}_4^*\frac{\hat{v}_{jSB1} n_j}{\hat{T}_{w0}^{1/2}} + \frac{\hat{C}_1}{\hat{p}_{w0}}\frac{\partial \hat{T}_{SB0}}{\partial x_j} n_j, \tag{3.162d}$$

where the slip coefficients $\hat{K}_1$, $\hat{C}_1$, and $\hat{C}_4^*$, derived by the Knudsen-layer analysis, are functions of $\hat{T}_{w0}$, whose functional forms are determined by the molecular model and kinetic boundary condition (3.134). They are related to the slip coefficients K_1, C_1, and C_4^* in the linear theory (Section 3.1.5). Their relations

are discussed in Section A.11. In the diffuse reflection or complete-condensation condition, the relations are, for a hard-sphere gas,

$$\hat{K}_1 = K_1\,(= -0.6463), \quad \hat{C}_1 = C_1\,(= 1.0947), \quad \hat{C}_4^* = C_4^*\,(= -2.1412),$$

and for the BKW model,

$$\hat{K}_1/\hat{T}_{w0}^{1/2} = K_1\,(= -0.38316),\ \hat{C}_1/\hat{T}_{w0}^{1/2} = C_1\,(= 0.55844),$$
$$\hat{C}_4^* = C_4^*\,(= -2.13204).$$

The effect of molecular property enters the above system only through the transport coefficients Γ_1, Γ_2, and Γ_7 and the slip coefficients $\hat{K}_1$, $\hat{C}_1$, and $\hat{C}_4^*$. Thus, the fundamental structure of the equations and boundary conditions is generally common to molecular models.

It may be better to add a comment on the process of determination of the macroscopic variables when the boundary is an interface of a gas and its condensed phase. From Eq. (3.153) and the boundary condition (3.162b), $\hat{p}_{SB0} = \hat{p}_0 = \hat{p}_{w0}$, which requires that $\hat{p}_{w0}$ is uniform. From the set of equations (3.155), (3.156) [or (3.160)], and (3.157) with Eq. (3.158a) and the boundary conditions (3.162a), (3.162c), and (3.162d), the variables $\hat{T}_{SB0}$, $\hat{\rho}_{SB0}$, $\hat{v}_{iSB1}$, and $\hat{p}_{SB2}$ are determined with the constant $\hat{p}_1$ in Eq. (3.154) as a parameter, leaving an undetermined integration constant (say, $\hat{p}_2$) in $\hat{p}_{SB2}$; the parameter $\hat{p}_1$ enters the variables $\hat{T}_{SB0}$, $\hat{\rho}_{SB0}$, $\hat{v}_{iSB1}$, and $\hat{p}_{SB2}$ through $\hat{p}_{SB1}\,(= \hat{p}_1)$ in the boundary condition (3.162d). The constant $\hat{p}_1$ cannot be arbitrary, because it is determined by the condition at infinity in an unbounded-domain problem, or because the quantity $\hat{\rho}_{SB0}\hat{v}_{iSB1}n_i$ integrated over the boundary must be zero from Eq. (3.155) in a bounded-domain problem. The present system is formally consistent, but a note should be made here. The saturated gas pressure $\hat{p}_w$ is generally an increasing function of temperature $\hat{T}_w$. Thus, $\hat{T}_{w0}$ is required to be uniform because $\hat{p}_{w0}$ is uniform as shown above. In a bounded-domain problem, the system for $\hat{T}_{SB0}$, $\hat{\rho}_{SB0}$, $\hat{v}_{iSB1}$, and $\hat{p}_{SB2}$ has a solution with $\hat{T}_{SB0} = \text{const}$ and $\hat{\rho}_{SB0} = \text{const}$; this case corresponds to that discussed in Section 3.2. In an unbounded-domain problem, the pressure $\hat{p}_\infty$ at infinity should be close to $\hat{p}_{w0}$ (with difference of the order of k) for Eq. (3.135a) or (3.143) to hold, but the temperature $\hat{T}_\infty$ at infinity may be arbitrary, for which the result of the present section is required. In this case, the gas is highly undersaturated or supersaturated at infinity.

3.3.4 Ghost effect and incompleteness of the classical gas dynamics

The system of equations (3.155)–(3.157) has a striking feature. It determines $\hat{T}_{SB0}$, $\hat{\rho}_{SB0}$, $\hat{v}_{iSB1}$, and $\hat{p}_{SB2}$ simultaneously. That is, the temperature field $\hat{T}_{SB0}$ in the continuum limit ($k \to 0$) cannot be independent of the component function $\hat{v}_{iSB1}$ at the first order of k. This is strange from the classical fluid-dynamic point of view. In the world of $k = 0_+$ or $\mathrm{Kn} = 0_+$ (in the world of the

continuum limit), one has no way to perceive the infinitesimal velocity $\hat{v}_{iSB1}k$ and thus, the quantity $\hat{v}_{iSB1}$. The temperature field is affected by something that does not exist in the world, which may be called a *ghost effect*.[62] The convection effect of the infinitesimal velocity cannot be neglected in Eq. (3.157), and the thermal stress of the second-order infinitesimal must be retained in Eq. (3.156) to determine $\hat{v}_{iSB1}$. Thus, the temperature field $\hat{T}_{SB0}$ is affected by non-Navier–Stokes stress (*non-Navier–Stokes effect* in the continuum limit).[63]

In the classical fluid dynamics, the temperature field of a gas at rest is obtained from the heat-conduction equation, i.e., Eq. (3.157) with $\hat{v}_{iSB1} = 0$. This is allowed only in special cases. We will discuss the condition that is required for

[62]The ghost effect, a finite effect produced by an infinitesimal quantity, is not unique to the present system. The corresponding situations are encountered in asymptotic analyses around singular points in various systems. Consider the following differential system for (u, v) containing a small parameter ε: the equations are symbolically given by

$$F_1(u,v) + \varepsilon H_1(u,v) = 0,\ \ F_2(u,v) + \varepsilon H_2(u,v) = 0, \tag{$*$}$$

where $F_1(0, v) = 0$ and $F_2(0, v) = 0$ for any v, and the boundary conditions for u and v are

$$u = \varepsilon U,\ \ v = V.$$

To make the discussion simpler, F_1 and F_2 are assumed to be bilinear with respect to u and v. Here, we look for the solution (u, v) in the power series of ε, i.e.,

$$u = u_0 + \varepsilon u_1 + \cdots, \quad v = v_0 + \varepsilon v_1 + \cdots.$$

Then, the leading-order equations are

$$F_1(u_0, v_0) = 0, \quad F_2(u_0, v_0) = 0,$$

and the boundary conditions are

$$u_0 = 0,\ \ v_0 = V_0, \tag{$**$}$$

where $V = V_0 + \varepsilon V_1 + \cdots$. The set $(0, v_0)$, where v_0 is an arbitrary function that satisfies the boundary condition $(**)$, is a solution. When $u_0 = 0$, the next-order equations are

$$F_1(u_1, v_0) + H_1(0, v_0) = 0, \quad F_2(u_1, v_0) + H_2(0, v_0) = 0, \tag{\#}$$

and the boundary conditions are

$$u_1 = U_1, \quad v_0 = V_0,$$

where $U = U_1 + \cdots$. The function u_1 cannot generally be zero owing to the boundary condition for u_1 and the terms $H_1(0, v_0)$ and $H_2(0, v_0)$ in Eq. (#). The leading-order function v_0 is determined together with the first-order function u_1 from Eq. (#). In other words, in the limiting world that $\varepsilon \to 0$, the infinitesimal field u produces a finite effect on the field v. There are various physical mechanisms that cause the field u. In the limit that $\varepsilon \to 0$, we cannot perceive the infinitesimal quantity u. Thus, the corresponding results in the field v are called their ghost effects.

[63]The non-Navier–Stokes effect and the ghost effect should not be confused. As is obvious from the discussion in the following paragraphs in the present subsection, thermal creep flow and nonlinear-thermal-stress flow, the latter of which contributes to the non-Navier–Stokes effect, are not required for the existence of the ghost effect (see also Sections 8.2 and 8.3). Kogan and Fridlender, who proposed the nonlinear-thermal-stress flow in a different way (Kogan, Galkin & Fridlender [1976]), misunderstand our claim in the way that nonlinear-thermal-stress flow = the ghost effect → ghost (what does not exist) and seem to be unhappy. It cannot be imagined that such a misunderstanding takes place from our various past descriptions and direct explanations. Expressions (definition, concept, and statement) should be taken precisely.

$\hat{v}_{iSB1} = 0$. First, from the boundary condition (3.161b) with (3.161a) or (3.162c) with (3.162a), it is required that $[\hat{v}_{wj1}\hat{T}_{w0}^{-1/2} - (\hat{K}_1/\hat{p}_0)\partial\hat{T}_{w0}/\partial x_j](\delta_{ij} - n_j n_i) = 0$. This condition may be conveniently split into the two conditions
(i) $\hat{v}_{wi1} = 0$,
(ii) $(\delta_{ij} - n_j n_i)\partial\hat{T}_{w0}/\partial x_j = 0$,
because $(\delta_{ij} - n_j n_i)\hat{v}_{wj1}$ and $(\delta_{ij} - n_j n_i)\partial\hat{T}_{w0}/\partial x_j$ may be chosen arbitrarily. That is, if the condition (i) or (ii) is not satisfied, $\hat{v}_{iSB1}$ does not generally vanish. Secondly, owing to the thermal stress term in Eq. (3.160), there is another condition that is required for $\hat{v}_{iSB1} = 0$. That is, eliminating $\hat{p}^{\dagger}_{SB2}$ from Eq. (3.160) by taking its curl and putting $\hat{v}_{iSB1} = 0$ in the result, we have the condition
(iii)

$$\frac{\partial\hat{T}_{SB0}}{\partial x_i}\frac{\partial}{\partial x_j}\left(\frac{\partial\hat{T}_{SB0}}{\partial x_k}\right)^2 - \frac{\partial\hat{T}_{SB0}}{\partial x_j}\frac{\partial}{\partial x_i}\left(\frac{\partial\hat{T}_{SB0}}{\partial x_k}\right)^2 + \frac{4\hat{p}_0^2}{f_\Gamma(\hat{T}_{SB0})}\left(\frac{\partial}{\partial x_j}\frac{\hat{F}_{i2}}{\hat{T}_{SB0}} - \frac{\partial}{\partial x_i}\frac{\hat{F}_{j2}}{\hat{T}_{SB0}}\right) = 0, \tag{3.163}$$

where $f_\Gamma(\hat{T}_{SB0}) = \Gamma_2^2 \mathrm{d}(\Gamma_7/\Gamma_2^2)/\mathrm{d}\hat{T}_{SB0}$.

The condition (ii) requires that the temperature be uniform on each boundary; the condition (iii) means that the isothermal lines are parallel when $\hat{F}_{i2} = 0$.[64] The flow induced when the condition (iii) is not satisfied is called *nonlinear-thermal-stress flow* (see Section 5.1.3). These conditions are satisfied only in very special cases. For example, when $\hat{F}_{i2} = 0$, this type of temperature field is possible in a gas between two parallel plane walls, coaxial cylinders, or concentric spheres with uniform temperature on each boundary. Even in the case of a gas between two parallel plane walls with uniform temperature on each boundary, the solution with nonzero $\hat{v}_{iSB1}$ is possible in a system under gravity (Bénard problem), and the temperature field is strongly distorted by the infinitesimal flow. This interesting example is discussed in Section 8.2.

In this way, we find that the flow $\hat{v}_{iSB1}(\neq 0)$ or a flow of the order of Kn is naturally induced by a nontrivial temperature field. The thermal creep flow (an effect of slip condition of the order of Kn) and the nonlinear thermal stress flow of the order of Kn (non-Navier–Stokes effect or an effect of nonlinear thermal stress of the second order of Kn) produce finite effects on the temperature field. That is, the situation considered in this section, i.e., Eq. (3.135a), is not a special situation but naturally occurs. The condition (i) or the component $\hat{v}_{wi1}$ cannot be identified in a gas in the continuum limit. That is, the temperature field is indefinite in the world of the continuum limit (or in the continuum world). The famous Taylor–Couette problem with different cylinder temperatures and infinitesimal speeds of rotation of the cylinders is an interesting example of this case, where the infinitesimal speeds of rotation of the cylinders induce strongly

[64] From Eq. (3.163), $(\partial\hat{T}_{SB0}/\partial x_k)^2$ is a function of $\hat{T}_{SB0}$ when $\hat{F}_{i2} = 0$ (see discussions related to the implicit function theorem in a standard textbook of analysis, e.g., Buck [1965], Takagi [1961], and Bronshtein & Semendyayev [1997]).

distorted temperature fields and the fields are subject to non-Navier–Stokes effect, as shown in Section 8.3. In a real gas the mean free path is not exactly zero, however small it may be. Then, a very small motion of the boundary (of the order of Kn) affects the temperature field considerably (of the order of unity).

We have seen the discrepancy of the classical fluid dynamics (or Navier–Stokes system) in describing the behavior of the temperature field of a gas at rest in the continuum limit ($\mathrm{Kn} = 0_+$). This discrepancy can be seen from the Navier–Stokes set of equations itself if we look at the set a little carefully.

The energy equation of the Navier–Stokes set of equations is given as follows:

$$\frac{5}{2}\rho v_i \frac{\partial RT}{\partial X_i} = \cdots + \frac{\partial}{\partial X_i}\lambda \frac{\partial T}{\partial X_i}, \tag{3.164}$$

where only the essential terms in the discussion are shown and λ is the thermal conductivity. In discussing the temperature field of a gas at rest, one usually puts $v_i = 0$ and solves the heat-conduction equation $\partial(\lambda \partial T/\partial X_i)/\partial X_i = 0$. However, we have to examine the equation (3.164) a little more carefully.

According to a very crude estimate by elementary kinetic theory (e.g., Kennard [1938], Vincenti & Kruger [1965]), or as we have seen in Eqs. (3.70) and (3.71), the viscosity μ and thermal conductivity λ of a gas are related to the mean free path ℓ of the gas, i.e.,

$$\mu/\rho = f(T)(2RT)^{1/2}\ell, \quad \lambda/\rho = g(T)(2RT)^{1/2}R\ell, \tag{3.165}$$

where f and g are nondimensional functions of T, whose functional forms are determined by the molecular model. For example, for a hard-sphere gas, $f = 0.56277$ and $g = 2.1295$. With the above order of λ, let us estimate the orders of the main terms of Eq. (3.164), the convection term on the left-hand side (say, Evec) and the conduction term, the last term, on the right-hand side (say, Educ). They are

$$O(\mathrm{Evec}) = \rho VRT/L, \qquad O(\mathrm{Educ}) = \rho(RT)^{3/2}\ell/L^2,$$

where V and L are, respectively, the characteristic flow speed and the length scale of variation of the gas temperature, and the temperature variation is assumed to be of the same order as the temperature itself (a fundamental assumption in this section). The two terms are comparable when the flow speed V is of the order of $(RT)^{1/2}\ell/L$. Thus, the flow vanishing as $\ell \to 0$ cannot be neglected in the energy equation. As a flow of this magnitude, we know the thermal creep flow or nonlinear-thermal-stress flow, which is inevitable except special cases. Thus, the heat-conduction equation is inappropriate in describing the temperature field of a gas at rest in the continuum limit.

Next, for the above size of flow speed, i.e., $V = O[(RT)^{1/2}\ell/L]$, let us estimate the orders of the main terms, the convection term (say, Mvec) and the viscous term (say, Visc), of the momentum equation of the Navier–Stokes set

$$\rho v_j \frac{\partial v_i}{\partial X_j} = \cdots + \frac{\partial}{\partial X_j}\mu\left(\frac{\partial v_i}{\partial X_j} + \frac{\partial v_j}{\partial X_i} - \frac{2}{3}\frac{\partial v_k}{\partial X_k}\delta_{ij}\right).$$

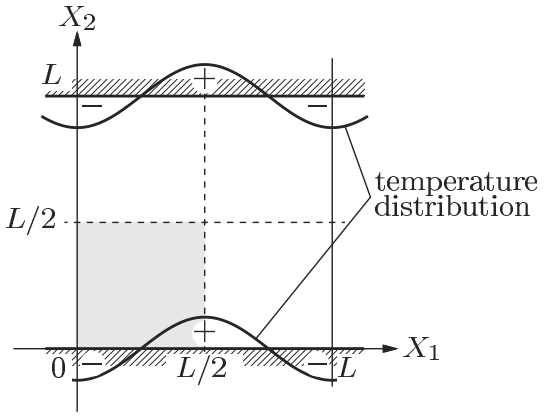

Figure 3.3. Geometry. In this example, the behavior of a gas between two parallel plane walls with the periodic temperature distribution $T_w = T_0(1 - \Delta\tau_w \cos 2\pi X_1/L)$ is considered.

The order of the convection term on the left-hand side and that of the viscous term, the last term, on the right-hand side are

$$O(\text{Mvec}) = \rho V^2/L = (\rho RT/L)(\ell/L)^2, \qquad O(\text{Visc}) = (\rho RT/L)(\ell/L)^2.$$

Both are of the second order of the Knudsen number. Thus, a stress p_{ij} of the order of $\rho RT(\ell/L)^2$ should be retained in the above equation. The thermal stress and the weak external force in Eq. (3.156) are a stress and force of this order. Another non-Navier–Stokes stress is shown in Chapter 9. Thus, we see the incompleteness of the Navier–Stokes set in describing the behavior of a gas in the continuum limit.

The ghost effect in the sense that something that does not exist in the world of a gas in the continuum limit produces a finite effect in this world is found in the flow-velocity field in the cylindrical Couette flow with evaporation or condensation on the cylinders in Sone, Takata & Sugimoto [1996], which is explained in Section 8.4.2 (see also Sone [1997, 2002]). The ghost effect appears combined with bifurcation of a flow in the famous Bénard and Taylor–Couette problems. These problems are discussed in Sections 8.2 and 8.3. A geometric parameter of the system such as infinitesimal curvature of the boundary can be a source of ghost and non-Navier–Stokes effects, which will be discussed in Chapter 9.

As we have seen, the classical fluid dynamics is incomplete. In order to analyze the ghost effect and to find the correct behavior of a gas in the continuum limit ($\text{Kn} = 0_+$), we have to rely on molecular gas dynamics or kinetic theory. This is a new important role of molecular gas dynamics.

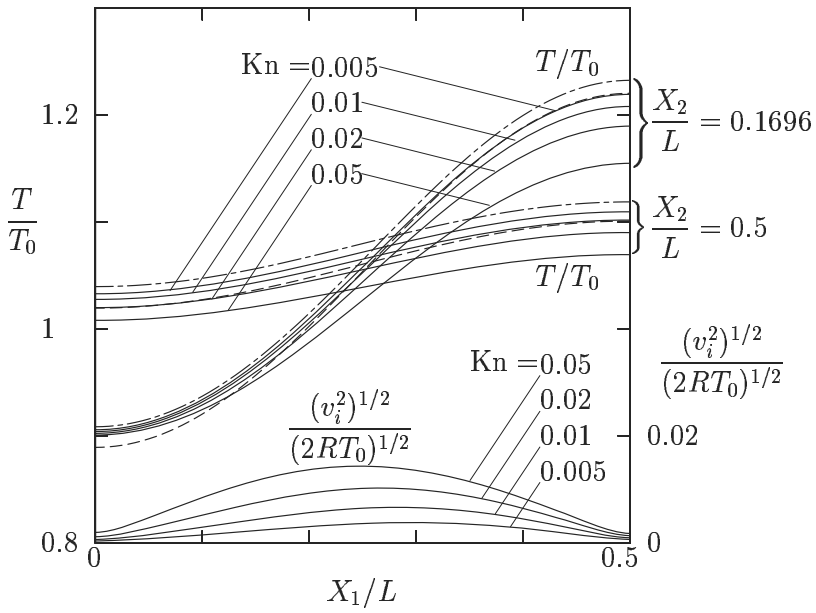

Figure 3.4. Comparison of the three kinds of solutions for the problem shown in Fig. 3.3 with $\Delta\tau_w = 0.5$ I: Temperature distributions along $X_2/L = 0.1696$ and $X_2/L = 0.5$ and flow-speed distribution along $X_2/L = 0.0227$. The solid lines ——: the BKW equation for Kn = 0.005, 0.01, 0.02, and 0.05, the dot-dash lines –·–: the asymptotic theory, and the dashed lines - - -: the heat-conduction equation. Note the difference of the ordinate of T/T_0 from that of $(v_i^2)^{1/2}/(2RT_0)^{1/2}$. The solution of the kinetic equation converges to the solution by the asymptotic theory.

3.3.5 Illustrative example

In order to understand the situation more clearly, we take a simple example and compare three kinds of solutions: the solution of the heat-conduction equation, the solution of the system derived by the asymptotic analysis [Eqs. (3.155)–(3.157), (3.161a), and (3.161b)], and the numerical solutions of the Boltzmann equation for various small Knudsen numbers. The example considered here is a gas between two parallel plane walls at $X_2 = 0$ and $X_2 = L$ in the absence of external force ($F_i = 0$); both walls are at rest[65] and have a common temperature distribution $T_w = T_0(1 - \Delta\tau_w \cos 2\pi X_1/L)$, where T_0 and $\Delta\tau_w$ are constants (Fig. 3.3). We look for the periodic solution with period L with respect to X_1. In Figs. 3.4 and 3.5, the three kinds of solutions for $\Delta\tau_w = 0.5$ are compared, where the BKW equation (and the corresponding asymptotic and heat-conduction equations) and the diffuse-reflection condition are used for simplicity

[65]The solution is indefinite unless $\hat{v}_{wi1}$ is specified as explained in Section 3.3.4. Thus, we consider the case $\hat{v}_{wi1} = 0$ as well as $\hat{v}_{wi0} = 0$.

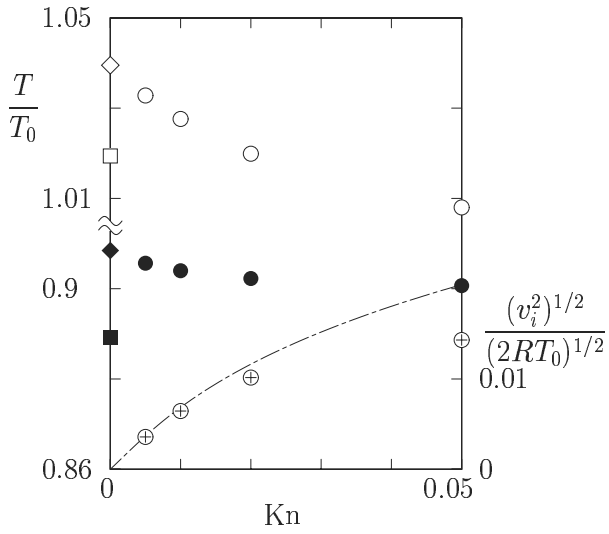

Figure 3.5. Comparison of the three kinds of solutions for the problem shown in Fig. 3.3 with $\Delta\tau_w = 0.5$ II: Temperatures at $(X_1/L, X_2/L) = (0, 0.1696)$ and $(0, 0.5)$ and flow speed at $(X_1/L, X_2/L) = (0.25, 0.0227)$ vs Kn. The white symbols (○, ◇, □): T/T_0 at $(X_1/L, X_2/L) = (0, 0.5)$, the black symbols (●, ♦, ■): T/T_0 at $(X_1/L, X_2/L) = (0, 0.1696)$, and the circled pluses ⊕: $(v_i^2)^{1/2}/(2RT_0)^{1/2}$ at $(X_1/L, X_2/L) = (0.25, 0.0227)$; the circles (○, ●, ⊕): the BKW equation, the diamonds (◇, ♦): the asymptotic theory, and the squares (□, ■): the heat-conduction equation; the dot-dash line –·–: $|(\hat{v}_{iSB1} + \hat{v}_{iK1})k|$ in the asymptotic theory (the explicit formula for $\hat{v}_{iK1}$ is not given in the main text, because it is not necessary for its purpose). Note the difference of the ordinate of T/T_0 from that of $(v_i^2)^{1/2}/(2RT_0)^{1/2}$. The solution of the kinetic equation converges to the solution by the asymptotic theory.

of numerical computation of the kinetic equation, because the principal features of the previous discussion are the same for the BKW equation and the standard Boltzmann equation. The temperature distributions along $X_2/L = 0.1696$ and $X_2/L = 0.5$, and the flow speed distribution along $X_2/L = 0.0227$ are shown in Fig. 3.4; the temperature at $(X_1/L, X_2/L) = (0, 0.1696)$ and $(0, 0.5)$ and the flow speed at $(0.25, 0.0227)$ vs Kn are shown in Fig. 3.5. The flow speed attains roughly the maximum value at this point. The Knudsen number Kn here is defined by the mean free path of the average density of the gas in the domain and the channel width L. From Figs. 3.4 and 3.5, it is clear that the temperature field of the kinetic equation approaches that of the system of the asymptotic theory and not that of the heat-conduction equation and that the flow vanishes as the Knudsen number tends to zero. In Figs. 3.6 (a) and (b), a comparison of the solution of the asymptotic system and that of the heat-conduction equation for a hard-sphere gas is shown for the same problem. The data in this subsection are taken from Sone, Aoki, Takata, Sugimoto & Bobylev [1996]. Incidentally,

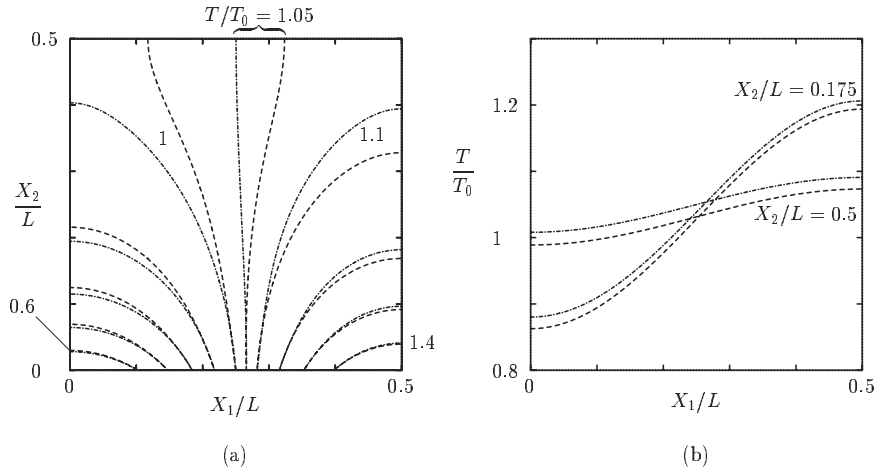

Figure 3.6. Comparison of the solutions of the asymptotic theory and heat-conduction equation for a hard-sphere gas in the problem shown in Fig. 3.3 with $\Delta\tau_w = 0.5$. (a) The isothermal lines $T/T_0 = 0.6 + 0.1m$ ($m = 0, 1, ..., 8$) and 1.05. (b) The temperature distributions along $X_2/L = 0.175$ and $X_2/L = 0.5$. Here, the dot-dash lines $-\cdot-$: asymptotic theory and the dashed lines - - -: heat-conduction equation.

examples of the ghost effect on flow velocity fields are given in Section 8.4.2.

3.4 Nonlinear problem II: Flow with a finite Mach number around a simple boundary

3.4.1 Problem and the outline of analysis

Up to now, we have considered the cases where the Mach number Ma of a gas flow is a small quantity much smaller than or of the same order as the Knudsen number Kn. In this section a flow with a finite Mach number around a simple boundary is considered. In this case, from the von Karman relation (3.74), the Reynolds number Re of the flow is very large, and in view of the result for the Navier–Stokes system,[66] a viscous boundary layer (or Prandtl boundary layer) with thickness of the order of $\mathrm{Re}^{-1/2}L$ or $\mathrm{Kn}^{1/2}L$ for a finite Ma is expected outside the Knudsen layer. Thus, the asymptotic analysis for small Knudsen numbers is developed by introducing an intermediate anisotropic layer with thickness of the order of $\mathrm{Kn}^{1/2}L$. In order to express this layer, the velocity distribution function and macroscopic variables are expanded in power

[66]The discussion of the viscous boundary layer in the Navier–Stokes system is found in most textbooks of classical fluid dynamics, e.g., Prandtl [1952], Tietjens [1957], Liepmann & Roshko [1957], Schlichting [1979], and Chorin & Marsden [1997]. The first stresses on the physical aspect and the last stresses on the mathematical aspect. Incidentally, asymptotic analyses of various problems in classical fluid dynamics are discussed in Zeytounian [2002, 2003].

series of $\mathrm{Kn}^{1/2}$ or $k^{1/2}$,[67] in contrast to the cases discussed in the foregoing sections, where they are expanded in power series of k. The analysis for a finite Mach number, with this anisotropy, does not cover the analyses in the foregoing sections, but this is a special case with a very large Reynolds number to be treated separately.

The problem is the asymptotic analysis for small Knudsen numbers (or small k) of the time-independent boundary-value problem of the Boltzmann equation (1.47a) with the boundary condition (1.64), or more simply the diffuse-reflection condition (1.63a) with (1.63b) on a simple boundary when the flow Mach number or $\hat{v}_i$ is of the order of unity (Sone, Bardos, Golse & Sugimoto [2000]). The nondimensional Boltzmann equation is

$$\zeta_i \frac{\partial \hat{f}}{\partial x_i} = \frac{1}{k} \hat{J}(\hat{f}, \hat{f}). \tag{3.166}$$

The boundary condition is symbolically expressed as

$$\hat{f}(x_i, \zeta_i) = \hat{f}_w \quad (\zeta_j n_j > 0). \tag{3.167}$$

Here, the boundary data $\hat{v}_{wi}$ and $\hat{T}_w$ are taken to be independent of k for simplicity.[68]

We will outline the analysis of the boundary-value problem, referring to the principal results summarized in Section 3.4.2.

The boundary condition being put aside, the solution $[\partial \hat{f}/\partial x_i = O(\hat{f})]$ describing the overall behavior of the gas is obtained in the power-series expansion in $k^{1/2}$, i.e.,

$$\hat{f} = \hat{f}_h = \hat{f}_{h0} + \hat{f}_{h1}\varepsilon + \cdots, \tag{3.168}$$

where $\varepsilon = k^{1/2}$ and the subscript h is attached to discriminate the expansion in ε.[69] Corresponding to the expansion of the velocity distribution function, the boundary data $\hat{f}_w$ and the macroscopic variables $\hat{\rho}$, $\hat{v}_i$, $\hat{T}$, etc. are also expanded in ε, i.e.,

$$\hat{f}_w = \hat{f}_{w0} + \hat{f}_{w1}\varepsilon + \cdots, \tag{3.169}$$

$$\hat{h}_h = \hat{h}_{h0} + \hat{h}_{h1}\varepsilon + \cdots, \tag{3.170}$$

where $\hat{h}$ represents $\hat{\rho}$, $\hat{v}_i$, $\hat{T}$, etc. Substituting the expansion (3.168) into Eq. (3.166) and arranging the same-order terms in ε, we obtain a series of integral equations

[67] The length scale of variation of the variables in the viscous boundary layer is $\mathrm{Re}^{-1/2}L$ or $\mathrm{Kn}^{1/2}L$ for a finite Ma. Thus, $\mathrm{Kn}^{1/2}$ or $k^{1/2}$ is the fundamental parameter instead of k. The solutions in the other regions are required to be expanded in $k^{1/2}$ in harmony with the solution in the layer.

[68] The boundary function $\hat{f}_w$ depends on k even when $\hat{v}_{wi}$ and $\hat{T}_w$ are independent of k, because $\hat{f}_w$ depends on $\hat{f}$ $(\zeta_i n_i < 0)$.

[69] See the first two sentences of Footnote 39 in Section 3.2.3.

for $\hat{f}_{hm}$, which are linear for $m \geq 1$, as in the previous analyses,[70] i.e.,

$$\hat{J}(\hat{f}_{h0}, \hat{f}_{h0}) = 0, \tag{3.171a}$$

$$\hat{J}(\hat{f}_{h0}, \hat{f}_{h1}) = 0, \tag{3.171b}$$

$$2\hat{J}(\hat{f}_{h0}, \hat{f}_{hm}) = \zeta_i \frac{\partial \hat{f}_{hm-2}}{\partial x_i} - \sum_{s=1}^{m-1} \hat{J}(\hat{f}_{hs}, \hat{f}_{hm-s}) \quad (m = 2, 3, \ldots). \tag{3.171c}$$

The leading term $\hat{f}_{h0}$ of the expansion is the local Maxwellian, as $\hat{f}_{SB0}$ in Section 3.3.2, i.e.,

$$\hat{f}_{h0} = \frac{\hat{\rho}_{h0}}{(\pi \hat{T}_{h0})^{3/2}} \exp\left(-\frac{(\zeta_i - \hat{v}_{ih0})^2}{\hat{T}_{h0}} \right). \tag{3.172}$$

The ε-order term $\hat{f}_{h1}$ being artificially introduced for adjusting $\hat{f}_h$ to the viscous boundary-layer solution to be discussed, the sum $\hat{f}_{h0} + \hat{f}_{h1}\varepsilon$ is practically Maxwellian, i.e.,

$$\hat{f}_{h0} + \hat{f}_{h1}\varepsilon = \frac{\hat{\rho}_{h0} + \hat{\rho}_{h1}\varepsilon}{[\pi(\hat{T}_{h0} + \hat{T}_{h1}\varepsilon)]^{3/2}} \exp\left(-\frac{[\zeta_i - (\hat{v}_{ih0} + \hat{v}_{ih1}\varepsilon)]^2}{\hat{T}_{h0} + \hat{T}_{h1}\varepsilon} \right) + O(\varepsilon^2). \tag{3.173}$$

We advance the analysis to the higher orders. From the condition for Eq. (1.83) to hold and the relation (1.53),[71] the condition (solvability condition)

$$\int (1, \zeta_i, \zeta_k^2) \zeta_j \frac{\partial \hat{f}_{hm-2}}{\partial x_j} \mathbf{d}\boldsymbol{\zeta} = 0 \quad (m = 2, 3, \ldots) \tag{3.174}$$

is required for Eq. (3.171c) to have a solution. From Eq. (3.174) with $m = 2$, the Euler set of equations for $\hat{\rho}_{h0}$, $\hat{v}_{ih0}$, and $\hat{T}_{h0}$ in the Maxwellian (3.172) is derived [Eqs. (3.192a)–(3.192c) in Section 3.4.2]. From Eq. (3.174) with $m = 3$, the linearized Euler set of equations for $\hat{\rho}_{h1}$, $\hat{v}_{ih1}$, and $\hat{T}_{h1}$, linearized around $\hat{\rho}_{h0}$, $\hat{v}_{ih0}$, and $\hat{T}_{h0}$, is derived [Eqs. (3.194a)–(3.194c)].[72]

The leading Maxwellian $\hat{f}_{h0}$ can apparently be made to satisfy the boundary condition (3.167) by taking $\hat{v}_{ih0} = \hat{v}_{wi}$ and $\hat{T}_{h0} = \hat{T}_w$, but these conditions are too strong as the boundary conditions for the Euler set, a set of the first-order equations. Thus, we have to loosen the assumption $\partial \hat{f}/\partial x_i = O(\hat{f})$ on the solution in a neighborhood of the boundary. The solution is looked for by inserting a layer expressing the viscous boundary layer with thickness of the order of εL. In the layer, we assume that the behavior of the gas varies appreciably within the layer in the direction normal to the boundary, i.e., $\varepsilon n_i \partial \hat{f}/\partial x_i = O(\hat{f})$, and introduce the variables (y, χ_1, χ_2) natural to this variation, i.e.,

$$x_i = \varepsilon y n_i(\chi_1, \chi_2) + x_{wi}(\chi_1, \chi_2), \tag{3.175}$$

[70] See Footnote 58 in Section 3.3.2.

[71] See Footnote 59 in Section 3.3.2.

[72] The $\hat{\rho}_{h0} + \hat{\rho}_{h1}\varepsilon$, $\hat{v}_{ih0} + \hat{v}_{ih1}\varepsilon$, and $\hat{T}_{h0} + \hat{T}_{h1}\varepsilon$, where the ε-order terms are artificially introduced in connection with the viscous boundary layer, are practically governed by the Euler set.

where $x_i = x_{wi}(\chi_1, \chi_2)$ is the boundary surface and y is a stretched coordinate normal to the boundary. In this coordinate system, the Boltzmann equation (3.166) is rewritten as

$$\frac{1}{\varepsilon}\zeta_i n_i \frac{\partial \hat{f}_V}{\partial y} + \zeta_i \left(\frac{\partial \chi_1}{\partial x_i}\frac{\partial \hat{f}_V}{\partial \chi_1} + \frac{\partial \chi_2}{\partial x_i}\frac{\partial \hat{f}_V}{\partial \chi_2} \right) = \frac{1}{\varepsilon^2}\hat{J}(\hat{f}_V, \hat{f}_V), \tag{3.176}$$

where the subscript V is attached to discriminate the viscous boundary-layer solution.[73]

The solution $\hat{f}_V$ in the layer, for which $\partial \hat{f}_V/\partial y = O(\hat{f}_V)$, is looked for in a power series of ε, i.e.,

$$\hat{f}_V = \hat{f}_{V0} + \hat{f}_{V1}\varepsilon + \cdots . \tag{3.177}$$

Corresponding to this expansion, the macroscopic variables $\hat{\rho}$, $\hat{v}_i$, $\hat{T}$, etc. are also expanded in power series of ε, i.e.,

$$\hat{h}_V = \hat{h}_{V0} + \hat{h}_{V1}\varepsilon + \cdots , \tag{3.178}$$

where $\hat{h}$ represents $\hat{\rho}, \hat{v}_i, \hat{T}$, etc. Substituting the expansion (3.177) into Eq. (3.176) and arranging the same-order terms, we obtain a series of integral equations for $\hat{f}_{Vm}$, which are linear for $m \geq 1$, as in the previous analyses,[74] i.e.,

$$\hat{J}(\hat{f}_{V0}, \hat{f}_{V0}) = 0, \tag{3.179a}$$

$$2\hat{J}(\hat{f}_{V0}, \hat{f}_{Vm}) = \mathrm{Ihv}_m \quad (m \geq 1), \tag{3.179b}$$

where Ihv_m is the inhomogeneous term determined by $\hat{f}_{Vn}$ $(n < m)$, e.g., $\mathrm{Ihv}_1 = \zeta_i n_i \partial \hat{f}_{V0}/\partial y$.

The leading term $\hat{f}_{V0}$ of the expansion is the local Maxwellian as $\hat{f}_{h0}$, i.e.,

$$\hat{f}_{V0} = \frac{\hat{\rho}_{V0}}{(\pi \hat{T}_{V0})^{3/2}} \exp\left(-\frac{(\zeta_i - \hat{v}_{iV0})^2}{\hat{T}_{V0}} \right). \tag{3.180}$$

The Maxwellian $\hat{f}_{V0}$ can be made to satisfy the boundary condition (3.167) by choosing the boundary values of the parameters $\hat{v}_{iV0}$, $\hat{T}_{V0}$ as[75]

$$\hat{v}_{iV0} = \hat{v}_{wi}, \quad \hat{T}_{V0} = \hat{T}_w \quad \text{at } y = 0. \tag{3.181}$$

From the condition for Eq. (1.83) to hold and the relation (1.53),[76] the following condition SCV_m^r (solvability condition) is required for Eq. (3.179b) for $\hat{f}_{Vm}$ $(m \geq 1)$ to have a solution:

$$\mathrm{SCV}_m^r : \int \psi_r \mathrm{Ihv}_m \mathbf{d}\boldsymbol{\zeta} = 0 \quad (\psi_0 = 1,\ \psi_i = \zeta_i,\ \psi_4 = \zeta_k^2),$$

[73] See the first two sentences of Footnote 39 in Section 3.2.3.

[74] See Footnote 58 in Section 3.3.2.

[75] (i) See Footnote 60 in Section 3.3.2.

(ii) The equations derived later are compatible with this nonslip condition in contrast to the Euler set for $\hat{\rho}_{h0}$, $\hat{v}_{ih0}$, and $\hat{T}_{h0}$.

[76] See Footnote 59 in Section 3.3.2.

from which relations among $\hat{\rho}_{Vn}$, $\hat{v}_{iVn}$, $\hat{T}_{Vn}$, $\hat{p}_{Vn}$ $(n \leq m-1)$ are derived.

The solvability conditions SCV_1^0 and $\mathrm{SCV}_1^i n_i$ give, respectively,

$$\frac{\partial \hat{\rho}_{V0} \hat{v}_{iV0} n_i}{\partial y} = 0 \quad \text{and} \quad \frac{\partial \hat{p}_{V0}}{\partial y} + \frac{\partial 2 \hat{\rho}_{V0} (\hat{v}_{iV0} n_i)^2}{\partial y} = 0. \tag{3.182}$$

From the first relations of Eq. (3.182) and Eq. (3.181), we find

$$\hat{v}_{iV0} n_i = 0, \ \text{thus} \ \frac{\partial \hat{p}_{V0}}{\partial y} = 0, \tag{3.183}$$

because $\hat{v}_{wi} n_i = 0$.[77] With this result,[78] the other conditions of SCV_1^r are reduced to identities. Then, Eq. (3.179b) with $m = 1$ for $\hat{f}_{V1}$ is solved. The analysis proceeds with repetition of derivation of the solvability condition and solution of the integral equation. Owing to the above degeneracy, the series of equations determines the component functions of the expansions of $\hat{\rho}_V$, $\hat{v}_{iV}$, $\hat{T}_V$, and $\hat{p}_V$ in a staggered combination of different order of the expansions.[79] That is, from the set of $\mathrm{SCV}_1^j n_j$, SCV_2^0, $\mathrm{SCV}_2^j(\delta_{ij} - n_i n_j)$, and SCV_2^4, the equations for $\hat{\rho}_{V0}$, $\hat{v}_{iV1} n_i$, $\hat{v}_{jV0}(\delta_{ij} - n_i n_j)$, $\hat{p}_{V0}$, and $\hat{T}_{V0}$ are obtained, from the set of $\mathrm{SCV}_2^j n_j$, SCV_3^0, $\mathrm{SCV}_3^j(\delta_{ij} - n_i n_j)$, and SCV_3^4, the equations for $\hat{\rho}_{V1}$, $\hat{v}_{iV2} n_i$, $\hat{v}_{jV1}(\delta_{ij} - n_i n_j)$, $\hat{p}_{V1}$, and $\hat{T}_{V1}$ are obtained, and so on. The derivation of the explicit equations requires a tedious lengthy manipulation and the result is also very lengthy. Thus, the result is summarized in Section 3.4.2 for the two-dimensional case (see Sone, Bardos, Golse & Sugimoto [2000] or Sone [2002] for the details of the analysis and the general results).

We could make $\hat{f}_{V0}$ satisfy the boundary condition (3.167) at the order of unity. To construct the solution that satisfies the boundary condition at the higher orders, we have to introduce the Knudsen-layer correction $\hat{f}_K$, for which $\varepsilon^2 n_i \partial \hat{f}_K / \partial x_i = O(\hat{f}_K)$. That is, the solution is put in the form[80]

$$\hat{f} = \hat{f}_V + \hat{f}_K. \tag{3.184}$$

The Knudsen-layer correction $\hat{f}_K$ is expanded in a power series of ε starting from the first order of ε, i.e.,

$$\hat{f}_K = \hat{f}_{K1} \varepsilon + \cdots, \tag{3.185}$$

for which the Knudsen-layer variables (η, χ_1, χ_2) introduced in Eq. (3.31), i.e.,

$$x_i = \varepsilon^2 \eta n_i(\chi_1, \chi_2) + x_{wi}(\chi_1, \chi_2),$$

[77] In Sone [2002] (Sone, Bardos, Golse & Sugimoto [2000]), the statement $\hat{v}_{iV0} n_i = 0$ on page 177 ($\hat{u}_{iV0} n_i = 0$ on page 335) should be put before $\partial \hat{p}_{V0} / \partial y = 0$, i.e., Eq. (6.53) [Eq. (52)].

[78] The lengthy manipulation becomes much lengthier unless the relation is not used in the early stage of analysis.

[79] Note that Eq. (1.54d), i.e., $\hat{p} = \hat{\rho} \hat{T}$, is implicitly used in the following discussion, in addition to the relations referred to.

[80] See Footnote 39 in Section 3.2.3.

are natural variables. We can proceed with the analysis in the same way as in Sections 3.1.4, 3.2.3, and 3.3.2 and obtain the (homogeneous or inhomogeneous) linearized one-dimensional Boltzmann equation for $\hat{f}_{Km}$

$$\zeta_i n_i \frac{\partial \hat{f}_{Km}}{\partial \eta} = 2\hat{J}((\hat{f}_{V0})_0, \hat{f}_{Km}) + \mathrm{Ihk}_m \quad (m \geq 1), \tag{3.186}$$

where the quantities in the parentheses with subscript 0 are evaluated on the boundary, and Ihk_m ($\mathrm{Ihk}_1 = 0$) is the inhomogeneous term determined by the solution of the previous stages. The boundary condition for $\hat{f}_{Km}$ is

$$\hat{f}_{Km} = \hat{f}_{wm} - \hat{f}_{Vm} \quad (\zeta_i n_i > 0) \text{ at } \eta = 0, \tag{3.187a}$$

$$\hat{f}_{Km} \to 0 \quad \text{as } \eta \to \infty. \tag{3.187b}$$

The speed of decay of $\hat{f}_{Km}$ is assumed to be faster than any inverse power of η.[81] The boundary-value problem (3.186)–(3.187b) is practically the same as that of the linear theory discussed in Section 3.1.4 (see Section A.11). According to the Grad–Bardos theorem, the slip conditions for $\hat{v}_{iVm}$ and $\hat{T}_{Vm}$ on the boundary are derived as the conditions that the problem (3.186)–(3.187b) has the solution $\hat{f}_{Km}$.[82]

As the final step of analysis, the condition to connect the overall solution $\hat{f}_h$ with the viscous boundary-layer solution $\hat{f}_V$ is discussed. In the viscous boundary layer with (nondimensional) thickness of the order of ε, the expansion of the overall solution $\hat{f}_h$

$$\hat{f}_h = (\hat{f}_{h0})_0 + \left[(\hat{f}_{h1})_0 + (\partial \hat{f}_{h0}/\partial x_i)_0 n_i y\right]\varepsilon + \cdots, \tag{3.188}$$

can be applied. Put the viscous boundary-layer solution $\hat{f}_V$ in the form

$$\hat{f}_V = \hat{f}_h + \hat{f}_{VC}. \tag{3.189}$$

If the residue $\hat{f}_{VC}$ decays rapidly (or faster than any inverse power of y) as $y \to \infty$,[83] the connection of $\hat{f}_V$ and $\hat{f}_h$ can be done. Consider Eq. (3.189) in the region where y is very large but εy is very small.[84] The residue $\hat{f}_{VC}$ is

[81] The fast decay with η is required for clear separation of $\hat{f}_V$ and $\hat{f}_K$. See Footnote 6 in Section 3.1.4.

[82] The solution $\hat{v}_{iKm} n_i$ can be obtained without full solution of the system in the same way as $u_{iKm} n_i$ is done in Footnote 11 in Section 3.1.4. That is, integrating Eq. (3.186) over the whole space of $\boldsymbol{\zeta}$ and noting that the integral of the collision term vanishes by integration, we obtain a simple equation for $\hat{v}_{iKm} n_i$, e.g., $\partial \hat{\rho}_{V0} \hat{v}_{iK1} n_i / \partial \eta = 0$. Thus, from the condition at $\eta = \infty$, $\hat{v}_{iK1} n_i = 0$. Then, from the condition $\hat{v}_i n_i = 0$ [or $(\hat{v}_{iV1} + \hat{v}_{iK1}) n_i = 0$] on a simple boundary, we have $\hat{v}_{iV1} n_i = 0$ there.

[83] The fast decay with y is required for clear separation of $\hat{f}_h$ and $\hat{f}_{VC}$. See Footnote 6 in Section 3.1.4.

[84] For example, $y = \varepsilon^{-1/n}$ (for arbitrarily large n). Then, $\hat{f}_{VC}$ is smaller than any inverse power of ε there, because of the assumption of the rapid decay of $\hat{f}_{VC}$ as $y \to \infty$. Further, this choice does not mix up the power terms of y in $\hat{f}_h$ that are of different order in ε for finite y [or terms of different orders in ε in Eq. (3.188) are not mixed up in the region].

negligibly small there. Comparing the two solutions $\hat{f}_V$ and $\hat{f}_h$ in this region with Eq. (3.188) in mind, we find that the two solutions match if the following conditions are satisfied:

$$\hat{\rho}_{V0} \sim (\hat{\rho}_{h0})_0 \quad \text{as } y \to \infty, \tag{3.190a}$$

$$\hat{v}_{iV0} \sim (\hat{v}_{ih0})_0 \quad \text{as } y \to \infty, \tag{3.190b}$$

$$\hat{T}_{V0} \sim (\hat{T}_{h0})_0 \quad \text{as } y \to \infty, \tag{3.190c}$$

$$\hat{\rho}_{V1} \sim (\hat{\rho}_{h1})_0 + y n_j \left(\frac{\partial \hat{\rho}_{h0}}{\partial x_j} \right)_0 \quad \text{as } y \to \infty, \tag{3.191a}$$

$$\hat{v}_{iV1} \sim (\hat{v}_{ih1})_0 + y n_j \left(\frac{\partial \hat{v}_{ih0}}{\partial x_j} \right)_0 \quad \text{as } y \to \infty, \tag{3.191b}$$

$$\hat{T}_{V1} \sim (\hat{T}_{h1})_0 + y n_j \left(\frac{\partial \hat{T}_{h0}}{\partial x_j} \right)_0 \quad \text{as } y \to \infty, \tag{3.191c}$$

and so on.

3.4.2 Fluid-dynamic-type equations and their boundary conditions and the recipe for solution

Here we summarize the equations and boundary conditions that determine the behavior of the gas up to the order of ε and describe the recipe for solution of the system. The viscous boundary-layer equations for the general three-dimensional case are complicated to see their character; thus, we here list the equations and boundary conditions in the two-dimensional case. In the viscous boundary-layer system, the quantities are assumed to be uniform along the χ_2 coordinate, and χ_1 is simply denoted by χ. For simplicity, the components of $\hat{v}_{iVm}$ along χ and η coordinates are denoted, respectively, by u_m and v_m. Generally, the order of expansion is denoted by the subscript of each quantity, and the subscript V is omitted.

System in the overall region:

The fluid-dynamic-type equations that determine the behavior of a gas in the overall region are the Euler set of equations at the leading order, i.e.,

$$\frac{\partial \hat{\rho}_{h0} \hat{v}_{ih0}}{\partial x_i} = 0, \tag{3.192a}$$

$$\hat{\rho}_{h0} \hat{v}_{jh0} \frac{\partial \hat{v}_{ih0}}{\partial x_j} + \frac{1}{2} \frac{\partial \hat{p}_{h0}}{\partial x_i} = 0, \tag{3.192b}$$

$$\hat{\rho}_{h0} \hat{v}_{jh0} \frac{\partial}{\partial x_j} \left(\hat{v}_{ih0}^2 + \frac{5}{2} \hat{T}_{h0} \right) = 0, \tag{3.192c}$$

where

$$\hat{p}_{h0} = \hat{\rho}_{h0} \hat{T}_{h0}.$$

The boundary condition on a simple boundary is

$$\hat{v}_{ih0} n_i = 0, \tag{3.193}$$

which is derived from Eqs. (3.183) and (3.190b).

Solving the above system, we proceed to the analysis of the viscous boundary-layer equations at the leading order (see the next item). After that, we return to the analysis of the next order. The equations at the next order are the linearized Euler set of equations, linearized around $\hat{\rho}_{h0}$, $\hat{v}_{ih0}$, and $\hat{T}_{h0}$, i.e.,

$$\frac{\partial(\hat{\rho}_{h0}\hat{v}_{ih1} + \hat{\rho}_{h1}\hat{v}_{ih0})}{\partial x_i} = 0, \tag{3.194a}$$

$$\hat{\rho}_{h0}\hat{v}_{jh0}\frac{\partial \hat{v}_{ih1}}{\partial x_j} + (\hat{\rho}_{h0}\hat{v}_{jh1} + \hat{\rho}_{h1}\hat{v}_{jh0})\frac{\partial \hat{v}_{ih0}}{\partial x_j} + \frac{1}{2}\frac{\partial \hat{p}_{h1}}{\partial x_i} = 0, \tag{3.194b}$$

$$\hat{\rho}_{h0}\hat{v}_{jh0}\frac{\partial}{\partial x_j}\left(2\hat{v}_{ih0}\hat{v}_{ih1} + \frac{5}{2}\hat{T}_{h1}\right) + (\hat{\rho}_{h0}\hat{v}_{jh1} + \hat{\rho}_{h1}\hat{v}_{jh0})\frac{\partial}{\partial x_j}\left(\hat{v}_{ih0}^2 + \frac{5}{2}\hat{T}_{h0}\right) = 0, \tag{3.194c}$$

where

$$\hat{p}_{h1} = \hat{\rho}_{h0}\hat{T}_{h1} + \hat{\rho}_{h1}\hat{T}_{h0}.$$

The boundary condition for the equations are derived from the viscous boundary-layer solution v_1 at the leading order [see Eq. (3.199)] and the connection condition (3.191b) as

$$(\hat{v}_{ih1})_0\, n_i = -\int_0^\infty \left[\left(\frac{\partial \hat{v}_{ih0}}{\partial x_j}\right)_0 n_i n_j + \frac{1}{(\hat{\rho}_{h0})_0}\frac{\partial \hat{\rho}_0 u_0}{\partial \chi}\right] \mathrm{d}y. \tag{3.195}$$

Here, we move to the analysis of the viscous boundary layer.

System in the viscous boundary layer:

From Eq. (3.183) with the connection conditions (3.190a) and (3.190c), v_0 and $\hat{p}_0$ are known, i.e.,

$$v_0 = 0, \qquad \hat{p}_0 = \hat{p}_0(\chi) = (\hat{p}_{h0})_0. \tag{3.196}$$

The variables u_0, $\hat{T}_0$, and v_1 are determined by the following system:

$$\hat{\rho}_0\left(u_0\frac{\partial u_0}{\partial \chi} + v_1\frac{\partial u_0}{\partial y}\right) = -\frac{1}{2}\frac{\mathrm{d}\hat{p}_0}{\mathrm{d}\chi} + \frac{1}{2}\frac{\partial}{\partial y}\left(\Gamma_1(\hat{T}_0)\frac{\partial u_0}{\partial y}\right), \tag{3.197}$$

$$\frac{3}{2}\hat{\rho}_0\left(u_0\frac{\partial \hat{T}_0}{\partial \chi} + v_1\frac{\partial \hat{T}_0}{\partial y}\right) = -\hat{p}_0\left(\frac{\partial u_0}{\partial \chi} + \frac{\partial v_1}{\partial y}\right) + \Gamma_1(\hat{T}_0)\left(\frac{\partial u_0}{\partial y}\right)^2 + \frac{5}{4}\frac{\partial}{\partial y}\left(\Gamma_2(\hat{T}_0)\frac{\partial \hat{T}_0}{\partial y}\right), \tag{3.198}$$

$$v_1 = -\frac{1}{\hat{\rho}_0}\int_0^y \frac{\partial \hat{\rho}_0 u_0}{\partial \chi}\mathrm{d}y, \tag{3.199}$$

where

$$\hat{\rho}_0 = \hat{p}_0/\hat{T}_0. \tag{3.200}$$

Their boundary conditions are

$$u_0 = \hat{v}_{wi}t_i, \qquad \hat{T}_0 = \hat{T}_w \qquad \text{at } y = 0, \tag{3.201}$$

$$u_0 \sim (\hat{v}_{ih0})_0 t_i, \qquad \hat{T}_0 \sim (\hat{T}_{h0})_0 \quad \text{as } y \to \infty, \tag{3.202}$$

where t_i is a unit vector tangent to the χ coordinate on the boundary, thus, $t_i = t_i(\chi)$, and $\Gamma_1(\hat{T}_0)$ and $\Gamma_2(\hat{T}_0)$ are positive functions of $\hat{T}_0$ whose functional forms are determined by the molecular model (see Section A.2.9). Equations (3.197) and (3.198) are, respectively, $\mathrm{SCV}_2^i t_i$ and SCV_2^4; Eq. (3.199) is derived from SCV_2^0 and the boundary condition for v_1 $(= 0)$ obtained by the Knudsen-layer analysis.[85] The boundary conditions (3.201) and (3.202) correspond, respectively, to Eq. (3.181) and the connection conditions (3.190b) and (3.190c).

After solving this system, we return to the analysis of the system (3.194a)–(3.195) for $\hat{\rho}_{h1}$, $\hat{v}_{ih1}$, and $\hat{T}_{h1}$. After that, we analyze the following viscous boundary-layer system at the next order. The equations are[86]

$$\begin{aligned}
&\hat{\rho}_0 u_0 \frac{\partial u_1}{\partial \chi} + (\hat{\rho}_0 u_1 + \hat{\rho}_1 u_0)\frac{\partial u_0}{\partial \chi} + \hat{\rho}_0 v_1 \frac{\partial u_1}{\partial y} \\
&+ (\hat{\rho}_0 v_2 + \hat{\rho}_1 v_1)\frac{\partial u_0}{\partial y} - \kappa \hat{\rho}_0 u_0 v_1 + \kappa y \hat{\rho}_0 u_0 \frac{\partial u_0}{\partial \chi} \\
&= -\frac{1}{2}\left(\frac{\partial \hat{p}_1}{\partial \chi} + \kappa y \frac{\mathrm{d}\hat{p}_0}{\mathrm{d}\chi}\right) \\
&\quad + \frac{1}{2}\frac{\partial}{\partial y}\left[\Gamma_1(\hat{T}_0)\left(\frac{\partial u_1}{\partial y} + \kappa u_0\right) + \hat{T}_1 \frac{\mathrm{d}\Gamma_1(\hat{T}_0)}{\mathrm{d}\hat{T}_0}\frac{\partial u_0}{\partial y}\right] \\
&\quad - \kappa \Gamma_1(\hat{T}_0)\frac{\partial u_0}{\partial y},
\end{aligned} \tag{3.203}$$

$$\frac{\partial \hat{p}_1}{\partial y} = -2\kappa \hat{\rho}_0 {u_0}^2, \tag{3.204}$$

[85] See Footnote 82 in Section 3.4.1.

[86] Equation (3.204) being first solved with the connection conditions (3.191a) and (3.191c), $\hat{p}_1$ is obtained independently of the other quantities, which is the same situation as that of $\hat{p}_0$.

$$
\begin{aligned}
&\frac{3}{2}\hat{\rho}_0 v_1 \frac{\partial \hat{T}_1}{\partial y} + \frac{3}{2}(\hat{\rho}_0 v_2 + \hat{\rho}_1 v_1)\frac{\partial \hat{T}_0}{\partial y} \\
&+ \frac{3}{2}\hat{\rho}_0 u_0 \frac{\partial \hat{T}_1}{\partial \chi} + \frac{3}{2}(\hat{\rho}_0 u_1 + \hat{\rho}_1 u_0)\frac{\partial \hat{T}_0}{\partial \chi} + \frac{3}{2}\kappa y \hat{\rho}_0 u_0 \frac{\partial \hat{T}_0}{\partial \chi} \\
&= -\hat{p}_0 \left[\frac{\partial v_2}{\partial y} + \frac{\partial u_1}{\partial \chi} + \kappa\left(y\frac{\partial u_0}{\partial \chi} - v_1\right)\right] - \hat{p}_1\left(\frac{\partial v_1}{\partial y} + \frac{\partial u_0}{\partial \chi}\right) \\
&\quad + \left[2\Gamma_1(\hat{T}_0)\left(\frac{\partial u_1}{\partial y} + \kappa u_0\right) + \hat{T}_1 \frac{\mathrm{d}\Gamma_1(\hat{T}_0)}{\mathrm{d}\hat{T}_0}\frac{\partial u_0}{\partial y}\right]\frac{\partial u_0}{\partial y} \\
&\quad + \frac{5}{4}\frac{\partial}{\partial y}\left[\Gamma_2(\hat{T}_0)\frac{\partial \hat{T}_1}{\partial y} + \hat{T}_1 \frac{\mathrm{d}\Gamma_2(\hat{T}_0)}{\mathrm{d}\hat{T}_0}\frac{\partial \hat{T}_0}{\partial y}\right] - \frac{5}{4}\kappa\Gamma_2(\hat{T}_0)\frac{\partial \hat{T}_0}{\partial y},
\end{aligned}
\tag{3.205}
$$

$$
v_2 = -\frac{\hat{\rho}_1 v_1}{\hat{\rho}_0} - \frac{1}{\hat{\rho}_0}\int_0^y \left(\frac{\partial(\hat{\rho}_0 u_1 + \hat{\rho}_1 u_0)}{\partial \chi} - \kappa\hat{\rho}_0 v_1 + \kappa y \frac{\partial \hat{\rho}_0 u_0}{\partial \chi}\right)\mathrm{d}y, \tag{3.206}
$$

where κ/L is the curvature of the boundary taken negative when the center of the curvature lies on the side of the gas, and $\hat{\rho}_1$ is given by

$$
\hat{\rho}_1 = \frac{\hat{p}_1 - \hat{\rho}_0 \hat{T}_1}{\hat{T}_0}. \tag{3.207}
$$

Equations (3.203), (3.204), and (3.205) are, respectively, $\mathrm{SCV}_3^i t_i$, $\mathrm{SCV}_2^i n_i$, and SCV_3^4, and Eq. (3.206) is derived from SCV_3^0 and the boundary value of v_2 obtained by the Knudsen-layer analysis.[87] The boundary conditions at $y = 0$, derived by the Knudsen-layer analysis, are

$$
u_1 = -\frac{\hat{k}_0}{\hat{\rho}_0}\frac{\partial u_0}{\partial y}, \quad \hat{T}_1 = \frac{\hat{d}_1}{\hat{\rho}_0}\frac{\partial \hat{T}_0}{\partial y}, \tag{3.208}
$$

where the slip coefficients $\hat{k}_0$ and $\hat{d}_1$ are related to those k_0 and d_1 in the linear theory in Section 3.1.5.[88] Their relations are discussed in Section A.11. For the diffuse-reflection condition, the relations are

$$
\begin{aligned}
&\hat{k}_0 = k_0\ (= -1.2540), \quad \hat{d}_1 = d_1\ (= 2.4001) \quad \text{(hard-sphere gas)}, \\
&\hat{k}_0/\hat{T}_w^{1/2} = k_0\ (= -1.01619), \quad \hat{d}_1/\hat{T}_w^{1/2} = d_1\ (= 1.30272) \quad \text{(BKW model)}.
\end{aligned}
$$

[87] See Footnote 82 in Section 3.4.1.

[88] The thermal creep flow appears at the order of ε^2, because the variations of the variables along the boundary are $O(\varepsilon)$ times smaller than those normal to the boundary in the viscous boundary layer.

The conditions at infinity are

$$\hat{\rho}_1 \sim (\hat{\rho}_{h1})_0 + y n_j \left(\frac{\partial \hat{\rho}_{h0}}{\partial x_j}\right)_0 \qquad \text{as } y \to \infty, \tag{3.209a}$$

$$u_1 \sim (\hat{v}_{ih1})_0 \, t_i + y n_j \left(\frac{\partial \hat{v}_{ih0}}{\partial x_j}\right)_0 t_i \quad \text{as } y \to \infty, \tag{3.209b}$$

$$\hat{T}_1 \sim \left(\hat{T}_{h1}\right)_0 + y n_j \left(\frac{\partial \hat{T}_{h0}}{\partial x_j}\right)_0 \qquad \text{as } y \to \infty, \tag{3.209c}$$

which are the connection conditions (3.191a)–(3.191c).

The Knudsen-layer correction for the macroscopic variables is given as

$$\hat{\rho}_{K1} = \frac{1}{\hat{T}_w}\left(\frac{\partial \hat{T}_0}{\partial y}\right)_0 \hat{\Omega}_1(\tilde{\eta}), \tag{3.210a}$$

$$\hat{v}_{iK1} t_i = -\frac{1}{(\hat{\rho}_0)_0}\left(\frac{\partial u_0}{\partial y}\right)_0 \hat{Y}_0(\tilde{\eta}), \quad \hat{v}_{iK1} n_i = 0, \tag{3.210b}$$

$$\hat{T}_{K1} = \frac{1}{(\hat{\rho}_0)_0}\left(\frac{\partial \hat{T}_0}{\partial y}\right)_0 \hat{\Theta}_1(\tilde{\eta}), \tag{3.210c}$$

where $\tilde{\eta} = (\hat{\rho}_0)_0 \eta$ and the Knudsen-layer functions $\hat{Y}_0(\tilde{\eta})$, $\hat{\Omega}_1(\tilde{\eta})$, and $\hat{\Theta}_1(\tilde{\eta})$ are related to those $Y_0(\eta)$, $\Omega_1(\eta)$, and $\Theta_1(\eta)$ in Section 3.1.5 and the relations, which depend on the choice of the reference quantities, are discussed in Section A.11.

The viscous boundary-layer equations (3.197)–(3.200) and boundary conditions (3.201) and (3.202) at the leading order are the same as those for the Navier–Stokes equations for a compressible fluid (the compressible fluid version of the Prandtl boundary-layer equations and their boundary conditions). Equations (3.203)–(3.207) for the next-order variables also do not contain the non-Navier–Stokes stress and heat-flow terms. The term containing $\hat{T}_1 \mathrm{d}\Gamma_1/\mathrm{d}\hat{T}_0$ or $\hat{T}_1 \mathrm{d}\Gamma_2/\mathrm{d}\hat{T}_0$ is due to the fact that the viscosity or thermal conductivity of the gas depends on its temperature. These equations are derived by a power series expansion in the inverse $\mathrm{Re}^{-1/2}$ of the square root of the Reynolds number Re from the Navier–Stokes set of equations for a compressible fluid where the coordinate normal to the boundary is stretched by the factor of $\mathrm{Re}^{1/2}$ [note the relation (3.74) for the transform from the $\mathrm{Re}^{-1/2}$-expansion to ε-expansion]. The result does not support the claim by Darrozes [1969] that the boundary-layer equations describing the leading effect of gas rarefaction (or $\hat{\rho}_1$, u_1, v_1, $\hat{p}_1$, and $\hat{T}_1$) should contain a non-Navier–Stokes stress term. (In his paper no explicit equations are given.) Owing to the anisotropic character of the viscous boundary layer, a higher-order quantity, or v_2, which is expressed by lower-order quantities, enters the equations that determine the behavior of $\hat{\rho}_1$, u_1, $\hat{p}_1$, and $\hat{T}_1$. However, in view of the fact that its boundary value $(v_2)_0$ vanishes owing to the displacement effect of the Knudsen layer being of higher order, the contributions up to the order of $\mathrm{Kn}^{1/2}$ are included in the system of the Navier–Stokes

equations (in the nonexpanded original form) and the (correspondingly rearranged) slip conditions consisting of tangential velocity slip due to the shear of flow and temperature jump due to the temperature gradient normal to the boundary.

In a system where the Euler set of equations is the leading set of the fluid-dynamic-type equations, a kinetic transition layer or shock layer, corresponding to a shock wave (Section 4.7), may appear in a gas (Grad [1969]). At the zeroth approximation, the solutions of the Euler set of equations across the shock layer are connected by the Rankine–Hugoniot relation for a plane shock wave, and the smooth transition between the two solutions is expressed by the solution of a plane shock wave.

3.5 Nonlinear problem III: Flow with a finite speed of evaporation or condensation

3.5.1 Problem and the outline of analysis

In Section 3.4, we discussed a flow with a finite Mach number around a simple boundary, across which there is no mass flux. In the present section (Section 3.5), we consider a flow of a gas around its condensed phase where evaporation or condensation with a speed of a finite Mach number is taking place. Owing to the convection effect of condensing or evaporating flow of a finite Mach number, the viscous boundary layer, which appears in a flow with a finite Mach number around a simple boundary (Section 3.4),[89] shrinks to merge into the Knudsen layer over a condensing boundary, or the layer spreads into the whole flow field (or the Euler region) over an evaporating boundary and the viscous effect is reduced to a secondary one there. The Euler region is connected directly to the Knudsen layer. Instead, the Knudsen layer is governed by a nonlinear equation in contrast to that in the foregoing sections.

Consider a time-independent system composed of a gas and its condensed phase of smooth shape, on the surface of which evaporation or condensation is taking place. The Mach number of the speed of evaporation and condensation of the gas on the interface of the gas and its condensed phase is of the order of unity. We will outline the asymptotic analysis of this system for small Knudsen numbers (see Sone [2002] for the details).

The problem is the time-independent boundary-value problem of the Boltzmann equation (1.47a) with the boundary condition (1.69), or more simply the complete-condensation condition (1.68). The nondimensional Boltzmann equation is

$$\zeta_i \frac{\partial \hat{f}}{\partial x_i} = \frac{1}{k} \hat{J}(\hat{f}, \hat{f}), \tag{3.211}$$

[89] The viscous boundary layer appears when $\mathrm{Ma} \gg \mathrm{Kn}$ or $\mathrm{Re} \gg 1$ even if $\mathrm{Ma} \ll 1$ (see Sone, Bardos, Golse & Sugimoto [2000] or Sone [2002]).

and the boundary condition is symbolically expressed as

$$\hat{f}(x_i, \zeta_i) = \hat{f}_w \quad (\zeta_j n_j > 0). \tag{3.212}$$

The solution of the boundary-value problem is expressed as the sum of the two terms, the overall solution and the Knudsen-layer correction, i.e.,

$$\hat{f} = \hat{f}_H + \hat{f}_K, \tag{3.213}$$

where the overall solution $\hat{f}_H$ is a solution of Eq. (3.211), with Eq. (3.212) put aside, whose length scale of variation is the reference length of the system, i.e., $\partial \hat{f}_H / \partial x_i = O(\hat{f}_H)$.[90] The Knudsen-layer correction $\hat{f}_K$ is appreciable only in a thin layer, with thickness of the order of the mean free path, adjacent to the boundary and decays rapidly in the layer in the direction normal to the boundary.[91]

The solution $\hat{f}_H$ is obtained in a power series of k, i.e.,

$$\hat{f}_H = \hat{f}_{H0} + \hat{f}_{H1} k + \cdots, \tag{3.214}$$

where the subscript H is the symbol showing the original *Hilbert expansion* (Hilbert [1912]). Corresponding to this expansion, the boundary data $\hat{f}_w$ and the macroscopic variables $\hat{\rho}$, $\hat{v}_i$, $\hat{T}$, etc. are also expanded in power series of k, i.e.,

$$\hat{f}_w = \hat{f}_{w0} + \hat{f}_{w1} k + \cdots, \tag{3.215}$$

$$\hat{h}_H = \hat{h}_{H0} + \hat{h}_{H1} k + \cdots, \tag{3.216}$$

where $\hat{h}$ represents $\hat{\rho}$, $\hat{v}_i$, $\hat{T}$, etc. The analysis of $\hat{f}_{Hm}$ is essentially the same as the previous analyses in Sections 3.1.2, 3.2.2, 3.3.2, and 3.4.1. The series (3.214) being substituted into Eq. (3.211), a series of integral equations for $\hat{f}_{Hm}$ is derived,[92] i.e.,

$$\hat{J}(\hat{f}_{H0}, \hat{f}_{H0}) = 0, \tag{3.217a}$$

$$2\hat{J}(\hat{f}_{H0}, \hat{f}_{Hm}) = \zeta_i \frac{\partial \hat{f}_{Hm-1}}{\partial x_i} - \sum_{s=1}^{m-1} \hat{J}(\hat{f}_{Hs}, \hat{f}_{Hm-s}) \quad (m = 1, 2, \ldots), \tag{3.217b}$$

where the $\sum$ term is absent when $m = 1$.

The leading distribution $\hat{f}_{H0}$ is Maxwellian, i.e.,

$$\hat{f}_{H0} = \frac{\hat{\rho}_{H0}}{(\pi \hat{T}_{H0})^{3/2}} \exp\left(-\frac{(\zeta_i - \hat{v}_{iH0})^2}{\hat{T}_{H0}} \right). \tag{3.218}$$

[90] See the first two sentences of Footnote 39 in Section 3.2.3.

[91] In addition to the condition $kn_i \partial \hat{f}_K / \partial x_i = O(\hat{f}_K)$, the decay faster than any inverse power of η, defined by Eq. (3.147), is assumed, which is required for clear separation of $\hat{f}_H$ and $\hat{f}_K$. See Footnote 6 in Section 3.1.4.

[92] See Footnote 58 in Section 3.3.2.

We advance the analysis without limiting the parametric functions $\hat{\rho}_{H0}$, $\hat{v}_{iH0}$, and $\hat{T}_{H0}$ in the Maxwellian to special values (e.g., $\hat{v}_{iH0} = 0$ in Section 3.3, or $\hat{\rho}_{H0}$ and $\hat{T}_{H0}$ are uniform in addition to $\hat{v}_{iH0} = 0$ in Section 3.2). From the condition for Eq. (1.83) to hold and the relation (1.53),[93] the condition (solvability condition)

$$\int (1, \zeta_i, \zeta_k^2)\zeta_j \frac{\partial \hat{f}_{Hm-1}}{\partial x_j} \mathbf{d}\boldsymbol{\zeta} = 0 \quad (m = 1, 2, \ldots) \tag{3.219}$$

is required for Eq. (3.217b) to have a solution. From Eq. (3.219) with $m = 1$, the equations that determine the variation of $\hat{\rho}_{H0}$, $\hat{v}_{iH0}$, and $\hat{T}_{H0}$, which are the Euler set of equations, are derived. In the higher-order analysis, a series of linearized Euler sets of equations, linearized around $(\hat{\rho}_{H0}, \hat{v}_{iH0}, \hat{T}_{H0})$, with additional inhomogeneous terms is obtained. In the present case, no degeneration of the solvability condition occurs in contrast to the cases of ϕ_G, ϕ_S, $\hat{f}_{SB}$, and $\hat{f}_V$ (see Sections 3.1.2, 3.2.2, 3.3.2, and 3.4.1).

When evaporation or condensation of a finite Mach number, or $\hat{v}_{iH0} n_i \neq 0$, is taking place on the interface, noting the condition (1.71c) with the uniqueness comment, we find that the Maxwellian (3.218) cannot be matched with the boundary condition (3.212). Thus, we have to introduce the Knudsen-layer correction $\hat{f}_K$ from the leading order. Substituting Eq. (3.213) into Eq. (3.211) and rewriting the result in the Knudsen-layer variables (3.147), we find that the Knudsen-layer correction $\hat{f}_K$ is governed by Eq. (3.148) with Eq. (3.147) where $\hat{F}_i$ is put zero and $\hat{f}_{SB}$ is replaced by $\hat{f}_H$. The function $\hat{f}_K$ is expanded in a power series of k, i.e.,

$$\hat{f}_K = \hat{f}_{K0} + \hat{f}_{K1} k + \cdots . \tag{3.220}$$

The series (3.214) and (3.220) are substituted into the above-mentioned equation for $\hat{f}_K$ and the same-order terms in k are arranged. In this process, the following expansion of $\hat{f}_H$ with respect to η is used:

$$\hat{f}_H = (\hat{f}_{H0})_0 + \left[(\hat{f}_{H1})_0 + (\partial \hat{f}_{H0}/\partial x_i)_0 n_i \eta \right] k + \cdots , \tag{3.221}$$

where the quantities in the parentheses with subscript 0 are evaluated on the interface, because $\hat{f}_H$ appears only as the product with $\hat{f}_K$ in the equation for $\hat{f}_K$. Then, we obtain the equation for $\hat{f}_{Km}$. With the new function $\hat{f}_{HK}$ defined by

$$\hat{f}_{HK} = (\hat{f}_{H0})_0 + \hat{f}_{K0}, \tag{3.222}$$

the leading-order Knudsen-layer equation is given in the form

$$\zeta_i n_i \frac{\partial \hat{f}_{HK}}{\partial \eta} = \hat{J}(\hat{f}_{HK}, \hat{f}_{HK}). \tag{3.223}$$

[93] See Footnote 59 in Section 3.3.2.

The boundary condition for $\hat{f}_{HK}$ is

$$\hat{f}_{HK} = \hat{f}_{w0} \qquad (\zeta_i n_i > 0) \qquad \text{at } \eta = 0, \tag{3.224a}$$

$$\hat{f}_{HK} \to \frac{(\hat{p}_{H0})_0}{\pi^{3/2}(\hat{T}_{H0})_0^{5/2}} \exp\left(-\frac{[\zeta_i - (\hat{v}_{iH0})_0]^2}{(\hat{T}_{H0})_0}\right) \quad \text{as } \eta \to \infty. \tag{3.224b}$$

The Knudsen layer is determined by the half-space problem of the original nonlinear Boltzmann equation, in contrast to that of the linearized Boltzmann equation for the Knudsen layer in the previous cases (Sections 3.1.4, 3.2.3, 3.3.2, and 3.4.1). The (nonlinear) half-space problem, i.e., Eqs. (3.223)–(3.224b), is studied analytically (Sone [1978b], Sone, Golse, Ohwada & Doi [1998]; see Chapter 7) and numerically (Sone, Aoki & Yamashita [1986], Sone, Aoki, Sugimoto & Yamada [1988], Sone & Sugimoto [1990], Aoki, Sone & Yamada [1990], and Aoki, Nishino, Sone & Sugimoto [1991]; see Section 6.1). The extensive numerical studies on the basis of the BKW equation and the complete-condensation condition give the comprehensive feature of the solution; the analytical studies clarify the key characteristics of the solution. According to them, for the half-space problem to have a solution, the parameters $(\hat{p}_{H0})_0$, $(\hat{v}_{iH0})_0$, and $(\hat{T}_{H0})_0$ in Eq. (3.224b) and the boundary data $\hat{p}_w$, $\hat{v}_{wi}$, and $\hat{T}_w$ of the interface must satisfy some relations.[94] The relations among $(\hat{p}_{H0})_0$, $(\hat{v}_{iH0})_0$, $(\hat{T}_{H0})_0$, and the boundary data give the boundary conditions for the Euler set of equations on the interface. They are summarized in the next subsection.

3.5.2 System of fluid-dynamic-type equations and boundary conditions in the continuum limit

Here we summarize the fluid-dynamic-type equations and their associated boundary conditions on the interface at the leading order of the expansion. We use the dimensional variables without the subscripts concerning the expansion.

The fluid-dynamic-type equations are the Euler set of equations

$$\frac{\partial \rho v_i}{\partial X_i} = 0, \tag{3.225a}$$

$$\rho v_j \frac{\partial v_i}{\partial X_j} + \frac{\partial p}{\partial X_i} = 0, \tag{3.225b}$$

[94] (i) The boundary data $\hat{p}_w$, $\hat{v}_{wi}$, and $\hat{T}_w$ are assumed to be independent of k for simplicity, because only the leading-order term is obtained explicitly here.

(ii) The mathematical theory, as the Grad–Bardos theorem in the linearized problem, is not developed yet for this nonlinear problem except for the analysis in Chapter 7. Thus, extensive numerical computation is carried out to derive the result given in Section 3.5.2. That is, the time-dependent behavior of a gas in the half-space domain ($\eta > 0$) is studied for many situations, and possible kinds of time-dependent solutions and their limiting time-independent solutions are examined, from which the relations between the condition of the condensed phase and that of the gas at infinity are found. The process of analysis is explained for the special case $(\hat{v}_{iH0} - \hat{v}_{jH0} n_j n_i)_0 = 0$ and $\hat{v}_{wi} = 0$ in Section 6.1. The case $(\hat{v}_{iH0} - \hat{v}_{jH0} n_j n_i)_0 \neq 0$ or $\hat{v}_{wi} \neq 0$ $(\hat{v}_{wi} n_i = 0)$ is studied in Aoki, Nishino, Sone & Sugimoto [1991].

Table 3.4. The functions $h_1(M_n)$ and $h_2(M_n)$ (BKW and complete condensation; Sone & Sugimoto [1990, 1993]).

M_n	h_1	h_2	M_n	h_1	h_2	M_n	h_1	h_2
0.0000	1.0000	1.0000	0.4000	0.4900	0.8470	0.8000	0.2695	0.7088
0.04999	0.9083	0.9798	0.4400	0.4593	0.8326	0.8400	0.2553	0.6956
0.07998	0.8582	0.9679	0.4800	0.4310	0.8184	0.8800	0.2420	0.6824
0.1200	0.7966	0.9521	0.5200	0.4050	0.8043	0.9200	0.2297	0.6693
0.1600	0.7404	0.9365	0.5600	0.3809	0.7904	0.9600	0.2182	0.6563
0.2000	0.6891	0.9212	0.6000	0.3586	0.7765	0.9700	0.2155	0.6530
0.2400	0.6421	0.9060	0.6400	0.3380	0.7628	0.9800	0.2128	0.6498
0.2800	0.5991	0.8910	0.6800	0.3189	0.7492	0.9900	0.2101	0.6466
0.3200	0.5596	0.8761	0.7200	0.3012	0.7356	1.0000	0.2075	0.6434
0.3600	0.5233	0.8615	0.7600	0.2848	0.7222			

$$v_j \frac{\partial}{\partial X_j}\left(\frac{5}{2}RT + \frac{1}{2}v_i^2\right) = 0, \tag{3.225c}$$

where

$$p = R\rho T. \tag{3.226}$$

The boundary condition for the Euler set of equations on the interface to which the complete-condensation condition applies is given in the following form, where the notation

$$M_n = \frac{v_i n_i}{(5RT/3)^{1/2}}, \quad \overline{M}_t = \frac{|v_i - v_j n_j n_i - v_{wi}|}{(5RT/3)^{1/2}}, \tag{3.227}$$

with v_{wi} ($v_{wi}n_i = 0$) being the velocity of the interface, is used.

(a) In the case of evaporation ($M_n \geq 0$)

$$p/p_w = h_1(M_n), \quad T/T_w = h_2(M_n), \quad \overline{M}_t = 0 \quad \text{when } 0 \leq M_n \leq 1, \tag{3.228a}$$

$$\text{No solution exists when } M_n > 1, \tag{3.228b}$$

where p_w is the saturated gas pressure at the temperature T_w of the condensed phase. The functions $h_1(M_n)$ and $h_2(M_n)$ for the BKW equation with the complete-condensation condition are tabulated in Table 3.4.

(b) In the case of condensation ($M_n < 0$)

$$p/p_w = F_s(M_n, \overline{M}_t, T/T_w) \quad \text{when } -1 < M_n < 0, \tag{3.229a}$$

$$p/p_w > F_b(M_n, \overline{M}_t, T/T_w) \quad \text{when } M_n < -1, \tag{3.229b}$$

$$p/p_w \geq F_b(-1_-, \overline{M}_t, T/T_w) = F_s(-1_+, \overline{M}_t, T/T_w). \tag{3.229c}$$

Examples of the functions F_s and F_b for the BKW equation with the complete-condensation condition are given in Figs. 3.7 and 3.8 (see also Tables 6.1 and 6.2 in Section 6.1 and more data in Sone, Aoki & Yamashita [1986], Aoki, Sone

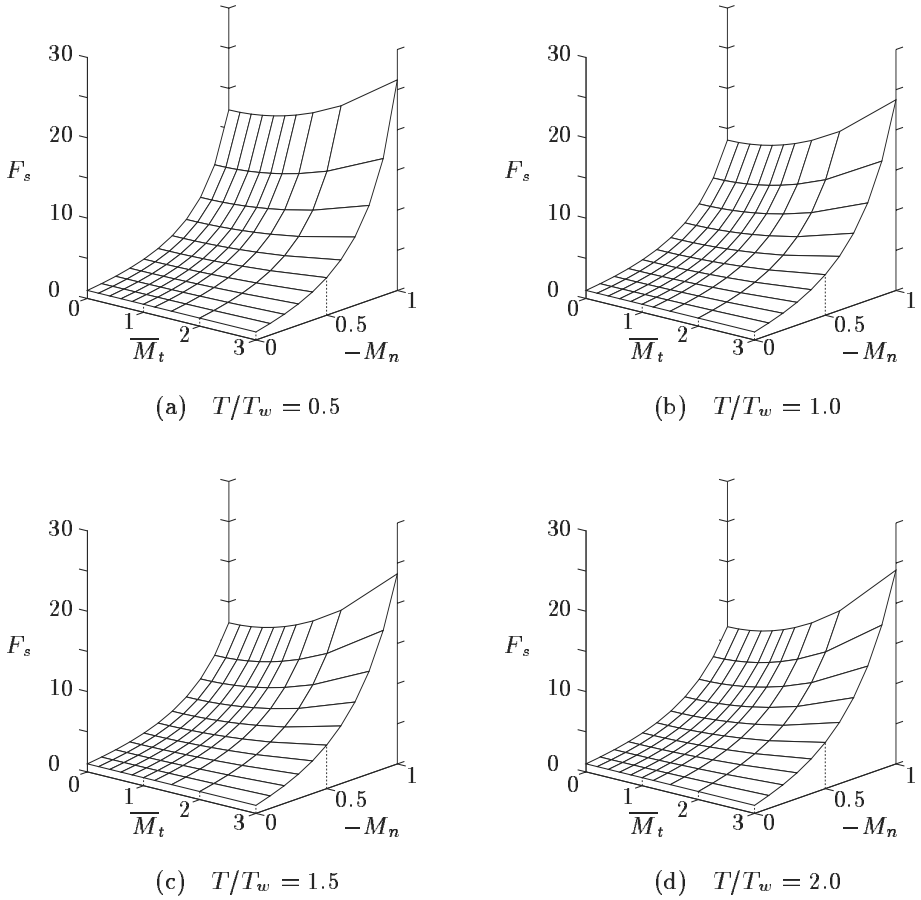

Figure 3.7. $F_s(M_n, \overline{M}_t, T/T_w)$ (BKW & complete condensation). (a) $T/T_w = 0.5$, (b) $T/T_w = 1.0$, (c) $T/T_w = 1.5$, and (d) $T/T_w = 2.0$.

& Yamada [1990], and Aoki, Nishino, Sone & Sugimoto [1991]).[95] The bounds of the functions h_1, h_2, F_s, and F_b are discussed in Sone, Takata & Sugimoto [1996], Sone, Takata & Golse [2001], and Bobylev, Grzhibovskis & Heintz [2001] (see also Sone [2002]).

The boundary conditions for evaporation and condensation for the complete-condensation condition can be generalized by a simple transformation to a more general mixed-type condition [Eqs. (1.28a) and (1.28b) with $\alpha = 1$ and α_c being arbitrary] (Section 6.6; see also Section 7.6 of Sone [2002]). This generalization

[95]Numerical computations of the subsonic condensation for hard-sphere molecules for the cases $\overline{M}_t = 0$ and $T/T_w = 0.5, 1, 2$ (Sone & Sasaki [unpublished]) show that their relative differences of p/p_w from the above BKW results are less than 1% except in the range $-1 \le M_n \le -0.9$ at $T/T_w = 0.5$, where the differences are bounded by 5%. The equivalent statement in Footnote 6 of Chapter 7 in Sone [2002] contains a misprint, where M_n should be replaced by $-M_n$.

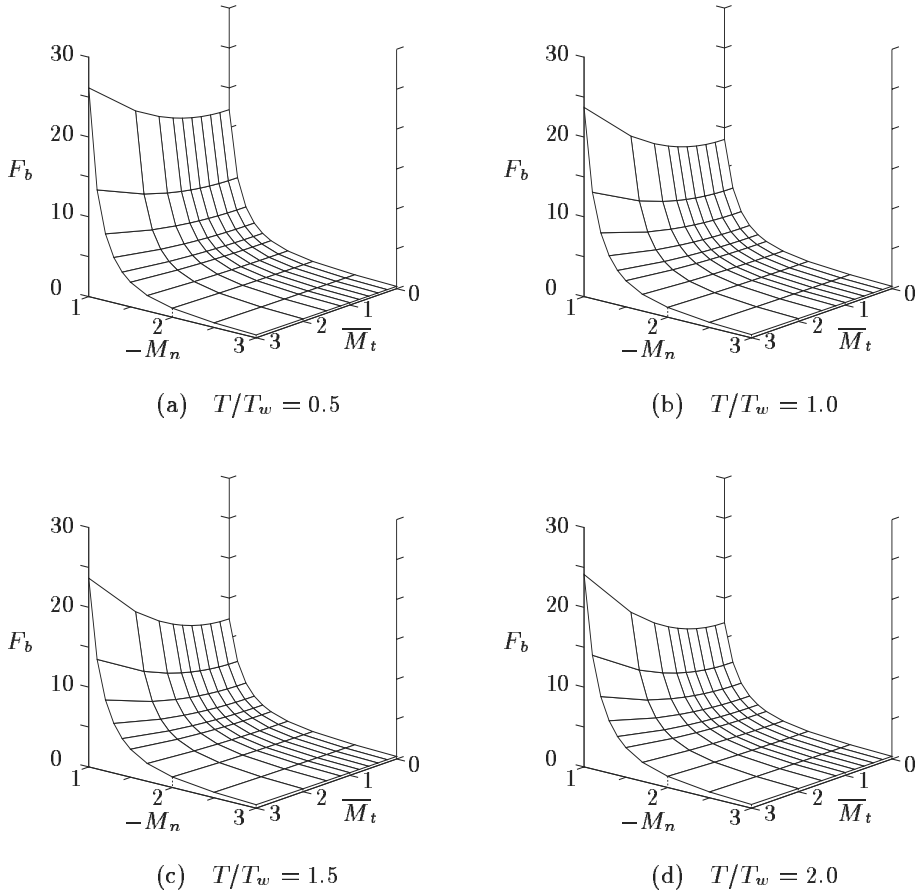

Figure 3.8. $F_b(M_n, \overline{M}_t, T/T_w)$ (BKW & complete condensation). (a) $T/T_w = 0.5$, (b) $T/T_w = 1.0$, (c) $T/T_w = 1.5$, and (d) $T/T_w = 2.0$.

is not limited to the BKW equation but also applies to the standard Boltzmann equation. According to it, the solution has the same feature as the solution under the complete-condensation condition when the condensation coefficient α_c (≤ 1) is larger than some value ($\alpha_c > \alpha_c^{cr}$), but no solution exists in a band region around $M_n = -1$ (say, $c_1 \leq -M_n \leq c_2$; $0 < c_1 \leq 1$, $c_2 \geq 1$) when $\alpha_c \leq \alpha_c^{cr}$.

The boundary condition on an interface shows qualitatively different characters depending on evaporation, subsonic condensation, or supersonic condensation. In the four-dimensional space $(M_n, \overline{M}_t, p/p_w, T/T_w)$, the boundary data are given on a hyper-curve for evaporation, on a hyper-surface for subsonic condensation, and in a domain for supersonic condensation. The analytical structure of this transition will be explained in Chapter 7 on the basis of Sone [1978b] and Sone, Golse, Ohwada & Doi [1998]. The mathematical study of the

half-space problem is in progress, but some difficulty has to be overcome (Ukai, Yang & Yu [2003, 2004], Bardos, Golse & Sone [2006]).

As in the case of Section 3.4, a shock layer may appear in a flow of the present problem. An example is given in Section 6.3.

3.6 Review of the fluid-dynamic-type systems

3.6.1 Classification

In Sections 3.1–3.5, we have discussed the time-independent behavior of a gas for small Knudsen numbers for various physical situations on the basis of the Boltzmann system. The fluid-dynamic-type equations and their associated boundary conditions (or fluid-dynamic-type system) derived in the continuum limit differ considerably depending on the situations. It may be in order to summarize these results.

The velocity distribution function describing the overall behavior of the gas approaches a Maxwell distribution f_e, whose parameters depend on the position in the gas, in the continuum limit. The fluid-dynamic-type equations that determine the macroscopic variables in the limit differ considerably depending on the character of the Maxwellian. The systems are classified by the size of $|f_e - f_{e0}|/f_{e0}$, where f_{e0} is the stationary Maxwellian

$$f_{e0} = \frac{\rho_0}{(2\pi RT_0)^{3/2}} \exp\left(-\frac{\xi_i^2}{2RT_0}\right).$$

Here, ρ_0 and T_0 are, respectively, the characteristic values of the density and temperature in the gas. The systems are classified as follows:

(i) $|f_e - f_{e0}|/f_{e0} = O(\mathrm{Kn})$: The continuum limit is a uniform state at rest. The nonuniform state of the first order of Knudsen number is described by the system derived in Section 3.2, where the leading set of equations is the incompressible Navier–Stokes set with the energy equation modified. (S system, for short)

(i′) $|f_e - f_{e0}|/f_{e0} = o(\mathrm{Kn})$: The system is reduced to the linear system discussed in Section 3.1, where the fluid-dynamic-type equations are given by the Stokes set.

(ii) $|f_e - f_{e0}|/f_{e0} = O(1)$ with $|v_i|/(2RT)^{1/2} = O(\mathrm{Kn})$ (v_i and T are the velocity and temperature of f_e, respectively): The behavior of the gas is described by the system derived in Section 3.3, where the temperature and density of the gas in the continuum limit are determined together with the flow velocity of the first order of Kn amplified by 1/Kn (the ghost effect), and the thermal stress of the order of $(\mathrm{Kn})^2$ must be retained in the momentum equations (a non-Navier–Stokes effect). The thermal creep in the boundary condition must be taken into account. (SB system)

(iii) $|f_e - f_{e0}|/f_{e0} = O(1)$ with $|v_i|/(2RT)^{1/2} = O(1)$:

(a) The behavior of the gas around a simple boundary is described by the system derived in Section 3.4, where the leading fluid-dynamic-type set is the combination of the Euler and viscous boundary-layer sets. (E+VB system)

(b) The behavior of the gas around the condensed phase of the gas, where evaporation or condensation of a finite Mach number, i.e., $|v_i n_i|/(2RT)^{1/2} = O(1)$, is taking place, is described by the system derived in Section 3.5, where the leading fluid-dynamic-type set is the Euler set. The Knudsen-layer correction is given by the nonlinear Boltzmann equation in contrast to the other cases, in which the Knudsen layer is governed by the linearized Boltzmann equation. (E system)

The fluid-dynamic-type equations describing the nontrivial leading-order behavior of a gas are further subclassified in marginal cases. For example, take the edge of Case (iii) between Cases (i) and (iii) where the difference $|f_e - f_{e0}|/f_{e0}$ is small but finite or much larger than the Knudsen number in the way that Mach number of the flow is so. The Euler set of equations in Case (iii) reduces to the incompressible Euler set.[96] In flows around a simple boundary [Case (iii-a)], the viscous boundary-layer equations reduce to the "incompressible viscous boundary-layer equations".[97] In flows with evaporation or condensation on an interface [Case (iii-b)], the Knudsen layer on an evaporating interface (the nonlinear half-space problem of the nonlinear Boltzmann equation) simply reduces to the Knudsen layer in the linearized problem (the half-space problem of the linearized Boltzmann equation); on the other hand, the Knudsen layer on a condensing interface (the corresponding nonlinear half-space problem) splits into two layers, i.e., the suction boundary-layer[98] and the Knudsen layer in the linearized problem. The thickness of the suction boundary layer is of the order of the mean free path divided by the Mach number. This separation is compared with that of the viscous boundary layer and the Knudsen layer in Case (iii-a). The analysis of the Knudsen layer in the linearized problem gives the boundary

[96]The work done by pressure, explained in Footnote 47 in Section 3.2.4 for Case (i), contributes to the energy equation but in a degenerate way. A constant is multiplied to that for an incompressible fluid. In both the cases, the variation of the temperature in the direction of the flow velocity vanishes.

[97](i) The quotation mark has the same meaning as that explained in Section 3.2.4. That is, there is a difference by the work done by pressure in the energy equation.

(ii) The rescalings of the thickness of the viscous boundary layer and thus the velocity component normal to the boundary are required. For example, when the Mach number is small but finite [say, $O(\delta)$], the thickness of the viscous boundary layer is thicker by the factor $\delta^{-1/2}$, that is, ε in Eq. (3.175) is to be replaced by $\varepsilon/\delta^{1/2}$ and thus, v_1 in Eq. (3.199) is of the order of $\delta^{1/2}$ [consider the balance between the first term in the parentheses on the left-hand side and the second term on the right-hand side of Eq. (3.197), and estimate the size of v_1 using Eq. (3.199)]. The discussion for other relative sizes of Mach and Knudsen numbers is given in Sone, Bardos, Golse & Sugimoto [2000]. In this discussion, the continuum limit is a uniform state at rest, and the fluid-dynamic-type equations, though similar to the present ones, describe the nontrivial leading-order state. The equations in the present case describe the behavior in the continuum limit.

[98]The half-space problem with suction on the boundary is studied by the Navier–Stokes equations and is called the *suction boundary layer* (see Schlichting [1979]). The above is the corresponding problem in the kinetic theory, which is explained in Section 7.2 in detail. The bifurcation of solution on the transition from evaporation to condensation on the interface is seen in this half-space problem. An example of flows with the suction boundary layer is given in Sone & Doi [2000] (see also Sone [2002]), where a flow between coaxial circular cylindrical condensed phases is studied and the bifurcation of solution is shown to occur under the axially symmetric and uniform condition (see also Section 8.4.2).

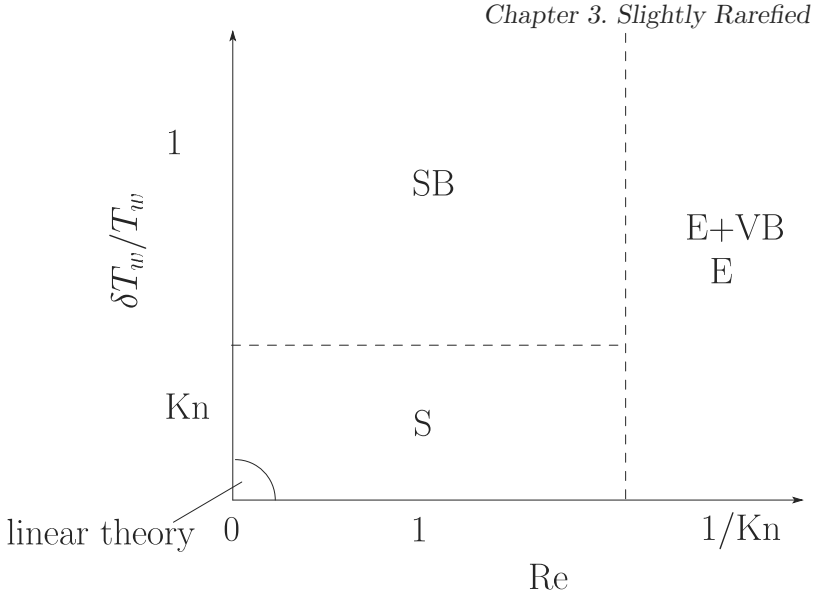

Figure 3.9. Fluid-dynamic-type systems describing the behavior of a gas of small Knudsen numbers ($\mathrm{Kn} \ll 1$) in the parameter plane (Re, $\delta T_w/T_w$). In the region SB, the classical gas dynamics is inapplicable.

condition for the Euler set on the evaporating interface and that for the suction-boundary-layer equations on the condensing interface. The connection of the solution of the Euler set and that of the suction-boundary-layer equations is done in the same way as that of the Euler equations and the viscous-boundary-layer equations. The equations in the marginal case have mixed features of Cases (i) and (iii). The difference between Cases (iii-a) and (iii-b) is the sizes of the velocity component normal to the boundary. Thus, as $|v_i n_i|/(2RT)^{1/2}$ decreases from $O(1)$, the nonlinear Knudsen layer in Case (iii-b) separates into a suction boundary layer and linear Knudsen layer with increasing the thickness of the former, and deforms into viscous boundary layer.

In view of the relation among the Mach number Ma, the Knudsen number Kn, and the Reynolds number Re noted in Section 3.1.9, i.e.,

$$\mathrm{Ma} = \left(\frac{3\pi}{40}\right)^{1/2} \gamma_1 \mathrm{ReKn},$$

the fluid-dynamic-type systems are classified in terms of the Reynolds number and the relative temperature variation of the boundary. Let T_w and δT_w be, respectively, the characteristic values of the temperature of the boundary and its variation, and let the Reynolds number Re be defined by $UL/(\mu_0/\rho_0)$, where U is the characteristic speed of the boundary (including infinity) and μ_0 is the reference viscosity. Then, the nontrivial leading-order fluid-dynamic-type systems for small Knudsen numbers are classified in the (Re, $\delta T_w/T_w$) plane as shown in Fig. 3.9, where S corresponds to the S system of Case (i) in the paragraph before the preceding one, SB corresponds to the SB system of Case

(ii), E+VB and E correspond, respectively, to E+VB and E systems in Case (iii). It may be noted here that when $\delta T_w/T_w$ is of the order of unity, the thermal creep or nonlinear-thermal-stress flows can be much larger than the boundary speed or U, e.g., in the case $U = 0$. In this case, the Reynolds number based on the boundary speed does not reflect the characteristic flow speed of the gas. When $\delta T_w/T_w$ is of the order of unity in the SB region of Fig. 3.9, the Reynolds number based on the characteristic speed of the gas is generally of the order of unity. In the SB region, the Mach number is small, i.e., $O(\mathrm{Kn})$. In the S region, the temperature variation $\delta T_w/T_w$ as well as the Mach number is small, i.e., $O(\mathrm{Kn})$, that is, nontrivial variations of variables are of the order of Kn. In the E or E+VB region, the Mach number is of the order of unity. Thus, the (nondimensional) temperature variation in the gas can be of the order of unity irrespective of $\delta T_w/T_w$.

The above classification is done for a general geometry. In some special geometries, the main equations degenerate, and the behavior in the continuum limit is determined by higher-order terms.[99] For example, in plane or cylindrical Couette flow, owing to the degeneracy of the convection effect, the viscous effect spreads over the whole field, and the Euler region disappears. A geometrical parameter of the system can be a source of the ghost effect. If a special geometry is considered, new non-Navier–Stokes and ghost effects, different from those mentioned above, enter the leading-order system. In Chapter 9, where the plane Couette flow is considered as the limit that the radii of the cylinders tend to infinity in the cylindrical Couette flow, the infinitesimal curvature of the boundary produces a finite effect on the flow, and in addition, the limiting equations contain a new non-Navier–Stokes term, i.e, the stress quadratic of the shear of flow, as well as nonlinear thermal stress term. In the (axially symmetric and uniform) cylindrical Couette flow with evaporation and condensation on the cylinders made of the condensed phase of the gas, the ghost effect on the circumferential flow field is produced by infinitesimal evaporation and condensation,[100] which will be discussed in Section 8.4.2.

In this way, the behavior for small Knudsen numbers depends largely on the behavior of the other parameters, and various kinds of equations appear as those governing the limiting behavior. Obviously, from the above discussion and Fig. 3.9, there are important classes of problems to which the classical fluid dynamics is inapplicable. That is, the classical fluid dynamics, which aims to describe the behavior of a gas in the continuum limit, fails to describe it correctly. The ghost effect and non-Navier–Stokes effect present themselves in well-known problems in the classical fluid dynamics, e.g., Bénard problem, Taylor–Couette problem with different boundary temperatures, which will be discussed in Sections 8.2 and 8.3. Thus, kinetic theory plays an essential role in correct understanding of the behavior of a gas that has been treated in the classical gas dynamics.

The asymptotic behavior for small Knudsen numbers is sometimes described

[99] See also Footnote 62 in Section 3.3.4.

[100] The infinitesimal evaporation and condensation are naturally established for a wide range of the parameters when the outer cylinder is rotating.

in the following way. In the continuum limit, the behavior of the macroscopic variables is determined by the Euler equations, their behavior at the next step of gas rarefaction is determined by the Navier–Stokes equations, their behavior at the further step by the Burnett equations, and so on. Clearly from the asymptotic analysis of this chapter, this is not a correct description. The continuum limit is not a point where the Knudsen number is zero, but it should be understood as a space where the further classification is required. Further, the combination of the fluid-dynamic-type equations and their associated boundary conditions is sometimes discussed carelessly. The correct combination is determined by the systematic asymptotic analysis of the Boltzmann system as shown in this chapter. These notes also apply to the time-dependent problem to be discussed in Section 3.7.

3.6.2 Supplementary discussion

It may be better to add some comments on the continuum limit for the cases of the S system of the weakly nonlinear theory and the Stokes system of the linear theory. The variation of solutions from a uniform state is of the order of the Knudsen number in the S system, and the variation of solutions is much smaller than the Knudsen number in the Stokes system.[101] In these cases, the state literally in the continuum limit, where the quantities of the order of the Knudsen number or smaller are neglected, is a uniform equilibrium state expressed with a uniform Maxwellian. When we mention nontrivial states, i.e., those other than uniform equilibrium states, of a gas in these cases, we take into account the effect of nonzero Knudsen number, i.e., the effect of gas rarefaction. The quantities of the order of the Knudsen number or smaller are of interest in discussing the behavior of a gas of a small Knudsen number.

When analyzing gas dynamic problems by the Navier–Stokes equations, people think that they are discussing the behavior of a gas in the continuum limit and do not think that they are discussing the effect of gas rarefaction. When they analyze problems of a gas in the atmospheric condition, where the Knudsen number is small but finite, on the basis of the Navier–Stokes equations, they think that the equations are for the case in the continuum limit but that the equations describe the system of finite variations very well because the Knudsen number is very small. However, it is not the case when the Reynolds number is small or of the order of unity. It is easily seen if we examine the data of our surroundings.

Take a system whose characteristic length is about 1 cm, e.g., a flow past a sphere of radius 1 cm and a flow through a channel of width 1 cm. The mean free path of the gas is 6×10^{-8} m at the atmospheric condition,[102] and therefore, the Knudsen number Kn is about 6×10^{-6}. If the flow speed is about 1 cm/s, the Mach number Ma is about 3×10^{-5}. The Mach number and the Knudsen

[101] See Footnote 3 in Section 3.1.2.

[102] The data for the air are given for a clear intuitive picture of the sizes of variables, although the air is not a single-component monatomic gas and does not correspond exactly to the gas described by the Boltzmann equation discussed in this book.

number are comparably small (Ma/Kn $\approx$ 5). This is the case to which the S system can be applied and the variation of the variables in the gas is of the order of the Knudsen number. When the characteristic length is about 0.3 mm and the flow speed is about 0.3 mm/s, the Knudsen number is about 2×10^{-4} and the Mach number is 1×10^{-6}. Both are small but the Mach number is much smaller than the Knudsen number (Ma/Kn $\approx 5 \times 10^{-3}$). These flows with small Mach numbers, of the order of the Knudsen number or much smaller, are well perceived by us.

When we treat a real gas of small mean free path (e.g., a gas under the atmospheric condition), we easily use the terminology 'the continuum limit.' It should be noted that we are not always discussing quantities of the order of unity but that the quantities of our interest are of the order of the Knudsen number or smaller in a large class of problems.

The conditions (3.12), (3.87), (3.153), and (3.154), i.e., the requirement of uniform pressure, may be strange or seem to be too strong to those who are working with the classical fluid-dynamic equations. These conditions are almost obvious if one examines the sizes of the quantities in the classical fluid-dynamic equations, paying attention to the relation (3.70) between the mean free path and viscosity. They are the conditions that the solutions satisfying the original setup of the problems can be obtained. That is, much larger flow velocity than that assumed before the analysis is induced if the pressure conditions are not satisfied. In other words, the pressure differences induced by such flows are higher-order quantities. This is not noticed very well but requires some care. For example, according to Eq. (3.22), the heat flow is proportional to the temperature gradient, but there is no heat flow due to the pressure gradient at the leading order; there is a heat flow due to the pressure gradient at the next order. This is of higher order only because the pressure gradient is of higher order; the coefficients are of the same order. Thus, we have to examine the higher-order heat flow in the discussion related to the coefficients. This discussion on the basis of a concrete example is given in the second part of Footnote 8 in Section 4.2.2.

3.7 Time-dependent problem

To extend the process in Sections 3.1.2, 3.2.2, 3.3.2, 3.4.1, and 3.5.1 to obtain the fluid-dynamic-type equations to time-dependent problems is simple and straightforward. We have only to carry out a similar expansion retaining the time-derivative term in the Boltzmann equation with some care about the time scale of variation of the velocity distribution function. We will explain only the outline of the time-dependent analysis because the analysis can be carried out parallel to the time-independent case.

We consider the case where the collision term is dominant in the Boltzmann equation as in the time-independent analysis, i.e., the time-derivative term as well as the space-derivative term in the Boltzmann equation is much smaller than its collision term. In the nondimensional form of the Boltzmann equation

(1.47a), (1.75a), or (1.96), k (or Kn) and $k\mathrm{Sh}$ are both small; thus Sh, the Strouhal number defined by Eq. (1.48a), is of the order of unity or small. The condition on $k\mathrm{Sh}$ corresponds to the condition that the mean free time (the inverse of the mean collision frequency) is much smaller than the time scale of variation of the velocity distribution function.

When Sh $[= L/t_0(2RT_0)^{1/2}]$ is of the order of unity, the time scale t_0 of variation is $t_0 \sim L/(2RT_0)^{1/2}$ and the ratio[103] of the time-derivative term to the collision term is of the order of k. This time scale t_0 is a time of the order that the sound wave propagates over the distance of the reference length L. Thus, wave propagation is described by this time scale. On the other hand, when Sh is small and of the order of k, the time scale t_0 is $t_0 \sim L^2/\ell_0(2RT_0)^{1/2}$ and the ratio of the time-derivative term to the collision term is of the order of k^2. In view of the relation between the viscosity μ_0 or thermal conductivity λ_0 and the mean free path ℓ_0 at the reference state, i.e., Eq. (3.70) or (3.71), $t_0 \sim \rho_0 L^2/\mu_0$ or $t_0 \sim R\rho_0 L^2/\lambda_0$. This is the characteristic time scale of viscous or thermal diffusion.[104]

When the time scale t_0 of variation is of the order of the time required for the gas flow to traverse the distance L, i.e., $t_0 = L/U$ (U: a characteristic flow speed), then $\mathrm{Sh} = O(\mathrm{Ma})$. In view of the von Karman relation (3.74), this time scale is comparable to the second one when the Reynolds number is finite (the case related to Sections 3.2 and 3.3); it is much longer than the second when the Reynolds number is small (the case related to Section 3.1, i.e., the linear theory); it is comparable to the first one when the Mach number is of the order of unity (the case related to Sections 3.4 and 3.5).

3.7.1 Fluid-dynamic-type equations I: Sh = $O(1)$

Consider the case where Sh is of the order of unity. We can take $\mathrm{Sh} = 1$ $[t_0 = L/(2RT_0)^{1/2}]$ without loss of generality. Then, the relation between the nondimensional time variable $\hat{t}$ and the original dimensional time variable t is $\hat{t} = t/L(2RT_0)^{-1/2}$.

Linear problem

First consider the linear problem in Section 3.1. Take the linearized Boltzmann equation (1.96) with the time-derivative term $\partial\phi/\partial\hat{t}$

$$\frac{\partial\phi}{\partial\hat{t}} + \zeta_i \frac{\partial\phi}{\partial x_i} = \frac{1}{k}\mathcal{L}(\phi), \tag{3.230}$$

[103] In Eq. (1.47a), the ratio is $(\mathrm{Sh}\,\partial\hat{f}/\partial\hat{t})/[\hat{J}(\hat{f},\hat{f})/k]$, where $\partial\hat{f}/\partial\hat{t}$ and $\hat{J}(\hat{f},\hat{f})$ are nondimensionalized so as to be of the order of unity by choosing the reference variables.

[104] The time scale of variation of the solution of the heat-conduction equation $\frac{5}{2}\rho_0\partial RT/\partial t = \lambda_0\partial^2 T/\partial X_i^2$, which corresponds to Eq. (3.258c) if the boundary condition on P_{G0} there is time-independent, is $R\rho_0 L^2/\lambda_0$. The diffusion of vorticity of a parallel flow $v_i = (v_1(X_2), 0, 0)$ by viscosity is determined by $\rho_0\partial v_1/\partial t = \mu_0\partial^2 v_1/\partial X_2^2$. The time scale of variation of the solution is given by $\rho_0 L^2/\mu_0$.

where Sh is taken to be unity. Put the distribution function ϕ in a power series of k, i.e.,

$$\phi = \phi_G = \phi_{G0} + \phi_{G1}k + \phi_{G2}k^2 + \cdots . \tag{3.231}$$

Corresponding to this expansion, the macroscopic variables ω, u_i, τ, etc., defined by Eqs. (1.97a)–(1.97f), are also expanded in k as

$$h_G = h_{G0} + h_{G1}k + h_{G2}k^2 + \cdots , \tag{3.232}$$

where $h = \omega$, u_i, τ, etc. The h_{Gm} is related to ϕ_{Gm} by Eqs. (1.97a)–(1.97f) with $\phi = \phi_{Gm}$ and $h = h_{Gm}$. The relation is the same as in the time-independent case. The analysis goes parallel to that in Section 3.1.2, with the additional $\partial\phi_{Gm}/\partial\hat{t}$ term. Substituting the expansion (3.231) into Eq. (3.230) and arranging the same-order terms in k, we obtain a series of integral equations for ϕ_{Gm}, i.e.,

$$\mathcal{L}(\phi_{G0}) = 0, \tag{3.233}$$

$$\mathcal{L}(\phi_{Gm}) = \frac{\partial\phi_{Gm-1}}{\partial\hat{t}} + \zeta_i\frac{\partial\phi_{Gm-1}}{\partial x_i} \quad (m = 1, 2, 3\ldots), \tag{3.234}$$

where the conditions $\partial\phi_G/\partial\hat{t} = O(\phi_G)$ and $\partial\phi_G/\partial x_i = O(\phi_G)$ are used.

The equation for ϕ_{Gm} (and that for ϕ_{Sm}, $\hat{f}_{SBm}$, or $\hat{f}_{Hm}$ to appear in the following analyses) has the same character as the corresponding equation in time-independent case. The homogeneous part of the equation is the same and the difference is the time-derivative term in its inhomogeneous term. Therefore, the analysis is carried out in a similar way with the repetition of solution of the equation and derivation of the solvability condition of the next-order equation. The solvability condition is in the form with the time-derivative term $\partial\phi_{Gm-1}/\partial\hat{t}$ added to $\zeta_i\partial\phi_{Gm-1}/\partial x_i$ in Eq. (3.8) (and similar modification in the other cases).

The leading-order solution ϕ_{G0} is the local Maxwellian in its linearized form, i.e.,

$$\phi_{G0} = \omega_{G0} + 2\zeta_i u_{iG0} + \left(\zeta_j^2 - \frac{3}{2}\right)\tau_{G0}. \tag{3.235}$$

From the solvability condition on the inhomogeneous term in Eq. (3.234) with $m = 1$, the set of equations that determines the macroscopic variables ω_{G0}, u_{iG0}, and τ_{G0} is derived as

$$\frac{\partial\omega_{G0}}{\partial\hat{t}} + \frac{\partial u_{iG0}}{\partial x_i} = 0, \tag{3.236a}$$

$$\frac{\partial u_{iG0}}{\partial\hat{t}} + \frac{1}{2}\frac{\partial P_{G0}}{\partial x_i} = 0, \tag{3.236b}$$

$$\frac{3}{2}\frac{\partial P_{G0}}{\partial\hat{t}} + \frac{5}{2}\frac{\partial u_{iG0}}{\partial x_i} = 0, \tag{3.236c}$$

where

$$P_{G0} = \omega_{G0} + \tau_{G0}.$$

Equations (3.236b) and (3.236c) are the *acoustic equations* for u_{iG0} and P_{G0} describing the propagation of sound waves. The other variables ω_{G0} and τ_{G0} are obtained from P_{G0} by the equations

$$\frac{\partial \omega_{G0}}{\partial \hat{t}} = \frac{3}{5}\frac{\partial P_{G0}}{\partial \hat{t}}, \qquad \tau_{G0} = P_{G0} - \omega_{G0}.$$

Proceeding to the higher-order analysis, we obtain the equations for ω_{Gm}, u_{iGm}, and τ_{Gm}, where the operator for ω_{Gm}, u_{iGm}, and τ_{Gm} is the same as that for ω_{G0}, u_{iG0}, and τ_{G0} in Eqs. (3.236a)–(3.236c) and there are inhomogeneous terms consisting of the viscous and heat-conduction terms etc. expressed with the macroscopic variables at the preceding stage. For example,

$$\frac{\partial \omega_{G1}}{\partial \hat{t}} + \frac{\partial u_{iG1}}{\partial x_i} = 0, \tag{3.237a}$$

$$\frac{\partial u_{iG1}}{\partial \hat{t}} + \frac{1}{2}\frac{\partial P_{G1}}{\partial x_i} = \frac{\gamma_1}{2}\frac{\partial}{\partial x_j}\left(\frac{\partial u_{iG0}}{\partial x_j} + \frac{\partial u_{jG0}}{\partial x_i} - \frac{2}{3}\frac{\partial u_{kG0}}{\partial x_k}\delta_{ij}\right), \tag{3.237b}$$

$$\frac{3}{2}\frac{\partial P_{G1}}{\partial \hat{t}} + \frac{5}{2}\frac{\partial u_{iG1}}{\partial x_i} = \frac{5\gamma_2}{4}\frac{\partial^2 \tau_{G0}}{\partial x_j^2}, \tag{3.237c}$$

where

$$P_{G1} = \omega_{G1} + \tau_{G1}.$$

Weakly nonlinear problem

Consider the case where the perturbed velocity distribution function ϕ is of the order of k. This case corresponds to Section 3.2. Take the Boltzmann equation (1.75a) with the time-derivative term $\partial\phi/\partial\hat{t}$

$$\frac{\partial \phi}{\partial \hat{t}} + \zeta_i \frac{\partial \phi}{\partial x_i} = \frac{1}{k}[\mathcal{L}(\phi) + \mathcal{J}(\phi, \phi)]. \tag{3.238}$$

The distribution function ϕ is expanded in the form

$$\phi = \phi_S = \phi_{S1}k + \phi_{S2}k^2 + \cdots. \tag{3.239}$$

Corresponding to this expansion, the macroscopic variables ω, u_i, τ, etc. are also expanded in k, i.e.,

$$h_S = h_{S1}k + h_{S2}k^2 + \cdots, \tag{3.240}$$

where $h = \omega$, u_i, τ, etc. The relation between h_{Sm} and ϕ_{Sm} is obtained by expanding Eqs. (1.78a)–(1.78f) with $\phi = \phi_S$ and $h = h_S$. It is the same as in the time-independent case [see Eqs. (3.79a)–(3.80f)]. Substituting the expansion (3.239) into Eq. (3.238), we obtain a series of integral equations for ϕ_{Sm}, i.e.,

$$\mathcal{L}(\phi_{S1}) = 0, \tag{3.241a}$$

$$\mathcal{L}(\phi_{Sm}) = \frac{\partial \phi_{Sm-1}}{\partial \hat{t}} + \zeta_i \frac{\partial \phi_{Sm-1}}{\partial x_i} - \sum_{r=1}^{m-1} \mathcal{J}(\phi_{Sm-r}, \phi_{Sr}) \quad (m = 2, 3, \ldots), \tag{3.241b}$$

where the conditions $\partial\phi_S/\partial\hat{t} = O(\phi_S)$ and $\partial\phi_S/\partial x_i = O(\phi_S)$ are used. These are the same type of equations as Eqs. (3.233) and (3.234) in the linear theory; the difference is the $\mathcal{J}$ terms in the inhomogeneous term.[105]

The leading-order solution ϕ_{S1} is given by

$$\phi_{S1} = \omega_{S1} + 2\zeta_i u_{iS1} + \left(\zeta_i^2 - \frac{3}{2}\right)\tau_{S1}. \tag{3.242}$$

From the solvability condition of Eq. (3.241b) with $m = 2$ for ϕ_{S2}, the equations that determine ω_{S1}, u_{iS1}, and τ_{S1} are derived as

$$\frac{\partial\omega_{S1}}{\partial\hat{t}} + \frac{\partial u_{iS1}}{\partial x_i} = 0, \tag{3.243a}$$

$$\frac{\partial u_{iS1}}{\partial\hat{t}} + \frac{1}{2}\frac{\partial P_{S1}}{\partial x_i} = 0, \tag{3.243b}$$

$$\frac{3}{2}\frac{\partial P_{S1}}{\partial\hat{t}} + \frac{5}{2}\frac{\partial u_{iS1}}{\partial x_i} = 0, \tag{3.243c}$$

where

$$P_{S1} = \omega_{S1} + \tau_{S1}.$$

They are the same as Eqs. (3.236a)–(3.236c) for ω_{G0}, u_{iG0}, and τ_{G0}. That is, Eqs. (3.243b) and (3.243c) are the acoustic equations describing the propagation of sound waves. The equations for the higher-order ω_{Sm}, u_{iSm}, and τ_{Sm}, the operator for which is the same as that for ω_{S1}, u_{iS1}, and τ_{S1} in Eqs. (3.243a)–(3.243c), have inhomogeneous terms consisting of the viscous and heat-conduction terms etc. expressed with the macroscopic variables at previous stages. For example,

$$\frac{\partial\omega_{S2}}{\partial\hat{t}} + \frac{\partial u_{iS2}}{\partial x_i} = -\frac{\partial\omega_{S1}u_{iS1}}{\partial x_i}, \tag{3.244a}$$

$$\begin{aligned}\frac{\partial u_{iS2}}{\partial\hat{t}} + \frac{1}{2}\frac{\partial P_{S2}}{\partial x_i} = &-\frac{\partial\omega_{S1}u_{iS1}}{\partial\hat{t}} - \frac{\partial u_{jS1}u_{iS1}}{\partial x_j} \\ &+ \frac{\gamma_1}{2}\frac{\partial}{\partial x_j}\left(\frac{\partial u_{iS1}}{\partial x_j} + \frac{\partial u_{jS1}}{\partial x_i} - \frac{2}{3}\frac{\partial u_{kS1}}{\partial x_k}\delta_{ij}\right),\end{aligned} \tag{3.244b}$$

$$\frac{3}{2}\frac{\partial P_{S2}}{\partial\hat{t}} + \frac{5}{2}\frac{\partial u_{iS2}}{\partial x_i} = -\frac{\partial u_{iS1}^2}{\partial\hat{t}} - \frac{5}{2}\frac{\partial P_{S1}u_{jS1}}{\partial x_j} + \frac{5\gamma_2}{4}\frac{\partial^2\tau_{S1}}{\partial x_j^2}, \tag{3.244c}$$

where

$$P_{S2} = \omega_{S2} + \tau_{S2} + \omega_{S1}\tau_{S1}.$$

Nonlinear problem

Consider the case where any special condition on the velocity distribution function, like Eq. (3.135a), is not imposed. Take the Boltzmann equation (1.47a) in the absence of an external force $\hat{F}_i = 0$

[105] See the explanation at the beginning of the paragraph next to that containing Eq. (3.234).

$$\frac{\partial \hat{f}}{\partial \hat{t}} + \zeta_i \frac{\partial \hat{f}}{\partial x_i} = \frac{1}{k} \hat{J}(\hat{f}, \hat{f}). \tag{3.245}$$

The distribution function $\hat{f}$ is expanded in a power series of k, i.e.,

$$\hat{f} = \hat{f}_H = \hat{f}_{H0} + \hat{f}_{H1} k + \cdots . \tag{3.246}$$

Corresponding to the expansion (3.246), the macroscopic variables $\hat{\rho}$, $\hat{v}_i$, $\hat{T}$, etc. [see Eqs. (1.54a)–(1.54f)] are also expanded in k, i.e.,

$$\hat{h}_H = \hat{h}_{H0} + \hat{h}_{H1} k + \cdots , \tag{3.247}$$

where $\hat{h} = \hat{\rho}$, $\hat{v}_i$, $\hat{T}$, etc. Substituting the series (3.246) into Eq. (3.245), we obtain a series of integral equations for $\hat{f}_{Hm}$, i.e.,

$$\hat{J}(\hat{f}_{H0}, \hat{f}_{H0}) = 0, \tag{3.248a}$$

$$2\hat{J}(\hat{f}_{H0}, \hat{f}_{Hm}) = \frac{\partial \hat{f}_{Hm-1}}{\partial \hat{t}} + \zeta_i \frac{\partial \hat{f}_{Hm-1}}{\partial x_i} - \sum_{s=1}^{m-1} \hat{J}(\hat{f}_{Hs}, \hat{f}_{Hm-s}) \quad (m = 1, 2, \ldots), \tag{3.248b}$$

where $\sum$ term is absent when $m = 1$, and the conditions $\partial \hat{f}_H / \partial \hat{t} = O(\hat{f}_H)$ and $\partial \hat{f}_H / \partial x_i = O(\hat{f}_H)$ are used in the derivation.

From Eq. (3.248a), we have

$$\hat{f}_{H0} = \frac{\hat{\rho}_{H0}}{(\pi \hat{T}_{H0})^{3/2}} \exp\left(- \frac{(\zeta_i - \hat{v}_{iH0})^2}{\hat{T}_{H0}} \right). \tag{3.249}$$

From the solvability condition of Eq. (3.248b) with $m = 1$ for $\hat{f}_{H1}$, the equations for $\hat{\rho}_{H0}$, $\hat{v}_{iH0}$, and $\hat{T}_{H0}$ are obtained as[106]

$$\frac{\partial \hat{\rho}_{H0}}{\partial \hat{t}} + \frac{\partial \hat{\rho}_{H0} \hat{v}_{iH0}}{\partial x_i} = 0, \tag{3.250a}$$

$$\frac{\partial \hat{\rho}_{H0} \hat{v}_{iH0}}{\partial \hat{t}} + \frac{\partial \hat{\rho}_{H0} \hat{v}_{jH0} \hat{v}_{iH0}}{\partial x_j} + \frac{1}{2} \frac{\partial \hat{p}_{H0}}{\partial x_i} = 0, \tag{3.250b}$$

$$\frac{\partial}{\partial \hat{t}} \left[\hat{\rho}_{H0} \left(\hat{v}_{iH0}^2 + \frac{3}{2} \hat{T}_{H0} \right) \right] + \frac{\partial}{\partial x_j} \left[\hat{\rho}_{H0} \hat{v}_{jH0} \left(\hat{v}_{iH0}^2 + \frac{5}{2} \hat{T}_{H0} \right) \right] = 0, \tag{3.250c}$$

where

$$\hat{p}_{H0} = \hat{\rho}_{H0} \hat{T}_{H0}.$$

Equations (3.250a)–(3.250c) are called the Euler set of equations. The higher-order equations are the linearized Euler set of equations, linearized around $\hat{\rho}_{H0}$, $\hat{v}_{iH0}$, and $\hat{T}_{H0}$, with inhomogeneous terms including viscous and heat-conduction terms, etc. For example,

[106] See the explanation at the beginning of the paragraph next to that containing Eq. (3.234).

$$\frac{\partial \hat{\rho}_{H1}}{\partial \hat{t}} + \frac{\partial \hat{\rho}_{H0}\hat{v}_{iH1}}{\partial x_i} + \frac{\partial \hat{\rho}_{H1}\hat{v}_{iH0}}{\partial x_i} = 0, \tag{3.251a}$$

$$\frac{\partial (\hat{\rho}_H \hat{v}_{iH})_1}{\partial \hat{t}} + \frac{\partial (\hat{\rho}_H \hat{v}_{jH}\hat{v}_{iH})_1}{\partial x_j} + \frac{1}{2}\frac{\partial \hat{p}_{H1}}{\partial x_i}$$
$$= \frac{1}{2}\frac{\partial}{\partial x_j}\left[\Gamma_1(\hat{T}_{H0})\left(\frac{\partial \hat{v}_{iH0}}{\partial x_j} + \frac{\partial \hat{v}_{jH0}}{\partial x_i} - \frac{2}{3}\frac{\partial \hat{v}_{kH0}}{\partial x_k}\delta_{ij}\right)\right], \tag{3.251b}$$

$$\frac{\partial}{\partial \hat{t}}\left[\hat{\rho}_{H0}\left(2\hat{v}_{iH0}\hat{v}_{iH1} + \frac{3}{2}\hat{T}_{H1}\right) + \hat{\rho}_{H1}\left(\hat{v}_{iH0}^2 + \frac{3}{2}\hat{T}_{H0}\right)\right]$$
$$+ \frac{\partial}{\partial x_j}\left[\hat{\rho}_{H0}\hat{v}_{jH0}\left(2\hat{v}_{iH0}\hat{v}_{iH1} + \frac{5}{2}\hat{T}_{H1}\right) + (\hat{\rho}_H\hat{v}_{jH})_1\left(\hat{v}_{iH0}^2 + \frac{5}{2}\hat{T}_{H0}\right)\right]$$
$$= \frac{\partial}{\partial x_j}\left[\Gamma_1(\hat{T}_{H0})\hat{v}_{iH0}\left(\frac{\partial \hat{v}_{iH0}}{\partial x_j} + \frac{\partial \hat{v}_{jH0}}{\partial x_i} - \frac{2}{3}\frac{\partial \hat{v}_{kH0}}{\partial x_k}\delta_{ij}\right)\right]$$
$$+ \frac{5}{4}\frac{\partial}{\partial x_i}\left(\Gamma_2(\hat{T}_{H0})\frac{\partial \hat{T}_{H0}}{\partial x_i}\right), \tag{3.251c}$$

where

$$\hat{p}_{H1} = \hat{\rho}_{H0}\hat{T}_{H1} + \hat{\rho}_{H1}\hat{T}_{H0},$$

and $(\hat{\rho}_H\hat{v}_{jH})_1$ and $(\hat{\rho}_H\hat{v}_{jH}\hat{v}_{iH})_1$ are the abbreviations

$$(\hat{\rho}_H\hat{v}_{jH})_1 = \hat{\rho}_{H0}\hat{v}_{jH1} + \hat{\rho}_{H1}\hat{v}_{jH0},$$
$$(\hat{\rho}_H\hat{v}_{jH}\hat{v}_{iH})_1 = \hat{\rho}_{H0}\hat{v}_{jH0}\hat{v}_{iH1} + \hat{\rho}_{H0}\hat{v}_{jH1}\hat{v}_{iH0} + \hat{\rho}_{H1}\hat{v}_{jH0}\hat{v}_{iH0}.$$

The present case is the original Hilbert expansion (Hilbert [1912]).

3.7.2 Fluid-dynamic-type equations II: Sh = $O(k)$

Consider the case where Sh is of the order of k. We can take Sh $= k$ [i.e., $t_0 = L/k(2RT_0)^{1/2}$] without loss of generality. Then, the relation between the nondimensional time variable $\hat{t}$ and the original dimensional time variable t is $\hat{t} = t/L(2RT_0)^{-1/2}k^{-1}$. To avoid the confusion with the case Sh $= O(1)$, we use the different notation $\tilde{t}$ for $\hat{t}$, i.e., $\tilde{t} = t/L(2RT_0)^{-1/2}k^{-1}$. Naturally, $\partial \hat{f}/\partial \tilde{t} = O(\hat{f})$ or $\partial \phi/\partial \tilde{t} = O(\phi)$.

Linear problem

With Sh $= k$ and the new notation $\tilde{t}$, the linearized Boltzmann equation (1.96) is given as

$$k\frac{\partial \phi}{\partial \tilde{t}} + \zeta_i\frac{\partial \phi}{\partial x_i} = \frac{1}{k}\mathcal{L}(\phi), \tag{3.252}$$

where $\partial\phi/\partial\tilde{t} = O(\phi)$ and $\partial\phi/\partial x_i = O(\phi)$. The distribution function ϕ is expanded in a power series of k, i.e.,

$$\phi = \phi_G = \phi_{G0} + \phi_{G1}k + \phi_{G2}k^2 + \cdots . \tag{3.253}$$

Corresponding to the above expansion of ϕ, the macroscopic variables ω, u_i, τ, etc., defined by Eqs. (1.97a)–(1.97f), are also expanded in k as

$$h_G = h_{G0} + h_{G1}k + h_{G2}k^2 + \cdots , \tag{3.254}$$

where $h = \omega$, u_i, τ, etc. Substituting the series (3.253) into Eq. (3.252), we obtain a series of integral equations for ϕ_{Gm} $(m = 0, 1, 2, \ldots)$ as

$$\mathcal{L}(\phi_{G0}) = 0, \tag{3.255a}$$

$$\mathcal{L}(\phi_{G1}) = \zeta_i \frac{\partial \phi_{G0}}{\partial x_i}, \tag{3.255b}$$

$$\mathcal{L}(\phi_{Gm}) = \frac{\partial \phi_{Gm-2}}{\partial \tilde{t}} + \zeta_i \frac{\partial \phi_{Gm-1}}{\partial x_i} \quad (m = 2, 3 \ldots). \tag{3.255c}$$

Repeating the process of solution and solvability condition, we obtain ϕ_{Gm} and a series of the sets of equations for h_{Gm}.[107] From Eqs. (3.255a) and (3.255b), it is seen that ϕ_{G0} and ϕ_{G1} are formally the same as those in the time-independent case, i.e.,

$$\phi_{G0} = \omega_{G0} + 2\zeta_i u_{iG0} + \left(\zeta_j^2 - \frac{3}{2}\right)\tau_{G0}, \tag{3.256a}$$

$$\phi_{G1} = \omega_{G1} + 2\zeta_i u_{iG1} + \left(\zeta_j^2 - \frac{3}{2}\right)\tau_{G1} - \zeta_i\zeta_j B(\zeta)\frac{\partial u_{iG0}}{\partial x_j} - \zeta_i A(\zeta)\frac{\partial \tau_{G0}}{\partial x_i}, \tag{3.256b}$$

where ϕ_{G0} is the linearized form of the Maxwellian. The fluid-dynamic-type equations that determine the macroscopic variables up to h_{G1} are

$$\frac{\partial P_{G0}}{\partial x_i} = 0, \tag{3.257}$$

$$\frac{\partial u_{jG0}}{\partial x_j} = 0, \tag{3.258a}$$

$$\frac{\partial u_{iG0}}{\partial \tilde{t}} = -\frac{1}{2}\frac{\partial P_{G1}}{\partial x_i} + \frac{\gamma_1}{2}\frac{\partial^2 u_{iG0}}{\partial x_j^2}, \tag{3.258b}$$

$$\frac{5}{2}\frac{\partial \tau_{G0}}{\partial \tilde{t}} - \frac{\partial P_{G0}}{\partial \tilde{t}} = \frac{5\gamma_2}{4}\frac{\partial^2 \tau_{G0}}{\partial x_j^2}, \tag{3.258c}$$

[107] See the explanation at the beginning of the paragraph next to that containing Eq. (3.234).

$$\frac{\partial u_{jG1}}{\partial x_j} = -\frac{\partial \omega_{G0}}{\partial \tilde{t}}, \tag{3.259a}$$

$$\frac{\partial u_{iG1}}{\partial \tilde{t}} = -\frac{1}{2}\frac{\partial P_{G2}}{\partial x_i} + \frac{\gamma_1}{2}\frac{\partial}{\partial x_j}\left(\frac{\partial u_{iG1}}{\partial x_j} + \frac{\partial u_{jG1}}{\partial x_i} - \frac{2}{3}\frac{\partial u_{kG1}}{\partial x_k}\delta_{ij}\right) - \frac{\gamma_3}{3}\frac{\partial}{\partial x_i}\frac{\partial^2 \tau_{G0}}{\partial x_j^2}, \tag{3.259b}$$

$$\frac{5}{2}\frac{\partial \tau_{G1}}{\partial \tilde{t}} - \frac{\partial P_{G1}}{\partial \tilde{t}} = \frac{5\gamma_2}{4}\frac{\partial^2 \tau_{G1}}{\partial x_j^2}, \tag{3.259c}$$

where

$$P_{Gm} = \omega_{Gm} + \tau_{Gm}.$$

The time-derivative terms $\partial u_{iG0}/\partial \tilde{t}$ in Eq. (3.258b) and $(5/2)\partial \tau_{G0}/\partial \tilde{t} - \partial P_{G0}/\partial \tilde{t}$ in Eq. (3.258c) in the set of equations (3.257)–(3.258c) are the corrections to Eqs. (3.12)–(3.13c) with $m = 0$ in the corresponding time-independent case. These equations are similar to the Stokes set of equations for an incompressible fluid, but there is a difference in Eq. (3.258c). Rewriting the time-derivative terms in Eq. (3.258c) in the form

$$\frac{5}{2}\frac{\partial \tau_{G0}}{\partial \tilde{t}} - \frac{\partial P_{G0}}{\partial \tilde{t}} = \frac{3}{2}\frac{\partial \tau_{G0}}{\partial \tilde{t}} - \frac{\partial \omega_{G0}}{\partial \tilde{t}},$$

and neglecting the last term $-\partial \omega_{G0}/\partial \tilde{t}$, we obtain the energy equation of the Stokes set for an incompressible fluid. From Eq. (3.259a) and the discussion in Footnote 47 in Section 3.2.4, $\partial \omega_{G0}/\partial \tilde{t}$ is the corresponding contribution to Eq. (3.258c) of the work done by pressure on a volume of a gas, which vanishes in an incompressible fluid in the present situation.[108] In Eq. (3.259b), the thermal stress term appears in contrast to the time-independent case, but it can be incorporated in the pressure term as was done by Eq. (3.126) in Section 3.2.4.

In Eqs. (3.257)–(3.259c), the variable P_{Gm} appears in somewhat awkward way, i.e., in a staggered combination with the other variables. This character is common to the weakly nonlinear problem and the first case of the nonlinear one to be discussed. The P_{G0} in Eq. (3.258c) is already determined by Eq. (3.257) with an additive arbitrary function of $\tilde{t}$, which is determined by the boundary condition in the process of solution of Eq. (3.258c).[109] From Eqs. (3.258a) and (3.258b), u_{iG0} and P_{G1} (except an additive function of $\tilde{t}$) are determined. The additive function in P_{G1} is determined by the boundary condition in the process of solution of Eq. (3.259c). In this way, we can consistently determine the solution. The boundary conditions on a simple boundary or an interface for Eqs. (3.257)–(3.259c) are given in Section 3.7.3.

[108] The relation $\partial \omega_{Gm}/\partial \tilde{t} = 0$ is the linearized form of the condition of incompressibility $\partial \rho/\partial t + v_i \partial \rho/\partial X_i = 0$.

[109] The pressure P_{Gm} is not specified on a simple boundary. However, its value at infinity is specified in an infinite domain problem or the total mass is invariant in time (and thus specified) in a closed domain problem.

Weakly nonlinear problem

Consider the case where $\phi = O(k)$. This case corresponds to Section 3.2. With $\mathrm{Sh} = k$ and the new notation $\tilde{t}$, the Boltzmann equation (1.75a) is given as

$$k\frac{\partial \phi}{\partial \tilde{t}} + \zeta_i \frac{\partial \phi}{\partial x_i} = \frac{1}{k}[\mathcal{L}(\phi) + \mathcal{J}(\phi, \phi)]. \tag{3.260}$$

The distribution function ϕ is expanded in a power series of k, i.e.,

$$\phi = \phi_S = \phi_{S1}k + \phi_{S2}k^2 + \cdots . \tag{3.261}$$

Corresponding to the expansion (3.261), the macroscopic variables ω, u_i, τ, etc. are also expanded in k, i.e.,

$$h_S = h_{S1}k + h_{S2}k^2 + \cdots , \tag{3.262}$$

where $h = \omega$, u_i, τ, etc. Substituting the series (3.261) into Eq. (3.260), we obtain a series of integral equations for ϕ_{Sm} $(m = 1, 2, \ldots)$, i.e.,

$$\mathcal{L}(\phi_{S1}) = 0, \tag{3.263a}$$

$$\mathcal{L}(\phi_{S2}) = \zeta_i \frac{\partial \phi_{S1}}{\partial x_i} - \mathcal{J}(\phi_{S1}, \phi_{S1}), \tag{3.263b}$$

$$\mathcal{L}(\phi_{Sm}) = \frac{\partial \phi_{Sm-2}}{\partial \tilde{t}} + \zeta_i \frac{\partial \phi_{Sm-1}}{\partial x_i} - \sum_{r=1}^{m-1} \mathcal{J}(\phi_{Sm-r}, \phi_{Sr}) \quad (m = 3, 4, \ldots). \tag{3.263c}$$

Repeating the process of solution and solvability condition, we obtain ϕ_{Sm} and a series of the sets of equations for h_{Sm}.[110] From Eqs. (3.263a) and (3.263b), it is seen that ϕ_{S1} and ϕ_{S2} are formally the same as those in the time-independent case, i.e.,

$$\phi_{S1} = \omega_{S1} + 2\zeta_i u_{iS1} + \left(\zeta_j^2 - \frac{3}{2}\right)\tau_{S1}, \tag{3.264a}$$

$$\phi_{S2} = \phi_{eS2} - \zeta_i\zeta_j B(\zeta)\frac{\partial u_{iS1}}{\partial x_j} - \zeta_i A(\zeta)\frac{\partial \tau_{S1}}{\partial x_i}, \tag{3.264b}$$

where ϕ_{eS2} is the second-order component function of the expansion of the local Maxwellian in k [see Eq. (3.94)], i.e.,

$$\begin{aligned}\phi_{eS2} = {} & \omega_{S2} + 2\zeta_i u_{iS2} + \left(\zeta_j^2 - \frac{3}{2}\right)\tau_{S2} + 2\zeta_i\omega_{S1}u_{iS1} \\ & + \left(\zeta_j^2 - \frac{3}{2}\right)\left(\frac{2}{3}u_{iS1}^2 + \omega_{S1}\tau_{S1}\right) + 2\left(\zeta_i\zeta_j - \frac{1}{3}\zeta_\ell^2\delta_{ij}\right)u_{iS1}u_{jS1} \\ & + 2\zeta_i\left(\zeta_j^2 - \frac{5}{2}\right)u_{iS1}\tau_{S1} + \left(\frac{1}{2}\zeta_i^2\zeta_j^2 - \frac{5}{2}\zeta_i^2 + \frac{15}{8}\right)\tau_{S1}^2.\end{aligned}$$

[110] See the explanation at the beginning of the paragraph next to that containing Eq. (3.234).

The fluid-dynamic-type equations that determine the macroscopic variables up to h_{S2} are

$$\frac{\partial P_{S1}}{\partial x_i} = 0, \tag{3.265}$$

$$\frac{\partial u_{iS1}}{\partial x_i} = 0, \tag{3.266a}$$

$$\frac{\partial u_{iS1}}{\partial \tilde{t}} + u_{jS1}\frac{\partial u_{iS1}}{\partial x_j} = -\frac{1}{2}\frac{\partial P_{S2}}{\partial x_i} + \frac{\gamma_1}{2}\frac{\partial^2 u_{iS1}}{\partial x_j^2}, \tag{3.266b}$$

$$\frac{5}{2}\frac{\partial \tau_{S1}}{\partial \tilde{t}} - \frac{\partial P_{S1}}{\partial \tilde{t}} + \frac{5}{2}u_{jS1}\frac{\partial \tau_{S1}}{\partial x_j} = \frac{5\gamma_2}{4}\frac{\partial^2 \tau_{S1}}{\partial x_j^2}, \tag{3.266c}$$

$$\frac{\partial u_{iS2}}{\partial x_i} = -\frac{\partial \omega_{S1}}{\partial \tilde{t}} - \frac{\partial \omega_{S1}u_{iS1}}{\partial x_i}, \tag{3.267a}$$

$$\begin{aligned}&\frac{\partial u_{iS2}}{\partial \tilde{t}} + u_{jS1}\frac{\partial u_{iS2}}{\partial x_j} + u_{jS2}\frac{\partial u_{iS1}}{\partial x_j}\\ &= -\frac{1}{2}\left(\frac{\partial P_{S3}}{\partial x_i} - \omega_{S1}\frac{\partial P_{S2}}{\partial x_i}\right) + \frac{\gamma_1}{2}\frac{\partial}{\partial x_j}\left(\frac{\partial u_{iS2}}{\partial x_j} + \frac{\partial u_{jS2}}{\partial x_i} - \frac{2}{3}\frac{\partial u_{kS2}}{\partial x_k}\delta_{ij}\right)\\ &\quad - \frac{\gamma_1\omega_{S1}}{2}\frac{\partial^2 u_{iS1}}{\partial x_j^2} + \frac{\gamma_4}{2}\frac{\partial}{\partial x_j}\left[\tau_{S1}\left(\frac{\partial u_{iS1}}{\partial x_j} + \frac{\partial u_{jS1}}{\partial x_i}\right)\right] - \frac{\gamma_3}{3}\frac{\partial}{\partial x_i}\frac{\partial^2 \tau_{S1}}{\partial x_j^2},\end{aligned} \tag{3.267b}$$

$$\begin{aligned}&\frac{3}{2}\frac{\partial P_{S2}}{\partial \tilde{t}} + \frac{3}{2}u_{jS1}\frac{\partial P_{S2}}{\partial x_j} + \frac{5}{2}\left(\frac{\partial P_{S1}u_{jS2}}{\partial x_j} - \frac{\partial \omega_{S2}}{\partial \tilde{t}} - \frac{\partial(\omega_{S2}u_{jS1} + \omega_{S1}u_{jS2})}{\partial x_j}\right)\\ &= \frac{5\gamma_2}{4}\frac{\partial^2 \tau_{S2}}{\partial x_j^2} + \frac{5\gamma_5}{4}\frac{\partial}{\partial x_j}\left(\tau_{S1}\frac{\partial \tau_{S1}}{\partial x_j}\right) + \frac{\gamma_1}{2}\left(\frac{\partial u_{iS1}}{\partial x_j} + \frac{\partial u_{jS1}}{\partial x_i}\right)^2,\end{aligned} \tag{3.267c}$$

where

$$P_{S1} = \omega_{S1} + \tau_{S1}, \quad P_{S2} = \omega_{S2} + \omega_{S1}\tau_{S1} + \tau_{S2}. \tag{3.268}$$

The time-derivative terms $\partial u_{iS1}/\partial\tilde{t}$ in Eq. (3.266b) and $5\partial\tau_{S1}/2\partial\tilde{t} - \partial P_{S1}/\partial\tilde{t}$ in Eq. (3.266c) in the set of equations (3.265)–(3.266c) are the corrections to Eqs. (3.87)–(3.88c) in the corresponding time-independent case. These equations are similar to the Navier–Stokes set of equations for an incompressible fluid, but there is a difference in Eq. (3.266c). Rewriting the left-hand side of Eq. (3.266c) with the aid of Eqs. (3.265) and (3.268) in the form

$$\begin{aligned}&\frac{5}{2}\frac{\partial \tau_{S1}}{\partial \tilde{t}} - \frac{\partial P_{S1}}{\partial \tilde{t}} + \frac{5}{2}u_{jS1}\frac{\partial \tau_{S1}}{\partial x_j}\\ &= \frac{3}{2}\frac{\partial \tau_{S1}}{\partial \tilde{t}} + \frac{3}{2}u_{jS1}\frac{\partial \tau_{S1}}{\partial x_j} - \left(\frac{\partial \omega_{S1}}{\partial \tilde{t}} + u_{jS1}\frac{\partial \omega_{S1}}{\partial x_j}\right),\end{aligned}$$

and neglecting the last term $\partial\omega_{S1}/\partial\tilde{t} + u_{jS1}\partial\omega_{S1}/\partial x_j$, we obtain the energy equation of the Navier–Stokes set of equations for an incompressible fluid. From Eqs. (3.266a), (3.267a), and the discussion in Footnote 47 in Section 3.2.4, $\partial\omega_{S1}/\partial\tilde{t} + u_{jS1}\partial\omega_{S1}/\partial x_j$ is the corresponding contribution to Eq. (3.266c) of the work done by pressure on a volume of a gas, which vanishes in an incompressible fluid.[111] An example showing a decisive difference of the solution of Eqs. (3.265)–(3.266c) and that of the corresponding Navier–Stokes equations for incompressible fluid is given in Sone [2002].

In Eqs. (3.265)–(3.267c), the variable P_{Sm} appears in a staggered combination with the other variables. The P_{S1} in Eq. (3.266c) is determined, except an additive arbitrary function of $\tilde{t}$, by Eq. (3.265) in the preceding step. The arbitrary function is determined by the boundary condition in the process of solution of u_{iS1}, τ_{S1}, ω_{S1}, and P_{S2} from Eqs. (3.266a)–(3.266c), where an arbitrary function of $\tilde{t}$ in P_{S2} is left undetermined.[112] An additive arbitrary function of $\tilde{t}$ in P_{S2} is determined by the boundary condition in the process of solution of u_{iS2}, τ_{S2}, ω_{S2}, and P_{S3} from Eqs. (3.267a)–(3.267c), where an arbitrary function of $\tilde{t}$ in P_{S3} is left undetermined. In this way, we can consistently determine the solution. The boundary conditions on a simple boundary or an interface for Eqs. (3.265)–(3.267c) are given in Section 3.7.3.

Nonlinear problem

First consider the case where the condition

$$\int \zeta_i \hat{f} \mathbf{d}\boldsymbol{\zeta} = O(k), \tag{3.269}$$

which is introduced in Section 3.3, is imposed. With $\mathrm{Sh} = k$ and the new notation $\tilde{t}$, the Boltzmann equation (1.47a) in the absence of an external force $\hat{F}_i = 0$ is given as

$$k\frac{\partial \hat{f}}{\partial \tilde{t}} + \zeta_i \frac{\partial \hat{f}}{\partial x_i} = \frac{1}{k}\hat{J}(\hat{f}, \hat{f}). \tag{3.270}$$

The distribution function $\hat{f}$ is expanded in a power series of k, i.e.,

$$\hat{f} = \hat{f}_{SB} = \hat{f}_{SB0} + \hat{f}_{SB1}k + \cdots . \tag{3.271}$$

Corresponding to the expansion (3.271), the macroscopic variables $\hat{\rho}$, $\hat{v}_i$, $\hat{T}$, etc. (see Section 1.9) are also expanded in k, i.e.,

$$\hat{h}_{SB} = \hat{h}_{SB0} + \hat{h}_{SB1}k + \cdots , \tag{3.272}$$

[111] The relation $\partial\omega_{S1}/\partial\tilde{t} + u_{jS1}\partial\omega_{S1}/\partial x_j = 0$ is the condition of incompressibility.
[112] See Footnote 109 in this subsection.

where $\hat{h} = \hat{\rho}$, $\hat{v}_i$, $\hat{T}$, etc. Substituting the series (3.271) into Eq. (3.270), we obtain a series of integral equations for $\hat{f}_{SBm}$ $(m = 0, 1, \ldots)$, i.e.,

$$\hat{J}(\hat{f}_{SB0}, \hat{f}_{SB0}) = 0, \tag{3.273a}$$

$$2\hat{J}(\hat{f}_{SB0}, \hat{f}_{SB1}) = \zeta_i \frac{\partial \hat{f}_{SB0}}{\partial x_i}, \tag{3.273b}$$

$$2\hat{J}(\hat{f}_{SB0}, \hat{f}_{SBm}) = \frac{\partial \hat{f}_{SBm-2}}{\partial \tilde{t}} + \zeta_i \frac{\partial \hat{f}_{SBm-1}}{\partial x_i} - \sum_{r=1}^{m-1} \hat{J}(\hat{f}_{SBr}, \hat{f}_{SBm-r}) \qquad (m \geq 2). \tag{3.273c}$$

Repeating the process of solution and solvability condition, we obtain $\hat{f}_{SBm}$ and a series of the sets of equations for $\hat{h}_{SBm}$.[113] The leading-order solution $\hat{f}_{SB0}$ is the Maxwellian

$$\hat{f}_{SB0} = \frac{\hat{\rho}_{SB0}}{(\pi \hat{T}_{SB0})^{3/2}} \exp\left(-\frac{\zeta_i^2}{\hat{T}_{SB0}}\right), \tag{3.274}$$

where the condition (3.269) is used. The set of equations that determines the leading-order macroscopic variables is given by

$$\hat{p}_{SB0} = \hat{p}_0, \tag{3.275}$$

$$\hat{p}_{SB1} = \hat{p}_1, \tag{3.276}$$

$$\frac{\partial \hat{\rho}_{SB0}}{\partial \tilde{t}} + \frac{\partial \hat{\rho}_{SB0} \hat{v}_{iSB1}}{\partial x_i} = 0, \tag{3.277a}$$

$$\begin{aligned}
&\frac{\partial \hat{\rho}_{SB0} \hat{v}_{iSB1}}{\partial \tilde{t}} + \frac{\partial \hat{\rho}_{SB0} \hat{v}_{jSB1} \hat{v}_{iSB1}}{\partial x_j} \\
&\quad = -\frac{1}{2}\frac{\partial \hat{p}^*_{SB2}}{\partial x_i} + \frac{1}{2}\frac{\partial}{\partial x_j}\left[\Gamma_1(\hat{T}_{SB0})\left(\frac{\partial \hat{v}_{iSB1}}{\partial x_j} + \frac{\partial \hat{v}_{jSB1}}{\partial x_i} - \frac{2}{3}\frac{\partial \hat{v}_{kSB1}}{\partial x_k}\delta_{ij}\right)\right] \\
&\qquad + \frac{1}{2\hat{p}_0}\frac{\partial}{\partial x_j}\left\{\Gamma_7(\hat{T}_{SB0})\left[\frac{\partial \hat{T}_{SB0}}{\partial x_i}\frac{\partial \hat{T}_{SB0}}{\partial x_j} - \frac{1}{3}\left(\frac{\partial \hat{T}_{SB0}}{\partial x_k}\right)^2 \delta_{ij}\right]\right\},
\end{aligned} \tag{3.277b}$$

$$\frac{3}{2}\frac{\partial \hat{\rho}_{SB0} \hat{T}_{SB0}}{\partial \tilde{t}} + \frac{5}{2}\frac{\partial \hat{\rho}_{SB0} \hat{v}_{iSB1} \hat{T}_{SB0}}{\partial x_i} = \frac{5}{4}\frac{\partial}{\partial x_i}\left(\Gamma_2(\hat{T}_{SB0})\frac{\partial \hat{T}_{SB0}}{\partial x_i}\right), \tag{3.277c}$$

where $\hat{p}_0$ and $\hat{p}_1$ depend only on $\tilde{t}$, and

$$\hat{\rho}_{SB0} = \frac{\hat{p}_0}{\hat{T}_{SB0}}, \tag{3.278a}$$

$$\hat{p}^*_{SB2} = \hat{p}_{SB2} + \frac{2}{3\hat{p}_0}\frac{\partial}{\partial x_k}\left(\Gamma_3(\hat{T}_{SB0})\frac{\partial \hat{T}_{SB0}}{\partial x_k}\right). \tag{3.278b}$$

[113] See the explanation at the beginning of the paragraph next to that containing Eq. (3.234).

The time-derivative terms $\partial\hat{\rho}_{SB0}/\partial\tilde{t}$ in Eq. (3.277a), $\partial\hat{\rho}_{SB0}\hat{v}_{iSB1}/\partial\tilde{t}$ in Eq. (3.277b), and $(3/2)\partial\hat{\rho}_{SB0}\hat{T}_{SB0}/\partial\tilde{t}$ in Eq. (3.277c) in the set of equations (3.275)–(3.278b) are the corrections to Eqs. (3.153)–(3.158b) in the corresponding time-independent case. The ghost and non-Navier–Stokes effects are the feature of this system as in the time-independent problem.

In Eqs. (3.275)–(3.277c), the variable $\hat{p}_{SBm}$ appears in a staggered combination with the other variables. The arbitrary function $\hat{p}_0$ of $\tilde{t}$ is determined by the boundary condition in the process of solution of $\hat{v}_{iSB1}$, $\hat{T}_{SB0}$, $\hat{\rho}_{SB0}$, and $\hat{p}_{SB2}$ from Eqs. (3.277a)–(3.277c), where an arbitrary function of $\tilde{t}$ in $\hat{p}_{SB2}$ is left undetermined.[114] The process of solution can be advanced in a similar way. The boundary conditions on a simple boundary or an interface for Eqs. (3.277a)–(3.277c) are given in Section 3.7.3.

Next, consider the case where the condition (3.269) is eliminated and $\int \zeta_i \hat{f}\mathbf{d}\boldsymbol{\zeta}$ is a quantity of the order unity. The process is similar to the preceding case with the formally same relations from Eq. (3.270) to Eq. (3.273c) where the subscript SB is replaced by H. Equation (3.274) is replaced by

$$\hat{f}_{H0} = \frac{\hat{\rho}_{H0}}{(\pi\hat{T}_{H0})^{3/2}} \exp\left(-\frac{(\zeta_i - \hat{v}_{iH0})^2}{\hat{T}_{H0}}\right). \tag{3.279}$$

The set of equations for $\hat{\rho}_{H0}$, $\hat{v}_{iH0}$, and $\hat{T}_{H0}$ is simply

$$\frac{\partial\hat{\rho}_{H0}\hat{v}_{iH0}}{\partial x_i} = 0, \tag{3.280a}$$

$$\frac{\partial\hat{\rho}_{H0}\hat{v}_{jH0}\hat{v}_{iH0}}{\partial x_j} + \frac{1}{2}\frac{\partial\hat{p}_{H0}}{\partial x_i} = 0, \tag{3.280b}$$

$$\frac{\partial}{\partial x_j}\left[\hat{\rho}_{H0}\hat{v}_{jH0}\left(\hat{v}_{iH0}^2 + \frac{5}{2}\hat{T}_{H0}\right)\right] = 0, \tag{3.280c}$$

where

$$\hat{p}_{H0} = \hat{\rho}_{H0}\hat{T}_{H0}.$$

This result is easily understood from the results (3.250a)–(3.250c) in the case $\mathrm{Sh} = O(1)$. The time-derivative terms in these equations are reduced to a higher order and do not enter Eqs. (3.280a)–(3.280c). The time variation of this system is determined by that of the data in the boundary conditions (or the connecting condition with the viscous boundary-layer solution).

The role of the uniform pressure conditions, i.e., Eqs. (3.257), (3.265), (3.275), and (3.276), is similar to that of Eqs. (3.12), (3.87), (3.153), and (3.154) discussed in the last paragraph of Section 3.6.2 for time-independent problems. Unless the conditions (3.257), (3.265), (3.275), and (3.276) are satisfied, flow fields with faster time variation (Section 3.7.1) or larger flow velocity than those of the setups of analysis are induced.

Some mathematical theories for initial-value problems are developed for linear and weakly nonlinear problems by Bardos, Golse & Levermore [1998, 2000]

[114] See Footnote 109 in this subsection.

and Golse & Saint-Raymond [2004] (see also the article by Golse in Bouchut, Golse & Pulvirenti [2000]).

3.7.3 Slip boundary condition and Knudsen-layer correction

We first discuss the boundary condition for the fluid-dynamic-type equations derived in the case $\mathrm{Sh} = O(k)$ of Section 3.7.2. Naturally, the condition of a boundary (e.g., the boundary temperature), a simple boundary or an interface, is assumed to vary in such a time scale t_0 that $\mathrm{Sh} = O(k)$. Here, the shape of the boundary is taken to be invariant and its velocity component normal to it to be zero ($u_{wi}n_i = 0$ or $\hat{v}_{wi}n_i = 0$).

To make the fluid-dynamic-type solution ϕ_G, ϕ_S, or $\hat{f}_{SB}$ match the kinetic boundary condition, we introduce the Knudsen-layer correction

$$\phi = \phi_G + \phi_K, \quad \phi = \phi_S + \phi_K, \quad \hat{f} = \hat{f}_{SB} + \hat{f}_K.$$

It is seen from Eqs. (3.255a) and (3.255b) for ϕ_{G0} and ϕ_{G1}, Eqs. (3.263a) and (3.263b) for ϕ_{S1} and ϕ_{S2}, or Eqs. (3.273a) and (3.273b) for $\hat{f}_{SB0}$ and $\hat{f}_{SB1}$ that the fluid-dynamic parts ϕ_{G0} and ϕ_{G1}, ϕ_{S1} and ϕ_{S2}, or $\hat{f}_{SB0}$ and $\hat{f}_{SB1}$ are of the same form as those in the time-independent case discussed in Section 3.1.2, 3.2.2, or 3.3.2, though the macroscopic variables contained in them parametrically are time-dependent. With this preliminary information, we will discuss the equation and boundary condition for the Knudsen-layer correction.

The boundary condition for the Knudsen-layer correction is determined by the original kinetic boundary condition for the full solution and the boundary data of the fluid-dynamic part ϕ_G, ϕ_S, or $\hat{f}_{SB}$, which contains undetermined quantities. That is, the boundary condition given by the scattering kernel on a simple boundary or on an interface (see Sections 1.9 and 1.11) is expressed symbolically in the form

$$\varphi_{Km} = \mathcal{K}(\varphi_{Km}) + \mathcal{K}(\varphi_{Fm}) + \mathfrak{g}_m - \varphi_{Fm} \quad (\zeta_i n_i > 0),$$

where

$$\varphi_{Fm} = \phi_{Gm},\ \phi_{Sm},\ \text{or}\ \hat{f}_{SBm},$$
$$\varphi_{Km} = \phi_{Km}\ (\text{for}\ \phi_{Gm}\ \text{and}\ \phi_{Sm})\ \text{or}\ \hat{f}_{Km},$$

$\mathcal{K}(*)$ is a linear integral operator, and $\mathfrak{g}_m$ is determined by the boundary parameter [and ϕ_{Sn}, $\hat{f}_{SBn}$, and φ_{Kn} $(n < m)$ for ϕ_S and $\hat{f}_{SB}$]. The Knudsen-layer correction ϕ_{Km} (for ϕ_{Gm} and ϕ_{Sm}) or $\hat{f}_{Km}$ vanishes as $\eta \to \infty$. From the property of the fluid-dynamic part ϕ_G, ϕ_S, or $\hat{f}_{SB}$ noted above, the boundary conditions for the Knudsen-layer corrections ϕ_{K0} and ϕ_{K1} (corresponding to ϕ_G), ϕ_{K1} and ϕ_{K2} (corresponding to ϕ_S), or $\hat{f}_{K1}$ are of the same form as those in the time-independent case.[115]

[115]The Knudsen-layer correction $\hat{f}_K$ starts from the first order of k, i.e., $\hat{f}_K = \hat{f}_{K1}k + \cdots$,

The equation for the Knudsen layer is derived in the same way as in the time-independent problem by introducing the Knudsen-layer variables [Eq. (3.31)]. Assuming that the correction ϕ_K or $\hat{f}_K$ varies in such a time scale t_0 that Sh$= O(k)$, we find that the relative size of the time-derivative term to the collision and the spatial derivative terms[116] is of the order of k^2. It should be noted that there is another time-dependent contribution from the ϕ_S and $\hat{f}_{SB}$. That is, in splitting the Boltzmann equation into that for the fluid-dynamic part and the remaining equation for the Knudsen-layer correction, we have to handle $\mathcal{J}(\phi_S, \phi_K)$ or $\hat{J}(\hat{f}_{SB}, \hat{f}_K)$ term. This process can be carried out in the same way as in the time-independent case (see Sections 3.2.3 and 3.3.2). There is no contribution of ϕ_S to the equation for ϕ_{K1}, and ϕ_{S1} enters the equation for ϕ_{K2}. Only $\hat{f}_{SB0}$ enters the equation for $\hat{f}_{K1}$. Thus, the equations for ϕ_{K0}, ϕ_{K1} (corresponding to ϕ_G), ϕ_{K1}, ϕ_{K2} (corresponding to ϕ_S), and $\hat{f}_{K1}$ are of the same form as those in the time-independent case. For this form of equation, the solution varies in such a time scale t_0 that Sh$= O(k)$, if the boundary condition varies similarly. Thus, the assumption introduced at the beginning of this paragraph is verified.

From the above discussion on the equation and boundary condition for the Knudsen-layer correction, we find that the time-independent results for the slip conditions and Knudsen-layer corrections derived in Sections 3.1, 3.2, and 3.3 apply to the time-dependent equations derived in Section 3.7.2 up to some stage. That is,

Linear problem

The first two stages of the slip boundary conditions and the Knudsen-layer corrections in Section 3.1.5, i.e., Eqs. (3.40a)–(3.40c), (3.41a)–(3.41c) on a simple boundary and Eqs. (3.56a)–(3.56c), (3.57a)–(3.57c) on an interface of the gas and its condensed phase, apply to the fluid-dynamic-type equations determining the macroscopic variables up to h_{G1}, i.e., Eq. (3.257), Eqs. (3.258a)–(3.258c), and Eqs. (3.259a)–(3.259c).

Weakly nonlinear problem

The first two stages of the slip boundary conditions and the Knudsen-layer corrections in Section 3.2.3, i.e., Eqs. (3.113a)–(3.113c), (3.114a)–(3.114c) on a simple boundary and Eqs. (3.119a)–(3.119c), (3.120a)–(3.120c) on an interface, apply to the fluid-dynamic-type equations determining the macroscopic variables up to h_{S2}, i.e., Eq. (3.265), Eqs. (3.266a)–(3.266c), and Eqs. (3.267a)–(3.267c).

Nonlinear problem 1

Equations (3.161a) and (3.161b) on a simple boundary and Eqs. (3.162a)–(3.162d) on an interface apply to the set of equations (3.277a)–(3.278b).

---

irrespective of a simple boundary or an interface, because $\hat{f}_{SB0}$ is a Maxwellian with zero velocity and the kinetic boundary condition is satisfied by taking $\hat{T}_{SB0} = \hat{T}_{w0}$ as in the time-independent case. Incidentally, for a simple boundary, we can take $\phi_{K0} = 0$ for ϕ_G and $\phi_{K1} = 0$ for ϕ_S as in the time-independent case.

[116] In the Knudsen layer, the spatial derivative term is upgraded by the factor $1/k$.

The fluid-dynamic-type equations derived in the case $\mathrm{Sh} = O(1)$ and in the last problem of the case $\mathrm{Sh} = O(k)$ are the first-order equations of the Euler type. Generally, a viscous boundary layer or a suction boundary layer intervenes between the Euler region and the Knudsen layer, as discussed in Section 3.4 or in Sone & Doi [2000] for time-independent problems. Applicability of the slip condition obtained for the time-independent case to time-dependent problems can be discussed similarly.

When evaporation or condensation with a finite Mach number is taking place on an interface of a gas and its condensed phase, the behavior of the gas is described by the Euler set of equations (3.250a)–(3.250c) or (3.280a)–(3.280c) with nonlinear Knudsen-layer corrections as in the time-independent case in Section 3.5. By a similar argument, we obtain the following result.

Nonlinear problem 2
Equations (3.228a)–(3.229c) apply to the set of equations (3.250a)–(3.250c) or (3.280a)–(3.280c) on an interface where evaporation or condensation of a finite Mach number is taking place.

3.7.4 Initial layer and others

Consider an initial-value problem in an infinite domain without a boundary, where Knudsen number or k based on the reference length L determined by the initial condition is small. When the initial velocity distribution function is not close to a local Maxwellian, the collision term $\hat{J}(\hat{f}, \hat{f})/k$ in the Boltzmann equation (1.47a) [or $\mathcal{L}(\phi)/k + \mathcal{J}(\phi, \phi)/k$ in Eq. (1.75a) or $\mathcal{L}(\phi)/k$ in Eq. (1.96)] is of the order of $1/k$. Then, the time-derivative term $\mathrm{Sh}\partial\hat{f}/\partial\hat{t}$ (or $\mathrm{Sh}\partial\phi/\partial\hat{t}$) is of the order of k^{-1}. Thus, for the time scale of variation of the velocity distribution function or the time scale for which $\partial\hat{f}/\partial\hat{t}$ (or $\partial\phi/\partial\hat{t}$) is of the order of unity, the Strouhal number Sh is of the order of $1/k$, that is, $t_0 \sim \ell_0/(2RT_0)^{1/2} \sim \bar{\tau}_c$, where $\bar{\tau}_c$ is the mean free time (see Section 1.5). That is, the state of the gas varies in the time scale of the mean free time. As time goes on, the molecules undergo molecular collisions, many collisions after many $\bar{\tau}_c$'s, and the velocity distribution function approaches a local Maxwellian. Then, the collision term, and thus the time-derivative term, degrades to the order of unity, which is the order of the space-derivative term.[117] That is, Sh is of the order of unity or the time scale of variation of the distribution function is $t_0 \sim L/(2RT_0)^{1/2}$, which is the time of the order that the sound wave propagates over the distance of the reference length L. This is the case discussed in Section 3.7.1, where the fluid-dynamic-type equations describing propagation of waves are derived. As time further goes on, the wave fronts escape from the field, and the spatial variation of the variables, as well as the collision term, becomes moderate. With decay of the combination of the spatial derivative and collision terms, the time-derivative

[117] A shock wave (Section 4.7), where the length scale of variation is of the order of the mean free path, may be formed locally as time goes on.

term in the Boltzmann equation becomes smaller. When it reduces to the order of k, the time scale t_0 of the variation of variables becomes $t_0 \sim \rho_0 L^2/\mu_0$ or $t_0 \sim R\rho_0 L^2/\lambda_0$, and the macroscopic variables are determined by the fluid-dynamic-type equations derived in Section 3.7.2. The first region with the time scale $\bar{\tau}_c$ is called an *initial layer,* the second region with the time scale $t_0 \sim L/(2RT_0)^{1/2}$ an *Euler* or *inviscid region*, and the last region with $t_0 \sim \rho_0 L^2/\mu_0$ a *diffusion* or *viscous region*.[118]

The initial-value problem in an infinite domain without a boundary is studied by Grad [1963a]. In this pioneering work of modern kinetic theory, the initial layer is introduced, and its general theory is developed to connect a smooth initial condition to the fluid-dynamic-type equations in the region with $\mathrm{Sh} = O(1)$. An example showing the behavior of a gas in a longer time scale, $\mathrm{Sh} = O(k)$, is given in Sone & Shibata [1965] and Sone [1968]. In an initial and boundary-value problem, where there is a boundary, the interaction of the initial layer with the boundary has to be discussed. Some simple examples have been studied (Sone [1964, 1965, 1966a]). Mathematical study of the time-evolution process through the initial layer to the fluid-dynamic region for a simple example is carried out by Ha, Liu & Yu [2006] (see the last paragraph of Section 4.7).

Recently, Liu & Yu [2004b, 2006a] derived the Green function of the linearized Boltzmann equation for an initial-value problem. Their rigorous mathematical work clarifies the structure of the time evolution of the solution of the Boltzmann equation, especially the character in the regions $\mathrm{Sh} = O(1)$ and $\mathrm{Sh} = O(k)$. Their study of the Green function is progressing to initial and boundary-value problems (e.g., Liu & Yu [2006b]).

Solutions with discontinuities can be constructed from the Euler set of equations where the conservations of mass, momentum, and energy fluxes (and the condition of nondecrease of the entropy along a fluid-particle path) hold across the discontinuity. These solutions are called *weak solutions* of the Euler set (Lax [1957], Liu [1975], Smoller [1983], Sone [1987]). The discontinuities are of two kinds, shock wave and contact discontinuity (see, e.g., Courant & Friedrichs [1948] and Liepmann & Roshko [1957]). There is no mass flux across the contact discontinuity, where the pressure is continuous but the temperature and the density or the flow velocity parallel to it or both are discontinuous. In the Boltzmann system, the contact discontinuity, if any at some instant, begins to diffuse immediately (thus may be called contact layer) and the variation extends to a wide range in a long time $\mathrm{Sh} = O(k)$. On the other hand, the shock wave, to be discussed in Section 4.7, is a thin layer with thickness of the order of the mean free path and can persist, depending on situations, for a long time up to the region $\mathrm{Sh} = O(k)$, without broadening. Thus, a smooth solution described by the Euler set coexists with shock waves of infinitesimal thickness. Yu [2005] extended the Hilbert expansion in Section 3.7.1 in such a way that the shock wave can be incorporated into the expansion. Numerical examples of the time evolution of shock waves and contact layers

[118] See Footnote 104 at the beginning of this section.

are given in Sections 4.8, 6.1.2, and 6.1.3. Examples of the contact layer of flow velocity parallel to the layer are given in Sone & Shibata [1965], Sone [1968], and Aoki, Nishino, Sone & Sugimoto [1991], in the first two of which the diffusion of an initial vortex layer (or discontinuity of tangential velocity) is discussed.

Chapter 4

Simple Flows

In this chapter, we discuss various fundamental physical problems of simple geometry, such as unidirectional flows, quasi-unidirectional flows, a uniform flow past a sphere, and a plane shock wave. Various fundamental properties of the solution of the Boltzmann equation are provided in these examples.

4.1 Couette-flow and heat-transfer problems between two parallel plates

Consider a gas between two parallel plane walls, one at $X_2 = 0$ is at rest and is kept at a uniform temperature T_0, and the other at $X_2 = L$ is moving with velocity $(U, 0, 0)$ and is kept at another uniform temperature T_1. We are interested in the time-independent behavior of the gas when the wall speed $|U|$ and the temperature difference $|T_1 - T_0|$ are small, i.e., $|U|/(2RT_0)^{1/2} \ll 1$ and $|T_1 - T_0|/T_0 \ll 1$. The linearized Boltzmann equation and the linearized diffuse-reflection condition are applied. The solution that is uniform with respect to X_1 and X_3 is looked for here. We use the notation in Section 1.10 and the relation in Section 1.11, where the temperature T_0 of the wall at $X_2 = 0$ and the average density of the gas over the channel are taken, respectively, as the reference temperature T_0 and the reference density ρ_0 in the definition of the nondimensional variables.

The linearized Boltzmann equation is given as

$$\zeta_2 \frac{\partial \phi}{\partial x_2} = \frac{1}{k} \mathcal{L}(\phi),$$

and the boundary conditions are, at $x_2 = 0$,

$$\phi(x_2, \zeta_i) = -2\sqrt{\pi} \int_{\zeta_2 < 0} \zeta_2 \phi E \mathbf{d}\boldsymbol{\zeta} \qquad (\zeta_2 > 0), \tag{4.1}$$

and at $x_2 = 1$,

$$\phi(x_2, \zeta_i) = \check{\sigma}_w + 2\zeta_1 \Delta u + \left(\zeta_j^2 - \frac{3}{2}\right)\Delta\tau \qquad (\zeta_2 < 0), \tag{4.2a}$$

$$\check{\sigma}_w = -\frac{1}{2}\Delta\tau + 2\sqrt{\pi}\int_{\zeta_2>0} \zeta_2 \phi E \mathbf{d\zeta}, \tag{4.2b}$$

where

$$\Delta u = \frac{U}{(2RT_0)^{1/2}}, \qquad \Delta\tau = \frac{T_1}{T_0} - 1.$$

In view of the discussion of the similarity solution in Section A.5, we put ϕ in the form

$$\phi = \Delta u \zeta_1 \Phi_{\mathrm{C}}(x_2, \zeta_2, \zeta) + \Delta\tau \Phi_{\mathrm{H}}(x_2, \zeta_2, \zeta), \quad \zeta = (\zeta_i^2)^{1/2}. \tag{4.3}$$

Then the problem is split into two independent problems, one for Φ_{C} (*plane-Couette-flow problem*) and the other for Φ_{H} (*heat-transfer problem*), i.e., the equations are

$$\zeta_2 \frac{\partial \Phi_{\mathrm{C}}}{\partial x_2} = \frac{1}{k\zeta_1}\mathcal{L}(\zeta_1 \Phi_{\mathrm{C}}), \qquad \zeta_2 \frac{\partial \Phi_{\mathrm{H}}}{\partial x_2} = \frac{1}{k}\mathcal{L}(\Phi_{\mathrm{H}}), \tag{4.4}$$

and the boundary conditions are

$$\Phi_{\mathrm{C}} = 0 \qquad (\zeta_2 > 0) \qquad \text{at } x_2 = 0, \tag{4.5a}$$

$$\Phi_{\mathrm{C}} = 2 \qquad (\zeta_2 < 0) \qquad \text{at } x_2 = 1, \tag{4.5b}$$

$$\Phi_{\mathrm{H}} = -2\sqrt{\pi}\int_{\zeta_2<0} \zeta_2 \Phi_{\mathrm{H}} E \mathbf{d\zeta} \qquad (\zeta_2 > 0) \quad \text{at } x_2 = 0, \tag{4.6a}$$

$$\Phi_{\mathrm{H}} = 2\sqrt{\pi}\int_{\zeta_2>0} \zeta_2 \Phi_{\mathrm{H}} E \mathbf{d\zeta} + \zeta^2 - 2 \quad (\zeta_2 < 0) \quad \text{at } x_2 = 1. \tag{4.6b}$$

The macroscopic variables, i.e., density ρ, velocity v_i, temperature T, stress tensor p_{ij}, and heat-flow vector q_i, corresponding to Φ_{C} are expressed as

$$\frac{v_{1\mathrm{C}}}{U} = \int \zeta_1^2 \Phi_{\mathrm{C}}(x_2, \zeta_2, \zeta) E \mathbf{d\zeta},$$

$$\frac{p_{12\mathrm{C}}}{p_0} = \frac{p_{21\mathrm{C}}}{p_0} = \frac{2U}{(2RT_0)^{1/2}} \int \zeta_1^2 \zeta_2 \Phi_{\mathrm{C}}(x_2, \zeta_2, \zeta) E \mathbf{d\zeta},$$

$$\frac{q_{1\mathrm{C}}}{p_0 U} = \int \zeta_1^2 \zeta^2 \Phi_{\mathrm{C}}(x_2, \zeta_2, \zeta) E \mathbf{d\zeta} - \frac{5}{2}\frac{v_{1\mathrm{C}}}{U},$$

where $p_{12\mathrm{C}}$ is independent of x_2 owing to the conservation equation (1.100). In view of the parity (even or odd) of $\zeta_1 \Phi_{\mathrm{C}}$ with respect to ζ_1 and ζ_3, the other quantities, i.e.,

$$v_{2\mathrm{C}}, \quad v_{3\mathrm{C}}, \quad \rho_{\mathrm{C}}/\rho_0 - 1, \quad T_{\mathrm{C}}/T_0 - 1,$$
$$p_{ij\mathrm{C}} - p_0\delta_{ij} \text{ except } (i,j) = (1,2) \text{ and } (2,1), \quad q_{2\mathrm{C}}, \quad q_{3\mathrm{C}},$$

all vanish. The macroscopic variables corresponding to $\Phi_{\rm H}$ are

$$\frac{\rho_{\rm H}}{\rho_0}-1=\ \Delta\tau\int\Phi_{\rm H}E\mathbf{d\zeta},\qquad \frac{T_{\rm H}}{T_0}-1=\ \Delta\tau\int\left(\frac{2}{3}\zeta^2-1\right)\Phi_{\rm H}E\mathbf{d\zeta},$$
$$\frac{p_{22{\rm H}}}{p_0}-1=2\ \Delta\tau\int\zeta_2^2\Phi_{\rm H}E\mathbf{d\zeta},\quad \frac{p_{11{\rm H}}}{p_0}-1=\frac{p_{33{\rm H}}}{p_0}-1=2\ \Delta\tau\int\zeta_1^2\Phi_{\rm H}E\mathbf{d\zeta},$$
$$\frac{q_{2{\rm H}}}{p_0(2RT_0)^{1/2}}=\ \Delta\tau\int\zeta_2\zeta^2\Phi_{\rm H}E\mathbf{d\zeta},$$

where $p_{22{\rm H}}$ and $q_{2{\rm H}}$ are independent of x_2 owing to the conservation equations (1.100) and (1.101). The other quantities, i.e.,

$$v_{i{\rm H}},\quad p_{ij{\rm H}}\ (i\neq j),\quad q_{1{\rm H}},\quad q_{3{\rm H}},$$

all vanish. The conservation equation (1.99) and the condition of a simple boundary are used to derive $v_{2{\rm H}}=0$. To summarize, the macroscopic variables for the original problem are given as

$$\left.\begin{aligned}&v_1\ =v_{1{\rm C}},\quad v_2\ =v_3=0,\quad \rho=\rho_{\rm H},\quad T=T_{\rm H},\\&p_{11}=p_{33}=p_{11{\rm H}}\ (=p_{33{\rm H}}),\quad p_{22}=p_{22{\rm H}},\\&p_{12}=p_{21}=p_{12{\rm C}}\ (=p_{21{\rm C}}),\quad p_{13}=p_{31}=p_{23}=p_{32}=0,\\&q_1=q_{1{\rm C}},\ q_2=q_{2{\rm H}},\ q_3=0.\end{aligned}\right\}\tag{4.7}$$

The solution for small k of the Couette-flow problem can be easily obtained by the asymptotic theory in Section 3.1.[1] The analysis can be easily extended to any order of k for the present simple problem. The function Φ_{CG}

$$\Phi_{CG}=c_1x_2+c_0-\frac{1}{2}kc_1\zeta_2B(\zeta),\tag{4.8}$$

where c_0 and c_1 are constants and $B(\zeta)$ is defined in Section A.2.9, satisfies the equation for $\Phi_{\rm C}$ in Eq. (4.4) for arbitrary k [see Eq. (3.19) or (A.130) and Eq. (A.124) with (A.128a)]. Let $u_{CG}=\int\zeta_1^2\Phi_{CG}E\mathbf{d\zeta}$. Then

$$u_{CG}=(c_1x_2+c_0)/2.\tag{4.9}$$

The solution $\Phi_{\rm C}$ satisfying the boundary conditions (4.5a) and (4.5b) is looked for in the form

$$\Phi_{\rm C}=\Phi_{CG}+\Phi_{CK}(\eta)+\Phi_{CK}^{-}(\eta_-),$$

where Φ_{CK} is the Knudsen-layer correction in the neighborhood of the wall on $x_2=0$ and Φ_{CK}^{-} is the one in the neighborhood of $x_2=1$, and the arguments η and η_- are the corresponding Knudsen-layer variables, i.e., $\eta=x_2/k$ and

[1] According to Footnote 3 in Section 3.1.2, it is required that $|U|/(2RT_0)^{1/2}\ll k^n$ and $|T_1-T_0|/T_0\ll k^n$. Similar assumptions apply to the results for small Knudsen numbers on the basis of the linearized Boltzmann equation.

$\eta_- = (1-x_2)/k$. Obviously, from the equation for $\Phi_{\rm C}$ in Eq. (4.4), the equations for Φ_{CK} and Φ^-_{CK} are

$$\zeta_2 \frac{\partial \zeta_1 \Phi_{CK}}{\partial \eta} = \mathcal{L}(\zeta_1 \Phi_{CK}), \quad -\zeta_2 \frac{\partial \zeta_1 \Phi^-_{CK}}{\partial \eta_-} = \mathcal{L}(\zeta_1 \Phi^-_{CK}). \tag{4.10}$$

From Eqs. (4.5a), (4.5b), and (4.8), the boundary conditions are[2]

$$\left.\begin{aligned} &\Phi_{CK} = -c_0 + \tfrac{1}{2} c_1 \zeta_2 B(\zeta) k \quad (\zeta_2 > 0) \quad \text{at } \eta = 0, \\ &\Phi^-_{CK} = 2 - c_0 - c_1 + \tfrac{1}{2} c_1 \zeta_2 B(\zeta) k \quad (\zeta_2 < 0) \quad \text{at } \eta_- = 0, \end{aligned}\right\} \tag{4.11}$$

$$\Phi_{CK} \to 0 \ \text{ as } \eta \to \infty, \quad \Phi^-_{CK} \to 0 \ \text{ as } \eta_- \to \infty. \tag{4.12}$$

The above system (4.10)–(4.12) for $\zeta_1 \Phi_{CK}$ or $\zeta_1 \Phi^-_{CK}$ is a special form of that for the Knudsen-layer correction ϕ_{K1} on a simple boundary in Section 3.1.4.[3] The $\zeta_1 \Phi_{CG}$ is the corresponding Grad–Hilbert part and $(u_{CG}, 0, 0)$ is its flow velocity. Applying the relation of the system for ϕ_{K1} and the slip condition (3.41a) to the system for $\zeta_1 \Phi_{CK}$ on $x_2 = 0$, we find that the constant c_0 is related to c_1 as

$$c_0 = -c_1 k_0 k, \tag{4.13}$$

where k_0 is the slip coefficient defined in Section 3.1.5. Similarly for the Knudsen layer on $x_2 = 1$, we have

$$2 - c_1 - c_0 = -c_1 k_0 k. \tag{4.14}$$

From Eqs. (4.13), (4.14),

$$c_1 = \frac{2}{1 - 2k_0 k}, \quad c_0 = -\frac{2k_0 k}{1 - 2k_0 k}.$$

Thus, from (4.8),

$$\Phi_{CG} = \frac{2}{1 - 2k_0 k} \left[x_2 - \left(k_0 + \frac{1}{2} \zeta_2 B(\zeta) \right) k \right]. \tag{4.15}$$

Noting the correspondence between the system for ϕ_{K1} in Footnote 12 in Section 3.1.4 and the Knudsen-layer corrections (3.41a), (3.50), and (3.53), we find the expression of the Knudsen-layer parts for $v_{1\rm C}$, $p_{12\rm C}$, and $q_{1\rm C}$. Collecting the results, we have

$$\frac{v_{1\rm C}}{U} = \frac{1}{1 - 2k_0 k} \left(\frac{X_2}{L} - [k_0 + Y_0(\eta) - Y_0(\eta_-)] k \right), \tag{4.16a}$$

$$\frac{p_{12\rm C}}{p_0 U (2RT_0)^{-1/2}} = -\frac{\gamma_1 k}{1 - 2k_0 k}, \tag{4.16b}$$

$$\frac{q_{1\rm C}}{p_0 U} = \frac{k}{1 - 2k_0 k} [H_A(\eta) - H_A(\eta_-)], \tag{4.16c}$$

[2]The decay of Φ_{CK} (Φ^-_{CK}) as η (η_-) $\to \infty$ is assumed to be faster than any inverse power of η (η_-) as in the Knudsen-layer analyses in Chapter 3, which is assured by the Grad–Bardos theorem. Thus, the error of the boundary condition for Φ_{CK} (Φ^-_{CK}) owing to the tail of the Knudsen layer Φ^-_{CK} (Φ_{CK}) on the other boundary is smaller than any power of k.

[3]See Footnote 12 in Section 3.1.4.

where γ_1 is the nondimensional viscosity defined in Section 3.1.3, and $Y_0(\eta)$ and $H_A(\eta)$ are Knudsen-layer functions defined in Section 3.1.5. The solution, i.e., Eqs. (4.16a)–(4.16c), where the terms of arbitrary order of k are taken into account, is inapplicable for a finite value of k. In fact, the limiting values as $k \to \infty$ of the results (4.16a)–(4.16c) do not agree with the corresponding free molecular results to be given by Eq. (4.17).[4] The reason is that for a finite k, η (η_-) is finite at the other wall for which the boundary condition as η (η_-) $\to \infty$ in Eq. (4.12) is inapplicable. In other words, the above result is the asymptotic solution where the terms as $\exp(-1/k)$ are neglected[5] and these terms are smaller than any power of k for a small k but are finite for a finite k. Physically, the asymptotic analysis neglects the effect of molecules impinging on a wall directly from the other wall.

The solution for the free molecular case ($k = \infty$) is easily obtained (see Section 2.3.3) as

$$\frac{v_{1\mathrm{C}}}{U} = \frac{1}{2}, \qquad \frac{p_{12\mathrm{C}}}{p_0 U (2RT_0)^{-1/2}} = -\frac{1}{\sqrt{\pi}}, \qquad \frac{q_{1\mathrm{C}}}{p_0 U} = 0. \tag{4.17}$$

The state of the gas is uniform.

The numerical results for a hard-sphere gas of the profiles $v_{1\mathrm{C}}/U$ and $q_{1\mathrm{C}}/p_0U$ vs X_2/L and the variations of $p_{12\mathrm{C}}/p_0U(2RT_0)^{-1/2}$ and $\int_0^{L/2} q_{1\mathrm{C}}\mathrm{d}X_2/p_0UL$ with k are shown in Figs. 4.1, 4.2, 4.3, and 4.4 (Sone, Takata & Ohwada [1990]). There is a heat flow in the absence of temperature gradient. More detailed information of the flow including the velocity distribution function is given in the above paper.

The solution for small k of the heat-transfer problem can be easily obtained by the asymptotic theory in Section 3.1. The analysis can be easily extended to any order of k for the present simple problem. The analysis goes parallel to that for Φ_{C} by putting

$$\Phi_{\mathrm{H}} = \Phi_{\mathrm{H}G} + \Phi_{\mathrm{H}K}(\eta) + \Phi^-_{\mathrm{H}K}(\eta_-),$$

where $\Phi_{\mathrm{H}G} = (\zeta^2 - 5/2)(\bar{c}_1 x_2 + \bar{c}_0) + \bar{c}_2 - \bar{c}_1\zeta_2 A(\zeta)k$ ($\bar{c}_0$, $\bar{c}_1$, $\bar{c}_2$: constants). The results are

$$\frac{\rho_{\mathrm{H}} - \rho_0}{\rho_0(T_1/T_0 - 1)} = \frac{1}{1 + 2d_1 k}\left(\frac{1}{2} - \frac{X_2}{L} + [\Omega_1(\eta) - \Omega_1(\eta_-)]k\right), \tag{4.18a}$$

$$\frac{T_{\mathrm{H}} - T_0}{T_0(T_1/T_0 - 1)} = \frac{1}{1 + 2d_1 k}\left(\frac{X_2}{L} + [d_1 + \Theta_1(\eta) - \Theta_1(\eta_-)]k\right), \tag{4.18b}$$

$$\frac{q_{2\mathrm{H}}}{p_0(2RT_0)^{1/2}(T_1/T_0 - 1)} = -\frac{5\gamma_2}{4}\frac{k}{1 + 2d_1 k}, \tag{4.18c}$$

where γ_2, the nondimensional thermal conductivity, is defined in Section 3.1.3 and d_1, the slip coefficient, and $\Omega_1(\eta)$ and $\Theta_1(\eta)$, Knudsen-layer functions, are defined in Section 3.1.5.

[4] The limiting value of $p_{12\mathrm{C}}$ as $k \to \infty$ of Eq. (4.16b) does not agree with $p_{12\mathrm{C}}$ in Eq. (4.17). The same thing applies to $q_{2\mathrm{H}}$ in Eqs. (4.18c) and (4.19).

[5] See Footnote 2 in this section.

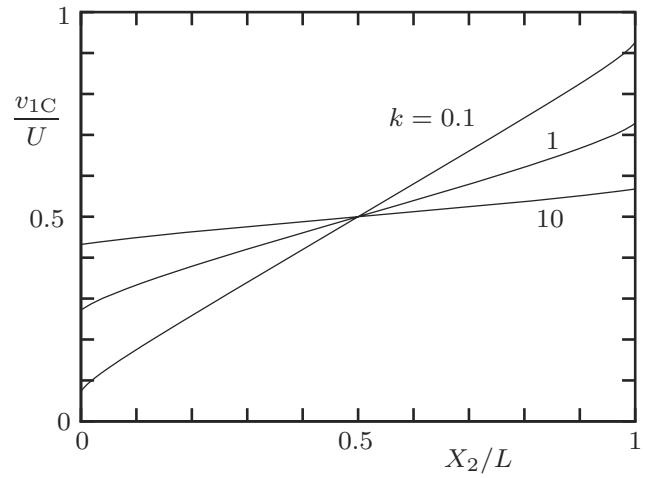

Figure 4.1. The velocity distribution, v_{1C}/U vs X_2/L, in the plane Couette flow (a hard-sphere gas).

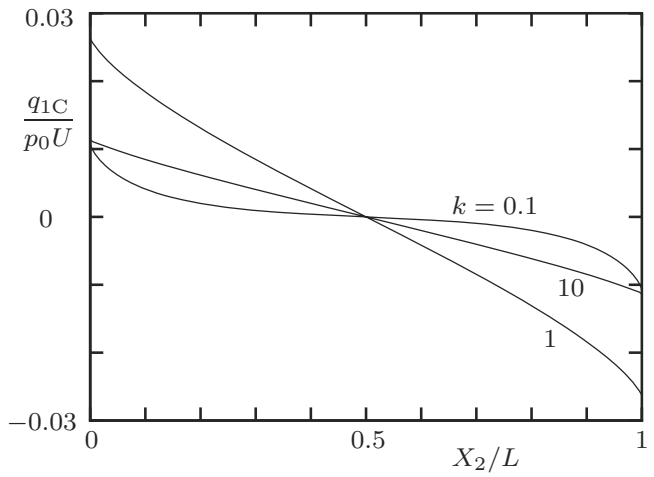

Figure 4.2. The heat-flux distribution, q_{1C}/p_0U vs X_2/L, in the plane Couette flow (a hard-sphere gas).

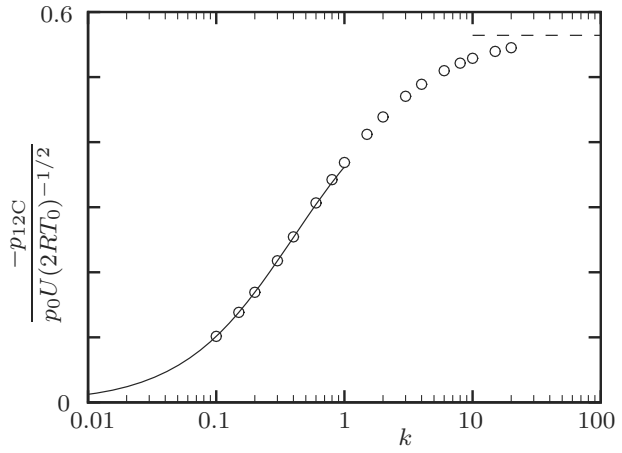

Figure 4.3. The shear stress, $p_{12C}/p_0U(2RT_0)^{-1/2}$ vs k, in the plane Couette flow (a hard-sphere gas). The white circles ∘ indicate the numerical solution, the solid line —— indicates the asymptotic solution (4.16b) for small k, and the dashed line – – – indicates the solution of the free molecular flow ($k = \infty$).

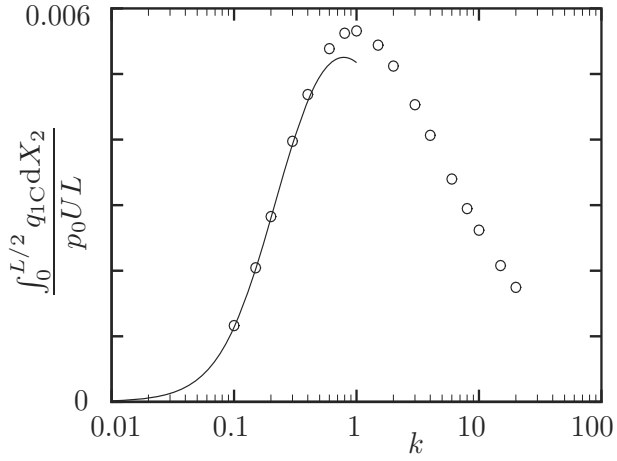

Figure 4.4. The heat-flow rate, $\int_0^{L/2} q_{1C}\mathrm{d}X_2/p_0UL$ vs k, through the half of the channel in the plane Couette flow (a hard-sphere gas). The white circles ∘ indicate the solution and the solid line —— indicates the asymptotic solution for small k derived from Eq. (4.16c). The heat flow vanishes in the free molecular flow ($k = \infty$).

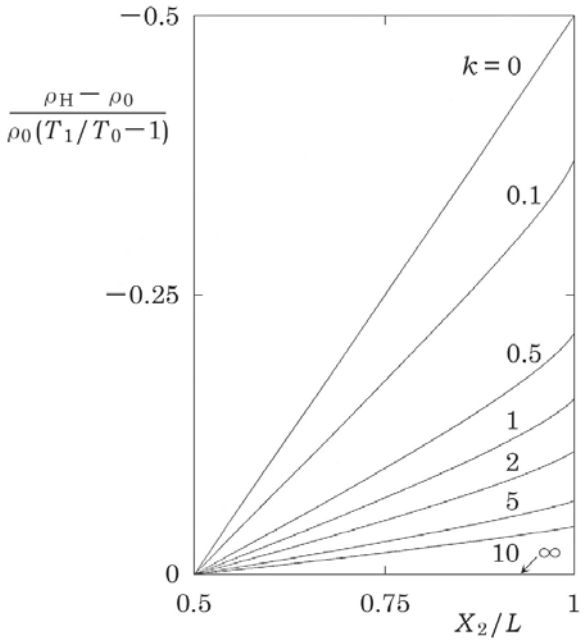

Figure 4.5. The density distribution, $(\rho_H - \rho_0)/\rho_0(T_1/T_0 - 1)$ vs X_2/L, in the heat-transfer problem between two parallel plane walls (a hard-sphere gas).

The solution for the free molecular case ($k = \infty$) is easily obtained (see Section 2.3.3) as

$$\frac{\rho_H}{\rho_0} = 1, \quad \frac{T_H}{T_0} = 1 + \frac{T_1 - T_0}{2T_0}, \quad \frac{q_{2H}}{p_0(2RT_0)^{1/2}} = -\frac{T_1 - T_0}{\sqrt{\pi}T_0}. \tag{4.19}$$

The state of the gas is uniform.

The numerical results (Ohwada, Aoki & Sone [1989]) for a hard-sphere gas of the profiles $(\rho_H - \rho_0)/\rho_0(T_1/T_0 - 1)$ and $(T_H - T_0)/(T_1 - T_0)$ vs X_2/L and the variation of $q_{2H}/p_0(2RT_0)^{1/2}(T_1/T_0 - 1)$ with k are shown in Figs. 4.5 and 4.6 and Table 4.1, in the last of which the data by Eq. (4.18c) are supplemented.

The case where the plate speed $|U|$ is not small, i.e., $|U|/(2RT_0)^{1/2} = O(1)$, is analyzed for small k in Sone & Yamamoto [1970], where the nonlinear effect on the slip condition and the Knudsen layer appears in the second order of k. Other aspects of the Couette flow, mainly not related to the direct effect of the boundaries, are discussed in the monograph by Garzó & Santos [2003].

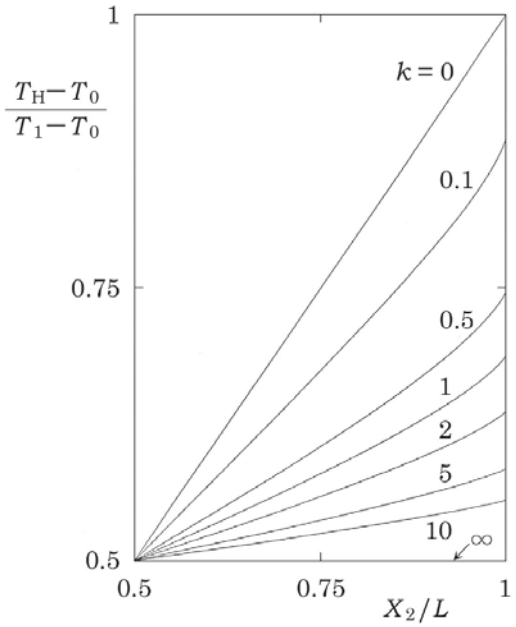

Figure 4.6. The temperature distribution, $(T_H - T_0)/(T_1 - T_0)$ vs X_2/L, in the heat-transfer problem between two parallel plane walls (a hard-sphere gas).

Table 4.1. Heat transfer, $q_{2H}/p_0(2RT_0)^{1/2}$ vs k, between the two parallel walls in the heat transfer problem (a hard-sphere gas). The data in parentheses are the results by the asymptotic theory, i.e., Eq. (4.18c).

k	$\dfrac{-2q_{2H}}{p_0(2RT_0)^{1/2}\left(\dfrac{T_1}{T_0}-1\right)}$		k	$\dfrac{-2q_{2H}}{p_0(2RT_0)^{1/2}\left(\dfrac{T_1}{T_0}-1\right)}$
0.033	0.1377	(0.1369)	5	1.046
0.1	0.3246	(0.3247)	6.310	1.061
0.1585	0.4329	(0.4326)	8	1.073
0.2512	0.5492	(0.5473)	10	1.083
0.3981	0.6637	(0.6572)	15.85	1.098
0.5	0.7170	(0.7067)	20	1.104
0.6310	0.7682	(0.7527)	25.12	1.109
1	0.8577	(0.8285)	40	1.116
1.585	0.9304		50	1.118
2	0.9609		63.10	1.120
2.512	0.9871		100	1.123
3.981	1.030		∞	1.128

4.2 Flows through a channel or pipe I: Straight pipe

4.2.1 Analysis by a similarity solution

Consider a gas in an infinitely long channel or pipe with a uniform cross section. The shape of the cross section may be arbitrary. Let the X_1 axis be parallel to the channel or pipe. The temperature T_w of the channel or pipe is given by

$$T_w = T_0 + \frac{\mathrm{d}T_w}{\mathrm{d}X_1} X_1,$$

where T_0 and $\mathrm{d}T_w/\mathrm{d}X_1$ are constants, and the gas is subject to a pressure gradient.[6] We assume that the temperature and pressure gradients are small, i.e.,

$$\frac{L}{T_0}\left|\frac{\mathrm{d}T_w}{\mathrm{d}X_1}\right| \ll 1, \qquad \frac{L}{p_0}\left|\frac{\mathrm{d}p}{\mathrm{d}X_1}\right| \ll 1, \tag{4.20}$$

where L is a characteristic size of the cross section and p_0 is a characteristic value of the pressure in the gas, and analyze the time-independent behavior of the gas on the basis of the linearized Boltzmann equation (1.96) introduced in Section 1.11.[7] As the boundary condition, we take the diffuse-reflection condition (1.105a) with (1.105b) for simplicity. Similar formulation can be carried out for the general boundary condition (1.107). Incidentally, the flow induced through a channel or pipe by a pressure gradient along it is called *Poiseuille flow* and the flow through a channel or pipe by a temperature gradient along it *thermal transpiration*.

With the notation introduced in Section 1.10, the linearized Boltzmann equation is given by

$$\zeta_i \frac{\partial \phi}{\partial x_i} = \frac{1}{k}\mathcal{L}(\phi), \tag{4.21}$$

and the diffuse-reflection condition on the channel or pipe surface is

$$\phi(x_i, \zeta_i) = \check{\sigma}_w + \left(\zeta_j^2 - \frac{3}{2}\right)\tau_w \qquad (\zeta_j n_j > 0), \tag{4.22a}$$

$$\check{\sigma}_w = -\frac{1}{2}\tau_w - 2\sqrt{\pi}\int_{\zeta_k n_k < 0} \zeta_j n_j \phi E \mathbf{d}\boldsymbol{\zeta}. \tag{4.22b}$$

[6] In contrast to the temperature distribution on the channel or pipe, we cannot impose the pressure gradient arbitrarily, though we can impose some pressure gradient. We will find that there is a solution that has a uniform pressure over a cross section and a uniform pressure gradient along the channel or pipe.

[7] (i) To be definite, the average pressure over the cross section at $X_1 = 0$ may be taken as the reference pressure p_0.

(ii) The pressure or temperature becomes infinite at infinity, however small the pressure or temperature gradient may be. From the discussion in Sections 4.2.3 and 4.3, the result in this section will be found to be valid locally [or up to $|X_1| = O(L)$] when the gradients are small, i.e., Eqs. (4.20) holds. When k is small, we have to be more careful to the use of the linearized equation [see Footnote 3 in Section 3.1.2 and Footnote 8 (ii) in Section 4.2.2].

In this subsection, τ_w is given by

$$\tau_w = (\mathrm{d}\tau_w/\mathrm{d}x_1)x_1, \quad \mathrm{d}\tau_w/\mathrm{d}x_1 : \text{ a constant},$$

and n_i is the unit normal vector to the channel or pipe surface, pointed to the gas region. Here n_1 is zero, i.e., $n_i = (0, n_2, n_3)$.

We put the solution ϕ in the form

$$\phi = x_1\Phi_0(\zeta, \zeta_2, \zeta_3) + \zeta_1\Phi_1(x_2, x_3, \zeta, \zeta_2, \zeta_3), \tag{4.23}$$

which is a similarity solution in Section A.5. Substituting Eq. (4.23) into the linearized Boltzmann equation (4.21) and the boundary condition (4.22a) with (4.22b), we have

$$\mathcal{L}(\Phi_0(\zeta, \zeta_2, \zeta_3)) = 0, \tag{4.24a}$$

$$\zeta_2\frac{\partial\Phi_1}{\partial x_2} + \zeta_3\frac{\partial\Phi_1}{\partial x_3} - \frac{1}{k\zeta_1}\mathcal{L}(\zeta_1\Phi_1) = -\Phi_0, \tag{4.24b}$$

and

$$\Phi_0 = \left(\zeta^2 - 2\right)\frac{\mathrm{d}\tau_w}{\mathrm{d}x_1} - 2\sqrt{\pi}\int_{\zeta_2 n_2 + \zeta_3 n_3 < 0}(\zeta_2 n_2 + \zeta_3 n_3)\Phi_0 E\mathbf{d\zeta} \qquad (\zeta_2 n_2 + \zeta_3 n_3 > 0), \tag{4.25a}$$

$$\Phi_1 = 0 \qquad (\zeta_2 n_2 + \zeta_3 n_3 > 0). \tag{4.25b}$$

It is easily seen that the function Φ_0 of the form

$$\Phi_0 = c_0 + \left(\zeta^2 - \frac{5}{2}\right)\frac{\mathrm{d}\tau_w}{\mathrm{d}x_1}, \tag{4.26}$$

where c_0 is an arbitrary constant, satisfies Eqs. (4.24a) and (4.25a).

The perturbed density ω, temperature τ, pressure P, and flow velocity u_i corresponding to the solution (4.23) with (4.26) are given as

$$\omega = \left(c_0 - \frac{\mathrm{d}\tau_w}{\mathrm{d}x_1}\right)x_1, \quad \tau = \frac{\mathrm{d}\tau_w}{\mathrm{d}x_1}x_1, \quad P = c_0 x_1, \tag{4.27a}$$

$$u_1 = \int \zeta_1^2\Phi_1 E\mathbf{d\zeta}, \quad u_2 = u_3 = 0. \tag{4.27b}$$

The density, temperature, and pressure are uniform over the cross section, and c_0 is

$$c_0 = \frac{\mathrm{d}P}{\mathrm{d}x_1} = \frac{L}{p_0}\frac{\mathrm{d}p}{\mathrm{d}X_1}.$$

With this relation, the solution Φ_0 is expressed as

$$\Phi_0 = \frac{L}{p_0}\frac{\mathrm{d}p}{\mathrm{d}X_1} + \left(\zeta^2 - \frac{5}{2}\right)\frac{L}{T_0}\frac{\mathrm{d}T_w}{\mathrm{d}X_1}. \tag{4.28}$$

The other solution Φ_1, the solution of Eq. (4.24b) with the inhomogeneous term (4.28), is expressed as

$$\Phi_1 = \left(\frac{L}{p_0}\frac{\mathrm{d}p}{\mathrm{d}X_1}\right)\Phi_{\mathrm{P}} + \left(\frac{L}{T_0}\frac{\mathrm{d}T_w}{\mathrm{d}X_1}\right)\Phi_{\mathrm{T}}, \tag{4.29}$$

where Φ_{P} and Φ_{T} are the solutions of the following two-dimensional inhomogeneous Boltzmann equations over the cross section:

$$\zeta_2\frac{\partial\Phi_{\mathrm{P}}}{\partial x_2} + \zeta_3\frac{\partial\Phi_{\mathrm{P}}}{\partial x_3} - \frac{1}{k\zeta_1}\mathcal{L}(\zeta_1\Phi_{\mathrm{P}}) = -1, \tag{4.30a}$$

$$\zeta_2\frac{\partial\Phi_{\mathrm{T}}}{\partial x_2} + \zeta_3\frac{\partial\Phi_{\mathrm{T}}}{\partial x_3} - \frac{1}{k\zeta_1}\mathcal{L}(\zeta_1\Phi_{\mathrm{T}}) = -\left(\zeta^2 - \frac{5}{2}\right), \tag{4.30b}$$

and the boundary condition

$$\Phi_{\mathrm{P}} = 0 \quad (\zeta_2 n_2 + \zeta_3 n_3 > 0), \tag{4.31a}$$

$$\Phi_{\mathrm{T}} = 0 \quad (\zeta_2 n_2 + \zeta_3 n_3 > 0), \tag{4.31b}$$

where the solutions Φ_{P} and Φ_{T} are functions of x_2, x_3, ζ_2, ζ_3, ζ, and k, and their functional forms are determined by the shape of the cross section. In the cases of a channel between two parallel plates and a circular pipe, the problem reduces to a spatially one-dimensional problem.

The flow velocity v_1 [$= (2RT_0)^{1/2}u_1$] and the heat flow q_1 [$= p_0(2RT_0)^{1/2}Q_1$] are expressed as

$$\frac{v_1}{(2RT_0)^{1/2}} = \left(\frac{L}{p_0}\frac{\mathrm{d}p}{\mathrm{d}X_1}\right)u_{\mathrm{P}} + \left(\frac{L}{T_0}\frac{\mathrm{d}T_w}{\mathrm{d}X_1}\right)u_{\mathrm{T}}, \tag{4.32a}$$

$$\frac{q_1}{p_0(2RT_0)^{1/2}} = \left(\frac{L}{p_0}\frac{\mathrm{d}p}{\mathrm{d}X_1}\right)Q_{\mathrm{P}} + \left(\frac{L}{T_0}\frac{\mathrm{d}T_w}{\mathrm{d}X_1}\right)Q_{\mathrm{T}}, \tag{4.32b}$$

where

$$u_{\mathrm{P}} = \int \zeta_1^2\Phi_{\mathrm{P}}E\mathbf{d\zeta}, \qquad u_{\mathrm{T}} = \int \zeta_1^2\Phi_{\mathrm{T}}E\mathbf{d\zeta}, \tag{4.33a}$$

$$Q_{\mathrm{P}} = \int \zeta_1^2\zeta^2\Phi_{\mathrm{P}}E\mathbf{d\zeta} - \frac{5}{2}u_{\mathrm{P}}, \qquad Q_{\mathrm{T}} = \int \zeta_1^2\zeta^2\Phi_{\mathrm{T}}E\mathbf{d\zeta} - \frac{5}{2}u_{\mathrm{T}}. \tag{4.33b}$$

The mass flow M per unit time (mass-flow rate) through the pipe defined by

$$M = \int_{\text{cross section}} \left(\int \xi_1 f\mathbf{d\xi}\right)\mathrm{d}X_2\mathrm{d}X_3$$

is expressed as follows:

$$\frac{M}{2p_0L^2/(2RT_0)^{1/2}} = \left(\frac{L}{p_0}\frac{\mathrm{d}p}{\mathrm{d}X_1}\right)\hat{M}_{\mathrm{P}} + \left(\frac{L}{T_0}\frac{\mathrm{d}T_w}{\mathrm{d}X_1}\right)\hat{M}_{\mathrm{T}}, \tag{4.34}$$

where

$$\hat{M}_{\mathrm{P}} = \int_S\int \zeta_1^2\Phi_{\mathrm{P}}E\mathbf{d\zeta}\mathrm{d}x_2\mathrm{d}x_3, \qquad \hat{M}_{\mathrm{T}} = \int_S\int \zeta_1^2\Phi_{\mathrm{T}}E\mathbf{d\zeta}\mathrm{d}x_2\mathrm{d}x_3, \tag{4.35}$$

with S representing the cross section in the nondimensional (x_2, x_3) space.

4.2.2 Example

As an example, consider the flow between two parallel plates, one at $X_2 = 0$ and the other at $X_2 = L$, where the state is uniform with respect to X_3. The problem is one-dimensional. The problem is to solve the following boundary-value problems of the inhomogeneous one-dimensional Boltzmann equation

$$\zeta_2 \frac{\partial \Phi_{\rm P}}{\partial x_2} - \frac{1}{k\zeta_1}\mathcal{L}(\zeta_1 \Phi_{\rm P}) = -1, \tag{4.36a}$$

$$\zeta_2 \frac{\partial \Phi_{\rm T}}{\partial x_2} - \frac{1}{k\zeta_1}\mathcal{L}(\zeta_1 \Phi_{\rm T}) = -\left(\zeta^2 - \frac{5}{2}\right), \tag{4.36b}$$

under the boundary conditions at $x_2 = 0$ and $x_2 = 1$

$$\Phi_{\rm P} = 0 \quad (\zeta_2 > 0 \ \text{ at } x_2 = 0 \ \text{ and } \zeta_2 < 0 \ \text{ at } x_2 = 1\ ), \tag{4.37a}$$

$$\Phi_{\rm T} = 0 \quad (\zeta_2 > 0 \ \text{ at } x_2 = 0 \ \text{ and } \zeta_2 < 0 \ \text{ at } x_2 = 1\ ). \tag{4.37b}$$

The flow velocity $v_1\,[= (2RT_0)^{1/2}u_1]$, the heat flow $q_1\,[= p_0(2RT_0)^{1/2}Q_1]$, and the mass flow M per unit time (or mass-flow rate) for unit width (in the X_3 direction) of the channel defined by $M = \int_0^L \left(\int \xi_1 f \mathbf{d\xi}\right) {\rm d}X_2$ are expressed as

$$\frac{v_1}{(2RT_0)^{1/2}} = \left(\frac{L}{p_0}\frac{{\rm d}p}{{\rm d}X_1}\right) u_{\rm P} + \left(\frac{L}{T_0}\frac{{\rm d}T_w}{{\rm d}X_1}\right) u_{\rm T}, \tag{4.38a}$$

$$\frac{q_1}{p_0(2RT_0)^{1/2}} = \left(\frac{L}{p_0}\frac{{\rm d}p}{{\rm d}X_1}\right) Q_{\rm P} + \left(\frac{L}{T_0}\frac{{\rm d}T_w}{{\rm d}X_1}\right) Q_{\rm T}, \tag{4.38b}$$

$$\frac{M}{2p_0L/(2RT_0)^{1/2}} = \left(\frac{L}{p_0}\frac{{\rm d}p}{{\rm d}X_1}\right) \hat{M}_{\rm P} + \left(\frac{L}{T_0}\frac{{\rm d}T_w}{{\rm d}X_1}\right) \hat{M}_{\rm T}, \tag{4.38c}$$

where

$$u_{\rm P} = \int \zeta_1^2 \Phi_{\rm P} E \mathbf{d\zeta}, \qquad u_{\rm T} = \int \zeta_1^2 \Phi_{\rm T} E \mathbf{d\zeta}, \tag{4.39a}$$

$$Q_{\rm P} = \int \zeta_1^2 \zeta^2 \Phi_{\rm P} E \mathbf{d\zeta} - \frac{5}{2} u_{\rm P}, \qquad Q_{\rm T} = \int \zeta_1^2 \zeta^2 \Phi_{\rm T} E \mathbf{d\zeta} - \frac{5}{2} u_{\rm T}, \tag{4.39b}$$

and $\hat{M}_{\rm P}$ and $\hat{M}_{\rm T}$, defined by Eq. (4.35), are modified as

$$\hat{M}_{\rm P} = \int_0^1 \int \zeta_1^2 \Phi_{\rm P} E \mathbf{d\zeta} {\rm d}x_2, \qquad \hat{M}_{\rm T} = \int_0^1 \int \zeta_1^2 \Phi_{\rm T} E \mathbf{d\zeta} {\rm d}x_2. \tag{4.40}$$

The solution for small Knudsen numbers (or $k \ll 1$) is easily obtained with the aid of the asymptotic theory discussed in Section 3.1. That is,

$$u_{\rm P} = -\frac{1}{2\gamma_1 k}\left\{x_2(1-x_2) - [k_0 + Y_0(\eta) + Y_0(\eta_-)]k \right. \\ \left. + 2[a_1 + Y_{a1}(\eta) + Y_{a1}(\eta_-)]k^2\right\}, \tag{4.41a}$$

$$Q_{\rm P} = -\frac{1}{2\gamma_1}\{H_A(\eta) + H_A(\eta_-) - [\gamma_3 + H_{A2}(\eta) + H_{A2}(\eta_-)]k\}, \tag{4.41b}$$

$$\hat{M}_{\rm P} = -\frac{1}{2\gamma_1 k}\left(\frac{1}{6} - k_0 k + 2(a_1 - 2b_1)k^2\right), \tag{4.41c}$$

and

$$u_{\rm T} = -\left(K_1 + \frac{1}{2}Y_1(\eta) + \frac{1}{2}Y_1(\eta_-)\right)k, \tag{4.42a}$$

$$Q_{\rm T} = -\left(\frac{5}{4}\gamma_2 - H_B(\eta) - H_B(\eta_-)\right)k, \tag{4.42b}$$

$$\hat{M}_{\rm T} = -(K_1 + 2b_2k)k. \tag{4.42c}$$

Here,

$$\eta = \frac{x_2}{k}, \quad \eta_- = \frac{1-x_2}{k};$$

the nondimensional viscosity γ_1, thermal conductivity γ_2, and thermal stress coefficient γ_3 are defined in Section 3.1.3; the slip coefficients k_0, K_1, a_1, b_1, and b_2 and the Knudsen-layer functions $Y_0(\eta)$, $Y_{a1}(\eta)$, $H_A(\eta)$, $Y_1(\eta)$, and $H_B(\eta)$ are defined in Section 3.1.5; and the function $H_{A2}(\eta)$ is the Knudsen-layer function related to $Q_{iK2}t_i$, which is determined by ϕ_{K2} (but is not shown explicitly) in Section 3.1.4. The solutions $\Phi_{\rm P}$ and $\Phi_{\rm T}$ for $k \ll 1$ on the basis of the asymptotic theory can be extended to any order of k by an argument similar to that in the Couette flow (Section 4.1).[8] The results (4.41a)–(4.41c) and (4.42a)–(4.42c) are the extended ones, which does not mean that the results are applicable to a finite Knudsen number, as noted in Section 4.1.

The asymptotic results for large Knudsen numbers (or $k \gg 1$) for the BKW model are obtained by Cercignani & Daneri [1963] for $\hat{M}_{\rm P}$ and by Niimi [1971] for $\hat{M}_{\rm T}$ as

$$\hat{M}_{\rm P} \sim -(2\sqrt{\pi})^{-1}\ln k, \tag{4.43a}$$

$$\hat{M}_{\rm T} \sim (4\sqrt{\pi})^{-1}(\ln k - 3\gamma_e/2 + 1/2), \tag{4.43b}$$

where γ_e $(= 0.57721\cdots)$ is the Euler constant. The logarithmic singularity in

[8] (i) The Grad–Hilbert solutions Φ_{PG} and Φ_{TG}, corresponding to Φ_{CG} or Φ_{HG} in Section 4.1, are taken as

$$\Phi_{PG} = \gamma_1^{-1}\{(x_2 - \tfrac{1}{2})^2k^{-1} - b(x_2 - \tfrac{1}{2})\zeta_2 B(\zeta) + [D_1(\zeta) + \zeta_2^2 D_2(\zeta)]k\} + c_0,$$
$$\Phi_{TG} = \bar{c}_0 - A(\zeta)k,$$

where b, c_0, and $\bar{c}_0$ are undetermined constants and $A(\zeta)$, $B(\zeta)$, $D_1(\zeta)$, and $D_2(\zeta)$ are introduced in Eq. (3.19). The Knudsen-layer corrections are made to Φ_{PG} and Φ_{TG}. The constants b, c_0, and $\bar{c}_0$ are determined together with the Knudsen-layer corrections.

(ii) The $u_{\rm P}$ diverges, i.e., $O(1/k)$, as $k \to 0$, that is, a flow is induced by a smaller pressure gradient by the order k, i.e., $(L/p_0)(\mathrm{d}p/\mathrm{d}X_1) = O(u_1k)$, which corresponds to Eq. (3.12). This difference of size should be noted in the heat flow due to temperature and pressure gradients. The coefficients of the temperature gradient and the pressure gradient for the heat flow outside the Knudsen layer are of the same order [see the γ_3 and γ_2 terms in Eqs. (4.41b) and (4.42b)], but the heat flow itself due to the pressure gradient is smaller by the order k than that due to the temperature gradient, because the pressure gradient is required to be smaller by the order k than other variables (see the discussion of the last paragraph of Section 3.6.2). Correspondingly, the contribution of H_{A2} reduces to the order of k^2.

(iii) See Footnote 3 in Section 3.1.2 for the condition on the size of $(L/p_0)(\mathrm{d}p/\mathrm{d}X_1)$ and $(L/T_0)(\mathrm{d}T_w/\mathrm{d}X_1)$ when $k \ll 1$ and the higher order terms of k are interested in.

the thermal transpiration for a hard-sphere gas is proved in Chen, Chen, Liu & Sone [2006].[9]

The numerical solution of the above system for a hard-sphere gas is obtained in Ohwada, Sone & Aoki [1989b]. The profiles of $u_{\rm P}$ and $Q_{\rm P}$ in the channel and $\hat{M}_{\rm P}$ vs k for the Poiseuille flow are shown, respectively, in Table 4.2, Fig. 4.7, and Table 4.3; the profiles of $u_{\rm T}$ and $Q_{\rm T}$ in the channel and $\hat{M}_{\rm T}$ vs k for the thermal transpiration in Table 4.4, Fig. 4.8, and Table 4.3. The nondimensional mass-flow rate $\hat{M}_{\rm P}$ of the Poiseuille flow takes the minimum value around $k = 0.8$, which is called *Knudsen minimum*. It may be noted that the heat flow is not zero ($Q_{\rm P} \neq 0$) in the gas with a uniform temperature.

The Poiseuille flow and thermal transpiration through a pipe are studied for various cross sections (Sone & Hasegawa [1987], Hasegawa & Sone [1988]; see Section 5.4.3 for a square cross section). A software that gives the flow profiles and mass-flow rates of the Poiseuille flow and thermal transpiration through a circular pipe or through a channel between parallel plates for BKW model immediately after inputting desired Knudsen numbers can be downloaded from http://fd.kuaero.kyoto-u.ac.jp/members/sone or http://www.users.kudpc.kyoto-u.ac.jp/~a51424/Sone/database-e.html (see Section B.3). The software is based on the data prepared by the modified Knudsen number expansion (see Section B.3). The counterpart of the Poiseuille flow or thermal transpiration through an infinitely long channel is the flow induced by pressure or temperature difference between two reservoirs joined by a slit (or infinitely short channel). These flows

[9]The free-molecular-flow solutions for $\Phi_{\rm P}$ and $\Phi_{\rm T}$, i.e., the solutions at $k = \infty$, can be easily obtained from Eqs. (4.36a)–(4.37b) as

$$\Phi_{\rm P} = -\zeta_2^{-1} x_2 \quad (\zeta_2 > 0), \qquad \Phi_{\rm P} = -\zeta_2^{-1}(x_2 - 1) \quad (\zeta_2 < 0),$$
$$\Phi_{\rm T} = -\zeta_2^{-1}(\zeta^2 - 5/2)x_2 \quad (\zeta_2 > 0), \quad \Phi_{\rm T} = -\zeta_2^{-1}(\zeta^2 - 5/2)(x_2 - 1) \quad (\zeta_2 < 0),$$

both of which have the nonintegrable singularity ζ_2^{-1} at $\zeta_2 = 0$. Owing to this singularity, $\hat{M}_{\rm P}$ and $\hat{M}_{\rm T}$ diverge. On the other hand, in the corresponding flow through a pipe, $\Phi_{\rm P}$ and $\Phi_{\rm T}$ have the integrable singularity $(\zeta_2^2 + \zeta_3^2)^{-1/2}$ at $(\zeta_2^2 + \zeta_3^2)^{1/2} = 0$ [see Eqs. (4.30a) and (4.30b)]. The difference between the two cases, the channel and the pipe, can be understood in the following way.

In the free molecular flows, the molecules reaching a point under consideration come from the channel or pipe wall or from infinity without collision with other molecules. The difference of states between the point (say, $x_1 = 0$) under consideration and the point at $x_1 = x_d$ is proportional to x_d (for example, the temperature difference). Thus, the average effect of a molecule coming from $x_1 = x_d$ is proportional to x_d. The number of molecules coming from the region $x_1 > x_d$ is proportional to the solid angle Ω_{x_d} viewing the portion of the channel or the pipe for $x_1 > x_d$, including infinity, from $x_1 = 0$; the angle Ω_{x_d} is proportional to $1/x_d$ for the channel and to $1/x_d^2$ for the pipe; and more molecules come from a long distance in the channel than in the pipe, because the side wall is absent for the channel. Thus, the effect of the molecules coming from the region $x_1 > x_d$ is proportional to

$$\int_{x_d}^{\infty} x_1 {\rm d}\Omega_{x_1}.$$

In view of the size of Ω_{x_d}, this diverges for the channel, but converges for the pipe.

The collision effect is not negligible for the molecules travelling for a long distance for large but finite Knudsen numbers, which is discussed in Section 2.6. As the combined effect of these contributions, the logarithmic singularity appears in $\hat{M}_{\rm P}$ and $\hat{M}_{\rm T}$ of the flow through the channel.

Table 4.2. The profiles of the nondimensional flow velocity u_{P} in the Poiseuille flow between two parallel plates (a hard-sphere gas).

	$-u_{\mathrm{P}}$				
X_2/L	$k = 0.1$	$k = 0.4$	$k = 1$	$k = 4$	$k = 10$
0	0.3784	0.4363	0.5129	0.6932	0.8530
0.0125	0.4843	0.4852			
0.025	0.5580	0.5196			
0.0375	0.6219	0.5489			
0.05	0.6800	0.5750	0.6123	0.7662	0.9179
0.1	0.8779	0.6602	0.6736	0.8121	0.9592
0.15	1.0404	0.7262	0.7205	0.8473	0.9909
0.2	1.1765	0.7792	0.7578	0.8752	1.0161
0.25	1.2895	0.8218	0.7876	0.8974	1.0362
0.3	1.3809	0.8555	0.8109	0.9149	1.0519
0.35	1.4515	0.8810	0.8285	0.9280	1.0637
0.4	1.5018	0.8990	0.8408	0.9371	1.0720
0.45	1.5318	0.9096	0.8481	0.9425	1.0768
0.5	1.5418	0.9132	0.8505	0.9443	1.0785

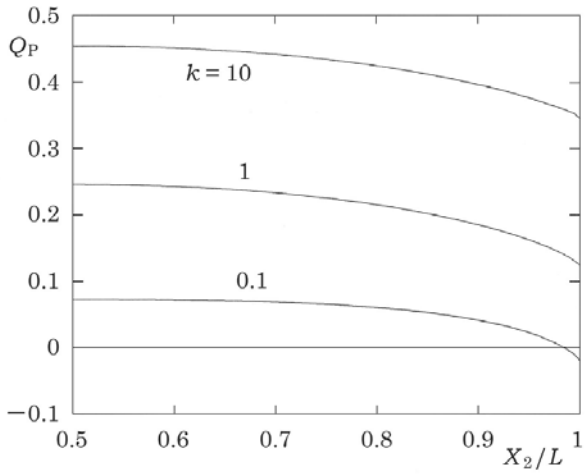

Figure 4.7. The profiles of the nondimensional heat flow Q_{P} in the Poiseuille flow between two parallel plates (a hard-sphere gas).

Table 4.3. Nondimensional mass-flow rates $\hat{M}_{\rm P}$ and $\hat{M}_{\rm T}$ (a hard-sphere gas). The data in parentheses are the results (4.41c) and (4.42c) by the asymptotic theory. The last term of $\hat{M}_{\rm P}$ [Eq. (4.41c)] is not included.

k	$-\hat{M}_{\rm P}$	$\hat{M}_{\rm T}$	k	$-\hat{M}_{\rm P}$	$\hat{M}_{\rm T}$
0.05	(1.8060)	(0.0299)	1	0.7574	0.2140
0.1	1.1930	0.0553	1.5	0.7771	0.2477
	(1.1498)	(0.0551)	2	0.7991	0.2724
0.15	0.9938	0.0761	3	0.8398	0.3082
	(0.9311)	(0.0755)	4	0.8749	0.3345
0.2	0.8999	0.0935	6	0.9321	0.3730
	(0.8218)	(0.0911)	8	0.9778	0.4015
0.3	0.8152	0.1209	10	1.0159	0.4242
0.4	0.7801	0.1419	15	1.0908	0.4669
0.6	0.7562	0.1730	20	1.1479	0.4984
0.8	0.7533	0.1958			

Table 4.4. The profiles of the nondimensional flow velocity $u_{\rm T}$ in the thermal transpiration between two parallel plates (a hard-sphere gas).

	$u_{\rm T}$				
X_2/L	$k=0.1$	$k=0.4$	$k=1$	$k=4$	$k=10$
0	0.0202	0.0719	0.1337	0.2542	0.3468
0.0125	0.0287	0.0836			
0.025	0.0337	0.0914			
0.0375	0.0375	0.0978			
0.05	0.0406	0.1034	0.1677	0.2869	0.3778
0.1	0.0490	0.1208	0.1878	0.3072	0.3974
0.15	0.0540	0.1334	0.2029	0.3226	0.4124
0.2	0.0573	0.1430	0.2146	0.3348	0.4243
0.25	0.0594	0.1504	0.2239	0.3445	0.4337
0.3	0.0609	0.1561	0.2310	0.3520	0.4411
0.35	0.0618	0.1603	0.2364	0.3577	0.4467
0.4	0.0624	0.1633	0.2401	0.3617	0.4506
0.45	0.0628	0.1650	0.2423	0.3640	0.4529
0.5	0.0629	0.1655	0.2430	0.3648	0.4536

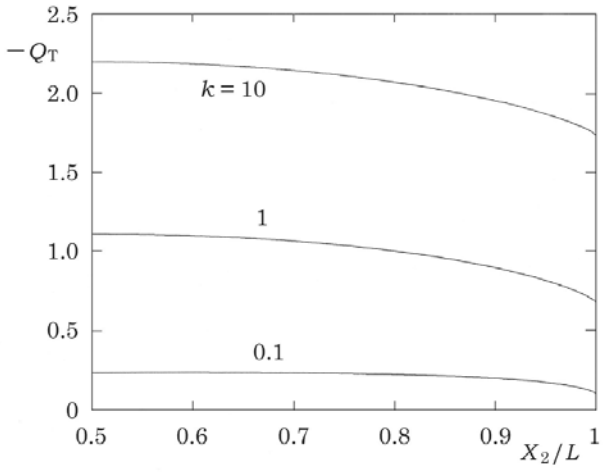

Figure 4.8. The profiles of the nondimensional heat flow Q_T in the thermal transpiration between two parallel plates (a hard-sphere gas).

are studied in Hasegawa & Sone [1991a,b].

4.2.3 Slowly varying approximation

The similarity solution can be applied locally to a more general case where the temperature or pressure gradient is not uniform along the pipe, if the state of the gas is slowly varying along the pipe (or with respect to x_1). In order to make this point clearer and to show the procedure to the higher-order analysis, we will analyze the flow through a straight pipe systematically for the slowly varying situation. The temperature T_w or τ_w of the pipe is assumed to depend only on x_1.

The state of the gas is assumed here to be slowly varying with respect to x_1, i.e., the length scale of variation in the X_1 direction is much larger than the characteristic size of the cross section. We introduce a shrunk variable χ_1

$$\chi_1 = \varepsilon x_1,$$

where ε is a small quantity ($0 < \varepsilon \ll 1$), e.g., $(L/T_w)|\mathrm{d}T_w/\mathrm{d}X_1|$ or $|\mathrm{d}\tau_w/\mathrm{d}x_1|$. Then, $\partial\phi/\partial\chi_1 = O(\phi)$. With the new variable, the linearized Boltzmann equation is rewritten as

$$\varepsilon\zeta_1\frac{\partial\phi}{\partial\chi_1}+\zeta_2\frac{\partial\phi}{\partial x_2}+\zeta_3\frac{\partial\phi}{\partial x_3} = \frac{1}{k}\mathcal{L}(\phi). \tag{4.44}$$

We look for the solution ϕ in a power series of ε, i.e.,

$$\phi = \phi_0(\chi_1, x_2, x_3, \zeta_i) + \phi_1(\chi_1, x_2, x_3, \zeta_i)\varepsilon + \cdots . \tag{4.45}$$

Substituting this series into Eq. (4.44) and arranging the same-order terms in ε, we have

$$\zeta_2\frac{\partial\phi_0}{\partial x_2}+\zeta_3\frac{\partial\phi_0}{\partial x_3}-\frac{1}{k}\mathcal{L}(\phi_0)=0, \tag{4.46a}$$

$$\zeta_2\frac{\partial\phi_1}{\partial x_2}+\zeta_3\frac{\partial\phi_1}{\partial x_3}-\frac{1}{k}\mathcal{L}(\phi_1)=-\zeta_1\frac{\partial\phi_0}{\partial\chi_1}. \tag{4.46b}$$

From the boundary condition (4.22a) with (4.22b) and the expansion (4.45),

$$\phi_0=\bar\sigma_{w0}+\left(\zeta_j^2-\frac{3}{2}\right)\bar\tau_w(\chi_1)\qquad(\zeta_2n_2+\zeta_3n_3>0), \tag{4.47a}$$

$$\bar\sigma_{w0}=-\frac{1}{2}\bar\tau_w-2\sqrt{\pi}\int_{\zeta_2n_2+\zeta_3n_3<0}(\zeta_2n_2+\zeta_3n_3)\phi_0E\mathbf{d}\boldsymbol{\zeta}, \tag{4.47b}$$

$$\phi_1=\bar\sigma_{w1}\qquad(\zeta_2n_2+\zeta_3n_3>0), \tag{4.48a}$$

$$\bar\sigma_{w1}=-2\sqrt{\pi}\int_{\zeta_2n_2+\zeta_3n_3<0}(\zeta_2n_2+\zeta_3n_3)\phi_1E\mathbf{d}\boldsymbol{\zeta}, \tag{4.48b}$$

where

$$\bar\tau_w(\chi_1)=\tau_w(x_1).$$

The boundary-value problem for ϕ_0, i.e., the system (4.46a), (4.47a), and (4.47b), has the following solution:[10]

$$\begin{aligned}\phi_0&=\left(\zeta_j^2-\frac{5}{2}\right)\bar\tau_w(\chi_1)+\bar C_0(\chi_1)\\&=\left(\zeta_j^2-\frac{5}{2}\right)\tau_w(x_1)+C_0(x_1),\end{aligned} \tag{4.49}$$

where $\bar C_0(\chi_1)$ is an arbitrary function of χ_1 and $C_0(x_1)=\bar C_0(\chi_1)$. The solution ϕ_0 agrees with $x_1\Phi_0$ in Eq. (4.23) with (4.26) through the correspondence $[\tau_w(x_1),C_0(x_1)]\iff[(\mathrm{d}\tau_w/\mathrm{d}x_1)x_1,\,c_0x_1]$.

With the above ϕ_0 in Eq. (4.46b), we have

$$\zeta_2\frac{\partial\phi_1}{\partial x_2}+\zeta_3\frac{\partial\phi_1}{\partial x_3}-\frac{1}{k}\mathcal{L}(\phi_1)=-\zeta_1\left[\left(\zeta_j^2-\frac{5}{2}\right)\frac{\mathrm{d}\bar\tau_w}{\mathrm{d}\chi_1}+\frac{\mathrm{d}\bar C_0}{\mathrm{d}\chi_1}\right]. \tag{4.50}$$

Putting ϕ_1 in the form

$$\phi_1=\zeta_1\Phi_1(\chi_1,x_2,x_3,\zeta_2,\zeta_3,\zeta), \tag{4.51}$$

and substituting Eq. (4.51) into Eqs. (4.50), (4.48a), and (4.48b), we obtain the equation and boundary condition for Φ_1, that is, the equation for Φ_1 is

$$\zeta_2\frac{\partial\Phi_1}{\partial x_2}+\zeta_3\frac{\partial\Phi_1}{\partial x_3}-\frac{1}{k\zeta_1}\mathcal{L}(\zeta_1\Phi_1)=-\left[\left(\zeta^2-\frac{5}{2}\right)\frac{\mathrm{d}\bar\tau_w}{\mathrm{d}\chi_1}+\frac{\mathrm{d}\bar C_0}{\mathrm{d}\chi_1}\right], \tag{4.52}$$

[10]The solution is shown to be unique in Section A.12. The proof is given for the three-dimensional problem. The proof is easily transferred to the one- and two-dimensional cases. The solution ϕ_1 as well as ϕ_0 is also unique. So is the solution in Section 4.1, etc.

and the boundary condition on the pipe is

$$\Phi_1 = 0 \quad (\zeta_2 n_2 + \zeta_3 n_3 > 0). \tag{4.53}$$

In the boundary-value problem, Eqs. (4.52) and (4.53), the variable χ_1 works as a parameter, and the problem is reduced to a two-dimensional problem over a cross section of the pipe. Comparing Eqs. (4.52) and (4.53) with Eqs. (4.24b), (4.25b), and (4.26), we find that the solution Φ_1 is expressed with $\Phi_{\rm P}$ and $\Phi_{\rm T}$ introduced in Section 4.2.1 as the solutions of Eq. (4.30a) with (4.31a) and Eq. (4.30b) with (4.31b) in the following form:

$$\Phi_1 = \varepsilon^{-1}\left(\frac{{\rm d}C_0}{{\rm d}x_1}\Phi_{\rm P} + \frac{{\rm d}\tau_w}{{\rm d}x_1}\Phi_{\rm T}\right). \tag{4.54}$$

The density, temperature, and pressure up to the order of ε are given by

$$\omega = \int \phi_0 E\mathbf{d}\boldsymbol{\zeta} = \bar{C}_0(\chi_1) - \bar{\tau}_w(\chi_1) = C_0(x_1) - \tau_w(x_1), \tag{4.55a}$$

$$\tau = \int \left(\frac{2}{3}\zeta^2 - 1\right)\phi_0 E\mathbf{d}\boldsymbol{\zeta} = \bar{\tau}_w(\chi_1) = \tau_w(x_1), \tag{4.55b}$$

$$P = \omega + \tau = \bar{C}_0(\chi_1) = C_0(x_1), \tag{4.55c}$$

because ϕ_1 is odd with respect to ζ_1. These variables are uniform over the cross section. The flow velocity u_i is given by

$$u_1 = \varepsilon\int \zeta_1^2\Phi_1 E\mathbf{d}\boldsymbol{\zeta} = \frac{{\rm d}P}{{\rm d}x_1}\int \zeta_1^2\Phi_{\rm P}E\mathbf{d}\boldsymbol{\zeta} + \frac{{\rm d}\tau_w}{{\rm d}x_1}\int \zeta_1^2\Phi_{\rm T}E\mathbf{d}\boldsymbol{\zeta}, \quad u_2 = u_3 = 0. \tag{4.56}$$

The solution $\phi_0 + \varepsilon\phi_1$ for arbitrary temperature and pressure distributions $\tau_w(x_1)$ and $C_0(x_1)$ is determined by the local temperature and pressure and their first derivatives. It is locally expressed with the similarity solution linear in x_1, i.e., $x_1\Phi_0 + \zeta_1\Phi_1$ in Eq. (4.23), discussed in Section 4.2.1.

We can control the temperature distribution along the pipe at our disposal, but the pressure in the gas is not such a quantity. We may impose the average pressure gradient, but cannot control the pressure locally. The variation of pressure along the pipe is determined by the solvability condition of the next-order equation. The equation and boundary condition for ϕ_2 are given by

$$\zeta_2\frac{\partial\phi_2}{\partial x_2} + \zeta_3\frac{\partial\phi_2}{\partial x_3} - \frac{1}{k}\mathcal{L}(\phi_2) = -\zeta_1\frac{\partial\phi_1}{\partial\chi_1}, \tag{4.57}$$

and

$$\phi_2 = \bar{\sigma}_{w2} \qquad (\zeta_2 n_2 + \zeta_3 n_3 > 0), \tag{4.58a}$$

$$\bar{\sigma}_{w2} = -2\sqrt{\pi}\int_{\zeta_2 n_2 + \zeta_3 n_3 < 0} (\zeta_2 n_2 + \zeta_3 n_3)\phi_2 E\mathbf{d}\boldsymbol{\zeta}. \tag{4.58b}$$

Multiplying Eq. (4.57) by E, integrating it over the whole space of $\boldsymbol{\zeta}$ and over a cross section S of the pipe, and noting Eq. (1.83), we have, with the aid of Gauss's divergence theorem,

$$-\int_{\partial S}\int(\zeta_2 n_2+\zeta_3 n_3)\phi_2 E\mathbf{d}\boldsymbol{\zeta}\mathrm{d}s=-\int_S\int\zeta_1\frac{\partial\phi_1}{\partial\chi_1}E\mathbf{d}\boldsymbol{\zeta}\mathrm{d}x_2\mathrm{d}x_3, \tag{4.59}$$

where ∂S is the boundary curve of the cross section S and $\mathrm{d}s$ is its line element of integration. From the boundary condition, i.e., Eqs. (4.58a) and (4.58b), the left-hand side of Eq. (4.59) vanishes. Thus, for Eq. (4.57) to have a solution ϕ_2, the solution ϕ_1 must satisfy the condition

$$\int_S\int\zeta_1\frac{\partial\phi_1}{\partial\chi_1}E\mathbf{d}\boldsymbol{\zeta}\mathrm{d}x_2\mathrm{d}x_3=0. \tag{4.60}$$

Substituting ϕ_1 given by Eqs. (4.51), (4.54), and (4.55c) into Eq. (4.60), we obtain

$$\hat{M}_{\mathrm{P}}\frac{\mathrm{d}P}{\mathrm{d}x_1}+\hat{M}_{\mathrm{T}}\frac{\mathrm{d}\tau_w}{\mathrm{d}x_1}=\mathrm{const}, \tag{4.61}$$

where $\hat{M}_{\mathrm{P}}$ and $\hat{M}_{\mathrm{T}}$ are defined by Eq. (4.35). This condition (4.61) corresponds to the conservation of mass-flow rate through the pipe.[11] That is, nonuniform mass-flow rate due to nonuniform temperature gradient is compensated by induction of the pressure gradient $\mathrm{d}P/\mathrm{d}x_1$ satisfying the condition (4.61).

4.3 Flow through a channel or pipe II: Quasi-unidirectional flow

In Section 4.2, the problem is analyzed on the basis of the linearized Boltzmann equation under the assumption that the state is close to an equilibrium state at rest, and further the analysis is limited to a straight pipe of a uniform cross section. Here, we will eliminate these restrictions. In this section we use the notation defined in Section 1.9. We consider a gas in a nearly straight channel or pipe (say, in the X_1 direction) under the assumptions: (i) the pipe surface is nearly parallel to the X_1 axis, and (ii) the state of the gas is slowly varying with respect to X_1. That is, let ε be a small quantity ($\varepsilon\ll 1$). Then, $\partial\hat{f}/\partial x_1=O(\varepsilon\hat{f})$, $n_1=O(\varepsilon)$, and $\partial n_i/\partial x_1=O(\varepsilon)$, where n_i is the unit normal vector to the pipe surface. This allows the case where the state of the gas, e.g., the temperature, pressure, and the size and direction[12] of the pipe may differ considerably between

[11] Without proceeding to the second-order analysis, we can simply obtain the condition (4.60) by applying the law of the conservation of mass. However, the condition should be derived naturally in the process of solving the Boltzmann equation. The present analysis is given to show this procedure. Now that we know the role of the conservation law in the process of the solution, we will use the law for simplicity of analysis in Section 4.3.

[12] The following analysis can be carried out in the same way and the same form of results is obtained when x_i (or X_i) is an orthogonal curvilinear coordinate system with small curvature $O(\varepsilon)$ and with the x_1 (or X_1) coordinate being the coordinate in the direction of the pipe (e.g., along the center of the cross section). See Footnote 13 in this section.

two points far apart. In the following discussion, we first analyze the case where the temperature T_w of the pipe depends only on X_1 and the pipe wall is at rest, and then extend the results to a case with weaker restrictions where T_w has a small variation along the circumference of the cross section and the pipe wall is making a time-independent nonuniform slow motion.

The basic equation is the Boltzmann equation (1.47a), i.e.,

$$\zeta_i \frac{\partial \hat{f}}{\partial x_i} = \frac{1}{k} \hat{J}(\hat{f}, \hat{f}), \tag{4.62}$$

and as the boundary condition, the diffuse-reflection condition, Eq. (1.63a) with (1.63b), is used for simplicity of explanation, i.e., on the pipe wall,

$$\hat{f}(x_i, \zeta_i) = \frac{\hat{\sigma}_w}{(\pi \hat{T}_w)^{3/2}} \exp\left(-\frac{(\zeta_i - \hat{v}_{wi})^2}{\hat{T}_w} \right) \qquad (\zeta_j n_j > 0), \tag{4.63a}$$

$$\hat{\sigma}_w = -2 \left(\frac{\pi}{\hat{T}_w} \right)^{1/2} \int_{\zeta_j n_j < 0} \zeta_j n_j \hat{f}(x_i, \zeta_i) \mathbf{d\zeta}. \tag{4.63b}$$

It is not difficult to extend the analysis to the more general condition (1.26) or (1.64). For the moment we leave the reference temperature T_0 and reference pressure p_0 unspecified.

First, the analysis is carried out under the assumptions that the temperature T_w of the pipe [or $\hat{T}_w$ in the boundary condition (4.63a) with (4.63b)] depends only on X_1 (or x_1) and that the pipe wall is at rest, i.e., $v_{wi} = 0$.

According to the slowly varying assumption, the same shrunk variable χ_1 as in Section 4.2.3, i.e.,

$$\chi_1 = \varepsilon x_1,$$

is used. We look for the solution in a power series of ε, i.e.,

$$\hat{f} = \hat{f}_0 + \hat{f}_1 \varepsilon + \cdots . \tag{4.64}$$

Here, $\hat{f}_0$ is assumed to be independent of x_2 and x_3 in view of the result in the preceding section. The analysis will be seen to be carried out consistently under this assumption. Substituting these expressions into Eq. (4.62) and arranging the same-order terms in ε, we have

$$\hat{J}(\hat{f}_0, \hat{f}_0) = 0, \tag{4.65}$$

$$\zeta_2 \frac{\partial \hat{f}_1}{\partial x_2} + \zeta_3 \frac{\partial \hat{f}_1}{\partial x_3} - \frac{2}{k} \hat{J}(\hat{f}_0, \hat{f}_1) = -\zeta_1 \frac{\partial \hat{f}_0}{\partial \chi_1}. \tag{4.66}$$

From Eq. (4.65), the leading term $\hat{f}_0$ is the Maxwellian uniform with respect to x_2 and x_3; the following Maxwellian $\hat{f}_0$ at rest with (nondimensional) temperature $\hat{T}_w(x_1)$ and pressure $\hat{\mathrm{p}}_0(x_1)$ satisfies the boundary condition (4.63a)

with (4.63b) and is the desired solution:[13]

$$\hat{f}_0 = \frac{\hat{\mathrm{p}}_0(x_1)}{\pi^{3/2}[\hat{T}_w(x_1)]^{5/2}} \exp\left(-\frac{{\zeta_i}^2}{\hat{T}_w(x_1)}\right), \tag{4.67}$$

where $\hat{\mathrm{p}}_0$ is defined as the leading-order component function of expansion of $\hat{p}$:

$$p = \mathrm{p}_0 + \mathrm{p}_1\varepsilon + \cdots, \qquad \hat{p} = p/p_0 = \hat{\mathrm{p}}_0 + \hat{\mathrm{p}}_1\varepsilon + \cdots.$$

With Eq. (4.67), the inhomogeneous term of Eq. (4.66) is expressed as

$$-\zeta_1 \frac{\partial \hat{f}_0}{\partial \chi_1} = -\zeta_1 \hat{f}_0 \left[\left(\frac{{\zeta_i}^2}{\hat{T}_w} - \frac{5}{2}\right)\frac{1}{\hat{T}_w}\frac{\mathrm{d}\hat{T}_w}{\mathrm{d}\chi_1} + \frac{1}{\hat{\mathrm{p}}_0}\frac{\mathrm{d}\hat{\mathrm{p}}_0}{\mathrm{d}\chi_1}\right]. \tag{4.68}$$

Substituting the expansion (4.64) into the boundary condition (4.63a) with (4.63b), and noting that $\hat{f}_0$ given by Eq. (4.67) satisfies Eq. (4.63a) with (4.63b) and that the first component n_1 of the normal vector to the boundary is of the order of ε, we have the boundary condition on $\hat{f}_1$ as

$$\hat{f}_1 = \frac{\hat{\sigma}_{w1}}{[\pi\hat{T}_w(x_1)]^{3/2}} \exp\left(-\frac{{\zeta_i}^2}{\hat{T}_w(x_1)}\right) \qquad (\zeta_2 n_2 + \zeta_3 n_3 > 0), \tag{4.69a}$$

$$\hat{\sigma}_{w1} = -2\left(\frac{\pi}{\hat{T}_w(x_1)}\right)^{1/2} \int_{\zeta_2 n_2 + \zeta_3 n_3 < 0} (\zeta_2 n_2 + \zeta_3 n_3)\hat{f}_1 \mathbf{d}\boldsymbol{\zeta}. \tag{4.69b}$$

In the boundary-value problem, Eqs. (4.66)–(4.69b), the variable χ_1 or x_1 works as a parameter and the problem for $\hat{f}_1$ is a two-dimensional boundary-value problem of the inhomogeneous linearized Boltzmann equation over a cross section of the pipe.[14] When the problem is considered on a cross section, we can conveniently choose $T_w(X_1)$ and $\mathrm{p}_0(X_1)$ as the reference temperature T_0 and the reference pressure p_0 respectively. This simplifies the expressions considerably, e.g., $\hat{f}_0 = E(\zeta)$ and $2\hat{J}(\hat{f}_0, \hat{f}_1) = E\mathcal{L}(\phi)$ with $\phi = \hat{f}_1/\hat{f}_0$. Noting that the inhomogeneous term (4.68) is odd in ζ_1 and that $2\hat{J}(\hat{f}_0, \hat{f}_1)$ $[= E\mathcal{L}(\phi)]$ is odd in ζ_1 if $\hat{f}_1$ is odd in ζ_1 [see Section A.2.7 about the parity of $\mathcal{L}(\phi)$], we can put $\hat{f}_1/\hat{f}_0$ consistently in the form

$$\hat{f}_1/\hat{f}_0 = \zeta_1 \Phi_1(\chi_1, x_2, x_3, \zeta, \zeta_2, \zeta_3). \tag{4.70}$$

[13] For the Maxwellian (4.67), the curvature contribution vanishes in the equation for $\hat{f}_1$ in the curvilinear system introduced in Footnote 12 in this section, and it is of the same form as Eq. (4.66).

[14] For analysis up to higher orders, we should use a curvilinear coordinate system with the pipe surface on a coordinate surface (and with a nearly straight coordinate corresponding to the X_1 axis). At the present order, the equation and boundary condition remain in the same form. At the higher orders, the treatment of the boundary condition, especially the range of integration, becomes obscure.

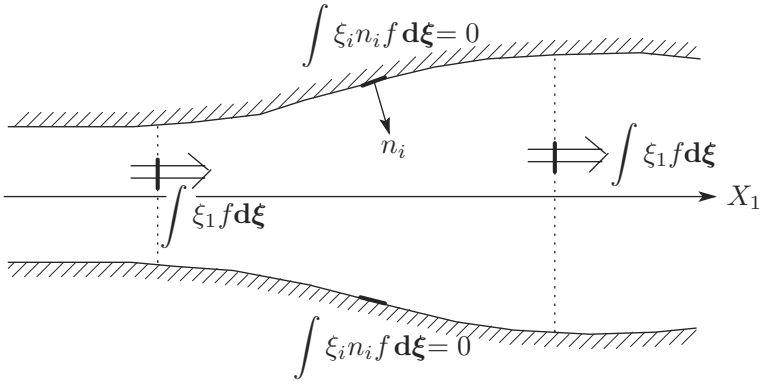

Figure 4.9. Conservation of mass. The law of the conservation of mass is applied to the control surface consisting of the dashed lines --- in the gas and the surface of the pipe between them.

Then, Eq. (4.66) and Eq. (4.69a) with (4.69b) are, respectively, reduced to

$$\zeta_2 \frac{\partial \Phi_1}{\partial x_2} + \zeta_3 \frac{\partial \Phi_1}{\partial x_3} - \frac{1}{k\zeta_1} \mathcal{L}(\zeta_1 \Phi_1) = -\varepsilon^{-1} \left[\left(\zeta^2 - \frac{5}{2} \right) \frac{L}{T_w} \frac{\mathrm{d}T_w}{\mathrm{d}X_1} + \frac{L}{\mathrm{p}_0} \frac{\mathrm{d}\mathrm{p}_0}{\mathrm{d}X_1} \right], \tag{4.71}$$

and

$$\Phi_1(\chi_1, x_2, x_3, \zeta, \zeta_2, \zeta_3) = 0 \quad (\zeta_2 n_2 + \zeta_3 n_3 > 0). \tag{4.72}$$

Comparing Eqs. (4.71) and (4.72) with Eqs. (4.52) and (4.53) and noting the solution (4.54) of the latter, we find that Φ_1 is expressed with Φ_P and Φ_T introduced in Section 4.2.1 as

$$\varepsilon \Phi_1 = \left(\frac{L}{\mathrm{p}_0(X_1)} \frac{\mathrm{d}\mathrm{p}_0(X_1)}{\mathrm{d}X_1} \right) \Phi_\mathrm{P} + \left(\frac{L}{T_w(X_1)} \frac{\mathrm{d}T_w(X_1)}{\mathrm{d}X_1} \right) \Phi_\mathrm{T}. \tag{4.73}$$

The solution $\hat{f}_0(1 + \zeta_1 \Phi_1 \varepsilon + \cdots)$ agrees, locally with respect to X_1, with the result of the linearized Boltzmann equation for a straight pipe up to the order of ε [or $(L/T_w)(\mathrm{d}T_w/\mathrm{d}X_1)$, $(L/\mathrm{p}_0)(\mathrm{d}\mathrm{p}_0/\mathrm{d}X_1)$].

In the analysis in Section 4.2.3, we saw that the solvability condition of the second-order equation corresponds to the conservation of mass. This condition adds a condition on the solution at the first order obtained. Here we examine the mass conservation condition instead of carrying out the second-order analysis, because the analysis is simpler.[15] Take a control surface consisting of two cross sections (two planes normal to the X_1 axis) and the pipe surface as shown in Fig. 4.9. There is no mass flow across the pipe surface. Therefore, the mass-flow rate through a cross section is invariant. That is,

$$\int_{\text{cross section}} \left(\int \xi_1 f \mathbf{d\xi} \right) \mathrm{d}X_2 \mathrm{d}X_3 = \text{const},$$

[15] See Footnote 11 in Section 4.2.3.

where the integration is carried out over the whole space of $\boldsymbol{\xi}$ and over a cross section. Accordingly,

$$\frac{2\mathrm{p}_0(X_1)L^2\varepsilon}{[2RT_w(X_1)]^{1/2}}\int_S\left(\int\zeta_1\hat{f}_1\mathbf{d\zeta}\right)\mathrm{d}x_2\mathrm{d}x_3=\text{const},$$

where S is the cross section in the (x_2,x_3) plane at X_1 under consideration. From Eqs. (4.70) and (4.73),

$$\varepsilon\int\zeta_1\hat{f}_1\mathbf{d\zeta}=\left(\frac{L}{\mathrm{p}_0}\frac{\mathrm{d}\mathrm{p}_0}{\mathrm{d}X_1}\right)\int\zeta_1^2\Phi_{\mathrm{P}}E\mathbf{d\zeta}+\left(\frac{L}{T_w}\frac{\mathrm{d}T_w}{\mathrm{d}X_1}\right)\int\zeta_1^2\Phi_{\mathrm{T}}E\mathbf{d\zeta}.$$

Therefore,

$$\left[\left(\frac{L}{\mathrm{p}_0}\frac{\mathrm{d}\mathrm{p}_0}{\mathrm{d}X_1}\right)\int_S\int\zeta_1^2\Phi_{\mathrm{P}}E\mathbf{d\zeta}\mathrm{d}x_2\mathrm{d}x_3+\left(\frac{L}{T_w}\frac{\mathrm{d}T_w}{\mathrm{d}X_1}\right)\int_S\int\zeta_1^2\Phi_{\mathrm{T}}E\mathbf{d\zeta}\mathrm{d}x_2\mathrm{d}x_3\right]$$
$$\times\frac{2\mathrm{p}_0(X_1)L^2}{[2RT_w(X_1)]^{1/2}}=\text{const}.$$

To summarize the results, the macroscopic variables, the temperature T, the pressure p, the velocity v_i, the heat-flow vector q_i, and the mass-flow rate M, (up to the order of ε) are expressed in the same form as those in Section 4.2.1, i.e.,

$$T(X_1)=T_w(X_1),\quad p(X_1)=\mathrm{p}_0(X_1),\tag{4.74}$$

where there is no contribution from $\hat{f}_1$, and

$$\frac{v_1}{(2RT_w)^{1/2}}=\left(\frac{L}{\mathrm{p}_0}\frac{\mathrm{d}\mathrm{p}_0}{\mathrm{d}X_1}\right)u_{\mathrm{P}}+\left(\frac{L}{T_w}\frac{\mathrm{d}T_w}{\mathrm{d}X_1}\right)u_{\mathrm{T}},\qquad v_2=v_3=0,\tag{4.75a}$$

$$\frac{q_1}{\mathrm{p}_0(2RT_w)^{1/2}}=\left(\frac{L}{\mathrm{p}_0}\frac{\mathrm{d}\mathrm{p}_0}{\mathrm{d}X_1}\right)Q_{\mathrm{P}}+\left(\frac{L}{T_w}\frac{\mathrm{d}T_w}{\mathrm{d}X_1}\right)Q_{\mathrm{T}},\quad q_2=q_3=0,\tag{4.75b}$$

$$\frac{M}{2\mathrm{p}_0L^2/(2RT_w)^{1/2}}=\left(\frac{L}{\mathrm{p}_0}\frac{\mathrm{d}\mathrm{p}_0}{\mathrm{d}X_1}\right)\hat{M}_{\mathrm{P}}+\left(\frac{L}{T_w}\frac{\mathrm{d}T_w}{\mathrm{d}X_1}\right)\hat{M}_{\mathrm{T}},\tag{4.75c}$$

where

$$u_{\mathrm{P}}=\int\zeta_1^2\Phi_{\mathrm{P}}E\mathbf{d\zeta},\qquad u_{\mathrm{T}}=\int\zeta_1^2\Phi_{\mathrm{T}}E\mathbf{d\zeta},\tag{4.76a}$$

$$Q_{\mathrm{P}}=\int\zeta_1^2\zeta^2\Phi_{\mathrm{P}}E\mathbf{d\zeta}-\frac{5}{2}u_{\mathrm{P}},\qquad Q_{\mathrm{T}}=\int\zeta_1^2\zeta^2\Phi_{\mathrm{T}}E\mathbf{d\zeta}-\frac{5}{2}u_{\mathrm{T}},\tag{4.76b}$$

$$\hat{M}_{\mathrm{P}}=\int_S\int\zeta_1^2\Phi_{\mathrm{P}}E\mathbf{d\zeta}\mathrm{d}x_2\mathrm{d}x_3,\qquad \hat{M}_{\mathrm{T}}=\int_S\int\zeta_1^2\Phi_{\mathrm{T}}E\mathbf{d\zeta}\mathrm{d}x_2\mathrm{d}x_3,\tag{4.76c}$$

and the subsidiary condition

$$\frac{2\mathrm{p}_0(X_1)L^2}{[2RT_w(X_1)]^{1/2}}\left[\left(\frac{L}{\mathrm{p}_0}\frac{\mathrm{d}\mathrm{p}_0}{\mathrm{d}X_1}\right)\hat{M}_{\mathrm{P}}+\left(\frac{L}{T_w}\frac{\mathrm{d}T_w}{\mathrm{d}X_1}\right)\hat{M}_{\mathrm{T}}\right]=\text{const}.\tag{4.77}$$

Apparently, the formulas are the same as those in Section 4.2.1, but some care is required about the reference quantities. In the transformation from Eq. (4.66) to Eq. (4.71) [or more directly to Eqs. (4.30a) and (4.30b)], the local variables $T_w(X_1)$ and $\mathrm{p}_0(X_1)$ are chosen as the reference T_0 and p_0. The reference L may be chosen universally or locally. The Knudsen number or k that appears in Eqs. (4.30a) and (4.30b) and thus in Φ_{P} and Φ_{T} is a local quantity with respect to X_1.

Up to this point, we have considered the case where the temperature of the pipe or channel is uniform along the circumference of each cross section, i.e., T_w is a function of X_1 only, and the pipe is at rest, i.e., $v_{wi} = 0$. We will slightly loosen this restriction. Let the surface of the channel or pipe be moving with slowly varying time-independent small velocity tangent to the surface, i.e., $\hat{v}_{wi}\,[= v_{wi}/(2RT_0)^{1/2}] = O(\varepsilon)$, $\partial\hat{v}_{wi}/\partial x_1 = O(\varepsilon\hat{v}_{wi})$, $\partial\hat{v}_{wi}/\partial\hat{t} = 0$, and $\hat{v}_{wi}n_i = 0$, and let the temperature $T_w(X_1)$ [or $T_0\hat{T}_w(x_1)$] of the pipe be slightly generalized as $T_w(X_1)[1+\tau_w(x_i)]$ (or $T_0\hat{T}_w(x_1)[1+\tau_w(x_i)]$), where $\tau_w = O(\varepsilon)$ and $\partial\tau_w/\partial x_1 = O(\varepsilon\tau_w)$. According to Eq. (1.63a) with (1.63b), the boundary condition (4.63a) with (4.63b) is modified as

$$\hat{f} = \frac{\hat{\sigma}_w}{[\pi\hat{T}_w(1+\tau_w)]^{3/2}} \exp\left(-\frac{(\zeta_i - \hat{v}_{wi})^2}{\hat{T}_w(1+\tau_w)}\right) \qquad (\zeta_j n_j > 0), \tag{4.78a}$$

$$\hat{\sigma}_w = -2\left(\frac{\pi}{\hat{T}_w(1+\tau_w)}\right)^{1/2} \int_{\zeta_j n_j<0} \zeta_j n_j \hat{f}(x_i,\zeta_i)\mathbf{d}\boldsymbol{\zeta}. \tag{4.78b}$$

Put the solution $\hat{f}$ in the form with a correction $\hat{f}_{\mathrm{C}}$

$$\hat{f} = \hat{f}_0 + \varepsilon\hat{f}_1 + \varepsilon\hat{f}_{\mathrm{C}} + \cdots, \tag{4.79a}$$

$$\varepsilon\hat{f}_{\mathrm{C}} = \hat{f}_0(\zeta_1\varphi_a + \varphi_b), \tag{4.79b}$$

where $\hat{f}_0$ and $\varepsilon\hat{f}_1$ are the solutions obtained previously [i.e., Eqs. (4.67), (4.70), and (4.73)], and φ_a and φ_b are even functions in ζ_1. Substituting this form of solution into Eqs. (4.62), (4.78a), and (4.78b), noting that $\hat{f}_0 + \varepsilon\hat{f}_1$ satisfies Eqs. (4.62), (4.78a), and (4.78b) with $\hat{v}_{wi} = 0$ and $\tau_w = 0$ up to the order of ε, and arranging the same-order terms in ε, we obtain the two independent systems for φ_a and φ_b. They are the two-dimensional boundary-value problems of the linearized Boltzmann equation on each cross section, where the variable χ_1 or x_1 works as a parameter. Thus, we take the local quantities $T_w(X_1)$ and $\mathrm{p}_0(X_1)$ as the reference temperature and pressure respectively. Then, the systems are given as follows: The equation for φ_a is

$$\zeta_2\frac{\partial\varphi_a}{\partial x_2} + \zeta_3\frac{\partial\varphi_a}{\partial x_3} - \frac{1}{k\zeta_1}\mathcal{L}(\zeta_1\varphi_a) = 0, \tag{4.80}$$

and its boundary condition on the pipe is

$$\varphi_a = 2\hat{v}_{w1}(x_1,x_2,x_3) \qquad (\zeta_2 n_2 + \zeta_3 n_3 > 0), \tag{4.81}$$

and the equation for φ_b is

$$\zeta_2 \frac{\partial \varphi_b}{\partial x_2} + \zeta_3 \frac{\partial \varphi_b}{\partial x_3} - \frac{1}{k}\mathcal{L}(\varphi_b) = 0, \tag{4.82}$$

and its boundary condition is

$$\varphi_b = \varpi_b + 2(\zeta_2 \hat{v}_{w2} + \zeta_3 \hat{v}_{w3}) + ({\zeta_i}^2 - 2)\tau_w \quad (\zeta_2 n_2 + \zeta_3 n_3 > 0), \tag{4.83a}$$

$$\varpi_b = -2\sqrt{\pi} \int_{\zeta_2 n_2 + \zeta_3 n_3 < 0} (\zeta_2 n_2 + \zeta_3 n_3)\varphi_b E(\zeta) \mathbf{d}\boldsymbol{\zeta}. \tag{4.83b}$$

The corrections $v_{1\mathrm{C}}$, $q_{1\mathrm{C}}$, and M_{C} to the velocity v_1, the heat-flow vector q_1, and the mass-flow rate M are determined only by φ_a as

$$\frac{v_{1\mathrm{C}}}{(2RT_w)^{1/2}} = \int \zeta_1^2 \varphi_a E \mathbf{d}\boldsymbol{\zeta}, \tag{4.84a}$$

$$\frac{q_{1\mathrm{C}}}{\mathrm{p}_0 (2RT_w)^{1/2}} = \int \zeta_1^2 \left(\zeta^2 - \frac{5}{2}\right) \varphi_a E \mathbf{d}\boldsymbol{\zeta}, \tag{4.84b}$$

$$\frac{M_{\mathrm{C}}}{2\mathrm{p}_0 L^2/(2RT_w)^{1/2}} = \int_S \int \zeta_1^2 \varphi_a E \mathbf{d}\boldsymbol{\zeta} \mathrm{d}x_2 \mathrm{d}x_3. \tag{4.84c}$$

The above quantities are to be added to Eqs. (4.75a)–(4.75c). The subsidiary condition (4.77) is modified as

$$\frac{2\mathrm{p}_0(X_1)L^2}{[2RT_w(X_1)]^{1/2}} \left[\left(\frac{L}{\mathrm{p}_0} \frac{\mathrm{d}\mathrm{p}_0}{\mathrm{d}X_1} \right) \hat{M}_{\mathrm{P}} + \left(\frac{L}{T_w} \frac{\mathrm{d}T_w}{\mathrm{d}X_1} \right) \hat{M}_{\mathrm{T}} + \hat{M}_{\mathrm{C}} \right] = \mathrm{const}, \tag{4.85}$$

where

$$\hat{M}_{\mathrm{C}} = \frac{M_{\mathrm{C}}}{2\mathrm{p}_0 L^2/(2RT_w)^{1/2}}.$$

The flow field (v_2, v_3) and the corrections to the temperature $T(X_1)$ $[= T_w(X_1)]$ and the pressure $p(X_1)$ $[= \mathrm{p}_0(X_1)]$ in a cross section are determined by φ_b. Let the temperature and the pressure on a cross section be $T_w(X_1)(1 + \tau)$ and $\mathrm{p}_0(X_1)(1 + P)$, respectively. Then, v_2, v_3, τ, and P are expressed with φ_b as

$$\frac{v_i}{(2RT_w)^{1/2}} = \int \zeta_i \varphi_b E \mathbf{d}\boldsymbol{\zeta} \quad (i = 2 \text{ and } 3),$$

$$\tau = \int \left(\frac{2}{3}\zeta^2 - 1 \right) \varphi_b E \mathbf{d}\boldsymbol{\zeta}, \quad P = \frac{2}{3} \int \zeta^2 \varphi_b E \mathbf{d}\boldsymbol{\zeta}.$$

Naturally, the temperature and pressure are no longer uniform over a cross section. It may be repeated that the slowly varying restriction on $\hat{v}_{wi}$ and τ_w that $\partial \hat{v}_{wi}/\partial x_1 = O(\varepsilon \hat{v}_{wi})$ and $\partial \tau_w/\partial x_1 = O(\varepsilon \tau_w)$ is required for the extended analysis to be valid.

From the analysis in this section, it is clear that the results by the similarity solutions of the Poiseuille flow and thermal transpiration in Section 4.2.1 and

those of the Couette-flow and heat-transfer problems in Section 4.1 have universal importance.[16] The rarefied-gas problems corresponding to the *lubrication* problems discussed in classical fluid dynamics (Sommerfeld [1964]), which has important applications in micro flows,[17] e.g., design of the system of a magnetic disk and sliders, can be discussed by simple application of the result in this section with the data in Sections 4.1 and 4.2.

Finally, we should make a comment on the behavior for small Knudsen numbers or small k. We have seen that the asymptotic behavior for small Knudsen numbers depends on the other parameters in Chapter 3 (see, especially, Section 3.6.1). In the present section, the analysis for small ε is carried out for a given finite k. When we are interested in the asymptotic behavior for small ε and k, their relative size is important. An interesting related example is given in Chapter 9. The small ε represents the scale characterizing the deviation of the nearly straight channel or pipe from a straight one as well as the scale of the (nondimensional) temperature or pressure gradient or $\hat{v}_{wi}$. The latter three are related to the scale of the flow speed $|\hat{v}_1|$.[18] Consider the former size separately and let it be $\bar{\varepsilon}$. Take the product of the reference curvature and the reference width of the boundary as $\bar{\varepsilon}$. In Chapter 9, a nearly parallel flow through a channel is considered and its behavior is investigated in the limit that $\bar{\varepsilon}$ and k tend to zero simultaneously with ε, the order of $\hat{v}_1$, fixed.[19] This concerns with flows of a gas in the continuum limit through a straight channel. The limiting behavior depends on the speed that $\bar{\varepsilon}$ vanishes relative to k. When $\bar{\varepsilon}$ tends to zero not faster than the order of $(k/\varepsilon)^2$, the limiting behavior depends on the infinitesimal curvature of the boundary. That is, the infinitesimal curvature produces a finite effect on the parallel flow. Thus, the limiting behavior for $k \to 0$ requires careful examination. One often refers to the continuum limit loosely in real situations, but careful classification should be done according to the data of the situations (see Section 3.6.2).

4.4 Gas over a plane wall

Concerning the behavior of a semi-infinite expanse of a gas bounded by a plane wall (a half-space problem), the following uniqueness statement is strangely unknown, and incorrect discussion is sometimes made. It may be in order to give its proof.

Consider semi-infinite expanse of a gas ($X_1 > 0$) bounded by a stationary plane wall with a uniform temperature T_w at $X_1 = 0$. There is no external force acting on the gas. The state of the gas is time-independent and uniform with

[16] Some engineers do not like the similarity solution because it is unbounded or it is the solution of the linearized equation.

[17] In a system whose characteristic size L is of the order of micron or smaller (but much larger than the molecular size), the mean free path is not negligible compared with L in the atmospheric condition. Thus, the kinetic theory analysis is required.

[18] As $k \to 0$, $|\hat{v}_1|$ is not of the order of the temperature or pressure gradient [see Section 4.2.2, including Footnote 8 (ii) and (iii) there].

[19] For simplicity, consider the case where $\hat{v}_{wi} = O(\varepsilon)$ (see the preceding Footnote 18).

respect to X_2 and X_3, i.e., $f = f(X_1, \boldsymbol{\xi})$, and it approaches an equilibrium state as $X_1 \to \infty$, i.e.,

$$f \to \frac{\rho_\infty}{(2\pi RT_\infty)^{3/2}} \exp\left(-\frac{(\xi_i - v_{i\infty})^2}{2RT_\infty}\right) \quad \text{as } X_1 \to \infty, \tag{4.86}$$

where ρ_∞, $v_{i\infty}$, and T_∞ are bounded. The plane wall is a simple boundary where the boundary condition is given by Eq. (1.26) with the conditions (1.27a)–(1.27c), i.e.,

$$f(0, \boldsymbol{\xi}) = \int_{\xi_{1*}<0} K_B(\boldsymbol{\xi}, \boldsymbol{\xi}_*) f(0, \boldsymbol{\xi}_*) \mathbf{d}\boldsymbol{\xi}_* \quad (\xi_1 > 0). \tag{4.87}$$

We will show[20] that the solution of the Boltzmann equation (1.5), i.e.,

$$\xi_1 \frac{\partial f}{\partial X_1} = J(f, f), \tag{4.88}$$

describing the above situation exists only when

$$v_{i\infty} = 0, \quad T_\infty = T_w,$$

and that the solution is uniquely given by the Maxwellian

$$f = \frac{\rho_\infty}{(2\pi RT_w)^{3/2}} \exp\left(-\frac{\xi_i^2}{2RT_w}\right). \tag{4.89}$$

From the integral of the Boltzmann equation (4.88) over the whole space of $\boldsymbol{\xi}$ [or the conservation equation (1.12)], i.e.,

$$\frac{\mathrm{d}}{\mathrm{d}X_1}\left(\int \xi_1 f \mathbf{d}\boldsymbol{\xi}\right) = 0,$$

and the condition ($\rho v_1 = \int \xi_1 f \mathbf{d}\boldsymbol{\xi} = 0$ at $X_1 = 0$) of a simple boundary that the mass flux through the boundary vanishes, we find that the mass flux vanishes for $X_1 \geq 0$, i.e.,

$$\int \xi_1 f \mathbf{d}\boldsymbol{\xi} = 0 \quad (0 \leq X_1 < \infty). \tag{4.90}$$

With this result in the condition (4.86) at infinity, it is easily found that

$$\int \xi_1 \xi_i^2 f \mathbf{d}\boldsymbol{\xi} = 0 \quad \text{at infinity.} \tag{4.91}$$

The integral of the Boltzmann equation (4.88) multiplied by ξ_j^2 over the whole space of $\boldsymbol{\xi}$ [or the conservation equation (1.14)] gives

$$\frac{\mathrm{d}}{\mathrm{d}X_1}\left(\int \xi_1 \xi_j^2 f \mathbf{d}\boldsymbol{\xi}\right) = 0. \tag{4.92}$$

[20] This is an extension of Golse's proof in Bardos, Golse & Sone [2006] for a similar problem under the complete-condensation condition. He proved the same statement for the complete-condensation condition on the plane wall and a Maxwellian with $v_1 = 0$ at infinity.

Thus, from Eqs. (4.91) and (4.92), we have

$$\int \xi_1 \xi_j^2 f \mathbf{d\xi} = 0 \quad (0 \le X_1 < \infty). \tag{4.93}$$

For the boundary condition (1.26) with the conditions (1.27a)–(1.27c), the following inequality (Darrozes & Guiraud [1966]) holds at $X_1 = 0$ [Eq. (A.262) in Section A.10]:

$$\int \xi_1 f \ln(f/c_0) \mathbf{d\xi} \le \int \xi_1 f \ln(f_0/c_0) \mathbf{d\xi}, \tag{4.94}$$

where f_0 is a Maxwellian with the temperature T_w and the velocity v_{wi} $(= 0)$ of the wall and an arbitrary density ρ_0, i.e.,

$$f_0 = \frac{\rho_0}{(2\pi R T_w)^{3/2}} \exp\left(-\frac{\xi_i^2}{2RT_w}\right),$$

and c_0 is a constant to make f/c_0 and f_0/c_0 in the argument of the $\ln(*)$ function dimensionless whose choice does not influence the result. With the aid of Eqs. (4.90) and (4.93),

$$\begin{aligned} \int \xi_1 f \ln(f/c_0) \mathbf{d\xi} &\le \int \xi_1 f \ln(f_0/c_0) \mathbf{d\xi} \\ &= -\frac{1}{2RT_w} \int \xi_1 \xi_i^2 f \mathbf{d\xi} = 0 \quad \text{at } X_1 = 0. \end{aligned} \tag{4.95}$$

On the other hand, from the H theorem, i.e., Eq. (1.36), in a time-independent one-dimensional case,

$$-\int \xi_1 f \ln(f/c_0) \mathbf{d\xi}\Big|_{X_1=0} + \int \xi_1 f \ln(f/c_0) \mathbf{d\xi}\Big|_{X_1=\infty} = \int_0^\infty G \mathrm{d}X_1 \le 0, \tag{4.96}$$

where

$$G = -\frac{1}{4m} \int (f' f_*' - f f_*) \ln\left(\frac{f' f_*'}{f f_*}\right) B \mathrm{d}\Omega \mathbf{d\xi}_* \mathbf{d\xi} \le 0.$$

From Eqs. (4.86), (4.90), and (4.91), the second term on the left-hand side of Eq. (4.96) vanishes, that is,

$$-\int \xi_1 f \ln(f/c_0) \mathbf{d\xi}\Big|_{X_1=0} = \int_0^\infty G \mathrm{d}X_1 \le 0. \tag{4.97}$$

Combining the two inequalities (4.95) and (4.97), we have

$$0 \le -\int \xi_1 f \ln(f/c_0) \mathbf{d\xi}\Big|_{X_1=0} = \int_0^\infty G \mathrm{d}X_1 \le 0.$$

Therefore, we have

$$\int_0^\infty G \mathrm{d}X_1 = 0, \tag{4.98}$$

and

$$\int \xi_1 f \ln(f/c_0)\mathbf{d}\boldsymbol{\xi}\Big|_{X_1=0} = 0.$$

From Eq. (4.98), f is Maxwellian in $0 < X_1 < \infty$, and Eq. (4.88) is reduced to $\xi_1 \partial f/\partial X_1 = 0$. That is, f is a uniform Maxwellian. From the condition (4.86) at infinity and Eq. (4.90),

$$f = \frac{\rho_\infty}{(2\pi R T_\infty)^{3/2}} \exp\left(-\frac{\xi_1^2 + (\xi_2 - v_{2\infty})^2 + (\xi_3 - v_{3\infty})^2}{2RT_\infty}\right) \quad (0 < X_1 < \infty).$$

From the condition (1.27c) with its note,

$$v_{2\infty} = v_{3\infty} = 0, \quad T_w = T_\infty.$$

Thus, the solution should be in the form (4.89), which is really a solution.

The same statement holds for the linearized Boltzmann equation with the corresponding general boundary condition (A.252) on a simple boundary. The temperature T_w of the wall and the density ρ_∞ at infinity being, respectively, taken as the reference temperature T_0 or $\tau_w = 0$ and the reference density ρ_0 or $\omega_\infty = 0$, the linearized Boltzmann equation is given in the form

$$\zeta_1 \frac{\partial \phi}{\partial \eta} = \mathcal{L}(\phi) \quad (0 < \eta < \infty), \tag{4.99}$$

and the boundary condition is expressed in the scattering kernel $\hat{K}_{B0}$

$$E(\zeta)\phi(\eta, \boldsymbol{\zeta}) = \int_{\zeta_{1*}<0} \hat{K}_{B0}(\boldsymbol{\zeta}, \boldsymbol{\zeta}_*)\phi(\eta, \boldsymbol{\zeta}_*)E(\zeta_*)\mathbf{d}\boldsymbol{\zeta}_* \quad (\zeta_1 > 0) \quad \text{at } \eta = 0, \tag{4.100a}$$

$$\phi(\eta, \boldsymbol{\zeta}) \to 2\zeta_i u_{i\infty} + \left(\zeta_i^2 - \frac{3}{2}\right)\tau_\infty \quad \text{as } \eta \to \infty, \tag{4.100b}$$

where $u_{i\infty}$ and τ_∞ are some constants and $\eta = x_1/k$ $(= 2X_1/\sqrt{\pi}\ell_0)$. Then, the solution of the boundary-value problem (4.99)–(4.100b) exists when and only when

$$u_{i\infty} = 0 \text{ and } \tau_\infty = 0,$$

and the unique solution is given by

$$\phi = 0.$$

The proof can be given in the same way as the preceding proof for the nonlinear case on the basis of the three relations: one is the equality

$$\int \zeta_1 \phi^2 E \mathbf{d}\boldsymbol{\zeta} = 0 \quad \text{at infinity},$$

which is derived from the conservation equation (1.99), the condition of a simple boundary ($u_1 = \int \zeta_1 \phi E \mathbf{d\zeta} = 0$ at $\eta = 0$), and the boundary condition (4.100b) at infinity; the second is the inequality

$$\int \zeta_1 \phi^2 E \mathbf{d\zeta} \le 0 \quad \text{at } \eta = 0, \tag{4.101}$$

which is proved in the second part of Section A.10; and the third is the linearized-Boltzmann-equation version of the equation for the H function given by Eq. (1.115), i.e.,

$$\frac{\partial}{\partial \eta} \int \zeta_1 \phi^2 E \mathbf{d\zeta} = LG, \tag{4.102}$$

where

$$LG = -\frac{1}{2} \int E E_* (\phi' + \phi'_* - \phi - \phi_*)^2 \widehat{B} \mathrm{d}\Omega \mathbf{d\zeta}_* \mathbf{d\zeta} \le 0.$$

4.5 Uniform flow past a sphere with a uniform temperature

Consider a uniform flow of a gas with density ρ_0, flow velocity $(U, 0, 0)$, and temperature T_0 past a sphere of radius L with a uniform surface temperature T_0, that is, the behavior of a gas disturbed by the sphere from the uniform flow, i.e., the Maxwellian with the above macroscopic variables. Taking the case where the flow is slow, i.e., $U/(2RT_0)^{1/2} \ll 1$, we analyze the time-independent behavior of the gas on the basis of the linearized Boltzmann equation and the diffuse-reflection boundary condition (see Section 1.11). We use the notation in Section 1.10, with L, ρ_0, and T_0 as the reference quantities, and the spherical coordinates

$$x_1 = \hat{r} \cos\theta, \ x_2 = \hat{r} \sin\theta \cos\varphi, \ x_3 = \hat{r} \sin\theta \sin\varphi,$$

where the origin is at the center of the sphere. The linearized Boltzmann equation for the perturbed velocity distribution function ϕ in the spherical coordinates for a time-independent axially symmetric state [Eq. (A.164) in Section A.3)] is

$$\begin{aligned} &\zeta_r \frac{\partial \phi}{\partial \hat{r}} + \frac{\zeta_\theta}{\hat{r}} \frac{\partial \phi}{\partial \theta} + \frac{\zeta_\theta^2 + \zeta_\varphi^2}{\hat{r}} \frac{\partial \phi}{\partial \zeta_r} + \left(\frac{\zeta_\varphi^2}{\hat{r}} \cot\theta - \frac{\zeta_r \zeta_\theta}{\hat{r}} \right) \frac{\partial \phi}{\partial \zeta_\theta} \\ &- \left(\frac{\zeta_\theta \zeta_\varphi}{\hat{r}} \cot\theta + \frac{\zeta_r \zeta_\varphi}{\hat{r}} \right) \frac{\partial \phi}{\partial \zeta_\varphi} - \frac{1}{k} \mathcal{L}(\phi) = 0. \end{aligned} \tag{4.103}$$

The diffuse-reflection condition on the sphere is

$$\phi = -2\sqrt{\pi} \int_{\zeta_r < 0} \zeta_r \phi E \mathbf{d\zeta} \quad (\zeta_r > 0) \quad \text{at } \hat{r} = 1, \tag{4.104}$$

and the condition at infinity, or the Maxwellian state, is

$$\phi = 2U(2RT_0)^{-1/2}\zeta_1 = 2U(2RT_0)^{-1/2}(\zeta_r\cos\theta - \zeta_\theta\sin\theta) \quad \text{as } \hat{r}\to\infty. \tag{4.105}$$

In view of the boundary conditions (4.104) and (4.105), the similarity solution (A.205) in Section A.5 can be applied. We put the solution in the form[21]

$$\phi = U(2RT_0)^{-1/2}[\Phi_c(\hat{r},\zeta_r,\zeta)\cos\theta + \zeta_\theta\Phi_s(\hat{r},\zeta_r,\zeta)\sin\theta]. \tag{4.106}$$

Then, Eq. (4.103) is reduced to the equations that do not include the θ variable

$$D_c(\Phi_c,\Phi_s) = \frac{1}{k}F_c, \qquad D_s(\Phi_c,\Phi_s) = \frac{1}{k}F_s, \tag{4.107}$$

where

$$D_c(\Phi_c,\Phi_s) = \zeta_r\frac{\partial\Phi_c}{\partial\hat{r}} + \frac{\zeta^2-\zeta_r^2}{\hat{r}}\frac{\partial\Phi_c}{\partial\zeta_r} + \frac{\zeta^2-\zeta_r^2}{\hat{r}}\Phi_s, \tag{4.108a}$$

$$D_s(\Phi_c,\Phi_s) = \zeta_r\frac{\partial\Phi_s}{\partial\hat{r}} + \frac{\zeta^2-\zeta_r^2}{\hat{r}}\frac{\partial\Phi_s}{\partial\zeta_r} - \frac{\zeta_r}{\hat{r}}\Phi_s - \frac{1}{\hat{r}}\Phi_c, \tag{4.108b}$$

and

$$F_c(\hat{r},\zeta_r,\zeta) = \mathcal{L}(\Phi_c), \qquad \zeta_\theta F_s(\hat{r},\zeta_r,\zeta) = \mathcal{L}(\zeta_\theta\Phi_s). \tag{4.109}$$

The boundary condition (4.104) is reduced to[22]

$$\Phi_c = -2\sqrt{\pi}\int_{\zeta_r<0}\zeta_r\Phi_c E\mathbf{d\zeta}, \quad \Phi_s = 0 \quad (\zeta_r>0) \ \text{ at } \hat{r}=1, \tag{4.110}$$

and the condition (4.105) is reduced to

$$\Phi_c \to 2\zeta_r, \quad \Phi_s\to -2 \quad \text{as } \hat{r}\to\infty. \tag{4.111}$$

The problem is reduced, without approximation, to a spatially one-dimensional one.

[21] The velocity distribution function ϕ around a sphere has discontinuities (see Fig. 3.1). Its discontinuities are on the cone $\zeta_r/\zeta = (\hat{r}^2-1)^{1/2}/\hat{r}$ $(\zeta_r>0)$, which is independent of θ in the present variables. The form of ϕ given by Eq. (4.106) is compatible with the discontinuities at the above position. In fact, the above discontinuities are on the characteristic of Eq. (4.107) for Φ_c and Φ_s.

[22] For a function f of ζ_r and ζ, like Φ_c, it is convenient to introduce the spherical coordinate expression $(\zeta,\theta_\zeta,\psi)$ for $\boldsymbol{\zeta}$ with the $\hat{r}$ direction (the radial direction) as its polar direction, i.e.,

$$\zeta_r = \zeta\cos\theta_\zeta,\ \zeta_\theta = \zeta\sin\theta_\zeta\cos\psi,\ \zeta_\varphi = \zeta\sin\theta_\zeta\sin\psi$$
$$(0\le\zeta<\infty,\ 0\le\theta_\zeta\le\pi,\ 0\le\psi<2\pi).$$

In these variables, $f(\zeta_r,\zeta)\mathbf{d\zeta} = f(\zeta\cos\theta_\zeta,\zeta)\zeta^2\sin\theta_\zeta\mathrm{d}\zeta\mathrm{d}\theta_\zeta\mathrm{d}\psi$.
(i) The intuitive image is simpler for such a velocity distribution function.
(ii) In carrying out the integral of $f(\zeta_r,\zeta)$ with respect to $\boldsymbol{\zeta}$ for $\zeta_r \lessgtr 0$ or the whole space, the three-dimensional integral is reduced to a two-dimensional one. For example,

$$\int_{\zeta_r<0} f(\zeta_r,\zeta)\mathbf{d\zeta} = 2\pi\int_0^\infty\int_{\pi/2}^\pi f(\zeta\cos\theta_\zeta,\zeta)\zeta^2\sin\theta_\zeta\mathrm{d}\theta_\zeta\mathrm{d}\zeta.$$

As shown in Section A.5, the macroscopic variables, i.e., density ρ, flow velocity $(v_r, v_\theta, v_\varphi)$, temperature T, etc., have a simple dependence on θ, i.e.,

$$\frac{\rho-\rho_0}{\rho_0\cos\theta},\quad \frac{v_r}{(2RT_0)^{1/2}\cos\theta},\quad \frac{v_\theta}{(2RT_0)^{1/2}\sin\theta},\quad \frac{T-T_0}{T_0\cos\theta},$$
$$\frac{p_{rr}-p_0}{p_0\cos\theta},\quad \frac{p_{r\theta}}{p_0\sin\theta},\quad \frac{p_{\theta\theta}-p_0}{p_0\cos\theta},\quad \frac{p_{\varphi\varphi}-p_0}{p_0\cos\theta},$$
$$\frac{q_r}{p_0(2RT_0)^{1/2}\cos\theta},\quad \frac{q_\theta}{p_0(2RT_0)^{1/2}\sin\theta}$$

are independent of θ, and $v_\varphi = p_{r\varphi} = p_{\theta\varphi} = q_\varphi = 0$.[23]

For small Knudsen numbers ($k \ll 1$), we can make use of the asymptotic theory explained in Section 3.1.[24] According to it,[25]

$$\frac{\rho-\rho_0}{U(2RT_0)^{-1/2}\rho_0\cos\theta} = -\frac{3\gamma_1}{2}\frac{k}{\hat r^2} + \left[-\left(\frac{3\gamma_1 k_0}{2}+6d_4\right)\frac{1}{\hat r^2}+6\Omega_4(\eta)\right]k^2+\cdots, \tag{4.112a}$$

$$\frac{v_r}{U\cos\theta} = 1-\frac{1}{2}\left(\frac{3}{\hat r}-\frac{1}{\hat r^3}\right)-\frac{3k_0}{2}\left(\frac{1}{\hat r}-\frac{1}{\hat r^3}\right)k + \left(2A_{\rm d}\frac{1}{\hat r}+2B_{\rm d}\frac{1}{\hat r^3}-3\int_\infty^\eta Y_0(\eta_0)\mathrm{d}\eta_0\right)k^2+\cdots, \tag{4.112b}$$

$$\frac{v_\theta}{U\sin\theta} = -1+\frac{1}{4}\left(\frac{3}{\hat r}+\frac{1}{\hat r^3}\right)+\frac{3}{4}\left[k_0\left(\frac{1}{\hat r}+\frac{1}{\hat r^3}\right)+2Y_0(\eta)\right]k + \left(-A_{\rm d}\frac{1}{\hat r}+B_{\rm d}\frac{1}{\hat r^3}+Y_{\rm d}(\eta)\right)k^2+\cdots, \tag{4.112c}$$

$$\frac{T-T_0}{U(2RT_0)^{-1/2}T_0\cos\theta} = 6\left(\frac{d_4}{\hat r^2}+\Theta_4(\eta)\right)k^2+\cdots, \tag{4.112d}$$

$$\frac{p-p_0}{U(2RT_0)^{-1/2}p_0\cos\theta} = -\frac{3\gamma_1}{2}\frac{k}{\hat r^2}\left(1+k_0k-\frac{4}{3}A_{\rm d}k^2\right)+6[\Omega_4(\eta)+\Theta_4(\eta)]k^2+\cdots, \tag{4.112e}$$

$$\frac{q_r}{p_0U\cos\theta} = \left(\frac{3\gamma_3}{2\hat r^3}+3\int_\infty^\eta H_A(\eta_0)\mathrm{d}\eta_0\right)k^2+\cdots, \tag{4.112f}$$

$$A_{\rm d} = -\tfrac{1}{4}\left(9k_0^2-12a_1+3a_2+3a_3+6b_1\right),$$
$$B_{\rm d} = \tfrac{1}{4}\left(9k_0^2-12a_1+3a_2+3a_3-6b_1\right),$$
$$Y_{\rm d}(\eta) = \tfrac{1}{2}[9k_0Y_0(\eta)-12Y_{a1}(\eta)+3Y_{a2}(\eta)+3Y_{a3}(\eta)],$$
$$\eta = (\hat r-1)/k.$$

[23] The symbols v_r, ..., p_{rr}, $p_{r\theta}$, ..., q_r, ... are the corresponding spherical components of v_i, p_{ij}, and q_i. That is, their relations to the velocity distribution function are given by Eqs. (1.2b), (1.2f), and (1.2g) with the subscript i or j being replaced by r, θ, or φ.

[24] See Footnote 3 in Section 3.1.2.

[25] As noted in Section 3.1.6, the macroscopic variables except v_r and q_r are subject to the S-layer correction at the order of k^2 at the bottom of the Knudsen layer or in the neighborhood $\eta = O(k)$ of the boundary.

Here, the nondimensional transport coefficients γ_1 and γ_3 are defined in Section 3.1.3; the slip coefficients k_0, d_4, a_1, a_2, a_3, and b_1 and the Knudsen-layer functions $\Omega_4(\eta)$, $Y_0(\eta)$, $\Theta_4(\eta)$, $H_A(\eta)$, $Y_{a1}(\eta)$, $Y_{a2}(\eta)$, and $Y_{a3}(\eta)$ are introduced in Section 3.1.5; the fluid-dynamic part of p is given up to the order of k^3 to obtain the force acting on the sphere in harmony with the other variables;[26] and $q_r/p_0U\cos\theta$ is shown because it is important in Section 4.6. With the aid of the discussion of Section 3.1.7, the force F_i acting on the sphere is obtained from these macroscopic variables as

$$\frac{F_1}{p_0UL^2/(2RT_0)^{1/2}} = 6\pi\gamma_1 k\left(1 + k_0 k - \frac{4}{3}A_{\rm d}k^2 + \cdots\right), \quad F_2 = F_3 = 0. \tag{4.113}$$

For the free molecular case ($k = \infty$), the solution ϕ (or Φ_c and Φ_s) is easily obtained by the simple recipe given in Section 2.3.2 as

$$\Phi_c = \begin{cases} 2\zeta\cos\theta_\zeta & [\mathrm{Arcsin}(1/\hat{r}) < \theta_\zeta \le \pi], \\ -\sqrt{\pi}[\cos\theta_\zeta(1-\hat{r}^2\sin^2\theta_\zeta)^{1/2} + \hat{r}\sin^2\theta_\zeta] & \\ \qquad\qquad [0 \le \theta_\zeta < \mathrm{Arcsin}(1/\hat{r})], & \end{cases} \tag{4.114a}$$

$$\Phi_s = \begin{cases} -2 & [\mathrm{Arcsin}(1/\hat{r}) < \theta_\zeta \le \pi], \\ -\sqrt{\pi}\zeta^{-1}[\hat{r}\cos\theta_\zeta - (1-\hat{r}^2\sin^2\theta_\zeta)^{1/2}] & \\ \qquad\qquad [0 \le \theta_\zeta < \mathrm{Arcsin}(1/\hat{r})], & \end{cases} \tag{4.114b}$$

where $\theta_\zeta = \mathrm{Arccos}(\zeta_r/\zeta)$, from which the macroscopic variables are obtained as

$$\frac{\rho-\rho_0}{U(2RT_0)^{-1/2}\rho_0\cos\theta} = -\frac{\sqrt{\pi}}{6}\left[\left(1+\frac{6}{\pi}\right)\frac{1}{\hat{r}^2} + 2\hat{r} - \left(2\hat{r}+\frac{1}{\hat{r}}\right)\left(1-\frac{1}{\hat{r}^2}\right)^{1/2}\right], \tag{4.115a}$$

$$\frac{v_r}{U\cos\theta} = \frac{1}{8}\left[3 - \frac{1}{\hat{r}^2} - \frac{2}{\hat{r}^3} + 4\left(1-\frac{1}{\hat{r}^2}\right)^{3/2} + \frac{\hat{r}}{2}\left(1-\frac{1}{\hat{r}^2}\right)^2\ln\frac{\hat{r}+1}{\hat{r}-1}\right], \tag{4.115b}$$

$$\frac{v_\theta}{U\sin\theta} = -\frac{1}{16}\left[5 + \frac{1}{\hat{r}^2} + \frac{2}{\hat{r}^3} + 8\left(1-\frac{1}{\hat{r}^2}\right)^{1/2}\left(1+\frac{1}{2\hat{r}^2}\right) + \frac{\hat{r}}{2}\left(3+\frac{1}{\hat{r}^2}\right)\left(1-\frac{1}{\hat{r}^2}\right)\ln\frac{\hat{r}+1}{\hat{r}-1}\right], \tag{4.115c}$$

$$\frac{T-T_0}{U(2RT_0)^{-1/2}T_0\cos\theta} = -\frac{1}{3\sqrt{\pi}\hat{r}^2}, \tag{4.115d}$$

$$\frac{q_r}{p_0U\cos\theta} = \frac{1}{16}\left[1 + \frac{1}{\hat{r}^2} + \frac{2}{\hat{r}^3} - \frac{\hat{r}}{2}\left(1-\frac{1}{\hat{r}^2}\right)^2\ln\frac{\hat{r}+1}{\hat{r}-1}\right]. \tag{4.115e}$$

[26] From the argument in Section 3.1.7 and the formulas of stress tensor in Section 3.1.3, we can obtain the force on a closed body up to the order of k^3 of the nondimensional force F_i/p_0L^2 with the additional information P_{G3}. The Knudsen-layer part P_{K3}, which does not contribute to the force, is not shown in Eq. (4.112e).

Especially, q_r at $\hat{r} = 1$, which is important to construct the solution of a uniform flow past a sphere with an arbitrary thermal conductivity in Section 4.6, is

$$\frac{q_r}{p_0 U \cos\theta} = \frac{1}{4}. \tag{4.116}$$

The force F_i acting on the sphere is

$$\frac{F_1}{p_0 U L^2/(2RT_0)^{1/2}} = \frac{2}{3}\sqrt{\pi}(\pi + 8), \quad F_2 = F_3 = 0. \tag{4.117}$$

The boundary-value problem for Φ_c and Φ_s is solved numerically for a hard-sphere gas in Takata, Sone & Aoki [1993]. The density, temperature, and velocity profiles are shown for $k = 0.1$, 1, and 10 in Figs. 4.10 and 4.11 (see the paper for more detailed data). The force F_i [$= (F_1, 0, 0)$] acting on the sphere is obtained from p_{rr} and $p_{r\theta}$. The result, i.e., F_1 vs k, is shown in Fig. 4.12 and tabulated as $F_1^{(\mathrm{d})}$ later (in Section 4.6.3) in Table 4.5. The free molecular solution ($k = \infty$) and the asymptotic solution for $k = 0$ or small k of a hard-sphere gas are also shown in Figs. 4.10–4.12. In the numerical computation, the discontinuity in the velocity distribution function, explained in Section 3.1.6, should be taken into account.[27] The behavior of the discontinuity, as well as other more detailed data, is shown in the above-mentioned paper.[28]

It may be noted that the temperature is not uniform except for the case $k = 0$ [Fig. 4.10(b) and Eq. (4.112d)]. In a rarefied gas ($k \neq 0$), the temperature is related to the velocity even in the linear theory. In classical fluid dynamics, the slow motion of the gas does not produce any effect on the temperature field. In a rarefied gas, a nonuniform temperature field is induced by a slow motion of the gas [thermal polarization; see the paragraph next to that of Eq. (3.48)].

We have discussed the case where the temperature of the sphere is kept at the same temperature as T_0 at infinity. When the surface temperature is kept at a uniform temperature T_w [$= T_0(1 + \tau_w)$] different from T_0, the solution can be obtained simply by the superposition of the above result and that of a uniformly heated (or cooled) sphere in the gas at rest. That is, let ϕ_{d} be the solution ϕ of the problem discussed in this section, and let ϕ_{h} be the solution ϕ of the problem where the sphere with the temperature $T_0(1 + \tau_w)$ lies in a gas at rest with temperature T_0 and density ρ_0. Then, the desired solution is given by $\phi_{\mathrm{d}} + \phi_{\mathrm{h}}$. The solution ϕ_{h} being spherically symmetric, the flow velocity and the force on the sphere are those given by ϕ_{d}. The numerical solution ϕ_{h} for a hard-sphere gas is found in Takata, Sone, Lhuillier & Wakabayashi [1998].

The corresponding problems where the sphere is made of the condensed phase of the gas and condensation or evaporation is taking place on the surface of the sphere are studied in Sone, Takata & Wakabayashi [1994] and Takata,

[27] The method of numerical computation in a similar situation, where the velocity distribution function has a discontinuity, is outlined in Section 6.2.2 (see the original paper for the details and also Sone, Ohwada & Aoki [1989a] and Ohwada, Sone & Aoki [1989a] for the computation of the linearized collision integral).

[28] Examples of the velocity distribution function with a discontinuity are given for more interesting situations in Sections 6.2, 6.3, and 6.4.

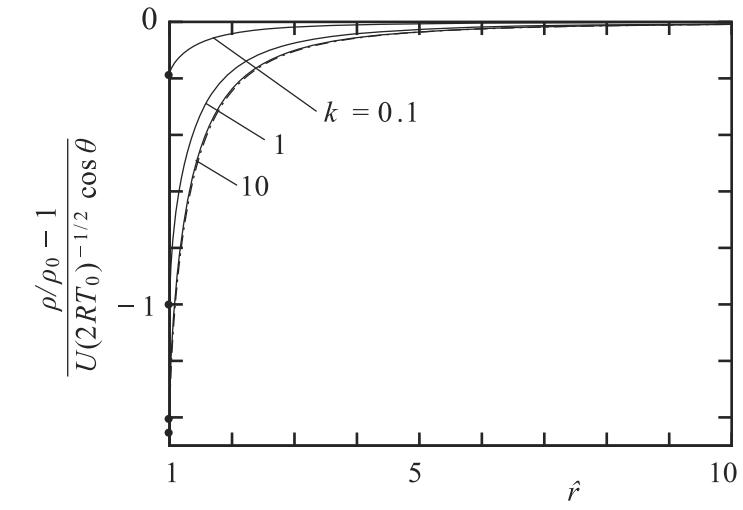

(a)

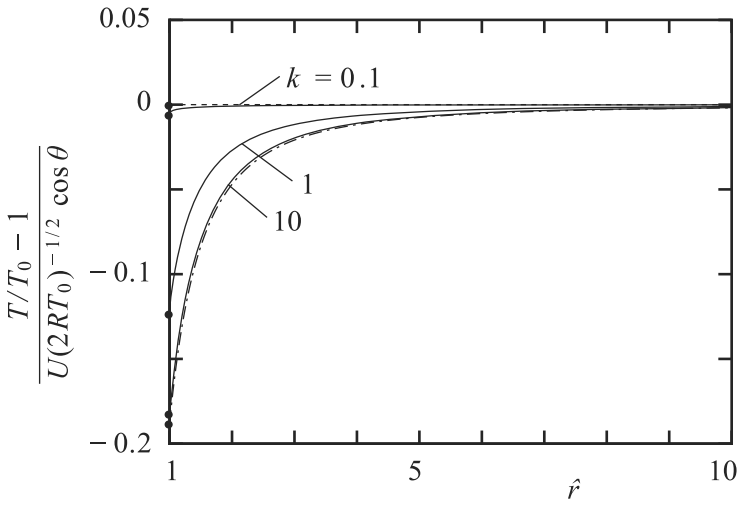

(b)

Figure 4.10. The density and temperature profiles in a uniform flow past a sphere with a uniform temperature (a hard-sphere gas). (a) $(\rho/\rho_0 - 1)/U(2RT_0)^{-1/2}\cos\theta$ vs $\hat{r}$ $(= r/L)$ and (b) $(T/T_0 - 1)/U(2RT_0)^{-1/2}\cos\theta$ vs $\hat{r}$. The solid lines —— are the numerical solution and the black circles • indicate the values on the sphere. The dashed line – – – is the asymptotic solution (4.112a) or (4.112d) with $k = 0$, the former of which coincides with the thick upper frame and is invisible, and the dot-dash lines –·– are the free molecular solution (4.115a) or (4.115d).

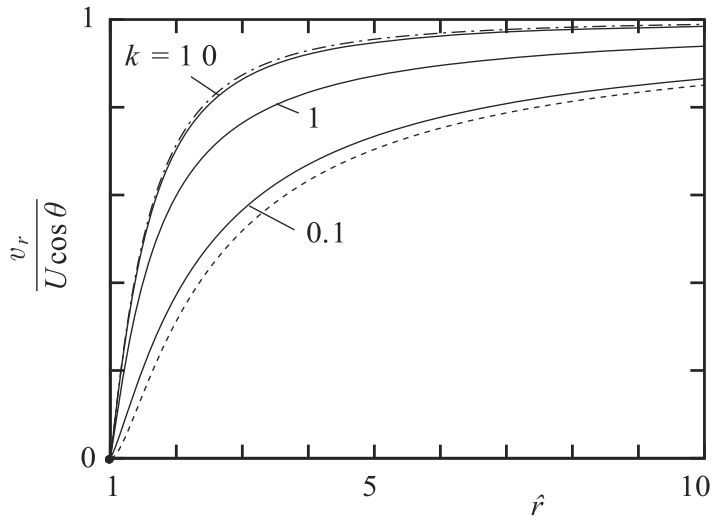

(a)

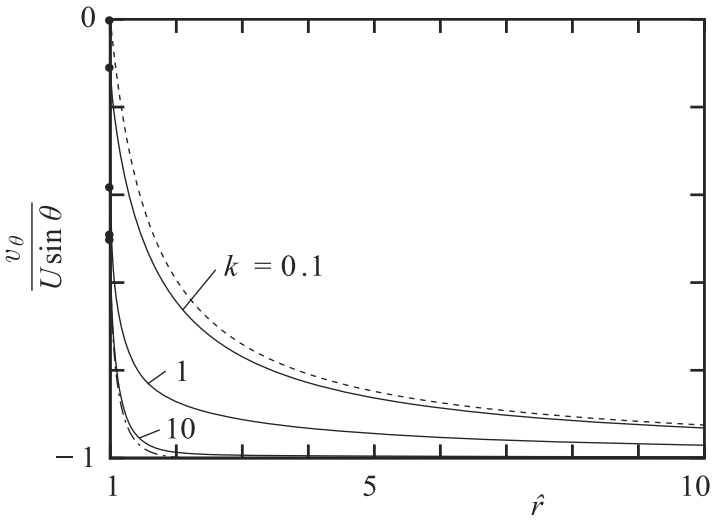

(b)

Figure 4.11. The velocity profile in a uniform flow past a sphere with a uniform temperature (a hard-sphere gas). (a) $v_r/U\cos\theta$ vs $\hat{r}$ $(= r/L)$ and (b) $v_\theta/U\sin\theta$ vs $\hat{r}$. The solid lines —— are the numerical solution and black circles • indicate the values on the sphere. The dashed lines – – – are the asymptotic solution (4.112b) or (4.112c) with $k = 0$, and the dot-dash lines –·– are the free molecular solution (4.115b) or (4.115c).

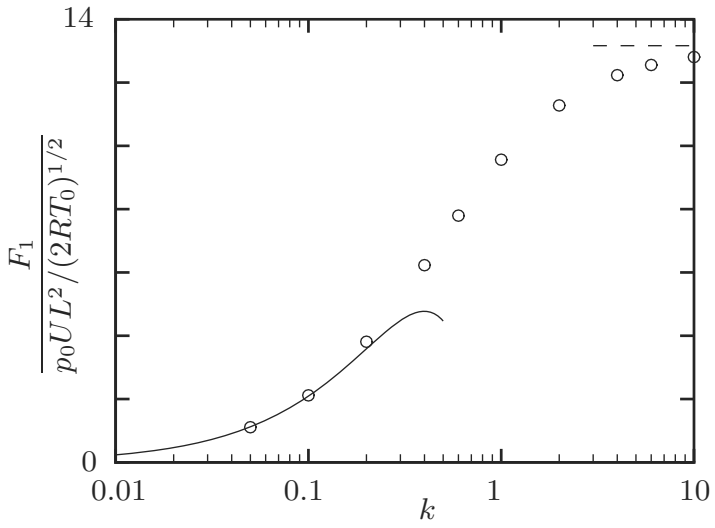

Figure 4.12. The force, $F_1/p_0UL^2(2RT_0)^{-1/2}$ vs k, acting on the sphere with a uniform temperature in a uniform flow (a hard-sphere gas). The white circles ∘ are the numerical solution, the solid line —— is the asymptotic solution (4.113) up to the order of k^2, and the dashed line – – – indicates the free molecular solution (4.117).

Sone, Lhuillier & Wakabayashi [1998]. Incidentally, in the latter paper, where a uniformly heated (or cooled) sphere made of the condensed phase of the gas is considered, the Onsager relation is confirmed between the fluxes of mass and energy from the sphere and their associated forces for the whole range of the Knudsen number numerically. The Onsager relation in relation to solutions of the linearized Boltzmann equation is also discussed in Sharipov [1994a, 1994b].

4.6 Uniform flow past a sphere with an arbitrary thermal conductivity

4.6.1 Formulation

In the preceding section (Section 4.5), the surface temperature of the sphere is kept at a uniform temperature T_0. Here, we extend the analysis to the case where the sphere is a uniform solid body with a uniform thermal conductivity. Then, the temperature field inside the sphere is determined by the heat-conduction equation

$$\frac{1}{\hat{r}^2}\frac{\partial}{\partial\hat{r}}\left(\hat{r}^2\frac{\partial\tau_p}{\partial\hat{r}}\right)+\frac{1}{\hat{r}^2\sin\theta}\frac{\partial}{\partial\theta}\left(\sin\theta\frac{\partial\tau_p}{\partial\theta}\right)=0 \qquad (\hat{r}<1), \tag{4.118}$$

where $T_0(1+\tau_p)$ is the temperature inside the sphere and the axial symmetry $(\partial/\partial\varphi = 0)$ of the field is taken into account.

The equation for the perturbed velocity distribution function ϕ of the gas and its boundary condition at infinity are the same as those in Section 4.5, i.e.,

$$\zeta_r \frac{\partial\phi}{\partial\hat{r}} + \frac{\zeta_\theta}{\hat{r}}\frac{\partial\phi}{\partial\theta} + \frac{\zeta_\theta^2+\zeta_\varphi^2}{\hat{r}}\frac{\partial\phi}{\partial\zeta_r} + \left(\frac{\zeta_\varphi^2}{\hat{r}}\cot\theta - \frac{\zeta_r\zeta_\theta}{\hat{r}}\right)\frac{\partial\phi}{\partial\zeta_\theta} - \left(\frac{\zeta_\theta\zeta_\varphi}{\hat{r}}\cot\theta + \frac{\zeta_r\zeta_\varphi}{\hat{r}}\right)\frac{\partial\phi}{\partial\zeta_\varphi} - \frac{1}{k}\mathcal{L}(\phi) = 0, \tag{4.119}$$

and

$$\phi = 2U(2RT_0)^{-1/2}(\zeta_r\cos\theta - \zeta_\theta\sin\theta) \quad \text{as } \hat{r}\to\infty. \tag{4.120}$$

On the surface of the sphere, in addition to the diffuse-reflection condition

$$\phi = (\zeta^2-2)\tau_p - 2\sqrt{\pi}\int_{\zeta_r<0}\zeta_r\phi E\mathbf{d}\boldsymbol{\zeta} \quad (\zeta_r>0) \ \text{ at } \hat{r}=1, \tag{4.121}$$

the condition of continuity of the energy flux through the surface is required,

$$-\frac{\lambda_p T_0}{L}\frac{\partial\tau_p}{\partial\hat{r}} = q_r \quad \text{at } \hat{r}=1, \tag{4.122}$$

where λ_p is the thermal conductivity of the sphere.

We put the solution ϕ in the sum

$$\phi = \phi_{\rm d} + c_{\rm D}U(2RT_0)^{-1/2}\phi_1. \tag{4.123}$$

Here, $\phi_{\rm d}$ is the solution for a uniform flow past a sphere with a uniform temperature T_0 in Section 4.5, $c_{\rm D}$ is an undetermined constant,[29] and ϕ_1 is a function to be determined. Then, ϕ_1 and τ_p of the similarity form[30]

$$\phi_1 = \Phi_c^{(1)}(\hat{r},\zeta_r,\zeta)\cos\theta + \zeta_\theta\Phi_s^{(1)}(\hat{r},\zeta_r,\zeta)\sin\theta, \tag{4.124a}$$

$$\tau_p = c_{\rm D}U(2RT_0)^{-1/2}\hat{r}\cos\theta, \tag{4.124b}$$

are easily seen to be consistent with the equations and the boundary conditions. The equations for $\Phi_c^{(1)}(\hat{r},\zeta_r,\zeta)$ and $\Phi_s^{(1)}(\hat{r},\zeta_r,\zeta)$ are given by Eqs. (4.107)–(4.109) with $(\Phi_c,\Phi_s) = (\Phi_c^{(1)},\Phi_s^{(1)})$, i.e.,

$$D_c(\Phi_c^{(1)},\Phi_s^{(1)}) = \frac{1}{k}F_c, \qquad D_s(\Phi_c^{(1)},\Phi_s^{(1)}) = \frac{1}{k}F_s, \tag{4.125}$$

where

$$D_c(\Phi_c^{(1)},\Phi_s^{(1)}) = \zeta_r\frac{\partial\Phi_c^{(1)}}{\partial\hat{r}} + \frac{\zeta^2-\zeta_r^2}{\hat{r}}\frac{\partial\Phi_c^{(1)}}{\partial\zeta_r} + \frac{\zeta^2-\zeta_r^2}{\hat{r}}\Phi_s^{(1)}, \tag{4.126a}$$

$$D_s(\Phi_c^{(1)},\Phi_s^{(1)}) = \zeta_r\frac{\partial\Phi_s^{(1)}}{\partial\hat{r}} + \frac{\zeta^2-\zeta_r^2}{\hat{r}}\frac{\partial\Phi_s^{(1)}}{\partial\zeta_r} - \frac{\zeta_r}{\hat{r}}\Phi_s^{(1)} - \frac{1}{\hat{r}}\Phi_c^{(1)}, \tag{4.126b}$$

[29] The temperature on the surface of the particle is not known (or specified) beforehand. The constant $c_{\rm D}$ in Eq. (4.124b) is introduced for this reason, but this constant in Eq. (4.123) is just for convenience.

[30] See Footnote 21 in Section 4.5.

and

$$F_c(\hat{r},\zeta_r,\zeta)=\mathcal{L}(\Phi_c^{(1)}),\qquad \zeta_\theta F_s(\hat{r},\zeta_r,\zeta)=\mathcal{L}(\zeta_\theta\Phi_s^{(1)}). \tag{4.127}$$

The boundary conditions on the sphere ($\hat{r}=1$), corresponding to Eqs. (4.121) and (4.122), are given by

$$\Phi_c^{(1)}=\zeta^2-2-2\pi^{3/2}\int_0^\infty\int_{\pi/2}^\pi \zeta^3\sin 2\theta_\zeta\Phi_c^{(1)}E\mathrm{d}\theta_\zeta\mathrm{d}\zeta\quad(\zeta_r>0), \tag{4.128a}$$

$$\Phi_s^{(1)}=0\quad(\zeta_r>0), \tag{4.128b}$$

and

$$c_{\mathrm{D}}=-\frac{4\pi}{5}\frac{\lambda_g}{k\gamma_2\lambda_p}\int_0^\infty\int_0^\pi \zeta^5\sin 2\theta_\zeta(\Phi_c^{(\mathrm{d})}|_{\hat{r}=1}+c_{\mathrm{D}}\Phi_c^{(1)}|_{\hat{r}=1})E\mathrm{d}\theta_\zeta\mathrm{d}\zeta, \tag{4.129}$$

where $\theta_\zeta=\mathrm{Arccos}(\zeta_r/\zeta)$,[31] $\Phi_c^{(\mathrm{d})}$ is Φ_c in Eq. (4.106) for the flow past the sphere with the uniform surface temperature T_0 in Section 4.5, and the thermal conductivity λ_g of the gas is introduced with the aid of the relation $\lambda_g T_0/L=5k\gamma_2 p_0(2RT_0)^{1/2}/4$ [see Eq. (3.71)] for the convenience of comparison with conventional formulas. The condition at infinity is

$$\Phi_c^{(1)}\to 0\ \text{ and }\ \Phi_s^{(1)}\to 0\quad\text{as }\hat{r}\to\infty. \tag{4.130}$$

From the condition (4.129), the undetermined constant c_{D} is determined as

$$c_{\mathrm{D}}=-\frac{C_q^{(\mathrm{d})}}{5k\gamma_2\lambda_p/4\lambda_g+C_q^{(1)}}, \tag{4.131}$$

where

$$C_q^{(\mathrm{d})}=\pi\int_0^\infty\int_0^\pi \zeta^5\sin 2\theta_\zeta\Phi_c^{(\mathrm{d})}|_{\hat{r}=1}E\mathrm{d}\theta_\zeta\mathrm{d}\zeta=\frac{q_r^{(\mathrm{d})}|_{\hat{r}=1}}{p_0U\cos\theta}, \tag{4.132a}$$

$$C_q^{(1)}=\pi\int_0^\infty\int_0^\pi \zeta^5\sin 2\theta_\zeta\Phi_c^{(1)}|_{\hat{r}=1}E\mathrm{d}\theta_\zeta\mathrm{d}\zeta=\frac{q_r^{(1)}|_{\hat{r}=1}}{p_0(2RT_0)^{1/2}\cos\theta}. \tag{4.132b}$$

Here, $q_r^{(\mathrm{d})}$ and $q_r^{(1)}$ are q_r's[32] corresponding to ϕ_{d} and ϕ_1 respectively. The $C_q^{(\mathrm{d})}$ and $C_q^{(1)}$ are determined by k.

The velocity distribution function ϕ_1 given by Eq. (4.124a) with the solution ($\Phi_c^{(1)}$, $\Phi_s^{(1)}$) of Eq. (4.125) with (4.126a)–(4.127) under the boundary conditions (4.128a), (4.128b), and (4.130) is the solution of the case where the sphere with its surface temperature $T_0(1+\cos\theta)$ lies in an infinite expanse of a gas at rest with density ρ_0 and temperature T_0. Thus, the desired solution of the problem introduced at the beginning of this section is given by the sum (4.123) of the two solutions, one is the solution for the uniform flow past the sphere with the uniform surface temperature, obtained in Section 4.5, and the other is the solution (4.124a) for a gas around the sphere whose surface temperature $T_0(1+\tau_w)$ is given by $T_0(1+\cos\theta)$ or $\tau_w=\cos\theta$.

[31] See Footnote 22 in Section 4.5.
[32] See Footnote 23 in Section 4.5.

4.6.2 A gas around a sphere with a nonuniform temperature

The solution for the gas around the sphere with the nonuniform temperature $\tau_w = \cos\theta$ also plays an important role in thermophoresis to be discussed in Section 5.3. Thus, it may be in order to summarize the result. Let us repeat the problem briefly. In an infinite expanse of a gas at rest with density ρ_0 and temperature T_0, there lies a sphere whose surface temperature is given by $T_0(1+\cos\theta)$. The behavior of the gas is governed by the linearized Boltzmann equation and the diffuse-reflection condition. The solution ϕ is expressed in the form[33]

$$\phi = \Phi_c(\hat{r}, \zeta_r, \zeta)\cos\theta + \zeta_\theta \Phi_s(\hat{r}, \zeta_r, \zeta)\sin\theta, \tag{4.133}$$

and $\Phi_c(\hat{r}, \zeta_r, \zeta)$ and $\Phi_s(\hat{r}, \zeta_r, \zeta)$ are governed by Eq. (4.125) with (4.126a)–(4.127) with $\Phi_c^{(1)}$ and $\Phi_s^{(1)}$ replaced by Φ_c and Φ_s. The boundary conditions for them are Eqs. (4.128a), (4.128b), and (4.130) with the same replacement, i.e.,

$$\Phi_c = \zeta^2 - 2 - 2\pi^{3/2}\int_0^\infty \int_{\pi/2}^\pi \zeta^3 \sin 2\theta_\zeta \Phi_c E \mathrm{d}\theta_\zeta \mathrm{d}\zeta \quad (\zeta_r > 0), \tag{4.134a}$$

$$\Phi_s = 0 \quad (\zeta_r > 0), \tag{4.134b}$$

and

$$\Phi_c \to 0 \ \text{ and } \ \Phi_s \to 0 \quad \text{as } \hat{r} \to \infty. \tag{4.135}$$

The solution for small Knudsen numbers ($k \ll 1$) is easily obtained by the asymptotic theory in Section 3.1 as[34]

$$\frac{v_r}{(2RT_0)^{1/2}\cos\theta} = -K_1\left(\frac{1}{\hat{r}} - \frac{1}{\hat{r}^3}\right)k + \left(\frac{2A_\mathrm{t}}{\hat{r}} + \frac{2B_\mathrm{t}}{\hat{r}^3} - \int_\infty^\eta Y_1(\eta_0)\mathrm{d}\eta_0\right)k^2 + \cdots, \tag{4.136a}$$

$$\frac{v_\theta}{(2RT_0)^{1/2}\sin\theta} = \frac{1}{2}\left[K_1\left(\frac{1}{\hat{r}} + \frac{1}{\hat{r}^3}\right) + Y_1(\eta)\right]k + \left(-\frac{A_\mathrm{t}}{\hat{r}} + \frac{B_\mathrm{t}}{\hat{r}^3} + Y_\mathrm{t}(\eta)\right)k^2 + \cdots, \tag{4.136b}$$

$$\frac{\rho - \rho_0}{\rho_0\cos\theta} = -\frac{1}{\hat{r}^2} + 2\left(\frac{d_1}{\hat{r}^2} - \Omega_1(\eta)\right)k + \left(-\frac{K_1\gamma_1 + D_\mathrm{t}}{\hat{r}^2} + \Omega_\mathrm{t}(\eta)\right)k^2 + \cdots, \tag{4.136c}$$

$$\frac{T - T_0}{T_0\cos\theta} = \frac{1}{\hat{r}^2} - 2\left(\frac{d_1}{\hat{r}^2} + \Theta_1(\eta)\right)k + \left(\frac{D_\mathrm{t}}{\hat{r}^2} + \Theta_\mathrm{t}(\eta)\right)k^2 + \cdots, \tag{4.136d}$$

$$\frac{p - p_0}{p_0\cos\theta} = -2[\Omega_1(\eta) + \Theta_1(\eta)]k + \left(-\frac{K_1\gamma_1}{\hat{r}^2} + \Omega_\mathrm{t}(\eta) + \Theta_\mathrm{t}(\eta)\right)k^2 + \frac{2A_\mathrm{t}\gamma_1}{\hat{r}^2}k^3 + \cdots, \tag{4.136e}$$

$$\frac{q_r}{p_0(2RT_0)^{1/2}\cos\theta} = \frac{5\gamma_2}{2\hat{r}^3}k - \left(\frac{5\gamma_2 d_1}{\hat{r}^3} - 2\int_\infty^\eta H_B(\eta_0)\mathrm{d}\eta_0\right)k^2 + \cdots, \tag{4.136f}$$

[33] See Footnote 21 in Section 4.5.

[34] See Footnotes 3 in Section 3.1.2 and 25 in Section 4.5.

$$
\begin{aligned}
&A_{\rm t} = -\tfrac{1}{2}(b_2 + 3K_1k_0 - 3a_4 + a_5 + a_6),\\
&B_{\rm t} = \tfrac{1}{2}(-b_2 + 3K_1k_0 - 3a_4 + a_5 + a_6),\\
&D_{\rm t} = 4d_1^2 + 6d_3 - 2d_5,\\
&Y_{\rm t}(\eta) = 3K_1Y_0(\eta) - 3Y_{a4}(\eta) + Y_{a5}(\eta) + Y_{a6}(\eta),\\
&\Omega_{\rm t}(\eta) = 4d_1\Omega_1(\eta) + 6\Omega_3(\eta) - 2\Omega_5(\eta),\\
&\Theta_{\rm t}(\eta) = 4d_1\Theta_1(\eta) + 6\Theta_3(\eta) - 2\Theta_5(\eta),\\
&\eta = (\hat{r} - 1)/k.
\end{aligned}
$$

Here, the nondimensional viscosity γ_1 and thermal conductivity γ_2 are defined in Section 3.1.3; the slip coefficients K_1, k_0, a_4, a_5, a_6, b_2, d_1, d_3, and d_5 and the Knudsen-layer functions $Y_0(\eta)$, $Y_1(\eta)$, $Y_{a4}(\eta)$, $Y_{a5}(\eta)$, $Y_{a6}(\eta)$, $\Omega_1(\eta)$, $\Omega_3(\eta)$, $\Omega_5(\eta)$, $\Theta_1(\eta)$, $\Theta_3(\eta)$, $\Theta_5(\eta)$, and $H_B(\eta)$ are introduced in Section 3.1.5; the fluid-dynamic part of the pressure $(p - p_0)/p_0 \cos\theta$ is given up to the order of k^3 to obtain the force acting on the sphere in harmony with other variables;[35] and $q_r/p_0(2RT_0)^{1/2}\cos\theta$ is shown because it is important in Sections 4.6.3 and 5.3.2. The force F_i on the sphere is

$$
\frac{F_1}{p_0L^2} = 4\pi\gamma_1(K_1k^2 - 2A_{\rm t}k^3) + \cdots, \quad F_2 = F_3 = 0. \tag{4.137}
$$

The free molecular solution ($k = \infty$) of the problem is given as follows:

$$
\Phi_c = \begin{cases} 0 & [\mathrm{Arcsin}(1/\hat{r}) < \theta_\zeta \le \pi],\\ (\zeta^2 - 2)[\hat{r}\sin^2\theta_\zeta + \cos\theta_\zeta(1 - \hat{r}^2\sin^2\theta_\zeta)^{1/2}] & \\ & [0 \le \theta_\zeta < \mathrm{Arcsin}(1/\hat{r})], \end{cases} \tag{4.138a}
$$

$$
\Phi_s = \begin{cases} 0 & [\mathrm{Arcsin}(1/\hat{r}) < \theta_\zeta \le \pi],\\ \zeta^{-1}(\zeta^2 - 2)[\hat{r}\cos\theta_\zeta - (1 - \hat{r}^2\sin^2\theta_\zeta)^{1/2}] & \\ & [0 \le \theta_\zeta < \mathrm{Arcsin}(1/\hat{r})], \end{cases} \tag{4.138b}
$$

where $\theta_\zeta = \mathrm{Arccos}(\zeta_r/\zeta)$, and

$$
\frac{\rho - \rho_0}{\rho_0\cos\theta} = -\frac{1}{12}\left[2\hat{r} - \left(2\hat{r} + \frac{1}{\hat{r}}\right)\left(1 - \frac{1}{\hat{r}^2}\right)^{1/2} + \frac{1}{\hat{r}^2}\right], \tag{4.139a}
$$

$$
\frac{T - T_0}{T_0\cos\theta} = \frac{1}{6}\left[2\hat{r} - \left(2\hat{r} + \frac{1}{\hat{r}}\right)\left(1 - \frac{1}{\hat{r}^2}\right)^{1/2} + \frac{1}{\hat{r}^2}\right], \tag{4.139b}
$$

$$
v_r = v_\theta = 0, \tag{4.139c}
$$

$$
\frac{q_r}{p_0(2RT_0)^{1/2}\cos\theta} = \frac{1}{4\sqrt{\pi}}\left[1 + \frac{1}{\hat{r}^2} + \frac{2}{\hat{r}^3} - \frac{\hat{r}}{2}\left(1 - \frac{1}{\hat{r}^2}\right)^2 \ln\frac{\hat{r} + 1}{\hat{r} - 1}\right]. \tag{4.139d}
$$

Especially, q_r at $\hat{r} = 1$, which is important in Eq. (4.132b), is

[35] See Footnote 26 in Section 4.5.

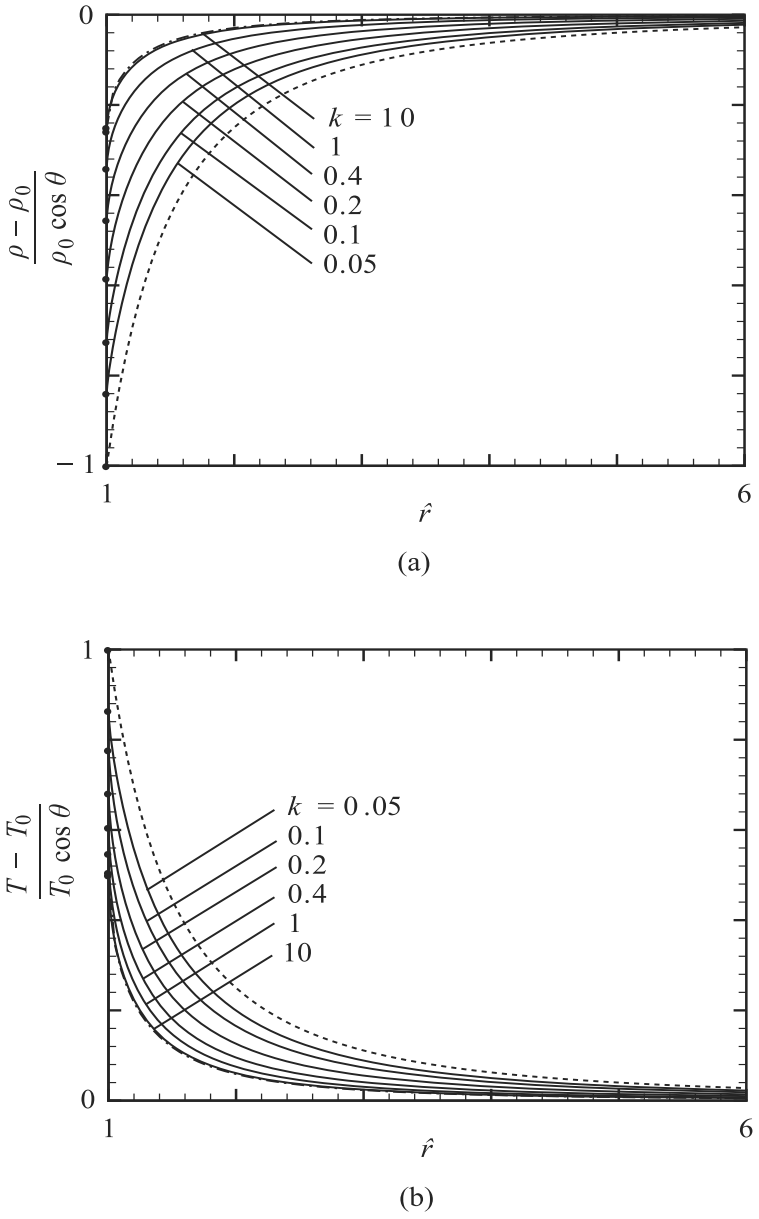

Figure 4.13. Density and temperature profiles in a gas around a sphere with a nonuniform temperature (a hard-sphere gas). (a) Density and (b) temperature. The solid lines —— are the numerical solution, the dashed lines – – – are the asymptotic solution (4.136c) or (4.136d) with $k = 0$, and the dot-dash lines –·– are the free molecular solution (4.139a) or (4.139b). The black circles • indicate the values on the sphere.

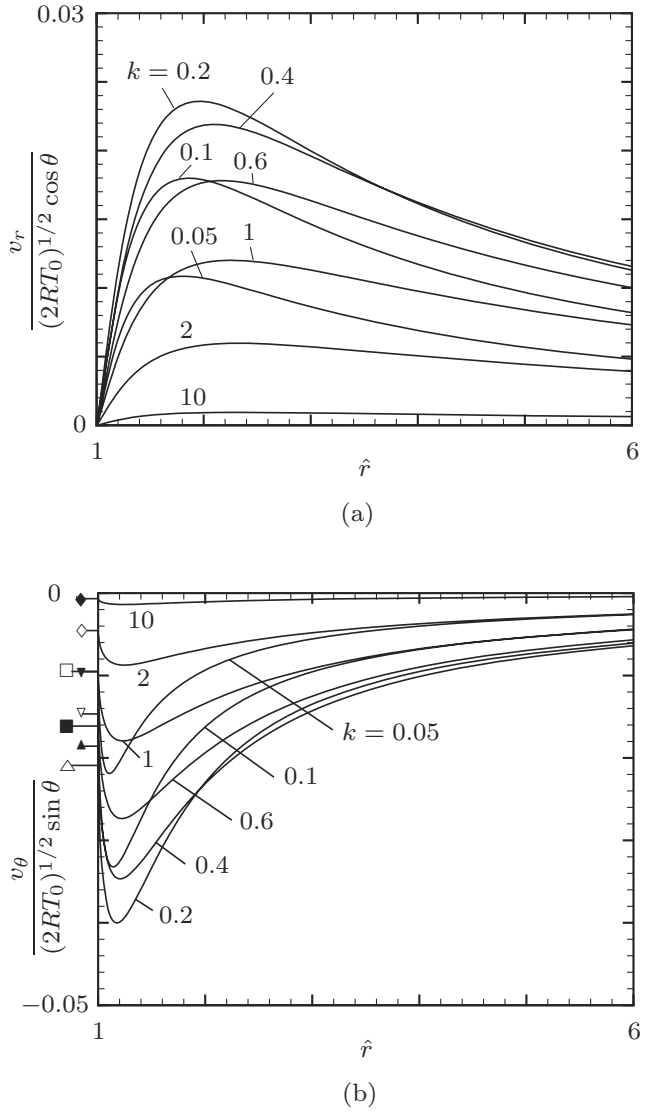

Figure 4.14. Velocity profiles in a gas around a sphere with a nonuniform temperature (a hard-sphere gas). (a) v_r and (b) v_θ. The solid lines —— are the numerical solution. The flow vanishes for the asymptotic solution (4.136a) and (4.136b) with $k = 0$ and the free molecular solution ($k = \infty$). In (b) the values on the sphere of the numerical results are marked by □ for $k = 0.05$, ■ for $k = 0.1$, △ for $k = 0.2$, ▲ for $k = 0.4$, ▽ for $k = 0.6$, ▼ for $k = 1$, ◇ for $k = 2$, and ♦ for $k = 10$.

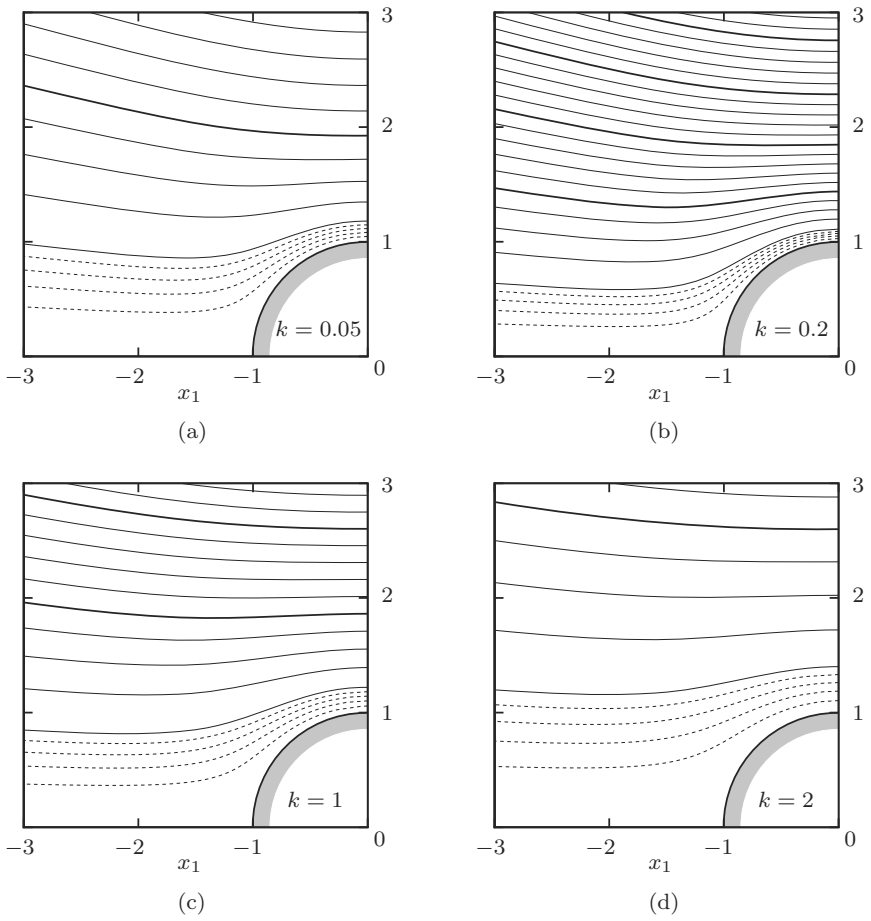

Figure 4.15. Streamlines of flow (in a plane containing x_1 axis) in a gas around a sphere with a nonuniform temperature (a hard-sphere gas). (a) $k = 0.05$, (b) $k = 0.2$, (c) $k = 1$, and (d) $k = 2$. The ordinates in the figures are commonly $(x_2^2 + x_3^2)^{1/2}$. The streamlines $\Psi = 4 \times 10^{-3} n$ ($n = 0, 1, 2, \ldots$) are shown in solid lines, the thick lines of which indicate the cases $n = 0, 5, 10, \ldots$, and the lines $\Psi = 4 \times 10^{-3}(n/5)$ ($n = 1, 2, 3,$ and 4) are shown in dashed lines, where Ψ is the Stokes stream function defined by $v_r/(2RT_0)^{1/2} = (\hat{r}^2 \sin\theta)^{-1} \partial\Psi/\partial\theta$ and $v_\theta/(2RT_0)^{1/2} = -(\hat{r} \sin\theta)^{-1} \partial\Psi/\partial\hat{r}$. A streamline closer to the sphere takes smaller value of Ψ; $\Psi = 0$ for the line on the x_1 axis. The arrows indicate the direction of the flow.

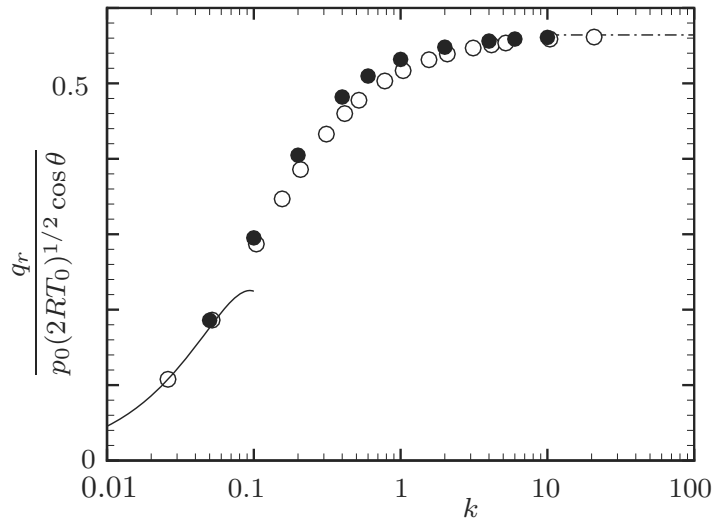

Figure 4.16. The heat flow, $q_r/p_0(2RT_0)^{1/2}\cos\theta$ at $\hat{r}=1$ vs k, from a sphere with a nonuniform temperature in a gas (a hard-sphere gas). The black circles • are the numerical solution for a hard-sphere gas, the white circles ∘ are the numerical solution for the BKW model, the solid line —— is the asymptotic solution for a hard-sphere gas for small k [Eq. (4.136f) up to the order of k^2], and the dot-dash line –·– indicates the free molecular solution (4.140). In the above figure, the data for the BKW model are those where the original k is replaced by $1.922284k$ (see Footnote 37 in Section 4.6.2).

$$\frac{q_r}{p_0(2RT_0)^{1/2}\cos\theta}=\frac{1}{\sqrt{\pi}}. \tag{4.140}$$

The force F_i ($F_2=F_3=0$) acting on the sphere is given by

$$\frac{F_1}{p_0L^2}=-\frac{\pi}{3}. \tag{4.141}$$

The solution of the problem is obtained numerically for a hard-sphere gas in Takata & Sone [1995].[36] The profiles of the density, temperature, and velocity fields are shown in Figs. 4.13 and 4.14. A flow is induced owing to the nonuniform temperature on the sphere. Some examples of the streamlines are shown in Fig. 4.15. The heat transfer on the sphere (per unit time) and the force acting on the sphere are shown in Figs. 4.16 and 4.17, where the results for the BKW model are also shown for comparison.[37]

[36]See Footnote 27 in Section 4.5.

[37]The way of comparing the results of different molecular models is not unique. The present problem contains the parameter k. The parameter can be replaced by $\mu_g/\rho_0L(RT_0)^{1/2}$, $\lambda_g(RT_0)^{1/2}/p_0LR$, or $(\mu_g\lambda_g)^{1/2}T_0{}^{1/2}/p_0L$, where μ_g and λ_g are, respectively, the viscosity

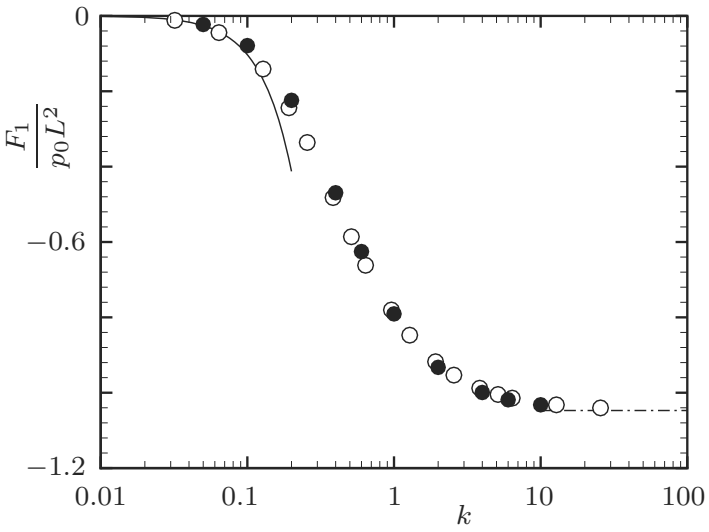

Figure 4.17. The force, F_1/p_0L^2 vs k, acting on a sphere with a nonuniform temperature in a gas (a hard-sphere gas). The black circles • are the numerical solution for a hard-sphere gas, the white circles ∘ are the numerical solution for the BKW model, the solid line —— is the asymptotic solution for a hard-sphere gas for small k [Eq. (4.137) up to the order of k^2], and the dot-dash line –·– indicates the free molecular solution (4.141). In the above figure, the data for the BKW model are those where the original k is replaced by $1.562492k$ (see Footnote 37 in Section 4.6.2).

A flow is induced around the sphere from the colder to the hotter side. The leading terms of Eqs. (4.136a) and (4.136b) for $k \ll 1$ are due to the thermal creep flow noted in Section 3.1.5 and to be discussed in more detail in Section

---

and thermal conductivity of the gas at the reference state [see Eqs. (3.70) and (3.71)]. The result of comparison depends on the choice of the parameter, because the relation between the mean free path ℓ_0 and μ_g, λ_g, or $(\mu_g\lambda_g)^{1/2}$ depends on molecular models owing to the dependence of γ_1 and γ_2 in Eqs. (3.70) and (3.71) on molecular models. When $\mu_g/\rho_0 L(RT_0)^{1/2}$ (or μ_g) is taken as the basic parameter instead of k (or ℓ_0), $\gamma_1 k$ is invariant among molecular models, that is, the relation between k's of a hard-sphere gas and the BKW model is

$$k \text{ (BKW)} = 1.270042k \text{ (hard sphere)};$$

when $\lambda_g(RT_0)^{1/2}/p_0LR$ (or λ_g) is taken, $\gamma_2 k$ is invariant, that is, the relation is

$$k \text{ (BKW)} = 1.922284k \text{ (hard sphere)};$$

when $(\mu_g\lambda_g)^{1/2}{T_0}^{1/2}/p_0L$ [or $(\mu_g\lambda_g)^{1/2}$] is taken, $(\gamma_1\gamma_2)^{1/2}k$ is invariant, that is, the relation is

$$k \text{ (BKW)} = 1.562492k \text{ (hard sphere)}.$$

The second relation is chosen in Fig. 4.16, and the third is chosen in Fig. 4.17. There are misprints in this kind of note after Eq. (25) in Takata & Sone [1995], that is, the correspondences are transposed.

5.1.1. In the free molecular case ($k = \infty$), no flow is induced. This is an example of the general proposition (see Section 2.5.4) for the class of solutions given in Section 2.5.

4.6.3 Solution for a sphere with an arbitrary thermal conductivity

The solution for a uniform flow past a sphere with an arbitrary thermal conductivity is obtained in the form (4.123), i.e.,

$$\phi = \phi_{\rm d} + c_{\rm D} U (2RT_0)^{-1/2} \phi_1, \tag{4.142}$$

where $\phi_{\rm d}$ is ϕ given in Section 4.5 and ϕ_1 is given by Eq. (4.124a). The constant $c_{\rm D}$ in Eq. (4.142) is given by Eq. (4.131), i.e.,

$$c_{\rm D} = -\frac{C_q^{({\rm d})}}{5k\gamma_2\lambda_p/4\lambda_g + C_q^{(1)}}. \tag{4.143}$$

Corresponding to Eq. (4.142), the perturbed macroscopic variables (corresponding to ϕ)[38]

$$\rho - \rho_0,\ v_r,\ v_\theta,\ T - T_0,\ p_{rr} - p_0,\ p_{r\theta},\ p_{\theta\theta} - p_0,\ p_{\varphi\varphi} - p_0,\ q_r,\ q_\theta,$$

are given by Eq. (4.142) where ϕ, $\phi_{\rm d}$, and ϕ_1 are replaced by the macroscopic variables corresponding to ϕ, $\phi_{\rm d}$, and ϕ_1 respectively. That is, the nondimensional macroscopic variables (say, $h = \omega$, u_i, etc.) expressed by the distribution function ϕ by Eqs. (1.97a)–(1.97f) are expressed by

$$h = h_{\rm d} + c_{\rm D} U (2RT_0)^{-1/2} h_1, \tag{4.144}$$

where $h_{\rm d}$ and h_1 are, respectively, given by Eqs. (1.97a)–(1.97f) with ϕ replaced by $\phi_{\rm d}$ and ϕ_1.

For $k \ll 1$, with the aid of Eqs. (4.112f) and (4.136f),

$$c_{\rm D} = \frac{-6\left(\gamma_3 - 2\displaystyle\int_0^\infty H_A(\eta){\rm d}\eta\right)k}{5\gamma_2(\lambda_p/\lambda_g + 2)} + \cdots. \tag{4.145}$$

For $k = \infty$, with the aid of Eqs. (4.116) and (4.140),

$$c_{\rm D} = 0. \tag{4.146}$$

In the two limiting cases, $k = 0$ and $k = \infty$, the solution reduces to the solution around the sphere with the uniform temperature T_0.

The numerical data of $C_q^{({\rm d})}$ and $C_q^{(1)}$ vs k, defined by Eqs. (4.132a) and (4.132b), are given for a hard-sphere gas in Table 4.5, from which the coefficient $c_{\rm D}$ is determined by Eq. (4.143). When $\lambda_p/\lambda_g \to \infty$, $c_{\rm D}$ reduces to zero and the

[38] See Footnote 23 in Section 4.5.

Table 4.5. The numerical data of $C_q^{(\mathrm{d})}$ and $C_q^{(1)}$ [or $q_r^{(\mathrm{d})}/p_0U\cos\theta$ and $q_r^{(1)}/p_0(2RT_0)^{1/2}\cos\theta$ at $\hat{r}=1$] and $F_1^{(\mathrm{d})}/p_0UL^2(2RT_0)^{-1/2}$ and $F_1^{(1)}/p_0L^2$ (a hard-sphere gas).

k	$C_q^{(\mathrm{d})}$	$C_q^{(1)}$	$\dfrac{F_1^{(\mathrm{d})}}{p_0UL^2/(2RT_0)^{1/2}}$	$\dfrac{F_1^{(1)}}{p_0L^2}$
0	0	0	0	0
0.05	0.0053	0.1859	1.1091	−0.0228
0.1	0.0189	0.2952	2.1168	−0.0788
0.2	0.0535	0.4048	3.8110	−0.2241
0.4	0.1118	0.4819	6.2292	−0.4694
0.6	0.1492	0.5097	7.7951	−0.6254
1	0.1887	0.5318	9.5625	−0.7908
2	0.2226	0.5480	11.2772	−0.9327
4	0.2386	0.5561	12.2333	−0.9994
6	0.2432	0.5588	12.5557	−1.0187
10	0.2464	0.5609	12.8071	−1.0321
∞	0.25	0.5642	13.1653	−1.0472

solution ϕ reduces to ϕ_{d}, i.e., the solution for the case of the uniform temperature in Section 4.5.

The force F_i ($F_2=F_3=0$) acting on the sphere is given as

$$\begin{aligned}\frac{F_1}{p_0UL^2/(2RT_0)^{1/2}} &= \frac{F_1^{(\mathrm{d})}}{p_0UL^2/(2RT_0)^{1/2}} + \frac{c_{\mathrm{D}}U}{(2RT_0)^{1/2}}\frac{F_1^{(1)}}{p_0UL^2/(2RT_0)^{1/2}} \\ &= \frac{F_1^{(\mathrm{d})}}{p_0UL^2/(2RT_0)^{1/2}} + \frac{c_{\mathrm{D}}F_1^{(1)}}{p_0L^2},\end{aligned} \tag{4.147}$$

where $F_1^{(\mathrm{d})}$ is F_1 in Section 4.5 and $F_1^{(1)}$ is F_1 in Section 4.6.2.

For small Knudsen numbers ($k \ll 1$), there is no contribution up to the order of k^2 from the second term on the right-hand side of Eq. (4.147), i.e.,

$$\begin{aligned}\frac{F_1}{p_0UL^2/(2RT_0)^{1/2}} = 6\pi\gamma_1 k\left[1+k_0k-4\left(\frac{A_{\mathrm{d}}}{3}+\frac{K_1[\gamma_3-2\int_0^\infty H_A(\eta)\mathrm{d}\eta]}{5\gamma_2(\lambda_p/\lambda_g+2)}\right)k^2\right] \\ +\cdots.\end{aligned} \tag{4.148}$$

For the free molecular case ($k=\infty$), the second term vanishes because $c_{\mathrm{D}}=0$, i.e.,

$$\frac{F_1}{p_0UL^2/(2RT_0)^{1/2}} = \frac{2}{3}\sqrt{\pi}(\pi+8). \tag{4.149}$$

The force F_1 is independent of λ_p/λ_g for $k=\infty$.

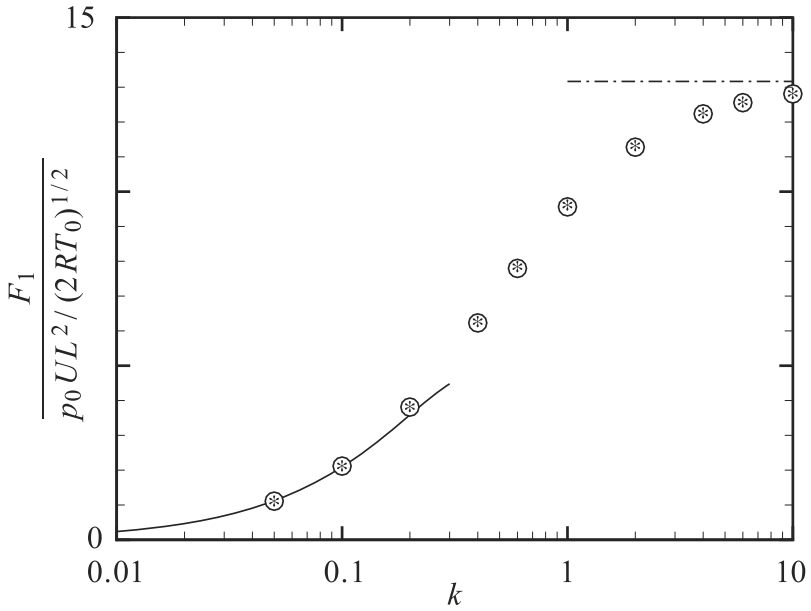

Figure 4.18. The force (or drag), $F_1/p_0UL^2(2RT_0)^{-1/2}$ vs k, acting on a sphere with arbitrary thermal conductivity in a uniform flow of a gas (a hard-sphere gas). The white circles $\circ$ are the numerical solution for $\lambda_p/\lambda_g = \infty$ (or for the sphere with a uniform temperature) and the stars $*$ are the numerical solution for $\lambda_p/\lambda_g = 1$. The solid line —— is the asymptotic solution for small k [Eq. (4.148) up to the order of k^2], and the dot-dash line –·– indicates the free molecular solution (4.149); they are independent of λ_p/λ_g.

The numerical data of $F_1^{(\mathrm{d})}/p_0UL^2(2RT_0)^{-1/2}$ and $F_1^{(1)}/p_0L^2$ in the formula (4.147) are given for a hard-sphere gas in Table 4.5. The force F_1 vs k for a hard-sphere gas obtained from these data is shown in Fig. 4.18, where Eq. (4.149) for $k = \infty$ and Eq. (4.148) for small k up to the order of k^2 are also shown. The effect of λ_p/λ_g is small.

4.7 Shock wave

Consider a time-independent unidirectional flow (say, in the X_1 direction) in an infinite expanse of a gas, where the states at infinities, or as $X_1 \to -\infty$ and as $X_1 \to \infty$, are both uniform, say $[\rho_{-\infty}, v_{1-\infty}(>0), T_{-\infty}, p_{-\infty}(= R\rho_{-\infty}T_{-\infty})]$ and $[\rho_\infty, v_{1\infty}, T_\infty, p_\infty(= R\rho_\infty T_\infty)]$. The states at infinities being uniform, their velocity distribution functions are Maxwellian. That is,

$$f \to \frac{\rho_{-\infty}}{(2\pi RT_{-\infty})^{3/2}} \exp\left(-\frac{(\xi_i - v_{1-\infty}\delta_{i1})^2}{2RT_{-\infty}}\right) \quad \text{as } X_1 \to -\infty, \tag{4.150a}$$

$$f \to \frac{\rho_\infty}{(2\pi RT_\infty)^{3/2}} \exp\left(-\frac{(\xi_i - v_{1\infty}\delta_{i1})^2}{2RT_\infty}\right) \quad \text{as } X_1 \to \infty. \tag{4.150b}$$

The two states at infinities cannot be chosen arbitrarily. According to the conservation equations (1.12)–(1.14), they are related as

$$\rho_{-\infty} v_{1-\infty} = \rho_\infty v_{1\infty}, \tag{4.151a}$$

$$\rho_{-\infty} v_{1-\infty}^2 + p_{-\infty} = \rho_\infty v_{1\infty}^2 + p_\infty, \tag{4.151b}$$

$$\rho_{-\infty} v_{1-\infty}\left(v_{1-\infty}^2 + \frac{5p_{-\infty}}{\rho_{-\infty}}\right) = \rho_\infty v_{1\infty}\left(v_{1\infty}^2 + \frac{5p_\infty}{\rho_\infty}\right). \tag{4.151c}$$

These relations are rewritten in the form

$$\frac{p_\infty}{p_{-\infty}} = \frac{5M_{-\infty}^2 - 1}{4}, \tag{4.152a}$$

$$\frac{\rho_\infty}{\rho_{-\infty}} = \frac{v_{1-\infty}}{v_{1\infty}} = \frac{4M_{-\infty}^2}{M_{-\infty}^2 + 3}, \tag{4.152b}$$

$$\frac{T_\infty}{T_{-\infty}} = \frac{(5M_{-\infty}^2 - 1)(M_{-\infty}^2 + 3)}{16M_{-\infty}^2}, \tag{4.152c}$$

where

$$M_{-\infty} = \frac{v_{1-\infty}}{(5RT_{-\infty}/3)^{1/2}}.$$

These conditions are called the *shock condition* or the *Rankine–Hugoniot relation* (Courant & Friedrichs [1948], Liepmann & Roshko [1957]). The ratios of the downstream and upstream data of pressure, density, flow velocity, and temperature are expressed in terms of the upstream Mach number $M_{-\infty}$. It may be noted that Eqs. (4.152a)–(4.152c) with the subscripts ∞ and $-\infty$ interchanged also hold because Eqs. (4.151a)–(4.151c) are symmetric with respect to the subscripts ∞ and $-\infty$, and that the possible ranges of $M_{-\infty}$ and M_∞ are $M_{-\infty}^2 \geq 1/5$ and $M_\infty^2 \geq 1/5$ because the pressure and temperature should be non-negative. The downstream Mach number M_∞ $(= v_{1\infty}/\sqrt{5RT_\infty/3})$ is related to the upstream one as

$$M_\infty^2 - 1 = -\frac{4(M_{-\infty}^2 - 1)}{5M_{-\infty}^2 - 1}, \tag{4.153}$$

which shows that $M_\infty^2 < 1$ or $M_\infty^2 > 1$ depending on $M_{-\infty}^2 > 1$ or $M_{-\infty}^2 < 1$ and that $M_\infty^2 = 1$ corresponds to $M_{-\infty}^2 = 1$.

According to the H theorem [or Eqs. (1.33)–(1.34b) in Section 1.7],

$$H_{1\infty} - H_{1-\infty} \leq 0, \tag{4.154}$$

where $H_1 = \int \xi_1 f \ln(f/c_0)\mathbf{d\xi}$. At infinities, f being Maxwellian, $H_{1\infty}$ and $H_{1-\infty}$ are expressed with the H function H $[= \int f \ln(f/c_0)\mathbf{d\xi}$; see Eq. (1.32)] as $H_{1\infty} = H_\infty v_{1\infty}$ and $H_{1-\infty} = H_{-\infty} v_{1-\infty}$. Thus, the inequality (4.154) is reduced to

$$\frac{H_\infty}{\rho_\infty} - \frac{H_{-\infty}}{\rho_{-\infty}} \leq 0. \tag{4.155}$$

On the other hand, for the Mawellians at infinities,

$$\frac{H_\infty}{\rho_\infty} - \frac{H_{-\infty}}{\rho_{-\infty}} = -\frac{3}{2}\left[\ln\left(\frac{p_\infty}{p_{-\infty}}\right) - \frac{5}{3}\ln\left(\frac{\rho_\infty}{\rho_{-\infty}}\right)\right],$$

where $p_\infty/p_{-\infty}$ and $\rho_\infty/\rho_{-\infty}$ are expressed in terms of $M^2_{-\infty}$ by Eqs. (4.152a) and (4.152b). The difference $\Delta H = H_\infty/\rho_\infty - H_{-\infty}/\rho_{-\infty}$ is zero at $M^2_{-\infty} = 1$ and is monotonically decreasing in the range $M^2_{-\infty} \geq 1/5$, because

$$\frac{\mathrm{d}\Delta H}{\mathrm{d}M^2_{-\infty}} = -\frac{3}{2}\frac{(M^2_{-\infty}-1)^2}{M^2_{-\infty}(M^2_{-\infty}-\frac{1}{5})(M^2_{-\infty}+3)} \leq 0.$$

Thus, by the condition (4.155), $M^2_{-\infty} \geq 1$, that is, the upstream state is supersonic. From the statement just after Eq. (4.153), $1/5 \leq M^2_\infty \leq 1$, that is, the downstream state is subsonic. Incidentally, the ratios of the downstream and upstream data of pressure, density, flow velocity, and temperature are all unity when $M^2_{-\infty} = 1$; the ratios of the downstream and upstream data of pressure and temperature are infinite ($p_\infty/p_{-\infty} = T_\infty/T_{-\infty} = \infty$), but those of density and flow velocity are finite ($\rho_\infty/\rho_{-\infty} = v_{1-\infty}/v_{1\infty} = 4$) when $M^2_{-\infty} = \infty$.

Our interest is the time-independent solution that connects the two states at infinities, which is called *shock wave* or *shock layer*. In the Euler set of equations in the classical fluid dynamics, the shock wave is treated as a discontinuity with the above-mentioned shock condition as the connection condition. Its internal structure is discussed by the Navier–Stokes set of equations. However, the thickness of the shock wave is of the order of the mean free path, and therefore, it is not correctly discussed by the Navier–Stokes set and should be discussed by the Boltzmann equation.

Obviously, when the two states at infinities are equal, the uniform state is a solution. The mathematical theory of the existence of a nontrivial solution is studied by Caflisch & Nicolaenko [1982] and Liu & Yu [2004a], and the existence and uniqueness of a weak shock wave solution, where the two uniform states at infinities are very close or $0 < M^2_{-\infty} - 1 \ll 1$, are proved. Its profile is given in Grad [1969]. It is obtained from the Boltzmann equation as a slowly varying solution and the velocity distribution function is expressed by the local Maxwellian and the parametric macroscopic variables are determined by fluid-dynamic-type equations (see the discussion of a slowly varying solution in a transonic region in Section 7.3.2). In Liu & Yu [2004a], besides their simple and clear description, they also demonstrated that the velocity distribution function is positive in the shock layer and that the solution is stable.

There are many numerical works on the shock wave structure (e.g., Mott-Smith [1951], Liepmann, Narashimha & Chahine [1962], Salwen, Grosch & Ziering [1964], Holway Jr. [1965], Bird [1965, 1967, 1994], Elliot & Baganoff [1974], Erwin, Pham-Van-Diep & Muntz [1991], Ohwada [1993], Cercignani, Frezzotti & Grosfils [1999], Takata, Aoki & Cercignani [2000]), among which the pioneering work by Mott-Smith [1951] is well known (see Section B.2.2). Many are discussions of their numerical or approximate works rather than the physical discussion of shock waves. When the strength of a shock wave is strong,

the profile of the temperature field is reported not to be monotonic; it first increases from the upstream value, reaches the maximum value, and decreases to the downstream value, though the overshoot is small. This is mainly discussed from the former point noted above. In the limit that the strength of the shock wave becomes infinite or the upstream Mach number becomes infinite, the width of the velocity distribution function at upstream infinity becomes diminishingly small compared with the scale of the flow velocity there, or the velocity distribution function at upstream infinity approaches a delta function on the scale of the flow velocity there. Grad [1969] proposed a method to approach this case. Takata, Aoki & Cercignani [2000] carried out the analysis on the basis of Grad [1969] and Caflisch [1985] for a hard-sphere gas, according to which the trace of the singular character at upstream infinity remains at downstream infinity. Ivanov and his collaborators (e.g., Ivanov, Markelov, Kudryavtev & Gimelshein [1998]) are actively carrying out engineering computation of flows with shock waves, especially the interaction of shock wave and boundary layer by DSMC method (see Section B.1).

Recently, Yu [2005] reported a very interesting mathematical work. The behavior of a gas where the length scale and the time scale of variation of the state are, respectively, much larger than the mean free path and the mean free time of the gas is studied by the Hilbert expansion. The leading term of the velocity distribution function is Maxwellian and its parameters, i.e., the density, velocity, and temperature, are governed by the Euler set of equations. The solution of the Euler set may contain discontinuity, which is determined by the shock condition mentioned above. Yu [2005] extended the Hilbert expansion to the case where there is shock-wave discontinuity in the solution. He constructed the systematic procedure to carry out the Hilbert expansion (the *generalized Hilbert expansion*) with shock waves for spatially one-dimensional problems. Further, he gave the rigorous mathematical proof that the solution thus obtained approximates the solution of the Boltzmann equation when the strength of the shock wave is weak. This restriction is a technical problem and not an essential one. Ha, Liu & Yu [2006] considered a spatially one-dimensional initial-value problem and studied the formation of a shock wave mathematically. That is, the two equilibrium states whose macroscopic variables are related by the shock condition are in contact with each other initially. The solution of the Euler set of equations for this initial condition is simply the propagation of the initial shock discontinuity, where no expansion wave appears. Thus, the time-evolution of the solution of the Boltzmann equation is the formation of a shock layer through the initial layer and its propagation. They studied this process by rigorous mathematical analysis. This supplements Yu's above-mentioned work (Yu [2005]).

4.8 Formation and propagation of a shock wave

As an example showing the formation of a shock wave and its propagation, we consider a semi-infinite expanse ($X_1 > 0$) of a gas bounded by a plane wall at

rest with temperature T_0 at $X_1 = 0$. Initially, the gas is in equilibrium with the wall at pressure p_0 and temperature T_0. At time $t = 0$, the temperature of the wall is suddenly changed to another value T_1 and is kept at T_1 for subsequent time. The time evolution of the behavior of the gas is studied numerically on the basis of the BKW equation and the diffuse-reflection condition on the wall.

The present spatially one-dimensional BKW system can be reduced to a simpler system where two molecular velocity components are eliminated. Here, we take ℓ_0, the mean free path of the gas in the equilibrium state at rest with density $\rho_0\,(= p_0/RT_0)$ and temperature T_0, as the reference length L and $\ell_0/(2RT_0)^{1/2}$ as the reference time t_0, and use the notation introduced in Section 1.9. Then, the BKW system is transformed into the following system for the marginal velocity distribution functions g and h (see Section A.6): The marginal velocity distribution functions g and h are defined by

$$g = \int\int \hat{f}\mathrm{d}\zeta_2\mathrm{d}\zeta_3, \quad h = \int\int (\zeta_2^2 + \zeta_3^2)\hat{f}\mathrm{d}\zeta_2\mathrm{d}\zeta_3, \tag{4.156}$$

and the macroscopic variables $\hat{\rho}$, $\hat{v}_1$, and $\hat{T}$ are given as

$$\hat{\rho} = \int g\mathrm{d}\zeta_1, \quad \hat{v}_1 = \frac{1}{\hat{\rho}}\int \zeta_1 g\mathrm{d}\zeta_1, \quad \hat{T} = \frac{2}{3\hat{\rho}}\int [(\zeta_1 - \hat{v}_1)^2 g + h]\mathrm{d}\zeta_1. \tag{4.157}$$

The BKW equation is reduced to

$$\frac{\partial}{\partial \hat{t}}\begin{bmatrix} g \\ h \end{bmatrix} + \zeta_1 \frac{\partial}{\partial x_1}\begin{bmatrix} g \\ h \end{bmatrix} = \frac{2}{\sqrt{\pi}}\hat{\rho}\begin{bmatrix} G - g \\ H - h \end{bmatrix}, \tag{4.158}$$

where

$$\begin{bmatrix} G \\ H \end{bmatrix} = \frac{\hat{\rho}}{(\pi\hat{T})^{1/2}}\begin{bmatrix} 1 \\ \hat{T} \end{bmatrix} \exp\left(-\frac{(\zeta_1 - \hat{v}_1)^2}{\hat{T}}\right).$$

The boundary condition on the wall is

$$\begin{bmatrix} g \\ h \end{bmatrix} = \frac{\hat{\sigma}_1}{(\pi\hat{T}_1)^{1/2}}\begin{bmatrix} 1 \\ \hat{T}_1 \end{bmatrix} \exp\left(-\frac{\zeta_1^2}{\hat{T}_1}\right) \quad (\zeta_1 > 0) \quad \text{at } x_1 = 0, \tag{4.159a}$$

$$\hat{\sigma}_1 = -2\left(\frac{\pi}{\hat{T}_1}\right)^{1/2} \int_{\zeta_1 < 0} \zeta_1 g\mathrm{d}\zeta_1, \tag{4.159b}$$

where $\hat{T}_1 = T_1/T_0$, and the condition at infinity is

$$\begin{bmatrix} g \\ h \end{bmatrix} \to \frac{1}{\sqrt{\pi}}\begin{bmatrix} 1 \\ 1 \end{bmatrix} \exp(-\zeta_1^2) \quad \text{as } x_1 \to \infty. \tag{4.160}$$

The initial condition at $\hat{t} = 0$ is

$$\begin{bmatrix} g \\ h \end{bmatrix} = \frac{1}{\sqrt{\pi}}\begin{bmatrix} 1 \\ 1 \end{bmatrix} \exp(-\zeta_1^2) \quad (x_1 > 0). \tag{4.161}$$

The marginal velocity distribution functions g and h have discontinuity at the corner $(x_1, \hat{t}) = (0, 0)$ of the domain $(x_1 > 0,\ \hat{t} > 0)$ for $\zeta_1 > 0$. In fact,

taking the limits of g and h ($\zeta_1 > 0$) in the two different orders, i.e., first $\hat{t} \to 0_+$ and then $x_1 \to 0_+$ and first $x_1 \to 0_+$ and then $\hat{t} \to 0_+$, we have

$$\lim_{x_1 \to 0_+} \left(\lim_{\hat{t} \to 0_+} \begin{bmatrix} g \\ h \end{bmatrix} \right) = \frac{1}{\sqrt{\pi}} \begin{bmatrix} 1 \\ 1 \end{bmatrix} \exp(-\zeta_1^2),$$

$$\lim_{\hat{t} \to 0_+} \left(\lim_{x_1 \to 0_+} \begin{bmatrix} g \\ h \end{bmatrix} \right) = \frac{\hat{\sigma}_{1+}}{(\pi \hat{T}_1)^{1/2}} \begin{bmatrix} 1 \\ \hat{T}_1 \end{bmatrix} \exp\left(-\frac{\zeta_1^2}{\hat{T}_1} \right),$$

where $\hat{\sigma}_{1+} = \lim_{\hat{t} \to 0_+} \hat{\sigma}_1$. The two limits do not agree unless $\hat{T}_1 = 1$. The differences of the above two kinds of the limits, i.e., the discontinuities of g and h at the corner $(x_1, \hat{t}) = (0, 0)$, propagate in the direction of the characteristic $x_1 - \zeta_1 \hat{t} = 0$ of Eq. (4.158) and decay owing to the collision term on its right-hand side. The direction of the propagation depends on ζ_1. For $\zeta_1 < 0$, the characteristic starts from infinity, where g and h are continuous, and therefore they are continuous for all x_1 and $\hat{t}$. In the numerical computation, the standard finite-difference scheme has a difficulty that it involves differentiation processes across the discontinuity; some improvement is required.

In the numerical computation of a time-evolution problem, the distributions g and h for each ζ_1 at the time step $\hat{t} = \hat{t}_{i+1}$ are obtained from the data of the previous stages independently of those for the other values of ζ_1, because the interaction between different ζ_1's enters through $\hat{\rho}$, $\hat{v}_1$, and $\hat{T}$ in G and H for which the data at $\hat{t} = \hat{t}_i$ and before are used. Thus, the discontinuity is only on the line $x_1 - \zeta_1 \hat{t} = 0$ (with ζ_1 under concern), and this enables us a simple modification to treat the discontinuity with a good accuracy.

For $\zeta_1 < 0$, there is no discontinuity, and g and h at $\hat{t} = \hat{t}_{i+1}$ are computed by a standard finite-difference scheme from $x_1 = \infty$ to $x_1 = 0$. For $\zeta_1 > 0$, we have to take care of the discontinuity $x_1 - \zeta_1 \hat{t} = 0$. When the standard finite-difference formula to obtain g and h at $(\hat{t}_{i+1}, x_{1j})$ contains the lattice points only on the same side of the discontinuity, we can use this formula to obtain the data at $(\hat{t}_{i+1}, x_{1j})$. The approach for the other case is explained for the first-order implicit scheme. First compute the data on both sides $x_1 - \zeta_1 \hat{t}_i = 0_\pm$ of the discontinuity by extrapolation from the data on the lattice points along $\hat{t} = \hat{t}_i$. With these as the initial data, integrate Eq. (4.158) along its characteristic (or the discontinuity) $x_1 - \zeta_1 \hat{t} = 0$ up to $\hat{t} = \hat{t}_{i+1}$, and prepare the data of g and h at the point where the characteristic crosses the lattice lines. If the point $(\hat{t}_i, x_{1j})$ is on the other side of $(\hat{t}_{i+1}, x_{1j})$ across the discontinuity, let the time derivatives of g and h be expressed by the data at $(\hat{t}_{i+1}, x_{1j})$ and at $(\hat{t}_{D+}, x_{1j})$, which is the point on the discontinuity on the side $x_1 - \zeta_1 \hat{t} = 0_-$. If the point $(\hat{t}_{i+1}, x_{1j-1})$ is on the other side of $(\hat{t}_{i+1}, x_{1j})$ across the discontinuity, which appears in the implicit formula, let the space derivatives of g and h be expressed by the data at $(\hat{t}_{i+1}, x_{1j})$ and at $(\hat{t}_{i+1}, x_{1D+})$, which is the point $x_1 - \zeta_1 \hat{t}_{i+1} = 0_+$ on the discontinuity. Thus, we obtain a *hybrid difference scheme* consisting of the standard finite-difference scheme and the characteristic method. The more explicit description of the hybrid scheme, which is devised by Sone & Sugimoto [1990], is given in Aoki, Sone, Nishino & Sugimoto [1991].

Two examples of the numerical computation of the problem in Aoki, Sone,

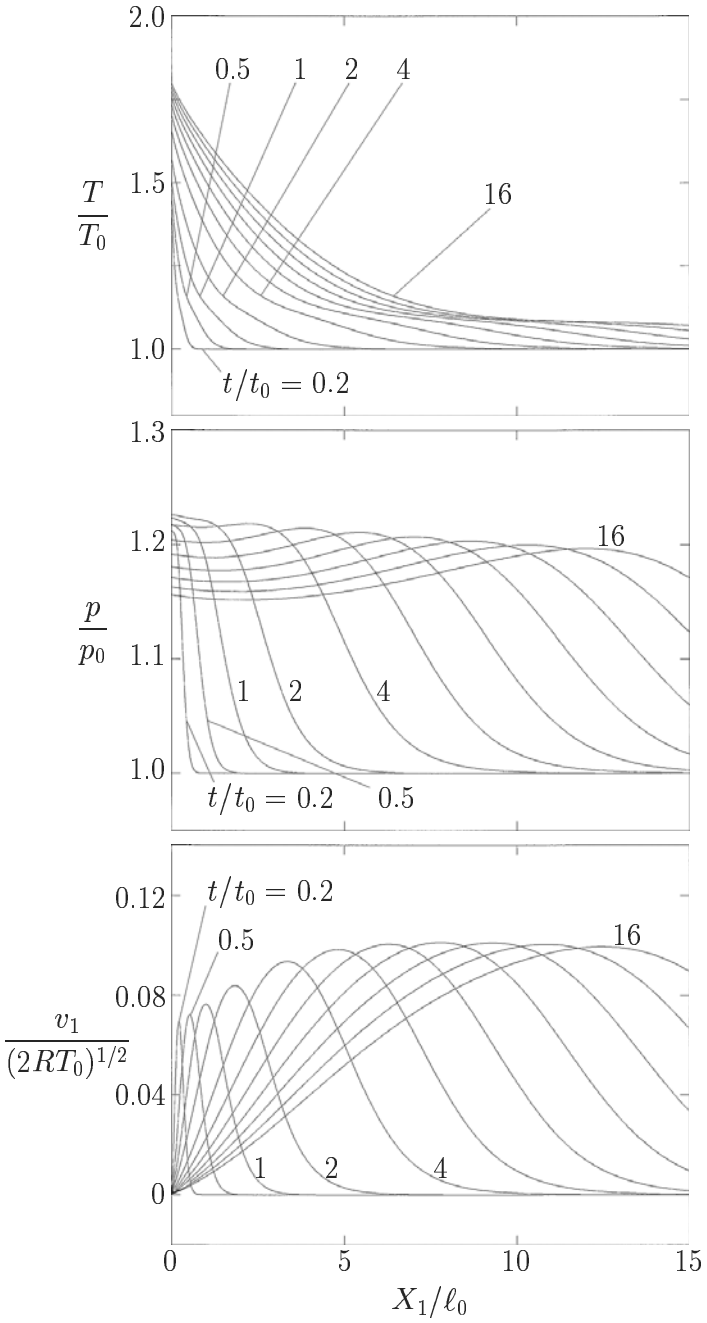

Figure 4.19. Formation of a shock wave by a sudden change of the wall temperature from T_0 to $2T_0$ at time $t = 0$ I: Initial stage.

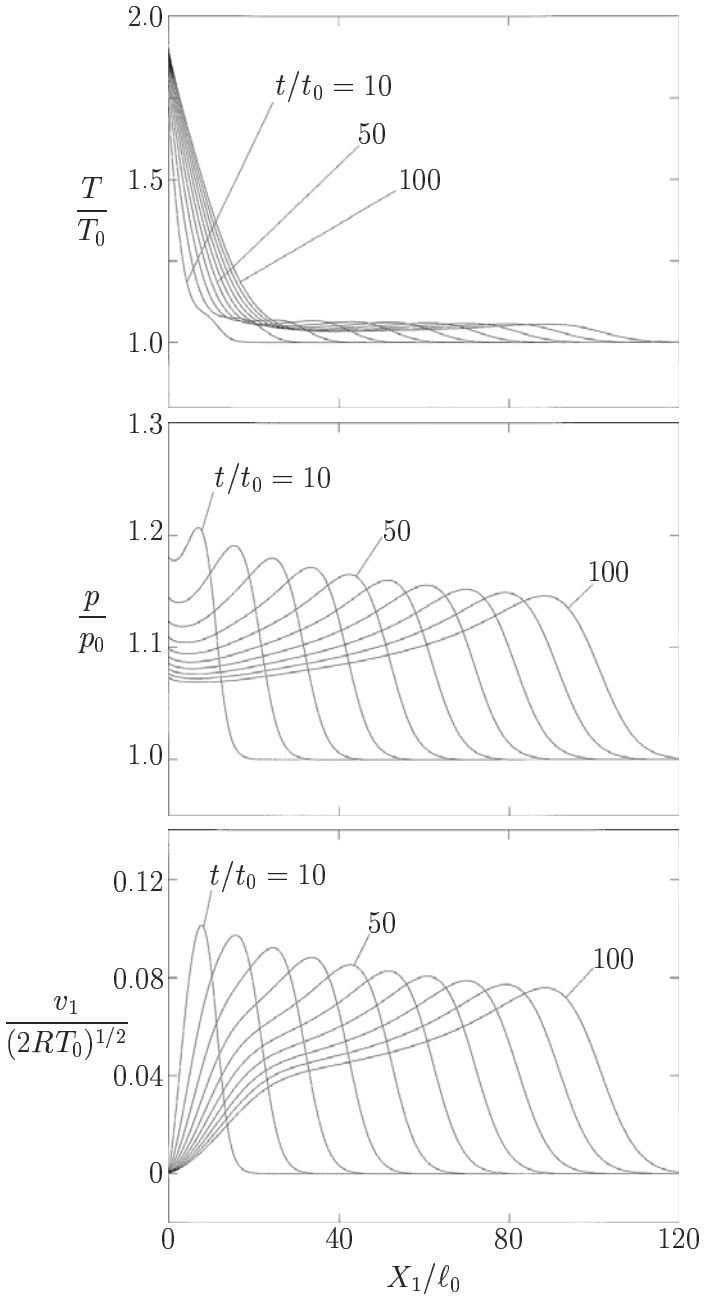

Figure 4.20. Formation of a shock wave by a sudden change of the wall temperature from T_0 to $2T_0$ at time $t = 0$ II: Intermediate stage.

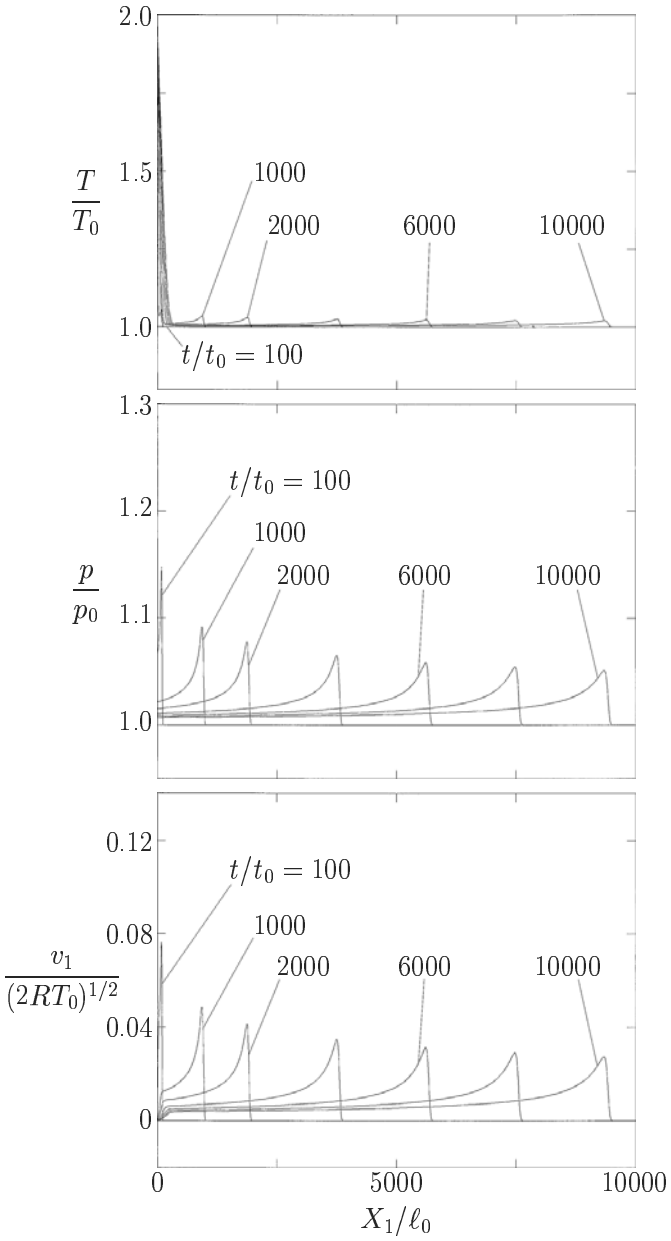

Figure 4.21. Formation of a shock wave by a sudden change of the wall temperature from T_0 to $2T_0$ at time $t = 0$ III: Long-time behavior.

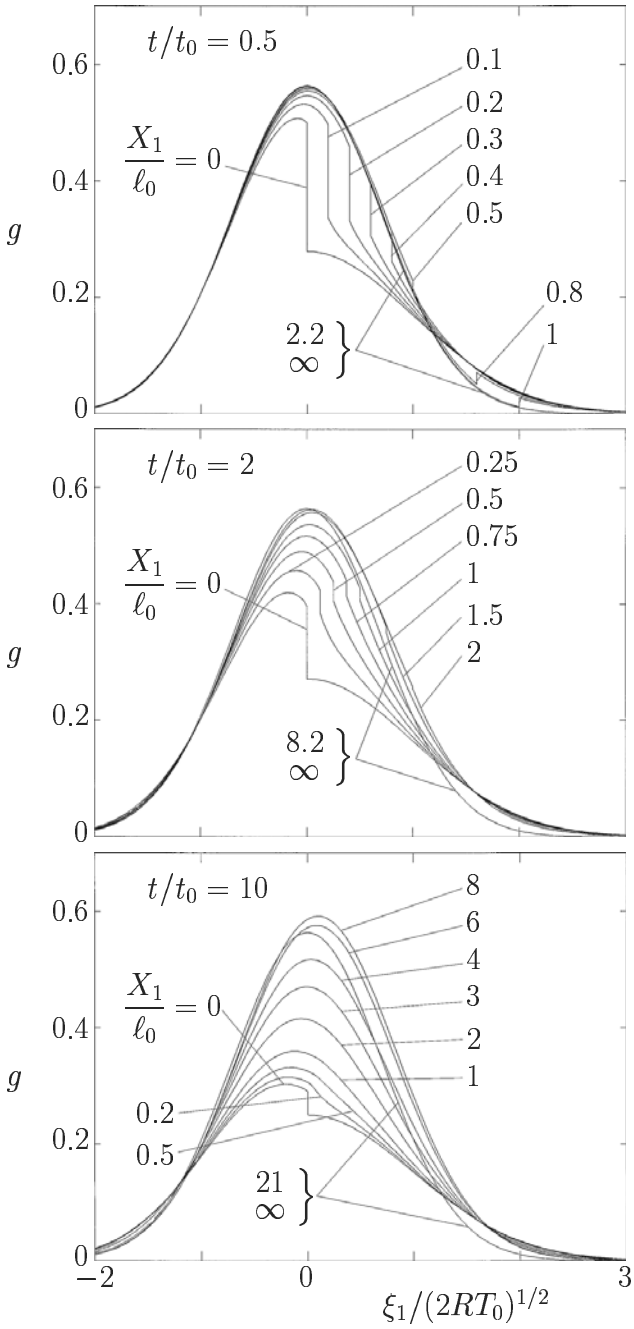

Figure 4.22. Discontinuity of the marginal velocity distribution function g by a sudden change of the wall temperature from T_0 to $2T_0$ at time $t = 0$.

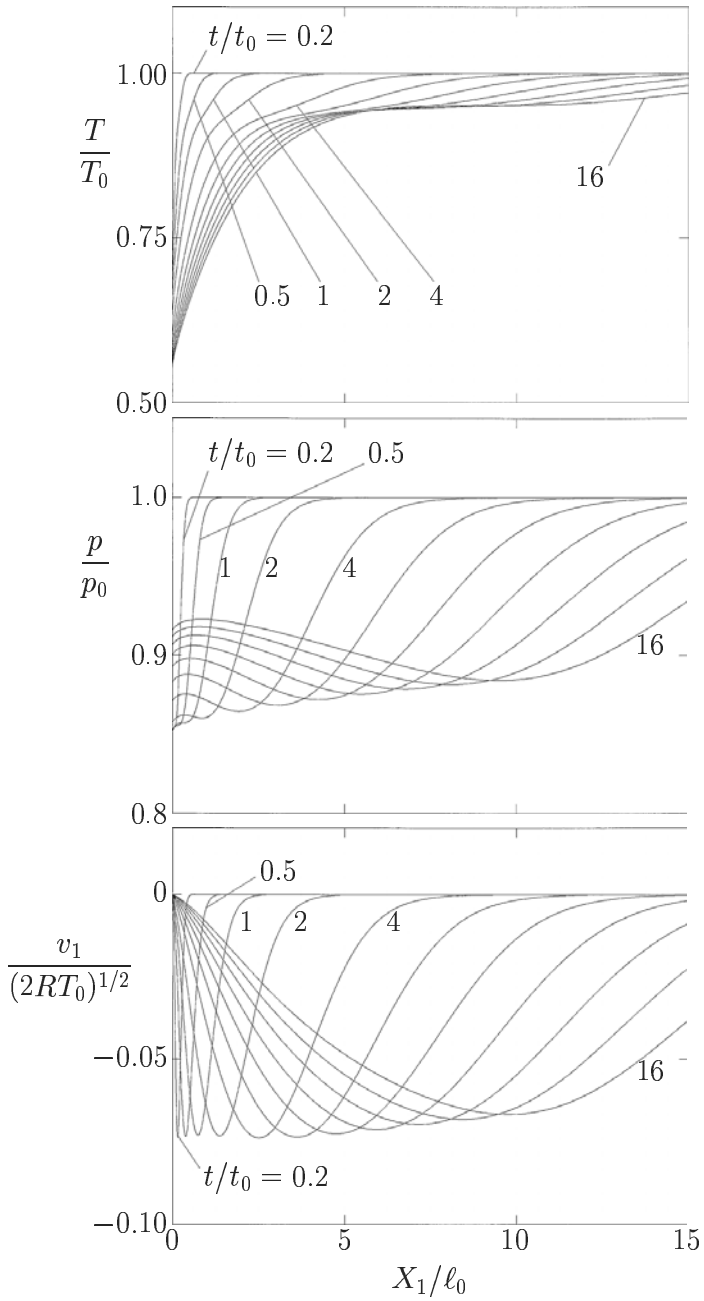

Figure 4.23. Formation of an expansion wave by a sudden change of the wall temperature from T_0 to $T_0/2$ at time $t = 0$ I: Initial stage.

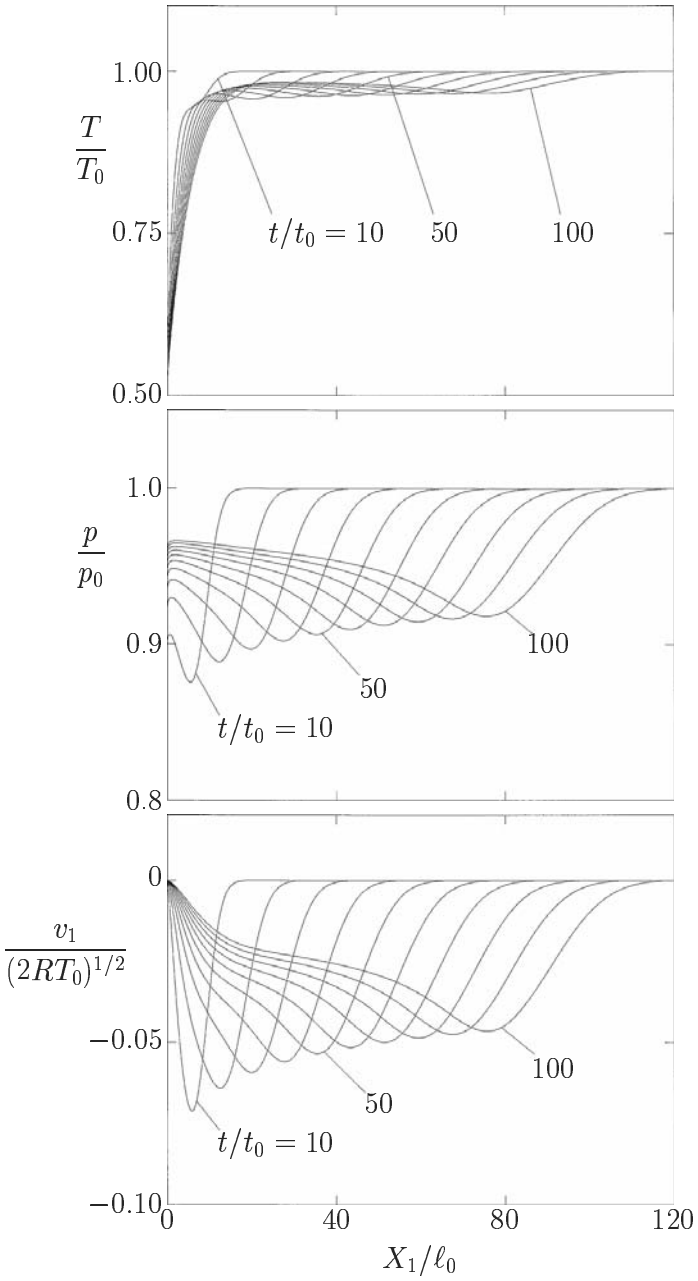

Figure 4.24. Formation of an expansion wave by a sudden change of the wall temperature from T_0 to $T_0/2$ at time $t = 0$ II: Intermediate stage.

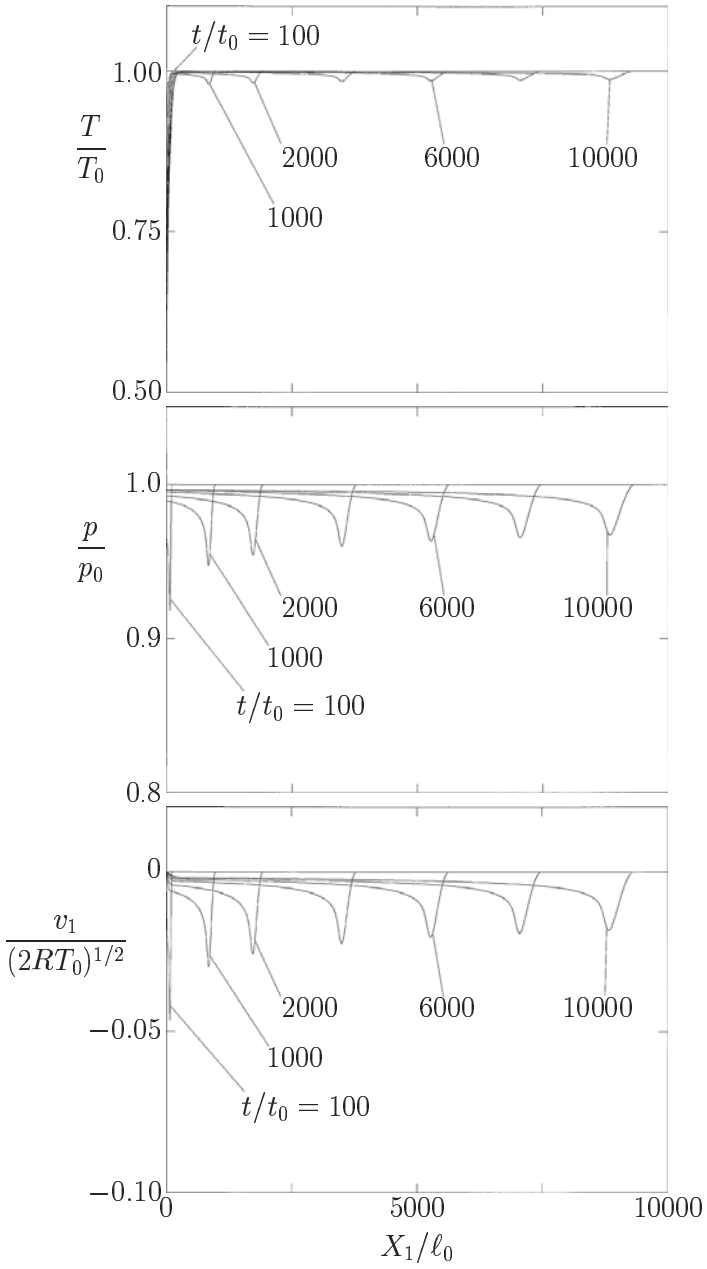

Figure 4.25. Formation of an expansion wave by a sudden change of the wall temperature from T_0 to $T_0/2$ at time $t = 0$ III: Long-time behavior.

Nishino & Sugimoto [1991], where the plate is suddenly heated and cooled, are shown here. The case where the temperature of the wall is suddenly raised from T_0 to $T_1 = 2T_0$ is given in Figs. 4.19–4.22. In Figs. 4.19–4.21, the time evolution of the temperature T, pressure p, and velocity v_1 fields are plotted.[39] With the sudden rise of the wall temperature, the gas close to the wall is heated and accordingly the pressure rises sharply near the wall, which pushes the gas away from the wall and a shock wave (or compression wave) propagates into the gas. As time goes on, the gas moves away from the wall but there is no gas supply from the wall, and the heat transferred from the wall to the gas decreases owing to the rise of the temperature of the gas near the wall. Accordingly, the pressure decrease due to the escape of the gas is not compensated by the heating, and the pressure gradually decreases. As a result, an expansion wave propagates toward the shock wave from behind and attenuates the shock wave together with another dissipation effect. The main temperature rise of the gas occurs gradually well after the shock wave passed; this process is due to the conduction of heat. In Fig. 4.22, the marginal velocity distribution function g at various X_1/L is plotted for $t/t_0 = 0.5$, 2, and 10. The marginal velocity distribution function g has discontinuity at $(t,\ X_1) = (0, 0)$ as shown above. As time goes on, the position of the discontinuity shifts to $X_1 = \zeta_1 t(2RT_0)^{1/2}$, and the size of the discontinuity decreases owing to molecular collisions.

The corresponding results for the case where the temperature of the wall is suddenly lowered from T_0 to $T_1 = T_0/2$ are given in Figs. 4.23–4.25, where the roughly opposite process occurs (compression wave $\rightarrow$ expansion wave). That is, by the cooling of the gas near the wall, the pressure decreases there and an expansion wave propagates into the gas. The expansion wave sends a gas towards the wall. As time goes on, with the decrease of the temperature of the gas near the wall, the suction of heat from the gas by the wall decreases and thus the pressure decrease becomes weaker. Thus, the gas begins to accumulate near the wall, because there is no suction on the wall and the pressure drop by cooling is not strong enough to compensate the gas flow. Then, a compression wave chases the expansion wave to attenuate. The main temperature drop of the gas occurs gradually well after the expansion wave passed, as in the first example.

When the temperature rise or drop of the wall is small, i.e., $|T_1/T_0 - 1| \ll 1$, the problem is studied analytically on the basis of the linearized BKW equation (Sone [1965]), which is compared with the numerical result for small data for $|T_1/T_0 - 1|$ in Aoki, Sone, Nishino & Sugimoto [1991].

[39] The time is measured in the scale of the mean free time in the computation. In the atmospheric condition the mean free time is about 2×10^{-10} s. Thus, one second is a very long time (more than $t/t_0 = 10^9$) in the reference time of the above computation. See Footnote 102 in Section 3.6.2.

Chapter 5

Flows Induced by Temperature Fields

In the framework of the classical fluid dynamics, no time-independent flow is induced in a gas without an external force, such as the gravity, by the effect of its temperature field. In a rarefied gas, on the other hand, the temperature field of a gas (often in combination with a solid boundary) plays an important role in inducing time-independent flows. Two examples were discussed in Sections 4.2, 4.3, and 4.6.2. In this chapter, we will discuss various flows induced by temperature fields and their application to a vacuum pump without a moving part.

5.1 Flows in a slightly rarefied gas

In Chapter 3, we carried out the asymptotic analysis of the Boltzmann system for small Knudsen numbers and derived the fluid-dynamic-type equations and their associated boundary conditions that describe the behavior of a gas for small Knudsen numbers. From this system we can find flows induced by temperature fields, as we have already pointed out. These are characterized by the local behavior of the temperature field of the gas.

5.1.1 Thermal creep flow

According to the slip boundary condition derived in Chapter 3, i.e., Eq. (3.41a), (3.57a), (3.114a), (3.120a), (3.161b), or (3.162c), a flow velocity along a boundary is imposed as the boundary condition for the fluid-dynamic-type equations in Sections 3.1.2, 3.2.2, or 3.3.3 when the temperature of the boundary is not uniform. This flow characterized by the temperature gradient of the boundary along it is called *thermal creep flow*.

Consider a gas ($X_2 > 0$) bounded by a plane wall at $X_2 = 0$ with a small temperature gradient $\mathrm{d}T_w/\mathrm{d}X_1$ along the wall. According to the Stokes set of

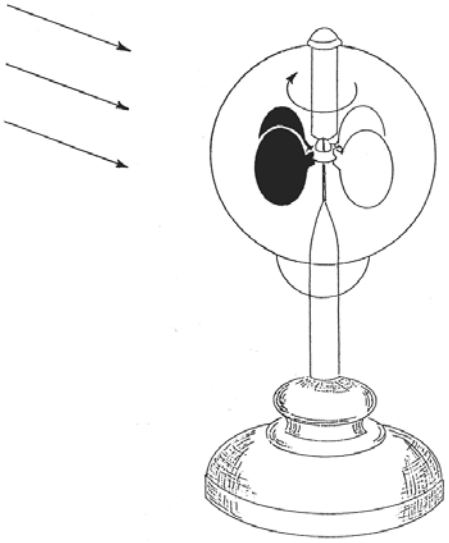

Figure 5.1. Radiometer.

equations in Section 3.1.2 and the slip boundary condition in Section 3.1.5, the velocity and temperature fields are found to be given as follows:[1]

$$\left.\begin{aligned} v_1 &= -\left(\frac{\pi RT_0}{2}\right)^{1/2} \frac{\ell_0}{T_0}\frac{\mathrm{d}T_w}{\mathrm{d}X_1}[K_1 + \tfrac{1}{2}Y_1(2X_2/\sqrt{\pi}\ell_0)], \\ v_2 &= v_3 = 0, \\ T &= T_0 + \frac{\mathrm{d}T_w}{\mathrm{d}X_1}X_1, \end{aligned}\right\} \tag{5.1}$$

where T_w is the temperature of the wall and T_0 is the temperature at $X_1 = 0$. The flow is in the direction of the temperature gradient of the wall[2] and uniform except in the neighborhood of the plane wall of the order of the mean free path ℓ_0, and the temperature of the gas is uniform with respect to X_2.

The thermal creep flow is known for a long time (Maxwell [1879]), but its rigorous formulation on the basis of the Boltzmann equation is done much later (Sone [1966b, 1970]).[3] The rotation of the windmill in the famous *radiometer*

[1] We are interested in the range $|X_1| < X_0$ of a gas over a plane wall, where $X_0 \gg \ell_0$. When the temperature variation in the range is small, i.e., $(X_0/T_0)|\mathrm{d}T_w/\mathrm{d}X_1| \ll \ell_0/X_0$, the Stokes set of equations and their associated boundary conditions can be applied in the range of the gas, and the flow field is expressed by Eq. (5.1). The present situation corresponds to the case where $\mathrm{d}p/\mathrm{d}X_1 = 0$ and the wall at $X_2 = L$ goes to infinity (or $L \to \infty$ and accordingly $k \to 0$) in Section 4.2.2.

[2] This is the case of a hard-sphere gas or the BKW model, for which K_1 is negative.

[3] In these papers, the problem over a plane wall is directly studied without using the asymptotic theory. Owing to the degeneracy due to the simple geometry, the thermal creep

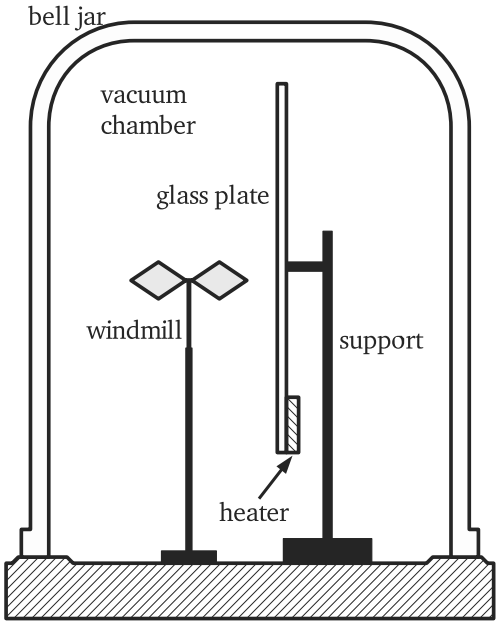

Figure 5.2. Experimental apparatus for the thermal creep flow.

(Fig. 5.1)[4] is explained by the thermal creep flow in, e.g., Kennard [1938]. This is not a direct demonstration of a flow induced along a wall with a temperature gradient. An experiment is devised to show this clearly by Sone [1991b].[5] The experimental apparatus as shown in Fig. 5.2 is prepared. A rectangular glass plate (70×200 mm) is set in space with its longer sides in the vertical direction, and an electric heater of Nichrome wire is placed near the lower end of the back of the plate. A windmill with cellophane vanes to detect vertical flow is placed in front of the plate. The whole system is placed in a cylindrical vacuum chamber (diameter 250 mm, height 300 mm) of a glass bell jar on a steel base, where the pressure can be controlled from the atmospheric condition down to several pascals (Pa = kg/m s^2). When the plate is heated, the temperature of the plate is about 34°C near its upper end, 65°C at the height of the windmill, and 140°C in the heated region. When the plate is not heated, the windmill remains at rest for the whole pressure range. When the plate is heated and the gas is at the atmospheric condition, the windmill rotates at 110 rpm (revolutions

flow appears with a different value (but of the same order) of the slip coefficient also in the limit that the accommodation coefficient α in the Maxwell-type boundary condition tends to zero, in contrast to the case of general situation. See the note (vii) after Eq. (3.42c) and compare Sone [1970] and the references there.

[4]A set of vanes blackened on one side is suspended on an axis in an exhausted glass vessel. The vanes rotate on exposure to sunlight. It is now sold as an ornament.

[5]The video file of the experiment can be downloaded at http://fd.kuaero.kyoto-u.ac.jp/members/sone.

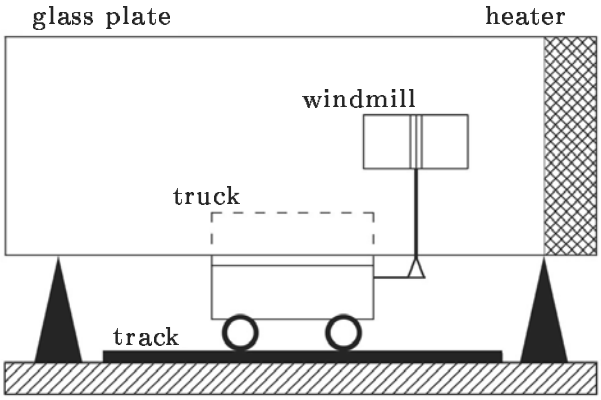

Figure 5.3. A plate with a heater and a movable windmill.

per minute), from which an upward flow is seen to be induced in front of the plate. This flow is attributed to natural convection. As the pressure in the chamber is decreased, the rotation of the windmill becomes gradually slower and stops at about 1400 Pa. As the pressure is decreased further, the windmill begins to rotate again at about 40 Pa but in the opposite direction, and its speed increases and reaches about 60 rpm at 13 Pa and about 140 rpm at 3 Pa. From the direction of rotation of the windmill, the flow is downwards or in the direction of the temperature gradient. Incidentally, the mean free path at 13 Pa is about 0.5 mm. The experiment, though only qualitative with rough data for reference, clearly demonstrates a flow induced by the temperature gradient of a wall in a simple way. The flow in a rarefied gas makes good contrast to the natural convection in atmospheric condition.

The above experiment is made a little quantitative by a simple improvement in Sone, Sawada & Hirano [1994], where the dependence of the flow on the temperature gradient of the wall and on the pressure of the gas is examined. A rectangular glass plate ($70 \times 200 \times 5$ mm) is set in space with its 70 mm side in the vertical direction, and an electric heater (70×32 mm) of Nichrome wire is attached on the back of one of the horizontal end of the plate. A track of a HO gauge model railway is placed parallel to and at the back of the plate. A truck with an electric motor and an arm stretching to the front side of the plate is on the track (Fig. 5.3). Thus, the position of the windmill along the plate can be adjusted freely by moving the truck. Polypropylene vanes (5.1 mg) of the windmill are suspended on a needle and rotate when there is a horizontal flow. The vane-tip speed is 57 mm/s when the vanes rotate at 100 rpm. The whole system is placed in a vacuum chamber of the bell jar used in the preceding experiment (Fig. 5.2). The temperature gradient is in the horizontal direction and decreases with the distance from the heater. Shifting the position of the truck and observing the speed of rotation of the windmill, we find the relation between the speed of rotation and the temperature gradient along the wall. The experimental result of the relation is given in Fig. 5.4. The experiment is done

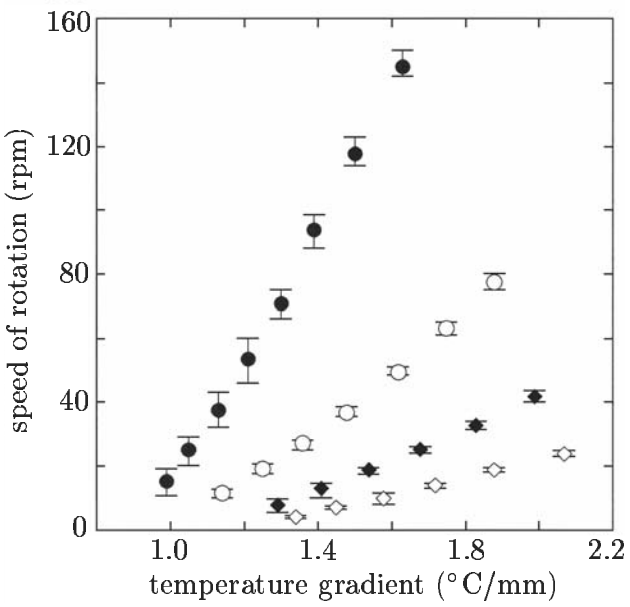

Figure 5.4. The speed of rotation (rpm) vs the temperature gradient (°C/mm) along the plate. Each mark shows the average value of several experiments. The two parallel bars on a mark show the variation of the data. The black circle • is the data at 6.7 Pa; ○ : at 13.3 Pa; ♦ : at 26.7 Pa; and ◇ : at 53 Pa. The vane-tip speed is 57 mm/s when the vanes rotates at 100 rpm.

in the pressure range 6 – 55 Pa, which is in a slip flow regime. The speed of rotation is roughly linear in the local temperature gradient of the plate. The slope of the approximate line, i.e., the speed of rotation vs the temperature gradient, is nearly inversely proportional to the pressure of the gas (or nearly proportional to the mean free path).

In order to understand the physical mechanism of the thermal creep flow, consider a gas at rest with a temperature gradient in the two situations shown in Figs. 5.5 (a) and (b), in the latter of which the gas is bounded by a wall. Let us examine the momentum transmitted by the molecules impinging on a small area dS from its upper side. The molecules impinging on dS come from various directions directly (or without molecular collisions) over a distance of the order of the mean free path, keeping the property of their origins. The average speed of molecules arriving from the hotter region is larger than that from the colder region. In the gas at rest, the pressure is uniform and the density is lower in the hotter side; the number of the molecules impinging on dS from the hotter side per unit time is the same as that from the colder side. Thus, the momentum transferred to dS by the molecules impinging on it has a component in the direction opposite to the temperature gradient, because the average speed of molecules from the hotter side is larger.

When the area dS lies in the middle of the gas [Fig. 5.5 (a)], where the state

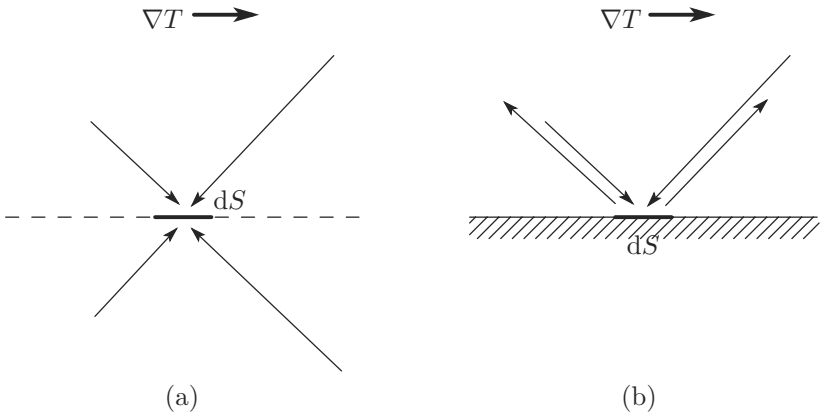

Figure 5.5. A gas with a temperature gradient. (a) A gas without a boundary and (b) a gas bounded by a wall.

is symmetric with respect to the dotted line, the molecules impinging on dS from its lower side carry the momentum in the direction opposite to the temperature gradient from the lower side to the upper side. Therefore, there is no exchange of momentum through dS. On the other hand, when the area dS is on the wall [Fig. 5.5 (b)], the situation is quite different. The contribution of the molecules leaving the wall to the tangential component of the momentum transfer is nothing in the case of the diffuse reflection. (Generally except in the specular reflection, the velocity distribution function of the molecules leaving the wall, characterized by the wall condition, is qualitatively different from that of the impinging molecules, formed by collisions of surrounding gas molecules. Thus the two contributions are generally different.) Thus, a momentum in the direction opposite to the temperature gradient is transferred to dS from the gas. As its reaction, the gas is subject to a force in the direction of the temperature gradient, and a flow is induced in that direction. In a gas in motion, a momentum in the direction of motion is transferred to the wall or dS. Thus, a time-independent flow is established when the two contributions of momentum transfer balance. Obviously from the above explanation, the boundary (or the qualitative difference between the velocity distribution functions of the molecules impinging on the boundary and of those leaving there) plays an essential role in inducing the thermal creep flow. Incidentally, by simple physical discussions similar to the above, we can easily understand flows induced over a wall in different situations, a straightforward extension of the thermal creep flow or a new situation. A flow induced over a wall with a discontinuous temperature distribution is the former example,[6] whose numerical example by the BKW equation is given in Aoki, Takata, Aikawa & Golse [2001]. The latter example that is not expected before is the thermal edge flow explained in Section 5.1.4.

[6]Needless to say, the discontinuity itself is not essential to induction of flow.

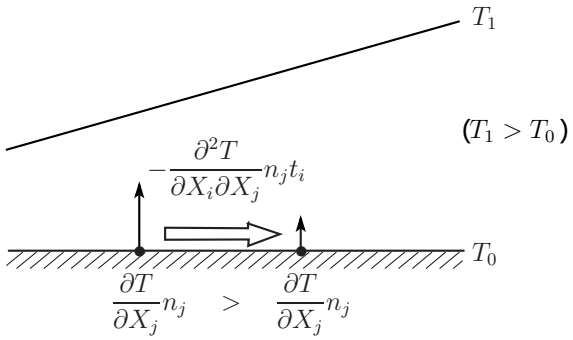

Figure 5.6. Thermal stress slip on a boundary with a uniform temperature. When the isothermal lines are not parallel in a neighborhood of the boundary, the thermal-stress slip flow is induced as shown by the white arrow.

5.1.2 Thermal-stress slip flow

This flow was pointed out on the basis of the asymptotic theory in Sone [1971]. In the slip boundary conditions (3.42a) and (3.42b) at the second order in k, there are various terms determined by the temperature field. However, all of them except the term $a_4 n_j t_i \partial G_{iG0}/\partial x_j$ in Eq. (3.42a) vanish when the temperature of the boundary is uniform, i.e., $t_i \partial \tau_w/\partial x_i = 0$, or when the thermal creep flow is absent. Corresponding to this remaining term, another type of flow, different from the thermal creep flow, is induced by the temperature field in the gas. Over a boundary of a uniform temperature, the term $a_4 n_j t_i \partial G_{iG0}/\partial x_j$ is rewritten as

$$a_4 \frac{\partial G_{iG0}}{\partial x_j} n_j t_i = -a_4 \frac{\partial^2 \tau_{G0}}{\partial x_i \partial x_j} n_j t_i = -a_4 t_j \frac{\partial}{\partial x_j} \left(n_i \frac{\partial \tau_{G0}}{\partial x_i} \right),$$

because the derivative of n_i along the boundary is parallel to the boundary. When the temperature gradient $n_i \partial \tau_{G0}/\partial x_i$ normal to the boundary is not uniform over the boundary or the isothermal surface ($\tau_{G0} = \text{const}$) is not parallel to the boundary, a flow is induced in the direction that the isothermal surfaces are diverging or converging, depending on whether the temperature of the boundary is lower or higher than that of the surrounding gas (Fig. 5.6).[7] The flow is called *thermal-stress slip flow* because the slip velocity $a_4 n_j t_i \partial G_{iG0}/\partial x_j$ is proportional to the thermal stress given in Eq. (3.21) and due to the thermal stress as explained below. One may naturally think that the flow is a kind of thermal creep flow due to the modified temperature field induced by the first-order temperature jump (3.41c); but this is in the direction opposite to the thermal-stress slip flow, and therefore the thermal-stress slip flow is a new type of flow. Several examples of the flow have been studied (Sone [1972, 1974], Sone

[7] This is the case of a hard-sphere gas or the BKW model under the Maxwell-type condition as well as the diffuse-reflection condition, for which a_4 in Eq. (3.42a) is positive (Sone, Aoki & Onishi [1977], Ohwada & Sone [1992]).

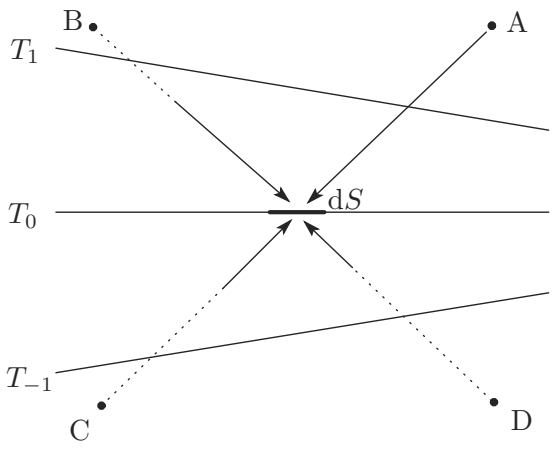

Figure 5.7. Source of thermal stress. The stress on the surface element dS is the momentum flux through dS. The difference of the average molecular speeds among the molecules arriving at the surface element dS from various directions (say from A, B, C, D) owing to their different temperatures at their origins causes a stress on dS.

& Tanaka [1980]).

Consider a small area dS in a gas with a nonuniform temperature gradient as shown in Fig. 5.7 and examine the momentum transfer through dS. The molecules impinging on dS come from various directions directly (or without molecular collisions) over a distance of the order of the mean free path ℓ, keeping the property of their origins. The average speed of molecules arriving from the hotter region is larger than that from the colder region. In view of the temperature field around dS, the molecules impinging on dS may be represented by those from the four points A, B, C, and D about one mean free path away from dS in the figure. By a discussion similar to that in the thermal creep flow (Section 5.1.1), the momentum transferred by the molecules from A, B, C, or D, compared with the uniform temperature case, is proportional to the temperature difference between the point A, B, C, or D and dS. Therefore, noting the sign of contribution, as discussed in Section 5.1.1, and the distance of A, B, C, or D from dS, we can estimate the tangential stress, i.e., the tangential momentum flux through dS from its lower side to it upper side, as

$$\text{Stress} \sim T_A - T_B + T_C - T_D \sim \ell^2 \frac{\partial^2 T}{\partial X_1 \partial X_2},$$

where the temperature T_0 at dS is cancelled out. This conforms with the thermal stress in Eq. (3.21).

Now, we consider how the thermal-stress slip flow is induced by the thermal stress. Take a control surface ABCD in a gas at rest with a nonuniform temperature gradient as shown in Fig. 5.8 (a). The contribution of the thermal force on the volume of the gas surrounded by ABCD vanishes when integrated

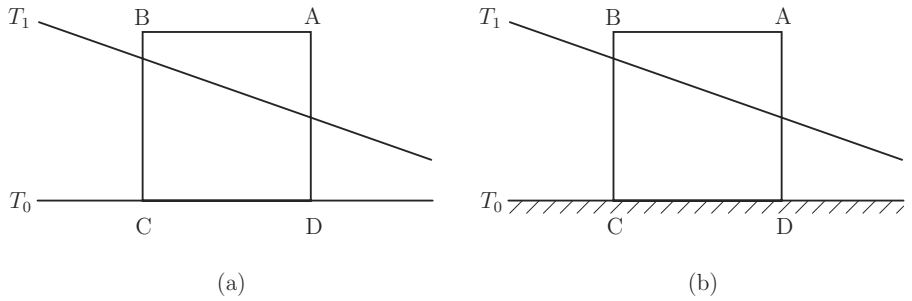

Figure 5.8. Control surface ABCD for explanation of the cause of thermal-stress slip flow. (a) The control surface is in a gas and (b) the part CD of the control surface is on a wall.

over ABCD if the linear theory in Section 3.1.3 is applicable.[8] When the gas is bounded by a wall as shown in Fig. 5.8 (b), the situation is different. The most part of the sides BC and AD (thus, AB) being taken outside the Knudsen layer, the thermal stress (the momentum transfer owing to the temperature variation) is roughly the same as before on AB, BC, and AD, but the momentum transfer on the wall (or CD) is quite different from that in the gas. The momentum transfer due to the molecules impinging on CD, which corresponds to the contribution $T_A - T_B$ in the preceding paragraph, is roughly a half of the total transfer on CD in the gas, and the transfer due to the molecules leaving CD on the wall has no tangential contribution in case of the diffuse reflection. Therefore, the momentum transfer on CD is reduced to about a half by replacing CD in the gas [Fig. 5.8 (a)] by a wall [Fig. 5.8 (b)]. Thus, the balance of the thermal stress on ABCD is violated and a flow is induced. This is the thermal-stress slip flow. As in the thermal creep flow, the boundary wall (or the qualitative difference between the velocity distribution functions of the molecules impinging on the boundary and of those leaving there) plays an essential role in inducing the flow.

As an example of the thermal-stress slip flow, consider a gas between two parallel noncoaxial circular cylinders with different uniform temperatures T_1 and T_2 (Sone & Tanaka [1980]). Then, no thermal creep flow is induced because of uniform temperature on each cylinder. The isothermal surfaces being not parallel between the noncoaxial cylinders, the thermal-stress slip flow is induced between the cylinders as shown in Fig. 5.9, where streamlines are shown with arrows indicating the direction of flow when the outer cylinder is heated ($T_2 > T_1$).[9] The thermal-stress slip flow plays an important role in causing negative thermophoresis (see Section 5.3).

[8] The thermal stress in Eq. (3.21) integrated over ABCD is seen to vanish with the aid of Eq. (3.13c). This corresponds to the absence of a thermal stress term in Eq. (3.13b) of the Stokes set of equations.

[9] The flow velocity differs only by a factor a_4 for different molecular models and kinetic boundary conditions. Thus, the profile of the streamlines is the same with the difference of a factor of their values.

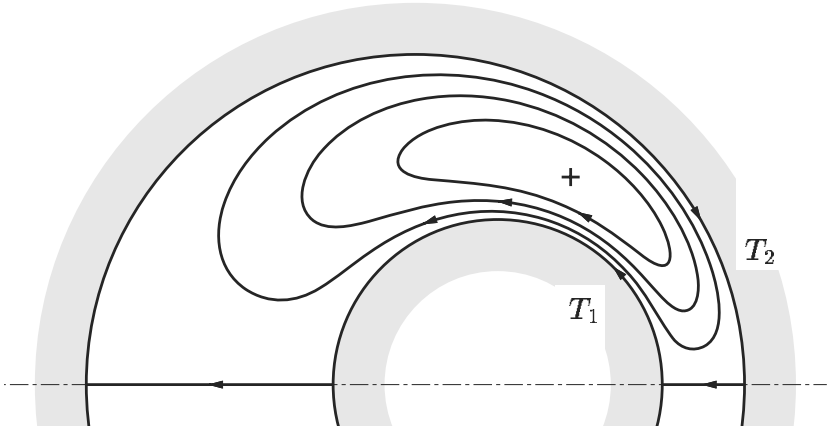

Figure 5.9. Thermal-stress slip flow induced in a gas between parallel noncoaxial circular cylinders with different uniform temperatures T_1 and T_2. The direction of flow is shown by arrows on streamlines when the temperature T_2 of the outer cylinder is higher than the temperature T_1 of the inner ($T_2 > T_1$).

5.1.3 Nonlinear-thermal-stress flow

In Section 3.3.4, we have seen that even in the absence of an external force, a gas cannot be at rest unless the isothermal lines are parallel or unless

$$\frac{\partial \hat{T}_{SB0}}{\partial x_i}\frac{\partial}{\partial x_j}\left(\frac{\partial \hat{T}_{SB0}}{\partial x_k}\right)^2 - \frac{\partial \hat{T}_{SB0}}{\partial x_j}\frac{\partial}{\partial x_i}\left(\frac{\partial \hat{T}_{SB0}}{\partial x_k}\right)^2 = 0. \tag{5.2}$$

The flow is called *nonlinear-thermal-stress flow*.

In a gas with a temperature variation, a stress, i.e., thermal stress, is induced. In the linear problem discussed in Section 3.1, the stress over a control surface in the gas balances[10] and there is no contribution to the Stokes set of equations (3.12)–(3.13c). In the weakly nonlinear problem in Section 3.2, there is a contribution to Eq. (3.89b) as

$$-\frac{\gamma_3}{3}\frac{\partial}{\partial x_i}\frac{\partial^2 \tau_{S1}}{\partial x_j^2}.$$

This term is, however, incorporated in the pressure term, and thus, does not work to induce a flow [see Sections 3.2.2 (the last paragraph) and 3.2.4].[11] When

[10] See Footnote 8 in Section 5.1.2.

[11] When the boundary is a simple boundary at rest and the flow speed at infinity vanishes (or no flow is imposed at infinity) if the domain extends to infinity, $\partial^2 \tau_{S1}/\partial x_j^2$ itself vanishes. In fact, from Eqs. (3.88a), (3.88b), (3.113a), and the condition at infinity, $u_{iS1} = 0$ and $P_{S2} =$ const [the uniqueness of solution is assumed; the uniqueness holds for a bounded domain (see Temam [1984])]. Thus, from Eq. (3.88c), $\partial^2 \tau_{S1}/\partial x_j^2 = 0$.

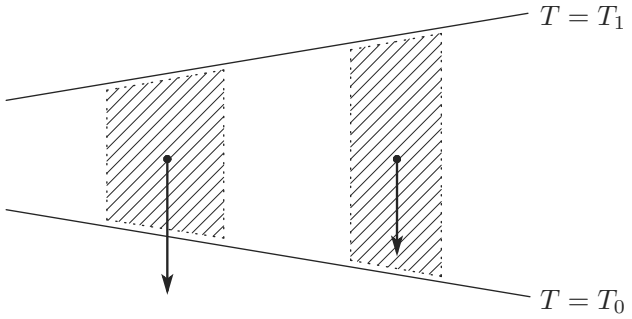

Figure 5.10. Body force due to the nonlinear thermal stress not incorporated in pressure term for $\hat{v}_{jSB1} = 0$, i.e., the contribution of the second term in the square brackets in the expression (5.4). The force acting on the shaded portion of the gas is shown by the arrow for a hard-sphere gas and the BKW model when $T_1 > T_0$.

the temperature variation is not small, the thermal stress appears in Eq. (3.160):

$$\hat{\rho}_{SB0}\hat{v}_{jSB1}\frac{\partial \hat{v}_{iSB1}}{\partial x_j} = -\frac{1}{2}\frac{\partial \hat{p}^{\dagger}_{SB2}}{\partial x_i} + \hat{\rho}_{SB0}\hat{F}_{i2} + \frac{1}{2}\frac{\partial}{\partial x_j}\left[\Gamma_1\left(\frac{\partial \hat{v}_{iSB1}}{\partial x_j} + \frac{\partial \hat{v}_{jSB1}}{\partial x_i} - \frac{2}{3}\frac{\partial \hat{v}_{kSB1}}{\partial x_k}\delta_{ij}\right)\right] + \left[\frac{\Gamma_7}{\Gamma_2}\frac{\hat{v}_{jSB1}}{\hat{T}_{SB0}}\frac{\partial \hat{T}_{SB0}}{\partial x_j} + \frac{\Gamma_2^2}{4\hat{p}_0}\frac{\mathrm{d}\Gamma_7/\Gamma_2^2}{\mathrm{d}\hat{T}_{SB0}}\left(\frac{\partial \hat{T}_{SB0}}{\partial x_j}\right)^2\right]\frac{\partial \hat{T}_{SB0}}{\partial x_i}, \quad (5.3)$$

where a part of the thermal stress is incorporated in the pressure term $\hat{p}^{\dagger}_{SB2}$, as shown in Eq. (3.159), and the remaining part of the thermal stress is the last term on the right-hand side.

Comparing $\hat{\rho}_{SB0}\hat{F}_{i2}$ and the thermal stress term, we find that

$$\frac{\hat{T}_{SB0}k^2}{\hat{p}_0}\left[\frac{\Gamma_7}{\Gamma_2}\frac{\hat{v}_{jSB1}}{\hat{T}_{SB0}}\frac{\partial \hat{T}_{SB0}}{\partial x_j} + \frac{\Gamma_2^2}{4\hat{p}_0}\frac{\mathrm{d}\Gamma_7/\Gamma_2^2}{\mathrm{d}\hat{T}_{SB0}}\left(\frac{\partial \hat{T}_{SB0}}{\partial x_j}\right)^2\right]\frac{\partial \hat{T}_{SB0}}{\partial x_i} \quad (5.4)$$

is the force acting on unit mass of the gas divided by $2RT_0/L$. At each point, the gas is subject to a force parallel to the temperature gradient (Fig. 5.10).[12] In the absence of a flow ($\hat{v}_{iSB1} = 0$), the thermal stress can be incorporated into the pressure term if the condition (5.2) is satisfied. If not, $\hat{v}_{iSB1} = 0$ is inconsistent with Eq. (5.3) for $\hat{F}_{i2} = 0$; that is, a flow is induced in the gas in the absence of an external force. This is the nonlinear-thermal-stress flow. The

[12]The factor $\Gamma_2^2\mathrm{d}(\Gamma_7/\Gamma_2^2)/\mathrm{d}\hat{T}_{SB0}$ in $(\Gamma_2^2/4\hat{p}_0)[\mathrm{d}(\Gamma_7/\Gamma_2^2)/\mathrm{d}\hat{T}_{SB0}](\partial\hat{T}_{SB0}/\partial x_j)^2$ term in Eq. (5.4) is $-\Gamma_7/\hat{T}_{SB0}$ ($= -1.758705/\hat{T}_{SB0}$) for a hard-sphere gas and -1 for the BKW model. Thus, the force in the absence of a flow is in the direction opposite to the temperature gradient for these molecular models.

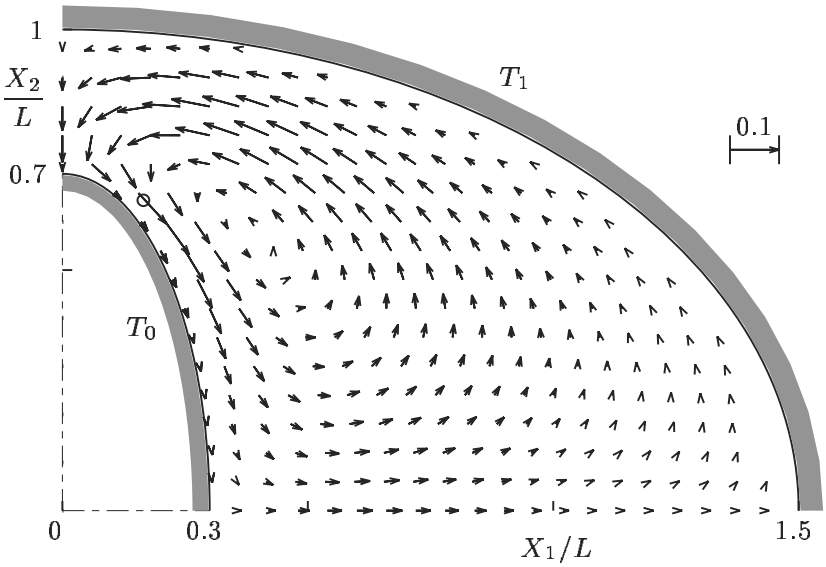

Figure 5.11. Nonlinear-thermal-stress flow induced between two coaxial elliptic cylinders with different uniform temperatures for a hard-sphere gas ($T_1/T_0 = 5$; T_0 : temperature of the inner cylinder and T_1 : temperature of the outer cylinder). In view of the symmetry situation, the result in the first quadrant is shown. The arrows indicate the flow velocity $\hat{v}_{iSB1}$ [$= \lim_{k\to 0} \boldsymbol{v}/(2RT_0)^{1/2}k$] at their starting points and the scale 0.1 of $(\hat{v}^2_{iSB1})^{1/2}$ is shown in the right upper space in the figure. The symbol $\circ$ represents the point of the maximum speed. As is apparent in the figure, L is the half length of the minor axis of the outer ellipse. See the corresponding flow at various Knudsen numbers in Fig. 5.13 and note the direction of the flow. (The numerical computation of the asymptotic equations in Section 3.3.3 is carried out by Doi.)

temperature field in the gas is the cause of the nonlinear-thermal-stress flow. The boundary wall plays only an indirect role to form such a temperature field in contrast to the thermal creep and thermal-stress slip flows.

An example of the nonlinear-thermal-stress flow is shown in Fig. 5.11. This example is chosen for comparison with the flow for finite Knudsen numbers in Section 5.2.

5.1.4 Thermal edge flow

We have discussed flows induced by temperature fields for small Knudsen numbers on the basis of the asymptotic theory explained in Chapter 3 and found the thermal creep flow and the nonlinear-thermal-stress flow at the first order of the Knudsen number and the thermal-stress slip flow at the second order of the Knudsen number. In the asymptotic theory, the shape of the boundary is assumed to be smooth, i.e., the Knudsen number based on the radius of curvature of the boundary is small. Thus the case where the boundary has a sharp edge is

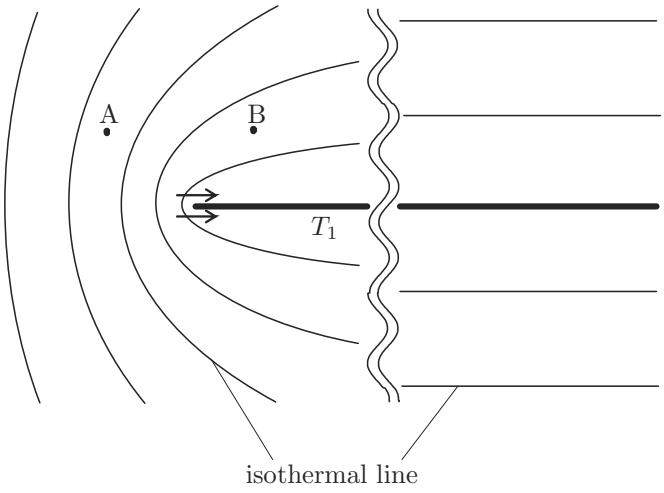

Figure 5.12. The temperature field near a uniformly heated plate. A flow is induced near the edge of the plate in the direction of the arrows. The points A and B are about one mean free path away from the edge.

excluded. Here, we will examine the possibility of a temperature-induced flow due to a sharp edge of a boundary.

Consider a uniformly heated plate in a gas, where the mean free path is much smaller than the size of the plate. In the neighborhood of the plate far away (on the scale of the mean free path) from its edges, the temperature of the gas is uniform along the plate, and the isothermal surfaces are parallel (Fig. 5.12). There is no cause of a flow along the plate. Near the edges of the plate, the isothermal surfaces are sharply curved. Kinetic theory approach of the field around the heated edge is not available. Thus we estimate the temperature field around the edge by the heat-conduction equation, though it is not guaranteed that the heat-conduction equation describes the field exactly even in the continuum limit (see Section 3.3). Then, it is given by $T_1[1 - ar^{1/2}\sin(\theta/2)+\cdots]$, where T_1 is the temperature of the plate and a is a constant ($a > 0$ for a heated plate), and (r, θ) is the plane polar coordinates with its origin at the edge and $\theta = 0$ on the plate. In this temperature field, the temperatures T_A at A and T_B at B in Fig. 5.12, where A and B are at about one mean free path ℓ_1 away from the edge, are, respectively, roughly estimated to be $T_1[1-(\alpha_0+\alpha_1)\ell_1^{1/2}]$ and $T_1[1-(\alpha_0-\alpha_1)\ell_1^{1/2}]$, where α_0 and α_1 are some constants ($\alpha_0 > \alpha_1 > 0$ for a heated plate). The character of the group of molecules impinging on the edge region is roughly represented by the combination of two groups: one from A and the other from B. The situation is similar to that over a plane wall with the temperature gradient $(T_B - T_A)/\sqrt{2}\ell_1 \sim \alpha_1 T_1 \ell_1^{-1/2}$, where the thermal creep flow is induced. Thus a flow proportional to the square root of the mean free path ($\sim \ell_1^{1/2}$) is induced near the edge, and the flow direction is from A to B as shown by the arrows in Fig. 5.12. The flow is called *thermal edge*

flow. In fact, the flow is confirmed experimentally by Sone & Yoshimoto [1997][13] as well as numerically by Aoki, Sone & Masukawa [1995] (see Sone [2002] for more detail). This flow is applied to the driving mechanism of a pump without a moving part (see Section 5.5.4).

5.2 Flow between elliptic cylinders with different temperatures

In Section 4.2.2, the thermal transpiration through a channel between two parallel plates is discussed for the whole range of the Knudsen number. The flow induced is unidirectional in the direction of the temperature gradient of the channel wall, though the flow profile varies considerably depending on the Knudsen number. Here, we present an example of non-unidirectional flows and examine its variation with the Knudsen number.

Consider a gas between two coaxial elliptic cylinders with different uniform temperatures. The major axes of the two ellipses are set orthogonal (Fig. 5.13). The temperature of the inner cylinder is kept at T_0 and the outer at T_1, whose difference $|T_1 - T_0|/T_0$ is of the order unity. In this example, no thermal creep flow is induced because the temperature on each of the cylinders is uniform, but the nonlinear-thermal-stress flow is to be induced because the isothermal lines are not parallel and the temperature difference $|T_1 - T_0|/T_0$ is not small. The time-independent behavior of the gas consisting of hard-sphere molecules is studied by the DSMC method (see Section B.1) under the diffuse-reflection condition for various Knudsen numbers in Aoki, Sone & Waniguchi [1998]. Some of the results are shown in Fig. 5.13.

The size and arrangement of the elliptic cylinders are obvious from the figure. The Knudsen number Kn is defined by ℓ_{av}/L, where L is the half length of the minor axis of the outer ellipse and ℓ_{av} is the mean free path of the gas in the equilibrium state at rest with the average gas density ρ_{av} in the whole domain. The flow velocity fields for $T_1/T_0 = 5$ are shown in Figs. 5.13 (a.1)–(b), where the arrows indicate the flow velocity $\boldsymbol{v}$ with $v_3 = 0$ at their starting points and the scale 0.01 of $|\boldsymbol{v}|/(2RT_0)^{1/2}$ is shown in each panel, and the white circles $\circ$ indicate the point with the maximum speed $|\boldsymbol{v}|_{\max}/(2RT_0)^{1/2}$ whose value is given in the caption. In view of the symmetry of the situation, the computation is carried out by the DSMC method in the first quadrant, which is divided into 775 cells and 1000 particles are put in each cell on the average or 775,000 particles in total in the cases (a.1)–(a.5), and 546 cells, 1000 particles in a cell, and 546,000 total number of particles in the case (b).

Figures 5.13 (a.1)–(a.5) show the variation of the flow field with the Knudsen number for a given set of elliptic cylinders. At Kn = 0.1 [Fig. 5.13 (a.1)], a clockwise circulating flow is induced along the inner cylinder and is dominant in the flow field. If we observe a little carefully, we notice that a slow counter-

[13]The video file of the experiment can be downloaded at http://fd.kuaero.kyoto-u.ac.jp/members/sone.

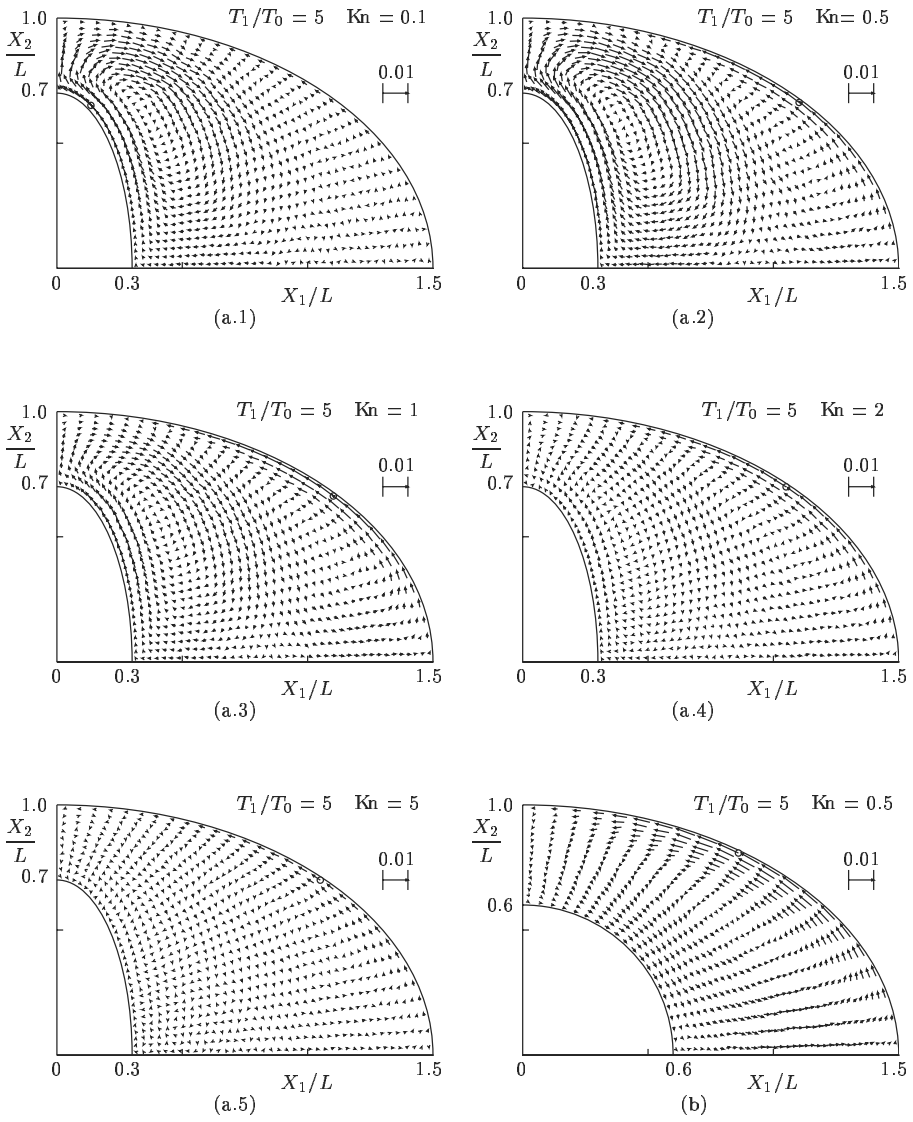

Figure 5.13. Flows induced between two coaxial elliptic cylinders with different uniform temperatures for a hard-sphere gas ($T_1/T_0 = 5$). (a.1) Kn = 0.1, (a.2) Kn = 0.5, (a.3) Kn = 1, (a.4) Kn = 2, (a.5) Kn = 5, and (b) the case with the inner cylinder being replaced by a circular cylinder, Kn = 0.5. The arrows indicate the flow velocity $\boldsymbol{v}$ with $v_3 = 0$ at their starting points and the scale 0.01 of $|\boldsymbol{v}|/(2RT_0)^{1/2}$ is shown in each panel. The white circles $\circ$ indicate the points with the maximum speed $|\boldsymbol{v}|_{\max}$, and the values of $|\boldsymbol{v}|_{\max}/(2RT_0)^{1/2}$ are 5.72×10^{-3} (Kn = 0.1) in (a.1), 6.58×10^{-3} (Kn = 0.5) in (a.2), 7.30×10^{-3} (Kn = 1) in (a.3), 5.72×10^{-3} (Kn = 2) in (a.4), 3.69×10^{-3} (Kn = 5) in (a.5), and 8.64×10^{-3} (Kn = 0.5) in (b). See the corresponding nonlinear-thermal-stress flow in Fig. 5.11 and note the direction of the flow.

clockwise circulating flow is also induced along the outer cylinder. At Kn = 0.5 [Fig. 5.13 (a.2)], the flow speed is increased on the whole; in particular, the flow along the outer cylinder is intensified significantly. As Kn increases to 1, the inner clockwise flow weakens considerably, whereas the counter-clockwise flow still grows slightly. With the further increase of Kn (Kn = 1 → 2 → 5), the inner flow attenuates rapidly, but the decay of the outer flow is slow. The flow vanishes in the free molecular case (Kn = ∞), which is proved in more general situation in Section 2.5. When the inner elliptic cylinder is replaced by a circular cylinder [Fig. 5.13 (b)], the flow induced near the inner cylinder weakens owing to its mild curvature, and the flow induced near the outer cylinder dominates over the whole domain.

According to the asymptotic theory for small Knudsen numbers in Section 3.3, the nonlinear-thermal-stress flow of the first order of the Knudsen number is induced as shown in Fig. 5.11 in Section 5.1.3. The flow is in the direction opposite to the main flow in Fig. 5.13 (a.1). The gas between the cylinders is at rest at Kn = 0. First, the nonlinear-thermal-stress flow is induced as Kn increases, but the flow is reversed and the flow in Fig. 5.13 (a.1) is established when Kn is further increased up to Kn = 0.1. At Kn = 0.1, the local mean free path ℓ_{loc} is about a half of ℓ_{av} near the top of the inner cylinder of the lower temperature, because the density is about $2\rho_{av}$ there. In the range of the order of the corresponding local mean free path near the top of the inner cylinder, the isothermal lines are well curved, and the molecules directly (or without intermolecular collision) impinging on the cylinder well perceive the curved isothermal lines. Thus, the discussion for the thermal edge flow in Section 5.1.4 applies to the present situation and the flow shown in Fig. 5.13 (a.1) is induced near the inner cylinder. The flow for intermediate or large Knudsen numbers requires more detailed discussion by taking account of the global feature of the field, which is made in Aoki, Sone & Waniguchi [1998].

Another similar example showing the flow induced between two parallel noncoaxial circular cylinders with slightly different uniform temperatures is studied for the whole range of the Knudsen number by a finite-difference numerical analysis of the integral equation form of the linearized BKW equation (see Section A.4.2) in Aoki, Sone & Yano [1989]. The flow for small Knudsen numbers is the thermal-stress slip flow explained in Section 5.1.2 with a figure of its streamlines (Fig. 5.9). The discussion on the flow for intermediate or large Knudsen numbers is made in a little different way in Aoki, Sone & Yano [1989] from that in Aoki, Sone & Waniguchi [1998].

5.3 Thermophoresis

Thermophoresis is a phenomenon of temperature-induced flows that has long been of interest, especially in the field of aerosol sciences, where the size of an aerosol particle is so small that the mean free path of the gas molecules of the surrounding gas is comparable to it and the effect of a finite Knudsen number is important. When a particle lies in a gas with a temperature gradient, a flow

is induced and the particle is subject to a force, called *thermal force*. If the particle is left free in the gas, it drifts because of the thermal force. These as a whole are called *thermophoresis*. There are a lot of attempts to attack this problem (e.g., Epstein [1929], Bakanov & Deryaguin [1959], Waldmann [1959], Schmitt [1959], Schadt & Cadle [1961], Brock [1962], Jacobsen & Brock [1965], Derjaguin, Storozhilova & Rabinovich [1966], Sone [1972], Phillips [1975], Sone & Aoki [1977a,b, 1979, 1981, 1983], Prodi, Santachiara & Prodi [1979], Beresnev & Chernyak [1985], Bakanov [1991], Takata, Aoki & Sone [1994], Takata & Sone [1995]). Most of the theoretical and numerical works discuss the thermophoresis of a spherical particle on the basis of the linearized Boltzmann equation and try to obtain a reasonable solution under various simplifying assumptions. The limitation to the linearized equation is legitimate in aerosol problems because the Mach number of a flow induced and the temperature variation, characterized by the surrounding temperature, over the distance of the particle size are both very small in such a small system. Recent development of computers made an accurate numerical analysis of the problem on the basis of the Boltzmann equation possible. Here, we will discuss the thermophoresis of a spherical particle with an arbitrary thermal conductivity. As in our discussion of a uniform flow past a sphere in Sections 4.5 and 4.6, we will discuss the problem on the basis of Takata & Sone [1995] in two steps.

5.3.1 A spherical particle with a uniform temperature

In this subsection, we discuss the thermophoresis of a spherical particle (or a sphere of radius L) kept at a uniform temperature T_0 in a gas at rest with a uniform pressure p_0 and a small temperature gradient [say, $(\partial T/\partial X_1)_\infty$]. That is, the state of gas is given by $v_i = 0$, $p = p_0$, and $T = T_0 + (\partial T/\partial X_1)_\infty X_1$, where $(L_{\rm O}/T_0)(\partial T/\partial X_1)_\infty \ll 1$ for $L_{\rm O} \gg L$, in the absence of the particle, and the particle is at $X_i = 0$; the time-independent behavior of the gas disturbed by the presence of the particle is studied on the basis of the linearized Boltzmann equation and the diffuse-reflection condition on the surface of the particle (Section 1.11).[14] We use the notation in Section 1.10, with L, T_0, and p_0 as the reference quantities, and the spherical coordinate system

$$x_1 = \hat{r}\cos\theta,\ x_2 = \hat{r}\sin\theta\cos\varphi,\ x_3 = \hat{r}\sin\theta\sin\varphi,$$

where the origin is at the center of the sphere. The linearized Boltzmann equation for the perturbed velocity distribution function ϕ with axial symmetry

[14] (i) The $L_{\rm O}$ is so large that the perturbations by the sphere are negligibly small compared with $(L_{\rm O}/T_0)(\partial T/\partial X_1)_\infty$ in the region $|X_i| \sim L_{\rm O}$. Then, the linearized Boltzmann equation and the boundary condition, especially at infinity shown below, is applicable.

(ii) When the temperature at $X_1 = 0$ of the gas unperturbed by the sphere is different from T_0 [say, T_1, i.e., $T = T_1 + (\partial T/\partial X_1)_\infty X_1$], the solution is obtained by simply adding the spherically symmetric solution with temperature T_1 at infinity as explained in the drag problem (see the last paragraph but one of Section 4.5).

$(\partial/\partial\varphi = 0)$ in the spherical coordinates [Eq. (A.164) in Section A.3] is

$$\zeta_r \frac{\partial \phi}{\partial \hat{r}} + \frac{\zeta_\theta}{\hat{r}} \frac{\partial \phi}{\partial \theta} + \frac{\zeta_\theta^2 + \zeta_\varphi^2}{\hat{r}} \frac{\partial \phi}{\partial \zeta_r} + \left(\frac{\zeta_\varphi^2}{\hat{r}} \cot\theta - \frac{\zeta_r \zeta_\theta}{\hat{r}} \right) \frac{\partial \phi}{\partial \zeta_\theta}$$
$$- \left(\frac{\zeta_\theta \zeta_\varphi}{\hat{r}} \cot\theta + \frac{\zeta_r \zeta_\varphi}{\hat{r}} \right) \frac{\partial \phi}{\partial \zeta_\varphi} - \frac{1}{k} \mathcal{L}(\phi) = 0, \tag{5.5}$$

and the diffuse-reflection condition is

$$\phi = -2\sqrt{\pi} \int_{\zeta_r < 0} \zeta_r \phi E \mathbf{d}\boldsymbol{\zeta} \qquad (\zeta_r > 0) \quad \text{at } \hat{r} = 1. \tag{5.6}$$

Take the distribution function, say ϕ_∞, in the form

$$\phi_\infty = \frac{L}{T_0} \left(\frac{\partial T}{\partial X_1} \right)_\infty \left[\left(\zeta^2 - \frac{5}{2} \right) x_1 - k\zeta_1 A(\zeta) \right], \tag{5.7}$$

where $A(\zeta)$ is equal to the function $\mathcal{A}(\zeta, 1)$ defined in Section A.2.9. It is easily seen that this ϕ_∞ satisfies the linearized Boltzmann equation (5.5) [more easily seen by the rectangular coordinate expression $\zeta_i \partial\phi/\partial x_i = \mathcal{L}(\phi)/k$] and that it expresses the state at rest with temperature $T_0 + (\partial T/\partial X_1)_\infty X_1$ and pressure p_0. Therefore, the distribution function ϕ of the present thermophoresis problem approaches Eq. (5.7) at infinity. That is, the boundary condition of ϕ at infinity is given by ϕ_∞, i.e.,

$$\phi \to \frac{L}{T_0} \left(\frac{\partial T}{\partial X_1} \right)_\infty \left[\left(\zeta^2 - \frac{5}{2} \right) \hat{r} \cos\theta - k(\zeta_r \cos\theta - \zeta_\theta \sin\theta) A(\zeta) \right] \quad \text{as } \hat{r} \to \infty. \tag{5.8}$$

The distribution function ϕ in the similarity form (Case 4 of Section A.5)[15]

$$\phi = \frac{L}{T_0} \left(\frac{\partial T}{\partial X_1} \right)_\infty [\Phi_c(\hat{r}, \zeta_r, \zeta) \cos\theta + \zeta_\theta \Phi_s(\hat{r}, \zeta_r, \zeta) \sin\theta],$$

is compatible with Eqs. (5.5), (5.6), and (5.8). The equation for $\Phi_c(\hat{r}, \zeta_r, \zeta)$ and $\Phi_s(\hat{r}, \zeta_r, \zeta)$ are given in Case 4 of Section A.5 [or by Eqs. (4.107)–(4.109)]. From the boundary condition (5.6),

$$\Phi_c = -2\sqrt{\pi} \int_{\zeta_r < 0} \zeta_r \Phi_c E \mathbf{d}\boldsymbol{\zeta}, \quad \Phi_s = 0 \qquad (\zeta_r > 0) \quad \text{at } \hat{r} = 1, \tag{5.9}$$

and from the condition (5.8) at infinity,

$$\Phi_c \to \left(\zeta^2 - \frac{5}{2} \right) \hat{r} - k\zeta_r A(\zeta), \quad \Phi_s \to kA(\zeta) \quad \text{as } \hat{r} \to \infty. \tag{5.10}$$

[15] See Footnote 21 in Section 4.5.

As shown in Section A.5, the macroscopic variables, i.e., density ρ, flow velocity $(v_r, v_\theta, v_\varphi)$, temperature T, etc., have a simple dependence on θ, i.e.,

$$\frac{\rho-\rho_0}{\rho_0\cos\theta},\quad \frac{v_r}{(2RT_0)^{1/2}\cos\theta},\quad \frac{v_\theta}{(2RT_0)^{1/2}\sin\theta},\quad \frac{T-T_0}{T_0\cos\theta},$$
$$\frac{p_{rr}-p_0}{p_0\cos\theta},\quad \frac{p_{r\theta}}{p_0\sin\theta},\quad \frac{p_{\theta\theta}-p_0}{p_0\cos\theta},\quad \frac{p_{\varphi\varphi}-p_0}{p_0\cos\theta},$$
$$\frac{q_r}{p_0(2RT_0)^{1/2}\cos\theta},\quad \frac{q_\theta}{p_0(2RT_0)^{1/2}\sin\theta},$$

are independent of θ, and $v_\varphi = p_{r\varphi} = p_{\theta\varphi} = q_\varphi = 0$.[16]

For small k, we can make use of the asymptotic theory in Section 3.1.[17] The solution can be easily obtained as[18]

$$\frac{v_r}{(2RT_0)^{1/2}\cos\theta} = \frac{L}{T_0}\left(\frac{\partial T}{\partial X_1}\right)_\infty \left[-3a_4\left(\frac{1}{\hat r}-\frac{1}{\hat r^3}\right)k^2+\cdots\right], \tag{5.11a}$$

$$\frac{v_\theta}{(2RT_0)^{1/2}\sin\theta} = \frac{L}{T_0}\left(\frac{\partial T}{\partial X_1}\right)_\infty \left[\frac{3}{2}a_4\left(\frac{1}{\hat r}+\frac{1}{\hat r^3}\right)+3Y_{a4}(\eta)\right]k^2+\cdots, \tag{5.11b}$$

$$\frac{\rho-\rho_0}{\rho_0\cos\theta} = \frac{L}{T_0}\left(\frac{\partial T}{\partial X_1}\right)_\infty \left[-\hat r+\frac{1}{\hat r^2}+\left(-\frac{3d_1}{\hat r^2}+3\Omega_1(\eta)\right)k + \left(-\frac{D_{\rm th}}{\hat r^2}+\Omega_{\rm th}(\eta)\right)k^2+\cdots\right], \tag{5.11c}$$

$$\frac{T-T_0}{T_0\cos\theta} = \frac{L}{T_0}\left(\frac{\partial T}{\partial X_1}\right)_\infty \left[\hat r-\frac{1}{\hat r^2}+\left(\frac{3d_1}{\hat r^2}+3\Theta_1(\eta)\right)k + \left(\frac{D_{\rm th}}{\hat r^2}+\Theta_{\rm th}(\eta)\right)k^2+\cdots\right], \tag{5.11d}$$

$$\frac{p-p_0}{p_0\cos\theta} = \frac{L}{T_0}\left(\frac{\partial T}{\partial X_1}\right)_\infty \left(3\big[\Omega_1(\eta)+\Theta_1(\eta)\big]k+\big[\Omega_{\rm th}(\eta)+\Theta_{\rm th}(\eta)\big]k^2 - \frac{3a_4\gamma_1}{\hat r^2}k^3+\cdots\right), \tag{5.11e}$$

$$\frac{q_r}{p_0(2RT_0)^{1/2}\cos\theta} = \frac{L}{T_0}\left(\frac{\partial T}{\partial X_1}\right)_\infty \left[-\frac{5\gamma_2}{4}\left(1+\frac{2}{\hat r^3}\right)k+\frac{15\gamma_2 d_1}{2\hat r^3}k^2+\cdots\right], \tag{5.11f}$$

[16] See Footnote 23 in Section 4.5.

[17] See Footnote 3 in Section 3.1.2.

[18] As noted in Section 3.1.6, the macroscopic variables except v_r and q_r are subject to the S-layer correction at the order of k^2 at the bottom of the Knudsen layer or in the neighborhood $\eta = O(k)$ of the boundary.

with

$$
\begin{aligned}
&D_{\rm th} = -6d_1^2 - 6d_3 + 3d_5,\\
&\Omega_{\rm th}(\eta) = -6d_1\Omega_1(\eta) - 6\Omega_3(\eta) + 3\Omega_5(\eta),\\
&\Theta_{\rm th}(\eta) = -6d_1\Theta_1(\eta) - 6\Theta_3(\eta) + 3\Theta_5(\eta),\\
&\eta = (\hat{r}-1)/k.
\end{aligned}
$$

Here, γ_1 and γ_2 are the nondimensional viscosity and thermal conductivity defined in Section 3.1.3 (see also Section 3.1.9); a_4, d_1, d_3, and d_5 are the slip coefficients and $Y_{a4}(\eta)$, $\Omega_1(\eta)$, $\Omega_3(\eta)$, $\Omega_5(\eta)$, $\Theta_1(\eta)$, $\Theta_3(\eta)$, and $\Theta_5(\eta)$ are the Knudsen-layer functions introduced in Section 3.1.5. The fluid-dynamic part of the pressure $(p-p_0)/p_0\cos\theta$ is given to the order of k^3 to obtain the thermal force on the sphere in harmony with the other variables;[19] $q_r/p_0(2RT_0)^{1/2}\cos\theta$ is also given because it is important in Section 5.3.2.[20] The flow induced is proportional to a_4 and is a thermal-stress slip flow. The force F_i acting on the particle is given by

$$
F_1 = \frac{\lambda_g L^2}{(2RT_0)^{1/2}}\left(\frac{\partial T}{\partial X_1}\right)_\infty\left(\frac{48\pi a_4\,{\rm Pr}}{5}k^2 + \cdots\right), \quad F_2 = F_3 = 0,
$$

where λ_g is the thermal conductivity of the gas [see Eq. (3.71)] and Pr $(= \gamma_1/\gamma_2)$ is the Prandtl number introduced in Section 3.1.9.[21]

The free-molecular-flow limit $(k \to \infty)$, where the particle radius is negligibly small compared with the mean free path of the gas, is studied in Bakanov & Deryaguin [1959] and Waldmann [1959], where ϕ_∞ given by Eq. (5.7) is taken as ϕ for the molecules impinging on the particle.[22] Then, the force F_i acting on the particle, the thermal force, is given as

$$
F_1 = \frac{\lambda_g L^2}{(2RT_0)^{1/2}}\left(\frac{\partial T}{\partial X_1}\right)_\infty\left[-\frac{4\pi}{\gamma_2}I_5(A)\right], \quad F_2 = F_3 = 0,
$$

[19] See Footnote 26 in Section 4.5.

[20] The expression $-3 - 6d_1k$ in the corresponding formula to q_r at $\hat{r} = 1$ for small k in the footnote to Table II in Takata & Sone [1995] should be $-3 + 6d_1k$.

[21] In the formula, the mean free path ℓ, thus k, is hidden in λ_g [see Eq. (3.71)].

[22] The situation they considered is as follows. There is an infinite expanse of a gas with a small temperature gradient. The small temperature gradient means that the variation of temperature of the gas over the distance of the mean free path is much smaller than the temperature of the gas. Then, the distribution function ϕ of the gas molecules is given by Eq. (5.7). A small particle in the gas is considered here. The small particle means that the size of the particle is much smaller than the mean free path. In a region far away from the particle in the scale of the size of the particle but close to it in the scale of the mean free path, the molecules from the particle come directly or without collision, and the relative number of these molecules is negligibly small. Thus the gas in this region is nearly the same as the gas in the absence of the particle. The molecules impinging on the particle from this region arrive at the particle directly or without molecular collision. Thus, in the limit $k \to \infty$, the distribution function ϕ in Eq. (5.7) at $\hat{r} = 0$ can be taken as the distribution function of the molecules impinging on the particle, because the difference between ϕ at $\hat{r} = 0$ and ϕ at $\hat{r} = 1$ is of higher order. The terminology "free-molecular-flow limit" is used to mean that the particle is much smaller than the mean free path. Molecular collisions are taken into account in the background gas as is seen from the function $A(\zeta)$ in Eq. (5.7).

where γ_2 is defined by Eq. (3.24) and $I_5(A)$ is the integral (3.25) of the function $A(\zeta)$.[23] The quantity in the square brackets is -1.94228 for a hard-sphere gas and $-16\sqrt{\pi}/15$ $(= -1.89062)$ for the BKW model.

The problem, i.e., Eqs. (4.107)–(4.109) with the boundary conditions (5.9) and (5.10), is solved numerically for a hard-sphere gas in Takata, Aoki & Sone [1994].[24] Some of the profiles of the macroscopic variables are shown in Figs. 5.14 and 5.15. The force F_i acting on the particle, the thermal force, is expressed as

$$F_1 = \frac{\lambda_g L^2}{(2RT_0)^{1/2}} \left(\frac{\partial T}{\partial X_1}\right)_\infty h^{(\mathrm{th})}, \quad F_2 = F_3 = 0, \tag{5.12}$$

and the force coefficient $h^{(\mathrm{th})}$ is tabulated later (in Section 5.3.2) in Table 5.1. The force coefficient $h^{(\mathrm{th})}$ for $k \ll 1$ or $k \to \infty$ is given, from the above-mentioned formulas of the force F_i, as

$$h^{(\mathrm{th})} = \begin{cases} \dfrac{48\pi a_4 \,\mathrm{Pr}}{5} k^2 + \cdots & (k \ll 1), \\ -\dfrac{4\pi}{\gamma_2} I_5(A) & (k \to \infty). \end{cases} \tag{5.13}$$

5.3.2 A spherical particle with an arbitrary thermal conductivity

Here, we extend the analysis to the case where the sphere is a uniform solid body with a uniform thermal conductivity. Then, the temperature field inside the particle is determined by the heat-conduction equation

$$\frac{1}{\hat{r}^2}\frac{\partial}{\partial \hat{r}}\left(\hat{r}^2 \frac{\partial \tau_p}{\partial \hat{r}}\right) + \frac{1}{\hat{r}^2 \sin\theta}\frac{\partial}{\partial \theta}\left(\sin\theta \frac{\partial \tau_p}{\partial \theta}\right) = 0 \qquad (\hat{r} < 1), \tag{5.14}$$

where $T_0(1 + \tau_p)$ is the temperature inside the particle and the axial symmetry $(\partial/\partial\varphi = 0)$ of the field is taken into account.

The equation for the perturbed velocity distribution function ϕ in the gas and its boundary condition at infinity are the same as those in Section 5.3.1, that is, the equation is Eq. (5.5) and the boundary condition at infinity is Eq. (5.8). On the surface of the spherical particle, in addition to the diffuse-reflection condition

$$\phi = (\zeta^2 - 2)\tau_p - 2\sqrt{\pi} \int_{\zeta_r < 0} \zeta_r \phi E \mathbf{d}\boldsymbol{\zeta} \quad (\zeta_r > 0) \ \text{ at } \hat{r} = 1, \tag{5.15}$$

[23] The somewhat strange expression, containing quantities related to the collision integral, in the square brackets of the thermal force for the free-molecular-flow limit is due to the two reasons: γ_2 comes from the choice of the conventional force formula with the thermal conductivity λ_g, and $I_5(A)$ comes from the collision effect in the infinite space of the background gas.

[24] See Footnote 27 in Section 4.5.

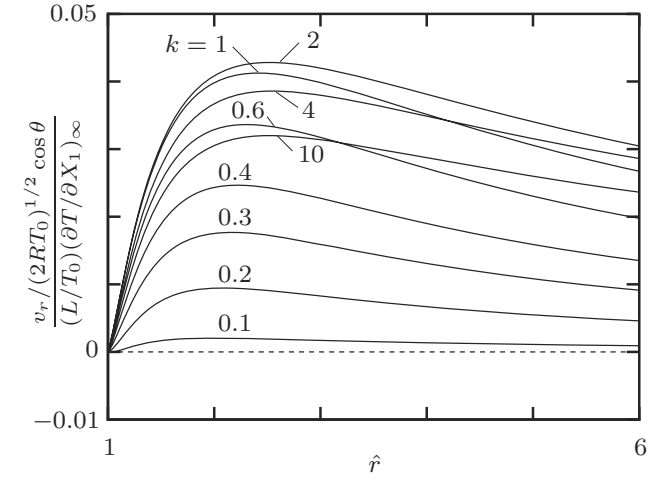

(a)

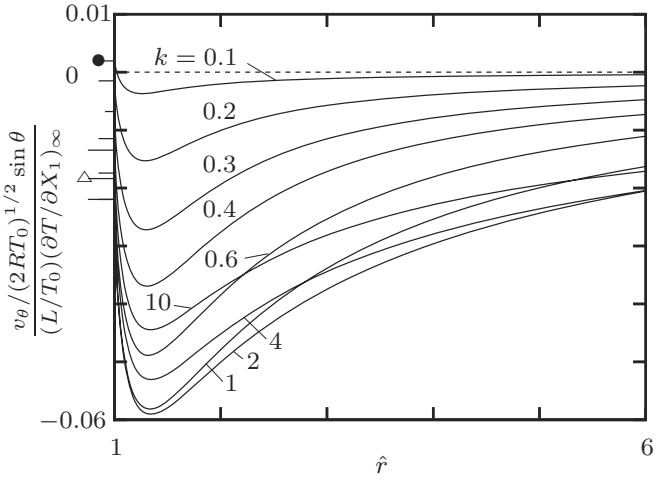

(b)

Figure 5.14. Velocity profiles in thermophoresis around a spherical particle with a uniform temperature for various k (a hard-sphere gas). (a) v_r and (b) v_θ. The solid lines —— are the numerical solution, and the dashed lines - - - are the asymptotic solution (5.11a) or (5.11b) with $k = 0$. In (b), the values on the sphere are marked by • for $k = 0.1$, ■ for $k = 0.2$, □ for $k = 0.3$, ⧫ for $k = 0.4$, ▲ for $k = 0.6$, ▼ for $k = 1$, ▽ for $k = 2$, △ for $k = 4$, and ◇ for $k = 10$.

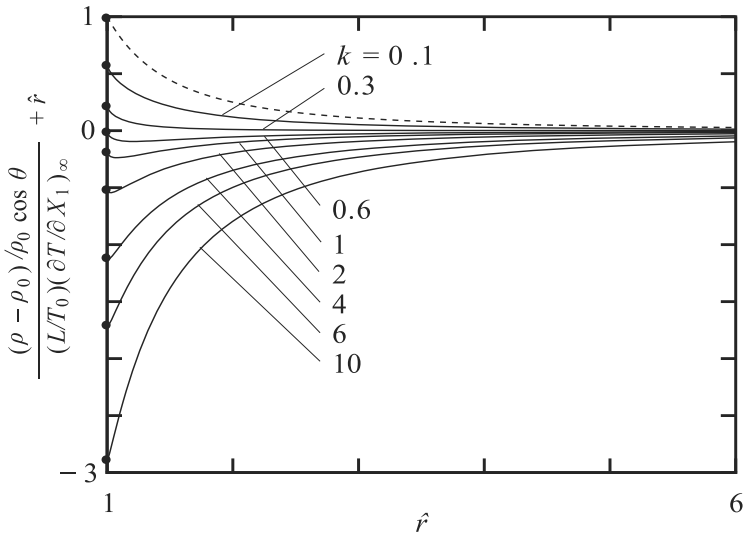

(a)

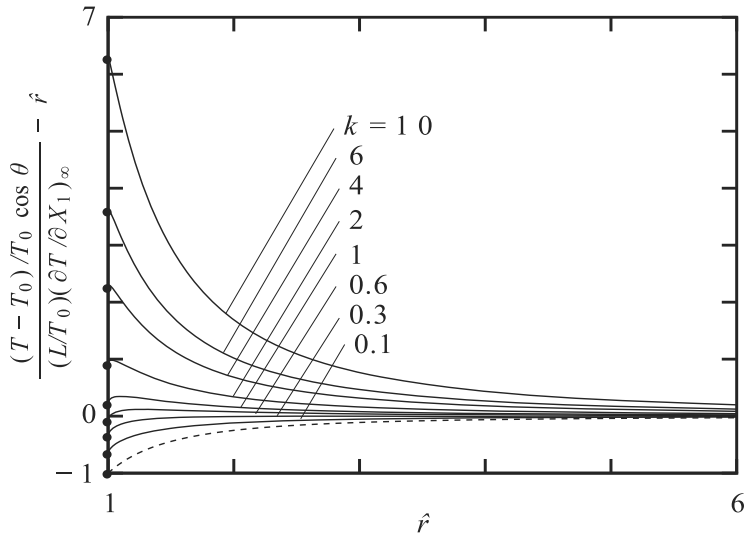

(b)

Figure 5.15. Density and temperature profiles in thermophoresis around a spherical particle with a uniform temperature for various k (a hard-sphere gas). (a) Density and (b) temperature. The solid lines —— are the numerical solution, and the dashed lines - - - are the asymptotic solution (5.11c) or (5.11d) with $k = 0$. The black circle • indicate the values on the sphere.

the condition of continuity of the energy flux through the surface of the particle is required,

$$-\frac{\lambda_p T_0}{L}\frac{\partial \tau_p}{\partial \hat{r}} = q_r \quad \text{at } \hat{r}=1, \tag{5.16}$$

where λ_p is the thermal conductivity of the spherical particle.

Here, we put the solution ϕ in the sum

$$\phi = \phi_{\rm th} + c_{\rm Th}\frac{L}{T_0}\left(\frac{\partial T}{\partial X_1}\right)_\infty \phi_1, \tag{5.17}$$

where $\phi_{\rm th}$ is the solution of the thermophoresis of a spherical particle with the uniform surface temperature T_0 in Section 5.3.1, and $c_{\rm Th}$ is an undetermined constant.[25] Then, the equation for ϕ_1 is Eq. (5.5) with $\phi=\phi_1$, and its condition at infinity is

$$\phi_1 \to 0 \ \text{ as } \hat{r}\to\infty. \tag{5.18}$$

We put ϕ_1 and τ_p in the similarity form[26]

$$\phi_1 = \Phi_c^{(1)}(\hat{r},\zeta_r,\zeta)\cos\theta + \zeta_\theta \Phi_s^{(1)}(\hat{r},\zeta_r,\zeta)\sin\theta, \tag{5.19a}$$

$$\tau_p = c_{\rm Th}\frac{L}{T_0}\left(\frac{\partial T}{\partial X_1}\right)_\infty \hat{r}\cos\theta, \tag{5.19b}$$

which is easily seen to be consistent with the equations and the boundary conditions. The equations for $\Phi_c^{(1)}(\hat{r},\zeta_r,\zeta)$ and $\Phi_s^{(1)}(\hat{r},\zeta_r,\zeta)$ are given by Eqs. (4.107)–(4.109) with $(\Phi_c,\Phi_s)=(\Phi_c^{(1)},\Phi_s^{(1)})$, i.e.,

$$D_c(\Phi_c^{(1)},\Phi_s^{(1)}) = \frac{1}{k}F_c, \qquad D_s(\Phi_c^{(1)},\Phi_s^{(1)}) = \frac{1}{k}F_s, \tag{5.20}$$

where

$$D_c(\Phi_c^{(1)},\Phi_s^{(1)}) = \zeta_r\frac{\partial \Phi_c^{(1)}}{\partial \hat{r}} + \frac{\zeta^2-\zeta_r^2}{\hat{r}}\frac{\partial \Phi_c^{(1)}}{\partial \zeta_r} + \frac{\zeta^2-\zeta_r^2}{\hat{r}}\Phi_s^{(1)}, \tag{5.21a}$$

$$D_s(\Phi_c^{(1)},\Phi_s^{(1)}) = \zeta_r\frac{\partial \Phi_s^{(1)}}{\partial \hat{r}} + \frac{\zeta^2-\zeta_r^2}{\hat{r}}\frac{\partial \Phi_s^{(1)}}{\partial \zeta_r} - \frac{\zeta_r}{\hat{r}}\Phi_s^{(1)} - \frac{1}{\hat{r}}\Phi_c^{(1)}, \tag{5.21b}$$

and

$$F_c(\hat{r},\zeta_r,\zeta) = \mathcal{L}(\Phi_c^{(1)}), \qquad \zeta_\theta F_s(\hat{r},\zeta_r,\zeta) = \mathcal{L}(\zeta_\theta\Phi_s^{(1)}). \tag{5.22}$$

The boundary conditions on the sphere ($\hat{r}=1$), corresponding to Eqs. (5.15) and (5.16), are reduced to

$$\Phi_c^{(1)} = \zeta^2 - 2 - 2\pi^{3/2}\int_0^\infty\int_{\pi/2}^\pi \zeta^3\sin 2\theta_\zeta \Phi_c^{(1)} E \mathrm{d}\theta_\zeta \mathrm{d}\zeta \quad (\zeta_r>0), \tag{5.23a}$$

$$\Phi_s^{(1)} = 0 \quad (\zeta_r>0), \tag{5.23b}$$

[25] The temperature on the surface of the particle is not known (or specified) beforehand. The constant $c_{\rm Th}$ in Eq. (5.19b) is introduced for this reason, but this constant in Eq. (5.17) is just for convenience.

[26] See Footnote 21 in Section 4.5.

and

$$c_{\rm Th} = -\frac{4\pi}{5}\frac{\lambda_g}{k\gamma_2\lambda_p}\int_0^\infty\int_0^\pi \zeta^5 \sin 2\theta_\zeta (\Phi_c^{(\rm th)} + c_{\rm Th}\Phi_c^{(1)})_{\hat r=1} E {\rm d}\theta_\zeta {\rm d}\zeta, \tag{5.24}$$

where $\theta_\zeta = {\rm Arccos}(\zeta_r/\zeta)$,[27] $\Phi_c^{(\rm th)}$ is Φ_c for the thermophoresis of a spherical particle with the uniform temperature T_0 in Section 5.3.1, and the thermal conductivity λ_g of the gas is used with the aid of the relation $\lambda_g T_0/L = 5k\gamma_2 p_0(2RT_0)^{1/2}/4$ (see Section 3.1.9). From Eq. (5.18), the condition at infinity is

$$\Phi_c^{(1)} \to 0 \ \text{ and } \ \Phi_s^{(1)} \to 0 \quad \text{as } \hat r \to \infty. \tag{5.25}$$

The problem for $(\Phi_c^{(1)}, \Phi_s^{(1)})$, i.e., Eqs. (5.20), (5.23a), (5.23b), and (5.25), is the same as that for (Φ_c, Φ_s) in Section 4.6.2, where a sphere whose surface temperature is given by $T_0(1+\cos\theta)$ lies in a gas at rest with temperature T_0 and pressure p_0. That is, ϕ_1 is ϕ in Section 4.6.2. From the condition (5.24), the constant $c_{\rm Th}$ is determined as

$$c_{\rm Th} = -\frac{C_q^{(\rm th)}}{5k\gamma_2\lambda_p/4\lambda_g + C_q^{(1)}}, \tag{5.26}$$

where

$$\begin{aligned} C_q^{(\rm th)} &= \pi\int_0^\infty\int_0^\pi \zeta^5 \sin 2\theta_\zeta \Phi_c^{(\rm th)}|_{\hat r=1} E {\rm d}\theta_\zeta {\rm d}\zeta \\ &= \frac{q_r^{(\rm th)}|_{\hat r=1}}{p_0(2RT_0)^{1/2}(L/T_0)(\partial T/\partial X_1)_\infty \cos\theta}, \end{aligned} \tag{5.27a}$$

$$\begin{aligned} C_q^{(1)} &= \pi\int_0^\infty\int_0^\pi \zeta^5 \sin 2\theta_\zeta \Phi_c^{(1)}|_{\hat r=1} E {\rm d}\theta_\zeta {\rm d}\zeta \\ &= \frac{q_r^{(1)}|_{\hat r=1}}{p_0(2RT_0)^{1/2}\cos\theta}. \end{aligned} \tag{5.27b}$$

Here, $q_r^{(\rm th)}$ and $q_r^{(1)}$ are q_r's corresponding to $\phi_{\rm th}$ and ϕ_1 respectively; $C_q^{(1)}$ and $q_r^{(1)}$ are those in Sections 4.6.1 and 4.6.3. With this $c_{\rm Th}$, the solution ϕ of thermophoresis of a spherical particle with an arbitrary thermal conductivity is obtained by Eq. (5.17) with $\phi_{\rm th}$ (ϕ in Section 5.3.1) and ϕ_1 (ϕ in Section 4.6.2).

Corresponding to Eq. (5.17), the perturbed macroscopic variables (corresponding to ϕ)

$$\rho - \rho_0,\ v_r,\ v_\theta,\ T - T_0,\ p_{rr} - p_0,\ p_{r\theta},\ p_{\theta\theta} - p_0,\ p_{\varphi\varphi} - p_0,\ q_r,\ q_\theta,$$

are given by Eq. (5.17) where ϕ, $\phi_{\rm th}$, and ϕ_1 are replaced by the macroscopic variables corresponding to ϕ, $\phi_{\rm th}$, and ϕ_1 respectively. That is, the nondimensional macroscopic variables (say, $h = \omega$, u_i, etc.) expressed by the distribution

[27] See Footnote 22 in Section 4.5.

function ϕ by Eqs. (1.97a)–(1.97f) are expressed by

$$h = h_{\rm th} + c_{\rm Th}\frac{L}{T_0}\left(\frac{\partial T}{\partial X_1}\right)_\infty h_1, \tag{5.28}$$

where $h_{\rm th}$ and h_1 are, respectively, given by Eqs. (1.97a)–(1.97f) with ϕ replaced by $\phi_{\rm th}$ and ϕ_1.

The $C_q^{(\rm th)}$ and $C_q^{(1)}$ in Eqs. (5.27a) and (5.27b) are functions of k that determine $c_{\rm Th}$. When k is small, from the results in Sections 4.6.2 and 5.3.1, they are

$$\begin{aligned} C_q^{(\rm th)} &= \frac{15}{4}\gamma_2 k(-1 + 2d_1 k + \cdots), \\ C_q^{(1)} &= \frac{5\gamma_2}{2}k - \left(5\gamma_2 d_1 + 2\int_0^\infty H_B(\eta){\rm d}\eta\right)k^2 + \cdots, \end{aligned}$$

and, therefore,

$$c_{\rm Th} = \frac{3}{2+\frac{\lambda_p}{\lambda_g}}\left[1 - \frac{2}{2+\frac{\lambda_p}{\lambda_g}}\left(\frac{d_1\lambda_p}{\lambda_g} - \frac{4}{5\gamma_2}\int_0^\infty H_B(\eta){\rm d}\eta\right)k + \cdots\right]. \tag{5.29}$$

When $k \to \infty$,

$$C_q^{(\rm th)} \to -\frac{5}{8}\gamma_2 k, \quad C_q^{(1)} \to \frac{1}{\sqrt{\pi}},$$

and, therefore,

$$c_{\rm Th} \to \frac{\lambda_g}{2\lambda_p}. \tag{5.30}$$

The numerical data of $C_q^{(\rm th)}$ and $C_q^{(1)}$ vs k are tabulated for a hard-sphere gas in Table 5.1. When $\lambda_p/\lambda_g \to \infty$, $c_{\rm Th}$ reduces to zero irrespective of k and the solution ϕ reduces to the solution $\phi_{\rm th}$ for the particle with the uniform temperature T_0 discussed in Section 5.3.1.

The force F_i ($F_2 = F_3 = 0$) on the sphere, or the thermal force on a sphere with an arbitrary thermal conductivity, is given as

$$\begin{aligned} \frac{F_1}{\frac{\lambda_g L^2}{(2RT_0)^{1/2}}\left(\frac{\partial T}{\partial X_1}\right)_\infty} &= \frac{F_1^{(\rm th)}}{\frac{\lambda_g L^2}{(2RT_0)^{1/2}}\left(\frac{\partial T}{\partial X_1}\right)_\infty} + \frac{c_{\rm Th}L}{T_0}\left(\frac{\partial T}{\partial X_1}\right)_\infty \frac{F_1^{(1)}}{\frac{\lambda_g L^2}{(2RT_0)^{1/2}}\left(\frac{\partial T}{\partial X_1}\right)_\infty} \\ &= h^{(\rm th)} + \frac{4c_{\rm Th}}{5\gamma_2 k}\frac{F_1^{(1)}}{p_0 L^2}, \end{aligned} \tag{5.31}$$

where $F_1^{(\rm th)}$ is F_1 in Section 5.3.1, $F_1^{(1)}$ is F_1 in Section 4.6.2, and $h^{(\rm th)}$ is defined in Eq. (5.12), i.e.,

$$F_1^{(\rm th)} = \frac{\lambda_g L^2}{(2RT_0)^{1/2}}\left(\frac{\partial T}{\partial X_1}\right)_\infty h^{(\rm th)}. \tag{5.32}$$

Table 5.1. The numerical data of $C_q^{(\mathrm{th})}$, $4C_q^{(\mathrm{th})}/5\gamma_2 k$, $C_q^{(1)}$, $h^{(\mathrm{th})}$, and $F_1^{(1)}/p_0L^2$ for a hard-sphere gas.

k	$C_q^{(\mathrm{th})}$	$\frac{4}{5\gamma_2 k}C_q^{(\mathrm{th})}$	$C_q^{(1)}$	$h^{(\mathrm{th})}$	$\frac{F_1^{(1)}}{p_0L^2}$
0	0	-3	0	0	0
0.05	-0.2878	-2.3955	0.1859	-0.0068	-0.0228
0.1	-0.4757	-1.9797	0.2952	-0.0457	-0.0788
0.2	-0.7166	-1.4911	0.4048	-0.2075	-0.2241
0.4	-1.0348	-1.0766	0.4819	-0.6017	-0.4694
0.6	-1.301	-0.9025	0.5097	-0.9034	-0.6254
1	-1.802	-0.7500	0.5318	-1.2585	-0.7908
2	-3.019	-0.6282	0.5480	-1.6001	-0.9327
4	-5.430	-0.5649	0.5561	-1.7818	-0.9994
6	-7.836	-0.5435	0.5588	-1.8399	-1.0187
10	-12.64	-0.5262	0.5609	-1.8838	-1.0321
∞	$-\infty$	-0.5	0.5642	-1.9423	-1.0472

From Eq. (5.26), the factor $4c_{\mathrm{Th}}/5\gamma_2 k$ is given by[28]

$$\frac{4c_{\mathrm{Th}}}{5\gamma_2 k} = -\frac{4C_q^{(\mathrm{th})}/5\gamma_2 k}{5k\gamma_2\lambda_p/4\lambda_g + C_q^{(1)}}. \tag{5.33}$$

For small k, the formula (5.33) is reduced to

$$\frac{4c_{\mathrm{Th}}}{5\gamma_2 k} = \frac{12}{5\gamma_2(2+\frac{\lambda_p}{\lambda_g})k}\left[1 - \frac{2}{2+\frac{\lambda_p}{\lambda_g}}\left(\frac{d_1\lambda_p}{\lambda_g} - \frac{4}{5\gamma_2}\int_0^\infty H_B(\eta)\mathrm{d}\eta\right)k + \cdots\right],$$

and, therefore, the thermal force F_i is given as

$$\frac{F_1}{\frac{\lambda_g L^2}{(2RT_0)^{1/2}}\left(\frac{\partial T}{\partial X_1}\right)_\infty} = \frac{48\pi\,\mathrm{Pr}}{5}\left(\frac{K_1}{2+\lambda_p/\lambda_g}k + (a_4 - A_{\mathrm{Th}})k^2 + \cdots\right), \tag{5.34}$$

where

$$A_{\mathrm{Th}} = \frac{2A_{\mathrm{t}}}{2+\frac{\lambda_p}{\lambda_g}} + \frac{2K_1}{(2+\frac{\lambda_p}{\lambda_g})^2}\left(d_1\frac{\lambda_p}{\lambda_g} - \frac{4}{5\gamma_2}\int_0^\infty H_B(\eta)\mathrm{d}\eta\right).$$

For $k \to \infty$, from Eq. (5.30),

$$\frac{4c_{\mathrm{Th}}}{5\gamma_2 k} \to 0,$$

[28]The extra factor $4/5\gamma_2 k$ of the linear combination in the thermal force formula, compared with Eq. (5.28), is due to the conventional force formula containing thermal conductivity.

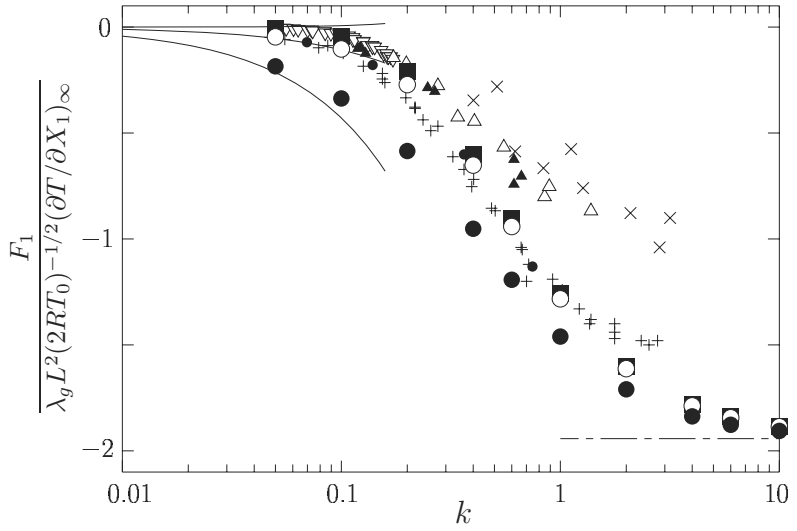

Figure 5.16. Thermal force [Eq. (5.31)] on a spherical particle with an arbitrary thermal conductivity: $F_1/\lambda_g L^2 (2RT_0)^{-1/2} (\partial T/\partial X_1)_\infty$ vs k (a hard-sphere gas). Here, ■ indicates the numerical solution for $\lambda_p/\lambda_g = \infty$, ○ for 10, and ● for 1 (Takata & Sone [1995]). The solid lines — are the asymptotic solutions for small k [from the top, $\lambda_p/\lambda_g = \infty$ (correct up to the order of k^2) in Ohwada & Sone [1992], 10 and 1 (correct up to the order of k) in Takata & Sone [1995]]. The dot-dash line – · – indicates the free molecular limit $k \to \infty$ in Waldmann [1959] and Bakanov & Deryaguin [1959]. Experimental data are shown by smaller symbols: × indicates the case $\lambda_p/\lambda_g = 475$ (Hg in Air), △ 263 (NaCl in Air), ▲ 8.14 (tricresyl phosphate in Air) in Schadt & Cadle [1961]; ▽ 366 (NaCl in Ar) in Jacobsen & Brock [1965]; • 8.14 (tricresyl phosphate in Air) in Phillips [1975]; + 7.41 (Oil in Ar) in Schmitt [1959].

and thus, thermal force F_i is reduced to that in Section 5.3.1 [see Eqs. (5.12) and (5.13)], i.e.,

$$\frac{F_1}{\dfrac{\lambda_g L^2}{(2RT_0)^{1/2}} \left(\dfrac{\partial T}{\partial X_1} \right)_\infty} = -\frac{4\pi}{\gamma_2} I_5(A). \tag{5.35}$$

The numerical data of $4C_q^{(\mathrm{th})}/5\gamma_2 k$ in Eq. (5.33), $h^{(\mathrm{th})}$ defined by Eq. (5.32), and $F_1^{(1)}/p_0 L^2$ in the formula (5.31) vs k are given for a hard-sphere gas in Table 5.1. The force F_1 vs k for a hard-sphere gas obtained from these data is shown in Fig. 5.16. Equation (5.35) for $k \to \infty$ and Eq. (5.34) for small k up to the order of k for finite λ_p/λ_g and up to the order of k^2 for infinite λ_p/λ_g are also shown in Fig. 5.16.

The thermal force depends considerably on the ratio λ_p/λ_g of the thermal conductivities of the particle and the gas as well as on the Knudsen number (or k). The ratio λ_p/λ_g is generally a large number. The force is in the direction

opposite to the temperature gradient for most of the range of k. When $k \ll 1$, the particle with a uniform temperature or very large λ_p/λ_g [$O(k^{-2})$ or the larger] is subject to a force in the direction of the temperature gradient for a hard-sphere gas and the BKW model [see Eq. (5.34)]. This is due to the thermal-stress slip flow discussed in Section 5.1.2. This case is specifically called *negative thermophoresis*.

5.4 One-way flows induced through a pipe without average pressure and temperature gradients

5.4.1 Background

In Section 4.2.2, we saw a flow induced through a channel between two plates with a temperature gradient along the plates. Generally, a flow is induced along a pipe with a temperature gradient. The flow is in the direction of the temperature gradient. This phenomenon is known as *thermal transpiration* for a long time (e.g., Maxwell [1879], Knudsen [1910a, 1910b], Kennard [1938], Loeb [1961], Sone [2000a]). Its application to a pumping system is considered by connecting two reservoirs with a pipe with a temperature gradient. However, to obtain a large pressure difference between the reservoirs, the temperature gradient of the pipe is to be large or the pipe is to be long, which makes the temperature difference at the two ends of the pipe large. This is not practical and some cascade process is required. As early as 1910, Knudsen devised an experiment with a cascade system to obtain a pressure ratio as large as ten (Knudsen [1910b]). No big progress was made for a while, but more attention to engineering application of the flow has been paid anew recently, for example, in relation to micro-mechanical systems (Huber [1995], Pham-Van-Diep, Keeley, Muntz & Weaver [1995], Sone, Waniguchi & Aoki [1996], Vargo & Muntz [1997], Hudson & Bartel [1999], Sone & Sato [2000], Aoki, Sone, Takata, Takahashi & Bird [2001], Sone, Fukuda, Hokazono & Sugimoto [2001], Sone & Sugimoto [2002, 2003], Young, Han, Muntz, Shiflett, Ketsdever & Green [2003], Karniadakis, Beskok & Aluru [2005], Sugimoto & Sone [2005], etc.).

One of the basic problems of the cascade system is to investigate the possibility of a one-way flow through an infinite pipe under a periodic condition along the pipe or through a finite pipe with its two ends at an equal pressure and temperature. We will discuss this problem in this section, and its application to a Knudsen compressor in Section 5.5.

5.4.2 Pipe with ditches

It is "almost sure" that a one-way flow cannot be induced in a straight pipe with a uniform cross section by devising the temperature distribution along it. This is shown mathematically by Golse [unpublished] (see his proof in Appendix A.4

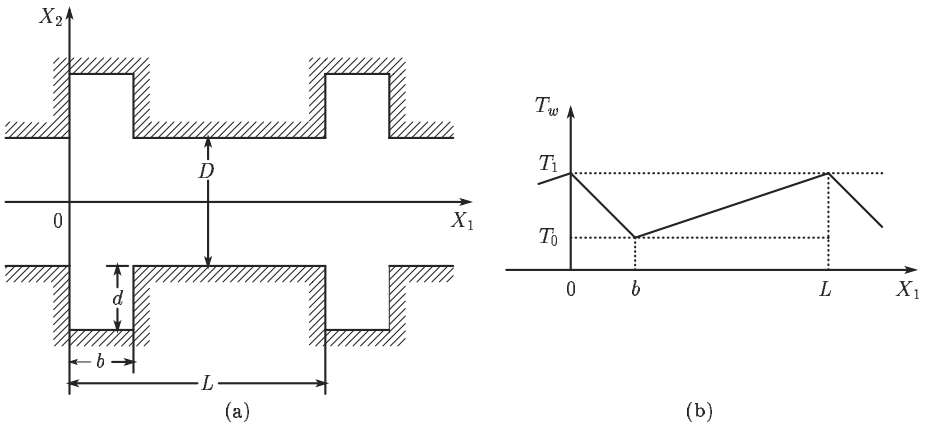

Figure 5.17. Channel configuration. (a) Channel between two parallel walls with ditches dug periodically and (b) its wall temperature distribution.

of Sone [2002]), numerically in Sone, Waniguchi & Aoki [1996] and Aoki, Sone, Takata, Takahashi & Bird [2001], and experimentally in Sone & Sato [2000]. The "almost sure" means that the mathematical proof is done on the basis of the *linearized* Boltzmann equation and, thus, a one-way flow due to a nonlinear effect is not excluded and that the numerical computation and experiment are done only for limited cases, though they are done in a nonlinear region.

Consider a rarefied gas in a channel between two parallel walls with ditches dug periodically and with a saw-like temperature distribution as shown in Fig. 5.17. The time-independent solution periodic in the direction of the channel is studied for a hard-sphere gas numerically by the DSMC method (see Section B.1) in Sone, Waniguchi & Aoki [1996] for various sets of parameters of the system. In the following discussion, the Knudsen number Kn is defined by ℓ_{av}/D, where ℓ_{av} is the mean free path of the gas in the equilibrium state at rest with the average density ρ_{av} over the whole gas domain. A one-way flow is shown to be induced in the X_1 direction as shown in Fig. 5.18. Locally, flows are induced in the direction of the temperature gradient of the wall, but the flow induced in the $-X_1$ direction on the bottom of a ditch is blocked by the side wall of the ditch, and therefore, a one-way flow is induced in the X_1 direction. Let Mf be the average mass flux over the cross section of the main part of the pipe or channel. That is, DMf is the mass flow per unit time (or the mass-flow rate) through the channel with unit width in X_3 direction. The nondimensional average mass flux $Mf/\rho_{av}(2RT_0)^{1/2}$ vs Kn is shown in Fig. 5.19. When there are no ditches on the walls ($d = 0$), the one-way flow or the mass flow through the channel vanishes although a local flow is induced. An example of the flow pattern is given in Fig. 5.20. The corresponding $Mf/\rho_{av}(2RT_0)^{1/2}$ is 2.064×10^{-4}, which is zero within the error of the numerical computation. A shallow ditch helps to induce a considerable one-way flow. For example, when the depth of the ditch is reduced to half of Fig. 5.18 ($d/D = 1/2 \to 1/4$, with

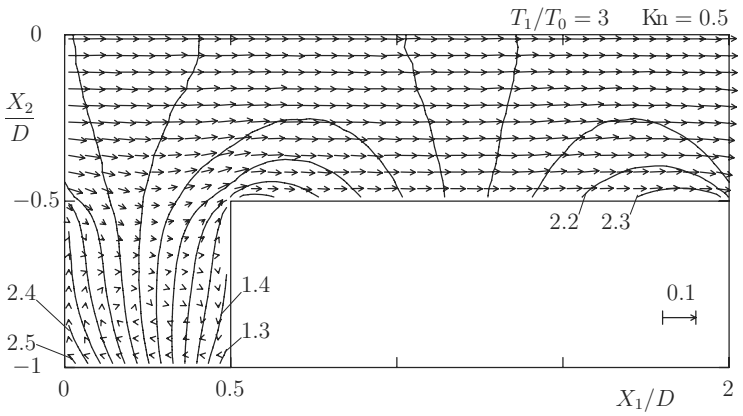

Figure 5.18. One-way flow induced in the channel with ditches in Fig. 5.17 ($L/D = 2$, $b/D = 1/2$, $d/D = 1/2$, $T_1/T_0 = 3$, Kn$= 0.5$). The arrows indicate the flow velocity v_i at their starting points; the scale 0.1 of $(v_i^2)^{1/2}/(2RT_0)^{1/2}$ is shown near the right lower corner in the figure. The solid curves indicate the isothermal lines $T/T_0 = 1.3$, $1.4, \ldots,$ 2.5. Here the Knudsen number is defined by Kn$= \ell_{av}/D$, where ℓ_{av} is the mean free path of the equilibrium state at rest with the average density ρ_{av} over the channel.

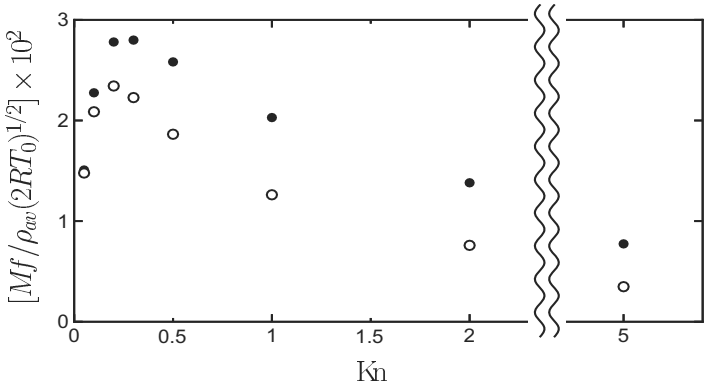

Figure 5.19. Mass flux Mf through the channel or the pipe with the periodic ditches ($L/D = 2$, $b/D = 1/2$, $d/D = 1/2$, $T_1/T_0 = 3$) : $Mf/\rho_{av}(2RT_0)^{1/2}$ vs Kn, where DMf is the mass-flow rate through the channel with unit width in X_3 direction, $\pi D^2 Mf/4$ is the mass-flow rate through the pipe, and ρ_{av} is the average density of the gas over the domain. The symbol • : the channel, ∘ : the pipe.

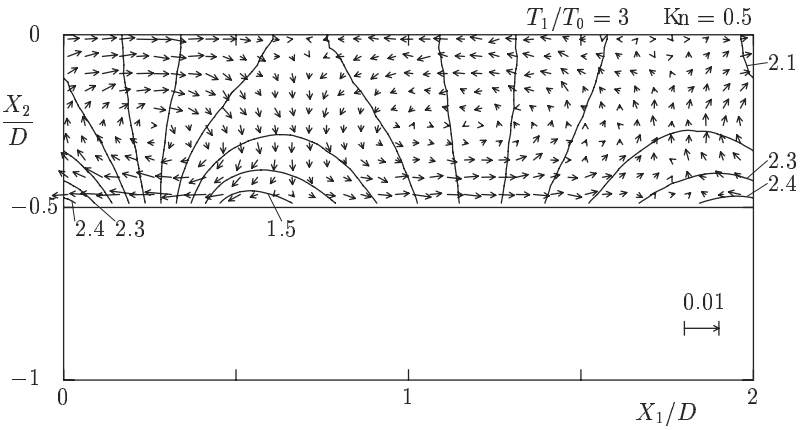

Figure 5.20. Flow field in a channel without a ditch in Fig. 5.17 ($L/D = 2, b/D = 1/2$, $d/D = 0$, $T_1/T_0 = 3$, Kn$= 0.5$). The arrows indicate the flow velocity v_i at their starting points; the scale 0.01 of $(v_i^2)^{1/2}/(2RT_0)^{1/2}$ is shown near the right lower corner in the figure. The solid curves indicate the isothermal lines $T/T_0 = 1.5, 1.6, \ldots, 2.4$. Here the Knudsen number is defined by Kn$= \ell_{av}/D$, where ℓ_{av} is the mean free path of the gas in the equilibrium state at rest with the average density ρ_{av} over the channel.

common $L/D = 2$, $b/D = 1/2$), $Mf/\rho_{av}(2RT_0)^{1/2}$ is reduced only by 15% of the original value when Kn $= 0.5$ and $T_1/T_0 = 3$.

If the system is closed at $X_1 = 0$ and $X_1 = \mathcal{N}L$ ($\mathcal{N}$: a positive integer) with walls at temperature T_1, the flow is blocked and the pressure difference is induced between the two ends. The pressure variation along the channel is shown in Fig. 5.21, where the average pressure $P_{D/5}$ in the central part of the channel of width $D/5$, i.e., $P_{D/5} = (5/D)\int_{-D/10}^{D/10} p\mathrm{d}X_2$, instead of the local pressure, is shown and the Knudsen number Kn is based on the average density ρ_{av} over the domain $0 < X_1 < \mathcal{N}L$. Some irregular behaviors are seen in the first and last sectors owing to the end effect. Let us define a semi-local Knudsen number $\mathrm{Kn}_L(X_1)$ at X_1 on the basis of the mean free path at the average density over the interval $(X_1, X_1 + L)$. It is a decreasing function of X_1 as shown in Fig. 5.21. Thus, $P_{D/5}$ is expressed as a function of Kn_L. The two relations, $P_{D/5}(* + L)/P_{D/5}(*)$ vs $\mathrm{Kn}_L(*)$ (the variation of the compression ratio with the semi-local Knudsen number) and $\mathrm{Kn}_L(* + L)$ vs $\mathrm{Kn}_L(*)$ (the relation between the neighboring semi-local Knudsen numbers), obtained from the data for various global Knudsen number Kn are shown in Fig. 5.22. They are on a smooth curve except the data on the end units, from which we can get the information of the effective range of the pump and its pumping strength. Further, the n-stage pressure ratio $P_{D/5}(nL)/P_{D/5}(0)$ can be obtained easily from the two curves with the aid of the subsidiary curve $\mathrm{Kn}_L(* + L) = \mathrm{Kn}_L(*)$. That is, let $\mathrm{Kn}_L(0)$ be given. Read $P_{D/5}(L)/P_{D/5}(0)$ and $\mathrm{Kn}_L(L)$ on the two curves. With the aid of the subsidiary curve $\mathrm{Kn}_L(* + L) = \mathrm{Kn}_L(*)$, shift the ordinate $\mathrm{Kn}_L(L)$ to the abscissa. Continue this process and obtain $P_{D/5}(2L)/P_{D/5}(L)$,

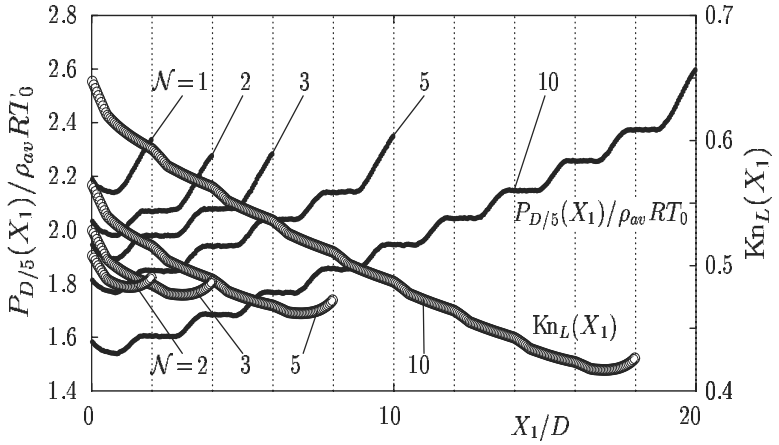

Figure 5.21. The distribution of the average pressure $P_{D/5}$ and the semi-local Knudsen number Kn_L in the channel closed with the walls with temperature T_1 at $X_1 = 0$ and $X_1 = \mathcal{N}L$ ($L/D = 2$, $b/D = 1/2$, $d/D = 1/2$, $T_1/T_0 = 3$, $\mathrm{Kn} = 0.5$). The average pressure $P_{D/5}$ is the average of the local pressure in the central part of the channel of width $D/5$, i.e., $P_{D/5} = (5/D)\int_{-D/10}^{D/10} p\mathrm{d}X_2$, and the semi-local Knudsen number $\mathrm{Kn}_L(X_1)$ at X_1 is defined on the basis of the mean free path at the average density over the interval $(X_1, X_1 + L)$.

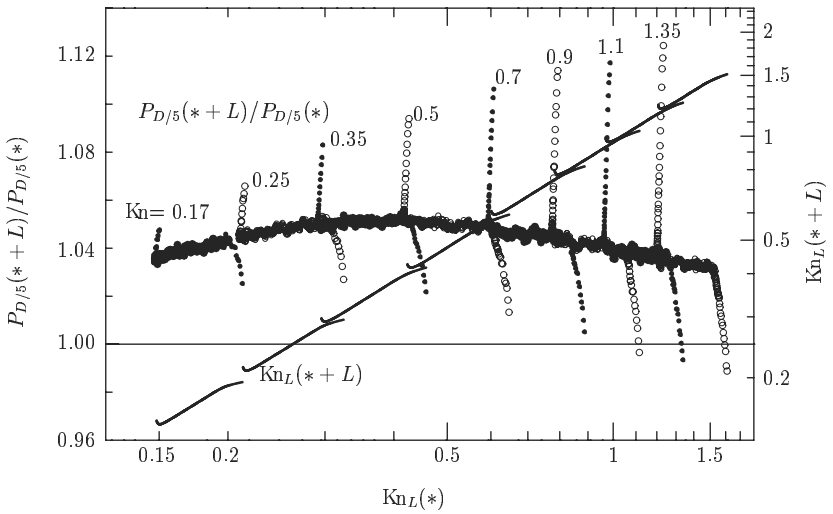

Figure 5.22. $P_{D/5}(*+L)/P_{D/5}(*)$ and $\mathrm{Kn}_L(*+L)$ vs $\mathrm{Kn}_L(*)$ for the closed channel ($L/D = 2$, $b/D = 1/2$, $d/D = 1/2$, $T_1/T_0 = 3$). The data for various global Knudsen number Kn over the domain for the closed pipe $\mathcal{N} = 10$ are shown. The data that divert from the main smooth curve are those taken from the end sectors of each pipe.

Table 5.2. The comparison of the average mass flux Mf through the pipe for various depths of the ditches (Kn = 0.5, $T_1/T_0 = 3$, $L/D = 2$, and $b/D = 1/2$).

d/D	0	1/8	1/4	1/2	1
$[Mf/\rho_{av}(2RT_0)^{1/2}] \times 10^2$	6.790×10^{-3}	1.040	1.506	1.863	1.921

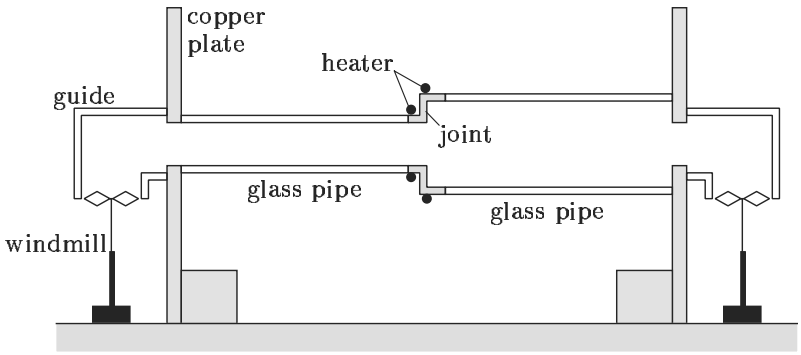

Figure 5.23. Experimental apparatus demonstrating a one-way flow induced in a pipe without average pressure and temperature gradients.

$P_{D/5}(3L)/P_{D/5}(2L), \ldots$. Then we obtain $P_{D/5}(nL)/P_{D/5}(0)$ by their product.

The corresponding analysis for a circular pipe with the periodic ditches is carried out in Aoki, Sone, Takata, Takahashi & Bird [2001], and one-way flows are shown to be induced through the pipe. The average mass flux Mf over the cross section of the main part through the pipe, from which the mass-flow rate through the pipe is given by $\pi D^2 Mf/4$, is compared with that through the channel in Fig. 5.19. The one-way flow is stronger in the case of the channel. The pumping effect is, however, found to be stronger for the pipe because of larger resistance to a pressure gradient. According to the method explained in the preceding paragraph, it is estimated that, for example, the pressure ratio about 15 is obtained with $\mathcal{N} = 40$ for the pipe system ($L/D = 2$, $b/D = 1/2$, $d/D = 1/2$, $T_1/T_0 = 3$) operated in the range $1 \le \mathrm{Kn}_L(0) \le 1.5$ of the semi-local Knudsen number at the low-pressure end, while the pressure ratio about 5 is obtained for the corresponding channel system. As in the case of the channel, a one-way flow is not induced, within the error of the numerical computation, when there are no ditches. Here, we list the data showing the effect of the depth of the ditches on the one-way flow in Table 5.2. Even a shallow ditch has a considerable effect, i.e., $Mf/\rho_{av}(2RT_0)^{1/2}$ for $d/D = 1/8$ is 56% of that for $d/D = 1/2$.

The one-way flow induced by a ditch is demonstrated by a simple experiment (Sone & Sato [2000]).[29] The experiment is done in the vacuum chamber in

[29]The video file of the experiment can be downloaded at http://fd.kuaero.kyoto-

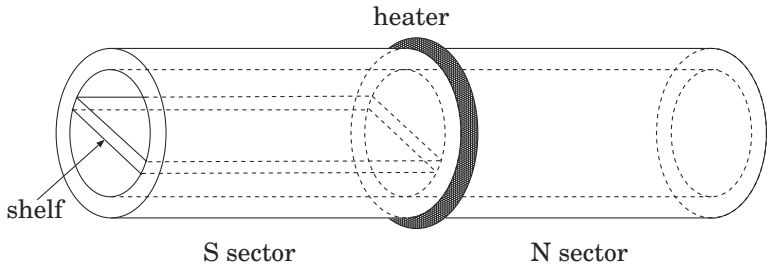

Figure 5.24. A pipe with a shelf put up in its half part.

Section 5.1.1. The pipe system consists of two circular glass pipes of different inner diameters, 12 and 24 mm, and of length 60 mm each (Fig. 5.23). They are connected with a brass joint, and the joint is heated to about 110°C with a Nichrome wire around it. At each of the other ends of the two pipes, a copper plate 4-mm thick is attached to keep the temperatures of both ends nearly the same. In fact the temperatures are about 20°C, and the difference is at most 1°C. The flow is detected by windmills set at both ends of the polycarbonate guides. The windmills rotate with speed about 180 rpm at 5 Pa, 110 rpm at 10 Pa, 60 rpm at 20 Pa, and 25 rpm at 40 Pa in the direction that the flow is from the thinner pipe to the thicker. At 100 Pa and above, no motion is observed. When only the thinner pipe is set, the speed is about 190 rpm at 10 Pa. When the pipe is of a uniform cross section, no flow is naturally induced. If the position of the heater is shifted away from the middle point of the pipe of a uniform cross section, no flow is induced.

5.4.3 Pipe with shelves

If we examine the mass-flow rate formulas for the Poiseuille flow and the thermal transpiration through a uniform straight pipe for small Knudsen numbers, we notice that a one-way flow can be induced in a pipe with a shelf (or shelves) partially put up in the half of the pipe as shown in Fig. 5.24, where the part with a shelf will be called S sector and the part without a shelf N sector. The mass-flow rates of the two flows are easily obtained by the asymptotic theory in Section 3.1 as

$$M_P = -\frac{c_P p S^2}{\mu R T_w}\frac{\mathrm{d}p}{\mathrm{d}X_1}, \quad M_T = \frac{c_T \ell p S}{T_w\sqrt{RT_w}}\frac{\mathrm{d}T_w}{\mathrm{d}X_1},$$

where M_P is the mass-flow rate through the pipe in the X_1 direction (or the axis of the pipe) of the Poiseuille flow and M_T is that of the thermal transpiration; T_w is the temperature of the pipe, p is the pressure, μ is the viscosity, and ℓ is the mean free path of the gas; S is the cross-sectional area of the pipe; c_P is a constant depending on the shape of the cross section and c_T is a constant

u.ac.jp/members/sone.

depending on the molecular model and the kinetic boundary condition, and R is the specific gas constant. It may be noted that the mass flow of the Poiseuille flow is proportional to S^2 and that of the thermal transpiration is proportional to S. When the pipe is heated in the middle of the pipe, the thermal transpiration is induced in both sides of the heater in the opposite directions, but the mass-flow rate is the same whether the pipe passage is divided by thin shelves into several (say, n) parts or not because $(S \div n) \times n = S$. The two flows encounter in the middle and the pressure there increases and a pressure gradient is induced in each sector of the pipe, which induces a flow away from the middle part of the pipe. This flow is weaker in the S sector because $(S \div n)^2 \times n = S^2/n$.[30] Therefore, a one-way flow is induced from the S sector to the N sector. More about the mass-flow and the pumping effect along this line are given in Sone [2002]. Here, we will extend the discussion when operated in larger Knudsen numbers.

According to Section 4.2.1, the mass-flow rate M through a straight pipe induced by the two effects, the pressure gradient in the gas and the temperature gradient on the pipe, is expressed in the form [Eq. (4.34)]

$$\frac{M}{2p_0L^2/(2RT_0)^{1/2}} = \left(\frac{L}{p_0}\frac{\mathrm{d}p}{\mathrm{d}X_1}\right)\hat{M}_\mathrm{P}(k) + \left(\frac{L}{T_0}\frac{\mathrm{d}T_w}{\mathrm{d}X_1}\right)\hat{M}_\mathrm{T}(k), \tag{5.36}$$

where $\hat{M}_\mathrm{P}$ (< 0) and $\hat{M}_\mathrm{T}$ (> 0) are determined by the Knudsen number (or k) and the shape of the cross section, and L is the reference size of the cross section. We will consider the case with a rectangular cross section to avoid the complexity coming from the shape difference when shelves are put up. Let this formula be for the N sector. Then the mass-flow rate M_sh through each passage of the pipe divided by shelves into $n \times n$ passages is given as follows:

$$\frac{M_\mathrm{sh}}{2p_0L^2/n^2(2RT_0)^{1/2}} = \frac{1}{n}\left[\left(\frac{L}{p_0}\frac{\mathrm{d}p}{\mathrm{d}X_1}\right)\hat{M}_\mathrm{P}(nk) + \left(\frac{L}{T_0}\frac{\mathrm{d}T_w}{\mathrm{d}X_1}\right)\hat{M}_\mathrm{T}(nk)\right], \tag{5.37}$$

because the reference length of the thinner pipe is L/n and thus, k is factored by n. This naturally agrees with the discussion in the preceding paragraph because $\hat{M}_\mathrm{P}(k) \propto 1/k$ and $\hat{M}_\mathrm{T}(k) \propto k$ for $k \ll 1$ (note that n^2 corresponds to n in the discussion there).

Let the length of the S sector be L_S and that of the N sector be L_N. The temperature at the heater is kept at T_1 and the temperature at both ends of the pipe is at T_0. The pressure at the ends is p_0 and that at the heater is p_1, which is unknown. Then, the mass-flow rate M_S through the S sector and that M_N through the N sector are given, respectively, as

$$\frac{M_\mathrm{S}}{2p_0L^2/(2RT_0)^{1/2}} = \frac{1}{n}\left(\frac{(p_1-p_0)L}{p_0L_\mathrm{S}}\hat{M}_\mathrm{P}(nk) + \frac{(T_1-T_0)L}{T_0L_\mathrm{S}}\hat{M}_\mathrm{T}(nk)\right), \tag{5.38a}$$

$$\frac{M_\mathrm{N}}{2p_0L^2/(2RT_0)^{1/2}} = -\frac{(p_1-p_0)L}{p_0L_\mathrm{N}}\hat{M}_\mathrm{P}(k) - \frac{(T_1-T_0)L}{T_0L_\mathrm{N}}\hat{M}_\mathrm{T}(k). \tag{5.38b}$$

[30] We neglect the effect of the shape constant c_P because we can choose a pipe of a rectangular cross section as an example and divide it into similar rectangular sections.

Owing to the conservation of mass-flow rate, these quantities, $M_{\rm S}$ and $M_{\rm N}$, are equal, from which the unknown p_1 is determined as

$$\frac{(p_1-p_0)}{p_0}\left(\frac{L_{\rm S}}{L_{\rm N}}+\frac{\hat{M}_{\rm P}(nk)}{n\hat{M}_{\rm P}(k)}\right)=-\frac{(T_1-T_0)}{T_0}\frac{\hat{M}_{\rm T}(k)}{\hat{M}_{\rm P}(k)}\left(\frac{L_{\rm S}}{L_{\rm N}}+\frac{\hat{M}_{\rm T}(nk)}{n\hat{M}_{\rm T}(k)}\right).$$

With this p_1-p_0 in Eq. (5.38a) or (5.38b), we obtain the mass-flow rate M $(=M_{\rm S}=M_{\rm N})$ through the pipe as

$$M=M_{\rm S0}\frac{m_{\rm T}}{n}\frac{1-\dfrac{m_{\rm P}}{m_{\rm T}}}{1+\dfrac{m_{\rm P}}{n}\dfrac{L_{\rm N}}{L_{\rm S}}}, \tag{5.39}$$

where

$$\frac{M_{\rm S0}}{2p_0L^2/(2RT_0)^{1/2}}=\frac{(T_1-T_0)L}{T_0L_{\rm S}}\hat{M}_{\rm T}(k), \tag{5.40a}$$

$$m_{\rm T}=\frac{\hat{M}_{\rm T}(nk)}{\hat{M}_{\rm T}(k)},\qquad m_{\rm P}=\frac{\hat{M}_{\rm P}(nk)}{\hat{M}_{\rm P}(k)}. \tag{5.40b}$$

Unless $m_{\rm P}/m_{\rm T}=1$, a one-way flow is induced in this system consisting of the S and N sectors. When $k\ll1$, $\hat{M}_{\rm T}(k)\propto k$ and $\hat{M}_{\rm P}(k)\propto1/k$. Thus, for $nk\ll1$, $m_{\rm T}=n$ and $m_{\rm P}=1/n$, and, therefore,

$$M=M_{\rm S0}\frac{n^2-1}{n^2+(L_{\rm N}/L_{\rm S})}. \tag{5.41}$$

The formula in Sone [2002] is its special case with $L_{\rm N}/L_{\rm S}=1$. The numerical data of $\hat{M}_{\rm T}(k)$ and $\hat{M}_{\rm P}(k)$ for a square cross section with the length of its side taken as L (BKW model, the diffuse reflection), taken from Sone & Hasegawa [1987], are shown in Table 5.3. The $\hat{M}_{\rm T}(k)$ increases monotonically with k; $|\hat{M}_{\rm P}(k)|$ first decreases as k increases, reaching the minimum value around $k=\sqrt{\pi}$ or ${\rm Kn}=2$ (Knudsen minimum) and increases slightly to the value at $k=\infty$. The data in the paper shows a similar behavior for the rectangular cross sections $L\times2L$ and $L\times4L$.[31]

[31] In Sone & Hasegawa [1987], the area S of the cross section is used instead of L^2 on the left-hand side of Eq. (5.36). Thus, the right-hand side expresses the average mass-flow rate per unit area (or the average mass flux) divided by $2p_0/(2RT_0)^{1/2}$. The length of the shorter side of the rectangular cross section being taken as the reference length, the average mass flux for the Poiseuille flow or the thermal transpiration increases as the aspect ratio of the cross section increases. In the channel or $L\times\infty$, the average mass flux diverges as $k\to\infty$ (see Section 4.2.2). Incidentally, the ratio $\hat{M}_{\rm T}/\hat{M}_{\rm P}\to-1/2$ as $k\to\infty$, irrespective of the shape of cross section including the channel [see Eqs. (4.43a) and (4.43b) in Section 4.2.2], from which the condition that no mass flow is induced in a free molecular gas is derived. The result is the linearized version of the condition (2.56) in Section 2.5.6. It may be noted that a half of the length of the shorter side of the cross section is taken as the reference length L in Sone & Hasegawa [1987] and that some care is required to transform the numerical data from it. The factor 4 in the table is for that reason.

Table 5.3. $\hat{M}_{\rm P}(k)$ and $\hat{M}_{\rm T}(k)$ for a square cross section.

$4k/\sqrt{\pi}$	$-4\hat{M}_{\rm P}$	$4\hat{M}_{\rm T}$	$4k/\sqrt{\pi}$	$-4\hat{M}_{\rm P}$	$4\hat{M}_{\rm T}$
0.05	7.457	0.0319	0.8	1.704	0.2806
0.06	6.467	0.0379	1	1.643	0.3147
0.07	5.708	0.0437	2	1.542	0.4226
0.08	5.119	0.0488	4	1.522	0.5250
0.09	4.686	0.0544	6	1.530	0.5789
0.1	4.337	0.0601	8	1.540	0.6137
0.2	2.800	0.1095	10	1.550	0.6386
0.3	2.298	0.1503	20	1.581	0.7038
0.4	2.047	0.1835	40	1.611	0.7515
0.5	1.905	0.2129	100	1.639	0.7923
0.6	1.814	0.2383	∞	1.677	0.8386
0.7	1.751	0.2607			

The first factor $M_{\rm S0}$ in Eq. (5.39), or Eq. (5.40a), is the mass-flow rate through the pipe only of the S sector with the shelves eliminated, where the temperature is different at the two ends, i.e., T_0 and T_1. The combination of the first and second factors, i.e., $M_{\rm S0}m_{\rm T}/n$, in Eq. (5.39) is the mass-flow rate through the pipe only of the S sector with shelves. From the data of $\hat{M}_{\rm T}(k)$ shown above, this is generally smaller than $M_{\rm S0}$ and approaches $M_{\rm S0}$ as $k \to 0$ with a fixed n; it decreases as n increases with a fixed k. The last factor, i.e., $(1 - m_{\rm P}/m_{\rm T})/(1 + m_{\rm P}L_{\rm N}/nL_{\rm S})$, which is smaller than unity for a finite k, expresses the reduction of the mass-flow rate by attaching the N sector to make the end conditions equal. For $nk \ll 1$, this factor reduces to $(n^2-1)/(n^2 + L_{\rm N}/L_{\rm S})$ and approaches unity as $n \to \infty$.

When a pipe with a temperature gradient is closed at their ends (or when $M = 0$), a pressure gradient is induced according to Eq. (5.36) as

$$\frac{{\rm d}p}{{\rm d}X_1} = -\frac{p_0}{T_0}\frac{{\rm d}T_w}{{\rm d}X_1}\frac{\hat{M}_{\rm T}(k)}{\hat{M}_{\rm P}(k)}.$$

Applying this formula to the present pipe consisting of the S and N sectors having the opposite temperature gradients, we find that there is a pressure rise

$$-\frac{T_1 - T_0}{T_0}\frac{\hat{M}_{\rm T}(nk)}{\hat{M}_{\rm P}(nk)}p_0$$

in the S sector and that there is a pressure drop

$$-\frac{T_1 - T_0}{T_0}\frac{\hat{M}_{\rm T}(k)}{\hat{M}_{\rm P}(k)}p_0$$

in the N sector. Therefore, the pressure difference between the two ends of the

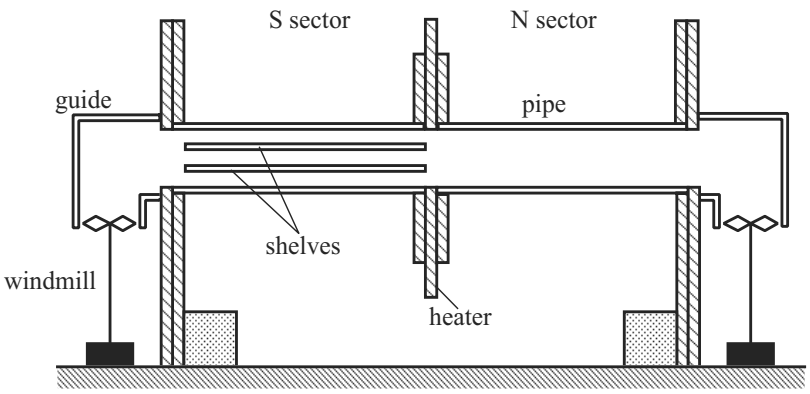

Figure 5.25. The pipe system with S and N sectors. In this figure, the S sector has two shelves.

pipe is given by

$$\frac{p_2 - p_0}{p_0} = -\frac{T_1 - T_0}{T_0} \frac{\hat{M}_{\mathrm{T}}(k)}{\hat{M}_{\mathrm{P}}(k)} \left(\frac{m_{\mathrm{T}}}{m_{\mathrm{P}}} - 1 \right), \tag{5.42}$$

where p_0 is the pressure at the end of the S sector and p_2 is the pressure at the end of the N sector. In the limiting case that $nk \to 0$, the factor $m_{\mathrm{T}}/m_{\mathrm{P}} - 1$ approaches $n^2 - 1$, and the formula (5.42) reduces to that given in Sone [2002]; the effect of the shelves on the pressure rise (or the pumping effect) increases indefinitely as $n \to \infty$. When k is a finite value, $m_{\mathrm{T}}/m_{\mathrm{P}}$ is bounded with respect to n; so is the effect of the shelves on the pressure rise.

The foregoing analysis to estimate a one-way flow, proposed by the author quite a long time ago, is based on the results for a slowly varying pipe flow along a pipe discussed in Section 4.2. At the connection point of the S and N sectors, the temperature gradient is discontinuous and the number of passage of flow changes from n^2 to one. Some correction is required for the formulas. The correction becomes larger when the length of the sectors decreases to a size comparable to the cross section of the pipe. From the simple analysis, however, a one-way flow is seen to be induced only by changing the number of passages in a part of a straight pipe, and the strength of the flow can be estimated.

The one-way flow induced in a pipe with the S and N sectors is demonstrated in a simple experiment (Sone, Fukuda, Hokazono & Sugimoto [2001]).[32] The pipe system consisting of S and N sectors shown in Fig. 5.25 is prepared. The inner diameter of the pipe is 11.5 mm and the length of sector S or N is 65 mm. The system is put in a vacuum chamber of the bell jar shown in Section 5.1.1, and a flow induced through the pipe is observed by windmills at the entrance of the pipe (Fig. 5.25). The windmill rotates with speed, for example, 34 rpm

[32]The video file of the experiment can be downloaded at http://fd.kuaero.kyoto-u.ac.jp/members/sone.

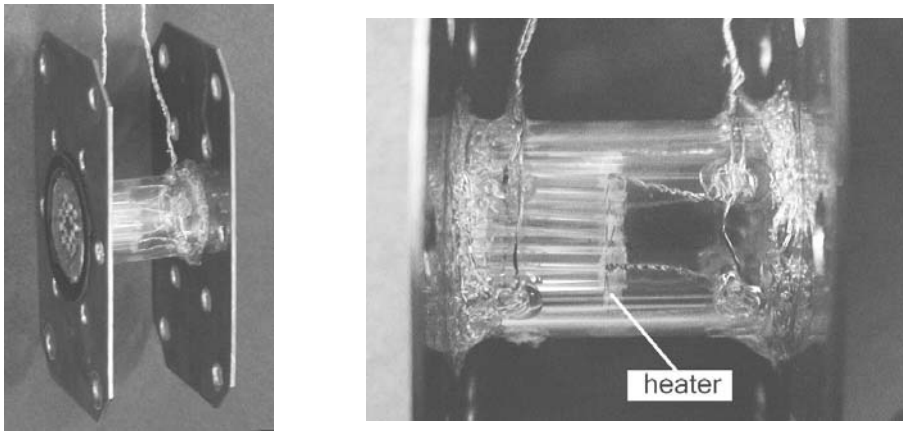

(a) (b)

Figure 5.26. Pump unit of the Knudsen compressor. (a) Overall view and (b) closer view.

at 40 Pa and 94 rpm at 10 Pa for the S sector with one shelf and 48 rpm at 40 Pa and 120 rpm at 10 Pa for the S sector with two shelves in the direction that the flow is from the S sector to the N sector, when the temperature of the pipe at the heater is 95°C and that at the entrance is 28°C.

A model of a pump without a moving part is constructed using the above-described system by Sone & Sugimoto [2002, 2003] (see the next section). Hudson & Bartel [1999] proposed to make use of an effect of accommodation in the kinetic boundary condition.

5.5 Compressors without a moving part

5.5.1 Knudsen compressor

Here, a simple pump model that demonstrates the pumping effect discussed in the preceding section (Section 5.4) is described. A cascade pumping system consisting of ten equal pump units is prepared by Sone & Sugimoto [2002, 2003] in the following way. The unit is a circular glass pipe with a heater at its middle position along its axis, and the pipe is divided into several passages on one side of the heater. That is, a bundle of 18 glass pipes of inner diameter 1.6 mm and length 15 mm is inserted in a half part of a circular glass pipe of inner diameter 15 mm and length 30 mm; a heater of Nichrome wire is wound around one end of each thinner pipe, and it is situated in the middle part of the pipe of length 30 mm; and a copper plate of thickness 1 mm is attached at each end of the unit (Fig. 5.26). The thinner-pipe side and the other side correspond, respectively, to the S sector and to the N sector in the preceding subsection (Section 5.4.3) and will also be called so here. The copper plate plays multiple

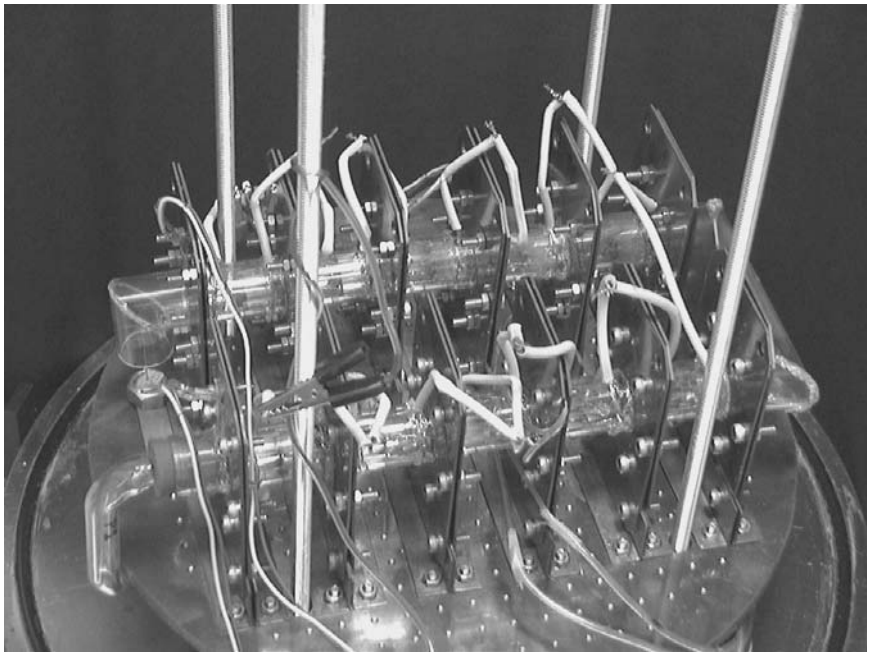

Figure 5.27. Pump system consisting of the ten units in Fig. 5.26.

roles: it is the joint to the next unit and the support, which is fixed to the base of a thick copper plate; the plate joined with the base serves to keep the temperature of the ends of the pipe units at a constant temperature close to the room temperature. In the real unit, the mass flow induced in the S sector by the temperature gradient is smaller than the corresponding flow in the N sector owing to the reduction of the cross-sectional area of the passage by the thickness of thinner pipes. However, some of the mass flow in the N sector is blocked by the change of cross section at the joint of the S and N sectors as in the system in Section 5.4.2. The five units are connected at the copper plates in a series and two of this series are joined with a glass pipe as shown in Fig. 5.27. This forms the pumping system consisting of ten units.

The experiment to examine the performance of the pumping system is carried out in the following system (Fig. 5.28). The pumping system is put in a glass bell jar of diameter 250 mm and height 300 mm put on a steel base, and the N-sector end of the pumping system is open in the bell jar. The pressure in the bell jar is controlled from atmospheric pressure down to several pascals by a rotary vacuum pump. The other end (or S-sector end) of the pumping system is connected to a steel tank of 8×10^3 cm^3 with a glass pipe of length 150 mm and a steel pipe of length 550 mm. The bell jar and the tank serve as reservoirs. The heating is controlled by electric current supplied from the outside of the bell jar. The performance of the pumping system is how fast it pumps a gas from the tank to the bell jar when the heater is put on.

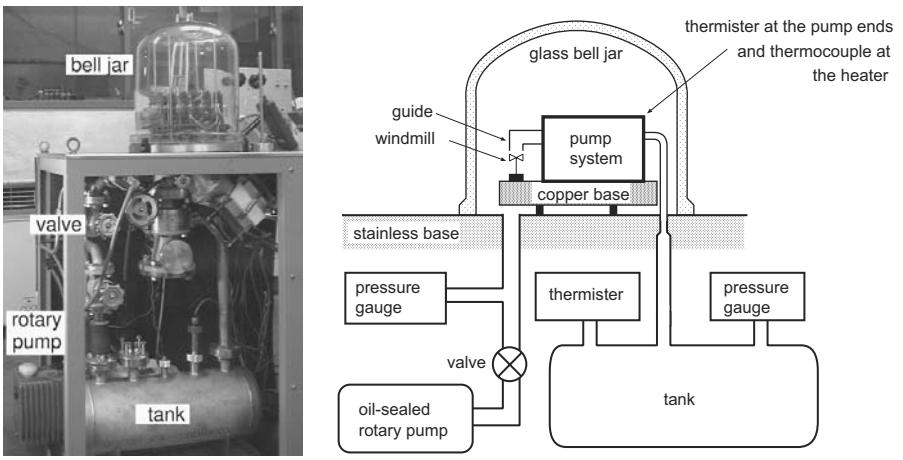

Figure 5.28. Experimental system. (a) Real system and (b) explanatory diagram.

5.5.2 Performance

The performance of the pumping system is examined in the following way. First, keep the whole experimental system at a desired uniform pressure by adjusting the valve between the rotary pump and the vacuum chamber. After confirming that the stationary state at a desired pressure is established, put on the heater, and observe the pressures in the vacuum chamber and in the tank and the temperatures at the heater, at the two ends of the pumping system, and in the tank. In this process, the pressure in the vacuum chamber is kept constant at the initial pressure by adjusting the valve.

Some of the results of the performance experiment in Sone & Sugimoto [2003] are presented here.[33] The time variations of the pressures in the tank and in the vacuum chamber (bell jar) are plotted in Fig. 5.29. In the experiments, the pressure in the bell jar is kept at a constant value p_0 within the error of $\pm 1\%$. The pressure in the tank during the initial period before the heater is put on is sometimes a little higher (the pressure difference: $-0.1 \sim 0.4$ Pa for $p_0 \leq 20$ Pa and $-0.5 \sim 0.8$ Pa for $p_0 \geq 40$ Pa) than that in the bell jar. Owing to the uncontrollable pressure variation in the bell jar and the conceivable errors (2%) between the two pressure gauges, this difference cannot be given a definite meaning for $p_0 \geq 40$ Pa, but the relative difference amounts to $2 \sim 6$ % for low pressures and is appreciable [see Fig. 5.29 (a)]. This difference may be attributed to desorption of gases from the tank or pumping system, because this difference reduces in the experiments after the tank is baked or after repeated experiments. The temperature difference between the two ends of the pumping system is less than 2 K. The temperatures of the two ends of the pumping system gradually increase after the heater is put on. Thus, a temperature gradient (20 K over 600

[33] The pump in this paper is a little improved from that in Sone & Sugimoto [2002].

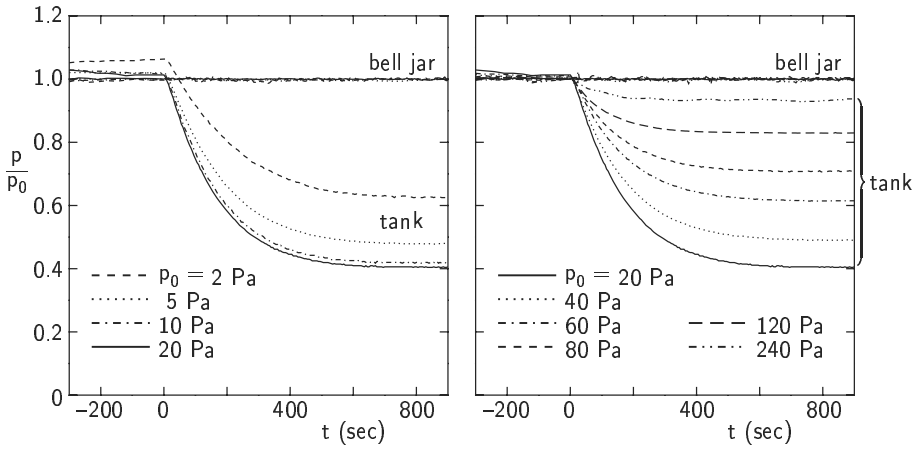

Figure 5.29. Time variation of the pressure p (Pa) in the tank and in the bell jar for the heating of 39 W. The t is the time after the heater is put on. The p_0 is the pressure in the bell jar that is aimed to be kept at that value.

mm) is induced along the pipe between the pumping system and the tank. These gradients are, however, too small to induce an appreciable flow. Incidentally, the temperature of the heater increases rapidly to around 500 K in 100 s and then gradually to about 550 K in 800 s.

The pumping speed [or the volume-flow rate (cm^3/s)] from the tank vs the pressure (Pa) in the tank during the pumping process at a constant pressure in the bell jar, estimated from Fig. 5.29, is shown in Fig. 5.30.

The gas flow is visualized by a windmill at the bell-jar-side end of the pumping system (Fig. 5.28). The performance (e.g., the pumping speed) is naturally reduced in the presence of the windmill. The results in Figs. 5.29 and 5.30 are for the experiments without the windmill.

5.5.3 Discussion

The above pump makes use of the features of the two kinds of flows: temperature-induced flow and pressure-driven flow. The cascade system works effectively in the model. The present system consists of ten equal units. Much larger pressure ratio can be obtained in a system consisting of much more units. However, in a system consisting of many units to obtain a large pressure ratio, the pressure in a unit differs much depending on its position in the series of units. Thus, a unit should be designed so as to work effectively in its pressure range with the aid of the discussion and data in Section 5.4. For example, when $p_0 = 240$ Pa, the pressure drop of only about 5% is obtained in the case of Fig. 5.29. This is expected to be improved, without losing mass-flow rate, by using more thinner pipes for the S sector; in this case, in view of Fig. 5.30, the mass-flow rate is enough as a pump unit in a series of other units working in a lower pressure

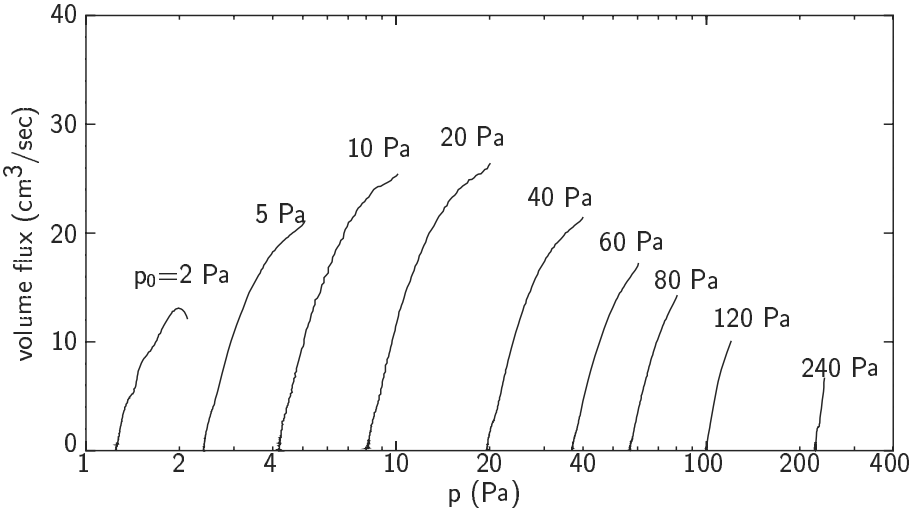

Figure 5.30. Pumping speed [volume-flow rate (cm^3/s) from the tank] vs the pressure p in the tank during pumping process at a constant pressure p_0 in the bell jar, corresponding to the experiment shown in Fig. 5.29.

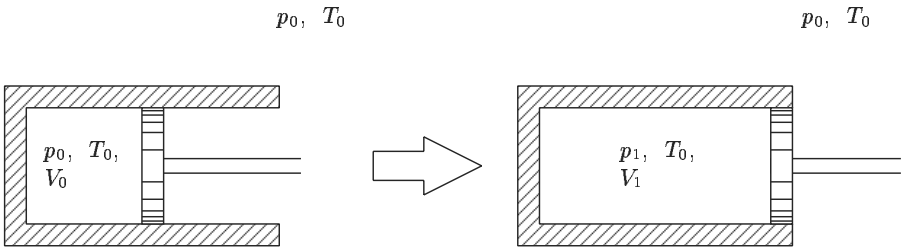

Figure 5.31. Thermodynamic process.

range, though the volume-flow rate decreases considerably. The principle and mechanism of the pump system is so simple that a larger system giving a larger flow rate can be made without difficulty.

The pump was made to demonstrate that a simple pumping system without a moving part has an appreciable pumping speed (volume-flow rate) and maintains a considerable pressure ratio between two reservoirs. Thus, no attention is paid to the energy efficiency of the system; any means is not taken to prevent unnecessary heat escape for a generally inefficient heat system. Thus the energy efficiency is expected to be very low. For example, in the experiment in Fig. 5.29 of 39 W (watt = $\mathrm{kg\,m}^2/\mathrm{s}^3$) electric supply, it takes 250 s to expand volume $V_0 = 4.8 \times 10^3$ cm^3 of air in the tank to the full volume 8×10^3 cm^3 of the tank when $p_0 = 40$ Pa, and thus the energy required in this process is $E = 39$

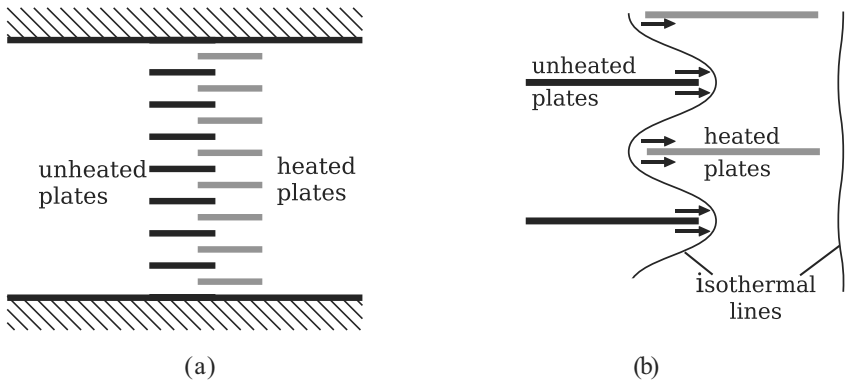

Figure 5.32. Thermal edge flow. (a) Arrays of heated plates and unheated plates and (b) isothermal lines and the thermal edge flow induced by the arrays of the plates in panel (a). See Section 5.1.4.

W×250 s = 9800 J. Here, consider a thermodynamic process to expand a gas. Take a heat-permeable cylinder with a piston in an infinite expanse of a gas at pressure p_0 and temperature T_0 (Fig. 5.31).Initially, the piston contains the same gas of the same pressure and temperature as the surrounding gas, and the volume of the cylinder is V_0. Then, move the piston so slowly to expand the volume to V_1 that the temperature of the gas in the piston is kept at T_0 during the expansion. The work W_T required to move the piston by an external force during this process is given by $p_0V_0[V_1/V_0 - 1 - \ln(V_1/V_0)]$. The work W_T corresponding to the above example is $W_T = 0.03$ J. Thus the ratio W_T/E is about 3×10^{-6}, which is by far smaller (1/1000) than that of a commercial turbo-molecular vacuum pump. However, the present system being very primitive, there is enough allowance to improve its performance, i.e., the enforcement of flow by devising the shape and size of the system and the prevention of heat escape.

5.5.4 Thermal-edge compressor

The system introduced above makes use of the thermal transpiration as its driving force. A temperature gradient along the pipe is essential, and heat flow through the solid part of the pipe accompanies the gradient. This is a loss of energy in the system. In order to reduce this energy loss considerably, we have recently devised a new driving system using the thermal edge flow (Section 5.1.4) as shown in Fig. 5.32 and made a prototype of the new pump system (Sugimoto & Sone [2005]; the patent is applied for). The pump we made is as follows. A short steel pipe, with bottom, of inner diameter 60 mm and length 15 mm is prepared (Fig. 5.33). A square hole (38 × 38 mm) is made in the middle of the bottom. The array of 18 unheated plates is set directly on the hole. The array of 19 heated plates is framed with heat insulator and is set on the cylinder bottom

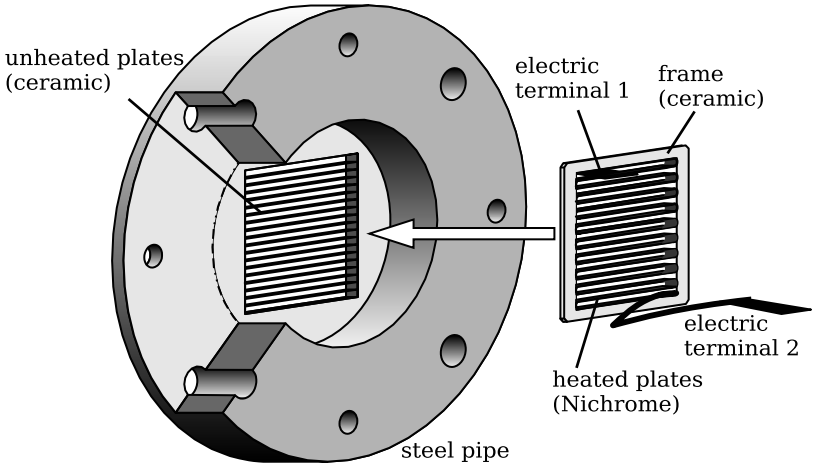

Figure 5.33. Pump unit of the thermal-edge compressor. The unheated plate is ceramic and the array of heated plates is made of a Nichrome band heater. The smaller holes are used as ducts for cooling water. The larger holes are for joint-bolts.

so as to be in the configuration as shown in Fig. 5.32 (a). This is a unit of the pump. The heated plates are themselves a heater made of Nichrome ribbon, and the unheated plates are made of ceramic. Smaller holes in the pipe are used as ducts for cooling water, and larger holes are used to connect the units. Five units are arranged in a series as shown in Fig. 5.34. The wires supply electric current to the heater and the cooling water flowing through the ducts keeps the pipe at a uniform and constant temperature. In the new system, which may be called a *thermal-edge compressor*, the heat flow from the hotter plates to the colder, which results in loss of energy, is determined by the heat flow through the gas, which is much smaller owing to smaller heat conductivity of the gas. Each of the plates is kept at (nearly) uniform temperature, and the heat flow through the solid part is small. Thus, we can expect that the loss of energy decreases considerably. Let the pressure at the entrance of the pump be p_1 and that at the exit be p_0. An example of the performance test, i.e., the relation between the volume flow rate V_1 of the gas at the entrance and the pressure ratio p_1/p_0 for the energy supply 32.2 W, is shown in Fig. 5.35. Incidentally, the temperature of a heated plate is about 419 K for $p_0 = 10$ Pa and 444 K for $p_0 = 4$ Pa and that of a unheated plate is 319 K. The energy efficiency of the new system is six times better than that of the system in Section 5.5.1.

In view of the decisive advantage of the system, clean and of very simple structure without a moving part, and the performance of the Knudsen and thermal-edge compressors, a pump without a moving part is promising as a real one. These compressors can be also applied to a valve system or a drying system working in low pressures because their structures are simple, their sizes can be chosen freely, and the working condition can be simply controlled by electric current.

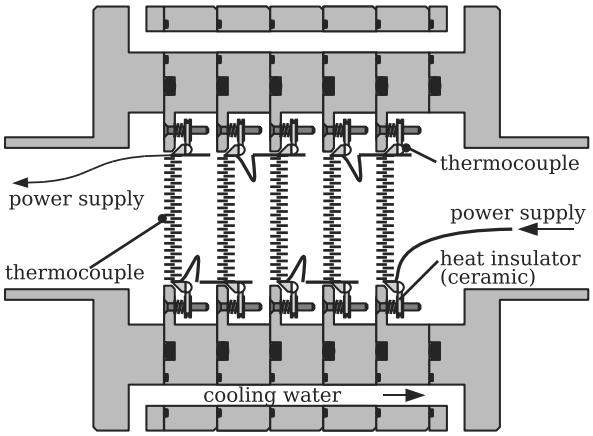

Figure 5.34. Pump system of the thermal-edge compressor. Five units are joined in a series. The ducts prepared by the smaller holes in the unit are used to flow cooling water to keep the pipe at a uniform and constant temperature. Electric current is supplied with a wire to the heater. The connection of the units is made tight with packing.

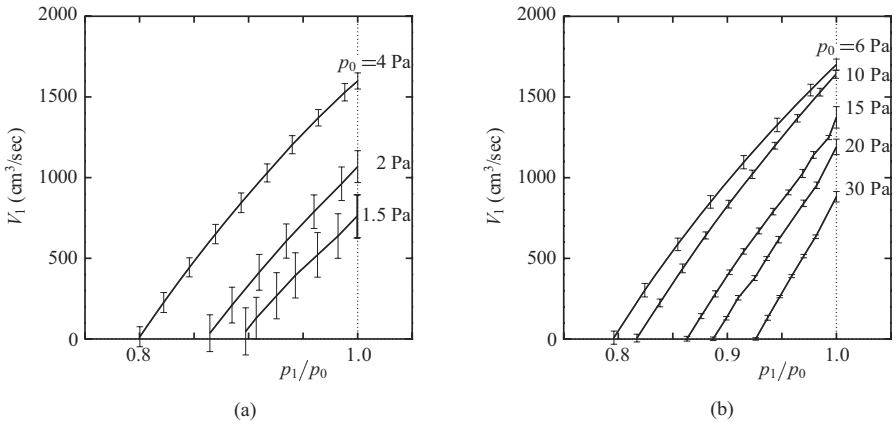

Figure 5.35. Performance of the pump driven by thermal edge flow (the volume flow rate V_1 and the pressure p_1 of the gas at the entrance of the pump for various pressure p_0 at the exit, i.e., V_1 vs p_1/p_0 for various p_0). (a) Smaller p_0 and (b) larger p_0. The energy supply is 32.2 W. Wide error bars in panel (a) are due to poor precision of the mass flow meter for small mass-flow rate.

5.6 Summary

In this chapter, various kinds of time-independent flows induced by temperature fields have been explained and some of them are demonstrated in simple experiments. They are typical of a rarefied gas. That is, they disappear in the continuum limit (or $\mathrm{Kn} \to 0$).[34] In the free molecular gas ($\mathrm{Kn} = \infty$), they also disappears in a bounded-domain system or in an unbounded-domain system with a common uniform state at rest at infinities, as we have seen in Section 2.5. In the free molecular case, however, a heated (or cooled) body in the gas at rest is generally subject to a force, in contrast to the case in the continuum limit. As the experiments show, appreciable flows are very easily induced by temperature fields, in contrast to general understanding. The flow velocity and temperature fields are closely related in a rarefied gas. Thermal polarization mentioned in Section 4.5 is another outcome of this relation.

Besides being interesting flows typical in a rarefied gas, the temperature-induced flows have a very important effect on the behavior of a gas in the continuum limit. Their infinitesimal trace in the continuum limit produces a finite effect on the behavior of the gas in the limit. We discussed this effect or the ghost effect in Section 3.3.4. Its examples in well-known problems in the classical fluid dynamics will be given in Sections 8.2 and 8.3.

[34] The flows induced by temperature fields are absent for the leading-order term of ϕ with respect to k in Sections 3.1 and 3.2.

Chapter 6

Flows with Evaporation and Condensation

Simple but fundamental flows with evaporation and condensation on a boundary are discussed in this chapter. Some examples are mentioned in Chapters 2 and 4, and those related to bifurcation of flows are discussed in Chapters 7 and 8.

6.1 Evaporation from or condensation onto a plane condensed phase

6.1.1 Problem and basic equations

Consider a semi-infinite expanse ($X_1 > 0$) of a gas bounded by its plane condensed phase at rest with temperature T_w at $X_1 = 0$. Let the saturated gas pressure at temperature T_w be p_w. At time $t = 0$, the gas is in the uniform equilibrium state with pressure p_∞, temperature T_∞, and flow velocity $(v_{1\infty}, 0, 0)$, which is not in equilibrium with the condensed phase. We discuss the time evolution of the disturbance produced by the interaction of the gas with the condensed phase on the basis of the numerical computation of the BKW equation and the complete-condensation condition.

As in Section 4.8, the present spatially one-dimensional BKW system can be reduced to a simpler system where two molecular velocity components are eliminated. Let ℓ_w $[= (8RT_w/\pi)^{1/2}/(A_c p_w/RT_w)]$ be the mean free path of the gas in the equilibrium state at rest with pressure p_w and temperature T_w. We take p_w as the reference pressure p_0, T_w as the reference temperature T_0, ℓ_w as the reference length L, and $t_w = \ell_w/(2RT_w)^{1/2}$ as the reference time t_0, and use the notation introduced in Section 1.9. Then, the BKW system is transformed into the following system for the marginal velocity distribution functions g and h (see Section A.6): The marginal velocity distribution functions g and h are

defined by

$$g = \int\int \hat{f} \mathrm{d}\zeta_2 \mathrm{d}\zeta_3, \quad h = \int\int (\zeta_2^2 + \zeta_3^2) \hat{f} \mathrm{d}\zeta_2 \mathrm{d}\zeta_3, \tag{6.1}$$

and the macroscopic variables $\hat{\rho}$, $\hat{v}_1$, and $\hat{T}$ are given as

$$\hat{\rho} = \int g \mathrm{d}\zeta_1, \quad \hat{v}_1 = \frac{1}{\hat{\rho}} \int \zeta_1 g \mathrm{d}\zeta_1, \quad \hat{T} = \frac{2}{3\hat{\rho}} \int [(\zeta_1 - \hat{v}_1)^2 g + h] \mathrm{d}\zeta_1. \tag{6.2}$$

The BKW equation is reduced to

$$\frac{\partial}{\partial \hat{t}} \begin{bmatrix} g \\ h \end{bmatrix} + \zeta_1 \frac{\partial}{\partial x_1} \begin{bmatrix} g \\ h \end{bmatrix} = \frac{2}{\sqrt{\pi}} \hat{\rho} \begin{bmatrix} G - g \\ H - h \end{bmatrix}, \tag{6.3}$$

where

$$\begin{bmatrix} G \\ H \end{bmatrix} = \frac{\hat{\rho}}{(\pi \hat{T})^{1/2}} \begin{bmatrix} 1 \\ \hat{T} \end{bmatrix} \exp\left(-\frac{(\zeta_1 - \hat{v}_1)^2}{\hat{T}} \right). \tag{6.4}$$

The boundary condition on the wall is, at $x_1 = 0$,

$$\begin{bmatrix} g \\ h \end{bmatrix} = \frac{1}{\sqrt{\pi}} \begin{bmatrix} 1 \\ 1 \end{bmatrix} \exp\left(-\zeta_1^2\right) \quad (\zeta_1 > 0), \tag{6.5}$$

and the condition at infinity is, as $x_1 \to \infty$,

$$\begin{bmatrix} g \\ h \end{bmatrix} \to \frac{\hat{p}_\infty}{\sqrt{\pi} \hat{T}_\infty^{3/2}} \begin{bmatrix} 1 \\ \hat{T}_\infty \end{bmatrix} \exp\left(-\frac{(\zeta_1 - \hat{v}_{1\infty})^2}{\hat{T}_\infty} \right), \tag{6.6}$$

where $\hat{p}_\infty = p_\infty / p_w$, $\hat{T}_\infty = T_\infty / T_w$, $\hat{v}_{1\infty} = v_{1\infty} / (2RT_w)^{1/2}$. The initial condition at $\hat{t} = 0$ is

$$\begin{bmatrix} g \\ h \end{bmatrix} = \frac{\hat{p}_\infty}{\sqrt{\pi} \hat{T}_\infty^{3/2}} \begin{bmatrix} 1 \\ \hat{T}_\infty \end{bmatrix} \exp\left(-\frac{(\zeta_1 - \hat{v}_{1\infty})^2}{\hat{T}_\infty} \right) \quad (x_1 > 0). \tag{6.7}$$

In the following discussion we often use, instead of $\hat{v}_{1\infty}$, the Mach number M_∞

$$M_\infty = \frac{v_{1\infty}}{(5RT_\infty/3)^{1/2}},$$

which is related to $\hat{v}_{1\infty}$ as $M_\infty = (6/5)^{1/2} \hat{v}_{1\infty} / \hat{T}_\infty^{1/2}$.

The marginal velocity distribution functions g and h have discontinuity at the corner $(x_1, \hat{t}) = (0, 0)$ of the domain $(x_1 > 0,\ \hat{t} > 0)$ for $\zeta_1 > 0$. In fact, taking the limits of g and h $(\zeta_1 > 0)$ in the two different orders, i.e., first $\hat{t} \to 0_+$ and then $x_1 \to 0_+$ and first $x_1 \to 0_+$ and then $\hat{t} \to 0_+$, we have

$$\lim_{x_1 \to 0_+} \left(\lim_{\hat{t} \to 0_+} \begin{bmatrix} g \\ h \end{bmatrix} \right) = \frac{\hat{p}_\infty}{\sqrt{\pi} \hat{T}_\infty^{3/2}} \begin{bmatrix} 1 \\ \hat{T}_\infty \end{bmatrix} \exp\left(-\frac{(\zeta_1 - \hat{v}_{1\infty})^2}{\hat{T}_\infty} \right),$$

and

$$\lim_{\hat{t} \to 0_+} \left(\lim_{x_1 \to 0_+} \begin{bmatrix} g \\ h \end{bmatrix} \right) = \frac{1}{\sqrt{\pi}} \begin{bmatrix} 1 \\ 1 \end{bmatrix} \exp\left(-\zeta_1^2\right).$$

The two kinds of limits do not agree unless $\hat{p}_\infty = 1$, $\hat{T}_\infty = 1$, and $\hat{v}_{1\infty} = 0$. The differences of the above two kinds of limits, i.e., the discontinuities of g and h at the corner $(x_1, \hat{t}) = (0, 0)$, propagate in the direction of the characteristic $x_1 - \zeta_1 \hat{t} = 0$ of Eq. (6.3) and decay owing to the collision term on its right-hand side. The direction of the propagation depends on ζ_1. For $\zeta_1 < 0$, the characteristic starts at an interior point of the gas, where g and h are continuous, and therefore they are continuous for all x_1 and $\hat{t}$. Owing to the discontinuity, the standard finite-difference scheme has a difficulty in the differentiation process across the discontinuity. A hybrid method to treat the discontinuity is explained in Section 4.8, according to which the numerical computation is carried out here.

6.1.2 Behavior of evaporating flows

First, we discuss the behavior of the gas evaporating from the plane condensed phase on the basis of the numerical computation by Sone & Sugimoto [1990].

Transient behavior

The transient behavior of the gas for $M_\infty = 0$, $\hat{p}_\infty\,(= p_\infty/p_w) = 0.25$, and $\hat{T}_\infty\,(= T_\infty/T_w) = 1$ is shown in Figs. 6.1–6.3. Figure 6.1 shows the time evolution of disturbance at the initial stage, and Fig. 6.2 shows the separation process of the disturbance into a shock layer, a contact layer, and a Knudsen layer, accompanying the development of uniform regions between the wave and layers. The front of disturbances, which is confirmed by investigation of the long time behavior to be propagating with its shape preserving at a constant speed, is a shock layer; the layer slowly widening with time across which the pressure is uniform or nearly uniform, the flow velocity varies slightly, and the temperature (thus, density) varies considerably is a *contact layer,* corresponding to a contact discontinuity of the Euler equations; and the thin layer adjacent to the condensed phase is a Knudsen layer. The shock layer propagates at a supersonic speed determined by its strength (Section 4.7), and the contact layer shifts nearly at the flow speed[1] accompanied by diffusion. The uniform regions escape from the flow field and the Knudsen layer converges quickly to a time-independent state. Finally, a time independent state with the uniform state between the contact layer and the Knudsen layer as the state at infinity is established. Figure 6.3 shows the decay of the discontinuity of the marginal velocity distribution function g, where the discontinuity is invisible at $\hat{t}\,(= t/t_w) = 50$.

The case with a smaller pressure ratio, i.e., $M_\infty = 0$, $\hat{p}_\infty\,(= p_\infty/p_w) = 0.05$, and $\hat{T}_\infty\,(= T_\infty/T_w) = 1$ is shown in Figs. 6.4 and 6.5. Figure 6.4 is the flow field after the separation of the shock layer, the contact layer, and the Knudsen layer, where uniform regions between the shock layer and the contact layer and between the contact layer and the Knudsen layer are developing. Owing to

[1] If the profile of the layer is shifting without deformation, and if the density varies considerably but the flow velocity is uniform across the layer, the shifting speed of the profile is easily seen to be the same as the flow velocity of the gas from the conservation equation of mass (1.12).

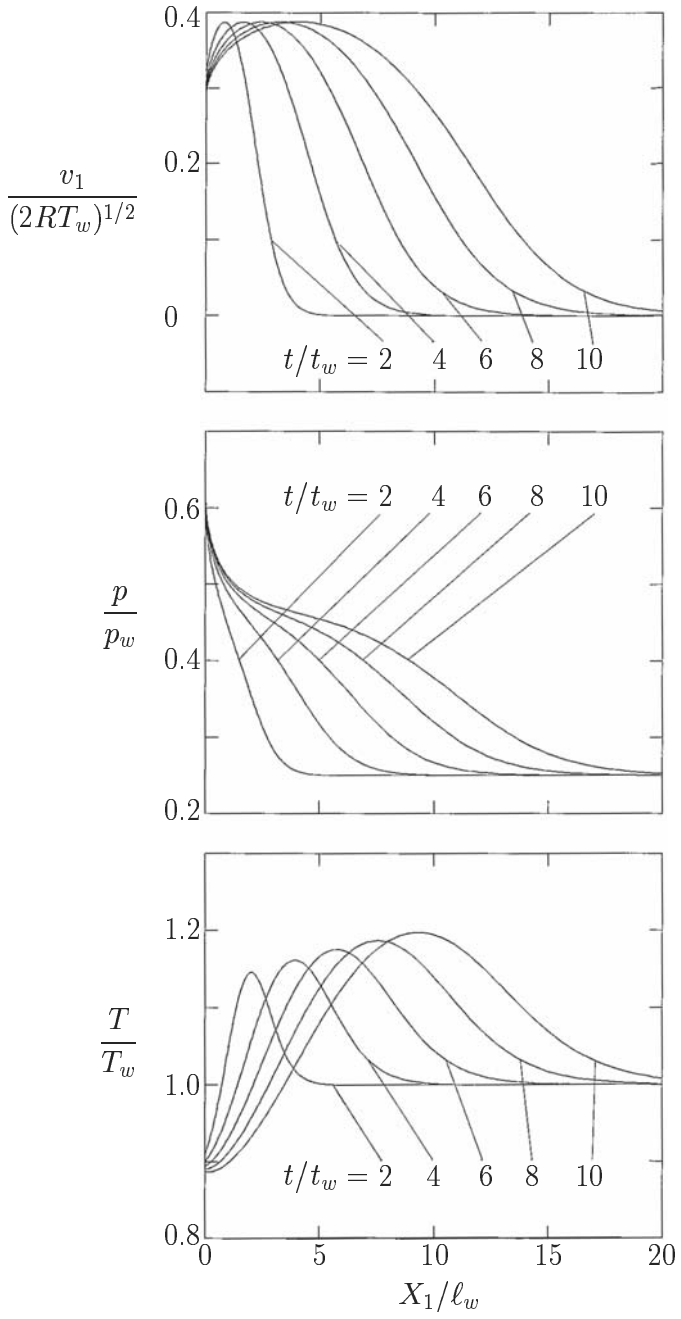

Figure 6.1. Transient process of the evaporating flow from a plane condensed phase for the initial condition ($M_\infty = 0$, $p_\infty/p_w = 0.25$, $T_\infty/T_w = 1$) I: Initial stage.

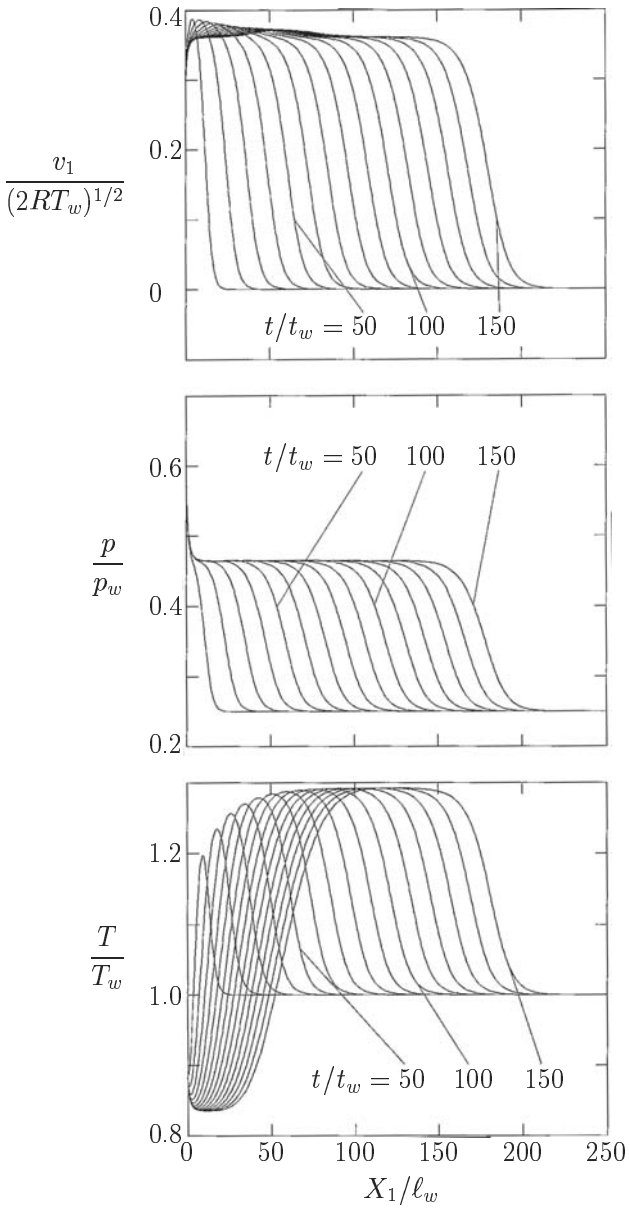

Figure 6.2. Transient process of the evaporating flow from a plane condensed phase for the initial condition ($M_\infty = 0$, $p_\infty/p_w = 0.25$, $T_\infty/T_w = 1$) II: Separation stage.

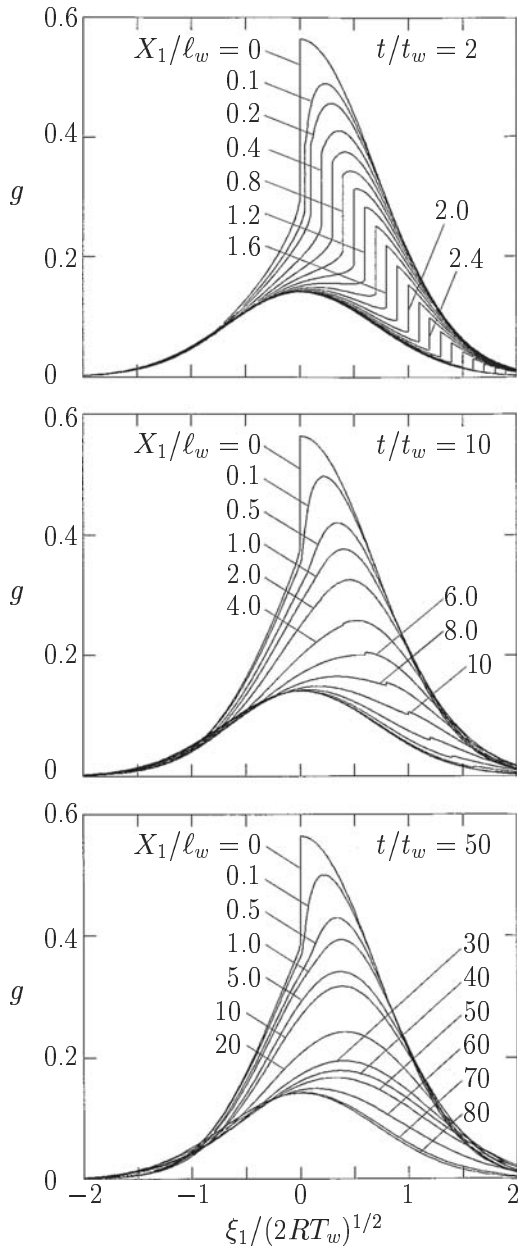

Figure 6.3. Propagation and decay of the discontinuity of the marginal velocity distribution function g in the evaporating flow from a plane condensed phase for the initial condition ($M_\infty = 0$, $p_\infty/p_w = 0.25$, $T_\infty/T_w = 1$).

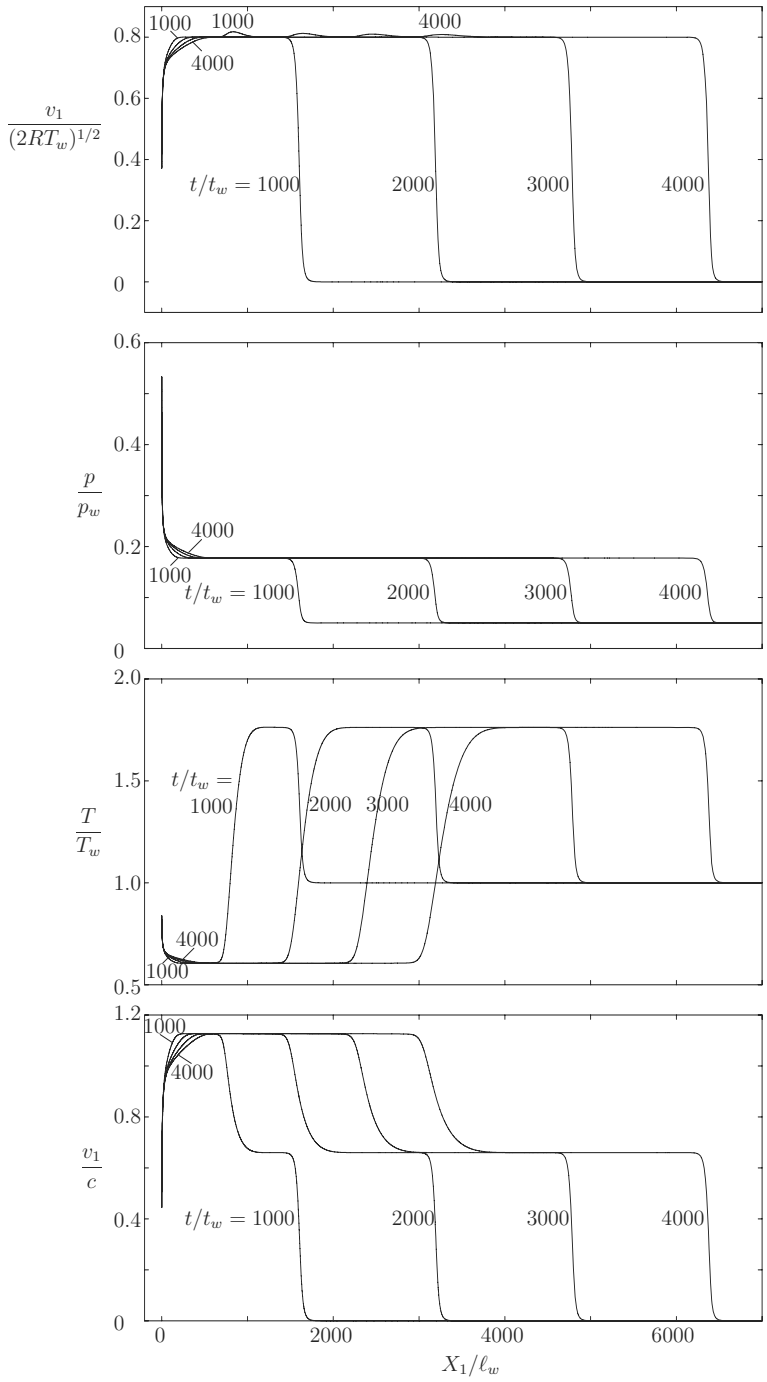

Figure 6.4. Transient process of the evaporating flow from a plane condensed phase for the initial condition ($M_\infty = 0$, $p_\infty/p_w = 0.05$, $T_\infty/T_w = 1$). (Computed newly by H. Sugimoto.)

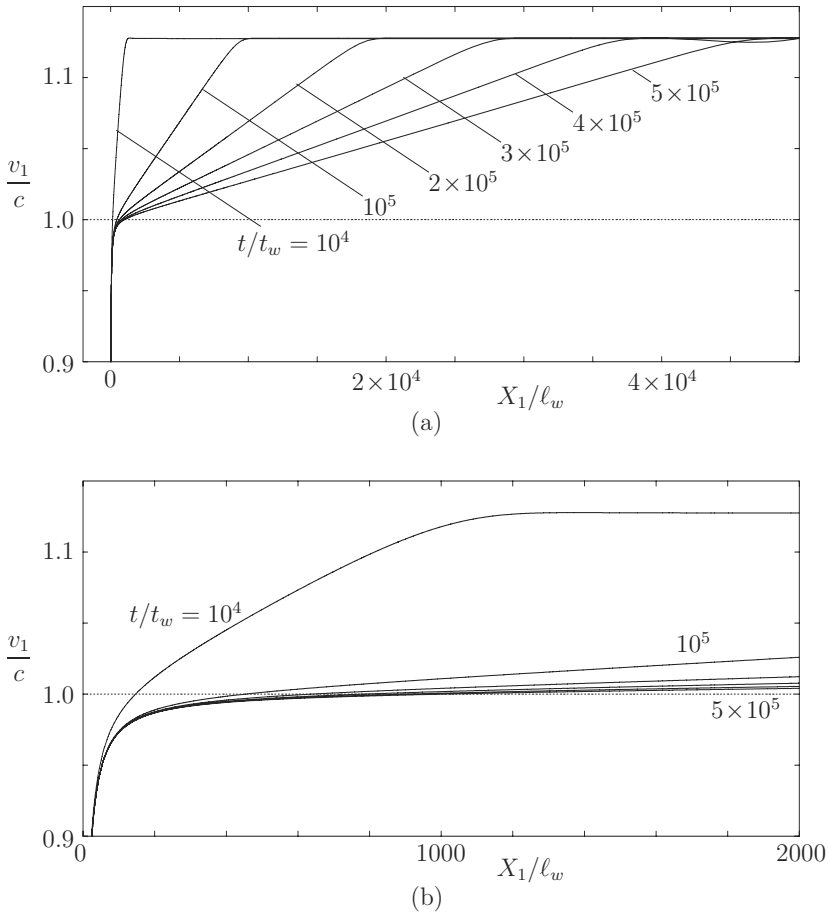

Figure 6.5. Shift of the supersonic region to infinity in the transient evaporating flow from a plane condensed phase for the initial condition ($M_\infty = 0$, $p_\infty/p_w = 0.05$, $T_\infty/T_w = 1$) I: v_1/c vs X_1/ℓ_w for various large values of t/t_w. (a) Wider range of X_1/ℓ_w and (b) Knudsen-layer region. The region with $v_1/c > 1$ is moving away to infinity as time goes on [panel (a)]. A point with $v_1/c < 1$ seems to converge to a finite X_1/ℓ_w [panel (b)]. The fine dotted line in panel (a) or (b) is the line $v_1/c = 1$. (Computed newly by H. Sugimoto up to much longer time than in Sone & Sugimoto [1990] to show the limiting behavior more clearly.)

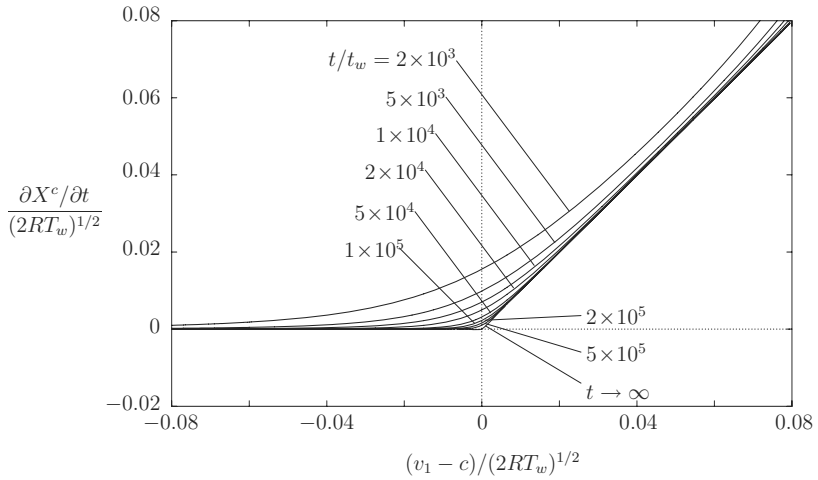

Figure 6.6. Shift of the supersonic region to infinity in the transient evaporating flow from a plane condensed phase for the initial condition ($M_\infty = 0$, $p_\infty/p_w = 0.05$, $T_\infty/T_w = 1$) II: $(\partial X^c/\partial t)/(2RT_w)^1/2$ vs $(v_1 - c)/(2RT_w)^1/2$ for various large values of t/t_w. The curve marked by $t \to \infty$ is the limiting curve estimated by extrapolating the data up to $t/t_w = 5\times10^5$. The $\partial X^c/\partial t$ converges to $v_1 - c$ in the supersonic region ($v_1 > c$) and it converges to 0 in the subsonic region ($v_1 < c$). The various limiting curves estimated with data up to the smaller t/t_w being compared, they are seen to approach the above-mentioned limiting curve $t \to \infty$ from below. (Computed newly by H. Sugimoto up to much longer time than in Sone & Sugimoto [1990] to obtain the limiting curve $t \to \infty$ more accurately.)

the small pressure ratio, a strong evaporating flow is induced accompanied by a large temperature drop in the neighborhood of the condensed phase, and a strong shock wave is formed, across which there is a large temperature jump. Thus, there is a large temperature difference across the contact layer. The variation of flow velocity across the contact layer being immaterial, there is large increase of Mach number v_1/c [$c = (5RT/3)^{1/2}$][2] across it, and the flow becomes supersonic behind the contact layer. The contact layer diffuses or its thickness increases with time. This is also clearly seen, besides the temperature profile itself, from widening of the region of nonuniform velocity in the contact layer as time goes on. The transition region in the neighborhood of the condensed phase is still in a time-dependent state in contrast to the preceding example, though the uniform region between the transition region and the contact layer is expanding. Figure 6.5 shows the profiles v_1/c vs X_1/ℓ_w for various large values of t/t_w.[3] The supersonic region ($v_1/c > 1$) seems to shift to infinity, but a sub-

[2]See Footnote 32 in Section 3.1.9.

[3]The time is measured in the scale of the mean free time in the computation. In the atmospheric condition the mean free time is about 2×10^{-10} s. Thus, one second is a very long time (more than $t/t_w = 10^9$) in the reference time of the above computation. See Footnote 102 in Section 3.6.2.

sonic point ($v_1/c < 1$) seems to converge to a finite X_1/ℓ_w. This is confirmed numerically in the next paragraph. After the supersonic region escapes from the flow field to infinity, time-independent Knudsen layer with sonic speed[4] at infinity is established.

Let X^c be the coordinate X_1 of the nearest point to $X_1 = 0$ where $(v_1 - c)/(2RT_w)^{1/2}$ takes a given value. It is a function of $(v_1 - c)/(2RT_w)^{1/2}$ and t/t_w. Figure 6.6 shows $\partial X^c/\partial t$ vs $(v_1 - c)/(2RT_w)^{1/2}$ [the shifting velocity of X^c of a given $(v_1-c)/(2RT_w)^{1/2}$ as a function of $(v_1-c)/(2RT_w)^{1/2}$] for various large values of t/t_w. Its limiting curve as $t \to \infty$ estimated by extrapolating the data up to $t/t_w = 5 \times 10^5$ is $\partial X^c/\partial t = v_1 - c$ for $v_1 > c$ (in the supersonic region) and $\partial X^c/\partial t = 0$ for $v_1 < c$ (in the subsonic region) with the errors unrecognizable in the figure. Any supersonic X^c point is moving away from the condensed phase at a speed larger than $v_1 - c$, and therefore, the supersonic region finally disappears from the flow field to infinity.

Figures 6.7 and 6.8 show the case with $M_\infty = 0.75$, $p_\infty/p_w = 1$, and $T_\infty/T_w = 1$. The gas initially receding from the condensed phase, a rarefaction region develops near the condensed phase, from which an expansion wave, a contact layer, and a Knudsen layer are separated, and uniform regions develop between the wave and layers.

Time-independent solution

From the long-time behavior of time-evolution solutions, time-independent solutions are constructed. That is, we pursue the time evolution until a uniform state ahead of the Knudsen layer develops enough and confirm that g and h there correspond to those of a Maxwellian; if necessary, we introduce the following cut and patch process several times: replace the contact layer etc. ahead of the nearly uniform region by a uniform state and pursue the time evolution. Being interested only in a time-independent solution, we do not have to follow the time evolution accurately, and the time-consuming hybrid method is unnecessary. Instead, various nonuniform initial conditions are tried in order to avoid missing any possible stable time-independent solution.

From a large number of time-independent solutions, we find that p_∞/p_w and T_∞/T_w are determined by M_∞, where p_∞, T_∞, and M_∞ are the data at infinity in the time-independent solution (but not those of the initial condition), i.e.,

$$\frac{p_\infty}{p_w} = h_1(M_\infty), \quad \frac{T_\infty}{T_w} = h_2(M_\infty) \quad (0 \le M_\infty \le 1). \tag{6.8}$$

The functions $h_1(M_\infty)$ and $h_2(M_\infty)$ are tabulated in Table 3.4, where M_n corresponds to M_∞.[5] No time-independent solution exists for $M_\infty > 1$. Three examples of the profiles of the flow velocity, pressure, and temperature of the time-independent solutions are shown in Fig. 6.9, where the crosses $\times$ denote

[4] See Footnote 32 in Section 3.1.9.

[5] If the general case with $\hat{v}_2$, $\hat{v}_3$, $\hat{v}_{2\infty}$, or $\hat{v}_{3\infty} \neq 0$ is considered, they all vanish in the limiting time-independent state (Aoki, Nishino, Sone & Sugimoto [1991]). Thus, the results are commonly given by Table 3.4.

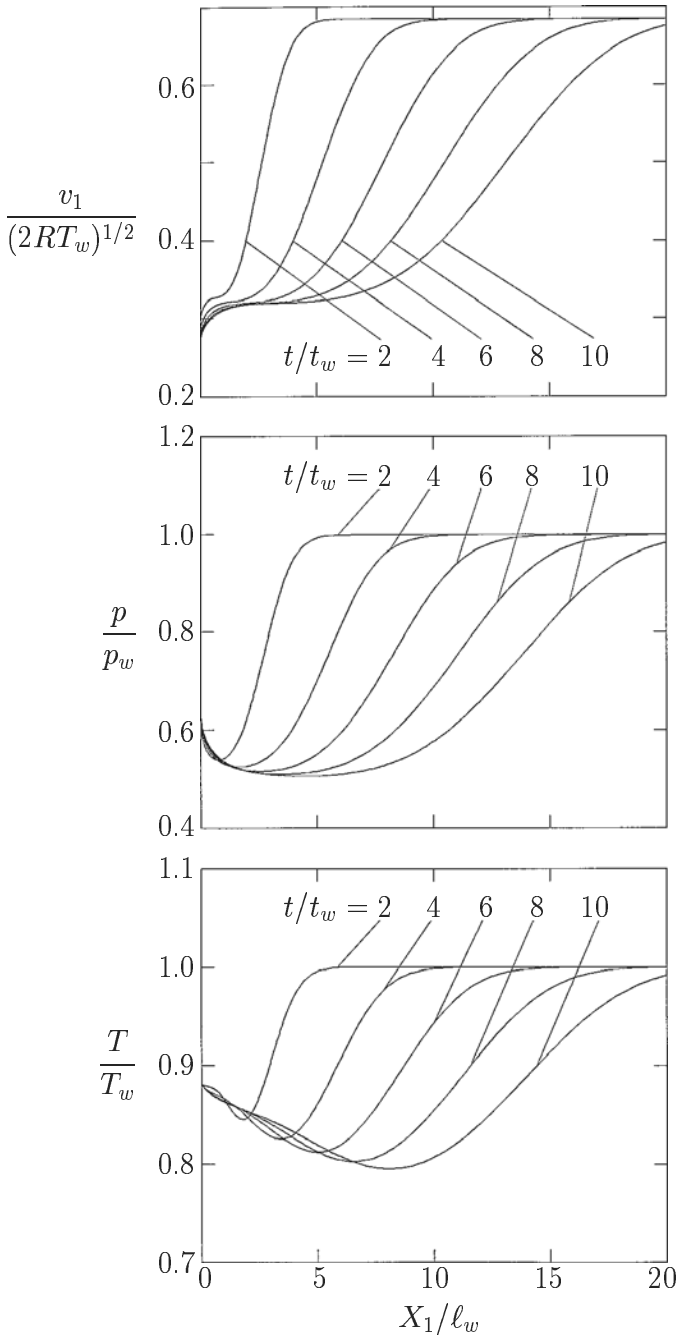

Figure 6.7. Transient process of the evaporating flow from a plane condensed phase for the initial condition ($M_\infty = 0.75$, $p_\infty/p_w = 1$, $T_\infty/T_w = 1$) I: Initial stage.

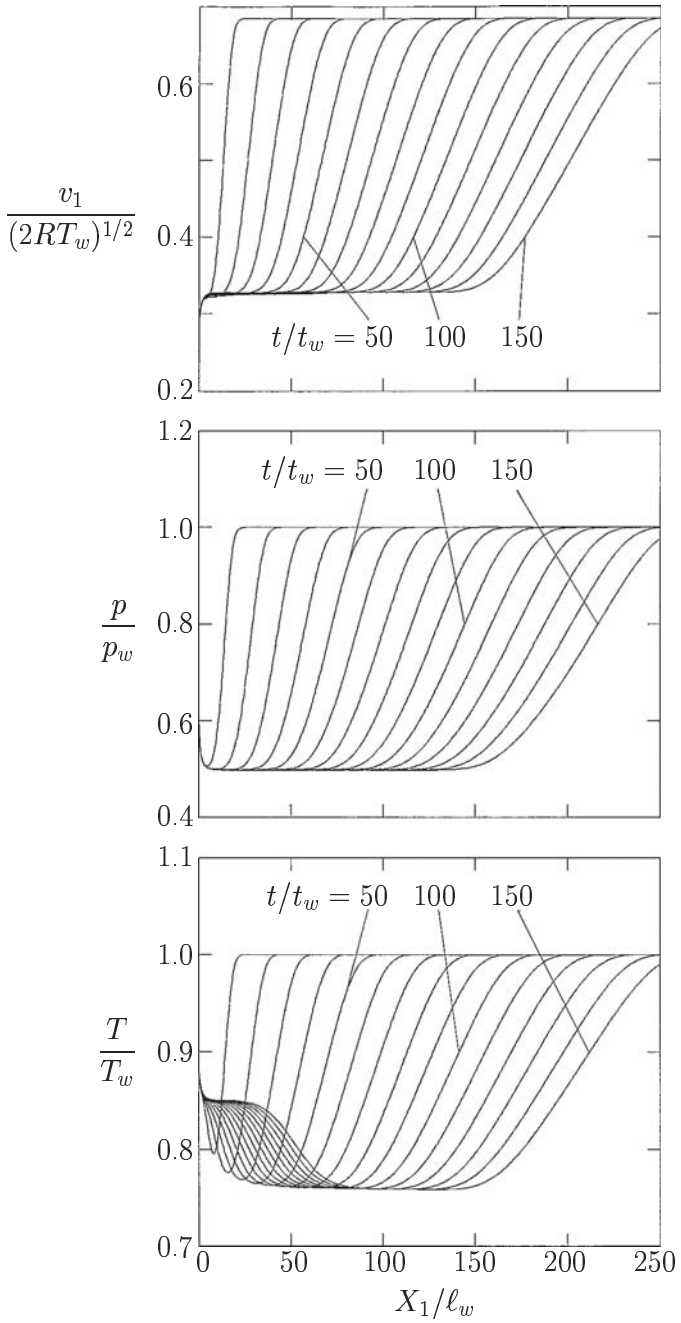

Figure 6.8. Transient process of the evaporating flow from a plane condensed phase for the initial condition ($M_\infty = 0.75$, $p_\infty/p_w = 1$, $T_\infty/T_w = 1$) II: Separation stage.

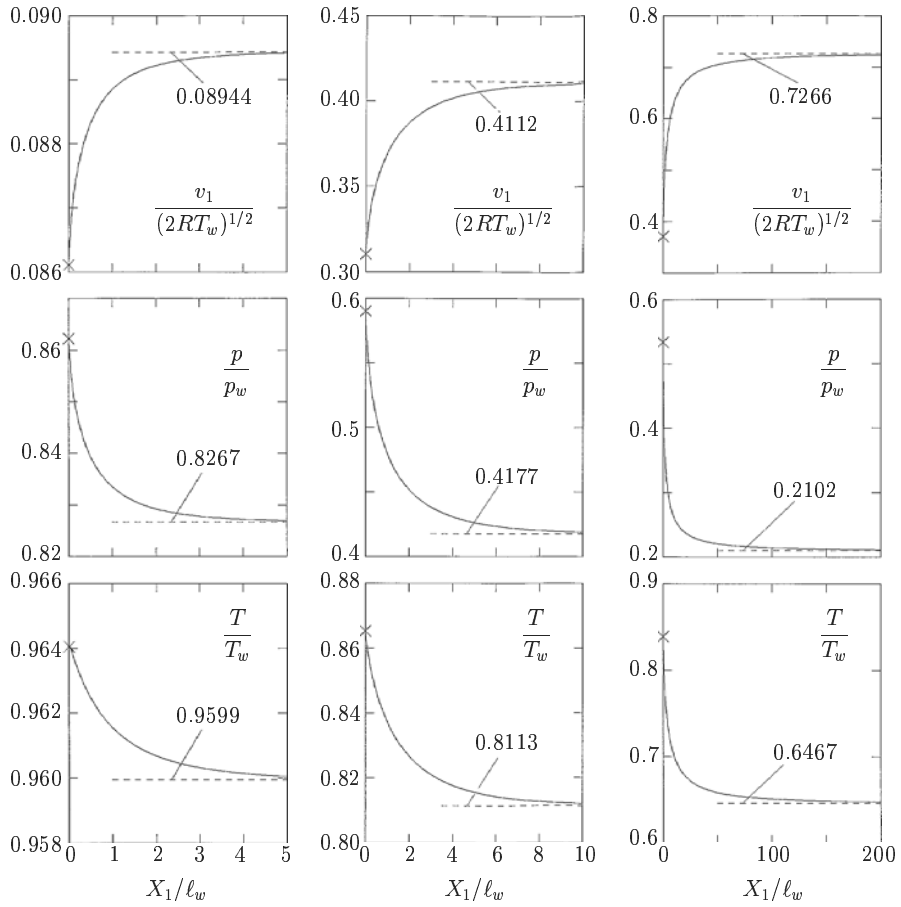

(a) $M_\infty = 0.1$ (b) $M_\infty = 0.5001$ (c) $M_\infty = 0.9897$

Figure 6.9. Profiles of flow velocity, pressure, and temperature, i.e., $v_1/(2RT_w)^{1/2}$, p/p_w, and T/T_w vs X_1/ℓ_w of time-independent solutions evaporating from a plane condensed phase. (a) $M_\infty = 0.1$, (b) $M_\infty = 0.5001$, and (c) $M_\infty = 0.9897$. The crosses $\times$ are the values at $X_1/\ell_w = 0$, and the dashed lines $---$ are the asymptotes at infinity. The approach to the state at infinity becomes slower as M_∞ tends to unity.

the values at $X_1/\ell_w = 0$. The approach to the state at infinity becomes slower as M_∞ tends to unity. The pressure ratio p_∞/p_w takes the minimum value 0.2075 at $M_\infty = 1$. No state with lower than this pressure is possible at infinity. When the state at infinity is vacuum initially, it is filled up with the gas in the final time-independent state. The situation is different in the evaporation from a cylinder or sphere to be discussed in Sections 6.2 and 6.4.

The case where the flow has a component parallel to the plane condensed phase initially and at infinity, or equivalently the condensed phase is moving along it, is discussed in Aoki, Nishino, Sone & Sugimoto [1991]. In the limit

$t/t_w \to \infty$, the parallel component vanishes or it approaches the motion of the condensed phase. Thus, the relation (6.8) holds in this case.

6.1.3 Behavior of condensing flows

Next, we discuss the behavior of the gas condensing onto the plane condensed phase on the basis of the numerical computation by Sone, Aoki & Yamashita [1986], Sone, Aoki, Sugimoto & Yamada [1988], and Aoki, Sone & Yamada [1990].

Transient behavior

The solution is obtained numerically by a finite difference method for many sets of parameters M_∞ (< 0), p_∞/p_w, and T_∞/T_w, and is classified into the following four types:
(I) The gas is compressed on the condensed phase, and the compression region propagates or diffuses toward upstream. The speed of propagation, however, slows down and finally vanishes. A time-independent state with the prescribed condition at infinity (M_∞, p_∞/p_w, T_∞/T_w) is established. [I-type solution; Fig. 6.10 (a)]
(II) The gas is compressed on the condensed phase, and the compression wave (shock wave) propagates up to upstream infinity. The region behind the wave approaches a time-independent state with a new subsonic state at infinity. [II-type solution; Fig. 6.10 (b)]
(III) Rarefaction region develops on the condensed phase and diffuses as time goes on. A time-independent state with the prescribed condition at infinity is established finally. [III-type solution; Fig. 6.10 (c)]
(IV) Rarefaction region develops on the condensed phase, and an expansion wave propagates up to infinity. The region behind the wave approaches a time-independent state with a new subsonic or sonic state at infinity. [IV-type solution; Fig. 6.10 (d)]

The type of solution is determined by the initial and boundary data (M_∞, p_∞/p_w, T_∞/T_w). The type of numerical solutions on the section of $T_\infty/T_w = 1$ of the space (M_∞, p_∞/p_w, T_∞/T_w) is shown in Fig. 6.11, where the points that give the I-, II-, III-, and IV-type solutions are marked by $\circ$, $\bullet$, $\triangle$, and $\blacktriangle$ respectively.[6] From close examination of a large number of the data, the regions I, II, III, and IV of the four types of solution are schematically given in Fig. 6.12. The boundary between regions I and II and that between regions II and IV intersect on the plane $M_\infty = -1$. For p_∞/p_w larger than the intersection, the region of the III-type solution appears between regions I and IV.

Supplementary explanation of the time evolution of solutions is given with the aid of Figs. 6.10, 6.13, and 6.14. The time evolution of solution at the point A

[6] To be more precise, the region II is subdivided into two regions. For p_∞/p_w smaller than some value that depends on M_∞ and T_∞/T_w [or in the region below the dashed line in Figs. 6.11 (a) and 6.12], the gas evaporates from the condensed phase, although the gas flow is blowing toward the condensed phase at infinity.

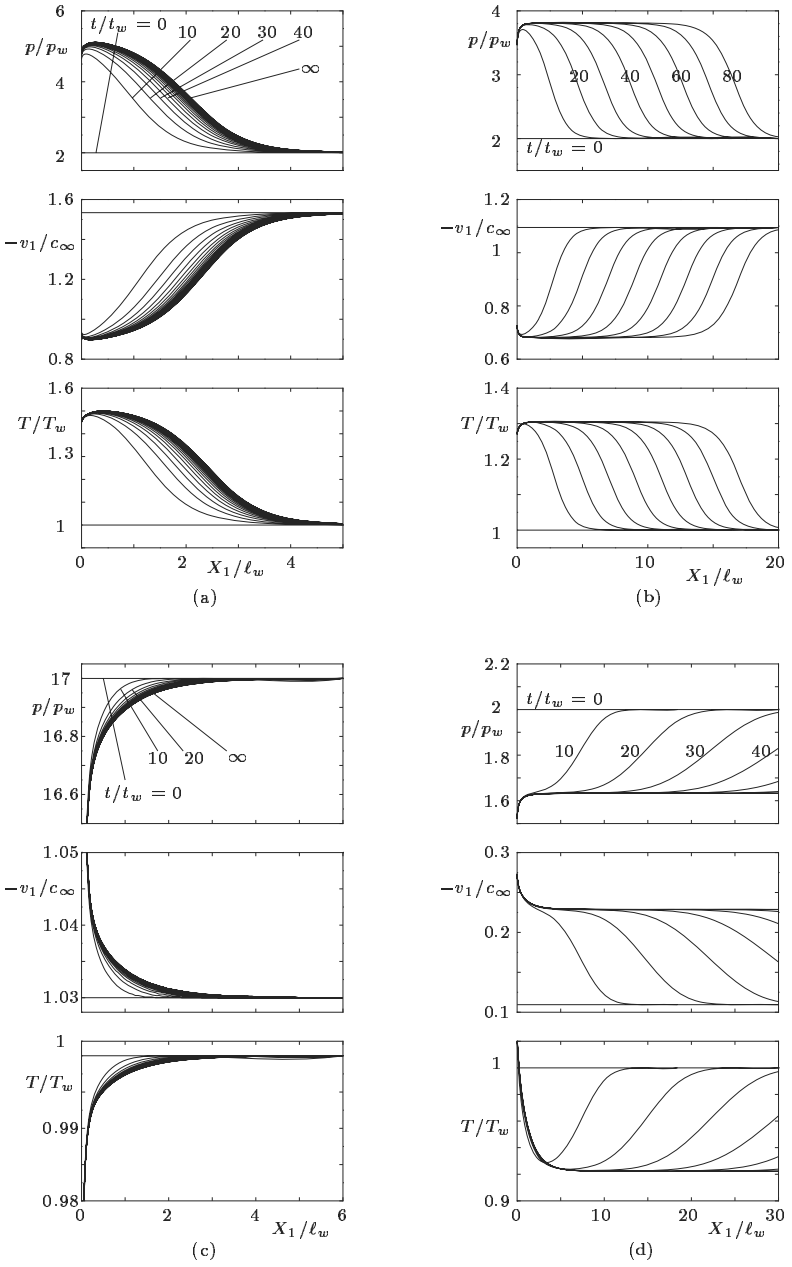

Figure 6.10. Typical time evolution of a flow condensing onto a plane condensed phase. (a) $M_\infty = -1.534$, $p_\infty/p_w = 2$, $T_\infty/T_w = 1$, (b) $M_\infty = -1.095$, $p_\infty/p_w = 2$, $T_\infty/T_w = 1$, (c) $M_\infty = -1.03$, $p_\infty/p_w = 17$, $T_\infty/T_w = 1$, and (d) $M_\infty = -0.1095$, $p_\infty/p_w = 2$, $T_\infty/T_w = 1$. The c_∞ is the sonic speed at infinity, i.e., $c_\infty = (5RT_\infty/3)^{1/2}$. The limiting profile at $t/t_w = \infty$ is a time-independent solution. (Recomputed by T. Doi for the figure.)

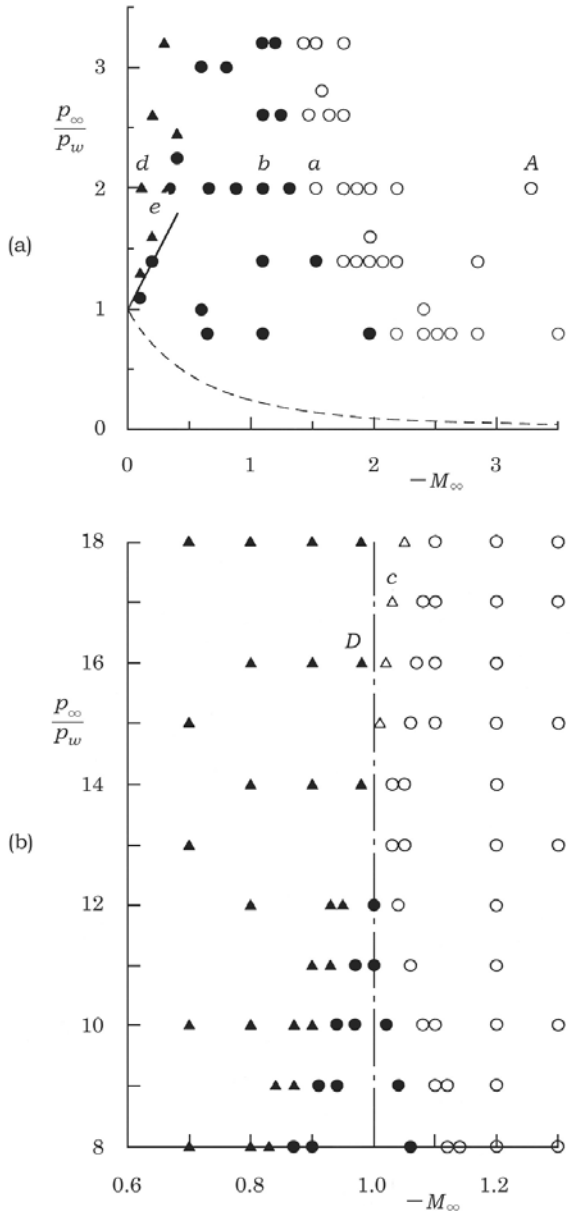

Figure 6.11. Type of solution on the cross section ($T_\infty/T_w = 1$) in the space $(M_\infty, p_\infty/p_w, T_\infty/T_w)$. (a) Smaller p_∞/p_w and (b) larger p_∞/p_w. Here, ○, ●, △, and ▲ indicate the I-, II-, III-, and IV-type solutions respectively. In panel (a), the solid line —— shows the analytical result for small $|M_\infty|$ in Section 7.2 on which a time-independent solution with (M_∞, p_∞, T_∞) at infinity exists, and the dashed line - - - indicates the boundary below which evaporation takes place on the condensed phase (see Footnote 6 in this subsection).

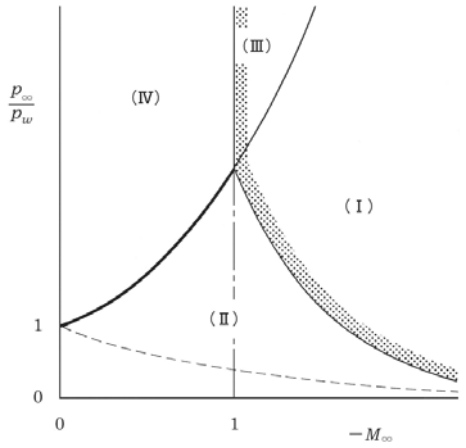

Figure 6.12. Schematic map of the type of solution and the existence range of a time-independent solution on the cross section $T_\infty/T_w = \text{const}$ in the three-dimensional space $(M_\infty, p_\infty/p_w, T_\infty/T_w)$. The I-, II-, III-, and IV-type solutions evolve, respectively, from the initial and boundary conditions in the regions marked by (I), (II), (III), and (IV). The dashed line - - - - in (II) indicates the boundary below which evaporation takes place on the condensed phase (see Footnote 6 in this subsection). In the case of the existence range of a time-independent solution, $(M_\infty, p_\infty/p_w, T_\infty/T_w)$ is taken as $(M, p/p_w, T/T_w)$ at infinity. A time-independent solution exists on the boundary between the regions II and IV and in the regions I and III.

in Fig. 6.11 (a) is given in Fig. 6.13 (a). The state approaches a time-independent state very rapidly and the disturbances are confined in a narrow region owing to strong convection of the flow from infinity. Only a partial profile (head) of a shock wave is observed. At the point a in Fig. 6.11 (a), the propagation of disturbance decelerates more slowly and almost the full profile of a shock wave is seen ahead of a thin Knudsen layer adjacent to the condensed phase [Fig. 6.10 (a)]. At the point b (or d) in Fig. 6.11 (a), a shock wave (or an expansion wave) propagates accompanied by a thin Knudsen layer on the condensed phase [Fig. 6.10 (b) or (d)]. As $|M_\infty|$ decreases from b or increases from d in Fig. 6.11 (a), the strength of the wave decreases. At some point [e in Fig. 6.11 (a)] in the middle, the disturbance propagates with damping and no finite disturbance propagates up to upstream infinity; the solution approaches a subsonic time-independent solution with the prescribed data at infinity (Fig. 6.14). Figure 6.10 (c) with the initial data at c in Fig. 6.11 (b) is an example of the solutions of type III, which is a supersonic accelerating flow. The time evolution of the solution at the point D in Fig. 6.11 (b), large p_∞/p_w and M_∞ close to -1, is shown in Fig. 6.13 (b). Close examination as done in Fig. 6.6 in Section 6.1.2 shows that the solution slowly approaches a time-independent state with a sonic condition at infinity.[7]

[7]See Footnote 3 in Section 6.1.2.

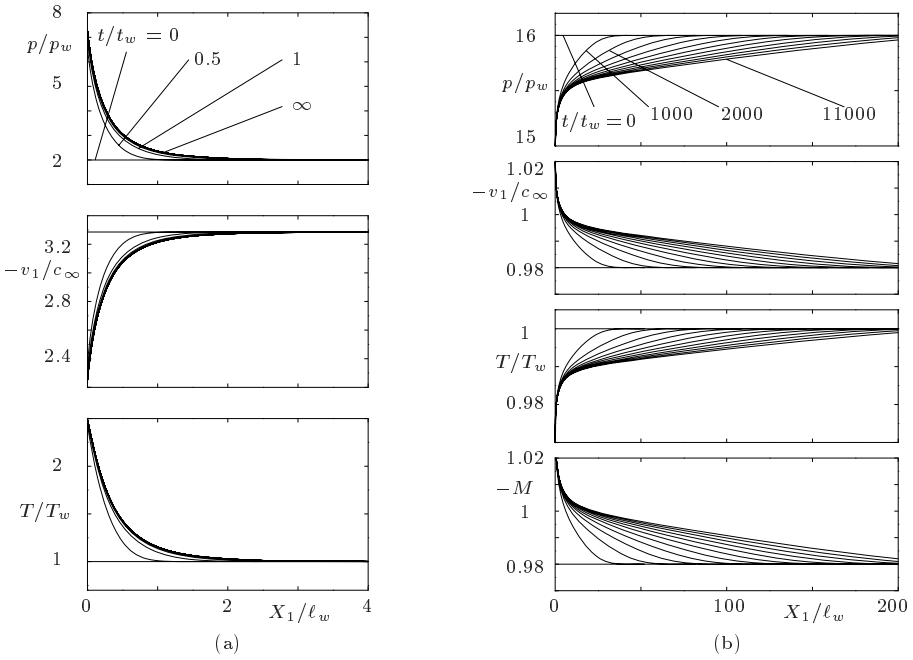

Figure 6.13. Time evolution of solutions I. (a) $M_\infty = -3.286$, $p_\infty/p_w = 2$, $T_\infty/T_w = 1$ [solution starting at A in Fig. 6.11 (a)] and (b) $M_\infty = -0.98$, $p_\infty/p_w = 16$, $T_\infty/T_w = 1$ [solution starting at D in Fig. 6.11 (b)]. The c_∞ is the sonic speed at infinity, i.e., $c_\infty = (5RT_\infty/3)^{1/2}$. (Recomputed by T. Doi for the figure.)

Time-independent solution

From the preceding discussion and extensive data of the numerical computation, we find that a time-independent solution exists for the set of parameters in the regions I and III and on the boundary between the regions II and IV (see Fig. 6.12), i.e.,

$$p_\infty/p_w = F_s(M_\infty, 0, T_\infty/T_w) \qquad (-1 < M_\infty < 0), \tag{6.9a}$$

$$p_\infty/p_w > F_b(M_\infty, 0, T_\infty/T_w) \qquad (M_\infty < -1), \tag{6.9b}$$

$$p_\infty/p_w \geq F_b(-1_-, 0, T_\infty/T_w) = F_s(-1_+, 0, T_\infty/T_w) \quad (M_\infty = -1), \tag{6.9c}$$

where M_∞, p_∞/p_w, and T_∞/T_w are, respectively, M, p/p_w, and T/T_w at infinity (but not those in the initial condition). The $F_s(M_\infty, 0, T_\infty/T_w)$ and $F_b(M_\infty, 0, T_\infty/T_w)$, which are special ones with $\overline{M}_t = 0$ of $F_s(M_\infty, \overline{M}_t, T_\infty/T_w)$ and $F_b(M_\infty, \overline{M}_t, T_\infty/T_w)$ introduced in Eqs. (3.229a)–(3.229c), are tabulated in Tables 6.1 and 6.2.[8]

[8]The data F_s and F_b with $\overline{M}_t \neq 0$ obtained by a similar numerical computation are shown in Figs. 3.7 and 3.8 in Section 3.5.2.

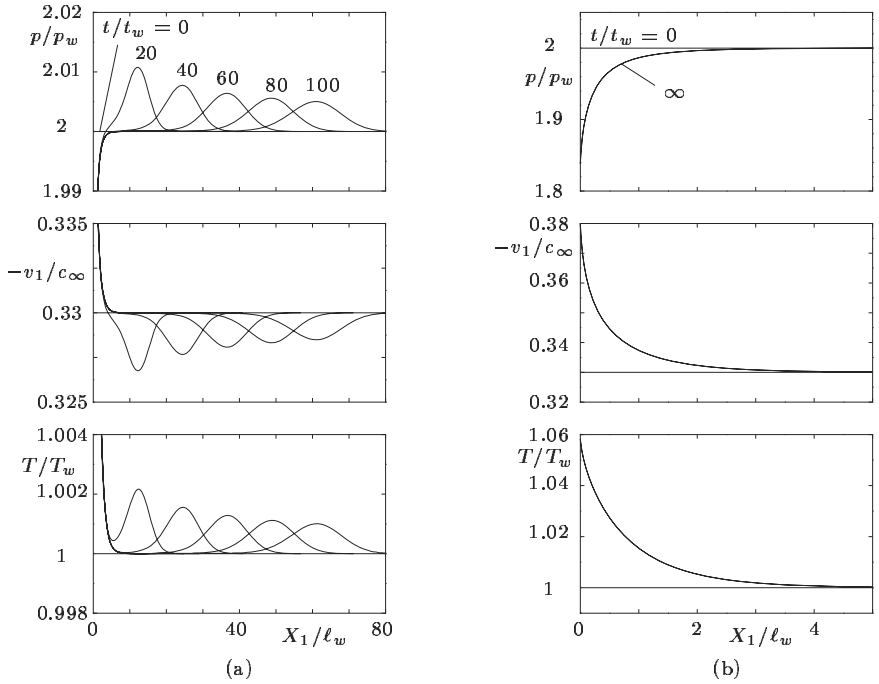

Figure 6.14. Time evolution of solution II: $M_\infty = -0.330$, $p_\infty/p_w = 2$, $T_\infty/T_w = 1$ [solution starting at e in Fig. 6.11 (a)]. (a) Profiles for various t/t_w and (b) the limiting profile at $t/t_w = \infty$, i.e., the time-independent profile. The c_∞ is the sonic speed at infinity, i.e., $c_\infty = (5RT_\infty/3)^{1/2}$. (Recomputed by T. Doi for the figure.)

The analytical structure of the boundary of the regions is discussed in Chapter 7. The profiles at $t/t_w = \infty$ in Figs. 6.10, 6.13, and 6.14 are time-independent solutions. The profiles at $t/t_w = \infty$ of the flows supersonic at infinity in Figs. 6.10 (a), (c), and 6.13 (a) show the feature of the time-independent solution clearly. Several examples of the flow subsonic at infinity are separately shown in Fig. 6.15, because the variations in the profiles are confined in a narrow region in Fig. 6.10, where most of the space is used to show the development of a new uniform state behind a wave front.

The profiles in Fig. 6.15 depend largely on the temperature ratio T_∞/T_w. The flow can be accelerating or decelerating depending on T_∞/T_w for each Mach number M_∞. Three types of profiles are found at $M_\infty = -0.3$, but the type of panel (a2) appears only for a narrow range of T_∞/T_w, inside of $1.13 - 1.15$. At $M_\infty = -0.9$, the type of panel (a1) does not appear even at $T_\infty/T_w = 0.02$, but the type of (a2) appears. In the figures, the profiles are given as functions of X_1/ℓ_w. If they are given as a function of X_1/ℓ_∞, where ℓ_∞ is the mean free path of the gas in the equilibrium state at rest with pressure p_∞ and temperature T_∞ and is related to ℓ_w as $\ell_\infty = (T_\infty/T_w)^{3/2}\ell_w$ [see Eq. (1.41)], the thickness of the transition region for a given M_∞ is nearly common to the three T_∞/T_w's and

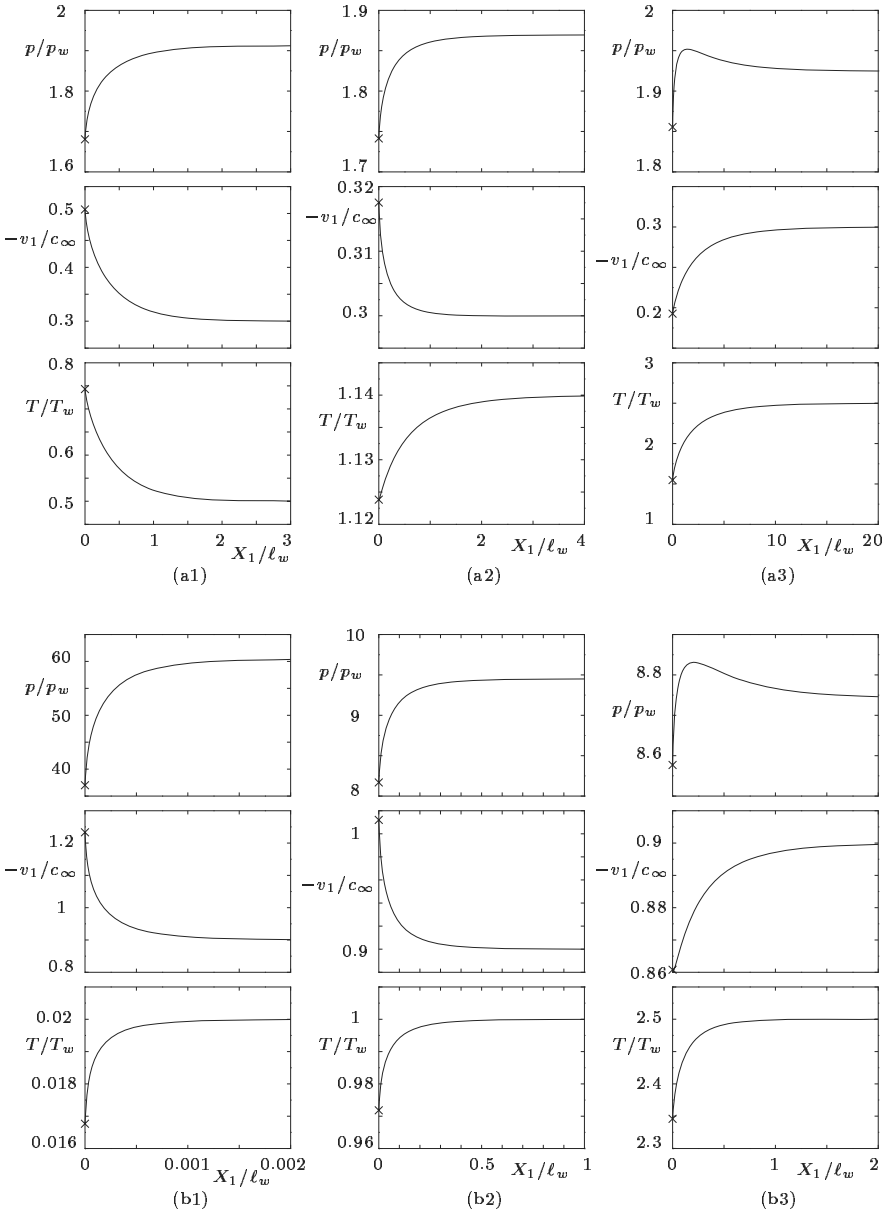

Figure 6.15. Profiles of subsonic time-independent solutions condensing onto a plane condensed phase. (a1) $M_\infty = -0.3$ and $T_\infty/T_w = 0.5$ (thus, $p_\infty/p_w = F_s = 1.9126$), (a2) $M_\infty = -0.3$ and $T_\infty/T_w = 1.14$ (thus, $p_\infty/p_w = F_s = 1.8696$), (a3) $M_\infty = -0.3$ and $T_\infty/T_w = 2.5$ (thus, $p_\infty/p_w = F_s = 1.9246$), (b1) $M_\infty = -0.9$ and $T_\infty/T_w = 0.02$ (thus, $p_\infty/p_w = F_s = 60.47$), (b2) $M_\infty = -0.9$ and $T_\infty/T_w = 1$ (thus, $p_\infty/p_w = F_s = 9.4508$), (b3) $M_\infty = -0.9$ and $T_\infty/T_w = 2.5$ (thus, $p_\infty/p_w = F_s = 8.7417$). The c_∞ is the sonic speed at infinity, i.e., $c_\infty = (5RT_\infty/3)^{1/2}$. The crosses $\times$ indicate the values at $X_1/\ell_w = 0$. (Computed by T. Doi for the figure.)

Table 6.1. $F_s(M_\infty, 0, T_\infty/T_w)$ (BKW and complete condensation). The superscript asterisk $*$ indicates the limiting value as M_∞ tends to zero. The solution at $M_\infty = 0$ exists only for $T_\infty/T_w = 1$.

	F_s						
$-M_\infty$	$T_\infty/T_w = 0.5$	0.75	1.0	1.5	2.0	3.0	4.0
0	1.000*	1.000*	1.000	1.000*	1.000*	1.000*	1.000*
0.05	1.114	1.104	1.104	1.106	1.112	1.119	1.130
0.10	1.232	1.221	1.220	1.225	1.233	1.250	1.267
0.15	1.367	1.354	1.352	1.359	1.370	1.396	1.421
0.20	1.525	1.506	1.502	1.511	1.526	1.559	1.592
0.25	1.707	1.679	1.673	1.683	1.701	1.742	1.785
0.30	1.914	1.878	1.869	1.879	1.900	1.951	2.002
0.35	2.146	2.106	2.092	2.103	2.130	2.186	2.254
0.40	2.427	2.369	2.350	2.359	2.385	2.454	2.521
0.45	2.757	2.675	2.649	2.654	2.685	2.761	2.838
0.50	3.122	3.031	2.998	2.995	3.026	3.111	3.212
0.55	3.583	3.449	3.396	3.389	3.423	3.513	3.612
0.60	4.092	3.942	3.869	3.849	3.870	3.975	4.107
0.65	4.734	4.525	4.424	4.385	4.411	4.509	4.639
0.70	5.527	5.225	5.077	5.014	5.029	5.124	5.284
0.75	6.411	6.074	5.873	5.758	5.747	5.838	5.993
0.80	7.626	7.105	6.826	6.640	6.597	6.666	6.829
0.85	9.092	8.385	8.040	7.695	7.602	7.630	7.758
0.90	11.11	9.993	9.443	8.968	8.790	8.754	8.902
1_	17.32		13.56	12.41	11.92		

Table 6.2. $F_b(M_\infty, 0, T_\infty/T_w)$ (BKW and complete condensation).

	F_b				
$-M_\infty$	$T_\infty/T_w = 0.5$	0.75	1.0	1.5	2.0
1.1	9.009	8.130	7.703	7.331	7.210
1.2	5.586	5.185	5.002	4.864	4.850
1.3	3.825	3.614	3.526	3.477	3.498
1.4	2.793	2.673	2.629	2.619	2.650
1.5	2.137	2.064	2.042	2.051	2.085
1.6	1.692	1.647	1.638	1.654	1.686
1.7	1.376	1.348	1.346	1.367	1.396
1.8	1.143	1.126	1.129	1.151	1.180
1.9	0.9666	0.9573	0.9623	0.9852	1.011
2.0	0.8296	0.8252	0.8318	0.8545	0.8797
2.1	0.7209	0.7199	0.7274	0.7496	0.7733
2.2	0.6331	0.6346	0.6428	0.6640	0.6861
2.3	0.5611	0.5644	0.5730	0.5936	0.6141
2.4	0.5014	0.5059	0.5145	0.5342	0.5534
2.5	0.4513	0.4566	0.4653	0.4841	0.5023
2.6	0.4086	0.4146	0.4231	0.4411	0.4583
2.7	0.3722	0.3799	0.3872	0.4044	0.4208
2.8	0.3407	0.3474	0.3557	0.3723	0.3879
2.9	0.3133	0.3202	0.3283	0.3443	0.3591
3.0	0.2893	0.2963	0.3043	0.3196	0.3338

it shrinks with increase of $|M_\infty|$ owing to convection. More detailed numerical data and discussions are given in Sone, Aoki & Yamashita [1986], Sone, Aoki, Sugimoto & Yamada [1988], Aoki, Sone & Yamada [1990], and Aoki, Nishino, Sone & Sugimoto [1991]. In the last paper, the case where the flow has a component parallel to the boundary is discussed.

6.2 Evaporation from a cylindrical condensed phase into a vacuum

6.2.1 Problem and basic equation

Consider a time-independent evaporating flow of a gas from a circular cylinder made of its condensed phase (radius: L, temperature: T_w, and the saturated gas pressure at temperature T_w : p_w) into an infinite expanse of a vacuum. Here, we discuss the behavior of the flow around the circular cylinder for a wide range of the Knudsen number Kn_w (the mean free path of the gas in the equilibrium state at rest with temperature T_w and pressure p_w divided by the radius of the cylinder) mainly on the basis of numerical analysis (Sone & Sugimoto [1995]) of the BKW equation and the complete-condensation condition. We consider the simple case where the state of the gas is axially symmetric and uniform and the flow is in the radial direction.

Basically, we use the notation introduced in Section 1.9 with L, p_w, and T_w as the reference length L, the reference pressure p_0, and the reference temperature T_0 respectively. Owing to the cylindrical geometry, the cylindrical coordinates (r, θ, z) and their nondimensional counterparts $(\hat{r}, \theta, \hat{z})$ are used here. We further introduce new notation. Let $(\zeta_r, \zeta_\theta, \zeta_z)$ be the cylindrical-coordinate components of the nondimensional molecular velocity $\boldsymbol{\zeta}$, and let ζ_r and ζ_θ be expressed as

$$\zeta_r = \zeta_\rho \cos\theta_\zeta, \ \ \zeta_\theta = \zeta_\rho \sin\theta_\zeta. \tag{6.10}$$

The range of the new variables is $(0 \le \zeta_\rho < \infty, -\pi < \theta_\zeta \le \pi, -\infty < \zeta_z < \infty)$. Owing to the symmetry of the problem, $\hat{f}$ is even in θ_ζ and the problem can be considered in the range $0 \le \theta_\zeta \le \pi$. The BKW equation (1.61) for the present situation is reduced to[9]

$$D_c \hat{f} = \frac{2}{\sqrt{\pi}\mathrm{Kn}_w} \hat{\rho}(\hat{f}_e - \hat{f}), \tag{6.11}$$

where

$$D_c = \zeta_\rho \cos\theta_\zeta \frac{\partial}{\partial \hat{r}} - \frac{\zeta_\rho \sin\theta_\zeta}{\hat{r}} \frac{\partial}{\partial \theta_\zeta}, \quad \mathrm{Kn}_w = \frac{\ell_w}{L},$$

$$\hat{f}_e = \frac{\hat{\rho}}{(\pi \hat{T})^{3/2}} \exp\left(- \frac{\zeta_\rho^2 + \hat{v}_r^2 - 2\hat{v}_r \zeta_\rho \cos\theta_\zeta + \zeta_z^2}{\hat{T}} \right),$$

[9] Equation (6.11) is derived easily from Eq. (A.157) in Section A.3. The former is simpler in the sense that it contains the derivatives with respect to only $\hat{r}$ and θ_ζ.

and

$$\hat{\rho} = 2\int \zeta_\rho \hat{f} \mathrm{d}\zeta_\rho \mathrm{d}\theta_\zeta \mathrm{d}\zeta_z, \tag{6.12a}$$

$$\hat{v}_r = \frac{2}{\hat{\rho}} \int \zeta_\rho^2 \hat{f} \cos\theta_\zeta \mathrm{d}\zeta_\rho \mathrm{d}\theta_\zeta \mathrm{d}\zeta_z, \tag{6.12b}$$

$$\hat{T} = \frac{2}{3\hat{\rho}} \left(2\int \zeta_\rho (\zeta_\rho^2 + \zeta_z^2) \hat{f} \mathrm{d}\zeta_\rho \mathrm{d}\theta_\zeta \mathrm{d}\zeta_z - \hat{\rho}\hat{v}_r^2 \right), \tag{6.12c}$$

$$\hat{p} = \hat{\rho}\hat{T}. \tag{6.12d}$$

Here, ℓ_w is the mean free path of the gas in the equilibrium state at rest with pressure p_w and temperature T_w [$\ell_w = (8RT_w/\pi)^{1/2}/(A_c\rho_w)$; $\rho_w = p_w/RT_w$] and the integration is carried out over the domain ($0 \le \zeta_\rho < \infty$, $0 \le \theta_\zeta \le \pi$, $-\infty < \zeta_z < \infty$), where the symmetry of $\hat{f}$ with respect to θ_ζ is taken into account. The boundary conditions on the cylinder and at infinity are

$$\hat{f} = \frac{1}{\pi^{3/2}} \exp(-\zeta_\rho^2 - \zeta_z^2) \quad (\hat{r} = 1,\ 0 \le \theta_\zeta < \pi/2), \tag{6.13a}$$

$$\hat{f} \to 0 \qquad\qquad (\hat{r} \to \infty,\ \pi/2 < \theta_\zeta \le \pi). \tag{6.13b}$$

We introduce the marginal velocity distribution functions (g, h)

$$(g, h) = \int_{-\infty}^{\infty} (1, \zeta_z^2) \hat{f} \mathrm{d}\zeta_z, \tag{6.14}$$

where the variable ζ_z is eliminated. Then, the equations for g and h are

$$D_c(g, h) = \frac{2}{\sqrt{\pi}\mathrm{Kn}_w} \hat{\rho}[(g_e, h_e) - (g, h)], \tag{6.15}$$

$$(g_e, h_e) = \left(\frac{1}{\hat{T}}, \frac{1}{2} \right) \frac{\hat{\rho}}{\pi} \exp\left(-\frac{\zeta_\rho^2 + \hat{v}_r^2 - 2\hat{v}_r \zeta_\rho \cos\theta_\zeta}{\hat{T}} \right). \tag{6.16}$$

The variables $\hat{\rho}$, $\hat{v}_r$, and $\hat{T}$ are expressed by g and h as

$$\hat{\rho} = 2\int \zeta_\rho g \mathrm{d}\zeta_\rho \mathrm{d}\theta_\zeta, \tag{6.17a}$$

$$\hat{v}_r = \frac{2}{\hat{\rho}} \int \zeta_\rho^2 g \cos\theta_\zeta \mathrm{d}\zeta_\rho \mathrm{d}\theta_\zeta, \tag{6.17b}$$

$$\hat{T} = \frac{2}{3\hat{\rho}} \left(2\int \zeta_\rho (\zeta_\rho^2 g + h) \mathrm{d}\zeta_\rho \mathrm{d}\theta_\zeta - \hat{\rho}\hat{v}_r^2 \right), \tag{6.17c}$$

where the integrations with respect to ζ_ρ and θ_ζ are carried out over the domain ($0 \le \zeta_\rho < \infty$, $0 \le \theta_\zeta \le \pi$). The boundary conditions on the cylinder and at infinity are

$$(g, h) = (1, 1/2)\pi^{-1} \exp(-\zeta_\rho^2) \quad (\hat{r} = 1,\ 0 \le \theta_\zeta < \pi/2), \tag{6.18a}$$

$$(g, h) \to (0, 0) \qquad\qquad (\hat{r} \to \infty,\ \pi/2 < \theta_\zeta \le \pi). \tag{6.18b}$$

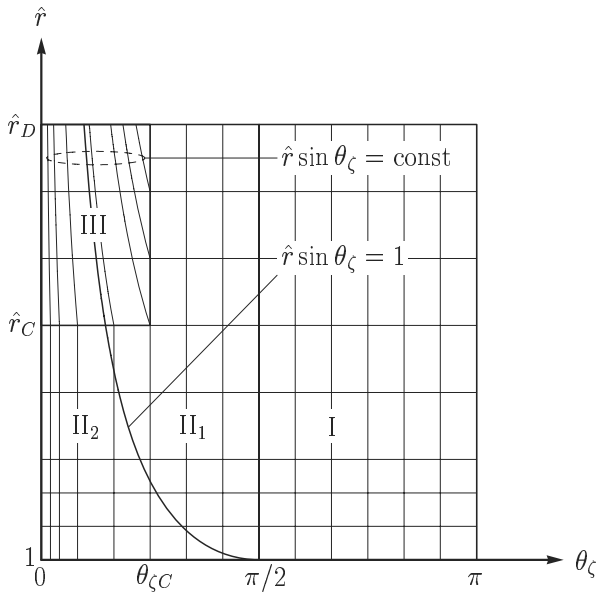

Figure 6.16. Lattice system for the time-independent evaporating flow from a cylinder. The figure corresponds to the explanation (i)–(iv) in Section 6.2.2.

6.2.2 Outline of numerical computation

The boundary-value problem (6.15), (6.18a), and (6.18b) will be solved numerically by a *hybrid finite-difference method* developed in Sugimoto & Sone [1992] and Sone & Sugimoto [1995]. The outline of the method is as follows:

(i) In the numerical computation we consider the problem in a finite domain $(1 \le \hat{r} \le \hat{r}_D,\ 0 \le \zeta_\rho \le \zeta_D,\ 0 \le \theta_\zeta \le \pi)$ in $(\hat{r}, \zeta_\rho, \theta_\zeta)$ space, where $\hat{r}_D$ and ζ_D are chosen properly depending on the situations (Fig. 6.16). The discrete solution $(g_\#, h_\#)$ of (g, h) at the lattice points in $(\hat{r}, \zeta_\rho, \theta_\zeta)$ space is constructed as the limit of the sequence $(g_\#^{(n)}, h_\#^{(n)})$ obtained as follows. The initial solution $(g_\#^{(0)}, h_\#^{(0)})$ is chosen properly. Let the solution $(g_\#^{(n)}, h_\#^{(n)})$ be known. The solution $(g_\#^{(n+1)}, h_\#^{(n+1)})$ for $(\pi/2 \le \theta_\zeta \le \pi)$ is constructed from $\hat{r} = \hat{r}_D$ to $\hat{r} = 1$ (the solution in region I in Fig. 6.16) and then $(g_\#^{(n+1)}, h_\#^{(n+1)})$ for $(0 \le \theta_\zeta < \pi/2)$ from $\hat{r} = 1$ to $\hat{r} = \hat{r}_D$ (the solution in regions II_1, II_2, and III in Fig. 6.16) with the aid of a finite-difference equation for Eq. (6.15), which is prepared in such a way that $(g_\#^{(n+1)}, h_\#^{(n+1)})$ is constructed in the direction from $(\hat{r} = \hat{r}_D,\ \theta_\zeta = \pi)$ to $(\hat{r} = 1,\ \theta_\zeta = \pi/2)$ in the region I and in the direction from $(\hat{r} = 1,\ \theta_\zeta = \pi/2)$ to $(\hat{r} = \hat{r}_D,\ \theta_\zeta = 0)$ in the regions II_1, II_2, and III. This direction of construction of solution conforms with the direction of the characteristics of Eq. (6.15) on the average.

(ii) On the surface of the cylinder, the marginal velocity distribution functions g and h are discontinuous at $\theta_\zeta = \pi/2$ (or $\zeta_r = 0$) because the nature of the

velocity distribution function of the impinging molecules ($\pi/2 < \theta_\zeta \leq \pi$ or $\zeta_r < 0$) and that of the outgoing molecules ($0 \leq \theta_\zeta < \pi/2$ or $\zeta_r > 0$) are different. The discontinuity propagates into the gas along the characteristic of Eq. (6.15). Therefore, the discontinuity of (g, h) lies on the surface

$$\hat{r} \sin \theta_\zeta = 1 \qquad (0 < \theta_\zeta \leq \pi/2). \tag{6.19}$$

The position of the discontinuity is independent of the molecular speed ζ_ρ. As the distance $\hat{r}$ increases, the discontinuity decays owing to molecular collisions. When we discretize Eq. (6.15), which includes derivative terms $\partial/\partial\hat{r}$ and $\partial/\partial\theta_\zeta$, we should not apply finite-difference approximation for differentiation to these terms across the discontinuity. Therefore, we divide $(\hat{r}, \zeta_\rho, \theta_\zeta)$ space into two regions (II_1 and II_2 in Fig. 6.16) by the discontinuity surface (6.19) and apply a standard finite-difference approximation in each region. In this scheme, the limiting values of $(g_\#^{(n)}, h_\#^{(n)})$ on the surface from both sides of it are needed as the boundary condition. They are obtained separately along the characteristic (6.19) as is done in Section 4.8. In the region where the discontinuity has decayed sufficiently, we use a standard finite-difference scheme in the whole region for efficiency.

(iii) The numerical computation is carried out over a finite domain ($1 \leq \hat{r} \leq \hat{r}_D,\ 0 \leq \zeta_\rho \leq \zeta_D,\ 0 \leq \theta_\zeta \leq \pi$) with the boundary condition at infinity applied at $\hat{r} = \hat{r}_D$ instead of the original infinite domain ($1 \leq \hat{r} < \infty,\ 0 \leq \zeta_\rho < \infty,\ 0 \leq \theta_\zeta \leq \pi$).[10] Because g and h are seen to decay rapidly with ζ_ρ from numerical tests, accurate computation of the problem can be carried out with a reasonable size of ζ_D. On the other hand, approach to the state at infinity as $\hat{r} \to \infty$ is very slow, and therefore we carry out detailed tests for different large $\hat{r}_D$ and confirm the accuracy of the computation.

(iv) The marginal velocity distribution functions g and h in the far field are concentrated around the characteristic $\hat{r} \sin \theta_\zeta = \text{const}$ for $0 \leq \theta_\zeta \leq \pi/2$ in evaporating flows into a vacuum, as you will see in the result to be shown. The characteristic $\hat{r} \sin \theta_\zeta = \text{const}$ for $0 \leq \theta_\zeta \leq \pi/2$ approaches the line $\theta_\zeta = 0$ as $\hat{r} \to \infty$. Therefore, g and h vary considerably in a narrow range of θ_ζ near $\theta_\zeta = 0$ for large $\hat{r}$. We need a fine lattice system in this region. Because a rectangular lattice system in $(\hat{r}, \theta_\zeta)$ is inconvenient for this purpose, we introduce a characteristic coordinate system $\hat{r} \sin \theta_\zeta = \text{const}$ and $\hat{r} = \text{const}$ in the region ($\hat{r} \geq \hat{r}_C,\ 0 \leq \theta_\zeta \leq \theta_{\zeta C}$, where $\hat{r}_C$ and $\theta_{\zeta C}$ are chosen properly) (region III in Fig. 6.16) and integrate the finite-difference system written in the characteristic coordinate system.

[10] One may suspect that it restricts the solution in a narrower class to apply the boundary condition (6.18b) at $\hat{r} = \hat{r}_D$ ($\gg 1$), instead of at $\hat{r} = \infty$, and that other solutions may exist from the following argument. The boundary condition $(g, h) = (g_0(\zeta_\rho), h_0(\zeta_\rho))\hat{r}_D^{-1}$ ($\pi/2 < \theta_\zeta \leq \pi$) at $\hat{r} = \hat{r}_D$, for example, is compatible with the condition (6.18b) at $\hat{r} = \infty$ in the limit $\hat{r}_D \to \infty$. The new boundary condition may allow another solution with different mass and energy flows from those of the solution considered here, because the mass and energy fluxes integrated around large circle $\hat{r} = \hat{r}_D$, which is introduced by the new boundary condition, remain finite owing to the factor $\hat{r}_D$ of the circumference. The discussion that this is not the case is given in Sone & Sugimoto [1995]. A similar argument applies to the spherical problem in Section 6.4.

6.2.3 The behavior of the gas

Before presenting the result of numerical computation, we give the solution of two limiting cases: the free molecular solution and that in the continuum limit.

Free molecular flow

The free molecular solution is easily obtained by the recipe in Chapter 2 as

$$\hat{f} = \begin{cases} \pi^{-3/2}\exp(-\zeta_\rho^2 - \zeta_z^2) & [0 \le |\theta_\zeta| < \mathrm{Arcsin}(L/r)], \\ 0 & [\mathrm{Arcsin}(L/r) < |\theta_\zeta| \le \pi], \end{cases} \tag{6.20}$$

and

$$(g,h) = \begin{cases} (1,1/2)\pi^{-1}\exp(-\zeta_\rho^2) & [0 \le |\theta_\zeta| < \mathrm{Arcsin}(L/r)], \\ (0,0) & [\mathrm{Arcsin}(L/r) < |\theta_\zeta| \le \pi]. \end{cases} \tag{6.21}$$

At a given point in the gas, only the molecules whose velocities are inside the wedge $|\theta_\zeta| < \mathrm{Arcsin}(L/r)$ or which come directly from the cylinder are present. The height of $\hat{f}$ is invariant with respect to the distance.

From the velocity distribution function $\hat{f}$, the macroscopic variables are easily obtained, e.g.,

$$\left.\begin{aligned} &\frac{\rho}{\rho_w} = \frac{L}{\pi r x}, \quad \frac{v_r}{(2RT_w)^{1/2}} = \frac{\sqrt{\pi}x}{2}, \quad M = \left(\frac{10}{3\pi x^2} - \frac{5}{9}\right)^{-1/2}, \\ &\frac{T}{T_w} = 1 - \frac{\pi x^2}{6}, \quad \frac{T_r}{T_w} = 1 - \frac{\pi x^2}{2} + xy, \quad \frac{T_\theta}{T_w} = 1 - xy, \quad \frac{T_z}{T_w} = 1, \end{aligned}\right\} \tag{6.22}$$

where

$$x = (L/r)/\mathrm{Arcsin}(L/r), \quad y = [1 - (L/r)^2]^{1/2},$$

M is the Mach number defined by

$$M = v_r/(5RT/3)^{1/2}, \tag{6.23}$$

and the temperatures T_r, T_θ, and T_z in the r, θ, and z directions, which are often referred to in experimental literatures, are defined by

$$\left.\begin{aligned} &R\rho T_r = \iiint (\xi_r - v_r)^2 f \mathrm{d}\xi_r \mathrm{d}\xi_\theta \mathrm{d}\xi_z, \qquad R\rho T_\theta = \iiint \xi_\theta^2 f \mathrm{d}\xi_r \mathrm{d}\xi_\theta \mathrm{d}\xi_z, \\ &R\rho T_z = \iiint \xi_z^2 f \mathrm{d}\xi_r \mathrm{d}\xi_\theta \mathrm{d}\xi_z, \qquad T = \frac{1}{3}(T_r + T_\theta + T_z), \end{aligned}\right\} \tag{6.24}$$

where $(\xi_r, \xi_\theta, \xi_z)$ are the cylindrical-coordinate components of the molecular velocity $\boldsymbol{\xi}$, corresponding to the nondimensional $(\zeta_r, \zeta_\theta, \zeta_z)$.

The macroscopic variables v_r, M, T, T_r, and T_z take nonzero values at infinity, because $x = 1$ and $y = 1$ there, and ρ and T_θ vanish with speeds

proportional to L/r and $(L/r)^2$ respectively as $r/L \to \infty$. The mass and energy flows m_f and e_f from the cylinder per unit time and per unit area of the cylinder (or the mass and energy fluxes from the cylinder) are

$$m_f/\rho_w(2RT_w)^{1/2} = 1/2\sqrt{\pi}, \quad e_f/p_w(2RT_w)^{1/2} = 1/\sqrt{\pi}. \tag{6.25}$$

Flow in the continuum limit

The solution in the continuum limit can also easily be obtained with the aid of the asymptotic theory described in Section 3.5. It is the solution of the Euler set of equations (3.225a)–(3.225c) under the boundary conditions (3.228a) and (3.228b) with its Knudsen layer flattened on the condensed phase. The isentropic expanding flow into a vacuum, given by the Euler set of equations, is supersonic ($M \geq 1$). In view of the boundary conditions (3.228a) and (3.228b), the solution of the Euler set should take the value $M = 1$ on the condensed phase, from which the solution is given by the parametric expression in M as follows:[11]

$$\left.\begin{aligned} &\frac{\rho}{\rho_*} = \frac{8}{(3+M^2)^{3/2}}, \quad \frac{v_r}{(5RT_*/3)^{1/2}} = \frac{2M}{(3+M^2)^{1/2}}, \\ &\frac{T}{T_*} = \frac{4}{3+M^2}, \qquad \frac{r}{L} = \frac{(3+M^2)^2}{16M}, \end{aligned}\right\} \tag{6.26}$$

or for large r/L,

$$\frac{\rho}{\rho_*} = \frac{L}{2r}, \ \frac{v_r}{(5RT_*/3)^{1/2}} = 2 - 3\left(\frac{L}{16r}\right)^{2/3}, \ \frac{T}{T_*} = 4\left(\frac{L}{16r}\right)^{2/3}, \ M = \left(\frac{16r}{L}\right)^{1/3},$$

where ρ_* and T_* are given by the functions $h_1(M)$ and $h_2(M)$ defined in Section 3.5.2 as

$$\rho_* = h_1(1)\rho_w/h_2(1), \qquad T_* = h_2(1)T_w.$$

The effect of the molecular model enters only through $h_1(1)$ and $h_2(1)$. For the BKW equation and the complete-condensation condition,

$$h_1(1)/h_2(1) = 0.3225, \quad h_2(1) = 0.6434.$$

The mass and energy flows m_f and e_f per unit time and per unit area from the cylinder are

$$\frac{m_f}{\rho_w(2RT_w)^{1/2}} = \left(\frac{5}{6}\right)^{1/2} \frac{h_1(1)}{h_2(1)^{1/2}}, \quad \frac{e_f}{p_w(2RT_w)^{1/2}} = 4\left(\frac{5}{6}\right)^{3/2} h_1(1)h_2(1)^{1/2}. \tag{6.27}$$

For the BKW equation and the complete-condensation condition,

$$m_f/\rho_w(2RT_w)^{1/2} = 0.2361, \quad e_f/p_w(2RT_w)^{1/2} = 0.5065.$$

[11] The fundamental properties of the gas flow governed by the Euler set of equations are discussed in Courant & Friedrichs [1948], Oswatitsch [1956], Liepmann & Roshko [1957], and so on.

In the far field from the cylinder, the length scale L_r of variation [e.g., $\rho/(\mathrm{d}\rho/\mathrm{d}r)$] of the above solution in the continuum limit is of the order of r, i.e.,

$$L_r \sim r,$$

and increases indefinitely with the distance from the cylinder. On the other hand, the local mean free path ℓ_{lc} is[12]

$$\ell_{lc} = v_r/A_c\rho \sim (5RT_*/3)^{1/2} r/A_c\rho_* L \sim \ell_w r/L.$$

Thus, the local Knudsen number $\mathrm{Kn}_r (= \ell_{lc}/L_r)$, which characterizes the feature of the variation of the flow, is

$$\mathrm{Kn}_r = \ell_{lc}/r \sim \ell_w/L = \mathrm{Kn}_w. \tag{6.28}$$

That is, the local Knudsen number is invariant along the flow from the cylinder. Therefore, the solution in the continuum limit is a good approximation for small Kn_w up to downstream infinity, where the density vanishes. This result depends on molecular models, for example, Kn_r increases indefinitely for a hard-sphere gas with the distance from the cylinder.[13] The above character applies to the pseudo-Maxwell molecule (Section A.2.4) as well as the BKW model.

It may be noted that the Mach number M of the Euler solution is unity at $r = L$ and that $\mathrm{d}\rho/\mathrm{d}r$, $\mathrm{d}v_r/\mathrm{d}r$, etc. are infinite at $r = L$. This violates the assumption imposed in the derivation of the Euler set of equations from the Boltzmann or BKW equation, which requires further discussion.

Numerical solution

The boundary-value problem, Eqs. (6.15), (6.18a), and (6.18b), is solved numerically for various Knudsen numbers by the finite-difference method outlined in Section 6.2.2.

Macroscopic variables The global profiles of the density, flow velocity, temperature, and Mach number, i.e., ρ/ρ_w, $v_r/(2RT_w)^{1/2}$, T/T_w, and M as functions of r/L, are shown in Figs. 6.17 and 6.18. The variables vary sharply near the cylinder and then approach the state at infinity very slowly. The density, which vanishes at infinity, is proportional to $1/r$ in the far field. This is found by close examination of the slope of the curve $\ln(\rho/\rho_w)$ vs $\ln(r/L)$. From this fact and the conservation of mass flow ($\rho v_r r = \mathrm{const}$), v_r approaches a finite value at infinity. The speed of approach becomes extremely slow as the Knudsen number

[12] In a hypersonic region, the characteristic molecular speed in the flow direction is the flow speed. Thus, in estimating the size of the transport term (say, $\xi_r \partial f/\partial r$) of the Boltzmann equation, we have to choose the flow speed (v_r) instead of the thermal speed ($\sqrt{2RT}$). Thus, the Knudsen number based on the mean free path calculated with the flow speed is appropriate to represent the ratio of the collision term to the transport term in the Boltzmann equation.

[13] The mean collision frequency of a Maxwellian for a molecule whose intermolecular force extends only to a finite radius d_m (e.g., a hard-sphere molecule with diameter d_m) is given, irrespectively of its flow velocity, by $4(\pi RT)^{1/2} d_m^2 \rho/m$ (Section A.8). Thus, $\mathrm{Kn}_r \sim \mathrm{Kn}_w (r/L)^{1/3}$.

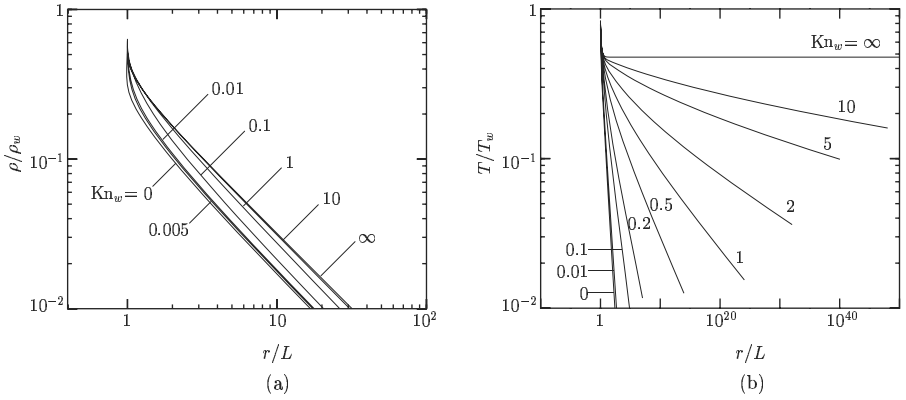

Figure 6.17. The profile of the macroscopic variables for various Knudsen numbers Kn_w of the evaporating flows from a cylinder into a vacuum I: density and temperature. (a) ρ/ρ_w vs r/L and (b) T/T_w vs r/L. In panel (a), the data for $\mathrm{Kn}_w = 0$ (the continuum limit), 0.005, 0.01, 0.1, 1, 10, and ∞ are shown. In panel (b), the data for $\mathrm{Kn}_w = 0$, 0.01, 0.1, 0.2, 0.5, 1, 2, 5, 10, and ∞ are shown.

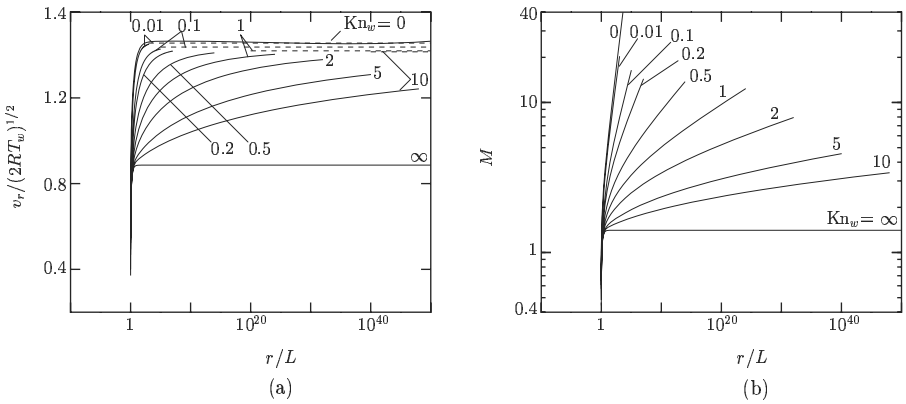

Figure 6.18. The profile of the macroscopic variables for various Knudsen numbers Kn_w in the evaporating flow from a cylinder into a vacuum II: flow velocity and Mach number. (a) $v_r/(2RT_w)^{1/2}$ vs r/L and (b) M vs r/L. The data for $\mathrm{Kn}_w = 0$, 0.01, 0.1, 0.2, 0.5, 1, 2, 5, 10, and ∞ are shown. The dashed lines in panel (a) indicate the limiting values of v_r (i.e., $v_{r\infty}$) as $r/L \to \infty$ [Eq. (6.29)] for $\mathrm{Kn}_w = 0.01$, 0.1, 1, and 10.

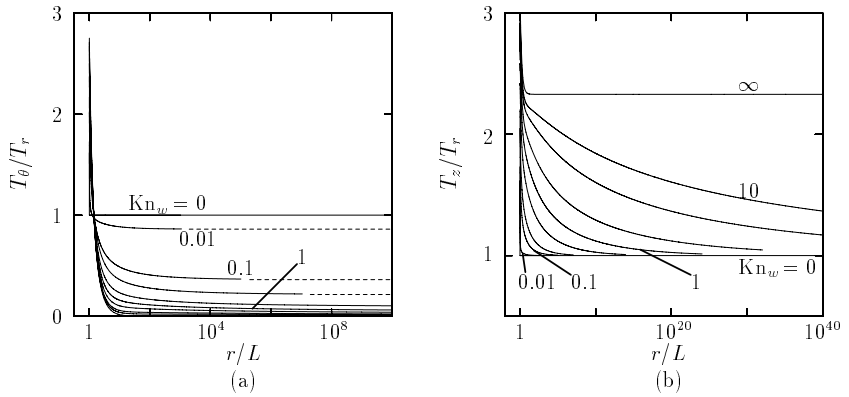

Figure 6.19. The ratios T_θ/T_r and T_z/T_r in the evaporating flow from a cylinder into a vacuum. (a) T_θ/T_r vs r/L and (b) T_z/T_r vs r/L. The data for $\mathrm{Kn}_w = 0$, 0.01, 0.1, 0.2, 0.5, 1, 2, 5, 10, and ∞ are shown. The dashed lines in panel (a) indicate the estimated values at infinity for $\mathrm{Kn}_w = 0.01$, 0.1, and 0.2.

increases [note the abscissa of Fig. 6.18 (a)]. Thus, it is impossible to carry out the computation up to the point where v_r is close enough to its value at infinity. Fortunately, by close examination of the numerical data of $(\hat{w} - \hat{\rho}\hat{v}_r^3)/\hat{\rho}\hat{v}_r$, where $p_w(2RT_w)^{1/2}\hat{w}$ is the energy flux in the gas in the r direction, it is estimated to vanish at infinity (see Sone & Sugimoto [1995]), from which

$$\hat{v}_{r\infty}^2 = \lim_{\hat{r}\to\infty} \hat{w}/\hat{\rho}\hat{v}_r = \lim_{\hat{r}\to\infty} 2\pi\hat{r}\hat{w}/2\pi\hat{r}\hat{\rho}\hat{v}_r = \rho_w e_f/p_w m_f.$$

Thus

$$v_{r\infty} = (2e_f/m_f)^{1/2}, \tag{6.29}$$

where $v_{r\infty} = \lim_{r\to\infty} v_r$ and $\hat{v}_{r\infty} = \lim_{\hat{r}\to\infty} \hat{v}_r$. The limiting velocity $v_{r\infty}$, calculated from m_f and e_f given below, is shown in dashed lines in Fig. 6.18 (a). The temperature of the gas decreases to vanish as r increases to infinity except in the free molecular flow. Its speed of approach to zero is extremely slow for moderate and large Knudsen numbers.

In experimental references, the temperatures T_r, T_θ, and T_z in the r, θ, and z directions [see Eq. (6.24)] are often referred to. They are all equal in an equilibrium state and thus, their ratios are a simple measure of deviation from an equilibrium state. The ratios T_θ/T_r and T_z/T_r are shown in Figs. 6.19 (a) and (b). Obviously, T_r, T_θ, and T_z vanish at infinity because T vanishes there. The ratio T_θ/T_r approaches a value between 0 and 1, which depends on Kn_w. The ratio T_z/T_r approaches unity irrespective of Kn_w except for $\mathrm{Kn}_w = \infty$, but the convergence is extremely slow for moderate and large Knudsen numbers.

The mass and energy flows m_f and e_f per unit time and per unit area from the cylinder are shown in Table 6.3 as $m_f/\rho_w(2RT_w)^{1/2}$ and $e_f/p_w(2RT_w)^{1/2}$ vs Kn_w.

Table 6.3. $m_f/\rho_w(2RT_w)^{1/2}$ and $e_f/p_w(2RT_w)^{1/2}$ vs Kn_w in the evaporating flow from a cylinder into a vacuum.

Kn_w	$\dfrac{m_f}{\rho_w(2RT_w)^{1/2}}$	$\dfrac{e_f}{p_w(2RT_w)^{1/2}}$	Kn_w	$\dfrac{m_f}{\rho_w(2RT_w)^{1/2}}$	$\dfrac{e_f}{p_w(2RT_w)^{1/2}}$
0	0.2361	0.5065	0.5	0.2761	0.5591
0.005	0.2429	0.5169	1	0.2786	0.5615
0.01	0.2463	0.5220	2	0.2802	0.5628
0.02	0.2509	0.5286	5	0.2813	0.5636
0.05	0.2586	0.5392	10	0.2817	0.5640
0.1	0.2649	0.5471	∞	0.2821	0.5642
0.2	0.2706	0.5536			

Velocity distribution function We will explain the behavior of the marginal velocity distribution function g referring to Figs. 6.20 and 6.21. The cases without figures can be inferred from these figures (see Sone & Sugimoto [1995]).

In the free molecular flow ($\mathrm{Kn}_w = \infty$) at the beginning in this subsection, the marginal velocity distribution function g is constant along the characteristics of Eq. (6.15) (or $\hat{r}\sin\theta_\zeta = \text{const}$). The function g, given by Eq. (6.21), is localized in the wedge $0 \le |\theta_\zeta| < \mathrm{Arcsin}(L/r)$ in the molecular velocity space. (All the molecules in the gas come directly from the cylinder and there are no other molecules.) The height of g is constant and the wedge becomes thinner and thinner along the flow. Thus, the height and the radial width of g take finite values at infinity.

For finite values of Kn_w, the above sharply localized distribution function is deformed by molecular collisions. It is noted that the distribution function g for outgoing molecules ($0 \le \theta_\zeta < \pi/2$) on the cylinder (at $r = L$) is the same for all Kn_w [Eq. (6.18a)] and that the nonzero part of g in the region $\pi/2 < \theta_\zeta \le \pi$ is a result of molecular collisions.

At $\mathrm{Kn}_w = 10$ (large Kn_w), the effect of molecular collisions in a region near the cylinder is appreciable only for small ζ_ρ, and very few molecules return to the cylinder [Fig. 6.20 (a) at $r/L = 1$ and Fig. 6.20 (b) at $r/L = 1.890$], because the molecules with small ζ_ρ have small free path, but the other molecules do not have much chance of collision in this distance from the cylinder.[14] Because the peak of g at $r/L = 1$ is at $\zeta_\rho = 0$, the peak or height of g is lowered considerably, but other overall feature of g retains much of that of the free molecular flow [note the dashed line in Fig. 6.20 (b)]. The effect of molecular collisions on g appears gradually but appreciably in a long distance along the flow [Fig. 6.20 (c) at $r/L = 11.96$ and Fig. 6.20 (d) at $r/L = 988.1$]. The height and the radial width of g decrease to vanish at infinity, which is confirmed by the test in Sone & Sugimoto [1995]. Correspondingly, the size of the discontinuity decreases to vanish, but its relative size to the height of g increases in the far field. The

[14] In the discussion of g and h, the free path in the z direction can be disregarded because the information with respect to ζ_z is averaged [see Eq. (6.14)].

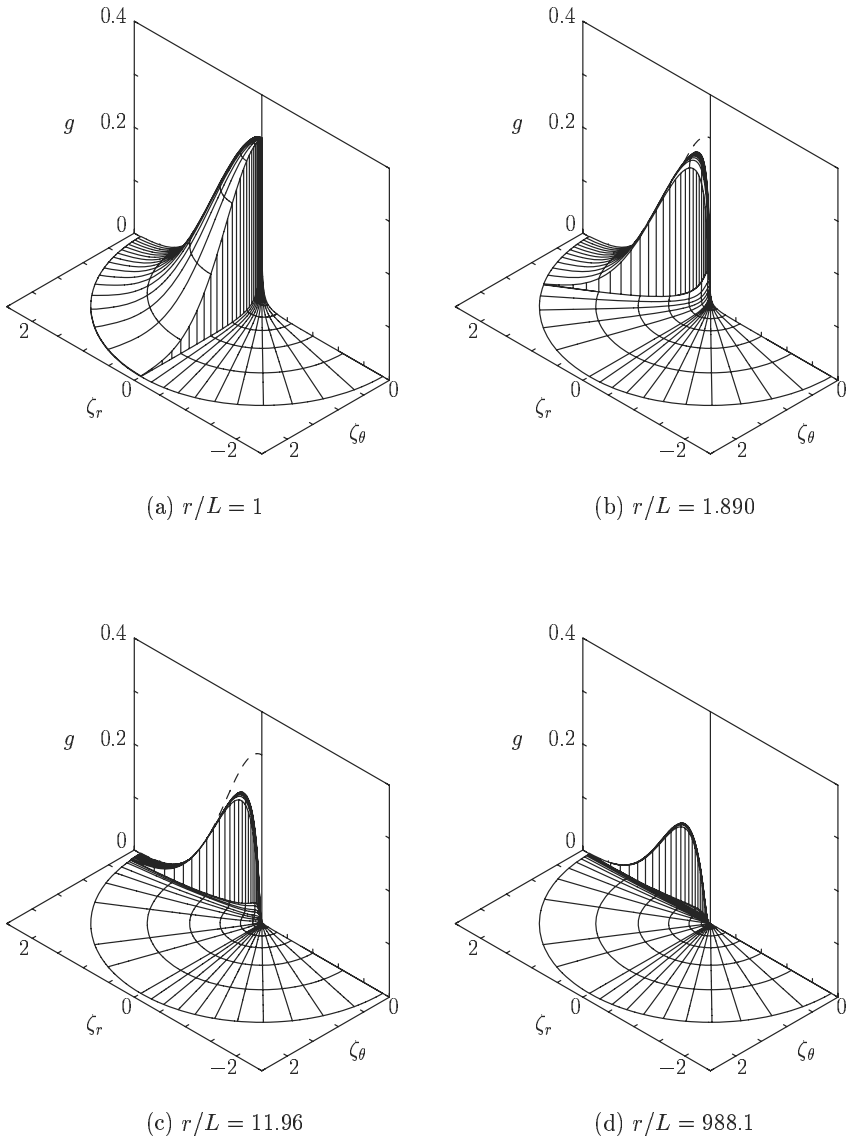

(a) $r/L = 1$ (b) $r/L = 1.890$

(c) $r/L = 11.96$ (d) $r/L = 988.1$

Figure 6.20. The marginal velocity distribution function g at various points in the evaporating flow from a cylinder into a vacuum I: $\mathrm{Kn}_w = 10$. (a) $r/L = 1$, (b) $r/L = 1.890$, (c) $r/L = 11.96$, and (d) $r/L = 988.1$. The surface g is shown by two sets of lines $\zeta_\rho = \text{const}$ and $\theta_\zeta = \text{const}$. Only the part for $0 \le \theta_\zeta \le \pi$ is shown because g is symmetric with respect to θ_ζ. The vertical stripes show the discontinuity of g. The dashed lines in (b) and (c) show the curve g along $\theta_\zeta = 0$ at $r/L = 1$ for comparison. Note that $\zeta_r = \zeta_\rho \cos\theta_\zeta$ and $\zeta_\theta = \zeta_\rho \sin\theta_\zeta$.

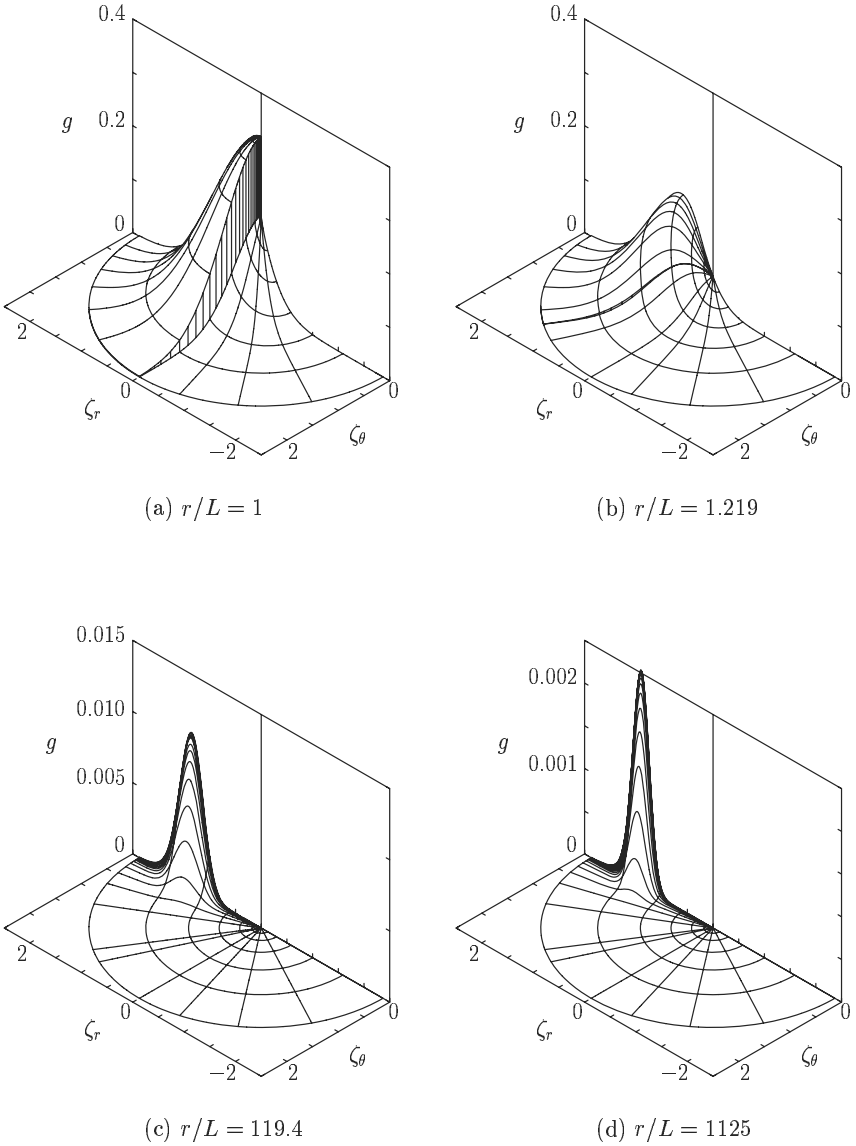

(a) $r/L = 1$ (b) $r/L = 1.219$

(c) $r/L = 119.4$ (d) $r/L = 1125$

Figure 6.21. The marginal velocity distribution function g at various points in the evaporating flow from a cylinder into a vacuum II: $\mathrm{Kn}_w = 0.1$. (a) $r/L = 1$, (b) $r/L = 1.219$, (c) $r/L = 119.4$, and (d) $r/L = 1125$. The surface g is shown by two sets of lines $\zeta_\rho = \text{const}$ and $\theta_\zeta = \text{const}$. Only the part for $0 \le \theta_\zeta \le \pi$ is shown because g is symmetric with respect to θ_ζ. The vertical stripes show the discontinuity of g. Note that $\zeta_r = \zeta_\rho \cos\theta_\zeta$ and $\zeta_\theta = \zeta_\rho \sin\theta_\zeta$.

decrease of the radial width of g is very slow; only its sign is seen in Fig. 6.20 (a) at $r/L = 1 \rightarrow$ Fig. 6.20 (d) at $r/L = 988.1$, but the width can be seen to vanish from the result that $T_r \rightarrow 0$ as $r/L \rightarrow \infty$. Over the whole flow field, the distribution function g in the $(\zeta_\rho \cos\theta_\zeta, \zeta_\rho \sin\theta_\zeta)$ plane is like a hill with large dislocation at $(r/L)\sin\theta_\zeta = 1$, and consists of two different parts. At $\mathrm{Kn}_w = 1$ (moderate Kn_w), the qualitative feature of g is similar to that at $\mathrm{Kn}_w = 10$, but the effect of molecular collisions is more pronounced [see Figs. 2 (a)–(d) in AIP document no. PAPS PHFLE-7-2072-9[15]].

At $\mathrm{Kn}_w = 0.1$ (fairly small Kn_w), the molecules that return to the cylinder by molecular collisions increase considerably, but the discontinuity of g is still large on the cylinder [Fig. 6.21 (a)]. As in the cases of $\mathrm{Kn}_w = 1$ and 10, the distribution function g on the cylinder is a hill with large dislocation, consisting of two different parts. The discontinuity decays rapidly along the flow and practically vanishes in several mean free paths from the cylinder [Fig. 6.21 (b) at $r/L = 1.219$]. The effect of molecular collisions prevails over the whole part of g there, and the distribution function g is a natural hill without additional bump [Fig. 6.21 (b)]. The distribution function is further deformed along the flow, but large deformation is got under in a distance of about 100 radii of the cylinder. Further downstream, its roughly shape-preserving deformation (or deformation expressed by scale changes) proceeds, as confirmed in Sone & Sugimoto [1995], and the height and expanse of g decrease more rapidly than in the case of $\mathrm{Kn}_w = 1$ [Fig. 6.21 (b) at $r/L = 1.219 \rightarrow$ Fig. 6.21 (d) at $r/L = 1125$]. Even at this fairly small Kn_w, the flow deviates considerably from the corresponding local equilibrium state over the whole flow field.

At $\mathrm{Kn}_w = 0.01$ (small Kn_w), the molecules that return to the cylinder further increase; the discontinuity of g on the cylinder shrinks but is still considerable. The distribution function g is, as before, a hill with dislocation, consisting of two different parts. The discontinuity practically vanishes in a very short distance of the order of ℓ_w^2/L. In this short distance, the deformation of g is limited to small ζ_ρ and the neighborhood of the discontinuity. Effects of molecular collisions prevail over the whole distribution function down the flow, and the distribution function becomes fairly close to a local equilibrium distribution in a distance of about $10\ell_w$ from the cylinder. Further downstream, the distribution function remains close to local equilibrium. The height of g decreases slower but the expanse of g shrinks faster than in the case of $\mathrm{Kn}_w = 0.1$.

The behavior of the field is proper to Kn_w. This is related to the relation (6.28) of Kn_r to Kn_w, which depends on molecular models.[16] The behavior proper to Kn_w in the far field is a good contrast to the free molecular behavior in the far field of the evaporating flow from a spherical condensed phase to be discussed in Section 6.4.

---

[15] The supplement to Sone & Sugimoto [1995]. Order by PAPS number and journal reference from AIP, Physics Auxiliary Publication Service, Carolyn Gehlbach, 500 Sunnyside Boulevard, Woodbury, NY 11797-2999. Fax: 516-576-2223, e-mail: janis@aip.org.

[16] The relation is derived for a Maxwellian. Thus, the correct relation requires to be calculated on the basis of its proper velocity distribution function when Kn_w is not small.

6.3 Evaporation from a cylindrical condensed phase into a gas

6.3.1 Problem and basic equation

Consider a time-independent evaporating flow of a gas from a circular cylinder made of its condensed phase (radius: L, temperature: T_w, and the saturated gas pressure at temperature T_w: p_w) into an infinite expanse of a gas at rest (pressure p_∞ and temperature T_∞). We discuss the behavior of the flow around the circular cylinder for a wide range of the pressure ratio p_∞/p_w and the Knudsen number Kn_w (the mean free path of the gas in the equilibrium state at rest with temperature T_w and pressure p_w divided by the radius of the cylinder) on the basis of numerical analysis (Sugimoto & Sone [1992]) of the BKW equation and the complete-condensation condition.

The equation for $\hat{f}$ and the boundary condition on the cylinder are given by Eqs. (6.11) and (6.13a). The boundary condition at infinity is

$$\hat{f} \to \frac{\hat{p}_\infty}{\pi^{3/2}\hat{T}_\infty^{5/2}} \exp\left(-\frac{\zeta_\rho^2 + \zeta_z^2}{\hat{T}_\infty}\right), \tag{6.30}$$

where $\hat{p}_\infty = p_\infty/p_w$ and $\hat{T}_\infty = T_\infty/T_w$. The equations for the marginal velocity distribution functions g and h and their boundary conditions on the cylinder are given by Eqs. (6.15) and (6.18a). Their boundary conditions at infinity are

$$(g, h) \to \left(\frac{1}{\hat{T}_\infty}, \frac{1}{2}\right) \frac{\hat{p}_\infty}{\pi\hat{T}_\infty} \exp\left(-\frac{\zeta_\rho^2}{\hat{T}_\infty}\right). \tag{6.31}$$

6.3.2 The behavior of the gas

Free molecular flow

The solution for the free molecular flow is obtained by a simple modification of the solution given in Section 6.2.3. That is, the velocity distribution function in the wedge region is the same as before, and that in the other region is given by the Maxwell distribution at infinity.

The free molecular solution is isolated from the solution for a finite Knudsen number. The length scale L_r of variation of variables [e.g., $\rho/(\mathrm{d}\rho/\mathrm{d}r)$] becomes longer and longer with the distance from the cylinder and it is infinite at infinity, i.e., $L_\infty = \infty$. Therefore, when the state at infinity is not vacuum (the density ρ_∞ at infinity is not zero), the effective Knudsen number Kn_∞ ($= \ell_\infty/L_\infty$; ℓ_∞ : the mean free path at infinity) at infinity vanishes, however small ρ_∞ may be [see Eqs. (1.22) and (1.41)]. The solution approaches a solution in the continuum limit in the far field. Thus, the behavior of the solution for the free molecular flow is different from that for a finite Kn_w. For example, the solution for the free molecular flow exists for an arbitrary set of the parameters $\hat{p}_\infty$ and $\hat{T}_\infty$, but, as will be shown in the followings, the solution for a finite Kn_w exists only when some relation is satisfied between $\hat{p}_\infty$ and $\hat{T}_\infty$.

Flow in the continuum limit

According to the asymptotic theory in Section 3.5, the solution is given by the Euler set of equations (3.225a)–(3.225c) with the boundary conditions (3.228a) and (3.228b) on the cylinder and the conditions at infinity.[17] Thus, the flow is isentropic except for the shock layer (see Section 4.7), if any. The temperature ratio T_∞/T_w and the mass and energy flows m_f and e_f from the cylinder per unit time and per unit area of the cylinder are determined by the pressure ratio p_∞/p_w as follows. The temperature T_∞ at infinity cannot be chosen at our disposal. The flow velocity $(v_{r\infty}, 0, 0)$ at infinity is imposed to vanish as the boundary condition.

(i) For $p_\infty/p_w > (4/3)^{5/2}h_1(1)$: The results are expressed with the aid of the parameter M_c (the Mach number of the Euler solution on the condensed phase) as

$$\frac{p_\infty}{p_w} = \left(\frac{M_c^2}{3}+1\right)^{5/2} h_1(M_c), \quad \frac{T_\infty}{T_w} = \left(\frac{M_c^2}{3}+1\right) h_2(M_c), \quad \frac{v_{r\infty}}{(2RT_w)^{1/2}} = 0, \tag{6.32}$$

$$\frac{m_f}{\rho_w(2RT_w)^{1/2}} = \left(\frac{5}{6}\right)^{1/2} \frac{M_c h_1(M_c)}{h_2(M_c)^{1/2}}, \tag{6.33a}$$

$$\frac{e_f}{p_w(2RT_w)^{1/2}} = \frac{1}{\sqrt{3}}\left(\frac{5}{2}\right)^{3/2}\left(\frac{M_c^2}{3}+1\right) M_c h_1(M_c) h_2(M_c)^{1/2}. \tag{6.33b}$$

(ii) For $0 < p_\infty/p_w < (4/3)^{5/2}h_1(1)$: A shock layer stands between the cylinder and infinity. The Mach number on the condensed phase is unity, i.e., $M_c = 1$. The quantities T_∞/T_w , $v_{r\infty}/(2RT_w)^{1/2}$, $m_f/\rho_w(2RT_w)^{1/2}$, and $e_f/p_w(2RT_w)^{1/2}$ are given by

$$\frac{T_\infty}{T_w} = \frac{4}{3}h_2(1) \ (= 0.8579), \qquad \frac{v_{r\infty}}{(2RT_w)^{1/2}} = 0, \tag{6.34}$$

$$\frac{m_f}{\rho_w(2RT_w)^{1/2}} = \left(\frac{5}{6}\right)^{1/2} \frac{h_1(1)}{h_2(1)^{1/2}} \ (= 0.2361), \tag{6.35a}$$

$$\frac{e_f}{p_w(2RT_w)^{1/2}} = \sqrt{2}\left(\frac{5}{3}\right)^{3/2} h_1(1)h_2(1)^{1/2} \ (= 0.5065), \tag{6.35b}$$

where the numerical data after the final equal sign in each equation are those for the BKW equation and the complete-condensation condition. For this pressure range, these quantities are independent of the pressure ratio p_∞/p_w. The limiting values of $v_{r\infty}/(2RT_w)^{1/2}$ and T_∞/T_w as $p_\infty/p_w \to 0$ do not approach those of the flow into a vacuum in Section 6.2.3. These two cases are two different states derived from different processes in taking the limit that $r/L \to \infty$ and $p_\infty/p_w \to 0$: one is the state derived by taking first $r/L \to \infty$ and then

[17] See Footnote 11 in Section 6.2.

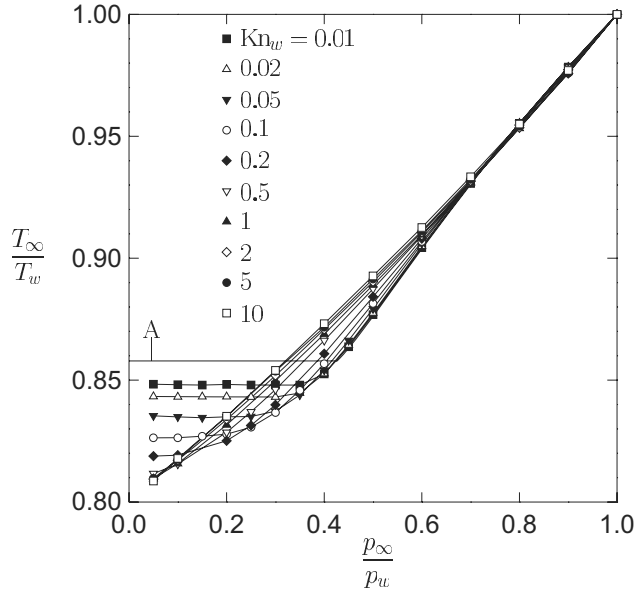

Figure 6.22. Temperature ratio T_∞/T_w vs pressure ratio p_∞/p_w for various Knudsen numbers Kn_w in the evaporating flow from a cylinder into a gas. The curve with the mark A is the solution in the continuum limit, i.e., Eqs. (6.32) and (6.34).

$p_\infty/p_w \to 0$, and the other is the state derived by taking first $p_\infty/p_w \to 0$ and then $r/L \to \infty$. In the latter, the shock wave shifts to infinity and disappears from the flow field in the first limit. Thus the state at infinity is ahead of the shock wave. On the other hand, in the former, the state behind the shock wave is chosen as the state at infinity in the first limit and then the pressure at infinity is brought to zero in the second limit.

Numerical solution

The boundary-value problem, Eqs. (6.15), (6.18a), and (6.31), is solved numerically for various Knudsen numbers by the finite-difference method outlined in Section 6.2.2.

Macroscopic variables The solution of the problem is determined by specifying the pressure ratio p_∞/p_w and the Knudsen number Kn_w. The temperature ratio T_∞/T_w is determined by them, i.e.,

$$T_\infty/T_w = \mathcal{T}(p_\infty/p_w, \mathrm{Kn}_w). \tag{6.36}$$

Their relation is shown in Fig. 6.22, where the solution in the continuum limit is marked by A.

The profiles of the density, flow velocity, temperature, and Mach number, i.e., ρ/ρ_w, $v_r/(2RT_w)^{1/2}$, T/T_w, and M $[= v_r/(5RT/3)^{1/2}]$ as functions of r/L,

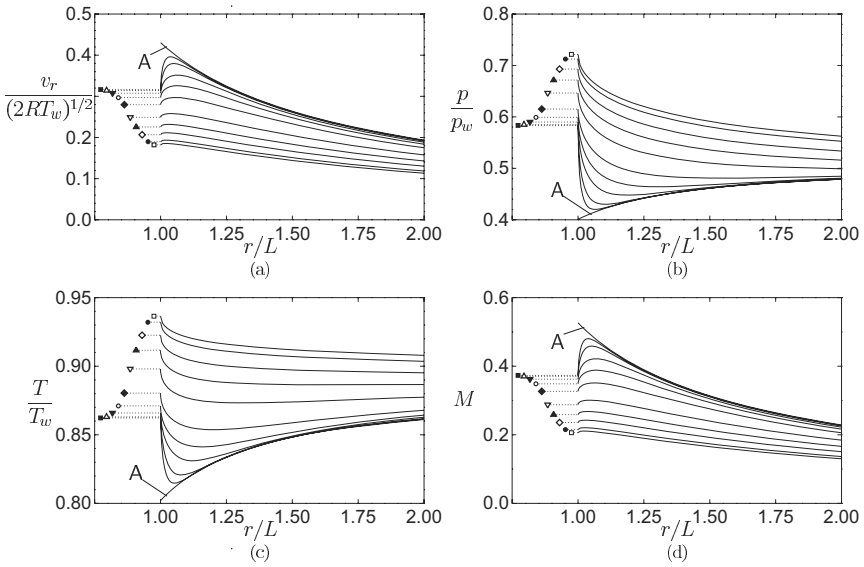

Figure 6.23. The profiles of the flow velocity v_r, the pressure p, the temperature T, and the Mach number M for various Knudsen numbers Kn_w in the evaporating flow from a cylinder into a gas I: $p_\infty/p_w = 0.5$. (a) $v_r/(2RT_w)^{1/2}$ vs r/L, (b) p/p_w vs r/L, (c) T/T_w vs r/L, and (d) M vs r/L. The curves for $\mathrm{Kn}_w = 0$ (the continuum limit), 0.01, 0.02, 0.05, 0.1, 0.2, 0.5, 1, 2, 5, and 10 are shown. The data are arranged in the order (or reverse order) of Kn_w except on or near the cylinder. The values on the cylinder are shown by the same symbols for Kn_w as in Fig. 6.22. The curve with the mark A is the solution in the continuum limit.

are shown for various values of the Knudsen number Kn_w in Figs. 6.23 and 6.24 representing two typical behaviors. Figure 6.23 is the case $p_\infty/p_w = 0.5$. The flow is accelerated near the cylinder and then is decelerated to the state at rest at infinity. It is subsonic over the whole flow field. The acceleration near the cylinder is smaller for larger Knudsen number. The pressure and temperature for small Kn_w decrease sharply near the cylinder, overshooting the uniform state at infinity, and then increase gradually to the state at infinity. As Kn_w becomes larger, their overshoots disappear and they decrease moderately and monotonically to the state at infinity. With decrease of p_∞/p_w, the acceleration and the overshoot are more intensified and extend in a wider region. At $p_\infty/p_w = 0.4260$, the flow (except for the Knudsen-layer correction) with $\mathrm{Kn}_w = 0$ reaches sonic ($M = 1$) on the cylinder, but the flow with $\mathrm{Kn}_w > 0$ is subsonic over the whole field. For smaller p_∞/p_w, the flow with small Kn_w is accelerated to supersonic speed and then is decelerated sharply, and with increase of Kn_w, the acceleration becomes weaker, its region shrinks, the deceleration becomes milder, and finally the flow becomes subsonic over the whole field. As p_∞/p_w becomes smaller, the flow is accelerated up to farther downstream and the acceleration to supersonic state occurs in larger Kn_w. Figure 6.24 is the case $p_\infty/p_w = 0.05$.

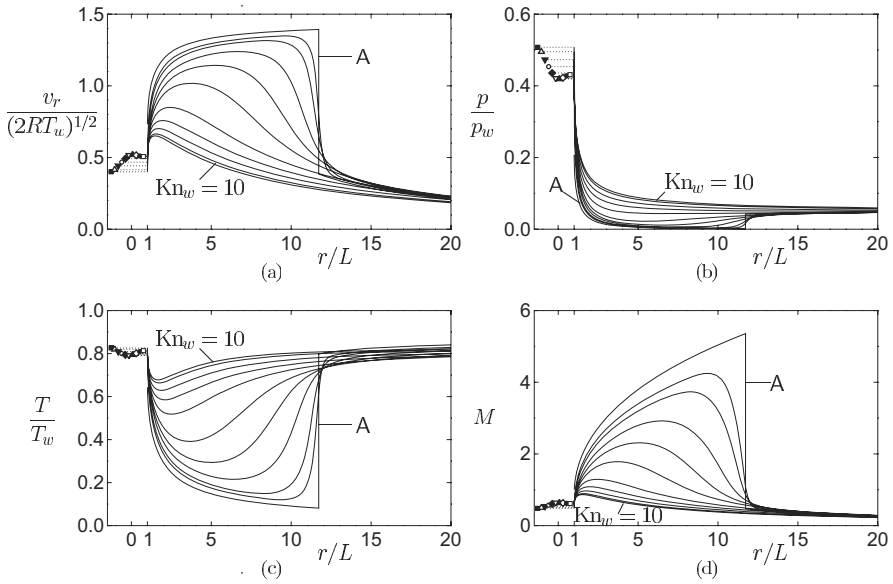

Figure 6.24. The profiles of the flow velocity v_r, the pressure p, the temperature T, and the Mach number M for various Knudsen numbers Kn_w in the evaporating flow from a cylinder into a gas II: $p_\infty/p_w = 0.05$. (a) $v_r/(2RT_w)^{1/2}$ vs r/L, (b) p/p_w vs r/L, (c) T/T_w vs r/L, and (d) M vs r/L. The curves for $\mathrm{Kn}_w = 0$ (the continuum limit), 0.01, 0.02, 0.05, 0.1, 0.2, 0.5, 1, 2, 5, and 10 are shown. The data are arranged in the order (or reverse order) of Kn_w except on or near the cylinder. The values on the cylinder are shown by the same symbols for Kn_w as in Fig. 6.22. The curve with the mark A is the solution in the continuum limit, accompanied by discontinuity, i.e., a shock wave.

The variations of the mass and energy flows m_f and e_f per unit time and per unit area from the cylinder with the pressure ratio are shown as $m_f/\rho_w(2RT_w)^{1/2}$ and $e_f/p_w(2RT_w)^{1/2}$ vs p_∞/p_w in Figs. 6.25 and 6.26.

Velocity distribution function We will explain the behavior of the marginal velocity distribution function g referring to Figs. 6.27 and 6.28 with the aid of the behavior of the macroscopic variables (Figs. 6.23 and 6.24). The cases without figures can be inferred from these figures (see Sugimoto & Sone [1992]).

For $p_\infty/p_w = 0.05$ and $\mathrm{Kn}_w = 0.01$, the discontinuity of the distribution function g is smoothed out by frequent molecular collisions in a short distance with a shift of its center of mass corresponding to acceleration of the gas flow [Fig. 6.27 (a) at $r/L = 1 \rightarrow$ Fig. 6.27 (b) at $r/L = 1.105$]. The center of mass of the distribution function is further shifted and its extent shrinks, corresponding to acceleration and temperature drop [Fig. 6.27 (b) at $r/L = 1.105 \rightarrow$ Fig. 6.27 (c) at $r/L = 10.23$; note the difference of the scale of the ordinate between the figures (b) and (c)]. Then the peak of the distribution function is lowered and another bump appears [Fig. 6.27 (c) at $r/L = 10.23 \rightarrow$ Fig. 6.27 (d) at

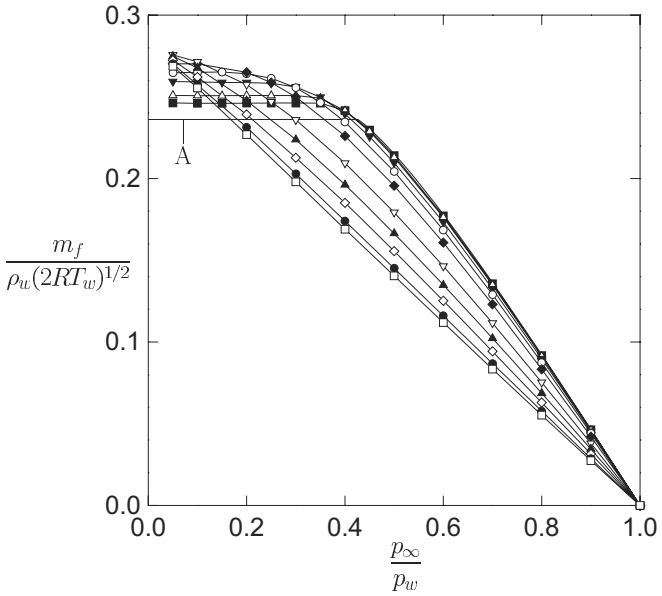

Figure 6.25. The nondimensional mass flux $m_f/\rho_w(2RT_w)^{1/2}$ versus the pressure ratio p_∞/p_w for various Knudsen numbers Kn_w in the evaporating flow from a cylinder into a gas. The same symbols as in Fig. 6.22 are used to indicate the Knudsen number. The curve with the mark A is the solution in the continuum limit, i.e., Eqs. (6.32), (6.33a), and (6.35a).

$r/L = 12.03$]. The peak disappears and a hill around the bump is established [Fig. 6.27 (d) at $r/L = 12.03 \rightarrow$ Fig. 6.27 (e) at $r/L = 13.02$]. The process Fig. 6.27 (c) $\rightarrow$ Fig. 6.27 (d) $\rightarrow$ Fig. 6.27 (e) corresponds to a shock wave, through which the gas is decelerated and heated. For $p_\infty/p_w = 0.05$ and $\mathrm{Kn}_w = 1$, the distribution function with a large discontinuity on the cylinder [Fig. 6.28 (a) at $r/L = 1$] is deformed from small molecular speed side (or small ζ_ρ side), and the peak is formed in positive ζ_r $(= \zeta_\rho \cos\theta_\zeta)$ region, which corresponds to acceleration [Fig. 6.28 (a) at $r/L = 1 \rightarrow$ Fig. 6.28 (b) at $r/L = 1.106$]. Then the peak is lowered gradually and the center of mass of the distribution function moves toward the origin, corresponding to deceleration [Fig. 6.28 (b) at $r/L = 1.106 \rightarrow$ Fig. 6.28 (c) at $r/L = 10.15 \rightarrow$ Fig. 6.28 (d) at $r/L = 19.98$; note the difference of the scale of the ordinate between the figures (b) and (c)]. There still remain a discontinuity and a strong anisotropy of the distribution function at $r/L = 19.98$.

When the pressure ratio is larger, the discontinuity of the distribution function is smaller and the variation is simple and no bump is formed corresponding to the simple variation of the macroscopic variables. For $p_\infty/p_w = 0.5$ and $\mathrm{Kn}_w = 0.01$, the velocity distribution function is smoothed out by frequent molecular collisions in a short distance with a slight shift of its center of mass corresponding to acceleration of the flow. The distribution function at about

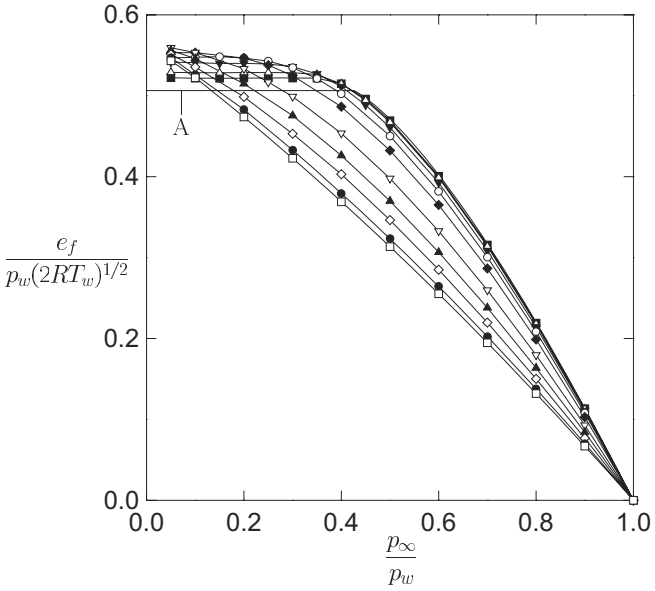

Figure 6.26. The nondimensional energy flux $e_f/p_w(2RT_w)^{1/2}$ versus the pressure ratio p_∞/p_w for various Knudsen numbers Kn_w in the evaporating flow from a cylinder into a gas. The same symbols as in Fig. 6.22 are used to indicate the Knudsen number. The curve with the mark A is the solution in the continuum limit, i.e., Eqs. (6.32), (6.33b), and (6.35b).

10 mean free paths and that about 150 mean free paths are quite similar. The similarity shows that the gas is in the continuum region. The difference can be figured out by the variation of the macroscopic variables in Fig. 6.23, e.g., the shift of its center of mass toward the origin corresponding to deceleration. For $p_\infty/p_w = 0.5$ and $\mathrm{Kn}_w = 1$, the discontinuity persists for a longer distance, and the deformation starts in the neighborhood of $\zeta_\rho = 0$.

6.4 Evaporation from a spherical condensed phase into a vacuum

6.4.1 Problem and basic equation

Consider a time-independent evaporating flow of a gas from a sphere made of its condensed phase (radius: L, temperature: T_w, and the saturated gas pressure at temperature T_w : p_w) into an infinite expanse of a vacuum. Here, we discuss the behavior of the flow around the sphere for a wide range of the Knudsen number Kn_w (the mean free path of the gas in the equilibrium state at rest with temperature T_w and pressure p_w divided by the radius of the sphere) on the basis of numerical analysis (Sone & Sugimoto [1993]) of the BKW equation and

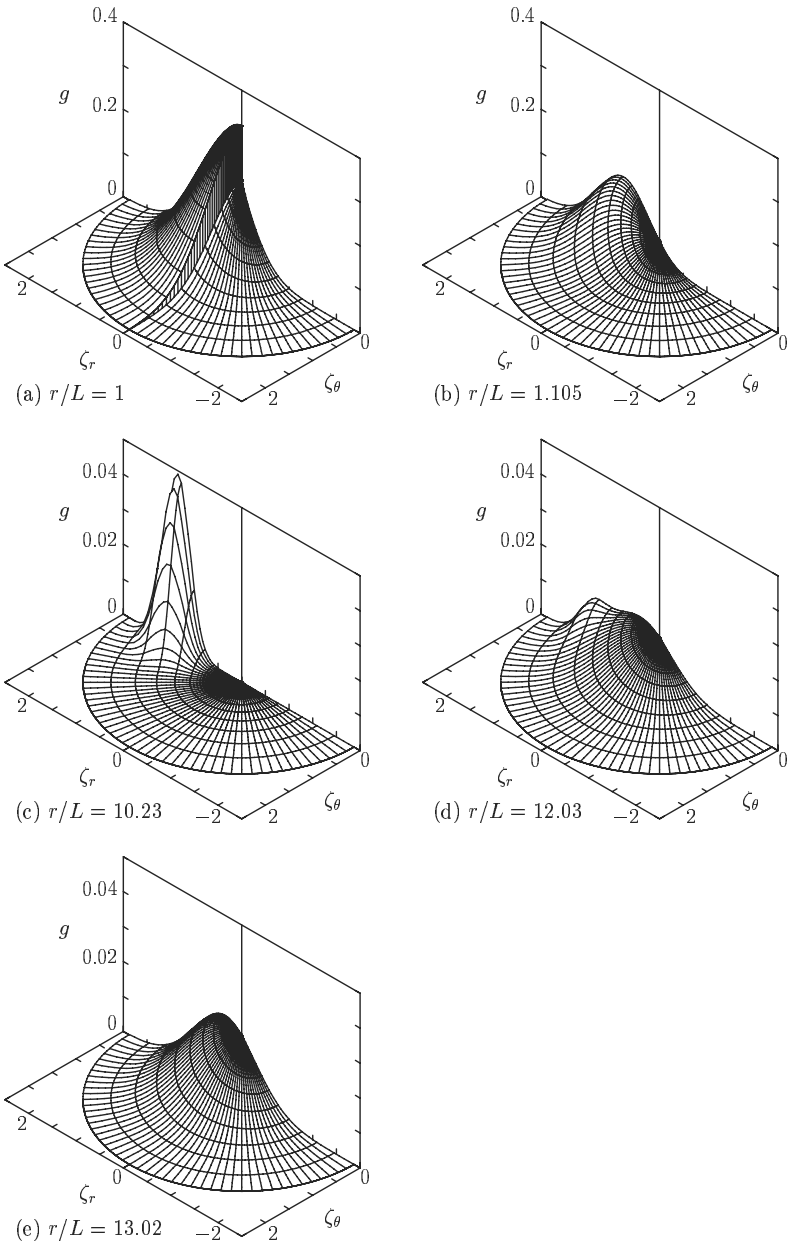

Figure 6.27. The marginal velocity distribution function g at various points in the evaporating flow from a cylinder into a gas I: $p_\infty/p_w = 0.05$ and $\mathrm{Kn}_w = 0.01$. (a) $r/L = 1$, (b) $r/L = 1.105$, (c) $r/L = 10.23$, (d) $r/L = 12.03$, and (e) $r/L = 13.02$. The surface g is shown by two sets of lines $\zeta_\rho = \text{const}$ and $\theta_\zeta = \text{const}$. Only the part for $0 \le \theta_\zeta \le \pi$ is shown because g is symmetric with respect to θ_ζ. The vertical stripes show the discontinuity of g. Note that $\zeta_r = \zeta_\rho \cos\theta_\zeta$ and $\zeta_\theta = \zeta_\rho \sin\theta_\zeta$.

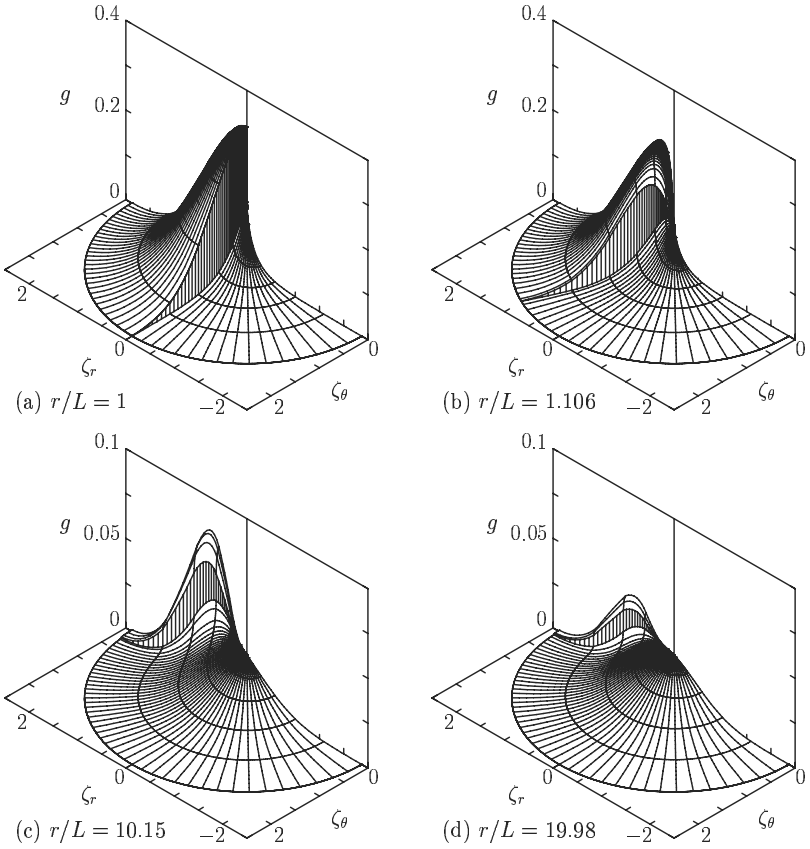

Figure 6.28. The marginal velocity distribution function g at various points in the evaporating flow from a cylinder into a gas II: $p_\infty/p_w = 0.05$ and $\mathrm{Kn}_w = 1$. (a) $r/L = 1$, (b) $r/L = 1.106$, (c) $r/L = 10.15$, and (d) $r/L = 19.98$. The surface g is shown by two sets of lines $\zeta_\rho = \text{const}$ and $\theta_\zeta = \text{const}$. Only the part for $0 \le \theta_\zeta \le \pi$ is shown because g is symmetric with respect to θ_ζ. The vertical stripes show the discontinuity of g. Note that $\zeta_r = \zeta_\rho \cos\theta_\zeta$ and $\zeta_\theta = \zeta_\rho \sin\theta_\zeta$.

the complete-condensation condition. We consider the simple case where the state of the gas is spherically symmetric and the flow is in the radial direction.

Basically, we use the notation introduced in Section 1.9 with L, p_w, and T_w as the reference length L, the reference pressure p_0, and the reference temperature T_0. The spherical coordinates (r, θ, φ) and their nondimensional counterparts $(\hat{r}, \theta, \varphi)$ are used here. We further introduce new notation. Let $(\zeta_r, \zeta_\theta, \zeta_\varphi)$ be the spherical components of the nondimensional velocity $\boldsymbol{\zeta}$, and let $(\zeta_r, \zeta_\theta, \zeta_\varphi)$ be expressed as

$$\zeta_r = \zeta \cos\theta_\zeta,\ \zeta_\theta = \zeta \sin\theta_\zeta \cos\psi,\ \zeta_\varphi = \zeta \sin\theta_\zeta \sin\psi, \tag{6.37}$$

where the range of $(\zeta, \theta_\zeta, \psi)$ is $(0 \le \zeta < \infty,\ 0 \le \theta_\zeta \le \pi,\ 0 \le \psi < 2\pi)$.[18] The velocity distribution function $\hat{f}$ is independent of ψ owing to the symmetry of the problem.[19] The BKW equation (1.61) for the present situation is reduced to[20]

$$D_s \hat{f} = \frac{2}{\sqrt{\pi}\mathrm{Kn}_w} \hat{\rho}(\hat{f}_e - \hat{f}), \tag{6.38}$$

where

$$D_s = \zeta \cos\theta_\zeta \frac{\partial}{\partial \hat{r}} - \frac{\zeta \sin\theta_\zeta}{\hat{r}} \frac{\partial}{\partial \theta_\zeta}, \quad \mathrm{Kn}_w = \frac{\ell_w}{L},$$

$$\hat{f}_e = \frac{\hat{\rho}}{(\pi \hat{T})^{3/2}} \exp\left(-\frac{\zeta^2 + \hat{v}_r^2 - 2\hat{v}_r \zeta \cos\theta_\zeta}{\hat{T}} \right),$$

and

$$\hat{\rho} = 2\pi \int \hat{f} \zeta^2 \sin\theta_\zeta \mathrm{d}\zeta \mathrm{d}\theta_\zeta, \tag{6.39a}$$

$$\hat{v}_r = \frac{2\pi}{\hat{\rho}} \int \hat{f} \zeta^3 \cos\theta_\zeta \sin\theta_\zeta \mathrm{d}\zeta \mathrm{d}\theta_\zeta, \tag{6.39b}$$

$$\hat{T} = \frac{2}{3\hat{\rho}} \left(2\pi \int \hat{f} \zeta^4 \sin\theta_\zeta \mathrm{d}\zeta \mathrm{d}\theta_\zeta - \hat{\rho} \hat{v}_r^2 \right), \tag{6.39c}$$

$$\hat{p} = \hat{\rho} \hat{T}. \tag{6.39d}$$

Here, ℓ_w is the mean free path of the gas in the equilibrium state at rest with pressure p_w and temperature T_w $[\ell_w = (8RT_w/\pi)^{1/2}/(A_c \rho_w); \rho_w = p_w/RT_w]$ and the integration is carried out over the domain $(0 \le \zeta < \infty,\ 0 \le \theta_\zeta \le \pi)$, where the integration with respect to ψ has been carried out, because $\hat{f}$ is

[18] See Footnote 22 in Section 4.5.

[19] In considering a spherical symmetry, it should be noted that the standard of direction on a sphere is the class of great circles passing a common point, e.g., $\varphi = \text{const}$. Thus, the velocity distribution function $\hat{f}$ expressing a *spherically symmetric state* is a function only of $\hat{r}$, ζ_r, and $\zeta_\theta^2 + \zeta_\varphi^2$ (and $\hat{t}$ for time-dependent problems); otherwise the uniqueness of $\hat{f}$ is violated at the common point. Therefore, $\hat{f}$ is a function of $\hat{r}$, ζ, and θ_ζ.

[20] Equation (6.38) is derived easily from Eq. (A.162) in Section A.3. The former is simpler in the sense that it contains the derivatives with respect to only $\hat{r}$ and θ_ζ.

independent of ψ. The boundary conditions on the cylinder and at infinity are

$$\left.\begin{array}{ll} \hat{f} = \dfrac{1}{\pi^{3/2}} \exp(-\zeta^2) & (\hat{r} = 1,\ 0 \le \theta_\zeta < \pi/2), \\ \hat{f} \to 0 & (\hat{r} \to \infty,\ \pi/2 < \theta_\zeta \le \pi). \end{array}\right\} \tag{6.40}$$

6.4.2 The behavior of the gas

Free molecular flow

The free molecular solution is easily obtained by the recipe in Chapter 2. The velocity distribution function $\hat{f}$ is

$$\hat{f} = \begin{cases} \pi^{-3/2} \exp(-\zeta^2) & [0 \le \theta_\zeta < \mathrm{Arcsin}(L/r)], \\ 0 & [\mathrm{Arcsin}(L/r) < \theta_\zeta \le \pi]. \end{cases} \tag{6.41}$$

At a given point in the gas, only the molecules whose velocities are inside the cone $0 \le \theta_\zeta < \mathrm{Arcsin}(L/r)$ or which come directly from the sphere are present. The height of $\hat{f}$ is invariant with respect to the distance. The density ρ, the flow velocity v_r, the temperatures T, and the parallel and normal temperatures[21] $T_\parallel$ and $T_\perp$ to the flow are

$$\begin{array}{l} \dfrac{\rho}{\rho_w} = \dfrac{1-y}{2}, \quad \dfrac{v_r}{(2RT_w)^{1/2}} = \dfrac{1+y}{\sqrt{\pi}}, \quad \dfrac{T}{T_w} = 1 - \dfrac{2(1+y)^2}{3\pi}, \\ \dfrac{T_\parallel}{T_w} = \left(1 - \dfrac{2}{\pi}\right)(1+y)^2 - y, \quad \dfrac{T_\perp}{T_w} = 1 - \dfrac{1}{2}(y + y^2), \end{array} \tag{6.42}$$

where

$$y = [1 - (L/r)^2]^{1/2}.$$

The flow velocity v_r, the temperature T, and the parallel temperature $T_\parallel$ take nonzero values at infinity, because $y = 1$ there, and ρ and $T_\perp$ vanish with speeds proportional to $(L/r)^2$ as $r/L \to \infty$. The mass and energy flows m_f and e_f per unit time and per unit area from the sphere are

$$m_f/\rho_w(2RT_w)^{1/2} = 1/2\sqrt{\pi}, \quad e_f/p_w(2RT_w)^{1/2} = 1/\sqrt{\pi}. \tag{6.43}$$

Flow in the continuum limit

The expanding isentropic flow into a vacuum is supersonic, and $M = 1$ on the condensed phase (or sphere) as explained in the case of the cylindrical

[21] The parallel and normal temperatures $(T_\parallel, T_\perp)$ are defined by

$$R\rho T_\parallel = \iiint (\xi_r - v_r)^2 f \mathrm{d}\xi_r \mathrm{d}\xi_\theta \mathrm{d}\xi_\varphi, \qquad 2R\rho T_\perp = \iiint (\xi_\theta^2 + \xi_\varphi^2) f \mathrm{d}\xi_r \mathrm{d}\xi_\theta \mathrm{d}\xi_\varphi,$$
$$T = (T_\parallel + 2T_\perp)/3,$$

where $(\xi_r, \xi_\theta, \xi_\varphi)$ are the spherical-coordinate components of the molecular velocity $\boldsymbol{\xi}$, corresponding to the nondimensional $(\zeta_r, \zeta_\theta, \zeta_\varphi)$.

condensed phase (Section 6.2.3). In view of this, the solution of the Euler set of equations (3.225a)–(3.225c) with the boundary conditions (3.228a) and (3.228b) that expresses expanding flows into a vacuum is obtained by the parametric expression in M $[= v_r/(5RT/3)^{1/2}]$ as[22]

$$\left.\begin{aligned} &\frac{\rho}{\rho_*} = \frac{8}{(3+M^2)^{3/2}}, \qquad \frac{v_r}{(5RT_*/3)^{1/2}} = \frac{2M}{(3+M^2)^{1/2}}, \\ &\frac{T}{T_*} = \frac{4}{3+M^2}, \qquad \frac{r}{L} = \frac{3+M^2}{4M^{1/2}}, \end{aligned}\right\} \tag{6.44}$$

or for large r/L,

$$\left.\begin{aligned} &\frac{\rho}{\rho_*} = \frac{1}{2}\left(\frac{L}{r}\right)^2, \qquad \frac{v_r}{(5RT_*/3)^{1/2}} = 2 - 3\left(\frac{L}{4r}\right)^{4/3}, \\ &\frac{T}{T_*} = 4^{-1/3}\left(\frac{L}{r}\right)^{4/3}, \qquad M = \left(\frac{4r}{L}\right)^{2/3}, \end{aligned}\right\} \tag{6.45}$$

where ρ_* and T_* are given by the functions $h_1(M)$ and $h_2(M)$, defined in Section 3.5.2, as

$$\rho_* = h_1(1)\rho_w/h_2(1), \qquad T_* = h_2(1)T_w,$$

where $h_1(1)/h_2(1) = 0.3225$ and $h_2(1) = 0.6434$ for the BKW equation and the complete-condensation condition. Incidentally,

$$T_\parallel = T_\perp = T,$$

because the velocity distribution function corresponding to the isentropic flow is Maxwellian. The mass and energy flows m_f and e_f per unit time and per unit area from the sphere are

$$\frac{m_f}{\rho_w(2RT_w)^{1/2}} = \left(\frac{5}{6}\right)^{1/2}\frac{h_1(1)}{h_2(1)^{1/2}}, \quad \frac{e_f}{p_w(2RT_w)^{1/2}} = 4\left(\frac{5}{6}\right)^{3/2} h_1(1)h_2(1)^{1/2}, \tag{6.46}$$

which are, respectively, 0.2361 and 0.5065 for the BKW equation and the complete-condensation condition.

In addition to the point that $\mathrm{d}\rho/\mathrm{d}r$, $\mathrm{d}v_r/\mathrm{d}r$, etc. are infinite at $r = L$, which is mentioned in Section 6.2.3, there is a more important point that requires improvement of the isentropic solution. It is the behavior of the solution for large r/L, where the density is low and the Mach number is large [Eq.(6.45)]. In the far field, the length scale L_r of variation of ρ etc., i.e., $\rho/(\mathrm{d}\rho/\mathrm{d}r)$ etc., is

$$L_r \sim r,$$

and the local mean free path ℓ_{lc} is

$$\ell_{lc} = v_r/A_c\rho \sim 4(5RT_*/3)^{1/2}r^2/A_c\rho_* L^2 \sim \ell_w(r/L)^2,$$

[22]See Footnote 11 in Section 6.2.

which is based on the flow speed instead of the thermal speed, because the far field with high Mach number is considered.[23] Thus, the local Knudsen number $\mathrm{Kn}_r (= \ell_{lc}/L_r)$ for large r/L increases with r as[24]

$$\mathrm{Kn}_r \sim \mathrm{Kn}_w r/L. \tag{6.47}$$

The local Knudsen number Kn_r, which characterizes the variation of the flow, is not uniformly small for small Kn_w, but it ranges from $O(\mathrm{Kn}_w)$ to ∞. Thus, the solution (6.44) is a poor approximation for small but finite Kn_w in the far field.

When Kn_w is very small, there is a region where Kn_r is small but M is large (e.g., take $r/L = \mathrm{Kn}_w^{-1/2}$). Then, the isentropic solution is valid up to this region, with the reservation of the first question raised in the preceding paragraph. The behavior downstream of this region can be studied by the *hypersonic approximation* (Hamel & Willis [1966] and Edwards & Cheng [1966]; see also Section B.5), where a simplification is made under the assumption that the width of the velocity distribution function is much smaller than the flow speed. According to Section B.5, the solution of the BKW equation under this approximation of a spherically expanding flow is expressed by the confluent hypergeometric functions as follows:

$$\hat{\rho} = c_0 \hat{r}^{-2}, \tag{6.48a}$$

$$\hat{v}_r = c_1, \tag{6.48b}$$

$$\hat{T} = \frac{1}{\hat{r}^2}\left[c_2 U\left(\frac{2}{3}, 3, \frac{\alpha}{\mathrm{Kn}_w \hat{r}}\right) + c_3 M\left(\frac{2}{3}, 3, \frac{\alpha}{\mathrm{Kn}_w \hat{r}}\right)\right], \tag{6.48c}$$

$$\alpha = 2c_0/\sqrt{\pi} c_1,$$

where c_0, c_1, c_2, and c_3 are undetermined constants, and $U(a, b, c)$ and $M(a, b, c)$ are Kummer's functions (of the same notation as in Abramowitz & Stegun [1972]; do not confuse with the Mach number M). The expansion for $\mathrm{Kn}_w \hat{r} \ll 1$ (what is called the inner expansion in Van Dyke [1964], Cole [1968], etc.) of the solution (6.48a)–(6.48c) is

$$\left.\begin{aligned} &\hat{\rho} = c_0 \hat{r}^{-2}, \quad \hat{v}_r = c_1, \\ &\hat{T} = c_2 \left(\frac{\mathrm{Kn}_w}{\alpha}\right)^{2/3} \frac{1}{\hat{r}^{4/3}} + \frac{2c_3}{\Gamma(2/3)} \left(\frac{\mathrm{Kn}_w}{\alpha}\right)^{7/3} \hat{r}^{1/3} \exp\left(\frac{\alpha}{\mathrm{Kn}_w \hat{r}}\right), \end{aligned}\right\} \tag{6.49}$$

where $\Gamma(x)$ is the gamma function. Matching Eq. (6.49) with the expansion of Eq. (6.44) for large $\hat{r}$, i.e., Eq. (6.45), of the isentropic solution, we have[25]

$$c_0 = \frac{h_1(1)}{2h_2(1)}, \quad c_1 = \left(\frac{10h_2(1)}{3}\right)^{1/2}, \quad c_2 = \left(\frac{3h_1(1)^2}{40\pi}\right)^{1/3} \frac{1}{\mathrm{Kn}_w^{2/3}}, \quad c_3 = 0. \tag{6.50}$$

[23] See Footnote 12 in Section 6.2.3.

[24] The relation depends on the molecular model. The relation applies to the pseudo-Maxwell molecule as well as the BKW model. For a hard-sphere molecule (or a molecule with a finite d_m,

$$\mathrm{Kn}_r \sim \mathrm{Kn}_w (r/L)^{5/3},$$

(see Footnote 13 in Section 6.2.3).

[25] The last condition $c_3 = 0$ is required for the smooth connection of the two solutions.

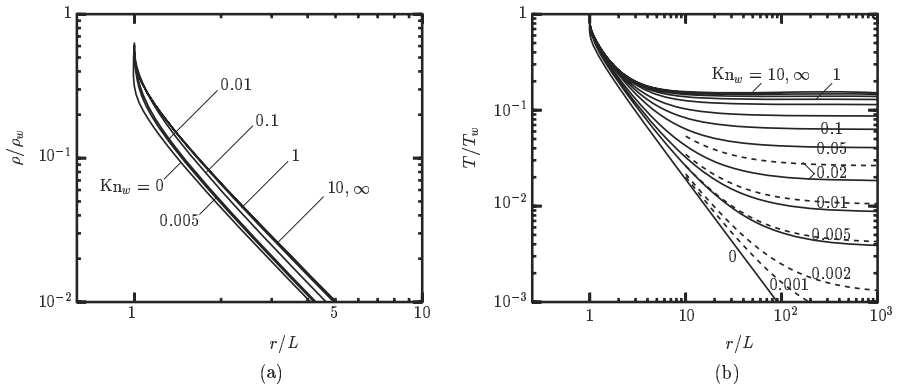

Figure 6.29. The profiles of the macroscopic variables for various Knudsen numbers Kn_w in the evaporating flow from a sphere into a vacuum. I: density and temperature. (a) ρ/ρ_w vs r/L and (b) T/T_w vs r/L. In panel (a), the curves for $\mathrm{Kn}_w = 0$, 0.005, 0.01, 0.1, 1, 10, and ∞ are shown. In panel (b), the curves for $\mathrm{Kn}_w = 0$, 0.005, 0.01, 0.02, 0.05, 0.1, 0.2, 0.5, 1, 2, 5, 10, and ∞ are shown, and the dashed lines are the solutions by the hypersonic approximation [Eq. (6.48c) with (6.50)].

The flow velocity does not vanish at infinity. From Eqs. (6.48c) and (6.50), we have, for $r/L \to \infty$,

$$T/T_w \to A_0 \mathrm{Kn}_w^{4/3}, \tag{6.51}$$
$$A_0 = \left(\frac{5\pi}{3}\right)^{2/3} \frac{h_2(1)^3}{\Gamma(2/3) h_1(1)^{4/3}} = 4.828,$$

The temperature at infinity takes nonzero value except for $\mathrm{Kn}_w = 0$. The normal temperature $T_\perp$ can be shown to decay as

$$T_\perp/T_w \to A_1 \mathrm{Kn}_w^{1/3} L/r, \quad \text{as } \mathrm{Kn}_w r/L \to \infty, \tag{6.52}$$
$$A_1 = \left(\frac{5\pi}{24}\right)^{1/6} \frac{h_2(1)^{3/2}}{\Gamma(2/3) h_1(1)^{1/3}} = 0.5999.$$

Numerical solution

The boundary-value problem, Eqs. (6.38) and (6.40), is solved numerically for various Knudsen numbers by a hybrid finite-difference method, which is practically the same as that outlined in Section 6.2.2.

Macroscopic variables The profiles of the density, flow velocity, temperature, and Mach number, i.e., ρ/ρ_w, $v_r/(2RT_w)^{1/2}$, T/T_w, and M as functions of r/L, are shown for various values of the Knudsen number Kn_w in Figs. 6.29 and 6.30. The data marked by $\mathrm{Kn}_w = 0$ and those by $\mathrm{Kn}_w = \infty$ are, respectively, the solution of the Euler set with the Knudsen layer and the free molecular solution.

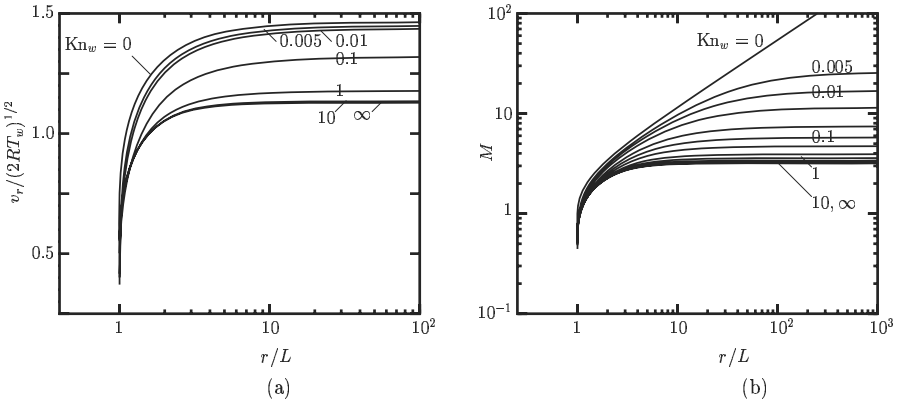

Figure 6.30. The profiles of the macroscopic variables for various Knudsen numbers Kn_w in the evaporating flow from a sphere into a vacuum II: flow velocity and Mach number. (a) $v_r/(2RT_w)^{1/2}$ vs r/L and (b) M vs r/L. In panel (a), the curves for $\mathrm{Kn}_w = 0$, 0.005, 0.01, 0.1, 1, 10, and ∞ are shown. In panel (b), the curves for $\mathrm{Kn}_w = 0$, 0.005, 0.01, 0.02, 0.05, 0.1, 0.2, 0.5, 1, 2, 5, 10, and ∞ are shown.

The solution of the Euler set takes $M = 1$ at $r/L = 1$ but the Knudsen layer, flattened on the sphere, has a finite amplitude. The part of the vertical line below $M = 1$ in Fig. 6.30 (b) is the flattened Knudsen layer. More detailed profiles of the above macroscopic variables near the sphere are given in Sone & Sugimoto [1993]. The dashed lines in Fig. 6.29 (b) are the corresponding solutions by the hypersonic approximation described above [Eq. (6.48c) with (6.50)].

The behavior of the gas varies very sharply near the sphere but approaches a vacuum state at infinity slowly. The density vanishes as fast as $r^{-\alpha}$ ($\alpha = 2.00$) for all Knudsen numbers. The flow velocity v_r and temperature T approach nonzero values at infinity (except for T at $\mathrm{Kn}_w = 0$), which depend on the Knudsen number. Their values $v_{r\infty}/(2RT_w)^{1/2}$ and T_∞/T_w at infinity, the latter of which is called *frozen temperature*, are tabulated in Table 6.4. The data in Table 6.4 are determined by close examination of the behavior of the variation of ρ, v_r, and T for large r. That is, $\ln\rho$, $\ln(\mathrm{d}v_r/\mathrm{d}r)$, and $\ln(\mathrm{d}T/\mathrm{d}r)$ vs $\ln r$ are found to be linear, with high accuracy, for large r, from which the asymptotic forms of ρ, v_r, and T are determined. Incidentally, the frozen temperatures for $\mathrm{Kn}_w = 0.005$ and 0.01 by the hypersonic approximation (6.51) are, respectively, 0.0041 and 0.0104, which are 0.0038 and 0.0086 by the numerical computation in Table 6.4. The velocity $v_{r\infty}/(2RT_w)^{1/2}$ at infinity by the hypersonic expansion, given by Eq. (6.48b) with (6.50), is 1.464, which agrees with the numerical value at $\mathrm{Kn}_w = 0$.

The normal and parallel temperatures, $T_\perp$ and $T_\parallel$, are often referred to in experimental studies of nonequilibrium flows. From the numerical result, the normal temperature $T_\perp$ vanishes as $r \to \infty$. From this result and Footnote 21 in this subsection,

$$T_\parallel \to 3T \quad \text{as } r \to \infty.$$

Table 6.4. $\dfrac{v_{r\infty}}{(2RT_w)^{1/2}}$, $\dfrac{T_\infty}{T_w}$, M_∞, $\dfrac{m_f}{\rho_w(2RT_w)^{1/2}}$, and $\dfrac{e_f}{p_w(2RT_w)^{1/2}}$ vs Kn_w in the evaporating flow from a sphere into a vacuum.

Kn_w	$\dfrac{v_{r\infty}}{(2RT_w)^{1/2}}$	$\dfrac{T_\infty}{T_w}$	M_∞	$\dfrac{m_f}{\rho_w(2RT_w)^{1/2}}$	$\dfrac{e_f}{p_w(2RT_w)^{1/2}}$
0	1.464	0	∞	0.2361	0.5065
0.005	1.4499	0.0038	26	0.2465	0.5222
0.01	1.4377	0.0086	17	0.2512	0.5290
0.02	1.4162	0.0183	11.5	0.2573	0.5374
0.05	1.3686	0.0406	7.44	0.2663	0.5487
0.1	1.3206	0.0630	5.76	0.2723	0.5554
0.2	1.2700	0.0867	4.72	0.2765	0.5596
0.5	1.2108	0.1141	3.927	0.2793	0.5616
1	1.1781	0.1290	3.593	0.2806	0.5628
2	1.1564	0.1388	3.400	0.2813	0.5634
5	1.1407	0.1458	3.273	0.2817	0.5637
10	1.1347	0.1484	3.227	0.2819	0.5640
∞	1.1284	0.1512	3.179	0.2821	0.5642

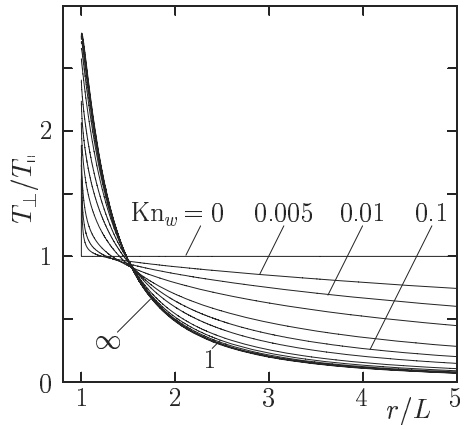

Figure 6.31. The profiles of the ratio $T_\perp/T_\parallel$ of the normal and parallel temperatures in the evaporating flow from a sphere into a vacuum for various Knudsen numbers Kn_w, i.e., $\mathrm{Kn}_w = 0$, 0.005, 0.01, 0.02, 0.05, 0.1, 0.2, 0.5, 1, 2, 5, 10, and ∞.

The ratio $T_\perp/T_\parallel$ is a measure of anisotropy of the velocity distribution function around the flow velocity ($T_\perp/T_\parallel = 1$ when it is isotropic). Its profile is shown in Fig. 6.31. The ratio $T_\perp/T_\parallel$ vanishes for all Kn_w, except for $\mathrm{Kn}_w = 0$, as $r \to \infty$. The velocity distribution function shows strong anisotropy over the whole flow field except for very small Knudsen numbers.

The variations of the mass and energy flows m_f and e_f per unit time and

per unit area from the sphere with the Knudsen number, i.e., $m_f/\rho_w(2RT_w)^{1/2}$ and $e_f/p_w(2RT_w)^{1/2}$ vs Kn_w, are tabulated in Table 6.4. They increase monotonically from the values at $\mathrm{Kn}_w = 0$ to those at $\mathrm{Kn}_w = \infty$. The contributions to m_f and e_f of the molecules leaving the sphere are equal to m_f and e_f at $\mathrm{Kn}_w = \infty$, respectively. Therefore, the differences from the free molecular values, which are negative, are the contributions of the molecules arriving on the sphere. For example, $m_f(\mathrm{Kn}_w = 0)/m_f(\mathrm{Kn}_w = \infty) = 0.8370$ and $e_f(\mathrm{Kn}_w = 0)/e_f(\mathrm{Kn}_w = \infty) = 0.8977$, and thus, 16.30% of the molecules leaving the sphere return to the sphere, but only 10.23% of the energy leaving the sphere return. This is because the returning molecules, on the average, have less energy than the leaving molecules. The rate 16.30% of the returning molecules at $\mathrm{Kn}_w = 0$ is equal to that in the evaporating flow from a plane condensed phase that reaches sonic speed at infinity. This is obvious from the structure of the solution, i.e., the isentropic evaporating flow that is sonic on the condensed phase and the Knudsen layer at the bottom of the isentropic flow.

Velocity distribution function We will explain the behavior of the velocity distribution function $\hat{f}$ referring to Figs. 6.32–6.36. The cases without figures can be inferred from these figures (see Sone & Sugimoto [1993]).

At $\mathrm{Kn}_w = \infty$ (free molecular flow), the molecular velocity is localized. That is, at a point r, the molecules with velocity $0 \le \theta_\zeta \le \mathrm{Arcsin}\,(L/r)$ come directly from the sphere and there are no molecules with the other velocity. The height of the velocity distribution function remains unchanged along the flow [see Eq. (6.41)]. At $\mathrm{Kn}_w = 10$ (large Knudsen number, Fig. 6.32), the feature of the free molecular flow is well preserved and only local correction in the $[\zeta_r, (\zeta_\theta^2 + \zeta_\varphi^2)^{1/2}]$ plane is seen. The effect of molecular collision is more eminent for smaller molecular speed (or small ζ) because of smaller free path. The height of the distribution function decreases very slowly.

On the other hand, at $\mathrm{Kn}_w = 0.01$ (very small Knudsen number, Figs. 6.33 and 6.34), the behavior is quite different. The discontinuity of the velocity distribution function on the sphere decays in a very short distance (much shorter than the mean free path ℓ_w) [Fig. 6.33 (a) at $r/L = 1 \rightarrow$ Fig. 6.33 (c) at $r/L = 1.0013$]. The distribution function is transformed into a distribution fairly close to the Maxwell distribution with the corresponding density, flow velocity, and temperature (the local Maxwellian f_e) in a distance of several mean free paths [Fig. 6.33 (a) at $r/L = 1 \rightarrow$ Fig. 6.33 (d) at $r/L = 1.015 \rightarrow$ Fig. 6.34 (a) at $r/L = 1.264$]. This is a kinetic transition process to a continuum region [Fig. 6.34 (a)]. The transition region is the Knudsen layer and the region with the discontinuity at the bottom of the Knudsen layer is the S layer, explained in Section 3.1.6. Along the flow, the density of the gas decreases and the collision effect becomes less important. Therefore, the velocity distribution function begins to deviate from the Maxwellian, i.e., its width normal to the flow shrinks [Fig. 6.34 (a) at $r/L = 1.264 \rightarrow$ Fig. 6.34 (b) at $r/L = 5.063 \rightarrow$ Fig. 6.34 (c) at $r/L = 60.76$]. In this stage, the collision effect is still appreciable and the height of the distribution function decreases considerably. Farther away from the sphere, where

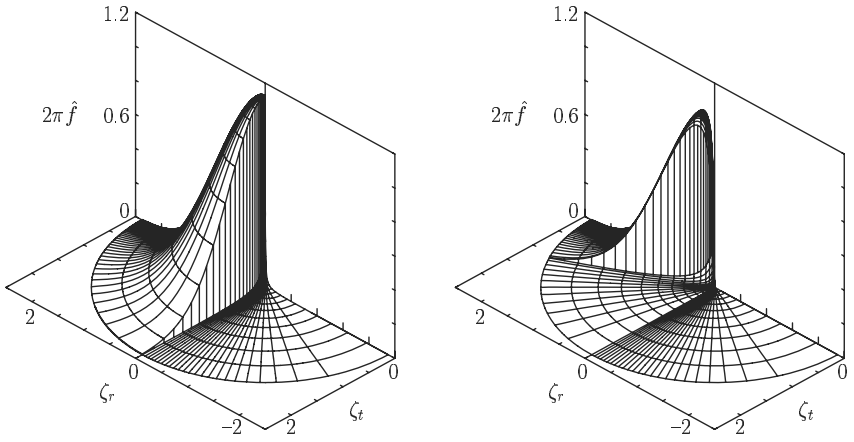

(a) $r/L = 1$ (b) $r/L = 2.205$

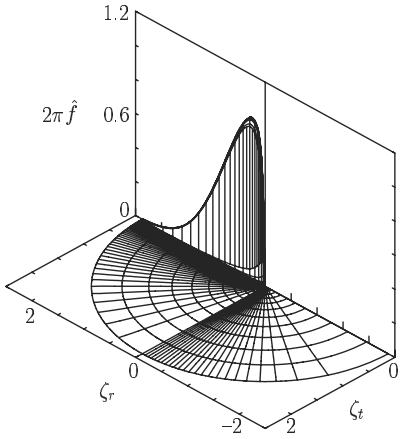

(c) $r/L = 99.94$

Figure 6.32. The velocity distribution function $\hat{f}$ at various points in the evaporating flow from a sphere into a vacuum at $\mathrm{Kn}_w = 10$. (a) $r/L = 1$, (b) $r/L = 2.205$, and (c) $r/L = 99.94$. The ζ_t is defined by $\zeta_t = (\zeta_\theta^2 + \zeta_\varphi^2)^{1/2}$. The vertical stripes show the discontinuity of $\hat{f}$.

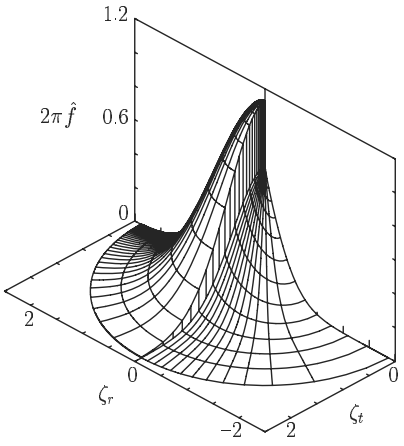

(a) $r/L = 1$

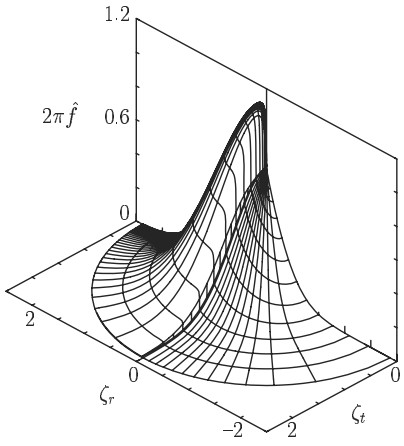

(b) $r/L = 1.00008$

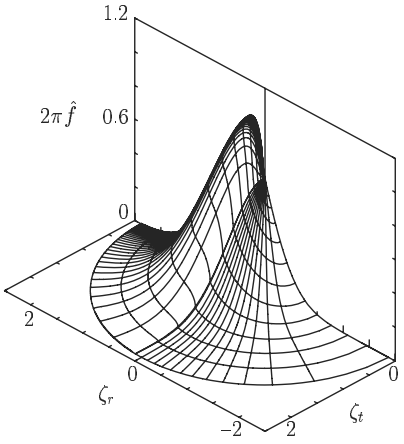

(c) $r/L = 1.0013$

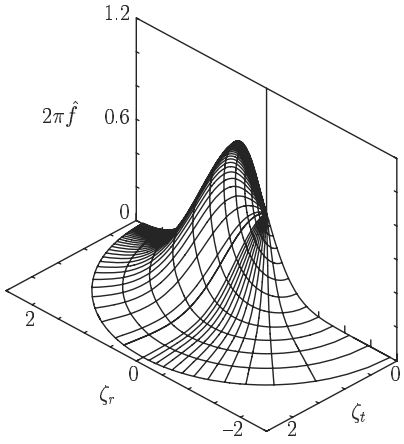

(d) $r/L = 1.015$

Figure 6.33. The velocity distribution function $\hat{f}$ at various points in the evaporating flow from a sphere into a vacuum at $\mathrm{Kn}_w = 0.01$ I. (a) $r/L = 1$, (b) $r/L = 1.00008$, (c) $r/L = 1.0013$, and (d) $r/L = 1.015$. The ζ_t is defined by $\zeta_t = (\zeta_\theta^2 + \zeta_\varphi^2)^{1/2}$. The vertical stripes show the discontinuity of $\hat{f}$.

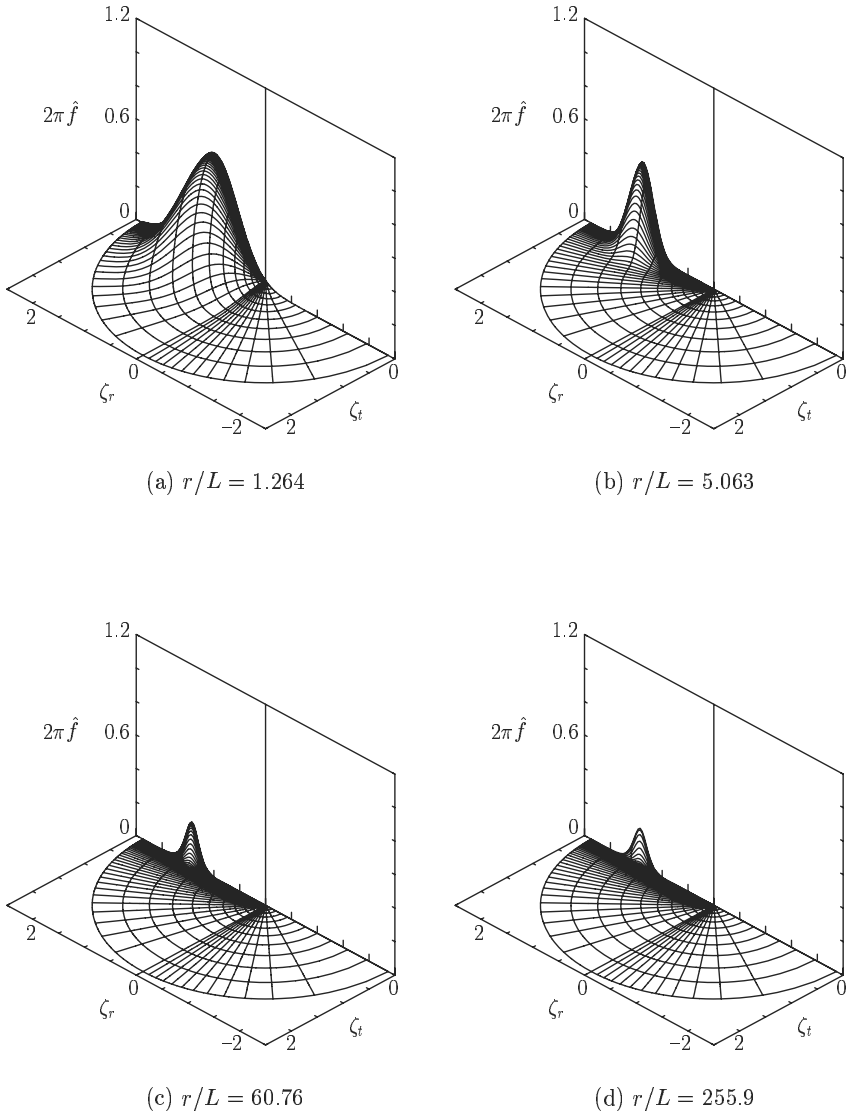

(a) $r/L = 1.264$ (b) $r/L = 5.063$

(c) $r/L = 60.76$ (d) $r/L = 255.9$

Figure 6.34. The velocity distribution function $\hat{f}$ at various points in the evaporating flow from a sphere into a vacuum at $\mathrm{Kn}_w = 0.01$ II. (a) $r/L = 1.264$, (b) $r/L = 5.063$, (c) $r/L = 60.76$, and (d) $r/L = 255.9$. The ζ_t is defined by $\zeta_t = (\zeta_\theta^2 + \zeta_\varphi^2)^{1/2}$.

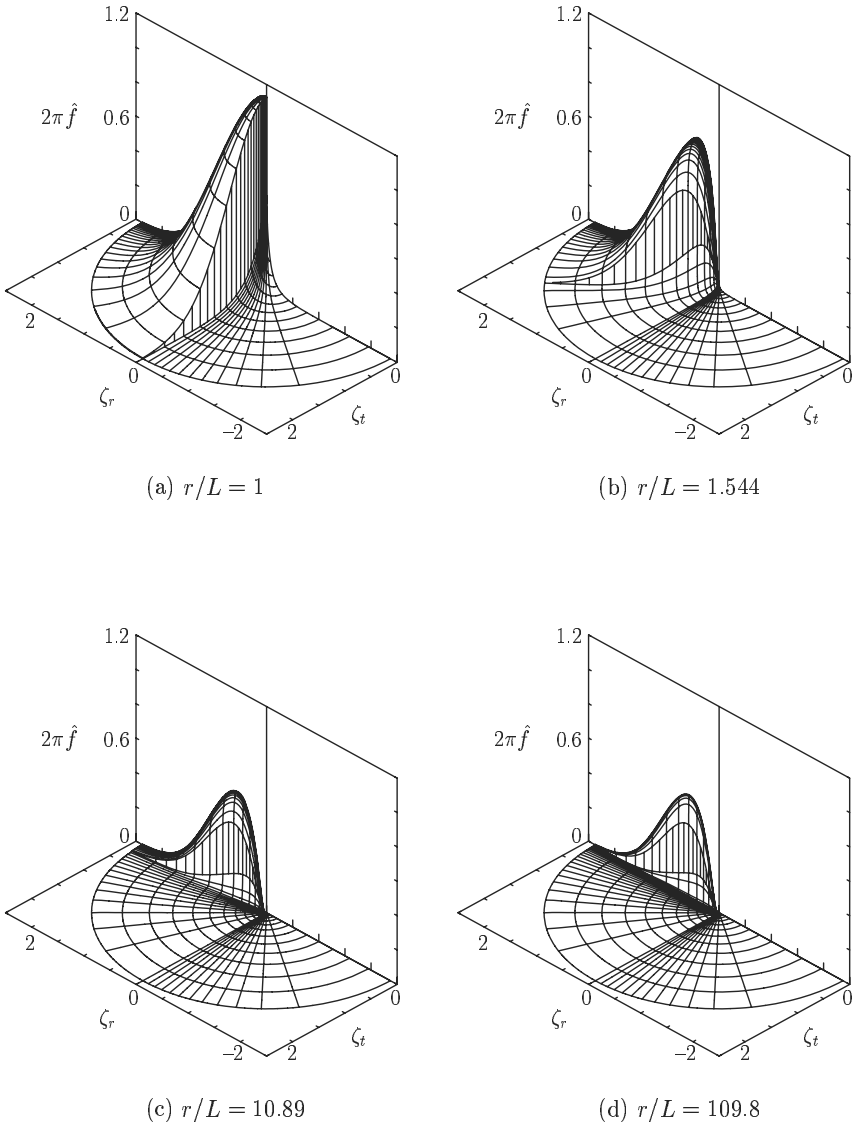

(a) $r/L = 1$ (b) $r/L = 1.544$

(c) $r/L = 10.89$ (d) $r/L = 109.8$

Figure 6.35. The velocity distribution function $\hat{f}$ at various points in the evaporating flow from a sphere into a vacuum at $\mathrm{Kn}_w = 1$. (a) $r/L = 1$, (b) $r/L = 1.544$, (c) $r/L = 10.89$, and (d) $r/L = 109.8$. The ζ_t is defined by $\zeta_t = (\zeta_\theta^2 + \zeta_\varphi^2)^{1/2}$. The vertical stripes show the discontinuity of $\hat{f}$.

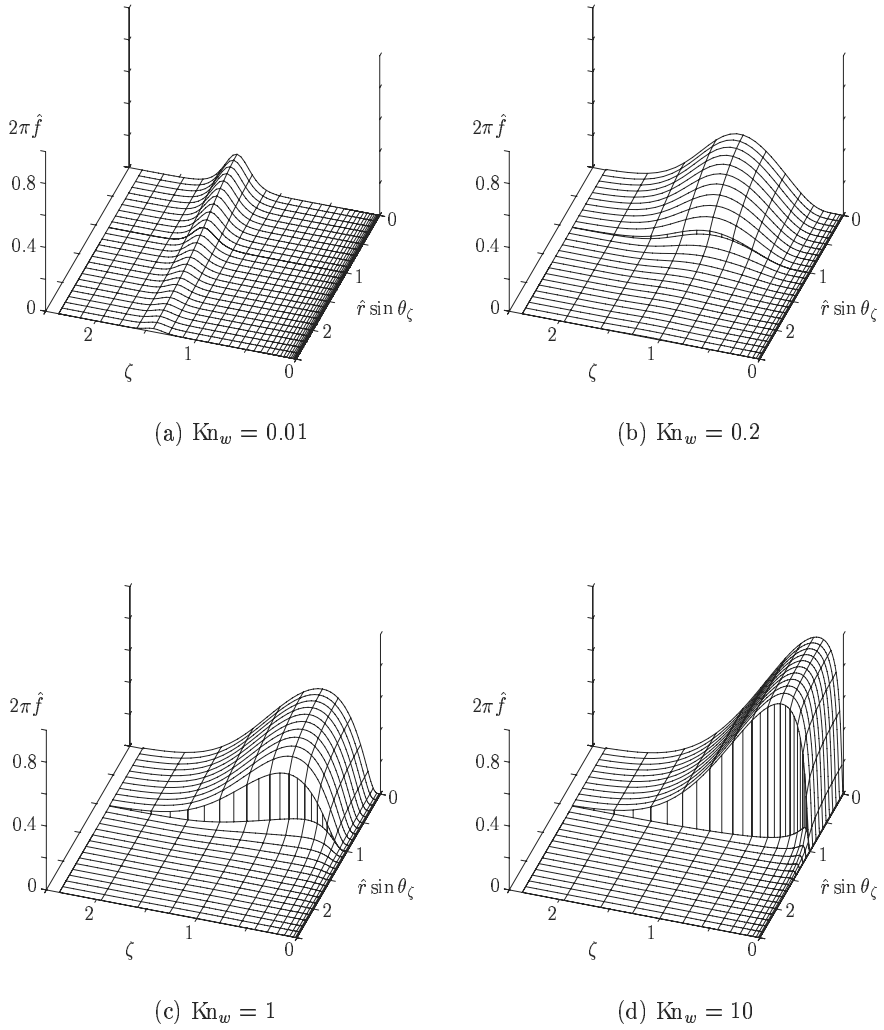

(a) $\mathrm{Kn}_w = 0.01$ (b) $\mathrm{Kn}_w = 0.2$

(c) $\mathrm{Kn}_w = 1$ (d) $\mathrm{Kn}_w = 10$

Figure 6.36. The velocity distribution function $\hat{f}$ at infinity in the neighborhood of the discontinuity ($\hat{r}\sin\theta_\zeta = 1$ with $0 \le \theta_\zeta < \pi/2$) in the evaporating flow from a sphere into a vacuum. (a) $\mathrm{Kn}_w = 0.01$, (b) $\mathrm{Kn}_w = 0.2$, (c) $\mathrm{Kn}_w = 1$, and (d) $\mathrm{Kn}_w = 10$. The data are extrapolated from the data for large r/L. The surface $\hat{f}$ is shown by $\zeta = \text{const}$ and $\hat{r}\sin\theta_\zeta = \text{const}$, and the discontinuity by the vertical stripes. The coordinate $\hat{r}\sin\theta_\zeta$ $(= \hat{r}\theta_\zeta + \cdots)$ is a coordinate stretched by $\hat{r}\,(= r/L)$.

the density of the gas is small, the height of the distribution function decreases very slowly as in the nearly free molecular flow [Fig. 6.34 (c) at $r/L = 60.76$ $\rightarrow$ Fig. 6.34 (d) at $r/L = 255.9$].

At $\mathrm{Kn}_w = 0.1$, the discontinuity decays in several mean free paths from the sphere ($r/L > 1.6$). The distribution function there is of the shape with $T_\perp/T_\parallel < 1$, and the ratio $T_\perp/T_\parallel$ decreases with the flow. That is, it is in a transition region that corresponds to the transition region in the downstream of the continuum region in the case $\mathrm{Kn}_w = 0.01$. The behavior farther downstream is similar to the case $\mathrm{Kn}_w = 0.01$, i.e., a transition region is followed by a free molecular region. There is no continuum region in the flow. At $\mathrm{Kn}_w = 1$, a transition region with large discontinuity [Fig. 6.35 (a) at $r/L = 1$ $\rightarrow$ Fig. 6.35 (c) at $r/L = 10.89$] is followed by a free molecular region with a large discontinuity [Fig. 6.35 (c) at $r/L = 10.89 \rightarrow$ Fig. 6.35 (d) at $r/L = 109.8$].

The transition to a free molecular flow region can be clearly seen from the profile of the distribution function $\hat{f}$ at a given ζ vs $\hat{r}\sin\theta_\zeta$ for various $\hat{r}$ $(= r/L)$. Because the characteristics of Eq. (6.38) are given by $\hat{r}\sin\theta_\zeta = \text{const}$, $\hat{f}$ at a given ζ is expressed by a single curve if the flow is free molecular. The flow approaches a free molecular condition for large $\hat{r}$ even for $\mathrm{Kn}_w = 0.01$. The discontinuity of the velocity distribution function remains appreciable at $r/L = 2000$ even for $\mathrm{Kn}_w = 0.2$. By extrapolation it is found to be appreciable at downstream infinity. Some examples of extrapolated distribution function $\hat{f}$ at infinity are shown in Fig. 6.36 (Sone & Sugimoto [1993]). This free molecular character, which is a good contrast to the evaporation from a cylindrical condensed phase into a vacuum discussed in Section 6.2, is related to Eq. (6.47).[26]

Supplementary discussion The evaporating flow from a spherical condensed phase into a vacuum is of free molecular type in the far field irrespective of Kn_w, in contrast to that from a cylindrical condensed phase, where the flow is proper to each Kn_w over the whole flow field.

In an apparently common situation, where the density of the gas and thus molecular collisions become less and less indefinitely with flow, the cylindrical and spherical flows into a vacuum show decisive difference in their behavior, especially in their velocity distribution functions, in the far field. Their difference, explained as the difference of the local Knudsen number Kn_r, can be explained more plainly as follows. The density of the gas decreases to vanish proportionally to $1/r$ in the cylindrical flow, but to $1/r^2$ in the spherical flow. Correspondingly, the mean free path ℓ, calculated with the flow speed as the average molecular speed, increases proportionally to r in the former case, but to r^2 in the latter. The average number of collisions per molecule while it proceeds from r_0 to infinity is given by $\int_{r_0}^{\infty} \ell^{-1} \mathrm{d}r$.[27] Therefore, it is infinite in the cylindrical flow, but finite in the spherical flow. Roughly speaking, in the spherical

[26] In view of Footnote 24 in this subsection, the tendency to the free molecular flow in the far field is stronger for a hard-sphere gas.

[27] We are not tracing a particular particle, but are simply considering the sum of the local expected number of collisions in the distance dr.

flow, after some distance, which depends on Kn_w, away from the sphere, there is no collision along the flow; therefore the flow shows free molecular behavior in the far field. In the cylindrical flow, on the other hand, the collision effect depends on Kn_w.

6.5 Negative temperature gradient phenomenon

Pao [1971] pointed out a phenomenon called the negative or inverted temperature gradient phenomenon in a flow of a gas between two parallel plates made of its condensed phase with different temperatures, where evaporation and condensation are taking place (two-surface problem of evaporation and condensation). We will discuss this phenomenon in this section.

Consider a gas between its two parallel plane condensed phases at rest with different temperatures T_0 and T_1 ($T_1 > T_0$).[28] Let the condensed phase at temperature T_0 be placed at $X_1 = 0$ and the other with T_1 be at $X_1 = L$. We are interested in the time-independent behavior of the gas when the state of the gas is uniform with respect to X_2 and X_3. The complete-condensation condition (1.29) is taken as the boundary condition on the condensed phase.[29] The saturated gas pressure p_w in the complete-condensation condition is an increasing function of the temperature of the condensed phase. Their relation is determined by the Clausius–Clapeyron relation (Reif [1965], Landau & Lifshitz [1963]).

First we consider the case where the temperature difference of the condensed phases is small [$(T_1 - T_0)/T_0 \ll 1$] and discuss the problem on the basis of the linearized Boltzmann equation introduced in Section 1.11. We put $T_1 = T_0(1+\Delta\tau_w)$ and $p_w(T_1) = p_0(1+\Delta P_w)$ with $p_0 = p_w(T_0)$ and use the notation in Sections 1.10 and 1.11 with p_0 and T_0 defined above as the reference quantities.

The behavior when the Knudsen number is small is very simply obtained by making use of the asymptotic theory for the linearized Boltzmann equation in Section 3.1. The macroscopic variables are governed by the Stokes set of equations (3.12)–(3.13c). The boundary conditions, and the Knudsen-layer corrections, for the set are given by Eqs. (3.56a)–(3.56c) for the leading-order quantities. According to Eqs. (3.12) and (3.13a) with $m = 0$, $P_{G0} = \text{const}$ and $u_{1G0} = \text{const}$, because the quantities depend only on x_1 ($= X_1/L$). From the boundary condition (3.56c) on each condensed phase, these constants are determined as

$$P_{G0} = \Delta P_w/2, \qquad u_{1G0} = \Delta P_w/2C_4^*. \tag{6.53}$$

For a hard-sphere gas and the BKW model, the jump coefficient C_4^* is negative. Thus, u_{1G0} is negative, that is, evaporation takes place at $x_1 = 1$, and condensation at $x_1 = 0$. Corresponding to the condensation at $x_1 = 0$ and the evaporation at $x_1 = 1$, according to the slip condition (3.56c), there are a temperature jump

[28] The inequality is introduced without loss of generality for convenience of explanation.

[29] The extension of the solution to a more general boundary condition is explained in Section 6.6 (v). From the relation of the two solutions, the negative temperature gradient phenomenon is seen to take place also for the generalized boundary condition.

$\tau_{G0} = (d_4^*/2C_4^*)\Delta P_w$ at $x_1 = 0$ and a drop $\tau_{G0} - \Delta\tau_w = -(d_4^*/2C_4^*)\Delta P_w$ at $x_1 = 1$. With these conditions at the condensed phases, τ_{G0}, the solution of Eq. (3.13c) with $m = 0$, obviously varies linearly in x_1 from $(d_4^*/2C_4^*)\Delta P_w$ to $\Delta\tau_w - (d_4^*/2C_4^*)\Delta P_w$ as

$$\tau_{G0} = \frac{d_4^*}{2C_4^*}\Delta P_w + \left(\Delta\tau_w - \frac{d_4^*}{C_4^*}\Delta P_w\right) x_1. \tag{6.54}$$

If the condition $\Delta P_w/\Delta\tau_w > C_4^*/d_4^*$ (= 4.6992 for a hard-sphere gas, = 4.7723 for the BKW model) or

$$\frac{T_0}{p_w(T_0)}\left(\frac{p_w(T_1) - p_w(T_0)}{T_1 - T_0}\right) > \frac{C_4^*}{d_4^*}, \tag{6.55}$$

is fulfilled, which is so for many kinds of gases (see "Thermophysical Properties of Fluid Systems" at http://webbook.nist.gov), then τ_{G0} at $x_1 = 1$ is smaller than τ_{G0} at $x_1 = 0$, and therefore the temperature gradient in the gas is in the direction opposite to that imposed between the two condensed phases. This phenomenon, first pointed out by Pao [1971], is called *negative* (or *inverted*) *temperature gradient phenomenon*.[30]

This phenomenon is due to the temperature drop or jump in the Knudsen layer resulting from the evaporation from or the condensation onto the condensed phase. The jump condition (3.56c) is derived from the analysis of the linearized Boltzmann equation of a half-space problem of weak evaporation and condensation, where the condition at infinity is uniform.[31] Thus, the negative temperature gradient is the result of adjusting the overshooting in the Knudsen layer (kinetic region) by the fluid-dynamic region. The condition (6.55) of the negative temperature gradient is determined only by the relation between the jump coefficients in the half-space problem and the Clausius–Clapeyron relation. Thus, this phenomenon is not limited to the gas between two plates. It is also seen for other geometries (e.g., Sone & Onishi [1978]). In the region where the negative temperature gradient is seen, the heat flow is in the direction from $x_1 = 0$ to $x_1 = 1$ in the above example, but the energy flow, to which the mass flow also contributes, is in the direction from $x_1 = 1$ to $x_1 = 0$ (the natural direction).

When the Knudsen number is not small, the kinetic region extends over the channel and the flow field is determined by the direct interaction of the kinetic regions extending from each of the two boundaries. The solution of the linearized Boltzmann equation for a hard-sphere gas is studied numerically for the whole range of the Knudsen number (or k) in Sone, Ohwada & Aoki [1991]. Some of the profiles of the density $(p_0/RT_0)(1+\omega)$ and the temperature $T_0(1+\tau)$ of the

[30] Overlooking the important condition in the Clausius statement, some people think that the present result, where heat is transferred from the colder wall to the hotter, contradicts the second law of thermodynamics. Clausius states that heat can in no way and by no process be transported from a colder to a warmer body without leaving further changes, i.e., without compensation (see Planck [1945]). In the present case, mass is transported.

[31] Some discussion about the jump or drop is made in Sone & Onishi [1978] and Sone [2002].

gas are shown for the two typical cases, i.e., $\Delta P_w/\Delta\tau_w = 2$ and $\Delta P_w/\Delta\tau_w = 12$, in Fig. 6.37, where the latter case satisfies the condition (6.55). Obviously, for the free molecular gas, the state is uniform in the gas. In the present notation, the flow velocity is expressed as $(2RT_0)^{1/2}(u_1, 0, 0)$. Let $p_0(2RT_0)^{1/2}(Q_1, 0, 0)$ and $p_0(2RT_0)^{1/2}(H_1, 0, 0)$ be, respectively, the heat-flow vector and the energy-flow vector. The mass-flow vector is given by $(p_0/RT_0)(2RT_0)^{1/2}(u_1, 0, 0)$ and $H_1 = Q_1 + 5u_1/2$ in the linearized problem. The variations of u_1, Q_1, and H_1, which are independent of x_1 here, with k are shown in Fig. 6.38. The energy flow H_1 is from the hotter condensed phase to the colder one for $\Delta P_w/\Delta\tau_w = 2$ and 12. On the other hand, the heat flow Q_1 is in that direction for $\Delta P_w/\Delta\tau_w = 2$ but in the opposite direction for $\Delta P_w/\Delta\tau_w = 12$. The latter is the case where τ_{G0} in Eq. (6.54) has the negative temperature gradient. The energy flow H_1 for $\Delta P_w/\Delta\tau_w = 12$ takes the minimum value at an intermediate Knudsen number, as in the (nondimensional) mass-flow rate in the Poiseuille flow (Knudsen minimum; see Section 4.2.2).

Limiting ourselves to the leading-order result for small Knudsen numbers, we will discuss the behavior of the gas when the differences of temperature and saturated gas pressure between the two condensed phases are larger. When the differences $\Delta\tau_w$ and ΔP_w are still small but one of them is comparable to the Knudsen number, the behavior of the gas is easily obtained with the aid of the weakly nonlinear theory in Section 3.2. The basic equations governing the macroscopic variables are given by Eqs. (3.87)–(3.88c), and their boundary conditions and the Knudsen-layer corrections are given by Eqs. (3.119a)–(3.119c). The boundary conditions and the Knudsen-layer corrections are practically the same as Eqs. (3.56a)–(3.56c) in the linear theory. Equations (3.88b) and (3.88c) among the basic equations Eqs. (3.87)–(3.88c) are different from the corresponding equations, Eqs. (3.13b) and (3.13c) with $m = 0$, in the linear theory, and they have convection terms. As is obvious from the discussion in the linear theory, the temperature jump in the present case is the same as in the linear theory. It is determined before the temperature field is solved. That is, from Eqs. (3.87), (3.88a), and (3.119c),

$$P_{S1}k = \Delta P_w/2, \qquad u_{1S1}k = \Delta P_w/2C_4^*. \tag{6.56}$$

With this u_{1S1} in the condition on τ_{S1} in Eq. (3.119c), we find that there are a temperature jump $\tau_{S1}k = (d_4^*/2C_4^*)\Delta P_w$ at $x_1 = 0$ and a drop $\tau_{S1}k - \Delta\tau_w = -(d_4^*/2C_4^*)\Delta P_w$ at $x_1 = 1$. The temperature field τ_{S1} connecting the two boundary values is given by the solution of Eq. (3.88c), i.e.,

$$\tau_{S1}k = \frac{d_4^*}{2C_4^*}\Delta P_w + \left(\Delta\tau_w - \frac{d_4^*}{C_4^*}\Delta P_w\right)\frac{1 - \exp(\Delta P_w x_1/\gamma_2 C_4^* k)}{1 - \exp(\Delta P_w/\gamma_2 C_4^* k)}, \tag{6.57}$$

where x_1 in Eq. (6.54) is simply replaced by $[1 - \exp(\Delta P_w x_1/\gamma_2 C_4^* k)]/[1 - \exp(\Delta P_w/\gamma_2 C_4^* k)]$. The linear function is recovered if $\Delta P_w/k \ll 1$, which is the assumption for the linear theory. The condition of the negative temperature gradient is the same as Eq. (6.55) in the linear theory. The difference is that the linear profile, negative or positive gradient, of the temperature field is curved by

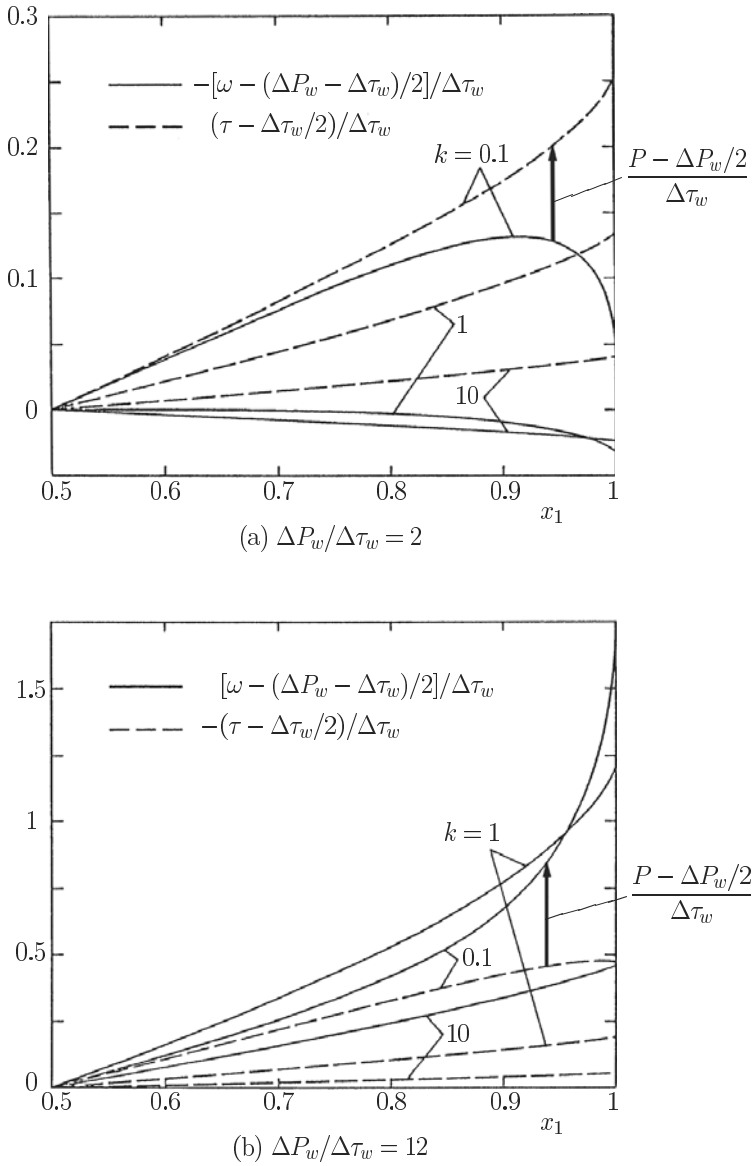

Figure 6.37. The distributions of the temperature τ and density ω in the gas for $k = 0.1$, 1, and 10 in the negative temperature gradient problem (a hard-sphere gas). (a) $\Delta P_w/\Delta\tau_w = 2$ and (b) $\Delta P_w/\Delta\tau_w = 12$. The profiles are antisymmetric with respect to $x_1 = 0.5$. Note the difference of the signs for the curves in panels (a) and (b).

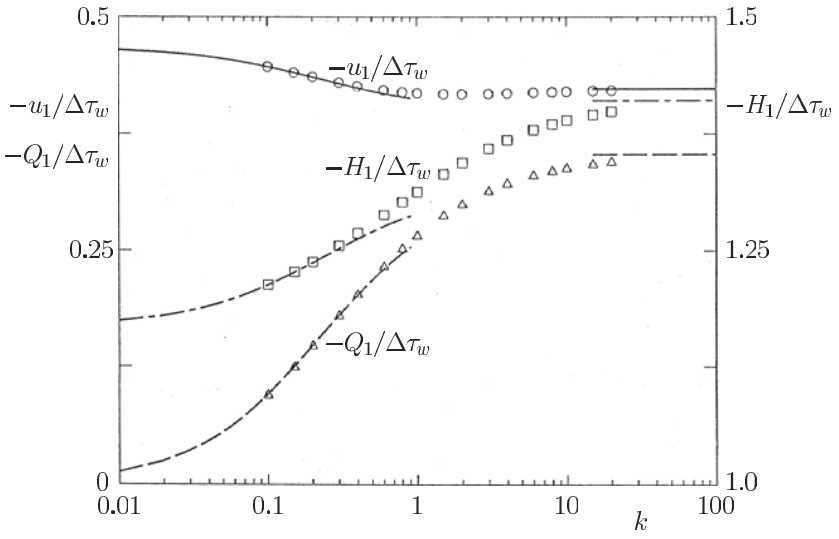

(a) $\Delta P_w/\Delta\tau_w = 2$

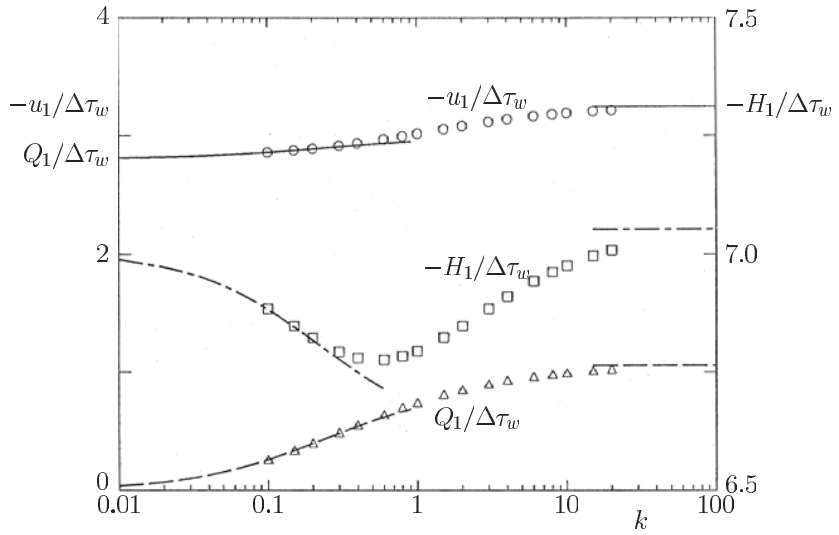

(b) $\Delta P_w/\Delta\tau_w = 12$

Figure 6.38. The variations of u_1, Q_1, and H_1 with k (a hard-sphere gas). (a) $\Delta P_w/\Delta\tau_w = 2$ and (b) $\Delta P_w/\Delta\tau_w = 12$. The symbols ◯, △, □ : the numerical results, the curves for small k : the analytical results by the asymptotic theory (Section 3.1), and the straight lines for large k : those for the free molecular flow (Chapter 2). Note the difference of the sign of Q_1 in panels (a) and (b).

the effect of convection of the flow. Thus, the negative temperature gradient is also seen in other geometries (e.g., Onishi & Sone [1983]). When $\Delta P_w \ll 1$ but $\Delta P_w/k \gg 1$, the weakly nonlinear theory is apparently inapplicable. However, the variation of the temperature field is limited in the range $x_1 = O(k/\Delta P_w)$ and it is practically uniform outside this range (or the variation is exponentially small). This means that the length scale of variation of τ_{S1} is $kL/\Delta P_w$, that is, the ratio of ΔP_w to the Knudsen number based on this length is of the order of unity, for which the weakly nonlinear theory is applicable. Thus, Eq. (6.57) is valid for any small ΔP_w and $\Delta\tau_w$ irrespective of their relative size to k.

When $\Delta P_w = O(1)$ and the Mach number of evaporating and condensing flow induced is of the order of unity, the behavior of the gas is described by the asymptotic theory in Section 3.5, where the macroscopic variables are governed by the Euler equations (3.225a)–(3.225c) and their boundary conditions are given by Eqs. (3.228a)–(3.229c). The solution of the one-dimensional Euler set of equations is piecewise uniform; the flow cannot be supersonic owing to the boundary conditions on the evaporating side. Thus, no shock wave exists in the flow field, and therefore the flow field is uniform. Owing to stronger convection, viscous effect is confined in a narrow region and merges into the Knudsen layer on the condensing side. Thus, the Knudsen layer, governed by the nonlinear Boltzmann equation, has some of the properties of the suction boundary layer[32] or the viscous boundary layer. As a result, the boundary condition, derived by the analysis of the Knudsen layer, is no longer symmetric on the condensing and evaporating sides. The boundary condition on the condensing side is weaker, that is, only one condition among the parameters, which is consistent with the Euler equations, where the differential order is lower than that of the Stokes equations or "the incompressible Navier–Stokes equations" in the previous cases. The boundary conditions being expressed with functions given only numerically, the solution of the problem requires some numerical computation, though the solution of the Euler equations is a simple uniform solution. The solution for the boundary conditions obtained by the BKW equation and the complete-condensation condition is given in Aoki & Sone [1991] (see also Sone [2002]).

For a while, there were some discussions about the negative temperature gradient phenomenon (Pao [1971], Matsushita [1976], Sone & Onishi [1978], Aoki & Cercignani [1983], Koffman, Plesset & Lees [1984], Ytrehus & Aukrust [1986], Hermans & Beenakker [1986], Mager, Adomeit & Wortberg [1989], Bedeaux, Hermans & Ytrehus [1990], Sone, Ohwada & Aoki [1991], Aoki & Masukawa [1994], Bobylev, Østomo & Ytrehus [1996], Ytrehus [1996]). However, the points are as described above, and the essence is due to Pao [1971].[33] For the system of the Boltzmann equation for a hard-sphere gas (or the BKW equation) and

[32] See Footnote 98 in Section 3.6.1.

[33] There is a work that tries to attribute the negative temperature gradient phenomenon to the nature of the solution of the Navier–Stokes equations under the assumption that the qualitative behavior of the whole field is described by these equations. Obviously from the above discussion, they assume the most important point that is to be investigated. The essence is the temperature drop (jump) in the kinetic region on an evaporating (condensing) boundary, whose mechanism is discussed in Sone & Onishi [1978] (see also Sone [2002]).

the complete-condensation condition, the range where the negative temperature gradient occurs is accurately obtained.[34] The experiment by Shankar & Deshpande [1990] indicates a temperature drop on the evaporating side and its jump on the condensing side.

Finally, it may be noted about the size of variables that we can perceive naturally. Flow speeds $1-10$ mm/s of a gas (e.g., air) can be perceived naturally, which correspond to Mach numbers $3\times10^{-6}-3\times10^{-5}$ at room temperature.[35] In the example of the negative temperature gradient phenomenon, the flow induced is of the same order as the nondimensional temperature difference $\Delta\tau_w$ between the two condensed phases. For the above size of the flow, the corresponding temperature difference is of the order of $10^{-3}-10^{-2}$ K. This difference (thus the negative temperature gradient) cannot be perceived naturally. This is not limited to the present problem. Let two (or more) physical variables be related by a physical law and let the variations of their nondimensional quantities be of the same order. The variations are not necessarily perceived equally. Some are perceived naturally but some are not. It is important to recognize this in the formulation of problems and understanding of results.

6.6 Generalized kinetic boundary condition

Up to now in this chapter, we have studied the problems under the complete-condensation boundary condition. The examples discussed are spatially one-dimensional, i.e., the velocity distribution function depends only on one space variable. In this case, we can extend the results to a more general boundary condition for time-independent problems. The condition we take here is the condition (1.67a) with $\alpha=1$, i.e.,

$$\hat{f}(x_i,\zeta_i)=\frac{\alpha_c\hat{\rho}_w+(1-\alpha_c)\hat{\sigma}_w}{(\pi\hat{T}_w)^{3/2}}\exp\left(-\frac{(\zeta_i-\hat{v}_{wi})^2}{\hat{T}_w}\right)\quad(\zeta_j n_j>0),\tag{6.58a}$$

$$\hat{\sigma}_w=-2\left(\frac{\pi}{\hat{T}_w}\right)^{1/2}\int_{\zeta_j n_j<0}\zeta_j n_j\hat{f}(x_i,\zeta_i)\mathbf{d}\boldsymbol{\zeta},\tag{6.58b}$$

where α_c $(0<\alpha_c\le1)$, called the condensation coefficient, is determined by the condition of the surface of the condensed phase, and $\hat{v}_{wi}n_i=0$ in the time-independent problems. In this boundary condition, the $1-\alpha_c$ part of the impinging molecules makes diffuse reflection. The complete-condensation condition is a special case of the above condition with $\alpha_c=1$, i.e.,

$$\hat{f}(x_i,\zeta_i)=\frac{\hat{\rho}_w}{(\pi\hat{T}_w)^{3/2}}\exp\left(-\frac{(\zeta_i-\hat{v}_{wi})^2}{\hat{T}_w}\right)\quad(\zeta_j n_j>0).\tag{6.59}$$

The difference between the two boundary conditions (6.58a) and (6.59) is the factors $\alpha_c\hat{\rho}_w+(1-\alpha_c)\hat{\sigma}_w$ and $\hat{\rho}_w$, which are constant when the condition on

[34] The effects of the molecular model and the kinetic boundary condition are condensed in the slip coefficients C_4^* and d_4^*.

[35] See Footnote 102 in Section 3.6.2.

the boundary is uniform. Owing to this simple difference, a solution under the generalized boundary condition is expressed with a solution under the complete-condensation condition. This process for the cases of evaporation from and condensation onto a plane condensed phase (the time-independent solution in Section 6.1) is explained in Sone [2002]. The extension for the cases in Sections 6.2–6.5 is similarly carried out. However, for the convenience of the reader, we will here explain the process of extension in a slightly different way.

The basic equation is the time-independent Boltzmann equation without external force, i.e.,

$$\zeta_i \frac{\partial \hat{f}}{\partial x_i} = \frac{1}{k} \hat{J}(\hat{f}, \hat{f}). \tag{6.60}$$

Let $\hat{f}_A$ be a solution of Eq. (6.60) with $k = k_A$ (or $\mathrm{Kn} = \mathrm{Kn}_A$).[36] Then $\hat{f}_B$ defined by

$$\hat{f}_B = \Gamma \hat{f}_A, \tag{6.61}$$

where Γ is a constant, is a solution of the Boltzmann equation with $k = k_B = \Gamma k_A$ (or $\mathrm{Kn} = \mathrm{Kn}_B = \Gamma \mathrm{Kn}_A$). Correspondingly, the extensive quantities $\hat{\rho}$, $\hat{p}$, $\hat{p}_{ij}$, and $\hat{q}_i$ are related as

$$(\hat{\rho}_B, \hat{p}_B, \hat{p}_{ijB}, \hat{q}_{iB}) = \Gamma(\hat{\rho}_A, \hat{p}_A, \hat{p}_{ijA}, \hat{q}_{iA}), \tag{6.62}$$

and the intensive quantities $\hat{v}_i$ and $\hat{T}$ remain unchanged, i.e.,

$$(\hat{v}_{iB}, \hat{T}_B) = (\hat{v}_{iA}, \hat{T}_A). \tag{6.63}$$

In the half-space problems in Section 6.1, where the Knudsen number does not enter the Boltzmann equation, the transformation ($\hat{f}_B = \Gamma \hat{f}_A$, $x_{iB} = x_i/\Gamma$) is convenient. Then, the set $(\hat{f}_B, x_{iB})$ satisfies the same form of the Boltzmann equation as $(\hat{f}_A, x_i)$, and the relations between the macroscopic variables are the same as Eqs. (6.62) and (6.63).

On the basis of these general relations and the fact that Eq. (6.58a) differs from Eq. (6.59) only by a factor independent of ζ_i, we will derive the relation between the solution under the complete-condensation condition (6.59) and the solution under the generalized condition (6.58a) with (6.58b).

Let $\hat{f}_{\mathsf{C}}$ be the solution for the complete-condensation condition. Put

$$\hat{f}_{\mathsf{G}} = \Gamma \hat{f}_{\mathsf{C}}, \qquad \mathrm{Kn}_{\mathsf{G}} = \Gamma \mathrm{Kn}_{\mathsf{C}} \quad (k_{\mathsf{G}} = \Gamma k_{\mathsf{C}}), \tag{6.64}$$

where Γ is defined with the data of one of the boundaries by the first line of the following expression:

$$\begin{aligned} \Gamma &= \frac{\alpha_c}{1 + \dfrac{2\sqrt{\pi}(1-\alpha_c)}{\hat{\rho}_w \hat{T}_w^{1/2}} \displaystyle\int_{\zeta_i n_i < 0} \zeta_i n_i \hat{f}_{\mathsf{C}}|_w \mathbf{d}\boldsymbol{\zeta}} \\ &= \frac{\alpha_c}{\alpha_c + 2\sqrt{\pi}(1-\alpha_c)\hat{m}_{f\mathsf{C}} \hat{\rho}_w^{-1} \hat{T}_w^{-1/2}}, \end{aligned} \tag{6.65}$$

[36] It should be noted that there is another parameter $U_0/k_B T_0$ in the problem (see Footnote 22 in Section 1.9 and more detailed discussion in Section A.2.4).

where the vertical bar $|_w$ with subscript w indicates that the quantities with it are evaluated on the boundary and

$$\hat{m}_f = \int \zeta_i n_i \hat{f}|_w \mathbf{d}\boldsymbol{\zeta}.$$

The last expression in Eq. (6.65) is derived with the aid of the complete-condensation condition (6.59) and the relation

$$\hat{m}_{f\mathsf{C}} = \int \zeta_i n_i \hat{f}_\mathsf{C}|_w \mathbf{d}\boldsymbol{\zeta} = \int_{\zeta_i n_i > 0} \zeta_i n_i \hat{f}_\mathsf{C}|_w \mathbf{d}\boldsymbol{\zeta} + \int_{\zeta_i n_i < 0} \zeta_i n_i \hat{f}_\mathsf{C}|_w \mathbf{d}\boldsymbol{\zeta}.$$

In time-independent problems with one space variable (one-dimensional, axially symmetric and uniform, or spherically symmetric case), Γ is a constant.

The function $\hat{f}_\mathsf{G}$ given by Eq. (6.64) is a solution of the Boltzmann equation (6.60) with $k = k_\mathsf{G}$ (or $\mathrm{Kn} = \mathrm{Kn}_\mathsf{G}$). On the boundary,

$$\hat{f}_\mathsf{G} = \Gamma \hat{f}_\mathsf{C} = \frac{\Gamma \hat{\rho}_w}{(\pi \hat{T}_w)^{3/2}} \exp\left(-\frac{(\zeta_i - \hat{v}_{wi})^2}{\hat{T}_w}\right) \quad (\zeta_i n_i > 0), \tag{6.66a}$$

$$\Gamma = \frac{\alpha_c}{1 + \dfrac{2\sqrt{\pi}(1-\alpha_c)}{\hat{\rho}_w \hat{T}_w^{1/2}} \displaystyle\int_{\zeta_i n_i < 0} \zeta_i n_i \hat{f}_\mathsf{C}|_w \mathbf{d}\boldsymbol{\zeta}}. \tag{6.66b}$$

From Eq. (6.66b) and the first relation of Eq. (6.64), we have another expression of Γ

$$\Gamma = \alpha_c - \frac{2\sqrt{\pi}(1-\alpha_c)}{\hat{\rho}_w \hat{T}_w^{1/2}} \int_{\zeta_i n_i < 0} \zeta_i n_i \hat{f}_\mathsf{G}|_w \mathbf{d}\boldsymbol{\zeta}.$$

With this Γ, Eq. (6.66a) is rewritten in the form

$$\hat{f}_\mathsf{G} = \frac{\alpha_c \hat{\rho}_w + (1-\alpha_c)\hat{\sigma}_w}{(\pi \hat{T}_w)^{3/2}} \exp\left(-\frac{(\zeta_i - \hat{v}_{wi})^2}{\hat{T}_w}\right) \quad (\zeta_i n_i > 0),$$

where

$$\hat{\sigma}_w = -2\left(\frac{\pi}{\hat{T}_w}\right)^{1/2} \int_{\zeta_i n_i < 0} \zeta_i n_i \hat{f}_\mathsf{G}|_w \mathbf{d}\boldsymbol{\zeta}.$$

The function $\hat{f}_\mathsf{G}$ satisfies the generalized boundary condition (6.58a) with (6.58b). That is, $\hat{f}_\mathsf{G}$ is the desired solution of the problem. The relations of the macroscopic variables between the two solutions are

$$(\hat{\rho}_\mathsf{G}, \hat{p}_\mathsf{G}, \hat{p}_{ij\mathsf{G}}, \hat{q}_{i\mathsf{G}}) = \Gamma(\hat{\rho}_\mathsf{C}, \hat{p}_\mathsf{C}, \hat{p}_{ij\mathsf{C}}, \hat{q}_{i\mathsf{C}}), \tag{6.67a}$$

$$(\hat{v}_{i\mathsf{G}}, \hat{T}_\mathsf{G}) = (\hat{v}_{i\mathsf{C}}, \hat{T}_\mathsf{C}). \tag{6.67b}$$

Reversely, let $\hat{f}_\mathsf{G}$ be a solution for the generalized boundary condition. Then, we will see in a similar way that $\hat{f}_\mathsf{C}$ given by

$$\hat{f}_\mathsf{C} = \Gamma_* \hat{f}_\mathsf{G}, \quad \mathrm{Kn}_\mathsf{C} = \Gamma_* \mathrm{Kn}_\mathsf{G}, \quad (k_\mathsf{C} = \Gamma_* k_\mathsf{G}),$$

where

$$\Gamma_* = \frac{1}{\alpha_c - \dfrac{2\sqrt{\pi}(1-\alpha_c)}{\hat{\rho}_w \hat{T}_w^{1/2}} \displaystyle\int_{\zeta_i n_i<0} \zeta_i n_i \hat{f}_{\mathsf{G}}|_w \mathbf{d}\boldsymbol{\zeta}} = \frac{\alpha_c}{\alpha_c - 2\sqrt{\pi}(1-\alpha_c)\hat{m}_{f\mathsf{G}}\hat{\rho}_w^{-1}\hat{T}_w^{-1/2}}$$

is the solution for the complete-condensation condition.

In the case of evaporation ($\hat{m}_{f\mathsf{C}} > 0$), Γ takes a positive finite value. In the case of condensation ($\hat{m}_{f\mathsf{C}} < 0$), Γ can be negative. The Γ_* always takes a positive finite value because $\int_{\zeta_i n_i<0} \zeta_i n_i \hat{f}_{\mathsf{G}}|_w \mathbf{d}\boldsymbol{\zeta} \le 0$. Therefore, in evaporating flows, there is one-to-one correspondence between the solutions for the complete-condensation condition and those for the generalized condition. On the other hand, in condensing flows, there is no solution for the generalized condition corresponding to a solution for the complete-condensation condition when α_c is small enough.

In the linearized problem, where only the linear terms of the perturbation around a uniform equilibrium state at rest are taken into account in the analysis, the relations are simplified in the following way. Let us use the perturbed quantities and linearized relations introduced in Sections 1.10 and 1.11. The linearized form of Γ defined by Eq. (6.65) is given by[37]

$$\Gamma = \frac{1}{1 + 2\sqrt{\pi}(1-\alpha_c)\alpha_c^{-1}\hat{m}_{f\mathsf{C}}\hat{\rho}_w^{-1}\hat{T}_w^{-1/2}} = 1 + \Delta\Gamma, \tag{6.68a}$$

$$\Delta\Gamma = -\frac{2\sqrt{\pi}(1-\alpha_c)\hat{m}_{f\mathsf{C}}}{\alpha_c}. \tag{6.68b}$$

The relations (6.64), (6.67a), and (6.67b) are reduced to

$$\phi_{\mathsf{G}} = \phi_{\mathsf{C}} + \Delta\Gamma, \qquad \mathrm{Kn}_{\mathsf{G}} = \mathrm{Kn}_{\mathsf{C}}, \tag{6.69a}$$

$$(\omega_{\mathsf{G}}, P_{\mathsf{G}}, P_{ij\mathsf{G}}, Q_{i\mathsf{G}}) = (\omega_{\mathsf{C}} + \Delta\Gamma, P_{\mathsf{C}} + \Delta\Gamma, P_{ij\mathsf{C}} + \Delta\Gamma\delta_{ij}, Q_{i\mathsf{C}}), \tag{6.69b}$$

$$(u_{i\mathsf{G}}, \tau_{\mathsf{G}}) = (u_{i\mathsf{C}}, \tau_{\mathsf{C}}). \tag{6.69c}$$

Here the results are summarized. In the cases (i), (ii), (iii), and (iv) of the following examples (i)–(v), the temperature T_w of the condensed phase and the corresponding saturated gas pressure p_w and density ρ_w (or $\rho_w = p_w/RT_w$) are taken as the reference quantities; thus, $\hat{T}_w = 1$, $\hat{p}_w = 1$, and $\hat{\rho}_w = 1$.

(i) Evaporation from or condensation onto a plane condensed phase

The two time-independent solutions evaporating from or condensing onto a plane condensed phase discussed in Section 6.1 are related as

$$(\hat{f}_{\mathsf{G}}, x_{1\mathsf{G}}) = (\Gamma \hat{f}_{\mathsf{C}}, x_1/\Gamma), \tag{6.70}$$

[37] The mass flux $\hat{m}_{f\mathsf{C}}$ is a small quantity and the leading term of $\hat{\rho}_w^{-1}\hat{T}_w^{-1/2}$ is unity.

$$(\hat{\rho}_{\mathsf{G}}, \hat{p}_{\mathsf{G}}, \hat{q}_{1\mathsf{G}}) = \Gamma(\hat{\rho}_{\mathsf{C}}, \hat{p}_{\mathsf{C}}, \hat{q}_{1\mathsf{C}}), \tag{6.71a}$$

$$(\hat{v}_{1\mathsf{G}}, \hat{T}_{\mathsf{G}}) = (\hat{v}_{1\mathsf{C}}, \hat{T}_{\mathsf{C}}), \tag{6.71b}$$

where

$$\begin{aligned}\Gamma &= \frac{\alpha_c}{1 + 2\sqrt{\pi}(1-\alpha_c)\displaystyle\int_{\zeta_1<0} \zeta_1 \hat{f}_{\mathsf{C}}|_{x_1=0} \mathbf{d}\boldsymbol{\zeta}} \\ &= \frac{\alpha_c}{\alpha_c + 2\sqrt{\pi}(1-\alpha_c)\hat{m}_{f\mathsf{C}}},\end{aligned} \tag{6.72}$$

with

$$\begin{aligned}\hat{m}_{f\mathsf{C}} &= \int_{\text{all } \boldsymbol{\zeta}} \zeta_1 \hat{f}_{\mathsf{C}}|_{x_1=0} \mathbf{d}\boldsymbol{\zeta} \\ &= \hat{\rho}_{\infty\mathsf{C}} \hat{v}_{1\infty\mathsf{C}},\end{aligned}$$

the last of which is the result of the conservation of mass flux, i.e., $\hat{\rho}\hat{v}_1 = \hat{\rho}_\infty \hat{v}_{1\infty}$. With the aid of Eqs. (6.70)–(6.71b), the expression of Γ in Eq. (6.72) is rewritten as

$$\begin{aligned}\Gamma &= \frac{1}{1 + \left(\dfrac{10\pi}{3}\right)^{1/2} \dfrac{(1-\alpha_c) M_{\infty\mathsf{C}} \hat{p}_{\infty\mathsf{C}}}{\alpha_c \hat{T}_{\infty\mathsf{C}}^{1/2}}} \\ &= \frac{1}{1 + \left(\dfrac{10\pi}{3}\right)^{1/2} \dfrac{(1-\alpha_c) M_{\infty\mathsf{G}} \hat{p}_{\infty\mathsf{G}}}{\alpha_c \Gamma \hat{T}_{\infty\mathsf{G}}^{1/2}}},\end{aligned} \tag{6.73}$$

which is used in the following discussion.

In view of the relation between the macroscopic variables of the two solutions, the condition (6.8) among the parameters M_∞, $\hat{p}_\infty$, and $\hat{T}_\infty$ under which the half-space problem of time-independent evaporating flows has a solution is transformed as

$$\hat{p}_{\infty\mathsf{G}} = \Gamma h_1(M_{\infty\mathsf{G}}), \quad \hat{T}_{\infty\mathsf{G}} = h_2(M_{\infty\mathsf{G}}) \quad (0 \le M_{\infty\mathsf{G}} \le 1). \tag{6.74}$$

From Eqs. (6.73) and (6.74), the factor Γ is expressed with $M_{\infty\mathsf{G}}$, i.e.,

$$\Gamma = \frac{1}{1 + \left(\dfrac{10\pi}{3}\right)^{1/2} \dfrac{(1-\alpha_c) M_{\infty\mathsf{G}} h_1(M_{\infty\mathsf{G}})}{\alpha_c h_2^{1/2}(M_{\infty\mathsf{G}})}}, \tag{6.75}$$

which is a positive finite value because $M_{\infty\mathsf{G}} \ge 0$. The curve $\hat{p}_{\infty\mathsf{G}}$ $(= \Gamma h_1)$ vs $M_{\infty\mathsf{G}}$ for the BKW equation is shown in Fig. 6.39.

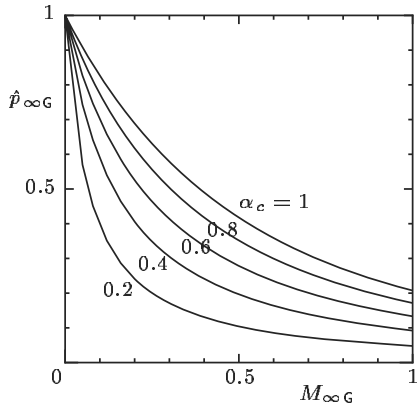

Figure 6.39. The curve $\hat{p}_{\infty \mathsf{G}} = \Gamma h_1(M_{\infty \mathsf{G}})$ for various α_c (the BKW equation).

With the aid of the relations (6.71a), (6.71b), and (6.73), the conditions (6.9a)–(6.9c) under which the half-space problem of time-independent condensing flows has a solution are transformed as[38]

$$\hat{p}_{\infty \mathsf{G}} = \Gamma F_s(M_{\infty \mathsf{G}}, 0, \hat{T}_{\infty \mathsf{G}}) \qquad (-1 < M_{\infty \mathsf{G}} < 0), \tag{6.76a}$$

$$\hat{p}_{\infty \mathsf{G}} > \Gamma_b F_b(M_{\infty \mathsf{G}}, 0, \hat{T}_{\infty \mathsf{G}}) \qquad (M_{\infty \mathsf{G}} < -1), \tag{6.76b}$$

$$\hat{p}_{\infty \mathsf{G}} \geq \Gamma_b F_b(-1_-, 0, \hat{T}_{\infty \mathsf{G}}) = \Gamma F_s(-1_+, 0, \hat{T}_{\infty \mathsf{G}}) \quad (M_{\infty \mathsf{G}} = -1). \tag{6.76c}$$

Here, Γ_b is Γ in Eq. (6.73) where $\hat{p}_{\infty \mathsf{C}}$ is replaced by its boundary value F_b; this process is legitimate because Γ increases continuously from Γ_b to infinity as $\hat{p}_{\infty \mathsf{C}}$ increases from F_b to $(3/10\pi)^{1/2}\alpha_c \hat{T}_{\infty \mathsf{C}}^{1/2}/(1-\alpha_c)(-M_{\infty \mathsf{C}})$.[39] The factor Γ or Γ_b is expressed with $M_{\infty \mathsf{G}}$ and $\hat{T}_{\infty \mathsf{G}}$ as

$$\Gamma = \frac{1}{1 + \left(\dfrac{10\pi}{3}\right)^{1/2} \dfrac{(1-\alpha_c) M_{\infty \mathsf{G}} F_s(M_{\infty \mathsf{G}}, 0, \hat{T}_{\infty \mathsf{G}})}{\alpha_c \hat{T}_{\infty \mathsf{G}}^{1/2}}} \qquad (-1 \leq M_{\infty \mathsf{G}} < 0), \tag{6.77a}$$

$$\Gamma_b = \frac{1}{1 + \left(\dfrac{10\pi}{3}\right)^{1/2} \dfrac{(1-\alpha_c) M_{\infty \mathsf{G}} F_b(M_{\infty \mathsf{G}}, 0, \hat{T}_{\infty \mathsf{G}})}{\alpha_c \hat{T}_{\infty \mathsf{G}}^{1/2}}} \qquad (M_{\infty \mathsf{G}} \leq -1). \tag{6.77b}$$

In the condensing flow, Γ or Γ_b can be negative for small α_c because $M_{\infty \mathsf{G}} < 0$. Then, there is no corresponding solution $\hat{f}_{\mathsf{G}}$ because $\hat{f}_{\mathsf{G}}$ must be non-negative.

[38] Here, we do not have to limit the second variable $\overline{M}_t$ in F_s and F_b, first introduced in Eqs. (3.229a)–(3.229c), to zero. Then, c_1 and c_2 to appear below depend also on $\overline{M}_t$.

[39] The solution $\hat{f}_{\mathsf{C}}$ for the parameters $M_{\infty \mathsf{C}} = M_{\infty \mathsf{G}}, \hat{T}_{\infty \mathsf{C}} = \hat{T}_{\infty \mathsf{G}}$, and $\hat{p}_{\infty \mathsf{C}}$ in the range $F_b(M_{\infty \mathsf{G}}, 0, \hat{T}_{\infty \mathsf{G}}) < \hat{p}_{\infty \mathsf{C}} < (3/10\pi)^{1/2}\alpha_c \hat{T}_{\infty \mathsf{G}}^{1/2}/(1-\alpha_c)(-M_{\infty \mathsf{G}})$ corresponds to the solution $\hat{f}_{\mathsf{G}}$ in the range $\Gamma_b F_b(M_{\infty \mathsf{G}}, 0, \hat{T}_{\infty \mathsf{G}}) < \hat{p}_{\infty \mathsf{G}} < \infty$.

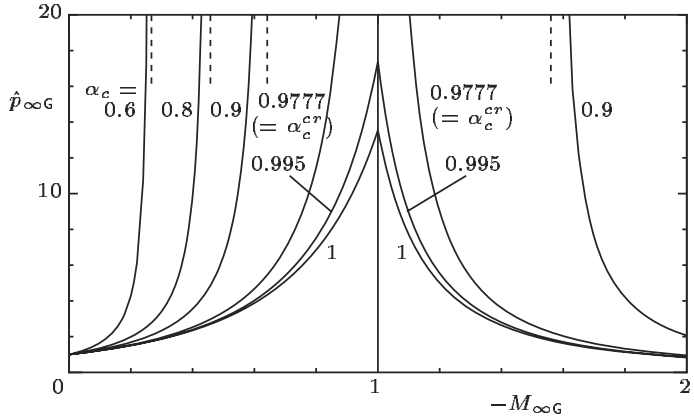

Figure 6.40. The section $\hat{p}_{\infty \mathsf{G}} = \Gamma F_s(M_{\infty \mathsf{G}}, 0, 1)$ $(-1 \le M_{\infty \mathsf{G}} < 0)$ of the solution surface and the section $\hat{p}_{\infty \mathsf{G}} = \Gamma_b F_b(M_{\infty \mathsf{G}}, 0, 1)$ $(M_{\infty \mathsf{G}} \le -1)$ of the boundary surface at $\hat{T}_{\infty \mathsf{G}} = 1$ (the BKW equation). The dashed lines are the asymptotes of the curves $\hat{p}_{\infty \mathsf{G}}$ vs $-M_{\infty \mathsf{G}}$. There is no solution between the two asymptotes when $\alpha_c \le \alpha_c^{cr} = 0.9777$ for which the two asymptotes degenerate into $M_{\infty \mathsf{G}} = -1$.

Therefore, the diagram shown in Fig. 6.12 remains qualitatively unchanged when the condensation coefficient α_c (≤ 1) is larger than some value $(\alpha_c > \alpha_c^{cr})$, but there appears a band region or regions $c_1 \le -M_{\infty \mathsf{G}} \le c_2$ where there is no solution when $\alpha_c \le \alpha_c^{cr}$. When $-M_{\infty \mathsf{G}} F_s$ is a decreasing function of $M_{\infty \mathsf{G}}$, $-M_{\infty \mathsf{G}} F_b$ is its increasing function,[40] and $F_s(-1_+, 0, \hat{T}_{\infty \mathsf{G}}) = F_b(-1_-, 0, \hat{T}_{\infty \mathsf{G}})$, as in the case of the BKW model, the band region is around $M_{\infty \mathsf{G}} = -1$ $(c_1 \le -M_{\infty \mathsf{G}} \le c_2;\ 0 < c_1 \le 1,\ c_2 \ge 1)$, where c_1 and c_2 depend on $\hat{T}_{\infty \mathsf{G}}$ as well as α_c. The section $\hat{p}_{\infty \mathsf{G}} = \Gamma F_s(M_{\infty \mathsf{G}}, 0, 1)$ $(-1 \le M_{\infty \mathsf{G}} < 0)$ of the solution surface and the section $\hat{p}_{\infty \mathsf{G}} = \Gamma_b F_b(M_{\infty \mathsf{G}}, 0, 1)$ $(M_{\infty \mathsf{G}} \le -1)$ of the boundary surface at $\hat{T}_{\infty \mathsf{G}} = 1$ are shown for the BKW equation in Fig. 6.40. This feature of the effect of incomplete condensation $(\alpha_c < 1)$ on the existence range of solution is similar to that of a noncondensable gas in a condensable gas (Sone, Aoki & Doi [1992]).

In the linearized problem, the flow velocities $u_{1\mathsf{G}}$ and $u_{1\mathsf{C}}$ are constants owing to the conservation of mass flux, i.e.,

$$\hat{m}_{f\mathsf{G}} = u_{1\mathsf{G}} = u_{1\infty \mathsf{G}} = u_{1\infty \mathsf{C}} = u_{1\mathsf{C}} = \hat{m}_{f\mathsf{C}}.$$

Correspondingly, from Eq. (6.68a) with (6.68b)

$$\Gamma = 1 - \frac{2\sqrt{\pi}(1 - \alpha_c) u_{1\infty \mathsf{C}}}{\alpha_c}.$$

According to Eq. (3.56c),

$$P_{\infty \mathsf{C}} = C^*_{4\mathsf{C}} u_{1\infty \mathsf{C}}, \qquad \tau_{\infty \mathsf{C}} = d^*_{4\mathsf{C}} u_{1\infty \mathsf{C}}.$$

[40] There are misprints in the corresponding statement on the fifth line of page 220 in Sone [2002]. The F_s and F_b there should be, respectively, replaced by $-M_n F_s$ and $-M_n F_b$.

Then, with the aid of Eqs. (6.69b) and (6.69c), the relations corresponding to those among $M_{\infty \mathsf{G}}$, $\hat{p}_{\infty \mathsf{G}}$, and $\hat{T}_{\infty \mathsf{G}}$ are, commonly for evaporation and condensation, given by

$$\left.\begin{aligned} &P_{\infty \mathsf{G}} = C^*_{4\mathsf{G}} u_{1\infty \mathsf{G}}, \qquad \tau_{\infty \mathsf{G}} = d^*_{4\mathsf{G}} u_{1\infty \mathsf{G}}, \\ &C^*_{4\mathsf{G}} = C^*_{4\mathsf{C}} - \frac{2\sqrt{\pi}(1-\alpha_c)}{\alpha_c}, \quad d^*_{4\mathsf{G}} = d^*_{4\mathsf{C}}. \end{aligned}\right\} \tag{6.78}$$

If $C^*_{4\mathsf{C}}$ is negative, $C^*_{4\mathsf{G}}$ is also negative because $0 < \alpha_c \leq 1$.

(ii) Evaporation from a cylindrical condensed phase into a vacuum

The two solutions for evaporating flows from a cylindrical condensed phase into a vacuum discussed in Section 6.2 are related as follows:

$$(\hat{f}_{\mathsf{G}}, g_{\mathsf{G}}, h_{\mathsf{G}}, \mathrm{Kn}_{w\mathsf{G}}) = \Gamma(\hat{f}_{\mathsf{C}}, g_{\mathsf{C}}, h_{\mathsf{C}}, \mathrm{Kn}_{w\mathsf{C}}), \tag{6.79}$$

$$(\hat{\rho}_{\mathsf{G}}, \hat{p}_{\mathsf{G}}, \hat{q}_{r\mathsf{G}}) = \Gamma(\hat{\rho}_{\mathsf{C}}, \hat{p}_{\mathsf{C}}, \hat{q}_{r\mathsf{C}}), \tag{6.80a}$$

$$(\hat{v}_{r\mathsf{G}}, \hat{T}_{\mathsf{G}}) = (\hat{v}_{r\mathsf{C}}, \hat{T}_{\mathsf{C}}), \tag{6.80b}$$

where

$$\begin{aligned} \Gamma &= \frac{\alpha_c}{1 + 2\sqrt{\pi}(1-\alpha_c)\displaystyle\int_{\zeta_r<0} \zeta_r \hat{f}_{\mathsf{C}}|_{\hat{r}=1} \mathbf{d}\boldsymbol{\zeta}} \\ &= \frac{\alpha_c}{\alpha_c + 2\sqrt{\pi}(1-\alpha_c)\hat{m}_{f\mathsf{C}}}, \end{aligned} \tag{6.81}$$

with

$$\hat{m}_{f\mathsf{C}} = \int_{\text{all } \boldsymbol{\zeta}} \zeta_r \hat{f}_{\mathsf{C}}|_{\hat{r}=1} \mathbf{d}\boldsymbol{\zeta}.$$

(iii) Evaporation from a cylindrical condensed phase into a gas

In the evaporating flows from a cylindrical condensed phase into a gas in Section 6.3, the same relations, Eqs. (6.79)–(6.81), as the flows into a vacuum hold for the two solutions. Corresponding to the relation (6.36) at infinity, we have

$$\hat{T}_{\infty \mathsf{G}} = \mathcal{T}(\hat{p}_{\infty \mathsf{G}}/\Gamma, \mathrm{Kn}_{w\mathsf{G}}/\Gamma).$$

(iv) Evaporation from a spherical condensed phase into a vacuum

The two solutions for evaporating flows from a spherical condensed phase into a vacuum discussed in Section 6.4 are related as follows:

$$(\hat{f}_{\mathsf{G}}, \mathrm{Kn}_{w\mathsf{G}}) = \Gamma(\hat{f}_{\mathsf{C}}, \mathrm{Kn}_{w\mathsf{C}}),$$

$$(\hat{\rho}_{\mathsf{G}}, \hat{p}_{\mathsf{G}}, \hat{q}_{r\mathsf{G}}) = \Gamma(\hat{\rho}_{\mathsf{C}}, \hat{p}_{\mathsf{C}}, \hat{q}_{r\mathsf{C}}),$$

$$(\hat{v}_{r\mathsf{G}}, \hat{T}_{\mathsf{G}}) = (\hat{v}_{r\mathsf{C}}, \hat{T}_{\mathsf{C}}),$$

where

$$\Gamma = \frac{\alpha_c}{1 + 2\sqrt{\pi}(1-\alpha_c)\displaystyle\int_{\zeta_r<0} \zeta_r \hat{f}_{\mathsf{C}}|_{\hat{r}=1}\mathbf{d}\boldsymbol{\zeta}} = \frac{\alpha_c}{\alpha_c + 2\sqrt{\pi}(1-\alpha_c)\hat{m}_{f\mathsf{C}}},$$

with

$$\hat{m}_{f\mathsf{C}} = \int_{\text{all } \boldsymbol{\zeta}} \zeta_r \hat{f}_{\mathsf{C}}|_{\hat{r}=1}\mathbf{d}\boldsymbol{\zeta}.$$

(v) Two-surface problem of evaporation and condensation

Consider a gas between its two parallel condensed phases discussed in Section 6.5 without limiting to the linearized Boltzmann equation, where the condensation coefficient α_c of the wall at $x_1 = 0$ is α_{c0}, and that at $x_1 = 1$ is α_{c1}. Let $p_1 = p_w(T_1)$, $\hat{p}_1 = p_1/p_0$, $\hat{T}_1 = T_1/T_0$, and $\hat{\rho}_1 = \hat{p}_1/\hat{T}_1$.[41]

Let the solution of the two-surface problem for the complete-condensation condition at $\mathrm{Kn} = \mathrm{Kn}_{\mathsf{C}}$ be $\hat{f}_{\mathsf{C}}$ with $\hat{p}_1 = \hat{p}_{1\mathsf{C}}$ and $\hat{T}_1 = \hat{T}_{1\mathsf{C}}$ ($\hat{\rho}_1 = \hat{\rho}_{1\mathsf{C}} = \hat{p}_{1\mathsf{C}}/\hat{T}_{1\mathsf{C}}$). Put

$$(\hat{f}_{\mathsf{G}}, \mathrm{Kn}_{\mathsf{G}}) = \Gamma(\hat{f}_{\mathsf{C}}, \mathrm{Kn}_{\mathsf{C}}), \tag{6.82}$$

where

$$\Gamma = \frac{\alpha_{c0}}{\alpha_{c0} + 2\sqrt{\pi}(1-\alpha_{c0})\hat{m}_{f\mathsf{C}}}, \tag{6.83}$$

with

$$\hat{m}_{f\mathsf{C}} = \int_{\text{all } \boldsymbol{\zeta}} \zeta_1 \hat{f}_{\mathsf{C}}|_{x_1=0}\mathbf{d}\boldsymbol{\zeta}.$$

Then, $\hat{f}_{\mathsf{G}}$ is the solution of the Boltzmann equation with $\mathrm{Kn} = \mathrm{Kn}_{\mathsf{G}} = \Gamma\mathrm{Kn}_{\mathsf{C}}$ that satisfies the generalized boundary condition on the wall at $x_1 = 0$. On the wall at $x_1 = 1$,

$$\hat{f}_{\mathsf{G}}|_{x_1=1} = \Gamma \hat{f}_{\mathsf{C}}|_{x_1=1} = \frac{\Gamma\hat{\rho}_{1\mathsf{C}}}{(\pi\hat{T}_{1\mathsf{C}})^{3/2}} \exp\left(-\frac{\zeta^2}{\hat{T}_{1\mathsf{C}}}\right) \quad (\zeta_1 < 0). \tag{6.84}$$

We will transform the expression $\Gamma\hat{\rho}_{1\mathsf{C}}$ as

$$\Gamma\hat{\rho}_{1\mathsf{C}} = \alpha_{c1}\Gamma\left[\hat{\rho}_{1\mathsf{C}} - \frac{2(1-\alpha_{c1})}{\alpha_{c1}}\left(\frac{\pi}{\hat{T}_{1\mathsf{C}}}\right)^{1/2}\hat{m}_{f\mathsf{C}}\right] + (1-\alpha_{c1})\Gamma\left[\hat{\rho}_{1\mathsf{C}} + 2\left(\frac{\pi}{\hat{T}_{1\mathsf{C}}}\right)^{1/2}\hat{m}_{f\mathsf{C}}\right]. \tag{6.85}$$

[41] (i) Here, $\hat{T}_1$ is not limited to $\hat{T}_1 > 1$, in contrast to the case in Section 6.5, where the restriction is only for convenience of explanation.

(ii) The above definition of $\hat{p}_1$ and $\hat{T}_1$ corresponds to choosing the values p_0 and T_0 on the wall at $x_1 = 0$ as the reference pressure and temperature. Thus, Kn is made with these quantities.

Here, we note the following relation obtained with the aid of the conservation of mass flux:

$$\begin{aligned}\hat{m}_{f\mathsf{C}} &= \int_{\text{all }\boldsymbol{\zeta}} \zeta_1 \hat{f}_{\mathsf{C}}|_{x_1=0}\mathbf{d}\boldsymbol{\zeta} = \int_{\text{all }\boldsymbol{\zeta}} \zeta_1 \hat{f}_{\mathsf{C}}|_{x_1=1}\mathbf{d}\boldsymbol{\zeta} \\ &= \int_{\zeta_1>0} \zeta_1 \hat{f}_{\mathsf{C}}|_{x_1=1}\mathbf{d}\boldsymbol{\zeta} + \int_{\zeta_1<0} \zeta_1 \hat{f}_{\mathsf{C}}|_{x_1=1}\mathbf{d}\boldsymbol{\zeta} \\ &= \frac{1}{\Gamma}\int_{\zeta_1>0} \zeta_1 \hat{f}_{\mathsf{G}}|_{x_1=1}\mathbf{d}\boldsymbol{\zeta} - \frac{\hat{\rho}_{1\mathsf{C}}\hat{T}_{1\mathsf{C}}^{1/2}}{2\sqrt{\pi}}.\end{aligned}$$

Using this relation in the second term of Eq. (6.85), we have

$$\begin{aligned}\Gamma\hat{\rho}_{1\mathsf{C}} = \alpha_{c1}\Gamma &\left(\hat{\rho}_{1\mathsf{C}} - \frac{2\sqrt{\pi}(1-\alpha_{c1})}{\alpha_{c1}\hat{T}_{1\mathsf{C}}^{1/2}}\hat{m}_{f\mathsf{C}}\right) \\ &- 2(1-\alpha_{c1})\left(\frac{\pi}{\hat{T}_{1\mathsf{C}}}\right)^{1/2}\int_{\zeta_1>0}(-\zeta_1)\hat{f}_{\mathsf{G}}|_{x_1=1}\mathbf{d}\boldsymbol{\zeta}. \qquad (6.86)\end{aligned}$$

Then, the boundary value of $\hat{f}_{\mathsf{G}}$ at $x_1 = 1$ for the molecules leaving there is expressed as

$$\hat{f}_{\mathsf{G}}|_{x_1=1} = \frac{\alpha_{c1}\hat{\rho}_1^* + (1-\alpha_{c1})\hat{\sigma}_1}{(\pi\hat{T}_{1\mathsf{C}})^{3/2}}\exp\left(-\frac{\zeta^2}{\hat{T}_{1\mathsf{C}}}\right) \quad (\zeta_1 < 0), \qquad (6.87)$$

where

$$\hat{\rho}_1^* = \Gamma\left(\hat{\rho}_{1\mathsf{C}} - \frac{2\sqrt{\pi}(1-\alpha_{c1})}{\alpha_{c1}\hat{T}_{1\mathsf{C}}^{1/2}}\hat{m}_{f\mathsf{C}}\right), \qquad (6.88a)$$

$$\hat{\sigma}_1 = -2\left(\frac{\pi}{\hat{T}_{1\mathsf{C}}}\right)^{1/2}\int_{\zeta_1>0}(-\zeta_1)\hat{f}_{\mathsf{G}}|_{x_1=1}\mathbf{d}\boldsymbol{\zeta}. \qquad (6.88b)$$

Equations (6.87)–(6.88b) show that $\hat{f}_{\mathsf{G}}$ satisfies the generalized boundary condition at $x_1 = 1$ if $\hat{p}_{1\mathsf{G}}$ and $\hat{T}_{1\mathsf{G}}$ are given by

$$\hat{p}_{1\mathsf{G}} = \Gamma\left(\hat{p}_{1\mathsf{C}} - \frac{2\sqrt{\pi}(1-\alpha_{c1})}{\alpha_{c1}}\hat{m}_{f\mathsf{C}}\hat{T}_{1\mathsf{C}}^{1/2}\right), \qquad (6.89)$$

$$\hat{T}_{1\mathsf{G}} = \hat{T}_{1\mathsf{C}}. \qquad (6.90)$$

That is, $\hat{f}_{\mathsf{G}} = \Gamma\hat{f}_{\mathsf{C}}$ is the solution of the two-surface problem at $\mathrm{Kn}_{\mathsf{G}} = \Gamma\mathrm{Kn}_{\mathsf{C}}$ under the generalized boundary condition (6.58a) with (6.58b) when $\hat{p}_{1\mathsf{G}}$ and $\hat{T}_{1\mathsf{G}}$ are given, respectively, by Eqs. (6.89) and (6.90).

The solution thus obtained loses its meaning when $\hat{f}_{\mathsf{G}} < 0$. In the above problem, we can assume $\hat{m}_{f\mathsf{C}} \geq 0$ without loss of generality. Then, from Eq. (6.83), $\Gamma > 0$. Thus, the condition to be satisfied is the positivity of $\hat{p}_{1\mathsf{G}}$, i.e.,

$$\alpha_{c1} > \frac{2\sqrt{\pi}\hat{m}_{f\mathsf{C}}\hat{T}_{1\mathsf{C}}^{1/2}}{\hat{p}_{1\mathsf{C}} + 2\sqrt{\pi}\hat{m}_{f\mathsf{C}}\hat{T}_{1\mathsf{C}}^{1/2}}.$$

In the linearized problem, the relation

$$\hat{m}_{f\mathsf{G}} = u_{1\mathsf{G}} = u_{1\mathsf{C}} = \hat{m}_{f\mathsf{C}}$$

holds in addition to Eqs. (6.69a)–(6.69c), and the relations (6.89) and (6.90) are reduced to

$$\Delta P_{w\mathsf{G}} = \Delta P_{w\mathsf{C}} - 2\sqrt{\pi}\left(\frac{1}{\alpha_{c1}} + \frac{1}{\alpha_{c0}} - 2\right)\hat{m}_{f\mathsf{C}},$$
$$\Delta \tau_{w\mathsf{G}} = \Delta \tau_{w\mathsf{C}},$$

where

$$\Delta P_w = (p_1 - p_0)/p_0, \quad \Delta \tau_w = (T_1 - T_0)/T_0.$$

They correspond to ΔP_w and $\Delta \tau_w$ in Section 6.5.

Chapter 7

Bifurcation in the Half-Space Problem of Evaporation and Condensation

In Section 3.5, we discussed the asymptotic behavior for small Knudsen numbers of a gas around a condensed phase of the gas where evaporation or condensation with a finite Mach number is taking place. In the continuum limit, the overall behavior of the gas is described by the Euler set of equations, and its boundary condition is derived from the analysis of the half-space problem of the Boltzmann equation. The boundary condition is qualitatively different depending on whether evaporation, subsonic condensation, or supersonic condensation is taking place. Here, we will discuss the transition from one type of the boundary condition to another, which takes place from evaporation to subsonic condensation and from subsonic condensation to supersonic condensation, on the basis of Sone [1978b, 2000b].

7.1 Problem

Consider a semi-infinite expanse ($X_1 > 0$) of a gas in a time-independent state, bounded by its plane condensed phase at $X_1 = 0$. The plane condensed phase is at rest and is kept at a uniform temperature T_w. The saturated gas pressure at this temperature (or T_w) is p_w. The state of the gas is uniform with respect to X_2 and X_3 coordinates and approaches a uniform state with pressure p_∞, temperature T_∞, and velocity $v_{i\infty}$ as $X_1 \to \infty$. We use the nondimensional variables introduced in Sections 1.9 and 1.10 with p_w and T_w as the reference pressure p_0 and the reference temperature T_0 respectively. The problem contains

no geometrical reference length. Thus, the nondimensional space coordinate η

$$\eta = 2X_1/\sqrt{\pi}\ell_w, \tag{7.1}$$

is used here, where ℓ_w is the mean free path of the gas in the equilibrium state at rest with pressure p_w and temperature T_w. Then, the basic equation is given as

$$\zeta_1 \frac{\partial \hat{f}}{\partial \eta} = \hat{J}(\hat{f}, \hat{f}), \tag{7.2}$$

and the boundary condition for $\hat{f}$ is

$$\hat{f} = \hat{f}_w \qquad (\zeta_1 > 0) \quad \text{at } \eta = 0, \tag{7.3a}$$

$$\hat{f} \to \frac{\hat{p}_\infty}{\pi^{3/2}\hat{T}_\infty^{5/2}} \exp\left(-\frac{(\zeta_i - \hat{v}_{i\infty})^2}{\hat{T}_\infty}\right) \quad \text{as } \eta \to \infty, \tag{7.3b}$$

where $\hat{f}_w$ is given by the corresponding nondimensional form of Eq. (1.30). The typical example of $\hat{f}_w$ is the complete-condensation condition (1.29), i.e.,

$$\hat{f}_w = E(\zeta) = \frac{1}{\pi^{3/2}} \exp\left(-{\zeta_i}^2\right). \tag{7.4}$$

The problem contains the five parameters $\hat{p}_\infty$ $(= p_\infty/p_w)$, $\hat{T}_\infty$ $(= T_\infty/T_w)$, and $\hat{v}_{i\infty}$ $[= v_{i\infty}/(2RT_w)^{1/2}]$. The Mach number M_∞ with sign

$$M_\infty = \frac{v_{1\infty}}{\sqrt{5RT_\infty/3}}$$

of the normal flow velocity $v_{1\infty}$ is also used instead of $\hat{v}_{1\infty}$.

First, in Section 7.2, we consider the problem for weak evaporation or condensation and construct the solution by introducing a slowly varying solution, for which nonlinear effect is of primary importance. The slowly varying solution is found to be a source of the different features of the solutions of evaporation and condensation. Then, in Section 7.3, where the restriction of weak flow is eliminated, slowly varying solutions are found around the sonic condition, and the structure of the transition from the solution of subsonic condensation to that of supersonic one is clarified with the aid of the slowly varying solutions.

7.2 Transition from evaporation to condensation

7.2.1 Basic equation and boundary condition

In this section, we discuss the case of weak evaporation and condensation, that is, $(p_\infty - p_w)/p_w$, $(T_\infty - T_w)/T_w$, and $v_{i\infty}/\sqrt{2RT_w}$, denoted by P_∞, τ_∞, and $u_{i\infty}$ respectively, are small quantities of the same order, say, of the order of ε. In this case it is convenient for the analysis to rewrite the equation (7.2) and the boundary conditions (7.3a) and (7.3b) in the notation defined in Section 1.10,

where the perturbed velocity distribution function ϕ ($= \hat{f}/E - 1$) is introduced. That is, the equation is

$$\zeta_1 \frac{\partial \phi}{\partial \eta} = \mathcal{L}(\phi) + \mathcal{J}(\phi, \phi), \tag{7.5}$$

where $\phi = \hat{f}/E - 1$, and the boundary condition is

$$\phi = \phi_w \quad (\zeta_1 > 0) \quad \text{at } \eta = 0, \tag{7.6a}$$
$$\phi \to \phi_{e\infty} \quad \text{as } \eta \to \infty, \tag{7.6b}$$

where $\phi_w = \hat{f}_w/E - 1$, especially for the complete-condensation condition,

$$\phi_w = 0, \tag{7.7}$$

and $\phi_{e\infty}$ is the perturbed velocity distribution function for the Maxwellian at infinity, i.e.,

$$E(\zeta)(1 + \phi_{e\infty}) = \frac{1 + P_\infty}{\pi^{3/2}(1 + \tau_\infty)^{5/2}} \exp\left(-\frac{(\zeta_i - u_{i\infty})^2}{1 + \tau_\infty}\right). \tag{7.8}$$

The small parameters P_∞, τ_∞, and $u_{i\infty}$ at infinity are expanded in ε, i.e.,

$$P_\infty = P_{\infty 1}\varepsilon + P_{\infty 2}\varepsilon^2 + \cdots, \tag{7.9a}$$
$$\tau_\infty = \tau_{\infty 1}\varepsilon + \tau_{\infty 2}\varepsilon^2 + \cdots, \tag{7.9b}$$
$$u_{i\infty} = u_{i\infty 1}\varepsilon + u_{i\infty 2}\varepsilon^2 + \cdots. \tag{7.9c}$$

Then,

$$\phi_{e\infty} = \phi_{e\infty 1}\varepsilon + \cdots, \tag{7.10}$$

where

$$\phi_{e\infty 1} = P_{\infty 1} + 2\zeta_i u_{i\infty 1} + \left(\zeta_i^2 - \frac{5}{2}\right)\tau_{\infty 1}. \tag{7.11}$$

7.2.2 Slowly varying solution

The nonlinear terms with respect to ϕ, as well as $(p_\infty - p_w)/p_w$, $(T_\infty - T_w)/T_w$, and $v_{i\infty}/\sqrt{2RT_w}$, in the above system, i.e., Eqs. (7.5)–(7.6b), being neglected formally under the assumption that they are small, the problem is reduced to the half-space problem of the linearized Boltzmann equation. Then, according to the Grad–Bardos theorem [see the paragraph containing Eq. (3.39) in Section 3.1.4], there exists a unique solution only when τ_∞/P_∞ and $u_{i\infty}/P_\infty$ take special values. When there is a solution that varies very slowly, i.e., with the length scale of variation of $1/\varepsilon$, the differential term $\zeta_1 \partial\phi/\partial\eta$ of Eq. (7.5) is of the order of ϕ^2 because $\partial\phi/\partial\eta = O(\varepsilon\phi)$, and the linear collision term $\mathcal{L}(\phi)$ is the only term of the order of ε and thus should vanish. Therefore, ϕ is the linearized version of a Maxwellian. The spatial variation of ϕ is determined by the terms

of the order of ϕ^2. Therefore, we can expect a solution with a quite different character from the solution of the linearized problem for the half-space problem. Thus we try to examine the existence of the slowly varying solution.

For the convenience of the analysis of the slowly varying solution, we introduce the shrunk variable x_1

$$x_1 = \varepsilon\eta. \tag{7.12}$$

Then, the condition of the slowly varying solution corresponds to

$$\frac{\partial\phi_{\rm s}}{\partial x_1} = O(\phi_{\rm s}), \tag{7.13}$$

where the lowercase roman subscript s indicates the slowly varying solution. With the new variable x_1, Eq. (7.5) is rewritten as

$$\zeta_1\frac{\partial\phi_{\rm s}}{\partial x_1} = \frac{1}{\varepsilon}[\mathcal{L}(\phi_{\rm s}) + \mathcal{J}(\phi_{\rm s},\phi_{\rm s})]. \tag{7.14}$$

The slowly varying solution $\phi_{\rm s}$ of Eq. (7.14), satisfying the condition (7.13), for small ε is practically the same as the one-dimensional version of the S solution discussed in Section 3.2.2. Thus, we can borrow the result with transcription of the notation. The solution is obtained in a power series of ε, i.e.,

$$\phi_{\rm s} = \phi_{\rm s1}\varepsilon + \phi_{\rm s2}\varepsilon^2 + \cdots. \tag{7.15}$$

Corresponding to the expansion of $\phi_{\rm s}$, the nondimensional perturbed macroscopic variables ω, u_i, τ, P, etc. are also expanded, i.e.,

$$h_{\rm s} = h_{\rm s1}\varepsilon + h_{\rm s2}\varepsilon^2 + \cdots, \tag{7.16}$$

where h represents ω, u_i, τ, P, etc. The relations between these macroscopic variables and the velocity distribution function are, for example,

$$\omega_{\rm s1} = \int \phi_{\rm s1}E\mathbf{d}\boldsymbol{\zeta}, \tag{7.17a}$$

$$u_{i{\rm s}1} = \int \zeta_i\phi_{\rm s1}E\mathbf{d}\boldsymbol{\zeta}, \tag{7.17b}$$

$$\frac{3}{2}\tau_{\rm s1} = \int\left(\zeta_i^2 - \frac{3}{2}\right)\phi_{\rm s1}E\mathbf{d}\boldsymbol{\zeta}, \tag{7.17c}$$

$$P_{\rm s1} = \omega_{\rm s1} + \tau_{\rm s1}. \tag{7.17d}$$

According to the results in Section 3.2.2, the component function $\phi_{\rm s1}$ of the velocity distribution function is given as

$$\phi_{\rm s1} = P_{\rm s1} + 2\zeta_i u_{i{\rm s}1} + \left(\zeta_i^2 - \frac{5}{2}\right)\tau_{\rm s1}, \tag{7.18}$$

and the functions $P_{\rm s1}$, $u_{i{\rm s}1}$, and $\tau_{\rm s1}$ in $\phi_{\rm s1}$ are determined by the following equations [see Eqs. (3.87)–(3.88c)]:

$$\frac{{\rm d}P_{\rm s1}}{{\rm d}x_1} = 0, \tag{7.19}$$

$$\frac{\mathrm{d}u_{1\mathrm{s}1}}{\mathrm{d}x_1} = 0, \tag{7.20a}$$

$$u_{1\mathrm{s}1}\frac{\mathrm{d}u_{i\mathrm{s}1}}{\mathrm{d}x_1} = -\frac{1}{2}\frac{\mathrm{d}P_{\mathrm{s}2}}{\mathrm{d}x_1}\delta_{i1} + \frac{1}{2}\gamma_1\frac{\mathrm{d}^2u_{i\mathrm{s}1}}{\mathrm{d}x_1^2}, \tag{7.20b}$$

$$u_{1\mathrm{s}1}\frac{\mathrm{d}\tau_{\mathrm{s}1}}{\mathrm{d}x_1} = \frac{1}{2}\gamma_2\frac{\mathrm{d}^2\tau_{\mathrm{s}1}}{\mathrm{d}x_1^2}. \tag{7.20c}$$

The solution of equations (7.19)–(7.20c) satisfying the expanded form (7.9a)–(7.9c) of the condition at infinity is given as follows:[1]

$$P_{\mathrm{s}1} = P_{\infty 1}, \tag{7.21a}$$

$$u_{1\mathrm{s}1} = u_{1\infty 1}, \tag{7.21b}$$

and when $u_{1\infty 1} \geq 0$

$$u_{i\mathrm{s}1} = u_{i\infty 1} \quad (i = 2 \text{ and } 3), \tag{7.22a}$$

$$\tau_{\mathrm{s}1} = \tau_{\infty 1}, \tag{7.22b}$$

and when $u_{1\infty 1} < 0$

$$u_{i\mathrm{s}1} = u_{i\infty 1} - c_i \exp\left(\frac{2u_{1\infty 1}}{\gamma_1}x_1\right) \quad (i = 2 \text{ and } 3), \tag{7.23a}$$

$$\tau_{\mathrm{s}1} = \tau_{\infty 1} - c_4 \exp\left(\frac{2u_{1\infty 1}}{\gamma_2}x_1\right), \tag{7.23b}$$

where c_i and c_4 are undetermined constants. In addition, we have $P_{\mathrm{s}2} = P_{\infty 2}$, which will be used in the higher-order analysis. When evaporation ($u_{1\infty 1} \geq 0$) is taking place, only a uniform solution is possible. On the other hand, when condensation ($u_{1\infty 1} < 0$) is taking place, there is a slowly varying solution with a structure and the solution has extra freedom.

7.2.3 Knudsen-layer correction

We will construct the solution of the half-space problem on the basis of the slowly varying solution obtained in Section 7.2.2. The slowly varying solution (7.18) cannot be made to satisfy the boundary condition (7.6a) on the condensed phase if evaporation or condensation is taking place, i.e., $u_{1\infty 1} \neq 0$.[2] The solution satisfying the condition on the condensed phase can be obtained by introducing a correction (Knudsen-layer correction) to the slowly varying solution in a neighborhood of the condensed phase. This is simply a transcription of the analysis in Section 3.2.3. That is, we put

$$\phi = \phi_{\mathrm{s}} + \phi_K,$$

[1] In the spatially one-dimensional problem, $u_{1\mathrm{s}1}$ is determined by Eq. (7.20a). Equation (7.20b) with $i = 1$ works only to determine $P_{\mathrm{s}2}$ in contrast to the two or three dimensional problem.

[2] Consider the condition (7.7) for simplicity.

where ϕ_K has the length scale of variation of the order of the mean free path, i.e., $\partial\phi_K/\partial\eta = O(\phi_K)$, and it is expanded as

$$\phi_K = \phi_{K1}\varepsilon + \cdots .$$

Corresponding to the expansion of ϕ_K, the Knudsen-layer correction h_K of a nondimensional perturbed macroscopic variable h, i.e., $h_K = h - h_{\rm s}$, where h represents ω, u_i, τ, P, etc. is also expanded, i.e.,

$$h_K = h_{K1}\varepsilon + h_{K2}\varepsilon^2 + \cdots .$$

The equation for ϕ_{K1} is given by

$$\zeta_1 \frac{\partial \phi_{K1}}{\partial \eta} = \mathcal{L}(\phi_{K1}), \tag{7.24}$$

and the boundary condition for ϕ_{K1} is

$$\begin{aligned}\phi_{K1} &= -\phi_{\rm s1} + \phi_w \\ &= -P_{\rm s1} - 2\zeta_2 u_{2{\rm s}1} - 2\zeta_3 u_{3{\rm s}1} - \left(\zeta_i^2 - \frac{5}{2}\right)\tau_{\rm s1} - 2\zeta_1 u_{1{\rm s}1} + \phi_w \\ &\qquad\qquad (\zeta_1 > 0) \quad \text{at } \eta = 0, \end{aligned} \tag{7.25a}$$

$$\phi_{K1} \to 0 \qquad \text{as } \eta \to \infty. \tag{7.25b}$$

According to the Grad–Bardos theorem, the solution ϕ_{K1} exists when and only when the boundary values of $P_{\rm s1}$, $u_{i{\rm s}1}$, and $\tau_{\rm s1}$ satisfy the relations

$$P_{\rm s1} = C_4^* u_{1{\rm s}1}, \quad \tau_{\rm s1} = d_4^* u_{1{\rm s}1}, \quad u_{2{\rm s}1} = 0, \quad u_{3{\rm s}1} = 0 \quad \text{at } x_1 = 0, \tag{7.26}$$

and the macroscopic variables of the Knudsen-layer correction are given by

$$u_{iK1} = 0, \quad \omega_{K1} = \Omega_4^*(\eta), \quad \tau_{K1} = \Theta_4^*(\eta),$$

where the slip coefficients C_4^* and d_4^* and the Knudsen-layer functions $\Omega_4^*(\eta)$ and $\Theta_4^*(\eta)$, determined by the molecular model and kinetic boundary condition, are the same as those in Sections 3.1.5 and 3.2.3. The relation (7.26) serves as the boundary conditions for Eqs. (7.19)–(7.20c).

7.2.4 Solution

When $u_{1\infty 1} \geq 0$, from Eqs. (7.21a)–(7.22b) and Eq. (7.26), the solution exists only when the state at infinity satisfies the conditions

$$u_{1\infty 1} = \frac{1}{C_4^*} P_{\infty 1}, \quad u_{2\infty 1} = u_{3\infty 1} = 0, \quad \tau_{\infty 1} = \frac{d_4^*}{C_4^*} P_{\infty 1},$$

and the solution is given by

$$u_{1{\rm s}1} = \frac{1}{C_4^*} P_{\infty 1}, \quad u_{2{\rm s}1} = 0, \quad u_{3{\rm s}1} = 0, \quad \tau_{\rm s1} = \frac{d_4^*}{C_4^*} P_{\infty 1}.$$

When $u_{1\infty 1} < 0$, from Eqs. (7.21a), (7.21b), (7.23a), (7.23b), and (7.26), the solution exists only when the state at infinity satisfies the condition

$$u_{1\infty 1} = \frac{1}{C_4^*} P_{\infty 1},$$

and the solution is given by

$$u_{1\mathrm{s}1} = \frac{1}{C_4^*} P_{\infty 1}, \quad u_{i\mathrm{s}1} = u_{i\infty 1} \left[1 - \exp\left(\frac{2u_{1\infty 1}}{\gamma_1} x_1 \right) \right] \quad (i = 2 \text{ and } 3),$$
$$\tau_{\mathrm{s}1} = \tau_{\infty 1} + \left(\frac{d_4^*}{C_4^*} P_{\infty 1} - \tau_{\infty 1} \right) \exp\left(\frac{2u_{1\infty 1}}{\gamma_2} x_1 \right).$$

The choice of the small parameter ε is not unique and can be chosen freely if it is of the order of P_∞. The ambiguity is compensated by the values of $P_{\infty 1}$, $\tau_{\infty 1}$, and $u_{i\infty 1}$. In fact, the solution in the original variables P_s, τ_s, and $u_{i\mathrm{s}}$ is expressed, with the error of $O(\varepsilon^2)$ neglected, as follows: Commonly for $P_\infty/(-C_4^*) \le 0$ and $P_\infty/(-C_4^*) > 0$, the condition at infinity should satisfy the condition

$$u_{1\infty} = \frac{1}{C_4^*} P_\infty, \tag{7.27}$$

and the variables P_s and $u_{1\mathrm{s}}$ are given by

$$P_\mathrm{s} = P_\infty, \quad u_{1\mathrm{s}} = \frac{1}{C_4^*} P_\infty. \tag{7.28}$$

When $P_\infty/(-C_4^*) \le 0$, the additional conditions

$$\tau_\infty = \frac{d_4^*}{C_4^*} P_\infty, \quad u_{2\infty} = u_{3\infty} = 0 \tag{7.29}$$

are required for the solution to exist, and the variables τ_s, $u_{2\mathrm{s}}$, and $u_{3\mathrm{s}}$ are given by

$$\tau_\mathrm{s} = \frac{d_4^*}{C_4^*} P_\mathrm{s}, \quad u_{2\mathrm{s}} = u_{3\mathrm{s}} = 0. \tag{7.30}$$

When $P_\infty/(-C_4^*) > 0$, the variables τ_s, $u_{2\mathrm{s}}$, and $u_{3\mathrm{s}}$ are given by

$$\left.\begin{aligned} \tau_\mathrm{s} &= \tau_\infty + \left(\frac{d_4^*}{C_4^*} P_\infty - \tau_\infty \right) \exp\left(\frac{2P_\infty}{\gamma_2 C_4^*} \eta \right), \\ u_{i\mathrm{s}} &= u_{i\infty} \left[1 - \exp\left(\frac{2P_\infty}{\gamma_1 C_4^*} \eta \right) \right] \qquad (i = 2, 3). \end{aligned} \right\} \tag{7.31}$$

To summarize, when $P_\infty/(-C_4^*) \le 0$, evaporation takes place ($u_{1\infty} \ge 0$),[3] and the solution is determined by specifying only one parameter, e.g., P_∞; and

[3]The slip coefficient C_4^* is negative ($C_4^* < 0$) for a hard-sphere gas and the BKW model under the complete-condensation condition [Eqs. (3.59) and (3.60)]. As explained in Section 6.6, generally, if $C_4^* < 0$ for the complete-condensation condition, it is also negative for its generalized boundary condition (6.58a) with (6.58b) [see Eq. (6.78)].

when $P_\infty/(-C_4^*) > 0$, condensation takes place ($u_{1\infty} < 0$), and the solution is determined by specifying four parameters P_∞ (or $u_{1\infty}$), $u_{2\infty}$, $u_{3\infty}$, and τ_∞. The decisive difference of the character of the solution depending on evaporation or condensation is due to whether there exists the slowly varying solution. In the next section, we will discuss the existence of a slowly varying solution when condensation is not weak, from which we can clarify the structure of the transition from subsonic to supersonic condensation.

7.3 Transonic condensation

Now consider the half-space problem described in Section 7.1 without the restriction of weak evaporation or condensation. Instead, we consider the case $\hat{v}_{i\infty} = (\hat{v}_{1\infty}, 0, 0)$ and analyze the problem under the restriction $\hat{v}_i = (\hat{v}_1, 0, 0)$ to avoid the complexity of expressions. The generalization to the case where $\hat{v}_2$ and $\hat{v}_3$ are not zero is straightforward with a note at the end of Section 7.3.2.

7.3.1 Preparation

In Sections 3.5.2 and 6.1.3, we explained, on the basis of a numerical study (Sone, Aoki & Yamashita [1986]), that bifurcation occurs at the sonic speed[4] in a condensing flow, as well as the bifurcation in the case of the transition from evaporation to condensation discussed in Section 7.2. The results, however, are numerical ones, and thus are of limited nature. We will discuss the analytical structure of the transition. First, the numerical results are summarized for the convenience of explanation.

The half-space problem does not necessarily have a solution for an arbitrary set of the three parameters $(M_\infty, p_\infty/p_w, T_\infty/T_w)$. As mentioned, the solution exists in the following region (Fig. 7.1). For $-1 < M_\infty < 0$, the solution exists when and only when the set of the three parameters lies on a surface in the $(M_\infty, p_\infty/p_w, T_\infty/T_w)$ space, or

$$p_\infty/p_w = F_s(M_\infty, T_\infty/T_w). \tag{7.32}$$

For $M_\infty \le -1$, the solution exists in a three-dimensional domain in the (M_∞, p_∞/p_w, T_∞/T_w) space, or

$$p_\infty/p_w > F_b(M_\infty, T_\infty/T_w) \quad (M_\infty < -1), \tag{7.33a}$$

$$p_\infty/p_w \ge F_b(-1, T_\infty/T_w), \tag{7.33b}$$

where F_s and F_b are those in Sections 3.5.2 and 6.1.3 with $\overline{M_t}$ eliminated, because the simpler case $\hat{v}_i = (\hat{v}_1, 0, 0)$ is considered here. The boundary $p_\infty/p_w = F_b(M_\infty, T_\infty/T_w)$ of the existence range of supersonic solutions is related to the surface $p_\infty/p_w = F_s(M_\infty, T_\infty/T_w)$. That is, a point on the boundary surface $p_\infty/p_w = F_b(M_\infty, T_\infty/T_w)$ is related to some point on the surface

[4] See Footnote 32 in Section 3.1.9.

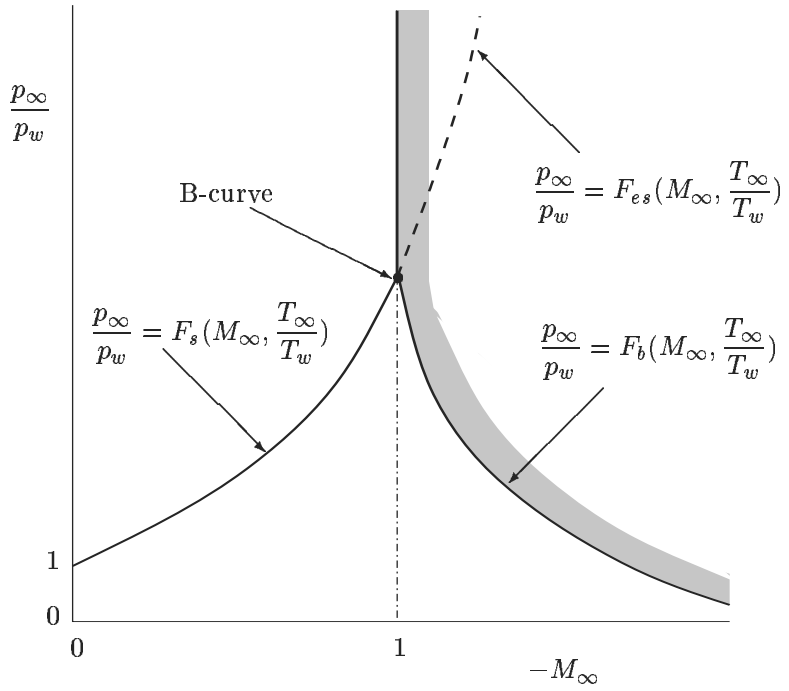

Figure 7.1. A schematic view of the section $T_\infty/T_w = \text{const}$ of the parameter space $(M_\infty, p_\infty/p_w, T_\infty/T_w)$ showing the range where a solution exists. A solution exists on the surface $p_\infty/p_w = F_s(M_\infty, T_\infty/T_w)$ and in the region $p_\infty/p_w \geq F_b(M_\infty, T_\infty/T_w)$, where the equal sign is applied only to the case $M_\infty = -1$. A supersonic Knudsen-layer-type solution exists on the surface $p_\infty/p_w = F_{es}(M_\infty, T_\infty/T_w)$.

(7.32) by the shock condition (or the Rankine–Hugoniot relation) introduced in Section 4.7.

The length scale of variation of the subsonic solution ($-1 < M_\infty < 0$) is of the order of the mean free path or the proper variable is η defined by Eq. (7.1), and the solution approaches the state at infinity exponentially fast, though confirmed only numerically. The solution with exponential approach can be extended to the supersonic range ($M_\infty \leq -1$), as shown in Fig. 7.2, which is confirmed for the BKW equation (Sone, Golse, Ohwada & Doi [1998]).

The solution of the half-space problem shows a striking feature across the sonic condition. Here, we will discuss the analytical structure of the solution in the transonic region. More precisely, we assume that there exists a solution on the surface $p_\infty/p_w = F_s(M_\infty, T_\infty/T_w)$ in $-1 < M_\infty < 0$ that approaches the state at infinity with exponential speed and that the solution with exponential approach is extended in the supersonic range, that is, there exists a solution with exponential approach on the surface $p_\infty/p_w = F_{es}(M_\infty, T_\infty/T_w)$ in $M_\infty \leq -1$. These solutions with exponential approach to the state at infinity will be called (subsonic or supersonic) *Knudsen-layer-type solutions*. Further,

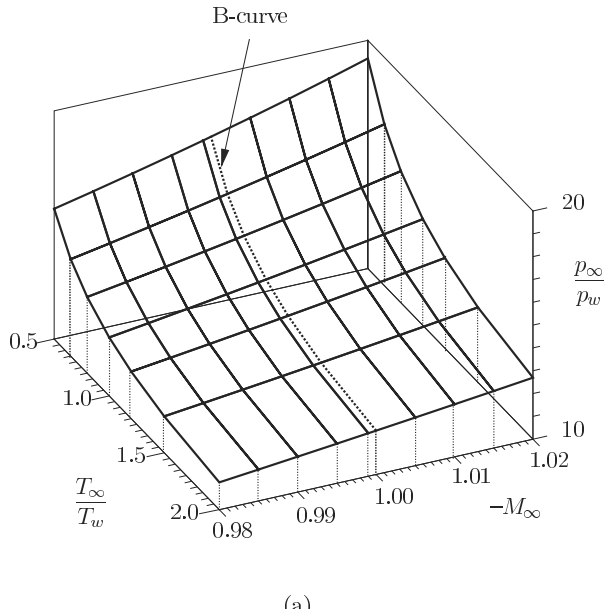

(a)

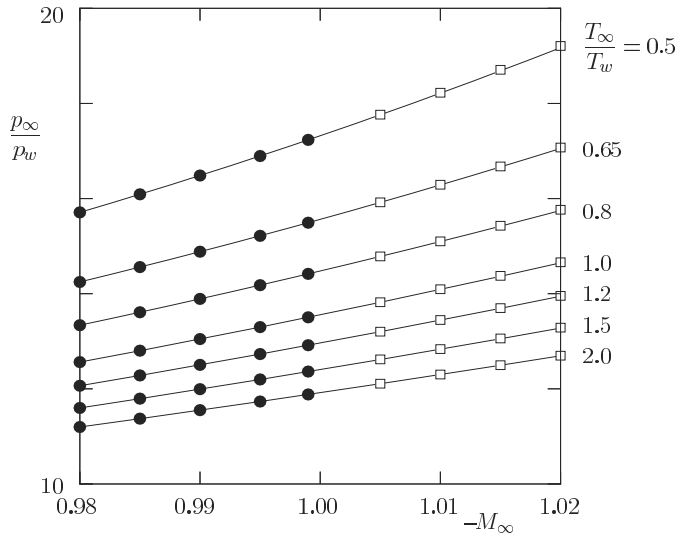

(b)

Figure 7.2. The surfaces F_s and F_{es}. (a) F_s and F_{es} in the neighborhood of $M_\infty = -1$; (b) Their sections $T_\infty/T_w = 0.5,\ 0.65,\ 0.8,\ 1,\ 1.2,\ 1.5$, and 2. In (a), the sonic line on the surfaces is shown as B-curve. In (b), the data (□) for F_{es} lie on the extrapolated curves (——) of the data (•) of F_s. The two surfaces are joined smoothly at the sonic points (along the B-curve).

we assume that the surface $p_\infty/p_w = F_s(M_\infty, T_\infty/T_w)$ intersects the plane $M_\infty = -1$ at a finite angle and that it is smoothly extended to the surface $p_\infty/p_w = F_{es}(M_\infty, T_\infty/T_w)$. Let the curve formed by the intersection of $M_\infty = -1$ and $p_\infty/p_w = F_s(M_\infty, T_\infty/T_w)$ in the $(M_\infty,\ p_\infty/p_w, T_\infty/T_w)$ space be called the B-curve. Under the assumptions stated above, we try to construct the supersonic solution in a neighborhood of the B-curve and confirm the result (7.33a) analytically.

The above numerical data are obtained for the complete-condensation condition on the condensed phase. The solution of the half-space problem is simply extended to the case of the boundary condition (1.28a) with $\alpha = 1$ as explained in Section 6.6. The extended solution has the same feature as the solution under the complete-condensation condition when the condensation coefficient α_c (≤ 1) is larger than some value ($\alpha_c > \alpha_c^{cr}$), but no solution exists in a band region or regions $c_1 \le -M_\infty \le c_2$ when $\alpha_c \le \alpha_c^{cr}$. When $-M_\infty F_s$ is a decreasing functions of M_∞, $-M_\infty F_b$ is its increasing function, and $F_s(-1_+, \hat{T}_\infty) = F_b(-1_-, \hat{T}_\infty)$, as for the BKW model, the band region is around $M_\infty = -1$ ($c_1 \le -M_\infty \le c_2$; $0 < c_1 \le 1$, $c_2 \ge 1$), where c_1 and c_2 depend on $\hat{T}_\infty$ as well as α_c (see Fig. 6.40 in Section 6.6). The effect of incomplete condensation ($\alpha_c < 1$) is similar to the effect of a noncondensable gas component in the gas (Sone, Aoki & Doi [1992]).

7.3.2 Slowly varying solution

In Section 7.2, we have seen that a slowly varying solution expands the dimension of the range of the parameter space where a solution exists. Thus, we examine whether there is another slowly varying solution with a nonsmall upstream Mach number.

Take an equilibrium state

$$\hat{f}_U = \frac{\hat{p}_U}{\pi^{3/2}\hat{T}_U^{5/2}} \exp\left(-\frac{(\zeta_i - \hat{v}_U\delta_{i1})^2}{\hat{T}_U}\right), \tag{7.34}$$

where $\hat{p}_U$, $\hat{T}_U$, and $\hat{v}_U$ are constants. We consider the case where the state of the gas is slightly perturbed from the uniform state (7.34) and the perturbation is slowly varying with respect to the space variable η, that is, $\partial\hat{f}/\partial\eta = O(\varepsilon\hat{f})$, where ε is the characteristic size of the perturbation. Using the shrunk variable x_1 defined by $x_1 = \varepsilon\eta$ [Eq. (7.12)], we have

$$\zeta_1 \frac{\partial \hat{f}}{\partial x_1} = \frac{1}{\varepsilon}\hat{J}(\hat{f}, \hat{f}). \tag{7.35}$$

The slowly varying solution, discriminated by the subscript s, is looked for in a power series of ε, i.e.,

$$\hat{f}_\mathrm{s} - \hat{f}_U = \hat{f}_{\mathrm{s}1}\varepsilon + \hat{f}_{\mathrm{s}2}\varepsilon^2 + \cdots. \tag{7.36}$$

Correspondingly, the macroscopic variables $\hat{\rho}_\mathrm{s}$, $\hat{v}_{1\mathrm{s}}$, $\hat{T}_\mathrm{s}$, and $\hat{p}_\mathrm{s}$ are also expanded similarly, i.e.,

$$\hat{h}_\mathrm{s} - \hat{h}_U = \hat{h}_{\mathrm{s}1}\varepsilon + \hat{h}_{\mathrm{s}2}\varepsilon^2 + \cdots, \tag{7.37}$$

where $\hat{h}$ represents any of $\hat{\rho}$, $\hat{v}_1$, $\hat{T}$, and $\hat{p}$. They are related to $\hat{f}_{\rm s}$ as

$$\hat{\rho}_{\rm s1} = \int \hat{f}_{\rm s1} \mathbf{d\zeta}, \tag{7.38a}$$

$$\hat{\rho}_U \hat{v}_{1{\rm s}1} = \int (\zeta_1 - \hat{v}_U) \hat{f}_{\rm s1} \mathbf{d\zeta}, \tag{7.38b}$$

$$\frac{3}{2}\hat{\rho}_U \hat{T}_{\rm s1} = \int \left((\zeta_i - \hat{v}_U \delta_{i1})^2 - \frac{3}{2}\hat{T}_U \right) \hat{f}_{\rm s1} \mathbf{d\zeta}, \tag{7.38c}$$

$$\hat{p}_{\rm s1} = \hat{\rho}_{\rm s1} \hat{T}_U + \hat{\rho}_U \hat{T}_{\rm s1}, \tag{7.38d}$$

$$\hat{\rho}_{\rm s2} = \int \hat{f}_{\rm s2} \mathbf{d\zeta}, \tag{7.39a}$$

$$\hat{\rho}_U \hat{v}_{1{\rm s}2} = \int (\zeta_1 - \hat{v}_U) \hat{f}_{\rm s2} \mathbf{d\zeta} - \hat{\rho}_{\rm s1}\, \hat{v}_{1{\rm s}1}, \tag{7.39b}$$

$$\frac{3}{2}\hat{\rho}_U \hat{T}_{\rm s2} = \int \left((\zeta_i - \hat{v}_U \delta_{i1})^2 - \frac{3}{2}\hat{T}_U \right) \hat{f}_{\rm s2} \mathbf{d\zeta} - \hat{\rho}_U \hat{v}_{1{\rm s}1}^2 - \frac{3}{2}\hat{\rho}_{\rm s1}\, \hat{T}_{\rm s1}, \tag{7.39c}$$

$$\hat{p}_{\rm s2} = \hat{\rho}_{\rm s2} \hat{T}_U + \hat{\rho}_U \hat{T}_{\rm s2} + \hat{\rho}_{\rm s1} \hat{T}_{\rm s1}. \tag{7.39d}$$

Substituting the expansion (7.36) into Eq. (7.35), we obtain the integral equation for $\hat{f}_{sm}$, i.e.,

$$\hat{J}(\hat{f}_U, \hat{f}_{\rm s1}) = 0, \tag{7.40}$$

$$2\hat{J}(\hat{f}_U, \hat{f}_{sm}) = \zeta_1 \frac{\partial \hat{f}_{sm-1}}{\partial x_1} - \sum_{l=1}^{m-1} \hat{J}(\hat{f}_{\rm sl}, \hat{f}_{sm-l}) \quad (m \geq 2). \tag{7.41}$$

In view of Eqs. (7.38a)–(7.38d), the solution of Eq. (7.40) is expressed as

$$\hat{f}_{\rm s1} = \hat{f}_U \left[\frac{\hat{\rho}_{\rm s1}}{\hat{\rho}_U} + \frac{2\hat{v}_{1{\rm s}1}(\zeta_1 - \hat{v}_U)}{\hat{T}_U} + \frac{\hat{T}_{\rm s1}}{\hat{T}_U} \left(\frac{(\zeta_i - \hat{v}_U \delta_{i1})^2}{\hat{T}_U} - \frac{3}{2} \right) \right]. \tag{7.42}$$

Then, $\hat{f}_U + \varepsilon \hat{f}_{\rm s1}$ is written as

$$\hat{f}_U + \varepsilon \hat{f}_{\rm s1} = \frac{\hat{p}_U + \varepsilon \hat{p}_{\rm s1}}{\pi^{3/2} (\hat{T}_U + \varepsilon \hat{T}_{\rm s1})^{5/2}} \exp\left(- \frac{[\zeta_i - (\hat{v}_U + \varepsilon \hat{v}_{1{\rm s}1})\delta_{i1}]^2}{\hat{T}_U + \varepsilon \hat{T}_{\rm s1}} \right) + O(\varepsilon^2). \tag{7.43}$$

The slowly varying solution $\hat{f}_{\rm s}$ is Maxwellian up to the order of ε. This property simplifies the later analysis and result considerably.

From the condition for Eq. (1.83) to hold and the relation (1.53),[5] the condition (solvability condition)

$$\int (1, \zeta_1, \zeta_i^2) \zeta_1 \frac{\partial \hat{f}_{sm-1}}{\partial x_1} \mathbf{d\zeta} = 0 \quad (m \geq 2) \tag{7.44}$$

is required for Eq. (7.41) to have a solution. With Eq. (7.42), the condition (7.44) for $m = 2$ is reduced to the following homogeneous linear equations for

[5] See Footnote 59 in Section 3.3.2.

$\mathrm{d}\hat{\rho}_{\mathrm{s}1}/\mathrm{d}x_1$, $\mathrm{d}\hat{v}_{1\mathrm{s}1}/\mathrm{d}x_1$, and $\mathrm{d}\hat{T}_{\mathrm{s}1}/\mathrm{d}x_1$:

$$\begin{pmatrix} \hat{v}_U & \hat{\rho}_U & 0 \\ \hat{T}_U/2 & \hat{\rho}_U\,\hat{v}_U & \hat{\rho}_U/2 \\ 0 & 2\hat{\rho}_U\hat{v}_U^2 & 5\hat{\rho}_U\hat{v}_U/2 \end{pmatrix} \begin{pmatrix} \mathrm{d}\hat{\rho}_{\mathrm{s}1}/\mathrm{d}x_1 \\ \mathrm{d}\hat{v}_{1\mathrm{s}1}/\mathrm{d}x_1 \\ \mathrm{d}\hat{T}_{\mathrm{s}1}/\mathrm{d}x_1 \end{pmatrix} = \begin{pmatrix} 0 \\ 0 \\ 0 \end{pmatrix}. \tag{7.45}$$

For the homogeneous equations (7.45) to have a nontrivial solution, the determinant composed of their coefficients must vanish, that is,

$$\hat{v}_U = 0, \quad \hat{v}_U = \pm(5\hat{T}_U/6)^{1/2}. \tag{7.46}$$

A slowly varying solution is possible only when the background uniform state is at rest or at a sonic state, defined as the state that the flow speed $|v_1|$ is equal to the sound speed $(5RT/3)^{1/2}$. The former case corresponds to the case discussed in Section 7.2.2. The solution of one of the latter cases, i.e., $\hat{v}_U = \pm(5\hat{T}_U/6)^{1/2}$, is obviously obtained from the other only by replacing the variables x_1 and $\hat{v}_{1\mathrm{s}1}$ by $-x_1$ and $-\hat{v}_{1\mathrm{s}1}$ respectively. Thus, hereafter, we consider the case $\hat{v}_U = -(5\hat{T}_U/6)^{1/2}$ whose result is directly used in the later analysis.

Let this state be indicated by the subscript B instead of U. That is,

$$\left.\begin{aligned} &\hat{v}_U = \hat{v}_B = -(5\hat{T}_B/6)^{1/2},\ \hat{T}_U = \hat{T}_B, \\ &\hat{p}_U = \hat{p}_B,\ \hat{\rho}_U = \hat{\rho}_B = \hat{p}_B/\hat{T}_B, \\ &\hat{f}_U = \hat{f}_B = \frac{\hat{p}_B}{\pi^{3/2}\hat{T}_B^{5/2}} \exp\left(-\frac{(\zeta_i - \hat{v}_B\delta_{i1})^2}{\hat{T}_B}\right). \end{aligned}\right\} \tag{7.47}$$

For this sonic background state, the three relations of the solvability condition (7.45) degenerate into two, and the following two independent equations are derived:

$$\frac{\mathrm{d}\hat{\rho}_{\mathrm{s}1}}{\mathrm{d}x_1} - \left(\frac{6}{5\hat{T}_B}\right)^{1/2} \hat{\rho}_B \frac{\mathrm{d}\hat{v}_{1\mathrm{s}1}}{\mathrm{d}x_1} = 0, \tag{7.48a}$$

$$\frac{\mathrm{d}\hat{T}_{\mathrm{s}1}}{\mathrm{d}x_1} - \left(\frac{8\hat{T}_B}{15}\right)^{1/2} \frac{\mathrm{d}\hat{v}_{1\mathrm{s}1}}{\mathrm{d}x_1} = 0. \tag{7.48b}$$

These equations are independent of molecular models. When Eqs. (7.48a) and (7.48b) with Eq. (7.47) are satisfied, the solution $\hat{f}_{\mathrm{s}2}$ is given in the form

$$\begin{aligned} \frac{\hat{f}_{\mathrm{s}2}}{\hat{f}_B} = {} & \frac{\hat{\rho}_{\mathrm{s}2}}{\hat{\rho}_B} + 2\tilde{\zeta}_1 \left(\frac{\hat{v}_{1\mathrm{s}2}}{\hat{T}_B^{1/2}} + \frac{\hat{\rho}_{\mathrm{s}1}\hat{v}_{1\mathrm{s}1}}{\hat{\rho}_B\hat{T}_B^{1/2}}\right) + \left(\tilde{\zeta}^2 - \frac{3}{2}\right)\left(\frac{\hat{T}_{\mathrm{s}2}}{\hat{T}_B} + \frac{2\hat{v}_{1\mathrm{s}1}^2}{3\hat{T}_B} + \frac{\hat{\rho}_{\mathrm{s}1}\hat{T}_{\mathrm{s}1}}{\hat{\rho}_B\hat{T}_B}\right) \\ & + 2\left(\tilde{\zeta}_1^2 - \frac{\tilde{\zeta}^2}{3}\right)\frac{\hat{v}_{1\mathrm{s}1}^2}{\hat{T}_B} + 2\tilde{\zeta}_1\left(\tilde{\zeta}^2 - \frac{5}{2}\right)\frac{\hat{v}_{1\mathrm{s}1}\hat{T}_{\mathrm{s}1}}{\hat{T}_B^{3/2}} + \left(\frac{1}{2}\tilde{\zeta}^4 - \frac{5}{2}\tilde{\zeta}^2 + \frac{15}{8}\right)\frac{\hat{T}_{\mathrm{s}1}^2}{\hat{T}_B^2} \\ & - \left(\tilde{\zeta}_1^2 - \frac{1}{3}\tilde{\zeta}^2\right)\mathcal{B}^{(0)}(\tilde{\zeta}, \hat{T}_B)\frac{1}{\hat{\rho}_B\hat{T}_B^{1/2}}\frac{\mathrm{d}\hat{v}_{1\mathrm{s}1}}{\mathrm{d}x_1} - \tilde{\zeta}_1\mathcal{A}(\tilde{\zeta}, \hat{T}_B)\frac{1}{\hat{\rho}_B\hat{T}_B}\frac{\mathrm{d}\hat{T}_{\mathrm{s}1}}{\mathrm{d}x_1}, \end{aligned} \tag{7.49}$$

where

$$\tilde{\zeta}_i = (\zeta_i - \hat{v}_B\delta_{i1})/\hat{T}_B^{1/2}, \quad \tilde{\zeta} = (\tilde{\zeta}_i^2)^{1/2}, \tag{7.50}$$

and $\mathcal{A}(\tilde{\zeta}, \hat{T}_B)$ and $\mathcal{B}^{(0)}(\tilde{\zeta}, \hat{T}_B)$ are functions defined in Section A.2.9.

The solvability condition (7.44) for $m = 3$ with Eq. (7.49) for $\hat{f}_{\rm s2}$ is reduced to the following linear equations for $\mathrm{d}\hat{\rho}_{\rm s2}/\mathrm{d}x_1$, $\mathrm{d}\hat{v}_{\rm 1s2}/\mathrm{d}x_1$, and $\mathrm{d}\hat{T}_{\rm s2}/\mathrm{d}x_1$:

$$\begin{aligned}
&\begin{pmatrix} \hat{v}_B & \hat{\rho}_B & 0 \\ \hat{T}_B/2 & \hat{\rho}_B\hat{v}_B & \hat{\rho}_B/2 \\ 0 & 2\hat{\rho}_B\hat{v}_B^2 & 5\hat{\rho}_B\hat{v}_B/2 \end{pmatrix} \begin{pmatrix} \mathrm{d}\hat{\rho}_{\rm s2}/\mathrm{d}x_1 \\ \mathrm{d}\hat{v}_{\rm 1s2}/\mathrm{d}x_1 \\ \mathrm{d}\hat{T}_{\rm s2}/\mathrm{d}x_1 \end{pmatrix} \\
&= -\begin{pmatrix} \dfrac{\mathrm{d}\hat{\rho}_{\rm s1}\hat{v}_{\rm 1s1}}{\mathrm{d}x_1} \\ \dfrac{1}{2}\dfrac{\mathrm{d}\hat{\rho}_{\rm s1}\hat{T}_{\rm s1}}{\mathrm{d}x_1} + (\hat{v}_B\hat{\rho}_{\rm s1} + \hat{\rho}_B\hat{v}_{\rm 1s1})\dfrac{\mathrm{d}\hat{v}_{\rm 1s1}}{\mathrm{d}x_1} - \dfrac{2}{3}\Gamma_1\dfrac{\mathrm{d}^2\hat{v}_{\rm 1s1}}{\mathrm{d}x_1^2} \\ \hat{\rho}_B\hat{v}_B\dfrac{\mathrm{d}\hat{v}_{\rm 1s1}^2}{\mathrm{d}x_1} - \dfrac{5}{4}\Gamma_2\dfrac{\mathrm{d}^2\hat{T}_{\rm s1}}{\mathrm{d}x_1^2} - \dfrac{4}{3}\Gamma_1\hat{v}_B\dfrac{\mathrm{d}^2\hat{v}_{\rm 1s1}}{\mathrm{d}x_1^2} \end{pmatrix},
\end{aligned} \tag{7.51}$$

where Γ_1 and Γ_2 are, respectively, the short forms of $\Gamma_1(\hat{T}_B)$ and $\Gamma_2(\hat{T}_B)$, functions of $\hat{T}_B$ determined by the molecular model, defined in Section A.2.9. The coefficient matrix on the left-hand side is the same as that of Eq. (7.45) whose determinant vanishes. Thus, the inhomogeneous terms must satisfy the following condition for Eq. (7.51) to have a solution:

$$\frac{\mathrm{d}\hat{v}_{\rm 1s1}^2}{\mathrm{d}x_1} - \frac{2\Gamma_1 + \Gamma_2}{4\hat{\rho}_B}\frac{\mathrm{d}^2\hat{v}_{\rm 1s1}}{\mathrm{d}x_1^2} = 0, \tag{7.52}$$

where $\hat{\rho}_{\rm s1}$ and $\hat{T}_{\rm s1}$ are taken to be zero when $\hat{v}_{\rm 1s1} = 0$ and thus, $\hat{v}_{\rm 1s1} = 0$ is the sonic point. The condition (7.52) being satisfied, the three equations of Eq. (7.51) degenerate into two equations for $\mathrm{d}\hat{\rho}_{\rm s2}/\mathrm{d}x_1$, $\mathrm{d}\hat{v}_{\rm 1s2}/\mathrm{d}x_1$, and $\mathrm{d}\hat{T}_{\rm s2}/\mathrm{d}x_1$. Equation (7.52) together with Eqs. (7.48a) and (7.48b), the two relations derived from the solvability condition (7.44) for $m = 2$, forms the set of equations for $\hat{\rho}_{\rm s1}$, $\hat{v}_{\rm 1s1}$, and $\hat{T}_{\rm s1}$.

From Eq. (7.52), under the condition $\mathrm{d}\hat{v}_{\rm 1s1}/\mathrm{d}x_1 \to 0$ as $x_1 \to \infty$ or $-\infty$,[6]

$$x_1 = \frac{1}{a^2}\int^{\hat{v}_{\rm 1s1}} \frac{\mathrm{d}\hat{v}_{\rm 1s1}}{\hat{v}_{\rm 1s1}^2 - C^2}, \tag{7.53}$$

where

$$a^2 = 4\hat{\rho}_B/(2\Gamma_1 + \Gamma_2),$$

and C (> 0) is an integration constant. Examining Eq. (7.53) with reference to Fig. 7.3, we find that $\hat{v}_{\rm 1s1} = -C$ corresponds to $x_1 = \infty$ (or $\hat{v}_{\rm 1s1} \to -C$ as $x_1 \to \infty$) and that $\hat{v}_{\rm 1s1} = C$ to $x_1 = -\infty$ (or $\hat{v}_{\rm 1s1} \to C$ as $x_1 \to -\infty$). The flow direction determined by $\hat{v}_B$ is shown by arrows in Fig. 7.3. There are three

[6] According to the last paragraph of Section A.2.9, $\Gamma_1 > 0$ and $\Gamma_2 > 0$.

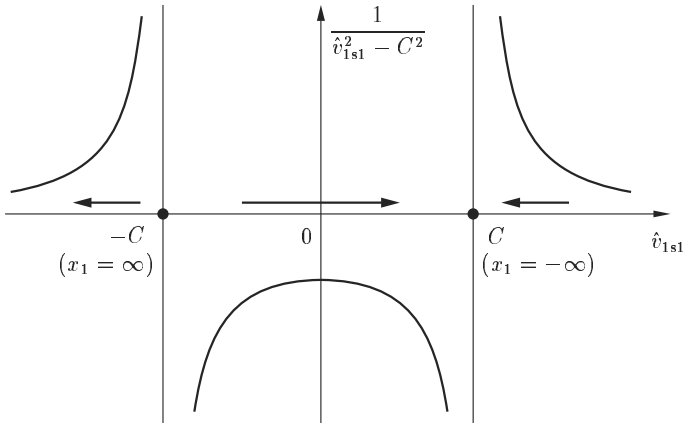

Figure 7.3. The integrand $1/(\hat{v}_{1s1}^2 - C^2)$.

kinds of solutions that tend to a uniform state as $x_1 \to \infty$ or $x_1 \to -\infty$, i.e.,

$$\hat{v}_{1s1} = -C \tanh X \quad (-\infty < X < \infty), \tag{7.54a}$$

$$\hat{v}_{1s1} = -C \coth X \quad (0 < X < \infty), \tag{7.54b}$$

$$\hat{v}_{1s1} = -C \coth X \quad (-\infty < X < 0), \tag{7.54c}$$

where

$$X + X_0 = Ca^2 x_1, \tag{7.55}$$

with an arbitrary constant X_0. The first solution (7.54a) is a *weak shock wave* solution (Grad [1969], Caflisch & Nicolaenko [1982]) from $x_1 = \infty$ to $-\infty$, the second solution (7.54b) in the region $(X_0/Ca^2 < x_1 < \infty)$ is a *supersonic accelerating flow* from $x_1 = \infty$, and the third solution (7.54c) in the region $(-\infty < x_1 < X_0/Ca^2)$ is a subsonic accelerating flow to $x_1 = -\infty$. The last two solutions diverge at a finite point $X = 0$ or $x_1 = X_0/Ca^2$. We can put any state in the range of X at the origin $x_1 = 0$ by choosing X_0 properly.

The other variables, i.e., $\hat{\rho}_{s1}$, $\hat{T}_{s1}$, and $\hat{p}_{s1}$, are easily obtained from $\hat{v}_{1s1}$ with the aid of Eqs. (7.48a), (7.48b), and (7.38d) as

$$\hat{\rho}_{s1} = -\frac{\hat{\rho}_B}{\hat{v}_B}\hat{v}_{1s1}, \tag{7.56a}$$

$$\hat{T}_{s1} = -\frac{4\hat{v}_B}{5}\hat{v}_{1s1}, \tag{7.56b}$$

$$\hat{p}_{s1} = -2\hat{\rho}_B \hat{v}_B \hat{v}_{1s1}, \tag{7.56c}$$

$$\hat{v}_B = -(5\hat{T}_B/6)^{1/2}. \tag{7.56d}$$

As we have noted before, the reflection of the solution with respect to $x_1 = 0$ (or $X = 0$) is the solution corresponding to $\hat{v}_B = (5\hat{T}_B/6)^{1/2}$. Thus, when we consider the half-space problem, there are four kinds of slowly varying solutions

that approach a uniform state as $x_1 \to \infty$, two condensing flows ($\hat{v}_{1\mathrm{s}} < 0$) supersonic at infinity and two evaporating flows ($\hat{v}_{1\mathrm{s}} > 0$) subsonic at infinity. The two condensing flows are the weak shock wave and the supersonic accelerating flow; the two evaporating flows are the weak shock wave and the subsonic accelerating flow.

Here, we express the results in a form convenient for later application to condensing flows (or $\hat{v}_{1\mathrm{s}} < 0$), where the Mach number M_∞

$$M_\infty = \frac{v_{1\infty}}{(5RT_\infty/3)^{1/2}} = \frac{\hat{v}_{1\infty}}{(5\hat{T}_\infty/6)^{1/2}} < 0,$$

is used instead of $\hat{v}_{1\infty}$; it has a sign in contrast to the conventional definition. It is noted that the terms of the order of ε^2 and higher are neglected in the equations that hereafter appear in this subsection, and that they are correct only up to the order of ε. The results are expressed with the same notation for the quantities with difference $O(\varepsilon^2)$, e.g., $\hat{v}_{1\mathrm{s}} = \hat{v}_B + \varepsilon\hat{v}_{1\mathrm{s}1}$. From Eqs. (7.37), (7.54a), (7.54b), and (7.56b),

$$\hat{v}_{1\infty} = \hat{v}_B - \varepsilon C, \quad \hat{v}_{1\mathrm{s}} = \hat{v}_B - \varepsilon C\hat{S}(X), \quad \hat{T}_\infty = \hat{T}_B + \frac{4\varepsilon\hat{v}_B}{5}C,$$

where $\hat{S}(X)$ is $\tanh X$ or $\coth X$, and $\hat{v}_B = -(5\hat{T}_B/6)^{1/2}$. Evaluating M_∞ by these relations, we find

$$\varepsilon C = \frac{3}{4}\hat{v}_B(M_\infty + 1),$$

from which $M_\infty < -1$. Then, the slowly varying solution around a sonic condition flowing in the $-X$ direction is expressed as follows:[7]

$$\hat{f}_{\mathrm{s}} = \frac{\hat{p}_{\mathrm{s}}}{\pi^{3/2}\hat{T}_{\mathrm{s}}{}^{5/2}} \exp\left(-\frac{(\zeta_i - \hat{v}_{1\mathrm{s}}\delta_{i1})^2}{\hat{T}_{\mathrm{s}}}\right), \tag{7.57a}$$

$$\hat{v}_{1\mathrm{s}} = \left(\frac{5\hat{T}_\infty}{6}\right)^{1/2}\left(M_\infty + \frac{3}{4}(M_\infty + 1)[\hat{S}(X) - 1]\right), \tag{7.57b}$$

$$\hat{\rho}_{\mathrm{s}} = \hat{\rho}_\infty\left(1 + \frac{3}{4}(M_\infty + 1)[\hat{S}(X) - 1]\right), \tag{7.57c}$$

$$\hat{T}_{\mathrm{s}} = \hat{T}_\infty\left(1 + \frac{1}{2}(M_\infty + 1)[\hat{S}(X) - 1]\right), \tag{7.57d}$$

$$\hat{p}_{\mathrm{s}} = \hat{p}_\infty\left(1 + \frac{5}{4}(M_\infty + 1)[\hat{S}(X) - 1]\right), \tag{7.57e}$$

$$M_{\mathrm{s}} = M_\infty + (M_\infty + 1)[\hat{S}(X) - 1], \tag{7.57f}$$

$$X + X_0 = -\sqrt{\frac{15}{2}}\frac{\hat{\rho}_B\hat{T}_B^{1/2}}{2\Gamma_1 + \Gamma_2}(M_\infty + 1)\eta = \sqrt{\frac{15}{2}}\frac{\hat{\rho}_B\hat{T}_B^{1/2}}{2\Gamma_1 + \Gamma_2}x_1, \tag{7.57g}$$

[7] If $\hat{\rho}_B$ and $\hat{T}_B$, including the arguments of Γ_1 and Γ_2, in Eq. (7.57g) are replaced by quantities with difference of $O(\varepsilon)$, e.g., by $\hat{\rho}_\infty$ and $\hat{T}_\infty$ respectively, the error in Eq. (7.57g) is $O(\varepsilon)$ for a finite x_1, but the errors in Eqs. (7.57a)–(7.57f) are $O(\varepsilon^2)$ because $\hat{S}(X)$ in Eqs. (7.57b)–(7.57f) is multiplied by the factor $M_\infty + 1$ of $O(\varepsilon)$.

where $M_\infty < -1$, M_s is the local Mach number given by $\hat{v}_{1\mathrm{s}}/(5\hat{T}_\mathrm{s}/6)^{1/2}$; the choice of ε, introduced in the definition of the shrunk variable x_1, has a freedom and $|M_\infty + 1|$ is taken as ε here; this difference appears only in the relation between η and x_1. When $\hat{S}(X) = \tanh X$, the above solution is a weak shock wave, and when $\hat{S}(X) = \coth X$, it is a supersonic accelerating flow. From these equations, the function $\hat{S}(X)$ is eliminated and the variables are expressed in terms of M_s. For example,

$$\hat{p}_\mathrm{s} = \hat{p}_\infty g_p(M_\mathrm{s}, M_\infty), \quad \hat{T}_\mathrm{s} = \hat{T}_\infty g_T(M_\mathrm{s}, M_\infty), \tag{7.58}$$

where

$$g_p(M_\mathrm{s}, M_\infty) = 1 + \frac{5}{4}(M_\mathrm{s} - M_\infty), \tag{7.59a}$$

$$g_T(M_\mathrm{s}, M_\infty) = 1 + \frac{1}{2}(M_\mathrm{s} - M_\infty). \tag{7.59b}$$

It should be noted that a slowly varying solution expressing a flow in the $-x_1$ direction exists only for $M_\infty < -1$, and M_s ranges in the domain

$$M_\infty \le M_\mathrm{s} \le -M_\infty - 2 \quad \text{(weak shock wave)}, \tag{7.60a}$$

$$M_\mathrm{s} \le M_\infty \qquad \text{(supersonic accelerating flow)}. \tag{7.60b}$$

Owing to the freedom of arbitrary X_0 in Eq. (7.57g), any set of the parameters $(M_\mathrm{s}, \hat{p}_\mathrm{s}, \hat{T}_\mathrm{s})$ satisfying the relation (7.58) can be located at the origin ($\eta = 0$ or $x_1 = 0$). For example, this is done by choosing X_0 by the relation

$$S(-X_0) = (M_\mathrm{s} + 1)/(M_\infty + 1). \tag{7.61}$$

The foregoing analysis of a slowly varying solution can be easily extended to the case where $\hat{v}_2$ and $\hat{v}_3$ are not zero. The solution is obtained by simply adding constant velocity components $\hat{v}_2 = \hat{v}_{2\infty}$ and $\hat{v}_3 = \hat{v}_{3\infty}$, that is, $\hat{f}_U + \varepsilon\hat{f}_{\mathrm{s}1}$ is a local Maxwellian given by

$$\hat{f}_U + \varepsilon\hat{f}_{\mathrm{s}1} = \frac{\hat{p}_U + \varepsilon\hat{p}_{\mathrm{s}1}}{\pi^{3/2}(\hat{T}_U + \varepsilon\hat{T}_{\mathrm{s}1})^{5/2}} \exp\left(-\frac{(\zeta_i - \hat{v}_i)^2}{\hat{T}_U + \varepsilon\hat{T}_{\mathrm{s}1}}\right) + O(\varepsilon^2), \tag{7.62}$$

where

$$\hat{v}_1 = \hat{v}_U + \varepsilon\hat{v}_{1\mathrm{s}1}, \quad \hat{v}_2 = \hat{v}_{2\infty}, \quad \hat{v}_3 = \hat{v}_{3\infty}.$$

The other variables as well as $\hat{v}_U$ and $\hat{v}_{1\mathrm{s}1}$ are the same as in the foregoing analysis.

7.3.3 Construction of the solution of the half-space problem

We try to construct supersonic condensing solutions in a transonic region on the basis of the slowly varying solution obtained in Section 7.3.2, as we have obtained weakly condensing solutions in Sections 7.2.3 and 7.2.4.

The slowly varying solution does not satisfy the boundary condition (7.3a), especially Eq. (7.4), on the condensed phase. Thus, we try to find the solution of the half-space problem by modifying the slowly varying function only in a neighborhood of the condensed phase. That is, we put the solution in the form

$$\hat{f} = \hat{f}_{\rm s} + \hat{f}_K, \tag{7.63}$$

where the correction term $\hat{f}_K$ is assumed to vary as $\partial \hat{f}_K/\partial\eta = O(\hat{f}_K)$, and vanishes very rapidly (or faster than any inverse power of η) as η tends to infinity (Knudsen-layer correction). We first rewrite Eq. (7.63) in the form

$$\hat{f} = \hat{f}_{\rm s} - \hat{f}_{e0} + \hat{f}^*, \tag{7.64}$$

with

$$\hat{f}_{e0} = \frac{(\hat{p}_{\rm s})_0}{\pi^{3/2}(\hat{T}_{\rm s}{}^{5/2})_0} \exp\left(-\frac{[\zeta_i - (\hat{v}_{1{\rm s}})_0\delta_{i1}]^2}{(\hat{T}_{\rm s})_0}\right), \tag{7.65a}$$

$$\hat{f}^* = \hat{f}_{e0} + \hat{f}_K, \tag{7.65b}$$

where the quantities in the parentheses with subscript zero $(\ )_0$ are evaluated at $x_1 = 0$, and $\hat{f}^*$ converges to $\hat{f}_{e0}$ exponentially as $\eta \to \infty$. The data $(\hat{p}_{\rm s})_0$, $(\hat{T}_{\rm s})_0$, and $(\hat{v}_{1{\rm s}})_0$ at $x_1 = 0$ contain an arbitrary constant X_0, which will be determined later. It is noted that the Maxwellian $\hat{f}_{e0}$ agrees with $(\hat{f}_{\rm s})_0$ up to the order of ε, because $\hat{f}_{\rm s}$ is Maxwellian up to this order [see Eq. (7.43)]. Substituting Eq. (7.64) into the Boltzmann equation (7.2), then we obtain the equation

$$\zeta_1 \frac{\partial \hat{f}^*}{\partial \eta} = \hat{J}(\hat{f}^*, \hat{f}^*) + 2\hat{J}(\hat{f}_{\rm s} - \hat{f}_{e0}, \hat{f}_K). \tag{7.66}$$

In this derivation, it is used that $\hat{f}_{\rm s}$ satisfies Eq. (7.2) and that $\hat{J}(\hat{f}_{e0}, \hat{f}_{e0}) = 0$. In the second term on the right-hand side of Eq. (7.66), the slowly varying function $\hat{f}_{\rm s} - \hat{f}_{e0}$ is multiplied by the rapidly decaying function $\hat{f}_K$, and therefore the former can be replaced by its series expansion

$$\hat{f}_{\rm s} = \hat{f}_B + \varepsilon(\hat{f}_{\rm s1})_0 + \varepsilon^2[(\hat{f}_{\rm s2})_0 + \eta(\partial \hat{f}_{\rm s1}/\partial x_1)_0] + \cdots. \tag{7.67}$$

From Eq. (7.67) and the fact that $\hat{f}_{\rm s}$ is Maxwellian up to the order of ε, the difference $\hat{f}_{\rm s} - \hat{f}_{e0}$ is $O(\varepsilon^2)$. Thus, we can estimate the second term on the right-hand side of Eq. (7.66) as

$$\hat{J}(\hat{f}_{\rm s} - \hat{f}_{e0}, \hat{f}_K) = O(\varepsilon^2 \hat{f}_K). \tag{7.68}$$

The integral $\hat{J}(\hat{f}_{\rm s} - \hat{f}_{e0}, \hat{f}_K)$ is exponentially small outside the region $\eta = O(1)$ and is of the order of ε^2 in the region $\eta = O(1)$. Therefore, the function $\hat{f}^*$, whose variation is confined in this region, is given within an error $O(\varepsilon^2)$ by the solution of the equation

$$\zeta_1 \frac{\partial \hat{f}^*}{\partial \eta} = \hat{J}(\hat{f}^*, \hat{f}^*). \tag{7.69}$$

From Eqs. (7.3a) and (7.64),

$$\hat{f}^* = \hat{f}_w - [(\hat{f}_{\rm s})_0 - \hat{f}_{e0}] \quad (\zeta_1 > 0) \quad \text{at } \eta = 0, \tag{7.70}$$

where $(\hat{f}_{\rm s})_0 - \hat{f}_{e0}$ is $O(\varepsilon^2)$. Thus, the difference of $O(\varepsilon^2)$ being neglected here, the condition (7.70) at $\eta = 0$ is reduced to the condition

$$\hat{f}^* = \hat{f}_w \quad (\zeta_1 > 0) \ \text{ at } \eta = 0, \tag{7.71}$$

especially for the complete-condensation condition,

$$\hat{f}^* = \pi^{-3/2} \exp(-\zeta_i^2) \quad (\zeta_1 > 0) \ \text{ at } \eta = 0. \tag{7.72}$$

From Eq. (7.65b) and the condition that $\hat{f}_K \to 0$ exponentially as $\eta \to \infty$, $\hat{f}^*$ approaches the Maxwellian $\hat{f}_{e0}$, i.e.,

$$\hat{f}^* \to \frac{(\hat{p}_{\rm s})_0}{\pi^{3/2}(\hat{T}_{\rm s})_0^{5/2}} \exp\left(-\frac{[\zeta_i - (\hat{v}_{1{\rm s}})_0\delta_{i1}]^2}{(\hat{T}_{\rm s})_0}\right) \quad \text{as } \eta \to \infty, \tag{7.73}$$

exponentially fast.

In the present study we are interested in the quantities up to the order of ε. Hereafter, we use the same notation for the quantities with difference $O(\varepsilon^2)$, e.g., $\hat{f}_{\rm s} = \hat{f}_B + \varepsilon\hat{f}_{\rm s1}$, $(\hat{f}_{\rm s})_0 = \hat{f}_{e0}$, $\hat{v}_{1{\rm s}} = \hat{v}_B + \varepsilon\hat{v}_{1{\rm s}1}$, $\hat{p}_{\rm s} = \hat{p}_B + \varepsilon\hat{p}_{\rm s1}$, $\hat{T}_{\rm s} = \hat{T}_B + \varepsilon\hat{T}_{\rm s1}$. Thus, from the above discussion, $\hat{f}^*$ is the solution of the boundary-value problem (7.69), (7.71), and (7.73) that approaches the state at infinity with an exponential speed. That is, $\hat{f}^*$ is the (subsonic or supersonic) Knudsen-layer-type solution in Section 7.3.1 where the parameters M_∞, p_∞/p_w, and T_∞/T_w are, respectively, replaced by $(M_{\rm s})_0$ $(= (\hat{v}_{1{\rm s}})_0/[5(\hat{T}_{\rm s})_0/6]^{1/2})$, $(\hat{p}_{\rm s})_0$, and $(\hat{T}_{\rm s})_0$. That is, the solution $\hat{f}^*$ exists when and only when the parameters $(M_{\rm s})_0$, $(\hat{p}_{\rm s})_0$, and $(\hat{T}_{\rm s})_0$ satisfy the relation

$$(\hat{p}_{\rm s})_0 = F_S((M_{\rm s})_0, (\hat{T}_{\rm s})_0), \tag{7.74}$$

where F_S is F_s or F_{es}.[8] This relation serves as the equation for undetermined X_0, which is contained in $(M_{\rm s})_0$, $(\hat{p}_{\rm s})_0$, and $(\hat{T}_{\rm s})_0$. If X_0 is determined, $(M_{\rm s})_0$, $(\hat{p}_{\rm s})_0$, and $(\hat{T}_{\rm s})_0$ are determined. That is, the solution of the half-space problem is determined. However, this equation may not always have a solution. To make this point clear and to derive the existence range of the supersonic solution in Fig. 7.1, we will construct a class of solutions of the half-space problem from a given Knudsen-layer-type solution $\hat{f}^*$ with the aid of the above discussion.

Let the values of M, $\hat{p}$, and $\hat{T}$ at infinity of a Knudsen-layer-type solution $\hat{f}^*$ be, respectively, $(M_{\rm s})_0$, $(\hat{p}_{\rm s})_0$, and $(\hat{T}_{\rm s})_0$, which satisfy the relation (7.74). Take the slowly varying solution $\hat{f}_{\rm s}$ with $(M_{\rm s})_0$, $(\hat{p}_{\rm s})_0$, and $(\hat{T}_{\rm s})_0$ as the values of $M_{\rm s}$, $\hat{p}_{\rm s}$, and $\hat{T}_{\rm s}$ at the origin. Then, the values $M_{\rm s}$, $\hat{p}_{\rm s}$, and $\hat{T}_{\rm s}$ at infinity, i.e.,

[8] Naturally, we are interested in the region in a neighborhood of the B-curve.

M_∞, $\hat{p}_\infty$, and $\hat{T}_\infty$, of this slowly varying solution are related to the values at the origin by the relation (7.58) with Eqs. (7.59a) and (7.59b), that is,

$$(\hat{p}_{\rm s})_0 = \hat{p}_\infty g_p((M_{\rm s})_0, M_\infty), \quad (\hat{T}_{\rm s})_0 = \hat{T}_\infty g_T((M_{\rm s})_0, M_\infty), \tag{7.75}$$

with

$$g_p((M_{\rm s})_0, M_\infty) = 1 + \frac{5}{4}((M_{\rm s})_0 - M_\infty), \tag{7.76a}$$

$$g_T((M_{\rm s})_0, M_\infty) = 1 + \frac{1}{2}((M_{\rm s})_0 - M_\infty), \tag{7.76b}$$

where $M_\infty \le (M_{\rm s})_0 \le -2 - M_\infty$ for the weak shock wave and $(M_{\rm s})_0 \le M_\infty$ for the supersonic accelerating flow. For a given $[(M_{\rm s})_0, (\hat{p}_{\rm s})_0, (\hat{T}_{\rm s})_0]$, the state $(M_\infty, \hat{p}_\infty, \hat{T}_\infty)$ allowed by the above relation is a one-parameter (say, M_∞) family, or a curve in $(M_\infty, \hat{p}_\infty, \hat{T}_\infty)$ space, i.e.,

$$\hat{p}_\infty = (\hat{p}_{\rm s})_0 g_p(M_\infty, (M_{\rm s})_0), \quad \hat{T}_\infty = (\hat{T}_{\rm s})_0 g_T(M_\infty, (M_{\rm s})_0), \tag{7.77}$$

where the range of the parameter M_∞ is $M_\infty \le \min[(M_{\rm s})_0, -2 - (M_{\rm s})_0]$ for the weak shock wave and $(M_{\rm s})_0 \le M_\infty \le -1$ for the supersonic accelerating flow. It may be noted that the slowly varying solution in the half space ($0 \le x_1 < \infty$) degenerates into the uniform state $M_{\rm s} = (M_{\rm s})_0$ in the two cases $M_\infty = -2 - (M_{\rm s})_0$ for $(M_{\rm s})_0 \ge -1$ and $M_\infty = (M_{\rm s})_0$ for $(M_{\rm s})_0 \le -1$. The latter is obvious, and the former is because the downstream infinity is set at the origin and the structure of the weak shock wave shifts to upstream infinity.

The solution $\hat{f}$ of the original half-space problem is obtained with these $\hat{f}^*$ and $\hat{f}_{\rm s}$ by Eq. (7.64). As is obvious from Eqs. (7.64) and (7.65b), $\hat{f} \to \hat{f}_{\rm s}$ as $x_1 \to \infty$, and thus $(M_\infty, \hat{p}_\infty, \hat{T}_\infty)$ given by Eq. (7.77) are the corresponding values of $\hat{f}$. In view of the one-parameter family relation (7.77), the dimension of the set $(M_\infty, \hat{p}_\infty, \hat{T}_\infty)$ that allows a solution $\hat{f}$ of the half-space problem is three, because the set $((M_{\rm s})_0, (\hat{p}_{\rm s})_0, (\hat{T}_{\rm s})_0)$ that allows a Knudsen-layer-type solution is given by Eq. (7.74). In the two degenerate cases $M_\infty = -2 - (M_{\rm s})_0$ $[(M_{\rm s})_0 \ge -1]$ and $M_\infty = (M_{\rm s})_0$ (≤ -1) mentioned at the end of the preceding paragraph, the solution $\hat{f}$ is given by $\hat{f}^*$ itself, and no new flow is created. Especially, in the former case, M of $\hat{f}$ at infinity is given by M_∞ $[= -2 - (M_{\rm s})_0]$ when M_∞ is approaching $-2 - (M_{\rm s})_0$, but M of $\hat{f}$ at infinity is $(M_{\rm s})_0$ at $M_\infty = -2 - (M_{\rm s})_0$. This fact is important to discuss the existence range of a solution in the next section.

In Figs. 7.4 and 7.5, we give some examples of the solution constructed from a subsonic or supersonic Knudsen-layer-type solution of the BKW equation under the complete-condensation condition. In these figures, the results are compared with the numerical results of the original half-space problem, i.e., Eqs. (7.2)–(7.4). The figures are taken from Sone, Golse, Ohwada & Doi [1998] with necessary transcriptions.

We can construct the solution of the half-space problem with nonzero $\hat{v}_{2\infty}$ and $\hat{v}_{3\infty}$ at infinity on the basis of Eq. (7.62) by a process similar to the foregoing one (see Bardos, Golse & Sone [2006]).

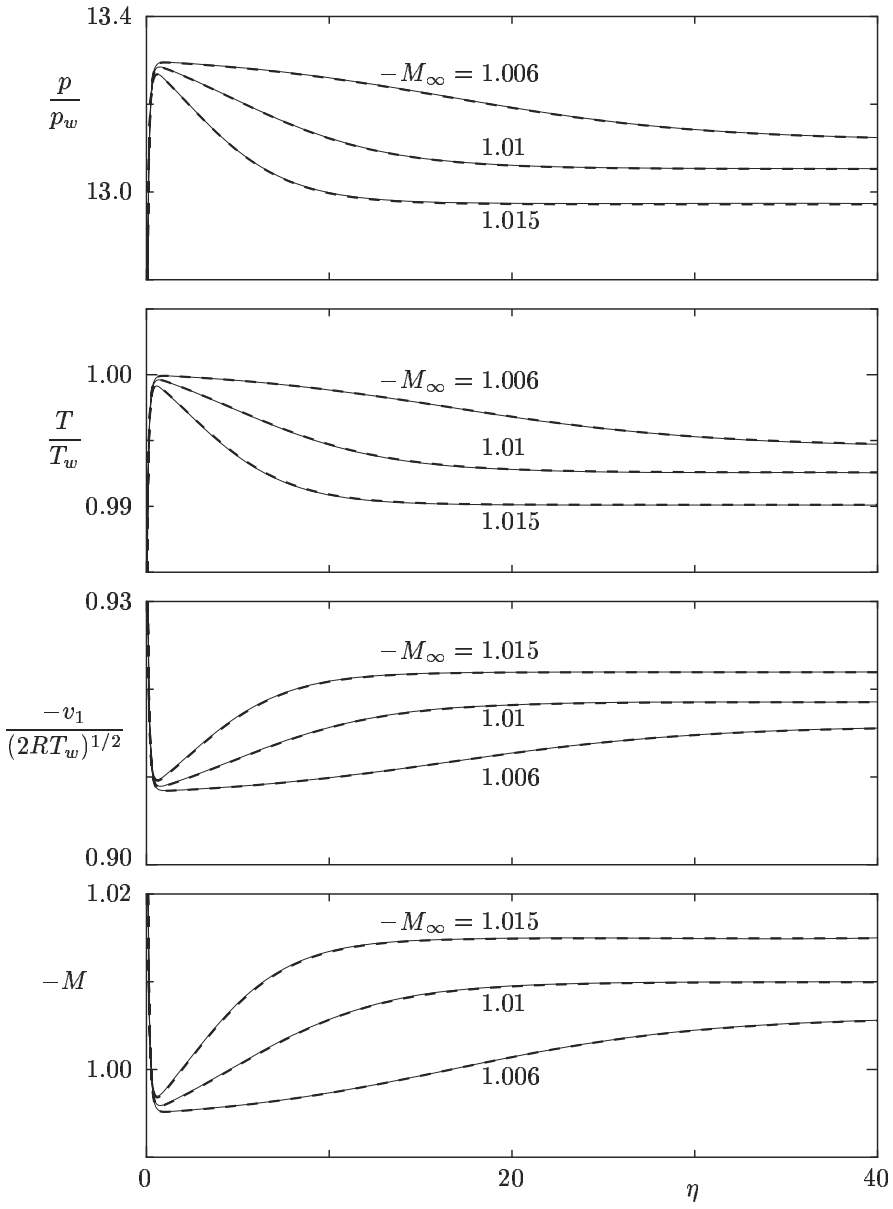

Figure 7.4. Various supersonic solutions generated from a subsonic Knudsen-layer-type solution $\hat{f}^*$ that takes $(M_s)_0 = -0.995$ and $(\hat{T}_s)_0 = 1$ [thus $(\hat{p}_s)_0 = 13.29786$] at $\eta = \infty$. The solid lines — indicate supersonic solutions for the BKW equation constructed by the recipe explained in Section 7.3.3. The dashed lines --- indicate numerical solutions with the corresponding values of M_∞, p_∞/p_w, and T_∞/T_w.

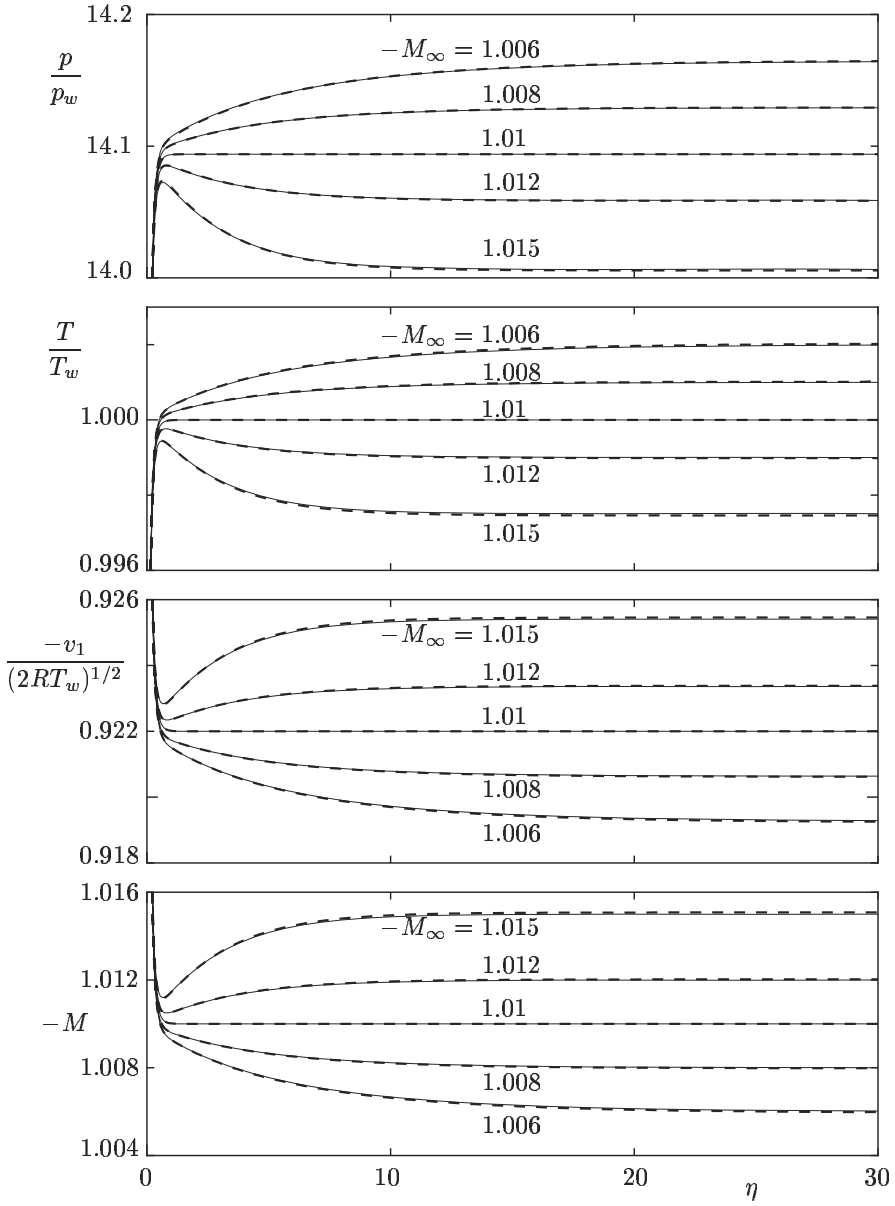

Figure 7.5. Various supersonic solutions generated from a supersonic Knudsen-layer-type solution $\hat{f}^*$ that takes $(M_s)_0 = -1.01$ and $(\hat{T}_s)_0 = 1$ [thus $(\hat{p}_s)_0 = 14.093889$] at $\eta = \infty$. The solid lines — indicate supersonic solutions for the BKW equation constructed by the recipe explained in Section 7.3.3. The dashed lines - - - indicate numerical solutions with the corresponding values of M_∞, p_∞/p_w, and T_∞/T_w. For the present $\hat{f}^*$, the slowly varying part of a solution is an accelerating flow if $M_\infty \geq -1.01$ and a weak shock wave if $M_\infty \leq -1.01$.

7.3.4 Existence range of a solution

Now we will discuss the range of the parameters $(M_\infty, \hat{p}_\infty, \hat{T}_\infty)$ in which the half-space problem has a solution. Substituting the relation (7.75) into the condition (7.74), we have

$$\hat{p}_\infty g_p((M_\mathrm{s})_0, M_\infty) = F_S((M_\mathrm{s})_0, \hat{T}_\infty g_T((M_\mathrm{s})_0, M_\infty)).$$

The relation is simplified in a neighborhood of the B-curve ($|M_\mathrm{s}+1| \ll 1$, $|M_\infty+1| \ll 1$) as

$$\hat{p}_\infty = F_S + \frac{\partial F_S}{\partial a_1}(M_\infty+1) + \left(-\frac{5}{4}F_S + \frac{\partial F_S}{\partial a_1} + \frac{1}{2}\frac{\partial F_S}{\partial a_2}\hat{T}_\infty\right)[(M_\mathrm{s})_0 - M_\infty], \quad (7.78)$$

where a_1 and a_2 are, respectively, the first and second arguments of F_S, that is, $F_S(a_1, a_2)$, and the function F_S and its derivatives $\partial F_S/\partial a_1$ and $\partial F_S/\partial a_2$ are evaluated at $(a_1, a_2) = (-1, \hat{T}_\infty)$. This is the relation among M_∞, $\hat{p}_\infty$, and $\hat{T}_\infty$ for which a solution of the half-space problem exists. This equation contains the parameter $(M_\mathrm{s})_0$ of the slowly varying solution. According to Eqs. (7.60a) and (7.60b), this parameter $(M_\mathrm{s})_0$ may take any value in the range

$$M_\infty \le (M_\mathrm{s})_0 < -(2+M_\infty) \quad \text{(weak shock wave)}, \quad (7.79a)$$

$$(M_\mathrm{s})_0 \le M_\infty \qquad \text{(supersonic accelerating flow)}, \quad (7.79b)$$

where the case $(M_\mathrm{s})_0 = -(2+M_\infty)$, included in Eq. (7.60a), is excluded, because the structure of the weak shock wave shifts to upstream infinity and no new solution is created as explained in the paragraph containing Eq. (7.77) of Section 7.3.3. Thus, the solution exists in the domain of $(M_\infty, \hat{p}_\infty, \hat{T}_\infty)$ given by the relations

$$\hat{p}_\infty = F_S + (M_\infty+1)\left(\frac{5}{2}F_S - \frac{\partial F_S}{\partial a_1} - \frac{\partial F_S}{\partial a_2}\hat{T}_\infty\right) + t\left(\frac{5}{4}F_S - \frac{\partial F_S}{\partial a_1} - \frac{1}{2}\frac{\partial F_S}{\partial a_2}\hat{T}_\infty\right), \quad (7.80a)$$

$$t > 0, \quad (7.80b)$$

where the parameter t is related to the parameter $(M_\mathrm{s})_0$ in Eq. (7.78) by $t = -(M_\mathrm{s})_0 - (2+M_\infty)$. Figure 7.1 corresponds to the case $5F_S/2 - \partial F_S/\partial a_1 - \hat{T}_\infty \partial F_S/\partial a_2 > 0$ and $5F_S/4 - \partial F_S/\partial a_1 - (\hat{T}_\infty/2)\partial F_S/\partial a_2 > 0$. In the figure, the region between $p_\infty/p_w = F_b$ and $p_\infty/p_w = F_{es}$ corresponds to $0 < t < -2(1+M_\infty)$, the surface $p_\infty/p_w = F_{es}$ to $t = -2(1+M_\infty)$, and the region above $p_\infty/p_w = F_{es}$ to $t > -2(1+M_\infty)$. For the BKW equation under the complete-condensation condition, $\partial F_S/\partial a_1$ and $\partial F_S/\partial a_2$ are both negative at $(a_1, a_2) = (-1, \hat{T}_\infty)$ so that the coefficient of t in Eq. (7.80a) is positive. Thus the solution exists in the region

$$\hat{p}_\infty > F_S + (M_\infty+1)\left(\frac{5}{2}F_S - \frac{\partial F_S}{\partial a_1} - \frac{\partial F_S}{\partial a_2}\hat{T}_\infty\right). \quad (7.81)$$

As discussed in the last paragraph but two of Section 7.3.3, the state (M_∞, $\hat{p}_\infty$, $\hat{T}_\infty$) given by Eq. (7.80a) with $t = 0$ corresponds to the upstream infinity of the weak shock wave whose downstream infinity is given by the state $[(M_\mathrm{s})_0, (\hat{p}_\mathrm{s})_0, (\hat{T}_\mathrm{s})_0]$. That is, a point on the surface $p_\infty/p_w = F_b(M_\infty, T_\infty/T_w)$ in Fig. 7.1 is related to some point on the surface $p_\infty/p_w = F_s(M_\infty, T_\infty/T_w)$ by the shock condition (or the Rankine–Hugoniot relation).

7.3.5 Supplementary discussion

In Sections 7.3.3 and 7.3.4, we constructed the solution with a slowly varying part of the half-space problem from a given Knudsen-layer-type solution, from which the range of the parameters where a solution exists is derived. On the basis of these results, the solution of the half-space problem when the parameters M_∞, $\hat{p}_\infty$, and $\hat{T}_\infty$ at infinity are given is obtained in the following process. First obtain t from Eq. (7.80a) for a given set of (M_∞, $\hat{p}_\infty$, $\hat{T}_\infty$). If $t \leq 0$, there is no solution. In the other case ($t > 0$), obtain $(M_\mathrm{s})_0$, $(\hat{p}_\mathrm{s})_0$, and $(\hat{T}_\mathrm{s})_0$ from the relation $(M_\mathrm{s})_0 = -(2+M_\infty)-t$ and Eq. (7.75) with Eqs. (7.76a) and (7.76b), and determine the value of X at which M_s takes the value $(M_\mathrm{s})_0$ from Eq. (7.57f). This X is chosen as $-X_0$, and then the slowly varying solution takes $(M_\mathrm{s})_0$, $(\hat{p}_\mathrm{s})_0$, and $(\hat{T}_\mathrm{s})_0$ at $x_1 = 0$. The desired slowly varying solution $\hat{f}_\mathrm{s}$ is given by Eq. (7.57a) with Eqs. (7.57b)–(7.57g).[9] The function $\hat{S}(X)$ there is $\tanh X$ for $0 < t < -2(1 + M_\infty)$ or $\coth X$ for $t > -2(1 + M_\infty)$. The data $(M_\mathrm{s})_0$, $(\hat{p}_\mathrm{s})_0$, and $(\hat{T}_\mathrm{s})_0$ thus obtained satisfy the relation (7.74). Thus, the Knudsen-layer-type solution $\hat{f}^*$ exists.

Choose the condition $(M_\infty, \hat{p}_\infty, \hat{T}_\infty)$ at infinity in the region where $t > -2(1 + M_\infty)$ and $|1 + M_\infty| \ll |\hat{p}_\infty - \hat{p}_B|/\hat{p}_B$, where $\hat{p}_B = F_S(-1, \hat{T}_\infty)$. Then, $|1 + M_\infty| \ll |(M_\mathrm{s})_0 - M_\infty|$, because $|(M_\mathrm{s})_0 - M_\infty|$ is of the same order as $|\hat{p}_\infty - \hat{p}_B|/\hat{p}_B$ owing to Eq. (7.78). In view of this condition, from Eq. (7.57f), $\hat{S}(X) = \coth X \gg 1$ near $M_\mathrm{s} = (M_\mathrm{s})_0$; thus, $|X| \ll 1$ and $|\mathrm{d}\hat{S}/\mathrm{d}X| \gg 1$. The slowly varying condition is violated there. Therefore, the analysis in Sections 7.3.2 and 7.3.3 is required refinement in the wedge region $|1 + M_\infty| \ll |\hat{p}_\infty - \hat{p}_B|/\hat{p}_B$. Some information about the behavior of the solution in the wedge region can be obtained from the result of Section 7.3.2, though it is incomplete in the region. The function $\coth X$ being approximated by $1/X$ there, $(1 + M_\infty)/X = M_\mathrm{s} + 1$ from Eq. (7.57f). Thus, from Eq. (7.57g), $X_0 = -(1 + M_\infty)/[(M_\mathrm{s})_0 + 1]$ at $\eta = 0$ and $X = (1 + M_\infty)\{-c_0\eta + [(M_\mathrm{s})_0 + 1]^{-1}\}$ (c_0: a positive constant). Consider the range of η where $|1+M_\infty|\eta \ll 1$ as well as $|1+M_\infty| \ll 1$, for which η can be very large. The function $(1 + M_\infty)\hat{S}(X)$ is $1/\{-c_0\eta + [(M_\mathrm{s})_0 + 1]^{-1}\}$. The solution is expected to decay as $1/c_0\eta$.

[9] In the relation (7.57g) between X and x_1, $\hat{\rho}_B$ and $\hat{T}_B$, including the argument $\hat{T}_B$ of Γ_1 and Γ_2, can be taken as $\hat{\rho}_\infty$ and $\hat{T}_\infty$ respectively in the present order of approximation (see Footnote 7 in Section 7.3.2).

Chapter 8

Ghost Effect and Bifurcation I: Bénard and Taylor–Couette Problems

In this chapter, typical bifurcation problems in classical fluid dynamics, the Bénard and Taylor–Couette problems, and related problems, are discussed on the basis of kinetic theory. In addition to the study of the effect of gas rarefaction in the Bénard problem, its behavior in the continuum limit is revisited in the framework of the asymptotic theory in Section 3.3 and is shown not to be correctly described by the classical fluid dynamics. In the Taylor–Couette problem, the effect of difference of the temperatures of the two cylinders is studied in the continuum limit on the basis of the asymptotic theory, and as in the Bénard problem, the classical fluid dynamics is shown to fail its correct description. The ghost and non-Navier–Stokes effects discussed in Section 3.3 play a central role in these bifurcations in the continuum limit. In the same geometrical configuration as the Taylor–Couette problem, we consider the bifurcation when the two cylinders are made of the condensed phase of the gas. Then, evaporation and condensation take place on the cylinders. Owing to the evaporation and condensation, bifurcation takes place in the simplest case where the field is axially symmetric and uniform. When the restriction of axial uniformity is eliminated, Taylor–Couette roll type of flow can stably exist in addition to the axially uniform flow.

8.1 Bénard problem I: Finite Knudsen number

8.1.1 Introduction

The Bénard problem (Bénard [1901], Rayleigh [1916]) concerning the instability of a layer of fluid heated from below has long been of interest to many scientists and engineers. In addition to a lot of works on the basis of classical fluid

dynamics (see, e.g., Chandrasekhar [1961], Koschmieder [1993], Bodenschatz, Pesch & Ahlers [2000]), the problem is also studied on the basis of kinetic theory (Garcia & Penland [1991], Stefanov & Cercignani [1992], Sone, Aoki, Sugimoto & Motohashi [1995], Sone, Aoki & Sugimoto [1997, 1999], Sone & Doi [2003a], etc.). The kinetic-theory works give not only the information of the gas rarefaction but also the important results for a gas in the continuum limit which are not reported in the classical fluid-dynamic approach or are not described correctly by it. First, in Section 8.1, we will discuss the Bénard problem of a gas of a finite Knudsen number. The behavior of the gas in the continuum limit, which shows the incompleteness of the classical fluid dynamics, will be discussed in the next section (Section 8.2).

Consider a gas in a rectangular domain ($0 < X_1 < L$, $0 < X_2 < D$), where the gas is subject to a uniform gravitational force in the negative X_2 direction, i.e., the acceleration g_i of gravity is $(0, -g, 0)$ with $g > 0$, the lower boundary at $X_2 = 0$ is at rest and is heated at a uniform temperature T_h, and the upper at $X_2 = D$ is at rest and is cooled at a uniform temperature T_c. We discuss the behavior of the gas on the basis of the numerical analyses carried out by a finite-difference method under the assumptions: (i) the behavior of the gas is described by the BKW equation; (ii) the molecules make the diffuse reflection on the upper and the lower boundaries; (iii) the molecules make the specular reflection on the side boundaries; (iv) the initial condition is appropriately chosen; and (v) the field of the gas is two dimensional, i.e., uniform in X_3. Let us list the basic equation and boundary conditions, which are given in Chapter 1, for the convenience of explanation. The BKW equation with the gravity is

$$\frac{\partial f}{\partial t} + \xi_1 \frac{\partial f}{\partial X_1} + \xi_2 \frac{\partial f}{\partial X_2} - g \frac{\partial f}{\partial \xi_2} = A_c \rho (f_e - f), \tag{8.1}$$

$$f_e = \frac{\rho}{(2\pi RT)^{3/2}} \exp\left(-\frac{(\xi_i - v_i)^2}{2RT} \right),$$

where ρ, v_i, and T are determined by f. The boundary conditions on the lower and upper boundaries are, at $X_2 = 0$,

$$f(X_1, 0, \xi_i, t) = \frac{\sigma_h}{(2\pi RT_h)^{3/2}} \exp\left(-\frac{\xi_i^2}{2RT_h} \right) \quad (\xi_2 > 0), \tag{8.2}$$

$$\sigma_h = -\left(\frac{2\pi}{RT_h} \right)^{1/2} \int_{\xi_2 < 0} \xi_2 f \, \mathbf{d}\boldsymbol{\xi},$$

and, at $X_2 = D$,

$$f(X_1, D, \xi_i, t) = \frac{\sigma_c}{(2\pi RT_c)^{3/2}} \exp\left(-\frac{\xi_i^2}{2RT_c} \right) \quad (\xi_2 < 0), \tag{8.3}$$

$$\sigma_c = \left(\frac{2\pi}{RT_c} \right)^{1/2} \int_{\xi_2 > 0} \xi_2 f \, \mathbf{d}\boldsymbol{\xi}.$$

The conditions on the side boundaries are commonly in the form

$$f(X_1, X_2, \xi_1, \xi_2, \xi_3, t) = f(X_1, X_2, -\xi_1, \xi_2, \xi_3, t) \\ (\xi_1 > 0) \ \text{ at } X_1 = 0 \text{ and } \ (\xi_1 < 0) \ \text{ at } X_1 = L. \tag{8.4}$$

The initial condition is

$$f(X_1, X_2, \xi_1, \xi_2, \xi_3, 0) = f_0 \quad \text{at } t = 0,$$

where f_0 is appropriately chosen depending on situations. The data in this section (Section 8.1) are taken from Sone, Aoki, Sugimoto & Motohashi [1995] and Sone, Aoki & Sugimoto [1997, 1999].

Let ρ_0 be the average density of the gas over the domain. Taking D, T_h, ρ_0, and $D/(2RT_h)^{1/2}$, respectively, as the reference length L, reference temperature T_0, reference density ρ_0, and reference time t_0 in Section 1.9, we find that the problem is characterized by the initial condition and the four parameters

$$\left.\begin{array}{ll} \text{Knudsen number Kn}: & (8RT_h/\pi)^{1/2}/(A_c\rho_0 D) = \ell_0/D, \\ \text{Froude number Fr}: & 2RT_h/Dg, \\ \text{Temperature ratio}: & T_c/T_h, \\ \text{Aspect ratio}: & L/D, \end{array}\right\} \tag{8.5}$$

where ℓ_0 is the mean free path of the gas in the equilibrium state at rest with density ρ_0 and temperature T_h.

8.1.2 Existence range of nonstationary solutions and their flow patterns

The system has a time-independent and spatially one-dimensional solution, uniform in X_1 and X_3, without flow ($v_i = 0$) for any set of parameters. Let us call the solution 1D solution and denote its velocity distribution function, density, and temperature, respectively, by f_U, ρ_U, and T_U. Depending on the strength of the gravity, the 1D solution f_U is classified into three types, type I: for strong gravity (or small Fr), the density ρ_U decreases as X_2 increases; type II: for weak gravity (or large Fr), ρ_U increases as X_2 increases; and type III: for the gravity of intermediate strength (or intermediate Fr), ρ_U first decreases, reaches its minimum, and then increases as X_2 increases.

Our interest is the possibility of another type of solution with nonzero flow velocity. For this purpose, the initial and boundary-value problem of the BKW equation stated in the preceding subsection (Section 8.1.1) is considered for the initial condition f_0

$$f_0 = \frac{\rho}{(2\pi RT)^{3/2}} \exp\left(-\frac{\xi_i^2}{2RT}\right), \tag{8.6a}$$

$$\rho = \rho_U(X_2), \qquad T = T_U(X_2)\left(1 + \varepsilon \cos\frac{\pi X_1}{L} \sin\frac{\pi X_2}{D}\right). \tag{8.6b}$$

Incidentally, the Maxwell distribution with ρ and T given by Eq. (8.6b) is noted not to satisfy the Boltzmann equation or BKW equation with the gravity.

The time evolution of the solution of the initial and boundary-value problem is studied numerically. From the long-time behavior of the solution, it is found that the solution approaches the 1D solution or a nonstationary solution depending on the parameters chosen. The diagram of the type of solutions in the case $L/D = 1$ and $\varepsilon = 0.5$ is shown for various Knudsen numbers in Fig. 8.1. For these parameters, the nonstationary solutions are time-independent single-roll-type solutions. In the figures, the symbol $\bullet$ indicates the 1D solution and $\circ$ the time-independent solution with a convection roll. A time-independent solution with a convection roll exists in a "triangular region" in the (Fr, T_c/T_h) plane. The region shrinks rapidly as the Knudsen number increases. According to the linear stability analysis based on the Boussinesq approximation of the Navier–Stokes equation, Rayleigh number $\mathrm{Ra} \approx 1700$ is the critical value above which the stationary solution is unstable (see, e.g., Chandrasekhar [1961]), where Ra is defined by

$$\mathrm{Ra} = \frac{16}{\pi \mathrm{Fr} \mathrm{Kn}^2} \left(\frac{T_h}{T_c} - 1 \right),$$

in terms of T_c/T_h, Fr, and Kn. The curve $\mathrm{Ra} = 1700$ is indicated by a dashed line in Fig. 8.1.[1] The dot-dash line in Fig. 8.1 indicates the approximate boundary of type I and type III of the 1D solution explained above.

Figure 8.1 is based on a special initial condition, Eqs. (8.6a) and (8.6b) with $\varepsilon = 0.5$, which is expected to induce a flow with a single roll. Therefore, in the triangular region of $\circ$ sign, another type of flow may take place. Similarly, in the region of $\bullet$ sign, the existence of a flow is not excluded. However, various tests, though not systematic, using different types of initial condition show that it is unlikely to exist in this region. The left-side boundary of two types of solutions, $\bullet$ and $\circ$, is first pointed out by kinetic-theory analysis.

Examples of the field of the single roll-type flow are shown in Figs. 8.2 (a), (b), and (c), where the fields of three Fr's, corresponding to three types of the 1D solution, are compared.

8.1.3 Array of rolls and its stability

Let us consider a time-independent solution $f(X_1, X_2, \xi_i)$ of the boundary-value problem, Eqs. (8.1)–(8.4), for $L = L_0$. Then, it can be shown with the help of Eq. (8.1) and the boundary condition (8.4) that $\partial^{2n} f / \partial X_1^{2n}$ are even and $\partial^{2n+1} f / \partial X_1^{2n+1}$ are odd with respect to ξ_1 at $X_1 = 0$ and L_0, where $n = 0, 1, 2, \ldots$. Now let us extend the function f to the region $0 < X_1 < 2L_0$ in such a manner that the part for $L_0 < X_1 < 2L_0$ is the mirror image of the part $0 < X_1 < L_0$, namely, by the rule

$$f(X_1, X_2, \xi_1, \xi_2, \xi_3) = f(2L_0 - X_1, X_2, -\xi_1, \xi_2, \xi_3) \quad (L_0 < X_1 < 2L_0). \tag{8.7}$$

[1] The curve based on Boussinesq approximation has meaning only when $|T_c/T_h - 1| \ll 1$. Further, the extension of the curve away from $T_c/T_h = 1$ is not unique because there is no difference between $(T_c - T_h)/T_h$ and $(T_c - T_h)/T_c$ in the Boussinesq approximation.

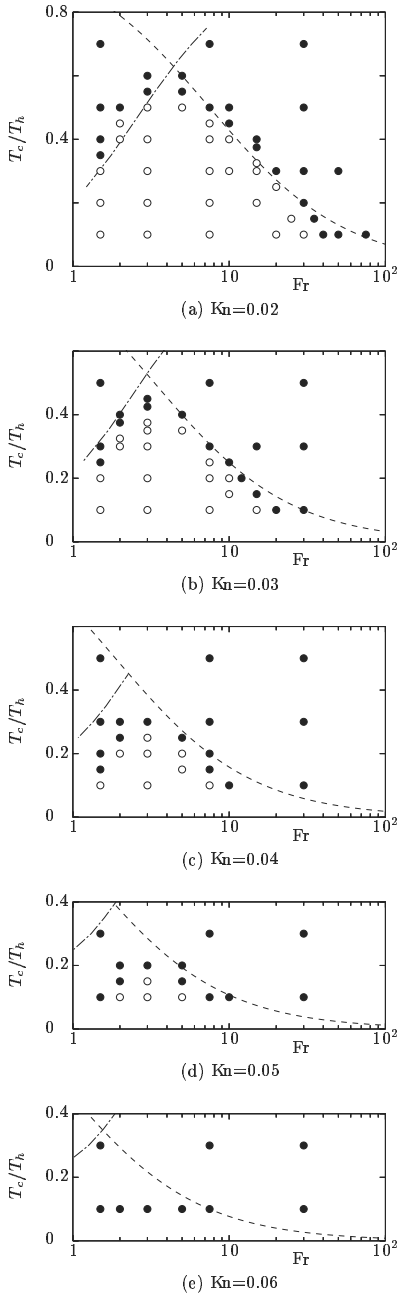

Figure 8.1. The range of the parameters Fr and T_c/T_h where a convection roll exists ($L/D = 1$ and $\varepsilon = 0.5$). (a) Kn = 0.02, (b) Kn = 0.03, (c) Kn = 0.04, (d) Kn = 0.05, and (e) Kn = 0.06. The white circle ∘ indicates that convection occurs there; the black circle • indicates that no flow occurs. See the main text for the dashed line - - - and the dot-dash line –·–.

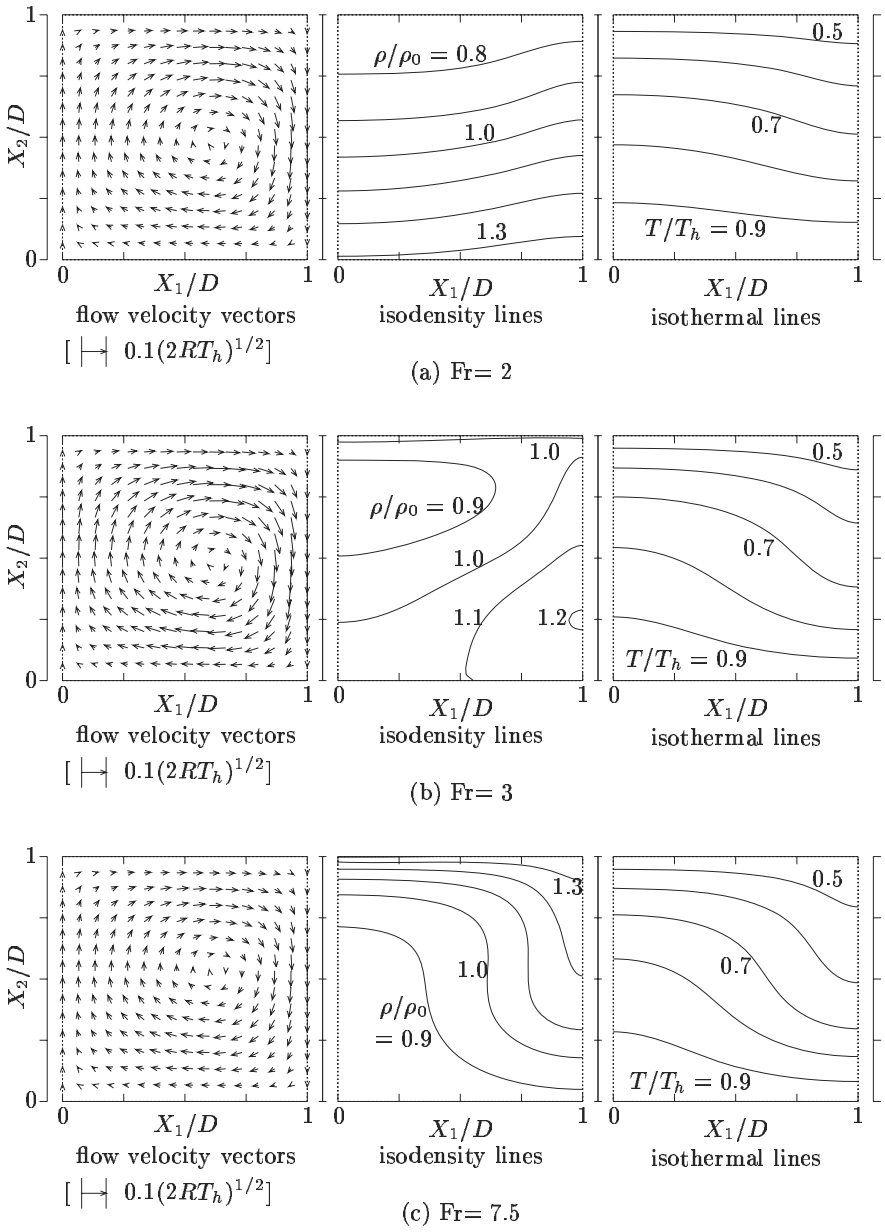

Figure 8.2. Flow velocity, isodensity lines, and isothermal lines ($L/D = 1$, $T_c/T_h = 0.4$, Kn $= 0.02$). (a) Fr $= 2$, (b) Fr $= 3$, and (c) Fr $= 7.5$. The contours of $\rho/\rho_0 = 0.1n$ and $T/T_h = 0.1m$ are shown in the figures. The arrows indicate the flow velocity at their starting points; the scale $(v_i^2)^{1/2}/(2RT_h)^{1/2} = 0.1$ is shown in the figures. The arrow is not shown on the upper and lower boundaries.

Then, from the property of $\partial^{2n} f/\partial X_1^{2n}$ and $\partial^{2n+1} f/\partial X_1^{2n+1}$ at $X_1 = L_0$, the derivatives of the resulting function with respect to X_1 are shown to be continuous in any order at $X_1 = L_0$. Therefore, the extended function gives a time-independent solution of Eqs. (8.1)–(8.4) for $L = 2L_0$, i.e., in the wider domain $0 < X_1 < 2L_0$. In general, by arranging a series of time-independent solutions of a kind laterally in such a way that the adjacent solutions are the mirror images of each other, we can generate a time-independent solution in a wider domain. Therefore, the array f_a^N of the N time-independent solutions of a single roll f_a^1 in the domain with the aspect ratio $L/D = a$ so arranged forms a solution consisting of N rolls in the domain with $L/D = Na$. For example, $f_{3/4}^4$ and f_1^3 are solutions consisting, respectively, of four and three rolls in the domain with $L/D = 3$. Here, for even N, we should discriminate two types of solutions, type A, where the leftmost roll is clockwise, and type B, where the leftmost roll is anti-clockwise. Hereafter, the type A is denoted by f_a^N and type B by $\overline{f_a^N}$.

The multiroll solution thus constructed may be unstable, even when the constituent single-roll solution is stable. We will discuss this problem. That is, taking a perturbed velocity distribution function of a time-independent multiroll solution f_a^N or $\overline{f_a^N}$ as the initial condition f_0, we pursue the time evolution of the distribution f and examine whether the distribution returns to the original multiroll solution or is transformed into a different flow pattern. As the perturbed distribution of the multiroll distribution, the following distribution is chosen: for even rolls (or even N),

$$f_0 = \left[1 - \varepsilon \sin\left(\frac{N\pi}{L} X_1\right)\right] f_{L/ND}^N, \tag{8.8}$$

and

$$= \left[1 - \varepsilon \sin\left(\frac{N\pi}{L} X_1\right)\right] \overline{f_{L/ND}^N}, \tag{8.9}$$

and for odd rolls (or odd N),

$$f_0 = \left[1 + \delta - \varepsilon \sin\left(\frac{N\pi}{L} X_1\right)\right] f_{L/ND}^N, \tag{8.10}$$

where ε is a parameter characterizing the size of the perturbation, and δ is a constant introduced to make the mass of the gas in the domain for the perturbed distribution equal to that for the original distribution, and thus determined by ε and $f_{L/ND}^N$. It is noted that the flow velocity and temperature fields are not perturbed for the above perturbed distributions (8.8)–(8.10).

The numerical computation of the stability analysis is carried out for the two- to six-roll solutions (two kinds of solutions for the even-roll solutions) to find the stable range with respect to the aspect ratio L/D of the domain with the other parameters fixed at $\mathrm{Fr} = 3$, $T_c/T_h = 0.4$, and $\mathrm{Kn} = 0.02$. The size ε of the perturbation is taken to be 0.01 for Eqs. (8.8) and (8.9), and $\varepsilon = 0.01$ and $\varepsilon = -0.01$ for Eq. (8.10) because the perturbations with ε of different signs have

Table 8.1. Stability of 2-roll solutions $f^2_{L/2D}$ and $\overline{f^2_{L/2D}}$ (Fr = 3, $T_c/T_h = 0.4$, and Kn = 0.02). The type of the limiting solution as $t \to \infty$ from the initial condition (8.8) or (8.9) is shown for various $L/2D$'s. The symbols **S**, **D**, and **T** show that the limiting solution is $f^M_{L/MD}$ with $M = 1, 2,$ and 3 respectively, and the bar over the letter represents $\overline{f^M_{L/MD}}$.

	$L/2D$							
N	0.55	0.6	0.68	0.685	0.7	1.3	1.35	1.36
2			**S**	**D**	**D**	**D**	$\overline{\mathbf{T}}$	
$\overline{2}$	**S**	$\overline{\mathbf{D}}$			$\overline{\mathbf{D}}$		$\overline{\mathbf{D}}$	$\overline{\mathbf{D}}$

Table 8.2. Stability of N-roll solutions $f^N_{L/ND}$ and $\overline{f^N_{L/ND}}$ ($N = 3, 4, 5, 6$; Fr = 3, $T_c/T_h = 0.4$, and Kn = 0.02). The type of the limiting solution as $t \to \infty$ from the initial condition (8.8), (8.9), or (8.10) is shown for various L/ND's and N's. The symbols **D**, **T**, **Q**, **V**, **VI**, **VII**, and **VIII** show that the limiting solution is $f^M_{L/MD}$ with $M = 2, 3, 4, 5, 6, 7,$ and 8, respectively, and the bar over the letter represents $\overline{f^M_{L/MD}}$.

	L/ND									
N	0.6	2/3	0.725	0.75	0.8	1.0	1.2	1.275	4/3	1.35
3+	**D**	**D**	**T**		**T**	**T**	**T**	**T**	$\overline{\mathbf{Q}}$	
3−	$\overline{\mathbf{D}}$	$\overline{\mathbf{D}}$	**T**		**T**	**T**	**T**	**T**	**V**	
4	**T**	**T**	**Q**		**Q**	**Q**	**Q**	**Q**		$\overline{\mathbf{V}}$
$\overline{4}$	**T**	**T**	$\overline{\mathbf{Q}}$		$\overline{\mathbf{Q}}$	$\overline{\mathbf{Q}}$	$\overline{\mathbf{Q}}$	$\overline{\mathbf{Q}}$		$\overline{\mathbf{VI}}$
5+	**T**	**Q**		**V**	**V**	**V**	**V**	**V**		$\overline{\mathbf{VI}}$
5−	$\overline{\mathbf{Q}}$	$\overline{\mathbf{Q}}$		**V**	**V**	**V**	**V**	**V**		**VII**
6	**T**	**V**		**VI**	**VI**	**VI**	**VI**	**VI**	$\overline{\mathbf{VII}}$	
$\overline{6}$	**Q**	**V**		$\overline{\mathbf{VI}}$	$\overline{\mathbf{VI}}$	$\overline{\mathbf{VI}}$	$\overline{\mathbf{VI}}$	$\overline{\mathbf{VI}}$	$\overline{\mathbf{VIII}}$	

different effects on the odd rolls. The basic method of numerical computation is explained in Sone, Aoki & Sugimoto [1997]. In all the cases, the flow converges to a time-independent multiroll solution consisting of single-roll solutions of an equal size, i.e., $f^M_{L/MD}$ or $\overline{f^M_{L/MD}}$ with M the same as or different from N in the initial condition. The type of flow established finally is shown in Tables 8.1 and 8.2, where the following symbols for the flow patterns are used: **S**, **D**, **T**, **Q**, **V**, **VI**, **VII**, and **VIII** show that the limiting solution is $f^M_{L/MD}$ with $M = 1, 2, 3, 4, 5, 6, 7,$ and 8, respectively, and the bar over the letter is used to represent $\overline{f^M_{L/MD}}$. In the leftmost column, the initial condition (8.9) is discriminated by the bar over the number N, and the positive or negative ε in Eq. (8.10) is indicated by + or − after N. Examples of transition to a different type of solution are shown in Figs. 8.3 and 8.4.

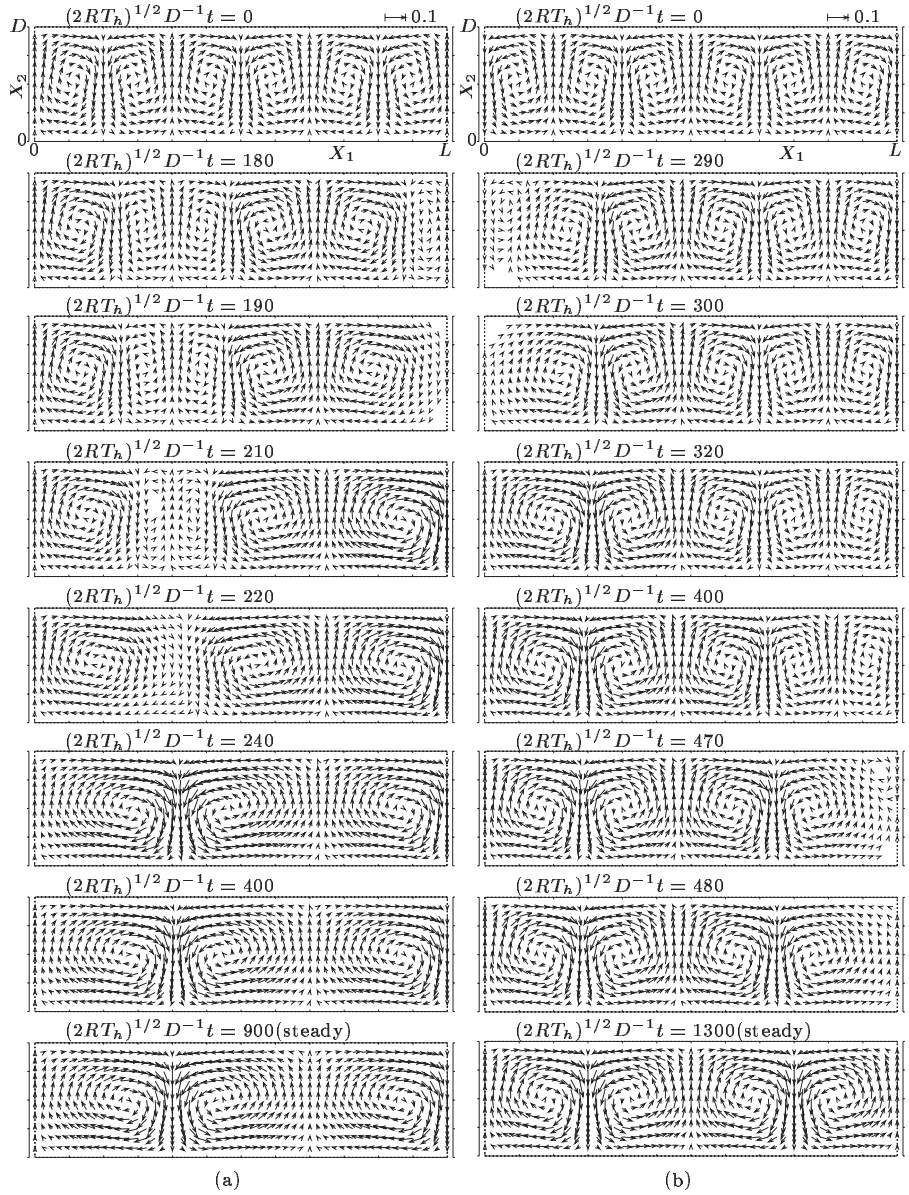

Figure 8.3. Transition process of the perturbed 6-roll solutions (8.8) and (8.9) with $\varepsilon = 0.01$ ($N = 6$, $L/D = 3.6$, $\mathrm{Fr} = 3$, $T_c/T_h = 0.4$, and $\mathrm{Kn} = 0.02$). (a) Initial condition (8.8) and (b) initial condition (8.9). The arrows indicate the flow velocity (v_1, v_2) at their starting points; the scale $(v_1^2 + v_2^2)^{1/2}/(2RT_h)^{1/2} = 0.1$ is shown in the figure. The arrow is not shown when $(v_1^2 + v_2^2)^{1/2}/(2RT_h)^{1/2} < 2 \times 10^{-3}$. The arrows on the upper and lower boundaries are omitted for clearness of the figure.

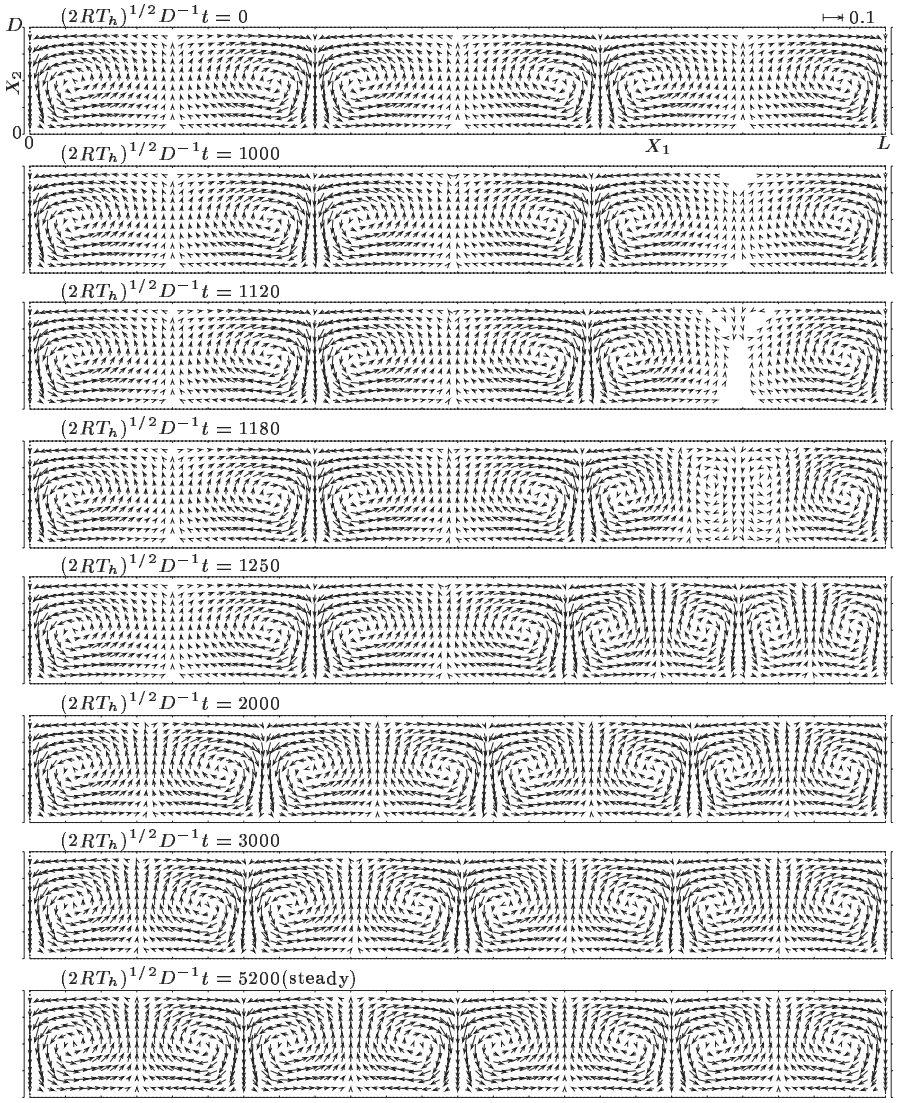

Figure 8.4. Transition process of the perturbed 6-roll solution (8.9) with $\varepsilon = 0.01$ ($N = 6$, $L/D = 8$, $\mathrm{Fr} = 3$, $T_c/T_h = 0.4$, and $\mathrm{Kn} = 0.02$). The arrows indicate the flow velocity (v_1, v_2) at their starting points; the scale $(v_1^2 + v_2^2)^{1/2}/(2RT_h)^{1/2} = 0.1$ is shown in the figure. The arrow is not shown when $(v_1^2 + v_2^2)^{1/2}/(2RT_h)^{1/2} < 2 \times 10^{-3}$. The arrows on the upper and lower boundaries are omitted for clearness of the figure.

8.2 Bénard problem II: Continuum limit

8.2.1 Introduction

In Section 3.3, we explained that the classical fluid dynamics is incomplete in describing the behavior of a gas in the continuum limit, that is, there is an important class of problems of a gas in the continuum limit that cannot be correctly described by the classical fluid dynamics. As its example, we will discuss the Bénard problem for a gas in the continuum limit, one of the most well-known and fundamental problems, on the basis of Sone & Doi [2003a] in this section.

Consider a gas in a time-independent state under a uniform gravity between two parallel plane walls at rest with different temperatures. The gravity is in the direction normal to the wall. Let D, T_h, T_c, ρ_0, g_i be, respectively, the distance between the walls, the temperature of the lower wall, that of the upper, the average density of the gas in the domain, and the acceleration of gravity (or gravity). We use the nondimensional variables defined in Section 1.9, with D and T_h as the reference length and temperature, instead of L and T_0 there. The Knudsen number Kn, or k, is based on the mean free path of the gas in the equilibrium state at rest with temperature T_h and the average density ρ_0 of the gas over the domain and the reference length D. The nondimensional gravity $\hat{g}_i = g_i D/2RT_h$ (see Section 3.3.1), whose magnitude (or $|\hat{g}_i|$) is the inverse of the Froude number Fr in Eq. (8.5), is used here. The coordinate system is taken in such a way that the lower wall is at $x_2 = 0$ and the upper wall is at $x_2 = 1$ and the gravity $\hat{g}_i$ is $(0, \hat{g}_2, 0)$ with $\hat{g}_2 < 0$. We are interested in the time-independent behavior of the gas in the limit that the Knudsen number Kn tends to zero (or $k \to 0$) for arbitrary values of T_c/T_h under the assumptions that the flow velocity $\hat{v}_i$ is of the order of k and the gravity $\hat{g}_2$ is of the second order of k (or say, $\hat{g}_2 = -\hat{g}k^2$), which corresponds to $\mathrm{Fr} = 1/\hat{g}k^2$ [see Eq. (8.5)]. Then, the behavior of the gas is described by the fluid-dynamic-type equations (3.155)–(3.158a), with $\hat{F}_{i2} = -\hat{g}\delta_{i2}$, and their associated boundary conditions (3.161a) and (3.161b) given in Section 3.3. The assumptions on the flow velocity and gravity are introduced by the following reasons: According to the discussion on the ghost effect in Section 3.3.4, an infinitesimal flow velocity of the first order of k produces a finite effect on the one-dimensional temperature field with parallel isothermal lines and $|T_c/T_h - 1|$ of the order unity, if it is induced by bifurcation. In view of the fluid-dynamic-type equations mentioned above, the bifurcation is expected to take place owing to the second-order infinitesimal gravity.

The analysis is limited to a two-dimensional case where the variables are independent of x_3 (or $\partial/\partial x_3 = 0$) and $\hat{v}_3 = 0$. The behavior in the limit that $\mathrm{Kn} \to 0$ being interested in, the variables $\hat{T}$, $\hat{\rho}$, u_i, and $\mathcal{P}$ (or $\mathcal{P}^*$) and the parameter $\hat{T}_B$ are, respectively, used for $\hat{T}_{SB0}$, $\hat{\rho}_{SB0}$, $\hat{v}_{iSB1}$, and $\hat{p}_{SB2}$ (or $\hat{p}^*_{SB2}$) and T_c/T_h. Thus, $\hat{\rho} = \hat{p}_0/\hat{T}$. The parameters included in Eqs. (3.155)–(3.158a), (3.161a), and (3.161b) are $\hat{T}_B$, $\hat{g}$, and $\hat{p}_0$. It may be better to add some comment on the parameter $\hat{p}_0$. At present, $\hat{p}_0$ is not specified in the problem stated above. The average density of the gas in the domain being taken as the reference density

ρ_0 in the definition of the nondimensional variables, the constant $\hat{p}_0$ is specified with the other parameters $\hat{T}_B$ and $\hat{g}$, but the explicit relation is given only after the solution is obtained. That is,

$$\hat{p}_0 = 1 \Big/ \left(\overline{1/\hat{T}}\right) , \tag{8.11}$$

where the bar — over $1/\hat{T}$ indicates its average over the domain.

8.2.2 One-dimensional solution

First consider the case where the behavior of the gas is uniform in the direction parallel to the walls (or $\partial/\partial x_1 = \partial/\partial x_3 = 0$). Then, the solution of Eqs. (3.155)–(3.158a) under the boundary conditions (3.161a) and (3.161b) is expressed in the form

$$\hat{T} = \hat{T}_U, \quad \hat{\rho} = \hat{\rho}_U = \hat{p}_0/\hat{T}_U, \tag{8.12a}$$

$$u_1 = u_2 = u_3 = 0, \tag{8.12b}$$

$$\mathcal{P} = \mathcal{P}_U = -2\hat{g}\hat{p}_0 \int^{\hat{T}_U} \frac{\Gamma_2(t)}{t}\mathrm{d}t \Big/ \int_1^{\hat{T}_B} \Gamma_2(t)\mathrm{d}t \, , \tag{8.12c}$$

where $\hat{T}_U$ is given by the implicit function

$$x_2 = \int_1^{\hat{T}_U} \Gamma_2(t)\mathrm{d}t \Big/ \int_1^{\hat{T}_B} \Gamma_2(t)\mathrm{d}t \, . \tag{8.13}$$

The nondimensional thermal conductivity $\Gamma_2(t)$ is defined in Eq. (A.131). When $\Gamma_2(t) = c_2 t^n$ [$n = 1/2$ (hard-sphere), $n = 1$ (BKW); c_2: a constant; see Eqs. (A.133) and (A.134)], the relation (8.13) can be made explicit, i.e.,

$$\hat{T}_U = [1 + (\hat{T}_B^{n+1} - 1)x_2]^{1/(n+1)}. \tag{8.14}$$

When the average density of the gas over the domain is taken as the reference density ρ_0, the undetermined constant $\hat{p}_0$ is determined as follows: By the definition of ρ_0,

$$\rho_0 = \frac{1}{D}\int_0^D \rho \mathrm{d}X_2 = \rho_0 \int_0^1 \frac{\hat{p}_0}{\hat{T}_U}\mathrm{d}x_2, \text{ thus, } \hat{p}_0 = \left(\int_0^1 \frac{1}{\hat{T}_U}\mathrm{d}x_2\right)^{-1} .$$

Substituting $\hat{T}_U$ given by Eq. (8.13) into the above equation, we have

$$\hat{p}_0 = \int_1^{\hat{T}_B} \Gamma_2(t)\mathrm{d}t \Big/ \int_1^{\hat{T}_B} t^{-1}\Gamma_2(t)\mathrm{d}t \, . \tag{8.15}$$

The above one-dimensional solution with the subscript U will be called the 1D solution for simplicity.

We will investigate the possibility of bifurcation from the 1D. In the following analysis, as mentioned at the end of Section 8.2.1, we consider only the case where the quantities are independent of x_3 ($\partial/\partial x_3 = 0$).

8.2.3 Bifurcation from the one-dimensional solution

Consider a solution that is periodic, with period $2\pi/\alpha$, with respect to the x_1 direction. We examine whether the periodic solution bifurcates from the 1D solution [Eqs. (8.12a)–(8.13)]. Let the values of the parameters $\hat{T}_B$ and $\hat{g}$ at a bifurcation point be $\hat{T}_{Bb}$ and $\hat{g}_b$. The corresponding value of $\hat{p}_0$, given by Eq. (8.15) for the 1D solution, is denoted by $\hat{p}_{0b}$. That is,

$$\hat{p}_{0b} = \int_1^{\hat{T}_{Bb}} \Gamma_2(t)\mathrm{d}t \Bigg/ \int_1^{\hat{T}_{Bb}} t^{-1}\Gamma_2(t)\mathrm{d}t. \tag{8.16}$$

For the solution periodic with respect to x_1 to be considered hereafter, from Eq. (8.11), $\hat{p}_0$ is given by

$$\hat{p}_0 = \left(\frac{\alpha}{2\pi} \int_0^1 \int_0^{2\pi/\alpha} \frac{1}{\hat{T}} \mathrm{d}x_1 \mathrm{d}x_2 \right)^{-1}. \tag{8.17}$$

For the present purpose, we try to find the solution (say, $\hat{h}$) as a perturbation to the 1D solution (say, $\hat{h}_{Ub}$) at the bifurcation point. Noting that the perturbation is from the 1D solution, or the coefficients of the equations for the perturbation are independent of x_1, and examining the order of differential operators with respect to x_1, we can consistently express the bifurcated solution in the form

$$\begin{aligned}
\hat{T} &= \hat{T}_{Ub}(x_2) + \delta\hat{T}_{11}(x_2)\cos\alpha x_1 \\
&\quad + \delta^2[\hat{T}_{20}(x_2) + \hat{T}_{21}(x_2)\cos\alpha x_1 + \hat{T}_{22}(x_2)\cos 2\alpha x_1] \\
&\quad + \delta^3[\hat{T}_{30}(x_2) + \hat{T}_{31}(x_2)\cos\alpha x_1 + \cdots + \hat{T}_{33}(x_2)\cos 3\alpha x_1] + \cdots, \qquad (8.18a) \\
\hat{\rho} &= \hat{\rho}_{Ub}(x_2) + \delta\hat{\rho}_{11}(x_2)\cos\alpha x_1 \\
&\quad + \delta^2[\hat{\rho}_{20}(x_2) + \hat{\rho}_{21}(x_2)\cos\alpha x_1 + \hat{\rho}_{22}(x_2)\cos 2\alpha x_1] \\
&\quad + \delta^3[\hat{\rho}_{30}(x_2) + \hat{\rho}_{31}(x_2)\cos\alpha x_1 + \cdots + \hat{\rho}_{33}(x_2)\cos 3\alpha x_1] + \cdots, \qquad (8.18b) \\
u_1 &= \delta U_{11}(x_2)\sin\alpha x_1 + \delta^2[U_{21}(x_2)\sin\alpha x_1 + U_{22}(x_2)\sin 2\alpha x_1] \\
&\quad + \delta^3[U_{31}(x_2)\sin\alpha x_1 + \cdots + U_{33}(x_2)\sin 3\alpha x_1] + \cdots, \qquad (8.18c) \\
u_2 &= \delta V_{11}(x_2)\cos\alpha x_1 + \delta^2[V_{20}(x_2) + V_{21}(x_2)\cos\alpha x_1 + V_{22}(x_2)\cos 2\alpha x_1] \\
&\quad + \delta^3[V_{30}(x_2) + V_{31}(x_2)\cos\alpha x_1 + \cdots + V_{33}(x_2)\cos 3\alpha x_1] + \cdots, \qquad (8.18d) \\
u_3 &= 0, \qquad (8.18e) \\
\mathcal{P}^* &= \mathcal{P}^*_{Ub}(x_2) + \delta\mathcal{P}^*_{11}(x_2)\cos\alpha x_1 \\
&\quad + \delta^2[\mathcal{P}^*_{20}(x_2) + \mathcal{P}^*_{21}(x_2)\cos\alpha x_1 + \mathcal{P}^*_{22}(x_2)\cos 2\alpha x_1] \\
&\quad + \delta^3[\mathcal{P}^*_{30}(x_2) + \mathcal{P}^*_{31}(x_2)\cos\alpha x_1 + \cdots + \mathcal{P}^*_{33}(x_2)\cos 3\alpha x_1] + \cdots, \qquad (8.18f)
\end{aligned}$$

where δ^2 indicates the deviation from the bifurcation point, for example, $\delta^2 = [(\hat{T}_B - \hat{T}_{Bb})^2 + (\hat{g} - \hat{g}_b)^2]^{1/2}$, but it is not necessary to be explicit here. Corresponding to the expansion using δ, the parameters $\hat{T}_B$ and $\hat{g}$ away from the bifurcation point $(\hat{T}_{Bb}, \hat{g}_b)$ are expressed as

$$\hat{T}_B = \hat{T}_{Bb} + \delta^2[(\hat{T}_B - \hat{T}_{Bb})/\delta^2], \quad \hat{g} = \hat{g}_b + \delta^2[(\hat{g} - \hat{g}_b)/\delta^2], \tag{8.19}$$

where $(\hat{T}_B - \hat{T}_{Bb})/\delta^2$ and $(\hat{g} - \hat{g}_b)/\delta^2$ are quantities of the order of unity. The difference between the order δ^2 of the deviation of the point $(\hat{T}_B, \hat{g})$ under interest from the bifurcation point and the order δ of the deviation of the bifurcated solution from the 1D solution is understood with the aid of the implicit function theorem.[2]

The basic equations are Eqs. (3.155)–(3.158a), with the new notation. It is, however, convenient here to eliminate the $\hat{p}^*_{SB2}$ (or $\mathcal{P}^*$) by taking the curl of Eq. (3.156) because $\hat{p}^*_{SB2}$ (or $\mathcal{P}^*$) does not appear in the boundary conditions and it is not a quantity of physical interest here. Substituting the series (8.18a)–(8.18e) and Eq. (8.19) into the basic equations (3.155), curl [Eq. (3.156)], (3.157), and (3.158a) and arranging the same-order terms in δ, we obtain a series of linear ordinary differential equations that determines the component functions $\hat{T}_{mn}$, $\hat{\rho}_{mn}$, U_{mn}, and V_{mn}. The $\mathcal{P}^*_{mn}$ is obtained from these quantities from Eq. (3.156). In the series of equations, the component functions appear in such a way that they can be formally determined successively from the lowest order (or in the order of m). The leading-order component functions $\hat{T}_{11}$, U_{11}, and V_{11} are governed by the following equations:

$$\alpha U_{11} + \frac{\mathrm{d}V_{11}}{\mathrm{d}x_2} + \frac{\mathrm{d}\ln\hat{\rho}_{Ub}}{\mathrm{d}x_2} V_{11} = 0, \tag{8.20a}$$

$$\frac{\mathrm{d}^3 U_{11}}{\mathrm{d}x_2^3} + A_1 \frac{\mathrm{d}^2 U_{11}}{\mathrm{d}x_2^2} + (A_2 - \alpha^2)\frac{\mathrm{d}U_{11}}{\mathrm{d}x_2} - \alpha^2 A_1 U_{11} + \alpha\left(\frac{\mathrm{d}^2 V_{11}}{\mathrm{d}x_2^2} - (A_2 + \alpha^2)V_{11}\right)$$
$$+ \frac{\alpha}{\hat{p}_{0b}}\left(B_1 \frac{\mathrm{d}^2\hat{T}_{11}}{\mathrm{d}x_2^2} + B_2 \frac{\mathrm{d}\hat{T}_{11}}{\mathrm{d}x_2} - (B_3 - B_4 + \alpha^2 B_1)\hat{T}_{11}\right) = 0, \tag{8.20b}$$

$$- C_1 V_{11} + \frac{\mathrm{d}^2\hat{T}_{11}}{\mathrm{d}x_2^2} + C_2 \frac{\mathrm{d}\hat{T}_{11}}{\mathrm{d}x_2} + (C_3 - \alpha^2)\hat{T}_{11} = 0, \tag{8.20c}$$

where A_1, B_1, C_1, etc. are expressed with the 1D solution and the nondimensional transport coefficients Γ_1, Γ_2, etc., defined by Eq. (A.131), as

$$A_1 = \frac{2\dot{\Gamma}_{1b}}{\Gamma_{1b}}\frac{\mathrm{d}\hat{T}_{Ub}}{\mathrm{d}x_2}, \qquad A_2 = \frac{\ddot{\Gamma}_{1b}}{\Gamma_{1b}}\left(\frac{\mathrm{d}\hat{T}_{Ub}}{\mathrm{d}x_2}\right)^2 + \frac{\dot{\Gamma}_{1b}}{\Gamma_{1b}}\frac{\mathrm{d}^2\hat{T}_{Ub}}{\mathrm{d}x_2^2},$$
$$B_1 = \frac{\Gamma_{7b}}{\Gamma_{1b}}\frac{\mathrm{d}\hat{T}_{Ub}}{\mathrm{d}x_2}, \qquad B_2 = \frac{\dot{\Gamma}_{7b}}{\Gamma_{1b}}\left(\frac{\mathrm{d}\hat{T}_{Ub}}{\mathrm{d}x_2}\right)^2,$$
$$B_3 = \frac{\dot{\Gamma}_{7b}}{\Gamma_{1b}}\frac{\mathrm{d}\hat{T}_{Ub}}{\mathrm{d}x_2}\frac{\mathrm{d}^2\hat{T}_{Ub}}{\mathrm{d}x_2^2} + \frac{\Gamma_{7b}}{\Gamma_{1b}}\frac{\mathrm{d}^3\hat{T}_{Ub}}{\mathrm{d}x_2^3}, \quad B_4 = \frac{2\hat{g}_b}{\Gamma_{1b}}\left(\frac{\hat{p}_{0b}}{\hat{T}_{Ub}}\right)^2,$$
$$C_1 = \frac{2\hat{\rho}_{Ub}}{\Gamma_{2b}}\frac{\mathrm{d}\hat{T}_{Ub}}{\mathrm{d}x_2}, \quad C_2 = \frac{2\dot{\Gamma}_{2b}}{\Gamma_{2b}}\frac{\mathrm{d}\hat{T}_{Ub}}{\mathrm{d}x_2}, \quad C_3 = \frac{\ddot{\Gamma}_{2b}}{\Gamma_{2b}}\left(\frac{\mathrm{d}\hat{T}_{Ub}}{\mathrm{d}x_2}\right)^2 + \frac{\dot{\Gamma}_{2b}}{\Gamma_{2b}}\frac{\mathrm{d}^2\hat{T}_{Ub}}{\mathrm{d}x_2^2},$$

[2] Consider two variables x and y related by $f(x, y) = 0$ with $f(0, 0) = 0$. According to the implicit function theorem (see, e.g., Buck [1965], Takagi [1961]), y is uniquely determined by x in a neighborhood of $x = 0$ unless $\partial f/\partial y = 0$ at $(x, y) = (0, 0)$. Thus, if $(x, y) = (0, 0)$ is a bifurcation point where $\partial f/\partial y = 0$, y is expressed, for example, as $y = x^{1/n} + \cdots$ with $n > 1$.

with

$$\Gamma_{1b} = \Gamma_1(\hat{T}_{Ub}),\ \Gamma_{2b} = \Gamma_2(\hat{T}_{Ub}),\ \Gamma_{7b} = \Gamma_7(\hat{T}_{Ub}),$$
$$\dot{\Gamma}_{mb} = \left(\mathrm{d}\Gamma_m/\mathrm{d}\hat{T}\right)_{\hat{T}=\hat{T}_{Ub}}, \quad \ddot{\Gamma}_{mb} = \left(\mathrm{d}^2\Gamma_m/\mathrm{d}\hat{T}^2\right)_{\hat{T}=\hat{T}_{Ub}}.$$

The functions $\hat{\rho}_{11}$ and $\mathcal{P}^*_{11}$ are expressed with $\hat{T}_{11}$, U_{11}, and V_{11} as

$$\hat{\rho}_{11} = -\frac{\hat{p}_{0b}}{\hat{T}_{Ub}}\frac{\hat{T}_{11}}{\hat{T}_{Ub}}, \tag{8.21}$$
$$\alpha\mathcal{P}^*_{11} = \frac{4\alpha^2\Gamma_{1b}}{3}U_{11} - \dot{\Gamma}_{1b}\frac{\mathrm{d}\hat{T}_{Ub}}{\mathrm{d}x_2}\frac{\mathrm{d}U_{11}}{\mathrm{d}x_2} - \Gamma_{1b}\frac{\mathrm{d}^2U_{11}}{\mathrm{d}x_2^2} + \alpha\dot{\Gamma}_{1b}\frac{\mathrm{d}\hat{T}_{Ub}}{\mathrm{d}x_2}V_{11} + \frac{\alpha\Gamma_{1b}}{3}\frac{\mathrm{d}V_{11}}{\mathrm{d}x_2}$$
$$+ \frac{\alpha}{p_{0b}}\left\{\left[\frac{2}{3}\dot{\Gamma}_{7b}\left(\frac{\mathrm{d}\hat{T}_{Ub}}{\mathrm{d}x_2}\right)^2 + \Gamma_{7b}\frac{\mathrm{d}^2\hat{T}_{Ub}}{\mathrm{d}x_2^2}\right]\hat{T}_{11} + \frac{1}{3}\Gamma_{7b}\frac{\mathrm{d}\hat{T}_{Ub}}{\mathrm{d}x_2}\frac{\mathrm{d}\hat{T}_{11}}{\mathrm{d}x_2}\right\}.$$

From Eqs. (3.161a) and (3.161b), the boundary conditions for Eqs. (8.20a)–(8.20c) are

$$\hat{T}_{11} = U_{11} = V_{11} = 0 \quad \text{at } x_2 = 0 \text{ and } x_2 = 1. \tag{8.22}$$

The boundary-value problem [(8.20a)–(8.20c) and (8.22)] is homogeneous. Thus, the problem can, generally, have a nontrivial solution only when the parameters $\hat{T}_{Bb}$, $\hat{g}_b$, and α satisfy some relation, say,

$$F_{\mathrm{Bbif}}(\hat{T}_{Bb}, \hat{g}_b, \alpha) = 0. \tag{8.23}$$

This is the relation among the parameters $\hat{T}_{Bb}$, $\hat{g}_b$, and α for which the solution (8.18a)–(8.18f) bifurcates from the one-dimensional solution (8.12a)–(8.13).

The relation (8.23), or the bifurcation relation, is studied numerically. The process of numerical analysis is, in principle, as follows: For simplicity of explanation, let $\hat{T}_{Bb}$ and α be given, and try to obtain $\hat{g}_b$ as their function. Choose $\hat{g}_b$ temporarily, and construct the three linearly independent solutions $\mathrm{S}_n(x_2)$ $(n = 1, 2, 3)$ of Eqs. (8.20a)–(8.20c) satisfying the condition (8.22) only at $x_2 = 0$ and one of the conditions $(\mathrm{d}\hat{T}_{11}/\mathrm{d}x_2, \mathrm{d}U_{11}/\mathrm{d}x_2, \mathrm{d}^2U_{11}/\mathrm{d}x_2^2) = (1,0,0), (0,1,0)$, or $(0,0,1)$ at $x_2 = 0$. Make their linear combination $\sum_{n=1}^{3} c_n\mathrm{S}_n$ (with $c_1 = 1$) satisfy the first two conditions of Eq. (8.22) at $x_2 = 1$. Then, V_{11} at $x_2 = 1$ is generally nonzero. Thus, carrying out this computation for various values of $\hat{g}_b$, obtain the variation of the value of V_{11} at $x_2 = 1$ with $\hat{g}_b$, from which the zero points of V_{11}, i.e., the required values of $\hat{g}_b$, are roughly estimated. Then, obtain accurate results of $\hat{g}_b$'s on the basis of the rough estimate. Some degeneracies occur for some parameters, for which some care should be taken. Each computation is easy and the bifurcation relation has been obtained for various cases.

The curve $\hat{g}_b$ vs $\hat{T}_{Bb}$ for a given α, which is obtained numerically for a hard-sphere gas, is shown in Fig. 8.5, where the corresponding curve when the thermal stress terms (the terms containing Γ_{7b} and $\dot{\Gamma}_{7b}$ through B_1, B_2, and

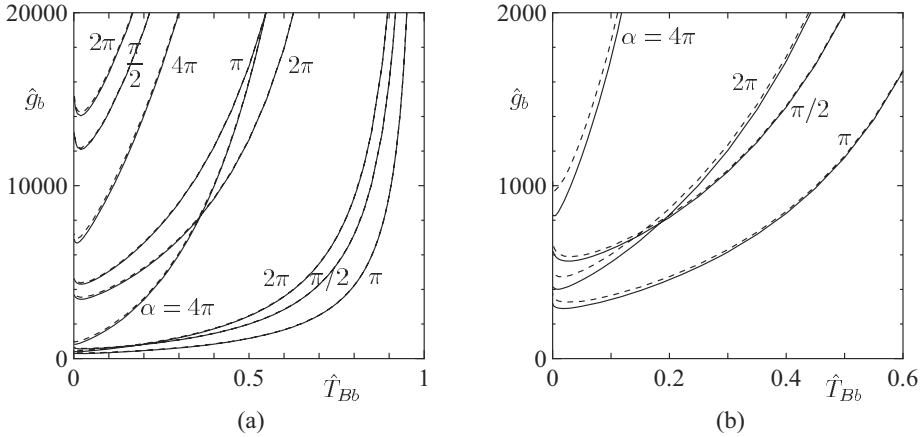

Figure 8.5. Bifurcation curves I: $\hat{g}_b$ vs $\hat{T}_{Bb}$ for various α. (a) Wider range of $\hat{g}_b$ showing several branches and (b) magnified figure of the the first branch. The solid lines —— indicate the bifurcation curve for a hard-sphere gas; the dashed lines – – – indicate the corresponding curve when the thermal stress terms are neglected.

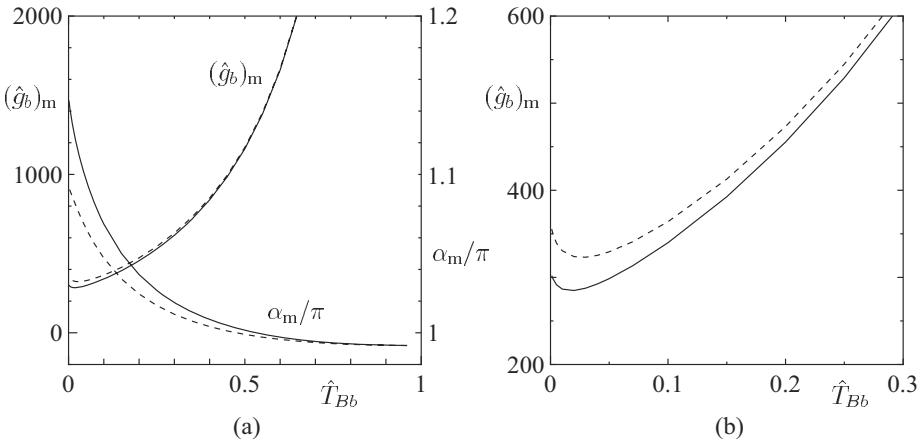

Figure 8.6. Bifurcation curves II: The curves $(\hat{g}_b)_{\rm m}$ and $\alpha_{\rm m}$ vs $\hat{T}_{Bb}$. (a) The two curves $(\hat{g}_b)_{\rm m}$ and $\alpha_{\rm m}$ vs $\hat{T}_{Bb}$ and (b) a magnified figure of the curve $(\hat{g}_b)_{\rm m}$ vs $\hat{T}_{Bb}$. The solid lines —— indicate the bifurcation curve for a hard-sphere gas; the dashed lines – – – indicate the corresponding curve when the thermal stress terms are neglected.

B_3) in Eq. (8.20b) are neglected is shown in dashed lines for comparison. There is appreciable difference between the two kinds of the curves for small $\hat{T}_{Bb}$. The relation being expressed as $\hat{g}_b = \hat{g}_b(\hat{T}_{Bb}, \alpha)$, consider the minimum value of $\hat{g}_b$ with respect to α with $\hat{T}_{Bb}$ being fixed and denote it by $(\hat{g}_b)_{\rm m}$ and the minimum point by $\alpha_{\rm m}$. The curves $(\hat{g}_b)_{\rm m}$ and $\alpha_{\rm m}$ vs $\hat{T}_{Bb}$ are shown in Fig. 8.6.

When the condition (8.23) is satisfied, the solution is determined except for a constant factor. This factor is determined by the higher-order analysis, which is only touched on here. The boundary-value problem for U_{21}, V_{21}, and $\hat{T}_{21}$ is homogeneous and of the same form as that for U_{11}, V_{11}, and $\hat{T}_{11}$. The problem for U_{m1}, V_{m1}, and $\hat{T}_{m1}$ ($m \geq 3$) is inhomogeneous, and its homogeneous part is of the same form as that for U_{11}, V_{11}, and $\hat{T}_{11}$. Thus, its inhomogeneous part must satisfy some relation (solvability condition) for the solution U_{m1}, V_{m1}, and $\hat{T}_{m1}$ to exist.[3] The homogeneous part of the boundary-value problem for U_{mn}, V_{mn}, and $\hat{T}_{mn}$ ($n \neq 1$) generally has no nontrivial solution unless an additional condition among $\hat{T}_{Bb}$, $\hat{g}_b$, and α is satisfied.

Let the undetermined constant factor (or the norm) of the set $\delta(U_{11}, V_{11}, \hat{T}_{11})$ be δA, where the norm may be defined, for example, as $A = [\int_0^1 (U_{11}^2 + V_{11}^2 + \hat{T}_{11}^2) \mathrm{d}x_2]^{1/2}$. Then, the solvability condition of the boundary-value problem for U_{31}, V_{31}, and $\hat{T}_{31}$ is expressed in the following form:

$$A[a_T(\hat{T}_B - \hat{T}_{Bb})/\delta^2 + a_g(\hat{g} - \hat{g}_b)/\delta^2 - a_O A^2] = 0. \tag{8.24}$$

Thus,

$$A^2 = \frac{a_T}{a_O}\frac{(\hat{T}_B - \hat{T}_{Bb})}{\delta^2} + \frac{a_g}{a_O}\frac{(\hat{g} - \hat{g}_b)}{\delta^2}, \text{ or } \quad A = 0,$$

where a_T/a_O and a_g/a_O are determined by $\hat{T}_{Bb}$, $\hat{g}_b$, and α. The first equation gives the amplitude of the bifurcated solution, and the second is the one-dimensional solution. The bifurcated solution extends to the range

$$\frac{a_T}{a_O}(\hat{T}_B - \hat{T}_{Bb}) + \frac{a_g}{a_O}(\hat{g} - \hat{g}_b) > 0, \tag{8.25}$$

in the parameter plane $(\hat{T}_B, \hat{g})$, and the amplitude A remains zero along the direction $(\hat{T}_B - \hat{T}_{Bb},\ \hat{g} - \hat{g}_b)$ given by

$$\frac{a_T}{a_O}(\hat{T}_B - \hat{T}_{Bb}) + \frac{a_g}{a_O}(\hat{g} - \hat{g}_b) = 0. \tag{8.26}$$

That is, this is the direction of the bifurcation curve $F_{\mathrm{Bbif}}(\hat{T}_{Bb}, \hat{g}_b, \alpha) = 0$ in the $(\hat{T}_{Bb}, \hat{g}_b)$ plane, which is shown in Fig. 8.5.

When $a_O = 0$, the coefficients a_T/a_O and a_g/a_O are infinite. This indicates that the amplitude δA is much larger than δ (the square root of the deviation from the bifurcation point), and thus the preceding analysis should be reconsidered. The solution bifurcating from the bifurcation point $(\hat{T}_{Bb}, \hat{g}_b, \alpha)$ where the condition $a_O = 0$ is satisfied can be obtained in the same way as the preceding solution by modifying the power series (8.18a)–(8.18f) of δ to power series of

[3] The solution of the adjoint problem of Eqs. (8.20a)–(8.20c) and (8.22) should be orthogonal to the inhomogeneous part. If the homogeneous system has no nontrivial solution, its adjoint system has no nontrivial solution; if the homogeneous system has a nontrivial solution, its adjoint system has a nontrivial solution. See, e.g., Coddington & Levinson [1955], Reid [1971], and Kato [1976].

$\delta^{1/2}$. That is,

$$\begin{aligned} f = {} & f_{Ub}(x_2) + \delta^{1/2} f_{11}(x_2)\cos\alpha x_1 \\ & + \delta[f_{20}(x_2) + f_{21}(x_2)\cos\alpha x_1 + f_{22}(x_2)\cos 2\alpha x_1] \\ & + \delta^{3/2}[f_{30}(x_2) + f_{31}(x_2)\cos\alpha x_1 + \cdots + f_{33}(x_2)\cos 3\alpha x_1] \\ & + \delta^2[f_{40}(x_2) + f_{41}(x_2)\cos\alpha x_1 + \cdots + f_{44}(x_2)\cos 4\alpha x_1] + \cdots , \end{aligned} \tag{8.27a}$$

$$\begin{aligned} u_1 = {} & \delta^{1/2} U_{11}(x_2)\sin\alpha x_1 + \delta[U_{21}(x_2)\sin\alpha x_1 + U_{22}(x_2)\sin 2\alpha x_1] \\ & + \delta^{3/2}[U_{31}(x_2)\sin\alpha x_1 + \cdots + U_{33}(x_2)\sin 3\alpha x_1] \\ & + \delta^2[U_{41}(x_2)\sin\alpha x_1 + \cdots + U_{44}(x_2)\sin 4\alpha x_1] + \cdots , \end{aligned} \tag{8.27b}$$

where $f = \hat{T}$, u_2, $\hat{\rho}$, or $\mathcal{P}^*$. The boundary-value problem for $(U_{11}, V_{11}, \hat{T}_{11})$ is the same as that for $(U_{11}, V_{11}, \hat{T}_{11})$ in the preceding analysis, as should be. In the higher-order analysis, the homogeneous part is the same as before but some inhomogeneous terms degenerate because of the condition on a_O, and the amplitude of the solution $(U_{11}, V_{11}, \hat{T}_{11})$ is determined by the solvability condition of the equations for $(U_{51}, V_{51}, \hat{T}_{51})$. As the result, the fourth power A^4, instead of A^2 in the general case, of the amplitude of $(U_{11}, V_{11}, \hat{T}_{11})$ is expressed by a linear combination of $\hat{T}_B - \hat{T}_{Bb}$ and $\hat{g} - \hat{g}_b$.

When $n\alpha$, as well as α, satisfies the bifurcation relation (8.23) for some set of integer n (n^*), some comments are in order. Then the leading terms [the terms of the order δ of Eqs. (8.18a)–(8.18f)] of the perturbation should be the sum of corresponding Fourier components, that is,

$$\delta \sum_{n=(n^*)} f_{1n}(x_2)\cos\alpha n(x_1 - c_n) \text{ or } \delta \sum_{n=(n^*)} U_{1n}(x_2)\sin\alpha n(x_1 - c_n),$$

where c_n is some constant, and the following terms correspondingly consist of more terms than before. With these modifications, the analysis can be carried out in a similar way. Incidentally, if the neighboring integers (say m and $m+1$) belong to the set (n^*), the corresponding amplitudes, say A_m and A_{m+1}, vanish.

8.2.4 Two-dimensional temperature field under infinitesimal flow velocity

In the preceding subsection (Section 8.2.3), we have found that there is a bifurcation of temperature field under infinitesimal flow velocity (the first-order infinitesimal) and gravity (the second-order infinitesimal) and that the nonlinear thermal stress, which is the second-order infinitesimal, affects the bifurcation of the temperature field. In this subsection, we will study the temperature field away from bifurcation points by numerical analysis of the system, Eqs. (3.155)–(3.158a), (3.161a), and (3.161b), summarized in Section 3.3.3.[4]

[4]Note that the simpler notation explained in the last paragraph of Section 8.2.1 is used here.

The numerical computation is carried out in the following way. Consider a gas in the finite domain ($0 < x_1 < x_{1B}$, $0 < x_2 < 1$) and take the following conditions on the side boundaries:

$$\frac{\partial \hat{T}}{\partial x_1} = 0, \quad u_1 = 0, \quad \frac{\partial u_2}{\partial x_1} = 0 \quad \text{at } x_1 = 0 \text{ and } x_1 = x_{1B}, \tag{8.28}$$

in addition to the conditions on the lower and upper boundaries, i.e.,

$$\hat{T} = 1, \ u_1 = u_2 = 0 \ \text{ at } x_2 = 0, \text{ and } \ \hat{T} = \hat{T}_B, \ u_1 = u_2 = 0 \ \text{ at } x_2 = 1, \tag{8.29}$$

and the condition corresponding to Eq. (8.17), i.e.,

$$\hat{p}_0 = \left(\frac{1}{x_{1B}} \int_0^1 \int_0^{x_{1B}} \frac{1}{\hat{T}} \mathrm{d}x_1 \mathrm{d}x_2 \right)^{-1}. \tag{8.30}$$

Incidentally, from Eqs. (3.155) and (3.158a) and the boundary condition (8.28), $\partial^2 u_1 / \partial x_1^2 = 0$ at $x_1 = 0$ and $x_1 = x_{1B}$, and then from Eq. (3.156) with $i = 1$, $\partial \mathcal{P}^* / \partial x_1 = 0$ there.

Let a solution for $x_{1B} = \pi/\alpha$ of the above problem in the rectangular domain be S1. Then its mirror image with respect to the vertical boundary is also a solution of the problem (say, S2). The two kinds of solutions S1 and S2 being alternately arranged laterally, the resulting flow field is found to be two times continuously differentiable across the vertical connection lines $x_1 = n\pi/\alpha$ ($n = 0, \pm 1, \pm 2, \ldots$), because it satisfies Eqs. (3.155)–(3.158a) except on the connection lines and satisfies the condition (8.28) at the connection lines (note the relations derived in the preceding paragraph). That is, the flow field thus constructed is a periodic solution with period $2\pi/\alpha$ with respect to x_1 in the infinite domain between the two plane walls at $x_2 = 0$ and $x_2 = 1$.

The boundary-value problem, i.e., Eqs. (3.155)–(3.158a), (8.28)–(8.30), is solved numerically by a finite-difference method. The solution of the boundary-value problem for the finite-difference equations is obtained by the method of iteration. In the computation, the equation derived from Eq. (3.156) by taking its curl is used instead of Eq. (3.156) in order to eliminate the variable $\hat{p}^*_{SB2}$; the vorticity $\omega = \partial u_2/\partial x_1 - \partial u_1/\partial x_2$ and the stream function Ψ, in place of the continuity equation (3.155), are introduced. The superscript with parentheses showing the step of iteration is attached to the resulting equations in the following way:

$$\frac{\partial}{\partial x_i} \left(\Gamma_2^{(n)} \frac{\partial \hat{T}^{(n+1)}}{\partial x_i} \right) = 2\hat{p}_0^{(n)} \frac{u_i^{(n)}}{\hat{T}^{(n)}} \frac{\partial \hat{T}^{(n)}}{\partial x_i}, \tag{8.31}$$

$$\hat{p}_0^{(n+1)} = \left(\frac{1}{x_{1B}} \int_0^1 \int_0^{x_{1B}} \frac{1}{\hat{T}^{(n+1)}} \mathrm{d}x_1 \mathrm{d}x_2 \right)^{-1}, \tag{8.32}$$

$$\Gamma_1^{(n+1)}\left(\frac{\partial^2}{\partial x_1^2}+\frac{\partial^2}{\partial x_2^2}\right)\omega^{(n+1)} = -\frac{2\hat{g}\hat{p}_0^{(n+1)}}{(\hat{T}^{(n+1)})^2}\frac{\partial\hat{T}^{(n+1)}}{\partial x_1} - \dot{\Gamma}_1^{(n+1)}\frac{\partial\hat{T}^{(n+1)}}{\partial x_i}\frac{\partial\omega^{(n)}}{\partial x_i}$$
$$+\frac{\partial}{\partial x_i}\left\{\dot{\Gamma}_1^{(n+1)}\left[\frac{\partial\hat{T}^{(n+1)}}{\partial x_2}\left(\frac{\partial u_1^{(n)}}{\partial x_i}+\frac{\partial u_i^{(n)}}{\partial x_1}\right)-\frac{\partial\hat{T}^{(n+1)}}{\partial x_1}\left(\frac{\partial u_2^{(n)}}{\partial x_i}+\frac{\partial u_i^{(n)}}{\partial x_2}\right)\right]\right\}$$
$$+\frac{1}{\hat{p}_0^{(n+1)}}\frac{\partial}{\partial x_i}\left[-\frac{\partial}{\partial x_1}\left(\Gamma_7^{(n+1)}\frac{\partial\hat{T}^{(n+1)}}{\partial x_2}\frac{\partial\hat{T}^{(n+1)}}{\partial x_i}\right)\right.$$
$$\left.+\frac{\partial}{\partial x_2}\left(\Gamma_7^{(n+1)}\frac{\partial\hat{T}^{(n+1)}}{\partial x_1}\frac{\partial\hat{T}^{(n+1)}}{\partial x_i}\right)\right]$$
$$-\frac{2\hat{p}_0^{(n+1)}u_i^{(n)}}{(\hat{T}^{(n+1)})^2}\left(\frac{\partial u_2^{(n)}}{\partial x_i}\frac{\partial\hat{T}^{(n+1)}}{\partial x_1}-\frac{\partial u_1^{(n)}}{\partial x_i}\frac{\partial\hat{T}^{(n+1)}}{\partial x_2}\right)+\frac{2\hat{p}_0^{(n+1)}}{\hat{T}^{(n+1)}}\frac{\partial u_i^{(n)}\omega^{(n)}}{\partial x_i}, \tag{8.33}$$

$$\left(\frac{\partial^2}{\partial x_1^2}+\frac{\partial^2}{\partial x_2^2}\right)\Psi^{(n+1)} = -\frac{1}{\hat{T}^{(n+1)}}\omega^{(n+1)}$$
$$+\frac{1}{(\hat{T}^{(n+1)})^2}\left(u_2^{(n)}\frac{\partial}{\partial x_1}-u_1^{(n)}\frac{\partial}{\partial x_2}\right)\hat{T}^{(n+1)}, \tag{8.34}$$

$$u_1^{(n+1)} = \hat{T}^{(n+1)}\frac{\partial\Psi^{(n+1)}}{\partial x_2}, \qquad u_2^{(n+1)} = -\hat{T}^{(n+1)}\frac{\partial\Psi^{(n+1)}}{\partial x_1}, \tag{8.35}$$

where

$$\Gamma_2^{(n)} = \Gamma_2(\hat{T}^{(n)}), \quad \Gamma_1^{(n+1)} = \Gamma_1(\hat{T}^{(n+1)}), \quad \Gamma_7^{(n+1)} = \Gamma_7(\hat{T}^{(n+1)}). \tag{8.36}$$

Here, Eq. (8.31) corresponds to Eq. (3.157), Eq. (8.33) to the curl of Eq. (3.156), Eq. (8.34) to the relation $\omega = \partial u_2/\partial x_1 - \partial u_1/\partial x_2$, and Eq. (8.35) to the definition of the stream function Ψ.

The boundary conditions for Eq. (8.31) are

$$\hat{T}^{(n+1)} = 1 \ \text{ at } x_2 = 0 \ \text{ and } \ \hat{T}^{(n+1)} = \hat{T}_B \ \text{ at } x_2 = 1, \tag{8.37a}$$

$$\frac{\partial\hat{T}^{(n+1)}}{\partial x_1} = 0 \ \text{ at } x_1 = 0 \ \text{ and } x_1 = x_{1B}. \tag{8.37b}$$

The boundary conditions for Eq. (8.33) are

$$\omega^{(n+1)} = \omega^{(n)} - \vartheta u_1^{(n)} \quad \text{at} \quad x_2 = 0, \tag{8.38a}$$

$$\omega^{(n+1)} = \omega^{(n)} + \vartheta u_1^{(n)} \quad \text{at} \quad x_2 = 1, \tag{8.38b}$$

$$\omega^{(n+1)} = 0 \quad \text{at} \quad x_1 = 0 \ \text{ and } x_1 = x_{1B}. \tag{8.38c}$$

The boundary conditions for Eq. (8.34) are

$$\Psi^{(n+1)} = 0 \ \text{ at } x_1 = 0,\ x_1 = x_{1B},\ x_2 = 0,\ \text{and } x_2 = 1. \tag{8.39}$$

These boundary conditions except Eqs. (8.38a) and (8.38b) are the straightforward results from the boundary conditions (8.28) and (8.29). When the

iteration converges, the conditions (8.38a) and (8.38b), where ϑ is chosen appropriately so as to make the iteration converge, are reduced to the conditions $u_1 = 0$ at $x_2 = 0$ and $x_2 = 1$, which are not guaranteed by the other boundary conditions. The above equations for iterative computation are rewritten in a finite-difference form.

The iteration process is carried out in the following way: (i) Choose an initial set of ($\hat{T}^{(0)}$, $\hat{p}_0^{(0)}$, $u_1^{(0)}$, $u_2^{(0)}$, $\omega^{(0)}$). (ii) Obtain $\hat{T}^{(n+1)}$, $\hat{p}_0^{(n+1)}$, $\omega^{(n+1)}$, $\Psi^{(n+1)}$, $u_1^{(n+1)}$, and $u_2^{(n+1)}$ successively using Eqs. (8.31)–(8.35) according to their order with the set ($\hat{T}^{(n)}$, $\hat{p}_0^{(n)}$, $\omega^{(n)}$, $u_1^{(n)}$, $u_2^{(n)}$) obtained at the preceding stage (or given as the initial set). That is, $\hat{T}^{(n+1)}$ from Eq. (8.31), $\hat{p}_0^{(n+1)}$ from Eq. (8.32), $\omega^{(n+1)}$ from Eq. (8.33), $\Psi^{(n+1)}$ from Eq. (8.34), $u_1^{(n+1)}$ and $u_2^{(n+1)}$ from Eq. (8.35) using the data obtained so far. (iii) Return to step (ii) and continue the process with newly obtained ($\hat{T}^{(n+1)}$, $\hat{p}_0^{(n+1)}$, $\omega^{(n+1)}$, $u_1^{(n+1)}$, $u_2^{(n+1)}$) as ($\hat{T}^{(n)}$, $\hat{p}_0^{(n)}$, $\omega^{(n)}$, $u_1^{(n)}$, $u_2^{(n)}$). The essential problem at each step is to solve the Poisson equation.[5]

Some of the results of computation are shown for $x_{1B} = 1$ in Figs. 8.7 and 8.8. When $\hat{T}_B = 0.1$ (Fig. 8.7), the bifurcated solution first extends to the direction of smaller $\hat{g}$ from the bifurcation point at $\hat{g} = 341.28$ and then to larger $\hat{g}$ after its amplitude grows to some size.[6] At $\hat{g} = 320$ [panel (a) of Fig. 8.7], there is no bifurcated solution for the system with the thermal stress terms neglected, for which the bifurcation point is at $\hat{g} = 364.96$; at $\hat{g} = 328$ [panel (b) of Fig. 8.7], the maximum difference of the temperature of the system without thermal stress from that of the correct system amounts to 20% of the correct solution; and for $\hat{g} = 1000$ and 7000 [panels (c) and (d) of Fig. 8.7], slight differences of isothermal lines are seen in the central regions. When $\hat{T}_B = 0.5$ (Fig. 8.8), the bifurcated solution extends to the direction of larger $\hat{g}$ from the bifurcation point at $\hat{g} = 1162.28$. At $\hat{g} = 1170$ [panel (a) of Fig. 8.8], there is no bifurcated solution for the system without thermal stress; at $\hat{g} = 1180$ [panel (b) of Fig. 8.8], there is clearly a difference between the two solutions with and without thermal stress. The results clearly show that the Navier–Stokes system fails to describe the temperature field in the continuum limit. The strongly deformed temperature field in the absence of gas motion is the ghost effect.

8.2.5 Discussions

In this section, the Bénard problem of a gas in the continuum limit between two parallel plane walls with different temperatures is studied on the basis of the asymptotic fluid-dynamic-type equations and their associated boundary conditions. The two-dimensional problem discussed in this work is, apparently, a plain problem which has already been studied sufficiently, but the result is not the one that is given by the classical fluid dynamics. In the problem the temperature field is determined together with the infinitesimal velocity field. The

[5]The term $\partial(\Gamma_2^{(n)}\partial\hat{T}^{(n+1)}/\partial x_i)/\partial x_i$ on the left-hand side of Eq. (8.31) can be transformed, with replacement of $\Gamma_2^{(n)}$ by $\Gamma_2^{(n+1)}$, into the form $(\partial^2/\partial x_1^2 + \partial^2/\partial x_2^2)\int^{\hat{T}^{(n+1)}} \Gamma_2 \mathrm{d}\hat{T}$.

[6]One of the solutions for $\hat{g} < \hat{g}_b$ cannot be obtained numerically.

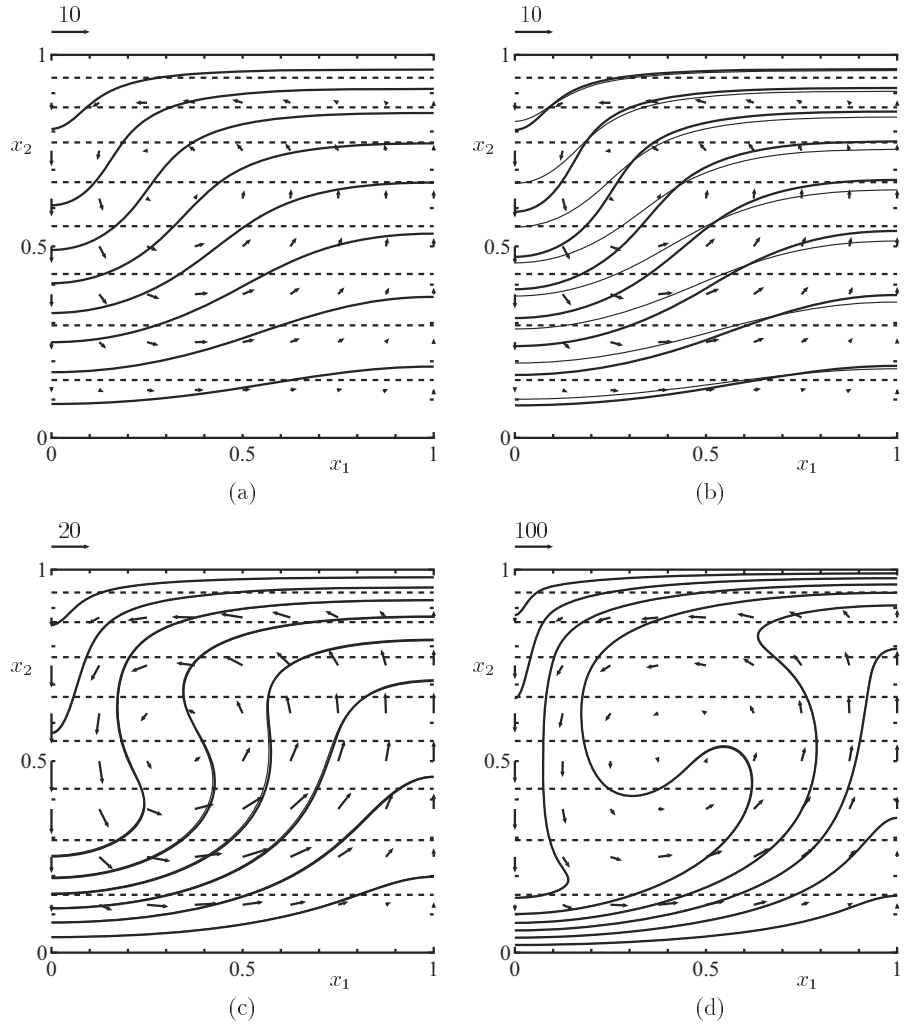

Figure 8.7. The bifurcated temperature field for a hard-sphere gas I: $\hat{T}_B = 0.1$ and $x_{1B} = 1$. (a) $\hat{g} = 320$, (b) $\hat{g} = 328$, (c) $\hat{g} = 1000$, (d) $\hat{g} = 7000$. The solid lines indicate the isothermal lines [$\hat{T} = 0.1n$ $(n = 1, 2, \ldots, 10)$ from the upper wall to the lower]; the arrows indicate u_i at their starting points and their scale is shown on the left shoulder of the figure. The thin lines indicate the corresponding results with the thermal stress effect neglected, and the dashed lines --- indicate the 1D solution.

infinitesimal velocity is not perceived in the continuum world (or in the world of the continuum limit). That is, the 1D temperature field bifurcates and its various strongly distorted fields appear when there is no flow at all. The distorted temperature field is determined by the infinitesimal flow velocity and gravity. In other words, the correct behavior of a gas in the continuum limit cannot be

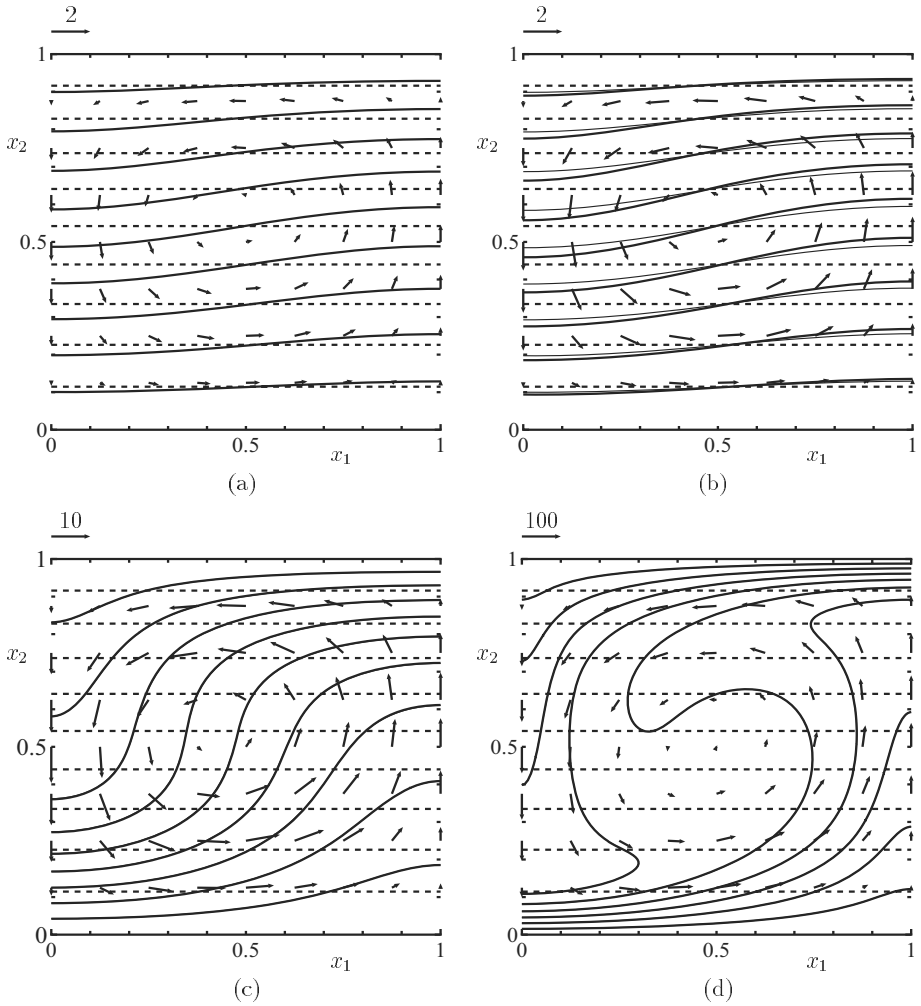

Figure 8.8. The bifurcated temperature field for a hard-sphere gas II: $\hat{T}_B = 0.5$ and $x_{1B} = 1$. (a) $\hat{g} = 1170$, (b) $\hat{g} = 1180$, (c) $\hat{g} = 2000$, (d) $\hat{g} = 30000$. The solid lines indicate the isothermal lines [$\hat{T} = 0.05n + 0.5$ ($n = 0, 1, \ldots, 10$) from the upper wall to the lower]; the arrows indicate u_i at their starting points and their scale is shown on the left shoulder of each panel. The thin lines indicate the corresponding results with the thermal stress effect neglected, and the dashed lines --- indicate the 1D solution.

obtained only by the quantities perceptible in its world.

A bifurcated and distorted temperature field is also obtained with the aid of the Navier–Stokes equations if the vanishing flow velocity is just retained. However, it does not give the correct answer. In the asymptotic fluid-dynamic-type equations, there is another contribution. It is the thermal stress. The thermal stress is of the second order in the Knudsen number and the viscous

stress is generally of the first order. In the present case, the velocity is of the first order and therefore the viscous stress degenerates to the second order. Thus the thermal stress should be retained together with the viscous stress. The difference between the two results has been studied. The dashed lines in Figs. 8.5 and 8.6 are the corresponding bifurcation curves for the set of equations (3.155)–(3.158a) where the thermal stress terms [or the terms containing Γ_7 in Eq. (3.156)] are eliminated. Some examples of isothermal lines for the two results are compared in Figs. 8.7 and 8.8, where the results for the thermal stress neglected are shown in thin solid lines. These results clearly show the ghost effect and inappropriateness of the Navier–Stokes system for the description of the behavior of a gas in the continuum limit.

In the atmospheric condition, the mean free path is very small but is not exactly zero. Then, the flow velocity is nonzero for the bifurcated temperature field. As an example, consider the following case: The distance D between the two walls is 10 m; the temperature T_c of the upper wall is 300 K; the gas between the channel is air (or nitrogen gas) and under atmospheric pressure.[7] Then, the mean free path near the upper wall is roughly 6×10^{-8} m. (i) When $T_c/T_h \ (= \hat{T}_B) = 0.1$, the mean free path near the lower wall is 6×10^{-7} m and thus the Knudsen number is 6×10^{-8}. The gravity $|g_i|$ at the bifurcation point for $\alpha = \pi$ is $|g_i| = 2 \times 10^{-7}$ m/s^2, which is 2×10^{-8} of the gravity on the earth. According to the numerical computation for $x_{1B} = 1$, $|u_i| \le 5$ for $\hat{g} = 320$ or $|u_i| \le 17$ for $\hat{g} = 1000$; that is, the flow velocity is, respectively, less than 0.4 or 2 mm/s. The corresponding temperature field is given in panels (a) and (c) of Fig. 8.7. In the case of Fig. 8.7 (a), there is no distortion of the temperature field if the thermal stress terms [or the terms containing Γ_7 in Eq. (3.156)] are neglected. (ii) When $T_c/T_h \ (= \hat{T}_B) = 0.5$, the mean free path near the lower wall is 10^{-7} m and thus the Knudsen number is 10^{-8}. The gravity $|g_i|$ at the bifurcation point for $\alpha = \pi$ is $|g_i| = 5 \times 10^{-9}$ m/s^2, which is 5×10^{-10} of the gravity on the earth. According to the numerical computation for $x_{1B} = 1$, $|u_i| \le 1$ for $\hat{g} = 1170$ or $|u_i| \le 10$ for $\hat{g} = 2000$; that is, the flow velocity is, respectively, less than 5×10^{-3} or 5×10^{-2} mm/s. The corresponding temperature field is given in panels (a) and (c) of Fig. 8.8. In the case of Fig. 8.8 (a), there is no distortion of the temperature field if the thermal stress terms [or the terms containing Γ_7 in Eq. (3.156)] are neglected. In view of the temperature field and the scale of the system, the velocity is practically a vanishingly small quantity. In the analysis, we considered the case where the plane walls were at rest. Unless the motion of the walls is kept at rest with accuracy much less than the above speed, the analysis taking into account of this small motion ($\hat{v}_{wi1}$) into the boundary condition (3.161b) is required for the correct description of the behavior of the temperature field. We have considered a perfectly time-independent problem. Infinitesimal time-dependent quantities (e.g., $\hat{v}_{wi1} n_i$) may induce time-dependent or time-independent effect on the behavior of a gas in the continuum limit.

The effect of infinitesimal velocity is more striking when we consider the

[7] See Footnote 102 in Section 3.6.2.

Bénard problem with the diffuse reflecting side walls. That is, a one-dimensional temperature field is impossible. In this case, from Eqs. (3.161a) and (3.161b), the boundary conditions for the fluid-dynamic-type equations on the side walls are given by

$$\hat{T} = \hat{T}_{ws}, \quad u_1 = 0, \quad \frac{u_2}{\hat{T}_{ws}^{1/2}} = -\frac{\hat{K}_1}{\hat{p}_0}\frac{\mathrm{d}\hat{T}_{ws}}{\mathrm{d}x_2} \quad \text{at } x_1 = 0 \text{ and } x_1 = x_{1B}, \tag{8.40}$$

where the slip coefficient $\hat{K}_1$ is related to that K_1 in the linear theory in Section 3.1.5 and their relation is discussed in Section A.11; $x_1 = 0$ and $x_1 = x_{1B}$ are the positions of the side walls[8] and $\hat{T}_{ws}$ is the temperature of the side walls, which cannot be uniform because the temperatures of the upper and lower walls are different. Thus, u_2 on the side wall is nonzero and therefore is so in the gas. On the other hand, if $\hat{T}$ (and therefore $\hat{\rho}$) depends only on x_2, then $\hat{\rho}u_2$ is independent of x_1 from Eq. (3.157). Then $\hat{\rho}u_1$ is found to be a linear function of x_1 from Eq. (3.155), and therefore $u_1 = 0$ from the boundary condition (8.40). Then $\hat{\rho}u_2$ is zero from Eqs. (3.155) and (8.29). Therefore, the temperature field $\hat{T}$ cannot be one-dimensional even in the absence of gas motion in the continuum limit. That is, the thermal creep flow (Section 5.1.1), or the flow of the order of the Knudsen number induced over a wall with nonuniform temperature, influences the temperature field in the continuum limit and makes a one-dimensional temperature field impossible. In classical fluid dynamics (the Navier–Stokes equations under nonslip condition), the one-dimensional temperature field given in Section 8.2.2 is possible when the temperature of the side walls is given in harmony with the 1D solution. Thus, the results of the two systems disagree at the starting point of the study of the Bénard problem.

The present study shows that the behavior of a gas in the continuum limit cannot be described by the Navier–Stokes equations for an important class of problems and that infinitesimal quantities play an important role for its description (ghost effect). Another example of the ghost effect owing to infinitesimal motion of a boundary is given in Section 8.3.

8.3 Taylor–Couette problem

8.3.1 Problem and basic equation

The Taylor–Couette problem of a gas between two rotating coaxial circular cylinders, as well as the Bénard problem, is one of the most famous problems of bifurcation of flows (Taylor [1923], Chandrasekhar [1961], Koschmieder [1993], Chossat & Iooss [1994]). Generally it is discussed for the case where the temperatures of the two cylinders are equal. When the temperatures of the two

[8]The problem has the corners where the assumption of the asymptotic theory is violated. If the corners are rounded, the asymptotic theory can be applied, which does not influence the following discussion.

cylinders are different, the bifurcation of the field is combined with the ghost effect, as in the case of the Bénard problem, and the result gives important information on the fundamental property of a gas in the continuum limit. We will discuss this problem on the basis of Sone, Handa & Doi [2003] in this section.

Consider a gas in a time-independent state between two rotating coaxial circular cylinders. Let the radius, temperature, and circumferential velocity of the inner cylinder be, respectively, L_A, T_A, and $V_{\theta A}$, and let the corresponding quantities of the outer cylinder be L_B, T_B, and $V_{\theta B}$. Without loss of generality, we can take $V_{\theta A}$ positive. We will investigate the asymptotic behavior of the gas in the limit that the Knudsen number tends to zero under the following assumptions: (i) the temperature difference of the two cylinders is finite, that is, $T_B/T_A - 1$ is of the order of unity; (ii) the speeds of rotation of the two cylinders are small, that is, $|V_{\theta A}|/(2RT_A)^{1/2}$ and $|V_{\theta B}|/(2RT_A)^{1/2}$ are of the order of the Knudsen number Kn of the system, where $\mathrm{Kn} = \ell_0/L_A$ with ℓ_0 being the mean free path of the gas in the equilibrium state at rest with temperature T_A and the average density ρ_0 of the gas over the domain. The second assumption is made because the bifurcation is expected to occur at this range of the speeds of the cylinders (see, e.g., Section 8.4.4) and discrimination of this order of speed is required.

The limiting behavior of the system as $\mathrm{Kn} \to 0$ is described by the fluid-dynamic-type equations (3.155)–(3.158a) with $\hat{F}_{i2} = 0$ and the boundary conditions (3.161a) and (3.161b). It is convenient to use their cylindrical coordinate expressions for the present problem. Let us introduce the following notation: $(L_A\hat{r}, \theta, L_A\hat{z})$ is the cylindrical coordinate system with its axial coordinate $L_A\hat{z}$ on the common axis of the cylinders; $\rho_0\hat{\rho}$, $(2RT_A)^{1/2}(\hat{v}_r, \hat{v}_\theta, \hat{v}_z)$, $T_A\hat{T}$, and $R\rho_0 T_A\hat{p}$ are, respectively, the density, the flow velocity in the cylindrical coordinate system, the temperature, and the pressure of the gas. The fluid-dynamic-type equations are given as

$$\frac{1}{\hat{r}}\frac{\partial \hat{\rho} u_r \hat{r}}{\partial \hat{r}} + \frac{1}{\hat{r}}\frac{\partial \hat{\rho} u_\theta}{\partial \theta} + \frac{\partial \hat{\rho} u_z}{\partial \hat{z}} = 0, \tag{8.41}$$

$$\begin{aligned}
&\hat{\rho} u_r \frac{\partial u_r}{\partial \hat{r}} + \frac{\hat{\rho} u_\theta}{\hat{r}}\frac{\partial u_r}{\partial \theta} + \hat{\rho} u_z \frac{\partial u_r}{\partial \hat{z}} - \frac{\hat{\rho} u_\theta^2}{\hat{r}} \\
&= -\frac{1}{2}\frac{\partial \hat{p}_2^{\natural}}{\partial \hat{r}} + \frac{1}{\hat{r}}\frac{\partial}{\partial \hat{r}}\left(\Gamma_1 \hat{r}\frac{\partial u_r}{\partial \hat{r}}\right) + \frac{1}{\hat{r}}\frac{\partial}{\partial \theta}\left[\frac{\Gamma_1}{2}\left(\frac{1}{\hat{r}}\frac{\partial u_r}{\partial \theta} + \frac{\partial u_\theta}{\partial \hat{r}} - \frac{u_\theta}{\hat{r}}\right)\right] \\
&\quad + \frac{\partial}{\partial \hat{z}}\left[\frac{\Gamma_1}{2}\left(\frac{\partial u_r}{\partial \hat{z}} + \frac{\partial u_z}{\partial \hat{r}}\right)\right] - \frac{\Gamma_1}{\hat{r}^2}\left(\frac{\partial u_\theta}{\partial \theta} + u_r\right) \\
&\quad + \frac{1}{\hat{r}}\frac{\partial}{\partial \hat{r}}\left[\frac{\Gamma_7 \hat{r}}{2\hat{p}_0}\left(\frac{\partial \hat{T}}{\partial \hat{r}}\right)^2\right] + \frac{1}{\hat{r}^2}\frac{\partial}{\partial \theta}\left(\frac{\Gamma_7}{2\hat{p}_0}\frac{\partial \hat{T}}{\partial \hat{r}}\frac{\partial \hat{T}}{\partial \theta}\right) \\
&\quad + \frac{\partial}{\partial \hat{z}}\left(\frac{\Gamma_7}{2\hat{p}_0}\frac{\partial \hat{T}}{\partial \hat{r}}\frac{\partial \hat{T}}{\partial \hat{z}}\right) - \frac{\Gamma_7}{2\hat{p}_0 \hat{r}^3}\left(\frac{\partial \hat{T}}{\partial \theta}\right)^2,
\end{aligned} \tag{8.42}$$

$$\hat\rho u_r\frac{\partial u_\theta}{\partial\hat r}+\frac{\hat\rho u_\theta}{\hat r}\frac{\partial u_\theta}{\partial\theta}+\hat\rho u_z\frac{\partial u_\theta}{\partial\hat z}+\frac{\hat\rho u_r u_\theta}{\hat r}$$
$$=-\frac{1}{2\hat r}\frac{\partial\hat p_2^\natural}{\partial\theta}+\frac{1}{\hat r}\frac{\partial}{\partial\hat r}\left[\frac{\Gamma_1\hat r}{2}\left(\frac{1}{\hat r}\frac{\partial u_r}{\partial\theta}+\frac{\partial u_\theta}{\partial\hat r}-\frac{u_\theta}{\hat r}\right)\right]$$
$$+\frac{1}{\hat r^2}\frac{\partial}{\partial\theta}\left[\Gamma_1\left(\frac{\partial u_\theta}{\partial\theta}+u_r\right)\right]+\frac{\partial}{\partial\hat z}\left[\frac{\Gamma_1}{2}\left(\frac{\partial u_\theta}{\partial\hat z}+\frac{1}{\hat r}\frac{\partial u_z}{\partial\theta}\right)\right]$$
$$+\frac{\Gamma_1}{2\hat r}\left(\frac{1}{\hat r}\frac{\partial u_r}{\partial\theta}+\frac{\partial u_\theta}{\partial\hat r}-\frac{u_\theta}{\hat r}\right)+\frac{1}{\hat r}\frac{\partial}{\partial\hat r}\left(\frac{\Gamma_7}{2\hat p_0}\frac{\partial\hat T}{\partial\hat r}\frac{\partial\hat T}{\partial\theta}\right)+\frac{1}{\hat r^3}\frac{\partial}{\partial\theta}\left[\frac{\Gamma_7}{2\hat p_0}\left(\frac{\partial\hat T}{\partial\theta}\right)^2\right]$$
$$+\frac{1}{\hat r}\frac{\partial}{\partial\hat z}\left(\frac{\Gamma_7}{2\hat p_0}\frac{\partial\hat T}{\partial\theta}\frac{\partial\hat T}{\partial\hat z}\right)+\frac{\Gamma_7}{2\hat p_0\hat r^2}\frac{\partial\hat T}{\partial\hat r}\frac{\partial\hat T}{\partial\theta},\tag{8.43}$$

$$\hat\rho u_r\frac{\partial u_z}{\partial\hat r}+\frac{\hat\rho u_\theta}{\hat r}\frac{\partial u_z}{\partial\theta}+\hat\rho u_z\frac{\partial u_z}{\partial\hat z}=-\frac{1}{2}\frac{\partial\hat p_2^\natural}{\partial\hat z}+\frac{1}{\hat r}\frac{\partial}{\partial\hat r}\left[\frac{\Gamma_1\hat r}{2}\left(\frac{\partial u_z}{\partial\hat r}+\frac{\partial u_r}{\partial\hat z}\right)\right]$$
$$+\frac{1}{\hat r}\frac{\partial}{\partial\theta}\left[\frac{\Gamma_1}{2}\left(\frac{\partial u_\theta}{\partial\hat z}+\frac{1}{\hat r}\frac{\partial u_z}{\partial\theta}\right)\right]+\frac{\partial}{\partial\hat z}\left(\Gamma_1\frac{\partial u_z}{\partial\hat z}\right)$$
$$+\frac{1}{\hat r}\frac{\partial}{\partial\hat r}\left(\frac{\Gamma_7\hat r}{2\hat p_0}\frac{\partial\hat T}{\partial\hat r}\frac{\partial\hat T}{\partial\hat z}\right)+\frac{1}{\hat r^2}\frac{\partial}{\partial\theta}\left(\frac{\Gamma_7}{2\hat p_0}\frac{\partial\hat T}{\partial\theta}\frac{\partial\hat T}{\partial\hat z}\right)+\frac{\partial}{\partial\hat z}\left[\frac{\Gamma_7}{2\hat p_0}\left(\frac{\partial\hat T}{\partial\hat z}\right)^2\right],\tag{8.44}$$

$$\hat\rho u_r\frac{\partial\hat T}{\partial\hat r}+\frac{\hat\rho u_\theta}{\hat r}\frac{\partial\hat T}{\partial\theta}+\hat\rho u_z\frac{\partial\hat T}{\partial\hat z}$$
$$=\frac{1}{\hat r}\frac{\partial}{\partial\hat r}\left(\frac{\Gamma_2\hat r}{2}\frac{\partial\hat T}{\partial\hat r}\right)+\frac{1}{\hat r}\frac{\partial}{\partial\theta}\left(\frac{\Gamma_2}{2\hat r}\frac{\partial\hat T}{\partial\theta}\right)+\frac{\partial}{\partial\hat z}\left(\frac{\Gamma_2}{2}\frac{\partial\hat T}{\partial\hat z}\right),\tag{8.45}$$

$$\hat\rho\,\hat T=\hat p_0,\tag{8.46}$$

where

$$(u_r,u_\theta,u_z)=\lim_{k\to0}(\hat v_r/k,\hat v_\theta/k,\hat v_z/k),\tag{8.47a}$$

$\hat\rho$ and $\hat T$ are their limiting values as $k\to0$, (8.47b)

$$\hat p_0=\lim_{k\to0}\hat p,\quad \hat p_1=\lim_{k\to0}(\hat p-\hat p_0)/k,\quad \hat p_2=\lim_{k\to0}(\hat p-\hat p_0-\hat p_1k)/k^2,\tag{8.47c}$$

$$\hat p_2^\natural=\hat p_2+\frac{2\Gamma_3}{3\hat p_0}\left[\frac{1}{\hat r}\frac{\partial}{\partial\hat r}\left(\hat r\frac{\partial\hat T}{\partial\hat r}\right)+\frac{1}{\hat r^2}\frac{\partial^2\hat T}{\partial\theta^2}+\frac{\partial^2\hat T}{\partial\hat z^2}\right]$$
$$+\frac{\bar\Gamma_7}{\hat p_0}\left[\left(\frac{\partial\hat T}{\partial\hat r}\right)^2+\frac{1}{\hat r^2}\left(\frac{\partial\hat T}{\partial\theta}\right)^2+\left(\frac{\partial\hat T}{\partial\hat z}\right)^2\right]+\frac{2\Gamma_1}{3}\left(\frac{1}{\hat r}\frac{\partial\hat r u_r}{\partial\hat r}+\frac{1}{\hat r}\frac{\partial u_\theta}{\partial\theta}+\frac{\partial u_z}{\partial\hat z}\right),$$

$$k=\sqrt{\pi}\mathrm{Kn}/2.\tag{8.47d}$$

In the above equations, the $\hat{p}_0$ and $\hat{p}_1$ are noted to be constants, which is the result of the assumption (ii) [see Eqs. (3.153) and (3.154)], and Γ_1, $\bar{\Gamma}_7$, etc. are the functions of $\hat{T}$ defined by Eq. (A.131). Incidentally, $\hat{\rho}$, $\hat{T}$, $\hat{p}_0$, $\hat{p}_1$, $\hat{p}_2$, and (u_r, u_θ, u_z) are, respectively, $\hat{\rho}_{SB0}$, $\hat{T}_{SB0}$, $\hat{p}_{SB0}$, $\hat{p}_{SB1}$, $\hat{p}_{SB2}$, and the cylindrical coordinate counterpart $(\hat{v}_{rSB1}, \hat{v}_{\theta SB1}, \hat{v}_{zSB1})$ of $\hat{v}_{iSB1}$ in Section 3.3.

The boundary conditions for these equations on the cylinders are

$$\hat{T} = 1, \quad u_\theta = U_A, \quad u_r = u_z = 0 \quad \text{at } \hat{r} = 1, \tag{8.48}$$

and

$$\hat{T} = \hat{T}_B, \quad u_\theta = U_B, \quad u_r = u_z = 0 \quad \text{at } \hat{r} = \hat{r}_B, \tag{8.49}$$

where $\hat{T}_B = T_B/T_A$, $\hat{r}_B = L_B/L_A$, and

$$U_A = \lim_{k\to 0} V_{\theta A}/(2RT_A)^{1/2}k, \quad U_B = \lim_{k\to 0} V_{\theta B}/(2RT_A)^{1/2}k,$$

which are quantities of the order of unity. The parameter $V_{\theta A}$ (thus, U_A) being taken positive, the two cylinders are rotating in the same direction when $U_B > 0$, and in opposite directions when $U_B < 0$. We specify the average density of the gas over the domain and take it as the reference density, which is another condition to fix the problem as shown in the process of analysis.

8.3.2 Analysis of bifurcation

Axially symmetric and uniform solution

The axially symmetric and uniform solution ($\partial/\partial\theta = \partial/\partial\hat{z} = 0$) of the fluid-dynamic-type equations (8.41)–(8.46) and the boundary conditions (8.48) and (8.49) is easily obtained as follows:

$$\hat{T} = \hat{T}_U(\hat{r}), \quad \hat{\rho} = \hat{\rho}_U(\hat{r}) = \frac{\hat{p}_0}{\hat{T}_U(\hat{r})}, \tag{8.50a}$$

$$u_\theta = u_{\theta U}(\hat{r}), \quad u_r = u_z = 0, \tag{8.50b}$$

where $\hat{T}_U(\hat{r})$ is given implicitly by

$$\hat{r} = \exp\left(\frac{(\ln \hat{r}_B)\displaystyle\int_1^{\hat{T}_U} \Gamma_2(\hat{T})\mathrm{d}\hat{T}}{\displaystyle\int_1^{\hat{T}_B} \Gamma_2(\hat{T})\mathrm{d}\hat{T}} \right), \tag{8.51}$$

and $u_{\theta U}(\hat{r})$ is given, with the aid of the above result, by

$$u_{\theta U} = \left(\frac{U_B}{\hat{r}_B} - U_A \right) \frac{\hat{r}\displaystyle\int_1^{\hat{r}} \frac{1}{\hat{r}^3\Gamma_1(\hat{T}_U)}\mathrm{d}\hat{r}}{\displaystyle\int_1^{\hat{r}_B} \frac{1}{\hat{r}^3\Gamma_1(\hat{T}_U)}\mathrm{d}\hat{r}} + U_A\hat{r}, \tag{8.52}$$

The nondimensional viscosity and thermal conductivity $\Gamma_1(\hat{T})$ and $\Gamma_2(\hat{T})$ are defined in Eq. (A.131). The axially symmetric and uniform solution introduced above will be called the ASU solution, for short. The thermal stress terms in Eqs. (8.43) and (8.44) vanish owing to the axially symmetric and uniform field.

When $\Gamma_1(\hat{T}) = c_1\hat{T}^n$ and $\Gamma_2(\hat{T}) = c_2\hat{T}^n$ [$n = 1/2$ (hard-sphere), $n = 1$ (BKW); c_1, c_2 : constants; see Eqs. (A.133) and (A.134)], the relation (8.51) can be made explicit, that is,

$$\hat{T}_U = \left[1 + \left(\hat{T}_B^{n+1} - 1\right)\frac{\ln\hat{r}}{\ln\hat{r}_B}\right]^{1/(n+1)}, \tag{8.53}$$

and further, with this expression of $\hat{T}_U$ in the integral $\int_1^{\hat{r}}[1/\hat{r}^3\Gamma_1(\hat{T}_U)]\mathrm{d}\hat{r}$, i.e.,

$$\int_1^{\hat{r}} \frac{1}{\hat{r}^3\Gamma_1(\hat{T}_U)}\mathrm{d}\hat{r} = \frac{1}{c_1}\int_1^{\hat{r}} \frac{1}{\hat{r}^3\left[1 + \left(\hat{T}_B^{n+1} - 1\right)\dfrac{\ln\hat{r}}{\ln\hat{r}_B}\right]^{n/(n+1)}}\mathrm{d}\hat{r},$$

the relation (8.52) becomes explicit.

When the average density of the gas over the domain is taken as the reference density ρ_0, the undetermined $\hat{p}_0$ is determined as follows: By the definition of ρ_0,

$$\rho_0 = \frac{2\rho_0}{\hat{r}_B^2 - 1}\int_1^{\hat{r}_B} \hat{\rho}\hat{r}\mathrm{d}\hat{r}.$$

Substituting $\hat{\rho}$ given by the second relation in Eq. (8.50a) into the above equation, we have

$$\hat{p}_0 = \frac{\hat{r}_B^2 - 1}{2}\left(\int_1^{\hat{r}_B} \frac{\hat{r}}{\hat{T}_U}\mathrm{d}\hat{r}\right)^{-1}. \tag{8.54}$$

Bifurcation from the axially symmetric and uniform solution

Consider an axially symmetric solution that is periodic, with period $2\pi/\alpha$, along the axial direction $\hat{z}$. We are interested in the bifurcation of this class of solution from the ASU solution, i.e., Eqs. (8.50a)–(8.52), and the behavior of the solution in the neighborhood of the bifurcation point, if any. Let the values of the parameters $\hat{T}_B$, U_A, and U_B at a bifurcation point be, respectively, $\hat{T}_{Bb}$, U_{Ab}, and U_{Bb}, and let the ASU solution ($\hat{T}_U$, $\hat{\rho}_U$, $u_{\theta U}$) with these parameters be denoted by ($\hat{T}_{Ub}$, $\hat{\rho}_{Ub}$, $u_{\theta Ub}$). The corresponding value of the parameter $\hat{p}_0$, given by Eq. (8.54) for the ASU solution, is denoted by $\hat{p}_{0b}$. That is,

$$\hat{p}_{0b} = \frac{\hat{r}_B^2 - 1}{2}\left(\int_1^{\hat{r}_B} \frac{\hat{r}}{\hat{T}_{Ub}}\mathrm{d}\hat{r}\right)^{-1}. \tag{8.55}$$

For a solution periodic with respect to $\hat{z}$, to be considered hereafter, $\hat{p}_0$ is given by

$$\hat{p}_0 = \frac{\pi(\hat{r}_B^2 - 1)}{\alpha}\left(\int_0^{2\pi/\alpha}\int_1^{\hat{r}_B} \frac{\hat{r}}{\hat{T}}\mathrm{d}\hat{r}\mathrm{d}\hat{z}\right)^{-1}. \tag{8.56}$$

The solution that bifurcates from the ASU solution is obtained as a perturbation to the ASU solution at the bifurcation point in the form[9]

$$\hat{T} = \hat{T}_{Ub}(\hat{r}) + \delta\hat{T}_{11}(\hat{r})\cos\alpha\hat{z} + \delta^2[\hat{T}_{20}(\hat{r}) + \hat{T}_{21}(\hat{r})\cos\alpha\hat{z} + \hat{T}_{22}(\hat{r})\cos 2\alpha\hat{z}] + \cdots, \tag{8.57a}$$

$$\hat{\rho} = \hat{\rho}_{Ub}(\hat{r}) + \delta\hat{\rho}_{11}(\hat{r})\cos\alpha\hat{z} + \delta^2[\hat{\rho}_{20}(\hat{r}) + \hat{\rho}_{21}(\hat{r})\cos\alpha\hat{z} + \hat{\rho}_{22}(\hat{r})\cos 2\alpha\hat{z}] + \cdots, \tag{8.57b}$$

$$u_\theta = u_{\theta Ub}(\hat{r}) + \delta U_{11}(\hat{r})\cos\alpha\hat{z} + \delta^2[U_{20}(\hat{r}) + U_{21}(\hat{r})\cos\alpha\hat{z} + U_{22}(\hat{r})\cos 2\alpha\hat{z}] + \cdots, \tag{8.57c}$$

$$u_r = \delta V_{11}(\hat{r})\cos\alpha\hat{z} + \delta^2[V_{20}(\hat{r}) + V_{21}(\hat{r})\cos\alpha\hat{z} + V_{22}(\hat{r})\cos 2\alpha\hat{z}] + \cdots, \tag{8.57d}$$

$$u_z = \delta W_{11}(\hat{r})\sin\alpha\hat{z} + \delta^2[W_{21}(\hat{r})\sin\alpha\hat{z} + W_{22}(\hat{r})\sin 2\alpha\hat{z}] + \cdots, \tag{8.57e}$$

where δ^2 indicates the deviation from the bifurcation point, for example, $\delta^2 = [(\hat{T}_B - \hat{T}_{Bb})^2 + (U_A - U_{Ab})^2 + (U_B - U_{Bb})^2]^{1/2}$, but it is not necessary to be explicit here. It is attached to make the size of a term explicit. Corresponding to the expansion using δ, the parameters $\hat{T}_B$, U_A, and U_B away from the bifurcation point $(\hat{T}_{Bb}, U_{Ab}, U_{Bb})$ are expressed as

$$\left.\begin{aligned} \hat{T}_B &= \hat{T}_{Bb} + \delta^2\left(\frac{\hat{T}_B - \hat{T}_{Bb}}{\delta^2}\right), \\ U_A &= U_{Ab} + \delta^2\left(\frac{U_A - U_{Ab}}{\delta^2}\right), \\ U_B &= U_{Bb} + \delta^2\left(\frac{U_B - U_{Bb}}{\delta^2}\right), \end{aligned}\right\} \tag{8.58}$$

where $(\hat{T}_B - \hat{T}_{Bb})/\delta^2$, $(U_A - U_{Ab})/\delta^2$, and $(U_B - U_{Bb})/\delta^2$ are quantities of the order of unity.

The basic equations are the conservation equations (8.41)–(8.45) and the equation of state (8.46), where the derivatives with respect to θ vanish ($\partial/\partial\theta = 0$). It is, however, convenient here to eliminate $\hat{p}_2^\natural$ from Eqs. (8.42) and (8.44), because $\hat{p}_2^\natural$ does not appear in the boundary conditions and is not a quantity of physical interest here. Substituting the series (8.57a)–(8.57e) and Eq. (8.58) into the basic equations (8.41)–(8.46) with $\hat{p}_2^\natural$ eliminated and the conditions (8.48), (8.49), and (8.56), and arranging the same-order terms in δ, we obtain a series of the linear ordinary differential equations and boundary conditions that determine the component functions $\hat{T}_{mn}$, $\hat{\rho}_{mn}$, U_{mn}, V_{mn}, and W_{mn}. In the series of equations, the component functions appear in such a way that they can be formally determined successively from the lowest order (or in the order of m).

[9] See Footnote 2 in Section 8.2.3.

The leading-order component functions $\hat{T}_{11}$, $\hat{\rho}_{11}$, U_{11}, V_{11}, and W_{11} are governed by the equations

$$\frac{\mathrm{d}V_{11}}{\mathrm{d}\hat{r}} + A_1 V_{11} + \alpha W_{11} = 0, \tag{8.59a}$$

$$\frac{\mathrm{d}^2 U_{11}}{\mathrm{d}\hat{r}^2} + B_1 \frac{\mathrm{d}U_{11}}{\mathrm{d}\hat{r}} - \left(\frac{B_1}{\hat{r}} + \alpha^2\right) U_{11} + B_2 V_{11} + B_3 \frac{\mathrm{d}\hat{T}_{11}}{\mathrm{d}\hat{r}} + B_4 \hat{T}_{11} = 0, \tag{8.59b}$$

$$\begin{aligned}
&\alpha C_1 U_{11} + \alpha \left(\frac{\mathrm{d}^2 V_{11}}{\mathrm{d}\hat{r}^2} + \frac{1}{\hat{r}}\frac{\mathrm{d}V_{11}}{\mathrm{d}\hat{r}} + (C_2 - \alpha^2) V_{11}\right) \\
&+ \alpha \left(C_3 \frac{\mathrm{d}^2 \hat{T}_{11}}{\mathrm{d}\hat{r}^2} + C_4 \frac{\mathrm{d}\hat{T}_{11}}{\mathrm{d}\hat{r}} + (C_5 - \alpha^2 C_3)\hat{T}_{11}\right) \\
&+ \frac{\mathrm{d}^3 W_{11}}{\mathrm{d}\hat{r}^3} + C_6 \frac{\mathrm{d}^2 W_{11}}{\mathrm{d}\hat{r}^2} + (C_7 - \alpha^2)\frac{\mathrm{d}W_{11}}{\mathrm{d}\hat{r}} + \alpha^2 C_8 W_{11} = 0,
\end{aligned} \tag{8.59c}$$

$$D_1 V_{11} + \frac{\mathrm{d}^2 \hat{T}_{11}}{\mathrm{d}\hat{r}^2} + D_2 \frac{\mathrm{d}\hat{T}_{11}}{\mathrm{d}\hat{r}} + (D_3 - \alpha^2)\hat{T}_{11} = 0, \tag{8.59d}$$

$$\hat{\rho}_{11} = -\hat{\rho}_{Ub}\hat{T}_{11}/\hat{T}_{Ub}, \tag{8.59e}$$

where $A_1, B_1, \ldots,$ and D_3 are determined by the ASU solution at the bifurcation point as

$$A_1 = \frac{1}{\hat{\rho}_{Ub}\hat{r}}\frac{\mathrm{d}\hat{\rho}_{Ub}\hat{r}}{\mathrm{d}\hat{r}}, \quad B_1 = \frac{\dot{\Gamma}_{1b}}{\Gamma_{1b}}\frac{\mathrm{d}\hat{T}_{Ub}}{\mathrm{d}\hat{r}} + \frac{1}{\hat{r}}, \qquad B_2 = -\frac{2\hat{\rho}_{Ub}}{\Gamma_{1b}}\left(\frac{\mathrm{d}u_{\theta Ub}}{\mathrm{d}\hat{r}} + \frac{u_{\theta Ub}}{\hat{r}}\right),$$

$$B_3 = \frac{\dot{\Gamma}_{1b}}{\Gamma_{1b}}\left(\frac{\mathrm{d}u_{\theta Ub}}{\mathrm{d}\hat{r}} - \frac{u_{\theta Ub}}{\hat{r}}\right), \quad B_4 = \left[\frac{\ddot{\Gamma}_{1b}}{\Gamma_{1b}} - \left(\frac{\dot{\Gamma}_{1b}}{\Gamma_{1b}}\right)^2\right]\frac{\mathrm{d}\hat{T}_{Ub}}{\mathrm{d}\hat{r}}\left(\frac{\mathrm{d}u_{\theta Ub}}{\mathrm{d}\hat{r}} - \frac{u_{\theta Ub}}{\hat{r}}\right),$$

$$C_1 = \frac{4\hat{\rho}_{Ub}u_{\theta Ub}}{\Gamma_{1b}\hat{r}}, \qquad C_2 = -\frac{\ddot{\Gamma}_{1b}}{\Gamma_{1b}}\left(\frac{\mathrm{d}\hat{T}_{Ub}}{\mathrm{d}\hat{r}}\right)^2 - \frac{\dot{\Gamma}_{1b}}{\Gamma_{1b}}\left(\frac{\mathrm{d}^2\hat{T}_{Ub}}{\mathrm{d}\hat{r}^2} + \frac{1}{\hat{r}}\frac{\mathrm{d}\hat{T}_{Ub}}{\mathrm{d}\hat{r}}\right) - \frac{1}{\hat{r}^2},$$

$$C_3\hat{p}_{0b} = \frac{\Gamma_{7b}}{\Gamma_{1b}}\frac{\mathrm{d}\hat{T}_{Ub}}{\mathrm{d}\hat{r}}, \qquad C_4\hat{p}_{0b} = \left(\frac{\dot{\Gamma}_{7b}}{\Gamma_{1b}}\frac{\mathrm{d}\hat{T}_{Ub}}{\mathrm{d}\hat{r}} + \frac{\Gamma_{7b}}{\Gamma_{1b}\hat{r}}\right)\frac{\mathrm{d}\hat{T}_{Ub}}{\mathrm{d}\hat{r}},$$

$$C_5\hat{p}_{0b} = -\left[\frac{\Gamma_{7b}}{\Gamma_{1b}}\left(\frac{\mathrm{d}^3\hat{T}_{Ub}}{\mathrm{d}\hat{r}^3} + \frac{1}{\hat{r}}\frac{\mathrm{d}^2\hat{T}_{Ub}}{\mathrm{d}\hat{r}^2} - \frac{1}{\hat{r}^2}\frac{\mathrm{d}\hat{T}_{Ub}}{\mathrm{d}\hat{r}}\right) + \frac{\dot{\Gamma}_{7b}}{2\Gamma_{1b}}\frac{\mathrm{d}}{\mathrm{d}\hat{r}}\left(\frac{\mathrm{d}\hat{T}_{Ub}}{\mathrm{d}\hat{r}}\right)^2 + \frac{2(\hat{\rho}_{Ub}u_{\theta Ub})^2}{\Gamma_{1b}\hat{r}}\right],$$

$$C_6 = \frac{2\dot{\Gamma}_{1b}}{\Gamma_{1b}}\frac{\mathrm{d}\hat{T}_{Ub}}{\mathrm{d}\hat{r}} + \frac{1}{\hat{r}}, \qquad C_7 = \frac{\ddot{\Gamma}_{1b}}{\Gamma_{1b}}\left(\frac{\mathrm{d}\hat{T}_{Ub}}{\mathrm{d}\hat{r}}\right)^2 + \frac{\dot{\Gamma}_{1b}}{\Gamma_{1b}}\left(\frac{\mathrm{d}^2\hat{T}_{Ub}}{\mathrm{d}\hat{r}^2} + \frac{1}{\hat{r}}\frac{\mathrm{d}\hat{T}_{Ub}}{\mathrm{d}\hat{r}}\right) - \frac{1}{\hat{r}^2},$$

$$C_8 = -\frac{2\dot{\Gamma}_{1b}}{\Gamma_{1b}}\frac{\mathrm{d}\hat{T}_{Ub}}{\mathrm{d}\hat{r}}, \quad D_1 = -\frac{2\hat{\rho}_{Ub}}{\Gamma_{2b}}\frac{\mathrm{d}\hat{T}_{Ub}}{\mathrm{d}\hat{r}}, \qquad D_2 = \frac{2\dot{\Gamma}_{2b}}{\Gamma_{2b}}\frac{\mathrm{d}\hat{T}_{Ub}}{\mathrm{d}\hat{r}} + \frac{1}{\hat{r}},$$

$$D_3 = \frac{\ddot{\Gamma}_{2b}}{\Gamma_{2b}}\left(\frac{\mathrm{d}\hat{T}_{Ub}}{\mathrm{d}\hat{r}}\right)^2 + \frac{\dot{\Gamma}_{2b}}{\Gamma_{2b}}\left(\frac{\mathrm{d}^2\hat{T}_{Ub}}{\mathrm{d}\hat{r}^2} + \frac{1}{\hat{r}}\frac{\mathrm{d}\hat{T}_{Ub}}{\mathrm{d}\hat{r}}\right),$$

with

$$\Gamma_{mb} = \Gamma_m(\hat{T}_{Ub}), \quad \dot{\Gamma}_{mb} = \left(\mathrm{d}\Gamma_m/\mathrm{d}\hat{T}\right)_{\hat{T}=\hat{T}_{Ub}}, \quad \ddot{\Gamma}_{mb} = \left(\mathrm{d}^2\Gamma_m/\mathrm{d}\hat{T}^2\right)_{\hat{T}=\hat{T}_{Ub}}.$$

Their boundary conditions are given by

$$\hat{T}_{11} = U_{11} = V_{11} = W_{11} = 0 \quad \text{at } \hat{r} = 1 \text{ and } \hat{r}_B. \tag{8.60}$$

The homogeneous boundary-value problem [Eqs. (8.59a)–(8.59d) and (8.60)] can have a nontrivial solution only when the parameters $\hat{T}_{Bb}$, U_{Ab}, U_{Bb}, α, and $\hat{r}_B$ satisfy some relation among them, say,

$$F_{\mathrm{Cbif}}(\hat{T}_{Bb}, U_{Ab}, U_{Bb}, \alpha, \hat{r}_B) = 0. \tag{8.61}$$

The relation (8.61), or the bifurcation relation, is studied numerically for a hard-sphere gas; the process of the numerical analysis is similar to the corresponding process in the Bénard problem in Section 8.2.3. In Fig. 8.9, the relation U_{Ab} vs $\hat{T}_{Bb}$ is shown for various α when $U_{Bb} = 0$ and $\hat{r}_B = 2$. There are infinitely many U_{Ab}'s for a given $\hat{T}_{Bb}$,[10] the first three of which are shown in Fig. 8.9 (a). The lowest branches of the curves are shown in a larger scale in Fig. 8.9 (b). In this figure, the corresponding results for the system of equations without the thermal stress terms [the terms coming from Γ_7 in Eqs. (8.42)–(8.44)] are shown in the dashed lines. The white and black circles in the figure indicate the DSMC results by Aoki, Sone & Yoshimoto [1999] (see the caption for the precise meaning). In Fig. 8.10, the relation U_{Ab} vs $\hat{T}_{Bb}$ for the sets $(\hat{r}_B, \alpha) = (1.5, 2\pi)$ and $(2, \pi)$ is shown for various U_{Bb}. (There are infinitely many curves above the curves in the figures.)

The result in this bifurcation analysis shows that the bifurcation occurs when $|V_{\theta A}|/(2RT_A)^{1/2}$ and $|V_{\theta B}|/(2RT_A)^{1/2}$ are of the order of the Knudsen number, which was expected at the beginning of the present study, and thus, the analysis limited to the case where the gas flow is of the order of the Knudsen number is appropriate to find the bifurcation point. In the world of the continuum limit, where one cannot discriminate the size of the quantities of the order of the Knudsen number, the bifurcation from the axially symmetric and uniform solution occurs in a gas when the cylinders are at rest.

8.3.3 Bifurcated temperature field under infinitesimal speeds of rotation of the cylinders

In the preceding subsection (Section 8.3.2), we have found that the bifurcation of the temperature field occurs when the speeds of rotation of the cylinders are the first-order infinitesimal and that the nonlinear thermal stress, which is the second-order infinitesimal, affects its bifurcation. In this subsection, we will study the bifurcated temperature field away from bifurcation points by numerical computation of the system given in Section 8.3.1 under the restriction that the solution is axially symmetric.

[10] "Infinitely many" is the plausible result suggested by detailed numerical study.

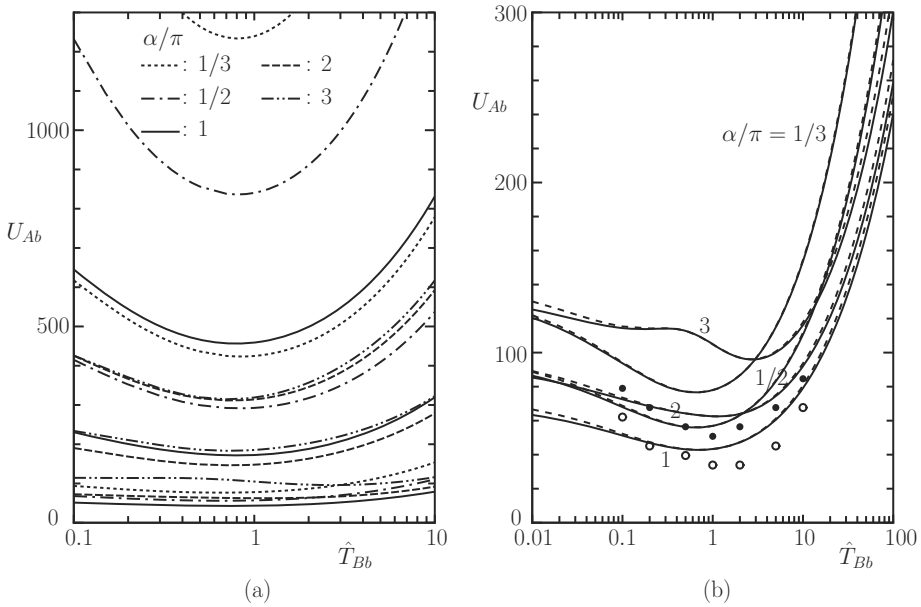

Figure 8.9. Bifurcation curves for a hard-sphere gas I: U_{Ab} vs $\hat{T}_{Bb}$ [Eq. (8.61)] with $U_{Bb} = 0$ and $\hat{r}_B = 2$ for various α. For a given α, there are infinitely many branches. (a) A wider range of U_{Ab} showing several branches and (b) a magnified figure of the first branch. In panel (b), the solid lines —— indicate the bifurcation curves for the full equations; the dashed lines – – – indicate the corresponding curves when the thermal stress terms are neglected. The white and black circles indicate the DSMC results with the specular-reflection condition at $\hat{z} = 0$ and $\hat{z} = 1$ at Kn = 0.02 in Aoki, Sone & Yoshimoto [1999]; the white circles ∘ are the largest values of $V_{\theta A}/(2RT_A)^{1/2}k$ where the ASU solution is stable, and the black circles • are the smallest values of $V_{\theta A}/(2RT_A)^{1/2}k$ at which a roll-type solution exists; the data $V_{\theta A}/(2RT_A)^{1/2}$ divided by k (or $0.01\sqrt{\pi}$) are shown as a rough estimate of the first-order coefficient of the expansion in k [see Eq. (8.47a)].

The numerical computation is carried out in the following way. Consider a gas in the finite domain in the $\hat{z}$ direction $(0 < \hat{z} < \hat{z}_B)$[11] and take the following conditions on the boundaries at $\hat{z} = 0$ and $\hat{z} = \hat{z}_B$:

$$\frac{\partial \hat{T}}{\partial \hat{z}} = 0, \quad u_z = 0, \quad \frac{\partial u_r}{\partial \hat{z}} = \frac{\partial u_\theta}{\partial \hat{z}} = 0 \quad \text{at } \hat{z} = 0 \text{ and } \hat{z} = \hat{z}_B, \tag{8.62}$$

in addition to the conditions on the cylinders [see Eqs. (8.48) and (8.49)], i.e.,

$$\hat{T} = 1, \quad u_\theta = U_A, \quad u_r = u_z = 0 \quad \text{at } \hat{r} = 1, \tag{8.63}$$

$$\hat{T} = \hat{T}_B, \quad u_\theta = U_B, \quad u_r = u_z = 0 \quad \text{at } \hat{r} = \hat{r}_B, \tag{8.64}$$

[11] See Fig. 8.19 for the related situation in Section 8.4.3.

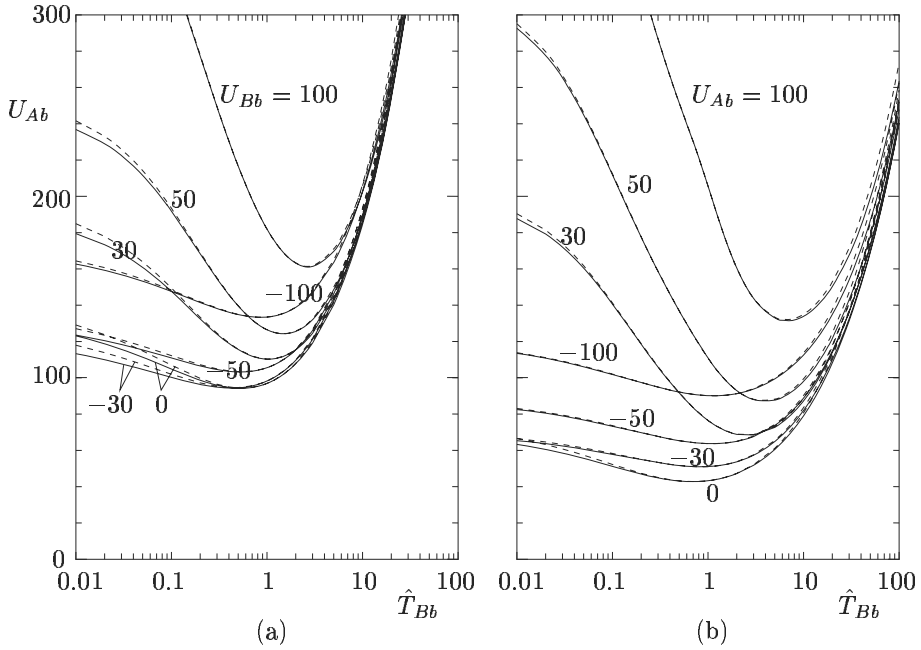

Figure 8.10. Bifurcation curves for a hard-sphere gas II: The first branches of U_{Ab} vs $\hat{T}_{Bb}$ [Eq. (8.61)] for various U_{Bb}. (a) $\hat{r}_B = 1.5$ and $\alpha = 2\pi$ and (b) $\hat{r}_B = 2$ and $\alpha = \pi$. The solid lines —— indicate the bifurcation curves for the full equations; the dashed lines – – – indicate the corresponding curves when the thermal stress terms are neglected.

and the condition corresponding to Eq. (8.56), i.e.,

$$\hat{p}_0 = \frac{\hat{z}_B(\hat{r}_B^2 - 1)}{2} \left(\int_0^{\hat{z}_B} \int_1^{\hat{r}_B} \frac{\hat{r}}{\hat{T}} \mathrm{d}\hat{r}\mathrm{d}\hat{z} \right)^{-1}. \tag{8.65}$$

Incidentally, from Eqs. (8.41) and (8.46) and the boundary condition (8.62), $\partial^2 u_z/\partial \hat{z}^2 = 0$ at $\hat{z} = 0$ and $\hat{z} = \hat{z}_B$, and then from Eq. (8.44), $\partial \hat{p}_2^\natural/\partial \hat{z} = 0$ there.

Let a solution of the above problem in the rectangular domain be S1. Then its mirror image (say, S2) with respect to the boundary at $\hat{z} = 0$ or $\hat{z} = \hat{z}_B$ is also a solution of the problem. The two kinds of solutions S1 and S2 being alternately arranged in the $\hat{z}$ direction, the resulting function is found to be two times continuously differentiable across the connection lines $\hat{z} = n\hat{z}_B$ ($n = 0, \pm 1, \pm 2, \ldots$), because it satisfies Eqs. (8.41)–(8.46) except on the connection lines and satisfies the condition (8.62) on the connection lines (note the relations derived in the preceding paragraph). That is, the function thus constructed is a periodic solution with period $2\hat{z}_B$ with respect to $\hat{z}$ in the infinite domain between the two coaxial circular cylinders at $\hat{r} = 1$ and $\hat{r} = \hat{r}_B$.

The boundary-value problem, i.e., Eqs. (8.41)–(8.46), (8.62)–(8.65), is solved

numerically by a finite-difference method. The system where $\hat{p}_2^\natural$ is eliminated by taking the difference of ∂[Eq. (8.42)]$/\partial\hat{z}$ and ∂[Eq. (8.44)]$/\partial\hat{r}$ is used in the computation [Eq. (8.43) does not contain $\hat{p}_2^\natural$ because of the axial symmetry]. The solution of the system is obtained by the method of iteration similar to that in the Bénard problem in Section 8.2.4 (see Sone, Handa & Doi [2003] for the details).

Bifurcated temperature fields of a hard-sphere gas for three U_A's are compared when $\hat{T}_B = 0.1$, $U_B = 0$, $\hat{r}_B = 2$, and $\hat{z}_B = 1$ in Fig. 8.11. According to the analysis in Section 8.3.2, bifurcation occurs at $U_A = 51.2239$. The bifurcated solution first extends from $U_A = 51.2239$ to smaller values of U_A and then to larger U_A.[12] Figure 8.11 (a) is the field for $U_A = 51$, where the isothermal lines of the bifurcated field are shown in solid lines and those of the axially symmetric and uniform field in dot-dash lines. The system where the thermal stress terms are neglected has no bifurcated solution at this value of U_A. Incidentally, the bifurcation occurs at $U_A = 52.2640$ for the system without the thermal stress. Figure 8.11 (b) is the field for $U_A = 53$, and Fig. 8.11 (c) is the field for $U_A = 100$. In these cases, the system with the thermal stress terms neglected has bifurcated solutions, whose isothermal lines are shown in dashed lines there. The (u_r, u_z), i.e., the infinitesimal velocity amplified by $1/k$ [or $\lim_{k\to 0}(\hat{v}_r/k, \hat{v}_z/k)$], is shown by arrows in these figures. The isothermal lines are strongly distorted by the infinitesimal flow. The difference between the correct temperature field and that of the Navier–Stokes equation with the infinitesimal velocity retained amounts to about 10% at $U_A = 53$ in Fig. 8.11 (b).

Figure 8.12 is a similar figure when $\hat{T}_B = 10$, $U_B = 0$, $\hat{r}_B = 2$, and $\hat{z}_B = 1$, where the same symbols as in Fig. 8.11 are used. Bifurcation occurs at $U_A = 79.1001$. The bifurcated solution extends from $U_A = 79.1001$ to smaller values of U_A and then to larger U_A.[13] Figure 8.12 (a) is the field for $U_A = 79$, where the system with the thermal stress terms neglected has no bifurcated solution. Incidentally, the bifurcation occurs at $U_A = 80.7446$ for the system without the thermal stress. Figure 8.12 (b) is the field for $U_A = 80$, and Fig. 8.12 (c) is the field for $U_A = 100$. In these cases, the system with the thermal stress terms neglected has bifurcated solutions. The isothermal lines are strongly distorted by the infinitesimal flow, as in Fig. 8.11. The difference between the correct temperature field and that of the Navier–Stokes equations with the infinitesimal velocity retained amounts to about 10% at $U_A = 80$ in Fig. 8.12 (b).

8.3.4 Discussion

In this section (Section 8.3), we have discussed the time-independent axially symmetric behavior of a gas in the continuum limit between two coaxial circular cylinders with different temperatures, with special interest in bifurcation of the solution from an axially uniform one. The bifurcation of the solution occurs at infinitesimal speeds of rotation of the two cylinders. Thus the velocity in the gas

[12] One of the solutions for $U_A < U_{Ab}$ cannot be obtained numerically.
[13] See the preceding footnote (Footnote 12).

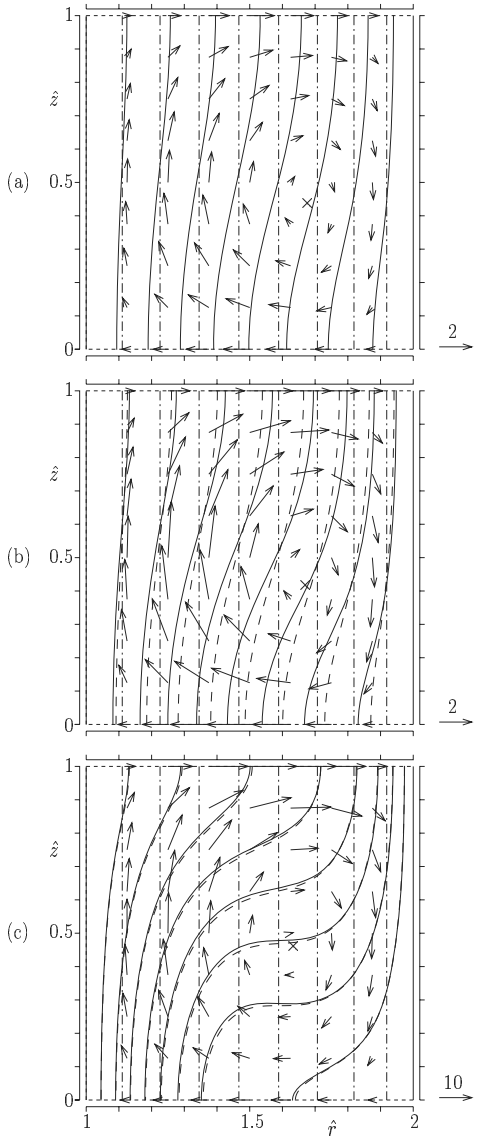

Figure 8.11. Bifurcated temperature fields for a hard-sphere gas I: $\hat{T}_B = 0.1$, $U_B = 0$, $\hat{r}_B = 2$, and $\hat{z}_B = 1$. (a) $U_A = 51$, (b) $U_A = 53$, and (c) $U_A = 100$. The solid lines —— indicate the isothermal lines of the bifurcated temperature field [$\hat{T} = 0.1n$ ($n = 1, 2, \ldots, 10$) from the right wall to the left]. The dashed lines – – – indicate the corresponding results with the thermal stress neglected, and the dot-dash lines – · – indicate the isothermal lines for the ASU solution. The arrows indicate (u_r, u_z) at their starting points and their scale is shown on the lower right corner of each panel, and $\times$ indicates the point where $u_r = u_z = 0$. The maximum of $(u_r^2 + u_z^2)^{1/2}$ is 1.97 at $U_A = 51$ in (a), 3.40 at $U_A = 53$ in (b), and 14.6 at $U_A = 100$ in (c).

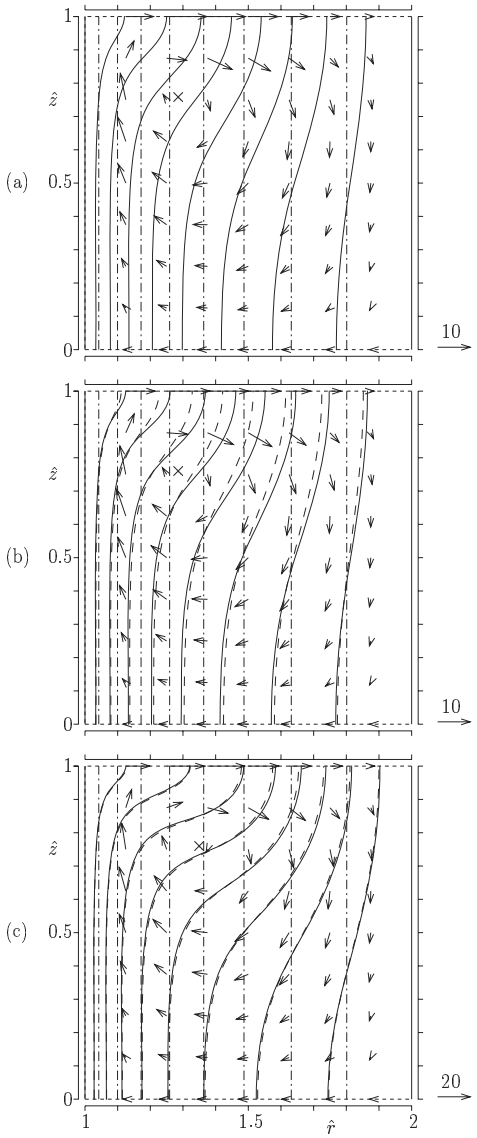

Figure 8.12. Bifurcated temperature fields for a hard-sphere gas II: $\hat{T}_B = 10, U_B = 0$, $\hat{r}_B = 2$, and $\hat{z}_B = 1$. (a) $U_A = 79$, (b) $U_A = 80$, and (c) $U_A = 100$. The solid lines —— indicate the isothermal lines of the bifurcated temperature field [$\hat{T} = n$ $(n = 1, 2, \ldots, 10)$ from the left wall to the right]. The dashed lines −−− indicate the corresponding results with the thermal stress neglected, and the dot-dash lines −·− indicate the isothermal lines for the ASU solution. The arrows indicate (u_r, u_z) at their starting points and their scale is shown on the lower right corner of each panel, and × indicates the point where $u_r = u_z = 0$. The maximum of $(u_r^2 + u_z^2)^{1/2}$ is 12.4 at $U_A = 79$ in (a), 13.3 at $U_A = 80$ in (b), and 23.8 at $U_A = 100$ in (c).

is infinitesimal, but the temperature field away from the bifurcation point has a finite deviation from the axially uniform one (the ghost effect). If one neglects the infinitesimal quantities in the analysis, one cannot find the bifurcation, only to obtain the axially uniform solution. The bifurcated temperature field differs considerably from that obtained by the Navier–Stokes set of equations with the infinitesimal velocity being retained, when the ratio of the temperatures of the two cylinders differs considerably from unity, say, $T_B/T_A = 0.1$ or 10 (a non-Navier–Stokes effect). These results show that the classical fluid dynamics is incomplete to describe the behavior of a gas in the continuum limit. The present problem, the Taylor–Couette problem where the temperatures of the two cylinders are different, is not a simple extension of that with equal temperatures but an important problem that presents an interesting result about the fundamental equations governing the behavior of a gas in the continuum limit.

As shown in Figs. 8.11 and 8.12, the temperature field changes largely with U_A and U_B (or with infinitesimal speeds $V_{\theta A}$ and $V_{\theta B}$ of rotation of the cylinders). In the world of the continuum limit, one has no way to know or determine these infinitesimal velocities. Thus, the temperature field is indeterminate. In a real gas, the Knudsen number may be very small but is not completely zero. To determine its temperature field, we cannot neglect very small motion of the cylinders, however small it may be.

In the atmospheric condition, the mean free path is very small but is not exactly zero. Then, the flow velocity is nonzero for the bifurcated temperature field. Let us estimate the rough size of the flow speed that induces the distorted temperature fields in Figs. 8.11 and 8.12. As an example, consider the following case: The radius L_A of the inner cylinder and that of the outer are, respectively, 10 m and 20 m; the temperature T_A of the inner cylinder is 300 K (or 3000 K); the gas between the cylinders is air or nitrogen gas and under atmospheric pressure.[14] Then, the mean free path near the inner cylinder is roughly 6×10^{-8} m (or 6×10^{-7} m) and thus the Knudsen number is 6×10^{-9} (or 6×10^{-8}). Then, for the case with $V_{\theta B} = 0$ mm/s, $T_A = 3000$ K, and $T_B = 300$ K, the bifurcation occurs at $V_{\theta A} = 4$ mm/s (corresponding to $U_A = 51.2239$ for $\alpha = \pi$); for the case with $V_{\theta B} = 0$ mm/s, $T_A = 300$ K, and $T_B = 3000$ K, it occurs at $V_{\theta A} = 0.2$ mm/s (corresponding to $U_A = 79.1001$ for $\alpha = \pi$). In view of these bifurcation speeds U_A shown in the parentheses, the well-distorted temperature fields in Figs. 8.11 (a) and (b) or Figs. 8.12 (a) and (b) can be seen about $V_{\theta A} = 4$ mm/s or $V_{\theta A} = 0.2$ mm/s. This speed is very small compared with the scale of the system (In the latter case, it takes more than 3 days for one rotation of the inner cylinder). Unless one controls this small speed of motion of the cylinders in experiment or analysis, one will obtain a quite different temperature field. If one analyzes the problem neglecting this size of velocity, one obtains only the axially uniform solution. The distorted temperature field is determined by the flow in the $(\hat{r}, \hat{z})$ plane, and the circumferential flow plays an indirect role to induce the motion in the $(\hat{r}, \hat{z})$ plane. The maximum speeds of this motion corresponding to the maximum $(u_r^2 + u_z^2)^{1/2}$ in Figs. 8.11 (a), (b), and (c) with

[14] See Footnote 102 in Section 3.6.2.

$T_A = 3000$ K and $T_B = 300$ K are, respectively, 0.16, 0.27, and 1.2 mm/s, and those in Figs. 8.12 (a), (b), and (c) with $T_A = 300$ K and $T_B = 3000$ K are, respectively, 3.1×10^{-2}, 3.3×10^{-2}, and 6×10^{-2} mm/s. In the experiment one must eliminate possible disturbances of these sizes.

The effect of the temperature difference of the two cylinders on the appearance of the roll-type solution is often discussed by the analogy with the Bénard problem in the following way. When the outer cylinder is heated, the centrifugal force acts in the same direction as the gravity in the Bénard problem, and therefore the bifurcation occurs more easily. However, the bifurcation curves U_{Ab} vs $\hat{T}_{Bb}$, for example in Fig. 8.9, at $\hat{T}_{Bb}$ considerably away from unity are well in higher positions than those at $\hat{T}_{Bb} = 1$. This is opposite to the guess by the analogy consideration. The minimum point of a bifurcation curve differs considerably depending on situations. This is discussed in details in Handa & Doi [2004]. When the temperature difference $|T_B/T_A - 1|$ is much larger than the Knudsen number but is small, the non-Navier–Stokes effect is negligible. Thus, the problem can be discussed by the Navier–Stokes equations with the infinitesimal velocity retained. There are some works on the effect of the temperature difference of the two cylinders by the Boussinesq approximation of the Navier–Stokes equations. Unfortunately, the terms of the temperature effect are inconsistently taken in and the same-order terms are discarded. That is, the effect of the temperature difference on the ASU solution, as well as the dependence of viscosity on temperature, is not correctly taken into account. As a result, for example, when the outer cylinder is at rest and the ratio of the radii of the two cylinders is less than about three, the effect of the temperature difference of the cylinders appears in wrong directions in the Boussinesq approximation analyses and in the analysis of the Navier–Stokes equation with constant viscosity.

8.4 Flows between rotating circular cylinders with evaporation and condensation

8.4.1 Introduction

In the preceding subsection (Section 8.3), we discussed the traditional Taylor–Couette problem of a gas in the continuum limit and showed the importance of kinetic theory even in this typically classical fluid-dynamic problem. In this section, we extend the problem to the case where the cylinders are made of the condensed phase of the gas. Then, condensation and evaporation take place on the cylinders. This freedom introduces interesting results. That is, even in the simple case where the state of the gas is axially symmetric and uniform, the solution of the problem is not unique and is affected by the ghost effect of infinitesimal convection (Sone, Takata & Sugimoto [1996], Sone, Sugimoto & Aoki [1999], Sone & Doi [2000]). We first explain this result in Section 8.4.2

and then, in Sections 8.4.3 and 8.4.4, discuss the effect of evaporation and condensation on the formation of the roll-type solution.

Consider a gas between two rotating coaxial circular cylinders made of the condensed phase of the gas. Let the radius, temperature, and circumferential velocity of the inner cylinder be, respectively, L_A, T_A, and $V_{\theta A}$, and let the corresponding quantities of the outer cylinder be L_B, T_B, and $V_{\theta B}$, where T_A, $V_{\theta A}$, T_B, and $V_{\theta B}$ are uniform on each cylinder; the saturated gas pressure at temperature T_A is denoted by p_A and that at T_B by p_B. We will discuss the behavior of the gas between the cylinders, with special interest in the stability and bifurcation of time-independent solutions, under the following assumptions: (i) the gas molecules leaving the cylinders follow the complete-condensation condition and (ii) the flow field is axially symmetric.

The system of the Boltzmann equation and the complete-condensation condition being made dimensionless by taking L_A, T_A, p_A, and $L_A/(2RT_A)^{1/2}$ as the reference quantities L, T_0, p_0, and t_0 in Section 1.9, the problem is found to be characterized by the initial condition and the following parameters:

$$\frac{L_B}{L_A},\quad \frac{V_{\theta A}}{\sqrt{2RT_A}},\quad \frac{V_{\theta B}}{\sqrt{2RT_A}},\quad \frac{T_B}{T_A},\quad \frac{p_B}{p_A},\quad \frac{\ell_A}{L_A}(=\mathrm{Kn}), \tag{8.66}$$

where ℓ_A is the mean free path of the gas in the equilibrium state at rest with temperature T_A and pressure p_A.

8.4.2 Axially symmetric and uniform case

We will first consider the case where the flow field is axially uniform as well as axially symmetric. The time-independent behavior of the gas is studied analytically and numerically. We will summarize the results related to the bifurcation of and the ghost effect on the flow.

Asymptotic analysis 1

Here, the problem for small Knudsen numbers is considered. We discuss the system of fluid-dynamic-type equations and their associated boundary conditions that describes the problem in the continuum limit, and give examples of the ghost effect of infinitesimal convection on the flow field as an application of the system (Sone, Takata & Sugimoto [1996]; see also Sone [1997, 2002]).

When the Mach numbers of the flows of evaporation or condensation on the cylinders are finite, we can analyze the problem on the basis of the Euler system, Eqs. (3.225a)–(3.226) and (3.228a)–(3.229c), discussed in Section 3.5. In the Euler system, the circumferential velocity component is imposed on an evaporating boundary, but is not on a condensing one. Owing to this feature, we will see that bifurcation of flow takes place in the system under consideration. When neither evaporation nor condensation is taking place and radial flow vanishes, the solution of the Euler set of equations is indefinite, and more careful

examination is required. We will consider the situation where radial velocity component vanishes when a cylinder is rotating.[15]

When both the cylinders are at rest and $p_B/p_A > 1$, a radial flow is obviously induced where evaporation takes place on the outer cylinder and condensation does on the inner cylinder.[16] When the outer cylinder is rotating slowly, the flow is deformed to a spiral flow evaporating from the outer cylinder. As the speed of rotation of the outer cylinder increases, the pressure of the gas increases on the outer cylinder by the centrifugal force of the rotation of the gas, and the speed of evaporation of the gas from the outer cylinder is reduced and finally vanishes. This process can be studied by the Euler system derived in Section 3.5. The limiting speed $|V_{\theta B}^{cr}|$ of the outer cylinder where the radial velocity component vanishes is given by

$$\frac{|V_{\theta B}^{cr}|}{(2RT_A)^{1/2}} = \left(\frac{5T_B}{2T_A}\right)^{1/2} \left[1 - \left(\frac{p_B}{p_A}\right)^{-2/5}\right]^{1/2} \left[\left(\frac{L_B}{L_A}\right)^2 - 1\right]^{-1/2}. \tag{8.67}$$

Beyond this speed, no flow evaporating from the outer cylinder is possible. The flow evaporating from the inner cylinder at rest, which is a radial flow,[17] is impossible, because the pressure of the gas on the outer cylinder of the radial-flow solution of the Euler equations satisfying the boundary condition on the inner cylinder is lower than p_B in the boundary condition on the outer cylinder.[18] Thus, the radial flow vanishes for the range $|V_{\theta B}| \geq |V_{\theta B}^{cr}|$ given by Eq. (8.67). For this range of $V_{\theta B}$, the asymptotic analysis for small Knudsen numbers (Kn or k) of the problem with radial velocity component of the first or higher order of the Knudsen number is required.

The asymptotic analysis can be carried out on the basis of the Boltzmann equation in the cylindrical coordinate expression in the same way as that in Section 3.3 under the axially symmetric and uniform condition and in the absence of the external force by replacing the supplementary condition (3.135a) by

$$\int \zeta_r \hat{f} \mathbf{d}\boldsymbol{\zeta} = O(k),$$

where ζ_r is the radial component of $\boldsymbol{\zeta}$. According to the asymptotic analysis in Sone, Takata & Sugimoto [1996], the leading-order behavior of the gas is

[15]The situation where the circumferential velocity component as well as the radial velocity component vanishes is possible only when $p_B = p_A$.

[16]The results in this subsection related to the functions h_1, h_2, F_s, and F_b in the boundary conditions (3.228a)–(3.229c) are based on their properties, e.g., $h_1 \leq 1$ and $F_s \geq 1$, that are proved partially or shown numerically for some molecular models. They are summarized in Sone, Takata & Golse [2001] (see also Sone [2002]).

[17]Note the boundary conditions for the Euler set of equations mentioned above.

[18]See Footnote 28 in Sone, Takata & Sugimoto [1996] and Section IV in Sone, Takata & Golse [2001]. More detailed explanation in the latter is for the case where both the cylinders are at rest, but it is simply extended to the present case, where the outer cylinder is rotating.

described by the following equations:

$$\frac{\mathrm{d}\hat{\rho}_{H0}\hat{v}_{rH1}\hat{r}}{\mathrm{d}\hat{r}} = 0, \tag{8.68a}$$

$$\frac{\hat{\rho}_{H0}\hat{v}_{\theta H0}^2}{\hat{r}} = \frac{1}{2}\frac{\mathrm{d}\hat{p}_{H0}}{\mathrm{d}\hat{r}}, \tag{8.68b}$$

$$\hat{\rho}_{H0}\hat{v}_{rH1}\left(\frac{\mathrm{d}\hat{v}_{\theta H0}}{\mathrm{d}\hat{r}} + \frac{\hat{v}_{\theta H0}}{\hat{r}}\right) = \frac{1}{2\hat{r}^2}\frac{\mathrm{d}}{\mathrm{d}\hat{r}}\left[\Gamma_1(\hat{T}_{H0})\hat{r}^2\left(\frac{\mathrm{d}\hat{v}_{\theta H0}}{\mathrm{d}\hat{r}} - \frac{\hat{v}_{\theta H0}}{\hat{r}}\right)\right], \tag{8.68c}$$

$$\hat{\rho}_{H0}\hat{v}_{rH1}\frac{\mathrm{d}}{\mathrm{d}\hat{r}}\left(\hat{v}_{\theta H0}^2 + \frac{5}{2}\hat{T}_{H0}\right) = \frac{1}{\hat{r}}\frac{\mathrm{d}}{\mathrm{d}\hat{r}}\left[\Gamma_1(\hat{T}_{H0})\hat{r}\hat{v}_{\theta H0}\left(\frac{\mathrm{d}\hat{v}_{\theta H0}}{\mathrm{d}\hat{r}} - \frac{\hat{v}_{\theta H0}}{\hat{r}}\right)\right] + \frac{5}{4\hat{r}}\frac{\mathrm{d}}{\mathrm{d}\hat{r}}\left(\Gamma_2(\hat{T}_{H0})\hat{r}\frac{\mathrm{d}\hat{T}_{H0}}{\mathrm{d}\hat{r}}\right), \tag{8.68d}$$

$$\hat{p}_{H0} = \hat{\rho}_{H0}\hat{T}_{H0}, \tag{8.68e}$$

where $(\hat{r}, \theta, \hat{z})$ and $(\hat{v}_r, \hat{v}_\theta, \hat{v}_z(=0))$ are, respectively, the cylindrical coordinate expressions of x_i and $\hat{v}_i$ with the axis of the cylinders on $\hat{r} = 0$, the subscript H is used instead of SB in Section 3.3,[19] and $\Gamma_1(\hat{T}_{H0})$ and $\Gamma_2(\hat{T}_{H0})$ are the nondimensional viscosity and thermal conductivity defined in Section A.2.9. The boundary condition for this set of equations is[20]

$$\hat{v}_{\theta H0} = \frac{V_{\theta A}}{(2RT_A)^{1/2}}, \quad \hat{p}_{H0} = 1, \quad \hat{T}_{H0} = 1 \quad \text{at } \hat{r} = 1, \tag{8.69a}$$

$$\hat{v}_{\theta H0} = \frac{V_{\theta B}}{(2RT_A)^{1/2}}, \quad \hat{p}_{H0} = \frac{p_B}{p_A}, \quad \hat{T}_{H0} = \frac{T_B}{T_A} \quad \text{at } \hat{r} = \frac{L_B}{L_A}. \tag{8.69b}$$

In view of the number of the equations and the boundary conditions and the order of the differential equations, the variables $\hat{\rho}_{H0}$, $\hat{v}_{\theta H0}$, $\hat{T}_{H0}$, $\hat{p}_{H0}$, and $\hat{v}_{rH1}$ are determined by the above system of equations and boundary conditions. Systems of similar character are obtained by higher-order analysis. The system (8.68a)–(8.69b) determines the variables $\hat{\rho}_{H0}$, $\hat{v}_{\theta H0}$, $\hat{T}_{H0}$, and $\hat{p}_{H0}$ of the order of unity simultaneously with the first-order variable $\hat{v}_{rH1}$. That is, the behavior of the gas in the continuum limit is influenced by the infinitesimal radial velocity component (ghost effect). No non-Navier–Stokes stress enters Eqs. (8.68b) and (8.68c).

The above example with $V_{\theta A} = 0$ is studied for $|V_{\theta B}| > |V_{\theta B}^{cr}|$ on the basis of the above system (8.68a)–(8.69b). Some of the results in Sone, Takata & Sugimoto [1996] are shown in Figs. 8.13 and 8.14.[21] Figures 8.13 (a) and (b) show the profiles $\hat{v}_{\theta H0}$ vs $\hat{r}$ of the circumferential velocity component, respectively,

[19] We used the same subscript H as in Section 3.5 without introducing a new symbol, because the present case is a very limited subclass of the original Hilbert expansion and a local discussion.

[20] As in the case in Section 3.3, $\hat{f}_{H0}$, corresponding to $\hat{f}_{SB0}$, is a Maxwellian without radial velocity component. Thus, the complete-condensation condition [more generally, the kinetic boundary condition (1.69)] is satisfied when the values of the parameters in the Maxwellian satisfy the conditions (8.69a) and (8.69b).

[21] (i) The saturated gas pressure is a rapidly increasing function of the temperature, and for

for various $V_{\theta B}/(2RT_A)^{1/2}$ and for various p_B/p_A. The dashed line $---$ is the profile for $|V_{\theta B}| \to |V_{\theta B}^{cr}|_-$.[22] The profiles with label ($\hat{v}_{rH1} = 0$) for which $\hat{v}_{rH1} = 0$ coincide with those of the Navier–Stokes equations under nonslip condition.[23] The $\hat{v}_{rH1}$ is negative for the smaller values of $V_{\theta B}/(2RT_A)^{1/2}$ in panel (a) and for larger values of p_B/p_A in panel (b) and vice versa. Figure 8.14 shows the profiles $\hat{T}_{H0}$ vs $\hat{r}$ of the temperature corresponding to Fig. 8.13. The profiles $\hat{v}_{\theta H0}$ and $\hat{T}_{H0}$ are deformed by the effect of the infinitesimal convection due to $\hat{v}_{rH1}$ from the profile for $\hat{v}_{rH1} = 0$. The numerical solutions of the kinetic (BKW) equation for small Knudsen numbers are compared with the solution of Eqs. (8.68a)–(8.69b) with $\Gamma_1(\hat{T}_{H0}) = \Gamma_2(\hat{T}_{H0}) = \hat{T}_{H0}$ corresponding to the BKW equation in Sone, Takata & Sugimoto [1996] in figures similar to Figs. 3.4 and 3.5 (see also Sone [1997]). The solutions of the kinetic equation approach those of Eqs. (8.68a)–(8.69b) as $\mathrm{Kn} \to 0$.

When the inner cylinder is at rest, as we have seen, the flow from the inner cylinder to the outer is impossible when $p_B/p_A > 1$. Consider the case where the inner cylinder is rotating, the outer cylinder is at rest, and $p_B/p_A > 1$. A spiral flow evaporating from the inner cylinder can have a pressure higher than p_B on the outer cylinder owing to the centrifugal force; thus, a flow from the inner cylinder to the outer is possible. On the other hand, a radial flow from the outer cylinder can be possible, because the flow is radial on the outer cylinder at rest and the circumferential velocity component is not imposed on the rotating inner cylinder. Therefore, two flows, from the outer cylinder to the inner and from the inner cylinder to the outer, are possible. In fact, the solid line for $\mathrm{Kn} = 0_+$ to be shown together with the numerical result for finite Knudsen numbers in Fig. 8.18 shows this. Thus, various situations can be imagined depending on the set of the parameters. The bifurcation problem for small Knudsen numbers can be studied more easily when the speeds of rotation of the cylinders are small, and the comprehensive feature of the bifurcation is clarified (Sone & Doi [2000]; see also Sone [2002]), which will be summarized in **Asymptotic analysis 2** in this subsection (Section 8.4.2).

Before the discussion of the bifurcation problem for small speeds of rota-

---

many gases, $1 < T_B/T_A < 1.02$ at $p_B/p_A = 1.2$ (see Table C.2 or "Thermophysical Properties of Fluid Systems" at http://webbook.nist.gov); thus $T_B/T_A = 1$ is chosen.

(ii) Figures 8.13 and 8.14 are the corrected figures of Figs. 3 and 4 in Sone, Takata & Sugimoto [1996] (see its erratum). Incidentally, Figs. 5 and 6 in Sone [1997], which correspond, respectively, to Fig. 8.13 (a) and Fig. 2 (a) in the former paper, are required corrections according to the present figure and the erratum.

[22] The two solutions with v_r of different orders, i.e., $\hat{v}_r = O(1)$ and $O(k)$, are connected by a transition solution in the neighborhood of $V_{\theta B}^{cr}$. The transition solution in a similar situation (the case discussed in **Asymptotic analysis 2** in this subsection) are constructed in Sone & Doi [2000] (see also Sone [2002]).

[23] The nonslip condition imposes that the velocity and temperature of a gas on the boundary coincide with those of the boundary; no condition on the pressure of the gas is imposed. Here, the reference pressure p_A is taken to be the pressure of the gas on the inner cylinder, that is, $\hat{p} = 1$ there. This is what is called the *cylindrical Couette flow* or, simply, *Couette flow* in classical fluid dynamics. Needless to say, the name is used for the problems with the same geometrical situation in kinetic theory. This kind of extension of old terminology is common, e.g., plane Couette flow and Poiseuille flow.

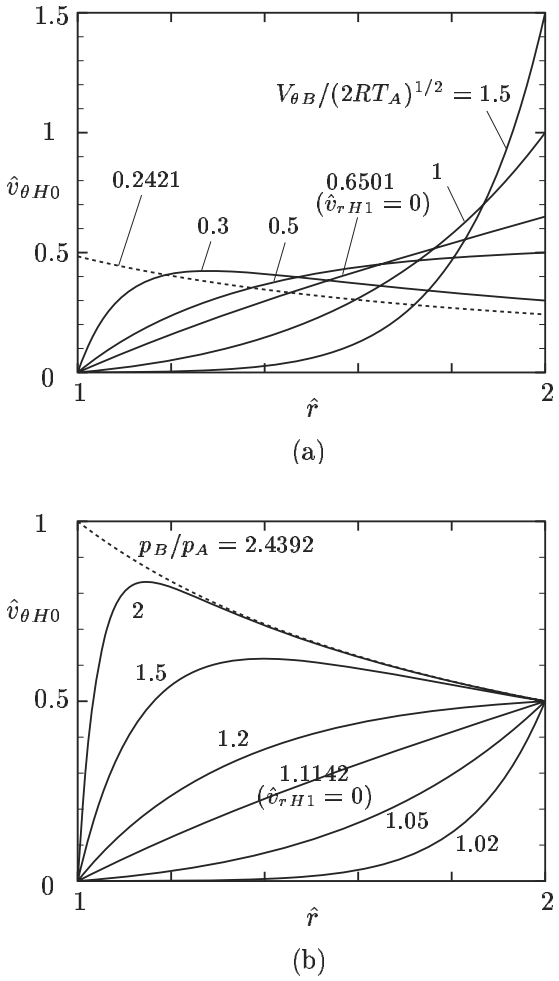

Figure 8.13. The circumferential velocity profiles $\hat{v}_{\theta H0}$ vs $\hat{r}$ for a hard-sphere gas $[V_{\theta A}/(2RT_A)^{1/2} = 0,\ T_B/T_A = 1,$ and $L_B/L_A = 2]$. (a) The profiles for various $V_{\theta B}/(2RT_A)^{1/2}$ at $p_B/p_A = 1.2$; (b) the profiles for various p_B/p_A at $V_{\theta B}/(2RT_A)^{1/2} = 0.5$. The dashed line $---$ is the profile for $V_{\theta B} \to V_{\theta B-}^{cr}$ in panel (a) and that for $p_B/p_A \to (p_B/p_A)_+^{cr}$ in panel (b), where $(p_B/p_A)^{cr}$ is p_B/p_A corresponding to $V_{\theta B}^{cr}$. The profiles with label $(\hat{v}_{rH1} = 0)$ for which $\hat{v}_{rH1} = 0$ coincide with those of the Navier–Stokes equations under nonslip condition (see Footnote 23 in this subsection).

tion of the cylinders, we briefly explain the framework of the governing system on the basis of the systems of equations and boundary conditions mentioned above. When the Mach number of the flow is small but finite, the Euler system, Eqs. (3.225a)–(3.226) and (3.228a)–(3.229c), reduces in the following way:

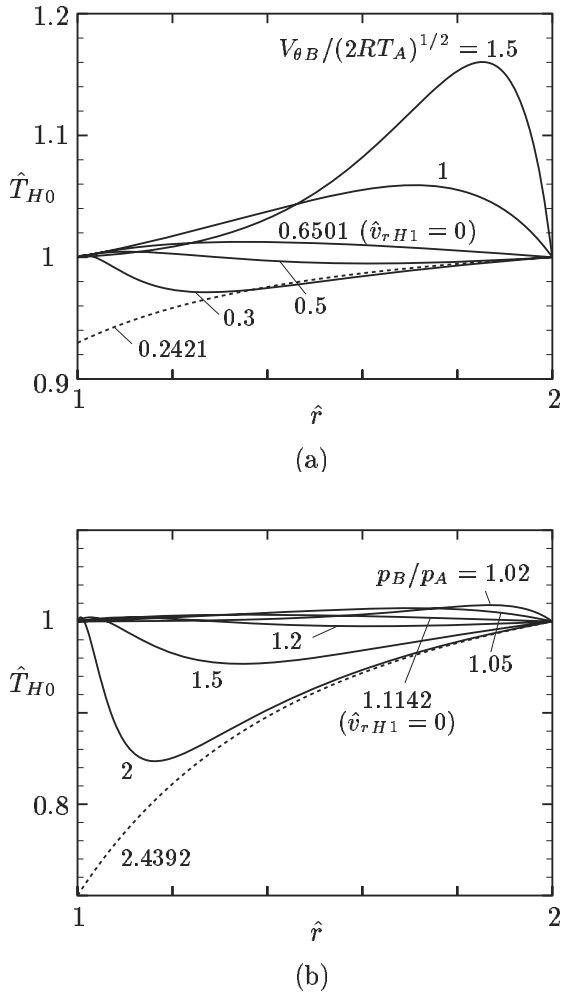

Figure 8.14. The temperature profiles $\hat{T}_{H0}$ vs $\hat{r}$ for a hard-sphere gas $[V_{\theta A}/(2RT_A)^{1/2} = 0,\ T_B/T_A = 1,$ and $L_B/L_A = 2]$. (a) The profiles for various $V_{\theta B}/(2RT_A)^{1/2}$ at $p_B/p_A = 1.2$; (b) the profiles for various p_B/p_A at $V_{\theta B}/(2RT_A)^{1/2} = 0.5$. The dashed line $---$ is the profile for $V_{\theta B} \to V_{\theta B-}^{cr}$ in panel (a) and that for $p_B/p_A \to (p_B/p_A)_+^{cr}$ in panel (b), where $(p_B/p_A)^{cr}$ is p_B/p_A corresponding to $V_{\theta B}^{cr}$. The profiles with label $(\hat{v}_{rH1} = 0)$ for which $\hat{v}_{rH1} = 0$ coincide with those of the Navier–Stokes equations under nonslip condition (see Footnote 23 in this subsection).

The Euler set of equations, Eqs. (3.225a)–(3.225c), is easily seen to reduce to incompressible Euler set. The boundary conditions, Eqs. (3.228a)–(3.229c), for the Euler set are derived by the analysis of Knudsen layer governed by the nonlinear Boltzmann equation. As explained in Section 3.6.1, the Knudsen layer

splits into the suction boundary layer and the Knudsen layer governed by the linearized Boltzmann equation on the condensing boundary and it reduces simply to the Knudsen layer governed by the linearized Boltzmann equation on the evaporating boundary. The boundary condition derived from the linearized Boltzmann equation is of the same feature (e.g., the number of conditions) as the condition (3.228a), and the condition derived from the combination of the suction boundary layer and the Knudsen layer governed by the linearized Boltzmann equation is also of the same feature as the condition (3.229a). Equations (8.68a)–(8.68d) reduce to "incompressible Navier–Stokes equations"[24] with infinitesimal radial velocity component retained. Thus the feature of the system for small but finite Mach numbers may be basically considered to be the same as the system with a finite Mach number.

As seen in the above examples, it is required for the ghost effect or bifurcation to occur that the pressure difference induced by the centrifugal force is comparable to or larger than $p_B - p_A$. When we consider the case where the speeds of rotation of the cylinders are small, i.e., $\hat{v}_\theta$ is a small quantity of the order of ε, the situation where the ghost effect or bifurcation occurs corresponds to the case where the difference $p_B/p_A - 1$ is $O(\varepsilon^2)$. Thus, for the study of the ghost effect and bifurcation for $V_{\theta A}/(2RT_A)^{1/2}$ or $V_{\theta B}/(2RT_A)^{1/2} = O(\varepsilon)$, the case $p_B/p_A - 1 = O(\varepsilon^2)$ should be considered. Thus, the ordering $\hat{v}_\theta = O(\varepsilon)$ and $\hat{v}_r = O(\varepsilon^2)$ should be taken into account in the derivation of the systems for small speeds of rotation of the cylinders in the preceding paragraph. In Sone & Doi [2000], the case where $\mathrm{Kn} = \varepsilon^m$ is considered under the above ordering, and the system of equations and boundary conditions for $m \geq 3$ is found to be basically the same as the case of finite Mach numbers.

Asymptotic analysis 2

Here, we consider the bifurcation problem for small Knudsen numbers when the speeds of rotation of the cylinders are small, and describe the main results of the bifurcation analysis in Sone & Doi [2000], where the comprehensive feature of the flow is clarified (the brief description of analysis is given in Sone [2002]).

In the work, the following case of the parameters is considered:

$$\left.\begin{aligned} &\frac{L_B}{L_A} - 1 = \hat{r}_B - 1 = O(1), \quad \mathrm{Kn} = \varepsilon^m, \\ &\frac{V_{\theta A}}{\sqrt{2RT_A}} = \varepsilon u_{\theta A1}, \quad \frac{V_{\theta B}}{\sqrt{2RT_A}} = \varepsilon u_{\theta B1}, \\ &\frac{T_B}{T_A} - 1 = \varepsilon^2 \tau_{B2}, \quad \frac{p_B}{p_A} - 1 = \varepsilon^2 P_{B2}, \end{aligned}\right\} \tag{8.70}$$

where $\varepsilon \ll 1$, and $u_{\theta A1}$, $u_{\theta B1}$, τ_{B2}, and P_{B2} are quantities of the order of unity. The solution shows different features depending on the value of m : $m \geq 3$, $m = 2$, and $m = 1$. In the last case ($m = 1$), no bifurcation occurs.

[24] See the first paragraph of Section 3.2.4 for the meaning of the quotation mark.

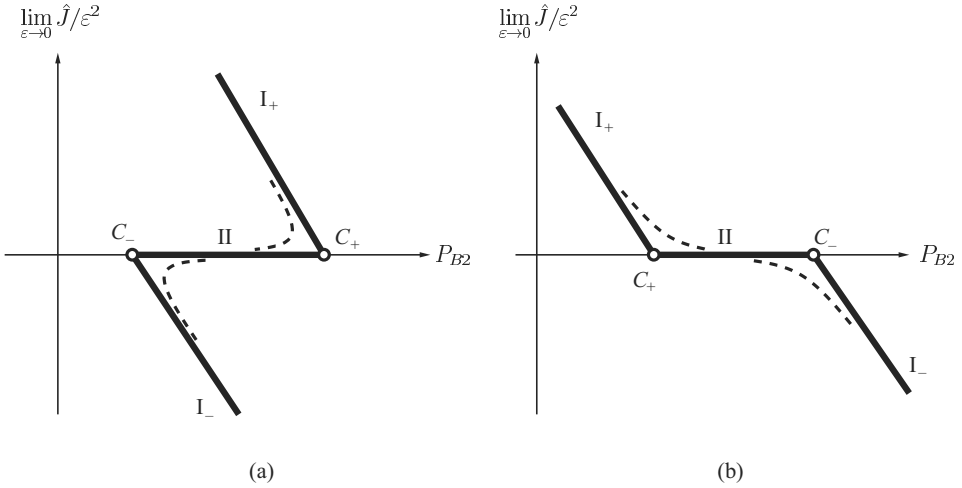

Figure 8.15. Bifurcation diagram (or schematic profiles $\lim_{\varepsilon\to 0}\hat{J}/\varepsilon^2$ vs P_{B2}) of the axially uniform flow in the limit $\varepsilon \to 0$ for the parameter size given by Eq. (8.70) with $m \geq 3$ I: The two cylinders are rotating in the same direction ($u_{\theta A1}u_{\theta B1} > 0$). (a) $u_{\theta A1}^2 > (u_{\theta B1}\hat{r}_B)^2$ and (b) $u_{\theta A1}^2 < (u_{\theta B1}\hat{r}_B)^2$. The solution is indicated by thick solid lines. The connection of the two solutions I and II by a transition solution is shown by a dashed line.

Let the mass flow from the inner cylinder to the outer cylinder per unit time and per unit length of the cylinders be J, and the nondimensional mass-flow rate $J/[2\sqrt{2}\pi L_A p_A/(RT_A)^{1/2}]$ be denoted by $\hat{J}$. The diagrams $\hat{J}/\varepsilon^2$ vs P_{B2} for $m \geq 3$ are given in Figs. 8.15 and 8.16. There are two kinds of solutions: one with $\hat{J}$ of the order of ε^2 (say I) and the other with $\hat{J}$ of the order of ε^m (say II). The first solution is subclassified into two: one with positive $\hat{J}$ denoted by I$_+$ and the other with negative $\hat{J}$ denoted by I$_-$. Figure 8.15 is the diagram when the two cylinders are rotating in the same direction, and Fig. 8.16 is that when the two cylinders are rotating in the opposite directions. The two solutions I$_+$ and I$_-$ are disjointed and connected with the solution II at C_+ and C_-. The P_{B2} at these points are

$$P_{B2} = \frac{(\hat{r}_B^2 - 1)u_{\theta A1}^2}{\hat{r}_B^2} \quad \text{at } C_+, \tag{8.71a}$$

$$P_{B2} = (\hat{r}_B^2 - 1)u_{\theta B1}^2 \quad \text{at } C_-. \tag{8.71b}$$

The solution connecting the two solutions (I$_+$ and II at C_+ or I$_-$ and II at C_-) of different orders of $\hat{J}$ smoothly is shown schematically by a dashed line in these figures.

When the two cylinders are rotating in the same direction ($u_{\theta A1}u_{\theta B1} > 0$), the bifurcation diagram is classified into two classes. When $|u_{\theta A1}| > |\hat{r}_B u_{\theta B1}|$ (the angular momentum of the gas on the inner cylinder is larger than that on

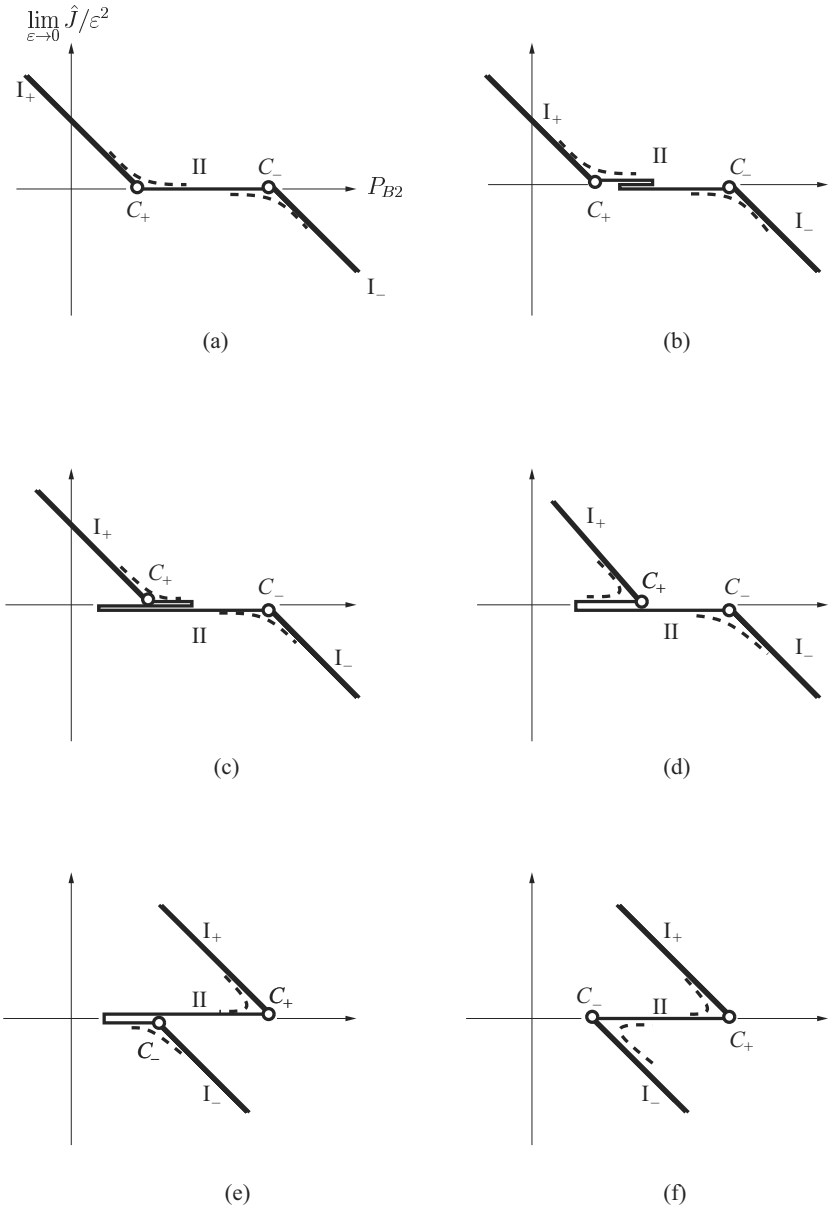

Figure 8.16. Bifurcation diagram (or schematic profiles $\lim_{\varepsilon\to 0} \hat{J}/\varepsilon^2$ vs P_{B2}) of the axially uniform flow in the limit $\varepsilon \to 0$ for the parameter size given by Eq. (8.70) with $m \geq 3$ II: The two cylinders are rotating in opposite directions ($u_{\theta A1}u_{\theta B1} < 0$). (a) $(u_{\theta A1}/u_{\theta B1}\hat{r}_B)^2 \leq 1/9c_1$, (b) $1/9c_1 < (u_{\theta A1}/u_{\theta B1}\hat{r}_B)^2 < 1/9c_2$, (c) $1/9c_2 < (u_{\theta A1}/u_{\theta B1}\hat{r}_B)^2 < 1/9$, (d) $1/9 \leq (u_{\theta A1}/u_{\theta B1}\hat{r}_B)^2 < 1$, (e) $1 < (u_{\theta A1}/u_{\theta B1}\hat{r}_B)^2 < 9$, and (f) $(u_{\theta A1}/u_{\theta B1}\hat{r}_B)^2 \geq 9$, where c_1 and c_2 depend on $\hat{r}_B$. The solution is indicated by thick or medium solid lines. The connection of the two solutions I and II by a transition solution is shown by a dashed line.

the outer), three solutions exist in the range

$$(\hat{r}_B^2 - 1)u_{\theta B1}^2 < P_{B2} < \frac{(\hat{r}_B^2 - 1)u_{\theta A1}^2}{\hat{r}_B^2}, \tag{8.72}$$

and the solution is unique in the other range of P_{B2}. When $|u_{\theta A1}| \leq |\hat{r}_B u_{\theta B1}|$ (the angular momentum of the gas on the inner cylinder is not larger than that on the outer), the solution is unique for the whole range of P_{B2}. When the two cylinders are rotating in the opposite directions ($u_{\theta A1}u_{\theta B1} < 0$), the bifurcation diagram is classified into six classes. The situation of the solution I_+ and I_- is the same as in the case when the cylinders are rotating in the same direction ($u_{\theta A1}u_{\theta B1} > 0$), but the solution II is classified into four kinds when $|u_{\theta A1}| \leq |\hat{r}_B u_{\theta B1}|$ and into two kinds when $|u_{\theta A1}| \geq |\hat{r}_B u_{\theta B1}|$.

The above feature of the diagram is common to $m \geq 3$. The solution II is determined by the interaction of the circumferential velocity of the order of ε with the radial velocity of the order of ε^m. The limiting case $m \to \infty$ corresponds to flows with small but finite Mach numbers [$O(\varepsilon)$] in the continuum limit (Kn $= 0_+$).[25] In this world, the radial velocity of the solution II vanishes, that is, there is no radial flow. However, if the radial velocity is neglected in the analysis, the correct solution is not obtained except for a special P_{B2}.[26] The solution II is determined by the ghost effect.

The bifurcation diagram for $m = 2$ is shown in Fig. 8.17. The solution is of a single kind with $\hat{J}$ of the order of ε^2. The diagram is classified into two classes as shown in Fig. 8.17, irrespective of the directions of rotation of the two cylinders.

Arkeryd & Nouri [2005] discussed a rigorous mathematical estimate of the residue of the above asymptotic solution (Sone & Doi [2000]) for a special case.

Numerical analysis

The effect of gas rarefaction or the Knudsen number on the bifurcation is explained on the basis of the numerical work by Sone, Sugimoto & Aoki [1999], where the problem is studied numerically on the basis of the BKW equation by a finite-difference method. The values of the parameters studied in the paper are as follows:

[25] Strictly, the solution in the continuum limit (Kn $\to$ 0) for small but finite ε should be carried out in the two steps (see Sections 9.3 and 3.6.1): (i) the asymptotic analysis for small Kn is carried out without the relation between ε and Kn being set (see Section 3.5), and then (ii) the approximation for small ε under the parameter setting of Eq. (8.70) excluding the relation Kn $= \varepsilon^m$ is carried out. In this process, the Knudsen layer governed by the nonlinear Boltzmann equation is split into the suction boundary layer and the Knudsen layer governed by the linearized equation. The present case corresponds to the above mentioned small ε simplification of the ghost effect solution for Kn $= 0_+$ with $\hat{J} = 0$ in Fig. 8.18, which is studied on the basis of Sone, Takata & Sugimoto [1996] [see **Asymptotic analysis 1** in this subsection (Section 8.4.2)].

[26] The solution satisfying the boundary condition on P_{B2} cannot be obtained. However, the circumferential velocity field is determined independently of P_{B2}. This is the solution under nonslip condition [see Footnote 23 in this subsection (Section 8.4.2)].

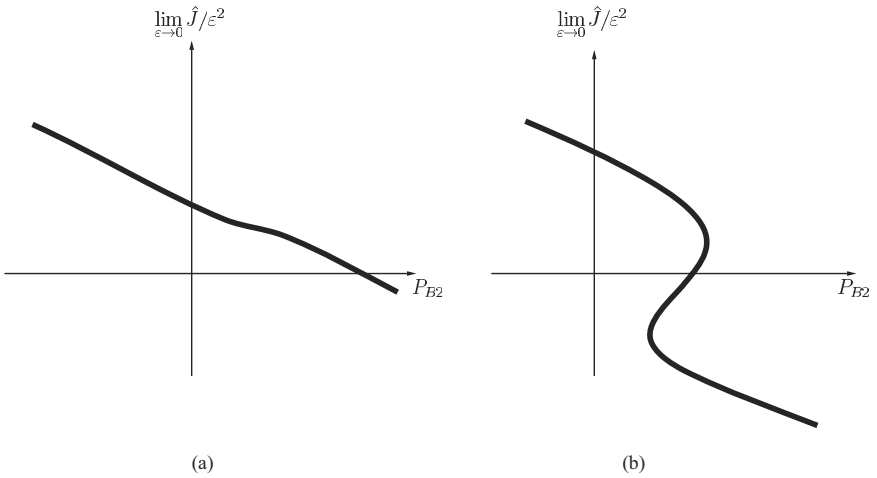

Figure 8.17. Bifurcation diagram (or schematic profiles $\lim_{\varepsilon\to 0}\hat{J}/\varepsilon^2$ vs P_{B2}) of the axially uniform flow in the limit $\varepsilon \to 0$ for the parameter size given by Eq. (8.70) with $m = 2$. (a) Unique solution and (b) bifurcation.

(i) The outer cylinder is at rest, i.e., $V_{\theta B} = 0$, and[27]

$$\frac{L_B}{L_A} = 2, \quad \frac{p_B}{p_A} = 1.2, \quad \frac{T_B}{T_A} = 1; \tag{8.73}$$

(ii) Various speeds $|V_{\theta A}|$ of rotation of the inner cylinder;
(iii) Various Knudsen numbers Kn.

Evaporation takes place on the outer cylinder and condensation on the inner cylinder for $p_B/p_A > 1$ when both the cylinders are at rest. Thus, the gas flow is from the outer cylinder to the inner cylinder. According to the numerical analysis, the variation of the flow with the speed of rotation of the inner cylinder and the Knudsen number shows an interesting behavior. The diagram $J/[2\sqrt{2}\pi L_A p_A/(RT_A)^{1/2}]$ (J : the mass flow from the inner cylinder to the outer per unit time and per unit length of the cylinders) vs $|V_{\theta A}|/(2RT_A)^{1/2}$ (the nondimensional speed of rotation of the inner cylinder) is shown for various Knudsen numbers in Fig. 8.18. In the free molecular flow ($\mathrm{Kn} = \infty$), $\hat{J} = -1/10\sqrt{\pi}$ ($= -0.05642$) irrespective of $|V_{\theta A}|/(2RT_A)^{1/2}$, where $\hat{J} = J/[2\sqrt{2}\pi L_A p_A/(RT_A)^{1/2}]$.[28] The flow is in the direction from the outer cylinder to the inner. For intermediate and large Knudsen numbers ($0.02 \lesssim \mathrm{Kn} < \infty$), the flow is from the outer cylinder to the inner for small $|V_{\theta A}|$, and $|\hat{J}|$ decreases as $|V_{\theta A}|$ increases and vanishes at some $|V_{\theta A}|$, which depends on the Knudsen number Kn. For larger $|V_{\theta A}|$, the flow is reversed from the inner cylinder to the outer and $|\hat{J}|$ increases as $|V_{\theta A}|$ increases. For smaller Knudsen numbers ($0 < \mathrm{Kn} \lesssim 0.01$), the flow is from the outer cylinder to the

[27] See Footnote 21 (i) in this subsection (Section 8.4.2).
[28] For $\mathrm{Kn} = \infty$, the analytic solution is easily obtained as $\hat{J} = [1-(p_B/p_A)(T_A/T_B)^{1/2}]/2\sqrt{\pi}$.

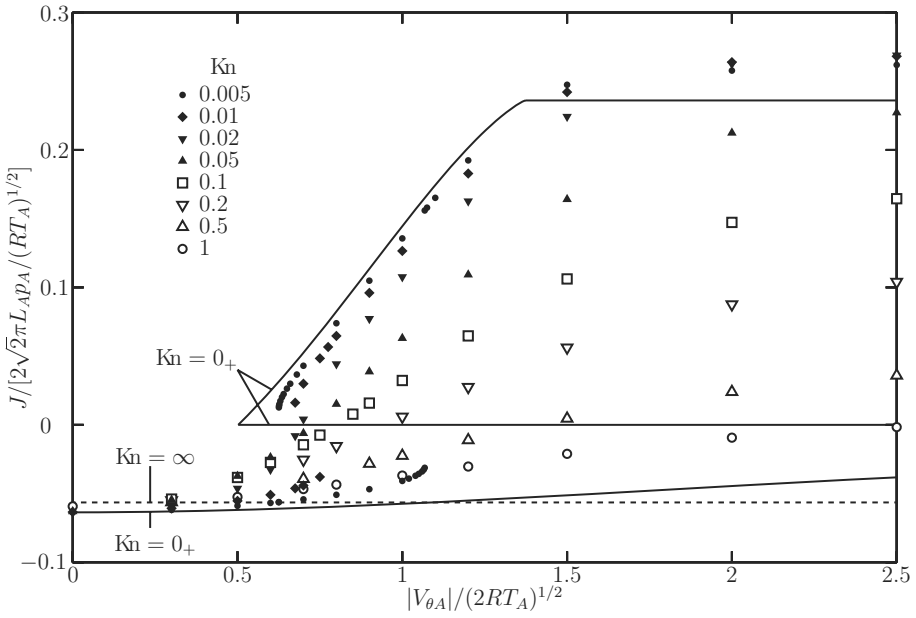

Figure 8.18. Bifurcation diagram: $J/[2\sqrt{2}\pi L_A p_A/(RT_A)^{1/2}]$ vs $|V_{\theta A}|/(2RT_A)^{1/2}$ (J : the mass flow from the inner cylinder to the outer per unit time and per unit length of the cylinders) of the axially symmetric and uniform solution for various Knudsen numbers Kn ($L_B/L_A = 2$, $V_{\theta B} = 0$, $p_B/p_A = 1.2$, $T_B/T_A = 1$).

inner ($\hat{J} < 0$) for small $|V_{\theta A}|$, and $|\hat{J}|$ decreases as $|V_{\theta A}|$ increases as in the cases for larger Knudsen numbers, but the flow suddenly changes its direction (or $\hat{J}$ suddenly jumps to a positive value) at some $|V_{\theta A}|$, which depends on Kn. Then, the mass-flow rate $\hat{J}$ (> 0) from the inner cylinder to the outer increases as $|V_{\theta A}|$ increases. This solution of a positive mass-flow rate exists also for smaller $|V_{\theta A}|$ than the jump point down to some $|V_{\theta A}|$, which depends on Kn. Thus, two solutions, positive and negative mass-flow rates $\hat{J}$, exist in some range of $|V_{\theta A}|$.

In the limit of $\mathrm{Kn} \to 0$, for which the asymptotic solution is obtained on the basis of **Asymptotic analysis 1** in this subsection, three kinds of solutions are obtained as shown by solid lines in Fig. 8.18. The limiting solution at $\mathrm{Kn} = 0_+$ on the line $\hat{J} = 0$ is obtained by the system (8.68a)–(8.69b), and the solutions on the other part of the solid line are obtained by the Euler system, Eqs. (3.225a)–(3.226) and (3.228a)–(3.229c), given in Section 3.5. The solutions on $\hat{J} = 0$ are subject to the ghost effect of an infinitesimal radial flow [$O(\mathrm{Kn})$] of evaporation and condensation on the cylinders except for a special value of $|V_{\theta A}|$. At the special point, the speed of evaporation and condensation is of a higher-order infinitesimal and the solution is the cylindrical Couette flow, i.e, the solution of the Navier–Stokes equations under nonslip condition on the cylinders.[29] At the

[29]See Footnote 23 in this subsection (Section 8.4.2).

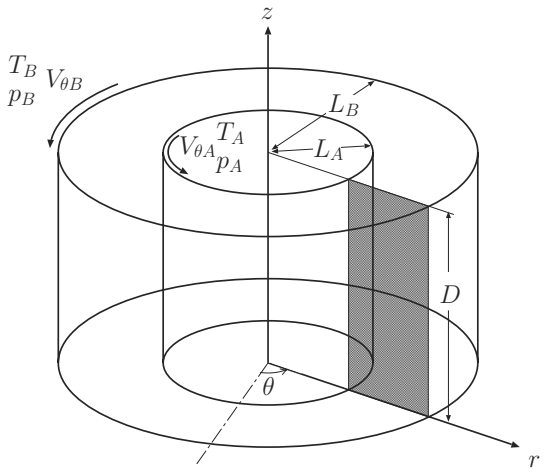

Figure 8.19. Geometry of the system. Here, (r, θ, z) is the (dimensional) cylindrical coordinate system, which is used for explanation in this section (Section 8.4.3). The axially symmetric problem considered in this section is discussed on the shaded rectangular domain.

other points on the line $\hat{J} = 0$, owing to the ghost effect of infinitesimal radial flow, the behavior of the gas, e.g., the profiles of the circumferential velocity component and temperature, deviates strongly from those of the cylindrical Couette flow. This feature is the same as that of the examples given in Figs. 8.13 and 8.14. The present bifurcation diagram corresponds to the panel (a) in Fig. 8.15 with C_- at the origin, where only one solution exists for P_{B2} on the right of the point C_+ [or $u_{\theta A1}^2 < P_{B2}\hat{r}_B^2/(\hat{r}_B^2 - 1)$] but three solutions exist for P_{B2} on the left of the point C_+ [or $u_{\theta A1}^2 > P_{B2}\hat{r}_B^2/(\hat{r}_B^2 - 1)$].

The problem is also studied as the long-time behavior of the solution of the time-evolution problem for a hard-sphere gas by DSMC computation in Sone, Ohwada & Makihara [1999] and Sone, Handa & Sugimoto [2002] (see Section B.1.6). The above two kinds of numerical solutions, positive and negative mass-flow rates $\hat{J}$, are obtained from two different kinds of initial conditions.

8.4.3 Axially symmetric and nonuniform case I: Finite Knudsen number

From now on, we discuss the problem by eliminating the restriction of axial uniformity. First, we explain the results for finite Knudsen numbers by DSMC computation obtained by Sone, Handa & Sugimoto [2002].

Here, we consider a hard-sphere gas between the cylinders of a finite length D with the two ends in their axial direction being bounded by specularly reflecting boundaries (Fig. 8.19). The discussion will be made on the shaded rectangular region, because the axially symmetric case is considered here. Let the time-independent solution of the above problem and its mirror image with respect to

the axial end be arranged alternately in the axial direction. This is a periodic solution between the infinitely long cylinders, with period $2D$ along the axis of the cylinders.[30] The axially uniform solution considered in the preceding subsection (Section 8.4.2) is, naturally, a solution in the domain of a finite length. We will investigate the stability of the axially uniform solutions by elimination of the condition of the axial uniformity and look for another type of solution with the direct simulation Monte Carlo (or DSMC) method explained in Section B.1. The stability is studied in the following way: First construct axially symmetric and uniform solutions with DSMC system of computation for the axially symmetric and uniform condition, and then investigate the time evolution of the axially uniform solutions with the DSMC system for the axially symmetric condition, where the axially uniform restriction is eliminated.[31] DSMC solutions at some instant inevitably deviate from the corresponding real solutions of the Boltzmann system, and thus no perturbation is required to study the stability.

The numerical computation is carried out in the following values of the parameters:

(i) The outer cylinder is at rest, i.e., $V_{\theta B} = 0$, and[32]

$$\frac{L_B}{L_A} = 2, \quad \frac{D}{L_A} = 1, \quad \frac{p_B}{p_A} = 1.2, \quad \frac{T_B}{T_A} = 1; \tag{8.74}$$

(ii) Two typical cases of the Knudsen number:

$$\mathrm{Kn} = 0.005, \text{ where bifurcation occurs in the axially uniform case,} \tag{8.75a}$$

$$\mathrm{Kn} = 0.02, \text{ where no bifurcation occurs in the axially uniform case;} \tag{8.75b}$$

(iii) Various speeds $|V_{\theta A}|$ of rotation of the inner cylinder.

The choice (i) is the same as (i) in Section 8.4.2 except for the additional data for D/L_A.

Case $\mathrm{Kn} = 0.005$

This is the case where bifurcation occurs in the axially uniform case. Let the mass flow per unit time from the inner cylinder to the outer of length D be J_D, and the nondimensional mass-flow rate $J_D/[2\sqrt{2}\pi L_A D p_A/(RT_A)^{1/2}]$ be denoted by $\hat{J}$. The diagram of the nondimensional mass-flow rate $\hat{J}$ vs the nondimensional circumferential speed $|V_{\theta A}|/(2RT_A)^{1/2}$ of rotation of the inner cylinder of the time-independent solutions is shown in Fig. 8.20, where the stability of axially uniform solutions is also indicated. The relation $\hat{J}$ vs $|V_{\theta A}|/(2RT_A)^{1/2}$ for the axially uniform solution, which consists of two branches, is shown by

[30] See the third paragraph in Section 8.3.3, where the corresponding solution in a similar situation is explained.

[31] Examples of the DSMC systems with symmetry are given in Section B.1.5.

[32] (i) See Footnote 21 (i) in Section 8.4.2.

(ii) In the present choice of the parameter, $D = L_B - L_A = L_A$, and the shaded region where the analysis is carried out is a square. Thus, z/D, used as the ordinates in Figs. 8.21, 8.22, and 8.24 for the domain with respect to z to be explicit, is equivalent to z/L_A.

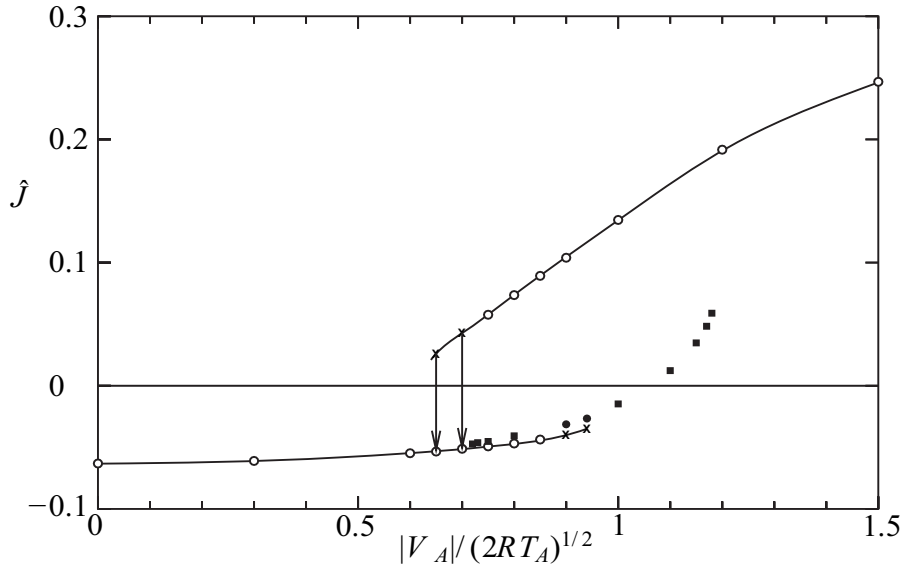

Figure 8.20. Bifurcation diagram [$\hat{J}$ (= $J_D/[2\sqrt{2}\pi L_A D p_A/(RT_A)^{1/2}]$) vs $|V_{\theta A}|/(2RT_A)^{1/2}$] of the axially symmetric solution (Kn = 0.005; $L_B/L_A = 2$, $D/L_A = 1$, $V_{\theta B} = 0$, $p_B/p_A = 1.2$, $T_B/T_A = 1$). See the main text.

solid lines in the diagram. The stability of an axially uniform solution on the curve is marked by the symbols ∘ and × in the diagram. That is, if the solution of time-evolution computation remains the original axially uniform solution, it is marked by the symbol ∘, and if the solution changes to another solution, it is marked by the symbol ×. The latter solution in the long-time limit is of two kinds: One is a stable axially uniform solution ∘, marked by the arrow ↓, on the other branch of the axially uniform solution; and the other is a new time-independent axially nonuniform solution, which is marked by •. The axially uniform solution is unstable only near the edge of each branch, where $|\hat{J}|$ is smaller than $|\hat{J}|$ on the other part of the corresponding branch.

The process of transition of the first type at $|V_{\theta A}|/(2RT_A)^{1/2} = 0.65$ is shown in Fig. 8.21. In Fig. 8.21, the flow velocity field (v_r, v_θ, v_z) in the cylindrical coordinate system is shown by the arrows expressing $(v_r, v_z)/(2RT_A)^{1/2}$ at their starting points and the level curves $|v_\theta|/(2RT_A)^{1/2} = \text{const}$. The axially uniform solution at $|V_{\theta A}|/(2RT_A)^{1/2} = 0.65$ on the upper branch, where evaporation is taking place on the inner cylinder, deviates slowly from its initial state and a roll is formed accompanying the decrease of $\hat{J}$. After the reversal of $\hat{J}$ from positive to negative, the roll decays and the flow approaches an axially uniform flow with evaporation on the outer cylinder. This flow is nearly radial and the circumferential motion is limited only in a close neighborhood of the inner cylinder. The process of transition of the second type at $|V_{\theta A}|/(2RT_A)^{1/2} = 0.94$ is shown in Fig. 8.22. The axially uniform solution at $|V_{\theta A}|/(2RT_A)^{1/2} = 0.94$ on the lower branch, where evaporation is taking place on the outer cylinder,

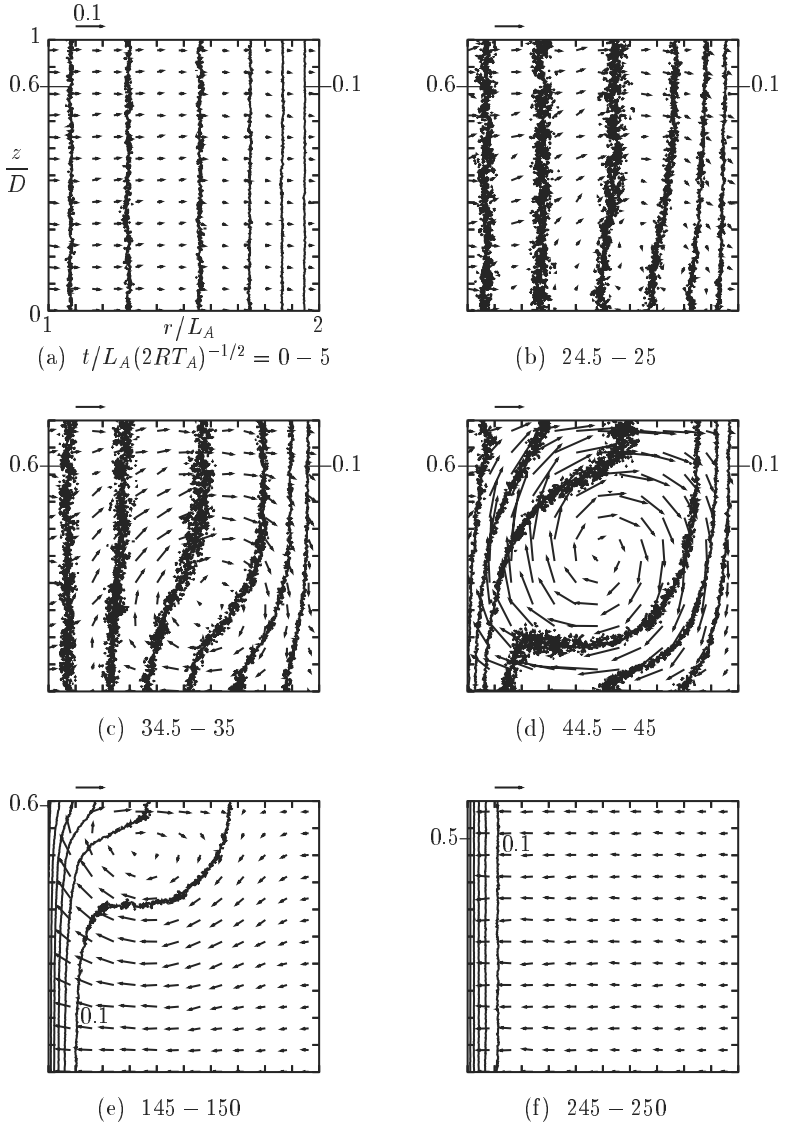

Figure 8.21. Transition process from the axially uniform solution at $|V_{\theta A}|/(2RT_A)^{1/2} = 0.65$ on the upper branch to that on the lower branch (Kn = 0.005). (a) The average of the data from $t/L_A(2RT_A)^{-1/2} = 0$ to 5, (b) 24.5 – 25, (c) 34.5 – 35, (d) 44.5 – 45, (e) 145 – 150, and (f) 245 – 250. The arrows indicate $(v_r, v_z)/(2RT_A)^{1/2}$ at their starting points. Their scale of 0.1 is shown by the arrow on the left shoulder of each panel. The level curves $|v_\theta|/(2RT_A)^{1/2} = 0.1n$ $(n = 1, 2, \ldots)$ are drawn in the figures. On some of the level curves, the level value is indicated.

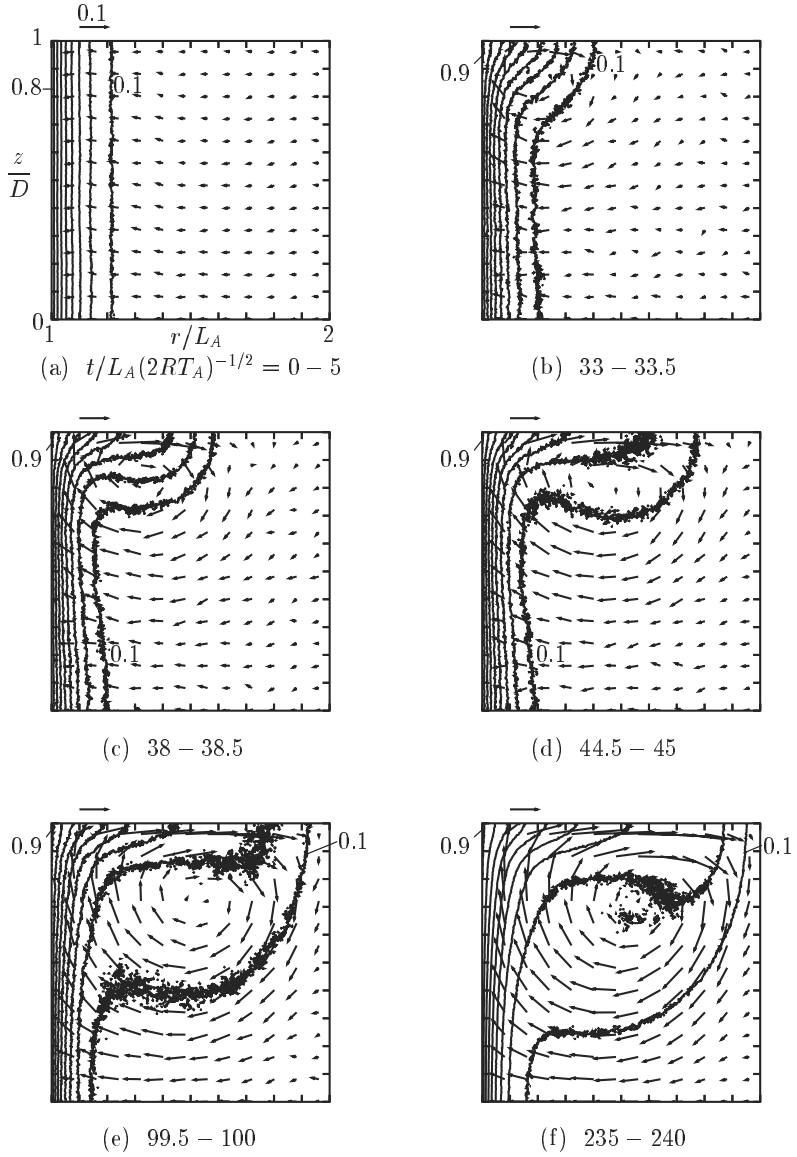

Figure 8.22. Transition process from the axially uniform solution at $|V_{\theta A}|/(2RT_A)^{1/2} = 0.94$ on the lower branch to the roll-type solution (Kn = 0.005). (a) The average of the data from $t/L_A(2RT_A)^{-1/2} = 0$ to 5, (b) 33 – 33.5, (c) 38 – 38.5, (d) 44.5 – 45, (e) 99.5 – 100, and (f) 235 – 240. The arrows indicate $(v_r, v_z)/(2RT_A)^{1/2}$ at their starting points. Their scale of 0.1 is shown by the arrow on the left shoulder of each panel. The level curves $|v_\theta|/(2RT_A)^{1/2} = 0.1n$ $(n = 1, 2, \ldots)$ are drawn in the figures. On some of the level curves, the level value is indicated.

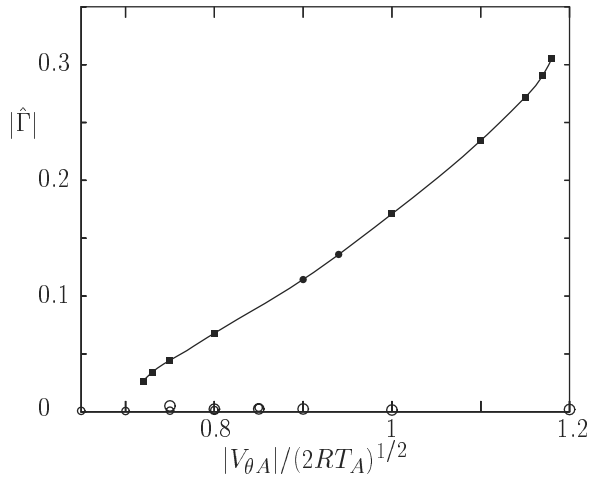

Figure 8.23. The circulation $\hat{\Gamma}$ [$= \Gamma/L_A(2RT_A)^{1/2}$] vs $|V_{\theta A}|/(2RT_A)^{1/2}$ on the branch of the roll-type solution (• and ■ in Fig. 8.20) I: Kn = 0.005. The circulation Γ is defined by the circulation around the circle on the section $\theta =$ const with the radius $0.3L_A$ and its center at the center of the domain under discussion (the shaded region in Fig. 8.19). The black circle • and black square ■ correspond, respectively, to the solutions marked by • and ■ in Fig.8.20; the smaller white circle corresponds to a stable axially uniform solution on the lower branch, and the larger one to that on the upper branch.

deviates gradually from its initial state and a roll-type solution is established with $\hat{J}$ not much different from $\hat{J}$ of the initial state.

The axially nonuniform solution • is of a roll type. This type of solution exists in a wider range of $|V_{\theta A}|/(2RT_A)^{1/2}$ than that shown by the symbol •. A roll-type solution at a new $|V_{\theta A}|/(2RT_A)^{1/2}$ is constructed from the long-time behavior of the initial and boundary-value problem with a roll-type solution nearby $|V_{\theta A}|/(2RT_A)^{1/2}$ as the initial condition. The solutions thus obtained are marked by the black square ■ in Fig. 8.20. The variation of the circulation Γ of the roll-type solution along the branch is shown in Fig. 8.23, where the circulation Γ is defined by the circulation around the circle on the section $\theta =$ const with the radius $0.3L_A$ and its center at the center of the domain under discussion (the shaded region in Fig. 8.19). As $|V_{\theta A}|/(2RT_A)^{1/2}$ becomes smaller, the circulation decreases to vanish and the nondimensional mass-flow rate $\hat{J}$ approaches that of the axially uniform solution on the lower branch. Thus, the bifurcation of the roll-type solution from the lower branch may be considered to occur at about $|V_{\theta A}|/(2RT_A)^{1/2} = 0.7$. The other end of the black symbols (a black square) in Fig. 8.20 is at $|V_{\theta A}|/(2RT_A)^{1/2} = 1.18$. The time evolution of the initial and boundary-value problem at $|V_{\theta A}|/(2RT_A)^{1/2} = 1.19$ with the roll-type solution at $|V_{\theta A}|/(2RT_A)^{1/2} = 1.18$ as the initial condition deviates from the initial condition and approaches the corresponding axially uniform solution on the upper branch. This indicates that the time-independent solution of a roll type does not exist at $|V_{\theta A}|/(2RT_A)^{1/2} = 1.19$ or that the time-independent

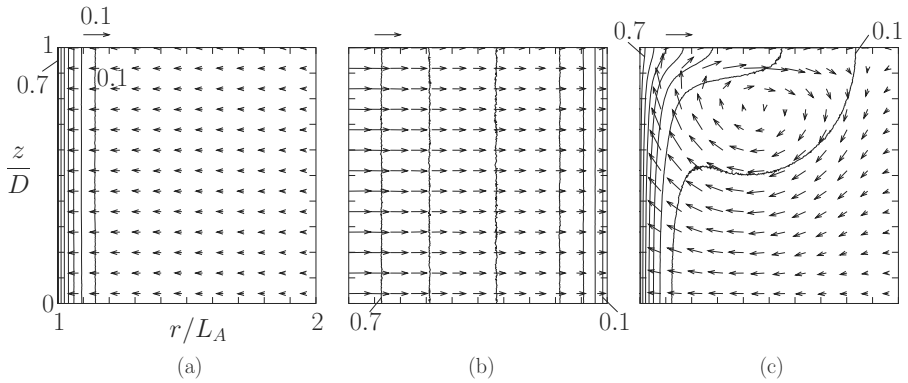

Figure 8.24. The velocity fields of three types of the flow at $|V_{\theta A}|/(2RT_A)^{1/2} = 0.8$ (Kn = 0.005). (a) A flow with negative mass-flow rate, (b) a flow with positive mass-flow rate, and (c) a flow of roll type. The arrows indicate $(v_r, v_z)/(2RT_A)^{1/2}$ at their starting points. Their scale of 0.1 is shown by the arrow on the left shoulder of each panel. The level curves $|v_\theta|/(2RT_A)^{1/2} = 0.1n$ $(n = 1, 2, \ldots)$ are drawn in the figures. On some of the level curves, the level value is indicated.

solution, if any, is unstable for a perturbation of the size of 0.01. The disappearance of a roll-type solution may be understood in the following way: Stronger convection $\hat{J}$ with increase of $|V_{\theta A}|/(2RT_A)^{1/2}$ sweeps away the seed of a roll out of the flow field.

From the bifurcation diagram given by Fig. 8.20, it is found that three kinds of solutions, two axially uniform solutions with positive and negative mass-flow rates and a roll-type solution, exist stably between $0.75 \lesssim |V_{\theta A}|/(2RT_A)^{1/2} \lesssim 0.85$. The three kinds of profiles of the flow field at $|V_{\theta A}|/(2RT_A)^{1/2} = 0.8$ are shown in Fig. 8.24.

Case Kn = 0.02

This is the case where no bifurcation occurs in the axially uniform case, where the relation $\hat{J}$ vs $|V_{\theta A}|/(2RT_A)^{1/2}$ is given by a single curve. The bifurcation diagram $\hat{J}$ vs $|V_{\theta A}|/(2RT_A)^{1/2}$ with stability indication of axially uniform solutions is shown in Fig. 8.25. In Fig. 8.25, the same symbols are used as in Fig. 8.20; the shaded circle is a new symbol indicating that the time evolution from the axially uniform solution keeps oscillating and does not approach a time-independent solution. This solution could not be confirmed to be a real solution, and further discussion is required. An example of false oscillatory solutions is given in Section B.1.6. The axially uniform solution is unstable only in a limited range of $|V_{\theta A}|/(2RT_A)^{1/2}$ or $\hat{J}$ [say, $c_L \le |V_{\theta A}|/(2RT_A)^{1/2} \le c_M$ $(c_L > 0)$ or $j_L \le \hat{J} \le j_M$ $(j_L < 0,\ j_M > 0)$]. The variation of the circulation Γ along the branch of the roll-type solution (• and ■) is shown in Fig. 8.26. As $|V_{\theta A}|/(2RT_A)^{1/2}$ becomes smaller, the circulation decreases to vanish and the mass-flow rate approaches that of the axially uniform solution. The bifurcation

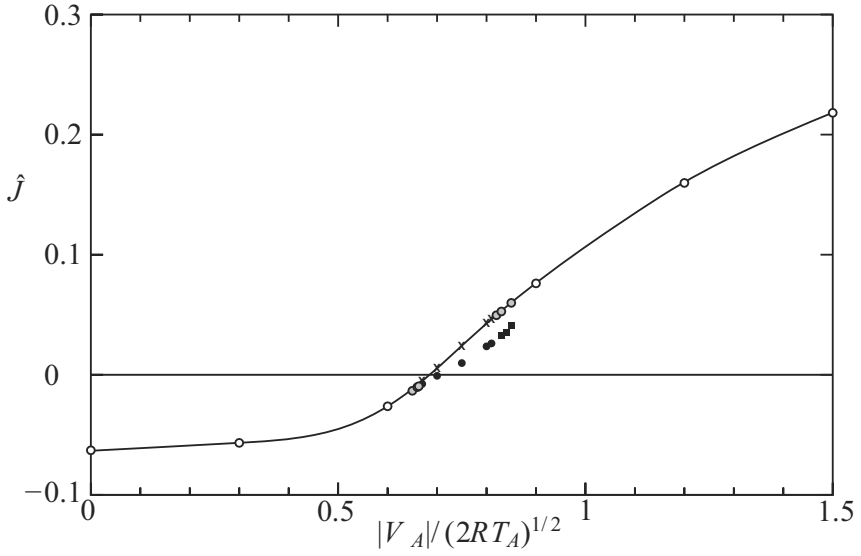

Figure 8.25. Bifurcation diagram [$\hat{J}$ (= $J_D/[2\sqrt{2}\pi L_A D p_A/(RT_A)^{1/2}]$) vs $|V_{\theta A}|/(2RT_A)^{1/2}$] of the axially symmetric solution (Kn = 0.02; $L_B/L_A = 2$, $D/L_A = 1$, $V_{\theta B} = 0$, $p_B/p_A = 1.2$, $T_B/T_A = 1$). See the main text.

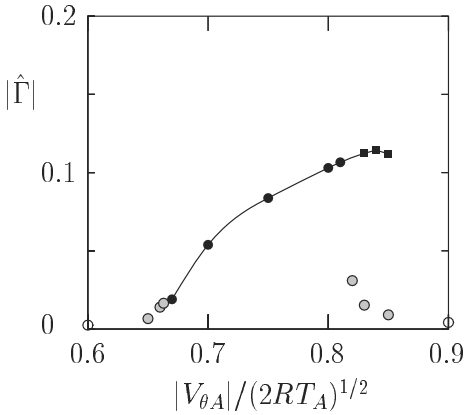

Figure 8.26. The circulation $\hat{\Gamma}$ [= $\Gamma/L_A(2RT_A)^{1/2}$] vs $|V_{\theta A}|/(2RT_A)^{1/2}$ on the branch of the roll-type solution (• and ■ in Fig. 8.25) II: Kn = 0.02. The circulation Γ is defined by the circulation around the circle on the section θ = const with the radius $0.3L_A$ and its center at the center of the domain under discussion (the shaded region in Fig. 8.19). The black circle • and black square ■ correspond, respectively, to the solutions marked by • and ■ in Fig. 8.25; the shaded circle is the maximum value of the oscillating solution marked by the same symbol in Fig. 8.25; and the white circle corresponds to an axially uniform solution.

of a roll-type solution from the branch of the axially uniform flow seems to occur at about $|V_{\theta A}|/(2RT_A)^{1/2} = 0.66$. The other end of the black symbols (a black square) in Fig. 8.25 is at $|V_{\theta A}|/(2RT_A)^{1/2} = 0.85$. The time evolution of the initial and boundary-value problem at $|V_{\theta A}|/(2RT_A)^{1/2} = 0.86$ with the roll-type solution at $|V_{\theta A}|/(2RT_A)^{1/2} = 0.85$ as the initial condition deviates from the initial condition and approaches the corresponding axially uniform solution with a slightly large fluctuation. This indicates that the time-independent solution of a roll type does not exist at $|V_{\theta A}|/(2RT_A)^{1/2} = 0.86$ or that the time-independent solution, if any, is unstable for a perturbation of the size of 0.01.

In the above DSMC computations, the domain $(L_A, L_B) \times (0, D)$ is divided into $m \times n$ uniform cells. The data for $\mathrm{Kn} = 0.005$ are the results of 400×400 cells and those for $\mathrm{Kn} = 0.02$ are those of 100×100; the average number of particles in a cell distributed initially is about 100 for both the cases.

8.4.4 Axially symmetric and nonuniform case II: Limiting solution as $\mathsf{Kn} \to 0$

In this subsection we discuss the bifurcation from the axially uniform solution when the Knudsen number of the system is small on the basis of Sone & Doi [2003b]. That is, taking a small quantity ε, we study the asymptotic behavior as $\varepsilon \to 0$ of the axially symmetric time-independent solution of the problem described in Section 8.4.1 when the six parameters (8.66) are limited to the following case:

$$\left.\begin{array}{lll} \dfrac{L_B}{L_A} - 1 = \hat{r}_B - 1 = O(1), & \dfrac{V_{\theta A}}{\sqrt{2RT_A}} = \varepsilon u_{\theta A}, & \dfrac{V_{\theta B}}{\sqrt{2RT_A}} = \varepsilon u_{\theta B}, \\ T_B/T_A - 1 = \varepsilon\tau_B, & p_B/p_A - 1 = \varepsilon P_B, & \mathrm{Kn} = 2\varepsilon/\sqrt{\pi}, \end{array}\right\} \tag{8.76}$$

where $u_{\theta A}\,(\geq 0)$, $u_{\theta B}$, τ_B, and P_B are of the order of unity. We will see, in the present analysis, that an axially symmetric but nonuniform solution bifurcates in the above range of the parameters from the axially uniform solution, which is unique in this range in contrast to the case in **Asymptotic analysis 2** of Section 8.4.2. From the result, the axially nonuniform solution bifurcated may be considered to continue to exist in the range of the parameters studied in **Asymptotic analysis 2** of Section 8.4.2.

Basic equation and boundary condition

The time-independent behavior of a gas around the condensed phase of the gas for the above range of the parameters are studied in Section 3.2, and the fluid-dynamic-type equations and their associated boundary conditions, describing the behavior of the gas, are derived. Let the cylindrical coordinate system with the axis of the cylinders as the axial direction, the flow velocity (in the cylindrical coordinates), pressure, and temperature of the gas be, respectively, $(L_A\hat{r}, \theta, L_A\hat{z})$, $\varepsilon(2RT_A)^{1/2}(u_r, u_\theta, u_z)$, $p_A(1+\varepsilon P)$, and $T_A(1+\varepsilon\tau)$. According to

Section 3.2, the equations and the boundary conditions governing the limiting values of the variables u_r, u_θ, u_z, P, and τ as $\varepsilon \to 0$ in an axially symmetric state ($\partial/\partial\theta = 0$) for the parameter range (8.76) are given in the following form with the same notation for the limiting values: The equations are

$$\frac{\partial P}{\partial \hat{r}} = \frac{\partial P}{\partial \hat{z}} = 0 \quad \Rightarrow \quad P : \text{uniform}, \tag{8.77}$$

$$\frac{1}{\hat{r}}\frac{\partial\, u_r \hat{r}}{\partial\, \hat{r}} + \frac{\partial u_z}{\partial \hat{z}} = 0, \tag{8.78a}$$

$$u_r \frac{\partial\, u_r}{\partial\, \hat{r}} + u_z \frac{\partial\, u_r}{\partial\, \hat{z}} - \frac{u_\theta^2}{\hat{r}} = -\frac{1}{2}\frac{\partial\, P_1}{\partial\, \hat{r}} + \frac{\gamma_1}{2}\left[\frac{1}{\hat{r}}\frac{\partial}{\partial\, \hat{r}}\left(\hat{r}\frac{\partial\, u_r}{\partial\, \hat{r}}\right) - \frac{u_r}{\hat{r}^2} + \frac{\partial^2 u_r}{\partial \hat{z}^2}\right], \tag{8.78b}$$

$$\frac{u_r}{\hat{r}}\frac{\partial\, u_\theta \hat{r}}{\partial\, \hat{r}} + u_z \frac{\partial u_\theta}{\partial \hat{z}} = \frac{\gamma_1}{2}\left[\frac{1}{\hat{r}}\frac{\partial}{\partial\, \hat{r}}\left(\hat{r}\frac{\partial\, u_\theta}{\partial\, \hat{r}}\right) - \frac{u_\theta}{\hat{r}^2} + \frac{\partial^2 u_\theta}{\partial \hat{z}^2}\right], \tag{8.78c}$$

$$u_r \frac{\partial\, u_z}{\partial\, \hat{r}} + u_z \frac{\partial\, u_z}{\partial\, \hat{z}} = -\frac{1}{2}\frac{\partial P_1}{\partial \hat{z}} + \frac{\gamma_1}{2}\left[\frac{1}{\hat{r}}\frac{\partial}{\partial\, \hat{r}}\left(\hat{r}\frac{\partial\, u_z}{\partial\, \hat{r}}\right) + \frac{\partial^2 u_z}{\partial \hat{z}^2}\right], \tag{8.78d}$$

$$u_r \frac{\partial\, \tau}{\partial\, \hat{r}} + u_z \frac{\partial\, \tau}{\partial\, \hat{z}} = \frac{\gamma_2}{2}\left[\frac{1}{\hat{r}}\frac{\partial}{\partial\, \hat{r}}\left(\hat{r}\frac{\partial\, \tau}{\partial\, \hat{r}}\right) + \frac{\partial^2 \tau}{\partial \hat{z}^2}\right], \tag{8.78e}$$

where P_1 is the next-order term in ε of P, divided by ε; γ_1 and γ_2 are constants depending on molecular models [see Eq. (3.24)], for example, $\gamma_1 = 1.2700424$, $\gamma_2 = 1.922284$ (a hard-sphere gas) or $\gamma_1 = \gamma_2 = 1$ (the BKW model). When the property of the cylinder surface is locally isotropic and the distribution of the reflected molecules has a finite complete condensation part,[33] the boundary conditions on the cylinders for Eqs. (8.77)–(8.78e) are given in the following form:

$$P = C_4^* u_r, \qquad \tau = d_4^* u_r, \qquad u_\theta = u_{\theta A}, \quad u_z = 0 \quad \text{at} \quad \hat{r} = 1, \tag{8.79a}$$

$$P = P_B - C_4^* u_r, \quad \tau = \tau_B - d_4^* u_r, \quad u_\theta = u_{\theta B}, \quad u_z = 0 \quad \text{at} \quad \hat{r} = \hat{r}_B, \tag{8.79b}$$

where C_4^* and d_4^* are constants depending on molecular models and kinetic boundary conditions. For the complete-condensation condition, for example, $C_4^* = -2.1412$ and $d_4^* = -0.4557$ (a hard-sphere gas) or $C_4^* = -2.13204$ and $d_4^* = -0.44675$ (the BKW model).

From Eqs. (8.78a)–(8.78d) and Eqs. (8.79a) and (8.79b) excluding their second relations, the velocity field is determined independently of the temperature field. Thus, we will mainly discuss the velocity field. Further, if this system is rewritten with the variables $(u_r, u_\theta, u_z)/\gamma_1$, $P/\gamma_1 C_4^*$, and P_1/γ_1^2 and the parameters $u_{\theta A}/\gamma_1$, $u_{\theta B}/\gamma_1$, and $P_B/\gamma_1 C_4^*$, the system does not contain the quantities that depend on molecular models or kinetic boundary conditions. Thus the results in these quantities obtained in the following analysis are independent of them.

[33] See Footnote 14 in Section 3.1.5 and Sone [2002].

Bifurcation analysis

First consider the case where the behavior of the gas is axially uniform (or $\partial/\partial\hat{z} = 0$). Then, the axially uniform solution, indicated by the subscript U, of Eqs. (8.77)–(8.78e) under the boundary conditions (8.79a) and (8.79b) is uniquely given in the following form:

$$\left.\begin{aligned} &u_{rU} = \frac{\gamma_1}{2}\frac{b}{\hat{r}}, \qquad u_{\theta U} = \gamma_1\left(c_1\hat{r}^{1+b} + \frac{c_0}{\hat{r}}\right), \qquad u_{zU} = 0, \\ &P_U = \frac{\hat{r}_B}{\hat{r}_B+1}P_B, \qquad \tau_U = d_1\hat{r}^\beta + d_0, \end{aligned}\right\} \tag{8.80}$$

where

$$b = \frac{2\hat{r}_B}{\hat{r}_B+1}\frac{P_B}{\gamma_1 C_4^*}, \qquad c_0 = \frac{\hat{r}_B}{\hat{r}_B^{2+b}-1}\left(\frac{\hat{r}_B^{1+b}u_{\theta A}}{\gamma_1} - \frac{u_{\theta B}}{\gamma_1}\right),$$
$$c_1 = \frac{1}{\hat{r}_B^{2+b}-1}\left(\frac{\hat{r}_B u_{\theta B}}{\gamma_1} - \frac{u_{\theta A}}{\gamma_1}\right), \qquad \beta = \frac{\gamma_1}{\gamma_2}b,$$
$$d_0 = \frac{-1}{\hat{r}_B^\beta - 1}\left(\tau_B - \frac{d_4^*(\hat{r}_B^{\beta+1}+1)}{C_4^*(\hat{r}_B+1)}P_B\right), \quad d_1 = \frac{1}{\hat{r}_B^\beta - 1}\left(\tau_B - \frac{d_4^*}{C_4^*}P_B\right),$$

and the solutions at the apparent singularities $b = 0$ and -2 are obtained as the limit of the above solution. The mass flow J per unit time from the inner cylinder to the outer per unit length is given by[34]

$$J = \frac{2\sqrt{2}\pi L_A p_A}{(1+L_A/L_B)(RT_A)^{1/2}}\frac{P_B}{C_4^*}\varepsilon = \frac{2\sqrt{2}\pi L_A p_A}{C_4^*(1+L_A/L_B)(RT_A)^{1/2}}\left(\frac{p_B}{p_A} - 1\right). \tag{8.81}$$

Evaporation takes place on the inner (outer) cylinder and condensation does on the outer (inner) cylinder when $P_B/C_4^* > 0$ (< 0), where $C_4^* < 0$ according to accurate results for a hard-sphere gas and the BKW model and approximate results for other molecular models.

Here, we consider a time-independent solution periodic with period $2\pi L_A/\alpha$ in the axial direction and investigate whether this solution bifurcates from the axially uniform solution and the behavior of the solution near the bifurcation point, if any. Let the bifurcation point be at $u_{\theta A} = u_{\theta Ab}$, $u_{\theta B} = u_{\theta Bb}$, $\tau_B = \tau_{Bb}$, and $P_B = P_{Bb}$ and the axially uniform solution f_U at this point be f_{Ub}. The solution in the neighborhood of the bifurcation point (or when $u_{\theta A} - u_{\theta Ab}$, $u_{\theta B} - u_{\theta Bb}$, $P_B - P_{Bb}$, and $\tau_B - \tau_{Bb}$ are of the order of δ^2, say) is found to be expressed in the following form:[35]

$$f(\hat{r},\hat{z}) = f_{Ub}(\hat{r}) + \delta f_{11}(\hat{r})\cos\alpha\hat{z} + \delta^2[f_{20}(\hat{r}) + f_{21}(\hat{r})\cos\alpha\hat{z} + f_{22}(\hat{r})\cos 2\alpha\hat{z}] + \cdots, \tag{8.82}$$

$$u_z(\hat{r},\hat{z}) = \delta W_{11}(\hat{r})\sin\alpha\hat{z} + \delta^2[W_{21}(\hat{r})\sin\alpha\hat{z} + W_{22}(\hat{r})\sin 2\alpha\hat{z}] + \cdots, \tag{8.83}$$

[34] In the formula (6) in Sone & Doi [2003b], M on the left-hand side is a misprint of $M/(p_A/RT_A)$.

[35] See Footnote 2 in Section 8.2.3.

where $f = u_r$, u_θ, P_1, or τ. Equations (8.82) and (8.83) with Eq. (8.80) being substituted into Eqs. (8.77)–(8.79b), it is found that the coefficient functions $f_{11}(\hat{r})$, $f_{20}(\hat{r})$, etc. of $\hat{r}$ are formally determined from the lowest order and that each Fourier component function is determined independently at each order of δ. Let $U_{mn}(\hat{r})$ and $V_{mn}(\hat{r})$ be $f_{mn}(\hat{r})$, respectively, corresponding to u_θ and u_r. From $U_{mn}(\hat{r})$ and $V_{mn}(\hat{r})$, the other variables are determined. For example, $n\alpha W_{mn} = -(\hat{r}V_{mn})'/\hat{r}$, where $(*)' = \mathrm{d}(*)/\mathrm{d}\hat{r}$. The temperature τ can be shown to be determined uniquely from the velocity.[36] Thus, the bifurcation can be discussed only with the velocity field, and τ_B does not influence the bifurcation. The mass-flow rate J remains the same as the axially uniform solution up to the order of δ.

The component functions $U_{11}(\hat{r})$ and $V_{11}(\hat{r})$ are the solution of the following homogeneous boundary-value problem of ordinary differential equations:

$$L_\theta(U_{11}) + q_\theta V_{11} = 0, \qquad L_r(V_{11}) + q_r U_{11} = 0; \tag{8.84}$$

$$U_{11}(\hat{r}) = V_{11}(\hat{r}) = V'_{11}(\hat{r}) = 0 \quad \text{at } \hat{r} = 1 \text{ and } \hat{r} = \hat{r}_B, \tag{8.85}$$

where

$$L_\theta(U) = U'' + (1-b)\hat{r}^{-1}U' - [(1+b)\hat{r}^{-2} + \alpha^2]U, \tag{8.86a}$$

$$\begin{aligned} L_r(V) = {} & V'''' + (2-b)\hat{r}^{-1}V''' - \left(3\hat{r}^{-2} + 2\alpha^2\right)V'' \\ & + [3(1+b)\hat{r}^{-3} - 2\alpha^2(1-b/2)\hat{r}^{-1}]V' \\ & + [-3(1+b)\hat{r}^{-4} + 2\alpha^2(1-b/2)\hat{r}^{-2} + \alpha^4]V, \end{aligned} \tag{8.86b}$$

$$q_\theta = -4c_1(1+b/2)\hat{r}^b, \qquad q_r = -4\alpha^2\left(c_1\hat{r}^b + c_0\hat{r}^{-2}\right). \tag{8.86c}$$

The homogeneous boundary-value problem has a nontrivial solution only when the parameters $u_{\theta Ab}/\gamma_1$, $u_{\theta Bb}/\gamma_1$, $P_{Bb}/\gamma_1 C_4^*$, $\hat{r}_B$, and α satisfy a relation, say,

$$F_{\mathrm{Cec}}(u_{\theta Ab}/\gamma_1,\, u_{\theta Bb}/\gamma_1,\, P_{Bb}/\gamma_1 C_4^*,\, \hat{r}_B,\, \alpha) = 0. \tag{8.87}$$

The relation can be found numerically by the method explained in the paragraph next to that of Eq. (8.23). The bifurcation relation when the outer cylinder is at rest is shown in Figs. 8.27 and 8.28 and Table 8.3. In Fig. 8.27, the relation $u_{\theta Ab}/\gamma_1$ vs $P_{Bb}/\gamma_1 C_4^*$ is shown for various values of α when $u_{\theta Bb} = 0$ and $\hat{r}_B = 2$. There are infinitely many $u_{\theta Ab}/\gamma_1$'s for a $P_{Bb}/\gamma_1 C_4^*$, the first three of which are shown in Fig. 8.27 (a).[37] The lowest branches of the curves for three α's are shown in a larger scale in panel (b) of Fig. 8.27. The minimum value of $u_{\theta Ab}/\gamma_1$ with respect to α at a given $P_{Bb}/\gamma_1 C_4^*$ is denoted by $(u_{\theta Ab}/\gamma_1)_m$ and the minimum point by α_m. They are shown in the second and third columns in Table 8.3.In Fig. 8.28, the bifurcation curves for the cases $\hat{r}_B = 1.5$ and 3,

[36] The uniqueness is easily seen to be equivalent to the proposition that the following system has only the trivial solution:

$$\mathrm{d}^2 g(\hat{r})/\mathrm{d}\hat{r}^2 + (\kappa/\hat{r})\mathrm{d}g(\hat{r})/\mathrm{d}\hat{r} - \alpha^2 g(\hat{r}) = 0, \quad g(1) = g(\hat{r}_B) = 0; \quad \kappa = 1 - \beta.$$

From the system it is easily derived that $\int_1^{\hat{r}_B}[\alpha^2 g^2 + (\mathrm{d}g/\mathrm{d}\hat{r})^2]\hat{r}^\kappa \mathrm{d}\hat{r} = 0$, from which the proposition, i.e., $g = 0$, follows.

[37] "Infinitely many" is the plausible result suggested by numerical study.

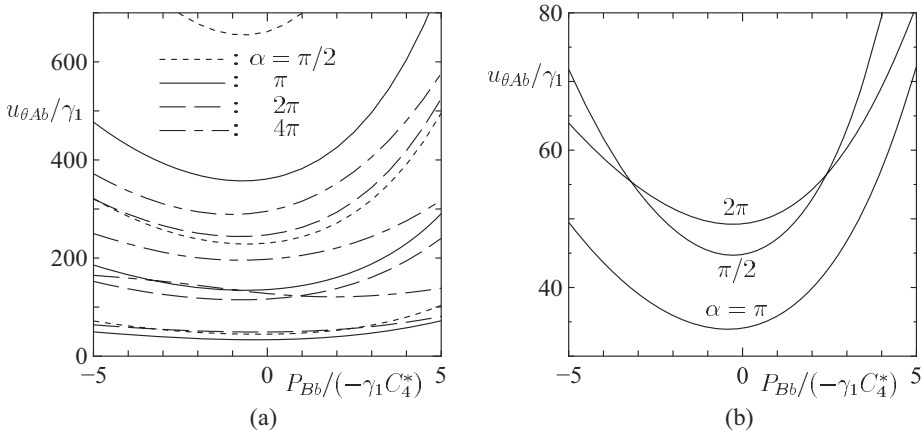

Figure 8.27. Bifurcation curve I: The relation $u_{\theta Ab}/\gamma_1$ vs $P_{Bb}/(-\gamma_1 C_4^*)$ for various α when the outer cylinder is at rest $u_{\theta Bb} = 0$ ($\hat{r}_B = 2$). (a) Wider range of $u_{\theta Ab}/\gamma_1$ and (b) the lowest (or first) branch for $\alpha = \pi/2$, π, and 2π.

Table 8.3. $(u_{\theta Ab}/\gamma_1)_m$, α_m, and $(a_A/a_O, a_B/a_O, a_P/a_O)$ at α_m for $u_{\theta Bb} = 0$, $\hat{r}_B = 2$, and various $P_{Bb}/(-\gamma_1 C_4^*)$.

$\dfrac{P_{Bb}}{(-\gamma_1 C_4^*)}$	$(u_{\theta Ab}/\gamma_1)_m$	α_m/π	a_A/a_O	a_B/a_O	a_P/a_O
−5	48.870	1.1408	−7.359	6.038	−44.95
−2	35.890	1.0356	7.270	−4.831	17.52
−1	34.201	1.0157	5.531	−3.062	5.177
0	34.093	1.0067	5.301	−2.061	−4.061
1	35.846	1.0110	6.176	−0.916	−17.33
2	39.858	1.0314	9.491	1.810	−50.35
5	70.599	1.2181	−6.142	−11.26	97.27

corresponding to Fig. 8.27 (b), are shown (there are infinitely many other curves above the curves in the figures). The bifurcation curves when the outer cylinder is rotating are shown in Figs. 8.29 and 8.30. In Fig. 8.29, the relation $u_{\theta Ab}/\gamma_1$ vs $P_{Bb}/\gamma_1 C_4^*$ for three sets of $(\hat{r}_B, \alpha)$ is shown for various $u_{\theta Bb}$ (there are infinitely many curves above the curves in the figures). The minimum $(u_{\theta Ab}/\gamma_1)_m$ of $u_{\theta Ab}/\gamma_1$ with respect to α with the other parameters fixed is shown as the curves $(u_{\theta Ab}/\gamma_1)_m$ vs $u_{\theta Bb}/\gamma_1$ for various $P_{Bb}/(-\gamma_1 C_4^*)$ in panel (a) of Fig. 8.30; the curve α_m (the minimum point) vs $u_{\theta Bb}/\gamma_1$ is shown for various $P_{Bb}/(-\gamma_1 C_4^*)$ in panel (b) of Fig. 8.30. The effect of $P_{Bb}/(-\gamma_1 C_4^*)$ or that of evaporation and condensation appears strongly when $u_{\theta Bb} < 0$ or the two cylinders are rotating in opposite directions.

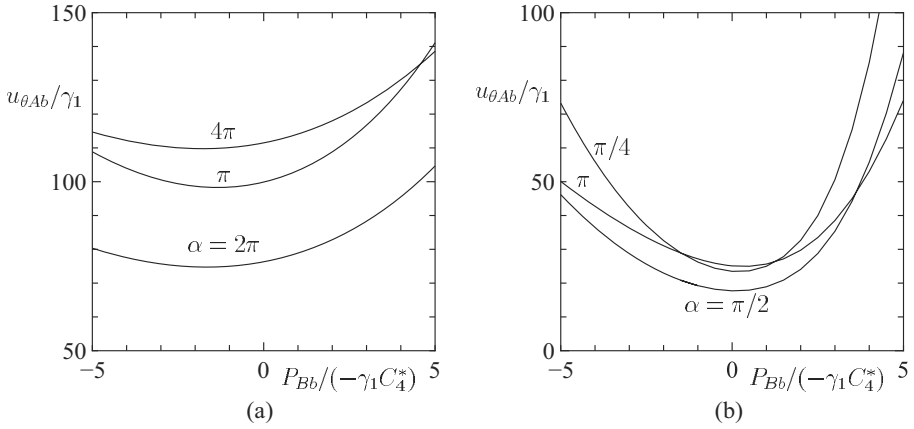

Figure 8.28. Bifurcation curve II: The first branch of the relation $u_{\theta Ab}/\gamma_1$ vs $P_{Bb}/(-\gamma_1 C_4^*)$ for various α when the outer cylinder is at rest $u_{\theta Bb} = 0$. (a) $\hat{r}_B = 1.5$ and (b) $\hat{r}_B = 3$.

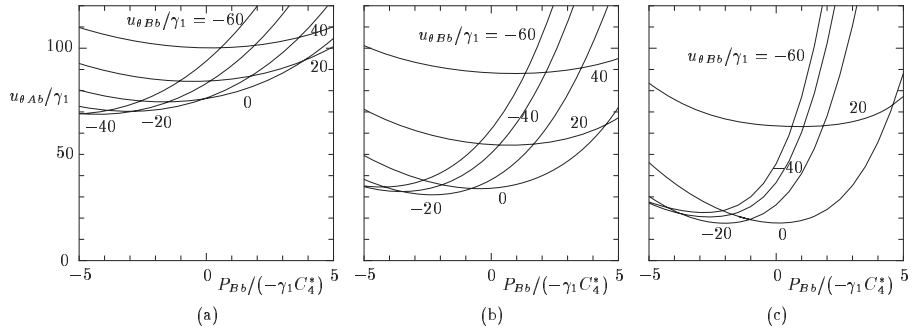

Figure 8.29. Bifurcation curve III: The first branch of the relation $u_{\theta Ab}/\gamma_1$ vs $P_{Bb}/(-\gamma_1 C_4^*)$ for various $u_{\theta Bb}/\gamma_1$. (a) $\hat{r}_B = 1.5$ and $\alpha = 2\pi$, (b) $\hat{r}_B = 2$ and $\alpha = \pi$, and (c) $\hat{r}_B = 3$ and $\alpha = \pi/2$.

When the relation (8.87) is satisfied, the boundary-value problem given by Eqs. (8.84) and (8.85) has a nontrivial solution. Some examples on the first branch for the case ($\alpha = \pi, \hat{r}_B = 2$) of the profiles $(U_{11}, V_{11})/||f_{11}||$ vs $\hat{r}$, where $||f_{11}|| = [\int_1^{\hat{r}_B}(U_{11}^2 + V_{11}^2)\hat{r}\mathrm{d}\hat{r}]^{1/2}$, are shown in Fig. 8.31. The flow field (V_{11}, W_{11}) in the $(\hat{r}, \hat{z})$ plane is a circulating flow of a single or multiple rolls depending on whether there is a node of V_{11} in $1 < \hat{r} < \hat{r}_B$. When $P_{Bb} = 0$ and $u_{\theta Bb} = 0$ (or there is neither evaporation nor condensation on the cylinders in the unperturbed flow and the outer cylinder is at rest), a single roll lies with its center in the central part of $(1, \hat{r}_B)$, and the $E_\perp (= \int_1^{\hat{r}_B} U_{11}^2 \hat{r}\mathrm{d}\hat{r})$ of the perturbed circumferential motion is comparable to $E_{\shortparallel}[= \int_1^{\hat{r}_B}(V_{11}^2 + W_{11}^2)\hat{r}\mathrm{d}\hat{r}]$

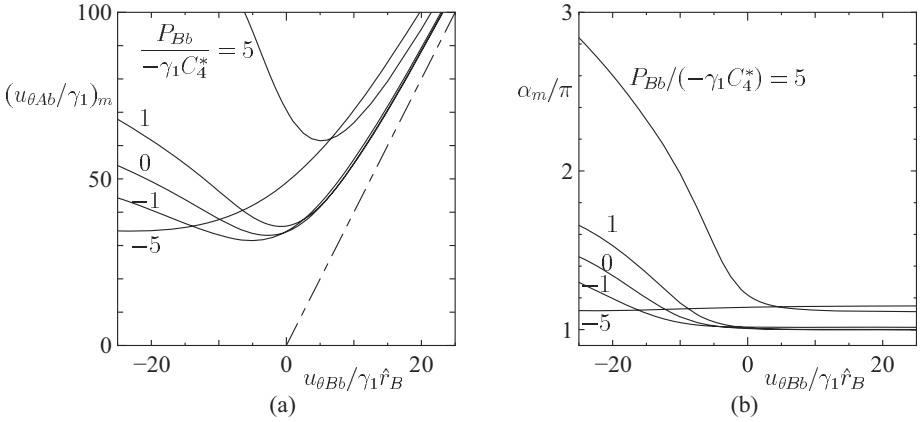

Figure 8.30. Bifurcation curve IV: the outer cylinder is rotating ($\hat{r}_B = 2$). (a) $(u_{\theta Ab}/\gamma_1)_m$ vs $u_{\theta Bb}/\gamma_1 \hat{r}_B$ and (b) α_m vs $u_{\theta Bb}/\gamma_1 \hat{r}_B$ The $(u_{\theta Ab}/\gamma_1)_m$ indicates the minimum of $u_{\theta Ab}/\gamma_1$ with respect to α, and α_m is the minimum point; the line $(u_{\theta Ab})_m = u_{\theta Bb}\hat{r}_B$ is shown by the dot-dash line $-\cdot-$.

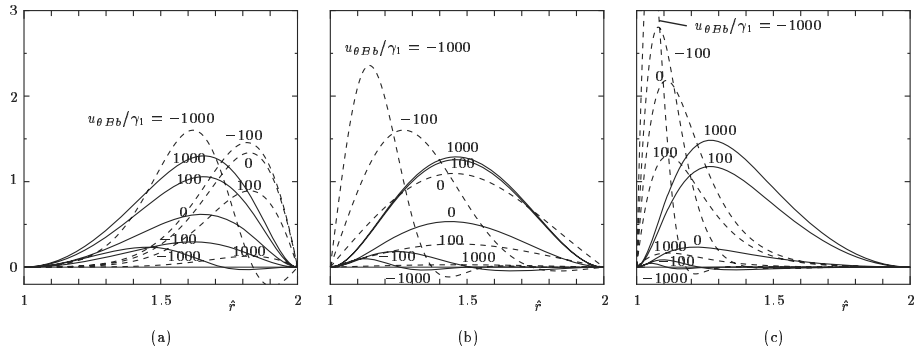

Figure 8.31. The various profiles $(U_{11}, V_{11})/||f_{11}||$ vs $\hat{r}$, where $||f_{11}|| = [\int_1^{\hat{r}_B}(U_{11}^2 + V_{11}^2)\hat{r}\mathrm{d}\hat{r}]^{1/2}$ ($\alpha = \pi$, $\hat{r}_B = 2$, the first branch of the bifurcation curves). (a) $P_{Bb}/(-\gamma_1 C_4^*) = -10$, (b) $P_{Bb}/(-\gamma_1 C_4^*) = 0$, and (c) $P_{Bb}/(-\gamma_1 C_4^*) = 10$. The dashed lines --- are $U_{11}/||f_{11}||$ and the solid lines —— are $V_{11}/||f_{11}||$.

of the motion in the $(\hat{r}, \hat{z})$ plane. When the outer cylinder is rotating, its effect appears differently for $u_{\theta Bb} > 0$ and for $u_{\theta Bb} < 0$. When $u_{\theta Bb} > 0$, the shape of the roll does not change much from that for $u_{\theta Bb} = 0$, but the ratio $E_\perp/E_{\shortparallel}$ decreases to vanish with the increase of $|u_{\theta Bb}|$. On the other hand, when $u_{\theta Bb} < 0$, the center of the roll moves towards the inner cylinder with increase of $|u_{\theta Bb}|$ and multiple rolls (two, three, ...) appear with its further increase; the ratio $E_\perp/E_{\shortparallel}$ increase with $|u_{\theta Bb}|$. When $P_{Bb} \neq 0$, the flow field is affected by the radial convection of the unperturbed flow, and the roll or rolls move

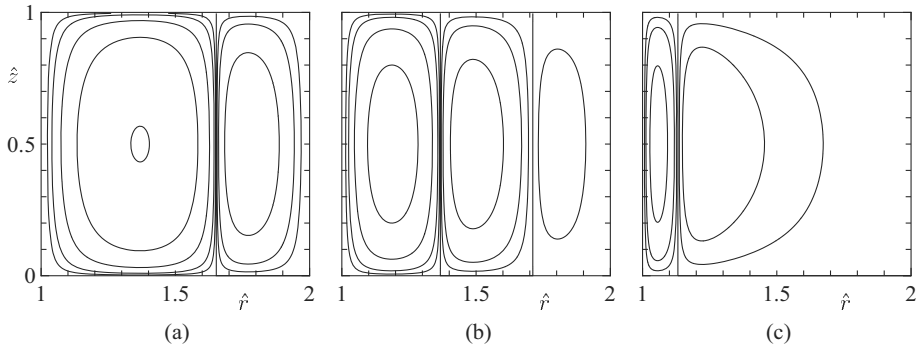

Figure 8.32. Collapse of a roll for large $|P_{Bb}|$ by the radial convection of the unperturbed flow ($\alpha = \pi$, $\hat{r}_B = 2$, $u_{\theta Bb}/\gamma_1 = -300$, the first branch curve). (a) $P_{Bb}/(-\gamma_1 C_4^*) = -5$, (b) $P_{Bb}/(-\gamma_1 C_4^*) = 0$, and (c) $P_{Bb}/(-\gamma_1 C_4^*) = 20$.

downstream. The roll on the side of the outer cylinder disappears with further increase of convection or $|P_{Bb}|$; this example is shown in Fig. 8.32. The variation of $E_\perp/E_{\shortparallel}$ with $u_{\theta Bb}$ is qualitatively similar to that for $P_{Bb} = 0$.

Solution in the neighborhood of a bifurcation point

The bifurcation point has been determined. However, the boundary-value problem for $U_{11}(\hat{r})$ and $V_{11}(\hat{r})$ [Eqs. (8.84) and (8.85)] being homogeneous, $U_{11}(\hat{r})$ and $V_{11}(\hat{r})$, the leading term of the bifurcated solution, are undetermined by a constant factor at this stage. It requires higher-order analysis to determine this factor, which is carried out here.

The equations for $U_{21}(\hat{r})$ and $V_{21}(\hat{r})$ are of the same form as those for $U_{11}(\hat{r})$ and $V_{11}(\hat{r})$; the boundary-value problem for $U_{m1}(\hat{r})$ and $V_{m1}(\hat{r})$ ($m \geq 3$) is inhomogeneous, and its homogeneous part is of the same form as that for $U_{11}(\hat{r})$ and $V_{11}(\hat{r})$. Thus, the inhomogeneous part of the boundary-value problem for $U_{m1}(\hat{r})$ and $V_{m1}(\hat{r})$ ($m \geq 3$) must satisfy some relation (solvability condition) for the solution $U_{m1}(\hat{r})$ and $V_{m1}(\hat{r})$ to exist.[38] The homogeneous part of the boundary-value problem for $U_{mn}(\hat{r})$ and $V_{mn}(\hat{r})$ ($n \neq 1$) has no nontrivial solution, unless an additional relation among $u_{\theta Ab}/\gamma_1, u_{\theta Bb}/\gamma_1, P_{Bb}/\gamma_1 C_4^*$, $\hat{r}_B$, and α is satisfied.

From the solvability condition of the boundary-value problem for $U_{31}(\hat{r})$ and $V_{31}(\hat{r})$, the undetermined norm (for example, $\delta||f_{11}|| = \delta[\int_1^{\hat{r}_B}(U_{11}^2+V_{11}^2)\hat{r}\mathrm{d}\hat{r}]^{1/2}$) of the solution $\delta(U_{11}(\hat{r}), V_{11}(\hat{r}))$ is determined by the following equation:

$$(\delta\|f_{11}\|)[\gamma_1(a_A\Delta u_{\theta A} + a_B\Delta u_{\theta B} - a_P\Delta P_B/C_4^*) - a_O(\delta\|f_{11}\|)^2] = 0, \quad (8.88)$$

[38] The solution of the adjoint problem of Eqs. (8.84) and (8.85) should be orthogonal to the inhomogeneous part. See Footnote 3 in Section 8.2.3.

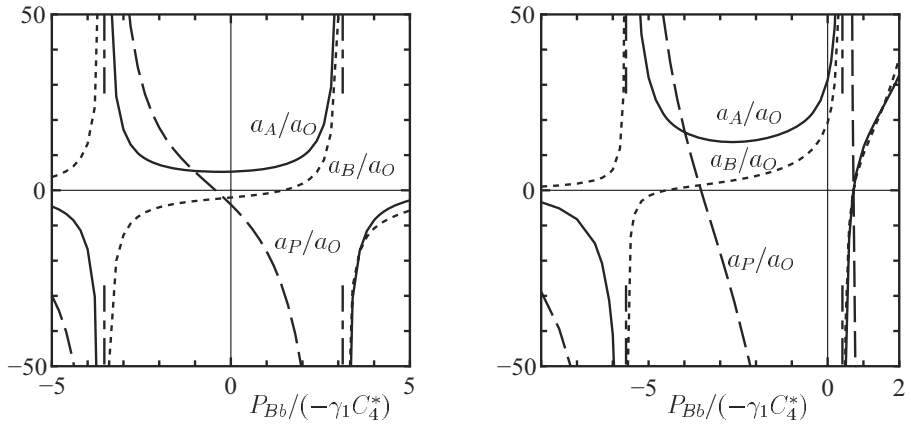

Figure 8.33. The coefficients a_A/a_O, a_B/a_O, and a_P/a_O vs $P_{Bb}/(-\gamma_1 C_4^*)$ ($\hat{r}_B = 2$, and $\alpha = \pi$) on the first branch. (a) $u_{\theta Bb} = 0$ and (b) $u_{\theta Bb}/\gamma_1 = -40$. The parameter $u_{\theta Ab}/\gamma_1$ is given in Figs. 8.27 and 8.29. The vertical dot-dash lines $-\cdot-$ at $P_{Bb}/(-\gamma_1 C_4^*) = -3.53365$ and 3.12345 in (a) and at $P_{Bb}/(-\gamma_1 C_4^*) = -5.63002$ and 0.41251 in (b) are the common asymptotes of the curves.

that is,

$$\left(\frac{\delta\|f_{11}\|}{\gamma_1}\right)^2 = \frac{a_A}{a_O}\frac{\Delta u_{\theta A}}{\gamma_1} + \frac{a_B}{a_O}\frac{\Delta u_{\theta B}}{\gamma_1} + \frac{a_P}{a_O}\frac{\Delta P_B}{(-\gamma_1 C_4^*)} \quad \text{or} \quad \delta\|f_{11}\| = 0, \tag{8.89}$$

where $\Delta u_{\theta A} = u_{\theta A} - u_{\theta Ab}$, $\Delta u_{\theta B} = u_{\theta B} - u_{\theta Bb}$, and $\Delta P_B = P_B - P_{Bb}$, and the coefficients a_A/a_O, a_B/a_O, and a_P/a_O, which depend on the definition of the norm, are constants determined by the parameters $u_{\theta Ab}/\gamma_1$, $u_{\theta Bb}/\gamma_1$, $P_{Bb}/(-\gamma_1 C_4^*)$, α, and $\hat{r}_B$.[39] Their examples are given in Fig. 8.33 and in the fourth to sixth columns of Table 8.3. The case $a_O = 0$ should be analyzed separately and requires the analysis to higher order, and then $(\delta\|f_{11}\|/\gamma_1)^4$, instead of $(\delta\|f_{11}\|/\gamma_1)^2$, is found to be the linear combination of $\Delta u_{\theta A}/\gamma_1$, $\Delta u_{\theta B}/\gamma_1$, and $\Delta P_B/(-\gamma_1 C_4^*)$.

The second relation of Eq. (8.89) corresponds to the axially uniform solution. The first relation gives the norm of bifurcated solution in the neighborhood of the bifurcation point. The $\delta\|f_{11}\|/\gamma_1$ can be real or time-independent bifurcated solutions are possible only when

$$\frac{a_A}{a_O}\frac{\Delta u_{\theta A}}{\gamma_1} + \frac{a_B}{a_O}\frac{\Delta u_{\theta B}}{\gamma_1} + \frac{a_P}{a_O}\frac{\Delta P_B}{(-\gamma_1 C_4^*)} > 0. \tag{8.90}$$

That is, the bifurcated solution is possible only when the variation of the parameters $u_{\theta A}$, $u_{\theta B}$, and P_B from $u_{\theta Ab}$, $u_{\theta Bb}$, and P_{Bb} satisfies the relation (8.90). For

[39] According to Eq. (8.87), one of these five parameters depends on the others.

example, consider the case on the first branch for $\hat{r}_B = 2$, $u_{\theta Bb} = 0$, and $\alpha = \pi$. The value a_A/a_O is positive in $-3.53365 < P_{Bb}/(-\gamma_1 C_4^*) < 3.12345$ [Fig. 8.33 (a)], and therefore the bifurcated solution exists for positive $\Delta u_{\theta A}/\gamma_1$, that is, it extends to the upper side of the bifurcation curve $u_{\theta Ab}/\gamma_1$ vs $P_{Bb}/(-\gamma_1 C_4^*)$ in Fig. 8.27 and in the other range of $P_{Bb}/(-\gamma_1 C_4^*)$ [within Fig. 8.33 (a)], the solution extends to the lower side.[40]

Discussion

The bifurcation curve corresponds to the neutral curve (or the boundary of linearly stable and unstable regions in the parameter space) of the axially uniform solution for the class of solutions with time scale of variation of the order of $L_A/(2RT_A)^{1/2}\varepsilon$ or $L_A^2\rho_0/\mu_0$, where μ_0/ρ_0 is the kinematic viscosity μ/ρ at the reference state. The side above the first branch in Fig. 8.27 is unstable one. The above-mentioned direction of extension of a bifurcated solution should not be confused with the linearly stable or the unstable side. The complete time-dependent analysis is not given here, but it is better to explain a little more.

The extension of the basic equations and boundary condition in the present subsection to a time-dependent problem where the time scale of variation is of the order of $L_A/(2RT_A)^{1/2}\varepsilon$ or $L_A^2\rho_0/\mu_0$ is discussed in Sections 3.7.2 and 3.7.3. That is, the equations are given by the set of equations (8.77)–(8.78e) with $\partial u_r/\partial\tilde{t}$, $\partial u_\theta/\partial\tilde{t}$, $\partial u_z/\partial\tilde{t}$, and $\partial(\tau - 2P/5)/\partial\tilde{t}$ being added, respectively, to the left-hand sides on Eqs. (8.78b)–(8.78e), where $\tilde{t} = t/L_A(2RT_A)^{-1/2}\varepsilon^{-1}$ (or $= 2t\mu_0/\rho_0 L_A^2\gamma_1$) with t being the time. The boundary conditions (8.79a) and (8.79b) apply to the time-dependent problem. From the linear-stability analysis of the axially uniform solution on the basis of this set of equations, each of the Fourier components with respect to $\hat{z}$ of the perturbation develops independently with $\tilde{t}$ and consists of infinitely many components, each of which also develops independently and exponentially with $\tilde{t}$ [say, $\exp(\kappa_n\tilde{t})$ $(n = 1, 2, \ldots)$]. The amplifying factor κ_n changes its sign from negative to positive when the parameter $u_{\theta Ab}/\gamma_1$ passes the n-th branch of the bifurcation curves in Fig. 8.27 from below. For the complete time-dependent study, solutions with shorter time scale of variation should be considered on the basis of the Boltzmann equation.[41]

We can construct the axially symmetric bifurcated solutions of the system (8.77)–(8.79b) in the parameter range above the bifurcation curve (or for $u_{\theta A} > u_{\theta Ab}$) in Fig. 8.27. The bifurcated solution can be inferred to be extended continuously with increase of $u_{\theta A}$ up to infinity. That is, this solution continues to exist up to the parameter size given by Eq. (8.70) with $m = 2$,

[40] Obviously, owing to the way of analysis, the statement applies only to the neighborhood of the bifurcation point. See Figs. 8.7 and 8.11 and their explanation in the text, where the bifurcated solutions first extend to one direction and then extends to another direction.

[41] For the solution to satisfy the above limitation of the time scale of variation, the initial velocity distribution function must be Maxwellian and its flow velocity must be solenoidal. The initial value of the Boltzmann system can be general, or non-Maxwellian with nonsolenoidal flow velocity. Though not related to the present problem, the stability discussion for initial-value problems of the Boltzmann equation in an infinite domain without boundary is found in Liu, Yang & Yu [2003] and Liu & Yu [2006a].

which corresponds to the case where $\varepsilon u_{\theta A}$ is much larger than εP_B and Kn (or $2\varepsilon/\sqrt{\pi}$).

When $P_B = 0$, with the aid of Eqs. (8.77), (8.78a), and the periodicity with respect to $\hat{z}$, the boundary conditions on u_r and τ in Eqs. (8.79a) and (8.79b) are reduced to $u_r = 0$ and $\tau = 0$ at $\hat{r} = 1$ and $u_r = 0$ and $\tau = \tau_B$ at $\hat{r} = \hat{r}_B$; that is, Eqs. (8.79a) and (8.79b) are reduced to the nonslip condition. Thus, the solution for this case gives that of the corresponding problem with a simple boundary. According to the analysis, the bifurcation is not affected by the amplified temperature difference τ_B $[= (T_B/T_A - 1)/\varepsilon]$ of the two cylinders.[42] The analysis in this section is limited to the case where the temperature difference $T_B/T_A - 1$ $(= \varepsilon\tau_B)$ of the two cylinders is of the same order as $\varepsilon u_{\theta A}$ and $\varepsilon u_{\theta B}$. That is, for this order of the variation of the temperature, the bifurcation is not subject to any effect. The analysis of the problem for a finite difference of the temperatures is discussed in Section 8.3, where the bifurcation occurs when the speeds of rotation of the cylinders are of the order of the Knudsen number i.e., the same order as $\varepsilon u_{\theta A}$ and $\varepsilon u_{\theta B}$ in this section. A finite difference of the temperatures of the cylinders affects the bifurcation speed only by the small order. Thus, apparent difference between the two results that the temperature difference of the boundaries affects the bifurcation in Section 8.3 and does not here does not contradict each other.

Arkeryd & Nouri [2006] have done a rigorous mathematical discussion of the above asymptotic analysis (Sone & Doi [2003b]) for a special case ($P_B = 0$, $\tau_B = 0$).

[42] See the paragraph next to that containing Eq. (8.79b) and Footnote 36 in this subsection.

Chapter 9

Ghost Effect and Bifurcation II: Ghost Effect of Infinitesimal Curvature and Bifurcation of the Plane Couette Flow

According to the asymptotic analysis for small Knudsen numbers in Chapter 3, the fluid-dynamic-type equations that describe the behavior of a gas in the continuum limit are classified depending on the size of the parameters in the problem under consideration (see, especially, Section 3.6). There is an important class of problems where the classical fluid dynamics, the Euler or Navier–Stokes system, is inapplicable and an infinitesimal flow velocity plays a decisive role to determine the behavior of the gas (the ghost and non-Navier–Stokes effects). Various examples of the ghost and non-Navier–Stokes effects are given in Chapter 8, in addition to that in Chapter 3. A geometrical parameter can be a source of the ghost effect. We will show an important case of this in this chapter. That is, taking a gas between two rotating coaxial circular cylinders, we consider the behavior of the gas in the limit that the Knudsen number and the inverse of radius (the curvature) of the inner cylinder tend to zero simultaneously, keeping the difference of the radii of the two cylinders fixed. The limiting behavior depends on the relative speed of decay of the two parameters. This singular character in the continuum limit introduces the ghost effect of infinitesimal curvature. Bifurcation of the plane Couette flow, a long-lasting problem of the classical fluid dynamics, occurs owing to the effect of infinitesimal curvature.

9.1 Problem and basic equations

Consider a gas in a time-independent state between two rotating coaxial circular cylinders. Let the radius, temperature, and circumferential velocity of the inner cylinder be, respectively, L_A, T_A, and V_A, and let the corresponding quantities of the outer cylinder be, respectively, $L_A + D$, T_B, and V_B. The nondimensional circumferential speeds $|V_A|/(2RT_A)^{1/2}$ and $|V_B|/(2RT_A)^{1/2}$ of rotation of the two cylinders, where R is the specific gas constant, are of the order of unity, and the nondimensional temperature difference $T_B/T_A - 1$ of the two cylinders is also of the order of unity. We will discuss the behavior of the gas in the limit that the Knudsen number $\mathrm{Kn} = \ell_0/D$ and the relative curvature D/L_A of the inner cylinder tend to zero simultaneously, keeping D fixed, where ℓ_0 is the mean free path of the gas in the equilibrium state at rest with temperature T_A and the average density ρ_0 of the gas in the domain. The discussion is based on Sone & Doi [2004].

Take D, T_A, and ρ_0, respectively, as the reference length, the reference temperature, and the reference density of the system and use the notation in Section 1.9. That is, we introduce the nondimensional space variable $\boldsymbol{x}$, the nondimensional molecular velocity $\boldsymbol{\zeta}$, and the nondimensional velocity distribution function $\hat{f}$ defined from the corresponding dimensional variables $\boldsymbol{X}$, $\boldsymbol{\xi}$, and f as follows:

$$\boldsymbol{x} = \frac{\boldsymbol{X}}{D}, \quad \boldsymbol{\zeta} = \frac{\boldsymbol{\xi}}{(2RT_A)^{1/2}}, \quad \hat{f} = \frac{f}{\rho_0/(2RT_A)^{3/2}}. \tag{9.1}$$

Let $(\hat{r}, \theta, \hat{z})$ and $(\zeta_r, \zeta_\theta, \zeta_z)$ be, respectively, the cylindrical coordinate expressions of $\boldsymbol{x}$ and $\boldsymbol{\zeta}$, where the $\hat{z}$ axis (or $\hat{r} = 0$) lies on the common axis of the cylinders. Then, in view of the formula in Section A.3, the nondimensional Boltzmann equation in the cylindrical coordinate expression for a time-independent state is given as

$$\zeta_r \frac{\partial \hat{f}}{\partial \hat{r}} + \frac{\zeta_\theta}{\hat{r}} \frac{\partial \hat{f}}{\partial \theta} + \zeta_z \frac{\partial \hat{f}}{\partial \hat{z}} + \frac{\zeta_\theta^2}{\hat{r}} \frac{\partial \hat{f}}{\partial \zeta_r} - \frac{\zeta_r \zeta_\theta}{\hat{r}} \frac{\partial \hat{f}}{\partial \zeta_\theta} = \frac{1}{k} \hat{J}(\hat{f}, \hat{f}), \tag{9.2a}$$

$$\hat{J}(\hat{f}, \hat{f}) = \int (\hat{f}' \hat{f}'_* - \hat{f} \hat{f}_*) \widehat{B} \mathrm{d}\Omega(\boldsymbol{\alpha}) \mathbf{d}\boldsymbol{\zeta}_*, \tag{9.2b}$$

where

$$k = \frac{\sqrt{\pi}}{2} \mathrm{Kn} = \frac{\sqrt{\pi} \ell_0}{2D}. \tag{9.3}$$

The boundary condition is generally given by Eq. (1.64) or more simply by Eq. (1.63a) with (1.63b) for the diffuse reflection. As the nondimensional data of the cylinders, we introduce

$$\hat{v}_A = \frac{V_A}{(2RT_A)^{1/2}}, \quad \hat{v}_B = \frac{V_B}{(2RT_A)^{1/2}}, \quad \hat{T}_B = \frac{T_B}{T_A}.$$

Here, it is noted that V_A and V_B are taken to be positive when the cylinders are rotating in the negative θ direction. We can take V_A positive without loss of generality.

In this chapter, we will investigate the problem in the limit that the two parameters, the Knudsen number Kn (or k) and the relative curvature D/L_A tend to zero simultaneously with the difference D of the radii of the two cylinders fixed. The analysis is carried out in detail when the relative curvature tends to zero with the same speed as the square of the Knudsen number (or $D/L_A \propto k^2$). On the basis of the result, we discuss the cases where D/L_A tends to zero with the other speeds. For the convenience of expression of the limiting state with infinite L_A/D, we introduce the notation

$$x = -\frac{L_A}{D}\theta, \quad y = \hat{r} - \frac{L_A}{D}, \quad z = \hat{z}, \tag{9.4a}$$

$$(\zeta_x,\ \zeta_y,\ \zeta_z) = (-\zeta_\theta,\ \zeta_r,\ \zeta_z), \tag{9.4b}$$

$$D/L_A = (k/c)^2, \tag{9.4c}$$

where c (> 0) is a constant of the order of unity. With this notation, the Boltzmann equation (9.2a) is rewritten as

$$\frac{\zeta_x}{1+(k/c)^2 y}\frac{\partial \hat{f}}{\partial x} + \zeta_y \frac{\partial \hat{f}}{\partial y} + \zeta_z \frac{\partial \hat{f}}{\partial z} + \frac{(k/c)^2 \zeta_x^2}{1+(k/c)^2 y}\frac{\partial \hat{f}}{\partial \zeta_y} - \frac{(k/c)^2 \zeta_x \zeta_y}{1+(k/c)^2 y}\frac{\partial \hat{f}}{\partial \zeta_x} = \frac{1}{k}\hat{J}(\hat{f},\hat{f}). \tag{9.5}$$

The boundary condition is symbolically expressed as

$$\hat{f} = \hat{f}_{wA} \quad (\zeta_y > 0) \ \text{ at } y = 0, \ \text{ and } \ \hat{f} = \hat{f}_{wB} \quad (\zeta_y < 0) \ \text{ at } y = 1. \tag{9.6}$$

One of our interests is the bifurcation from the plane parallel Couette flow between two parallel plane walls. Thus, we start our analysis under the assumption that the flow is nearly parallel. That is, we consider the solution in the limit of $k \to 0$ with $D/L_A = (k/c)^2$ that has the following properties: (i)

$$\int \zeta_x \hat{f}\, \mathbf{d\zeta} = O(1), \tag{9.7a}$$

$$\int \zeta_y \hat{f}\, \mathbf{d\zeta} = O(k), \ \int \zeta_z \hat{f}\, \mathbf{d\zeta} = O(k), \tag{9.7b}$$

and (ii) $\hat{f}$ varies slowly in the direction of the motion of the walls, i.e., $\partial \hat{f}/\partial x$ is of the order of $k\hat{f}$ or smaller, which is consistent with the assumption (i) in view of the law of mass conservation, as will be noted after the definition of the macroscopic variables is given. Corresponding to this variation, a shrunk coordinate χ is introduced, i.e.,

$$\chi = kx. \tag{9.8}$$

With the new variable χ, the Boltzmann equation is rewritten as

$$\frac{k\zeta_x}{1+(k/c)^2 y}\frac{\partial \hat{f}}{\partial \chi} + \zeta_y \frac{\partial \hat{f}}{\partial y} + \zeta_z \frac{\partial \hat{f}}{\partial z} + \frac{(k/c)^2 \zeta_x^2}{1+(k/c)^2 y}\frac{\partial \hat{f}}{\partial \zeta_y} - \frac{(k/c)^2 \zeta_x \zeta_y}{1+(k/c)^2 y}\frac{\partial \hat{f}}{\partial \zeta_x} = \frac{1}{k}\hat{J}(\hat{f},\hat{f}). \tag{9.9}$$

The macroscopic variables, the density ρ, the velocity v_ι, the temperature T, the pressure p, the stress tensor $p_{\iota\gamma}$, and the heat-flow vector q_ι, of the gas are defined by the velocity distribution function f, where the subscripts ι and γ are x, y, or z. The corresponding nondimensional variables $\hat{\rho}$, $\hat{v}_\iota$, $\hat{T}$, $\hat{p}$, $\hat{p}_{\iota\gamma}$, and $\hat{q}_\iota$ are defined, respectively, by ρ/ρ_0, $v_\iota/(2RT_A)^{1/2}$, T/T_A, p/p_0, $p_{\iota\gamma}/p_0$, and $q_\iota/p_0(2RT_A)^{1/2}$, where $p_0 = R\rho_0 T_A$. They are related to $\hat{f}$ as follows:

$$\hat{\rho} = \int \hat{f}\mathbf{d}\boldsymbol{\zeta}, \tag{9.10a}$$

$$\hat{\rho}\hat{v}_\iota = \int \zeta_\iota \hat{f}\mathbf{d}\boldsymbol{\zeta}, \tag{9.10b}$$

$$\frac{3}{2}\hat{\rho}\hat{T} = \int (\boldsymbol{\zeta} - \widehat{\boldsymbol{v}})^2 \hat{f}\mathbf{d}\boldsymbol{\zeta}, \tag{9.10c}$$

$$\hat{p} = \hat{\rho}\hat{T}, \tag{9.10d}$$

$$\hat{p}_{\iota\gamma} = 2\int (\zeta_\iota - \hat{v}_\iota)(\zeta_\gamma - \hat{v}_\gamma)\hat{f}\mathbf{d}\boldsymbol{\zeta}, \tag{9.10e}$$

$$\hat{q}_\iota = \int (\zeta_\iota - \hat{v}_\iota)(\boldsymbol{\zeta} - \widehat{\boldsymbol{v}})^2 \hat{f}\mathbf{d}\boldsymbol{\zeta}, \tag{9.10f}$$

where the bold face letter $\widehat{\boldsymbol{v}}$ is another expression for $\hat{v}_\iota$, introduced for brevity.

To summarize, we will discuss the asymptotic behavior of the solution $\hat{f}$ of the Boltzmann equation (9.9) with a finite c under the boundary condition (9.6) in the limit $k \to 0$ for the class of solution $\hat{f}$ that satisfies the conditions (9.7a) and (9.7b) and those on the variation of $\hat{f}$

$$\frac{\partial \hat{f}}{\partial \chi} = O(\hat{f}), \qquad \frac{\partial \hat{f}}{\partial y} = O(\hat{f}), \qquad \frac{\partial \hat{f}}{\partial z} = O(\hat{f}). \tag{9.11}$$

The condition (9.11) is easily seen to be consistent with the conditions (9.7a) and (9.7b) from the equation of mass conservation derived from the Boltzmann equation.[1] It may be noted that the constant c^2 is the ratio of k^2 to D/L_A [see Eq. (9.4c)].

9.2 Asymptotic analysis

In this section, we will carry out the asymptotic analysis for small k of the boundary-value problem stated at the end of the preceding section (Section 9.1) by making use of the procedure developed in Chapter 3.

[1] The Boltzmann equation (9.2a) being integrated over the whole space of $\boldsymbol{\zeta}$,

$$\partial \hat{r}\hat{\rho}\hat{v}_r/\hat{r}\partial\hat{r} + \partial\hat{\rho}\hat{v}_\theta/\hat{r}\partial\theta + \partial\hat{\rho}\hat{v}_z/\partial z = 0,$$

where $(\hat{v}_r, \hat{v}_\theta, \hat{v}_z)$ is the cylindrical coordinate expression of $\widehat{\boldsymbol{v}}$. Noting that $\hat{\rho}\hat{v}_r = O(k)$, $\hat{\rho}\hat{v}_z = O(k)$, $\hat{\rho}\hat{v}_\theta = O(1)$, and $\partial(*)/\partial y = O(*)$, we will find that $\partial\hat{\rho}\hat{v}_\theta/\hat{r}\partial\theta = O(k)$ and that the length scale of variation of variables in x is $O(k^{-1})$.

9.2.1 $\mathfrak{S}$ solution

First, putting aside the boundary condition, we consider the solution of Eq. (9.9) under the conditions (9.7a), (9.7b), and (9.11) for small k. This class of solution is looked for in a power series of k, i.e.,

$$\hat{f} = \hat{f}_{\mathfrak{S}} = \hat{f}_{\mathfrak{S}0} + \hat{f}_{\mathfrak{S}1}k + \hat{f}_{\mathfrak{S}2}k^2 + \cdots, \tag{9.12}$$

where the subscript $\mathfrak{S}$ is attached to discriminate this class of solution ($\mathfrak{S}$ solution or expansion). The condition (9.7b) corresponds to the condition on $\hat{f}_{\mathfrak{S}0}$

$$\int \zeta_y \hat{f}_{\mathfrak{S}0} \mathbf{d}\boldsymbol{\zeta} = \int \zeta_z \hat{f}_{\mathfrak{S}0} \mathbf{d}\boldsymbol{\zeta} = 0. \tag{9.13}$$

The relation between the macroscopic variables and the velocity distribution function is given by Eqs. (9.10a)–(9.10f) with the subscript $\mathfrak{S}$ attached. Corresponding to the expansion (9.12), the macroscopic variable $\hat{h}_{\mathfrak{S}}$, where $\hat{h}$ represents $\hat{\rho}$, $\hat{v}_\iota$, $\hat{T}$, etc., is also expanded in k, i.e.,

$$\hat{h}_{\mathfrak{S}} = \hat{h}_{\mathfrak{S}0} + \hat{h}_{\mathfrak{S}1}k + \hat{h}_{\mathfrak{S}2}k^2 + \cdots. \tag{9.14}$$

The component function $\hat{h}_{\mathfrak{S}m}$ is related to the component function of the velocity distribution function as follows:

$$\hat{\rho}_{\mathfrak{S}0} = \int \hat{f}_{\mathfrak{S}0} \mathbf{d}\boldsymbol{\zeta}, \tag{9.15a}$$

$$\hat{\rho}_{\mathfrak{S}0}\hat{v}_{x\mathfrak{S}0} = \int \zeta_x \hat{f}_{\mathfrak{S}0} \mathbf{d}\boldsymbol{\zeta}, \tag{9.15b}$$

$$\hat{\rho}_{\mathfrak{S}0}\hat{v}_{y\mathfrak{S}0} = \int \zeta_y \hat{f}_{\mathfrak{S}0} \mathbf{d}\boldsymbol{\zeta} = 0, \tag{9.15c}$$

$$\hat{\rho}_{\mathfrak{S}0}\hat{v}_{z\mathfrak{S}0} = \int \zeta_z \hat{f}_{\mathfrak{S}0} \mathbf{d}\boldsymbol{\zeta} = 0, \tag{9.15d}$$

$$\frac{3}{2}\hat{\rho}_{\mathfrak{S}0}\hat{T}_{\mathfrak{S}0} = \int \boldsymbol{\zeta}^2 \hat{f}_{\mathfrak{S}0} \mathbf{d}\boldsymbol{\zeta} - \hat{\rho}_{\mathfrak{S}0}\hat{v}_{x\mathfrak{S}0}^2, \tag{9.15e}$$

$$\hat{p}_{\mathfrak{S}0} = \hat{\rho}_{\mathfrak{S}0}\hat{T}_{\mathfrak{S}0}, \tag{9.15f}$$

$$\hat{p}_{\iota\gamma\mathfrak{S}0} = 2\int (\zeta_\iota - \hat{v}_{\iota\mathfrak{S}0})(\zeta_\gamma - \hat{v}_{\gamma\mathfrak{S}0})\hat{f}_{\mathfrak{S}0} \mathbf{d}\boldsymbol{\zeta}, \tag{9.15g}$$

$$\hat{q}_{\iota\mathfrak{S}0} = \int (\zeta_\iota - \hat{v}_{\iota\mathfrak{S}0})(\boldsymbol{\zeta} - \widehat{\boldsymbol{v}}_{\mathfrak{S}0})^2 \hat{f}_{\mathfrak{S}0} \mathbf{d}\boldsymbol{\zeta}, \tag{9.15h}$$

$$\hat{\rho}_{\mathfrak{S}1} = \int \hat{f}_{\mathfrak{S}1} \mathbf{d}\boldsymbol{\zeta}, \tag{9.16a}$$

$$\hat{\rho}_{\mathfrak{S}0}\hat{v}_{\iota\mathfrak{S}1} = \int (\zeta_\iota - \hat{v}_{\iota\mathfrak{S}0})\hat{f}_{\mathfrak{S}1}\mathbf{d}\boldsymbol{\zeta}, \tag{9.16b}$$

$$\frac{3}{2}\hat{\rho}_{\mathfrak{S}0}\hat{T}_{\mathfrak{S}1} = \int (\boldsymbol{\zeta} - \widehat{\boldsymbol{v}}_{\mathfrak{S}0})^2 \hat{f}_{\mathfrak{S}1}\mathbf{d}\boldsymbol{\zeta} - \frac{3}{2}\hat{\rho}_{\mathfrak{S}1}\hat{T}_{\mathfrak{S}0}, \tag{9.16c}$$

$$\hat{p}_{\mathfrak{S}1} = \hat{\rho}_{\mathfrak{S}0}\hat{T}_{\mathfrak{S}1} + \hat{\rho}_{\mathfrak{S}1}\hat{T}_{\mathfrak{S}0}, \tag{9.16d}$$

$$\hat{p}_{\iota\gamma\mathfrak{S}1} = 2\int (\zeta_\iota - \hat{v}_{\iota\mathfrak{S}0})(\zeta_\gamma - \hat{v}_{\gamma\mathfrak{S}0})\hat{f}_{\mathfrak{S}1}\mathbf{d}\boldsymbol{\zeta}, \tag{9.16e}$$

$$\begin{aligned}\hat{q}_{\iota\mathfrak{S}1} = \int (\zeta_\iota - \hat{v}_{\iota\mathfrak{S}0})(\boldsymbol{\zeta} - \widehat{\boldsymbol{v}}_{\mathfrak{S}0})^2 \hat{f}_{\mathfrak{S}1}\mathbf{d}\boldsymbol{\zeta} - \frac{3}{2}\hat{\rho}_{\mathfrak{S}0}\hat{T}_{\mathfrak{S}0}\hat{v}_{\iota\mathfrak{S}1} \\ - \hat{p}_{\iota x\mathfrak{S}0}\hat{v}_{x\mathfrak{S}1} - \hat{p}_{\iota y\mathfrak{S}0}\hat{v}_{y\mathfrak{S}1} - \hat{p}_{\iota z\mathfrak{S}0}\hat{v}_{z\mathfrak{S}1}.\end{aligned} \tag{9.16f}$$

Now, return to obtaining the $\mathfrak{S}$ solution. Substituting Eq. (9.12) into the Boltzmann equation (9.9) and arranging the same-order terms in k, we obtain a series of integral equations for $\hat{f}_{\mathfrak{S}m}$:[2]

$$\hat{J}(\hat{f}_{\mathfrak{S}0}, \hat{f}_{\mathfrak{S}0}) = 0, \tag{9.17}$$

$$2\hat{J}(\hat{f}_{\mathfrak{S}0}, \hat{f}_{\mathfrak{S}1}) = \zeta_y \frac{\partial \hat{f}_{\mathfrak{S}0}}{\partial y} + \zeta_z \frac{\partial \hat{f}_{\mathfrak{S}0}}{\partial z}, \tag{9.18a}$$

$$2\hat{J}(\hat{f}_{\mathfrak{S}0}, \hat{f}_{\mathfrak{S}2}) = \zeta_y \frac{\partial \hat{f}_{\mathfrak{S}1}}{\partial y} + \zeta_z \frac{\partial \hat{f}_{\mathfrak{S}1}}{\partial z} + \zeta_x \frac{\partial \hat{f}_{\mathfrak{S}0}}{\partial \chi} - \hat{J}(\hat{f}_{\mathfrak{S}1}, \hat{f}_{\mathfrak{S}1}), \tag{9.18b}$$

$$\begin{aligned}2\hat{J}(\hat{f}_{\mathfrak{S}0}, \hat{f}_{\mathfrak{S}3}) = \zeta_y \frac{\partial \hat{f}_{\mathfrak{S}2}}{\partial y} + \zeta_z \frac{\partial \hat{f}_{\mathfrak{S}2}}{\partial z} + \zeta_x \frac{\partial \hat{f}_{\mathfrak{S}1}}{\partial \chi} + \frac{\zeta_x^2}{c^2}\frac{\partial \hat{f}_{\mathfrak{S}0}}{\partial \zeta_y} \\ - \frac{\zeta_x\zeta_y}{c^2}\frac{\partial \hat{f}_{\mathfrak{S}0}}{\partial \zeta_x} - 2\hat{J}(\hat{f}_{\mathfrak{S}1}, \hat{f}_{\mathfrak{S}2}).\end{aligned} \tag{9.18c}$$

The solution $\hat{f}_{\mathfrak{S}0}$ of Eq. (9.17) satisfying the condition (9.13) is given by

$$\hat{f}_{\mathfrak{S}0} = \frac{\hat{\rho}_{\mathfrak{S}0}}{(\pi\hat{T}_{\mathfrak{S}0})^{3/2}} \exp\left(-\frac{(\zeta_x - \hat{v}_{x\mathfrak{S}0})^2 + \zeta_y^2 + \zeta_z^2}{\hat{T}_{\mathfrak{S}0}}\right), \tag{9.19}$$

where the relations (9.15a)–(9.15e) are used. The solution (9.19) is incomplete to determine $\hat{f}_{\mathfrak{S}0}$, because the spatial variations of the parameter functions $\hat{\rho}_{\mathfrak{S}0}$, $\hat{v}_{x\mathfrak{S}0}$, and $\hat{T}_{\mathfrak{S}0}$ are not specified. With this $\hat{f}_{\mathfrak{S}0}$, Eqs. (9.18a)–(9.18c), etc. are the inhomogeneous linear integral equations for $\hat{f}_{\mathfrak{S}m}$ ($m \geq 1$). The collision integral $\hat{J}(\hat{f}, \hat{g})$ satisfies the relation

$$\int \psi \hat{J}(\hat{f}, \hat{g})\mathbf{d}\boldsymbol{\zeta} = 0, \tag{9.20}$$

[2]See Footnote 58 in Section 3.3.2.

where

$$\psi = 1, \quad \zeta_x, \quad \zeta_y, \quad \zeta_z, \quad \boldsymbol{\zeta}^2, \tag{9.21}$$

for arbitrary $\hat{f}$ and $\hat{g}$ [see Eq. (1.53)]. From the condition for Eq. (1.83) to hold and the relation (9.20),[3] the inhomogeneous terms of the integral equations (9.18a)–(9.18c), etc. have to satisfy solvability conditions for them to have solutions. That is, the solvability conditions for Eqs. (9.18a)–(9.18c) are, respectively,

$$\int \psi \left(\zeta_y \frac{\partial \hat{f}_{\mathfrak{S}0}}{\partial y} + \zeta_z \frac{\partial \hat{f}_{\mathfrak{S}0}}{\partial z} \right) \mathbf{d}\boldsymbol{\zeta} = 0, \tag{9.22a}$$

$$\int \psi \left(\zeta_y \frac{\partial \hat{f}_{\mathfrak{S}1}}{\partial y} + \zeta_z \frac{\partial \hat{f}_{\mathfrak{S}1}}{\partial z} + \zeta_x \frac{\partial \hat{f}_{\mathfrak{S}0}}{\partial \chi} \right) \mathbf{d}\boldsymbol{\zeta} = 0, \tag{9.22b}$$

$$\int \psi \left(\zeta_y \frac{\partial \hat{f}_{\mathfrak{S}2}}{\partial y} + \zeta_z \frac{\partial \hat{f}_{\mathfrak{S}2}}{\partial z} + \zeta_x \frac{\partial \hat{f}_{\mathfrak{S}1}}{\partial \chi} + \frac{\zeta_x^2}{c^2} \frac{\partial \hat{f}_{\mathfrak{S}0}}{\partial \zeta_y} - \frac{\zeta_x \zeta_y}{c^2} \frac{\partial \hat{f}_{\mathfrak{S}0}}{\partial \zeta_x} \right) \mathbf{d}\boldsymbol{\zeta} = 0. \tag{9.22c}$$

The solvability condition for the integral equation for $\hat{f}_{\mathfrak{S}m}$ is reduced to a set of partial differential equations containing $\hat{\rho}_{\mathfrak{S}n}$, $\hat{v}_{x\mathfrak{S}n}$, $\hat{v}_{y\mathfrak{S}n}$, $\hat{v}_{z\mathfrak{S}n}$, $\hat{T}_{\mathfrak{S}n}$, and $\hat{p}_{\mathfrak{S}n}$ $(n \leq m-1)$.

As we have seen in Chapter 3, repeating the process of solvability condition and solution of the integral equation, we obtain a series of partial differential equations for the above macroscopic variables. The solvability conditions (9.22a) for $\psi = 1$, ζ_x, and $\boldsymbol{\zeta}^2$ with Eq. (9.19) degenerate into the identity. Owing to this degeneracy, staggered combination of the solvability conditions gives appropriate set of fluid-dynamic-type equations to determine the behavior of the gas successively from the lowest order of the expansion. In order to save space, we explain only the process referring to the final result summarized in Section 9.2.3. The solvability conditions (9.22a) for $\psi = \zeta_y$ and ζ_z correspond to Eq. (9.33). The solvability conditions (9.22b) for $\psi = 1$, ζ_x, and $\boldsymbol{\zeta}^2$ are, respectively, Eqs. (9.34), (9.35), and (9.38). The conditions (9.22b) for $\psi = \zeta_y$ and ζ_z are

$$\frac{\partial \hat{p}_{\mathfrak{S}1}}{\partial y} = \frac{\partial \hat{p}_{\mathfrak{S}1}}{\partial z} = 0. \tag{9.23}$$

We proceed with the analysis in a similar way, that is, to the solvability condition (9.22c). The solvability conditions (9.22c) for $\psi = \zeta_y$ and ζ_z are, respectively, Eqs. (9.36) and (9.37). The conditions (9.22c) for $\psi = 1$, ζ_x, and $\boldsymbol{\zeta}^2$, as well as Eq. (9.23), are the equations for the next-order set.

9.2.2 Knudsen-layer analysis

The leading term of the $\mathfrak{S}$ solution, i.e., $\hat{f}_{\mathfrak{S}0}$, is a Maxwellian with flow velocity $(\hat{v}_{x\mathfrak{S}0}, 0, 0)$ and temperature $\hat{T}_{\mathfrak{S}0}$. In view of the condition (iii) to the boundary condition (1.64), $\hat{f}_{\mathfrak{S}0}$ satisfies the general boundary condition (1.64) on a simple

[3] See Footnote 59 in Section 3.3.2.

boundary, as well as the diffuse-reflection condition (1.63a), if the boundary values of $\hat{v}_{x\mathfrak{S}0}$ and $\hat{T}_{\mathfrak{S}0}$ are taken as[4]

$$\hat{v}_{x\mathfrak{S}0} = \hat{v}_A, \quad \hat{T}_{\mathfrak{S}0} = 1 \quad \text{at } y = 0, \tag{9.24a}$$

$$\hat{v}_{x\mathfrak{S}0} = \hat{v}_B, \quad \hat{T}_{\mathfrak{S}0} = \hat{T}_B \quad \text{at } y = 1. \tag{9.24b}$$

The next-order distribution $\hat{f}_{\mathfrak{S}1}$, which is not Maxwellian, cannot be made to satisfy the boundary condition owing to its special form in $\boldsymbol{\zeta}$. Thus, we introduce the correction in a neighborhood of the boundary, i.e., a Knudsen-layer correction, to the $\mathfrak{S}$ solution. The analysis of the Knudsen layer can be carried out according to the recipe explained in Section 3.1.4. Here, we briefly explain it for the Knudsen layer on the inner cylinder ($y = 0$). That is, we put the solution $\hat{f}$ in the form

$$\hat{f} = \hat{f}_{\mathfrak{S}} + \hat{f}_K, \tag{9.25}$$

where $\hat{f}_K$ is the Knudsen-layer correction,[5] for which the condition on the $\mathfrak{S}$ solution is loosened. That is, the length scale of variation of $\hat{f}_K$ in the y direction is of the order of the mean free path, or $\partial \hat{f}_K/\partial \eta = O(\hat{f}_K)$ in the stretched coordinate η normal to the boundary

$$\eta = y/k. \tag{9.26}$$

The Knudsen-layer correction $\hat{f}_K$ vanishes as $\eta \to \infty$. The analysis is carried out under the stronger assumption that the speed of decay is faster than any inverse power of η,[6] which is verified by the Grad–Bardos theorem (Section 3.1.4).

Substituting Eq. (9.25) into Eq. (9.9) and noting that $\hat{f}_{\mathfrak{S}}$ satisfies Eq. (9.9), we have

$$\begin{aligned}&\zeta_y \frac{\partial \hat{f}_K}{\partial \eta} + \frac{k^2 \zeta_x}{1+(k/c)^2 k\eta} \frac{\partial \hat{f}_K}{\partial \chi} + k\zeta_z \frac{\partial \hat{f}_K}{\partial z} + \frac{k(k/c)^2 \zeta_x^2}{1+(k/c)^2 k\eta} \frac{\partial \hat{f}_K}{\partial \zeta_y} - \frac{k(k/c)^2 \zeta_x \zeta_y}{1+(k/c)^2 k\eta} \frac{\partial \hat{f}_K}{\partial \zeta_x} \\ &= 2\hat{J}(\hat{f}_{\mathfrak{S}}, \hat{f}_K) + \hat{J}(\hat{f}_K, \hat{f}_K).\end{aligned} \tag{9.27}$$

The interaction term $\hat{J}(\hat{f}_{\mathfrak{S}}, \hat{f}_K)$ can be simplified. Owing to the rapid decay of $\hat{f}_K$ as $\eta \to \infty$, we can use the the following expanded form for $\hat{f}_{\mathfrak{S}}$ in $\hat{J}(\hat{f}_{\mathfrak{S}}, \hat{f}_K)$:

$$\hat{f}_{\mathfrak{S}} = (\hat{f}_{\mathfrak{S}0})_0 + \left[(\hat{f}_{\mathfrak{S}1})_0 + \left(\frac{\partial \hat{f}_{\mathfrak{S}0}}{\partial y} \right)_0 \eta \right] k + \cdots, \tag{9.28}$$

where the quantities in the parentheses with subscript 0 are evaluated at $y = 0$ and the orders of the terms in k are reshuffled. The boundary condition being satisfied by $\hat{f}_{\mathfrak{S}0}$ at the order of unity, the Knudsen-layer correction is required only from the order of k. That is,

$$\hat{f}_K = \hat{f}_{K1} k + \cdots. \tag{9.29}$$

[4] See Footnote 60 in Section 3.3.2 for the uniqueness of this choice.

[5] The macroscopic variables are also put in the sum $\hat{h} = \hat{h}_{\mathfrak{S}} + \hat{h}_K$. Owing to the nonlinearity of Eqs. (9.10b)–(9.10f), $\hat{h}_K$ is expressed with $\hat{f}_{\mathfrak{S}}$ and $\hat{f}_K$.

[6] See Footnote 6 in Section 3.1.4.

Substituting the series (9.28) and (9.29) into Eq. (9.27) and arranging the terms with respect to k, we obtain the series of one-dimensional Boltzmann equations for $\hat{f}_{Km}$, e.g.,

$$\zeta_y \frac{\partial \hat{f}_{K1}}{\partial \eta} = 2\hat{J}((\hat{f}_{\mathfrak{S}0})_0, \hat{f}_{K1}). \tag{9.30}$$

The effects of the variation of the quantities parallel to the boundary including the curvature effect appear at higher orders as inhomogeneous terms, as is seen by examination of the order of each term in k in Eq. (9.27). The sum $\hat{f}_{\mathfrak{S}} + \hat{f}_K$ being substituted into the boundary condition (9.6) and the result being expanded in k, the boundary condition for $\hat{f}_{Km}$ on the inner cylinder is obtained:

$$\hat{f}_{Km} = \hat{f}_{wAm} - \hat{f}_{\mathfrak{S}m} \quad (\zeta_y > 0) \text{ at } \eta = 0, \tag{9.31}$$

where $\hat{f}_{wAm}$ is the coefficient of k^m of the expansion of $\hat{f}_{wA}$ in k. The other condition on $\hat{f}_{Km}$ is

$$\hat{f}_{Km} \to 0, \quad \text{as } \eta \to \infty, \tag{9.32}$$

with a speed faster than any inverse power of η.

According to the discussion in Section A.11, the solution $\hat{f}_{K1}$ of the Knudsen-layer correction and the slip condition are practically the same as those in the linear theory in Section 3.1.5, i.e., Eqs. (3.41a)–(3.41c) with the derivatives parallel to the x direction degraded corresponding to Eq. (9.11). The slip condition gives the relation among the boundary values of $\hat{v}_{x\mathfrak{S}1}$, $\hat{v}_{y\mathfrak{S}1}$, $\hat{v}_{z\mathfrak{S}1}$, $\hat{T}_{\mathfrak{S}1}$, $\hat{\rho}_{\mathfrak{S}1}$, $\partial \hat{v}_{x\mathfrak{S}0}/\partial y$, and $\partial \hat{T}_{\mathfrak{S}0}/\partial y$ in view of the condition (9.13), i.e., $\hat{v}_{y\mathfrak{S}0} = \hat{v}_{z\mathfrak{S}0} = 0$. For the purpose to obtain the boundary conditions for the set of equations (9.33)–(9.39b), in addition to Eqs. (9.24a) and (9.24b), we need only the conditions on the boundary data of $\hat{v}_{y\mathfrak{S}1}$ and $\hat{v}_{z\mathfrak{S}1}$. They simply vanish, i.e., $\hat{v}_{y\mathfrak{S}1} = \hat{v}_{z\mathfrak{S}1} = 0$ at $y = 0$. Similarly, $\hat{v}_{y\mathfrak{S}1} = \hat{v}_{z\mathfrak{S}1} = 0$ at $y = 1$.

9.2.3 Asymptotic fluid-dynamic-type equations and their boundary conditions

We summarize the fluid-dynamic-type equations and their associated boundary conditions that describe the behavior of a gas in the continuum limit satisfying the conditions given at the end of Section 9.1. The fluid-dynamic-type equations are

$$\frac{\partial \hat{p}_{\mathfrak{S}0}}{\partial y} = \frac{\partial \hat{p}_{\mathfrak{S}0}}{\partial z} = 0, \tag{9.33}$$

$$\frac{\partial \hat{\rho}_{\mathfrak{S}0} \hat{v}_{x\mathfrak{S}0}}{\partial \chi} + \frac{\partial \hat{\rho}_{\mathfrak{S}0} \hat{v}_{y\mathfrak{S}1}}{\partial y} + \frac{\partial \hat{\rho}_{\mathfrak{S}0} \hat{v}_{z\mathfrak{S}1}}{\partial z} = 0, \tag{9.34}$$

$$\begin{aligned} &\hat{\rho}_{\mathfrak{S}0} \left(\hat{v}_{x\mathfrak{S}0} \frac{\partial \hat{v}_{x\mathfrak{S}0}}{\partial \chi} + \hat{v}_{y\mathfrak{S}1} \frac{\partial \hat{v}_{x\mathfrak{S}0}}{\partial y} + \hat{v}_{z\mathfrak{S}1} \frac{\partial \hat{v}_{x\mathfrak{S}0}}{\partial z} \right) \\ &= -\frac{1}{2} \frac{\partial \hat{p}_{\mathfrak{S}0}}{\partial \chi} + \frac{1}{2} \frac{\partial}{\partial y} \left(\Gamma_1 \frac{\partial \hat{v}_{x\mathfrak{S}0}}{\partial y} \right) + \frac{1}{2} \frac{\partial}{\partial z} \left(\Gamma_1 \frac{\partial \hat{v}_{x\mathfrak{S}0}}{\partial z} \right), \end{aligned} \tag{9.35}$$

$$
\begin{aligned}
&\hat{\rho}_{\mathfrak{S}0}\left(\hat{v}_{x\mathfrak{S}0}\frac{\partial\hat{v}_{y\mathfrak{S}1}}{\partial\chi}+\hat{v}_{y\mathfrak{S}1}\frac{\partial\hat{v}_{y\mathfrak{S}1}}{\partial y}+\hat{v}_{z\mathfrak{S}1}\frac{\partial\hat{v}_{y\mathfrak{S}1}}{\partial z}-\frac{1}{c^2}\hat{v}_{x\mathfrak{S}0}^2\right)\\
&=-\frac{1}{2}\frac{\partial\hat{p}^c_{\mathfrak{S}2}}{\partial y}+\frac{1}{2}\frac{\partial}{\partial\chi}\left(\Gamma_1\frac{\partial\hat{v}_{x\mathfrak{S}0}}{\partial y}\right)\\
&\quad+\frac{\partial}{\partial y}\left(\Gamma_1\frac{\partial\hat{v}_{y\mathfrak{S}1}}{\partial y}\right)+\frac{1}{2}\frac{\partial}{\partial z}\left[\Gamma_1\left(\frac{\partial\hat{v}_{y\mathfrak{S}1}}{\partial z}+\frac{\partial\hat{v}_{z\mathfrak{S}1}}{\partial y}\right)\right]\\
&\quad+\frac{1}{2\hat{p}_{\mathfrak{S}0}}\left\{\frac{\partial}{\partial y}\left[\Gamma_7\left(\frac{\partial\hat{T}_{\mathfrak{S}0}}{\partial y}\right)^2\right]+\frac{\partial}{\partial z}\left(\Gamma_7\frac{\partial\hat{T}_{\mathfrak{S}0}}{\partial y}\frac{\partial\hat{T}_{\mathfrak{S}0}}{\partial z}\right)\right\}\\
&\quad+\frac{1}{\hat{p}_{\mathfrak{S}0}}\left\{\frac{\partial}{\partial y}\left[\Gamma_8\left(\frac{\partial\hat{v}_{x\mathfrak{S}0}}{\partial y}\right)^2\right]+\frac{\partial}{\partial z}\left(\Gamma_8\frac{\partial\hat{v}_{x\mathfrak{S}0}}{\partial y}\frac{\partial\hat{v}_{x\mathfrak{S}0}}{\partial z}\right)\right\},
\end{aligned}
\tag{9.36}
$$

$$
\begin{aligned}
&\hat{\rho}_{\mathfrak{S}0}\left(\hat{v}_{x\mathfrak{S}0}\frac{\partial\hat{v}_{z\mathfrak{S}1}}{\partial\chi}+\hat{v}_{y\mathfrak{S}1}\frac{\partial\hat{v}_{z\mathfrak{S}1}}{\partial y}+\hat{v}_{z\mathfrak{S}1}\frac{\partial\hat{v}_{z\mathfrak{S}1}}{\partial z}\right)\\
&=-\frac{1}{2}\frac{\partial\hat{p}^c_{\mathfrak{S}2}}{\partial z}+\frac{1}{2}\frac{\partial}{\partial\chi}\left(\Gamma_1\frac{\partial\hat{v}_{x\mathfrak{S}0}}{\partial z}\right)\\
&\quad+\frac{1}{2}\frac{\partial}{\partial y}\left[\Gamma_1\left(\frac{\partial\hat{v}_{y\mathfrak{S}1}}{\partial z}+\frac{\partial\hat{v}_{z\mathfrak{S}1}}{\partial y}\right)\right]+\frac{\partial}{\partial z}\left(\Gamma_1\frac{\partial\hat{v}_{z\mathfrak{S}1}}{\partial z}\right)\\
&\quad+\frac{1}{2\hat{p}_{\mathfrak{S}0}}\left\{\frac{\partial}{\partial y}\left(\Gamma_7\frac{\partial\hat{T}_{\mathfrak{S}0}}{\partial y}\frac{\partial\hat{T}_{\mathfrak{S}0}}{\partial z}\right)+\frac{\partial}{\partial z}\left[\Gamma_7\left(\frac{\partial\hat{T}_{\mathfrak{S}0}}{\partial z}\right)^2\right]\right\}\\
&\quad+\frac{1}{\hat{p}_{\mathfrak{S}0}}\left\{\frac{\partial}{\partial y}\left(\Gamma_8\frac{\partial\hat{v}_{x\mathfrak{S}0}}{\partial y}\frac{\partial\hat{v}_{x\mathfrak{S}0}}{\partial z}\right)+\frac{\partial}{\partial z}\left[\Gamma_8\left(\frac{\partial\hat{v}_{x\mathfrak{S}0}}{\partial z}\right)^2\right]\right\},
\end{aligned}
\tag{9.37}
$$

$$
\begin{aligned}
&\frac{5}{2}\hat{\rho}_{\mathfrak{S}0}\left(\hat{v}_{x\mathfrak{S}0}\frac{\partial\hat{T}_{\mathfrak{S}0}}{\partial\chi}+\hat{v}_{y\mathfrak{S}1}\frac{\partial\hat{T}_{\mathfrak{S}0}}{\partial y}+\hat{v}_{z\mathfrak{S}1}\frac{\partial\hat{T}_{\mathfrak{S}0}}{\partial z}\right)-\hat{v}_{x\mathfrak{S}0}\frac{\partial\hat{p}_{\mathfrak{S}0}}{\partial\chi}\\
&\quad=\frac{5}{4}\frac{\partial}{\partial y}\left(\Gamma_2\frac{\partial\hat{T}_{\mathfrak{S}0}}{\partial y}\right)+\frac{5}{4}\frac{\partial}{\partial z}\left(\Gamma_2\frac{\partial\hat{T}_{\mathfrak{S}0}}{\partial z}\right)+\Gamma_1\left[\left(\frac{\partial\hat{v}_{x\mathfrak{S}0}}{\partial y}\right)^2+\left(\frac{\partial\hat{v}_{x\mathfrak{S}0}}{\partial z}\right)^2\right],
\end{aligned}
\tag{9.38}
$$

and[7] the subsidiary relations on $\hat{\rho}_{\mathfrak{S}0}$ and $\hat{p}^c_{\mathfrak{S}2}$

$$
\hat{\rho}_{\mathfrak{S}0}=\hat{p}_{\mathfrak{S}0}(\chi)/\hat{T}_{\mathfrak{S}0}\quad\text{[see Eq. (9.15f)]},
\tag{9.39a}
$$

[7] The left-hand side of Eq. (9.38) is transformed as

$$
\hat{p}_{\mathfrak{S}0}\left(\hat{v}_{x\mathfrak{S}0}\frac{\partial}{\partial\chi}+\hat{v}_{y\mathfrak{S}1}\frac{\partial}{\partial y}+\hat{v}_{z\mathfrak{S}1}\frac{\partial}{\partial z}\right)\ln\left(\frac{\hat{T}^{5/2}_{\mathfrak{S}0}}{\hat{p}_{\mathfrak{S}0}}\right),
$$

which, except for the first factor $\hat{p}_{\mathfrak{S}0}$, corresponds to the variation of the entropy of a fluid particle along a streamline [see Eq. (1.35)].

$$\hat{p}^{c}_{\mathfrak{S}2} = \hat{p}_{\mathfrak{S}2} + \frac{2\Gamma_1}{3}\left(\frac{\partial \hat{v}_{x\mathfrak{S}0}}{\partial \chi} + \frac{\partial \hat{v}_{y\mathfrak{S}1}}{\partial y} + \frac{\partial \hat{v}_{z\mathfrak{S}1}}{\partial z}\right) + \frac{\Gamma_7}{3\hat{p}_{\mathfrak{S}0}}\left[\left(\frac{\partial \hat{T}_{\mathfrak{S}0}}{\partial y}\right)^2 + \left(\frac{\partial \hat{T}_{\mathfrak{S}0}}{\partial z}\right)^2\right] + \frac{2}{3\hat{p}_{\mathfrak{S}0}}\left[\frac{\partial}{\partial y}\left(\Gamma_3 \frac{\partial \hat{T}_{\mathfrak{S}0}}{\partial y}\right) + \frac{\partial}{\partial z}\left(\Gamma_3 \frac{\partial \hat{T}_{\mathfrak{S}0}}{\partial z}\right)\right] - \frac{2\Gamma_9}{3\hat{p}_{\mathfrak{S}0}}\left[\left(\frac{\partial \hat{v}_{x\mathfrak{S}0}}{\partial y}\right)^2 + \left(\frac{\partial \hat{v}_{x\mathfrak{S}0}}{\partial z}\right)^2\right], \tag{9.39b}$$

where Γ_1, Γ_2, Γ_3, Γ_7, Γ_8, and Γ_9 are short forms of the functions $\Gamma_1(\hat{T}_{\mathfrak{S}0})$, $\Gamma_2(\hat{T}_{\mathfrak{S}0}), \ldots, \Gamma_9(\hat{T}_{\mathfrak{S}0})$ of $\hat{T}_{\mathfrak{S}0}$ defined in Section A.2.9. Their functional forms are determined by the molecular model.

The boundary conditions are

$$\hat{v}_{x\mathfrak{S}0} = \hat{v}_A, \quad \hat{v}_{y\mathfrak{S}1} = \hat{v}_{z\mathfrak{S}1} = 0, \quad \hat{T}_{\mathfrak{S}0} = 1 \quad \text{at } y = 0, \tag{9.40a}$$

$$\hat{v}_{x\mathfrak{S}0} = \hat{v}_B, \quad \hat{v}_{y\mathfrak{S}1} = \hat{v}_{z\mathfrak{S}1} = 0, \quad \hat{T}_{\mathfrak{S}0} = \hat{T}_B \quad \text{at } y = 1. \tag{9.40b}$$

The coordinate system (x, y, z) given by Eq. (9.4a) is expressed in this symbol under the understanding that it reduces to a Cartesian system in the limit under consideration. For this, the range of x is naturally limited. Here, we are interested in the region where $|x|$ is finite or infinitely large but infinitely small compared with $1/k$ [or $o(1/k)$]. Then, $\hat{v}_{x\mathfrak{S}0}$ is obviously the x component (in the Cartesian system) of the (nondimensional) flow velocity at the leading order in k; in view of the relation (9.4c), $\hat{v}_{y\mathfrak{S}1}$ and $\hat{v}_{z\mathfrak{S}1}$ are seen to be, respectively the y and z component (in the Cartesian system) of the flow velocity at the first order of k.[8] The deviation of (x, y, z) from the corresponding exact Cartesian system enters in the higher-order equations, because the system derived above is the nontrivial leading-order equations. Thus, the system of fluid-dynamic-type equations (9.33)–(9.39b) and the boundary conditions (9.40a) and (9.40a) can be taken to be expressed in the Cartesian coordinate system.

The effect of molecular property enters the above system only through the transport coefficients $\Gamma_1, \Gamma_2, \Gamma_3, \Gamma_7, \Gamma_8$, and Γ_9. Thus, the fundamental structure of the equations and boundary conditions is generally common to molecular models.

The fluid-dynamic-type equations (9.33)–(9.39b) governing the behavior of the gas in the limiting state have the following important features:
(i) The velocity $\hat{v}_{x\mathfrak{S}0}$, the temperature $\hat{T}_{\mathfrak{S}0}$, and the density $\hat{\rho}_{\mathfrak{S}0}$ in the continuum limit are determined simultaneously with $\hat{v}_{y\mathfrak{S}1}$ and $\hat{v}_{z\mathfrak{S}1}$, the infinitesimal $\hat{v}_y$ and $\hat{v}_z$ amplified by $1/k$ (ghost effect).
(ii) Equations (9.36) and (9.37), the momentum equations in the y and z directions, have two kinds of non-Navier–Stokes stress terms, the thermal stress and the stress quadratic of the shear of flow.

[8] The original $\hat{v}_x$ being the circumferential component, it contributes to the y component (in the Cartesian coordinate in the limit), but it is of the order higher than k in the range of x of our interest owing to the relation (9.4c).

(iii) In the limiting state that we have taken, the (x, y, z) is a rectangular coordinate system. Equation (9.36), which expresses the conservation of the momentum in the y direction, has the term $\hat{\rho}_{\mathfrak{S}0}\hat{v}^2_{x\mathfrak{S}0}/c^2$ that is not found in the convection term of the conservation equations in a rectangular coordinate system. This works as an apparent external force. This quantity contributes to the convection of the momentum in the y direction into a volume element in a gas when the x axis has a curvature. That is, the curvature effect remains in the limit that the curvature vanishes. The infinitesimal curvature produces a finite effect on the parallel flow $\hat{v}_{x\mathfrak{S}0}$. This is a new kind of ghost effect and may be called the *ghost effect of infinitesimal curvature*.

9.2.4 Supplementary notes

The importance of the infinitesimal curvature is easily understood by examining the radial momentum convection into a small volume element $\hat{r}\mathrm{d}\hat{r}\mathrm{d}\theta\mathrm{d}\hat{z}$, which is given by

$$-\left(\frac{1}{\hat{r}}\frac{\partial\hat{\rho}\hat{r}\hat{v}_r^2}{\partial\hat{r}}+\frac{1}{\hat{r}}\frac{\partial\hat{\rho}\hat{v}_r\hat{v}_\theta}{\partial\theta}+\frac{\partial\hat{\rho}\hat{v}_r\hat{v}_z}{\partial\hat{z}}-\frac{\hat{\rho}\hat{v}_\theta^2}{\hat{r}}\right)\hat{r}\mathrm{d}\hat{r}\mathrm{d}\theta\mathrm{d}\hat{z},$$

where $(\hat{v}_r, \hat{v}_\theta, \hat{v}_z)$ is the cylindrical coordinate expression of $\hat{\boldsymbol{v}}$. In the present study, $\hat{v}_r = O(k)$, $\hat{v}_\theta = O(1)$, $\hat{v}_z = O(k)$, $\hat{r} = O(k^{-2})$, $\partial(*)/\partial\hat{r} = O(*)$, $\partial(*)/\partial\hat{z} = O(*)$, and $\partial(*)/\hat{r}\partial\theta = O(k*)$. It should be noted here that $\hat{r}$ is normalized by the distance D between the walls for which the condition $\partial(*)/\partial\hat{r} = O(*)$ is a natural one. The condition $\partial(*)/\hat{r}\partial\theta = O(k*)$ is a weak variation parallel to the walls and is consistent with the first three conditions listed above. Under this situation, all the terms in the parentheses of the above expression are of the same order, i.e., $O(k^2)$. We cannot neglect the term $\hat{\rho}\hat{v}_\theta^2/\hat{r}$ due to centripetal acceleration in the momentum equation in the limit of vanishing curvature.

Up to this point, we considered the case where the relative curvature D/L_A of the cylinder tends to zero with the same speed as k^2. If it tends to zero faster than k^2, it is easily seen that the $\hat{v}^2_{x\mathfrak{S}0}/c^2$ term becomes of higher order and disappears from Eq. (9.36).[9] The ghost effect of infinitesimal curvature is absent. For the other case, let D/L_A vanish as $D/L_A = (k^\varpi/c)^2$, where $0 < \varpi < 1$. The analysis in Section 9.2.1 can be carried out consistently under the assumption

$$\left.\begin{aligned}&\int\zeta_x\hat{f}\mathbf{d}\boldsymbol{\zeta}=O(1),\quad \int(\zeta_y,\zeta_z)\hat{f}\mathbf{d}\boldsymbol{\zeta}=O(k^\varpi),\\&\partial\hat{f}/\partial\chi=O(\hat{f}),\quad \partial\hat{f}/\partial y=O(\hat{f}),\quad \partial\hat{f}/\partial z=O(\hat{f}),\quad \chi=k^\varpi x.\end{aligned}\right\}\tag{9.41}$$

That is, the leading term of the flow velocity is taken as $\hat{v}_x = O(1)$, $\hat{v}_y = O(k^\varpi)$, and $\hat{v}_z = O(k^\varpi)$. We express $\hat{v}_x$, $\hat{v}_y$, $\hat{v}_z$, $\hat{T}$, and $\hat{p}$ as $\hat{v}_x = \hat{v}_{x\mathfrak{S}0} + \cdots$, $\hat{v}_y =$

[9] If the sizes of $\hat{v}_y$ and $\hat{v}_z$ are downgraded in such a way that the curvature term $\hat{v}^2_{x\mathfrak{S}0}/c^2$ is comparable to the other terms, the effect of $\hat{v}_y$ and $\hat{v}_z$ on $\hat{v}_x$ degenerates, and $\hat{v}_{x\mathfrak{S}0}$, $\hat{T}_{\mathfrak{S}0}$, and $\hat{\rho}_{\mathfrak{S}0}$ are determined by themselves, independently of $\hat{v}_y$, $\hat{v}_z$, and the curvature term.

$k^{\varpi}(\hat{v}_{y\mathfrak{S}1}+\cdots)$, and $\hat{v}_z = k^{\varpi}(\hat{v}_{z\mathfrak{S}1}+\cdots)$, $\hat{T} = \hat{T}_{\mathfrak{S}0}+\cdots$, $\hat{p} = \hat{p}_{\mathfrak{S}0}+k^{2\varpi}\hat{p}_{\mathfrak{S}2}+\hat{p}^*_{\mathfrak{S}1}$, where $\hat{v}_{x\mathfrak{S}0}$, $\hat{v}_{y\mathfrak{S}1}$, $\hat{v}_{z\mathfrak{S}1}$, $\hat{T}_{\mathfrak{S}0}$, $\hat{p}_{\mathfrak{S}0}$, and $\hat{p}_{\mathfrak{S}2}$ are quantities of the order of unity and $\hat{p}^*_{\mathfrak{S}1}$ is the remainder but contains the terms of the order between 1 and $k^{2\varpi}$; for the other quantities, the remainders are of the higher order of the form $k^{m\varpi+n}$. Then, the equations that govern $\hat{v}_{x\mathfrak{S}0}$, $\hat{v}_{y\mathfrak{S}1}$, $\hat{v}_{z\mathfrak{S}1}$, $\hat{T}_{\mathfrak{S}0}$, $\hat{p}_{\mathfrak{S}0}$, and $\hat{p}_{\mathfrak{S}2}$ are Eqs. (9.33)–(9.39b) where all the terms with Γ_s are eliminated, to which the remainders, including $\hat{p}^*_{\mathfrak{S}1}$, do not contribute. They are the first-order partial differential equations in contrast to Eqs. (9.33)–(9.39b). The solution of the new equations cannot directly be connected to the Knudsen-layer solution because the condition derived by the Knudsen-layer analysis is too strong to the first-order equations. Another layer, viscous boundary layer, intervenes between the two solutions (see Section 3.4). This case will not be discussed further.

The extension of the present analysis to a time-dependent problem is straightforward. The analysis can be carried out in a similar way, only retaining the time-derivative term in the Boltzmann equation. The result of extension is shown below when the time scale t_0 of variation of the distribution function f is

$$t_0 \sim \frac{D^2}{\ell_0(2RT_A)^{1/2}} \sim \frac{D^2}{\mu_0/\rho_0},$$

in the last expression of which the mean free path ℓ_0 is replaced by the viscosity μ_0 [$\mu_0 = \sqrt{\pi}\gamma_1 p_0\ell_0/(8RT_A)^{1/2}$] [see Eq. (3.70)]. This is the time scale of viscous diffusion.[10] The extension of the fluid-dynamic-type equations (9.34)–(9.38) to the time-dependent case is simply to add

$$\frac{\partial\hat{\rho}_{\mathfrak{S}0}}{\partial\hat{t}},\ \hat{\rho}_{\mathfrak{S}0}\frac{\partial\hat{v}_{x\mathfrak{S}0}}{\partial\hat{t}},\ \hat{\rho}_{\mathfrak{S}0}\frac{\partial\hat{v}_{y\mathfrak{S}1}}{\partial\hat{t}},\ \hat{\rho}_{\mathfrak{S}0}\frac{\partial\hat{v}_{z\mathfrak{S}1}}{\partial\hat{t}},\ \frac{5\hat{\rho}_{\mathfrak{S}0}}{2}\frac{\partial\hat{T}_{\mathfrak{S}0}}{\partial\hat{t}} - \frac{\partial\hat{p}_{\mathfrak{S}0}}{\partial\hat{t}}, \tag{9.42}$$

to the left-hand sides of Eqs. (9.34), (9.35), (9.36), (9.37), and (9.38) respectively.[11] Here, $\hat{t}$ is the nondimensional time defined by

$$\hat{t} = \frac{t}{D/(2RT_A)^{1/2}k}, \tag{9.43}$$

where t is the time. No correction is required to Eqs. (9.33), (9.39a), and (9.39b). The time-derivative term in the Boltzmann equation, the extended version of Eq. (9.2a), is given by $k\partial\hat{f}/\partial\hat{t}$ for the above-mentioned time scale of variation of $\hat{f}$. Comparing the order of this term in k with the others in the equation, we easily see that no correction is required to the boundary conditions (9.40a) and (9.40b) (see the discussion in Section 3.7.3).

[10] See Footnote 104 in Section 3.7.

[11] The expression $(5\hat{\rho}_{\mathfrak{S}0}/2)(\partial\hat{T}_{\mathfrak{S}0}/\partial\hat{t}) - \partial\hat{p}_{\mathfrak{S}0}/\partial\hat{t}$ is transformed as

$$\hat{p}_{\mathfrak{S}0}\frac{\partial}{\partial\hat{t}}\ln\left(\frac{\hat{T}^{5/2}_{\mathfrak{S}0}}{\hat{p}_{\mathfrak{S}0}}\right).$$

This expression, except for the first factor $\hat{p}_{\mathfrak{S}0}$, combined with the expression in Footnote 7 in Section 9.2.3 corresponds to the variation of the entropy of a fluid particle along a fluid-particle path.

9.3 System for small Mach numbers and small temperature variations

The fluid-dynamic-type equations (9.33)–(9.39b) contain various terms. Here, we consider the case where the Mach number of the flow is small [say, $\hat{v}_x = O(\varepsilon)$; ε is small but finite] and see how the fluid-dynamic-type equations are simplified and whether the effect of infinitesimal curvature remains there. That is, consider the case where the main flow field $\hat{v}_x$ is of the order of ε and the cross velocity field $(\hat{v}_y, \hat{v}_z)$ is of the order of k, the latter of which is the same order as in the preceding section (Section 9.2). That is,

$$\int \zeta_x \hat{f} \mathbf{d\zeta} = O(\varepsilon), \tag{9.44a}$$

$$\int \zeta_y \hat{f} \mathbf{d\zeta} = O(k), \ \int \zeta_z \hat{f} \mathbf{d\zeta} = O(k). \tag{9.44b}$$

We can consistently assume that the variations of $\hat{T}$ and $\hat{\rho}$ are of the order of ε.[12] This is the case where the variation of the distribution function from a uniform Maxwellian at rest is of the order of ε. Corresponding to the assumptions (9.44a) and (9.44b), the length scale of variation of $\hat{f}$ in the main flow direction can be a little smaller than the preceding case, that is, $\partial \hat{f}/\partial x = O(k\hat{f}/\varepsilon)$ owing to the mass conservation. Thus, we put

$$\tilde{\chi} = \chi/\varepsilon. \tag{9.45}$$

Then,

$$\frac{\partial \hat{f}}{\partial \tilde{\chi}} = O(\hat{f}), \quad \frac{\partial \hat{f}}{\partial y} = O(\hat{f}), \quad \frac{\partial \hat{f}}{\partial z} = O(\hat{f}). \tag{9.46}$$

The curvature effect is degraded according to the degrade of $\hat{v}_x$. In view of the discussion of the estimate of the convection terms in the first paragraph of Section 9.2.4, we consider the limiting case where the radius of the inner cylinder L_A tends to ∞ a little slower to compensate the degrade of $\hat{v}_x$. That is, the constant c in Eq. (9.4c), i.e., $D/L_A = (k/c)^2$, where it is assumed to be of the order of unity, is degraded as

$$c = C\varepsilon, \quad C = O(1). \tag{9.47}$$

With the above preparation, we try to simplify the fluid-dynamic-type equations (9.33)–(9.39b) and the boundary conditions (9.40a) and (9.40b) under the assumption that $\hat{v}_{x\mathfrak{S}0}$ and the variation of $\hat{\rho}_{\mathfrak{S}0}$ and $\hat{T}_{\mathfrak{S}0}$ are small but finite (say,

[12] When the flow speed is not small, the temperature variation is not small owing to viscous heating [Γ_1 term in Eq. (9.38)] even when there is no temperature difference between the two walls.

of the order of ε) with the rescalings (9.45) and (9.47). That is, we put

$$\left.\begin{aligned} &\hat{v}_{x\mathfrak{S}0} = \varepsilon(u_x + \cdots), \quad \hat{v}_{y\mathfrak{S}1} = u_y + \cdots, \quad \hat{v}_{z\mathfrak{S}1} = u_z + \cdots, \\ &\hat{p}_{\mathfrak{S}0} = 1 + \varepsilon P_{01} + \varepsilon^2 P_{02} + \cdots, \quad \hat{p}_{\mathfrak{S}2} = P_{20} + \cdots, \\ &\hat{T}_{\mathfrak{S}0} = 1 + \varepsilon(\tau + \cdots), \quad \hat{\rho}_{\mathfrak{S}0} = 1 + \varepsilon(\omega + \cdots), \end{aligned}\right\} \tag{9.48}$$

where u_x, u_y, u_z, τ, ω, P_{01}, P_{02}, and P_{20} are quantities of the order of unity, and substitute Eqs. (9.45), (9.47), and (9.48) into Eqs. (9.33)–(9.39b), and arrange the same-order terms in ε. Then, we obtain the equations that determine the leading-order quantities as follows:

$$\frac{\partial P_{01}}{\partial \tilde{\chi}} = \frac{\partial P_{01}}{\partial y} = \frac{\partial P_{01}}{\partial z} = 0, \quad P_{01} = \omega + \tau, \tag{9.49a}$$

$$\frac{\partial P_{02}}{\partial y} = \frac{\partial P_{02}}{\partial z} = 0, \tag{9.49b}$$

$$\frac{\partial u_x}{\partial \tilde{\chi}} + \frac{\partial u_y}{\partial y} + \frac{\partial u_z}{\partial z} = 0, \tag{9.50a}$$

$$u_x \frac{\partial u_x}{\partial \tilde{\chi}} + u_y \frac{\partial u_x}{\partial y} + u_z \frac{\partial u_x}{\partial z} = -\frac{1}{2}\frac{\partial P_{02}}{\partial \tilde{\chi}} + \frac{\gamma_1}{2}\left(\frac{\partial^2 u_x}{\partial y^2} + \frac{\partial^2 u_x}{\partial z^2}\right), \tag{9.50b}$$

$$u_x \frac{\partial u_y}{\partial \tilde{\chi}} + u_y \frac{\partial u_y}{\partial y} + u_z \frac{\partial u_y}{\partial z} - \frac{u_x^2}{C^2} = -\frac{1}{2}\frac{\partial P_{20}}{\partial y} + \frac{\gamma_1}{2}\left(\frac{\partial^2 u_y}{\partial y^2} + \frac{\partial^2 u_y}{\partial z^2}\right), \tag{9.50c}$$

$$u_x \frac{\partial u_z}{\partial \tilde{\chi}} + u_y \frac{\partial u_z}{\partial y} + u_z \frac{\partial u_z}{\partial z} = -\frac{1}{2}\frac{\partial P_{20}}{\partial z} + \frac{\gamma_1}{2}\left(\frac{\partial^2 u_z}{\partial y^2} + \frac{\partial^2 u_z}{\partial z^2}\right), \tag{9.50d}$$

$$u_x \frac{\partial \tau}{\partial \tilde{\chi}} + u_y \frac{\partial \tau}{\partial y} + u_z \frac{\partial \tau}{\partial z} = \frac{\gamma_2}{2}\left(\frac{\partial^2 \tau}{\partial y^2} + \frac{\partial^2 \tau}{\partial z^2}\right), \tag{9.50e}$$

where $\gamma_1 = \Gamma_1(1)$ and $\gamma_2 = \Gamma_2(1)$. In this system, u_x^2/C^2 enters Eq. (9.50c), but the thermal stress and the stress quadratic of the shear of flow do not enter Eqs. (9.50c) and (9.50d). The boundary conditions corresponding to Eqs. (9.40a) and (9.40b) are

$$u_x = u_A, \ u_y = u_z = 0, \ \tau = 0 \quad \text{at } y = 0, \tag{9.51a}$$

$$u_x = u_B, \ u_y = u_z = 0, \ \tau = \tau_B \quad \text{at } y = 1, \tag{9.51b}$$

where

$$u_A = V_A/\varepsilon(2RT_A)^{1/2}, \ u_B = V_B/\varepsilon(2RT_A)^{1/2}, \ \ \tau_B = (T_B - T_A)/\varepsilon T_A. \tag{9.52}$$

Here, it may be noted that we are considering the case where the quantities $V_A/\varepsilon(2RT_A)^{1/2}$, $V_B/\varepsilon(2RT_A)^{1/2}$, and $(T_B - T_A)/\varepsilon T_A$ are of the order of unity.

In the system of Eqs. (9.49b)–(9.50e) with the boundary conditions (9.51a) and (9.51b), the velocity field is determined from Eqs. (9.49b)–(9.50d) and the

conditions for u_x, u_y, and u_z in Eqs. (9.51a) and (9.51b), independently of the temperature field.

Incidentally, it may be noted that the same system as above, i.e., Eqs. (9.49a)–(9.51b) with the rescalings (9.45) and (9.47) and the expansion (9.48), is obtained by the asymptotic analysis when the parameter ε is related to k but k is smaller than any power of ε ($k \ll \varepsilon^n$ for any n), e.g., $\varepsilon = O(1/|\ln k|)$.

The system of equations and boundary conditions (9.49b)–(9.51b) are also derived for different scales of the variables. Put

$$\left.\begin{aligned} &\hat{v}_r = \varepsilon^s(u_y + \cdots),\ \hat{v}_\theta = -\varepsilon(u_x + \cdots),\ \hat{v}_z = \varepsilon^s(u_z + \cdots), \\ &\hat{p} = 1 + \varepsilon P_{01} + \cdots + \varepsilon^2 P_{02} + \cdots + \varepsilon^{2s} P_{20} + \cdots, \\ &\hat{T} = 1 + \varepsilon(\tau + \cdots),\quad \hat{\rho} = 1 + \varepsilon(\omega + \cdots),\quad P_{01} = \omega + \tau, \\ &k = \varepsilon^s,\quad D/L_A = (\varepsilon^{s-1}/C)^2 \quad (s > 1), \end{aligned}\right\} \tag{9.53}$$

where u_x, u_y, u_z, P_{01}, P_{02}, P_{20}, τ, ω, and C are quantities of the order of unity and s may not necessarily be an integer.[13] The variables x, y, and z are the same as before, i.e.,

$$x = -L_A\theta/D,\quad y = \hat{r} - L_A/D,$$

and the length scale of variation in the x direction is taken to be of the order of the ratio of $\hat{v}_x$ to $\hat{v}_y$ or $\hat{v}_z$, i.e., $1/\varepsilon^{s-1}$. Correspondingly,

$$\tilde{\chi} = \varepsilon^{s-1}x. \tag{9.54}$$

Then, P_{01} is uniform as before; Eqs. (9.49b)–(9.50e) and Eqs. (9.51a) and (9.51b) are, respectively, the governing equations and boundary conditions for the new u_x, u_y, u_z, τ, P_{01}, and P_{20}.[14] The process deriving this system from the Boltzmann equation is very similar to that deriving the system for the type II solution in Sone & Doi [2000] (see Chapter 8 in Sone [2002]).

Similarly to the comment in the second paragraph in Section 9.2.4, when D/L_A tends to zero faster than that given in Eq. (9.53), i.e., $D/L_A = (\varepsilon^{\kappa-1}/C)^2$ ($\kappa > s > 1$), the curvature term u_x^2/C^2 is reduced to a higher order and disappears from the system. When D/L_A tends to zero slower than that given in Eq. (9.53), i.e., $D/L_A = (\varepsilon^{\kappa-1}/C)^2$ ($1 < \kappa < s$), then for the scale of the variables given by Eqs. (9.53) and (9.54) with s replaced by κ except the relation $k = \varepsilon^s$, Eqs. (9.49b)–(9.50e) with the terms containing γ_1 and γ_2 eliminated (or the equations without the viscous and thermal conduction terms) are derived. In the complete description of this case, not treated here, a thin layer (or viscous boundary layer) intervenes between the above solution and the Knudsen layer as in the case in Section 3.4 (note the comment in Section 3.6.1). The process

[13] When s is not an integer, terms of the order of $\varepsilon^{m+n(s-1)}$ ($m = 1, 2, \ldots$, $n = 0, 1, 2, \ldots$) appear, and the analysis is more complicated than that for an integer s but can be carried out consistently.

[14] The terms, not explicitly shown between εP_{01} and $\varepsilon^2 P_{02}$ and between $\varepsilon^2 P_{02}$ and $\varepsilon^{2s} P_{20}$ in $\hat{p}$, if any, do not contribute to Eqs. (9.49a)–(9.50e) as the other terms not shown explicitly in Eq. (9.53).

deriving the system is very similar to that for the type I solution in Sone & Doi [2000] (see Chapter 8 in Sone [2002]).

Finally it may be noted that the parameters γ_1 and C in Eqs. (9.49b)–(9.50d) can be eliminated. That is, putting

$$\left.\begin{aligned} &\hat{u}_x = 2u_x/\gamma_1 C, \quad \hat{u}_y = 2u_y/\gamma_1, \ \hat{u}_z = 2u_z/\gamma_1, \\ &\hat{P}_{02} = 2P_{02}/(\gamma_1 C)^2, \quad \hat{P}_{20} = 2P_{20}/\gamma_1^2, \ \bar{\chi} = \tilde{\chi}/C, \end{aligned}\right\} \tag{9.55}$$

we have

$$\frac{\partial \hat{P}_{02}}{\partial y} = \frac{\partial \hat{P}_{02}}{\partial z} = 0, \tag{9.56}$$

$$\frac{\partial \hat{u}_x}{\partial \bar{\chi}} + \frac{\partial \hat{u}_y}{\partial y} + \frac{\partial \hat{u}_z}{\partial z} = 0, \tag{9.57a}$$

$$\hat{u}_x \frac{\partial \hat{u}_x}{\partial \bar{\chi}} + \hat{u}_y \frac{\partial \hat{u}_x}{\partial y} + \hat{u}_z \frac{\partial \hat{u}_x}{\partial z} = -\frac{\partial \hat{P}_{02}}{\partial \bar{\chi}} + \frac{\partial^2 \hat{u}_x}{\partial y^2} + \frac{\partial^2 \hat{u}_x}{\partial z^2}, \tag{9.57b}$$

$$\hat{u}_x \frac{\partial \hat{u}_y}{\partial \bar{\chi}} + \hat{u}_y \frac{\partial \hat{u}_y}{\partial y} + \hat{u}_z \frac{\partial \hat{u}_y}{\partial z} - \hat{u}_x^2 = -\frac{\partial \hat{P}_{20}}{\partial y} + \frac{\partial^2 \hat{u}_y}{\partial y^2} + \frac{\partial^2 \hat{u}_y}{\partial z^2}, \tag{9.57c}$$

$$\hat{u}_x \frac{\partial \hat{u}_z}{\partial \bar{\chi}} + \hat{u}_y \frac{\partial \hat{u}_z}{\partial y} + \hat{u}_z \frac{\partial \hat{u}_z}{\partial z} = -\frac{\partial \hat{P}_{20}}{\partial z} + \frac{\partial^2 \hat{u}_z}{\partial y^2} + \frac{\partial^2 \hat{u}_z}{\partial z^2}. \tag{9.57d}$$

The corresponding boundary conditions are

$$\hat{u}_x = \hat{u}_A, \ \hat{u}_y = \hat{u}_z = 0 \ \text{ at } y = 0, \tag{9.58a}$$

$$\hat{u}_x = \hat{u}_B, \ \hat{u}_y = \hat{u}_z = 0 \ \text{ at } y = 1, \tag{9.58b}$$

where

$$\hat{u}_A = 2u_A/\gamma_1 C, \quad \hat{u}_B = 2u_B/\gamma_1 C. \tag{9.59}$$

The extension to the time-dependent problems with the characteristic time scale $t_0 = D/(2RT_A)^{1/2}k$, mentioned at the end of Section 9.2.4, is simple. For the system (9.49a)–(9.50e), we have only to add

$$\frac{\partial u_x}{\partial \hat{t}}, \quad \frac{\partial u_y}{\partial \hat{t}}, \quad \frac{\partial u_z}{\partial \hat{t}}, \quad \frac{\partial \tau}{\partial \hat{t}} - \frac{2}{5}\frac{\partial P_{01}}{\partial \hat{t}},$$

where $\hat{t} = t/[D/(2RT_A)^{1/2}k]$, to the left-hand sides of Eqs. (9.50b), (9.50c), (9.50d), and (9.50e) respectively.[15] For the system (9.56)–(9.57d), we have only to add

$$\frac{\partial \hat{u}_x}{\partial \tilde{t}}, \quad \frac{\partial \hat{u}_y}{\partial \tilde{t}}, \quad \frac{\partial \hat{u}_z}{\partial \tilde{t}},$$

where $\tilde{t} = \gamma_1 \hat{t}/2$, to the left-hand sides of Eqs. (9.57b), (9.57c), and (9.57d) respectively.[16] The boundary conditions, i.e., Eqs. (9.51a) and (9.51b) and

[15] Owing to Eq. (9.49a), the two variables τ and P_{01} in the extended form of Eq. (9.50e) are replaced by a single variable τ^*

$$\tau^* = \tau - 2P_{01}/5.$$

[16] The relation between $\tilde{t}$ and $\hat{t}$ in Sone & Doi [2005] is a misprint.

Eqs. (9.58a) and (9.58b), are not required any correction.

In this section (Section 9.3), we have discussed the system where the variation ε of the velocity distribution function from a uniform Maxwellian at rest is small (thus, the Mach number and the temperature variation are small), paying attention to the relative sizes of ε to the Knudsen number (or k), i.e., the limit $k \to 0$ with ε being small but finite, the case with k being smaller than any power of ε, and the case with $k = O(\varepsilon^s)$ $(s > 1)$. The common system (9.49a)–(9.51b), including the time-derivative terms in the extension to the time-dependent problem, is derived for these three cases. In the first case, the curvature of the boundary and the cross field are infinitesimal, but they influence the main flow u_x through u_x^2/C^2 in Eq. (9.50c) and (u_y, u_z). That is, the infinitesimal curvature produces a finite effect on the main flow. This is the ghost effect of infinitesimal curvature in a low Mach number flow. In the other cases, where ε and k are related and tend to zero simultaneously, the curvature and the cross flow, which are, respectively, of the orders of $\varepsilon^{2(s-1)}$ and ε^s in the third case, are not infinitesimal but perceivable if the flow speed or ε is small but finite or perceivable.[17] These are not the case of the ghost effect.

9.4 Bifurcation of the plane Couette flow

9.4.1 Bifurcation analysis

In this section, we study the bifurcation of the plane Couette flow and the effect of the infinitesimal curvature as an application of the asymptotic theory. To find the effect of infinitesimal curvature as simple as possible, we consider the case with small but finite Mach number and (nondimensional) temperature variation, and analyze the problem on the basis of Eqs. (9.56)–(9.58b).[18]

Obviously, Eqs. (9.56)–(9.58b) have the following solution with $\hat{u}_y = \hat{u}_z = 0$ and $\partial/\partial\bar{\chi} = 0$:

$$\left.\begin{aligned} &\hat{u}_x = U_U = \hat{u}_A + (\hat{u}_B - \hat{u}_A)y, \\ &\hat{u}_y = \hat{u}_z = 0, \\ &\hat{P}_{02} = 0, \\ &\hat{P}_{20} = \mathcal{P}_U = \tfrac{1}{3}(\hat{u}_B - \hat{u}_A)^2 y^3 + \hat{u}_A(\hat{u}_B - \hat{u}_A)y^2 + \hat{u}_A^2 y + \text{const.} \end{aligned}\right\} \tag{9.60}$$

This is the plane Couette flow of a small but finite Mach number in the continuum limit, i.e., $u_x = u_A + (u_B - u_A)y$, $u_y = u_z = 0$, $P_{02} = 0$, and the contribution from P_{20} to the pressure is infinitesimal. We will consider a bifurcation from this parallel flow. To make the problem simpler, we consider the case where the variables are independent of $\bar{\chi}$ (or $\partial/\partial\bar{\chi} = 0$). Let the bifurcation

[17] In the second and third cases, the curvature and the cross flow are much smaller than ε (for large s in the third case), but it is a technical problem whether they are perceivable or not. On the other hand, in the first case, it is theoretically impossible to perceive the cross flow and the curvature of the boundary.

[18] Naturally, the analysis is the same for the other two cases discussed in the preceding section.

occur at ($\hat{u}_A = \hat{u}_{Ab}$, $\hat{u}_B = \hat{u}_{Bb}$) [or ($u_A = u_{Ab}$, $u_B = u_{Bb}$)], and let U_{Ub} and $\mathcal{P}_{Ub}$ be, respectively, U_U and $\mathcal{P}_U$ at this point, i.e.,

$$U_{Ub} = \hat{u}_{Ab} + (\hat{u}_{Bb} - \hat{u}_{Ab})y. \tag{9.61}$$

We examine the bifurcated solution in a close neighborhood of the bifurcation point (say, of the order of δ^2). To make the ordering clear, we express the boundary data $\hat{u}_A$ and $\hat{u}_B$ using a quantity δ expressing the deviation from the bifurcation point in the form

$$\hat{u}_A = \hat{u}_{Ab} + \frac{(\hat{u}_A - \hat{u}_{Ab})}{\delta^2}\delta^2, \quad \hat{u}_B = \hat{u}_{Bb} + \frac{(\hat{u}_B - \hat{u}_{Bb})}{\delta^2}\delta^2,$$

where $(\hat{u}_A - \hat{u}_{Ab})/\delta^2$ and $(\hat{u}_B - \hat{u}_{Bb})/\delta^2$ are of the order of unity. Then, the bifurcated solution is expressed in a power series of δ, i.e.,[19]

$$\hat{u}_x = U_{Ub} + \delta U_1 + \delta^2 U_2 + \cdots, \tag{9.62a}$$

$$\hat{u}_y = \delta V_1 + \delta^2 V_2 + \cdots, \tag{9.62b}$$

$$\hat{u}_z = \delta W_1 + \delta^2 W_2 + \cdots, \tag{9.62c}$$

$$\hat{P}_{20} = \mathcal{P}_{Ub} + \delta \mathcal{P}_1 + \delta^2 \mathcal{P}_2 + \cdots. \tag{9.62d}$$

Substituting the series (9.62a)–(9.62d) into Eqs. (9.57a)–(9.57d), we obtain a series of equations governing the perturbations $(U_1, V_1, W_1, \mathcal{P}_1)$, $(U_2, V_2, W_2, \mathcal{P}_2)$, etc. The equations for the first-order perturbations U_1, V_1, W_1, and $\mathcal{P}_1$ are

$$\frac{\partial V_1}{\partial y} + \frac{\partial W_1}{\partial z} = 0, \tag{9.63a}$$

$$\frac{\mathrm{d}\, U_{Ub}}{\mathrm{d}\, y} V_1 = \frac{\partial^2 U_1}{\partial y^2} + \frac{\partial^2 U_1}{\partial z^2}, \tag{9.63b}$$

$$-2U_{Ub}U_1 = -\frac{\partial \mathcal{P}_1}{\partial y} + \frac{\partial^2 V_1}{\partial y^2} + \frac{\partial^2 V_1}{\partial z^2}, \tag{9.63c}$$

$$0 = -\frac{\partial \mathcal{P}_1}{\partial z} + \frac{\partial^2 W_1}{\partial y^2} + \frac{\partial^2 W_1}{\partial z^2}, \tag{9.63d}$$

and the boundary conditions are

$$U_1 = V_1 = W_1 = 0 \ \text{ at } y = 0 \text{ and } y = 1. \tag{9.64}$$

We look for a solution periodic with respect to z, which is possible from the form of Eqs. (9.63a)–(9.63d). The solution can be put in the form

$$\left.\begin{aligned} U_1 &= U_{11}(y)\cos\alpha z, \quad V_1 = V_{11}(y)\cos\alpha z, \\ W_1 &= W_{11}(y)\sin\alpha z, \quad \mathcal{P}_1 = \mathcal{P}_{11}(y)\cos\alpha z. \end{aligned}\right\} \tag{9.65}$$

[19] See Footnote 2 in Section 8.2.3.

Then, we obtain the equations for U_{11} and V_{11} in the form

$$\frac{\mathrm{d}^2 U_{11}}{\mathrm{d}\, y^2} - \alpha^2 U_{11} - \frac{\mathrm{d}\, U_{Ub}}{\mathrm{d}\, y} V_{11} = 0, \tag{9.66a}$$

$$2\alpha^2 U_{Ub} U_{11} - \frac{\mathrm{d}^4 V_{11}}{\mathrm{d}\, y^4} + 2\alpha^2 \frac{\mathrm{d}^2 V_{11}}{\mathrm{d}\, y^2} - \alpha^4 V_{11} = 0. \tag{9.66b}$$

The boundary conditions for U_{11} and V_{11} are

$$U_{11} = V_{11} = \frac{\mathrm{d}\, V_{11}}{\mathrm{d}\, y} = 0 \quad \text{at } y = 0 \text{ and } y = 1. \tag{9.67}$$

The components W_{11} and $\mathcal{P}_{11}$ are expressed with V_{11} as

$$W_{11} = -\frac{1}{\alpha} \frac{\mathrm{d}\, V_{11}}{\mathrm{d}\, y}, \quad \mathcal{P}_{11} = \frac{1}{\alpha^2} \left(\frac{\mathrm{d}^3 V_{11}}{\mathrm{d}\, y^3} - \alpha^2 \frac{\mathrm{d}\, V_{11}}{\mathrm{d}\, y} \right). \tag{9.68}$$

The boundary-value problem (9.66a)–(9.67) is linear and homogeneous and contains the three parameters $\hat{u}_{Ab}$, $\hat{u}_{Bb}$, and α (or $2u_{Ab}/\gamma_1 C, 2u_{Bb}/\gamma_1 C$, and α), the first two of which are through U_{Ub}. Thus, the problem can, generally, have a nontrivial solution only when the parameters satisfy some relation, say,

$$F_{\mathrm{PC}}(2u_{Ab}/\gamma_1 C, 2u_{Bb}/\gamma_1 C, \alpha) = 0. \tag{9.69}$$

The solution (9.62a)–(9.62d) bifurcates from the parallel-flow solution (9.60) at the point $(2u_A/\gamma_1 C, 2u_B/\gamma_1 C, \alpha) = (2u_{Ab}/\gamma_1 C, 2u_{Bb}/\gamma_1 C, \alpha)$ that satisfies Eq. (9.69). The curves $2u_{Ab}/\gamma_1 C$ vs $2u_{Bb}/\gamma_1 C$ for $\alpha = \pi/2$, π, and 2π, which are obtained numerically [see the paragraph next to that containing Eq. (8.23) for the method], are shown in Fig. 9.1. There are infinitely many curves for a given α.[20] Two examples of the profiles $U_{11}/||f_{11}||$ and $V_{11}/||f_{11}||$, where $||f_{11}|| = [\int_0^1 (U_{11}^2 + V_{11}^2)\mathrm{d}y]^{1/2}$, are shown in Fig. 9.2. The flow in the (y, z) plane is of roll type. In the example where the two walls are moving in the opposite directions, the $V_{11}/||f_{11}||$ has a zero point, that is, two rolls are arranged in the y direction. It may be noted that the bifurcation curve is to be given by the straight line $u_{Ab} - u_{Bb} = \text{const}$ owing to the Galilean invariance for a uniform motion if the effect of infinitesimal curvature is absent. We will add some notes on the Galilean invariance and the ghost effect to avoid misunderstanding in the three paragraphs after next.

When the condition (9.69) is satisfied, the solution of Eqs. (9.66a)–(9.67) is determined except for a constant factor. This factor is determined by the standard procedure of the higher-order analysis, which is not given here (see Section 8.4.4). Instead, we will obtain some bifurcated solutions away from the bifurcation curve numerically in the next subsection (Section 9.4.2).

The Boltzmann system is invariant with respect to the Galilean transformation. In the present example of the continuum limit, however, equivalence of the limiting processes is required for the same physical behavior to take place

[20] "Infinitely many" is the plausible result suggested by numerical study.

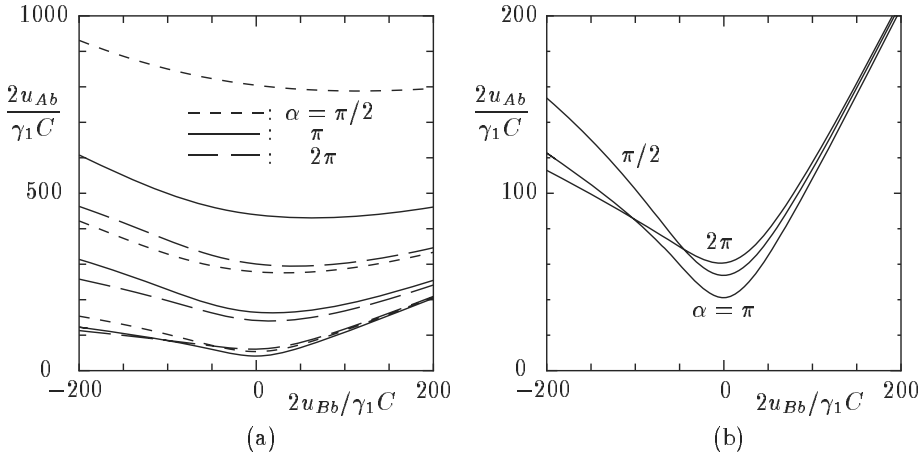

Figure 9.1. Bifurcation curves: $2u_{Ab}/\gamma_1 C$ vs $2u_{Bb}/\gamma_1 C$ for $\alpha = \pi/2$, π, and 2π. (a) Wider range of $2u_{Ab}/\gamma_1 C$ showing three branches and (b) magnified figure of the first branch.

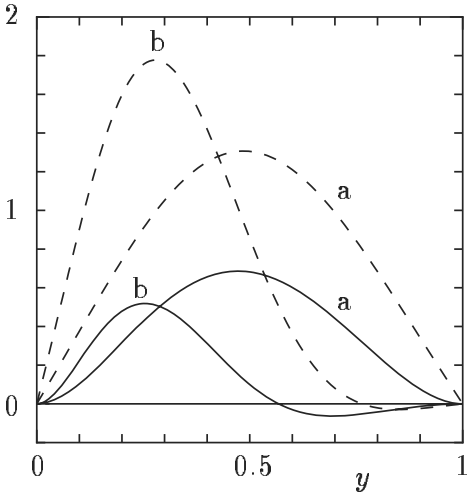

Figure 9.2. The profile $U_{11}/||f_{11}||$ and $V_{11}/||f_{11}||$ vs y, where $||f_{11}|| = [\int_0^1 (U_{11}^2 + V_{11}^2)\mathrm{d}y]^{1/2}$. The dashed lines $---$ are $U_{11}/||f_{11}||$ and the solid lines —— are$V_{11}/||f_{11}||$. The symbol a is for the case $\alpha = \pi$ and $2u_{Bb}/\gamma_1 C = 0$, for which $2u_{Ab}/\gamma_1 C = 41.1705$, and the symbol b is for $\alpha = 2\pi$ and $2u_{Bb}/\gamma_1 C = -150$, for which $2u_{Ab}/\gamma_1 C = 99.4753$.

in the same situation in two inertial systems. Let the two inertial systems be indicated by I and II, and let the limiting situations of the present problem in the systems I and II be, respectively, indicated by $I(\mathrm{u}_A, \mathrm{u}_B)_\mathrm{C}$ and $II(\mathrm{u}_A, \mathrm{u}_B)_\mathrm{C}$ when $u_A = \mathrm{u}_A$, $u_B = \mathrm{u}_B$, and $C = \mathrm{C}$. The $I(\mathrm{u}_A, \mathrm{u}_B)_\mathrm{C}$ and $II(\mathrm{u}_A, \mathrm{u}_B)_\mathrm{C}$ are the corresponding situations in the two systems I and II; that is, $I(\mathrm{u}_A, \mathrm{u}_B)_\mathrm{C}$ and $II(\mathrm{u}_A, \mathrm{u}_B)_\mathrm{C}$ are the same limiting situation viewed, respectively, from the system I and from the system II. The governing systems for $I(\mathrm{u}_A, \mathrm{u}_B)_\mathrm{C}$ and $II(\mathrm{u}_A, \mathrm{u}_B)_\mathrm{C}$ are the same in the expression of each system, because the Boltzmann system is Galilean invariant. Thus, the physical behavior is the same in the systems $I(\mathrm{u}_A, \mathrm{u}_B)_\mathrm{C}$ and $II(\mathrm{u}_A, \mathrm{u}_B)_\mathrm{C}$. On the other hand, if C is modified in one of the two systems, the physical behavior is different, e.g., the bifurcation point is different,[21] in the two systems, though the physical setup in the limit is the same in the two systems, i.e., the plane-Couette-flow problem with the same wall velocities. In the continuum limit ($\mathrm{Kn} = 0$ or $k = 0$), where the Boltzmann equation is singular, the solution is not unique and the correspondence including the limiting process is required for identification.

The bifurcation of the Couette flow is not Galilean invariant as mentioned in the paragraph containing Eq. (9.69). This does not mean that the bifurcation is different in two inertial systems. Let System II be moving with (nondimensional) velocity $(\mathrm{u}_B, 0, 0)$ relative to System I. Let bifurcation take place at $u_A = (\mathrm{u}_A)_b$ in the situation $I(\mathrm{u}_A, 0)_\mathrm{C}$. Then, the bifurcation takes place at $u_A = (\mathrm{u}_A)_b - \mathrm{u}_B$ in System II owing to the Galilean invariance. Apparently, $II(\mathrm{u}_A - \mathrm{u}_B, -\mathrm{u}_B)_\mathrm{C}$ corresponds to $I(\mathrm{u}_A, 0)_\mathrm{C}$, that is, the boundary velocities and the parallel flows (the plane Couette flow) in the two systems are related with the Galilean transformation. However, the bifurcation analysis in this subsection shows that the above relation does not hold. The reason is that the situation $II(\mathrm{u}_A - \mathrm{u}_B, -\mathrm{u}_B)_\mathrm{C}$ does not correspond to $I(\mathrm{u}_A, 0)_\mathrm{C}$ in the limiting process as explained below.

The situation $I(\mathrm{u}_A, 0)_\mathrm{C}$ is the state where the two coaxial cylinders with their common axis fixed in System I are rotating with the speeds corresponding to $u_A = \mathrm{u}_A$ and $u_B = 0$ and the limiting process with $C = \mathrm{C}$ is taken, and the situation $II(\mathrm{u}_A - \mathrm{u}_B, -\mathrm{u}_B)_\mathrm{C}$ is the state where the two coaxial cylinders with their common axis fixed in System II are rotating with the speeds corresponding to $u_A = \mathrm{u}_A - \mathrm{u}_B$ and $u_B = -\mathrm{u}_B$ and the limiting process with $C = \mathrm{C}$ is taken. They are not the two situations that we observe a given limiting situation from I and II. The situation where the common axis of the two cylinders is moving with velocity $(-\mathrm{u}_B, 0, 0)$, the cylinders are rotating with the speeds corresponding to $(\mathrm{u}_A, 0)$ in System II, and the limiting process with $C = \mathrm{C}$ is taken [say, $II(\mathrm{u}_A, 0)_{[\mathrm{C},(-\mathrm{u}_B,0,0)]}$] corresponds to $I(\mathrm{u}_A, 0)_\mathrm{C}$. In the situation $II(\mathrm{u}_A, 0)_{[\mathrm{C},(-\mathrm{u}_B,0,0)]}$, the (infinitesimal) curvature of the fluid-particle path is different from that in $II(\mathrm{u}_A - \mathrm{u}_B, -\mathrm{u}_B)_\mathrm{C}$ and thus the effective C changes, e.g., the curvature decreases when $\mathrm{u}_A > 0$ and $\mathrm{u}_B < 0$. Thus, the infinitesimal curvature in the situation $II(\mathrm{u}_A - \mathrm{u}_B, -\mathrm{u}_B)_\mathrm{C}$ is obviously different from that

[21] For example, from Eq. (9.69), $2u_{Ab}/\gamma_1 C$ is determined by α when $u_B = 0$. Thus, u_{Ab} depends on C.

in $\mathit{\Pi}(\mathrm{u}_A, 0)_{[\mathrm{C},(-\mathrm{u}_B,0,0)]}$. Thus, if we simply transform the boundary conditions in the system (9.49a)–(9.51b),[22] we cannot obtain the corresponding solution in another inertial system. To summarize, the solution for the limiting state as the Knudsen number vanishes is not unique; they depend on the limiting process. The solutions in two inertial systems of a physical problem are related by the Galilean transformation when the corresponding states in their limiting processes are related by the transformation.

9.4.2 Bifurcated flow field under infinitesimal curvature

In Section 9.4.1 we have found that there is a bifurcation from the parallel flow with a linear profile by the effect of infinitesimal curvature of the boundary. In this section, we will study the bifurcated velocity field away from bifurcation points by numerical analysis of the system (9.56)–(9.58b) for the case where the state of the gas is uniform with respect to $\bar{\chi}$ (or $\partial/\partial\bar{\chi} = 0$).

The numerical computation is carried out in the following way. Consider a gas in the finite domain ($0 < y < 1$, $0 < z < z_B$) and take the following conditions on the side boundaries:

$$\frac{\partial \hat{u}_x}{\partial z} = \frac{\partial \hat{u}_y}{\partial z} = 0, \ \hat{u}_z = 0 \ \text{ at } z = 0 \text{ and } z = z_B, \tag{9.70}$$

in addition to the conditions on the plane walls

$$\hat{u}_x = \hat{u}_A, \quad \hat{u}_y = \hat{u}_z = 0 \quad \text{at} \ \ y = 0, \tag{9.71a}$$

$$\hat{u}_x = \hat{u}_B, \quad \hat{u}_y = \hat{u}_z = 0 \quad \text{at} \ \ y = 1. \tag{9.71b}$$

Incidentally, from the basic equations (9.57a) and (9.57d) and the boundary condition (9.70), it is found that $\partial \hat{P}_{20}/\partial z = 0$ at $z = 0$ and $z = z_B$.

Let a solution of the above problem in the rectangular domain be S1. Then, its mirror image with respect to the side boundary ($z = 0$ or z_B) is also a solution of the problem (say, S2). The two kinds of solutions S1 and S2 being alternately arranged in the z direction, the resulting function is found to be two times continuously differentiable across the connection lines $z = nz_B$ ($n = 0, \pm 1, \pm 2, \ldots$), because it satisfies Eqs. (9.56)–(9.57d) except on the connection lines and satisfies the condition (9.70) on the connection lines. That is, the smooth function thus constructed is a periodic solution with period $2z_B$ with respect to z in the infinite domain between the two plane walls at $y = 0$ and $y = 1$.

The boundary-value problem, Eqs. (9.56)–(9.57d) with Eqs. (9.70)–(9.71b), is solved numerically by a finite-difference method. The solution of the finite-difference scheme derived from the above system where $\hat{P}_{20}$ is eliminated by taking the difference of ∂[Eq. (9.57c)]$/\partial z$ and ∂[Eq. (9.57d)]$/\partial y$ is obtained by the method of iteration similar to that described in Section 8.2.4 in the Bénard

[22] In the present form of solution, the solution in the transformed system is also time-independent. Generally, we have to discuss on the basis of the system that describes the time-dependent problem.

problem. Here, the equations are much more simpler than those in the Bénard problem.

Some of the results of computation are shown in Figs. 9.3–9.6. Figures 9.3 and 9.4 are, respectively, the velocity profiles $2u_x/\gamma_1 C$ vs y on various cross sections $z =$ const and the infinitesimal cross velocity field $(2u_y/\gamma_1, 2u_z/\gamma_1)$ for the case $z_B = 1$ and $2u_B/\gamma_1 C = 0$ (the wall at $y = 1$ is at rest). Figures 9.5 and 9.6 are the corresponding figures for the case $z_B = 1$ and $2u_B/\gamma_1 C = -150$ (the two walls are moving in the opposite directions). In these figures, the flow fields for three different values of $2u_A/\gamma_1 C$ away from the bifurcation points are shown in panels (a), (b), and (c). The main flow $2u_x/\gamma_1 C$ is disturbed owing to the convection of the infinitesimal cross flow $(2u_y/\gamma_1, 2u_z/\gamma_1)$ induced by the infinitesimal curvature. The three cases of $2u_B/\gamma_1 C = -150$ are the common results for the two kinds of the initial flow fields of iteration, the results for $2u_B/\gamma_1 C = 0$ and the eigenfunction of Eqs. (9.66a)–(9.68) for $2u_B/\gamma_1 C = -150$ and $\alpha = \pi$, both of which are of one-roll type in the z direction; however, two rolls are arranged in the z direction in the final result, and two rolls, one of which is weak, are arranged in the y direction for the parameter not far from the bifurcation curve. The bifurcated solution exists in the region with a little smaller values of $2u_A/\gamma_1 C$ than the bifurcation point $2u_{Ab}/\gamma_1 C$ $(= 99.4753)$ [see Figs. 9.5 (a) and 9.6 (a)], as well as in the region with the larger values of $2u_A/\gamma_1 C$.

The apparently strange effect of infinitesimal curvature can be understood in the following way. The infinitesimal curvature modifies the main flow substantially in the two processes. The small curvature induces a small cross flow as naturally expected. Owing to the cross flow, a fluid particle flows downstream circulating slowly as in Figs. 9.4 and 9.6. In this process, the momentum of the main flow in a region is convected to another region with different velocity originally, and the two walls reset the velocity in the main stream direction of the circulating fluid particle owing to the nonslip boundary condition. It takes a long time for a fluid particle to reach a region with substantially different flow velocity originally, but owing to large Reynolds number [$\propto$ Ma/Kn, see Eq. (3.74)] (or small viscosity), the particle reaches the region exchanging the momentum of the main flow gradually during translation and retaining a substantial part of its original momentum and gives a substantial effect on the main flow. The flow fields shown in Figs. 9.3–9.6 well reflect this process.

9.5 Summary and supplementary discussion

The behavior of parallel flows of a gas in the continuum limit between two parallel plane walls has been studied as the limit of nearly parallel flows between two coaxial circular cylinders when the mean free path (or Knudsen number Kn) and the inverse of the radius (or the relative curvature D/L_A) of the inner cylinder simultaneously tend to zero with the difference D of the radii of the two cylinders fixed. The process of analysis is explained for time-independent problems, but the main result is given also for time-dependent problems. The fluid-dynamic-

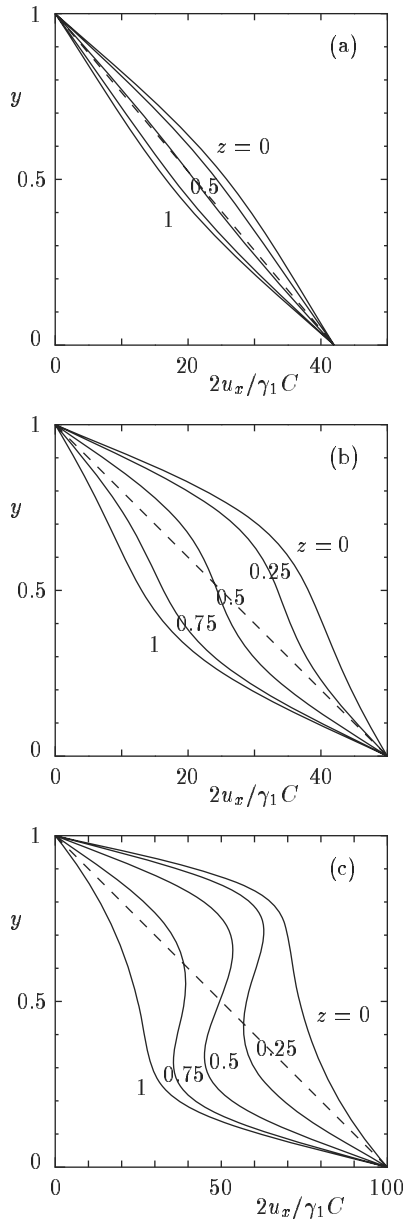

Figure 9.3. The bifurcated main velocity profiles, i.e., $2u_x/\gamma_1 C$ vs y, on various sections $z = \text{const}$ I: $z_B = 1$ and $2u_B/\gamma_1 C = 0$. (a) $2u_A/\gamma_1 C = 42$, (b) $2u_A/\gamma_1 C = 50$, (c) $2u_A/\gamma_1 C = 100$. The profiles $2u_x/\gamma_1 C$ on the sections $z = 0$, 0.25, 0.5, 0.75, and 1 between $z = 0$ and $z = 1$ are shown. The dashed lines ----- indicate the solution (9.60). Incidentally, the bifurcation point obtained in Section 9.4.1 is $2u_{Ab}/\gamma_1 C = 41.1705$ for $\alpha = \pi$ and $2u_{Bb}/\gamma_1 C = 0$.

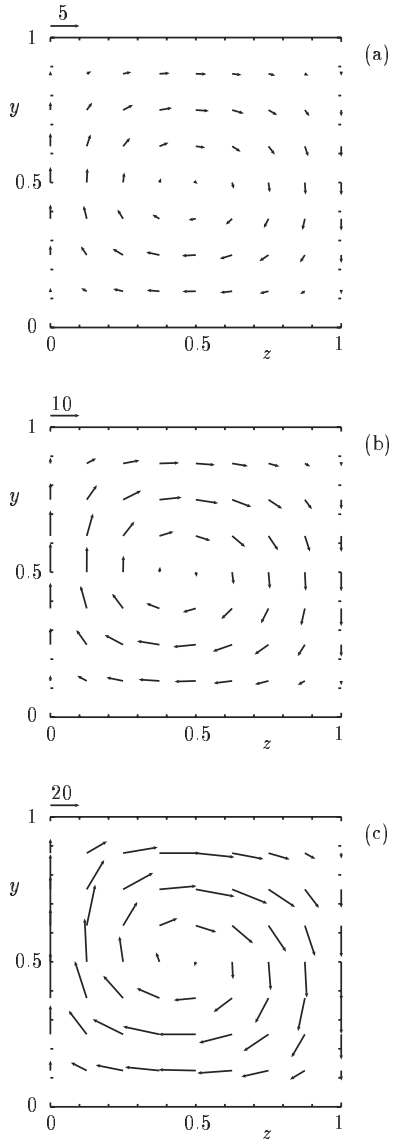

Figure 9.4. The bifurcated infinitesimal cross velocity field $(2u_y/\gamma_1, 2u_z/\gamma_1)$ I: $z_B = 1$ and $2u_B/\gamma_1 C = 0$. (a) $2u_A/\gamma_1 C = 42$, (b) $2u_A/\gamma_1 C = 50$, (c) $2u_A/\gamma_1 C = 100$. The arrows indicate $(2u_y/\gamma_1, 2u_z/\gamma_1)$ at their starting points and their scale is shown on the left shoulder of each panel. Note the difference of the scale of the arrow in panels (a), (b), and (c). Incidentally, the bifurcation point obtained in Section 9.4.1 is $2u_{Ab}/\gamma_1 C = 41.1705$ for $\alpha = \pi$ and $2u_{Bb}/\gamma_1 C = 0$.

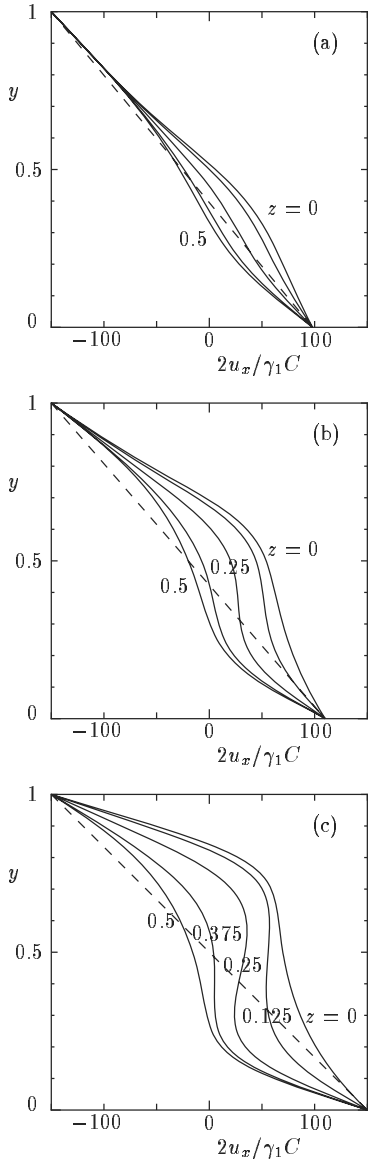

Figure 9.5. The bifurcated main velocity profiles, i.e., $2u_x/\gamma_1 C$ vs y, on various sections $z = \text{const}$ II: $z_B = 1$ and $2u_B/\gamma_1 C = -150$. (a) $2u_A/\gamma_1 C = 98$, (b) $2u_A/\gamma_1 C = 110$, (c) $2u_A/\gamma_1 C = 150$. The profiles $2u_x/\gamma_1 C$ on the sections $z = 0$, 0.125, 0.25, 0.375, and 0.5 are shown. The flow field in $0.5 < z \leq 1$ is the mirror image of the field $0 \leq z < 0.5$ with respect to the plane $z = 0.5$. The dashed lines - - - - - indicate the solution (9.60). Incidentally, the bifurcation point obtained in Section 9.4.1 is $2u_{Ab}/\gamma_1 C = 99.4753$ for $\alpha = 2\pi$ and $2u_{Bb}/\gamma_1 C = -150$.

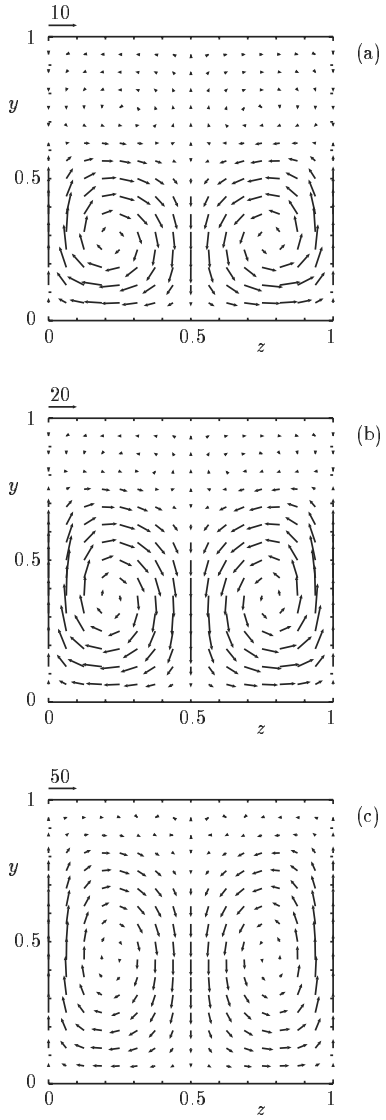

Figure 9.6. The bifurcated infinitesimal cross velocity field $(2u_y/\gamma_1, 2u_z/\gamma_1)$ II: $z_B = 1$ and $2u_B/\gamma_1 C = -150$. (a) $2u_A/\gamma_1 C = 98$, (b) $2u_A/\gamma_1 C = 110$, (c) $2u_A/\gamma_1 C = 150$. The arrows indicate $(2u_y/\gamma_1, 2u_z/\gamma_1)$ at their starting points and their scale is shown on the left shoulder of each panel. Note the difference of the scale of the arrow in panels (a), (b), and (c). Incidentally, the bifurcation point obtained in Section 9.4.1 is $2u_{Ab}/\gamma_1 C = 99.4753$ for $\alpha = 2\pi$ and $2u_{Bb}/\gamma_1 C = -150$.

type equations and their boundary conditions describing the limiting behavior, derived by asymptotic analysis of the Boltzmann system, depend on the relative speed of decay of the two quantities, the Knudsen number and the relative curvature of the inner cylinder. Generally, when the speed of decay of the curvature is not faster than the square of the mean free path [$D/L_A \geq (k/c)^2$; see Eq. (9.4c)], the limiting parallel flow is determined simultaneously with the infinitesimal cross flow by the fluid-dynamic-type equations with an infinitesimal curvature term. The detailed analysis and complete result were given for the threshold case, i.e., $D/L_A = (k/c)^2$, where the effect of infinitesimal curvature first enters the system. The fluid-dynamic-type equations contain non-Navier–Stokes terms as well as the infinitesimal curvature term. When the flow speed (or Mach number) and the temperature difference are small but finite [say $O(\varepsilon)$], the non-Navier–Stokes terms disappear, but the infinitesimal curvature term remains if the decay of the curvature is not faster than the square of the mean free path divided by the square of the flow speed [$D/L_A \geq (k/C\varepsilon)^2$; see Eqs. (9.4c) and (9.47) or Eq. (9.53)]. The two conditions $D/L_A \geq (k/c)^2$ and $D/L_A \geq (k/C\varepsilon)^2$, which give the range of existence of the infinitesimal-curvature effect, can be combined into the single formula $D/L_A \geq (\mathrm{Kn}/C_0\mathrm{Ma})^2$, where Ma and Kn are, respectively, the Mach number and the Knudsen number of the system, and C_0 is a constant. To summarize, the infinitesimal curvature of the boundary produces a finite effect on flows when the decay of the curvature is not faster than the square of the ratio of the Knudsen number to the Mach number. This is a new kind of ghost effect on a gas in the continuum limit. As an example, the bifurcation from the plane Couette flow with a linear profile is studied and found to occur owing to the infinitesimal curvature effect. The bifurcation relation and the bifurcated flow field are obtained. The profile of the bifurcated main parallel flow is considerably deformed from the linear profile by the infinitesimal cross flow.

In the atmospheric condition, the mean free path is small but not exactly zero. Thus, the radius L_A of the inner cylinder for which the curvature effect is appreciable is of a finite value. Let us estimate L_A for which the curvature effect is appreciable when the outer cylinder is at rest. Let the velocity of the inner cylinder of the bifurcation point be V_{Ab}. From Eq. (9.4c) with (9.47), or Eq. (9.53), and Eqs. (9.52) and (9.59), L_A/D is related to $V_{Ab}/(2RT_A)^{1/2}$ and k as

$$\frac{L_A}{D} = \left(\frac{2}{\gamma_1 \hat{u}_{Ab}}\right)^2 \frac{V_{Ab}^2}{2RT_A} \frac{1}{k^2}, \tag{9.72}$$

where $\hat{u}_{Ab}$ is about 40, as given in Fig. 9.1. Take the air at room temperature, i.e., $T_A \sim 300$ K, and atmospheric pressure.[23] Then, the mean free path ℓ_0 of the gas is roughly 6×10^{-8} m. When $V_{Ab} = 30$ cm/s and $D = 10$ cm, the parameters $V_{Ab}/(2RT_A)^{1/2}$ and Kn are roughly 10^{-3} and 6×10^{-7} respectively. Thus, from Eq. (9.72), L_A/D is about 4×10^3, i.e., L_A is about 400 m. For a little larger V_{Ab} and D, say $V_{Ab} = 10$ m/s and $D = 1$ m, the corresponding value of L_A/D is about 4×10^8, i.e., L_A is about 4×10^5 km, which is more than

[23] See Footnote 102 in Section 3.6.2.

60 times the radius of the Earth. For the curvature effect to be negligible, L_A is required to be much larger than these values in the atmospheric condition.

We have considered the limiting case that the Knudsen number tends to zero. Thus, one may naturally ask whether the same effect can be found starting from the Navier–Stokes equations. The answer is yes. In the kinetic-theory analysis, the flow velocity (or more precisely the Mach number Ma of the flow) is taken much larger than the Knudsen number (or $\hat{v}_x \gg k$). Thus, the Reynolds number Re of the system is very large in view of the von Karman relation (3.74). Now, take the Navier–Stokes equations for an incompressible fluid[24] and see how the infinitesimal curvature effect (ghost effect) appears in the limit that $\mathrm{Re} \to \infty$. This is some repetition, but this new effect may be better understood by nonspecialists in kinetic theory. In the kinetic theory approach, the infinitesimal curvature effect appears in the equation of momentum in the direction normal to the wall (or radial direction) and induces an infinitesimal velocity component normal to the wall (the radial velocity component), and this infinitesimal flow produces a finite effect on the main flow parallel to the wall. We first see this mechanism less formally on the basis of the Navier–Stokes equations for an incompressible fluid in the cylindrical coordinate system:

$$\frac{1}{r}\frac{\partial\, v_r r}{\partial r} + \frac{1}{r}\frac{\partial v_\theta}{\partial \theta} + \frac{\partial v_z}{\partial Z} = 0, \tag{9.73a}$$

$$\begin{aligned} &v_r \frac{\partial\, v_r}{\partial\, r} + \frac{v_\theta}{r}\frac{\partial v_r}{\partial \theta} + v_z \frac{\partial v_r}{\partial Z} - \frac{v_\theta^2}{r} \\ &\quad = -\frac{1}{\rho}\frac{\partial p}{\partial\, r} + \frac{\mu}{\rho}\left[\frac{1}{r}\frac{\partial}{\partial r}\left(r\frac{\partial v_r}{\partial r}\right) - \frac{v_r}{r^2} + \frac{1}{r^2}\frac{\partial^2 v_r}{\partial \theta^2} + \frac{\partial^2 v_r}{\partial Z^2} - \frac{2}{r^2}\frac{\partial v_\theta}{\partial \theta}\right], \end{aligned} \tag{9.73b}$$

$$\begin{aligned} &v_r \frac{\partial v_\theta}{\partial r} + \frac{v_\theta}{r}\frac{\partial v_\theta}{\partial \theta} + v_z \frac{\partial v_\theta}{\partial Z} + \frac{v_r v_\theta}{r} \\ &\quad = -\frac{1}{\rho r}\frac{\partial p}{\partial \theta} + \frac{\mu}{\rho}\left[\frac{1}{r}\frac{\partial}{\partial r}\left(r\frac{\partial\, v_\theta}{\partial r}\right) - \frac{v_\theta}{r^2} + \frac{1}{r^2}\frac{\partial^2 v_\theta}{\partial \theta^2} + \frac{\partial^2 v_\theta}{\partial Z^2} + \frac{2}{r^2}\frac{\partial v_r}{\partial \theta}\right], \end{aligned} \tag{9.73c}$$

$$v_r \frac{\partial v_z}{\partial r} + \frac{v_\theta}{r}\frac{\partial v_z}{\partial \theta} + v_z \frac{\partial v_z}{\partial Z} = -\frac{1}{\rho}\frac{\partial p}{\partial Z} + \frac{\mu}{\rho}\left[\frac{1}{r}\frac{\partial}{\partial r}\left(r\frac{\partial v_z}{\partial r}\right) + \frac{1}{r^2}\frac{\partial^2 v_z}{\partial \theta^2} + \frac{\partial^2 v_z}{\partial Z^2}\right], \tag{9.73d}$$

where (r, θ, Z) is the cylindrical space coordinate system, (v_r, v_θ, v_z) is the flow velocity in the cylindrical coordinate system, p is the pressure, ρ is the density (constant), and μ/ρ is the kinematic viscosity (constant).

Let U be a characteristic speed, e.g., circumferential speed of rotation of the inner cylinder. Let D and U be given. Consider the limiting process that $L_A \to \infty$ and ρ/μ (or $\mathrm{Re} = UD\rho/\mu$) $\to \infty$ keeping $L_A(\mu/\rho)^2$ (or $L_A/D\mathrm{Re}^2$) fixed, or $\mathrm{Re} \to \infty$ and $L_A = O(\mathrm{Re}^2)$. Thus, the parameter expressing the limiting process is only Re. Taking a nearly parallel flow (v_r, v_θ, v_z), where $v_\theta = O(1)$

[24] As we have seen, non-Navier–Stokes terms exist in the limiting fluid-dynamic-type equations when the Mach number is not small. Thus, it is sufficient to consider the incompressible Navier–Stokes equations.

and v_r and v_z are small, say $O(\delta)$, we examine how the main flow v_θ is determined together with the weak cross field (v_r, v_z) by their mutual interactions in the above limit with the aid of the Navier–Stokes equations in the cylindrical coordinates. Owing to the mass conservation (9.73a), the variation of the variables in the direction of θ is small, i.e., $(1/r)\partial(*)/\partial\theta = O(\delta*)$ when $\partial(*)/\partial r = O(*)$ and $\partial(*)/\partial Z = O(*)$. The term $-v_\theta^2/r$ on the left-hand side of Eq. (9.73b) is $O(\mathrm{Re}^{-2})$ because v_θ is $O(1)$ but r is $O(\mathrm{Re}^2)$. The convection terms $v_r\partial v_r/\partial r$ and $v_z\partial v_r/\partial Z$ are $O(\delta^2)$; the remaining convection term $(v_\theta/r)\partial v_r/\partial\theta$ is also $O(\delta^2)$, because $(1/r)\partial(*)/\partial\theta = O(\delta*)$. The viscous term on the right-hand side of Eq. (9.73b) is $O(\mathrm{Re}^{-1}\delta)$, because $v_r = O(\delta)$ and the kinematic viscosity μ/ρ is $O(\mathrm{Re}^{-1})$. These terms in Eq. (9.73b) are balanced when $\delta = O(\mathrm{Re}^{-1})$. Thus, the infinitesimal term v_θ^2/r induces infinitesimal cross flow (v_r, v_z) of the order of Re^{-1}. This infinitesimal cross flow (v_r, v_z) is reflected on the main flow v_θ through Eq. (9.73c). The terms $v_r\partial v_\theta/\partial r$ and $v_z\partial v_\theta/\partial Z$ on the left-hand side of Eq. (9.73c) express the convection effect by the infinitesimal velocity v_r and v_z. These terms are $O(\mathrm{Re}^{-1})$ and are of the same order as $(v_\theta/r)\partial v_\theta/\partial\theta$, because $(1/r)\partial(*)/\partial\theta = O(\mathrm{Re}^{-1}*)$. The viscous term on the right-hand side is also $O(\mathrm{Re}^{-1})$ owing to the kinematic viscosity μ/ρ. Thus, the infinitesimal cross flow (v_r, v_z) affects the main flow v_θ by the order of unity. This ordering consideration is in a good harmony with the physical explanation in the last paragraph of Section 9.4.2.

Formal derivation of the limiting equations is very simple. We put

$$\left.\begin{aligned} &\hat{u}_x = -\frac{v_\theta}{CU}, \quad \hat{u}_y = \frac{\mathrm{Re}v_r}{U}, \quad \hat{u}_z = \frac{\mathrm{Re}v_z}{U}, \quad C^2\hat{P}_{02} + \frac{\hat{P}_{20}}{\mathrm{Re}^2} = \frac{p}{\rho U^2}, \\ &x = -\frac{L_A\theta}{D}, \quad y = \frac{r - L_A}{D}, \quad z = \frac{Z}{D}, \quad \bar{\chi} = \frac{x}{\mathrm{Re}C}, \\ &\frac{L_A}{D} = C^2\mathrm{Re}^2, \quad \mathrm{Re} = \frac{UD\rho}{\mu}, \end{aligned}\right\} \tag{9.74}$$

where C is a constant. Here, we consider that $\hat{u}_x$, $\hat{u}_y$, $\hat{u}_z$, $\hat{P}_{02}$, $\hat{P}_{20}$, and C are quantities of the order of unity. That is, we are interested in the situation where the main flow v_θ/U parallel to the wall is of the order of unity but the cross components v_r/U and v_z/U are small quantities of the order of Re^{-1}. Naturally the length scale of variation with respect to r and Z is of the order of the channel width D. In view of Eq. (9.73a), the length scale of variation in the circumferential direction is of the order of $\mathrm{Re}D$ for the above scale of (v_r, v_θ, v_z), and thus the variable $\bar{\chi}$ is introduced. Substituting the relations given in Eq. (9.74) into the Navier–Stokes equations (9.73a)–(9.73d), arranging the same-order terms in Re^{-1}, and taking the limit as $\mathrm{Re} \to \infty$, then we obtain Eqs. (9.56)–(9.57d).[25]

For time-dependent problems, we have only to add

$$\frac{\partial\hat{u}_x}{\partial\tilde{t}}, \quad \frac{\partial\hat{u}_y}{\partial\tilde{t}}, \quad \text{and} \quad \frac{\partial\hat{u}_z}{\partial\tilde{t}},$$

[25] Note the discussion in the paragraph next to that containing Eq. (9.40b). A similar discussion can be carried out with $1/\mathrm{Re}$ in place of k.

where $\tilde{t} = t/(D^2\rho/\mu)$ with t being the time, to the left-hand sides of Eqs. (9.57b), (9.57c), and (9.57d), respectively. Equations (9.56) and (9.57a) remain unchanged. The linear stability analysis of the plane Couette flow on the basis of the extended equations is carried out in Sone & Doi [2005]. The bifurcation curves obtained in Section 9.4.1 are the threshold of the linear stability. When the Reynolds number is large but finite, the bifurcation occurs only when L_A is finite, but it is very large. When $\mathrm{Re} = 5 \times 10^3$, the bifurcation occurs at about $L_A/D = 1.5 \times 10^4$, because $\hat{u}_{Ab}$ is about 40 and thus C is about 40^{-1}.

In the linear stability analysis of the incompressible Navier–Stokes equations for the plane Couette flow with a linear profile between parallel plane walls, it is proved by Romanov [1973] that the flow is stable in the whole range of the Reynolds number. The above discussion with the result in Section 9.4.1 shows that the bifurcation occurs at infinite Reynolds number by the effect of infinitesimal curvature. This was one of the long-lasting problems in the classical fluid dynamics.

The results derived in this chapter for two inertial systems apparently is not related by the Galilean transformation. This is due to nonuniqueness of solution. That is, the limiting result as the Knudsen number tends to zero is not unique; they depend on the limiting process. The solutions in the two systems of a physical problem are related by the Galilean transformation if their states in their limiting processes are related by the transformation.

Appendix A

Supplement to the Boltzmann Equation

A.1 Derivation of the Boltzmann equation

We will give a formal derivation of the Boltzmann equation from the Liouville equation on the basis of Grad [1958]. Consider a system consisting of N identical particles each of which has mass m. Take the $6N$-dimensional Γ space consisting of the position $\boldsymbol{X}^{(i)}$ and velocity $\boldsymbol{\xi}^{(i)}$ of the particle i $(i = 1, 2, \ldots, N)$. Let f^N, a function of the $6N + 1$ variables $\boldsymbol{X}^{(1)}, \ldots, \boldsymbol{X}^{(N)}$, $\boldsymbol{\xi}^{(1)}, \ldots, \boldsymbol{\xi}^{(N)}$, and t, be the N-particle probability density function finding the particle i $(i = 1, 2, \ldots, N)$ at the position $\boldsymbol{X}^{(i)}$ and at velocity $\boldsymbol{\xi}^{(i)}$ in the Γ space with $6N$ dimensions at time t. The behavior of the density function f^N is determined by the *Liouville equation*[1] given by

$$\frac{\partial f^N}{\partial t} + \sum_{i=1}^{N} \left(\boldsymbol{\xi}^{(i)} \frac{\partial f^N}{\partial \boldsymbol{X}^{(i)}} + \boldsymbol{F}^{(i)} \frac{\partial f^N}{\partial \boldsymbol{\xi}^{(i)}} \right) = 0, \tag{A.1}$$

where $m\boldsymbol{F}^{(i)}$ is the force acting on the particle i. The meaning of the simplified notation of the gradients $\partial f^N / \partial \boldsymbol{X}^{(i)}$ and $\partial f^N / \partial \boldsymbol{\xi}^{(i)}$ and the scalar products $\boldsymbol{\xi}^{(i)} \partial f^N / \partial \boldsymbol{X}^{(i)}$ and $\boldsymbol{F}^{(i)} \partial f^N / \partial \boldsymbol{\xi}^{(i)}$, without dot $\cdot$, may be obvious. Here, the force $m\boldsymbol{F}^{(i)}$ acting on the particle i consists only of the interparticle force, that is,

$$\boldsymbol{F}^{(i)} = \sum_{j=1\,(j\neq i)}^{N} \boldsymbol{F}_{i,j},$$

[1]The Liouville equation is the exact equation describing the behavior of the probability density function f^N in Γ space of the N-particle system obeying Newton's law of motion. Its derivation is found in a textbook of statistical mechanics (e.g., Tolman [1979], Hill [1987], Reif [1965], Diu, Guthmann, Lederer & Roulet [1989]).

where $m\boldsymbol{F}_{i,j}$ is the force by the particle j (thus, $\boldsymbol{F}_{i,j} = -\boldsymbol{F}_{j,i}$ by the law of action and its reaction). The extension to a system with an external force is straightforward. We further assume that the force $\boldsymbol{F}_{i,j}$ is given by a potential determined by the interparticle distance $|\boldsymbol{X}^{(j)} - \boldsymbol{X}^{(i)}|$ and extends to only a finite distance d_m (or $\boldsymbol{F}_{i,j} = 0$ for $|\boldsymbol{X}^{(j)} - \boldsymbol{X}^{(i)}| \geq d_m$)[2] and that the density function is symmetric with respect to the N sets $(\boldsymbol{X}^{(i)}, \boldsymbol{\xi}^{(i)})$ $(i = 1, \ldots, N)$ of variables.

Now, we introduce the following *truncated probability density functions* $\tilde{f}_1$, $\tilde{f}_2$, $\tilde{f}_3, \ldots$:

$$\tilde{f}_1 = \int_{\Omega_1,\, \text{all } \boldsymbol{\xi}^{(2)},\ldots,\, \text{all } \boldsymbol{\xi}^{(N)}} f^N \mathbf{d}\boldsymbol{X}^{(2)} \cdots \mathbf{d}\boldsymbol{X}^{(N)} \mathbf{d}\boldsymbol{\xi}^{(2)} \cdots \mathbf{d}\boldsymbol{\xi}^{(N)}, \tag{A.2a}$$

$$\tilde{f}_2 = \int_{\Omega_{12},\, \text{all } \boldsymbol{\xi}^{(3)},\ldots,\, \text{all } \boldsymbol{\xi}^{(N)}} f^N \mathbf{d}\boldsymbol{X}^{(3)} \cdots \mathbf{d}\boldsymbol{X}^{(N)} \mathbf{d}\boldsymbol{\xi}^{(3)} \cdots \mathbf{d}\boldsymbol{\xi}^{(N)}, \tag{A.2b}$$

$$\tilde{f}_3 = \int_{\Omega_{123},\, \text{all } \boldsymbol{\xi}^{(4)},\ldots,\, \text{all } \boldsymbol{\xi}^{(N)}} f^N \mathbf{d}\boldsymbol{X}^{(4)} \cdots \mathbf{d}\boldsymbol{X}^{(N)} \mathbf{d}\boldsymbol{\xi}^{(4)} \cdots \mathbf{d}\boldsymbol{\xi}^{(N)}, \tag{A.2c}$$

$$\cdots\cdots\cdots,$$

where the ranges Ω_1, Ω_{12}, $\Omega_{123}, \ldots$ are defined as follows: Let $\boldsymbol{X}^{(1)}$ be fixed and let the domain D_1^r $(r = 2, \ldots, N)$ of the space $\boldsymbol{X}^{(r)}$ be defined by

$$D_1^r = \{|\boldsymbol{X}^{(r)} - \boldsymbol{X}^{(1)}| \geq d_m\}.$$

That is, the particle r in D_1^r is not subject to the interparticle force $\boldsymbol{F}_{r,1}$ due to the particle 1. Then, Ω_1, Ω_{12}, $\Omega_{123}, \ldots$ are

$$\begin{aligned}
\Omega_1 &= D_1^2 \times D_1^3 \times \cdots \times D_1^N, \\
\Omega_{12} &= D_1^3 \times D_1^4 \times \cdots \times D_1^N, \\
\Omega_{123} &= D_1^4 \times D_1^5 \times \cdots \times D_1^N, \\
&\cdots\cdots\cdots.
\end{aligned}$$

The functions $\tilde{f}_1$, $\tilde{f}_2$, etc. are, respectively, functions of $(\boldsymbol{X}^{(1)}, \boldsymbol{\xi}^{(1)}, t)$, $(\boldsymbol{X}^{(1)}, \boldsymbol{\xi}^{(1)}, \boldsymbol{X}^{(2)}, \boldsymbol{\xi}^{(2)}, t)$, etc.; $\tilde{f}_2$ is not symmetric with respect to the two sets $(\boldsymbol{X}^{(1)}, \boldsymbol{\xi}^{(1)})$ and $(\boldsymbol{X}^{(2)}, \boldsymbol{\xi}^{(2)})$ of variables. Incidentally, we introduce the notation S_i^r for the sphere in the space $\boldsymbol{X}^{(r)}$ with $\boldsymbol{X}^{(i)}$ as its center:

$$S_i^r = \{|\boldsymbol{X}^{(r)} - \boldsymbol{X}^{(i)}| < d_m\}.$$

Thus, D_1^r is the complement of S_1^r.

Integrating the Liouville equation (A.1) with respect to $\boldsymbol{X}^{(2)}$, …, $\boldsymbol{X}^{(N)}$, $\boldsymbol{\xi}^{(2)}$, …, $\boldsymbol{\xi}^{(N)}$ over the domain Ω_1 and the whole spaces of $\boldsymbol{\xi}^{(2)}$, …, $\boldsymbol{\xi}^{(N)}$ or

[2]For a hard-sphere particle, d_m is the diameter of the particle.

with respect to $\boldsymbol{X}^{(3)}, \ldots, \boldsymbol{X}^{(N)}$, $\boldsymbol{\xi}^{(3)}, \ldots, \boldsymbol{\xi}^{(N)}$ over the domain Ω_{12} and the whole spaces of $\boldsymbol{\xi}^{(3)}, \ldots, \boldsymbol{\xi}^{(N)}$ or $\ldots$, we obtain the following series of equations for $\tilde{f}_1$, $\tilde{f}_2$, $\ldots$ called *Grad hierarchy* (Grad [1958]):

$$\frac{\partial \tilde{f}_1}{\partial t} + \boldsymbol{\xi}^{(1)} \frac{\partial \tilde{f}_1}{\partial \boldsymbol{X}^{(1)}} = (N-1) \int_{\partial S_1^2,\, \text{all } \boldsymbol{\xi}^{(2)}} (\boldsymbol{\xi}^{(2)} - \boldsymbol{\xi}^{(1)}) \cdot \boldsymbol{n}_1^2 \tilde{f}_2 \mathrm{d}^2 \boldsymbol{X}^{(2)} \mathbf{d}\boldsymbol{\xi}^{(2)}, \quad \text{(A.3a)}$$

$$\begin{aligned} \frac{\partial \tilde{f}_2}{\partial t} + \boldsymbol{\xi}^{(1)} \frac{\partial \tilde{f}_2}{\partial \boldsymbol{X}^{(1)}} + \boldsymbol{\xi}^{(2)} \frac{\partial \tilde{f}_2}{\partial \boldsymbol{X}^{(2)}} + \boldsymbol{F}_{1,2} \frac{\partial \tilde{f}_2}{\partial \boldsymbol{\xi}^{(1)}} + \boldsymbol{F}_{2,1} \frac{\partial \tilde{f}_2}{\partial \boldsymbol{\xi}^{(2)}} \\ = (N-2) \int_{\partial S_1^3,\, \text{all } \boldsymbol{\xi}^{(3)}} (\boldsymbol{\xi}^{(3)} - \boldsymbol{\xi}^{(1)}) \cdot \boldsymbol{n}_1^3 \tilde{f}_3 \mathrm{d}^2 \boldsymbol{X}^{(3)} \mathbf{d}\boldsymbol{\xi}^{(3)} \\ - (N-2) \int_{D_1^3,\, \text{all } \boldsymbol{\xi}^{(3)}} \boldsymbol{F}_{2,3} \frac{\partial \tilde{f}_3}{\partial \boldsymbol{\xi}^{(2)}} \mathbf{d}\boldsymbol{X}^{(3)} \mathbf{d}\boldsymbol{\xi}^{(3)}, \end{aligned} \quad \text{(A.3b)}$$

$$\ldots\ldots\ldots\ldots\ldots,$$

where $\boldsymbol{n}_i^j = (\boldsymbol{X}^{(j)} - \boldsymbol{X}^{(i)})/|\boldsymbol{X}^{(j)} - \boldsymbol{X}^{(i)}|$; the range ∂S_1^2 of integration $\mathrm{d}^2\boldsymbol{X}^{(2)}$ with respect to $\boldsymbol{X}^{(2)}$ in Eq. (A.3a) is the surface ∂S_1^2 of the sphere S_1^2; the range ∂S_1^3 of integration $\mathrm{d}^2\boldsymbol{X}^{(3)}$ with respect to $\boldsymbol{X}^{(3)}$ in Eq. (A.3b) is the surface ∂S_1^3 of the sphere S_1^3; and the range D_1^3 of integration $\mathbf{d}\boldsymbol{X}^{(3)}$ with respect to $\boldsymbol{X}^{(3)}$ in the last term is practically $D_1^3 \cap S_2^3$ because the force $\boldsymbol{F}_{2,3}$ vanishes outside S_2^3. The above equations are considerably simplified by the assumptions of the symmetry of f^N with respect to the N sets $(\boldsymbol{X}^{(i)}, \boldsymbol{\xi}^{(i)})$ $(i = 1, \ldots, N)$ of variables and a finite range d_m of the interparticle force $\boldsymbol{F}_{i,j}$. Owing to the choice of the ranges of integration Ω_1, Ω_{12}, etc., instead of the whole spaces of $\boldsymbol{X}^{(2)}, \ldots, \boldsymbol{X}^{(N)}$, those of $\boldsymbol{X}^{(3)}, \ldots, \boldsymbol{X}^{(N)}$, etc., the interaction forces $\boldsymbol{F}_{i,j}$ do not appear in Eq. (A.3a), the interaction forces other than $\boldsymbol{F}_{1,2}$, $\boldsymbol{F}_{2,1}$, and $\boldsymbol{F}_{2,3}$ do not in Eq. (A.3b), etc. In place of these simplifications, the surface integrals over ∂S_1^2 and ∂S_1^3 on the right-hand sides of Eqs. (A.3a) and (A.3b) arise from the boundaries of the domains Ω_1 and Ω_{12}. Some supplementary explanations may be in order on the derivation of the right-hand sides.

With the aid of Gauss's divergence theorem, the integral of $\boldsymbol{\xi}^{(k)} \partial f^N / \partial \boldsymbol{X}^{(k)}$ $(k \geq 2)$ over Ω_1 or that of $\boldsymbol{\xi}^{(k)} \partial f^N / \partial \boldsymbol{X}^{(k)}$ $(k \geq 3)$ over Ω_{12} can be transformed into an integral over the boundary of Ω_1 (or ∂S_1^k) or Ω_{12} (or ∂S_1^k). For example,

$$\begin{aligned} &\int_{\Omega_1,\, \text{all } \boldsymbol{\xi}^{(2)}, \ldots,\, \text{all } \boldsymbol{\xi}^{(N)}} \boldsymbol{\xi}^{(2)} \frac{\partial f^N}{\partial \boldsymbol{X}^{(2)}} \mathbf{d}\boldsymbol{X}^{(2)} \cdots \mathbf{d}\boldsymbol{X}^{(N)} \mathbf{d}\boldsymbol{\xi}^{(2)} \cdots \mathbf{d}\boldsymbol{\xi}^{(N)} \\ &\quad = - \int_{\partial S_1^2,\, \text{all } \boldsymbol{\xi}^{(2)}} \boldsymbol{\xi}^{(2)} \cdot \boldsymbol{n}_1^2 \tilde{f}_2 \mathrm{d}^2 \boldsymbol{X}^{(2)} \mathbf{d}\boldsymbol{\xi}^{(2)}, \\ &\int_{\Omega_{12},\, \text{all } \boldsymbol{\xi}^{(3)}, \ldots, \text{all } \boldsymbol{\xi}^{(N)}} \boldsymbol{\xi}^{(3)} \frac{\partial f^N}{\partial \boldsymbol{X}^{(3)}} \mathbf{d}\boldsymbol{X}^{(3)} \cdots \mathbf{d}\boldsymbol{X}^{(N)} \mathbf{d}\boldsymbol{\xi}^{(3)} \cdots \mathbf{d}\boldsymbol{\xi}^{(N)} \\ &\quad = - \int_{\partial S_1^3,\, \text{all } \boldsymbol{\xi}^{(3)}} \boldsymbol{\xi}^{(3)} \cdot \boldsymbol{n}_1^3 \tilde{f}_3 \mathrm{d}^2 \boldsymbol{X}^{(3)} \mathbf{d}\boldsymbol{\xi}^{(3)}. \end{aligned}$$

In the integral of $\boldsymbol{\xi}^{(1)}\partial f^N/\partial \boldsymbol{X}^{(1)}$ over Ω_1 or Ω_{12}, a boundary term comes in through the process of interchanging the order of integration and differentiation because the domain (Ω_1 or Ω_{12}) of integration varies with $\boldsymbol{X}^{(1)}$. The derivative, with respect to ϑ, of the integral $\int_{\mathcal{D}(\vartheta)} g(\boldsymbol{X},\vartheta)\mathbf{d}\boldsymbol{X}$ over the domain $\mathcal{D}(\vartheta)$ deformable with ϑ is given in the following form:

$$\frac{\mathrm{d}}{\mathrm{d}\vartheta}\int_{\mathcal{D}(\vartheta)} g(\boldsymbol{X},\vartheta)\mathbf{d}\boldsymbol{X} = \int_{\mathcal{D}(\vartheta)} \frac{\partial g(\boldsymbol{X},\vartheta)}{\partial\vartheta}\mathbf{d}\boldsymbol{X} + \int_{\partial\mathcal{D}(\vartheta)} g(\boldsymbol{X},\vartheta)\frac{\partial \boldsymbol{X}_w}{\partial\vartheta}\cdot\boldsymbol{n}_w \mathrm{d}^2\boldsymbol{X}, \tag{A.4}$$

where $\boldsymbol{X}_w$ is a point on the boundary $\partial\mathcal{D}(\vartheta)$ of $\mathcal{D}(\vartheta)$, $\boldsymbol{n}_w$ is the outward unit normal vector to the boundary, and $\mathrm{d}^2\boldsymbol{X}$ is the surface element on $\partial\mathcal{D}(\vartheta)$; $\partial\boldsymbol{X}_w/\partial\vartheta$ is not unique but $\boldsymbol{n}_w\cdot\partial\boldsymbol{X}_w/\partial\vartheta$ is unique. The derivation of the formula is given at the end of this section as a lemma. With the aid of this formula, the above-mentioned integrals are transformed into the following forms:[3]

$$\begin{aligned}
&\int_{\Omega_1,\,\text{all }\boldsymbol{\xi}^{(2)},\ldots,\,\text{all }\boldsymbol{\xi}^{(N)}} \boldsymbol{\xi}^{(1)}\frac{\partial f^N}{\partial \boldsymbol{X}^{(1)}}\mathbf{d}\boldsymbol{X}^{(2)}\cdots\mathbf{d}\boldsymbol{X}^{(N)}\mathbf{d}\boldsymbol{\xi}^{(2)}\cdots\mathbf{d}\boldsymbol{\xi}^{(N)} \\
&\qquad = \boldsymbol{\xi}^{(1)}\frac{\partial \tilde{f}_1}{\partial \boldsymbol{X}^{(1)}} + (N-1)\int_{\partial S_1^2,\,\text{all }\boldsymbol{\xi}^{(2)}} \boldsymbol{\xi}^{(1)}\cdot\boldsymbol{n}_1^2\tilde{f}_2\mathrm{d}^2\boldsymbol{X}^{(2)}\mathbf{d}\boldsymbol{\xi}^{(2)}, \\
&\int_{\Omega_{12},\,\text{all }\boldsymbol{\xi}^{(3)},\ldots,\,\text{all }\boldsymbol{\xi}^{(N)}} \boldsymbol{\xi}^{(1)}\frac{\partial f^N}{\partial \boldsymbol{X}^{(1)}}\mathbf{d}\boldsymbol{X}^{(3)}\cdots\mathbf{d}\boldsymbol{X}^{(N)}\mathbf{d}\boldsymbol{\xi}^{(3)}\cdots\mathbf{d}\boldsymbol{\xi}^{(N)} \\
&\qquad = \boldsymbol{\xi}^{(1)}\frac{\partial \tilde{f}_2}{\partial \boldsymbol{X}^{(1)}} + (N-2)\int_{\partial S_1^3,\,\text{all }\boldsymbol{\xi}^{(3)}} \boldsymbol{\xi}^{(1)}\cdot\boldsymbol{n}_1^3\tilde{f}_3\mathrm{d}^2\boldsymbol{X}^{(3)}\mathbf{d}\boldsymbol{\xi}^{(3)},
\end{aligned}$$

where the factors $N-1$ and $N-2$ are due to the symmetry of the density function.

Let us return to the mainstream of the discussion. The series of equations (A.3a), (A.3b), ... is not a closed system, that is, Eq. (A.3a) contains $\tilde{f}_2$ as well as $\tilde{f}_1$, Eq. (A.3b) contains $\tilde{f}_3$ as well as $\tilde{f}_2$, and so on. That is, Eq. (A.3a) shows that the variation of $\tilde{f}_1$ along the path of one-particle system is determined by $\tilde{f}_2$; Eq. (A.3b) shows that the variation of $\tilde{f}_2$ along the path of two-particle system is determined by $\tilde{f}_3$; and so on. Now, we will see how Eqs. (A.3a) and (A.3b) can be simplified in the Grad–Boltzmann limit. Here, we consider the N particles in an infinite space without boundary, but a greater portion of the N particles is assumed to lie in a finite volume (say, L^3). The *Grad–Boltzmann limit* is the limiting process that the number of particles tends to infinite ($N\to\infty$) and the range of the interparticle force vanishes ($d_m\to 0$) keeping Nd_m^2 at a fixed value,[4] and thus, inevitably, $Nd_m^3\to 0$. Taking the coordinate system moving with the center of mass of the system, we can choose $(\sum_{i=1}^N|\boldsymbol{\xi}^{(i)}|^2/N)^{1/2}$ as

[3] The integration over Ω_1 ($=D_1^2\times D_1^3\times\cdots\times D_1^N$) is carried out successively, for example, over D_1^N, $D_1^{N-1},\ldots,$ and D_1^2, and the formula (A.4) is applied at each step of integration.

[4] Under the assumption of the second part of the preceding sentence, Nd_m^2/L^3 is of the order of the inverse of the mean free path [see Eq. (1.22) or (A.243)]. The nondimensional fixed value Nd_m^2/L^2 can be small or large. When the particles lie over an infinite domain with

the characteristic particle speed (say ξ_0) if it is finite. Then, the characteristic size $||\tilde{f}_n||$ of the truncated probability density function $\tilde{f}_n$ is $(L\xi_0)^{-3n}$ by the definition of the probability. With this note, we evaluate the size of the right-hand sides of Eqs. (A.3a) and (A.3b). The right-hand side of Eq. (A.3a) and the first term on the right-hand side of Eq. (A.3b) are integrals over the surface ∂S_1^2 or ∂S_1^3 with area $O(d_m^2)$, and therefore they are, respectively, $O(||\tilde{f}_2||\xi_0^4 N d_m^2)$ [or $O(||\tilde{f}_1||\xi_0 N d_m^2/L^3)$] and $O(||\tilde{f}_3||\xi_0^4 N d_m^2)$ [or $O(||\tilde{f}_2||\xi_0 N d_m^2/L^3)$] if none of $\tilde{f}_2$ and $\tilde{f}_3$ is singularly large on the surface ∂S_1^2 or ∂S_1^3.[5] The second term on the right-hand side of Eq. (A.3b) is an integral over the small region $D_1^3 \cap S_2^3$ of the order of d_m^3; but it does not vanish as $N d_m^3$ and is roughly estimated to be $O(||\tilde{f}_2||\xi_0 N d_m^2/L^3)$ because the interaction force $\boldsymbol{F}_{2,3}$ can be infinitely large as $|\boldsymbol{X}^{(2)} - \boldsymbol{X}^{(3)}| \to 0$.[6]

The range ∂S_1^2 of integration in the integral in Eq. (A.3a) is conveniently split into two parts, one is the part ∂S_{1+}^2 of the sphere where $(\boldsymbol{\xi}^{(2)} - \boldsymbol{\xi}^{(1)}) \cdot \boldsymbol{n}_1^2 > 0$ and the other is ∂S_{1-}^2 where $(\boldsymbol{\xi}^{(2)} - \boldsymbol{\xi}^{(1)}) \cdot \boldsymbol{n}_1^2 < 0$ for a given set of $\boldsymbol{\xi}^{(1)}$ and $\boldsymbol{\xi}^{(2)}$. On ∂S_{1+}^2 the two particles 1 and 2 are going to separate after their interaction by interparticle force, and on ∂S_{1-}^2 the two particles are going to enter the range of influence of their interparticle force. Let the position of the particle 2 on ∂S_{1+}^2 be $\boldsymbol{X}_+^{(2)}$ and that on ∂S_{1-}^2 be $\boldsymbol{X}_-^{(2)}$. Here we introduce an important assumption, called *molecular chaos*, that the two-particle truncated density function $\tilde{f}_2$ at $(\boldsymbol{X}^{(1)}, \boldsymbol{\xi}^{(1)}, \boldsymbol{X}_-^{(2)}, \boldsymbol{\xi}^{(2)}, t)$ on ∂S_{1-}^2 can be expressed by the product of the two one-particle truncated density functions,[7] that is,

$$\tilde{f}_2(\boldsymbol{X}^{(1)}, \boldsymbol{\xi}^{(1)}, \boldsymbol{X}_-^{(2)}, \boldsymbol{\xi}^{(2)}, t) = \tilde{f}_1(\boldsymbol{X}^{(1)}, \boldsymbol{\xi}^{(1)}, t)\tilde{f}_1(\boldsymbol{X}_-^{(2)}, \boldsymbol{\xi}^{(2)}, t). \tag{A.5}$$

We will try to express the two-particle truncated density function $\tilde{f}_2$ on the part ∂S_{1+}^2 in terms of the one-particle truncated density function $\tilde{f}_1$. That is, first, $\tilde{f}_2$ on the part ∂S_{1+}^2 is expressed in terms of $\tilde{f}_2$ on the part ∂S_{1-}^2, and then the assumption of molecular chaos is applied to this $\tilde{f}_2$. Equation (A.3b)

---

a substantial number density, the Grad–Boltzmann limit should be taken to be the limit that $n_0 \to \infty$ and $d_m \to 0$ with $n_0 d_m^2 = \text{const}$, where n_0 is a characteristic number of particles per unit volume.

[5]This kind of note applies to the ordering of a local integration of vanishing domain, e.g., Eq. (A.16).

[6]The interparticle force $\boldsymbol{F}_{2,3}$ in the integral over $D_1^3 \cap S_2^3$ can be very large (or diverge) as $\boldsymbol{X}^{(3)}$ approaches $\boldsymbol{X}^{(2)}$. For a repulsive force, however, $\tilde{f}_3$ is going to vanish there because the particles $\boldsymbol{X}^{(2)}$ and $\boldsymbol{X}^{(3)}$ cannot approach in a strong repulsive force field. That is, the two particles cannot be closer than the distance d_{sp} limited by $|\boldsymbol{F}_{2,3}|(d_m - d_{sp}) < O(|\boldsymbol{\xi}^{(2)}|^2 + |\boldsymbol{\xi}^{(3)}|^2)$, that is, $\tilde{f}_3$ vanishes inside the sphere d_{sp}. Thus, the integral with respect to the radial direction of the sphere D_1^3 is bounded by ξ_0^2 multiplied by the factors of the integrand other than $\boldsymbol{F}_{2,3}$. Thus, the second term on the right-hand side of Eq. (A.3b) is roughly estimated to be of the order of $N d_m^2$ as shown above. This can also be seen in the following way: The velocity $\boldsymbol{\xi}^{(3)}$ of the particle $\boldsymbol{X}^{(3)}$ is subject to a change of the order of $|\boldsymbol{F}_{2,3}|d_m/|\boldsymbol{\xi}^{(3)} - \boldsymbol{\xi}^{(2)}|$ during a short interaction period $d_m/|\boldsymbol{\xi}^{(3)} - \boldsymbol{\xi}^{(2)}|$, which is, on the other hand, of the order of $|\boldsymbol{\xi}^{(3)}|$. Thus, the average size of $\boldsymbol{F}_{2,3}$ during the interaction is of the order of ξ_0^2/d_m. Together with the other integrands, the second term is estimated as shown above.

[7]The assumption of molecular chaos is discussed in Grad [1958].

describes the variation of $\tilde{f}_2$ along the characteristic of Eq. (A.3b) or the trajectory in the space $(\boldsymbol{X}^{(1)}, \boldsymbol{\xi}^{(1)}, \boldsymbol{X}^{(2)}, \boldsymbol{\xi}^{(2)}, t)$ of the system of the two particles $\boldsymbol{X}^{(1)}$ and $\boldsymbol{X}^{(2)}$ interacting with each other by the interparticle forces $\boldsymbol{F}_{1,2}$ and $\boldsymbol{F}_{2,1}$. The variation is determined by the right-hand side of Eq. (A.3b) or $\tilde{f}_3$. The trajectory passes the region $|\boldsymbol{X}^{(2)} - \boldsymbol{X}^{(1)}| < d_m$ in a short time of the order of $d_m/|\boldsymbol{\xi}^{(2)} - \boldsymbol{\xi}^{(1)}|$. In other words, in this short time, the two particles $\boldsymbol{X}^{(1)}$ and $\boldsymbol{X}^{(2)}$ move from ∂S^2_{1-} to ∂S^2_{1+}. During this short period (or collision process), the two particles are subject to the strong interparticle forces $\boldsymbol{F}_{1,2}$ and $\boldsymbol{F}_{2,1}$ and their velocities $\boldsymbol{\xi}^{(1)}$ and $\boldsymbol{\xi}^{(2)}$ vary considerably. On the other hand, the contribution of the right-hand side of Eq. (A.3b) during this short period to the variation of $\tilde{f}_2$ is $O(||\tilde{f}_2||Nd_m^3/L^3)$ because the size of the right-hand side is $O(||\tilde{f}_2||\xi_0 N d_m^2/L^3)$ as shown in the paragraph before the preceding one. Therefore, the two-particle truncated density function $\tilde{f}_2$ takes the same value at the two ends of the trajectory of this short interaction period in the Grad–Boltzmann limit.

Let the two particles 1 and 2 be at $(\boldsymbol{X}^{(1)}, \boldsymbol{\xi}^{(1)})$ and $(\boldsymbol{X}^{(2)}_+, \boldsymbol{\xi}^{(2)})$, which is in the situation ∂S^2_{1+}. In view of their situation that they are on ∂S^2_{1+}, they were at the points $(\boldsymbol{X}^{(1)\prime}, \boldsymbol{\xi}^{(1)\prime})$ and $(\boldsymbol{X}^{(2)\prime}_-, \boldsymbol{\xi}^{(2)\prime})$ in the situation ∂S^2_{1-} at a close past time $t - \Delta t$, where Δt is of the order of $d_m/|\boldsymbol{\xi}^{(2)} - \boldsymbol{\xi}^{(1)}|$. Then, the particle velocities $\boldsymbol{\xi}^{(1)\prime}$ and $\boldsymbol{\xi}^{(2)\prime}$ at $t - \Delta t$ are expressed by the original ones $\boldsymbol{\xi}^{(1)}$ and $\boldsymbol{\xi}^{(2)}$ with a unit vector $\boldsymbol{\alpha}$ as a parameter as follows (see Fig. A.1):

$$\boldsymbol{\xi}^{(1)\prime} = \boldsymbol{\xi}^{(1)} + [\boldsymbol{\alpha} \cdot (\boldsymbol{\xi}^{(2)} - \boldsymbol{\xi}^{(1)})]\boldsymbol{\alpha}, \qquad \boldsymbol{\xi}^{(2)\prime} = \boldsymbol{\xi}^{(2)} - [\boldsymbol{\alpha} \cdot (\boldsymbol{\xi}^{(2)} - \boldsymbol{\xi}^{(1)})]\boldsymbol{\alpha}, \quad \text{(A.6)}$$

where the dot $\cdot$ for the scalar product serves to avoid confusion and the unit vectors $\boldsymbol{\alpha}$ and $-\boldsymbol{\alpha}$ give the same result. This relation is the result of conservation of momentum and energy before and after the interaction (see Section A.2.1). The dynamics of the system (in the past and future) is uniquely determined by $(\boldsymbol{X}^{(1)}, \boldsymbol{\xi}^{(1)}, \boldsymbol{X}^{(2)}_+, \boldsymbol{\xi}^{(2)})$ on ∂S^2_{1+}, and the parameter $\boldsymbol{\alpha}$ is expressed with $\boldsymbol{n}^2_{1+}$ $[= (\boldsymbol{X}^{(2)}_+ - \boldsymbol{X}^{(1)})/d_m]$ and $\boldsymbol{\xi}^{(2)} - \boldsymbol{\xi}^{(1)}$, i.e., $\boldsymbol{\alpha} = \boldsymbol{\alpha}(\boldsymbol{n}^2_{1+}, \boldsymbol{\xi}^{(2)} - \boldsymbol{\xi}^{(1)})$, the functional form of which is determined by the interparticle potential, containing d_m (see Section A.2.4 and also, for example, Goldstein [1950], Landau & Lifshitz [1960], Sone & Aoki [1994]).

According to the discussion in the paragraph before the preceding one,

$$\tilde{f}_2(\boldsymbol{X}^{(1)}, \boldsymbol{\xi}^{(1)}, \boldsymbol{X}^{(2)}_+, \boldsymbol{\xi}^{(2)}, t) = \tilde{f}_2(\boldsymbol{X}^{(1)\prime}, \boldsymbol{\xi}^{(1)\prime}, \boldsymbol{X}^{(2)\prime}_-, \boldsymbol{\xi}^{(2)\prime}, t - \Delta t).$$

For $\tilde{f}_2$ on ∂S^2_{1-}, i.e., $\tilde{f}_2(\boldsymbol{X}^{(1)\prime}, \boldsymbol{\xi}^{(1)\prime}, \boldsymbol{X}^{(2)\prime}_-, \boldsymbol{\xi}^{(2)\prime}, t - \Delta t)$, the assumption of molecular chaos can be applied. Thus, the two-particle truncated density function $\tilde{f}_2$ at $(\boldsymbol{X}^{(1)}, \boldsymbol{\xi}^{(1)}, \boldsymbol{X}^{(2)}_+, \boldsymbol{\xi}^{(2)}, t)$ is expressed by the product of the one-particle truncated density functions in the form

$$\begin{aligned}\tilde{f}_2(\boldsymbol{X}^{(1)}, \boldsymbol{\xi}^{(1)}, \boldsymbol{X}^{(2)}_+, \boldsymbol{\xi}^{(2)}, t) &= \tilde{f}_2(\boldsymbol{X}^{(1)\prime}, \boldsymbol{\xi}^{(1)\prime}, \boldsymbol{X}^{(2)\prime}_-, \boldsymbol{\xi}^{(2)\prime}, t - \Delta t) \\ &= \tilde{f}_1(\boldsymbol{X}^{(1)\prime}, \boldsymbol{\xi}^{(1)\prime}, t - \Delta t)\tilde{f}_1(\boldsymbol{X}^{(2)\prime}_-, \boldsymbol{\xi}^{(2)\prime}, t - \Delta t). \quad \text{(A.7)}\end{aligned}$$

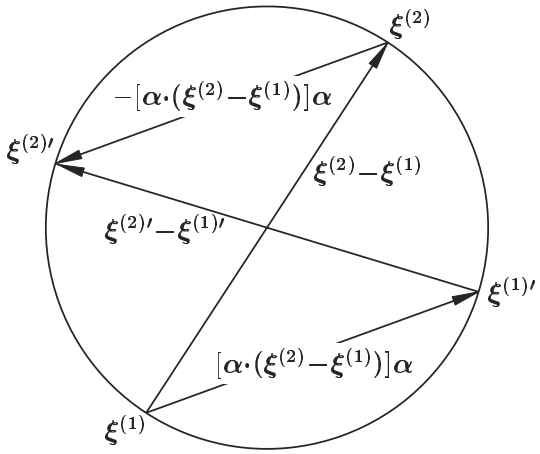

Figure A.1. Relation between $(\boldsymbol{\xi}^{(1)}, \boldsymbol{\xi}^{(2)})$ and $(\boldsymbol{\xi}^{(1)\prime}, \boldsymbol{\xi}^{(2)\prime})$. The velocities $\boldsymbol{\xi}^{(1)\prime}$ and $\boldsymbol{\xi}^{(2)\prime}$ are antipodal points on the sphere with $\boldsymbol{\xi}^{(1)}$ and $\boldsymbol{\xi}^{(2)}$ as its antipodal points.

Now, we introduce another assumption that the one-particle truncated density function $\tilde{f}_1$ is a *slowly varying* function in space $\boldsymbol{X}^{(1)}$ on the scale of d_m and in time t on the scale of d_m/ξ_0.[8] Then, in the function $\tilde{f}_1$ of Eqs. (A.5) and (A.7), the arguments $\boldsymbol{X}_-^{(2)}$, $\boldsymbol{X}^{(1)\prime}$, and $\boldsymbol{X}_-^{(2)\prime}$ can be replaced by $\boldsymbol{X}^{(1)}$, and the argument $t-\Delta t$ by t, because $|\boldsymbol{X}_-^{(2)}-\boldsymbol{X}^{(1)}|$, $|\boldsymbol{X}^{(1)\prime}-\boldsymbol{X}^{(1)}|$, and $|\boldsymbol{X}_-^{(2)\prime}-\boldsymbol{X}^{(1)}|$ are all of the order of d_m and Δt is of the order of d_m/ξ_0. With Eqs. (A.5) and (A.7) thus simplified, the integral on the right-hand side of Eq. (A.3a) is expressed by the one-particle truncated density function $\tilde{f}_1$ as

$$\int_{\partial S_1^2,\,\text{all }\boldsymbol{\xi}^{(2)}} (\boldsymbol{\xi}^{(2)}-\boldsymbol{\xi}^{(1)})\cdot\boldsymbol{n}_1^2\tilde{f}_2\mathrm{d}^2\boldsymbol{X}^{(2)}\mathbf{d}\boldsymbol{\xi}^{(2)} = I_- + I_+, \tag{A.8}$$

where

$$I_- = \int_{\substack{\partial S_{1-}^2\\ \text{all }\boldsymbol{\xi}^{(2)}}} (\boldsymbol{\xi}^{(2)}-\boldsymbol{\xi}^{(1)})\cdot\boldsymbol{n}_1^2\tilde{f}_1(\boldsymbol{X}^{(1)},\boldsymbol{\xi}^{(1)},t)\tilde{f}_1(\boldsymbol{X}^{(1)},\boldsymbol{\xi}^{(2)},t)\mathrm{d}^2\boldsymbol{X}^{(2)}\mathbf{d}\boldsymbol{\xi}^{(2)}, \tag{A.9a}$$

$$I_+ = \int_{\substack{\partial S_{1+}^2\\ \text{all }\boldsymbol{\xi}^{(2)}}} (\boldsymbol{\xi}^{(2)}-\boldsymbol{\xi}^{(1)})\cdot\boldsymbol{n}_1^2\tilde{f}_1(\boldsymbol{X}^{(1)},\boldsymbol{\xi}^{(1)\prime},t)\tilde{f}_1(\boldsymbol{X}^{(1)},\boldsymbol{\xi}^{(2)\prime},t)\mathrm{d}^2\boldsymbol{X}^{(2)}\mathbf{d}\boldsymbol{\xi}^{(2)}. \tag{A.9b}$$

The arguments $\boldsymbol{X}^{(1)}$ and t of $\tilde{f}_1$ being common, the integral over the hemisphere ∂S_{1-}^2 in I_- can be extended to the whole sphere ∂S_1^2 simply by replacing $(\boldsymbol{\xi}^{(2)}-$

[8] (i) The d_m/ξ_0 is the time that is taken to pass the distance d_m with the characteristic speed ξ_0 of the particles or the sound speed of the gas.

(ii) Owing to the slowly varying assumption, the Boltzmann equation to be derived cannot describe the behavior of the molecular scale.

$\boldsymbol{\xi}^{(1)})\cdot\boldsymbol{n}_1^2$ by $-|(\boldsymbol{\xi}^{(2)}-\boldsymbol{\xi}^{(1)})\cdot\boldsymbol{n}_1^2|/2$, that is,

$$I_- = -\frac{1}{2}\int_{\substack{\partial S_1^2 \\ \text{all } \boldsymbol{\xi}^{(2)}}} |(\boldsymbol{\xi}^{(2)}-\boldsymbol{\xi}^{(1)})\cdot\boldsymbol{n}_1^2|\tilde{f}_1(\boldsymbol{X}^{(1)},\boldsymbol{\xi}^{(1)},t)\tilde{f}_1(\boldsymbol{X}^{(1)},\boldsymbol{\xi}^{(2)},t)\mathrm{d}^2\boldsymbol{X}^{(2)}\mathbf{d}\boldsymbol{\xi}^{(2)}$$

$$= -\frac{d_m^2}{2}\int_{\substack{\text{all } \boldsymbol{e} \\ \text{all } \boldsymbol{\xi}^{(2)}}} |(\boldsymbol{\xi}^{(2)}-\boldsymbol{\xi}^{(1)})\cdot\boldsymbol{e}|\tilde{f}_1(\boldsymbol{X}^{(1)},\boldsymbol{\xi}^{(1)},t)\tilde{f}_1(\boldsymbol{X}^{(1)},\boldsymbol{\xi}^{(2)},t)\mathrm{d}\Omega(\boldsymbol{e})\mathbf{d}\boldsymbol{\xi}^{(2)}, \tag{A.10}$$

where $\boldsymbol{e}$ is a unit vector and $\mathrm{d}\Omega(\boldsymbol{e})$ is the solid angle element in the direction of $\boldsymbol{e}$. The extension of the range of integration of the integral I_+ needs some care. The parameter $\boldsymbol{\alpha}$ in the expressions $\boldsymbol{\xi}^{(1)\prime}$ and $\boldsymbol{\xi}^{(2)\prime}$ given by Eq. (A.6) is a function of $\boldsymbol{e}$ and $\boldsymbol{\xi}^{(2)}-\boldsymbol{\xi}^{(1)}$, that is,

$$\boldsymbol{\alpha} = \boldsymbol{\alpha}(\boldsymbol{e},\ \boldsymbol{\xi}^{(2)}-\boldsymbol{\xi}^{(1)}), \tag{A.11}$$

where $\boldsymbol{e} = \boldsymbol{n}_1^2$ [$= (\boldsymbol{X}^{(2)}-\boldsymbol{X}^{(1)})/|\boldsymbol{X}^{(2)}-\boldsymbol{X}^{(1)}|$]. The relation (A.11) is determined by the two-body interaction under interparticle potential, and $\boldsymbol{\alpha}$ is in the plane made by the two vectors $\boldsymbol{e}$ and $\boldsymbol{\xi}^{(2)}-\boldsymbol{\xi}^{(1)}$ (Section A.2.4). The relation is not unique because $\boldsymbol{\alpha}$ and $-\boldsymbol{\alpha}$ give the same result in Eq. (A.6). The relation can be made unique without loss of generality by choosing $(\boldsymbol{\xi}^{(2)}-\boldsymbol{\xi}^{(1)})\cdot\boldsymbol{\alpha} > 0$ here [when $(\boldsymbol{\xi}^{(2)}-\boldsymbol{\xi}^{(1)})\cdot\boldsymbol{e} > 0$]. We extend the relation (A.11) for $(\boldsymbol{\xi}^{(2)}-\boldsymbol{\xi}^{(1)})\cdot\boldsymbol{e} < 0$ as

$$\boldsymbol{\alpha}(\boldsymbol{e},\ \boldsymbol{\xi}^{(2)}-\boldsymbol{\xi}^{(1)}) = -\boldsymbol{\alpha}(-\boldsymbol{e},\ \boldsymbol{\xi}^{(2)}-\boldsymbol{\xi}^{(1)}). \tag{A.12}$$

For example, $\boldsymbol{\alpha} = \boldsymbol{e}$ for a hard-sphere particle. With the extension (A.12), the functions $\tilde{f}_1(\boldsymbol{X}^{(1)},\boldsymbol{\xi}^{(1)\prime},t)$ and $\tilde{f}_1(\boldsymbol{X}^{(1)},\boldsymbol{\xi}^{(2)\prime},t)$ in the integral I_+ are symmetrically extended with respect to $(\boldsymbol{\xi}^{(2)}-\boldsymbol{\xi}^{(1)})\cdot\boldsymbol{e} = 0$ to the whole ∂S_1^2, and thus, the integral I_+ is expressed with its range of integration extended as

$$I_+ = \frac{d_m^2}{2}\int_{\substack{\text{all } \boldsymbol{e} \\ \text{all } \boldsymbol{\xi}^{(2)}}} |(\boldsymbol{\xi}^{(2)}-\boldsymbol{\xi}^{(1)})\cdot\boldsymbol{e}|\tilde{f}_1(\boldsymbol{X}^{(1)},\boldsymbol{\xi}^{(1)\prime},t)\tilde{f}_1(\boldsymbol{X}^{(1)},\boldsymbol{\xi}^{(2)\prime},t)\mathrm{d}\Omega(\boldsymbol{e})\mathbf{d}\boldsymbol{\xi}^{(2)}. \tag{A.13}$$

Then, with Eqs. (A.8)–(A.13) in Eq. (A.3a), the equation for $\tilde{f}_1(\boldsymbol{X}^{(1)},\boldsymbol{\xi}^{(1)},t)$ is given as

$$\frac{\partial\tilde{f}_1}{\partial t} + \boldsymbol{\xi}^{(1)}\frac{\partial\tilde{f}_1}{\partial\boldsymbol{X}^{(1)}}$$

$$= \frac{Nd_m^2}{2}\int_{\substack{\text{all } \boldsymbol{e} \\ \text{all } \boldsymbol{\xi}^{(2)}}} |(\boldsymbol{\xi}^{(2)}-\boldsymbol{\xi}^{(1)})\cdot\boldsymbol{e}|[\tilde{f}_1(\boldsymbol{\xi}^{(1)\prime})\tilde{f}_1(\boldsymbol{\xi}^{(2)\prime}) - \tilde{f}_1(\boldsymbol{\xi}^{(1)})\tilde{f}_1(\boldsymbol{\xi}^{(2)})]\mathrm{d}\Omega(\boldsymbol{e})\mathbf{d}\boldsymbol{\xi}^{(2)}, \tag{A.14}$$

where $(N-1)d_m^2$ is identified with Nd_m^2 in the Grad–Boltzmann limit, and the arguments for the space and time variables of the truncated density function $\tilde{f}_1$ are not shown, because they are commonly $\boldsymbol{X}^{(1)}$ and t.

Now consider the following marginal probability density functions f_1, f_2, ...:

$$f_1 = \int_{\substack{\text{all } \boldsymbol{X}^{(2)},\ldots,\text{all } \boldsymbol{X}^{(N)} \\ \text{all } \boldsymbol{\xi}^{(2)},\ldots,\text{all } \boldsymbol{\xi}^{(N)}}} f^N \mathbf{d}\boldsymbol{X}^{(2)} \cdots \mathbf{d}\boldsymbol{X}^{(N)} \mathbf{d}\boldsymbol{\xi}^{(2)} \cdots \mathbf{d}\boldsymbol{\xi}^{(N)}, \tag{A.15a}$$

$$f_2 = \int_{\substack{\text{all } \boldsymbol{X}^{(3)},\ldots,\text{all } \boldsymbol{X}^{(N)} \\ \text{all } \boldsymbol{\xi}^{(3)},\ldots,\text{all } \boldsymbol{\xi}^{(N)}}} f^N \mathbf{d}\boldsymbol{X}^{(3)} \cdots \mathbf{d}\boldsymbol{X}^{(N)} \mathbf{d}\boldsymbol{\xi}^{(3)} \cdots \mathbf{d}\boldsymbol{\xi}^{(N)}, \tag{A.15b}$$

$$\cdots\cdots\cdots .$$

The f_1 is the probability density of finding the particle 1 with velocity $\boldsymbol{\xi}^{(1)}$ at position $\boldsymbol{X}^{(1)}$ and at time t, irrespective of the positions and the velocities of the other particles (or the particles $2, 3, \ldots, N$) and so on.

The difference between f_1 and $\tilde{f}_1$ is only the domains of integration with respect to the space variables $\boldsymbol{X}^{(2)}, \ldots, \boldsymbol{X}^{(N)}$ in their definitions. Noting that the whole space of $\boldsymbol{X}^{(2)} \times \cdots \times \boldsymbol{X}^{(N)}$ is $(S_1^2 + D_1^2) \times \cdots \times (S_1^N + D_1^N)$ and that the function f^N is symmetric with respect to the N sets of the variables $(\boldsymbol{X}^{(r)}, \boldsymbol{\xi}^{(r)})$ $(r = 1, 2, \ldots, N)$, we have[9]

$$\begin{aligned} f_1 &= \tilde{f}_1 + (N-1) \int_{S_1^2} \tilde{f}_2 \mathbf{d}\boldsymbol{X}^{(2)} \mathbf{d}\boldsymbol{\xi}^{(2)} + \cdots \\ &= \tilde{f}_1 + O(||\tilde{f}_1||(N-1)d_m^3/L^3) + \cdots . \end{aligned} \tag{A.16}$$

Thus, in the Grad–Boltzmann limit, we can identify $\tilde{f}_1$ with f_1. Put

$$f(\boldsymbol{X}, \boldsymbol{\xi}, t) = mN\tilde{f}_1(\boldsymbol{X}, \boldsymbol{\xi}, t). \tag{A.17}$$

Then $f(\boldsymbol{X}, \boldsymbol{\xi}, t)\mathbf{d}\boldsymbol{X}\mathbf{d}\boldsymbol{\xi}$ is the expected value of the mass of the particles at time t in the volume element $\mathbf{d}\boldsymbol{X}\mathbf{d}\boldsymbol{\xi}$ around $(\boldsymbol{X}, \boldsymbol{\xi})$ in the 6-dimensional space.[10]

From Eqs. (A.14) and (A.17), the equation for $f(\boldsymbol{X}, \boldsymbol{\xi}, t)$ is given in the form

$$\begin{aligned} &\frac{\partial f}{\partial t} + \boldsymbol{\xi} \frac{\partial f}{\partial \boldsymbol{X}} \\ &= \frac{N d_m^2}{2} \left(\frac{1}{mN} \right) \int_{\substack{\text{all } \boldsymbol{e} \\ \text{all } \boldsymbol{\xi}_*}} |(\boldsymbol{\xi}_* - \boldsymbol{\xi}) \cdot \boldsymbol{e}| [f(\boldsymbol{\xi}') f(\boldsymbol{\xi}_*') - f(\boldsymbol{\xi}) f(\boldsymbol{\xi}_*)] \mathrm{d}\Omega(\boldsymbol{e}) \mathbf{d}\boldsymbol{\xi}_*, \end{aligned} \tag{A.18}$$

---

[9] See Footnote 5 in this section.

[10] Let $\varphi(\boldsymbol{X}^{(1)}, \ldots, \boldsymbol{X}^{(N)}, \boldsymbol{\xi}^{(1)}, \ldots, \boldsymbol{\xi}^{(N)})$ be the function in the $6N$-dimensional space $\boldsymbol{X}^{(1)}, \ldots, \boldsymbol{X}^{(N)}, \boldsymbol{\xi}^{(1)}, \ldots, \boldsymbol{\xi}^{(N)}$ giving the number of the sets $(\boldsymbol{X}^{(i)}, \boldsymbol{\xi}^{(i)})$ $(i = 1, \ldots, N)$ that lie in a 6-dimensional domain I (for example, $X_{ai} \le X_i^{(r)} \le X_{bi}$, $\xi_{ai} \le \xi_i^{(r)} \le \xi_{bi}$). Then, the expected value $\bar{\varphi}$ of φ is given by

$$\begin{aligned} \bar{\varphi} &= \int_{\text{all } \boldsymbol{X}^{(1)},\ldots,\text{all } \boldsymbol{X}^{(N)},\ \text{all } \boldsymbol{\xi}^{(1)},\ldots,\text{all } \boldsymbol{\xi}^{(N)}} \varphi f^N \mathbf{d}\boldsymbol{X}^{(1)} \cdots \mathbf{d}\boldsymbol{X}^{(N)} \mathbf{d}\boldsymbol{\xi}^{(1)} \cdots \mathbf{d}\boldsymbol{\xi}^{(N)} \\ &= \int_I N f_1 \mathbf{d}\boldsymbol{X}^{(1)} \mathbf{d}\boldsymbol{\xi}^{(1)}, \end{aligned}$$

for a symmetric f^N in view of the decomposition $\varphi = \sum_{i=1}^N \varphi_I(\boldsymbol{X}^{(i)}, \boldsymbol{\xi}^{(i)})$, where $\varphi_I(\boldsymbol{X}^{(i)}, \boldsymbol{\xi}^{(i)}) = 1$ for $(\boldsymbol{X}^{(i)}, \boldsymbol{\xi}^{(i)})$ in I and $= 0$ outside I.

where

$$\boldsymbol{\xi}' = \boldsymbol{\xi} + [\boldsymbol{\alpha}\cdot(\boldsymbol{\xi}_* - \boldsymbol{\xi})]\boldsymbol{\alpha}, \quad \boldsymbol{\xi}'_* = \boldsymbol{\xi}_* - [\boldsymbol{\alpha}\cdot(\boldsymbol{\xi}_* - \boldsymbol{\xi})]\boldsymbol{\alpha}, \tag{A.19}$$

and the relation between $\boldsymbol{e}$ and $\boldsymbol{\alpha}$ is given by Eq. (A.11). The following function B, which is closely related to the differential cross-section (e.g., Reif [1965]), is often introduced to relate $\boldsymbol{e}$ to $\boldsymbol{\alpha}$:

$$|\boldsymbol{e}\cdot(\boldsymbol{\xi}_* - \boldsymbol{\xi})|\mathrm{d}\Omega(\boldsymbol{e}) = \frac{2}{d_m^2} B\mathrm{d}\Omega(\boldsymbol{\alpha}). \tag{A.20}$$

In view of the extension of the relation between $\boldsymbol{\alpha}$ and $\boldsymbol{e}$ for $(\boldsymbol{\xi}^{(2)} - \boldsymbol{\xi}^{(1)})\cdot\boldsymbol{e} < 0$ by Eq. (A.12), B is even with respect to $\boldsymbol{\alpha}$. According to the discussion in Section A.2.4, which relates B to the interparticle potential, B is a function of $|\boldsymbol{\alpha}\cdot(\boldsymbol{\xi}_* - \boldsymbol{\xi})|/|\boldsymbol{\xi}_* - \boldsymbol{\xi}|$ and $|\boldsymbol{\xi}_* - \boldsymbol{\xi}|$, i.e., $B = B(|\boldsymbol{\alpha}\cdot(\boldsymbol{\xi}_* - \boldsymbol{\xi})|/|\boldsymbol{\xi}_* - \boldsymbol{\xi}|, |\boldsymbol{\xi}_* - \boldsymbol{\xi}|)$. For a hard-sphere particle, $B = d_m^2|\boldsymbol{\alpha}\cdot(\boldsymbol{\xi}_* - \boldsymbol{\xi})|/2$ because $\boldsymbol{\alpha} = \boldsymbol{e}$. Then,

$$\frac{\partial f}{\partial t} + \boldsymbol{\xi}\frac{\partial f}{\partial \boldsymbol{X}} = \frac{1}{m}\int_{\substack{\text{all } \boldsymbol{\alpha} \\ \text{all } \boldsymbol{\xi}_*}} [f(\boldsymbol{\xi}')f(\boldsymbol{\xi}'_*) - f(\boldsymbol{\xi})f(\boldsymbol{\xi}_*)]B\mathrm{d}\Omega(\boldsymbol{\alpha})\mathbf{d}\boldsymbol{\xi}_*, \tag{A.21}$$

$$B = B(|\boldsymbol{\alpha}\cdot(\boldsymbol{\xi}_* - \boldsymbol{\xi})|/|\boldsymbol{\xi}_* - \boldsymbol{\xi}|, |\boldsymbol{\xi}_* - \boldsymbol{\xi}|).$$

Here, some comments may be in order about the relation between $\boldsymbol{e}$ and $\boldsymbol{\alpha}$. While $\boldsymbol{e}$ is moving over the unit sphere, $\boldsymbol{\alpha}$ also moves there, but the correspondence between $\boldsymbol{e}$ and $\boldsymbol{\alpha}$ is not generally one-to-one. Several $\boldsymbol{e}$'s may correspond to a single $\boldsymbol{\alpha}$, though the opposite is unique. For such $\boldsymbol{\alpha}$, the sum of B defined by the differential relation (A.20) at each $\boldsymbol{e}$ must be adopted as B in Eq. (A.21) [see Eq. (A.58) in Section A.2.4].

Equation (A.21) is the Boltzmann equation [Eq. (1.5) with (1.6), (1.7), and $F_i = 0$] introduced in Section 1.2.

In the derivation of the Boltzmann equation, the molecular-chaos assumption is introduced for the two-particle truncated density function $\tilde{f}_2$ for the situation that two particles are going to interact (or in I_-). If this assumption is also introduced for the situation that two particles have just finished interaction (or in I_+),[11] then the interaction term $(I_- + I_+)$ vanishes[12] and the Boltzmann equation is reduced to the equation for a free molecular gas (or the equation without the collision term) given by Eq. (2.1). If the density function f^N is factorized initially, the particles undergo molecular collision as time goes on, and then f^N (thus, $\tilde{f}_2$) is no longer factorized for the pair of the variables that undergoes particle collision. Thus, the molecular-chaos assumption in the analysis implicitly assumes that the chance of collision of the set of particles

[11] Obviously from the form of the distribution function $\tilde{f}_2$ after interaction derived under the assumption of molecular chaos before the interaction, the assumption of molecular chaos after the interaction is not compatible with that before interaction.

[12] In Eq. (A.3a), the slowly varying assumption on $\tilde{f}_1$ being used after the replacement of $\tilde{f}_2$ by the product of $\tilde{f}_1$ on its right-hand side of Eq. (A.3a), it is reduced to Eq. (A.8) where the arguments $\boldsymbol{\xi}^{(1)\prime}$ and $\boldsymbol{\xi}^{(2)\prime}$ of the two $\tilde{f}_1$'s in I_+ given by Eq. (A.9b) are replaced by $\boldsymbol{\xi}^{(1)}$ and $\boldsymbol{\xi}^{(2)}$ respectively. Then the integral with respect to $\mathrm{d}^2\boldsymbol{X}^{(2)}$ over the sphere ∂S_1^2 in I_+ is reduced to that of $(\boldsymbol{\xi}^{(2)} - \boldsymbol{\xi}^{(1)})\cdot\boldsymbol{n}_1^2$ over the sphere, which is easily seen to vanish.

that experienced collision between them is negligibly small.[13] The mathematical verification of the Boltzmann equation for a hard-sphere gas from the Liouville equation is studied by Lanford [1975] (see also Spohn [1991], Cercignani, Illner & Pulvirenti [1994]).[14]

---

[13]The period of time that this condition holds is roughly estimated as follows. In the first mean free time $\bar{\tau}_c$, all the molecules make their first collision on the average. In the next mean free time, the chance that any of the molecules collides with the molecule that it collided is $1/N$. Continuing this estimate, we find that the condition holds for $0 \le t < N_h\bar{\tau}_c$ where $N_h \gg 1$ but $N_h/N \ll 1$. Here, we considered the simple case where the order of the mean free time is invariant of time, e.g., the spatially uniform or periodic case.

[14]The proof is done by comparison of three systems, the BBGKY hierarchy, the Boltzmann hierarchy, and the Boltzmann equation. The *BBGKY hierarchy* for the N-particle system is a set of N equations for the marginal probability density functions f_s^N's ($s = 1, 2, \ldots, N$) derived from the Liouville equation by the same procedure as the Grad hierarchy for $\tilde{f}_s$, with the difference of the definition of f_s^N from that of $\tilde{f}_s$. That is, the definition of f_s^N is formally given by Eqs. (A.2a), (A.2b), etc., but their ranges Ω_1, Ω_{12}, etc. of integration are limited to the region where the hard-sphere particles can move, e.g., all the spheres S_i^j for any pair (i, j) are excluded from Ω_1. Then, in the resulting equations, the singular potentials of the hard-sphere particles disappear; instead, the boundary terms on the modified Ω_1, Ω_{12}, etc. appear [e.g., the right-hand side of Eq. (A.3a)], where the data after collision should be replaced by those before the collision by the interaction relation to complete the system of time evolution. The *Boltzmann hierarchy* is an infinite set of equations for f_s corresponding to f_s^N derived formally from the BBGKY hierarchy in the Grad–Boltzmann limit ($N \to \infty$, $d_m \to 0$, with Nd_m^2 fixed).

The framework of Lanford's work is to prove the following statements (i)–(iv). Then, the relation between the particle system and the Boltzmann equation is established in the Grad–Boltzmann limit.

(i) The BBGKY hierarchy is equivalent to the Liouville equation or the dynamics for a hard-sphere system.

(ii) The solution f_s^N of the initial-value problem of the BBGKY hierarchy converges, *in some sense,* to the solution f_s of the Boltzmann hierarchy in the Grad–Boltzmann limit, when its initial value g_s^N is in the factorized form $g_s^N = \prod_{l=1}^s [g(\boldsymbol{X}^{(l)}, \boldsymbol{\xi}^{(l)})]$.

(iii) Let $f(\boldsymbol{X}, \boldsymbol{\xi}, t)$ be the solution of the Boltzmann equation with the initial data $f(\boldsymbol{X}, \boldsymbol{\xi}, 0) = f_0(\boldsymbol{X}, \boldsymbol{\xi})$. Then, the function $f_s = \prod_{l=1}^s [f(\boldsymbol{X}^{(l)}, \boldsymbol{\xi}^{(l)}, t)/\mathsf{M}]$, where $s = 1, 2, \ldots$ and $\mathsf{M} = \lim_{N\to\infty} mN$, is a solution of the Boltzmann hierarchy for the initial data f_{s0} in the factorized form $f_{s0} = \prod_{l=1}^s [f_0(\boldsymbol{X}^{(l)}, \boldsymbol{\xi}^{(l)})/\mathsf{M}]$. Note the process from Eq. (A.17) to Eq. (A.21) for the factor $1/\mathsf{M}$.

(iv) The solution of the Boltzmann hierarchy with the initial data in a factorized form exists uniquely (the solution itself is not limited to a factorized form).

The proof is given for a limited time interval $0 \le t < t_0$, where t_0 is a fraction of the mean free time. This range $0 \le t < t_0$ is much smaller than the range where gas dynamic problems are discussed. Incidentally, the solution of the Boltzmann hierarchy exists as long as that of the Boltzmann equation exists. (Frankly speaking, the author has not examined the details of the proof by Lanford [1975].)

In the problem in an infinite domain without boundary discussed in the process of the Grad–Boltzmann limit, the particles extend to a wider range indefinitely as time goes on, and the local mean free path or time becomes larger. The average number of collisions of a particle up to time t is given by $\int_0^t \bar{\nu}_c \mathrm{d}t$, where $\bar{\nu}_c$ is the local mean collision frequency. The initial mean free path ℓ_0 and collision frequency $\bar{\nu}_{c0}$ are, respectively, of the orders of L^3/Nd_m^2 and $Nd_m^2\xi_0/L^3$. Their variations with time are roughly estimated in the following way: The particles substantially extend in the region of volume $L^3(1+\xi_0 t/L)^3$, and thus, the mean free path ℓ increases with time as $L^3(1+\xi_0 t/L)^3/Nd_m^2$ and the mean collision frequency $\bar{\nu}_c$ decreases and is bounded by $Nd_m^2\xi_0/L^3(1+\xi_0 t/L)^3$, because the range of particle speed at a point in space $\boldsymbol{X}$ decreases from ξ_0. Therefore, $\int_0^t \bar{\nu}_c \mathrm{d}t$ is bounded by $\bar{\nu}_{c0}L/\xi_0$ for any t. Thus, the average number of collisions of a particle up to $t = \infty$ can be much less than

Before closing this appendix, the formula (A.4) is derived.

Lemma.

$$\frac{\mathrm{d}}{\mathrm{d}\vartheta}\int_{\mathcal{D}(\vartheta)} g(\boldsymbol{X},\vartheta)\mathbf{d}\boldsymbol{X} = \int_{\mathcal{D}(\vartheta)} \frac{\partial g(\boldsymbol{X},\vartheta)}{\partial\vartheta}\mathbf{d}\boldsymbol{X} + \int_{\partial\mathcal{D}(\vartheta)} g(\boldsymbol{X},\vartheta)\left(\frac{\partial \boldsymbol{X}_w}{\partial\vartheta}\cdot\boldsymbol{n}_w\right)\mathrm{d}^2\boldsymbol{X},$$

where $\boldsymbol{X}_w$ is a point on the boundary $\partial\mathcal{D}(\vartheta)$ of $\mathcal{D}(\vartheta)$, $\boldsymbol{n}_w$ is the outward unit normal vector to the boundary, and $\mathrm{d}^2\boldsymbol{X}$ is the surface element on $\partial\mathcal{D}(\vartheta)$; the quantity $(\boldsymbol{n}_w\cdot\partial\boldsymbol{X}_w/\partial\vartheta)$ as a whole has a definite meaning for the deformable domain $\mathcal{D}(\vartheta)$. This formula applies to the space $\boldsymbol{X}$ with arbitrary dimension (say N).

Proof. Let $\mathcal{D}(0)$ be a fixed domain and Y_j be a point in it, which has a one-to-one correspondence to the domain $\mathcal{D}(\vartheta)$ as $X_i = X_i(Y_j,\vartheta)$. Then, the integral over the variable domain $\mathcal{D}(\vartheta)$ is expressed by that over the fixed domain $\mathcal{D}(0)$, for which the differentiation with respect to ϑ is carried out:

$$\begin{aligned}
&\frac{\mathrm{d}}{\mathrm{d}\vartheta}\int_{\mathcal{D}(\vartheta)} g(\boldsymbol{X},\vartheta)\mathbf{d}\boldsymbol{X}\\
&= \frac{\mathrm{d}}{\mathrm{d}\vartheta}\int_{\mathcal{D}(0)} g(\boldsymbol{X}(\boldsymbol{Y},\vartheta),\vartheta)J(\boldsymbol{Y},\vartheta)\mathbf{d}\boldsymbol{Y}\\
&= \int_{\mathcal{D}(0)}\left(\frac{\partial g(\boldsymbol{X},\vartheta)}{\partial\vartheta} + \frac{\partial g(\boldsymbol{X},\vartheta)}{\partial X_i}\frac{\partial X_i}{\partial\vartheta}\right)J(\boldsymbol{Y},\vartheta)\mathbf{d}\boldsymbol{Y} + \int_{\mathcal{D}(0)} g(\boldsymbol{X},\vartheta)\frac{\partial J}{\partial\vartheta}\mathbf{d}\boldsymbol{Y}\\
&= \int_{\mathcal{D}(\vartheta)}\left(\frac{\partial g(\boldsymbol{X},\vartheta)}{\partial\vartheta} + \frac{\partial g(\boldsymbol{X},\vartheta)}{\partial X_i}\frac{\partial X_i}{\partial\vartheta}\right)\mathbf{d}\boldsymbol{X} + \int_{\mathcal{D}(0)} g(\boldsymbol{X},\vartheta)\frac{\partial J}{\partial\vartheta}\mathbf{d}\boldsymbol{Y}, \qquad \text{(A.22)}
\end{aligned}$$

where J is the Jacobian of the transformation from Y_i to X_i. Let $\mathbb{T}$ be the transformation matrix whose (i,j) element T_{ij} is given by

$$T_{ij} = \frac{\partial X_i}{\partial Y_j}, \quad \text{that is,} \quad \mathbb{T} = \langle T_{ij}\rangle = \left\langle \frac{\partial X_i}{\partial Y_j}\right\rangle.$$

---

unity for small $\bar{\nu}_{c0}L/\xi_0$. Thus, the global validity of the proposition for small $\bar{\nu}_{c0}L/\xi_0$ does not help much for the understanding of the validity of the Boltzmann equation on the basis of the particle system. Real extension of the range is required.

The discussion in the preceding footnote (Footnote 13) suggests that the probability density function f^N or f_N^N is no longer in the form of the product $\prod_{l=1}^N[f(\boldsymbol{X}^{(l)},\boldsymbol{\xi}^{(l)},t)/mN]$ after the mean free time $\bar{\tau}_c$. On the other hand, the marginal distribution function f_2^N is well approximated by the product $\prod_{l=1}^2[f(\boldsymbol{X}^{(l)},\boldsymbol{\xi}^{(l)},t)/mN]$ for much longer time than the mean free time $\bar{\tau}_c$ when N is large. The above properties of f_N^N at the mean free time does not contradict the solution of the Boltzmann hierarchy in the form of the product. The following case is compatible with the preceding solution of the Boltzmann hierarchy: the solution f_s^N $(s=1,\ldots,n)$ of the BBGKY hierarchy is in the form of the product for some $n<N$, and it retains the form in the limit $N\to\infty$ for some n such that $n\ll N$ and $n\to\infty$. Incidentally, the relation between the BBGKY hierarchy and the Boltzmann equation is established if the convergence of f_1^N to f_1 and the uniqueness of f_1 of the Boltzmann hierarchy are proved.

The Jacobian is the determinant derived from the matrix $\langle T_{ij}\rangle$,[15] i.e.,

$$J = \left\| \frac{\partial X_i}{\partial Y_j} \right\|, \text{ and thus, } \frac{\partial J}{\partial \vartheta} = \frac{\partial}{\partial \vartheta} \left\| \frac{\partial X_i}{\partial Y_j} \right\|.$$

Then its inverse $\mathbb{T}^{-1}$ (or $\langle T_{ij}\rangle^{-1}$) is given by

$$\mathbb{T}^{-1} = \langle T_{ij}\rangle^{-1} = \left\langle \frac{\partial X_i}{\partial Y_j} \right\rangle^{-1} = \left\langle (-1)^{i+j} \frac{\Delta_{ji}}{J} \right\rangle,$$

where the element Δ_{ij} is the determinant of the submatrix of the matrix $\mathbb{T}$ with respect to its element T_{ij}.[16] The derivative $\partial J/\partial\vartheta$ of the Jacobian is transformed into the following form:

$$\begin{aligned}
\frac{\partial J}{\partial \vartheta} &= \frac{\partial}{\partial \vartheta} \left\| \frac{\partial X_i}{\partial Y_j} \right\| \\
&= \sum_{j=1}^{N} \sum_{i=1}^{N} (-1)^{i+j} \Delta_{ij} \frac{\partial}{\partial \vartheta} \left(\frac{\partial X_i}{\partial Y_j} \right) = \sum_{j=1}^{N} \sum_{i=1}^{N} (-1)^{i+j} \Delta_{ij} \frac{\partial}{\partial Y_j} \left(\frac{\partial X_i}{\partial \vartheta} \right) \\
&= \sum_{j=1}^{N} \sum_{i=1}^{N} (-1)^{i+j} \Delta_{ij} \sum_{k=1}^{N} \frac{\partial X_k}{\partial Y_j} \frac{\partial}{\partial X_k} \left(\frac{\partial X_i}{\partial \vartheta} \right) \\
&= \sum_{i=1}^{N} \sum_{k=1}^{N} \frac{\partial}{\partial X_k} \left(\frac{\partial X_i}{\partial \vartheta} \right) \left(\sum_{j=1}^{N} (-1)^{i+j} \Delta_{ij} \frac{\partial X_k}{\partial Y_j} \right) = \sum_{i=1}^{N} \sum_{k=1}^{N} J \delta_{ik} \frac{\partial}{\partial X_k} \left(\frac{\partial X_i}{\partial \vartheta} \right) \\
&= J \sum_{i=1}^{N} \frac{\partial}{\partial X_i} \left(\frac{\partial X_i}{\partial \vartheta} \right), \qquad \text{(A.23)}
\end{aligned}$$

where the following relation is used:

$$\sum_{j=1}^{N} (-1)^{i+j} \Delta_{ij} \frac{\partial X_k}{\partial Y_j} = J \delta_{ik},$$

and the summation sign $\sum$ is shown explicitly to make the order of summation explicit for clarity of deformation. With the aid of Eq. (A.23), the last integral in Eq. (A.22) is deformed into an integral over the domain $\mathcal{D}(\vartheta)$:

$$\begin{aligned}
\int_{\mathcal{D}(0)} g(\boldsymbol{X}, \vartheta) \frac{\partial J}{\partial \vartheta} \mathbf{d}\boldsymbol{Y} &= \int_{\mathcal{D}(0)} g(\boldsymbol{X}, \vartheta) \sum_{i=1}^{N} \frac{\partial}{\partial X_i} \left(\frac{\partial X_i}{\partial \vartheta} \right) J \mathbf{d}\boldsymbol{Y} \\
&= \int_{\mathcal{D}(\vartheta)} g(\boldsymbol{X}, \vartheta) \sum_{i=1}^{N} \frac{\partial}{\partial X_i} \left(\frac{\partial X_i}{\partial \vartheta} \right) \mathbf{d}\boldsymbol{X}.
\end{aligned}$$

[15] Consideration of the transformation $\mathbb{T}$ with a positive determinant is sufficient for the present purpose.

[16] The submatrix is defined as the matrix obtained by deleting the row and column containing the element T_{ij} from the matrix $\mathbb{T}$. The $(-1)^{i+j}\Delta_{ij}$ is called the cofactor of the element T_{ij}.

With this relation in Eq. (A.22), we obtain

$$\begin{aligned}
&\frac{\mathrm{d}}{\mathrm{d}\vartheta}\int_{\mathcal{D}(\vartheta)} g(\boldsymbol{X},\vartheta)\mathbf{d}\boldsymbol{X} \\
&\quad=\int_{\mathcal{D}(\vartheta)}\left[\frac{\partial g(\boldsymbol{X},\vartheta)}{\partial\vartheta}+\sum_{i=1}^{N}\frac{\partial}{\partial X_i}\left(\frac{\partial X_i}{\partial\vartheta}g(\boldsymbol{X},\vartheta)\right)\right]\mathbf{d}\boldsymbol{X} \\
&\quad=\int_{\mathcal{D}(\vartheta)}\frac{\partial g(\boldsymbol{X},\vartheta)}{\partial\vartheta}\mathbf{d}\boldsymbol{X}+\int_{\partial\mathcal{D}(\vartheta)} g(\boldsymbol{X},\vartheta)\left(\frac{\partial \boldsymbol{X}_w}{\partial\vartheta}\cdot\boldsymbol{n}_w\right)\mathrm{d}^2\boldsymbol{X}.
\end{aligned}$$

The last equation is obtained with the aid of Gauss's divergence theorem. The transformation $X_i = X_i(Y_j,\vartheta)$ is not unique for a given deformable $\mathcal{D}(\vartheta)$, but the quantity $(\boldsymbol{n}_w\cdot\partial\boldsymbol{X}_w/\partial\vartheta)$ in the last integral is uniquely determined by $\mathcal{D}(\vartheta)$, irrespective of the choice of $X_i = X_i(Y_j,\vartheta)$. ■

A.2 Collision integral

A.2.1 Binary collision

In the Boltzmann equation [Eq. (A.21) or Eq. (1.5) with (1.6)] or in its derivation in Section A.1, we encounter the relation [Eq. (A.19), (1.7), or (A.6)] between the initial and final velocities of collision of two molecules. Here, we will give its derivation.

Two molecules, molecule 0 and molecule 1, are in motion under the intermolecular potential. In the derivation of the Boltzmann equation, it is assumed that the intermolecular potential is a function of the distance between the two molecules and that its effect extends to a finite distance d_m. What we are interested in here is the relation between the velocities of the two molecules before and after the interaction. Let $\boldsymbol{\xi}$ and $\boldsymbol{\xi}'$ be, respectively, the velocities of the molecule 0 before and after the interaction, and let $\boldsymbol{\xi}_*$ and $\boldsymbol{\xi}'_*$ be those of the molecule 1. Then, owing to the conservation laws of the momentum and energy of the system,

$$\boldsymbol{\xi}+\boldsymbol{\xi}_* = \boldsymbol{\xi}'+\boldsymbol{\xi}'_*, \tag{A.24}$$

$$\boldsymbol{\xi}^2+\boldsymbol{\xi}_*^2 = \boldsymbol{\xi}'^2+\boldsymbol{\xi}_*'^2. \tag{A.25}$$

Generally, an external force, if any, is so small compared to the short-range intermolecular force that it does not produce an appreciable effect on the above conservation equations. The velocities after the interaction can be determined by those of before with additional two parameters.

As these parameters, we introduce a unit vector $\boldsymbol{\alpha}$ specifying the change of the direction of the velocity of molecule 0 by the interaction, i.e.,

$$\boldsymbol{\xi}'-\boldsymbol{\xi} = A\boldsymbol{\alpha}, \tag{A.26}$$

where A is an undetermined constant. From Eqs. (A.24) and (A.26),

$$\boldsymbol{\xi}'_*-\boldsymbol{\xi}_* = -A\boldsymbol{\alpha}. \tag{A.27}$$

Eliminating $\boldsymbol{\xi}'^2$ and $\boldsymbol{\xi}_*'^2$ in Eq. (A.25) with the aid of Eqs. (A.26) and (A.27), we have

$$A = \boldsymbol{\alpha} \cdot (\boldsymbol{\xi}_* - \boldsymbol{\xi}).$$

Therefore, we have

$$\boldsymbol{\xi}' = \boldsymbol{\xi} + [\boldsymbol{\alpha} \cdot (\boldsymbol{\xi}_* - \boldsymbol{\xi})]\boldsymbol{\alpha}, \tag{A.28a}$$

$$\boldsymbol{\xi}_*' = \boldsymbol{\xi}_* - [\boldsymbol{\alpha} \cdot (\boldsymbol{\xi}_* - \boldsymbol{\xi})]\boldsymbol{\alpha}, \tag{A.28b}$$

where $\boldsymbol{\alpha}$ and $-\boldsymbol{\alpha}$ are noted to give the same final velocities $(\boldsymbol{\xi}', \boldsymbol{\xi}_*')$. The relative velocity $\boldsymbol{\xi}_*' - \boldsymbol{\xi}'$ after collision is calculated as

$$\boldsymbol{\xi}_*' - \boldsymbol{\xi}' = \boldsymbol{\xi}_* - \boldsymbol{\xi} - 2[\boldsymbol{\alpha} \cdot (\boldsymbol{\xi}_* - \boldsymbol{\xi})]\boldsymbol{\alpha}. \tag{A.29}$$

Thus,

$$\boldsymbol{\alpha} \cdot (\boldsymbol{\xi}_*' - \boldsymbol{\xi}') = -\boldsymbol{\alpha} \cdot (\boldsymbol{\xi}_* - \boldsymbol{\xi}), \tag{A.30}$$

and further from Eq. (A.29),

$$(\boldsymbol{\xi}_*' - \boldsymbol{\xi}')^2 = (\boldsymbol{\xi}_* - \boldsymbol{\xi})^2. \tag{A.31}$$

The relative speed remains unchanged.

The transformation from the initial velocities to the final is a linear transformation. Its inverse is easily obtained from Eqs. (A.28a) and (A.28b) with the aid of Eq. (A.30) as

$$\boldsymbol{\xi} = \boldsymbol{\xi}' + [\boldsymbol{\alpha} \cdot (\boldsymbol{\xi}_*' - \boldsymbol{\xi}')]\boldsymbol{\alpha}, \tag{A.32a}$$

$$\boldsymbol{\xi}_* = \boldsymbol{\xi}_*' - [\boldsymbol{\alpha} \cdot (\boldsymbol{\xi}_*' - \boldsymbol{\xi}')]\boldsymbol{\alpha}. \tag{A.32b}$$

The transformation given by Eqs. (A.28a) and (A.28b) and its inverse, Eqs. (A.32a) and (A.32b), being of the same form, it is easily seen that the absolute value of the Jacobian of the transformation given by Eqs. (A.28a) and (A.28b) is unity. That is,

$$\left| \frac{\partial(\boldsymbol{\xi}', \boldsymbol{\xi}_*')}{\partial(\boldsymbol{\xi}, \boldsymbol{\xi}_*)} \right| = 1. \tag{A.33}$$

The Jacobian is easily seen to be -1 by direct calculation.

Finally, it is noted that a simple geometrical representation of the relations (A.28a) and (A.28b) is given in Fig. A.1 in Section A.1, where $(\boldsymbol{\xi}^{(1)}, \boldsymbol{\xi}^{(2)})$ and $(\boldsymbol{\xi}^{(1)\prime}, \boldsymbol{\xi}^{(2)\prime})$ correspond, respectively, to $(\boldsymbol{\xi}', \boldsymbol{\xi}_*')$ and $(\boldsymbol{\xi}, \boldsymbol{\xi}_*)$ in this subsection.[17]

A.2.2 Symmetry relation and its applications

Consider the following bilinear form related to the collision integral:

$$J(f, g) = \frac{1}{2m} \int_{\substack{\text{all } \boldsymbol{\alpha} \\ \text{all } \boldsymbol{\xi}_*}} (f' g_*' + f_*' g' - f g_* - f_* g) B \mathrm{d}\Omega(\boldsymbol{\alpha}) \mathbf{d}\boldsymbol{\xi}_*, \tag{A.34}$$

$$B = B(|\boldsymbol{\alpha} \cdot (\boldsymbol{\xi}_* - \boldsymbol{\xi})|/|\boldsymbol{\xi}_* - \boldsymbol{\xi}|, |\boldsymbol{\xi}_* - \boldsymbol{\xi}|).$$

[17] The relation between $(\boldsymbol{\xi}, \boldsymbol{\xi}_*)$ and $(\boldsymbol{\xi}', \boldsymbol{\xi}_*')$ is symmetric. We do not have to distinguish which is before or after the interaction and use the notation interchangeably.

The collision integral of the Boltzmann equation is expressed as $J(f,f)$. For a given function $\varphi(\boldsymbol{\xi})$ of $\boldsymbol{\xi}$, we define the integral $In_\varphi[J(f,g)]$

$$\begin{aligned} In_\varphi[J(f,g)] &= \int_{\text{all } \boldsymbol{\xi}} \varphi(\boldsymbol{\xi}) J(f,g) \mathbf{d}\boldsymbol{\xi} \\ &= \frac{1}{2m} \int \varphi(\boldsymbol{\xi})(f'g'_* + f'_* g' - fg_* - f_* g) B \mathrm{d}\Omega(\boldsymbol{\alpha}) \mathbf{d}\boldsymbol{\xi}_* \mathbf{d}\boldsymbol{\xi}. \end{aligned} \tag{A.35}$$

We will derive different expressions of $In_\varphi[J(f,g)]$ with the aid of the following transformation:
(TrA): Transcribe the letters $(\boldsymbol{\xi}, \boldsymbol{\xi}_*) \to (\boldsymbol{\xi}_*, \boldsymbol{\xi})$. By this transcription, $|\boldsymbol{\xi}_* - \boldsymbol{\xi}|$ and $|\boldsymbol{\alpha} \cdot (\boldsymbol{\xi}_* - \boldsymbol{\xi})|$ remain unchanged, but $(\boldsymbol{\xi}', \boldsymbol{\xi}'_*)$ changes to $(\boldsymbol{\xi}'_*, \boldsymbol{\xi}')$ owing to Eqs. (A.28a) and (A.28b). As a result, $B(|\boldsymbol{\alpha} \cdot (\boldsymbol{\xi}_* - \boldsymbol{\xi})|/|\boldsymbol{\xi}_* - \boldsymbol{\xi}|, |\boldsymbol{\xi}_* - \boldsymbol{\xi}|)$ and $f'g'_* + f'_* g' - fg_* - f_* g$ remain unchanged.
(TrB): First perform the change of variables of integration $(\boldsymbol{\xi}, \boldsymbol{\xi}_*, \boldsymbol{\alpha}) \to (\boldsymbol{\xi}', \boldsymbol{\xi}'_*, \boldsymbol{\alpha})$. According to the discussion in Section A.2.1, the absolute value of the Jacobian of the transformation is unity [Eq. (A.33)], $|\boldsymbol{\alpha} \cdot (\boldsymbol{\xi}'_* - \boldsymbol{\xi}')| = |\boldsymbol{\alpha} \cdot (\boldsymbol{\xi}_* - \boldsymbol{\xi})|$ [Eq. (A.30)], $|\boldsymbol{\xi}'_* - \boldsymbol{\xi}'| = |\boldsymbol{\xi}_* - \boldsymbol{\xi}|$ [Eq. (A.31)], and $(\boldsymbol{\xi}, \boldsymbol{\xi}_*)$ is expressed in $(\boldsymbol{\xi}', \boldsymbol{\xi}'_*)$ by Eqs. (A.32a) and (A.32b). Then, transcribe the letters $(\boldsymbol{\xi}', \boldsymbol{\xi}'_*) \to (\boldsymbol{\xi}, \boldsymbol{\xi}_*)$. As a result, the original $B(|\boldsymbol{\alpha} \cdot (\boldsymbol{\xi}_* - \boldsymbol{\xi})|/|\boldsymbol{\xi}_* - \boldsymbol{\xi}|, |\boldsymbol{\xi}_* - \boldsymbol{\xi}|)$ remains unchanged; the old $\boldsymbol{\xi}$ and $\boldsymbol{\xi}_*$ are replaced by the new $\boldsymbol{\xi}'$ and $\boldsymbol{\xi}'_*$ given by Eqs. (A.28a) and (A.28b) with the new $\boldsymbol{\xi}$ and $\boldsymbol{\xi}_*$, and thus, $f'g'_* + f'_* g' - fg_* - f_* g$ changes its sign.

Performing the transformation (TrA) or (TrB) to Eq. (A.35) or the result of the transformation, we obtain its four different expressions

$$In_\varphi[J(f,g)] = \frac{1}{2m} \int \varphi(\boldsymbol{\xi})(f'g'_* + f'_* g' - fg_* - f_* g) B \mathrm{d}\Omega(\boldsymbol{\alpha}) \mathbf{d}\boldsymbol{\xi}_* \mathbf{d}\boldsymbol{\xi}; \tag{A.36a}$$

applying the transformation (TrA) to Eq. (A.35),

$$= \frac{1}{2m} \int \varphi(\boldsymbol{\xi}_*)(f'g'_* + f'_* g' - fg_* - f_* g) B \mathrm{d}\Omega(\boldsymbol{\alpha}) \mathbf{d}\boldsymbol{\xi}_* \mathbf{d}\boldsymbol{\xi}; \tag{A.36b}$$

applying the transformation (TrB) to Eq. (A.35),

$$= \frac{-1}{2m} \int \varphi(\boldsymbol{\xi}')(f'g'_* + f'_* g' - fg_* - f_* g) B \mathrm{d}\Omega(\boldsymbol{\alpha}) \mathbf{d}\boldsymbol{\xi}_* \mathbf{d}\boldsymbol{\xi}; \tag{A.36c}$$

and applying the transformation (TrB) to Eq. (A.36b),

$$= \frac{-1}{2m} \int \varphi(\boldsymbol{\xi}'_*)(f'g'_* + f'_* g' - fg_* - f_* g) B \mathrm{d}\Omega(\boldsymbol{\alpha}) \mathbf{d}\boldsymbol{\xi}_* \mathbf{d}\boldsymbol{\xi}. \tag{A.36d}$$

Combining the two equations (A.36a) and (A.36b) or the four (A.36a)–(A.36d), we have

$$\begin{aligned} In_\varphi[J(f,g)] &= \frac{1}{4m} \int (\varphi + \varphi_*)(f'g'_* + f'_* g' - fg_* - f_* g) B \mathrm{d}\Omega(\boldsymbol{\alpha}) \mathbf{d}\boldsymbol{\xi}_* \mathbf{d}\boldsymbol{\xi} \\ &= \frac{1}{8m} \int (\varphi + \varphi_* - \varphi' - \varphi'_*)(f'g'_* + f'_* g' - fg_* - f_* g) B \mathrm{d}\Omega(\boldsymbol{\alpha}) \mathbf{d}\boldsymbol{\xi}_* \mathbf{d}\boldsymbol{\xi}, \end{aligned} \tag{A.36e}$$

where

$$\varphi = \varphi(\boldsymbol{\xi}), \quad \varphi_* = \varphi(\boldsymbol{\xi}_*), \quad \varphi' = \varphi(\boldsymbol{\xi}'), \quad \varphi'_* = \varphi(\boldsymbol{\xi}'_*).$$

Then, rewriting Eq. (A.36e) a little bit as

$$In_\varphi[J(f,g)] = \frac{1}{8m}\int(\varphi+\varphi_*-\varphi'-\varphi'_*)(f'g'_*+f'_*g')B\mathrm{d}\Omega(\boldsymbol{\alpha})\mathbf{d}\boldsymbol{\xi}_*\mathbf{d}\boldsymbol{\xi} - \frac{1}{8m}\int(\varphi+\varphi_*-\varphi'-\varphi'_*)(fg_*+f_*g)B\mathrm{d}\Omega(\boldsymbol{\alpha})\mathbf{d}\boldsymbol{\xi}_*\mathbf{d}\boldsymbol{\xi},$$

and applying the transformation (TrB) to the first integral on the right-hand side, we have

$$In_\varphi[J(f,g)] = \frac{1}{4m}\int(\varphi'+\varphi'_*-\varphi-\varphi_*)(fg_*+f_*g)B\mathrm{d}\Omega(\boldsymbol{\alpha})\mathbf{d}\boldsymbol{\xi}_*\mathbf{d}\boldsymbol{\xi}. \quad \text{(A.36f)}$$

Further, noting $(\varphi'+\varphi'_*-\varphi-\varphi_*) = (\varphi'-\varphi)+(\varphi'_*-\varphi_*)$ and applying the transformation (TrA) to the integral containing $(\varphi'_*-\varphi_*)$ in Eq. (A.36f), we have

$$In_\varphi[J(f,g)] = \frac{1}{2m}\int(\varphi'-\varphi)(fg_*+f_*g)B\mathrm{d}\Omega(\boldsymbol{\alpha})\mathbf{d}\boldsymbol{\xi}_*\mathbf{d}\boldsymbol{\xi}. \quad \text{(A.36g)}$$

Taking

$$\varphi(\boldsymbol{\xi}) = a_0 + \boldsymbol{a}\cdot\boldsymbol{\xi} + a_4\boldsymbol{\xi}^2,$$

where a_r is independent of $\boldsymbol{\xi}$ but may depend on $\boldsymbol{X}$ and t, in Eq. (A.36e) or (A.36f), we have

$$In_\varphi[J(f,g)] = 0,$$

owing to Eqs. (A.24) and (A.25).

Similar symmetry relations are naturally derived in the same way as above for the nondimensional collision integrals $\hat{J}(\hat{f},\hat{g})$ defined by Eq. (1.47b), $\mathcal{J}(\phi,\psi)$ by Eq. (1.75c), and their extensions $\hat{J}_a(\hat{f},\hat{g})$ by Eq. (A.114b) and $\mathcal{J}_a(\phi,\psi)$ by Eq. (A.114a), and also for the linearized collision integral and its extension $\mathcal{L}(\phi)$ by Eq. (1.75b) and $\mathcal{L}_a(\phi)$ by Eq. (A.111). The formulas corresponding to Eq. (A.36e) are listed here.

$$\int_{\text{all }\boldsymbol{\zeta}}\varphi(\boldsymbol{\zeta})\hat{J}_a(\hat{f},\hat{g})\mathbf{d}\boldsymbol{\zeta} = \frac{1}{2}\int\varphi(\boldsymbol{\zeta})(\hat{f}'\hat{g}'_*+\hat{f}'_*\hat{g}'-\hat{f}\hat{g}_*-\hat{f}_*\hat{g})\widehat{B}_a\mathrm{d}\Omega(\boldsymbol{\alpha})\mathbf{d}\boldsymbol{\zeta}_*\mathbf{d}\boldsymbol{\zeta}$$
$$= \frac{1}{8}\int(\varphi+\varphi_*-\varphi'-\varphi'_*)(\hat{f}'\hat{g}'_*+\hat{f}'_*\hat{g}'-\hat{f}\hat{g}_*-\hat{f}_*\hat{g})\widehat{B}_a\mathrm{d}\Omega(\boldsymbol{\alpha})\mathbf{d}\boldsymbol{\zeta}_*\mathbf{d}\boldsymbol{\zeta}, \quad \text{(A.37)}$$

$$\int_{\text{all }\boldsymbol{\zeta}}\varphi(\boldsymbol{\zeta})\mathcal{J}_a(\phi,\psi)E\mathbf{d}\boldsymbol{\zeta}$$
$$= \frac{1}{2}\int\varphi(\boldsymbol{\zeta})(\phi'\psi'_*+\phi'_*\psi'-\phi\psi_*-\phi_*\psi)\widehat{B}_a\mathrm{d}\Omega(\boldsymbol{\alpha})E_*E\mathbf{d}\boldsymbol{\zeta}_*\mathbf{d}\boldsymbol{\zeta}$$
$$= \frac{1}{8}\int(\varphi+\varphi_*-\varphi'-\varphi'_*)(\phi'\psi'_*+\phi'_*\psi'-\phi\psi_*-\phi_*\psi)\widehat{B}_aE_*E\mathrm{d}\Omega(\boldsymbol{\alpha})\mathbf{d}\boldsymbol{\zeta}_*\mathbf{d}\boldsymbol{\zeta}, \quad \text{(A.38)}$$

$$\begin{aligned}
&\int_{\text{all } \boldsymbol{\zeta}} \varphi(\boldsymbol{\zeta})\mathcal{L}_a(\phi)E\mathbf{d}\boldsymbol{\zeta} \\
&= \int \varphi(\boldsymbol{\zeta})(\phi' + \phi'_* - \phi - \phi_*)\widehat{B}_a E_* E\mathrm{d}\Omega(\boldsymbol{\alpha})\mathbf{d}\boldsymbol{\zeta}_*\mathbf{d}\boldsymbol{\zeta} \\
&= \frac{1}{4}\int (\varphi + \varphi_* - \varphi' - \varphi'_*)(\phi' + \phi'_* - \phi - \phi_*)\widehat{B}_a E_* E\mathrm{d}\Omega(\boldsymbol{\alpha})\mathbf{d}\boldsymbol{\zeta}_*\mathbf{d}\boldsymbol{\zeta}, \qquad \text{(A.39)}
\end{aligned}$$

where

$$\begin{aligned}
&\varphi = \varphi(\boldsymbol{\zeta}), \quad \varphi_* = \varphi(\boldsymbol{\zeta}_*), \quad \varphi' = \varphi(\boldsymbol{\zeta}'), \quad \varphi'_* = \varphi(\boldsymbol{\zeta}'_*), \\
&\boldsymbol{\zeta}' = \boldsymbol{\zeta} + [\boldsymbol{\alpha}\cdot(\boldsymbol{\zeta}_* - \boldsymbol{\zeta})]\boldsymbol{\alpha}, \quad \boldsymbol{\zeta}'_* = \boldsymbol{\zeta}_* - [\boldsymbol{\alpha}\cdot(\boldsymbol{\zeta}_* - \boldsymbol{\zeta})]\boldsymbol{\alpha},
\end{aligned}$$

and the formulas for $\hat{J}(\hat{f},\hat{g})$, $\mathcal{J}(\phi,\psi)$, and $\mathcal{L}(\phi)$ are omitted, because $\hat{J}(\hat{f},\hat{g}) = \hat{J}_1(\hat{f},\hat{g})$, $\mathcal{J}(\phi,\psi) = \mathcal{J}_1(\phi,\psi)$, and $\mathcal{L}(\phi) = \mathcal{L}_1(\phi)$.

Some important properties of the linearized collision integral $\mathcal{L}_a(\phi)$ are derived from the symmetry relation (A.39).

Obviously, from Eq. (A.39),

$$\int_{\text{all } \boldsymbol{\zeta}} \varphi(\boldsymbol{\zeta})\mathcal{L}_a(\phi)E\mathbf{d}\boldsymbol{\zeta} = \int_{\text{all } \boldsymbol{\zeta}} \phi(\boldsymbol{\zeta})\mathcal{L}_a(\varphi)E\mathbf{d}\boldsymbol{\zeta}. \qquad \text{(A.40)}$$

That is, the linearized collision operator is self-adjoint.

Putting $\varphi = \phi$ in Eq. (A.39), we have

$$\begin{aligned}
\int_{\text{all } \boldsymbol{\zeta}} \phi(\boldsymbol{\zeta})\mathcal{L}_a(\phi)E\mathbf{d}\boldsymbol{\zeta} &= -\frac{1}{4}\int (\phi' + \phi'_* - \phi - \phi_*)^2 \widehat{B}_a E_* E\mathrm{d}\Omega(\boldsymbol{\alpha})\mathbf{d}\boldsymbol{\zeta}_*\mathbf{d}\boldsymbol{\zeta} \\
&\le 0, \qquad \text{(A.41)}
\end{aligned}$$

where the equality holds when and only when

$$\phi' + \phi'_* - \phi - \phi_* = 0 \quad \text{ almost everywhere,}$$

because $\widehat{B}_a > 0$ almost everywhere.[18] The function ϕ that satisfies this relation is expressed by a linear combination of 1, ζ_i, and ζ_i^2 as to be shown in Section A.2.3. Thus, the equality in Eq. (A.41) holds when and only when ϕ is a linear combination of 1, ζ_i, and ζ_i^2.

Obviously, from the first relation of Eq. (A.41), the solution of the homogeneous equation

$$\mathcal{L}_a(\phi) = 0 \qquad \text{(A.42)}$$

satisfies $\phi' + \phi'_* - \phi - \phi_* = 0$ almost everywhere, that is,

$$\phi = a_0 + a_i\zeta_i + a_4\zeta_i^2. \qquad \text{(A.43)}$$

Obviously, Eq. (A.43) is the solution of Eq. (A.42) by the definition, Eq. (A.111), of $\mathcal{L}_a$. That is, Eq. (A.43) is the only solution of Eq. (A.42).

[18] See Footnote 5 in Section 1.2 for the definition of almost everywhere.

From the self-adjoint property (A.40) and the form of the solution of Eq. (A.43), the relation

$$\int_{\text{all } \boldsymbol{\zeta}} \varphi(\boldsymbol{\zeta}) \mathcal{L}_a(\phi) E \mathbf{d}\boldsymbol{\zeta} = 0 \quad \text{for any } \phi \tag{A.44}$$

holds when and only when φ is a linear combination of 1, ζ_i, and ζ_i^2.

A.2.3 Summational invariant

Let $(\boldsymbol{\xi}, \boldsymbol{\xi}_*)$ be the velocities of two molecules before their collision, and let $(\boldsymbol{\xi}', \boldsymbol{\xi}'_*)$ be those after the collision.[19] A function $\varphi(\boldsymbol{\xi})$ that satisfies the equation

$$\varphi(\boldsymbol{\xi}') + \varphi(\boldsymbol{\xi}'_*) = \varphi(\boldsymbol{\xi}) + \varphi(\boldsymbol{\xi}_*) \tag{A.45}$$

is called a *summational invariant of the collision*. The function

$$\varphi(\boldsymbol{\xi}) = a_0 + a_i \xi_i + a_4 \xi_i^2, \tag{A.46}$$

where a_r $(r = 0, 1, \ldots, 4)$ is independent of ξ_i, obviously satisfies Eq. (A.45) or the function (A.46) is a summational invariant. Our interest here is the general form of the function $\varphi(\boldsymbol{\xi})$ that satisfies the relation (A.45).

In view of the discussion in Section A.2.1 and Fig. A.1 in Section A.1, in the latter of which $(\boldsymbol{\xi}^{(1)}, \boldsymbol{\xi}^{(2)})$ and $(\boldsymbol{\xi}^{(1)\prime}, \boldsymbol{\xi}^{(2)\prime})$ should be replaced, respectively, by $(\boldsymbol{\xi}, \boldsymbol{\xi}_*)$ and $(\boldsymbol{\xi}', \boldsymbol{\xi}'_*)$, the sum $\varphi(\boldsymbol{\xi}) + \varphi(\boldsymbol{\xi}_*)$ for any set of antipodal points $(\boldsymbol{\xi}, \boldsymbol{\xi}_*)$ on a sphere takes the same value or the sum is constant on the sphere. The constant may, obviously, vary sphere from sphere. Here, we define an antipodal function. That is, an antipodal function is defined as a function $\varphi(\boldsymbol{\xi})$ that satisfies the condition

$$\varphi(\boldsymbol{\xi}) + \varphi(\boldsymbol{\xi}_*) = \text{const}, \tag{A.47}$$

for any antipodal points $(\boldsymbol{\xi}, \boldsymbol{\xi}_*)$ on an arbitrary sphere. The constant may depend on the sphere. The function given by Eq. (A.46) is obviously an antipodal function. The general form of the antipodal function is discussed by Kennard [1938] and Grad [1949]. We will give its derivation for the class of continuous functions according to Grad [1949].

First we show that a continuous antipodal function vanishes identically if it vanishes at the following five points:

$$\boldsymbol{\xi} = (0,0,0),\ (1,0,0),\ (0,1,0),\ (0,0,1),\ (-1,0,0). \tag{A.48}$$

Take the (ξ_1, ξ_2) plane as shown in Fig. A.2, where the first three and the last points in Eq. (A.48) are marked by A, B, C, and E, respectively. With the aid of Eq. (A.47), $\varphi(\boldsymbol{\xi})$ vanishes at all the lattice points with integer coordinates in the (ξ_1, ξ_2) plane, because starting from the pairs $[(B, E),\ (C, 1)]$, $[(E, 1),\ (A, 2)]$, $[(C, E),\ (A, 3)]$, $[(B, C),\ (A, 4)]$, we can successively find pairs of antipodal points at three points of which $\varphi(\boldsymbol{\xi}) = 0$, for example, in the order of the numbers in the figure. With the result, we can show that $\varphi(\boldsymbol{\xi})$ vanishes at all the centers

[19] See Footnote 17 in Section A.2.1.

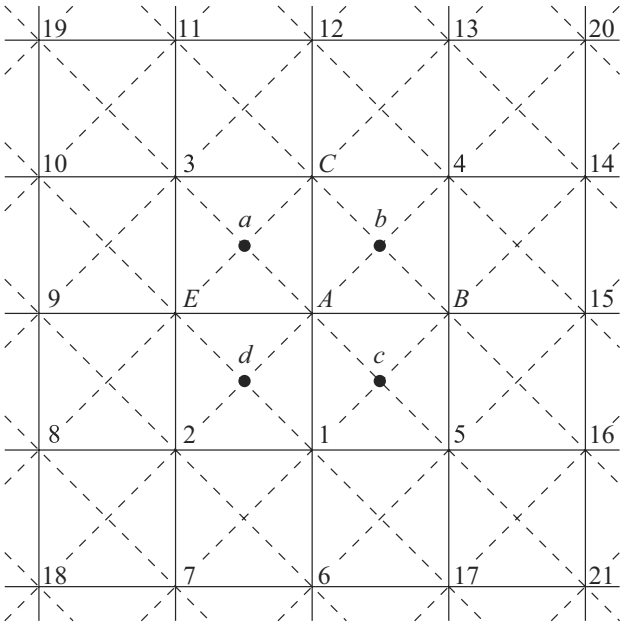

Figure A.2. Lattice points in the (ξ_1, ξ_2) plane and determination of the φ at the lattice points and so on.

of the squares with integer corners and unit sides. For example, taking the five pairs of antipodal points $[(a,b),\ (A,C)]$, $[(b,c),\ (A,B)]$, $[(c,d),\ (A,1)]$, $[(a,d),\ (A,E)]$, $[(a,c),\ (b,d)]$ in Fig. A.2, we have

$$\varphi(a)+\varphi(b)=\varphi(A)+\varphi(C)=0,\quad \varphi(b)+\varphi(c)=\varphi(A)+\varphi(B)=0,$$
$$\varphi(c)+\varphi(d)=\varphi(A)+\varphi(1)=0,\quad \varphi(a)+\varphi(d)=\varphi(A)+\varphi(E)=0,$$
$$\varphi(a)+\varphi(c)=\varphi(b)+\varphi(d),$$

from which

$$\varphi(a)=\varphi(b)=\varphi(c)=\varphi(d)=0.$$

Thus, we find that $\varphi(\boldsymbol{\xi})=0$ at all the lattice points of the oblique system of size $1/\sqrt{2}$, and therefore the process can be continued to smaller and smaller lattice. Thus, $\varphi(\boldsymbol{\xi})$ vanishes at points dense[20] in the (ξ_1, ξ_2) plane. The function $\varphi(\boldsymbol{\xi})$ being assumed continuous, $\varphi(\boldsymbol{\xi})=0$ in the (ξ_1, ξ_2) plane. With additional data at $\boldsymbol{\xi}=(0,0,1)$, we can show that $\varphi(\boldsymbol{\xi})=0$ in the (ξ_1, ξ_3) plane in a similar way. Then, for any point $\boldsymbol{\xi}\,[=(\xi_1,\xi_2,\xi_3)]$ in the $\boldsymbol{\xi}$ space, taking the pair $[((\xi_1,\xi_2,0),\ (\xi_1,0,\xi_3)),\ ((\xi_1,0,0),\ (\xi_1,\xi_2,\xi_3))]$, we find that $\varphi(\xi_1,\xi_2,\xi_3)=0$.

With this preparation, we show the general form of the antipodal function. Given an antipodal function $\psi(\boldsymbol{\xi})$, we construct the function (A.46) that takes

[20] Let X be a metric space, e.g., the $\boldsymbol{X}$ or $\boldsymbol{\xi}$ space and the (ξ_1, ξ_2) plane, and let S be a subset of X. The subset S is called *dense* in X if every point of X is a limit point of S, or a point of S (or both) (Rudin [1976]). Continuous functions that coincide on S coincide on X.

the values of $\psi(\boldsymbol{\xi})$ at the five points (A.48) by choosing a_r properly. From the discussion of the preceding paragraph, the function thus constructed coincides with the antipodal function $\psi(\boldsymbol{\xi})$ for all $\boldsymbol{\xi}$. That is, the general form of the antipodal function is given by Eq. (A.46).

The above result that a continuous summational invariant $\varphi(\boldsymbol{\xi})$ of collision is expressed by a linear combination of 1, ξ_i, and ξ_i^2 is extended to a wider class of functions by Arkeryd [1972]. That is, a summational invariant φ that is locally integrable is similarly expressed by a linear combination of 1, ξ_i, and ξ_i^2 almost everywhere, that is, it coincides with a continuous summational invariant (A.46) almost everywhere.[21] The φ may be discontinuous at the points with measure zero in the $\boldsymbol{\xi}$ space, but it is expressed by Eq. (A.46) at the other points.[22] The extension apparently seems to be only of mathematical interest. However, the velocity distribution function generally has discontinuities as explained in Section 3.1.6, and the summational invariant plays an important role in the derivation of a Maxwell distribution in Section A.7.1. If the above statement is not true for the class of functions that allow discontinuities, the velocity distribution function that describes an equilibrium state (Section A.7.1) is not necessarily a Maxwellian, and the equalities in Eq. (1.33) with (1.34b) and Eq. (1.36) for the H function hold for a velocity distribution function other than a Maxwellian, that is, a Maxwellian is no longer the only special function in the statement of the H theorem in Section 1.7. Thus, the extension is important though it requires sophisticated mathematics.

A.2.4 Function $B(|\boldsymbol{\alpha}\cdot(\boldsymbol{\xi}_*-\boldsymbol{\xi})|/|\boldsymbol{\xi}_*-\boldsymbol{\xi}|, |\boldsymbol{\xi}_*-\boldsymbol{\xi}|)$

The function $B(|\boldsymbol{\alpha}\cdot(\boldsymbol{\xi}_*-\boldsymbol{\xi})|/|\boldsymbol{\xi}_*-\boldsymbol{\xi}|, |\boldsymbol{\xi}_*-\boldsymbol{\xi}|)$ in the Boltzmann equation (1.5) with (1.6) in Section 1.2 is defined by Eq. (A.20) in Section A.1. According to it, the function $B(|\boldsymbol{\alpha}\cdot(\boldsymbol{\xi}_*-\boldsymbol{\xi})|/|\boldsymbol{\xi}_*-\boldsymbol{\xi}|, |\boldsymbol{\xi}_*-\boldsymbol{\xi}|)$ is determined by the relation between the two unit vectors $\boldsymbol{e}$ and $\boldsymbol{\alpha}$ in the binary collision of two molecules. However, the relation between $B(|\boldsymbol{\alpha}\cdot(\boldsymbol{\xi}_*-\boldsymbol{\xi})|/|\boldsymbol{\xi}_*-\boldsymbol{\xi}|, |\boldsymbol{\xi}_*-\boldsymbol{\xi}|)$ and the intermolecular potential is not explicitly seen from the definition. We will here discuss this relation.

Consider the binary collision of two molecules, say, molecule 0 and molecule 1, under the intermolecular potential $U(r)$ [$U(r)=0$ for $r>d_m$ (≥ 0)], where r is the distance between the two molecules. Let the velocities of the molecule 0 and molecule 1 when they are going to leave the influence range of the intermolecular potential at $r=d_m$ be, respectively, $\boldsymbol{\xi}$ and $\boldsymbol{\xi}_*$, and let the position of the molecule 1 relative to the molecule 0 be $d_m\boldsymbol{e}$ at that instant.[23] The motion of the molecule 1 relative to the molecule 0 is in the plane determined by the two vectors $\boldsymbol{\xi}_*-\boldsymbol{\xi}$ and $\boldsymbol{e}$. Take the plane polar coordinate system (r,θ) in the plane

[21] See Footnote 5 in Section 1.2 for the definition of almost everywhere and measure zero.

[22] More precisely, a locally integrable function φ that satisfies Eq. (A.45) almost everywhere in the $(\boldsymbol{\xi},\boldsymbol{\xi}_*)$ space. Incidentally, detailed discussion of the local behavior of the function related to the domain of $\boldsymbol{\xi}$ is discussed in Wennberg [1992].

[23] Corresponding to the discussion from Eqs. (A.10) to (A.13) in Section A.1, we choose the state where the interaction of the two particles ends as the reference state.

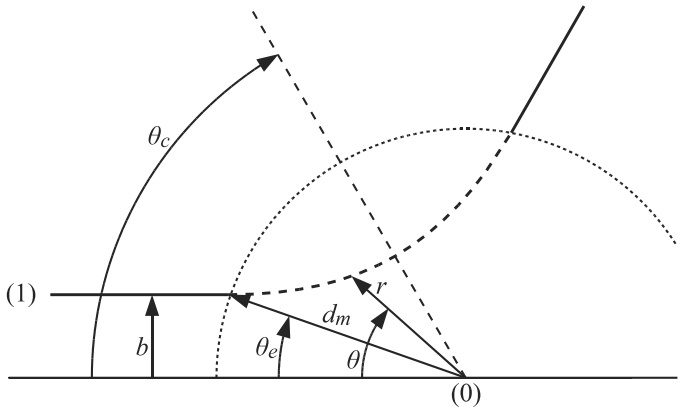

Figure A.3. Binary collision and the parameters θ_e, θ_c, and b. Molecule 0 and molecule 1 are, respectively, indicated by (0) and (1).

with its origin at the molecule 0 and $\theta = 0$ in the direction $\boldsymbol{\xi}_* - \boldsymbol{\xi}$, and let the position of the molecule 1 at the end of the interaction in the plane be (d_m, θ_e) $(0 \le \theta_e \le \pi/2$; see Fig. A.3). The motion of the molecule 1 is determined by the equations (the energy and angular momentum equations)

$$\frac{1}{4}m\left(\dot{r}^2 + r^2\dot{\theta}^2\right) + U(r) = \frac{1}{4}m\mathcal{V}^2, \tag{A.49a}$$

$$r^2\dot{\theta} = -\mathcal{V}b, \tag{A.49b}$$

where $\dot{r} = \mathrm{d}r/\mathrm{d}t$, $\dot{\theta} = \mathrm{d}\theta/\mathrm{d}t$, $\mathcal{V} = |\boldsymbol{\xi}_* - \boldsymbol{\xi}|$, and $b = d_m|\sin\theta_e|$. Thus, the trajectory of the relative motion of the molecule 1 is determined by the equation

$$\frac{b^2}{r^4}\left(\frac{\mathrm{d}r}{\mathrm{d}\theta}\right)^2 = 1 - \frac{4U(r)}{m\mathcal{V}^2} - \frac{b^2}{r^2}. \tag{A.50}$$

Let r_c be the largest solution of the equation

$$1 - \frac{4U(r)}{m\mathcal{V}^2} - \frac{b^2}{r^2} = 0,$$

and θ_c is the value of θ at $r = r_c$. Then the trajectory that extends to d_m (and thus infinity) exists only in the range $r \ge r_c$, and the trajectory is obviously symmetric with respect to $\theta = \theta_c$. From the latter property and the relations (A.30) and (A.31), we find that $\boldsymbol{\alpha}$ is in the direction of $\theta = \theta_c$ or $\theta_c + \pi$. From Eq. (A.50),

$$\begin{aligned}\theta_c - \theta_e &= -b\int_{d_m}^{r_c} r^{-2}\left(1 - \frac{4U(r)}{m\mathcal{V}^2} - \frac{b^2}{r^2}\right)^{-1/2}\mathrm{d}r \\ &= |\sin\theta_e|\int_{x_c}^{1} x^{-2}\left(1 - \frac{4U_0}{m\mathcal{V}^2}\hat{U}(x) - \frac{\sin^2\theta_e}{x^2}\right)^{-1/2}\mathrm{d}x,\end{aligned} \tag{A.51}$$

where $\hat{U}(x) = U(r)/U_0$, $x = r/d_m$, and x_c is the largest solution of the equation

$$1 - \frac{4U_0}{m\mathcal{V}^2}\hat{U}(x) - \frac{\sin^2\theta_e}{x^2} = 0.$$

The nondimensional potential $\hat{U}(x)$ vanishes for $x > 1$. The solution x_c is a function of θ_e and $U_0/m\mathcal{V}^2$, and its functional form is determined by $\hat{U}(x)$. So is θ_c. Owing to the symmetry of the trajectory with respect to the line $\theta = \theta_c$, the relation between θ_e and θ_c is the same when the configuration (d_m, θ_e) with $0 \le \theta_e \le \pi/2$ in Fig. A.3 is the state where the molecule 1 is going to interact with the molecule 0.

To derive the concrete expression of $B(|\boldsymbol{\alpha}\cdot(\boldsymbol{\xi}_*-\boldsymbol{\xi})|/|\boldsymbol{\xi}_*-\boldsymbol{\xi}|, |\boldsymbol{\xi}_*-\boldsymbol{\xi}|)$ in terms of the intermolecular potential, we have to express the relation (A.11), i.e.,

$$\boldsymbol{\alpha} = \boldsymbol{\alpha}(\boldsymbol{e}, \boldsymbol{\xi}_* - \boldsymbol{\xi}), \tag{A.52}$$

in terms of the potential. Let $\boldsymbol{\xi}'$ and $\boldsymbol{\xi}'_*$ be, respectively, the velocities before the interaction of the two particles corresponding to $\boldsymbol{\xi}$ and $\boldsymbol{\xi}_*$. According to the discussion of Section A.2.1, the vector $\boldsymbol{\alpha}$ is on the plane made by the two vectors $\boldsymbol{\xi}_* - \boldsymbol{\xi}$ and $\boldsymbol{\xi}' - \boldsymbol{\xi}'_*$ and equally divides the angle between them (see Fig. A.1, where $\boldsymbol{\xi}^{(1)}$, $\boldsymbol{\xi}^{(2)}$, $\boldsymbol{\xi}^{(1)\prime}$, and $\boldsymbol{\xi}^{(2)\prime}$ correspond, respectively, to $\boldsymbol{\xi}$, $\boldsymbol{\xi}_*$, $\boldsymbol{\xi}'$, and $\boldsymbol{\xi}'_*$). From the symmetry of the relative trajectory of the molecule 1 with respect to $\theta = \theta_c$, the unit vector $\boldsymbol{\alpha}$ is in the direction θ_c (or $\theta_c + \pi$) on the plane of the relative trajectory. Let the spherical coordinate representations of $\boldsymbol{e}$ and $\boldsymbol{\alpha}$ be, respectively, $(1, \tilde{\theta}_e, \varphi_e)$ and $(1, \theta_\alpha, \varphi_\alpha)$. Then, we can take $\tilde{\theta}_e = \theta_e$ and $\theta_\alpha = \bar{\theta}_c, \varphi_\alpha = \varphi_e$ ($\bar{\theta}_c = \theta_c + m\pi$; $0 \le \bar{\theta}_c \le \pi/2$) and $\theta_\alpha = \pi - \bar{\theta}_c, \varphi_\alpha = \varphi_e + \pi$ ($\bar{\theta}_c = \theta_c + m\pi$; $\pi/2 \le \bar{\theta}_c \le \pi$), where $\boldsymbol{\alpha}$ is made unique in such a way that $\boldsymbol{\alpha}\cdot(\boldsymbol{\xi}_* - \boldsymbol{\xi}) > 0$, which is adopted in the following discussion. From the relation between θ_e and θ_c obtained in the preceding paragraph, we can derive the expression of $B(|\boldsymbol{\alpha}\cdot(\boldsymbol{\xi}_*-\boldsymbol{\xi})|/|\boldsymbol{\xi}_*-\boldsymbol{\xi}|, |\boldsymbol{\xi}_*-\boldsymbol{\xi}|)$.

The solid angle elements $\mathrm{d}\Omega(\boldsymbol{e})$ and $\mathrm{d}\Omega(\boldsymbol{\alpha})$ are expressed in the spherical coordinates as

$$\mathrm{d}\Omega(\boldsymbol{e}) = \sin\tilde{\theta}_e \mathrm{d}\tilde{\theta}_e \mathrm{d}\varphi_e, \quad \mathrm{d}\Omega(\boldsymbol{\alpha}) = \sin\theta_\alpha \mathrm{d}\theta_\alpha \mathrm{d}\varphi_\alpha.$$

In view of the relation among $\tilde{\theta}_e$, φ_e, θ_α, φ_α, θ_e, θ_c, and $\bar{\theta}_c$ given in the preceding paragraph,

$$\mathrm{d}\Omega(\boldsymbol{e}) = \left|\frac{\sin\theta_e}{\sin\theta_c}\frac{\mathrm{d}\theta_e}{\mathrm{d}\theta_c}\right| \mathrm{d}\Omega(\boldsymbol{\alpha}), \tag{A.53}$$

where θ_e is a function of θ_c with the parameter $U_0/m\mathcal{V}^2$, given by inverting Eq. (A.51). In view of the relations

$$|\cos\theta_c| = |\boldsymbol{\alpha}\cdot(\boldsymbol{\xi}_* - \boldsymbol{\xi})|/|\boldsymbol{\xi}_* - \boldsymbol{\xi}| \ \text{ and } \ \mathcal{V} = |\boldsymbol{\xi}_* - \boldsymbol{\xi}|, \tag{A.54}$$

the function $|(\sin\theta_e/\sin\theta_c)\mathrm{d}\theta_e/\mathrm{d}\theta_c|$, as well as θ_e, is a function of $|\boldsymbol{\alpha}\cdot(\boldsymbol{\xi}_* - \boldsymbol{\xi})|/|\boldsymbol{\xi}_* - \boldsymbol{\xi}|$ and $(m/U_0)^{1/2}|\boldsymbol{\xi}_* - \boldsymbol{\xi}|$. On the other hand, from the definition (A.20) of B,

$$\mathrm{d}\Omega(\boldsymbol{e}) = \frac{2B}{d_m^2|\boldsymbol{\xi}_* - \boldsymbol{\xi}||\cos\theta_e|}\mathrm{d}\Omega(\boldsymbol{\alpha}), \tag{A.55}$$

because $|\boldsymbol{e}\cdot(\boldsymbol{\xi}_*-\boldsymbol{\xi})| = |\boldsymbol{\xi}_*-\boldsymbol{\xi}||\cos\theta_e|$. Comparing the two relations (A.53) and (A.55), and noting the comment just after Eq. (A.54), we find that the function B is expressed with the aid of a nondimensional function of $|\boldsymbol{\alpha}\cdot(\boldsymbol{\xi}_*-\boldsymbol{\xi})|/|\boldsymbol{\xi}_*-\boldsymbol{\xi}|$ and $(m/U_0)^{1/2}|\boldsymbol{\xi}_*-\boldsymbol{\xi}|$ in the form

$$B = \frac{d_m^2|\boldsymbol{\xi}_*-\boldsymbol{\xi}|}{2} f_B(|\boldsymbol{\alpha}\cdot(\boldsymbol{\xi}_*-\boldsymbol{\xi})|/|\boldsymbol{\xi}_*-\boldsymbol{\xi}|, (m/U_0)^{1/2}|\boldsymbol{\xi}_*-\boldsymbol{\xi}|), \tag{A.56a}$$

where

$$f_B(|\boldsymbol{\alpha}\cdot(\boldsymbol{\xi}_*-\boldsymbol{\xi})|/|\boldsymbol{\xi}_*-\boldsymbol{\xi}|, (m/U_0)^{1/2}|\boldsymbol{\xi}_*-\boldsymbol{\xi}|) = \frac{1}{2}\left|\frac{\sin 2\theta_e}{\sin\theta_c}\frac{\mathrm{d}\theta_e}{\mathrm{d}\theta_c}\right|. \tag{A.56b}$$

The following function $\underline{B}$ is sometimes used instead of B :

$$\underline{B}(\theta_\alpha, |\boldsymbol{\xi}_*-\boldsymbol{\xi}|) = B(|\boldsymbol{\alpha}\cdot(\boldsymbol{\xi}_*-\boldsymbol{\xi})|/|\boldsymbol{\xi}_*-\boldsymbol{\xi}|, |\boldsymbol{\xi}_*-\boldsymbol{\xi}|)\sin\theta_\alpha. \tag{A.57}$$

In the above discussion, the range of $\boldsymbol{e}$ is $\boldsymbol{e}\cdot(\boldsymbol{\xi}_*-\boldsymbol{\xi}) \geq 0$. In the derivation of the Boltzmann equation in Section A.1, the range of $\boldsymbol{e}$ is extended to the whole sphere ($0 \leq \tilde{\theta}_e \leq \pi$, $0 \leq \varphi_e < 2\pi$). Correspondingly, $\boldsymbol{\alpha}$ is extended in such a way that $-\boldsymbol{e}$ gives $-\boldsymbol{\alpha}$ [see from Eqs. (A.10) to (A.13)] and the function B is extended in such a way that $-\boldsymbol{\alpha}$ gives the same value as $\boldsymbol{\alpha}$, i.e., B is even with respect to $\boldsymbol{\alpha}$. With this extension in mind, we have taken the redundant absolute value of $\boldsymbol{\alpha}\cdot(\boldsymbol{\xi}_*-\boldsymbol{\xi})$ in the above discussion. Thus, the function B in Eq. (A.56a) applies in the extended domain as it is. Incidentally, B in the whole domain is also obtained directly by Eq. (A.56a) with (A.56b) if the relation (A.51) between θ_e and θ_c is used (this is the reason why the absolute sign is used there).[24]

It should be noted here that several $\boldsymbol{e}$'s may correspond to a single $\boldsymbol{\alpha}$, although the opposite correspondence ($\boldsymbol{e} \to \boldsymbol{\alpha}$) is unique.[25] Let $f_{B1}, f_{B2}, \ldots, f_{Bm}$ correspond to a single $\boldsymbol{\alpha}$ according to the multiple correspondence of $\boldsymbol{e}$. Then the function $B(|\boldsymbol{\alpha}\cdot(\boldsymbol{\xi}_*-\boldsymbol{\xi})|/|\boldsymbol{\xi}_*-\boldsymbol{\xi}|, |\boldsymbol{\xi}_*-\boldsymbol{\xi}|)$ is given by

$$B = \frac{d_m^2|\boldsymbol{\xi}_*-\boldsymbol{\xi}|}{2}\sum_{n=1}^{m} f_{Bn}. \tag{A.58}$$

In the derivation of the Boltzmann equation in Section A.1, the intermolecular potential $U(r)$ is assumed to be effective only in the finite range $r \leq d_m$. The two terms of its collision integral

$$J_G = \frac{1}{m}\int f' f'_* B(|\boldsymbol{\alpha}\cdot(\boldsymbol{\xi}_*-\boldsymbol{\xi})|/|\boldsymbol{\xi}_*-\boldsymbol{\xi}|, |\boldsymbol{\xi}_*-\boldsymbol{\xi}|)\mathrm{d}\Omega(\boldsymbol{\alpha})\mathbf{d}\boldsymbol{\xi}_*,$$
$$J_L = \frac{1}{m}\int f\, f_* B(|\boldsymbol{\alpha}\cdot(\boldsymbol{\xi}_*-\boldsymbol{\xi})|/|\boldsymbol{\xi}_*-\boldsymbol{\xi}|, |\boldsymbol{\xi}_*-\boldsymbol{\xi}|)\mathrm{d}\Omega(\boldsymbol{\alpha})\mathbf{d}\boldsymbol{\xi}_*,$$

[24] Here, $\boldsymbol{\alpha} = (1, \theta_\alpha, \varphi_\alpha)$ corresponds to $\boldsymbol{e} = (1, \tilde{\theta}_e, \varphi_e)$ with $\varphi_\alpha = \varphi_e$ in the damin ($0 \leq \tilde{\theta}_e \leq \pi/2$, $0 \leq \varphi_e < 2\pi$). The correspondence is extended in the domain ($0 \leq \tilde{\theta}_e \leq \pi$, $0 \leq \varphi_e < 2\pi$) in such a way that $-\boldsymbol{e} = (1, \pi-\tilde{\theta}_e, \varphi_e+\pi)$ corresponds to $-\boldsymbol{\alpha} = (1, \pi-\theta_\alpha, \varphi_\alpha+\pi)$. In terms of θ_e and θ_c, the correspondence $-\boldsymbol{e}$ to $-\boldsymbol{\alpha}$ is $\theta_e+\pi$ to $\theta_c+\pi$. Equation (A.51) with the absolute value for $\sin\theta_e$ gives the corresponding extension.

[25] We have chosen one of $\boldsymbol{\alpha}$ and $-\boldsymbol{\alpha}$ according to the discussion from Eqs. (A.10) to (A.13) in Section A.1.

which correspond, respectively, to I_+ given by Eq. (A.13) and I_- by Eq. (A.10), take finite values and are called, respectively, the gain and loss terms of the collision integral.

In the Boltzmann equation (1.5) with (1.6), the effect of intermolecular potential is condensed in the function $B(|\boldsymbol{\alpha}\cdot(\boldsymbol{\xi}_*-\boldsymbol{\xi})|/|\boldsymbol{\xi}_*-\boldsymbol{\xi}|, |\boldsymbol{\xi}_*-\boldsymbol{\xi}|)$. The function B can be defined even for an intermolecular force extending up to infinity. That is, first taking the limit of Eq. (A.51) as $d_m \to \infty$ with b kept at a finite value, we have

$$\theta_c = b\int_{r_c}^{\infty} r^{-2}\left(1-\frac{4U(r)}{m\mathcal{V}^2}-\frac{b^2}{r^2}\right)^{-1/2}\mathrm{d}r, \tag{A.59}$$

where r_c is the largest solution of the equation

$$1-4(m\mathcal{V}^2)^{-1}U(r)-b^2r^{-2}=0,$$

and from Eq. (A.59), b is expressed as an inverse function $b(\theta_c)$. Then, substitute this function $b(\theta_c)$ into the following expression of $B(|\boldsymbol{\alpha}\cdot(\boldsymbol{\xi}_*-\boldsymbol{\xi})|/|\boldsymbol{\xi}_*-\boldsymbol{\xi}|, |\boldsymbol{\xi}_*-\boldsymbol{\xi}|)$ obtained from Eqs. (A.53) and (A.55),

$$\begin{aligned} B(|\boldsymbol{\alpha}\cdot(\boldsymbol{\xi}_*-\boldsymbol{\xi})|/|\boldsymbol{\xi}_*-\boldsymbol{\xi}|, |\boldsymbol{\xi}_*-\boldsymbol{\xi}|) &= \frac{1}{4}|\boldsymbol{\xi}_*-\boldsymbol{\xi}|d_m^2\left|\frac{1}{\sin\theta_c}\frac{\partial\sin^2\theta_e}{\partial\theta_c}\right| \\ &= \frac{1}{4}|\boldsymbol{\xi}_*-\boldsymbol{\xi}|\left|\frac{1}{\sin\theta_c}\frac{\partial b^2}{\partial\theta_c}\right|. \end{aligned} \tag{A.60}$$

The Boltzmann equation (1.5) with (1.6) where the function B obtained for an intermolecular force extending to infinity is substituted is called the Boltzmann equation with an infinite-range intermolecular potential without verification. Each of the two terms of the collision integral, J_G or J_L, is divergent. However, when the potential decays faster than some speed, the collision integral as a whole converges.

Consider the potential of an inverse power of r, i.e.,

$$U(r)=\frac{a_0}{r^{n-1}} \qquad (a_0>0,\ n>1).$$

Then, from Eq. (A.59), by the change of variable $y=b/r$,

$$\theta_c=\int_0^{y_c}\left[1-\left(\frac{4a_0}{m\mathcal{V}^2b^{n-1}}\right)y^{n-1}-y^2\right]^{-1/2}\mathrm{d}y,$$

where $y_c\,(>0)$ is the smallest solution of the equation

$$1-\left(\frac{4a_0}{m\mathcal{V}^2b^{n-1}}\right)y^{n-1}-y^2=0.$$

Obviously, y_c and thus θ_c are functions of $4a_0/m\mathcal{V}^2b^{n-1}$. Therefore, b is expressed in the product of a function of $\mathcal{V}$ $(=|\boldsymbol{\xi}_*-\boldsymbol{\xi}|)$ and that of θ_c, i.e.,

$$b=\left(\frac{4a_0}{m}\right)^{1/(n-1)}|\boldsymbol{\xi}_*-\boldsymbol{\xi}|^{-2/(n-1)}g(\theta_c). \tag{A.61}$$

The function $g(\theta_c)$ is the inverse function of the integral

$$\theta_c = \int_0^{y_c(g)} \left[1 - \left(\frac{y}{g}\right)^{n-1} - y^2\right]^{-1/2} \mathrm{d}y, \tag{A.62a}$$

where $y_c(g)$ is the positive solution, which is unique, of the equation

$$1 - (y/g)^{n-1} - y^2 = 0. \tag{A.62b}$$

When g varies from 0 to ∞, from Eq. (A.62b), $y_c(g)$ increases monotonically from 0 and approaches 1 as $y_c = 1 - g^{-(n-1)}/2$; then, from Eq. (A.62a), $\theta_c(g)$ increases monotonically from 0 and approaches $\pi/2$.[26] The speed of approach is estimated in Eqs. (A.67)–(A.69).

From Eq. (A.60), with b in Eq. (A.61), the function B or $\underline{B}$ for the inverse-power potential is given by

$$\begin{aligned}\underline{B}(\theta_\alpha, |\boldsymbol{\xi}_* - \boldsymbol{\xi}|) &= B(|\boldsymbol{\alpha}\cdot(\boldsymbol{\xi}_* - \boldsymbol{\xi})|/|\boldsymbol{\xi}_* - \boldsymbol{\xi}|, |\boldsymbol{\xi}_* - \boldsymbol{\xi}|)\sin\theta_\alpha \\ &= \frac{1}{4}\left(\frac{4a_0}{m}\right)^{2/(n-1)} |\boldsymbol{\xi}_* - \boldsymbol{\xi}|^{\frac{n-5}{n-1}} \frac{\mathrm{d}g^2}{\mathrm{d}\theta_c} \quad (0 \le \theta_\alpha \le \pi/2),\end{aligned} \tag{A.63}$$

and it is symmetric with respect to $\theta_c = \pi/2$. The collision integral for the inverse-power potential is expressed, with g as an integration variable, as

$$J(f,f) = \frac{1}{m}\left(\frac{4a_0}{m}\right)^{2/(n-1)} \int_{\substack{0\le g<\infty \\ 0\le\varphi<2\pi \\ \text{all } \boldsymbol{\xi}_*}} (f'f'_* - f\,f_*)|\boldsymbol{\xi}_* - \boldsymbol{\xi}|^{(n-5)/(n-1)} g\mathrm{d}g\mathrm{d}\varphi\mathbf{d}\boldsymbol{\xi}_*, \tag{A.64}$$

where $\boldsymbol{\alpha}$ in $f'f'_*$ is a function of g and φ through Eq. (A.62a) because it is a function of θ_c and φ. Owing to the integration with respect to g, the gain and loss terms in the integral (A.64) diverge, but the integral as a whole converges for $n > 3$ for smooth f (or f with the continuous first derivative with respect to $\boldsymbol{\xi}$) as shown in the next paragraph. When $n = 5$, the factor $|\boldsymbol{\xi}_* - \boldsymbol{\xi}|^{(n-5)/(n-1)}$ is reduced to unity, which simplifies analyses, and the molecule with this potential is called the *Maxwell molecule*. From Eq. (A.63), the function B or $\underline{B}$ for the Maxwell molecule is given by

$$\begin{aligned}\underline{B}(\theta_\alpha, |\boldsymbol{\xi}_* - \boldsymbol{\xi}|) &= B(|\boldsymbol{\alpha}\cdot(\boldsymbol{\xi}_* - \boldsymbol{\xi})|/|\boldsymbol{\xi}_* - \boldsymbol{\xi}|, |\boldsymbol{\xi}_* - \boldsymbol{\xi}|)\sin\theta_\alpha \\ &= \frac{1}{4}\left(\frac{4a_0}{m}\right)^{1/2} \frac{\mathrm{d}g^2}{\mathrm{d}\theta_c} \quad (0 \le \theta_\alpha \le \pi/2).\end{aligned} \tag{A.65}$$

The difference $f'f'_* - f\,f_*$ in the integrand of Eq. (A.64) is estimated to be

$$|f'f'_* - f\,f_*| = O(|\pi/2 - \theta_c|), \tag{A.66}$$

[26] In view of the range of θ_c, $\theta_c = \theta_\alpha$ from the definition given after Eq. (A.52).

for a smooth f with the aid of the relations (1.7) [or (A.19)] and (A.54). The relation (A.62a) between θ_c and g can easily be integrated for $n = 2$ and 3 as

$$\theta_c = \frac{\pi}{2} - \mathrm{Arcsin}\left(\frac{1}{\sqrt{4g^2+1}}\right) = \frac{\pi}{2} - \frac{1}{2g} + \cdots \qquad (n=2), \tag{A.67}$$

$$\theta_c = \frac{\pi}{2}\frac{g}{\sqrt{1+g^2}} = \frac{\pi}{2}\left(1 - \frac{1}{2g^2} + \cdots\right) \qquad (n=3). \tag{A.68}$$

For other values of n, θ_c for large values of g is estimated as follows. First we put

$$x^2 = y^2\left(1 + \frac{y^{n-3}}{g^{n-1}}\right).$$

Then, x ranges from 0 to 1 while y varies from 0 to y_c. When $n > 3$ (n : not necessarily integer), we have

$$y = x\left(1 + \frac{y^{n-3}}{g^{n-1}}\right)^{-1/2} = x\left(1 - \frac{x^{n-3}}{2g^{n-1}} + \cdots\right),$$

and

$$\frac{\mathrm{d}\,y}{\mathrm{d}x} = 1 - \frac{(n-2)x^{n-3}}{2g^{n-1}} + \cdots.$$

Then,

$$\begin{aligned}\theta_c &= \int_0^{y_c(g)} \left[1 - (y/g)^{n-1} - y^2\right]^{-1/2} \mathrm{d}y \\ &= \int_0^1 \frac{1}{(1-x^2)^{1/2}}\left(1 - \frac{(n-2)x^{n-3}}{2g^{n-1}} + \cdots\right)\mathrm{d}x \\ &= \frac{\pi}{2} - O\left(\frac{1}{g^{n-1}}\right).\end{aligned} \tag{A.69}$$

Collecting these estimates (A.66)–(A.69), we find that the collision integral (A.64) converges as a whole for smooth f when $n > 3$.

The range of integral with respect to g is sometimes limited artificially to a finite range $0 \le g \le g_0$ in the collision integral (A.64). Then each term of the integral takes a finite value. The cutoff integral is called the *collision integral for the pseudo inverse-power potential* and the imaginary molecule is called the *pseudo inverse-power molecule*, especially the *pseudo Maxwell molecule* for $n = 5$. For the pseudo Maxwell molecule, the collision integral (A.64) is reduced to

$$J(f,f) = \left(\frac{4a_0}{m^3}\right)^{1/2} \int_{\substack{0\le g\le g_0 \\ 0\le\varphi<2\pi \\ \text{all } \boldsymbol{\xi}_*}} f' f'_* g \mathrm{d}g\mathrm{d}\varphi \mathbf{d}\boldsymbol{\xi}_* - A_c \rho f, \tag{A.70}$$

$$A_c = \pi\left(\frac{4a_0}{m^3}\right)^{1/2} g_0^2, \qquad \rho = \int_{\text{all } \boldsymbol{\xi}} f \mathbf{d}\boldsymbol{\xi}.$$

To limit the integration to the finite range $0 \le g \le g_0$ means that the pairs of molecules whose deflections by the interaction are smaller than some value, i.e., $|\theta_c(g) - \pi/2| < \varepsilon$ with $g_0 = g(\pi/2 - \varepsilon)$, are not counted to have made collision. Generally, not only for the inverse-power potential, the collision integral where the range of integration is limited to make its gain and loss terms converge separately is called the *collision integral with a cutoff potential.*[27]

The nondimensional form $\widehat{B}$ of the function B is introduced in Section 1.9, that is,

$$\widehat{B} = \frac{B(|\boldsymbol{\alpha}\cdot(\boldsymbol{\xi}_* - \boldsymbol{\xi})|/|\boldsymbol{\xi}_* - \boldsymbol{\xi}|, |\boldsymbol{\xi}_* - \boldsymbol{\xi}|)}{B_0},$$
$$B_0 = 4\sqrt{\pi} d_m^2 (RT_0)^{1/2}.$$

In view of Eqs. (A.56a),

$$\widehat{B} = \frac{1}{4\sqrt{2\pi}} |\boldsymbol{\zeta}_* - \boldsymbol{\zeta}| f_B(|\boldsymbol{\alpha}\cdot(\boldsymbol{\zeta}_* - \boldsymbol{\zeta})|/|\boldsymbol{\zeta}_* - \boldsymbol{\zeta}|, (2mRT_0/U_0)^{1/2}|\boldsymbol{\zeta}_* - \boldsymbol{\zeta}|). \quad \text{(A.71)}$$

Thus, the nondimensional function $\widehat{B}$ is a function of $|\boldsymbol{\alpha}\cdot(\boldsymbol{\zeta}_* - \boldsymbol{\zeta})|/|\boldsymbol{\zeta}_* - \boldsymbol{\zeta}|$ and $|\boldsymbol{\zeta}_* - \boldsymbol{\zeta}|$ with the parameter $(mRT_0/U_0)^{1/2}$. The function $\widehat{B}$ is proportional to $(mRT_0/U_0)^{-1/2}$ when it is considered as a function of $|\boldsymbol{\alpha}\cdot(\boldsymbol{\zeta}_* - \boldsymbol{\zeta})|/|\boldsymbol{\zeta}_* - \boldsymbol{\zeta}|$ and $(mRT_0/U_0)^{1/2}|\boldsymbol{\zeta}_* - \boldsymbol{\zeta}|$. The nondimensional form $\underline{\widehat{B}}$ of $\underline{B}$ is defined by

$$\underline{\widehat{B}} = \underline{B}/B_0 = \widehat{B}\sin\theta_\alpha. \quad \text{(A.72)}$$

In the case of the inverse-power potential, according to the second formula of Eq. (1.48d), the formal calculation of B_0 and $\widehat{B}$ gives

$$B_0 = \pi \left(\frac{4a_0}{m}\right)^{\frac{2}{n-1}} (2RT_0)^{\frac{n-5}{2(n-1)}} \int E E_* |\boldsymbol{\zeta}_* - \boldsymbol{\zeta}|^{\frac{n-5}{n-1}} \mathbf{d}\boldsymbol{\zeta}_* \mathbf{d}\boldsymbol{\zeta} \int_0^{\pi/2} \frac{\mathrm{d}g^2}{\mathrm{d}\theta_c} \mathrm{d}\theta_c, \quad \text{(A.73a)}$$

$$\underline{\widehat{B}} = \widehat{B}\sin\theta_\alpha = C_0 |\boldsymbol{\zeta}_* - \boldsymbol{\zeta}|^{(n-5)/(n-1)} \frac{\mathrm{d}g^2}{\mathrm{d}\theta_c}, \quad \text{(A.73b)}$$

where

$$C_0 = \frac{1}{4\pi \displaystyle\int E E_* |\boldsymbol{\zeta}_* - \boldsymbol{\zeta}|^{(n-5)/(n-1)} \mathbf{d}\boldsymbol{\zeta}_* \mathbf{d}\boldsymbol{\zeta} \int_0^{\pi/2} \frac{\mathrm{d}g^2}{\mathrm{d}\theta_c} \mathrm{d}\theta_c}.$$

The integral $\int_0^{\pi/2} (\mathrm{d}g^2/\mathrm{d}\theta_c)\mathrm{d}\theta_c$ in B_0 or C_0 diverges because g increases fast enough indefinitely as θ_c tends to $\pi/2$ [see the estimate just after Eq. (A.62b)],

[27] The cutoff potential where the range of θ_c is limited is called an angular cutoff potential. The angular cutoff potential, including the pseudo inverse-power potential, is not a fixed potential which is obtained by modifying the original potential. That is, in the angular cutoff potential, the two molecules, molecule 0 and molecule 1, interact in the following way. The molecules 1 that approach the molecule 0 in the range $0 \le b \le b_\mathrm{c}$ (see Fig. A.3 with the molecular velocities reversed), where b_c is determined by the relative speed, the cutoff angle, and the potential, behave as if they are in the original potential field. Those outside of this range ($b > b_\mathrm{c}$) are not subject to any force and continue their rectilinear constant motion.

and therefore this B_0 has no meaning as a nondimensionalizing factor and another quantity should be chosen as the factor. In the cutoff potential (or pseudo inverse-power potential), the contribution in a neighborhood of $\theta_c = \pi/2$ is neglected and the integral is made to take a finite value. With this value of B_0 or C_0, Eq. (A.73b) gives the function $\underline{\widehat{B}}$ or $\widehat{B}$ for the pseudo inverse-power potential.[28]

A.2.5 Spherically symmetric field of a symmetric tensor

Let l_{ij} be a three-dimensional orthogonal transformation matrix, i.e.,

$$l_{ik}l_{jk} = \delta_{ij}. \tag{A.74}$$

A tensor field $\hat{F}_{i_1,\ldots,i_m}(\zeta_i)$ that satisfies the relation

$$\hat{F}_{i_1,\ldots,i_m}(l_{ij}\zeta_j) = l_{i_1 j_1}\cdots l_{i_m j_m}\hat{F}_{j_1,\ldots,j_m}(\zeta_i), \tag{A.75}$$

is called *spherically symmetric*. A tensor field $\hat{F}_{i_1,\ldots,i_m}(\zeta_i)$ is called *axially symmetric* with respect to an axis a_i, when the relation (A.75) holds for the limited set of l_{ij} that satisfies the relation

$$a_i = l_{ij}a_j,$$

for a fixed a_i in addition to Eq. (A.74).

Put

$$F(\zeta_i) = Op[\phi_1(\zeta_i), \phi_2(\zeta_i), \ldots],$$

where $Op[*, \ldots]$ is an operator and $\phi_s(\zeta_i)$ is a function of ζ_i. Take the new function $\phi_{sR}(\zeta_i)$ defined by

$$\phi_{sR}(\zeta_i) = \phi_s(l_{ij}\zeta_j).$$

If the operator $Op[*, \ldots]$ satisfies the relation

$$F(l_{ij}\zeta_j) = Op[\phi_{1R}(\zeta_i), \phi_{2R}(\zeta_i), \ldots], \tag{A.76}$$

for arbitrary ϕ_s, then the operator $Op[*, \ldots]$ is called *isotropic*. The collision operators $\hat{J}(*,*)$, $\hat{J}_a(*,*)$, $\mathcal{J}(*,*)$, $\mathcal{J}_a(*,*)$, $\mathcal{L}(*)$, and $\mathcal{L}_a(*)$, which are defined, respectively by Eqs. (1.47b), (A.114b), (1.75c), (A.114a), (1.75b), and (A.111), are isotropic (see Section A.2.6).

Put

$$\hat{F}_{i_1,\ldots,i_m,i_n,\ldots,i_s}(\zeta_i) = [\mathcal{J}](\zeta_{i_1}\cdots\zeta_{i_m}\mathsf{f}(\zeta), \zeta_{i_n}\cdots\zeta_{i_s}\mathsf{g}(\zeta)),$$
$$\hat{G}_{i_1,\ldots,i_m}(\zeta_i) = [\mathcal{L}](\zeta_{i_1}\cdots\zeta_{i_m}\mathsf{f}(\zeta)),$$

where $[\mathcal{J}](*,*)$ represents $\hat{J}(*,*)$, $\hat{J}_a(*,*)$, $\mathcal{J}(*,*)$, or $\mathcal{J}_a(*,*)$ and $[\mathcal{L}](*)$ represents $\mathcal{L}(*)$ or $\mathcal{L}_a(*)$, and $\mathsf{f}(\zeta)$ and $\mathsf{g}(\zeta)$ are functions of ζ. The $\hat{F}_{i_1,\ldots,i_m,i_n,\ldots,i_s}(\zeta_i)$

[28] This B_0 may be taken as a B_0 for the corresponding non-cutoff potential. See Footnote 21 in Section 1.9.

is obviously symmetric with respect to the subscripts $i_1, \ldots, i_m$ and to $i_n, \ldots, i_s$, and so is $\hat{G}_{i_1,\ldots,i_m}(\zeta_i)$ with respect to the subscripts $i_1, \ldots, i_m$. From the isotropic property (A.76) of the collision operators and the bilinearity of $[\mathcal{J}](\hat{f}(\zeta_i), \hat{g}(\zeta_i))$ with respect to $\hat{f}(\zeta_i)$ and $\hat{g}(\zeta_i)$ or the linearity of $[\mathcal{L}](\hat{f}(\zeta_i))$ with respect to $\hat{f}(\zeta_i)$, we have

$$\hat{F}_{i_1,\ldots,i_m,i_n,\ldots,i_s}(l_{ij}\zeta_j) = l_{i_1 j_1} \cdots l_{i_m j_m} l_{i_n j_n} \cdots l_{i_s j_s} \hat{F}_{j_1,\ldots,j_m,j_n,\ldots,j_s}(\zeta_i), \quad \text{(A.77a)}$$

$$\hat{G}_{i_1,\ldots,i_m}(l_{ij}\zeta_j) = l_{i_1 j_1} \cdots l_{i_m j_m} \hat{G}_{j_1,\ldots,j_m}(\zeta_i). \quad \text{(A.77b)}$$

Thus the tensor fields $[\mathcal{J}](\zeta_{i_1} \cdots \zeta_{i_m} \mathsf{f}(\zeta), \zeta_{i_n} \cdots \zeta_{i_s} \mathsf{g}(\zeta))$ and $[\mathcal{L}](\zeta_{i_1} \cdots \zeta_{i_m} \mathsf{f}(\zeta))$ are spherically symmetric.

Let $\Phi_{i_1,\ldots,i_m}(\zeta_k)$ be a tensor field spherically symmetric of a symmetric tensor, i.e., $\Phi_{i_1,\ldots,i_m}(\zeta_k)$ is symmetric with respect to the subscripts $(i_1, \ldots, i_m)$ and satisfies the relation

$$\Phi_{i_1,\ldots,i_m}(l_{kh}\zeta_h) = l_{i_1 j_1} \cdots l_{i_m j_m} \Phi_{j_1,\ldots,j_m}(\zeta_k), \quad \text{(A.78)}$$

where

$$l_{ik} l_{jk} = \delta_{ij}.$$

The general form of $\Phi_{i_1,\ldots,i_m}(\zeta_k)$ is known to be expressed in the following form (see, for example, Sone [2002] for elementary derivation):

$$\Phi_{i_1,\ldots,i_m}(\zeta_h) = \sum_{n=0}^{[m/2]} g_n(\zeta) \sum_{*(m,2n)} \underbrace{\zeta_{i_a} \cdots \zeta_{i_b}}_{m-2n} \underbrace{\delta_{i_c i_d} \cdots \delta_{i_e i_f}}_{n}, \quad \text{(A.79)}$$

where $g_n(\zeta)$ is an arbitrary function of ζ, the symbol $[m/2]$ is the largest integer that does not exceed $m/2$, and the summation $\sum_{*(m,2n)}$ is carried out over $m!/2^n n!(m-2n)!$ terms in the following way: Divide m subscripts $(i_1, \ldots, i_m)$ into two sets: one with $m-2n$ elements $i_a, \ldots, i_b$ and the other with $2n$ elements $i_c, \ldots, i_f$, for which there are $m!/(2n)!(m-2n)!$ ways of division. For each division, consider all possible ways to make n pairs $(i_c, i_d), \ldots, (i_e, i_f)$ from the $2n$ elements $i_c, \ldots, i_f$, which are $(2n)!/2^n n!$. Then there are $m!/(2n)!(m-2n)! \times (2n)!/2^n n!$ terms. The $\sum_{*(m,2n)}$ means to sum up all these terms. For some small values of m, $\Phi_{i_1,\ldots,i_m}(\zeta_h)$ is given as follows:

$$\begin{aligned}
&m = 0: \ \Phi(\zeta_h) = g_0(\zeta),\\
&m = 1: \ \Phi_i(\zeta_h) = \zeta_i g_0(\zeta),\\
&m = 2: \ \Phi_{i,j}(\zeta_h) = \zeta_i\zeta_j g_0(\zeta) + \delta_{ij} g_1(\zeta),\\
&m = 3: \ \Phi_{i,j,k}(\zeta_h) = \zeta_i\zeta_j\zeta_k g_0(\zeta) + (\zeta_i\delta_{jk} + \zeta_j\delta_{ki} + \zeta_k\delta_{ij}) g_1(\zeta),\\
&m = 4: \ \Phi_{i,j,k,l}(\zeta_h) = \zeta_i\zeta_j\zeta_k\zeta_l g_0(\zeta)\\
&\qquad\qquad + (\zeta_i\zeta_j\delta_{kl} + \zeta_i\zeta_k\delta_{jl} + \zeta_i\zeta_l\delta_{jk} + \zeta_j\zeta_k\delta_{il} + \zeta_j\zeta_l\delta_{ik} + \zeta_k\zeta_l\delta_{ij}) g_1(\zeta)\\
&\qquad\qquad + (\delta_{ij}\delta_{kl} + \delta_{ik}\delta_{jl} + \delta_{il}\delta_{jk}) g_2(\zeta).
\end{aligned} \quad \text{(A.80)}$$

Let $\Phi_{i_1,\dots,i_m}(\zeta_k)$ be a tensor field axially symmetric with respect to axis a_i of a symmetric tensor, i.e., $\Phi_{i_1,\dots,i_m}(\zeta_k)$ is symmetric with respect to the subscripts $(i_1,\dots,i_m)$ and satisfies the relation

$$\Phi_{i_1,\dots,i_m}(l_{kj}\zeta_j) = l_{i_1 j_1}\cdots l_{i_m j_m}\Phi_{j_1,\dots,j_m}(\zeta_k), \tag{A.81}$$

where

$$l_{ik}l_{jk} = \delta_{ij}, \qquad l_{ij}a_j = a_i.$$

The general form of $\Phi_{i_1,\dots,i_m}(\zeta_k)$ for $a_i = (0,0,1)$ is expressed in the following form (see Sone [2002]):

$$\Phi_{\underbrace{i_1,\dots,i_h}_{h},\underbrace{3,\dots,3}_{m-h}}(\boldsymbol{\zeta}) = \sum_{N=0}^{[h/2]} g_N(\zeta,\zeta_3) \sum_{*(h,2N)} \underbrace{\zeta_{i_a}\cdots\zeta_{i_b}}_{h-2N}\underbrace{\delta_{i_c i_d}\cdots\delta_{i_e i_f}}_{N}, \tag{A.82}$$

where any of the indices $(i_1,\dots,i_h)$ does not take the value 3, $g_N(\zeta,\zeta_3)$ is an arbitrary function of ζ and ζ_3 [or $(\zeta_1^2+\zeta_2^2)^{1/2}$ and ζ_3], and the definition of $\sum_{*(h,2N)}$ just below Eq. (A.79) is applied here with h for m there. For some small values of h, $\Phi_{\underbrace{i_1,\dots,i_h}_{h},\underbrace{3,\dots,3}_{m-h}}(\zeta_h)$ is given as follows:

$$\begin{aligned}
h=0:\ & \Phi_{\underbrace{3,\dots,3}_{m}}(\boldsymbol{\zeta}) = g_0(\zeta,\zeta_3),\\
h=1:\ & \Phi_{i,\underbrace{3,\dots,3}_{m-1}}(\boldsymbol{\zeta}) = \zeta_i g_0(\zeta,\zeta_3),\\
h=2:\ & \Phi_{i,j,\underbrace{3,\dots,3}_{m-2}}(\boldsymbol{\zeta}) = \zeta_i\zeta_j g_0(\zeta,\zeta_3) + \delta_{ij} g_1(\zeta,\zeta_3),\\
h=3:\ & \Phi_{i,j,k,\underbrace{3,\dots,3}_{m-3}}(\boldsymbol{\zeta}) = \zeta_i\zeta_j\zeta_k g_0(\zeta,\zeta_3) + (\zeta_i\delta_{jk}+\zeta_j\delta_{ki}+\zeta_k\delta_{ij}) g_1(\zeta,\zeta_3),\\
h=4:\ & \Phi_{i,j,k,l,\underbrace{3,\dots,3}_{m-4}}(\boldsymbol{\zeta}) = \zeta_i\zeta_j\zeta_k\zeta_l g_0(\zeta,\zeta_3)\\
& \qquad + (\zeta_i\zeta_j\delta_{kl}+\zeta_i\zeta_k\delta_{jl}+\zeta_i\zeta_l\delta_{jk}+\zeta_j\zeta_k\delta_{il}+\zeta_j\zeta_l\delta_{ik}+\zeta_k\zeta_l\delta_{ij}) g_1(\zeta,\zeta_3)\\
& \qquad + (\delta_{ij}\delta_{kl}+\delta_{ik}\delta_{jl}+\delta_{il}\delta_{jk}) g_2(\zeta,\zeta_3),
\end{aligned} \tag{A.83}$$

where i, j, k, and l take the value 1 or 2.

A.2.6 Isotropic property of collision operator

For the convenience of discussion, the definition of isotropic operator in Section A.2.5 is repeated here. Put

$$F(\zeta_i) = Op[\phi_1(\zeta_i), \phi_2(\zeta_i), \dots], \tag{A.84}$$

where $Op[*,\ldots]$ is an operator and $\phi_s(\zeta_i)$ is a function of ζ_i. Take the new function $\phi_{sR}(\zeta_i)$ defined by

$$\phi_{sR}(\zeta_i) = \phi_s(l_{ij}\zeta_j),$$

where

$$l_{ik}l_{jk} = \delta_{ij}. \tag{A.85}$$

If the operator $Op[*,\ldots]$ satisfies the relation

$$F(l_{ij}\zeta_j) = Op[\phi_{1R}(\zeta_i), \phi_{2R}(\zeta_i), \ldots], \tag{A.86}$$

for arbitrary ϕ_s, then the operator $Op[*,\ldots]$ is called isotropic. We will show that the collision operators $\hat{J}(*,*)$ and $\mathcal{L}(*)$ [thus, $\hat{J}_a(*,*)$, $\mathcal{J}(*,*)$, $\mathcal{J}_a(*,*)$, and $\mathcal{L}_a(*)$], which are defined, respectively by Eqs. (1.47b) and (1.75b) [Eqs. (A.114b), (1.75c), (A.114a), and (A.111)], are isotropic.

First take the collision integral $\hat{J}(\hat{f},\hat{g})$

$$\hat{J}(\hat{f},\hat{g}) = \frac{1}{2}\int (\hat{f}'\hat{g}'_* + \hat{f}'_*\hat{g}' - \hat{f}\hat{g}_* - \hat{f}_*\hat{g})\widehat{B}(|\alpha_i V_i|/V, V)\,\mathrm{d}\Omega(\boldsymbol{\alpha})\,\mathbf{d}\boldsymbol{\zeta}_*, \tag{A.87}$$

where

$$\hat{f} = \hat{f}(\zeta_i), \qquad \hat{f}_* = \hat{f}(\zeta_{i*}), \qquad \hat{f}' = \hat{f}(\zeta'_i), \qquad \hat{f}'_* = \hat{f}(\zeta'_{i*}), \tag{A.88}$$

$$\zeta'_i = \zeta_i + \alpha_i\alpha_j V_j, \qquad \zeta'_{i*} = \zeta_{i*} - \alpha_i\alpha_j V_j, \quad V_i = \zeta_{i*} - \zeta_i, \quad V = (V_i^2)^{1/2}. \tag{A.89}$$

For the convenience of the following discussion, we introduce the notation

$$\bar{f}(\zeta_i) = \hat{f}(\bar{\zeta}_i), \qquad \bar{g}(\zeta_i) = \hat{g}(\bar{\zeta}_i), \qquad \bar{\zeta}_i = l_{ij}\zeta_j. \tag{A.90}$$

With this notation, the isotropic condition on $\hat{J}(*,*)$ is expressed as

$$\hat{J}(\bar{f},\bar{g}) = h_{f,g}(\bar{\zeta}_i),$$

for

$$\hat{J}(\hat{f},\hat{g}) = h_{f,g}(\zeta_i).$$

By definition,

$$\begin{aligned}\hat{J}(\bar{f},\bar{g}) &= \frac{1}{2}\int [\bar{f}(\zeta'_i)\bar{g}(\zeta'_{i*}) + \bar{f}(\zeta'_{i*})\bar{g}(\zeta'_i) - \bar{f}(\zeta_i)\bar{g}(\zeta_{i*}) - \bar{f}(\zeta_{i*})\bar{g}(\zeta_i)] \\ &\qquad \times \widehat{B}(|\alpha_i V_i|/V, V)\mathrm{d}\Omega(\boldsymbol{\alpha})\,\mathbf{d}\boldsymbol{\zeta}_* \\ &= \frac{1}{2}\int [\hat{f}(l_{ij}\zeta'_j)\hat{g}(l_{ij}\zeta'_{j*}) + \hat{f}(l_{ij}\zeta'_{j*})\hat{g}(l_{ij}\zeta'_j) - \hat{f}(\bar{\zeta}_i)\hat{g}(l_{ij}\zeta_{j*}) \\ &\qquad - \hat{f}(l_{ij}\zeta_{j*})\hat{g}(\bar{\zeta}_i)]\widehat{B}(|\alpha_i V_i|/V, V)\mathrm{d}\Omega(\boldsymbol{\alpha})\,\mathbf{d}\boldsymbol{\zeta}_*. \end{aligned} \tag{A.91}$$

Here, we introduce the change of variables of integration from ($\boldsymbol{\alpha}$, $\boldsymbol{\zeta}_*$) to ($\bar{\boldsymbol{\alpha}}$, $\bar{\boldsymbol{\zeta}}_*$) defined by

$$\bar{\zeta}_{i*} = l_{ij}\zeta_{j*}, \qquad \bar{\alpha}_i = l_{ij}\alpha_j, \tag{A.92}$$

and the notation

$$\bar{V}_i = \bar{\zeta}_{i*} - \bar{\zeta}_i \ (= l_{ij} V_j), \quad \bar{V} = (\bar{V}_i^2)^{1/2}. \tag{A.93}$$

Then, owing to Eq. (A.85),[29]

$$\bar{\alpha}_i \bar{V}_i = \alpha_i V_i, \quad \bar{V} = V, \quad (\bar{\alpha}_i^2)^{1/2} = 1, \quad \mathrm{d}\Omega(\boldsymbol{\alpha})\, \mathbf{d}\boldsymbol{\zeta}_* = \mathrm{d}\Omega(\bar{\boldsymbol{\alpha}})\, \mathbf{d}\bar{\boldsymbol{\zeta}}_*, \tag{A.94}$$

and from Eqs. (A.89), (A.90), (A.92), and (A.94),

$$l_{ij}\zeta'_j = l_{ij}(\zeta_j + \alpha_j \alpha_k V_k) = \ \bar{\zeta}_i + \bar{\alpha}_i \bar{\alpha}_k \bar{V}_k, \tag{A.95a}$$

$$l_{ij}\zeta'_{j*} = l_{ij}(\zeta_{j*} - \alpha_j \alpha_k V_k) = \ \bar{\zeta}_{i*} - \bar{\alpha}_i \bar{\alpha}_k \bar{V}_k. \tag{A.95b}$$

Further, with the aid of Eqs. (A.94), (A.95a), and (A.95b),

$$\left.\begin{aligned} &\bar{f}(\zeta_i) = \hat{f}(\bar{\zeta}_i), \qquad \bar{f}(\zeta_{i*}) = \hat{f}(\bar{\zeta}_{i*}), \\ &\bar{f}(\zeta'_i) = \hat{f}(l_{ij}\zeta'_j) = \hat{f}(\bar{\zeta}_i + \bar{\alpha}_i \bar{\alpha}_k \bar{V}_k) = \hat{f}(\widetilde{\zeta}'_i), \\ &\bar{f}(\zeta'_{i*}) = \hat{f}(l_{ij}\zeta'_{j*}) = \hat{f}(\bar{\zeta}_{i*} - \bar{\alpha}_i \bar{\alpha}_k \bar{V}_k) = \hat{f}(\widetilde{\zeta}'_{i*}), \\ &\widehat{B}(|\alpha_i V_i|/V, V) = \widehat{B}(|\bar{\alpha}_i \bar{V}_i|/\bar{V}, \bar{V}), \end{aligned}\right\} \tag{A.96}$$

where

$$\widetilde{\zeta}'_i = \bar{\zeta}_i + \bar{\alpha}_i \bar{\alpha}_k \bar{V}_k, \quad \widetilde{\zeta}'_{i*} = \ \bar{\zeta}_{i*} - \bar{\alpha}_i \bar{\alpha}_k \bar{V}_k. \tag{A.97}$$

With the aid of these relations, we have

$$\begin{aligned} \hat{J}(\bar{f}, \bar{g}) = \frac{1}{2} \int &[\hat{f}(\widetilde{\zeta}'_i)\hat{g}(\widetilde{\zeta}'_{i*}) + \hat{f}(\widetilde{\zeta}'_{i*})\hat{g}(\widetilde{\zeta}'_i) - \hat{f}(\bar{\zeta}_i)\hat{g}(\bar{\zeta}_{i*}) - \hat{f}(\bar{\zeta}_{i*})\hat{g}(\bar{\zeta}_i)] \\ &\times \widehat{B}(|\bar{\alpha}_i \bar{V}_i|/\bar{V}, \bar{V}) \mathrm{d}\Omega(\bar{\boldsymbol{\alpha}})\, \mathbf{d}\bar{\boldsymbol{\zeta}}_*. \end{aligned} \tag{A.98}$$

Here, we transcribe the letters of the variables of integration from ($\bar{\boldsymbol{\alpha}}$, $\bar{\boldsymbol{\zeta}}_*$) to ($\boldsymbol{\alpha}$, $\boldsymbol{\zeta}_*$).[30] Corresponding to this transcription, we also introduce the transcription

$$\widetilde{\zeta}'_i \to \zeta'_i, \quad \widetilde{\zeta}'_{i*} \to \ \zeta'_{i*}, \quad \bar{V}_i \to V_i, \quad \bar{V} \to V,$$

which is safely done because the new letters are not included in Eq. (A.98). With these transcriptions, Eq. (A.98) and the new transcribed letters (ζ'_i, ζ'_{i*}, V_i, V) are expressed as follows:

$$\begin{aligned} \hat{J}(\bar{f}, \bar{g}) = \frac{1}{2} \int &[\hat{f}(\zeta'_i)\hat{g}(\zeta'_{i*}) + \hat{f}(\zeta'_{i*})\hat{g}(\zeta'_i) - \hat{f}(\bar{\zeta}_i)\hat{g}(\zeta_{i*}) - \hat{f}(\zeta_{i*})\hat{g}(\bar{\zeta}_i)] \\ &\times \widehat{B}(|\alpha_i V_i|/V, V) \mathrm{d}\Omega(\boldsymbol{\alpha})\, \mathbf{d}\boldsymbol{\zeta}_*, \end{aligned} \tag{A.99}$$

and

$$V_i = \zeta_{i*} - \bar{\zeta}_i, \quad V = (V_i^2)^{1/2}, \tag{A.100a}$$

$$\zeta'_i = \bar{\zeta}_i + \alpha_i \alpha_j V_j, \qquad \zeta'_{i*} = \zeta_{i*} - \alpha_i \alpha_j V_j, \tag{A.100b}$$

[29] $\bar{a}_i \bar{b}_i = l_{ij} a_j l_{ik} b_k = \delta_{jk} a_j b_k = a_j b_j$.

[30] This is just a transcription but not a change of the variables.

with the aid of Eqs. (A.93) and (A.97).

Equation (A.99) with Eqs. (A.100a) and (A.100b) being compared with Eq. (A.87) with Eqs. (A.88) and (A.89), the only difference is that ζ_i in the latter (or in the original collision integral) is replaced by $\bar{\zeta}_i$ in the former (or in the collision integral with $\bar{f}$ and $\bar{g}$). That is,

$$\hat{J}(\bar{f},\bar{g}) = h_{f,g}(\bar{\zeta}_i). \tag{A.101}$$

Therefore, the collision operator $\hat{J}(*,*)$ is isotropic.

Next, take the linearized collision integral defined by Eq. (1.75b)

$$\begin{aligned}\mathcal{L}(\phi) &= \int E_*(\phi' + \phi'_* - \phi - \phi_*)\widehat{B}(|\alpha_i V_i|/V, V)\mathrm{d}\Omega(\boldsymbol{\alpha})\,\mathbf{d}\boldsymbol{\zeta}_*, \\ \phi &= \phi(\zeta_i), \quad \phi_* = \phi(\zeta_{i*}), \quad \phi' = \phi(\zeta'_i), \quad \phi'_* = \phi(\zeta'_{i*}).\end{aligned} \tag{A.102}$$

Putting

$$f = E\phi, \quad g = E,$$

in another expression of Eq. (A.102)[31]

$$E\mathcal{L}(\phi) = \int (E'\phi' E'_* + E'_*\phi'_* E' - E\phi E_* - E_*\phi_* E)\widehat{B}(|\alpha_i V_i|/V, V)\mathrm{d}\Omega(\boldsymbol{\alpha})\,\mathbf{d}\boldsymbol{\zeta}_*,$$

we have

$$\begin{aligned}E\mathcal{L}(\phi) &= \int (f'g'_* + f'_*g' - fg_* - f_*g)\widehat{B}(|\alpha_i V_i|/V, V)\mathrm{d}\Omega(\boldsymbol{\alpha})\,\mathbf{d}\boldsymbol{\zeta}_* \\ &= 2\hat{J}(E\phi, E) = 2h_{E\phi,E}(\zeta_i).\end{aligned} \tag{A.103}$$

Noting the relation

$$E = \bar{E}, \quad \bar{f}\bar{g} = \overline{fg},$$

we have

$$E\mathcal{L}(\bar{\phi}) = 2\hat{J}(E\bar{\phi}, E) = 2\hat{J}(\bar{E}\bar{\phi}, \bar{E}) = 2\hat{J}(\overline{E\phi}, \bar{E}) = 2h_{E\phi,E}(\bar{\zeta}_i). \tag{A.104}$$

The last relation is due to the isotropic property (A.101) of $\hat{J}(*,*)$. Comparing Eq. (A.104) with Eq. (A.103), we find that the linearized collision operator $E\mathcal{L}(*)$, thus $\mathcal{L}(*)$, is isotropic.

A.2.7 Parity of the linearized collision integral $\mathcal{L}(\phi)$

Take the linearized collision integral $\mathcal{L}(\phi)$ defined by Eq. (1.75b), i.e.,

$$\begin{aligned}&\mathcal{L}(\phi) = \int E_*(\phi' + \phi'_* - \phi - \phi_*)\widehat{B}\,\mathrm{d}\Omega(\boldsymbol{\alpha})\,\mathbf{d}\boldsymbol{V}, \\ &\widehat{B} = \widehat{B}(|\boldsymbol{\alpha}\cdot\boldsymbol{V}|/|\boldsymbol{V}|, |\boldsymbol{V}|), \\ &\phi = \phi(\zeta_i),\ \phi_* = \phi(\zeta_{i*}),\ \phi' = \phi(\zeta'_i),\ \phi'_* = \phi(\zeta'_{i*}), \\ &\zeta'_i = \zeta_i + \alpha_j V_j \alpha_i,\ \zeta'_{i*} = \zeta_{i*} - \alpha_j V_j \alpha_i,\ \zeta_{i*} = V_i + \zeta_i,\end{aligned} \tag{A.105}$$

[31] Note $E'E'_* = EE_*$.

where the variable of integration is changed from $\boldsymbol{\zeta}_*$ to $\boldsymbol{V}\,(=\boldsymbol{\zeta}_*-\boldsymbol{\zeta})$. We will show that the parity (even or odd) of $\mathcal{L}(\phi)$ with respect to a component of $\boldsymbol{\zeta}$, i.e., ζ_1, ζ_2, or ζ_3, agrees with that of ϕ.

Consider the integral of the form

$$\int \Psi(\chi_1,\chi_2,\chi_3)\Phi_E(\zeta_{1*},\zeta_{2*},\zeta_{3*})\,\widehat{B}\,(|\alpha_i V_i|/|V_i|,|V_i|)\mathrm{d}\Omega(\boldsymbol{\alpha})\,\mathbf{d}\boldsymbol{V}, \tag{A.106}$$

where $\Phi_E(\zeta_1,\zeta_2,\zeta_3)$ is an even function with respect to ζ_1, i.e., $\Phi_E(\zeta_1,\zeta_2,\zeta_3)=\Phi_E(-\zeta_1,\zeta_2,\zeta_3)$. The integral (A.106) is denoted, depending on the definition of χ_i, by

$$I:\ \text{Eq. (A.106) for } \chi_i=\zeta_{i*}=V_i+\zeta_i \text{ and } \Phi_E=1, \tag{A.107a}$$

$$II:\ \text{Eq. (A.106) for } \chi_i=\zeta_i'=\zeta_i+\alpha_j V_j\alpha_i, \tag{A.107b}$$

$$III:\ \text{Eq. (A.106) for } \chi_i=\zeta_{i*}'=\zeta_{i*}-\alpha_j V_j\alpha_i=V_i+\zeta_i-\alpha_j V_j\alpha_i. \tag{A.107c}$$

When the function $\Psi(\chi_1,\chi_2,\chi_3)$ is even with respect to the first argument, i.e., χ_1, it is denoted by Ψ_E and the subscript 0 is attached to the integral I, II, or III, and when Ψ is odd with respect to χ_1, it is denoted by Ψ_O and the subscript 1 is attached to the integral. We will examine the parity of the integrals I, II, and III. In the following manipulation, the change of variables of integration from V_i and α_i to $\widetilde{V}_i$ and $\widetilde{\alpha}_i$ defined by

$$\widetilde{V}_1=-V_1,\quad \widetilde{V}_s=V_s,\quad \widetilde{\alpha}_1=-\alpha_1,\quad \widetilde{\alpha}_s=\alpha_s\quad (s=2,3),$$

is performed. Noting that

$$\zeta_{i*}=V_i+\zeta_i,\qquad |\widetilde{V}_i|=|V_i|,\qquad \widetilde{\alpha}_i\widetilde{V}_i=\alpha_i V_i,$$

we can transform the integrals I, II, and III in the following way, where the subscript s indicates $s=2$ and 3:

$$\begin{aligned}
I_0(\zeta_1,\zeta_s)&=\int \Psi_E(V_1+\zeta_1,V_s+\zeta_s)\,\widehat{B}\,(|\alpha_i V_i|/|V_i|,|V_i|)\mathrm{d}\Omega(\boldsymbol{\alpha})\,\mathbf{d}\boldsymbol{V}\\
&=\int \Psi_E(-\widetilde{V}_1+\zeta_1,\widetilde{V}_s+\zeta_s)\,\widehat{B}\,(|\widetilde{\alpha}_i\widetilde{V}_i|/|\widetilde{V}_i|,|\widetilde{V}_i|)\mathrm{d}\Omega(\widetilde{\boldsymbol{\alpha}})\,\mathbf{d}\widetilde{\boldsymbol{V}}\\
&=\int \Psi_E(\widetilde{V}_1-\zeta_1,\widetilde{V}_s+\zeta_s)\,\widehat{B}\,(|\widetilde{\alpha}_i\widetilde{V}_i|/|\widetilde{V}_i|,|\widetilde{V}_i|)\mathrm{d}\Omega(\widetilde{\boldsymbol{\alpha}})\,\mathbf{d}\widetilde{\boldsymbol{V}}\\
&=I_0(-\zeta_1,\zeta_s),
\end{aligned}$$

$$\begin{aligned}
I_1(\zeta_1,\zeta_s)&=\int \Psi_O(V_1+\zeta_1,V_s+\zeta_s)\,\widehat{B}\,(|\alpha_i V_i|/|V_i|,|V_i|)\mathrm{d}\Omega(\boldsymbol{\alpha})\,\mathbf{d}\boldsymbol{V}\\
&=\int \Psi_O(-\widetilde{V}_1+\zeta_1,\widetilde{V}_s+\zeta_s)\,\widehat{B}\,(|\widetilde{\alpha}_i\widetilde{V}_i|/|\widetilde{V}_i|,|\widetilde{V}_i|)\mathrm{d}\Omega(\widetilde{\boldsymbol{\alpha}})\,\mathbf{d}\widetilde{\boldsymbol{V}}\\
&=-\int \Psi_O(\widetilde{V}_1-\zeta_1,\widetilde{V}_s+\zeta_s)\,\widehat{B}\,(|\widetilde{\alpha}_i\widetilde{V}_i|/|\widetilde{V}_i|,|\widetilde{V}_i|)\mathrm{d}\Omega(\widetilde{\boldsymbol{\alpha}})\,\mathbf{d}\widetilde{\boldsymbol{V}}\\
&=-I_1(-\zeta_1,\zeta_s),
\end{aligned}$$

$$
\begin{aligned}
\mathit{II}_0(\zeta_1,\zeta_s) &= \int \Psi_E(\zeta_i+\alpha_j V_j\alpha_i)\Phi_E(V_i+\zeta_i)\,\widehat{B}\left(|\alpha_i V_i|/|V_i|,|V_i|\right)\mathrm{d}\Omega(\boldsymbol{\alpha})\,\mathbf{d}\boldsymbol{V}\\
&= \int \Psi_E(\zeta_1-\widetilde{\alpha}_j\widetilde{V}_j\widetilde{\alpha}_1,\zeta_s+\widetilde{\alpha}_j\widetilde{V}_j\widetilde{\alpha}_s)\Phi_E(-\widetilde{V}_1+\zeta_1,\widetilde{V}_s+\zeta_s)\\
&\qquad\times\,\widehat{B}\left(|\widetilde{\alpha}_i\widetilde{V}_i|/|\widetilde{V}_i|,|\widetilde{V}_i|\right)\mathrm{d}\Omega(\widetilde{\boldsymbol{\alpha}})\,\mathbf{d}\widetilde{\boldsymbol{V}}\\
&= \int \Psi_E(-\zeta_1+\widetilde{\alpha}_j\widetilde{V}_j\widetilde{\alpha}_1,\zeta_s+\widetilde{\alpha}_j\widetilde{V}_j\widetilde{\alpha}_s)\Phi_E(\widetilde{V}_1-\zeta_1,\widetilde{V}_s+\zeta_s)\\
&\qquad\times\,\widehat{B}\left(|\widetilde{\alpha}_i\widetilde{V}_i|/|\widetilde{V}_i|,|\widetilde{V}_i|\right)\mathrm{d}\Omega(\widetilde{\boldsymbol{\alpha}})\,\mathbf{d}\widetilde{\boldsymbol{V}}\\
&= \mathit{II}_0(-\zeta_1,\zeta_s),
\end{aligned}
$$

$$
\begin{aligned}
\mathit{II}_1(\zeta_1,\zeta_s) &= \int \Psi_O(\zeta_i+\alpha_j V_j\alpha_i)\Phi_E(V_i+\zeta_i)\,\widehat{B}\left(|\alpha_i V_i|/|V_i|,|V_i|\right)\mathrm{d}\Omega(\boldsymbol{\alpha})\,\mathbf{d}\boldsymbol{V}\\
&= \int \Psi_O(\zeta_1-\widetilde{\alpha}_j\widetilde{V}_j\widetilde{\alpha}_1,\zeta_s+\widetilde{\alpha}_j\widetilde{V}_j\widetilde{\alpha}_s)\Phi_E(-\widetilde{V}_1+\zeta_1,\widetilde{V}_s+\zeta_s)\\
&\qquad\times\,\widehat{B}\left(|\widetilde{\alpha}_i\widetilde{V}_i|/|\widetilde{V}_i|,|\widetilde{V}_i|\right)\mathrm{d}\Omega(\widetilde{\boldsymbol{\alpha}})\,\mathbf{d}\widetilde{\boldsymbol{V}}\\
&= -\int \Psi_O(-\zeta_1+\widetilde{\alpha}_j\widetilde{V}_j\widetilde{\alpha}_1,\zeta_s+\widetilde{\alpha}_j\widetilde{V}_j\widetilde{\alpha}_s)\Phi_E(\widetilde{V}_1-\zeta_1,\widetilde{V}_s+\zeta_s)\\
&\qquad\times\,\widehat{B}\left(|\widetilde{\alpha}_i\widetilde{V}_i|/|\widetilde{V}_i|,|\widetilde{V}_i|\right)\mathrm{d}\Omega(\widetilde{\boldsymbol{\alpha}})\,\mathbf{d}\widetilde{\boldsymbol{V}}\\
&= -\mathit{II}_1(-\zeta_1,\zeta_s),
\end{aligned}
$$

$$
\begin{aligned}
\mathit{III}_0(\zeta_1,\zeta_s) &= \int \Psi_E(V_i+\zeta_i-\alpha_j V_j\alpha_i)\Phi_E(V_i+\zeta_i)\,\widehat{B}\left(|\alpha_i V_i|/|V_i|,|V_i|\right)\mathrm{d}\Omega(\boldsymbol{\alpha})\,\mathbf{d}\boldsymbol{V}\\
&= \int \Psi_E(-\widetilde{V}_1+\zeta_1+\widetilde{\alpha}_j\widetilde{V}_j\widetilde{\alpha}_1,\widetilde{V}_s+\zeta_s-\widetilde{\alpha}_j\widetilde{V}_j\widetilde{\alpha}_s)\\
&\quad\times\Phi_E(-\widetilde{V}_1+\zeta_1,\widetilde{V}_s+\zeta_s)\,\widehat{B}\left(|\widetilde{\alpha}_i\widetilde{V}_i|/|\widetilde{V}_i|,|\widetilde{V}_i|\right)\mathrm{d}\Omega(\widetilde{\boldsymbol{\alpha}})\,\mathbf{d}\widetilde{\boldsymbol{V}}\\
&= \int \Psi_E(\widetilde{V}_1-\zeta_1-\widetilde{\alpha}_j\widetilde{V}_j\widetilde{\alpha}_1,\widetilde{V}_s+\zeta_s-\widetilde{\alpha}_j\widetilde{V}_j\widetilde{\alpha}_s)\\
&\quad\times\Phi_E(\widetilde{V}_1-\zeta_1,\widetilde{V}_s+\zeta_s)\,\widehat{B}\left(|\widetilde{\alpha}_i\widetilde{V}_i|/|\widetilde{V}_i|,|\widetilde{V}_i|\right)\mathrm{d}\Omega(\widetilde{\boldsymbol{\alpha}})\,\mathbf{d}\widetilde{\boldsymbol{V}}\\
&= \mathit{III}_0(-\zeta_1,\zeta_s),
\end{aligned}
$$

$$
\begin{aligned}
\mathit{III}_1(\zeta_1,\zeta_s) &= \int \Psi_O(V_i+\zeta_i-\alpha_j V_j\alpha_i)\Phi_E(V_i+\zeta_i)\,\widehat{B}\left(|\alpha_i V_i|/|V_i|,|V_i|\right)\mathrm{d}\Omega(\boldsymbol{\alpha})\,\mathbf{d}\boldsymbol{V}\\
&= \int \Psi_O(-\widetilde{V}_1+\zeta_1+\widetilde{\alpha}_j\widetilde{V}_j\widetilde{\alpha}_1,\widetilde{V}_s+\zeta_s-\widetilde{\alpha}_j\widetilde{V}_j\widetilde{\alpha}_s)\\
&\quad\times\Phi_E(-\widetilde{V}_1+\zeta_1,\widetilde{V}_s+\zeta_s)\,\widehat{B}\left(|\widetilde{\alpha}_i\widetilde{V}_i|/|\widetilde{V}_i|,|\widetilde{V}_i|\right)\mathrm{d}\Omega(\widetilde{\boldsymbol{\alpha}})\,\mathbf{d}\widetilde{\boldsymbol{V}}\\
&= -\int \Psi_O(\widetilde{V}_1-\zeta_1-\widetilde{\alpha}_j\widetilde{V}_j\widetilde{\alpha}_1,\widetilde{V}_s+\zeta_s-\widetilde{\alpha}_j\widetilde{V}_j\widetilde{\alpha}_s)\\
&\quad\times\Phi_E(\widetilde{V}_1-\zeta_1,\widetilde{V}_s+\zeta_s)\,\widehat{B}\left(|\widetilde{\alpha}_i\widetilde{V}_i|/|\widetilde{V}_i|,|\widetilde{V}_i|\right)\mathrm{d}\Omega(\widetilde{\boldsymbol{\alpha}})\,\mathbf{d}\widetilde{\boldsymbol{V}}\\
&= -\mathit{III}_1(-\zeta_1,\zeta_s).
\end{aligned}
$$

Similar relations hold for the variables ζ_2 and ζ_3. Thus, the parity of the integrals I, II, and III with respect to a component of $\boldsymbol{\zeta}$, i.e., ζ_1, ζ_2, or ζ_3, agrees with that of Ψ.

The linearized collision integral $\mathcal{L}(\phi)$ is expressed as the sum of the three types of the integrals I, II, and III as

$$\begin{aligned}\mathcal{L}(\phi) &= \int E_*(\phi' + \phi'_* - \phi - \phi_*)\widehat{B}\,\mathrm{d}\Omega(\boldsymbol{\alpha})\,\mathbf{d}\boldsymbol{\zeta}_* \\ &= II(\Psi = \phi, \Phi_E = E) + III(\Psi = \phi, \Phi_E = E) \\ &\quad - \phi I_0(\Psi_E = E) - I(\Psi = \phi E).\end{aligned}$$

Therefore, the parity (even or odd) of $\mathcal{L}(\phi)$ with respect to a component of $\boldsymbol{\zeta}$, i.e., ζ_1, ζ_2, or ζ_3, agrees with that of ϕ.

Incidentally, the collision integral $\hat{J}(\hat{f}, \hat{f})$ can be easily shown to be even with respect to ζ_1, ζ_2, or ζ_3 when $\hat{f}$ is even with respect to ζ_1, ζ_2, or ζ_3 with the aid of a similar transformation of the variables.

A.2.8 Linearized collision integral $\mathcal{L}_a(\phi)$ and integral equation $\mathcal{L}_a(\phi) = \mathbb{h}$

The linearized collision integral $\mathcal{L}(\phi)$

$$\mathcal{L}(\phi(\boldsymbol{\zeta})) = \int E(\zeta_*)(\phi' + \phi'_* - \phi - \phi_*)\widehat{B}\,\mathrm{d}\Omega(\boldsymbol{\alpha})\,\mathbf{d}\boldsymbol{\zeta}_*, \tag{A.108}$$

where

$$\widehat{B} = \widehat{B}(|\boldsymbol{\alpha}\cdot(\boldsymbol{\zeta}_* - \boldsymbol{\zeta})|/|\boldsymbol{\zeta}_* - \boldsymbol{\zeta}|, |\boldsymbol{\zeta}_* - \boldsymbol{\zeta}|), \tag{A.109a}$$

$$\phi = \phi(\boldsymbol{\zeta}), \quad \phi_* = \phi(\boldsymbol{\zeta}_*), \quad \phi' = \phi(\boldsymbol{\zeta}'), \quad \phi'_* = \phi(\boldsymbol{\zeta}'_*), \tag{A.109b}$$

$$\boldsymbol{\zeta}' = \boldsymbol{\zeta} + [\boldsymbol{\alpha}\cdot(\boldsymbol{\zeta}_* - \boldsymbol{\zeta})]\boldsymbol{\alpha}, \quad \boldsymbol{\zeta}'_* = \boldsymbol{\zeta}_* - [\boldsymbol{\alpha}\cdot(\boldsymbol{\zeta}_* - \boldsymbol{\zeta})]\boldsymbol{\alpha}, \tag{A.109c}$$

is introduced in Section 1.10. This is related to the linear part, with respect to the perturbation ϕ, of the collision integral $\hat{J}(\hat{f}, \hat{f})$ defined by Eq. (1.47b) when $\hat{f}$ is given in the form

$$\hat{f} = E(\zeta)(1 + \phi), \quad E(\zeta) = \pi^{-3/2}\exp(-\zeta^2), \quad \zeta = (\zeta_i^2)^{1/2}.$$

That is,

$$\hat{J}(E(1+\phi), E(1+\phi)) = 2\hat{J}(E, E\phi) + \hat{J}(E\phi, E\phi).$$

Then, $\mathcal{L}(\phi)$ and $\mathcal{J}(\phi, \phi)$, defined by Eq. (1.75c), are related to $\hat{J}$ as

$$E\mathcal{L}(\phi) = 2\hat{J}(E, E\phi), \tag{A.110a}$$

$$E\mathcal{J}(\phi, \phi) = \hat{J}(E\phi, E\phi). \tag{A.110b}$$

In this sense, $\mathcal{L}(\phi)$ is called the collision integral linearized around the equilibrium state E.

We introduce a slight extension of $\mathcal{L}(\phi)$, i.e.,

$$\mathcal{L}_a(\phi(\boldsymbol{\zeta})) = \int E(\zeta_*)(\phi' + \phi'_* - \phi - \phi_*)\widehat{B}_a \mathrm{d}\Omega(\boldsymbol{\alpha})\, \mathbf{d}\boldsymbol{\zeta}_*, \tag{A.111}$$

$$\begin{aligned}\widehat{B}_a &= \widehat{B}_a(|\boldsymbol{\alpha}\cdot(\boldsymbol{\zeta}_* - \boldsymbol{\zeta})|/|\boldsymbol{\zeta}_* - \boldsymbol{\zeta}|, |\boldsymbol{\zeta}_* - \boldsymbol{\zeta}|) \\ &= \frac{\widehat{B}(|\boldsymbol{\alpha}\cdot(\boldsymbol{\zeta}_* - \boldsymbol{\zeta})|/|\boldsymbol{\zeta}_* - \boldsymbol{\zeta}|, |\boldsymbol{\zeta}_* - \boldsymbol{\zeta}|a^{1/2})}{a^{1/2}},\end{aligned} \tag{A.112}$$

where $a\,(>0)$ may depend on $\boldsymbol{x}$ and $\hat{t}$ but is independent of $\boldsymbol{\zeta}$. The operator $\mathcal{L}(\phi)$ is the special case $a = 1$ of $\mathcal{L}_a(\phi)$, i.e.,

$$\mathcal{L}(\phi) = \mathcal{L}_1(\phi).$$

For a hard-sphere gas, $\widehat{B}_a = |\alpha_i(\zeta_{i*} - \zeta_i)|/4(2\pi)^{1/2}$. For the BKW equation, the operator $\mathcal{L}_a(*)$ is consistently defined as linearized in the above sense in the form

$$a^{1/2}\mathcal{L}_a(\phi) = \int \left[1 + 2\zeta_i\zeta_{i*} + \frac{2}{3}\left({\zeta_i}^2 - \frac{3}{2}\right)\left({\zeta_{j*}}^2 - \frac{3}{2}\right)\right]\phi(\zeta_{k*})E(\zeta_*)\mathbf{d}\boldsymbol{\zeta}_* - \phi. \tag{A.113}$$

Incidentally, we introduce the extensions $\mathcal{J}_a(\phi,\psi)$ and $\hat{J}_a(\hat{f},\hat{g})$ of $\mathcal{J}(\phi,\psi)$ and $\hat{J}(\hat{f},\hat{g})$ [see Eqs. (1.75c) and (1.47b)] as

$$\mathcal{J}_a(\phi(\boldsymbol{\zeta}),\psi(\boldsymbol{\zeta})) = \frac{1}{2}\int E_*(\phi'\psi'_* + \phi'_*\psi' - \phi\psi_* - \phi_*\psi)\widehat{B}_a\, \mathrm{d}\Omega(\boldsymbol{\alpha})\, \mathbf{d}\boldsymbol{\zeta}_*, \tag{A.114a}$$

$$\hat{J}_a(\hat{f}(\boldsymbol{\zeta}),\hat{g}(\boldsymbol{\zeta})) = \frac{1}{2}\int (\hat{f}'\hat{g}'_* + \hat{f}'_*\hat{g}' - \hat{f}\hat{g}_* - \hat{f}_*\hat{g})\widehat{B}_a\, \mathrm{d}\Omega(\boldsymbol{\alpha})\, \mathbf{d}\boldsymbol{\zeta}_*. \tag{A.114b}$$

The linearized collision integral around a general Maxwellian is related to $\mathcal{L}_a(\phi)$. That is, let $\hat{f}$ be the Maxwellian

$$\hat{f} = \frac{\hat{\rho}}{(\pi\hat{T})^{3/2}}\exp\left(-\frac{(\zeta_i - \hat{v}_i)^2}{\hat{T}}\right). \tag{A.115}$$

The linearized collision integral $2\hat{J}(\hat{f},\hat{f}\Phi)$ is expressed with $\mathcal{L}_a(*)$ as

$$2\hat{J}(\hat{f},\hat{f}\Phi(\zeta_i)) = \frac{\hat{\rho}^2}{\hat{T}}E(\tilde{\zeta})\mathcal{L}_{\hat{T}}(\phi(\tilde{\zeta}_i)), \tag{A.116}$$

where

$$\tilde{\zeta}_i = (\zeta_i - \hat{v}_i)/\hat{T}^{1/2}, \qquad \phi(\tilde{\zeta}_i) = \Phi(\zeta_i), \tag{A.117}$$

and $\mathcal{L}_{\hat{T}}(\phi(\tilde{\zeta}_i))$ means that ζ_i, ζ_{i*}, ζ'_i, and ζ'_{i*} in Eqs. (A.111), (A.112), (A.109b), and (A.109c) are replaced by $\tilde{\zeta}_i$, $\tilde{\zeta}_{i*}$, $\tilde{\zeta}'_i$, and $\tilde{\zeta}'_{i*}$ respectively.

Now take the group of integral equations

$$\mathcal{L}_a[\phi_{i_1,\ldots,i_m}(\zeta_k)] = H_{i_1,\ldots,i_m}(\zeta_k), \tag{A.118}$$

where the inhomogeneous term $H_{i_1,\ldots,i_m}(\zeta_k)$, which satisfies the solvability condition[32]

$$\int (1, \zeta_i, \zeta^2) H_{i_1,\ldots,i_m}(\zeta_k) E(\zeta) \mathbf{d\zeta} = 0,$$

is assumed to be symmetric with respect to the subscripts $(i_1, \ldots, i_m)$ and spherically symmetric, i.e.,

$$H_{i_1,\ldots,i_m}(l_{kh}\zeta_h) = l_{i_1 j_1} \cdots l_{i_m j_m} H_{j_1,\ldots,j_m}(\zeta_k) \quad \text{with } l_{ik} l_{jk} = \delta_{ij}. \tag{A.119}$$

We will show that the solution $\phi_{i_1,\ldots,i_m}(\zeta_k)$ of Eq. (A.118) that is orthogonal to 1, ζ_i, and ζ^2 (the solutions of the associated homogeneous equation), i.e.,

$$\int (1,\ \zeta_i,\ \zeta^2) \phi_{i_1,\ldots,i_m}(\zeta_k) E(\zeta) \mathbf{d\zeta} = 0, \tag{A.120}$$

is spherically symmetric, i.e.,

$$\phi_{i_1,\ldots,i_m}(l_{kh}\zeta_h) = l_{i_1 j_1} \cdots l_{i_m j_m} \phi_{j_1,\ldots,j_m}(\zeta_k), \tag{A.121}$$

and symmetric with respect to the subscripts $(i_1, \ldots, i_m)$.

The operator $\mathcal{L}_a(*)$ being isotropic [see Eq. (A.76)],

$$\begin{aligned} \mathcal{L}_a[\phi_{i_1,\ldots,i_m}(l_{kh}\zeta_h)] &= H_{i_1,\ldots,i_m}(l_{kh}\zeta_h) \\ &= l_{i_1 j_1} \cdots l_{i_m j_m} H_{j_1,\ldots,j_m}(\zeta_k) \\ &= l_{i_1 j_1} \cdots l_{i_m j_m} \mathcal{L}_a[\phi_{j_1,\ldots,j_m}(\zeta_k)], \end{aligned}$$

with the aid of Eqs. (A.118) and (A.119). By the linearity of $\mathcal{L}_a(*)$,

$$\mathcal{L}_a[\phi_{i_1,\ldots,i_m}(l_{kh}\zeta_h) - l_{i_1 j_1} \cdots l_{i_m j_m} \phi_{j_1,\ldots,j_m}(\zeta_k)] = 0. \tag{A.122}$$

With the aid of Eq. (A.120), it is easy to show that $\phi_{i_1,\ldots,i_m}(l_{kh}\zeta_h)$, and therefore $\phi_{i_1,\ldots,i_m}(l_{kh}\zeta_h) - l_{i_1 j_1} \cdots l_{i_m j_m} \phi_{j_1,\ldots,j_m}(\zeta_k)$, is orthogonal to 1, ζ_i, and ζ^2. On the other hand, the functions 1, ζ_i, and ζ^2 are the only possible independent solutions of the homogeneous equation $\mathcal{L}_a(\phi) = 0$ [see the last paragraph of Section A.2.2]. Therefore, $\phi_{i_1,\ldots,i_m}(l_{kh}\zeta_h) - l_{i_1 j_1} \cdots l_{i_m j_m} \phi_{j_1,\ldots,j_m}(\zeta_k) = 0$ is the unique solution of Eq. (A.122). That is,

$$\phi_{i_1,\ldots,i_m}(l_{kh}\zeta_h) = l_{i_1 j_1} \cdots l_{i_m j_m} \phi_{j_1,\ldots,j_m}(\zeta_k).$$

The solution $\phi_{i_1,\ldots,i_m}(\zeta_k)$ of Eq. (A.118) subject to the orthogonal condition (A.120) is spherically symmetric. Further,

$$\begin{aligned} \mathcal{L}_a[\phi_{i_1,\ldots,i_p,\ldots,i_n,\ldots,i_m}(\zeta_k)] &= H_{i_1,\ldots,i_p,\ldots,i_n,\ldots,i_m}(\zeta_k), \\ \mathcal{L}_a[\phi_{i_1,\ldots,i_n,\ldots,i_p,\ldots,i_m}(\zeta_k)] &= H_{i_1,\ldots,i_n,\ldots,i_p,\ldots,i_m}(\zeta_k). \end{aligned}$$

Owing to the symmetry of $H_{i_1,\ldots,i_m}(\zeta_k)$ with respect to the subscripts $i_1, \ldots, i_m$,

$$\mathcal{L}_a[\phi_{i_1,\ldots,i_p,\ldots,i_n,\ldots,i_m}(\zeta_k) - \phi_{i_1,\ldots,i_n,\ldots,i_p,\ldots,i_m}(\zeta_k)] = 0.$$

The solution $\phi_{i_1,\ldots,i_p,\ldots,i_n,\ldots,i_m}(\zeta_k) - \phi_{i_1,\ldots,i_n,\ldots,i_p,\ldots,i_m}(\zeta_k)$ is orthogonal to 1, ζ_i, and ζ^2, and therefore is zero, that is, $\phi_{i_1,\ldots,i_m}(\zeta_k)$ is symmetric with respect to the subscripts $i_1, \ldots, i_m$. Thus, the solution $\phi_{i_1,\ldots,i_m}(\zeta_k)$ is expressed in the form given by Eq. (A.79).

[32] The relation is required for Eq. (A.118) to have a solution owing to the relation (A.44).

A.2.9 Functions defined by $\mathcal{L}_a(\phi) = \mathrm{Ih}$ and transport coefficients

Here, we give the definitions of the functions $\mathcal{A}(\zeta, a)$, $\mathcal{B}^{(0)}(\zeta, a)$, etc., and the transport coefficients $\Gamma_1(a)$, $\Gamma_2(a)$, etc., which appear in the main text. They are expressed with the solutions or their linear combinations of the following integral equations of the form $\mathcal{L}_a(\phi) = \mathrm{Ih}$, the general form of the solution of which is discussed in Section A.2.8.[33]

$$\mathcal{L}_a[\zeta_i \mathcal{A}(\zeta, a)] = -\zeta_i \left(\zeta^2 - \frac{5}{2}\right), \tag{A.123}$$

with the subsidiary condition $\displaystyle\int_0^\infty \zeta^4 \mathcal{A}(\zeta, a) E(\zeta) \mathrm{d}\zeta = 0$;

$$\mathcal{L}_a\left[\left(\zeta_i\zeta_j - \frac{1}{3}\zeta^2\delta_{ij}\right)\mathcal{B}^{(m)}(\zeta, a)\right] = IB_{ij}^{(m)}; \tag{A.124}$$

$$\begin{aligned}
&\mathcal{L}_a\left[\left(\zeta_i\delta_{jk} + \zeta_j\delta_{ki} + \zeta_k\delta_{ij}\right)\mathcal{T}_1^{(0)}(\zeta, a) + \zeta_i\zeta_j\zeta_k\mathcal{T}_2^{(0)}(\zeta, a)\right] \\
&= -\zeta_i\zeta_j\zeta_k\mathcal{B}^{(0)}(\zeta, a) + I_6(\mathcal{B}^{(0)}(\zeta, a))\left(\zeta_i\delta_{jk} + \zeta_j\delta_{ki} + \zeta_k\delta_{ij}\right),
\end{aligned} \tag{A.125}$$

with the subsidiary condition $\displaystyle\int_0^\infty \left(5\zeta^4\mathcal{T}_1^{(0)} + \zeta^6\mathcal{T}_2^{(0)}\right) E(\zeta)\mathrm{d}\zeta = 0$;

$$\begin{aligned}
&\mathcal{L}_a\Big[\left(\delta_{ij}\delta_{kl} + \delta_{ik}\delta_{jl} + \delta_{il}\delta_{jk}\right)\mathcal{Q}_1^{(0)}(\zeta, a) \\
&\quad + \left(\zeta_i\zeta_j\delta_{kl} + \zeta_i\zeta_k\delta_{jl} + \zeta_i\zeta_l\delta_{jk} + \zeta_j\zeta_k\delta_{il} + \zeta_j\zeta_l\delta_{ik} + \zeta_k\zeta_l\delta_{ij}\right)\mathcal{Q}_2^{(0)}(\zeta, a) \\
&\quad + \zeta_i\zeta_j\zeta_k\zeta_l\mathcal{Q}_3^{(0)}(\zeta, a)\Big] = -\zeta_i\zeta_j\zeta_k\zeta_l\left(2\mathcal{B}^{(0)}(\zeta, a) - \frac{1}{\zeta}\frac{\partial\mathcal{B}^{(0)}(\zeta, a)}{\partial\zeta}\right) \\
&\quad + \frac{1}{3}\left[\zeta^2\mathcal{B}^{(0)}(\zeta, a) + 2I_6(\mathcal{B}^{(0)}(\zeta, a))\left(\zeta^2 - \frac{3}{2}\right)\right]\left(\delta_{ij}\delta_{kl} + \delta_{ik}\delta_{jl} + \delta_{il}\delta_{jk}\right),
\end{aligned} \tag{A.126}$$

with the subsidiary conditions

$$\int_0^\infty (1,\ \zeta^2)\left(15\zeta^2\mathcal{Q}_1^{(0)} + 10\zeta^4\mathcal{Q}_2^{(0)} + \zeta^6\mathcal{Q}_3^{(0)}\right) E(\zeta)\mathrm{d}\zeta = 0;$$

[33] (i) The possible forms of the solutions corresponding to the inhomogeneous terms are put in Eqs. (A.123)–(A.127). Thus, they are equations for scalar functions.

(ii) The inhomogeneous term of Eq. (A.127) does not have the symmetry used in the discussion in Section A.2.8. However, we can show that the solution is in the form given in Eq. (A.127) by an argument (without symmetry condition but for a tensor of the fourth-order) similar to that in Appendix B of Sone [2002].

(iii) Some relations in the orthogonal condition (A.120), which makes the solution unique, are automatically satisfied by the solution of the form required from the inhomogeneous term. The remaining relations are given as the subsidiary conditions.

$$\mathcal{L}_a\left[\delta_{ij}\delta_{kl}\tilde{\mathcal{Q}}_{11}^{(0)}(\zeta,a)+(\delta_{ik}\delta_{jl}+\delta_{il}\delta_{jk})\,\tilde{\mathcal{Q}}_{12}^{(0)}(\zeta,a)+(\zeta_i\zeta_j\delta_{kl}+\zeta_k\zeta_l\delta_{ij})\tilde{\mathcal{Q}}_{21}^{(0)}(\zeta,a)\right.$$
$$\left.+(\zeta_i\zeta_k\delta_{jl}+\zeta_i\zeta_l\delta_{jk}+\zeta_j\zeta_k\delta_{il}+\zeta_j\zeta_l\delta_{ik})\tilde{\mathcal{Q}}_{22}^{(0)}(\zeta,a)+\zeta_i\zeta_j\zeta_k\zeta_l\tilde{\mathcal{Q}}_3^{(0)}(\zeta,a)\right]$$
$$=\mathcal{J}_a(\zeta_i\zeta_j\mathcal{B}^{(0)}(\zeta,a),\,\zeta_k\zeta_l\mathcal{B}^{(0)}(\zeta,a)), \tag{A.127}$$

with the subsidiary conditions

$$\int_0^\infty(1,\ \zeta^2)\left(15\zeta^2\tilde{\mathcal{Q}}_{11}^{(0)}+10\zeta^4\tilde{\mathcal{Q}}_{21}^{(0)}+\zeta^6\tilde{\mathcal{Q}}_3^{(0)}\right)E(\zeta)\mathrm{d}\zeta=0,$$
$$\int_0^\infty(1,\ \zeta^2)\left(15\zeta^2\tilde{\mathcal{Q}}_{12}^{(0)}+10\zeta^4\tilde{\mathcal{Q}}_{22}^{(0)}+\zeta^6\tilde{\mathcal{Q}}_3^{(0)}\right)E(\zeta)\mathrm{d}\zeta=0.$$

Here, the inhomogeneous term $IB_{ij}^{(m)}$ is given by

$$IB_{ij}^{(0)}=-2\left(\zeta_i\zeta_j-\frac{\zeta^2}{3}\delta_{ij}\right), \tag{A.128a}$$

$$IB_{ij}^{(1)}=\left(\zeta_i\zeta_j-\frac{\zeta^2}{3}\delta_{ij}\right)\mathcal{A}(\zeta,a), \tag{A.128b}$$

$$IB_{ij}^{(2)}=\left(\zeta_i\zeta_j-\frac{\zeta^2}{3}\delta_{ij}\right)\left(2(\zeta^2-3)\mathcal{A}(\zeta,a)-\zeta\frac{\partial\mathcal{A}(\zeta,a)}{\partial\zeta}+2a\frac{\partial\mathcal{A}(\zeta,a)}{\partial a}\right), \tag{A.128c}$$

$$IB_{ij}^{(3)}=\mathcal{J}_a(\zeta_i\mathcal{A}(\zeta,a),\zeta_j\mathcal{A}(\zeta,a))-\frac{\delta_{ij}}{3}\sum_{k=1}^{3}\mathcal{J}_a(\zeta_k\mathcal{A}(\zeta,a),\zeta_k\mathcal{A}(\zeta,a)), \tag{A.128d}$$

$$IB_{ij}^{(4)}=\left(\zeta_i\zeta_j-\frac{\zeta^2}{3}\delta_{ij}\right)\mathcal{B}^{(0)}(\zeta,a), \tag{A.128e}$$

and $I_n(Z(\zeta))$ is the integral

$$I_n(Z(\zeta))=\frac{8}{15\sqrt{\pi}}\int_0^\infty\zeta^nZ(\zeta)\exp(-\zeta^2)\mathrm{d}\zeta. \tag{A.129}$$

The functions $A(\zeta)$, $B(\zeta)$, etc. introduced in Section 3.1.2 are related to some of the solutions defined above as

$$\left.\begin{array}{l}A(\zeta)=\mathcal{A}(\zeta,1),\quad B(\zeta)=\mathcal{B}^{(0)}(\zeta,1),\quad F(\zeta)=\mathcal{B}^{(1)}(\zeta,1),\\ D_1(\zeta)=\mathcal{T}_1^{(0)}(\zeta,1),\quad D_2(\zeta)=\mathcal{T}_2^{(0)}(\zeta,1).\end{array}\right\} \tag{A.130}$$

The nondimensional transport coefficients $\Gamma_1(a)$, $\Gamma_2(a)$, etc. are expressed

in the following integrals of the functions defined above:[34]

$$\left.\begin{aligned}
&\Gamma_1(a)/a^{1/2} = I_6(\mathcal{B}^{(0)}(\zeta,a)), \quad \Gamma_2(a)/a^{1/2} = 2I_6(\mathcal{A}(\zeta,a)),\\
&\Gamma_3(a)/a = I_6(\mathcal{A}(\zeta,a)\mathcal{B}^{(0)}(\zeta,a)) = -2I_6(\mathcal{B}^{(1)}(\zeta,a)),\\
&\Gamma_7(a) = \frac{\mathrm{d}\Gamma_3(a)}{\mathrm{d}a} + I_6(\mathcal{B}^{(2)}(\zeta,a) + 2\mathcal{B}^{(3)}(\zeta,a)),\\
&\bar{\Gamma}_7(a) = \Gamma_7(a) - \tfrac{2}{3}I_6(\mathcal{B}^{(2)}(\zeta,a) + 2\mathcal{B}^{(3)}(\zeta,a)),\\
&\Gamma_8(a)/a = -I_6(\mathcal{Q}_3) - \tfrac{1}{7}I_8(\mathcal{Q}_4),\\
&\Gamma_9(a)/a = I_6(2\mathcal{Q}_3 - \mathcal{B}^{(4)}) + \tfrac{2}{7}I_8(\mathcal{Q}_4),
\end{aligned}\right\} \tag{A.131}$$

where

$$\mathcal{Q}_3 = \mathcal{Q}_2^{(0)} - \tilde{\mathcal{Q}}_{22}^{(0)} + \mathcal{B}^{(4)}, \quad \mathcal{Q}_4 = \mathcal{Q}_3^{(0)} - \tilde{\mathcal{Q}}_3^{(0)}, \tag{A.132}$$

and the second expression of $\Gamma_3(a)/a$ is derived from the first with the aid of the self-adjoint property of $\mathcal{L}_a$ [Eq. (A.40)]. The functional forms of the transport coefficients are determined by molecular models. For example, for a hard-sphere gas, the quantity on the right-hand side of each equation in the set (A.131) of formulas is constant, e.g.,

$$\left.\begin{aligned}
&\Gamma_1(a)/a^{1/2} = 1.270\,042\,427, \quad \Gamma_2(a)/a^{1/2} = 1.922\,284\,066,\\
&\Gamma_3(a)/a = 1.947\,906\,335, \quad \Gamma_7(a) = 1.758\,705, \quad \bar{\Gamma}_7(a) = 1.884\,839,
\end{aligned}\right\} \tag{A.133}$$

and for the BKW model,

$$\left.\begin{aligned}
&\Gamma_1(a)/a = \Gamma_2(a)/a = \Gamma_3(a)/a^2 = \Gamma_7(a)/a = \Gamma_9(a)/a = 1,\\
&\Gamma_8(a) = 0, \quad \bar{\Gamma}_7(a)/a = 5/3.
\end{aligned}\right\} \tag{A.134}$$

It can be shown generally that the nondimensional viscosity and thermal conductivity, i.e., $\Gamma_1(a)$ and $\Gamma_2(a)$ are positive with the aid of the inequality (A.41). Putting $\phi = \zeta_i\mathcal{A}(\zeta,a)$ in the inequality (A.41), we have

$$\int \zeta_i\mathcal{A}(\zeta,a)\mathcal{L}_a[\zeta_i\mathcal{A}(\zeta,a)]E(\zeta)\mathbf{d}\boldsymbol{\zeta} < 0,$$

where the equality sign is eliminated because $\zeta_i\mathcal{A}(\zeta,a)$ is obviously nonzero. Substituting Eq. (A.123) into the above inequality, we have

$$\begin{aligned}
0 &< \int \zeta^2\left(\zeta^2 - \frac{5}{2}\right)\mathcal{A}(\zeta,a)E(\zeta)\mathbf{d}\boldsymbol{\zeta} = 4\pi\int_0^\infty \zeta^4\left(\zeta^2 - \frac{5}{2}\right)\mathcal{A}(\zeta,a)E(\zeta)\mathrm{d}\zeta\\
&= 4\pi\int_0^\infty \zeta^6\mathcal{A}(\zeta,a)E(\zeta)\mathrm{d}\zeta = \frac{15}{2}I_6(\mathcal{A}(\zeta,a)),
\end{aligned}$$

where the subsidiary condition to Eq. (A.123) is used. Thus,

$$\Gamma_2(a) > 0. \tag{A.135}$$

[34] For the BKW equation, the following convention should be taken:
$\mathcal{B}^{(3)} = \tilde{\mathcal{Q}}_{12}^{(0)} = \tilde{\mathcal{Q}}_{22}^{(0)} = \tilde{\mathcal{Q}}_3^{(0)} = 0.$
This is due to the exceptional form of the BKW equation (see Footnote 35 in Section 3.2.2).

Similarly, from Eq. (A.124) for $m = 0$ with (A.128a),

$$\Gamma_1(a) > 0. \tag{A.136}$$

A.2.10 Kernel representation of the linearized collision integral $\mathcal{L}(\phi)$

The linearized collision integral $\mathcal{L}(\phi)$, defined by Eq. (1.75b) with (1.48c),

$$\mathcal{L}(\phi) = \int E_*(\phi' + \phi'_* - \phi - \phi_*)\widehat{B}\,\mathrm{d}\Omega(\boldsymbol{\alpha})\,\mathbf{d}\boldsymbol{\zeta}_*, \tag{A.137a}$$

$$\widehat{B} = \widehat{B}(|\boldsymbol{\alpha}\cdot(\boldsymbol{\zeta}_* - \boldsymbol{\zeta})|/|\boldsymbol{\zeta}_* - \boldsymbol{\zeta}|, |\boldsymbol{\zeta}_* - \boldsymbol{\zeta}|), \tag{A.137b}$$

is reduced to a standard *kernel form*, i.e., $\int K(\boldsymbol{\zeta},\boldsymbol{\zeta}_*)\phi(\boldsymbol{\zeta}_*)\mathbf{d}\boldsymbol{\zeta}_* + \kappa(\boldsymbol{\zeta})\phi(\boldsymbol{\zeta})$, in a clear way by Grad [1963b]. This form is very useful for analysis and numerical computation of the Boltzmann equation. The process and result are given here.

The integral is split into three parts as[35]

$$\mathcal{L}(\phi) = \mathcal{L}^G(\phi) - \mathcal{L}^{L2}(\phi) - \nu_L(\boldsymbol{\zeta})\phi, \tag{A.138}$$

where

$$\mathcal{L}^G(\phi) = \int E_*(\phi' + \phi'_*)\widehat{B}\mathrm{d}\Omega(\boldsymbol{\alpha})\,\mathbf{d}\boldsymbol{\zeta}_*, \tag{A.139a}$$

$$\mathcal{L}^{L2}(\phi) = \int E_*\phi_*\widehat{B}\,\mathrm{d}\Omega(\boldsymbol{\alpha})\,\mathbf{d}\boldsymbol{\zeta}_*, \tag{A.139b}$$

$$\nu_L(\boldsymbol{\zeta}) = \int E_*\widehat{B}\,\mathrm{d}\Omega(\boldsymbol{\alpha})\,\mathbf{d}\boldsymbol{\zeta}_*. \tag{A.139c}$$

Obviously, $\nu_L(\boldsymbol{\zeta})\phi$ and $\mathcal{L}^{L2}(\phi)$ are of desired forms. They can further be reduced to simpler forms for manipulation.

Take the spherical coordinate representation of $\boldsymbol{\alpha}$ with the direction of $\boldsymbol{\zeta}_*-\boldsymbol{\zeta}$ as its polar direction. Let the angle between $\boldsymbol{\alpha}$ and $\boldsymbol{\zeta}_*-\boldsymbol{\zeta}$ be θ and the angle of $\boldsymbol{\alpha}$ around $\boldsymbol{\zeta}_*-\boldsymbol{\zeta}$ be φ. Then[36]

$$\boldsymbol{\alpha} = (\cos\theta,\ \sin\theta\cos\varphi,\ \sin\theta\sin\varphi),\quad \mathrm{d}\Omega(\boldsymbol{\alpha}) = \sin\theta\mathrm{d}\theta\mathrm{d}\varphi,$$
$$|\boldsymbol{\alpha}\cdot(\boldsymbol{\zeta}_* - \boldsymbol{\zeta})| = |\boldsymbol{\zeta}_* - \boldsymbol{\zeta}||\cos\theta|.$$

The notation $\underline{\widehat{B}}(\theta, |\boldsymbol{\zeta}_* - \boldsymbol{\zeta}|)$

$$\underline{\widehat{B}}(\theta, |\boldsymbol{\zeta}_* - \boldsymbol{\zeta}|) = \widehat{B}(|\boldsymbol{\alpha}\cdot(\boldsymbol{\zeta}_* - \boldsymbol{\zeta})|/|\boldsymbol{\zeta}_* - \boldsymbol{\zeta}|, |\boldsymbol{\zeta}_* - \boldsymbol{\zeta}|)\sin\theta,$$

[35]Here, we consider the case where each of the gain and loss terms of the collision integral takes a finite value. It may be noted that $\mathcal{L}^G(\phi)$ is the gain term and $\mathcal{L}^{L2}(\phi) + \nu_L\phi$ is the loss term.

[36]The θ and φ correspond to θ_α and φ_α, respectively, in Section A.2.4.

is introduced, and the notation $\boldsymbol{V}$ is used for $\boldsymbol{\zeta}_* - \boldsymbol{\zeta}$, when convenient. Then, in view of their integrands being independent of φ, the integrals $\mathcal{L}^{L2}(\phi)$ and $\nu_L(\boldsymbol{\zeta})$ are expressed as

$$\mathcal{L}^{L2}(\phi) = 2\pi \int_{\text{all } \boldsymbol{\zeta}_*} \int_0^\pi E(\zeta_*)\phi(\boldsymbol{\zeta}_*)\underline{\widehat{B}}(\theta, |\boldsymbol{\zeta}_* - \boldsymbol{\zeta}|)\, \mathrm{d}\theta\, \mathbf{d}\boldsymbol{\zeta}_*, \tag{A.140a}$$

$$\nu_L(\boldsymbol{\zeta}) = 2\pi \int_{\text{all } \boldsymbol{\zeta}_*} \int_0^\pi E(\zeta_*)\underline{\widehat{B}}(\theta, |\boldsymbol{\zeta}_* - \boldsymbol{\zeta}|)\, \mathrm{d}\theta\, \mathbf{d}\boldsymbol{\zeta}_*. \tag{A.140b}$$

Putting

$$K_2(\boldsymbol{\zeta}, \boldsymbol{\zeta}_*) = 2\pi E(\zeta_*) \int_0^\pi \underline{\widehat{B}}(\theta, |\boldsymbol{\zeta}_* - \boldsymbol{\zeta}|)\, \mathrm{d}\theta\,, \tag{A.141}$$

we have

$$\mathcal{L}^{L2}(\phi) = \int K_2(\boldsymbol{\zeta}, \boldsymbol{\zeta}_*)\phi(\boldsymbol{\zeta}_*)\mathbf{d}\boldsymbol{\zeta}_*. \tag{A.142}$$

The transformation of $\mathcal{L}^G(\phi)$, or Eq. (A.139a), requires some manipulation, which will be performed in the rest of this subsection.

First, some relations, which are derived with the aid of elementary formulas of vector analysis (Jeffreys & Jeffreys [1946], Bronshtein & Semendyayev [1979]), are prepared. Take a vector $\boldsymbol{V}$ and a unit vector $\boldsymbol{\alpha}$. Consider the vector $\boldsymbol{\beta}$ defined for $\boldsymbol{V} \cdot \boldsymbol{\alpha} \geq 0$ by

$$\boldsymbol{\beta} = \frac{\boldsymbol{\alpha} \times \boldsymbol{V} \times \boldsymbol{\alpha}}{|\boldsymbol{V} \times \boldsymbol{\alpha}|} = \frac{\boldsymbol{V} - (\boldsymbol{V} \cdot \boldsymbol{\alpha})\boldsymbol{\alpha}}{|\boldsymbol{V} \times \boldsymbol{\alpha}|}, \tag{A.143}$$

where the symbol $\times$ indicates the vector product. Then, with the aid of the relations in the footnote below[37]

$$|\boldsymbol{\beta}| = 1, \quad \boldsymbol{\beta} \cdot \boldsymbol{\alpha} = 0, \quad \boldsymbol{V} \cdot \boldsymbol{\beta} = |\boldsymbol{V} \times \boldsymbol{\alpha}| \geq 0, \quad |\boldsymbol{V} \times \boldsymbol{\beta}| = |\boldsymbol{V} \cdot \boldsymbol{\alpha}|.$$

With these formulas, the relation (A.143) can be inverted in the symmetric form

$$\boldsymbol{\alpha} = \frac{\boldsymbol{\beta} \times \boldsymbol{V} \times \boldsymbol{\beta}}{|\boldsymbol{V} \times \boldsymbol{\beta}|} = \frac{\boldsymbol{V} - (\boldsymbol{V} \cdot \boldsymbol{\beta})\boldsymbol{\beta}}{|\boldsymbol{V} \times \boldsymbol{\beta}|},$$

for which the condition $\boldsymbol{V} \cdot \boldsymbol{\alpha} \geq 0$ is required.

With the above preparation, the vector $\boldsymbol{\zeta}'_*$ in the argument of ϕ'_* is transformed as follows:

$$\begin{aligned} \boldsymbol{\zeta}'_* &= \boldsymbol{\zeta}_* - (\boldsymbol{V} \cdot \boldsymbol{\alpha})\boldsymbol{\alpha} = \boldsymbol{\zeta} + \boldsymbol{V} - |\boldsymbol{V} \times \boldsymbol{\beta}|\boldsymbol{\alpha} \\ &= \boldsymbol{\zeta} + (\boldsymbol{V} \cdot \boldsymbol{\beta})\boldsymbol{\beta} \qquad (\boldsymbol{V} \cdot \boldsymbol{\alpha} > 0), \end{aligned}$$

---

[37]

$$\begin{aligned} (\boldsymbol{V} \times \boldsymbol{\alpha})^2 &= \varepsilon_{ijk} V_j \alpha_k \varepsilon_{ilm} V_l \alpha_m = (\delta_{jl}\delta_{km} - \delta_{jm}\delta_{kl}) V_j V_l \alpha_k \alpha_m \\ &= \boldsymbol{V}^2 - (\boldsymbol{V} \cdot \boldsymbol{\alpha})^2 = [\boldsymbol{V} - (\boldsymbol{V} \cdot \boldsymbol{\alpha})\boldsymbol{\alpha}]^2. \end{aligned}$$

$$\begin{aligned} \boldsymbol{\beta} \times \boldsymbol{V} &= \frac{\boldsymbol{V} - (\boldsymbol{V} \cdot \boldsymbol{\alpha})\boldsymbol{\alpha}}{|\boldsymbol{V} \times \boldsymbol{\alpha}|} \times \boldsymbol{V} = \frac{\boldsymbol{V} \cdot \boldsymbol{\alpha}}{|\boldsymbol{V} \times \boldsymbol{\alpha}|}(\boldsymbol{V} \times \boldsymbol{\alpha}), \\ &\therefore \ |\boldsymbol{\beta} \times \boldsymbol{V}| = |\boldsymbol{V} \cdot \boldsymbol{\alpha}|. \end{aligned}$$

and the differential element $\mathrm{d}\Omega(\boldsymbol{\alpha})\,\mathbf{d}\boldsymbol{\zeta}_*$ of the variables $(\boldsymbol{\alpha},\ \boldsymbol{\zeta}_*)$ is related to $\mathrm{d}\Omega(\boldsymbol{\beta})\,\mathbf{d}\boldsymbol{\zeta}_*$ of the variables $(\boldsymbol{\beta},\ \boldsymbol{\zeta}_*)$ [or $\mathrm{d}\Omega(\boldsymbol{\beta})\,\mathbf{d}\boldsymbol{V}$ of the variables $(\boldsymbol{\beta},\ \boldsymbol{V})$], i.e.,

$$\mathrm{d}\Omega(\boldsymbol{\alpha})\,\mathbf{d}\boldsymbol{\zeta}_* = \frac{|\boldsymbol{V}\cdot\boldsymbol{\beta}|}{|\boldsymbol{V}\times\boldsymbol{\beta}|}\mathrm{d}\Omega(\boldsymbol{\beta})\,\mathbf{d}\boldsymbol{\zeta}_* = \frac{|\boldsymbol{V}\cdot\boldsymbol{\beta}|}{|\boldsymbol{V}\times\boldsymbol{\beta}|}\mathrm{d}\Omega(\boldsymbol{\beta})\,\mathbf{d}\boldsymbol{V}.$$

With the aid of these relations, the part of $\mathcal{L}^G(\phi)$ containing ϕ'_* is transformed as

$$\begin{aligned}
&\int_{\text{all }\boldsymbol{\alpha},\ \text{all }\boldsymbol{\zeta}_*} E_*\phi'_*\widehat{B}\mathrm{d}\Omega(\boldsymbol{\alpha})\,\mathbf{d}\boldsymbol{\zeta}_* = 2\int_{\boldsymbol{V}\cdot\boldsymbol{\alpha}>0,\ \text{all }\boldsymbol{\zeta}_*} E_*\phi'_*\widehat{B}\mathrm{d}\Omega(\boldsymbol{\alpha})\,\mathbf{d}\boldsymbol{\zeta}_* \\
&= 2\int_{\substack{\boldsymbol{V}\cdot\boldsymbol{\beta}>0\\ \text{all }\boldsymbol{V}}} E_*\phi(\boldsymbol{\zeta}+(\boldsymbol{V}\cdot\boldsymbol{\beta})\boldsymbol{\beta})\widehat{B}(|\boldsymbol{V}\times\boldsymbol{\beta}|/|\boldsymbol{V}|,|\boldsymbol{V}|)\frac{|\boldsymbol{V}\cdot\boldsymbol{\beta}|}{|\boldsymbol{V}\times\boldsymbol{\beta}|}\mathrm{d}\Omega(\boldsymbol{\beta})\,\mathbf{d}\boldsymbol{V} \\
&= \int_{\substack{\text{all }\boldsymbol{\beta}\\ \text{all }\boldsymbol{V}}} E_*\phi(\boldsymbol{\zeta}+(\boldsymbol{V}\cdot\boldsymbol{\beta})\boldsymbol{\beta})\widehat{B}(|\boldsymbol{V}\times\boldsymbol{\beta}|/|\boldsymbol{V}|,|\boldsymbol{V}|)\frac{|\boldsymbol{V}\cdot\boldsymbol{\beta}|}{|\boldsymbol{V}\times\boldsymbol{\beta}|}\mathrm{d}\Omega(\boldsymbol{\beta})\,\mathbf{d}\boldsymbol{V}.
\end{aligned}$$

With $\widehat{B}^*$defined by

$$\widehat{B}^* = \widehat{B}(|\boldsymbol{\alpha}\cdot\boldsymbol{V}|/|\boldsymbol{V}|,|\boldsymbol{V}|) + \frac{|\boldsymbol{V}\cdot\boldsymbol{\alpha}|}{|\boldsymbol{V}\times\boldsymbol{\alpha}|}\widehat{B}(|\boldsymbol{V}\times\boldsymbol{\alpha}|/|\boldsymbol{V}|,|\boldsymbol{V}|),$$

the integral $\mathcal{L}^G(\phi)$ is expressed as

$$\mathcal{L}^G(\phi) = \int E(|\boldsymbol{V}+\boldsymbol{\zeta}|)\phi(\boldsymbol{\zeta}+(\boldsymbol{V}\cdot\boldsymbol{\alpha})\boldsymbol{\alpha})\widehat{B}^*\mathrm{d}\Omega(\boldsymbol{\alpha})\,\mathbf{d}\boldsymbol{V}, \tag{A.144}$$

where the argument $\boldsymbol{\zeta}'_*$ is eliminated from ϕ. The form is further deformed.

The vector $\boldsymbol{V}$ is decomposed into two components: the one parallel to $\boldsymbol{\alpha}$ and the other perpendicular to $\boldsymbol{\alpha}$, i.e.,

$$\boldsymbol{V} = \boldsymbol{w} + \boldsymbol{W},$$

where

$$\begin{aligned}
\boldsymbol{w} &= (\boldsymbol{\alpha}\cdot\boldsymbol{V})\boldsymbol{\alpha}, \\
\boldsymbol{W} &= \boldsymbol{V} - (\boldsymbol{\alpha}\cdot\boldsymbol{V})\boldsymbol{\alpha} = \boldsymbol{\alpha}\times\boldsymbol{V}\times\boldsymbol{\alpha}.
\end{aligned}$$

The variables $(\boldsymbol{\alpha},\boldsymbol{V})$ of integration in Eq. (A.144) are transformed to $(\boldsymbol{w},\ \boldsymbol{W})$. This requires a little care. First, we express the arguments of the integrand in Eq. (A.144) in the new variables $\boldsymbol{w}$ and $\boldsymbol{W}$. That is,

$$E(|\boldsymbol{V}+\boldsymbol{\zeta}|)\phi(\boldsymbol{\zeta}+(\boldsymbol{V}\cdot\boldsymbol{\alpha})\boldsymbol{\alpha}) = E(|\boldsymbol{w}+\boldsymbol{W}+\boldsymbol{\zeta}|)\phi(\boldsymbol{\zeta}+\boldsymbol{w}),$$

and

$$\begin{aligned}
\widehat{B}^* &= \widehat{B}(|\boldsymbol{\alpha}\cdot\boldsymbol{V}|/|\boldsymbol{V}|,|\boldsymbol{V}|) + \frac{|\boldsymbol{V}\cdot\boldsymbol{\alpha}|}{|\boldsymbol{V}\times\boldsymbol{\alpha}|}\widehat{B}(|\boldsymbol{V}\times\boldsymbol{\alpha}|/|\boldsymbol{V}|,|\boldsymbol{V}|) \\
&= \widehat{B}(|\cos\theta|,|\boldsymbol{V}|) + \frac{|\cos\theta|}{|\sin\theta|}\widehat{B}(|\sin\theta|,|\boldsymbol{V}|) \\
&= \widehat{B}^{\#}(|\boldsymbol{V}\cos\theta|,|\boldsymbol{V}\sin\theta|) \\
&= \widehat{B}^{\#}(|\boldsymbol{w}|,|\boldsymbol{W}|),
\end{aligned} \tag{A.145}$$

where the new symbol $\widehat{B}^{\#}$ is introduced for the function $\widehat{B}^{*}$ in the new variables.

In Eq. (A.144), the integral with respect to $\boldsymbol{V}$ for a given $\boldsymbol{\alpha}$ is performed first in the order: the integral with respect to $\boldsymbol{W}$ in the plane perpendicular to $\boldsymbol{\alpha}$ and the integral with respect to $|\boldsymbol{w}|$ in the direction of $\boldsymbol{\alpha}$; and then the integral with respect to $\boldsymbol{\alpha}$ is performed. Here, we combine the integral with respect to $|\boldsymbol{w}|$ and that with respect to $\boldsymbol{\alpha}$. This gives a three-dimensional integration over the three rectangular components of $\boldsymbol{w}$ $(=|\boldsymbol{w}|\boldsymbol{\alpha})$. Noting the arguments of the integrand shown above, the integral can be transformed as follows:

$$\begin{aligned}\int(*)\mathrm{d}\Omega(\boldsymbol{\alpha})\mathbf{d}\boldsymbol{V} &= \int_{\text{all }\boldsymbol{\alpha}}\int_{\text{all }\boldsymbol{V}}(*)\mathbf{d}\boldsymbol{V}\mathrm{d}\Omega(\boldsymbol{\alpha})\\ &= \int_{\text{all }\boldsymbol{\alpha}}\int_{-\infty}^{\infty}\int_{\text{all }\boldsymbol{W}\perp\boldsymbol{\alpha}}(*)\mathrm{d}\boldsymbol{W}\mathrm{d}(\boldsymbol{\alpha}\cdot\boldsymbol{V})\mathrm{d}\Omega(\boldsymbol{\alpha})\\ &= 2\int\int_{0}^{\infty}\left(\int(*)\mathrm{d}\boldsymbol{W}\right)\mathrm{d}|\boldsymbol{w}|\mathrm{d}\Omega(\boldsymbol{\alpha})\\ &= \int_{\text{all }\boldsymbol{w}}\frac{2}{|\boldsymbol{w}|^{2}}\left(\int_{\text{all }\boldsymbol{W}\perp\boldsymbol{w}}(*)\mathrm{d}\boldsymbol{W}\right)\mathbf{d}\boldsymbol{w}.\end{aligned}$$

With this formula, the integral $\mathcal{L}^{G}(\phi)$ is transformed as

$$\mathcal{L}^{G}(\phi) = 2\int\frac{1}{|\boldsymbol{w}|^{2}}E(|\boldsymbol{w}+\boldsymbol{W}+\boldsymbol{\zeta}|)\phi(\boldsymbol{\zeta}+\boldsymbol{w})\widehat{B}^{\#}(|\boldsymbol{w}|,|\boldsymbol{W}|)\mathrm{d}\boldsymbol{W}\,\mathbf{d}\boldsymbol{w}. \quad \text{(A.146)}$$

Introducing the translated variable $\boldsymbol{\eta}$, in place of $\boldsymbol{w}$,

$$\boldsymbol{\eta} = \boldsymbol{w}+\boldsymbol{\zeta},$$

we see that $\mathcal{L}^{G}(\phi)$ takes the kernel form

$$\mathcal{L}^{G}(\phi) = \int_{\text{all }\boldsymbol{\eta}}K_{1}(\boldsymbol{\zeta},\boldsymbol{\eta})\phi(\boldsymbol{\eta})\mathbf{d}\boldsymbol{\eta},$$

where

$$K_{1}(\boldsymbol{\zeta},\boldsymbol{\eta}) = \frac{2\exp(-\boldsymbol{\eta}^{2})}{\pi^{3/2}|\boldsymbol{\eta}-\boldsymbol{\zeta}|^{2}}\int\exp(-\boldsymbol{W}^{2}-2\boldsymbol{\eta}\cdot\boldsymbol{W})\widehat{B}^{\#}(|\boldsymbol{\eta}-\boldsymbol{\zeta}|,|\boldsymbol{W}|)\mathrm{d}\boldsymbol{W}. \quad \text{(A.147)}$$

Here, the integral with respect to $\boldsymbol{W}$ is performed over the whole two-dimensional space of $\boldsymbol{W}$ perpendicular to $\boldsymbol{\eta}-\boldsymbol{\zeta}$.

For a hard-sphere gas, $\widehat{B}(|\boldsymbol{\alpha}\cdot\boldsymbol{V}|/|\boldsymbol{V}|,|\boldsymbol{V}|)$, $\underline{\widehat{B}}(\theta,|\boldsymbol{V}|)$, and $\widehat{B}^{\#}(|\boldsymbol{w}|,|\boldsymbol{W}|)$ are given as

$$\frac{\underline{\widehat{B}}(\theta,|\boldsymbol{V}|)}{\sin\theta} = \widehat{B}(|\boldsymbol{\alpha}\cdot\boldsymbol{V}|/|\boldsymbol{V}|,|\boldsymbol{V}|) = \frac{|\boldsymbol{\alpha}\cdot\boldsymbol{V}|}{4(2\pi)^{1/2}} = \frac{|\boldsymbol{V}||\cos\theta|}{4(2\pi)^{1/2}}, \quad \text{(A.148a)}$$

$$\widehat{B}^{*} = \frac{|\boldsymbol{V}\cos\theta|}{4(2\pi)^{1/2}} + \frac{|\cos\theta|}{|\sin\theta|}\frac{|\boldsymbol{V}\sin\theta|}{4(2\pi)^{1/2}} = \frac{|\boldsymbol{w}|}{2(2\pi)^{1/2}} = \widehat{B}^{\#}(|\boldsymbol{w}|,|\boldsymbol{W}|). \quad \text{(A.148b)}$$

The derivation of K_2 and ν_L by Eqs. (A.141) and (A.140b) is straightforward, but that of K_1 needs some explanation. With $\widehat{B}^{\#}$ given by Eq. (A.148b) being substituted into Eq. (A.147),

$$K_1(\boldsymbol{\zeta},\boldsymbol{\eta}) = \frac{\exp(-\boldsymbol{\eta}^2)}{\sqrt{2}\pi^2|\boldsymbol{\eta}-\boldsymbol{\zeta}|}\int_{\text{all } \boldsymbol{W}\perp\boldsymbol{\eta}-\boldsymbol{\zeta}} \exp(-\boldsymbol{W}^2 - 2\boldsymbol{\eta}\cdot\boldsymbol{W})\mathrm{d}\boldsymbol{W}.$$

The integral is transformed in the following way:

$$\begin{aligned}\int_{\text{all } \boldsymbol{W}\perp\boldsymbol{\eta}-\boldsymbol{\zeta}} \exp(-\boldsymbol{W}^2 - 2\boldsymbol{\eta}\cdot\boldsymbol{W})\mathrm{d}\boldsymbol{W} &= \exp\left(\boldsymbol{a}^2\right)\int \exp[-(\boldsymbol{W}+\boldsymbol{a})^2]\mathrm{d}\boldsymbol{W} \\ &= \exp\left(\boldsymbol{a}^2\right)\int_0^{2\pi}\int_0^{\infty}\exp(-r^2)r\mathrm{d}r\mathrm{d}\varphi \\ &= \pi\exp\left(\boldsymbol{a}^2\right),\end{aligned}$$

where

$$\boldsymbol{a} = \boldsymbol{\eta} - \frac{[\boldsymbol{\eta}\cdot(\boldsymbol{\eta}-\boldsymbol{\zeta})]}{|\boldsymbol{\eta}-\boldsymbol{\zeta}|}\frac{(\boldsymbol{\eta}-\boldsymbol{\zeta})}{|\boldsymbol{\eta}-\boldsymbol{\zeta}|} = \frac{\boldsymbol{\eta}-\boldsymbol{\zeta}}{|\boldsymbol{\eta}-\boldsymbol{\zeta}|}\times\boldsymbol{\eta}\times\frac{\boldsymbol{\eta}-\boldsymbol{\zeta}}{|\boldsymbol{\eta}-\boldsymbol{\zeta}|},$$

which is the component of $\boldsymbol{\eta}$ perpendicular to $\boldsymbol{\eta}-\boldsymbol{\zeta}$. The magnitude of $\boldsymbol{a}$ is easily seen to be

$$|\boldsymbol{a}| = \frac{|\boldsymbol{\eta}\times\boldsymbol{\zeta}|}{|\boldsymbol{\eta}-\boldsymbol{\zeta}|}.$$

With these results,

$$K_1(\boldsymbol{\zeta},\boldsymbol{\eta}) = \frac{1}{\sqrt{2}\pi|\boldsymbol{\eta}-\boldsymbol{\zeta}|}\exp\left(-\boldsymbol{\eta}^2 + \frac{|\boldsymbol{\eta}\times\boldsymbol{\zeta}|^2}{|\boldsymbol{\eta}-\boldsymbol{\zeta}|^2}\right).$$

Summarizing the results, the kernel for a hard-sphere gas is

$$K_1(\boldsymbol{\zeta},\boldsymbol{\zeta}_*) = \frac{1}{\sqrt{2}\pi|\boldsymbol{\zeta}_*-\boldsymbol{\zeta}|}\exp\left(-\zeta_*^2 + \frac{(\boldsymbol{\zeta}_*\times\boldsymbol{\zeta})^2}{|\boldsymbol{\zeta}_*-\boldsymbol{\zeta}|^2}\right), \tag{A.149a}$$

$$K_2(\boldsymbol{\zeta},\boldsymbol{\zeta}_*) = \frac{|\boldsymbol{\zeta}_*-\boldsymbol{\zeta}|}{2\sqrt{2}\pi}\exp(-\zeta_*^2), \tag{A.149b}$$

$$\nu_L(\boldsymbol{\zeta}) = \frac{1}{2\sqrt{2}}\left[\exp(-\zeta^2) + \left(2\zeta + \frac{1}{\zeta}\right)\int_0^{\zeta}\exp(-\zeta_*^2)\mathrm{d}\zeta_*\right] \quad (\zeta = |\boldsymbol{\zeta}|). \tag{A.149c}$$

For the pseudo inverse-power potential (see Section A.2.4),

$$\widehat{B}\sin\theta = |\boldsymbol{V}|^{(n-5)/(n-1)}\beta(\theta) = \underline{\widehat{B}}(\theta,|\boldsymbol{V}|),$$

where $\beta(\theta_c)$ is the symmetric extension of $C_0\mathrm{d}g^2(\theta_c)/\mathrm{d}\theta_c$ in Eq. (A.73b) with respect to $\theta_c = \pi/2$ to $\pi/2 < \theta_c \le \pi$ with its value for $|\pi/2-\theta_c| < \delta$ (δ : some small constant) set zero by cutoff. By the definition (A.145),

$$\begin{aligned}\widehat{B}^* &= 2|\boldsymbol{V}|^{(n-5)/(n-1)}\bar{\beta}(\theta)/\sin\theta \\ &= 2|\boldsymbol{w}+\boldsymbol{W}|^{(n-5)/(n-1)}Q(|\boldsymbol{w}|/|\boldsymbol{W}|) \\ &= \widehat{B}^{\#}(|\boldsymbol{w}|,|\boldsymbol{W}|),\end{aligned}$$

where we put

$$\bar{\beta}(\theta) = \frac{1}{2}[\beta(\theta) + \beta(\tfrac{\pi}{2} - \theta)], \quad Q(|\boldsymbol{w}|/|\boldsymbol{W}|) = \bar{\beta}(\theta)/\sin\theta.$$

Substituting these $\underline{\widehat{B}}(\theta, |\boldsymbol{V}|)$ and $\widehat{B}^{\#}$ into Eqs. (A.147), (A.141), and (A.140b), we have

$$K_1(\boldsymbol{\zeta}, \boldsymbol{\eta}) = \frac{4\exp(-\boldsymbol{\eta}^2)}{\pi^{3/2}|\boldsymbol{\eta} - \boldsymbol{\zeta}|^2} \times \int_{\text{all } \boldsymbol{W} \perp \boldsymbol{\eta} - \boldsymbol{\zeta}} |\boldsymbol{\eta} - \boldsymbol{\zeta} + \boldsymbol{W}|^{\frac{n-5}{n-1}} \exp(-\boldsymbol{W}^2 - 2\boldsymbol{\eta} \cdot \boldsymbol{W}) Q(|\boldsymbol{\eta} - \boldsymbol{\zeta}|/|\boldsymbol{W}|) \mathrm{d}\boldsymbol{W}, \tag{A.150a}$$

$$\begin{aligned} K_2 &= 2\pi E(\zeta_*) \int_0^\pi \underline{\widehat{B}}(\theta, |\boldsymbol{\zeta}_* - \boldsymbol{\zeta}|)\, \mathrm{d}\theta \\ &= \beta_0 |\boldsymbol{\zeta}_* - \boldsymbol{\zeta}|^{(n-5)/(n-1)} \exp(-\zeta_*^2), \end{aligned} \tag{A.150b}$$

$$\begin{aligned} \nu_L(\boldsymbol{\zeta}) &= 2\pi \int_{\text{all } \boldsymbol{\zeta}_*} \int_0^\pi E(\zeta_*) \underline{\widehat{B}}(\theta, |\boldsymbol{\zeta}_* - \boldsymbol{\zeta}|) \mathrm{d}\theta\, \mathbf{d}\boldsymbol{\zeta}_* \\ &= \beta_0 \int_{\text{all } \boldsymbol{\zeta}_*} \exp(-\zeta_*^2) |\boldsymbol{\zeta}_* - \boldsymbol{\zeta}|^{(n-5)/(n-1)} \mathbf{d}\boldsymbol{\zeta}_*, \end{aligned} \tag{A.150c}$$

where

$$\beta_0 = \frac{4}{\sqrt{\pi}} \int_0^{\pi/2} \beta(\theta) \mathrm{d}\theta.$$

A.3 Boltzmann equation in the cylindrical and spherical coordinate systems

It is convenient to list the formulas of the transport derivative term

$$\frac{\partial f}{\partial t} + \xi_i \frac{\partial f}{\partial X_i} + \frac{\partial F_i f}{\partial \xi_i} \tag{A.151}$$

of the Boltzmann equation in the cylindrical and spherical coordinate systems.

In the cylindrical coordinate system (r, θ, z), where the relation to the rectangular coordinate system X_i is given, for example, as

$$X_1 = r\cos\theta, \ X_2 = r\sin\theta, \ X_3 = z, \tag{A.152}$$

the following relations hold:

$$\frac{\partial f}{\partial t} + \xi_i \frac{\partial f}{\partial X_i} = \frac{\partial f}{\partial t} + \xi_r \frac{\partial f}{\partial r} + \frac{\xi_\theta}{r} \frac{\partial f}{\partial \theta} + \xi_z \frac{\partial f}{\partial z} + \frac{\xi_\theta^2}{r} \frac{\partial f}{\partial \xi_r} - \frac{\xi_r \xi_\theta}{r} \frac{\partial f}{\partial \xi_\theta}, \tag{A.153a}$$

$$\frac{\partial F_i f}{\partial \xi_i} = \frac{\partial F_r f}{\partial \xi_r} + \frac{\partial F_\theta f}{\partial \xi_\theta} + \frac{\partial F_z f}{\partial \xi_z}, \tag{A.153b}$$

where ξ_r, ξ_θ, and ξ_z are, respectively, the r, θ, and z components of ξ_i (or $\boldsymbol{\xi}$), and F_r, F_θ, and F_z are, respectively, the corresponding components of F_i (or $\boldsymbol{F}$).

In the spherical coordinate system (r, θ, φ), where the relation to the rectangular coordinate system X_i is given, for example, as

$$X_1 = r\cos\theta,\ X_2 = r\sin\theta\cos\varphi,\ X_3 = r\sin\theta\sin\varphi, \tag{A.154}$$

the following relations hold:

$$\begin{aligned}\frac{\partial f}{\partial t} + \xi_i\frac{\partial f}{\partial X_i} = \frac{\partial f}{\partial t} + \xi_r\frac{\partial f}{\partial r} + \frac{\xi_\theta}{r}\frac{\partial f}{\partial \theta} + \frac{\xi_\varphi}{r\sin\theta}\frac{\partial f}{\partial \varphi}\\ + \frac{\xi_\theta^2+\xi_\varphi^2}{r}\frac{\partial f}{\partial \xi_r} + \left(\frac{\xi_\varphi^2}{r}\cot\theta - \frac{\xi_r\xi_\theta}{r}\right)\frac{\partial f}{\partial \xi_\theta}\\ - \left(\frac{\xi_\theta\xi_\varphi}{r}\cot\theta + \frac{\xi_r\xi_\varphi}{r}\right)\frac{\partial f}{\partial \xi_\varphi},\end{aligned} \tag{A.155a}$$

$$\frac{\partial F_i f}{\partial \xi_i} = \frac{\partial F_r f}{\partial \xi_r} + \frac{\partial F_\theta f}{\partial \xi_\theta} + \frac{\partial F_\varphi f}{\partial \xi_\varphi}, \tag{A.155b}$$

where ξ_r, ξ_θ, and ξ_φ are, respectively, the r, θ, and φ components of ξ_i (or $\boldsymbol{\xi}$), and F_r, F_θ, and F_φ are, respectively, the corresponding components of F_i (or $\boldsymbol{F}$).

Equations (A.153a) and (A.155a) contain derivatives with respect to molecular velocity components in the cylindrical or spherical coordinate system, which is better to be explained to beginners because the relation between the coordinate systems does not contain the molecular velocity. Let X_i be rectangular coordinates, χ_i be curvilinear coordinates, and their relation be given by

$$\chi_i = \chi_i(X_k) \quad (i = 1, 2, 3).$$

Let ξ_i be the X_i component of the molecular velocity and Ξ_i be its χ_i component. Then, the relation between them contains space coordinates as

$$\Xi_i = \Xi_i(\xi_k, X_k).$$

Therefore, the derivative $\partial/\partial X_i$ expressed in terms of the curvilinear coordinates is given as

$$\frac{\partial}{\partial X_i} = \frac{\partial \chi_k}{\partial X_i}\frac{\partial}{\partial \chi_k} + \frac{\partial \Xi_k}{\partial X_i}\frac{\partial}{\partial \Xi_k}.$$

In this way, the derivative $\partial/\partial X_i$ contains the derivatives with respect to Ξ_k. The expressions $\partial\chi_k/\partial X_i$ and $\partial\Xi_k/\partial X_i$ in a general coordinate system are given in the textbook by Kogan [1969] using Lamé coefficients (see Cartan [1946]).

Here, we summarize the corresponding forms of the nondimensional Boltzmann equation in Sections 1.9–1.11.

In the nondimensional cylindrical coordinate system $(\hat{r}, \theta, \hat{z})$, where

$$x_1 = \hat{r}\cos\theta,\ x_2 = \hat{r}\sin\theta,\ x_3 = \hat{z}, \tag{A.156}$$

and $(\zeta_r, \zeta_\theta, \zeta_z)$ is the $(\hat{r}, \theta, \hat{z})$ component of ζ_i,

(i) the Boltzmann equation (1.47a) for $\hat{f}$ is expressed as

$$\frac{D_{cy}\hat{f}}{D\hat{t}} + \frac{\partial \hat{F}_r \hat{f}}{\partial \zeta_r} + \frac{\partial \hat{F}_\theta \hat{f}}{\partial \zeta_\theta} + \frac{\partial \hat{F}_z \hat{f}}{\partial \zeta_z} = \frac{1}{k}\hat{J}(\hat{f},\hat{f}), \tag{A.157}$$

(ii) the Boltzmann equation (1.75a) for the perturbed velocity distribution function ϕ is

$$\frac{D_{cy}\phi}{D\hat{t}} = \frac{1}{k}[\mathcal{L}(\phi) + \mathcal{J}(\phi,\phi)], \tag{A.158}$$

(iii) the linearized Boltzmann equation (1.96) for ϕ is

$$\frac{D_{cy}\phi}{D\hat{t}} = \frac{1}{k}\mathcal{L}(\phi), \tag{A.159}$$

where

$$\frac{D_{cy}}{D\hat{t}} = \mathrm{Sh}\frac{\partial}{\partial \hat{t}} + \zeta_r \frac{\partial}{\partial \hat{r}} + \frac{\zeta_\theta}{\hat{r}}\frac{\partial}{\partial \theta} + \zeta_z \frac{\partial}{\partial \hat{z}} + \frac{\zeta_\theta^2}{\hat{r}}\frac{\partial}{\partial \zeta_r} - \frac{\zeta_r \zeta_\theta}{\hat{r}}\frac{\partial}{\partial \zeta_\theta}, \tag{A.160}$$

and $(\hat{F}_r, \hat{F}_\theta, \hat{F}_z)$ is the $(\hat{r},\theta,\hat{z})$ component of $\hat{F}_i$.

In the nondimensional spherical coordinate system $(\hat{r},\theta,\varphi)$, where

$$x_1 = \hat{r}\cos\theta,\ x_2 = \hat{r}\sin\theta\cos\varphi,\ x_3 = \hat{r}\sin\theta\sin\varphi, \tag{A.161}$$

and $(\zeta_r, \zeta_\theta, \zeta_\varphi)$ is the $(\hat{r},\theta,\varphi)$ component of ζ_i,

(i) the Boltzmann equation (1.47a) for $\hat{f}$ is expressed as

$$\frac{D_{sp}\hat{f}}{D\hat{t}} + \frac{\partial \hat{F}_r \hat{f}}{\partial \zeta_r} + \frac{\partial \hat{F}_\theta \hat{f}}{\partial \zeta_\theta} + \frac{\partial \hat{F}_\varphi \hat{f}}{\partial \zeta_\varphi} = \frac{1}{k}\hat{J}(\hat{f},\hat{f}), \tag{A.162}$$

(ii) the Boltzmann equation (1.75a) for the perturbed velocity distribution function ϕ is

$$\frac{D_{sp}\phi}{D\hat{t}} = \frac{1}{k}[\mathcal{L}(\phi) + \mathcal{J}(\phi,\phi)], \tag{A.163}$$

(iii) the linearized Boltzmann equation (1.96) for ϕ is

$$\frac{D_{sp}\phi}{D\hat{t}} = \frac{1}{k}\mathcal{L}(\phi), \tag{A.164}$$

where

$$\begin{aligned}\frac{D_{sp}}{D\hat{t}} = {} & \mathrm{Sh}\frac{\partial}{\partial \hat{t}} + \zeta_r \frac{\partial}{\partial \hat{r}} + \frac{\zeta_\theta}{\hat{r}}\frac{\partial}{\partial \theta} + \frac{\zeta_\varphi}{\hat{r}\sin\theta}\frac{\partial}{\partial \varphi} + \frac{\zeta_\theta^2 + \zeta_\varphi^2}{\hat{r}}\frac{\partial}{\partial \zeta_r} \\ & + \left(\frac{\zeta_\varphi^2}{\hat{r}}\cot\theta - \frac{\zeta_r\zeta_\theta}{\hat{r}}\right)\frac{\partial}{\partial \zeta_\theta} - \left(\frac{\zeta_\theta\zeta_\varphi}{\hat{r}}\cot\theta + \frac{\zeta_r\zeta_\varphi}{\hat{r}}\right)\frac{\partial}{\partial \zeta_\varphi},\end{aligned} \tag{A.165}$$

and $(\hat{F}_r, \hat{F}_\theta, \hat{F}_\varphi)$ is the $(\hat{r},\theta,\varphi)$ component of $\hat{F}_i$.

In the above formulas, the expression of the collision integrals $\hat{J}(\hat{f},\hat{f})$, $\mathcal{J}(\phi,\phi)$, and $\mathcal{L}(\phi)$ may not need explanation because no operation with respect to space variables is included and the coordinates in the systems are orthogonal at each point.

A.4 Integral form of the Boltzmann equation

A.4.1 General case

Consider the Boltzmann equation (1.5) with an intermolecular force of a finite range or a cutoff potential and rewrite it in the following form:

$$\frac{\partial f}{\partial t} + \xi_i \frac{\partial f}{\partial X_i} + \nu_c f = J_G, \tag{A.166}$$

where

$$\nu_c = \frac{1}{m} \int_{\text{all } \boldsymbol{\alpha},\ \text{all } \boldsymbol{\xi}_*} f_* B(|\boldsymbol{\alpha} \cdot (\boldsymbol{\xi}_* - \boldsymbol{\xi})|/|\boldsymbol{\xi}_* - \boldsymbol{\xi}|, |\boldsymbol{\xi}_* - \boldsymbol{\xi}|) \mathrm{d}\Omega(\boldsymbol{\alpha}) \mathbf{d}\boldsymbol{\xi}_*, \tag{A.167a}$$

$$J_G = \frac{1}{m} \int_{\text{all } \boldsymbol{\alpha},\ \text{all } \boldsymbol{\xi}_*} f' f'_* B(|\boldsymbol{\alpha} \cdot (\boldsymbol{\xi}_* - \boldsymbol{\xi})|/|\boldsymbol{\xi}_* - \boldsymbol{\xi}|, |\boldsymbol{\xi}_* - \boldsymbol{\xi}|) \mathrm{d}\Omega(\boldsymbol{\alpha}) \mathbf{d}\boldsymbol{\xi}_*, \tag{A.167b}$$

and the external force F_i is assumed to be absent for simplicity.

Considering ν_c and J_G in Eq. (A.166) being given, and integrating (A.166) along its characteristic, we obtain an *integral-equation expression of the Boltzmann equation* in the form

$$\begin{aligned} f(\boldsymbol{X}, \boldsymbol{\xi}, t) = {} & f(\boldsymbol{X} - \boldsymbol{\xi}(t - t_0), \boldsymbol{\xi}, t_0) \exp\left(- \int_{t_0}^{t} \nu_c(\boldsymbol{X} - \boldsymbol{\xi}(t - t_1), \boldsymbol{\xi}, t_1) \mathrm{d}t_1 \right) \\ & + \int_{t_0}^{t} J_G(\boldsymbol{X} - \boldsymbol{\xi}(t - \tau), \boldsymbol{\xi}, \tau) \exp\left(- \int_{\tau}^{t} \nu_c(\boldsymbol{X} - \boldsymbol{\xi}(t - t_1), \boldsymbol{\xi}, t_1) \mathrm{d}t_1 \right) \mathrm{d}\tau, \end{aligned} \tag{A.168}$$

which is called the *exponential* (*multiplier*) *form* of the Boltzmann equation to discriminate it from the other integral-equation expression, which is obtained by simply integrating the Boltzmann equation along the characteristic and called *integrated form* of the Boltzmann equation. The t_0 in Eq. (A.168) is given in the following way. Let $(\boldsymbol{X}, \boldsymbol{\xi}, t)$ be given. If we trace back a particle with velocity $\boldsymbol{\xi}$ from $(\boldsymbol{X}, t)$, we encounter some point on the boundary at some time $t_B(\boldsymbol{X}, \boldsymbol{\xi}, t)$ before the initial time $t = 0$, or do not encounter any point on the boundary until the initial time. We take $t_0 = t_B$ in the former case, and $t_0 = 0$ in the latter. The boundary condition, say Eq. (1.26) or Eq. (1.30), is applied to the factor $f(\boldsymbol{X} - \boldsymbol{\xi}(t - t_0), \boldsymbol{\xi}, t_0)$ in the first term on the right-hand side of Eq. (A.168) when $t_0 > 0$, and the initial condition to it when $t_0 = 0$. The first term on the right-hand side of Eq. (A.168) represents the contribution of the molecules heading to the point $(\boldsymbol{X}, t)$ from the boundary or initial state, and its exponential factor expresses the decay of the molecules reaching the point owing to molecular collisions. The second term represents the contribution of the molecules reaching the point $(\boldsymbol{X}, t)$ that are created along the characteristic by molecular collisions, the first factor of which expresses the

creation of such molecules by molecular collisions and the second (exponential) factor of which expresses the decay of the created molecules reaching the point owing to molecular collisions. Equation (A.168) is convenient to understand physical processes and to estimate the size of various contributions.

For a time-independent problem, this formula is still valid but with the following note: the third arguments (time arguments) in all functions are eliminated, the variables t_1 and τ of integration are transformed to $\bar{t}_1 = t - t_1$ and $\bar{\tau} = t - \tau$, and they are written as t_1 and τ anew; the $(t - t_0)$ in the first term on the right-hand side is the time required for a molecule with velocity $-\boldsymbol{\xi}$ to reach the boundary from the point $\boldsymbol{X}$ and is denoted by t_B. That is,

$$\begin{aligned} f(\boldsymbol{X},\boldsymbol{\xi}) &= f(\boldsymbol{X}-\boldsymbol{\xi}t_B,\boldsymbol{\xi})\exp\left(-\int_0^{t_B}\nu_c(\boldsymbol{X}-\boldsymbol{\xi}t_1,\boldsymbol{\xi})\mathrm{d}t_1\right) \\ &\quad + \int_0^{t_B} J_G(\boldsymbol{X}-\boldsymbol{\xi}\tau,\boldsymbol{\xi})\exp\left(-\int_0^{\tau}\nu_c(\boldsymbol{X}-\boldsymbol{\xi}t_1,\boldsymbol{\xi})\mathrm{d}t_1\right)\mathrm{d}\tau \\ &= f(\boldsymbol{X}-d_B\boldsymbol{\xi}/\xi,\boldsymbol{\xi})\exp\left(-\frac{1}{\xi}\int_0^{d_B(\boldsymbol{X},\boldsymbol{\xi}/\xi)}\nu_c(\boldsymbol{X}-s_1\boldsymbol{\xi}/\xi,\boldsymbol{\xi})\mathrm{d}s_1\right) \\ &\quad + \frac{1}{\xi}\int_0^{d_B(\boldsymbol{X},\boldsymbol{\xi}/\xi)} J_G(\boldsymbol{X}-s\boldsymbol{\xi}/\xi,\boldsymbol{\xi})\exp\left(-\frac{1}{\xi}\int_0^{s}\nu_c(\boldsymbol{X}-s_1\boldsymbol{\xi}/\xi,\boldsymbol{\xi})\mathrm{d}s_1\right)\mathrm{d}s, \end{aligned} \tag{A.169}$$

where $\xi = |\boldsymbol{\xi}|$, $s_1 = \xi t_1$, $s = \xi\tau$, and $d_B(\boldsymbol{X},\boldsymbol{\xi}/\xi)$ $(= \xi t_B)$ is the distance from $\boldsymbol{X}$ to the nearest point on the boundary in the $-\boldsymbol{\xi}$ direction and is determined by $\boldsymbol{X}$ and $\boldsymbol{\xi}/\xi$.

A.4.2 Linearized BKW equation with the diffuse-reflection or complete-condensation condition

The integral-equation expression (A.168) of the Boltzmann equation is reduced to a considerably simple form when we consider the case where the system is described by the linearized BKW equation (1.102) and the linearized diffuse-reflection boundary condition (1.105a) with (1.105b) on a simple boundary or the linearized complete-condensation condition (1.111) on an interface of the gas and its condensed phase. That is, the velocity distribution function is eliminated and the system is reduced to a system of integral equations for the density, the flow velocity, and the temperature of the gas. Here, we will derive the system.

We consider an initial and boundary-value problem of the linearized BKW equation under the linearized diffuse-reflection boundary condition or the linearized complete-condensation condition. The analysis is limited to the case where the boundary shape does not vary in time but the surface of the boundary may have a velocity along it, that is, $u_{wi}n_i = 0$ but $u_{wi}t_i$ may be different

from zero. The linearized BKW equation is

$$\mathrm{Sh}\frac{\partial\phi}{\partial\hat{t}}+\zeta_i\frac{\partial\phi}{\partial x_i}=\frac{1}{k}\left[-\phi+\omega+2\zeta_i u_i+\left(\zeta_i^2-\frac{3}{2}\right)\tau\right], \tag{A.170a}$$

$$\omega=\int\phi E\mathbf{d}\boldsymbol{\zeta}, \tag{A.170b}$$

$$u_i=\int\zeta_i\phi E\mathbf{d}\boldsymbol{\zeta}, \tag{A.170c}$$

$$\frac{3}{2}\tau=\int\left(\zeta_i^2-\frac{3}{2}\right)\phi E\mathbf{d}\boldsymbol{\zeta}. \tag{A.170d}$$

The linearized diffuse-reflection condition is

$$\phi(x_i,\zeta_i,\hat{t})=\sigma_w+2\zeta_j u_{wj}+\left(\zeta_j^2-\frac{3}{2}\right)\tau_w\qquad(\zeta_j n_j>0), \tag{A.171a}$$

$$\sigma_w=-\frac{1}{2}\tau_w-2\sqrt{\pi}\int_{\zeta_k n_k<0}\zeta_j n_j\phi E\mathbf{d}\boldsymbol{\zeta}. \tag{A.171b}$$

The linearized complete-condensation condition is

$$\phi(x_i,\zeta_i,\hat{t})=\omega_w+2\zeta_j u_{wj}+\left(\zeta_j^2-\frac{3}{2}\right)\tau_w\qquad(\zeta_j n_j>0). \tag{A.172}$$

The initial condition is given as

$$\phi=\phi_0\quad\text{ at }\ \hat{t}=0. \tag{A.173}$$

Here we can take $\mathrm{Sh}=1$ without loss of generality, because we do not evaluate the orders of the terms here and can choose the reference time arbitrarily.

Take the Laplace transform of Eqs. (A.170a)–(A.172). Then we have, from Eq. (A.170a) with $\mathrm{Sh}=1$,

$$\zeta_i\frac{\partial\tilde{\phi}}{\partial x_i}+(s+k^{-1})\tilde{\phi}=k^{-1}\left[\tilde{\omega}+2\zeta_i\tilde{u}_i+\left(\zeta_i^2-\frac{3}{2}\right)\tilde{\tau}\right]+\phi_0, \tag{A.174}$$

with

$$\tilde{\omega}=\int\tilde{\phi}E\mathbf{d}\boldsymbol{\zeta}, \tag{A.175a}$$

$$\tilde{u}_i=\int\zeta_i\tilde{\phi}E\mathbf{d}\boldsymbol{\zeta}, \tag{A.175b}$$

$$\frac{3}{2}\tilde{\tau}=\int\left(\zeta_i^2-\frac{3}{2}\right)\tilde{\phi}E\mathbf{d}\boldsymbol{\zeta}, \tag{A.175c}$$

from Eq. (A.171a) with (A.171b),

$$\tilde{\phi}=\tilde{\sigma}_w+2\zeta_j\tilde{u}_{wj}+\left(\zeta_j^2-\frac{3}{2}\right)\tilde{\tau}_w\qquad(\zeta_j n_j>0), \tag{A.176a}$$

$$\tilde{\sigma}_w=-\frac{1}{2}\tilde{\tau}_w-2\sqrt{\pi}\int_{\zeta_k n_k<0}\zeta_j n_j\tilde{\phi}E\mathbf{d}\boldsymbol{\zeta}, \tag{A.176b}$$

and from Eq. (A.172),

$$\tilde{\phi} = \tilde{\omega}_w + 2\zeta_j \tilde{u}_{wj} + \left(\zeta_j^2 - \frac{3}{2}\right)\tilde{\tau}_w \qquad (\zeta_j n_j > 0), \tag{A.177}$$

where the tilde $\sim$ over a character indicates its Laplace transform, for example,

$$\tilde{\phi} = \int_0^\infty \phi \exp(-s\hat{t})\mathrm{d}\hat{t}. \tag{A.178}$$

In the following analysis, we write $\tilde{\omega}_w$ instead of $\tilde{\sigma}_w$ in the diffuse-reflection condition (A.176a) and make a comment on the additional condition (A.176b) when necessary.

Considering the right-hand side of Eq. (A.174) being given, and integrating Eq. (A.174) along its characteristic, as we have done in Section A.4.1, we have the expression for $\tilde{\phi}$ corresponding to Eq. (A.169) as

$$\begin{aligned}\tilde{\phi}(\boldsymbol{x},\boldsymbol{\zeta}) = {}& \tilde{\phi}_w(\boldsymbol{x} - \hat{d}_B\boldsymbol{\zeta}/\zeta, \boldsymbol{\zeta}) \exp\left[-(s+k^{-1})\hat{d}_B/\zeta\right] \\ & + \frac{1}{k\zeta}\int_0^{\hat{d}_B(\boldsymbol{x},\boldsymbol{\zeta}/\zeta)} \tilde{\phi}_e(\boldsymbol{x} - \tau\boldsymbol{\zeta}/\zeta, \boldsymbol{\zeta}) \exp\left[-(s+k^{-1})\tau/\zeta\right] \mathrm{d}\tau \\ & + \frac{1}{\zeta}\int_0^{\hat{d}_B(\boldsymbol{x},\boldsymbol{\zeta}/\zeta)} \phi_0(\boldsymbol{x} - \tau\boldsymbol{\zeta}/\zeta, \boldsymbol{\zeta}) \exp\left[-(s+k^{-1})\tau/\zeta\right] \mathrm{d}\tau,\end{aligned} \tag{A.179}$$

where $\zeta = |\boldsymbol{\zeta}|$ and $\hat{d}_B$ is the distance (in the nondimensional $\boldsymbol{x}$ space) from $\boldsymbol{x}$ to the nearest point on the boundary in the $-\boldsymbol{\zeta}$ direction and a function of $\boldsymbol{x}$ and $\boldsymbol{\zeta}/\zeta$, and

$$\tilde{\phi}_w = \tilde{\omega}_w + 2\zeta_j \tilde{u}_{wj} + \left(\zeta^2 - \frac{3}{2}\right)\tilde{\tau}_w, \tag{A.180a}$$

$$\tilde{\phi}_e = \tilde{\omega} + 2\zeta_j \tilde{u}_j + \left(\zeta^2 - \frac{3}{2}\right)\tilde{\tau}. \tag{A.180b}$$

Substituting the expression (A.179) for $\tilde{\phi}$ into Eqs. (A.175a)–(A.175c), we obtain the integral equations for $\tilde{\omega}$, $\tilde{u}_i$, and $\tilde{\tau}$. We will explain this process explicitly.

Let $\bar{\boldsymbol{l}} = -\boldsymbol{\zeta}/\zeta$ (or $\bar{l}_i = -\zeta_i/\zeta$) and use the variables $(\zeta, \bar{\boldsymbol{l}})$ representation for $\boldsymbol{\zeta}$ (or choose a spherical coordinate system for the nondimensional molecular velocity $\boldsymbol{\zeta}$). Then, noting that $\mathbf{d}\boldsymbol{\zeta} = \zeta^2 \mathrm{d}\zeta \mathrm{d}\Omega(\bar{\boldsymbol{l}})$, where $\mathrm{d}\Omega(\bar{\boldsymbol{l}})$ is the solid-angle element in the direction $\bar{\boldsymbol{l}}$, and carrying out the integration with respect to ζ first

in Eqs. (A.175a)–(A.175c) with $\tilde{\phi}$ given by Eq. (A.179), we have, for example,

$$\begin{aligned}\tilde{\omega} &= \frac{1}{\pi^{3/2}}\int_{\text{all }\bar{\boldsymbol{l}}}[\tilde{\omega}_w(\boldsymbol{x}+\hat{d}_B\bar{\boldsymbol{l}})J_2((s+k^{-1})\hat{d}_B)+\cdots]\mathrm{d}\Omega(\bar{\boldsymbol{l}})\\ &+\frac{1}{k\pi^{3/2}}\int_{\text{all }\bar{\boldsymbol{l}}}\int_0^{\hat{d}_B(\boldsymbol{x},\bar{\boldsymbol{l}})}[\tilde{\omega}(\boldsymbol{x}+\tau\bar{\boldsymbol{l}})J_1((s+k^{-1})\tau)+\cdots]\mathrm{d}\tau\mathrm{d}\Omega(\bar{\boldsymbol{l}})\\ &+\frac{1}{\pi^{3/2}}\int_{\text{all }\bar{\boldsymbol{l}}}\int_0^{\hat{d}_B}\int_0^{\infty}\phi_0(\boldsymbol{x}+\tau\bar{\boldsymbol{l}},-\zeta\bar{\boldsymbol{l}})\zeta\exp\left(-\zeta^2-\frac{(s+k^{-1})\tau}{\zeta}\right)\mathrm{d}\zeta\mathrm{d}\tau\mathrm{d}\Omega(\bar{\boldsymbol{l}}),\end{aligned} \tag{A.181}$$

where $J_n(x)$ is the *Abramowitz function* (Abramowitz & Stegun [1972]) defined by

$$J_n(x)=\int_0^{\infty}\zeta^n\exp\left(-\zeta^2-\frac{x}{\zeta}\right)\mathrm{d}\zeta. \tag{A.182}$$

The argument $\boldsymbol{x}+\hat{d}_B\bar{\boldsymbol{l}}$ of $\tilde{\omega}_w$ is the nearest boundary point from $\boldsymbol{x}$ in the direction of $\bar{\boldsymbol{l}}$. Now put

$$\boldsymbol{x}_*=\boldsymbol{x}+\tau\bar{\boldsymbol{l}}\qquad(0\le\tau\le\hat{d}_B).$$

Then, $\boldsymbol{x}_*$ is a point on the line between $\boldsymbol{x}$ and $\boldsymbol{x}+\hat{d}_B\bar{\boldsymbol{l}}$. With the new variable $\boldsymbol{x}_*$, we have

$$\mathbf{d}\boldsymbol{x}_*=|\boldsymbol{x}_*-\boldsymbol{x}|^2\mathrm{d}\tau\mathrm{d}\Omega(\bar{\boldsymbol{l}}),\quad\frac{(x_i-x_{i*})n_i(\boldsymbol{x}_*)}{|\boldsymbol{x}_*-\boldsymbol{x}|}\mathrm{d}S(\boldsymbol{x}_*)=|\boldsymbol{x}_*-\boldsymbol{x}|^2\mathrm{d}\Omega(\bar{\boldsymbol{l}}),$$

where $\mathbf{d}\boldsymbol{x}_*$ is the volume element of the $\boldsymbol{x}_*$ space and $\mathrm{d}S(\boldsymbol{x}_*)$ is the boundary surface element at $\boldsymbol{x}_*$. Thus, Eq. (A.181) is rewritten as follows:

$$\begin{aligned}\tilde{\omega} &= \frac{1}{\pi^{3/2}}\int_{S^*(\boldsymbol{x})}\left(\tilde{\omega}_w(\boldsymbol{x}_*)\frac{J_2((s+k^{-1})|\boldsymbol{x}_*-\boldsymbol{x}|)}{|\boldsymbol{x}_*-\boldsymbol{x}|^2}+\cdots\right)\frac{(x_i-x_{i*})n_i(\boldsymbol{x}_*)}{|\boldsymbol{x}_*-\boldsymbol{x}|}\mathrm{d}S(\boldsymbol{x}_*)\\ &+\frac{1}{k\pi^{3/2}}\int_{V^*(\boldsymbol{x})}\left(\tilde{\omega}(\boldsymbol{x}_*)\frac{J_1((s+k^{-1})|\boldsymbol{x}_*-\boldsymbol{x}|)}{|\boldsymbol{x}_*-\boldsymbol{x}|^2}+\cdots\right)\mathbf{d}\boldsymbol{x}_*\\ &+\frac{1}{\pi^{3/2}}\int_{V^*(\boldsymbol{x})}\frac{1}{|\boldsymbol{x}_*-\boldsymbol{x}|^2}\int_0^{\infty}\phi_0(\boldsymbol{x}_*,\zeta(x_i-x_{i*})|\boldsymbol{x}_*-\boldsymbol{x}|^{-1})\\ &\qquad\times\zeta\exp\left[-\zeta^2-(s+k^{-1})|\boldsymbol{x}_*-\boldsymbol{x}|/\zeta\right]\mathrm{d}\zeta\mathbf{d}\boldsymbol{x}_*,\end{aligned}$$

where $V^*(\boldsymbol{x})$ and $S^*(\boldsymbol{x})$ are, respectively, the gas domain and the boundary surface that can be seen from the point $\boldsymbol{x}$ (see Fig. A.4).

In this way, we obtain the integral equations for $\tilde{\omega}$, $\tilde{u}_i$, and $\tilde{\tau}$ in the form

$$\begin{aligned}&\begin{pmatrix}\tilde{\omega}(\boldsymbol{x})\\ \tilde{u}_i(\boldsymbol{x})\\ \frac{3}{2}\tilde{\tau}(\boldsymbol{x})\end{pmatrix}-\frac{1}{k\pi^{3/2}}\int_{V^*(\boldsymbol{x})}\frac{1}{|\boldsymbol{x}_*-\boldsymbol{x}|^2}\mathbb{K}_5\begin{pmatrix}\tilde{\omega}(\boldsymbol{x}_*)\\ \tilde{u}_j(\boldsymbol{x}_*)\\ \tilde{\tau}(\boldsymbol{x}_*)\end{pmatrix}\mathbf{d}\boldsymbol{x}_*\\ &=-\frac{1}{\pi^{3/2}}\int_{S^*(\boldsymbol{x})}\frac{\mathfrak{r}_k n_k(\boldsymbol{x}_*)}{|\boldsymbol{x}_*-\boldsymbol{x}|^2}\mathbb{K}_{w5}\begin{pmatrix}\tilde{\omega}_w(\boldsymbol{x}_*)\\ \tilde{u}_{wj}(\boldsymbol{x}_*)\\ \tilde{\tau}_w(\boldsymbol{x}_*)\end{pmatrix}\mathrm{d}S(\boldsymbol{x}_*)+\begin{pmatrix}\mathrm{Ih}_\omega\\ \mathrm{Ih}_i\\ \mathrm{Ih}_\tau\end{pmatrix},\end{aligned} \tag{A.183}$$

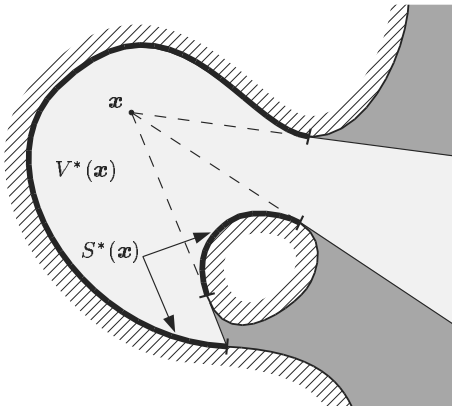

Figure A.4. The gas domain $V^*(\boldsymbol{x})$ and the boundary surface $S^*(\boldsymbol{x})$ that can be seen from $\boldsymbol{x}$. The integration is carried out over there.

$$\mathfrak{r}_i = \frac{x_{i*} - x_i}{|\boldsymbol{x}_* - \boldsymbol{x}|}. \tag{A.184}$$

Here, the kernels $\mathbb{K}_5$ and $\mathbb{K}_{w5}$ are the 5×5 matrices given by

$$\mathbb{K}_5 = \begin{pmatrix} J_1 & -2J_2\mathfrak{r}_j & J_3 - \frac{3}{2}J_1 \\ -J_2\mathfrak{r}_i & 2J_3\mathfrak{r}_i\mathfrak{r}_j & -(J_4 - \frac{3}{2}J_2)\mathfrak{r}_i \\ J_3 - \frac{3}{2}J_1 & -2(J_4 - \frac{3}{2}J_2)\mathfrak{r}_j & J_5 - 3J_3 + \frac{9}{4}J_1 \end{pmatrix}, \tag{A.185a}$$

$$\mathbb{K}_{w5} = \begin{pmatrix} J_2 & -2J_3\mathfrak{r}_j & J_4 - \frac{3}{2}J_2 \\ -J_3\mathfrak{r}_i & 2J_4\mathfrak{r}_i\mathfrak{r}_j & -(J_5 - \frac{3}{2}J_3)\mathfrak{r}_i \\ J_4 - \frac{3}{2}J_2 & -2(J_5 - \frac{3}{2}J_3)\mathfrak{r}_j & J_6 - 3J_4 + \frac{9}{4}J_2 \end{pmatrix}, \tag{A.185b}$$

where the arguments of the Abramowitz functions J_n's in the matrices are commonly

$$\left(s + k^{-1}\right)|\boldsymbol{x}_* - \boldsymbol{x}|, \text{ i.e., } J_n = J_n(\left(s + k^{-1}\right)|\boldsymbol{x}_* - \boldsymbol{x}|). \tag{A.186}$$

The inhomogeneous terms (Ih_ω, Ih_i, Ih_τ) due to the initial condition ϕ_0 are

$$\begin{pmatrix} \mathrm{Ih}_\omega \\ \mathrm{Ih}_i \\ \mathrm{Ih}_\tau \end{pmatrix} = \frac{1}{\pi^{3/2}} \int_{V^*(\boldsymbol{x})} \frac{1}{|\boldsymbol{x}_* - \boldsymbol{x}|^2} \int_0^\infty \begin{pmatrix} \zeta \\ -\zeta^2\mathfrak{r}_i \\ \zeta^3 - \frac{3}{2}\zeta \end{pmatrix} \times \phi_0(\boldsymbol{x}_*, -\zeta\mathfrak{r}_i) \exp\left[-\zeta^2 - (s + k^{-1})|\boldsymbol{x}_* - \boldsymbol{x}|/\zeta\right] \mathrm{d}\zeta \mathbf{d}\boldsymbol{x}_*. \tag{A.187}$$

The above system of integral equations is complete in the case of the complete-condensation boundary condition, but in the case of the diffuse reflection, $\tilde{\omega}_w(\boldsymbol{x})$

is subject to the condition

$$\tilde{\omega}_w(\boldsymbol{x}) = -\frac{1}{2}\tilde{\tau}_w(\boldsymbol{x}) + \frac{2}{k\pi}\int_{V^*(\boldsymbol{x})} \frac{\mathfrak{r}_i n_i(\boldsymbol{x})}{|\boldsymbol{x}_* - \boldsymbol{x}|^2}\mathbb{W}_5 \begin{pmatrix} \tilde{\omega}(\boldsymbol{x}_*) \\ \tilde{u}_j(\boldsymbol{x}_*) \\ \tilde{\tau}(\boldsymbol{x}_*) \end{pmatrix} \mathbf{d}\boldsymbol{x}_* \\ - \frac{2}{\pi}\int_{S^*(\boldsymbol{x})} \frac{\mathfrak{r}_i n_i(\boldsymbol{x})\mathfrak{r}_k n_k(\boldsymbol{x}_*)}{|\boldsymbol{x}_* - \boldsymbol{x}|^2}\mathbb{W}_{w5} \begin{pmatrix} \tilde{\omega}_w(\boldsymbol{x}_*) \\ \tilde{u}_{wj}(\boldsymbol{x}_*) \\ \tilde{\tau}_w(\boldsymbol{x}_*) \end{pmatrix} \mathrm{d}S(\boldsymbol{x}_*) - 2\sqrt{\pi}\mathrm{Ih}_i n_i(\boldsymbol{x}), \tag{A.188}$$

$$\mathbb{W}_5 = (J_2,\ -2J_3\mathfrak{r}_j,\ J_4 - \tfrac{3}{2}J_2), \tag{A.189a}$$

$$\mathbb{W}_{w5} = (J_3,\ -2J_4\mathfrak{r}_j,\ J_5 - \tfrac{3}{2}J_3), \tag{A.189b}$$

where the argument of J_n is given by Eq. (A.186). Here, it should be noted that the argument $\boldsymbol{x}$ is on the boundary, and $S^*(\boldsymbol{x})$ and $V^*(\boldsymbol{x})$ are the corresponding surface and domain seen from the boundary point $\boldsymbol{x}$. In the above system of integral equations, the boundary condition at infinity is not explicitly included, and thus the condition at infinity should be supplemented to the system.

In a time-independent problem, we have only to eliminate the Ih_* terms, the variable s, and the tildes over the characters, i.e., $(\mathrm{Ih}_\omega,\ \mathrm{Ih}_i,\ \mathrm{Ih}_\tau) = (0,\ 0,\ 0)$ and $(s,\ \tilde{\omega},\ \tilde{u}_i,\ \tilde{\tau},\ \tilde{\omega}_w,\ \tilde{u}_{wi},\ \tilde{\tau}_w) \to (0,\ \omega,\ u_i,\ \tau,\ \omega_w,\ u_{wi},\ \tau_w)$ in each of the above equations, where the argument of J_n given in Eq. (A.186) is reduced to $|\boldsymbol{x}_* - \boldsymbol{x}|/k$.

In various situations, we have a chance to discuss spatially one or two-dimensional solutions, where the distribution function ϕ or $\tilde{\phi}$ is independent of one or two of the space variables, say x_3, or x_2 and x_3, of the Boltzmann equation without or with an inhomogeneous term, the latter case of which is derived by simplification of three-dimensional problems [see, e.g., Eq. (A.208b) in Section A.5]. The lower-dimensional forms of Eqs. (A.183), (A.185a), (A.185b), and (A.187) [or with Eqs. (A.188)–(A.189b)] are derived from the original BKW system directly in the same way as the above three-dimensional integral equations by treating the ζ_3 variable (the two-dimensional case) or the ζ_2 and ζ_3 variables (the one-dimensional case) separately. This is simpler than to derive them from the three-dimensional integral equations.

Here, we list only the results for the two-dimensional case. The notation should be interpreted in the following degenerate way:

$$\boldsymbol{x} = (x_1, x_2),\quad \boldsymbol{x}_* = (x_{1*}, x_{2*}),\quad \mathbf{d}\boldsymbol{x}_* = \mathrm{d}x_{1*}\mathrm{d}x_{2*},\quad \boldsymbol{x}_* - \boldsymbol{x} = (x_{1*} - x_1, x_{2*} - x_2),$$

the third component of a vector, except $\tilde{u}_i$ and $\tilde{u}_{wi}$, is absent, i.e., $n_3 = 0$ and $x_{3*} - x_3 = 0$, and $V^*(\boldsymbol{x})$ and $S^*(\boldsymbol{x})$ are, respectively, a domain and a boundary in the two-dimensional plane, say, $x_3 = 0$. In their derivation, $\bar{\boldsymbol{l}} = (\bar{l}_1, \bar{l}_2, 0)$, $\mathrm{d}\Omega(\bar{\boldsymbol{l}})$ is the angle element in the direction $(\bar{l}_1, \bar{l}_2, 0)$, and the relations

$$\mathbf{d}\boldsymbol{\zeta} = \zeta\mathrm{d}\zeta\mathrm{d}\Omega(\bar{\boldsymbol{l}})\mathrm{d}\zeta_3,\ \zeta = (\zeta_1^2 + \zeta_2^2)^{1/2},\quad |\boldsymbol{x}_* - \boldsymbol{x}|\mathrm{d}\tau\mathrm{d}\Omega(\bar{\boldsymbol{l}}) = \mathbf{d}\boldsymbol{x}_*,$$

$$|\boldsymbol{x}_* - \boldsymbol{x}|\mathrm{d}\Omega(\bar{\boldsymbol{l}}) = \frac{(x_i - x_{i*})n_i(\boldsymbol{x}_*)}{|\boldsymbol{x}_* - \boldsymbol{x}|}\mathrm{d}S(\boldsymbol{x}_*)$$

are used. The integral equations for $\tilde{\omega}(\boldsymbol{x})$, $\tilde{u}_i(\boldsymbol{x})$, and $\tilde{\tau}(\boldsymbol{x})$ are given in the following equations (A.190)–(A.197b), where (i, j, k) run only on 1 and 2 :

$$\begin{aligned}
&\begin{pmatrix} \tilde{\omega}(\boldsymbol{x}) \\ \tilde{u}_i(\boldsymbol{x}) \\ \frac{3}{2}\tilde{\tau}(\boldsymbol{x}) \end{pmatrix} - \frac{1}{k\pi}\int_{V^*(\boldsymbol{x})} \frac{1}{|\boldsymbol{x}_* - \boldsymbol{x}|}\mathbb{K}_4 \begin{pmatrix} \tilde{\omega}(\boldsymbol{x}_*) \\ \tilde{u}_j(\boldsymbol{x}_*) \\ \tilde{\tau}(\boldsymbol{x}_*) \end{pmatrix} \mathbf{d}\boldsymbol{x}_* \\
&\quad = -\frac{1}{\pi}\int_{S^*(\boldsymbol{x})} \frac{\mathfrak{r}_k n_k(\boldsymbol{x}_*)}{|\boldsymbol{x}_* - \boldsymbol{x}|}\mathbb{K}_{w4} \begin{pmatrix} \tilde{\omega}_w(\boldsymbol{x}_*) \\ \tilde{u}_{wj}(\boldsymbol{x}_*) \\ \tilde{\tau}_w(\boldsymbol{x}_*) \end{pmatrix} \mathrm{d}S(\boldsymbol{x}_*) + \begin{pmatrix} \mathrm{Ih}_\omega \\ \mathrm{Ih}_i \\ \mathrm{Ih}_\tau \end{pmatrix}, \qquad \text{(A.190)}
\end{aligned}$$

$$\begin{aligned}
&\tilde{u}_3(\boldsymbol{x}) - \frac{1}{k\pi}\int_{V^*(\boldsymbol{x})} \frac{1}{|\boldsymbol{x}_* - \boldsymbol{x}|} J_0((s + k^{-1})|\boldsymbol{x}_* - \boldsymbol{x}|)\tilde{u}_3(\boldsymbol{x}_*)\mathbf{d}\boldsymbol{x}_* \\
&\quad = -\frac{1}{\pi}\int_{S^*(\boldsymbol{x})} \frac{\mathfrak{r}_k n_k(\boldsymbol{x}_*)}{|\boldsymbol{x}_* - \boldsymbol{x}|} J_1((s + k^{-1})|\boldsymbol{x}_* - \boldsymbol{x}|)\tilde{u}_{w3}(\boldsymbol{x}_*)\mathrm{d}S(\boldsymbol{x}_*) + \mathrm{Ih}_3, \qquad \text{(A.191)}
\end{aligned}$$

$$\mathfrak{r}_i = \frac{x_{i*} - x_i}{|\boldsymbol{x}_* - \boldsymbol{x}|}. \qquad \text{(A.192)}$$

Here, the kernels $\mathbb{K}_4$ and $\mathbb{K}_{w4}$ are the 4×4 matrices given by

$$\mathbb{K}_4 = \begin{pmatrix} J_0 & -2J_1\mathfrak{r}_j & J_2 - J_0 \\ -J_1\mathfrak{r}_i & 2J_2\mathfrak{r}_i\mathfrak{r}_j & -(J_3 - J_1)\mathfrak{r}_i \\ J_2 - J_0 & -2(J_3 - J_1)\mathfrak{r}_j & J_4 - 2J_2 + \frac{3}{2}J_0 \end{pmatrix}, \qquad \text{(A.193a)}$$

$$\mathbb{K}_{w4} = \begin{pmatrix} J_1 & -2J_2\mathfrak{r}_j & J_3 - J_1 \\ -J_2\mathfrak{r}_i & 2J_3\mathfrak{r}_i\mathfrak{r}_j & -(J_4 - J_2)\mathfrak{r}_i \\ J_3 - J_1 & -2(J_4 - J_2)\mathfrak{r}_j & J_5 - 2J_3 + \frac{3}{2}J_1 \end{pmatrix}, \qquad \text{(A.193b)}$$

where the arguments of the Abramowitz functions J_n's in the matrices are commonly

$$\left(s + k^{-1}\right)|\boldsymbol{x}_* - \boldsymbol{x}|, \text{ i.e., } \ J_n = J_n(\left(s + k^{-1}\right)|\boldsymbol{x}_* - \boldsymbol{x}|). \qquad \text{(A.194)}$$

The inhomogeneous terms (Ih_ω, Ih_i, Ih_3 Ih_τ) are

$$\begin{aligned}
\begin{pmatrix} \mathrm{Ih}_\omega \\ \mathrm{Ih}_i \\ \mathrm{Ih}_3 \\ \mathrm{Ih}_\tau \end{pmatrix} &= \frac{1}{\pi^{3/2}}\int_{V^*(\boldsymbol{x})} \frac{1}{|\boldsymbol{x}_* - \boldsymbol{x}|}\int_0^\infty\int_{-\infty}^\infty \begin{pmatrix} 1 \\ -\zeta\mathfrak{r}_i \\ \zeta_3 \\ \zeta^2 + \zeta_3^2 - \frac{3}{2} \end{pmatrix} \phi_0(\boldsymbol{x}_*, -\zeta\mathfrak{r}_i, \zeta_3) \\
&\quad \times \exp\left[-\zeta^2 - \zeta_3^2 - (s + k^{-1})|\boldsymbol{x}_* - \boldsymbol{x}|/\zeta\right] \mathrm{d}\zeta_3\mathrm{d}\zeta\mathbf{d}\boldsymbol{x}_*. \qquad \text{(A.195)}
\end{aligned}$$

In the case of the diffuse-reflection condition, $\tilde{\omega}_w(\boldsymbol{x})$ should satisfy the condition

$$\begin{aligned}
\tilde{\omega}_w(\boldsymbol{x}) &= -\frac{1}{2}\tilde{\tau}_w(\boldsymbol{x}) + \frac{2}{\sqrt{\pi}k}\int_{V^*(\boldsymbol{x})} \frac{\mathfrak{r}_i n_i(\boldsymbol{x})}{|\boldsymbol{x}_* - \boldsymbol{x}|}\mathbb{W}_4 \begin{pmatrix} \tilde{\omega}(\boldsymbol{x}_*) \\ \tilde{u}_j(\boldsymbol{x}_*) \\ \tilde{\tau}(\boldsymbol{x}_*) \end{pmatrix} \mathbf{d}\boldsymbol{x}_* \\
&\quad - \frac{2}{\sqrt{\pi}}\int_{S^*(\boldsymbol{x})} \frac{\mathfrak{r}_i n_i(\boldsymbol{x})\mathfrak{r}_k n_k(\boldsymbol{x}_*)}{|\boldsymbol{x}_* - \boldsymbol{x}|}\mathbb{W}_{w4} \begin{pmatrix} \tilde{\omega}_w(\boldsymbol{x}_*) \\ \tilde{u}_{wj}(\boldsymbol{x}_*) \\ \tilde{\tau}_w(\boldsymbol{x}_*) \end{pmatrix} \mathrm{d}S(\boldsymbol{x}_*) - 2\sqrt{\pi}\mathrm{Ih}_i n_i(\boldsymbol{x}), \qquad \text{(A.196)}
\end{aligned}$$

$$\mathbb{W}_4 = (J_1, \ -2J_2\mathfrak{r}_j, \ J_3 - J_1), \tag{A.197a}$$

$$\mathbb{W}_{w4} = (J_2, \ -2J_3\mathfrak{r}_j, \ J_4 - J_2), \tag{A.197b}$$

where the argument of J_n is given by Eq. (A.194). As in the three-dimensional case, the boundary condition at infinity should be supplemented to the above system of the integral equations.

As in the three-dimensional case, in a time-independent problem, we have only to eliminate the Ih_* terms, the variable s, and the tilde over the characters, i.e., $(\mathrm{Ih}_\omega, \mathrm{Ih}_i, \mathrm{Ih}_3, \mathrm{Ih}_\tau) = (0, 0, 0, 0)$ and $(0, \tilde{\omega}, \tilde{u}_i, \tilde{u}_3, \tilde{\tau}, \tilde{\omega}_w, \tilde{u}_{wi}, \tilde{u}_{w3}, \tilde{\tau}_w) \to (0, \omega, u_i, u_3, \tau, \omega_w, u_{wi}, u_{w3}, \tau_w)$ in each of the above equations, where the argument of J_n given in Eq. (A.194) is reduced to $|\boldsymbol{x}_* - \boldsymbol{x}|/k$. Some three-dimensional problems are reduced to those of the two-dimensional Boltzmann equation with an inhomogeneous term, as shown in Section A.5 [see Eq. (A.208b)]. In such cases, its Laplace transform has to be added to ϕ_0 in the formulas of Ih_ω, Ih_i, Ih_3, and Ih_τ.

In the one-dimensional case (say, $\partial/\partial x_2 = \partial/\partial x_3 = 0$ and the gas domain is $0 < x_1 < 1$ or ∞), the characteristic is the x_1 axis independently of $\boldsymbol{\zeta}$, and the integration with respect to $\boldsymbol{\zeta}$ is done first without combining $\mathrm{d}\Omega(\bar{\boldsymbol{l}})$ and $\mathrm{d}\tau$. Thus, the computation is much simpler. What is to be noted is the direction of integration, that is, the integration along the characteristic (or along x_1) is done from $x_1 = 0$ for $\zeta_1 > 0$ and from $x_1 = 1$ or ∞ for $\zeta_1 < 0$. The results are omitted here.

The integral equations derived here have various advantages. The velocity distribution function is eliminated in these equations, and the molecular velocity $\boldsymbol{\zeta}$ is eliminated. Therefore, various subtleties of the velocity distribution function, such as the discontinuity of the velocity distribution function and its singular behavior for small ζ (and $\zeta_i n_i$), do not enter these equations directly. From the behavior of the tail of the function $J_n(x)$, which is $c_0 x^{n/3} \exp(-c_1 x^{2/3})$ (c_0, c_1 : consts, $n \geq 1$) (see Abramowitz & Stegun [1972]), we can see the dependence on the Knudsen number of the effect of the surrounding gas and the boundary condition on the point $\boldsymbol{x}$ under consideration.[38]

A.5 Similarity solution

The velocity distribution function that is independent of the time variable or any of rectangular components of the space variable is obviously compatible with the (full or linearized) Boltzmann equation without an external force

$$\mathrm{Sh}\frac{\partial \hat{f}}{\partial \hat{t}} + \zeta_i \frac{\partial \hat{f}}{\partial x_i} = \frac{1}{k}\hat{J}(\hat{f}, \hat{f}), \tag{A.198a}$$

$$\hat{J}(\hat{f}, \hat{f}) = \int (\hat{f}'\hat{f}'_* - \hat{f}\hat{f}_*)\widehat{B}\,\mathrm{d}\Omega(\boldsymbol{\alpha})\,\mathbf{d}\boldsymbol{\zeta}_*, \tag{A.198b}$$

[38] In fact, various results for the asymptotic behavior of a gas for large or small Knudsen numbers are first obtained on the basis of the integral equations derived from the BKW equation in this section, and they are extended to the standard Boltzmann equation.

$$\mathrm{Sh}\frac{\partial \phi}{\partial \hat{t}} + \zeta_i \frac{\partial \phi}{\partial x_i} = \frac{1}{k}\mathcal{L}(\phi), \tag{A.199a}$$

$$\mathcal{L}(\phi) = \int E_*(\phi' + \phi'_* - \phi - \phi_*)\widehat{B}\,\mathrm{d}\Omega(\boldsymbol{\alpha})\,\mathbf{d}\boldsymbol{\zeta}_*. \tag{A.199b}$$

That is, the streaming operator $\mathrm{Sh}\partial/\partial\hat{t} + \zeta_i\partial/\partial x_i$ and the collision operator $\hat{J}(*,*)$ or $\mathcal{L}(*)$ in the Boltzmann equation do not violate this degenerate property. The analysis is generally simpler for the degenerate cases. For example, consider the spatially uniform case. Take Eq. (A.198a) without the space derivative terms

$$\mathrm{Sh}\frac{\partial \hat{f}}{\partial \hat{t}} = \frac{1}{k}\hat{J}(\hat{f},\hat{f}). \tag{A.200}$$

Then, from the conservation equations (1.57)–(1.59), which are derived by integrating the equation (A.200) multiplied by 1, ζ_i, or ζ_i^2 over the whole space of $\boldsymbol{\zeta}$, the density $\hat{\rho}$, the flow velocity $\hat{v}_i$, and the temperature $\hat{T}$ are time-independent, and thus they are constant. There are some other cases where the number of the independent variables, including the molecular velocity, is decreased with combination of the variables. They are called *similarity solutions*, which are discussed below.

First review the property of the collision integrals $\hat{J}(\hat{f},\hat{f})$ and $\mathcal{L}(\phi)$ (see Section A.2.5). The operators $\hat{J}(*,*)$ and $\mathcal{L}(*)$ are isotropic. Thus, for $\hat{f}$ or ϕ of the form $\Phi(\zeta)$, the integrals $\hat{J}(\hat{f},\hat{f})$ and $\mathcal{L}(\phi)$ are spherically symmetric, and therefore, according to Eq. (A.79) or (A.80) with $m = 0$, they are of the form

$$\hat{J}(\hat{f},\hat{f}) = F(\zeta), \qquad \mathcal{L}(\phi) = F(\zeta). \tag{A.201}$$

Let l_{ij} be

$$l_{ik}l_{jk} = \delta_{ij} \quad \text{with} \quad l_{11} = 1,\ l_{12} = 0,\ l_{13} = 0.$$

Noting $l_{1j}\zeta_j = \zeta_1$, $(l_{2j}\zeta_j)^2 + (l_{3j}\zeta_j)^2 = \zeta_2^2 + \zeta_3^2$, we find that for $\hat{f}$ or ϕ of the form $\Phi(\zeta_1, (\zeta_2^2 + \zeta_3^2)^{1/2})$,

$$\hat{J}(\hat{f}(l_{ij}\zeta_j), \hat{f}(l_{ij}\zeta_j)) = \hat{J}(\hat{f}(\zeta_i), \hat{f}(\zeta_i)), \qquad \mathcal{L}(\phi(l_{ij}\zeta_j)) = \mathcal{L}(\phi(\zeta_i)),$$

and that for ϕ_i defined by $\phi_1 = 0$, $\phi_s = \zeta_s\Phi(\zeta_1, (\zeta_2^2 + \zeta_3^2)^{1/2})$ with $s = 2$ or 3,

$$\mathcal{L}(\phi_i(l_{kj}\zeta_j)) = l_{ij}\mathcal{L}(\phi_j(\zeta_k)).$$

That is, $\hat{J}(\Phi(\zeta_1, (\zeta_2^2 + \zeta_3^2)^{1/2}), \Phi(\zeta_1, (\zeta_2^2 + \zeta_3^2)^{1/2}))$, $\mathcal{L}(\Phi(\zeta_1, (\zeta_2^2 + \zeta_3^2)^{1/2}))$, and $\mathcal{L}(\phi_i(\zeta_k))$ are axially symmetric with respect to the ζ_1 axis. Therefore, according to Eq. (A.83) with ($m = 0$, $h = 0$) or ($m = 1$, $h = 1$), the integrals for the two types of functions are of the form

$$\hat{J}(\Phi(\zeta_1,\zeta_\rho), \Phi(\zeta_1,\zeta_\rho)) = F(\zeta_1,\zeta_\rho), \qquad \mathcal{L}(\Phi(\zeta_1,\zeta_\rho)) = F(\zeta_1,\zeta_\rho), \tag{A.202a}$$

$$\mathcal{L}(\zeta_s\Phi(\zeta_1,\zeta_\rho)) = \zeta_s F(\zeta_1,\zeta_\rho) \qquad (s = 2,3), \tag{A.202b}$$

where

$$\zeta_\rho = (\zeta_2^2 + \zeta_3^2)^{1/2}. \tag{A.203}$$

Some examples of the similarity solutions are given here. The label (B, liB) applies to both of Eqs. (A.198a) and (A.199a); the label (liB) applies only to the linearized Boltzmann equation (A.199a).

Case 1 (B, liB): $\Phi(\zeta, \hat{t})$

Take a function of the form

$$\hat{f} = \Phi(\zeta, \hat{t}), \quad \phi = \Phi(\zeta, \hat{t}).$$

Owing to Eq. (A.201), it is easily seen that this form of the distribution function is compatible with Eqs. (A.198a) and (A.199a).

Case 2 (B, liB): $\Phi(x_1, \zeta_1, \zeta_\rho, \hat{t})$

Take a function of the form

$$\hat{f} = \Phi(x_1, \zeta_1, \zeta_\rho, \hat{t}), \quad \phi = \Phi(x_1, \zeta_1, \zeta_\rho, \hat{t}).$$

Owing to Eq. (A.202a), it is easily seen that this form of the distribution function is compatible with Eqs. (A.198a) and (A.199a).

Case 3 (liB): $\zeta_s \Phi(x_1, \zeta_1, \zeta_\rho, \hat{t})$ with $s = 2$ or 3

Take a function of the form

$$\phi = \zeta_s \Phi(x_1, \zeta_1, \zeta_\rho, \hat{t}) \quad (s = 2, 3).$$

Then, streaming part of Eq. (A.199a) is

$$\mathrm{Sh}\frac{\partial \phi}{\partial \hat{t}} + \zeta_i \frac{\partial \phi}{\partial x_i} = \zeta_s \left(\mathrm{Sh}\frac{\partial \Phi}{\partial \hat{t}} + \zeta_1 \frac{\partial \Phi}{\partial x_1} \right).$$

Owing to Eq. (A.202b), the collision integral $\mathcal{L}(\phi)$ can be expressed in the form

$$\mathcal{L}(\phi) = \mathcal{L}(\zeta_s \Phi(x_1, \zeta_1, \zeta_\rho, \hat{t})) = \zeta_s F(x_1, \zeta_1, \zeta_\rho, \hat{t}).$$

Thus, the present form of ϕ is compatible with Eq. (A.199a), i.e.,

$$\mathrm{Sh}\frac{\partial \Phi}{\partial \hat{t}} + \zeta_1 \frac{\partial \Phi}{\partial x_1} = \frac{1}{k} F(x_1, \zeta_1, \zeta_\rho, \hat{t}).$$

Case 4 (liB): $\Phi_c(\hat{r}, \zeta_r, \zeta, \hat{t}) \cos\theta + \zeta_\theta \Phi_s(\hat{r}, \zeta_r, \zeta, \hat{t}) \sin\theta$ (Sone & Aoki [1983])

Take the linearized Boltzmann equation in the spherical coordinate system $(\hat{r}, \theta, \varphi)$, i.e.,

$$\begin{aligned} &\mathrm{Sh}\frac{\partial \phi}{\partial \hat{t}} + \zeta_r \frac{\partial \phi}{\partial \hat{r}} + \frac{\zeta_\theta}{\hat{r}} \frac{\partial \phi}{\partial \theta} + \frac{\zeta_\varphi}{\hat{r} \sin\theta} \frac{\partial \phi}{\partial \varphi} + \frac{\zeta_\theta^2 + \zeta_\varphi^2}{\hat{r}} \frac{\partial \phi}{\partial \zeta_r} \\ &\quad + \left(\frac{\zeta_\varphi^2}{\hat{r}} \cot\theta - \frac{\zeta_r \zeta_\theta}{\hat{r}} \right) \frac{\partial \phi}{\partial \zeta_\theta} - \left(\frac{\zeta_\theta \zeta_\varphi}{\hat{r}} \cot\theta + \frac{\zeta_r \zeta_\varphi}{\hat{r}} \right) \frac{\partial \phi}{\partial \zeta_\varphi} = \frac{1}{k} \mathcal{L}(\phi). \end{aligned} \tag{A.204}$$

We will examine whether the function of the form

$$\phi = \Phi_c(\hat{r}, \zeta_r, \zeta, \hat{t}) \cos\theta + \zeta_\theta \Phi_s(\hat{r}, \zeta_r, \zeta, \hat{t}) \sin\theta, \tag{A.205}$$

where

$$\zeta = (\zeta_r^2 + \zeta_\theta^2 + \zeta_\varphi^2)^{1/2},$$

is compatible with Eq. (A.204). Substituting Eq. (A.205) into the left-hand side of Eq. (A.204), we have

$$\text{the left-hand side } = D_c(\Phi_c, \Phi_s) \cos\theta + \zeta_\theta D_s(\Phi_c, \Phi_s) \sin\theta,$$

where

$$D_c(\Phi_c, \Phi_s) = \mathrm{Sh} \frac{\partial \Phi_c}{\partial \hat{t}} + \zeta_r \frac{\partial \Phi_c}{\partial \hat{r}} + \frac{\zeta^2 - \zeta_r^2}{\hat{r}} \frac{\partial \Phi_c}{\partial \zeta_r} + \frac{\zeta^2 - \zeta_r^2}{\hat{r}} \Phi_s, \tag{A.206a}$$

$$D_s(\Phi_c, \Phi_s) = \mathrm{Sh} \frac{\partial \Phi_s}{\partial \hat{t}} + \zeta_r \frac{\partial \Phi_s}{\partial \hat{r}} + \frac{\zeta^2 - \zeta_r^2}{\hat{r}} \frac{\partial \Phi_s}{\partial \zeta_r} - \frac{\zeta_r}{\hat{r}} \Phi_s - \frac{1}{\hat{r}} \Phi_c. \tag{A.206b}$$

Here, $D_c(\Phi_c, \Phi_s)$ and $D_s(\Phi_c, \Phi_s)$ are functions of $\hat{r}$, ζ_r, ζ, and $\hat{t}$ only.

Substituting Eq. (A.205) into the right-hand side of Eq. (A.204), we have

$$\mathcal{L}(\phi) = \mathcal{L}(\Phi_c) \cos\theta + \mathcal{L}(\zeta_\theta \Phi_s) \sin\theta.$$

Owing to Eqs. (A.202a) and (A.202b), $\mathcal{L}(\Phi_c)$ and $\mathcal{L}(\zeta_\theta \Phi_s)$ can be expressed in the form[39]

$$\mathcal{L}(\Phi_c) = F_c(\hat{r}, \zeta_r, \zeta, \hat{t}), \qquad \mathcal{L}(\zeta_\theta \Phi_s) = \zeta_\theta F_s(\hat{r}, \zeta_r, \zeta, \hat{t}).$$

Therefore, the Boltzmann equation (A.204) is split into two parts, that is,

$$D_c(\Phi_c, \Phi_s) = \frac{1}{k} F_c, \qquad D_s(\Phi_c, \Phi_s) = \frac{1}{k} F_s,$$

where the independent variables are $\hat{r}$, ζ_r, ζ, and $\hat{t}$ only.

For this type of velocity distribution function, the macroscopic variables are

[39] The collision operator $\mathcal{L}(*)$ does not contain the operation with respect to the space and time variables. Thus, the formulas apply to the expression in terms of $(\zeta_r, \zeta_\theta, \zeta_\varphi)$ as well as the Cartesian coordinates ζ_i.

given as[40]

$$
\begin{aligned}
\frac{\omega}{\cos\theta} &= 2\pi\int_0^\infty\int_0^\pi \zeta^2\sin\theta_\zeta\Phi_c E\mathrm{d}\theta_\zeta\mathrm{d}\zeta,\\
\frac{u_r}{\cos\theta} &= \pi\int_0^\infty\int_0^\pi \zeta^3\sin 2\theta_\zeta\Phi_c E\mathrm{d}\theta_\zeta\mathrm{d}\zeta,\\
\frac{u_\theta}{\sin\theta} &= \pi\int_0^\infty\int_0^\pi \zeta^4\sin^3\theta_\zeta\Phi_s E\mathrm{d}\theta_\zeta\mathrm{d}\zeta,\\
\frac{\tau}{\cos\theta} &= 2\pi\int_0^\infty\int_0^\pi \left(\frac{2}{3}\zeta^2-1\right)\zeta^2\sin\theta_\zeta\Phi_c E\mathrm{d}\theta_\zeta\mathrm{d}\zeta,\\
\frac{P_{rr}}{\cos\theta} &= 4\pi\int_0^\infty\int_0^\pi \zeta^4\cos^2\theta_\zeta\sin\theta_\zeta\Phi_c E\mathrm{d}\theta_\zeta\mathrm{d}\zeta,\\
\frac{P_{r\theta}}{\sin\theta} &= 2\pi\int_0^\infty\int_0^\pi \zeta^5\cos\theta_\zeta\sin^3\theta_\zeta\Phi_s E\mathrm{d}\theta_\zeta\mathrm{d}\zeta,\\
\frac{P_{\theta\theta}}{\cos\theta} &= 2\pi\int_0^\infty\int_0^\pi \zeta^4\sin^3\theta_\zeta\Phi_c E\mathrm{d}\theta_\zeta\mathrm{d}\zeta,\\
P_{\varphi\varphi} &= 3(\omega+\tau)-P_{rr}-P_{\theta\theta},\\
\frac{Q_r}{\cos\theta} &= \pi\int_0^\infty\int_0^\pi \left(\zeta^2-\frac{5}{2}\right)\zeta^3\sin 2\theta_\zeta\Phi_c E\mathrm{d}\theta_\zeta\mathrm{d}\zeta,\\
\frac{Q_\theta}{\sin\theta} &= \pi\int_0^\infty\int_0^\pi \left(\zeta^2-\frac{5}{2}\right)\zeta^4\sin^3\theta_\zeta\Phi_s E\mathrm{d}\theta_\zeta\mathrm{d}\zeta,\\
u_\varphi &= P_{r\varphi}=P_{\theta\varphi}=Q_\varphi=0,
\end{aligned}
$$

where the variable θ_ζ is introduced instead of ζ_r by the relation $\zeta_r=\zeta\cos\theta_\zeta$ $(0\le\theta_\zeta\le\pi)$.[41] The integrals on the right-hand sides are functions of $\hat{r}$ and $\hat{t}$.

Case 5 (liB): $x_1\Phi_0(\zeta,\zeta_2,\zeta_3)+\zeta_1\Phi_1(x_2,x_3,\zeta,\zeta_2,\zeta_3)$

Take a function of the form

$$\phi = x_1\Phi_0(\zeta,\zeta_2,\zeta_3)+\zeta_1\Phi_1(x_2,x_3,\zeta,\zeta_2,\zeta_3). \tag{A.207}$$

Substituting Eq. (A.207) into the linearized Boltzmann equation (A.199a), we have

$$\mathcal{L}(\Phi_0(\zeta,\zeta_2,\zeta_3))=0, \tag{A.208a}$$

$$\zeta_2\frac{\partial\Phi_1}{\partial x_2}+\zeta_3\frac{\partial\Phi_1}{\partial x_3}=\frac{1}{k\zeta_1}\mathcal{L}(\zeta_1\Phi_1)-\Phi_0, \tag{A.208b}$$

both of which are compatible. In fact, from Eq. (A.208a),

$$\Phi_0(\zeta_i)=c_0+c_2\zeta_2+c_3\zeta_3+c_4\zeta^2,$$

[40]The definition of the quantities with the subscripts r, θ, or φ is obvious by Footnote 23 in Section 4.5 and the definition (1.74).

[41]See Footnote 22 in Section 4.5.

where c_0, c_2, c_3, and c_4 are arbitrary constants. The parity (even or odd) of $\mathcal{L}(\phi)$ with respect to a component of $\boldsymbol{\zeta}$ agrees with that of ϕ (see Section A.2.7), and therefore, $\mathcal{L}(\zeta_1\Phi_1)/\zeta_1$ is even with respect to ζ_1. Thus, the above form of Φ_1 is compatible with Eq. (A.208b).

A.6 Reduced BKW equation

According to Chu [1965], two components of the molecular velocities in the BKW equation (1.40a) or (1.61) can be eliminated in spatially one-dimensional problems, which is a big simplification. Here, we will explain the process. Take the following one-dimensional BKW equation without an external force ($\hat{F}_i = 0$)[42] in the nondimensional variables introduced in Section 1.9:

$$\mathrm{Sh}\frac{\partial \hat{f}}{\partial \hat{t}} + \zeta_1 \frac{\partial \hat{f}}{\partial x_1} = \frac{1}{k}\hat{\rho}(\hat{f}_e - \hat{f}), \tag{A.209}$$

where x_1 is the nontrivial space variable and

$$\hat{f}_e = \frac{\hat{\rho}}{(\pi\hat{T})^{3/2}} \exp\left(-\frac{(\zeta_i - \hat{v}_i)^2}{\hat{T}}\right), \tag{A.210a}$$

$$k = \frac{\sqrt{\pi}\ell_0}{2L} = \frac{(2RT_0)^{1/2}}{A_c\rho_0 L}, \quad \mathrm{Sh} = \frac{L}{t_0(2RT_0)^{1/2}}. \tag{A.210b}$$

The parameters $\hat{\rho}$, $\hat{v}_i$, and $\hat{T}$ of the local Maxwellian $\hat{f}_e$ is defined with $\hat{f}$ by Eqs. (1.54a)–(1.54c). It may be repeated that ℓ_0 is the mean free path of the gas in the equilibrium state at rest with density ρ_0 and temperature T_0, t_0 is the reference time, and L is the reference length.

Let us introduce the four marginal velocity distribution functions g, g_2, g_3, and h

$$\left.\begin{aligned} &g = \int\int \hat{f}\mathrm{d}\zeta_2\mathrm{d}\zeta_3, \quad g_2 = \int\int \zeta_2\hat{f}\mathrm{d}\zeta_2\mathrm{d}\zeta_3, \quad g_3 = \int\int \zeta_3\hat{f}\mathrm{d}\zeta_2\mathrm{d}\zeta_3, \\ &h = \int\int (\zeta_2^2 + \zeta_3^2)\hat{f}\mathrm{d}\zeta_2\mathrm{d}\zeta_3. \end{aligned}\right\} \tag{A.211}$$

Then,

$$\left.\begin{aligned} &\hat{\rho} = \int g\mathrm{d}\zeta_1, \quad \hat{v}_1 = \frac{1}{\hat{\rho}}\int \zeta_1 g\mathrm{d}\zeta_1, \quad \hat{v}_2 = \frac{1}{\hat{\rho}}\int g_2\mathrm{d}\zeta_1, \quad \hat{v}_3 = \frac{1}{\hat{\rho}}\int g_3\mathrm{d}\zeta_1, \\ &\hat{T} = \frac{2}{3\hat{\rho}}\int [(\zeta_1 - \hat{v}_1)^2 g + h]\mathrm{d}\zeta_1 - \frac{2}{3}(\hat{v}_2^2 + \hat{v}_3^2). \end{aligned}\right\} \tag{A.212}$$

[42] The extension to the case where $\hat{F}_i = (\hat{F}_1, 0, 0)$ and $\hat{F}_1$ is independent of ζ_i is straightforward.

Multiplying the BKW equation (A.209) by 1, ζ_2, ζ_3, or $\zeta_2^2+\zeta_3^2$ and integrating the result over the whole space of (ζ_2,ζ_3), we have

$$\mathrm{Sh}\frac{\partial}{\partial\hat{t}}\begin{bmatrix} g \\ g_2 \\ g_3 \\ h \end{bmatrix} + \zeta_1\frac{\partial}{\partial x_1}\begin{bmatrix} g \\ g_2 \\ g_3 \\ h \end{bmatrix} = \frac{1}{k}\hat{\rho}\begin{bmatrix} G-g \\ \hat{v}_2 G - g_2 \\ \hat{v}_3 G - g_3 \\ H-h \end{bmatrix}, \tag{A.213}$$

$$\begin{aligned}\begin{bmatrix} G \\ H \end{bmatrix} &= \int \begin{bmatrix} 1 \\ \zeta_2^2+\zeta_3^2 \end{bmatrix} \hat{f}_e \mathrm{d}\zeta_2\mathrm{d}\zeta_3 \\ &= \frac{\hat{\rho}}{(\pi\hat{T})^{1/2}}\begin{bmatrix} 1 \\ \hat{T}+\hat{v}_2^2+\hat{v}_3^2 \end{bmatrix}\exp\left(-\frac{(\zeta_1-\hat{v}_1)^2}{\hat{T}}\right).\end{aligned} \tag{A.214}$$

The new functions G and H are the marginal velocity distribution functions g and h corresponding to the Maxwellian $\hat{f}_e$.

The diffuse-reflection condition, Eqs. (1.63a) and (1.63b), with $n_2=n_3=0$, i.e.,

$$\hat{f}(x_1,\zeta_i,\hat{t}) = \frac{\hat{\sigma}_w}{(\pi\hat{T}_w)^{3/2}}\exp\left(-\frac{(\zeta_i-\hat{v}_{wi})^2}{\hat{T}_w}\right) \qquad [(\zeta_1-\hat{v}_{w1})n_1>0], \tag{A.215a}$$

$$\hat{\sigma}_w = -2\left(\frac{\pi}{\hat{T}_w}\right)^{1/2}\int_{(\zeta_1-\hat{v}_{w1})n_1<0}(\zeta_1-\hat{v}_{w1})n_1\hat{f}(x_1,\zeta_i,\hat{t})\mathbf{d\zeta}, \tag{A.215b}$$

is transformed into

$$\begin{bmatrix} g \\ g_2 \\ g_3 \\ h \end{bmatrix} = \frac{\hat{\sigma}_w}{(\pi\hat{T}_w)^{1/2}}\begin{bmatrix} 1 \\ \hat{v}_{w2} \\ \hat{v}_{w3} \\ \hat{T}_w+\hat{v}_{w2}^2+\hat{v}_{w3}^2 \end{bmatrix}\exp\left(-\frac{(\zeta_1-\hat{v}_{w1})^2}{\hat{T}_w}\right) \qquad [(\zeta_1-\hat{v}_{w1})n_1>0], \tag{A.216a}$$

$$\hat{\sigma}_w = -2\left(\frac{\pi}{\hat{T}_w}\right)^{1/2}\int_{(\zeta_1-\hat{v}_{w1})n_1<0}(\zeta_1-\hat{v}_{w1})n_1 g\mathrm{d}\zeta_1. \tag{A.216b}$$

The complete-condensation condition (1.68) with $n_2=n_3=0$, i.e.,

$$\hat{f}(x_1,\zeta_i,\hat{t}) = \frac{\hat{\rho}_w}{(\pi\hat{T}_w)^{3/2}}\exp\left(-\frac{(\zeta_i-\hat{v}_{wi})^2}{\hat{T}_w}\right) \qquad [(\zeta_1-\hat{v}_{w1})n_1>0], \tag{A.217}$$

is transformed into

$$\begin{bmatrix} g \\ g_2 \\ g_3 \\ h \end{bmatrix} = \frac{\hat{\rho}_w}{(\pi\hat{T}_w)^{1/2}}\begin{bmatrix} 1 \\ \hat{v}_{w2} \\ \hat{v}_{w3} \\ \hat{T}_w+\hat{v}_{w2}^2+\hat{v}_{w3}^2 \end{bmatrix}\exp\left(-\frac{(\zeta_1-\hat{v}_{w1})^2}{\hat{T}_w}\right) \qquad [(\zeta_1-\hat{v}_{w1})n_1>0]. \tag{A.218}$$

The initial and boundary-value problem for $\hat{f}$ with the five independent variables x_1, $\hat{t}$, ζ_1, ζ_2, and ζ_3 is reduced to that for the simultaneous system for g, g_2, g_3, and h with the three independent variables x_1, $\hat{t}$, and ζ_1.

When the initial condition satisfies $g_2 = g_3 = 0$ and the boundary data satisfy $\hat{v}_{w2} = \hat{v}_{w3} = 0$, the solution $(g, g_2, g_3, h) = (g, 0, 0, h)$ [thus, $\hat{v}_2 = \hat{v}_3 = 0$] is consistent with the reduced BKW equation (A.213) and the reduced diffuse-reflection condition (A.216a) with (A.216b) or the reduced complete-condensation condition (A.218). Then, the problem is reduced to that for the two marginal velocity distribution functions g and h.

Finally, in two-dimensional problems, where $\partial/\partial x_3 = 0$, the molecular velocity component ζ_3 can be similarly eliminated; further, in the cylindrical problem with the corresponding symmetry as in Sections 6.2 and 6.3, the axial component ξ_z or ζ_z of the molecular velocity can be eliminated in a similar way.

A.7 Maxwell distribution

A.7.1 Equilibrium distribution

We will look for the solution of the Boltzmann equation (1.5) describing an equilibrium state (or a time-independent and spatially uniform state) of the system under no external force ($F_i = 0$). The solution is assumed here to be continuous and positive. For the equilibrium solution f_E, the Boltzmann equation is reduced to

$$\int (f'_E f'_{E*} - f_E f_{E*}) B \mathrm{d}\Omega(\boldsymbol{\alpha}) \mathbf{d}\boldsymbol{\xi}_* = 0. \tag{A.219}$$

Multiplying Eq. (A.219) by $\ln c_0^{-1} f_E$, where c_0 is a nondimensionalizing constant, and integrating the result over the whole space of $\boldsymbol{\xi}$, we have

$$\begin{aligned}
&\int (\ln c_0^{-1} f_E)(f'_E f'_{E*} - f_E f_{E*}) B \mathrm{d}\Omega(\boldsymbol{\alpha}) \mathbf{d}\boldsymbol{\xi}_* \mathbf{d}\boldsymbol{\xi} \\
&\qquad = \frac{1}{4} \int (\ln c_0^{-1} f_E + \ln c_0^{-1} f_{E*} - \ln c_0^{-1} f'_E - \ln c_0^{-1} f'_{E*}) \\
&\qquad\qquad \times (f'_E f'_{E*} - f_E f_{E*}) B \mathrm{d}\Omega(\boldsymbol{\alpha}) \mathbf{d}\boldsymbol{\xi}_* \mathbf{d}\boldsymbol{\xi} \\
&\qquad = \frac{1}{4} \int (f'_E f'_{E*} - f_E f_{E*}) \ln \left(\frac{f_E f_{E*}}{f'_E f'_{E*}} \right) B \mathrm{d}\Omega(\boldsymbol{\alpha}) \mathbf{d}\boldsymbol{\xi}_* \mathbf{d}\boldsymbol{\xi} = 0,
\end{aligned} \tag{A.220}$$

where the symmetry relation (A.36e) is used for the transformation from the first expression to the second. The function B being positive almost everywhere,[43] f_E being positive, and $(x - y)\ln(y/x) \leq 0$, where the equal sign holds at $x = y$, the solution f_E must satisfy the *detailed-balance* condition

$$f'_E f'_{E*} = f_E \, f_{E*}, \tag{A.221}$$

[43] See Footnote 5 in Section 1.2.

from which

$$\ln c_0^{-1} f'_E + \ln c_0^{-1} f'_{E*} = \ln c_0^{-1} f_E + \ln c_0^{-1} f_{E*}, \tag{A.222}$$

for all $\boldsymbol{\xi}$, $\boldsymbol{\xi}_*$, and $\boldsymbol{\alpha}$. That is, $\ln c_0^{-1} f_E$ is a summational invariant of the collision. According to Section A.2.3, its general form is given by

$$\ln c_0^{-1} f_E = \Upsilon_0 + \Upsilon_i \xi_i + \Upsilon_4 \xi_i^2, \tag{A.223a}$$

that is,

$$f_E = (c_0 \exp \Upsilon_0) \exp(\Upsilon_i \xi_i + \Upsilon_4 \xi_i^2), \tag{A.223b}$$

where Υ_0, Υ_i, and Υ_4 are constants. Inversely, if f_E (or $\ln c_0^{-1} f_E$) is given by Eq. (A.223b) [or Eq. (A.223a)], f_E satisfies Eq. (A.219).

The relations between the above five parameters ($c_0 \exp \Upsilon_0$), Υ_i, and Υ_4 and the macroscopic variables ρ, v_i, and T are obtained with the aid of Eqs. (1.2a)–(1.2c) as

$$RT = -\frac{1}{2\Upsilon_4}, \quad v_i = -\frac{\Upsilon_i}{2\Upsilon_4}, \quad \frac{\rho}{(2\pi RT)^{3/2}} = (c_0 \exp \Upsilon_0) \exp\left(-\frac{\Upsilon_i^2}{4\Upsilon_4}\right).$$

With these relations, the velocity distribution function f_E describing an equilibrium state is given by

$$f_E = \frac{\rho}{(2\pi RT)^{3/2}} \exp\left(-\frac{(\xi_i - v_i)^2}{2RT}\right). \tag{A.224}$$

This distribution is called a Maxwell distribution (or Maxwellian), especially a Maxwell distribution at rest if $v_i = 0$.

Obviously from the above derivation, Eq. (A.224) is the unique positive continuous solution of Eq. (A.219) [or the solution of the Boltzmann equation (1.5) with $F_i = 0$ describing an equilibrium state]. If we review the proof, the logarithm $\ln c_0^{-1} f_E$ is first introduced. Thus, unless f_E is positive ($f_E > 0$), we cannot proceed any more. Thus, the positivity condition is required for the proof. A very simple proof that the non-negative continuous function f_E (≥ 0) satisfying $J(f_E, f_E) = 0$ is positive ($f_E > 0$) is given in Sone [1978a]. Thus, the uniqueness of the Maxwellian is extended to the class of non-negative continuous functions. Arkeryd [1972] made an important extension of the uniqueness. He considered the initial-value problem of the Boltzmann equation for spatially homogeneous initial data (or data uniform in $\boldsymbol{X}$). With the aid of the exponential (multiplier) form (A.168) of the Boltzmann equation, he could prove that nonnegativity of the solution f leads to strict positivity everywhere for f at positive time when the initial value is strictly positive on a set of positive measure.[44] He made another extension about the summational invariant explained in the last paragraph of Section A.2.3. Thus, the uniqueness of the Maxwellian is extended

[44]His positivity result in 1972 is only for the space-homogeneous case, but according to Arkeryd (private communication), this is less important because his particular result can be extended, with the same idea of proof (i.e., by inspection of the exponential form), to time and space-dependent cases as well as to time-independent cases.

to the class of locally integrable functions.[45] The extension is essential because the velocity distribution function generally has discontinuities as explained in Section A.2.3.

The Maxwell distribution (A.224) is spherically symmetric with respect to the *peculiar* (or *thermal*) *velocity* C_i $(= \xi_i - v_i)$ of a molecule. Thus, we introduce $f_{\mathrm{Sp}E}$

$$\begin{aligned} f_{\mathrm{Sp}E}\mathrm{d}\mathsf{C} &= \left(\int_0^{2\pi}\int_0^{\pi} f_E \mathsf{C}^2 \sin\theta \mathrm{d}\theta\mathrm{d}\varphi\right)\mathrm{d}\mathsf{C} \\ &= \frac{4\rho}{(2\pi RT)^{1/2}}\left(\frac{\mathsf{C}^2}{2RT}\right)\exp\left(-\frac{\mathsf{C}^2}{2RT}\right)\mathrm{d}\mathsf{C}, \end{aligned} \tag{A.225}$$

where we introduced the spherical coordinate representation of C_i

$$\mathsf{C}_1 = \mathsf{C}\sin\theta\cos\varphi, \quad \mathsf{C}_2 = \mathsf{C}\sin\theta\sin\varphi, \quad \mathsf{C}_3 = \mathsf{C}\cos\theta. \tag{A.226}$$

From Eq. (A.225), the most probable peculiar speed C_{mp}, i.e., the maximum point of $f_{\mathrm{Sp}E}$, the average peculiar speed $\bar{\mathsf{C}}$, and the root mean square $\left(\overline{\mathsf{C}^2}\right)^{1/2}$ of the peculiar speed C for the Maxwell distribution are given as

$$\mathsf{C}_{mp} = (2RT)^{1/2}, \quad \bar{\mathsf{C}} = \frac{2}{\sqrt{\pi}}(2RT)^{1/2}, \quad \left(\overline{\mathsf{C}^2}\right)^{1/2} = \sqrt{\frac{3}{2}}(2RT)^{1/2}. \tag{A.227}$$

The distribution (A.225), together with C_{mp}, $\bar{\mathsf{C}}$, and $\left(\overline{\mathsf{C}^2}\right)^{1/2}$, is shown in Fig. A.5.

Finally, it may be noted that, obviously from the above derivation, the Maxwell distribution (A.224), where ρ, v_i, and T are arbitrary functions of X_i and t, is the unique distribution that makes the collision integral $J(f, f)$ vanish.

A.7.2 Local Maxwell distribution

In the preceding subsection (Section A.7.1), we have found that the velocity distribution function f of the form (A.224) or Maxwellian, irrespective of ρ, v_i, and T being time-independent and spatially uniform or not, is the only distribution function that makes the collision integral of the Boltzmann equation vanish. When it is time-independent and spatially uniform or Υ_0, Υ_i, and Υ_4 in Eq. (A.223b) are constants, the Maxwellian (A.224) or Eq. (A.223b) is the solution of the Boltzmann equation (1.5) without an external force ($F_i = 0$). When ρ, v_i, and T or Υ_0, Υ_i, and Υ_4 are functions of t and/or X_j, the corresponding distribution, which is called a local Maxwell distribution (or local Maxwellian), does not necessarily satisfy the Boltzmann equation (1.5) with $F_i = 0$. Here, we examine the condition that the local Maxwell distribution satisfies the Boltzmann equation with $F_i = 0$ according to Grad [1949].

[45] The functions that differ only on a set of measure zero are identified.

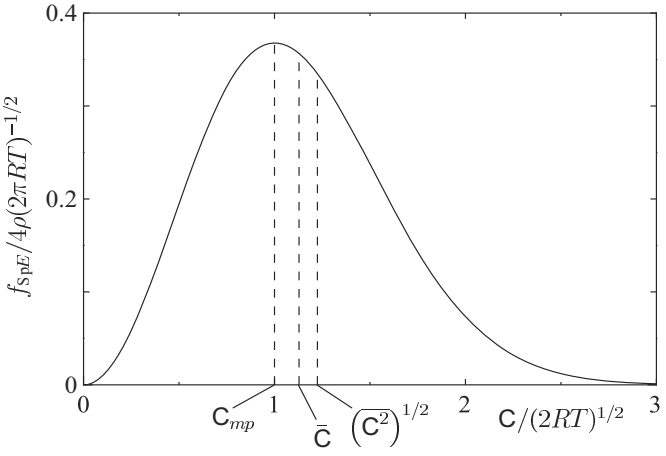

Figure A.5. The distribution f_{SpE} given by Eq. (A.225). The points marked by C_{mp}, $\bar{\mathsf{C}}$, and $\left(\overline{\mathsf{C}^2}\right)^{1/2}$ are, respectively, the points $\mathsf{C}_{mp}/(2RT)^{1/2}$, $\bar{\mathsf{C}}/(2RT)^{1/2}$, and $\left(\overline{\mathsf{C}^2}\right)^{1/2}/(2RT)^{1/2}$.

The local Maxwell distribution f_e is expressed in the same way as the equilibrium distribution (A.223a) in the form

$$\ln c_0^{-1} f_e = \Upsilon_0(\boldsymbol{X}, t) + \Upsilon_i(\boldsymbol{X}, t)\xi_i + \Upsilon_4(\boldsymbol{X}, t)\xi_i^2, \tag{A.228}$$

where c_0 is a nondimensionalizing constant. Noting that $\mathrm{d} \ln c_0^{-1} f_e = \mathrm{d}f_e/f_e$ and that the collision integral vanishes for f_e, i.e., $J(f_e, f_e) = 0$, we find that

$$\frac{\partial \ln c_0^{-1} f_e}{\partial t} + \xi_j \frac{\partial \ln c_0^{-1} f_e}{\partial X_j} = 0. \tag{A.229}$$

The functions $\Upsilon_0(\boldsymbol{X}, t)$, $\Upsilon_i(\boldsymbol{X}, t)$, and $\Upsilon_4(\boldsymbol{X}, t)$ are determined by Eq. (A.229) in the following way.

Substituting Eq. (A.228) into Eq. (A.229), and arranging the same-order terms in ξ_i, we have

$$\frac{\partial \Upsilon_0}{\partial t} = 0, \tag{A.230a}$$

$$\frac{\partial \Upsilon_i}{\partial t} + \frac{\partial \Upsilon_0}{\partial X_i} = 0, \tag{A.230b}$$

$$\delta_{ij} \frac{\partial \Upsilon_4}{\partial t} + \frac{1}{2}\left(\frac{\partial \Upsilon_i}{\partial X_j} + \frac{\partial \Upsilon_j}{\partial X_i}\right) = 0, \tag{A.230c}$$

$$\frac{\partial \Upsilon_4}{\partial X_i} = 0. \tag{A.230d}$$

From Eq. (A.230a), Υ_0 is a function of X_j only, and from Eq. (A.230d), Υ_4 is a function of t only. From Eq. (A.230b) with the former result, Υ_i is linear

with respect to t. Thus, from Eq. (A.230c), Υ_4 is quadratic in t. Differentiating Eq. (A.230c) with respect to X_k, and using Eq. (A.230d), we have

$$\frac{\partial^2 \Upsilon_i}{\partial X_j \partial X_k} + \frac{\partial^2 \Upsilon_j}{\partial X_k \partial X_i} = 0. \tag{A.231}$$

Replacing the set of subscripts (i, j, k) by (j, k, i) or (k, i, j), and assembling these three equations in the way $(i, j, k) + (k, i, j) - (j, k, i)$, we obtain

$$\frac{\partial^2 \Upsilon_i}{\partial X_j \partial X_k} = 0, \tag{A.232}$$

from which Υ_i is linear in X_j. Thus, from Eq. (A.230b), Υ_0 is quadratic in X_j.

To summarize the results up to this point,

$$\left.\begin{aligned} \Upsilon_0 &= a_0 + k_i X_i + \tfrac{1}{2}(\alpha_{ij} + \alpha_{ji}) X_i X_j, \\ \Upsilon_i &= a_i + b_i t + c_{ij} X_j + d_{ij} X_j t, \\ \Upsilon_4 &= a_4 + \beta t + \alpha t^2, \end{aligned}\right\} \tag{A.233}$$

where a_r, k_i, α_{ij}, b_i, c_{ij}, d_{ij}, α, and β are constants. From the above discussion, Eq. (A.233) obviously satisfies Eqs. (A.230a) and (A.230d), but is not guaranteed to satisfy Eqs. (A.230b) and (A.230c). Substituting Eq. (A.233) into Eqs. (A.230b) and (A.230c), we have

$$\left.\begin{aligned} &k_i + (\alpha_{ij} + \alpha_{ji}) X_j + b_i + d_{ij} X_j = 0, \\ &\delta_{ij}(\beta + 2\alpha t) + \tfrac{1}{2}[(c_{ij} + c_{ji}) + (d_{ij} + d_{ji}) t] = 0, \end{aligned}\right\} \tag{A.234}$$

from which we have

$$\left.\begin{aligned} b_i &= -k_i, \\ d_{ij} &= -2\alpha \delta_{ij}, \\ \alpha_{ij} + \alpha_{ji} &= 2\alpha \delta_{ij}, \\ c_{ij} &= \Omega_{ij} - \beta \delta_{ij}, \end{aligned}\right\} \tag{A.235}$$

where Ω_{ij} is an arbitrary antisymmetric constant tensor ($\Omega_{ij} + \Omega_{ji} = 0$).

The general form of a local Maxwell distribution that satisfies the Boltzmann equation (1.5) without an external force F_i is given by Eq. (A.228) where Υ_0, Υ_i, and Υ_4 are in the form

$$\left.\begin{aligned} \Upsilon_0 &= a_0 + k_i X_i + \alpha X_j^2, \\ \Upsilon_i &= a_i - k_i t - (2\alpha t + \beta) X_i + \Omega_{ij} X_j, \\ \Upsilon_4 &= a_4 + \beta t + \alpha t^2, \end{aligned}\right\} \tag{A.236}$$

with arbitrary constants a_r, k_i, α, β, and Ω_{ij} ($\Omega_{ij} + \Omega_{ji} = 0$). The macroscopic variables ρ, v_i, and T in the local Maxwellian

$$f_e = \frac{\rho}{(2\pi RT)^{3/2}} \exp\left(-\frac{(\xi_i - v_i)^2}{2RT}\right) \tag{A.237}$$

that satisfies the Boltzmann equation are given with the aid of Υ_0, Υ_i, and Υ_4 given by Eq. (A.236) as[46]

$$RT = -\frac{1}{2\Upsilon_4}, \quad v_i = -\frac{\Upsilon_i}{2\Upsilon_4}, \quad \frac{\rho}{(2\pi RT)^{3/2}} = c_0 \exp\left(\Upsilon_0 - \frac{\Upsilon_i^2}{4\Upsilon_4}\right). \quad \text{(A.238)}$$

Finally, we will examine the flow field that is described by the local Maxwellian satisfying the Boltzmann equation. It should be noted that the temperature is spatially uniform, irrespective of the parameters included in the solution.

(i) Time-independent and spatially uniform solution ($\alpha = \beta = k_i = \Omega_{ij} = 0$) :

In this case, Υ_0, Υ_i, and Υ_4 are reduced to constants ($\Upsilon_0 = a_0$, $\Upsilon_i = a_i$, $\Upsilon_4 = a_4$). This is the solution given in the preceding subsection (Section A.7.1). This is sometimes called an *absolute Maxwell distribution*.

(ii) Time-independent solution ($\alpha = \beta = k_i = 0$) :

In this case

$$\Upsilon_0 = a_0, \quad \Upsilon_i = a_i + \Omega_{ij} X_j, \quad \Upsilon_4 = a_4.$$

Thus, the gas motion is the superposition of a uniform flow with velocity $-a_i/2a_4$ and a rigid body rotation with angular velocity $\Omega_{ij}\varepsilon_{ijk}/4a_4$, where ε_{ijk} is Eddington's epsilon.[47] The density has a gradient in accordance with the pressure gradient induced by the rigid body rotation.

(iii) $\alpha = \beta = 0$, $k_i \neq 0$:

$$\Upsilon_0 = a_0 + k_i X_i, \quad \Upsilon_i = a_i - k_i t + \Omega_{ij} X_j, \quad \Upsilon_4 = a_4.$$

The difference from the case (ii) is that the uniform flow is time-dependent with density variation in time being induced correspondingly.

(iv) $\alpha \neq 0$ or $\beta \neq 0$:

When $\alpha \neq 0$, β can be eliminated by taking $t + (\beta/2\alpha)$ as new t. Irrespective of $\alpha = 0$ or $\alpha \neq 0$, the gas motion is the superposition of a spatially uniform flow, a rigid body rotation, and a radial flow, where the velocity or angular speed of rotation is time-dependent. The radial flow is an expanding flow if $\alpha < 0$ or ($\alpha = 0$, $\beta < 0$) and a converging flow if $\alpha > 0$ or ($\alpha = 0$, $\beta > 0$). In the latter case, Υ_4 becomes positive at some t, and thus the moments or the macroscopic variables (1.2a)–(1.2g) diverge. The solution is valid only up to this time. In the former case, the solution is valid from some t.

A.8 Mean free path for a Maxwellian

According to the definition in Section 1.5, the mean collision frequency $\bar{\nu}_c$ and the mean free path ℓ are determined by the velocity distribution function f [see Eqs. (1.19) and (1.20)]. We will obtain their expressions for a gas consisting of molecules with their intermolecular force extending only within a finite range d_m

[46] The c_0 can be incorporated into a_0 in Υ_0 by taking $a_0 + \ln c_0$ as new a_0.

[47] See the definition in Footnote 30 in Section 3.1.7.

(e.g., hard-sphere molecules with diameter d_m) when the velocity distribution function is the Maxwellian f_e

$$f_e = \frac{\rho}{(2\pi RT)^{3/2}} \exp\left(-\frac{(\xi_i - v_i)^2}{2RT}\right). \tag{A.239}$$

By definition, the mean collision frequency $\bar{\nu}_c$ is

$$\bar{\nu}_c = \frac{1}{\rho m} \int f(\boldsymbol{\xi}) f(\boldsymbol{\xi}_*) B \mathrm{d}\Omega(\boldsymbol{\alpha}) \mathbf{d}\boldsymbol{\xi}_* \mathbf{d}\boldsymbol{\xi}. \tag{A.240}$$

Noting the relation (A.20), we have

$$\bar{\nu}_c = \frac{d_m^2}{2\rho m} \int_{\text{all } \boldsymbol{e},\ \text{all } \boldsymbol{\xi}_*,\ \text{all } \boldsymbol{\xi}} |(\boldsymbol{\xi}_* - \boldsymbol{\xi}) \cdot \boldsymbol{e}| f(\boldsymbol{\xi}) f(\boldsymbol{\xi}_*) \mathrm{d}\Omega(\boldsymbol{e}) \mathbf{d}\boldsymbol{\xi}_* \mathbf{d}\boldsymbol{\xi}. \tag{A.241}$$

With the new variables

$$x_i = \frac{\xi_i + \xi_{i*} - 2v_i}{2(RT)^{1/2}}, \qquad y_i = \frac{\xi_i - \xi_{i*}}{2(RT)^{1/2}},$$

the product of the Maxwellians $f_e(\boldsymbol{\xi}) f_e(\boldsymbol{\xi}_*)$ is reduced to

$$f_e(\boldsymbol{\xi}) f_e(\boldsymbol{\xi}_*) = \frac{\rho^2}{(2\pi RT)^3} \exp\left(-x_i^2 - y_i^2\right).$$

Then, $\bar{\nu}_c$ for the Maxwellian (A.239) is given by

$$\begin{aligned} \bar{\nu}_c &= \frac{d_m^2 \rho (RT)^{1/2}}{\pi^3 m} \int |y_i e_i| \exp\left(-x_i^2 - y_i^2\right) \mathrm{d}\Omega(\boldsymbol{e}) \mathbf{d}\boldsymbol{x} \mathbf{d}\boldsymbol{y} \\ &= \frac{d_m^2 \rho (RT)^{1/2}}{\pi^{3/2} m} \int |y_i e_i| \exp\left(-y_i^2\right) \mathrm{d}\Omega(\boldsymbol{e}) \mathbf{d}\boldsymbol{y} \\ &= 4 d_m^2 (\pi RT)^{1/2} (\rho/m), \end{aligned} \tag{A.242}$$

where ρ/m is the number density of the molecules. The mean collision frequency $\bar{\nu}_c$ is independent of v_i.

The mean free path is easily obtained by the definition $\ell = \overline{\xi}/\bar{\nu}_c$. For the Maxwellian with $v_i = 0$,

$$\ell = \frac{1}{\sqrt{2}\pi d_m^2 (\rho/m)}, \tag{A.243}$$

because $\overline{\xi} = \overline{\mathsf{C}} = 2(2RT/\pi)^{1/2}$ [see Eq. (A.227)].[48]

[48] A gas consisting of very small hard-sphere molecules (diameter : d_c) with a very weak potential extending to d_m around it has the same mean collision frequency $\bar{\nu}_c$ and the same mean free path ℓ as the gas of a hard-sphere molecule with diameter d_m. The collision effect is quite different for the two gases, or the two gases behave quite differently for the same Knudsen number when $d_c \ll d_m$.

A.9 Kinetic boundary condition in the linearized problem

In this section, we simplify the kinetic boundary conditions (1.64) and (1.69) expressed with the scattering kernels $\hat{K}_B$ and $\hat{K}_I$ for the linearized system. First consider the case where $\hat{v}_{wi}n_i\ (= u_{wi}n_i) = 0$. The boundary condition can be put in the common form

$$\hat{f}(\boldsymbol{x},\boldsymbol{\zeta},\hat{t}) = \hat{g}(\boldsymbol{x},\boldsymbol{\zeta},\hat{t}) + \int_{\zeta_{i*}n_i<0} \hat{K}(\boldsymbol{\zeta},\boldsymbol{\zeta}_*,\boldsymbol{x},\hat{t})\hat{f}(\boldsymbol{x},\boldsymbol{\zeta}_*,\hat{t})\mathbf{d}\boldsymbol{\zeta}_*\ (\zeta_i n_i > 0), \quad \text{(A.244)}$$

where

$$\hat{g} = 0, \quad \hat{K} = \hat{K}_B \quad \text{for a simple boundary,}$$
$$\hat{g} = \hat{g}_I, \ \hat{K} = \hat{K}_I \quad \text{for an interface.}$$

Let $E(1+\phi_{ew})$ be the Maxwellian that is determined by the condition of the boundary. Thus, it satisfies the condition (1.66c) or (1.71c). That is,

$$E(1+\phi_{ew}) = \hat{g} + \int_{\zeta_{i*}n_i<0} \hat{K}E_*(1+\phi_{ew})_*\mathbf{d}\boldsymbol{\zeta}_* \quad (\zeta_i n_i > 0). \quad \text{(A.245)}$$

Hereafter, in this section the subscript $*$ indicates the argument $\boldsymbol{\zeta}_*$. The first-order expression of ϕ_{ew} is

$$\phi_{ew} = \omega_a + 2\zeta_i u_{wi} + \left(\zeta_i^2 - \frac{3}{2}\right)\tau_w,$$

where

$$\omega_a : \text{ arbitrary for a simple boundary,}$$
$$\omega_a = \omega_w \quad \text{for an interface.}$$

Let $\hat{K}$ and $\hat{g}$ at the reference state be, respectively, indicated by $\hat{K}_0\,(\geq 0)$ and $\hat{g}_0\,(\geq 0)$ with the subscript 0 and put $\hat{K} = \hat{K}_0 + \hat{K}_1$ and $\hat{g} = \hat{g}_0 + \hat{g}_1$. The leading order term of Eq. (A.245) is

$$E = \hat{g}_0 + \int_{\zeta_{i*}n_i<0} \hat{K}_0 E_*\mathbf{d}\boldsymbol{\zeta}_* \quad (\zeta_i n_i > 0). \quad \text{(A.246)}$$

That is,

$$E = \int_{\zeta_{i*}n_i<0} \hat{K}_{B0}E_*\mathbf{d}\boldsymbol{\zeta}_* \quad (\zeta_i n_i > 0), \quad \text{(A.247)}$$

$$E = \hat{g}_{I0} + \int_{\zeta_{i*}n_i<0} \hat{K}_{I0}E_*\mathbf{d}\boldsymbol{\zeta}_* \quad (\zeta_i n_i > 0). \quad \text{(A.248)}$$

These are the conditions on $\hat{K}_{B0}$, $\hat{K}_{I0}$, and $\hat{g}_{I0}$.

The boundary condition (A.244) is rewritten as

$$E(1+\phi) = \hat{g}_0 + \hat{g}_1 + \int_{\zeta_{i*}n_i<0} (\hat{K}_0 + \hat{K}_1)E_*(1+\phi)_* \mathbf{d}\boldsymbol{\zeta}_* \quad (\zeta_i n_i > 0). \tag{A.249}$$

Subtracting Eq. (A.245) from Eq. (A.249), and neglecting the second and higher-order terms of the perturbations, we have

$$E(\phi - \phi_{ew}) = \int_{\zeta_{i*}n_i<0} \hat{K}_0(\phi - \phi_{ew})_* E_* \mathbf{d}\boldsymbol{\zeta}_* \quad (\zeta_i n_i > 0). \tag{A.250}$$

That is,

$$\begin{aligned} E(\zeta)\phi(\boldsymbol{\zeta}) = &\left[\omega_a + 2\zeta_i u_{wi} + \left(\zeta_i^2 - \frac{3}{2}\right)\tau_w\right] E(\zeta) \\ &- \int_{\zeta_{i*}n_i<0} \hat{K}_0(\boldsymbol{\zeta}, \boldsymbol{\zeta}_*) \left[\omega_a + 2\zeta_{i*}u_{wi} + \left(\zeta_{i*}^2 - \frac{3}{2}\right)\tau_w\right] E(\zeta_*)\mathbf{d}\boldsymbol{\zeta}_* \\ &+ \int_{\zeta_{i*}n_i<0} \hat{K}_0(\boldsymbol{\zeta}, \boldsymbol{\zeta}_*)\phi(\boldsymbol{\zeta}_*)E(\zeta_*)\mathbf{d}\boldsymbol{\zeta}_* \qquad (\zeta_i n_i > 0). \end{aligned} \tag{A.251}$$

Thus, we have the boundary condition for the linearized system in the case $u_{wi}n_i = 0$ in the following form:
On a simple boundary,

$$\begin{aligned} E(\zeta)\phi(\boldsymbol{\zeta}) = &\left[2\zeta_i u_{wi} + \left(\zeta_i^2 - \frac{3}{2}\right)\tau_w\right] E(\zeta) \\ &- \int_{\zeta_{i*}n_i<0} \hat{K}_{B0}(\boldsymbol{\zeta}, \boldsymbol{\zeta}_*) \left[2\zeta_{i*}u_{wi} + \left(\zeta_{i*}^2 - \frac{3}{2}\right)\tau_w\right] E(\zeta_*)\mathbf{d}\boldsymbol{\zeta}_* \\ &+ \int_{\zeta_{i*}n_i<0} \hat{K}_{B0}(\boldsymbol{\zeta}, \boldsymbol{\zeta}_*)\phi(\boldsymbol{\zeta}_*)E(\zeta_*)\mathbf{d}\boldsymbol{\zeta}_* \quad (\zeta_i n_i > 0), \end{aligned} \tag{A.252}$$

where ω_a terms cancel out owing to Eq. (A.247). Transformation of the conditions (1.66a) and (1.66b) is straightforward, and the condition (1.66c) reduces to Eq. (A.247). The conditions on $\hat{K}_{B0}$ are summarized in the following way if the uniqueness condition attached to Eq. (1.66c) is combined:

(i) $\hat{K}_{B0}(\boldsymbol{\zeta}, \boldsymbol{\zeta}_*) \geq 0 \quad (\zeta_i n_i > 0,\ \zeta_{i*}n_i < 0).$ (A.253a)

(ii) $-\int_{\zeta_i n_i>0} \frac{\zeta_k n_k}{\zeta_{j*}n_j} \hat{K}_{B0}(\boldsymbol{\zeta}, \boldsymbol{\zeta}_*)\mathbf{d}\boldsymbol{\zeta} = 1 \quad (\zeta_{i*}n_i < 0).$ (A.253b)

(iii) Let φ be $\varphi = c_0 + c_i\zeta_i + c_4\zeta_i^2$, where c_0, c_i, and c_4 are independent of $\boldsymbol{\zeta}$. Among this φ, only $\varphi = c_0$ satisfies the relation

$$E(\zeta)\varphi(\boldsymbol{\zeta}) = \int_{\zeta_{i*}n_i<0} \hat{K}_{B0}(\boldsymbol{\zeta}, \boldsymbol{\zeta}_*)\varphi(\boldsymbol{\zeta}_*)E(\zeta_*)\mathbf{d}\boldsymbol{\zeta}_* \quad (\zeta_i n_i > 0). \tag{A.253c}$$

On an interface,

$$E(\zeta)\phi(\boldsymbol{\zeta}) = \left[\omega_w + 2\zeta_i u_{wi} + \left(\zeta_i^2 - \frac{3}{2}\right)\tau_w\right] E(\zeta) - \int_{\zeta_{i*}n_i<0} \hat{K}_{I0}(\boldsymbol{\zeta},\boldsymbol{\zeta}_*)\left[\omega_w + 2\zeta_{i*}u_{wi} + \left(\zeta_{i*}^2 - \frac{3}{2}\right)\tau_w\right] E(\zeta_*)\mathbf{d}\boldsymbol{\zeta}_* + \int_{\zeta_{i*}n_i<0} \hat{K}_{I0}(\boldsymbol{\zeta},\boldsymbol{\zeta}_*)\phi(\boldsymbol{\zeta}_*)E(\zeta_*)\mathbf{d}\boldsymbol{\zeta}_* \qquad (\zeta_i n_i > 0). \tag{A.255}$$

Obviously, transformation of the condition (1.71b) is straightforward and the condition (1.71c) is obviously satisfied because the Maxwellian ϕ_{ew} obviously satisfies Eq. (A.255). The conditions on $\hat{K}_{I0}$ are summarized in the following way if the uniqueness condition attached to Eq. (1.71c) is combined:

(i) $\hat{K}_{I0}(\boldsymbol{\zeta},\boldsymbol{\zeta}_*) \geq 0 \qquad (\zeta_i n_i > 0,\ \zeta_{i*}n_i < 0).$ (A.256b)

(ii-a) $E = \hat{g}_{I0} + \displaystyle\int_{\zeta_{i*}n_i<0} \hat{K}_{I0}(\boldsymbol{\zeta},\boldsymbol{\zeta}_*)E_*\mathbf{d}\boldsymbol{\zeta}_* \quad (\zeta_i n_i > 0);$ (A.256c)

(ii-b) Let φ be $\varphi = c_0 + c_i\zeta_i + c_4\zeta_i^2$, where c_0, c_i, and c_4 are independent of $\boldsymbol{\zeta}$. Among this φ, only $\varphi = 0$ satisfies the relation

$$E(\zeta)\varphi(\boldsymbol{\zeta}) = \int_{\zeta_{i*}n_i<0} \hat{K}_{I0}(\boldsymbol{\zeta},\boldsymbol{\zeta}_*)\varphi(\boldsymbol{\zeta}_*)E(\zeta_*)\mathbf{d}\boldsymbol{\zeta}_* \quad (\zeta_i n_i > 0). \tag{A.256d}$$

The linearized boundary condition is expressed with $\hat{K}_{B0}$ and $\hat{K}_{I0}$, i.e., the kernels at the reference state, in a simple form. In the above formulas, u_{wi} is equivalent to $u_{wi} - u_{wj}n_jn_i$ because the case $u_{wj}n_j = 0$ is considered.

Now, consider the case $u_{wj}n_j \neq 0$. The boundary condition (A.244) is the local relation that is determined by the quantities of the point and time under consideration.[49] Thus, consider it in the coordinate system moving with $u_{wj}n_jn_i$ at the point and time under consideration. The quantities in the new system are indicated by the circle $\circ$ over the corresponding symbol in the original system. Then, $\mathring{u}_{wj}n_j = 0$ in the new system.

$$\mathring{u}_{wj}n_j = 0,\ \ \mathring{\zeta}_i = \zeta_i - u_{wj}n_jn_i,\ \mathring{u}_{wi} = u_{wi} - u_{wj}n_jn_i,\ \mathring{\omega}_a = \omega_a,\ \mathring{\tau}_w = \tau_w,$$
$$E(\mathring{\zeta})[1 + \mathring{\phi}(\mathring{\boldsymbol{\zeta}})] = E(\zeta)[1 + \phi(\boldsymbol{\zeta})],\ \ E(\mathring{\zeta})[1 + \mathring{\phi}_{ew}(\mathring{\boldsymbol{\zeta}})] = E(\zeta)[1 + \phi_{ew}(\boldsymbol{\zeta})],$$
$$\mathring{\zeta}_i n_i = (\zeta_i - u_{wj}n_jn_i)n_i = (\zeta_i - u_{wi})n_i.$$

The Maxwellian $E(\mathring{\zeta})$ is at rest in the new system or $E(\zeta)$ is an expression for the Gaussian of its argument. Thus, $\mathring{\phi}(\mathring{\boldsymbol{\zeta}}) \neq \phi(\boldsymbol{\zeta})$. The second-order quantities

[49] See Footnote 14 in Section 1.6.1.

being neglected,

$$
\begin{aligned}
&E(\mathring{\zeta}) = E(\zeta)(1+2\zeta_i u_{wj} n_j n_i), \quad \mathring{\phi}(\mathring{\boldsymbol{\zeta}}) = \phi(\boldsymbol{\zeta}) - 2\zeta_i u_{wj} n_j n_i,\\
&\mathring{\zeta}_i \mathring{u}_{wi} = \zeta_i (u_{wi} - u_{wj} n_j n_i), \qquad \mathring{\zeta}_i^2 \mathring{\tau}_w = \zeta_i^2 \tau_w,\\
&\mathring{\phi}_{ew}(\mathring{\boldsymbol{\zeta}}) = \phi_{ew}(\boldsymbol{\zeta}) - 2\zeta_i u_{wj} n_j n_i = \omega_a + 2\zeta_i u_{wi} + \left(\zeta_i^2 - \tfrac{3}{2}\right)\tau_w - 2\zeta_i u_{wj} n_j n_i,\\
&\mathring{\phi}(\mathring{\boldsymbol{\zeta}}) - \mathring{\phi}_{ew}(\mathring{\boldsymbol{\zeta}}) = \phi(\boldsymbol{\zeta}) - \phi_{ew}(\boldsymbol{\zeta}).
\end{aligned}
$$

On a boundary where $\mathring{u}_{wj} n_j = 0$, Eq. (A.250) or (A.251) or Eqs. (A.252) and (A.255) can be applied with the circle $\circ$ over a letter. That is,

$$
E(\mathring{\zeta})[\mathring{\phi}(\mathring{\boldsymbol{\zeta}}) - \mathring{\phi}_{ew}(\mathring{\boldsymbol{\zeta}})] = \int_{\mathring{\zeta}_{i*} n_i < 0} \hat{K}_0(\mathring{\boldsymbol{\zeta}}, \mathring{\boldsymbol{\zeta}}_*)[\mathring{\phi}(\mathring{\boldsymbol{\zeta}}_*) - \mathring{\phi}_{ew}(\mathring{\boldsymbol{\zeta}}_*)] E(\mathring{\zeta}_*) \mathbf{d}\mathring{\boldsymbol{\zeta}}_* \quad (\mathring{\zeta}_i n_i > 0), \tag{A.257}
$$

where ω_a in $\mathring{\phi}_{ew}$ can be put zero without loss of generality for a simple boundary. Using the relation shown above and changing the variable of integration from $\mathring{\boldsymbol{\zeta}}_*$ to $\boldsymbol{\zeta}_*$, we have

$$
E(\zeta)[\phi(\boldsymbol{\zeta}) - \phi_{ew}(\boldsymbol{\zeta})] = \int_{(\zeta_{i*} - u_{wi}) n_i < 0} \hat{K}_0(\mathring{\boldsymbol{\zeta}}, \mathring{\boldsymbol{\zeta}}_*)[\phi(\boldsymbol{\zeta}_*) - \phi_{ew}(\boldsymbol{\zeta}_*)] E(\zeta_*) \mathbf{d}\boldsymbol{\zeta}_* \qquad [(\zeta_i - u_{wi}) n_i > 0]. \tag{A.258}
$$

Let the kernel $\hat{K}_0(\mathring{\boldsymbol{\zeta}}, \mathring{\boldsymbol{\zeta}}_*)$ be a sufficiently well-behaved function. In Eq. (A.258), if we shift the arguments $(\mathring{\boldsymbol{\zeta}}, \mathring{\boldsymbol{\zeta}}_*)$ of the kernel $\hat{K}_0$ to $(\boldsymbol{\zeta}, \boldsymbol{\zeta}_*)$, the difference between the kernels $\hat{K}_0(\mathring{\boldsymbol{\zeta}}, \mathring{\boldsymbol{\zeta}}_*)$ and $\hat{K}_0(\boldsymbol{\zeta}, \boldsymbol{\zeta}_*)$ is small in most of the region, but there appears a small region, i.e., $u_{wi} n_i < \zeta_i n_i < 0$ or $0 < \zeta_{i*} n_i < u_{wi} n_i$ depending on $u_{wi} n_i < 0$ or $u_{wi} n_i > 0$, where $\hat{K}_0(\boldsymbol{\zeta}, \boldsymbol{\zeta}_*)$ is undefined. Extending the kernel properly, especially in the $\boldsymbol{\zeta}$ side for $u_{wi} n_i < 0$,[50] we can control the error within the higher order. Thus, we have

$$
E(\zeta)[\phi(\boldsymbol{\zeta}) - \phi_{ew}(\boldsymbol{\zeta})] = \int_{(\zeta_{i*} - u_{wi}) n_i < 0} \hat{K}_0(\boldsymbol{\zeta}, \boldsymbol{\zeta}_*)[\phi(\boldsymbol{\zeta}_*) - \phi_{ew}(\boldsymbol{\zeta}_*)] E(\zeta_*) \mathbf{d}\boldsymbol{\zeta}_* \qquad [(\zeta_i - u_{wi}) n_i > 0]. \tag{A.259}
$$

On a simple boundary,

$$
\begin{aligned}
E(\zeta)\phi(\boldsymbol{\zeta}) = {} & \left[2\zeta_i u_{wi} + \left(\zeta_i^2 - \frac{3}{2}\right)\tau_w\right] E(\zeta)\\
& - \int_{(\zeta_{i*} - u_{wi}) n_i < 0} \hat{K}_{B0}(\boldsymbol{\zeta}, \boldsymbol{\zeta}_*) \left[2\zeta_{i*} u_{wi} + \left(\zeta_{i*}^2 - \frac{3}{2}\right)\tau_w\right] E(\zeta_*) \mathbf{d}\boldsymbol{\zeta}_*\\
& + \int_{(\zeta_{i*} - u_{wi}) n_i < 0} \hat{K}_{B0}(\boldsymbol{\zeta}, \boldsymbol{\zeta}_*) \phi(\boldsymbol{\zeta}_*) E(\zeta_*) \mathbf{d}\boldsymbol{\zeta}_* \quad [(\zeta_i - u_{wi}) n_i > 0].
\end{aligned} \tag{A.260}
$$

[50] For $u_{wi} n_i > 0$, the error is of higher order if we put $\hat{K}_0(\boldsymbol{\zeta}, \boldsymbol{\zeta}_*) = 0$ where it is not defined in the $\boldsymbol{\zeta}_*$ side.

On an interface,

$$E(\zeta)\phi(\boldsymbol{\zeta}) = \left[\omega_w + 2\zeta_i u_{wi} + \left(\zeta_i^2 - \frac{3}{2}\right)\tau_w\right] E(\zeta) - \int_{(\zeta_{i*}-u_{wi})n_i<0} \hat{K}_{I0}(\boldsymbol{\zeta},\boldsymbol{\zeta}_*)\left[\omega_w + 2\zeta_{i*}u_{wi} + \left(\zeta_{i*}^2 - \frac{3}{2}\right)\tau_w\right] E(\zeta_*)\mathbf{d}\boldsymbol{\zeta}_* + \int_{(\zeta_{i*}-u_{wi})n_i<0} \hat{K}_{I0}(\boldsymbol{\zeta},\boldsymbol{\zeta}_*)\phi(\boldsymbol{\zeta}_*)E(\zeta_*)\mathbf{d}\boldsymbol{\zeta}_* \quad [(\zeta_i - u_{wi})n_i > 0]. \quad \text{(A.261)}$$

In Eqs. (A.259)–(A.261), the apparent differences from Eqs. (A.251), (A.252), and (A.255) are the range of integration and that of definition of $\phi(\boldsymbol{\zeta})$ on the left-hand side.

In the above discussion, we used the conditions (1.66c) and (1.71c) with the attached uniqueness conditions and carried out a perturbation analysis. Thus, the above formulas cannot be applied to the specular-reflection condition and the kernel of singular type such as a kernel containing the specular-reflection part.

In this occasion, it may be in order to comment on the linearized system. From the discussion in the next two paragraphs, the linearized system should be taken as an independent system and be clearly posed when one poses the system.

The linearization is carried out formally neglecting the higher-order terms of formal expansion. It is not a rigorous mathematical process assuring that the linearized system really approximates the original system, that is, the solution of the linearized equation does not necessarily approximate the solution of the original nonlinear equation when the parameter of the basis of linearization is small. In fact, the solution of the linearized Boltzmann equation is insufficient to describe the weak condensation of the half-space problem discussed in Section 7.2, however small the rate of condensation and the other perturbed variables from a uniform equilibrium state may be.

The range $(\zeta_i - u_{wi})n_i \gtrless 0$ differs from $\zeta_i n_i \gtrless 0$ only by small amount $u_{wi}n_i$. For a smooth function, the shift of its variables by a small amount modifies its value only by a small amount of the same order. For a discontinuous function, like the velocity distribution function, especially on a boundary, as noted in Section 3.1.6, the difference is a finite amount in a narrow range of the order of the shift in a neighborhood of the discontinuity. How this difference is taken depends on the norm[51] that we choose for expressing the difference of two functions. In a boundary-value problem of the Boltzmann system, the simplification to shift the range by a small amount, e.g., from $(\zeta_i - u_{wi})n_i \gtrless 0$ to $\zeta_i n_i \gtrless 0$, can be considered. This is to be discussed with the choice of the norm; the error estimate requires detailed mathematical argument.

[51] Its exact definition being put aside, the norm of a function $g(\boldsymbol{x})$ in the domain D is defined by $\max_{\boldsymbol{x}\in D}|g|$, $\left(\int_D g^2 \mathbf{d}\boldsymbol{x}\right)^{1/2}$, etc.

A.10 Darrozes–Guiraud inequality

Darrozes & Guiraud [1966] proved an inequality on an integral of a function f satisfying the boundary condition (1.26) on a simple boundary. The *Darrozes–Guiraud inequality* is expressed as

$$\int_{\text{all } \boldsymbol{\xi}} (\xi_i - v_{wi}) n_i f(\boldsymbol{\xi}) \ln[f(\boldsymbol{\xi})/c_0] \mathbf{d}\boldsymbol{\xi} \le \int_{\text{all } \boldsymbol{\xi}} (\xi_i - v_{wi}) n_i f(\boldsymbol{\xi}) \ln[f_0(\boldsymbol{\xi})/c_0] \mathbf{d}\boldsymbol{\xi}. \tag{A.262}$$

Here,
(i) f satisfies the boundary condition (1.26), i.e.,

$$f(\boldsymbol{X}, \boldsymbol{\xi}, t) = \int_{(\xi_{i*} - v_{wi}) n_i < 0} K_B(\boldsymbol{\xi}, \boldsymbol{\xi}_*, \boldsymbol{X}, t) f(\boldsymbol{X}, \boldsymbol{\xi}_*, t) \mathbf{d}\boldsymbol{\xi}_* \quad [(\xi_i - v_{wi}) n_i > 0], \tag{A.263}$$

where K_B satisfies the conditions (1.27a)–(1.27c).
(ii) f_0 is the Maxwellian determined by the temperature and velocity of the boundary, that is,

$$f_0(\boldsymbol{\xi}) = \frac{\rho_0}{(2\pi R T_w)^{3/2}} \exp\left(-\frac{(\xi_i - v_{wi})^2}{2RT_w} \right), \tag{A.264}$$

with arbitrary ρ_0.
(iii) c_0 is a constant to make the arguments f/c_0 and f_0/c_0 of the $\ln(*)$ function dimensionless.
The equality of the relation (A.262) holds when and only when $f(\boldsymbol{\xi})/f_0(\boldsymbol{\xi})$ is independent of $\boldsymbol{\xi}$.

We will show its derivation (see also Cercignani [1988]). The inequality is proved with the aid of the Jensen inequality (Jensen [1906], see also Parzen [1960], Rudin [1987], or Lieb & Loss [2001])

$$F\left(\int \phi\psi \mathbf{d}\boldsymbol{\xi} \Big/ \int \psi \mathbf{d}\boldsymbol{\xi} \right) \le \int \psi F(\phi) \mathbf{d}\boldsymbol{\xi} \Big/ \int \psi \mathbf{d}\boldsymbol{\xi} \qquad (\psi \ge 0), \tag{A.265}$$

where $F(x)$ is a strictly convex function, ϕ and ψ ($\psi \ge 0$) are arbitrary functions of $\boldsymbol{\xi}$, and the equality sign holds when and only when ϕ is independent of $\boldsymbol{\xi}$.[52]

[52](i) The *strictly convex function* $F(x)$ in the interval $a \le x \le b$ is defined by the function $F(x)$ that satisfies the relation

$$F(c_1 x_1 + c_2 x_2) < c_1 F(x_1) + c_2 F(x_2),$$

for arbitrary x_1 and x_2 ($x_1 \ne x_2$) in the interval and for positive c_1 and c_2 satisfying $c_1 + c_2 = 1$.

(ii) Rough derivation of the Jensen inequality: By successive application of the above relation, we have

$$F\left(\sum_{m=1}^{n} c_m x_m \right) \le \sum_{m=1}^{n} c_m F(x_m) \quad \left(\sum_{m=1}^{n} c_m = 1,\ c_m \ge 0 \right),$$

where equality holds only when $x_1 = x_2 = \cdots = x_n$ or $c_m = 1$ for some m. With the correspondence $(c_1, c_2, \cdots, c_n) \to \psi \mathbf{d}\boldsymbol{\xi} / \int \psi \mathbf{d}\boldsymbol{\xi}$ and $(x_1, x_2, \cdots, x_n) \to \phi$, the Jensen inequality is obtained by taking the limiting process $n \to \infty$. See Lieb & Loss [2001] for the proof of the equality condition.

Let $F(x)$ be a convex function and consider the function $F(f(\boldsymbol{\xi})/f_0(\boldsymbol{\xi}))$. The function is expressed in another way with the aid of Eq. (A.263), i.e.,

$$F(f(\boldsymbol{\xi})/f_0(\boldsymbol{\xi})) = F\left(\int_{(\xi_{i*}-v_{wi})n_i<0} \frac{K_B(\boldsymbol{\xi},\boldsymbol{\xi}_*)f(\boldsymbol{\xi}_*)}{f_0(\boldsymbol{\xi})}\mathbf{d}\boldsymbol{\xi}_*\right) \quad [(\xi_i - v_{wi})n_i > 0].$$

Now apply the Jensen inequality to the function on the right-hand side. Here we choose $\phi(\boldsymbol{\xi}_*)$ and $\psi(\boldsymbol{\xi}_*)$ as

$$\phi(\boldsymbol{\xi}_*) = \frac{f(\boldsymbol{\xi}_*)}{f_0(\boldsymbol{\xi}_*)},$$

$$\psi(\boldsymbol{\xi}_*) = \frac{K_B(\boldsymbol{\xi},\boldsymbol{\xi}_*)f_0(\boldsymbol{\xi}_*)}{f_0(\boldsymbol{\xi})} \geq 0 \quad [(\xi_i - v_{wi})n_i > 0, \quad (\xi_{i*} - v_{wi})n_i < 0].$$

It should be noted here that $\phi(\boldsymbol{\xi}_*)$ is defined for the whole range of $\boldsymbol{\xi}_*$ and that $\psi(\boldsymbol{\xi}_*)$ satisfies the relation

$$\int_{(\xi_{i*}-v_{wi})n_i<0} \psi(\boldsymbol{\xi}_*)\mathbf{d}\boldsymbol{\xi}_* = 1 \quad [(\xi_i - v_{wi})n_i > 0] \quad [\text{see Eq. (1.27c)}].$$

With the above preparation, the Jensen inequality is applied as

$$\begin{aligned} F(f(\boldsymbol{\xi})/f_0(\boldsymbol{\xi})) &= F\left(\int_{(\xi_{i*}-v_{wi})n_i<0} \frac{K_B(\boldsymbol{\xi},\boldsymbol{\xi}_*)f_0(\boldsymbol{\xi}_*)}{f_0(\boldsymbol{\xi})}\frac{f(\boldsymbol{\xi}_*)}{f_0(\boldsymbol{\xi}_*)}\mathbf{d}\boldsymbol{\xi}_*\right) \\ &\leq \int_{(\xi_{i*}-v_{wi})n_i<0} \frac{K_B(\boldsymbol{\xi},\boldsymbol{\xi}_*)f_0(\boldsymbol{\xi}_*)}{f_0(\boldsymbol{\xi})} F\left(\frac{f(\boldsymbol{\xi}_*)}{f_0(\boldsymbol{\xi}_*)}\right)\mathbf{d}\boldsymbol{\xi}_* \\ &\qquad [(\xi_i - v_{wi})n_i > 0], \quad \text{(A.266)} \end{aligned}$$

where the equality sign holds when and only when $\phi(\boldsymbol{\xi})$ is independent of $\boldsymbol{\xi}$, that is, $f(\boldsymbol{\xi}) = cf_0(\boldsymbol{\xi})$ (c : a constant). Multiplying the inequality (A.266) by $(\xi_i - v_{wi})n_i f_0(\boldsymbol{\xi})$ and integrating with respect to $\boldsymbol{\xi}$ over $0 < (\xi_i - v_{wi})n_i < \infty$, we have

$$\begin{aligned} &\int_{(\xi_i-v_{wi})n_i>0} (\xi_i - v_{wi})n_i f_0(\boldsymbol{\xi})\, F\left(\frac{f(\boldsymbol{\xi})}{f_0(\boldsymbol{\xi})}\right)\mathbf{d}\boldsymbol{\xi} \\ &\leq \int_{(\xi_i-v_{wi})n_i>0} (\xi_i - v_{wi})n_i f_0(\boldsymbol{\xi}) \int_{(\xi_{i*}-v_{wi})n_i<0} \frac{K_B(\boldsymbol{\xi},\boldsymbol{\xi}_*)f_0(\boldsymbol{\xi}_*)}{f_0(\boldsymbol{\xi})} F\left(\frac{f(\boldsymbol{\xi}_*)}{f_0(\boldsymbol{\xi}_*)}\right)\mathbf{d}\boldsymbol{\xi}_*\mathbf{d}\boldsymbol{\xi} \\ &= \int_{(\xi_{i*}-v_{wi})n_i<0} f_0(\boldsymbol{\xi}_*)\, F\left(\frac{f(\boldsymbol{\xi}_*)}{f_0(\boldsymbol{\xi}_*)}\right) \int_{(\xi_i-v_{wi})n_i>0} (\xi_i - v_{wi})n_i K_B(\boldsymbol{\xi},\boldsymbol{\xi}_*)\mathbf{d}\boldsymbol{\xi}\mathbf{d}\boldsymbol{\xi}_* \\ &= -\int_{(\xi_{i*}-v_{wi})n_i<0} (\xi_{i*} - v_{wi})n_i f_0(\boldsymbol{\xi}_*)\, F\left(\frac{f(\boldsymbol{\xi}_*)}{f_0(\boldsymbol{\xi}_*)}\right)\mathbf{d}\boldsymbol{\xi}_*, \end{aligned}$$

where Eq. (1.27b) is used in the last transformation. From the first and the last expressions of the above relations,

$$\int_{\text{all } \boldsymbol{\xi}} (\xi_i - v_{wi})n_i f_0(\boldsymbol{\xi})\, F\left(\frac{f(\boldsymbol{\xi})}{f_0(\boldsymbol{\xi})}\right)\mathbf{d}\boldsymbol{\xi} \leq 0. \quad \text{(A.267)}$$

Choosing $\phi \ln \phi$ as $F(\phi)$ here, we obtain the Darrozes–Guiraud inequality

$$\int_{\text{all } \boldsymbol{\xi}} (\xi_i - v_{wi}) n_i f(\boldsymbol{\xi}) \ln[f(\boldsymbol{\xi})/c_0] \mathbf{d}\boldsymbol{\xi} \leq \int_{\text{all } \boldsymbol{\xi}} (\xi_i - v_{wi}) n_i f(\boldsymbol{\xi}) \ln[f_0(\boldsymbol{\xi})/c_0] \mathbf{d}\boldsymbol{\xi}.$$

In view of Eq. (A.264), the expression on the right-hand side is rewritten as

$$\int_{\text{all } \boldsymbol{\xi}} (\xi_i - v_{wi}) n_i f(\boldsymbol{\xi}) \ln[f_0(\boldsymbol{\xi})/c_0] \mathbf{d}\boldsymbol{\xi} = -\frac{1}{RT_w} [p_{ij}(v_j - v_{wj}) n_i + q_i n_i].$$

On the other hand, by definition (see Section 1.7),

$$\int_{\text{all } \boldsymbol{\xi}} (\xi_i - v_{wi}) n_i f(\boldsymbol{\xi}) \ln[f(\boldsymbol{\xi})/c_0] \mathbf{d}\boldsymbol{\xi} = (H_i - H v_{wi}) n_i.$$

Therefore,

$$(H_i - H v_{wi}) n_i \leq -\frac{1}{RT_w} [p_{ij}(v_j - v_{wj}) n_i + q_i n_i]. \tag{A.268}$$

Similarly, we can prove the following inequality used in Sections 4.4 and A.12:

$$\int \zeta_i n_i \phi^2 E \mathbf{d}\boldsymbol{\zeta} \leq 0 \quad \text{on a boundary}, \tag{A.269}$$

for the boundary condition (A.252) with $u_{wi} = 0$ and $\tau_w = 0$,[53] and for the condition (A.255) with $\omega_w = 0$, $u_{wi} = 0$, and $\tau_w = 0$, i.e.,

$$E(\zeta)\phi(\boldsymbol{\zeta}) = \int_{\zeta_{i*} n_i < 0} \hat{K}_0(\boldsymbol{\zeta}, \boldsymbol{\zeta}_*) \phi(\boldsymbol{\zeta}_*) E(\zeta_*) \mathbf{d}\boldsymbol{\zeta}_* \quad (\zeta_i n_i > 0), \tag{A.270}$$

where $\hat{K}_0 = \hat{K}_{B0}$ for the condition (A.252), and $\hat{K}_0 = \hat{K}_{I0}$ for the condition (A.255). The inequality (A.269) for the condition (A.252) is the linearized-boundary-condition version of the Darrozes–Guiraud inequality (A.262) for a boundary at rest. Here, we impose the following condition[54] on $\hat{K}_{I0}$ in addition to (i), (ii-a), and (ii-b) after Eq. (A.255):

$$-\int_{\zeta_i n_i > 0} \frac{\zeta_k n_k}{\zeta_{j*} n_j} \hat{K}_{I0}(\boldsymbol{\zeta}, \boldsymbol{\zeta}_*) \mathbf{d}\boldsymbol{\zeta} \leq 1 \quad (\zeta_{i*} n_i < 0). \tag{A.271}$$

We transform the integral $\int_{\zeta_i n_i > 0} \zeta_i n_i \phi^2 E \mathbf{d}\boldsymbol{\zeta}$ in the following way, the ex-

[53] This means that the reference temperature T_0 coincides with the temperature T_w on the point of the boundary under consideration.

[54] The condition requires that all the molecules with a given molecular velocity $\boldsymbol{\zeta}_*$ impinging on the boundary do not reflect on the boundary and that some of them are trapped there [note the discussion on the condition (1.27b) in Footnote 13 in Section 1.6.1].

planation of which is given after the equation:

$$\begin{aligned}
\int_{\zeta_i n_i>0} \zeta_i n_i \phi^2 E \mathbf{d}\boldsymbol{\zeta} &= \int_{\zeta_i n_i>0} \left(\int_{\zeta_{i*} n_i<0} \frac{\hat{K}_0(\boldsymbol{\zeta},\boldsymbol{\zeta}_*) E(\zeta_*)}{E(\zeta)} \phi(\boldsymbol{\zeta}_*) \mathbf{d}\boldsymbol{\zeta}_* \right)^2 \zeta_i n_i E(\zeta) \mathbf{d}\boldsymbol{\zeta} \\
&\le \int_{\zeta_i n_i>0} \left(\int_{\zeta_{i*} n_i<0} \frac{\hat{K}_0(\boldsymbol{\zeta},\boldsymbol{\zeta}_*) E(\zeta_*)}{E(\zeta)} \phi^2(\boldsymbol{\zeta}_*) \mathbf{d}\boldsymbol{\zeta}_* \right) c_1(\boldsymbol{\zeta}) \zeta_i n_i E(\zeta) \mathbf{d}\boldsymbol{\zeta} \\
&= \int_{\zeta_{i*} n_i<0} \zeta_{i*} n_i \phi^2(\boldsymbol{\zeta}_*) E(\zeta_*) \left(\int_{\zeta_i n_i>0} \frac{\hat{K}_0(\boldsymbol{\zeta},\boldsymbol{\zeta}_*)}{\zeta_{k*} n_k} c_1(\boldsymbol{\zeta}) \zeta_i n_i \mathbf{d}\boldsymbol{\zeta} \right) \mathbf{d}\boldsymbol{\zeta}_* \\
&= -\int_{\zeta_{i*} n_i<0} c_2(\boldsymbol{\zeta}_*) \zeta_{i*} n_i \phi^2(\boldsymbol{\zeta}_*) E(\zeta_*) \mathbf{d}\boldsymbol{\zeta}_* \\
&\le -\int_{\zeta_{i*} n_i<0} \zeta_{i*} n_i \phi^2(\boldsymbol{\zeta}_*) E(\zeta_*) \mathbf{d}\boldsymbol{\zeta}_*, \qquad \text{(A.272)}
\end{aligned}$$

where

$$\begin{aligned}
c_1(\boldsymbol{\zeta}) &= \int_{\zeta_{i*} n_i<0} \frac{\hat{K}_0(\boldsymbol{\zeta},\boldsymbol{\zeta}_*) E(\zeta_*)}{E(\zeta)} \mathbf{d}\boldsymbol{\zeta}_* \quad (\zeta_i n_i > 0), \\
c_2(\boldsymbol{\zeta}_*) &= -\int_{\zeta_i n_i>0} \frac{\hat{K}_0(\boldsymbol{\zeta},\boldsymbol{\zeta}_*)}{\zeta_{k*} n_k} c_1(\boldsymbol{\zeta}) \zeta_i n_i \mathbf{d}\boldsymbol{\zeta} \quad (\zeta_{i*} n_i < 0).
\end{aligned}$$

In the above process of transformation, (i) the boundary condition (A.270) is used in the first line; (ii) the Jensen inequality (A.265) is applied from the first to the second line with the replacement: after the change of notation $\boldsymbol{\xi} \to \boldsymbol{\zeta}_*$, the substitutions

$$\phi(\boldsymbol{\zeta}_*) = \phi(\boldsymbol{\zeta}_*), \quad \psi(\boldsymbol{\zeta}_*) = \frac{\hat{K}_0(\boldsymbol{\zeta},\boldsymbol{\zeta}_*) E(\zeta_*)}{E(\zeta)}, \quad F(x) = x^2,$$

are made in the Jensen inequality (A.265); (iii) the order of integration is interchanged from the second to the third line; and (iv) the last inequality results from the following bounds of $c_1(\boldsymbol{\zeta})$ and $c_2(\boldsymbol{\zeta}_*)$:

$$\begin{aligned}
&c_1(\boldsymbol{\zeta}) = 1 \ \text{ for } \hat{K}_0 = \hat{K}_{B0}, \\
&0 \le c_1(\boldsymbol{\zeta}) \le 1 \ \text{ for } \hat{K}_0 = \hat{K}_{I0},
\end{aligned}$$

which are derived from Eqs. (A.247) and (A.248), and

$$\begin{aligned}
&c_2(\boldsymbol{\zeta}_*) = 1 \ \text{ for } \hat{K}_0 = \hat{K}_{B0}, \\
&0 \le c_2(\boldsymbol{\zeta}_*) \le 1 \ \text{ for } \hat{K}_0 = \hat{K}_{I0},
\end{aligned}$$

which are derived from Eqs. (A.253b) and (A.271) together with the above inequalities for $c_1(\boldsymbol{\zeta})$. Then, from Eq. (A.272), we have

$$\int \zeta_i n_i \phi^2 E \mathbf{d}\boldsymbol{\zeta} \le 0.$$

A.11 Equation for Knudsen layer

The equations for $\hat{f}_{Km}$ of the Knudsen-layer correction in Sections 3.3, 3.4, and 9.2.2 are given in the forms

$$\zeta_i n_i \frac{\partial \hat{f}_{Km}}{\partial \eta} = 2\hat{J}((\hat{f}_{SB0})_0, \hat{f}_{Km}) + \mathrm{Ihk}_m, \tag{A.273a}$$

$$\zeta_i n_i \frac{\partial \hat{f}_{Km}}{\partial \eta} = 2\hat{J}((\hat{f}_{V0})_0, \hat{f}_{Km}) + \mathrm{Ihk}_m, \tag{A.273b}$$

$$\zeta_y \frac{\partial \hat{f}_{K1}}{\partial \eta} = 2\hat{J}((\hat{f}_{\mathfrak{S}0})_0, \hat{f}_{K1}), \tag{A.273c}$$

where Ihk_m (especially, $\mathrm{Ihk}_1 = 0$) represents the inhomogeneous term that decays rapidly (faster than any inverse power of η). These three quasi-one-dimensional equations, where the coordinates in the surface $\eta = \text{const}$ enter as parameters, are reduced to the same type of equation in the following way.

Introduce the new variables $\tilde{\eta}$ and $\tilde{\zeta}_i$, in place of η and ζ_i, defined by

$$\tilde{\eta} = (\hat{\rho}_{SB0})_0 \eta, \quad \tilde{\zeta}_i = \frac{\zeta_i}{\hat{T}_{w0}^{1/2}} \quad \text{for Eq. (A.273a)}, \tag{A.274a}$$

$$\tilde{\eta} = (\hat{\rho}_{V0})_0 \eta, \quad \tilde{\zeta}_i = \frac{\zeta_i - \hat{v}_{wi}}{\hat{T}_w^{1/2}} \quad \text{for Eq. (A.273b)}, \tag{A.274b}$$

$$\tilde{\eta} = (\hat{\rho}_{\mathfrak{S}0})_0 \eta, \quad \tilde{\zeta}_i = \frac{\zeta_i - \hat{v}_{wi}}{\hat{T}_w^{1/2}} \quad \text{for Eq. (A.273c)}. \tag{A.274c}$$

In Eq. (A.274c), i is used instead of ι $(= x, y, z)$ and $\hat{v}_{wi} = (\hat{v}_A, 0, 0)$ or $(\hat{v}_B, 0, 0)$ and $\hat{T}_w = 1$ or $\hat{T}_B$. Then, in view of the conditions (3.145), (3.181), (9.24a), and (9.24b),

$$(\hat{f}_{SB0})_0 = \frac{(\hat{\rho}_{SB0})_0}{\hat{T}_{w0}^{3/2}} E(\tilde{\zeta}), \quad (\hat{f}_{V0})_0 = \frac{(\hat{\rho}_{V0})_0}{\hat{T}_w^{3/2}} E(\tilde{\zeta}), \quad (\hat{f}_{\mathfrak{S}0})_0 = \frac{(\hat{\rho}_{\mathfrak{S}0})_0}{\hat{T}_w^{3/2}} E(\tilde{\zeta}).$$

Further, in view of the above relations, introduce $\phi_{Km}(\tilde{\eta}, \tilde{\zeta}_i)$ defined by

$$\hat{f}_{Km} = \frac{(\hat{\rho}_{SB0})_0}{\hat{T}_{w0}^{3/2}} E(\tilde{\zeta}) \phi_{Km}(\tilde{\eta}, \tilde{\zeta}_i) \quad \text{for Eq. (A.273a)},$$

$$\hat{f}_{Km} = \frac{(\hat{\rho}_{V0})_0}{\hat{T}_w^{3/2}} E(\tilde{\zeta}) \phi_{Km}(\tilde{\eta}, \tilde{\zeta}_i) \quad \text{for Eq. (A.273b)},$$

$$\hat{f}_{K1} = \frac{(\hat{\rho}_{\mathfrak{S}0})_0}{\hat{T}_w^{3/2}} E(\tilde{\zeta}) \phi_{K1}(\tilde{\eta}, \tilde{\zeta}_i) \quad \text{for Eq. (A.273c)}.$$

Then with the aid of Eqs. (A.115)–(A.117) in Section A.2.8, the Knudsen-layer equations (A.273a), (A.273b), and (A.273c) are reduced to the common form[55]

$$\tilde{\zeta}_i n_i \frac{\partial \phi_{Km}(\tilde{\eta}, \tilde{\zeta}_i)}{\partial \tilde{\eta}} = \mathcal{L}_a(\phi_{Km}(\tilde{\eta}, \tilde{\zeta}_i)) + \mathbb{IHK}_m, \tag{A.275}$$

[55] Equation (A.275) with Eq. (A.113) holds for the BKW equation.

where $a = \hat{T}_{w0}$ for Eq. (A.273a) and $a = \hat{T}_w$ for Eqs. (A.273b) and (A.273c), the operator $\mathcal{L}_a(*)$ is defined by Eqs. (A.111) and (A.112), and $\mathbb{IHK}_m$ is the appropriately transformed form of the inhomogeneous term Ihk_m. The boundary conditions are Eqs. (3.152a) and (3.152b), Eqs. (3.187a) and (3.187b), or Eqs. (9.31) and (9.32).

Equation (A.275) is a quasi-one-dimensional equation, where the coordinates in the surface $\tilde{\eta} = \text{const}$ appear only as parameters, and can be discussed only along an $\tilde{\eta}$ coordinate (or for a given set of the coordinates in the surface $\tilde{\eta} = \text{const}$). Thus, when we start from the nondimensional Boltzmann equation (1.47a) introduced in Section 1.9, it is convenient to choose the reference temperature T_0 and the reference density ρ_0 in such a way that $\hat{T}_{w0}$ or $\hat{T}_w$ and $(\hat{\rho}_{SB0})_0$, $(\hat{\rho}_{V0})_0$, or $(\hat{\rho}_{\mathfrak{S}0})_0$ on the $\tilde{\eta}$ coordinate under consideration take the value unity. Then, $a = 1$. That is,

$$\tilde{\zeta}_i n_i \frac{\partial \phi_{Km}(\tilde{\eta}, \tilde{\zeta}_i)}{\partial \tilde{\eta}} = \mathcal{L}(\phi_{Km}(\tilde{\eta}, \tilde{\zeta}_i)) + \mathbb{IHK}_m, \quad \Updownarrow \tag{A.276}$$

especially, for the leading-order Knudsen layer, where $\mathbb{IHK}_1 = 0$,

$$\tilde{\zeta}_i n_i \frac{\partial \phi_{K1}(\tilde{\eta}, \tilde{\zeta}_i)}{\partial \tilde{\eta}} = \mathcal{L}(\phi_{K1}(\tilde{\eta}, \tilde{\zeta}_i)). \quad \Updownarrow \tag{A.277}$$

The equations that apply on the special η coordinate line as Eqs. (A.276) and (A.277) are marked by $\Updownarrow$ at their ends in this section (Section A.11). Equation (A.277) is the same equation as Eq. (3.34) [or Eq. (3.35) without its inhomogeneous term] in the linear theory in Section 3.1.4. It may be added that for the present choice of the reference state, $(\hat{f}_{SB0})_0 = E(\tilde{\zeta})$, $(\hat{f}_{V0})_0 = E(\tilde{\zeta})$, $(\hat{f}_{\mathfrak{S}0})_0 = E(\tilde{\zeta})$, $\hat{f}_{K1} = E(\tilde{\zeta})\phi_{K1}(\tilde{\eta}, \tilde{\zeta}_i)$, $\tilde{\eta} = \eta$, and $\tilde{\zeta}_i = \zeta_i$ or $\tilde{\zeta}_i = \zeta_i - \hat{v}_{wi}$.

We will consider the boundary conditions for $\phi_{K1}(\tilde{\eta}, \tilde{\zeta}_i)$ corresponding to Eqs. (3.152a), (3.187a), and (9.31), where $\hat{f}_{SB1}$, $\hat{f}_{V1}$, or $\hat{f}_{\mathfrak{S}1}$ enters. These three functions are determined by Eq. (3.141), (3.179b), or (9.18a). These equations are commonly expressed by

$$2\hat{J}(\hat{f}_{*0}, \hat{f}_{*1}) = (a^{1/2}\tilde{\zeta}_i + \hat{v}_{wi0})\frac{\partial \hat{f}_{*0}}{\partial x_i},$$

where $\hat{f}_{*0}$ is a Maxwellian, $\hat{v}_{wi0} = 0$ and $a = \hat{T}_{w0}$ for Eq. (A.273a), and $\hat{v}_{wi0} = \hat{v}_{wi}$ and $a = \hat{T}_w$ for Eqs. (A.273b) and (A.273c). It may be noted that some terms in the expression degenerate and are of higher order. Especially, the $\hat{v}_{wi0}$ term on the right-hand side is of higher order and can be neglected in the cases of Eqs. (3.152a), (3.187a), and (9.31) because $\hat{v}_{wi0} = 0$ for Eq. (3.152a), and the derivatives parallel to the boundary are of higher order and $\hat{v}_{wi0} n_i = 0$ for Eqs. (3.187a) and (9.31). Thus, $\hat{f}_{*1}$ on the boundary, i.e., $(\hat{f}_{*1})_0$, is determined by

$$2\hat{J}((\hat{f}_{*0})_0, (\hat{f}_{*1})_0) = a^{1/2}\tilde{\zeta}_i \left(\frac{\partial \hat{f}_{*0}}{\partial x_i}\right)_0, \tag{A.278}$$

We are interested in $\hat{f}_{*1}$ at the point of the boundary that is on the η coordinate under consideration. Noting that $(\hat{f}_{*0})_0 = E(\tilde{\zeta})$ and $a = 1$ in the present choice of the reference state, we find that Eq. (A.278) is reduced to

$$\mathcal{L}(\phi_{*1}(x_{wi}, \tilde{\zeta}_i)) = \tilde{\zeta}_i \left(\frac{\partial \hat{\rho}_{*0}}{\partial x_i}\right)_0 + 2\tilde{\zeta}_i\tilde{\zeta}_j \left(\frac{\partial \hat{v}_{j*0}}{\partial x_i}\right)_0 + \tilde{\zeta}_i \left(\tilde{\zeta}_j^2 - \frac{3}{2}\right) \left(\frac{\partial \hat{T}_{*0}}{\partial x_i}\right)_0, \quad \Updownarrow$$

where we put $(\hat{f}_{*1})_0 = E(\tilde{\zeta})\phi_{*1}(x_{wi}, \tilde{\zeta}_i)$, and x_{wi} is the point under consideration. This is practically the same as Eq. (3.6) with $m = 1$ in Section 3.1.2.

The $\hat{f}_w$ part of the boundary conditions [say, Eq. (1.64) or (1.69)] being written using the new reference quantities and the expansion of $\hat{f}$

$$\begin{aligned}(\hat{f})_0 &= (\hat{f}_{*0})_0 + k[(\hat{f}_{*1})_0 + (\hat{f}_{K1})_0] + \cdots \\ &= E(\tilde{\zeta})(1 + k[\phi_{*1}(x_{wi}, \tilde{\zeta}_i) + \phi_{K1}(\tilde{\eta} = 0, \tilde{\zeta}_i)] + \cdots) \quad \Updownarrow\end{aligned}$$

being substituted there, we find that the boundary conditions of $\phi_{K1}(\tilde{\eta}, \tilde{\zeta}_i)$ for the three cases are of the same form as the condition at the first order of k in the linear theory, i.e., Eq. (3.36) with $m = 1$.[56] Therefore, the Knudsen-layer solution $\phi_{K1}(\tilde{\eta}, \tilde{\zeta}_i)$ is found to be expressed by the solution of the linear system. Thus, the slip conditions and the Knudsen-layer correction at the order of k on a simple boundary are obtained from Eqs. (3.41a)–(3.41c) for the three systems in Sections 3.3, 3.4, and 9.2.2 simply by transcription of notation. The formulas at the order of k on an interface in the case of Section 3.3 are from Eqs. (3.57a)–(3.57c) with $u_{iG0} = 0$ and $u_{wi0} = 0$.

Transforming these expressions of the original notation in each section, we obtain the relations between the slip coefficients $\hat{K}_1, \hat{C}_4^*, \hat{C}_1, \hat{k}_0, \hat{d}_1$ and the Knudsen-layer functions $\hat{Y}_0(\tilde{\eta}), \hat{\Omega}_1(\tilde{\eta}), \hat{\Theta}_1(\tilde{\eta})$ in Sections 3.3.3 and 3.4.2 and those $K_1, C_4^*, C_1, k_0, d_1$ and $Y_0(\eta), \Omega_1(\eta), \Theta_1(\eta)$ in the linear theory in Section 3.1.5. For example, the first relation of the slip condition (3.161b) is expressed as

$$(\hat{v}^\dagger_{jSB1} - \hat{v}^\dagger_{wj1})(\delta_{ij} - n_j n_i) = -K_1 \frac{\partial \hat{T}^\dagger_{SB0}}{\partial x_j}(\delta_{ij} - n_j n_i),$$

where the quantities with † indicate that they are nondimensionalized by the new reference quantities. Let the new reference temperature be indicated with a dagger † as $T_0^\dagger$. The two expressions $(2RT_0^\dagger)^{1/2}\hat{v}^\dagger_{jSB1}k^\dagger$ and $(2RT_0)^{1/2}\hat{v}_{jSB1}k$ are commonly the dimensional flow velocity of the leading order, and $T_0^\dagger\hat{T}^\dagger_{SB0}$ and $T_0\hat{T}_{SB0}$ are commonly the dimensional temperature of the leading order. Comparing the two expressions of a common quantity (or slip-flow velocity), we find that

$$K_1 \frac{\partial \hat{T}^\dagger_{SB0}}{\partial x_j}k^\dagger = \frac{\hat{K}_1}{\hat{p}_0}\frac{\partial \hat{T}_{SB0}}{\partial x_j}k, \text{ i.e., } \hat{K}_1 = \frac{(\hat{\rho}_{SB0})_0\rho_0 k^\dagger}{\rho_0 k}K_1,$$

[56] (i) Note the condition (1.66c) to Eq. (1.64) and the condition (1.71c) to Eq. (1.69).

(ii) In the present discussion, the condition $\hat{v}_{iSB0} = 0$ is important for the boundary condition (1.69).

(iii) The case in Section 3.4, ε $(= k^{1/2})$ should be taken as k here owing to the difference of the characteristic length in the viscous boundary layer.

from which, with the aid of the formula (1.48b), we have

$$\hat{K}_1 = \left(\frac{T_0^\dagger}{T_0}\right)^{1/2} \frac{B_0}{B_0^\dagger} K_1, \tag{A.279}$$

where $B_0^\dagger$ is defined by Eq. (1.48d) with the new reference quantities or more simply by the second or third expression of Eq. (1.48d) with T_0 being replaced by $T_0^\dagger$.[57] Similarly, we have, for $\hat{C}_1$ and $\hat{C}_4^*$ in the formula (3.162d) and for $\hat{k}_0$ and $\hat{d}_1$ in the formula (3.208),

$$\hat{C}_1 = \left(\frac{T_0^\dagger}{T_0}\right)^{1/2} \frac{B_0}{B_0^\dagger} C_1, \qquad \hat{C}_4^* = C_4^*, \tag{A.280a}$$

$$\hat{k}_0 = \left(\frac{T_0^\dagger}{T_0}\right)^{1/2} \frac{B_0}{B_0^\dagger} k_0, \qquad \hat{d}_1 = \left(\frac{T_0^\dagger}{T_0}\right)^{1/2} \frac{B_0}{B_0^\dagger} d_1. \tag{A.280b}$$

It is noted that y in the formula (3.208) differs for the two cases, because it contains k and should be discriminated as y and $y^\dagger$ in contrast to x_j in the formula (3.162c). For the Knudsen-layer functions $\hat{Y}_0(\tilde{\eta})$, $\hat{\Omega}_1(\tilde{\eta})$, and $\hat{\Theta}_1(\tilde{\eta})$, take the case of $\hat{Y}_0(\tilde{\eta})$. By a similar discussion to the above, from Eq. (3.210b),

$$\frac{(2RT_0)^{1/2}}{(\hat{\rho}_0)_0} \left(\frac{\partial u_0}{\partial y}\right)_0 \hat{Y}_0(\tilde{\eta})\, k^{1/2} = (2RT_0^\dagger)^{1/2} \left(\frac{\partial u_0^\dagger}{\partial y^\dagger}\right)_0 Y_0(\eta)\, (k^\dagger)^{1/2}.$$

Thus,

$$\hat{Y}_0(\tilde{\eta}) = \frac{k^\dagger (\hat{\rho}_0)_0 \rho_0}{k \rho_0} Y_0(\eta) = \left(\frac{T_0^\dagger}{T_0}\right)^{1/2} \frac{B_0}{B_0^\dagger} Y_0(\eta). \tag{A.281}$$

Similarly,

$$\hat{\Omega}_1(\tilde{\eta}) = \left(\frac{T_0^\dagger}{T_0}\right)^{1/2} \frac{B_0}{B_0^\dagger} \Omega_1(\eta), \quad \hat{\Theta}_1(\tilde{\eta}) = \left(\frac{T_0^\dagger}{T_0}\right)^{1/2} \frac{B_0}{B_0^\dagger} \Theta_1(\eta). \tag{A.282}$$

The factor $(T_0^\dagger/T_0)^{1/2} B_0/B_0^\dagger$ commonly appears in the formulas (A.279)–(A.282). For an intermolecular force extending to a finite distance (e.g., a hard-sphere gas), $(T_0^\dagger/T_0)^{1/2} B_0/B_0^\dagger = 1$ from the third expression of Eq. (1.48d). For the other molecules (an intermolecular force extending to infinity or a cutoff potential), the modified definition of B_0 is to be used as noted before.[58] For the BKW model, B_0 should be taken as $B_0/m = A_c$ from the comparison of Eqs. (1.48b) and (1.60b); thus, for the BKW model, $(T_0^\dagger/T_0)^{1/2} B_0/B_0^\dagger = (T_0^\dagger/T_0)^{1/2}$.

[57] See Footnote 21 in Section 1.9 and the last paragraph of Section A.2.4 for the intermolecular force extending to infinity or the cutoff potential.

[58] See Section A.2.4, especially its last paragraph, and Footnote 21 in Section 1.9.

From the formulas (3.41a) and (3.41b) of the slip condition for the linear theory, it is obvious that

$$\hat{v}_{y\mathfrak{S}1} = \hat{v}_{z\mathfrak{S}1} = 0 \quad \text{on the boundary,}$$

because $\hat{v}_{y\mathfrak{S}0} = \hat{v}_{z\mathfrak{S}0} = 0$.

A.12 Uniqueness of solution of the boundary-value problem of the linearized Boltzmann equation

Consider the time-independent boundary-value problem of the linearized Boltzmann equation (1.96) with the diffuse-reflection or complete-condensation boundary condition, i.e., Eq. (1.105a) with (1.105b) or Eq. (1.111), where $\partial/\partial\hat{t} = 0$ and $u_{wi}n_i = 0$. We will show that the solution is unique, except for an additive constant in the case of the diffuse reflection, for a bounded domain problem. For the uniqueness, we have only to show that the solution of the problem is a constant for the diffuse reflection when $u_{wi} = 0$ and $\tau_w = 0$, or it is zero for the complete condensation when $u_{wi} = 0$, $\tau_w = 0$, and $\omega_w = 0$. That is, the solution of the following boundary-value problem is a constant or zero: The linearized Boltzmann equation

$$\zeta_i \frac{\partial \phi}{\partial x_i} = \frac{1}{k}\mathcal{L}(\phi), \tag{A.283}$$

with the diffuse-reflection condition

$$\phi(x_i, \zeta_i) = \check{\sigma}_w \qquad (\zeta_j n_j > 0), \tag{A.284a}$$

$$\check{\sigma}_w = -2\sqrt{\pi} \int_{\zeta_k n_k < 0} \zeta_j n_j \phi E \mathbf{d}\boldsymbol{\zeta}, \tag{A.284b}$$

or with the complete-condensation condition

$$\phi(x_i, \zeta_i) = 0 \qquad (\zeta_j n_j > 0). \tag{A.285}$$

Integrating Eq. (A.283) multiplied by ϕE over the gas domain V and over the whole space of $\boldsymbol{\zeta}$ and using Gauss's divergence theorem, we obtain

$$-\frac{1}{2}\int_{\partial V}\int \zeta_i n_i \phi^2 E \mathbf{d}\boldsymbol{\zeta} \mathrm{d}S = \frac{1}{k}\int_V \int \phi \mathcal{L}(\phi) E \mathbf{d}\boldsymbol{\zeta}\mathbf{d}\boldsymbol{x}, \tag{A.286}$$

where ∂V is the boundary of the gas domain V and $\mathrm{d}S$ is the surface element on ∂V. Owing to Eq. (1.80),

$$\int_V \int \phi \mathcal{L}(\phi) E \mathbf{d}\boldsymbol{\zeta}\mathbf{d}\boldsymbol{x} \le 0, \tag{A.287}$$

where the equal sign holds when and only when $\phi' + \phi'_* - \phi - \phi_* = 0$, or ϕ is a summational invariant. Thus,

$$-\frac{1}{2}\int_{\partial V}\int \zeta_i n_i \phi^2 E \mathbf{d\zeta} \mathrm{d}S = \frac{1}{k}\int_V \int \phi \mathcal{L}(\phi) E \mathbf{d\zeta} \mathbf{d}\boldsymbol{x} \leq 0. \tag{A.288}$$

This is the linearized-Boltzmann-equation version of Eq. (1.36).

For the complete-condensation condition (A.285), Eq. (A.288) reduces to

$$-\frac{1}{2}\int_{\partial V}\int_{\zeta_i n_i<0} \zeta_i n_i \phi^2 E \mathbf{d\zeta} \mathrm{d}S = \frac{1}{k}\int_V \int \phi \mathcal{L}(\phi) E \mathbf{d\zeta} \mathbf{d}\boldsymbol{x} \leq 0, \tag{A.289}$$

where the left-hand side is obviously non-negative. Thus,

$$\int_V \int \phi \mathcal{L}(\phi) E \mathbf{d\zeta} \mathbf{d}\boldsymbol{x} = 0.$$

With the aid of Eq. (1.80),

$$\int \phi \mathcal{L}(\phi) E \mathbf{d\zeta} = 0.$$

From the symmetry relation (A.39),

$$0 = \int \phi \mathcal{L}(\phi) E \mathbf{d\zeta} = -\frac{1}{4}\int E E_* (\phi' + \phi'_* - \phi - \phi_*)^2 \widehat{B} \mathrm{d}\Omega \mathbf{d\zeta}_* \mathbf{d\zeta}.$$

Thus, $\phi' + \phi'_* - \phi - \phi_* = 0$, i.e., ϕ is a summational invariant. Then,

$$\mathcal{L}(\phi) = 0.$$

Therefore, Eq. (A.283) reduces to

$$\zeta_i \frac{\partial \phi}{\partial x_i} = 0. \tag{A.290}$$

From Eqs. (A.290) and (A.285), we find

$$\phi = 0.$$

Thus, in the case of the complete-condensation boundary condition, the solution of the boundary-value problem is unique.

For the diffuse-reflection condition, the left-hand side of Eq. (A.288) is rewritten. Splitting the integral into two parts, $\zeta_i n_i < 0$ and $\zeta_i n_i > 0$, and noting that the relation

$$\int_{\zeta_i n_i>0} \zeta_i n_i \breve{\sigma}_w^2 E \mathbf{d\zeta} = -\breve{\sigma}_w \int_{\zeta_k n_k<0} \zeta_j n_j \phi E \mathbf{d\zeta},$$

holds for the diffuse-reflection condition (A.284a) with (A.284b), we have

$$\begin{aligned}\int \zeta_i n_i \phi^2 E \mathbf{d}\boldsymbol{\zeta} &= \int_{\zeta_i n_i<0} \zeta_i n_i \phi^2 E \mathbf{d}\boldsymbol{\zeta} + \int_{\zeta_i n_i>0} \zeta_i n_i \check{\sigma}_w^2 E \mathbf{d}\boldsymbol{\zeta} \\ &= \int_{\zeta_i n_i<0} \zeta_i n_i \phi^2 E \mathbf{d}\boldsymbol{\zeta} - 2\check{\sigma}_w \int_{\zeta_k n_k<0} \zeta_i n_i \phi E \mathbf{d}\boldsymbol{\zeta} - \int_{\zeta_i n_i>0} \zeta_i n_i \check{\sigma}_w^2 E \mathbf{d}\boldsymbol{\zeta} \\ &= -\int_{\zeta_i n_i<0} |\zeta_i n_i| (\phi - \check{\sigma}_w)^2 E \mathbf{d}\boldsymbol{\zeta} \le 0. \end{aligned} \tag{A.291}$$

From Eqs. (A.288) and (A.291), on the boundary ∂V,

$$\int \zeta_i n_i \phi^2 E \mathbf{d}\boldsymbol{\zeta} = 0, \tag{A.292a}$$

$$\int_{\zeta_i n_i<0} \zeta_i n_i (\phi - \check{\sigma}_w)^2 E \mathbf{d}\boldsymbol{\zeta} = 0. \tag{A.292b}$$

From Eqs. (A.284a) and (A.292b),

$$\phi = \check{\sigma}_w \quad \text{for all } \zeta_i \quad \text{on } \partial V. \tag{A.293}$$

From Eqs. (A.288) and (A.292a),

$$\int_V \int \phi \mathcal{L}(\phi) E \mathbf{d}\boldsymbol{\zeta} \mathbf{d}\boldsymbol{x} = 0.$$

With the aid of Eq. (1.80),

$$\int \phi \mathcal{L}(\phi) E \mathbf{d}\boldsymbol{\zeta} = 0.$$

By the same way as in the complete condensation, $\phi' + \phi'_* - \phi - \phi_* = 0$, i.e., ϕ is a summational invariant. Then,

$$\mathcal{L}(\phi) = 0.$$

Therefore, Eq. (A.283) reduces to

$$\zeta_i \frac{\partial \phi}{\partial x_i} = 0. \tag{A.294}$$

From Eqs. (A.294) and (A.293), the boundary value of ϕ or $\check{\sigma}_w$ at two points on ∂V that can be connected with a straight line without intersecting the boundary ∂V are equal. Thus, if the shape of the domain V is such that any two points on ∂V can be connected by a broken line inside V with broken points on ∂V,[59] the boundary value of ϕ or $\check{\sigma}_w$ is uniform (or independent of the position on ∂V). Thus, from Eq. (A.294), ϕ is constant with respect to x_i and ζ_i. Thus, the

[59] Obviously, this assumption, which is called bridge or ergodicity assumption (Sone [1984a, 1985], Aoki, Bardos, Golse, Kogan & Sone [1993]), holds for most domains.

solution of the boundary-value problem with the diffuse-reflection condition is unique except for an additive constant. The proof for the diffuse reflection is practically the same as Golse's proof in Section A.4 of Sone [2002].

It may be noted that the proof given above applies to the class of functions with discontinuities[60] as described in Section 3.1.6. For this class of functions, the relations in the above analysis do not hold everywhere, but they hold almost everywhere.[61] Thus, the uniqueness theorem holds because two functions that agree almost everywhere are identified. It is important to include functions with discontinuity in the discussion because the velocity distribution function generally has discontinuities as shown in Section 3.1.6.

The points of the proof are the two inequalities (A.287) and (A.291), from which ϕ is derived to be a summational invariant. The inequality (A.287) derived with the aid of the symmetry relation for the linearized collision integral is independent of the boundary condition. The inequality (A.291) is derived in the second part of Section A.10 for general boundary conditions expressed with scattering kernels, i.e., the boundary condition (A.252) with $u_{wi} = 0$ and $\tau_w = 0$ and the boundary condition (A.255) with $\omega_w = 0$, $u_{wi} = 0$, and $\tau_w = 0$ where the extra condition (A.271) on the kernel $\hat{K}_{I0}$ is imposed. Thus, ϕ is a summational invariant for these boundary conditions, i.e.,

$$\phi = c_0 + c_i\zeta_i + c_4\zeta_i^2 \quad \text{almost everywhere,} \tag{A.295}$$

where c_0, c_i, and c_4 are independent of $\boldsymbol{\zeta}$, and

$$\zeta_i \frac{\partial \phi}{\partial x_i} = 0. \tag{A.296}$$

From Eqs. (A.295) and (A.296) together with the subsidiary conditions (iii) to Eq. (A.252) and (ii-b) to Eq. (A.255),[62] we find that for the boundary condition (A.252) with $u_{wi} = 0$ and $\tau_w = 0$,

$$\phi = c_0,$$

and for the boundary condition (A.255) with $\omega_w = 0$, $u_{wi} = 0$, and $\tau_w = 0$,

$$\phi = 0.$$

Thus, the uniqueness holds for the general boundary conditions (A.252) and (A.255) with the extra condition (A.271) on the kernel $\hat{K}_{I0}$ imposed.

[60] Appropriate integrability is assumed.

[61] See Footnote 5 in Section 1.2 for the definition of almost everywhere.

[62] Here, we used the explicit form (A.295) of ϕ, in contrast to the preceding proof. With this form, the proof is simpler, but Arkeryd's sophisticated result explained in the last paragraph of Section A.2.3 is required when the class of solutions with discontinuities is considered.

Appendix B

Methods of Solution

B.1 Direct simulation Monte Carlo method

B.1.1 Introduction

The direct simulation Monte Carlo method (DSMC method, in short), introduced by Bird [1963] (see also Bird [1994]), is a numerical method of solution of the Boltzmann equation, quite different from the finite-difference method.[1] In this method, (i) a group of many molecules at neighboring positions and with similar velocities is represented by a single particle, (ii) the laws of motion of the system of the particles are formulated according to the assumptions that are introduced in derivation of the Boltzmann equation, and (iii) the behavior of the system is simulated by numerical computation according to the laws, from which the behavior of the gas is determined. The process to carry out the computation is simple, but it requires a large-scale computation. In this appendix (Section B.1), the fundamental process of computation is briefly described, its theoretical background (or the relation to the Boltzmann equation) is given in an elementary form, which is not rigorous but is easily accessible to nonmathematicians, and an example of computation is given. The theoretical discussion and example will be helpful to develop the improvement and extension of the method with a sound background. It is not the purpose of the appendix to present a variety of technique.

B.1.2 Preparation

For preparation of the following discussion, we will explain the way to approximate the velocity distribution function with a series of the Dirac delta functions.

Let the domain D of a gas under consideration be divided into M small domains (or cells) $\mathbf{d}\boldsymbol{X}^{(l)}$ $(l = 1, 2, \ldots, M)$, and let $\boldsymbol{X}^{(l)}$ be the representative point in $\mathbf{d}\boldsymbol{X}^{(l)}$. We will show that the velocity distribution function $f(\boldsymbol{X}, \boldsymbol{\xi}, t)$ is

[1] Kogan's group in Russia was using a similar computation.

approximated in the following forms by choosing a constant Δ, an integer $N^{(l)}$, which depends on l, and $\boldsymbol{\xi}_{(l)}^{(j)}$ $(j = 1, 2, \ldots, N^{(l)})$:

$$f(\boldsymbol{X}, \boldsymbol{\xi}, t)\mathbf{d}\boldsymbol{X}^{(l)} = \Delta \sum_{j=1}^{N^{(l)}} \delta(\boldsymbol{\xi} - \boldsymbol{\xi}_{(l)}^{(j)}) \quad (\boldsymbol{X} \text{ is in } \mathbf{d}\boldsymbol{X}^{(l)}), \tag{B.1a}$$

$$f(\boldsymbol{X}, \boldsymbol{\xi}, t) = \Delta \sum_{l=1}^{M} \sum_{j=1}^{N^{(l)}} \delta(\boldsymbol{X} - \boldsymbol{X}_{(l)}^{(j)})\delta(\boldsymbol{\xi} - \boldsymbol{\xi}_{(l)}^{(j)}) \quad (\boldsymbol{X} \text{ is arbitrary}), \tag{B.1b}$$

where δ is the (three-dimensional) Dirac delta function and $\boldsymbol{X}_{(l)}^{(j)}$ is an arbitrary point in $\mathbf{d}\boldsymbol{X}^{(l)}$.

Take a moment of a function $f(\boldsymbol{X}, \boldsymbol{\xi}, t)$ with respect to $\boldsymbol{\xi}$, i.e.,

$$\left(\int_{\text{all } \boldsymbol{\xi}} \Phi(\boldsymbol{\xi}) f(\boldsymbol{X}^{(l)}, \boldsymbol{\xi}, t) \mathbf{d}\boldsymbol{\xi} \right) \mathbf{d}\boldsymbol{X}^{(l)}, \tag{B.2}$$

where $\Phi(\boldsymbol{\xi})$ is an arbitrary function of $\boldsymbol{\xi}$, and the integration with respect to $\boldsymbol{\xi}$ is carried out over the whole space of $\boldsymbol{\xi}$. We introduce a new vector $\boldsymbol{\eta}$

$$\boldsymbol{\eta} = \boldsymbol{\eta}(\boldsymbol{\xi}; \boldsymbol{X}^{(l)}, \mathbf{d}\boldsymbol{X}^{(l)}) \quad \text{or} \quad \boldsymbol{\xi} = \boldsymbol{\xi}(\boldsymbol{\eta}; \boldsymbol{X}^{(l)}, \mathbf{d}\boldsymbol{X}^{(l)}),$$

where the transformation from $\boldsymbol{\xi}$ to $\boldsymbol{\eta}$ is chosen in such a way that its Jacobian is $f(\boldsymbol{X}^{(l)}, \boldsymbol{\xi}, t)\ \mathbf{d}\boldsymbol{X}^{(l)}$, which can always be found.[2] Then,

$$\mathbf{d}\boldsymbol{\eta} = [f(\boldsymbol{X}^{(l)}, \boldsymbol{\xi}, t)\mathbf{d}\boldsymbol{X}^{(l)}]\mathbf{d}\boldsymbol{\xi},$$

and the range of $\boldsymbol{\eta}$ is reduced to a finite range. Then, the moment (B.2) is reduced to

$$\left(\int_{\text{all } \boldsymbol{\xi}} \Phi(\boldsymbol{\xi}) f(\boldsymbol{X}^{(l)}, \boldsymbol{\xi}, t) \mathbf{d}\boldsymbol{\xi} \right) \mathbf{d}\boldsymbol{X}^{(l)} = \int_{V^{(l)}} \Phi(\boldsymbol{\xi}(\boldsymbol{\eta}; \boldsymbol{X}^{(l)}, \mathbf{d}\boldsymbol{X}^{(l)})) \mathbf{d}\boldsymbol{\eta}, \tag{B.3}$$

where the domain $V^{(l)}$ of integration depends on l in its shape and volume.

Now, we divide each of $V^{(l)}$ $(l = 1, 2, \ldots, M)$ in $\boldsymbol{\eta}$ space into small cells of a common volume Δ independent of l. The number $N^{(l)}$ of the cells in $V^{(l)}$ is $V^{(l)}/\Delta$, where $V^{(l)}$ is used as the volume as well as the name of the domain, as $\mathbf{d}\boldsymbol{X}^{(l)}$. Let the representative point of each of the small cells be denoted as

[2] Let the Jacobian be $G(\boldsymbol{\xi})$ for simplicity. Put

$$g(\xi_2, \xi_3) = \int_{-\infty}^{\infty} G(\bar{\xi}_1, \xi_2, \xi_3) \mathrm{d}\bar{\xi}_1, \quad h(\xi_3) = \int_{-\infty}^{\infty} \int_{-\infty}^{\infty} G(\bar{\xi}_1, \bar{\xi}_2, \xi_3) \mathrm{d}\bar{\xi}_1 \mathrm{d}\bar{\xi}_2.$$

Then, the following transformation has the desired Jacobian:

$$\eta_1 = \frac{1}{g(\xi_2, \xi_3)} \int_{-\infty}^{\xi_1} G(\bar{\xi}_1, \xi_2, \xi_3) \mathrm{d}\bar{\xi}_1, \quad \eta_2 = \frac{1}{h(\xi_3)} \int_{-\infty}^{\xi_2} g(\bar{\xi}_2, \xi_3) \mathrm{d}\bar{\xi}_2, \quad \eta_3 = \int_{-\infty}^{\xi_3} h(\bar{\xi}_3) \mathrm{d}\bar{\xi}_3.$$

In this case, the domain of integration $V^{(l)}$ in Eq. (B.3) is the rectangular parallelepiped $[0 \le \eta_1 \le 1,\ 0 \le \eta_2 \le 1,\ 0 \le \eta_3 \le \rho(\boldsymbol{X}^{(l)}, t)\mathbf{d}\boldsymbol{X}^{(l)}]$.

$\boldsymbol{\eta}^{(j)}$ $(j = 1, 2, \ldots, N^{(l)})$. Then, the integral (B.3) [thus, the moment (B.2)] is approximated as

$$\text{Integral (B.3)} = \Delta \sum_{j=1}^{N^{(l)}} \Phi(\boldsymbol{\xi}_{(l)}^{(j)}), \qquad \boldsymbol{\xi}_{(l)}^{(j)} = \boldsymbol{\xi}(\boldsymbol{\eta}^{(j)}; \boldsymbol{X}^{(l)}, \mathbf{d}\boldsymbol{X}^{(l)}). \tag{B.4}$$

On the other hand, it is seen by direct substitution that the function on the right-hand side of the first relation of Eq. (B.4) is obtained by the moment (B.2) at $\boldsymbol{X} = \boldsymbol{X}^{(l)}$ of the function f given by Eq. (B.1a). Therefore, by taking Δ small (or $N^{(l)}$ large), any moment (B.2) of a function f is approximated with any accuracy by the corresponding moment of the function (B.1a) expressed in the series of the Dirac delta functions.[3] The convergence in this sense is called weak convergence.

Next, take a moment of a function $f(\boldsymbol{X}, \boldsymbol{\xi}, t)$ with respect to $\boldsymbol{X}$ and $\boldsymbol{\xi}$, i.e.,

$$\int_{\text{all } \boldsymbol{X},\, \text{all } \boldsymbol{\xi}} \varphi(\boldsymbol{X}, \boldsymbol{\xi}) f(\boldsymbol{X}, \boldsymbol{\xi}, t) \mathbf{d}\boldsymbol{X} \mathbf{d}\boldsymbol{\xi}, \tag{B.5}$$

where $\varphi(\boldsymbol{X}, \boldsymbol{\xi})$ can be nonzero only in a finite domain in D (the support[4] of φ, with respect to $\boldsymbol{X}$, is compact and in D). Here, applying the process leading to Eq. (B.3) from Eq. (B.2) to the integral on each cell $\mathbf{d}\boldsymbol{X}^{(l)}$ (the subdivision of the domain of $\boldsymbol{X}$), we can obtain

$$\text{Integral (B.5)} = \sum_{l=1}^{M} \int_{V^{(l)}} \varphi(\boldsymbol{X}^{(l)}, \boldsymbol{\xi}(\boldsymbol{\eta}; \boldsymbol{X}^{(l)}, \mathbf{d}\boldsymbol{X}^{(l)})) \mathbf{d}\boldsymbol{\eta}. \tag{B.6}$$

Then, applying the process leading to Eq. (B.4) to the integral over $V^{(l)}$, we find that the integral (B.5) is approximated by

$$\text{Integral (B.5)} = \Delta \sum_{l=1}^{M} \sum_{j=1}^{N^{(l)}} \varphi(\boldsymbol{X}^{(l)}, \boldsymbol{\xi}_{(l)}^{(j)}). \tag{B.7}$$

For infinitesimal cell $\mathbf{d}\boldsymbol{X}^{(l)}$, $\boldsymbol{X}^{(l)}$ can be replaced by an arbitrary point $\boldsymbol{X}_{(l)}^{(j)}$ in the cell. That is,

$$\text{Integral (B.5)} = \Delta \sum_{l=1}^{M} \sum_{j=1}^{N^{(l)}} \varphi(\boldsymbol{X}_{(l)}^{(j)}, \boldsymbol{\xi}_{(l)}^{(j)}). \tag{B.8}$$

[3]The divided region in $\boldsymbol{\xi}$ space corresponding to a small cell in $\boldsymbol{\eta}$ space is preferable not to be too elongated for the approximation to be efficient. Thus, the division of $V^{(l)}$ into small cells is appropriately done so as to make the number of such cells elongated in $\boldsymbol{\eta}$ space as small as possible. The outermost Δ cells extend to infinity in $\boldsymbol{\xi}$ space. Thus, the arbitrariness of the representative $\boldsymbol{\xi}$ is too large, and the error of $\Phi(\boldsymbol{\xi})$ is $O(\Phi(\boldsymbol{\xi}))$. However, for the distribution function rapidly vanishing as $|\boldsymbol{\xi}| \to \infty$, which we are considering here, their contribution is small for large $N^{(l)}$ because the number of such cells relative to $N^{(l)}$ vanishes rapidly as $N^{(l)} \to \infty$.

[4]The support of a function $\varphi(\boldsymbol{X})$ of $\boldsymbol{X}$ is the closure of the set of $\boldsymbol{X}$ where $\varphi(\boldsymbol{X}) \neq 0$. A compact set is a bounded closed set. See, e.g., Rudin [1976].

On the other hand, the series (B.1b) being substituted into Eq. (B.5), Eq. (B.8) is derived. That is, by taking M large and Δ small (or $N^{(l)}$ large), any moment of f with respect to $\boldsymbol{X}$ and $\boldsymbol{\xi}$ is approximated with any accuracy by the moment of the series (B.1b) (weak convergence).

The macroscopic variables of a gas, such as density, flow velocity, and temperature, are expressed by moments of the velocity distribution function f

$$\int_{\text{all } \boldsymbol{\xi}} \Phi(\boldsymbol{\xi}) f(\boldsymbol{X}, \boldsymbol{\xi}, t) \mathbf{d}\boldsymbol{\xi}. \tag{B.9}$$

This moment is expressed in the following form for f given by Eq. (B.1a):

$$\text{Integral (B.9)} = \frac{\Delta}{\mathbf{d}\boldsymbol{X}^{(l)}} \sum_{j=1}^{N^{(l)}} \Phi(\boldsymbol{\xi}_{(l)}^{(j)}). \tag{B.10}$$

The density ρ, the flow velocity $\boldsymbol{v}$, and the temperature T of the gas in the cell $\mathbf{d}\boldsymbol{X}^{(l)}$ are given by

$$\rho = \frac{N^{(l)}\Delta}{\mathbf{d}\boldsymbol{X}^{(l)}}, \tag{B.11a}$$

$$\boldsymbol{v} = \frac{1}{N^{(l)}} \sum_{j=1}^{N^{(l)}} \boldsymbol{\xi}_{(l)}^{(j)}, \tag{B.11b}$$

$$3RT = \frac{1}{N^{(l)}} \sum_{j=1}^{N^{(l)}} \left(\boldsymbol{\xi}_{(l)}^{(j)} - \frac{1}{N^{(l)}} \sum_{k=1}^{N^{(l)}} \boldsymbol{\xi}_{(l)}^{(k)} \right)^2. \tag{B.11c}$$

B.1.3 Process of DSMC method

In the present section, the DSMC process of solution of an initial and boundary-value problem of the Boltzmann equation

$$\frac{\partial f}{\partial t} + \xi_i \frac{\partial f}{\partial X_i} + \frac{\partial F_i f}{\partial \xi_i} = J(f, f), \tag{B.12a}$$

$$J(f, f) = \frac{1}{m} \int_{\text{all } \boldsymbol{\alpha},\ \text{all } \boldsymbol{\xi}_*} (f' f'_* - f f_*) B \mathrm{d}\Omega\,(\boldsymbol{\alpha}) \mathbf{d}\boldsymbol{\xi}_*, \tag{B.12b}$$

$$B = B(|(\boldsymbol{\xi}_* - \boldsymbol{\xi}) \cdot \boldsymbol{\alpha}|/|\boldsymbol{\xi}_* - \boldsymbol{\xi}|, |\boldsymbol{\xi}_* - \boldsymbol{\xi}|),$$

(see Section 1.2 for more details) is described. The boundary condition is given in terms of scattering kernel by Eq. (1.26) on a simple boundary or by Eq. (1.30) on an interface of the gas and its condensed phase. The velocity distribution function is given at initial time (say, $t = 0$) as the initial condition. The physical domain D of interest in a numerical computation is limited to a finite domain, and therefore some parts of the boundary are artificial boundaries.

First, we expand the initial velocity distribution function in the form of Eq. (B.1b), the practical procedure of which is explained at the end of this section. We identify each term [or the delta function $\delta(\boldsymbol{X}-\boldsymbol{X}_{(l)}^{(j)})\delta(\boldsymbol{\xi}-\boldsymbol{\xi}_{(l)}^{(j)})$] of the series as a particle and the centers $\boldsymbol{X}_{(l)}^{(j)}$ and $\boldsymbol{\xi}_{(l)}^{(j)}$ of the delta function, respectively, as the position and the velocity of the particle. Given an initial velocity distribution function (or the initial positions and velocities of all the particles), change the positions and velocities of the particles according to the following steps. Then, the velocity distribution function at $\mathrm{d}t$ is determined from Eq. (B.1b) with the new positions and velocities of the particles. Repeating this process successively with the new state as the initial condition, we determine the positions and velocities of the particles (or the velocity distribution function) at the successive time steps. The domain D of interest of the physical space $\boldsymbol{X}$ is initially divided into the set of cells $\mathbf{d}\boldsymbol{X}^{(l)}$ $(l=1,2,\ldots,M)$. This division remains fixed in the course of analysis.

Step (i): Let the position $\boldsymbol{X}_{(l)}^{(j)}$ and velocity $\boldsymbol{\xi}_{(l)}^{(j)}$ of all the particles at time t be given. Shift the position $\boldsymbol{X}_{(l)}^{(j)}$ and velocity $\boldsymbol{\xi}_{(l)}^{(j)}$ of each particle to $\boldsymbol{X}_{(l)}^{(j)}+\boldsymbol{\xi}_{(l)}^{(j)}\mathrm{d}t$ and $\boldsymbol{\xi}_{(l)}^{(j)}+\boldsymbol{F}(\boldsymbol{X}_{(l)}^{(j)},\boldsymbol{\xi}_{(l)}^{(j)},t)\mathrm{d}t$. Then, the velocity distribution function f is shifted to

$$f=\Delta\sum_{l=1}^{M}\sum_{j=1}^{N^{(l)}}\delta(\boldsymbol{X}-\boldsymbol{X}_{(l)}^{(j)}-\boldsymbol{\xi}_{(l)}^{(j)}\mathrm{d}t)\delta(\boldsymbol{\xi}-\boldsymbol{\xi}_{(l)}^{(j)}-\boldsymbol{F}(\boldsymbol{X}_{(l)}^{(j)},\boldsymbol{\xi}_{(l)}^{(j)},t)\mathrm{d}t). \tag{B.13}$$

A particle (in $\mathbf{d}\boldsymbol{X}^{(l)}$, say) generally enters a different cell ($\mathbf{d}\boldsymbol{X}^{(\bar{l})}$, say) after the shift. Then, we relabel the particle $[(l,j)\to(\bar{l},\bar{j})$, say] according to Eq. (B.1b) [or Eq. (B.1a)]. The parameter Δ, introduced in developing the initial velocity distribution function in the forms (B.1a) and (B.1b), is a fixed constant (throughout the process of computation).[5]

Step (ii): After the step (i), some particles go out of the domain D. They are got rid of from the analysis, but instead, new particles are introduced in the domain according to the boundary condition. The explicit description of this process is given at the end of this section.

Step (iii): The computation of this step is carried out independently in each cell $\mathbf{d}\boldsymbol{X}^{(l)}$. Consider one of the cells, which is denoted as $\mathbf{d}\boldsymbol{X}^{*}$. The velocity distribution function in this cell is expressed in the form of Eq. (B.1a). That is, the label discriminating the cell being eliminated, it is given by

$$f=\frac{\Delta}{\mathbf{d}\boldsymbol{X}^{*}}\sum_{j=1}^{N^{*}}\delta(\boldsymbol{\xi}-\boldsymbol{\xi}^{(j)}), \tag{B.14}$$

where N^{*} is the number of particles in the cell $\mathbf{d}\boldsymbol{X}^{*}$ after the steps (i) and (ii). Let the probability $\bar{P}^{(s)}(\boldsymbol{\xi}^{(j)},\boldsymbol{\xi}^{(k)})\mathrm{d}\Omega^{(s)}$ of finding a unit vector $\boldsymbol{\alpha}$ (to be called

[5] A particle is allotted to the collection with mass Δ of the molecules in $\mathbf{d}\boldsymbol{X}^{(l)}$ with neighboring molecular velocities.

collision parameter) in a solid-angle element $\mathrm{d}\Omega^{(s)}$ for the pair $(\boldsymbol{\xi}^{(j)}, \boldsymbol{\xi}^{(k)})$ (or the pair of the particles with $\boldsymbol{\xi}^{(j)}$ and $\boldsymbol{\xi}^{(k)}$ in $\mathbf{d}\boldsymbol{X}^*$) be defined by[6]

$$\bar{P}^{(s)}(\boldsymbol{\xi}^{(j)}, \boldsymbol{\xi}^{(k)})\mathrm{d}\Omega^{(s)} = \frac{\Delta \mathrm{d}t}{m\mathbf{d}\boldsymbol{X}^*} B(|(\boldsymbol{\xi}^{(k)}-\boldsymbol{\xi}^{(j)})\cdot\boldsymbol{\alpha}^{(s)}|/|\boldsymbol{\xi}^{(k)}-\boldsymbol{\xi}^{(j)}|, |\boldsymbol{\xi}^{(k)}-\boldsymbol{\xi}^{(j)}|)\mathrm{d}\Omega^{(s)}, \tag{B.15}$$

where $\boldsymbol{\alpha}^{(s)}$ is the representative point in $\mathrm{d}\Omega^{(s)}$. Now, for each of the pairs of the particles in $\mathbf{d}\boldsymbol{X}^*$[or $N^*(N^*-1)/2$ pairs of $(\boldsymbol{\xi}^{(j)}, \boldsymbol{\xi}^{(k)})$ with $j<k$], we carry out the following trial, on the basis of the probability (B.15), whether $\boldsymbol{\alpha}$ is found in $\mathrm{d}\Omega^{(s)}$ for some s or not and in which $\mathrm{d}\Omega^{(s)}$ if it is. If $\boldsymbol{\alpha}$ realizes in $\mathrm{d}\Omega^{(s)}$ for the pair $(\boldsymbol{\xi}^{(j)}, \boldsymbol{\xi}^{(k)})$, then the pair $(\boldsymbol{\xi}^{(j)}, \boldsymbol{\xi}^{(k)})$ in Eq. (B.14) is transformed to $(\widehat{\boldsymbol{\xi}}^{(j)}, \widehat{\boldsymbol{\xi}}^{(k)})$ given by the formula

$$\widehat{\boldsymbol{\xi}}^{(j)} = \boldsymbol{\xi}^{(j)} + [(\boldsymbol{\xi}^{(k)} - \boldsymbol{\xi}^{(j)})\cdot\boldsymbol{\alpha}^{(s)}]\boldsymbol{\alpha}^{(s)}, \tag{B.16a}$$

$$\widehat{\boldsymbol{\xi}}^{(k)} = \boldsymbol{\xi}^{(k)} - [(\boldsymbol{\xi}^{(k)} - \boldsymbol{\xi}^{(j)})\cdot\boldsymbol{\alpha}^{(s)}]\boldsymbol{\alpha}^{(s)}. \tag{B.16b}$$

If $\boldsymbol{\alpha}$ does not realize, the pair $(\boldsymbol{\xi}^{(j)}, \boldsymbol{\xi}^{(k)})$ in Eq. (B.14) is left unchanged. The velocity distribution function in the form (B.1a) or (B.1b) thus obtained is that at time $t+\mathrm{d}t$. Some comments on the parameter sizes in this step are required, but it is postponed until the end of the description of the final step.

Step (iv): Return to the step (i), and continue the computation to obtain the velocity distribution function at the subsequent times.

Supplementary notes to the explanation of the step (iii) are given here.

If $\boldsymbol{\alpha}$ realizes in $\mathrm{d}\Omega^{(s)}$ for some s, we say that the particles (j,k) have collided, and otherwise, no collision has taken place. The probability of the pair (j,k) that makes a collision is given by

$$\begin{aligned} P(\boldsymbol{\xi}^{(j)}, \boldsymbol{\xi}^{(k)}) &= \sum_s \bar{P}^{(s)}(\boldsymbol{\xi}^{(j)}, \boldsymbol{\xi}^{(k)})\mathrm{d}\Omega^{(s)} \\ &= \frac{\pi d_m^2 \Delta}{m}\frac{\mathrm{d}t}{\mathbf{d}\boldsymbol{X}^*}|\boldsymbol{\xi}^{(k)} - \boldsymbol{\xi}^{(j)}| \\ &= \frac{\pi d_m^2 \mathrm{d}t \rho(\boldsymbol{X}^*, t)|\boldsymbol{\xi}^{(k)} - \boldsymbol{\xi}^{(j)}|}{mN^*}, \end{aligned} \tag{B.17}$$

and the probability of no collision is $1 - P(\boldsymbol{\xi}^{(j)}, \boldsymbol{\xi}^{(k)})$. The second line on the right-hand side of Eq. (B.17) is derived from the first with the aid of Eqs. (B.15) and (A.20). The $P(\boldsymbol{\xi}^{(j)}, \boldsymbol{\xi}^{(k)})$ in Eq. (B.17) exceeds unity for very large particle-velocities ($|\boldsymbol{\xi}^{(k)} - \boldsymbol{\xi}^{(j)}| \to \infty$) even if we take the parameters Δ and $\mathrm{d}t$ small, which is inappropriate as a probability. However, the velocity distribution function decays very rapidly as $|\boldsymbol{\xi}| \to \infty$ and the contribution to the collision term (B.12b) of the Boltzmann equation (B.12a) from large molecular velocities is negligible. Thus, we can consider the problem within a reasonable size of particle speed. The speed of a particle may get higher and higher with repeated

[6] In the numerical computation, the whole direction of $\boldsymbol{\alpha}$ (or the unit sphere surface) is divided into a finite number of small elements $\mathrm{d}\Omega^{(s)}$.

collisions because the velocity distribution function approaches an equilibrium state or Maxwellian from the distribution with a finite range for the molecular speed, but this possibility is very small. In the conventional computation, no care is taken for it because it does not produce any important influence (e.g., it goes out of the domain of interest in a short time), or some cutoff is introduced (e.g., to try the process to determine $\boldsymbol{\alpha}$ again).

As we will discuss in the paragraph containing Eq. (B.59a), we have to choose $\mathrm{d}t$ so small that $P(\boldsymbol{\xi}^{(j)}, \boldsymbol{\xi}^{(k)})N^* \ll 1$. Then, the number of the pairs in the cell $\mathbf{d}\boldsymbol{X}^*$ that collide in the time interval $\mathrm{d}t$ is much smaller than the number N^* of the particles there. Therefore, a particle rarely has a chance to collide more than once in $\mathrm{d}t$. In conventional computation, the computation is continued or the second collision is neglected, if this happens in the process.[7]

The probability given by Eq. (B.17), where d_m is contained, is for molecules with a finite range of force. For molecules with an intermolecular force of infinite range ($d_m = \infty$), setting $\bar{P}^{(s)}(\boldsymbol{\xi}^{(j)}, \boldsymbol{\xi}^{(k)}) = 0$ in Eq. (B.15) when $|(\boldsymbol{\xi}^{(k)} - \boldsymbol{\xi}^{(j)}) \cdot \boldsymbol{\alpha}^{(s)}|$ is smaller than a small value chosen appropriately, then we get the result for a cutoff intermolecular potential. The cutoff is a natural one that corresponds to the convergence of the collision integral considered as a whole, or a forced cutoff, depending on the choice of the effective range of $|(\boldsymbol{\xi}^{(k)} - \boldsymbol{\xi}^{(j)}) \cdot \boldsymbol{\alpha}^{(s)}|$.

The process of DSMC method is a simple one as stated above. Some additional comments on the initial condition and the boundary condition may be in order.

The initial position $\boldsymbol{X}_{(l)}^{(j)}$ and velocity $\boldsymbol{\xi}_{(l)}^{(j)}$ of the particles are determined from the initial condition by the procedure described in Section B.1.2. In practical computation, however, the following method, which is in harmony with the flow of DSMC computation, is widely used. First choose the total number N of the particles, on which the accuracy of the solution depends. From the initial velocity distribution function, compute the initial density distribution $\rho(\boldsymbol{X}, 0)$. Determine the initial number $N^{(l)}$ of the particles in the cell $\mathbf{d}\boldsymbol{X}^{(l)}$ in such a way that it is proportional to $\rho(\boldsymbol{X}^{(l)}, 0)\mathbf{d}\boldsymbol{X}^{(l)}$. The velocities of these $N^{(l)}$ particles are determined according to the initial velocity distribution $f(\boldsymbol{X}^{(l)}, \boldsymbol{\xi}, 0)$. That is, for each particle in $\mathbf{d}\boldsymbol{X}^{(l)}$, its initial velocity $\boldsymbol{\xi}_{(l)}^{(j)}$ is chosen by the trial finding $\boldsymbol{\xi}$ in a small range $\mathbf{d}\boldsymbol{\xi}$ around $\boldsymbol{\xi}_{(l)}^{(j)}$ under the probability $f(\boldsymbol{X}^{(l)}, \boldsymbol{\xi}_{(l)}^{(j)}, 0)\mathbf{d}\boldsymbol{\xi}/\rho(\boldsymbol{X}^{(l)}, 0)$.[8] From the above initial $N^{(l)}$ and Eq. (B.11a) with the initial density, the constant Δ is determined. Incidentally, the number $N^{(l)}$ of the particles in the cell $\mathbf{d}\boldsymbol{X}^{(l)}$ and the total number N of the particles generally vary with time.

The boundary condition is assumed to be given by the scattering kernel [see Eqs. (1.26) and (1.30)]. The boundary surface is divided into small domains $\mathrm{d}S^{(r)}$ corresponding to the division of the $\boldsymbol{X}$ domain into $\mathbf{d}\boldsymbol{X}^{(l)}$. First consider

[7] If this produces a nonnegligible effect, the choice of the parameters [$\mathbf{d}\boldsymbol{X}^{(l)}$, Δ (or N), $\mathrm{d}t$] is inappropriate.

[8] This division of the velocity space is only for the determination of initial particle velocities and is not retained in the later times.

the case of a simple boundary (Section 1.6.1). Define $R_B(\boldsymbol{\xi}, \widetilde{\boldsymbol{\xi}}, \boldsymbol{X}, t)$ by

$$R_B(\boldsymbol{\xi}, \widetilde{\boldsymbol{\xi}}, \boldsymbol{X}, t) = -K_B(\boldsymbol{\xi}, \widetilde{\boldsymbol{\xi}}, \boldsymbol{X}, t)(\boldsymbol{\xi} - \boldsymbol{v}_w) \cdot \boldsymbol{n}/(\widetilde{\boldsymbol{\xi}} - \boldsymbol{v}_w) \cdot \boldsymbol{n}, \tag{B.18}$$

where K_B is introduced in Eq. (1.26). The representative value of $R_B(\boldsymbol{\xi}, \widetilde{\boldsymbol{\xi}}, \boldsymbol{X}, t)$ in $\mathrm{d}S^{(r)}$ between the time interval $(t, t+\mathrm{d}t)$ (or simply at t) is denoted by $R_B^{(r)}(\boldsymbol{\xi}, \widetilde{\boldsymbol{\xi}})$. Let a particle with velocity $\widetilde{\boldsymbol{\xi}}$ arrive at the boundary $\mathrm{d}S^{(r)}$ at $t + c\mathrm{d}t$ before the end of the time interval $t+\mathrm{d}t$ when the step (i) is performed. Then, the velocity $\boldsymbol{\xi}$ of the particle after the collision with the boundary is chosen by the probability $R_B^{(r)}(\boldsymbol{\xi}, \widetilde{\boldsymbol{\xi}})\mathbf{d}\boldsymbol{\xi}$, where the size of $\mathbf{d}\boldsymbol{\xi}$ should be chosen appropriately in the computation and $\boldsymbol{\xi}$ is its representative value, and the particle is shifted with this velocity for the remaining time interval $(1 - c)\mathrm{d}t$ according to the step (i). For example, for the specular-reflection condition (1.25), the velocity of the particle after the collision is uniquely given by

$$\boldsymbol{\xi} = \widetilde{\boldsymbol{\xi}} - 2[(\widetilde{\boldsymbol{\xi}} - \boldsymbol{v}_w^{(r)}) \cdot \boldsymbol{n}^{(r)}]\boldsymbol{n}^{(r)},$$

and for the diffuse-reflection condition (1.24a), the probability $R_B^{(r)}(\boldsymbol{\xi}, \widetilde{\boldsymbol{\xi}})\mathbf{d}\boldsymbol{\xi}$ is given by

$$R_B^{(r)}(\boldsymbol{\xi}, \widetilde{\boldsymbol{\xi}})\mathbf{d}\boldsymbol{\xi} = \frac{(\boldsymbol{\xi} - \boldsymbol{v}_w^{(r)}) \cdot \boldsymbol{n}^{(r)}}{2\pi(RT_w^{(r)})^2} \exp\left(-\frac{(\boldsymbol{\xi} - \boldsymbol{v}_w^{(r)})^2}{2RT_w^{(r)}}\right) \mathbf{d}\boldsymbol{\xi},$$

where $\boldsymbol{v}_w^{(r)}$, $T_w^{(r)}$, and $\boldsymbol{n}^{(r)}$ are their representative values in $\mathrm{d}S^{(r)}$. In the latter case, the probability is independent of $\widetilde{\boldsymbol{\xi}}$.

Next, consider the case of an interface of a gas and its condensed phase (Section 1.6.2). Similarly to the case of the simple boundary, let $R_I(\boldsymbol{\xi}, \widetilde{\boldsymbol{\xi}}, \boldsymbol{X}, t) = -K_I(\boldsymbol{\xi}, \widetilde{\boldsymbol{\xi}}, \boldsymbol{X}, t)(\boldsymbol{\xi} - \boldsymbol{v}_w) \cdot \boldsymbol{n}/(\widetilde{\boldsymbol{\xi}} - \boldsymbol{v}_w) \cdot \boldsymbol{n}$, where K_I is introduced in Eq. (1.30), and let $R_I^{(r)}(\boldsymbol{\xi}, \widetilde{\boldsymbol{\xi}})$ be its representative value in $\mathrm{d}S^{(r)}$ between $(t, t+\mathrm{d}t)$ (or at t). For a particle incident to the interface, it is reflected with the probability $R_I^{(r)}(\boldsymbol{\xi}, \widetilde{\boldsymbol{\xi}})\mathbf{d}\boldsymbol{\xi}$. However, a molecular velocity $\boldsymbol{\xi}$ is not always given to each of the molecules arriving at the boundary (or no reflection occurs for some incident particles), because the kernel K_I (or R_I) does not satisfy the condition corresponding to Eq. (1.27b) on K_B (or R_B). In Eq. (1.30), there is the contribution (or g_I term), which is independent of the incident particles. This contribution is determined in the following way. The number $N_w^{(r)}$ of the particles from the cell $\mathrm{d}S^{(r)}$ between $(t, t+\mathrm{d}t)$ owing to this term is given by

$$N_w^{(r)} = \left(\int_{(\boldsymbol{\xi} - \boldsymbol{v}_w^{(r)}) \cdot \boldsymbol{n}^{(r)} > 0} (\boldsymbol{\xi} - \boldsymbol{v}_w^{(r)}) \cdot \boldsymbol{n}^{(r)} g_I^{(r)} \mathbf{d}\boldsymbol{\xi}\right) \mathrm{d}S^{(r)}\mathrm{d}t/\Delta,$$

where $g_I^{(r)}$ is the corresponding representative value. The velocities of these particles are allotted by the probability

$$(\boldsymbol{\xi} - \boldsymbol{v}_w^{(r)}) \cdot \boldsymbol{n}^{(r)} g_I^{(r)} \mathbf{d}\boldsymbol{\xi} \left(\int_{(\boldsymbol{\xi} - \boldsymbol{v}_w^{(r)}) \cdot \boldsymbol{n}^{(r)} > 0} (\boldsymbol{\xi} - \boldsymbol{v}_w^{(r)}) \cdot \boldsymbol{n}^{(r)} g_I^{(r)} \mathbf{d}\boldsymbol{\xi}\right)^{-1},$$

and their positions are shifted from $\mathrm{d}S^{(r)}$ according to the step (i) until $t+\mathrm{d}t$, where the initial position and time of the particles are distributed, for example, uniformly over $\mathrm{d}S^{(r)}$ and $(t, t+\mathrm{d}t)$. For the complete-condensation condition (1.29), for example, there is no kernel K_I part, and

$$N_w^{(r)} = \rho_w (RT_w^{(r)}/2\pi)^{1/2} \mathrm{d}S^{(r)} \mathrm{d}t/\Delta,$$
$$\text{the probability} = \frac{(\boldsymbol{\xi} - \boldsymbol{v}_w^{(r)}) \cdot \boldsymbol{n}^{(r)}}{2\pi (RT_w^{(r)})^2} \exp\left(-\frac{(\boldsymbol{\xi} - \boldsymbol{v}_w^{(r)})^2}{2RT_w^{(r)}} \right) \mathbf{d}\boldsymbol{\xi}.$$

B.1.4 Theoretical background of DSMC method

In the DSMC method, whose process of computation is described in the preceding subsection (Section B.1.3), direct solution of the Boltzmann equation is not considered, but a large number of particles (or delta functions) that approximate the velocity distribution function are taken, and their motions (translation and collision) are simulated by the rules constructed on the basis of the assumptions in the derivation of the Boltzmann equation. Thus, the behavior of the macroscopic variables is expected to approach the corresponding solution of the Boltzmann equation when the number of the particles is increased indefinitely. However, in the description of Section B.1.3, the relation between the solutions of the two systems is not so transparent as that between the solution of the finite-difference method and that of the Boltzmann equation. Here, we discuss this direct relation in an elementary way without detailed rigor, which is accessible to nonmathematicians, for the purpose to give the understanding of their relation at the level of the understanding of the relation of a finite-difference system to the original equation shared among nonmathematicians. Its rigorous mathematical discussion is given by Wagner [1992].

We introduce the moment equation (or weak form) of the Boltzmann equation (B.12a), which is obtained by multiplying a function $\varphi(\boldsymbol{X}, \boldsymbol{\xi})$ of $\boldsymbol{X}$ and $\boldsymbol{\xi}$ and integrating with respect to $\boldsymbol{X}$ and $\boldsymbol{\xi}$ over the gas region D and the whole space of $\boldsymbol{\xi}$. For $\varphi(\boldsymbol{X}, \boldsymbol{\xi})$ whose support with respect to $\boldsymbol{X}$ is compact and lies inside the gas region D, it is given in the following form after integration by part:

$$\frac{\partial}{\partial t}[\varphi, f] - \left[\xi_i \frac{\partial \varphi}{\partial X_i} + F_i \frac{\partial \varphi}{\partial \xi_i}, f \right] = [\varphi, J(f, f)], \tag{B.19}$$

where $[g, h]$ is the inner product of functions $g(\boldsymbol{X}, \boldsymbol{\xi})$ and $h(\boldsymbol{X}, \boldsymbol{\xi})$ of $\boldsymbol{X}$ and $\boldsymbol{\xi}$ defined by

$$[g(\boldsymbol{X}, \boldsymbol{\xi}), h(\boldsymbol{X}, \boldsymbol{\xi})] = \int_{\boldsymbol{X}:\,\text{gas region, all } \boldsymbol{\xi}} g(\boldsymbol{X}, \boldsymbol{\xi}) h(\boldsymbol{X}, \boldsymbol{\xi}) \mathbf{d}\boldsymbol{X} \mathbf{d}\boldsymbol{\xi}. \tag{B.20}$$

From Eq. (B.19), the moment of the velocity distribution function f at $t+\mathrm{d}t$ is expressed in the form

$$[\varphi, f_{(1)}] = [\varphi, f_{(0)}] + \left[\xi_i \frac{\partial \varphi}{\partial X_i} + F_{i(0)} \frac{\partial \varphi}{\partial \xi_i}, f_{(0)} \right] \mathrm{d}t + [\varphi, J(f_{(0)}, f_{(0)})] \mathrm{d}t + O[(\mathrm{d}t)^2],$$

where[9]

$$f_{(0)} = f(\boldsymbol{X}, \boldsymbol{\xi}, t), \quad f_{(1)} = f(\boldsymbol{X}, \boldsymbol{\xi}, t + \mathrm{d}t), \quad \boldsymbol{F}_{(0)} = \boldsymbol{F}(\boldsymbol{X}, \boldsymbol{\xi}, t).$$

The terms of the order of $(\mathrm{d}t)^2$ being neglected, the moment $[\varphi, f_{(1)}]$ is given by

$$[\varphi, f_{(1)}] = [\varphi(\boldsymbol{X}+\boldsymbol{\xi}\mathrm{d}t, \boldsymbol{\xi} + \boldsymbol{F}_{(0)}\mathrm{d}t), f_{(0)}] + [\varphi(\boldsymbol{X}, \boldsymbol{\xi}), J(f_{(0)}, f_{(0)})]\mathrm{d}t. \tag{B.21}$$

Let f^A and f^B be defined by the equations

$$[\varphi, f^A] = [\varphi(\boldsymbol{X}+\boldsymbol{\xi}\mathrm{d}t, \boldsymbol{\xi} + \boldsymbol{F}_{(0)}\mathrm{d}t), f_{(0)}], \tag{B.22a}$$

$$[\varphi, f^B] = [\varphi(\boldsymbol{X}, \boldsymbol{\xi}), J(f_{(0)}, f_{(0)})]\mathrm{d}t. \tag{B.22b}$$

Then, the velocity distribution function $f_{(1)}$ at $t+\mathrm{d}t$ is given by their sum, i.e.,

$$f_{(1)} = f^A + f^B. \tag{B.23}$$

Especially when $\boldsymbol{F}= \boldsymbol{0}$ and $f_{(0)}$ is independent of $\boldsymbol{X}$, $f_{(1)}$ is simply given by

$$f_{(1)} = f_{(0)} + f^B. \tag{B.24}$$

In fact, in Eq. (B.22a) for f^A, putting $\boldsymbol{F}= \boldsymbol{0}$, changing the variable of integration ($\boldsymbol{X}\to\boldsymbol{X}-\boldsymbol{\xi}\mathrm{d}t$, $\boldsymbol{\xi} \to \boldsymbol{\xi}$), and noting that $f_{(0)}$ is independent of $\boldsymbol{X}$, we have $[\varphi, f^A] = [\varphi, f_{(0)}]$, i.e., $f^A = f_{(0)}$.

Substituting the expression (B.1b) of $f_{(0)}$ into Eq. (B.22a), we have

$$[\varphi, f^A] = \Delta \sum_{l=1}^{M} \sum_{j=1}^{N^{(l)}} \varphi(\boldsymbol{X}_{(l)}^{(j)}+\boldsymbol{\xi}_{(l)}^{(j)}\mathrm{d}t, \boldsymbol{\xi}_{(l)}^{(j)} + \boldsymbol{F}_{(0)}(\boldsymbol{X}_{(l)}^{(j)}, \boldsymbol{\xi}_{(l)}^{(j)})\mathrm{d}t). \tag{B.25}$$

The expression (B.25) being valid for arbitrary φ, the function f^A is expressed in the form

$$f^A = \Delta \sum_{l=1}^{M} \sum_{j=1}^{N^{(l)}} \delta(\boldsymbol{X}-\boldsymbol{X}_{(l)}^{(j)} - \boldsymbol{\xi}_{(l)}^{(j)}\mathrm{d}t)\delta(\boldsymbol{\xi} - \boldsymbol{\xi}_{(l)}^{(j)} - \boldsymbol{F}_{(0)}(\boldsymbol{X}_{(l)}^{(j)}, \boldsymbol{\xi}_{(l)}^{(j)})\mathrm{d}t). \tag{B.26}$$

Comparing Eq. (B.26) with Eq. (B.1b), we find that f^A is obtained from the initial distribution (B.1b) only by translation of the variables $\boldsymbol{X} \to \boldsymbol{X}-\boldsymbol{X}_{(l)}^{(j)} - \boldsymbol{\xi}_{(l)}^{(j)}\mathrm{d}t$ and $\boldsymbol{\xi} \to \boldsymbol{\xi} - \boldsymbol{\xi}_{(l)}^{(j)} - \boldsymbol{F}_{(0)}(\boldsymbol{X}_{(l)}^{(j)}, \boldsymbol{\xi}_{(l)}^{(j)})\mathrm{d}t$. Thus, $[\varphi, f^A]$ is the corresponding moment.

Consider the moment $[\varphi, f^B]$, which is the contribution of molecular collisions to the moment $[\varphi, f_{(1)}]$. For $\varphi(\boldsymbol{X}, \boldsymbol{\xi})$ in the form $\varphi(\boldsymbol{X}, \boldsymbol{\xi}) = \Psi(\boldsymbol{X})\Phi(\boldsymbol{\xi})$,

[9]The subscripts (0) and (1) are used to indicate the value of the time variable t, i.e., (0) for $t = t$ and (1) for $t = t+\mathrm{d}t$. They do not specify the variables $\boldsymbol{X}$ and $\boldsymbol{\xi}$. When they have to be specified, they are shown as the arguments of the corresponding function, e.g., $f_{(1)}(\boldsymbol{X}^*, \boldsymbol{\xi})$, which means $f(\boldsymbol{X}^*, \boldsymbol{\xi}, t+\mathrm{d}t)$.

where $\Psi(\boldsymbol{X})$ has a support containing $\boldsymbol{X}^*$ and of the size L^* and $\int \Psi(\boldsymbol{X})\mathbf{d}\boldsymbol{X}=1$, it is easily seen that

$$[\varphi, f^B] = \left\langle \Phi(\boldsymbol{\xi}), f^B(\boldsymbol{X}^*, \boldsymbol{\xi}) \right\rangle + O((L^*)^3), \tag{B.27}$$

where

$$\left\langle \bar{g}(\boldsymbol{\xi}), \bar{h}(\boldsymbol{\xi}) \right\rangle = \int_{\text{all } \boldsymbol{\xi}} \bar{g}(\boldsymbol{\xi})\bar{h}(\boldsymbol{\xi})\mathbf{d}\boldsymbol{\xi}. \tag{B.28}$$

On the other hand, from Eqs.(B.22b) and (1.10),

$$\begin{aligned}[\varphi, f^B] &= \mathrm{d}t \int_D \Psi(\boldsymbol{X}) \left\{ \frac{1}{2m} \int [\Phi(\boldsymbol{\xi}') + \Phi(\boldsymbol{\xi}'_*) - \Phi(\boldsymbol{\xi}) - \Phi(\boldsymbol{\xi}_*)] \right. \\ &\qquad \left. \times f_{(0)}(\boldsymbol{X}, \boldsymbol{\xi}) f_{(0)}(\boldsymbol{X}, \boldsymbol{\xi}_*) B \mathrm{d}\Omega(\boldsymbol{\alpha}) \mathbf{d}\boldsymbol{\xi}_* \mathbf{d}\boldsymbol{\xi} \right\} \mathbf{d}\boldsymbol{X} \\ &= \frac{\mathrm{d}t}{2m} \int [\Phi(\boldsymbol{\xi}') + \Phi(\boldsymbol{\xi}'_*) - \Phi(\boldsymbol{\xi}) - \Phi(\boldsymbol{\xi}_*)] \\ &\qquad \times f_{(0)}(\boldsymbol{X}^*, \boldsymbol{\xi}) f_{(0)}(\boldsymbol{X}^*, \boldsymbol{\xi}_*) B \mathrm{d}\Omega(\boldsymbol{\alpha}) \mathbf{d}\boldsymbol{\xi}_* \mathbf{d}\boldsymbol{\xi} + O((L^*)^3), \end{aligned} \tag{B.29}$$

where

$$\boldsymbol{\xi}' = \boldsymbol{\xi} + [(\boldsymbol{\xi}_* - \boldsymbol{\xi}) \cdot \boldsymbol{\alpha}]\boldsymbol{\alpha}, \qquad \boldsymbol{\xi}'_* = \boldsymbol{\xi}_* - [(\boldsymbol{\xi}_* - \boldsymbol{\xi}) \cdot \boldsymbol{\alpha}]\boldsymbol{\alpha}.$$

From Eqs. (B.27) and (B.29), in the limit as $L^* \to 0$,

$$\begin{aligned}&\left\langle \Phi(\boldsymbol{\xi}), f^B(\boldsymbol{X}^*, \boldsymbol{\xi}) \right\rangle \\ &= \frac{\mathrm{d}t}{2m} \int [\Phi(\boldsymbol{\xi}') + \Phi(\boldsymbol{\xi}'_*) - \Phi(\boldsymbol{\xi}) - \Phi(\boldsymbol{\xi}_*)] f_{(0)}(\boldsymbol{X}^*, \boldsymbol{\xi}) f_{(0)}(\boldsymbol{X}^*, \boldsymbol{\xi}_*) B \mathrm{d}\Omega(\boldsymbol{\alpha}) \mathbf{d}\boldsymbol{\xi}_* \mathbf{d}\boldsymbol{\xi}. \end{aligned} \tag{B.30}$$

An arbitrary moment $\left\langle \Phi(\boldsymbol{\xi}), f^B(\boldsymbol{X}^*, \boldsymbol{\xi}) \right\rangle$ of $f^B(\boldsymbol{X}^*, \boldsymbol{\xi})$, with respect to $\boldsymbol{\xi}$, at $\boldsymbol{X}^*$ is determined by $f_{(0)}$ at the same point $\boldsymbol{X}^*$.

Now, take the velocity distribution function at a point of space given by Eq. (B.1a). That is, for the point $\boldsymbol{X}^*$,

$$f_{(0)}(\boldsymbol{X}^*, \boldsymbol{\xi})\mathbf{d}\boldsymbol{X}^* = \Delta \sum_{j=1}^{N^*} \delta(\boldsymbol{\xi} - \boldsymbol{\xi}^{(j)}), \tag{B.31}$$

where the cell $\mathbf{d}\boldsymbol{X}^{(l)}$ that contains $\boldsymbol{X}^*$ is denoted by $\mathbf{d}\boldsymbol{X}^*$. Then, Eq. (B.30) is expressed as

$$\begin{aligned}&\left\langle \Phi(\boldsymbol{\xi}), f^B(\boldsymbol{X}^*, \boldsymbol{\xi}) \right\rangle \\ &= \frac{\mathrm{d}t}{m} \frac{\Delta^2}{(\mathbf{d}\boldsymbol{X}^*)^2} \sum_{j=1}^{N^*-1} \sum_{k=j+1}^{N^*} \int_{\text{all } \boldsymbol{\alpha}} [\Phi(\bar{\boldsymbol{\xi}}^{(j)}) + \Phi(\bar{\boldsymbol{\xi}}^{(k)}) - \Phi(\boldsymbol{\xi}^{(j)}) - \Phi(\boldsymbol{\xi}^{(k)})] \\ &\qquad \times B(|(\boldsymbol{\xi}^{(k)} - \boldsymbol{\xi}^{(j)}) \cdot \boldsymbol{\alpha}|/|\boldsymbol{\xi}^{(k)} - \boldsymbol{\xi}^{(j)}|, |\boldsymbol{\xi}^{(k)} - \boldsymbol{\xi}^{(j)}|)\mathrm{d}\Omega(\boldsymbol{\alpha}), \end{aligned} \tag{B.32}$$

where

$$\overline{\boldsymbol{\xi}}^{(j)} = \boldsymbol{\xi}^{(j)} + [(\boldsymbol{\xi}^{(k)} - \boldsymbol{\xi}^{(j)}) \cdot \boldsymbol{\alpha}]\boldsymbol{\alpha}, \quad \overline{\boldsymbol{\xi}}^{(k)} = \boldsymbol{\xi}^{(k)} - [(\boldsymbol{\xi}^{(k)} - \boldsymbol{\xi}^{(j)}) \cdot \boldsymbol{\alpha}]\boldsymbol{\alpha}. \quad \text{(B.33)}$$

The moment $\left\langle \Phi(\boldsymbol{\xi}), f^B(\boldsymbol{X}^*, \boldsymbol{\xi}) \right\rangle$ of f^B with respect to $\boldsymbol{\xi}$ at an arbitrary point $\boldsymbol{X}^*$ is expressed by Eq. (B.32) with the information of the initial distribution function (B.31). The moment $[\varphi, f^B]$ of f^B with respect to $\boldsymbol{X}$ and $\boldsymbol{\xi}$ is obtained from this expression. Thus, following the process explained in Section B.1.2, we can obtain the expression of f^B in the form of Eqs. (B.1a) and (B.1b).

Up to this point, we have discussed the variation of the velocity distribution function f on the basis of the Boltzmann equation (B.12a). That is, we have derived the formulas of the velocity distribution function and its moments at time $t+\mathrm{d}t$ from the velocity distribution function given in the forms (B.1a) and (B.1b) at time t. Now we will show that the velocity distribution function (or the moments of the velocity distribution function) at time $t+\mathrm{d}t$ obtained by the DSMC process from that at t given in the forms (B.1a) and (B.1b) agrees with the above expression derived from the Boltzmann equation.

From Eq. (B.26), the velocity distribution function (B.13) that is obtained by the step (i) of the process of the DSMC computation is obviously the solution f^A of Eq. (B.22a). Thus, we here discuss the relation between the result of the step (iii) (or the collision of particles) and the solution f^B of Eq. (B.22b), for which the discussion in a cell is sufficient.

Let the velocity distribution function $f_{(0)}$ at time t be given by Eq. (B.1a). That is, the velocity distribution function $f_{(0)}$ and its moment $\left\langle \Phi(\boldsymbol{\xi}), f_{(0)}(\boldsymbol{\xi}) \right\rangle$ in the cell $\mathbf{d}\boldsymbol{X}^*$ with representing point $\boldsymbol{X}^*$ are given by

$$f_{(0)}(\boldsymbol{X}^*, \boldsymbol{\xi}) = \frac{\Delta}{\mathbf{d}\boldsymbol{X}^*} \sum_{j=1}^{N^*} \delta(\boldsymbol{\xi} - \boldsymbol{\xi}^{(j)}), \quad \text{(B.34)}$$

$$\left\langle \Phi(\boldsymbol{\xi}), f_{(0)}(\boldsymbol{X}^*, \boldsymbol{\xi}) \right\rangle = \frac{\Delta}{\mathbf{d}\boldsymbol{X}^*} \sum_{j=1}^{N^*} \Phi(\boldsymbol{\xi}^{(j)}). \quad \text{(B.35)}$$

We carry out the step (iii) in Section B.1.3 to the particles arranged according to Eq. (B.34). After the trial for each of $N^*(N^*-1)/2$ pairs (j,k) that determines the collision of the pair, let the pair (j_n, k_n), where $j_n < k_n$, $n = 1, 2, \ldots, N_c$, make the collision with $\boldsymbol{\alpha}$ in $\mathrm{d}\Omega^{(s_n)}$ whose representative point is $\boldsymbol{\alpha}^{(s_n)}$. Here we assume that j_n and k_n $(n = 1, \ldots, N_c)$ are all different [see the paragraph next to that containing Eq. (B.17)]. Then the velocities $(\boldsymbol{\xi}^{(j_n)}, \boldsymbol{\xi}^{(k_n)})$ of the pair (j_n, k_n) are transformed to the velocities $(\widehat{\boldsymbol{\xi}}^{(j_n)}, \widehat{\boldsymbol{\xi}}^{(k_n)})$:

$$\widehat{\boldsymbol{\xi}}^{(j_n)} = \boldsymbol{\xi}^{(j_n)} + [(\boldsymbol{\xi}^{(k_n)} - \boldsymbol{\xi}^{(j_n)}) \cdot \boldsymbol{\alpha}^{(s_n)}]\boldsymbol{\alpha}^{(s_n)}, \quad \text{(B.36a)}$$

$$\widehat{\boldsymbol{\xi}}^{(k_n)} = \boldsymbol{\xi}^{(k_n)} - [(\boldsymbol{\xi}^{(k_n)} - \boldsymbol{\xi}^{(j_n)}) \cdot \boldsymbol{\alpha}^{(s_n)}]\boldsymbol{\alpha}^{(s_n)}. \quad \text{(B.36b)}$$

For the pairs (j,k) that do not collide, the velocities $(\boldsymbol{\xi}^{(j)}, \boldsymbol{\xi}^{(k)})$ are kept unchanged. As the result of this trial, the velocity distribution and its moment at

$t+\mathrm{d}t$, are transformed from Eqs. (B.34) and (B.35) to

$$S_{(\mathrm{iii})}\left\{f_{(0)}\right\}_{\mathbf{d}\boldsymbol{X}^*} = \frac{\Delta}{\mathbf{d}\boldsymbol{X}^*}\left[\sum_{\substack{j=1\\(j\neq j_n,k_n)}}^{N^*}\delta(\boldsymbol{\xi}-\boldsymbol{\xi}^{(j)}) + \sum_{n=1}^{N_c}\left(\delta(\boldsymbol{\xi}-\widehat{\boldsymbol{\xi}}^{(j_n)}) + \delta(\boldsymbol{\xi}-\widehat{\boldsymbol{\xi}}^{(k_n)})\right)\right], \quad \text{(B.37)}$$

$$\left\langle \Phi(\boldsymbol{\xi}), S_{(\mathrm{iii})}\left\{f_{(0)}\right\}_{\mathbf{d}\boldsymbol{X}^*}\right\rangle = \frac{\Delta}{\mathbf{d}\boldsymbol{X}^*}\left[\sum_{\substack{j=1\\(j\neq j_n,k_n)}}^{N^*}\Phi(\boldsymbol{\xi}^{(j)}) + \sum_{n=1}^{N_c}\left(\Phi(\widehat{\boldsymbol{\xi}}^{(j_n)}) + \Phi(\widehat{\boldsymbol{\xi}}^{(k_n)})\right)\right], \quad \text{(B.38)}$$

where $S_{(\mathrm{iii})}\left\{f_{(0)}\right\}$ is the result of the step (iii) on $f_{(0)}$ and the subscript $\mathbf{d}\boldsymbol{X}^*$ indicates that the indicated operation is carried out in the cell $\mathbf{d}\boldsymbol{X}^*$.

Now we will show that the DSMC result is consistent with the solution of the Boltzmann equation. For this purpose, the following random variables[10] Z_{jk} for the independent $N^*(N^*-1)/2$ trials are introduced:

$$Z_{jk} = \begin{cases} \Phi(\widehat{\boldsymbol{\xi}}^{(j)}) + \Phi(\widehat{\boldsymbol{\xi}}^{(k)}) - \Phi(\boldsymbol{\xi}^{(j)}) - \Phi(\boldsymbol{\xi}^{(k)}) \\ \text{when the pair } (j,k) \text{ collides,} \\ 0 \quad \text{when the pair } (j,k) \text{ does not collide,} \end{cases} \quad \text{(B.39)}$$

where $\widehat{\boldsymbol{\xi}}^{(j)}$ and $\widehat{\boldsymbol{\xi}}^{(k)}$ are given by Eqs. (B.36a) and (B.36b). Then, the random variable Z is defined by their sum

$$Z = \frac{\Delta}{\mathbf{d}\boldsymbol{X}^*}\sum_{j=1}^{N^*-1}\sum_{k=j+1}^{N^*} Z_{jk}. \quad \text{(B.40)}$$

The variable Z takes the following value $\hat{Z}$ when the pair (j_n, k_n) with $n = 1,\ldots,N_c$ makes the collision with $\boldsymbol{\alpha}^{(s_n)}$ and the other pairs make no collision:[11]

$$\hat{Z} = \frac{\Delta}{\mathbf{d}\boldsymbol{X}^*}\sum_{n=1}^{N_c}\left(\Phi(\widehat{\boldsymbol{\xi}}^{(j_n)}) + \Phi(\widehat{\boldsymbol{\xi}}^{(k_n)}) - \Phi(\boldsymbol{\xi}^{(j_n)}) - \Phi(\boldsymbol{\xi}^{(k_n)})\right). \quad \text{(B.41)}$$

From Eqs. (B.35) and (B.38), the value $\hat{Z}$ is equal to the difference of the moment of the velocity distribution function after the step (iii) and that before the step.

$$\hat{Z} = \left\langle \Phi(\boldsymbol{\xi}), S_{(\mathrm{iii})}\left\{f_{(0)}\right\}_{\mathbf{d}\boldsymbol{X}^*}\right\rangle - \left\langle \Phi(\boldsymbol{\xi}), f_{(0)}(\boldsymbol{X}^*,\boldsymbol{\xi})\right\rangle. \quad \text{(B.42)}$$

[10] See, e.g., Feller [1968], Parzen [1960], or Rényi [1966].

[11] The $\hat{Z}$ is the value that the random variable Z takes as the result of a trial.

Now consider the expectation $\mathrm{Ep}(Z_{jk})$ of Z_{jk}. From Eqs. (B.15) and (B.39), it is expressed in the form

$$\begin{aligned}\mathrm{Ep}(Z_{jk}) &= \sum_s \left(\Phi(\widehat{\boldsymbol{\xi}}^{(j)}) + \Phi(\widehat{\boldsymbol{\xi}}^{(k)}) - \Phi(\boldsymbol{\xi}^{(j)}) - \Phi(\boldsymbol{\xi}^{(k)})\right) \bar{P}^{(s)}(\boldsymbol{\xi}^{(j)}, \boldsymbol{\xi}^{(k)}) \mathrm{d}\Omega^{(s)} \\ &= \frac{\Delta \mathrm{d}t}{m \mathbf{d}\boldsymbol{X}^*} \sum_s \left(\Phi(\widehat{\boldsymbol{\xi}}^{(j)}) + \Phi(\widehat{\boldsymbol{\xi}}^{(k)}) - \Phi(\boldsymbol{\xi}^{(j)}) - \Phi(\boldsymbol{\xi}^{(k)})\right) \\ &\qquad \times B(|(\boldsymbol{\xi}^{(k)} - \boldsymbol{\xi}^{(j)}) \cdot \boldsymbol{\alpha}^{(s)}|/|\boldsymbol{\xi}^{(k)} - \boldsymbol{\xi}^{(j)}|, |\boldsymbol{\xi}^{(k)} - \boldsymbol{\xi}^{(j)}|) \mathrm{d}\Omega^{(s)}. \quad \text{(B.43)}\end{aligned}$$

From Eqs. (B.40) and (B.43), the expectation $\mathrm{Ep}(Z)$ of Z is expressed as

$$\begin{aligned}\mathrm{Ep}(Z) &= \frac{\Delta}{\mathbf{d}\boldsymbol{X}^*} \sum_{j=1}^{N^*-1} \sum_{k=j+1}^{N^*} \mathrm{Ep}(Z_{jk}) \\ &= \frac{\Delta^2 \mathrm{d}t}{m(\mathbf{d}\boldsymbol{X}^*)^2} \sum_{j=1}^{N^*-1} \sum_{k=j+1}^{N^*} \sum_s \left(\Phi(\widehat{\boldsymbol{\xi}}^{(j)}) + \Phi(\widehat{\boldsymbol{\xi}}^{(k)}) - \Phi(\boldsymbol{\xi}^{(j)}) - \Phi(\boldsymbol{\xi}^{(k)})\right) \\ &\qquad \times B(|(\boldsymbol{\xi}^{(k)} - \boldsymbol{\xi}^{(j)}) \cdot \boldsymbol{\alpha}^{(s)}|/|\boldsymbol{\xi}^{(k)} - \boldsymbol{\xi}^{(j)}|, |\boldsymbol{\xi}^{(k)} - \boldsymbol{\xi}^{(j)}|) \mathrm{d}\Omega^{(s)}. \quad \text{(B.44)}\end{aligned}$$

Comparing Eq. (B.44) with Eq. (B.32), we find that the expectation $\mathrm{Ep}(Z)$ approaches the right-hand side of Eq. (B.32) as $\mathrm{d}\Omega^{(s)} \to 0$. That is,

$$\left\langle \Phi(\boldsymbol{\xi}), f^B(\boldsymbol{X}^*, \boldsymbol{\xi}) \right\rangle = \mathrm{Ep}(Z) \qquad \text{as } \mathrm{d}\Omega^{(s)} \to 0. \quad \text{(B.45)}$$

The velocity distribution function $f^B(\boldsymbol{X}^*, \boldsymbol{\xi})$ is expressed by the expectation $\mathrm{Ep}(Z)$ of the random variable Z related to the step (iii) of the DSMC process.

According to the *law of large number* (see Feller [1968], Parzen [1960], Rényi [1966]), the expectation $\mathrm{Ep}(Z)$ is approximately obtained by taking the average of the results of very large repetitions of the trial consisting of the $N^*(N^*-1)/2$ independent trials.[12] Thus, the moment $\left\langle \Phi(\boldsymbol{\xi}), f^B(\boldsymbol{X}^*, \boldsymbol{\xi}) \right\rangle$ corresponding to the initial condition (B.34) is obtained by taking the average of $\hat{Z}$ obtained by many trials of the step (iii) of the DSMC process. Taking the representative value of $\varphi(\boldsymbol{X}, \boldsymbol{\xi})$ in the cell $\mathbf{d}\boldsymbol{X}^*$ as $\Phi(\boldsymbol{\xi})$, computing $\mathrm{Ep}(Z)$ by the DSMC process, and summing it up over all the cells, we find that the result is equal to $[\varphi, f^B]$.

In the above discussion, we found that f^B is obtained by the step (iii) of the DSMC process, but with very many trials of the step (iii). However, when the number N^* of the particles in a cell is very large, which is the basic assumption in the DSMC method, we can show that f^B is obtained approximately by one trial as follows.

The velocities of the particles in the DSMC procedure are $\boldsymbol{\xi}_{(l)}^{(j)}$ (or $\boldsymbol{\xi}^{(j)}$) in the velocity distribution function expressed in the form given by Eq. (B.1a) [or

[12] More explicitly, the probability that the difference between the average of the repeated trials and the expectation of the random variable is less than an arbitrary small value approaches unity as the number of the trials tends to infinity. In the following discussions, we, for convenience, use the expression "(the average of the infinitely many repeated trials) = (the expectation of the random variable) in the probabilistic sense" or "In the limit of infinite trials, the probability that the above equality holds is unity".

(B.34)]. In expressing the velocity distribution function in the form of Eq. (B.1a) [or (B.34)] in Section B.1.2, the $\boldsymbol{\eta}$ space transformed from the $\boldsymbol{\xi}$ space is divided into $N^{(l)}$ (or N^*) of equal volume, and a delta function (a particle in DSMC) is allotted to each of the volumes (say, $\boldsymbol{\xi}$ cell) in the $\boldsymbol{\xi}$ space corresponding to the divided volumes in $\boldsymbol{\eta}$ space. Collecting S neighboring $\boldsymbol{\xi}$ cells, where $S \gg 1$ but $S \ll N^*$, we call it a Ξ cell, and then the particles in $\mathbf{d}\boldsymbol{X}^*$ are grouped into N^*/S of the Ξ cells, in each of which the velocities of the particles are close. The Ξ cells are labeled from 1 to N^*/S. In each Ξ cell, there are S particles, which are labeled from 1 to S. The velocity of the βth particle in the Jth Ξ cell is denoted by $\boldsymbol{\xi}^{(J)}(\beta)$, where $\beta = 1, 2, \ldots, S$ and $J = 1, 2, \ldots, N^*/S$. Corresponding to this labeling, the random variable Z_{jk} is named in more detail. That is, if the jth particle in $\mathbf{d}\boldsymbol{X}^*$ corresponds to the βth particle in the Jth Ξ cell and the kth particle to the γth particle in the Kth Ξ cell, then Z_{jk} is denoted by $Z_{JK}(\beta, \gamma)$. The indices J and K range from 1 to N^*/S, and $J \leq K$ if $j < k$. The indices β and γ range from 1 to S, and $\beta < \gamma$ if $J = K$ but β and γ are arbitrary if $J < K$. Then, the random variable Z defined by Eq. (B.40) is rewritten in the form

$$Z = \frac{\Delta}{\mathbf{d}\boldsymbol{X}^*} \left(\sum_{J=1}^{N^*/S-1} \sum_{K=J+1}^{N^*/S} \sum_{\beta=1}^{S} \sum_{\gamma=1}^{S} Z_{JK}(\beta, \gamma) + \sum_{J=1}^{N^*/S} \sum_{\beta=1}^{S-1} \sum_{\gamma=\beta+1}^{S} Z_{JJ}(\beta, \gamma) \right). \tag{B.46}$$

The second group containing $Z_{JJ}(\beta, \gamma)$ on the right-hand side is the contribution of collisions between particles in the same Ξ cell. The difference of the velocities between particles in the same Ξ cell being small, their probability of collision is small [see Eq. (B.17)] and further the velocity change owing to collision, if occurs, is small (or of the order of the size of Ξ). Thus, the absolute values taken by the random variable $Z_{JJ}(\beta, \gamma)$ are also small [see Eq. (B.39)]. Therefore, their contribution to Eq. (B.46) is small, that is,

$$Z = \frac{\Delta}{\mathbf{d}\boldsymbol{X}^*} \sum_{J=1}^{N^*/S-1} \sum_{K=J+1}^{N^*/S} \sum_{\beta=1}^{S} \sum_{\gamma=1}^{S} Z_{JK}(\beta, \gamma). \tag{B.47}$$

The difference of $\boldsymbol{\xi}$ for different β or γ being small for small Ξ, the random variable $Z_{JK}(\beta, \gamma)$ for a fixed set of (J, K) is independent of (β, γ) and identically distributed irrespective of (β, γ). Therefore, the expectation of Z is given in the form

$$\mathrm{Ep}(Z) = \frac{\Delta S^2}{\mathbf{d}\boldsymbol{X}^*} \sum_{J=1}^{N^*/S-1} \sum_{K=J+1}^{N^*/S} \mathrm{Ep}(Z_{JK}(\beta', \gamma')), \tag{B.48}$$

where $\mathrm{Ep}(Z_{JK}(\beta', \gamma'))$ is the expectation of $Z_{JK}(\beta, \gamma)$ for an arbitrary set (β', γ') of (β, γ). According to the extended law of large number, the sum $\sum_{\beta=1}^{S} \sum_{\gamma=1}^{S} \hat{Z}_{JK}(\beta, \gamma)$ of the result $\hat{Z}_{JK}(\beta, \gamma)$ of the S^2 independent trials is, in the probabilistic sense, equal to

$$\sum_{\beta=1}^{S} \sum_{\gamma=1}^{S} \hat{Z}_{JK}(\beta, \gamma) = S^2 \mathrm{Ep}(Z_{JK}(\beta', \gamma')), \tag{B.49}$$

in the limit that $N^* \to \infty$ and $S \to \infty$ with $N^*/S \to \infty$ and $S^2/N^* \to \infty$. Here the condition $S^2/N^* \to \infty$ is required to the law of large number because the probability $\bar{P}^{(s)}(\boldsymbol{\xi}^{(j)}, \boldsymbol{\xi}^{(k)})\mathrm{d}\Omega^{(s)}$ vanishes with speed $1/N^*$ as $N^* \to \infty$. This is the reason that the adjective "extended" is attached. Supplementary explanation is given in the next paragraph. The condition $N^*/S \to \infty$ is the condition that the Ξ cell is small, which is used to derive Eq. (B.48). On the other hand, from Eq. (B.47),

$$\hat{Z} = \frac{\Delta}{\mathbf{d}\boldsymbol{X}^*} \sum_{J=1}^{N^*/S-1} \sum_{K=J+1}^{N^*/S} \sum_{\beta=1}^{S} \sum_{\gamma=1}^{S} \hat{Z}_{JK}(\beta, \gamma). \tag{B.50}$$

Thus, from Eqs. (B.48), (B.49), and (B.50), $\mathrm{Ep}(Z)$ is given by the result $\hat{Z}$ of a trial of the step (iii), i.e.,

$$\mathrm{Ep}(Z) = \hat{Z}. \tag{B.51}$$

The above discussion shows that carrying out the trials for all the pairs (β, γ) for a given set (J, K) corresponds to carrying out S^2 repeated trials for a representative pair in the (J, K)th Ξ cell.

To supplement the discussion in the preceding paragraph, first consider an event A that occurs with probability p in a trial. The probability $P_N(r)$ that the event A occurs r times in the repeated trials of N times is given by $P_N(r) = [N!/r!(N-r)!]p^r(1-p)^{N-r}$. Then, the probability that r satisfies $r = Np$ [with width εNp (ε : arbitrarily small positive number)] approaches unity in the limit that $N \to \infty$ (the law of large number; see Feller [1968], Parzen [1960], Rényi [1966]). That is, for arbitrarily small ε and δ, if we take $N \geq N_0$, where N_0 depends on ε and δ, then

$$\text{Probability } (|r - Np| < \varepsilon Np) \geq 1 - \delta. \tag{B.52}$$

The corresponding statement for the situation where p depends on N and vanishes ($p \to 0$) as $N \to \infty$ is required in this appendix. With a slight extension of the discussion in Section 17 of Chapter 3 in Rényi [1966], it can be shown that the above statement holds if the condition $Np \to \infty$ as $N \to \infty$ is imposed.[13] An example is given in Fig. B.1. Next, consider a trial where M mutually exclusive events $A_1, A_2, \ldots, A_M$ occur with probabilities of success $p_1, p_2, \ldots, p_M$.

[13] The expression (B.52) is equivalent to

$$\sum_{|r-Np|<\varepsilon Np} \binom{N}{r} p^r (1-p)^{N-r} \geq 1 - \delta,$$

because

$$\text{Probability } (|r - Np| < \varepsilon Np) = \sum_{|r-Np|<\varepsilon Np} \binom{N}{r} p^r (1-p)^{N-r}.$$

From the well-known equality (see p. 102 of Rényi [1966])

$$\sum_{r=0}^{N} (r - Np)^2 \binom{N}{r} p^r (1-p)^{N-r} = Np(1-p),$$

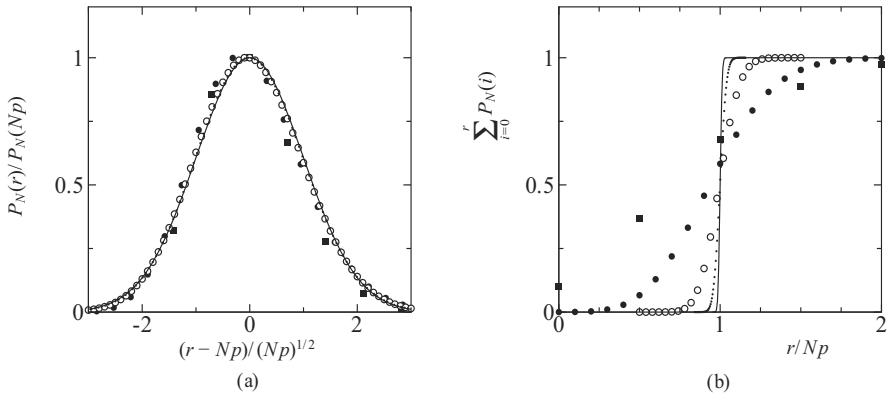

Figure B.1. The extended law of large number for $p = N^{-2/3}$. (a) $P_N(r)/P_N(Np)$ vs $(r - Np)/(Np)^{1/2}$ and (b) $\sum_{i=0}^{r} P_N(i)$ vs r/Np. The black square ■: $N = 8$, the black circle • : $N = 10^3$, the white circle ∘ : $N = 10^6$, and the dot · : $N = 10^9$. The solid line —— is $\exp[-(r - Np)^2/2Np]$ in panel (a) and $N = 10^{12}$ in panel (b).

From the preceding result, the probability that the numbers $r_1, r_2, \ldots, r_M$ of their success satisfy $r_1 r_2 \cdots r_M = N^M p_1 p_2 \cdots p_M$ in its N trials approaches unity in the limit $N \to \infty$ with $Np_1, Np_2, \ldots, Np_M \to \infty$. These statements may be called the *extended* law of large number.

From Eqs. (B.45) and (B.51),

$$\left\langle \Phi(\boldsymbol{\xi}), f^B(\boldsymbol{X}^*, \boldsymbol{\xi}) \right\rangle = \hat{Z}. \tag{B.53}$$

With this result into Eq. (B.42), the result of the step (iii) applied to $f_{(0)}$ is expressed as

$$\left\langle \Phi(\boldsymbol{\xi}), S_{(\mathrm{iii})} \left\{ f_{(0)} \right\}_{\mathbf{d}\boldsymbol{X}^*} \right\rangle = \left\langle \Phi(\boldsymbol{\xi}), f_{(0)}(\boldsymbol{X}^*, \boldsymbol{\xi}) + f^B(\boldsymbol{X}^*, \boldsymbol{\xi}) \right\rangle.$$

Thus,

$$\left[\varphi, S_{(\mathrm{iii})} \left\{ f_{(0)} \right\} \right] = \left[\varphi, f_{(0)}(\boldsymbol{X}, \boldsymbol{\xi}) + f^B(\boldsymbol{X}, \boldsymbol{\xi}) \right], \tag{B.54}$$

---

we have

$$\begin{aligned} Np(1-p) &\geq \sum_{|r-Np| \geq \varepsilon Np} (r - Np)^2 \binom{N}{r} p^r (1-p)^{N-r} \\ &\geq \varepsilon^2 (Np)^2 \sum_{|r-Np| \geq \varepsilon Np} \binom{N}{r} p^r (1-p)^{N-r}, \end{aligned}$$

from which

$$\begin{aligned} \sum_{|r-Np| < \varepsilon Np} \binom{N}{r} p^r (1-p)^{N-r} &= 1 - \sum_{|r-Np| \geq \varepsilon Np} \binom{N}{r} p^r (1-p)^{N-r} \\ &\geq 1 - \frac{1-p}{\varepsilon^2 Np} \geq 1 - \frac{1}{\varepsilon^2 Np}. \end{aligned}$$

Thus, if $Np \to \infty$ as $N \to \infty$, we can choose N_0 such that $Np \geq 1/\delta\varepsilon^2$ for $N \geq N_0$.

or

$$S_{(\mathrm{iii})}\left\{f_{(0)}\right\} = f_{(0)}(\boldsymbol{X},\boldsymbol{\xi}) + f^B(\boldsymbol{X},\boldsymbol{\xi}). \tag{B.55}$$

That is, the velocity distribution function obtained by applying the step (iii) to the initial distribution $f_{(0)}$ is found to be the sum of the initial distribution $f_{(0)}$ and the solution f^B of Eq. (B.22b).

Now, consider the case where the steps (i) and (iii) are applied successively to the initial distribution $f_{(0)}$ (the unit process of DSMC). As we have seen, the step (i) applied to $f_{(0)}$ gives f^A, that is,

$$S_{(\mathrm{i})}\left\{f_{(0)}\right\} = f^A, \tag{B.56}$$

where $S_{(\mathrm{i})}\{f_{(0)}\}$ means that the step (i) is applied to $f_{(0)}$. The application of the step (iii) after the step (i) gives

$$S_{(\mathrm{iii})}\left\{S_{(\mathrm{i})}\left\{f_{(0)}\right\}\right\} = f^A + f^B(f_{(0)} = f^A), \tag{B.57}$$

where Eq. (B.55) is used and $f^B(f_{(0)} = f^A)$ is the solution of Eq. (B.22b) with $f_{(0)} = f^A$. The difference between $f^B(f_{(0)} = f^A)$ and $f^B(f_{(0)} = f_{(0)})$ (or the original f^B) is of the order of $(\mathrm{d}t)^2$, because the difference between f^A and $f_{(0)}$ is of the order of $\mathrm{d}t$. Therefore, we have

$$\begin{aligned} S_{(\mathrm{iii})}\left\{S_{(\mathrm{i})}\left\{f_{(0)}\right\}\right\} &= f^A + f^B \\ &= f_{(1)}, \end{aligned} \tag{B.58}$$

which is the solution of Eq. (B.21). That is, the successive application of the steps (i) and (iii) to the initial distribution gives the solution of the Boltzmann equation at the next time step.

Supplementary remarks on the size of the parameters in the DSMC computation may be in order.

(i) The process from Eq. (B.19) to Eq. (B.21) is done under the assumption of small perturbation. The perturbed term must be small, that is,

$$\frac{[\varphi, J(f_{(0)}, f_{(0)})]\mathrm{d}t}{[\varphi, f_{(0)}]} \ll 1 \quad \text{or} \quad \frac{\left\langle \Phi, J(f_{(0)}, f_{(0)})\right\rangle \mathrm{d}t}{\left\langle \Phi, f_{(0)}\right\rangle} \ll 1.$$

In view of Eqs. (B.15), (B.17), (B.22b), (B.27), (B.32), and (B.35), the following condition is derived from the preceding relation:

$$N^* P(\boldsymbol{\xi}^{(j)}, \boldsymbol{\xi}^{(k)}) \ll 1, \tag{B.59a}$$

or

$$(\rho/m)\pi d_m^2 |\boldsymbol{\xi}|_{\mathrm{rmax}} \mathrm{d}t \ll 1. \tag{B.59b}$$

Here, $|\boldsymbol{\xi}|_{\mathrm{rmax}}$ indicates the size of range of $|\boldsymbol{\xi}|$ where the contribution to f in the computation is not negligible, which is roughly of the order of $(RT)^{1/2}$, and it is not a real maximum of $|\boldsymbol{\xi}|$, which is generally infinite. The relation means that the number $[N^{*2} P(\boldsymbol{\xi}^{(j)}, \boldsymbol{\xi}^{(k)})]$ of the pairs that collided in time $\mathrm{d}t$

in the cell $\mathbf{d}\boldsymbol{X}^*$ is much smaller than the number N^* of the particles in the cell. Thus, we have to choose $\mathrm{d}t$ so as to satisfy the above relation in the numerical computation. When this condition is satisfied, the probability for a particle to make a collision twice in the time interval $\mathrm{d}t$ is small, and therefore the treatment in the paragraph next to that containing Eq. (B.17) in the process of the step (iii) is allowed.
(ii) Consider the integral form of the Boltzmann equation (B.12a), which is derived by integrating the equation along its characteristic (see Section A.4.1). Then the velocity distribution function is expressed by the integral of the collision term along the characteristic from the initial or boundary surface in addition to the initial and boundary terms. The expression of the collision effect in the form of Eq. (B.22b) is allowed only for a narrow time interval where the characteristic is approximated by a straight line. However, the characteristic may pass several $\mathbf{d}\boldsymbol{X}$ cells during $(t, t+\mathrm{d}t)$ even when the condition is satisfied. In this case, the collision effect is not determined by $J(f, f)$ in a single cell but is expressed by a weighted average of $J(f, f)$ on the characteristic. Thus, the expression (B.22b) is valid only when $|\boldsymbol{\xi}|_{\mathrm{emax}}\mathrm{d}t = O(L)$, where L is the size of the cell $\mathbf{d}\boldsymbol{X}$ and $|\boldsymbol{\xi}|_{\mathrm{emax}}$ is the effective maximum speed of the molecules, which is roughly of the order of $|\boldsymbol{v}|_{\max} + (RT)^{1/2}$. The numerical computation should be carried out under the restriction $|\boldsymbol{\xi}|_{\mathrm{emax}}\mathrm{d}t \sim L$.

To summarize, the arbitrary moment of the velocity distribution function (the velocity distribution function itself) after a time interval $\mathrm{d}t$ is obtained from that at time t by the steps (i)–(iii) of the DSMC method explained in Section B.1.3. Thus, repeating the process, we can obtain the velocity distribution function at an arbitrary time.

In addition to the above discussion, the DSMC method can be understood in a different way. In the DSMC scheme, a collection of molecules is treated as a single molecule (called a particle), and the calculation of the translation and collision of particles is parallel to Boltzmann's derivation of his equation (Boltzmann [1896–98]). The relation between them can be made quantitatively. The translation process may not need discussion. We will discuss the collision process along this line.

The variation of the number $(f/m)\mathbf{d}\boldsymbol{\xi}\mathbf{d}\boldsymbol{X}$ of the molecules in $\mathbf{d}\boldsymbol{\xi}\mathbf{d}\boldsymbol{X}$ by intermolecular collision in time $\mathrm{d}t$ is expressed with the collision term (B.12b) of the Boltzmann equation (B.12a) as

$$\frac{1}{m}J(f, f)\mathbf{d}\boldsymbol{\xi}\mathbf{d}\boldsymbol{X}\mathrm{d}t. \tag{B.60}$$

The contribution to this by the loss term of the collision integral, i.e.,

$$\frac{1}{m^2}\left(\int_{\text{all }\boldsymbol{\alpha},\,\text{all }\boldsymbol{\xi}_*} ff_*B\mathrm{d}\Omega(\boldsymbol{\alpha})\mathbf{d}\boldsymbol{\xi}_*\right)\mathbf{d}\boldsymbol{\xi}\mathbf{d}\boldsymbol{X}\mathrm{d}t, \tag{B.61}$$

is the number of molecules in $\mathbf{d}\boldsymbol{\xi}\mathbf{d}\boldsymbol{X}$ around $(\boldsymbol{\xi}, \boldsymbol{X})$ that collide with any other molecules in time $\mathrm{d}t$. The number of the molecules in $\mathbf{d}\boldsymbol{\xi}\mathbf{d}\boldsymbol{X}$ that collide with

molecules in $\mathbf{d}\boldsymbol{\xi}_*$ around $\boldsymbol{\xi}_*$ in time $\mathrm{d}t$ is[14]

$$m^{-2} f f_* \left(\int_{\text{all } \boldsymbol{\alpha}} B \mathrm{d}\Omega(\boldsymbol{\alpha}) \right) \mathbf{d}\boldsymbol{\xi}_* \mathbf{d}\boldsymbol{\xi} \mathbf{d}\boldsymbol{X} \mathrm{d}t. \tag{B.62}$$

The time interval $\mathrm{d}t$ being taken to be small, only the molecules $\boldsymbol{\xi}_*$ in $\mathbf{d}\boldsymbol{X}$ participate in the collision given in Eq. (B.62). Then, from Eq. (B.62), the probability that any pair of molecules in $\mathbf{d}\boldsymbol{X}$, one with velocity $\boldsymbol{\xi}$ and the other with $\boldsymbol{\xi}_*$, makes a collision in time $\mathrm{d}t$ is $[\int_{\text{all } \boldsymbol{\alpha}} B \mathrm{d}\Omega(\boldsymbol{\alpha})]\mathrm{d}t/\mathbf{d}\boldsymbol{X}$. The velocities of the collided pair are given by Eqs. (A.28a) and (A.28b), i.e.,

$$\boldsymbol{\xi}' = \boldsymbol{\xi} + [\boldsymbol{\alpha} \cdot (\boldsymbol{\xi}_* - \boldsymbol{\xi})]\boldsymbol{\alpha}, \qquad \boldsymbol{\xi}'_* = \boldsymbol{\xi}_* - [\boldsymbol{\alpha} \cdot (\boldsymbol{\xi}_* - \boldsymbol{\xi})]\boldsymbol{\alpha}, \tag{B.63}$$

where $\boldsymbol{\alpha}$ is distributed according to the distribution $B\mathrm{d}\Omega(\boldsymbol{\alpha})/\int_{\text{all } \boldsymbol{\alpha}} B\mathrm{d}\Omega(\boldsymbol{\alpha})$.

In view of the above discussion, the contribution of the collision term can be computed in the following way. For all the pairs $(\boldsymbol{\xi}, \boldsymbol{\xi}_*)$ of the molecules in $\mathbf{d}\boldsymbol{X}$, determine whether they collide or not according to the probability $[\int_{\text{all } \boldsymbol{\alpha}} B\mathrm{d}\Omega(\boldsymbol{\alpha})]\mathrm{d}t/\mathbf{d}\boldsymbol{X}$ of collision given above. For the collided pairs, determine their $\boldsymbol{\alpha}$ according to the distribution $B\mathrm{d}\Omega(\boldsymbol{\alpha})/\int_{\text{all } \boldsymbol{\alpha}} B\mathrm{d}\Omega(\boldsymbol{\alpha})$ of $\boldsymbol{\alpha}$, from which the resulting pairs $(\boldsymbol{\xi}', \boldsymbol{\xi}'_*)$ of velocities are determined by Eq. (B.63). Then, the original molecular velocities $\boldsymbol{\xi}$ and $\boldsymbol{\xi}_*$ for the collided pairs are replaced by $\boldsymbol{\xi}'$ and $\boldsymbol{\xi}'_*$ just obtained. The new velocity distribution of the molecules is the distribution obtained by the collision integral after time $\mathrm{d}t$.

This process is carried out for a large number of particles, each of which represents a large number of molecules, in the DSMC computation. This process is verified by modifying the probability between the particles from that between the molecules in the following way. Consider two groups A and B of identical molecules, A consisting of M molecules $(a_1, a_2, \ldots, a_M)$ with neighboring molecular velocities and B consisting of N molecules $(b_1, b_2, \ldots, b_N)$ with another neighboring molecular velocities. Any pair (a_i, b_j) of molecules in A and B collides with a common probability p. Perform MN trials for MN pairs whether they collide or not. Then, for large M and N, the number of pairs that collide is MNp in the probabilistic sense. By the collision, MNp molecules leave each of A and B groups. Now, n molecules in each of A and B are represented by a particle. Then we obtain two groups $\mathfrak{A}$ and $\mathfrak{B}$, $\mathfrak{A}$ consisting of M/n particles $(\mathfrak{a}_1, \mathfrak{a}_2, \ldots, \mathfrak{a}_{M/n})$ and $\mathfrak{B}$ consisting of N/n particles $(\mathfrak{b}_1, \mathfrak{b}_2 \ldots, \mathfrak{b}_{N/n})$. Any pair $(\mathfrak{a}_i, \mathfrak{b}_j)$ in $\mathfrak{A}$ and $\mathfrak{B}$ collides with a common probability P. Perform similar trials for MN/n^2 pairs whether they collide or not. Then, for large M/n and N/n, the number of pairs that collide is MNP/n^2 in the probabilistic sense. By the collision, MNP/n^2 particles leave each of $\mathfrak{A}$ and $\mathfrak{B}$ groups, that is, MNP/n molecules leave each of A and B. For the simplified computation by the system of particles to approximate the collision process of the molecular systems A and B, MNP/n should be equal to MNp, that is, we should take

$$P = np. \tag{B.64}$$

[14] The derivation of the Boltzmann equation in Boltzmann [1896–98] proceeds in the opposite direction, i.e., from Eq. (B.62) to Eq. (B.61).

This result corresponds to the factor Δ/m in Eq. (B.15), because the factor is equal to the number of molecules represented by a particle in the DSMC computation.[15] The molecules after collision take various velocities, which is expressed by the parameter $\boldsymbol{\alpha}$. If the number MNp/n of the particles leaving $\mathfrak{A}$ and $\mathfrak{B}$ is large enough, the distribution of the particles after collision can simulate the distribution of the molecules.

We have shown the relation between the Boltzmann equation and the DSMC method described in Section B.1.3, which is in principle the method introduced by Bird, in two different ways. These give the background when one tries to improve the method of computation in efficiency and accuracy, and also give a guideline to introduce a similar method of computation in different systems. These are the benefit of theoretical study. Unfortunately, for some period in the past, it was said among some people that Bird's method is not related to the Boltzmann equation.[16] The theoretical discussion also eliminates the misunderstanding.[17]

B.1.5 Economy of computation

The DSMC method of solution is simple but requires a large computation because the computation for a large number of the particles is required. Most of the time of computation is obviously spent on the step (iii) in Section B.1.3, where the collision parameter $\boldsymbol{\alpha}^{(s)}$ is chosen with very low probability for very large pairs of the particles in each cell. We first explain an economy of computation with this process in mind.

In the step (iii), the collision parameter $\boldsymbol{\alpha}^{(s)}$ is generally chosen in the two steps. That is, first determine whether the pairs $(\boldsymbol{\xi}^{(j)}, \boldsymbol{\xi}^{(k)})$ of the particles collide or not by the probability $[P(\boldsymbol{\xi}^{(j)}, \boldsymbol{\xi}^{(k)}),\ 1 - P(\boldsymbol{\xi}^{(j)}, \boldsymbol{\xi}^{(k)})]$ for all the pairs in $\mathbf{d}\boldsymbol{X}^*$, and then choose the parameter $\boldsymbol{\alpha}^{(s)}$ by the probability $\bar{P}^{(s)}(\boldsymbol{\xi}^{(j)}, \boldsymbol{\xi}^{(k)})\mathrm{d}\Omega^{(s)}/P(\boldsymbol{\xi}^{(j)}, \boldsymbol{\xi}^{(k)})$. For the first step it requires $N^*(N^* - 1)/2$ trials. There are various attempts to reduce the number of this trial (e.g., Bird [1967, 1976, 1989], Koura [1986], Ivanov, Rogasinsky & Rudyak [1989], Baganoff & McDonald [1990]) in view of the property that the probability of the collision is very low and that only a very small portion of the pairs in the cell collides. We will show an example.

[15] See Footnote 5 in Section B.1.3.

[16] Especially, in presenting his work well after Bird's method was widely used, an author strongly claimed that his method is the only legitimate method. However, this method treated the collision of particles as a pair in an unnatural way, and thus, in numerical computation, where only a finite number of particles are considered, one comes across an unreasonable result that the temperature of a gas continues to decrease with time (see Greengard & Reyna [1992] for its mathematical proof and example). This may be attributed to unfavorable arrangement of terms, and thus the convergence is slow. Further, the economizing technique explained in the beginning of Section B.1.5, which was already widely adopted at that time, is not introduced. The technique is later introduced by Babovsky [1986], but the advantage of the later-introduced method is not clear owing to the above-mentioned defect.

[17] Rigorous mathematical discussion is given by Wagner [1992], but it is not accessible to nonmathematicians.

In the trials of collision or non for the $N^*(N^*-1)/2$ pairs, the probability $P(\boldsymbol{\xi}^{(j)}, \boldsymbol{\xi}^{(k)})$ of collision being less than $1/N^*$ and very small, the result is non for almost all the pairs. That is, the chance that the number of pairs that collide exceeds $[N^*(N^*-1)/2] \max P(\boldsymbol{\xi}^{(j)}, \boldsymbol{\xi}^{(k)})$ considerably in the trials is very low. Thus, we choose a number M^* in such a way that $N^*(N^*-1)/2 \gg M^* \gg [N^*(N^*-1)/2] \max P(\boldsymbol{\xi}^{(j)}, \boldsymbol{\xi}^{(k)})$. Selecting M^* pairs among $N^*(N^*-1)/2$ at random, we carry out the trial for each [say, (j,k)] of the M^* pairs to determine the collision with the probability $P(\boldsymbol{\xi}^{(j)}, \boldsymbol{\xi}^{(k)}) N^*(N^*-1)/2M^*$, which is amplified by the factor $N^*(N^*-1)/2M^*$. The pairs that are not selected as M^* pairs are judged not to collide. In this way we can finish the decision of collision by M^* trials instead of $N^*(N^*-1)/2$ with considerable economy of computation. The validity of this process is explained in the following paragraphs.

We will prepare before the discussion of the validity. Consider mutually exclusive S events $A_1, \ldots, A_S$ with a common probability p of their occurrence. Let p depend on S and vanish as $S \to \infty$ keeping the condition $Sp \to \infty$. The probability that some n events among the $A_1, \ldots, A_S$ occur and the remaining $(S-n)$ events do not is $[S!/n!(S-n)!]p^n(1-p)^{S-n}$. In the limit $S \to \infty$ with $Sp \to \infty$, the probability that the number n of occurrence (or success) takes the value $n = Sp$ [with the allowance of width εSp (ε : arbitrarily small positive number)] approaches unity [see the paragraph containing Eq. (B.52) and Fig. B.1]. On the other hand, first choose M^* of the events $A_1, \ldots, A_S$ at random, and make a trial of the occurrence or non for each of M^* with the probability pS/M^* of success, which is amplified by factor S/M^*. The event that is not chosen among M^* is taken to be non (or unsuccessful). Then, the probability of n success is $[M^*!/n!(M^*-n)!](pS/M^*)^n(1-pS/M^*)^{M^*-n}$. In the limit $S \to \infty$ with $M^* \to \infty$ and $Sp \to \infty$, the probability that the number n of occurrence takes the value $n = M^*(pS/M^*)$ (or $n = Sp$) [with allowance of width $\varepsilon M^* pS/M^* = \varepsilon Sp$ (ε : arbitrarily small positive number)] approaches unity.

Now, we will show the validity of the economizing process explained in the paragraph before the preceding one. Here, the Ξ cell of the particle velocity space $\boldsymbol{\xi}$ consisting of S particles is introduced, just as in the discussion in replacing the average of repeated computations by the average in a single computation in the paragraph containing Eq. (B.46) of Section B.1.4. The particles $\boldsymbol{\xi}^{(j)}$ are renumbered as $\boldsymbol{\xi}^{(J)}(\beta)$ [or $\boldsymbol{\xi}^{(K)}(\gamma)$]. Corresponding to this renumbering, the pair (j,k) of the particles and the probability $P(\boldsymbol{\xi}^{(j)}, \boldsymbol{\xi}^{(k)})$ are, respectively, denoted by $(J(\beta), K(\gamma))$ and $P^{(J,K)}(\beta, \gamma)$. The Ξ cell contains many particles, but the differences of the velocities among them are so small that they can be represented by a velocity. Thus, $P^{(J,K)}(\beta, \gamma)$ can be represented by a single $P^{(J,K)}$ determined by the (J,K) pair of the Ξ cells. We compare the number $n^{(J,K)}$ of success among the S^2 pairs in the Ξ cell pair (J,K) for the two cases, the one with direct trial for $N^*(N^*-1)/2$ and the other with preliminary selection of M^* pairs. First perform the trial for each (j,k) of the $N^*(N^*-1)/2$ pairs of the particles in the cell $\mathbf{d}\boldsymbol{X}^*$ whether the collision occurs or not with the probability $P(\boldsymbol{\xi}^{(j)}, \boldsymbol{\xi}^{(k)})$ of success, where we use a common probability $P^{(J,K)}$ for the pairs

that belong to the same pair (J, K) of the Ξ cells. Estimate the number $n^{(J,K)}$ of success among the S^2 pairs in the Ξ cell pair (J, K). According to the preceding paragraph, in the limit $S^2 \to \infty$ with $S^2 P^{(J,K)} \to \infty$,[18] the probability that $n^{(J,K)}$ of success satisfies $n^{(J,K)} = S^2 P^{(J,K)}$ with the allowance of width $o(S^2 P^{(J,K)})$ approaches unity. That is, the number $n^{(J,K)}$ of the pairs that collide is given by $n^{(J,K)} = S^2 P^{(J,K)}$ in the probabilistic sense. Next, choose M^* pairs at random from the $N^*(N^*-1)/2$ pairs in $\mathbf{d}\boldsymbol{X}^*$. The number of pairs in each of the Ξ cell pairs being commonly S^2, the probability that the number $r_{(J,K)}$ of the pairs that is chosen in the Ξ cell pair (J, K) satisfies $r_{(J,K)} = S^2 M^*/[N^*(N^*-1)/2]$ approaches unity in the limit $N^* \to \infty$ with $M^* \to \infty$, $S \to \infty$, $S^2 M^*/N^{*2} \to \infty$. That is, $r_{(J,K)}$ approaches $S^2 M^*/[N^*(N^*-1)/2]$ independently of the pair (J, K) in the probabilistic sense. Then, perform the trial of success or non for each of the $r_{(J,K)}$ pairs thus chosen with the probability $P^{(J,K)} S^2/r_{(J,K)}$ [or $P^{(J,K)} N^*(N^*-1)/2M^*$] of success. The probability that the number $n^{(J,K)}$ of success satisfies $n^{(J,K)} = r_{(J,K)}(P^{(J,K)} S^2/r_{(J,K)})$ (or $n^{(J,K)} = P^{(J,K)} S^2$) approaches unity in the limit $S \to \infty$, with $S^2 M^*/N^{*2} \to \infty$ (or $r_{(J,K)} \to \infty$) and $P^{(J,K)} S^2 \to \infty$. That is, $n^{(J,K)}$ approaches $P^{(J,K)} S^2$ in the probabilistic sense. The distributions $n^{(J,K)}$ of the two ways of trials have the same distribution. Therefore, the above-mentioned way of economizing the computation is legitimate in the case $N^* \to \infty$ with $N^{*2} \gg S^2 \gg N^*$ and $M^* \gg [N^*(N^*-1)/2] \max P^{(J,K)}$.[19]

Next, we consider the DSMC process when the dimension of a problem degenerates. First consider the spatially homogeneous case where $\boldsymbol{F} = \mathbf{0}$ and $f_{(0)}$ is independent of $\boldsymbol{X}$. From Eq. (B.24), we can obtain f at the next time step (or $f_{(1)}$) only from f^B. Therefore, we have only to carry out the computation to obtain f^B in a cell $\mathbf{d}\boldsymbol{X}^{(l)}$, that is, to repeat the step (iii) in a single cell. Next, consider the one-dimensional case where $\boldsymbol{F} = (F_1, 0, 0)$ and $f_{(0)}$ as well as F_1 is independent of X_2 and X_3. Then, applying the discussion from Eq. (B.23) to Eq. (B.24) for the variables X_2 and X_3, we have $[\varphi, f^A] = [\varphi(X_1 + \xi_1 \mathrm{d}t, X_2, X_3, \xi_1 + F_{1(0)}\mathrm{d}t, \xi_2, \xi_3), f_{(0)}]$. Thus, the expressions corresponding to Eqs. (B.25) and (B.26) are reduced to

$$[\varphi, f^A] = \Delta \sum_{l=1}^{M} \sum_{j=1}^{N^{(l)}} \varphi(X^{(j)}_{(l)1} + \xi^{(j)}_{(l)1}\mathrm{d}t, X^{(j)}_{(l)s}, \xi^{(j)}_{(l)1} + F_{1(0)}(X^{(j)}_{(l)1}, \boldsymbol{\xi}^{(j)}_{(l)})\mathrm{d}t, \xi^{(j)}_{(l)s}), \tag{B.65a}$$

$$f^A = \Delta \sum_{l=1}^{M} \sum_{j=1}^{N^{(l)}} \delta(X_1 - X^{(j)}_{(l)1} - \xi^{(j)}_{(l)1}\mathrm{d}t, X_s - X^{(j)}_{(l)s}) \times \delta(\xi_1 - \xi^{(j)}_{(l)1} - F_{1(0)}(X^{(j)}_{(l)1}, \boldsymbol{\xi}^{(j)}_{(l)})\mathrm{d}t, \xi_s - \xi^{(j)}_{(l)s}), \tag{B.65b}$$

where s indicates 2 and 3, and $X^{(j)}_{(l)i}$, $\xi^{(j)}_{(l)i}$, and F_i are the i-th component of $\boldsymbol{X}^{(j)}_{(l)}$,

[18] We determine the size of the Ξ cell in such a way that $N^{*2} \gg S^2 \gg N^* (\gg 1)$ because $P^{(J,K)} = O(1/N^*)$.

[19] In view of $P^{(J,K)} = O(1/N^*)$, the second condition reduces to $M^* \gg N^*$. The conditions $S^2 M^*/N^{*2} \to \infty$ and $P^{(J,K)} S^2 \to \infty$ are satisfied under the two conditions on S and M^*.

$\boldsymbol{\xi}_{(l)}^{(j)}$, and $\boldsymbol{F}$. Thus, we find that the DSMC process can be carried out only by distributing the particles on the X_1 axis. In the step (i), the positions and velocities of the particles are shifted in such a way that $X_{(l)1}^{(j)} \to X_{(l)1}^{(j)} + \xi_{(l)1}^{(j)} \mathrm{d}t$ and $\xi_{(l)1}^{(j)} \to \xi_{(l)1}^{(j)} + F_{1(0)}(X_{(l)1}^{(j)}, \boldsymbol{\xi}_{(l)}^{(j)})\mathrm{d}t$, and in the step (iii), the same process as in the general case is carried out in each cell. The simplified process of the two-dimensional problem can be constructed in a similar way.

In order to obtain the solution of a problem in a good approximation with the DSMC computation, we have to carry out the computation with a very large number of particles in the system, as is seen from the discussion in Section B.1.4. It is practically impossible at present to obtain a smooth flow-velocity profile or temperature distribution by one run of computation, though the severe condition is partly due to a rough estimate by elementary analysis. The results averaged in some way are usually presented, e.g., the average of many cases of computation. In the first stage of the discussion in Section B.1.4 of the background of the step (iii) of the DSMC process in Section B.1.3, we mentioned that the correct result is obtained by averaging many trials. This discussion, however, does not validate the averaging process done in conventional numerical computations. In that discussion, we showed only that the solution after the time step $\mathrm{d}t$ is correctly obtained by the averaging, but does not guarantee the result of the further steps. That is, the desired solution is obtained, if we take the average of the result at the first step, proceed to the next step with the resulting velocity distribution function as the initial condition, and repeat the same procedure. The averaging process used in practical computations, where independent computations up to some time steps are averaged, requires another verification. For example, the following confirmation is required: the computation is carried out for each of a group of initial conditions whose average gives the correct initial condition, and the average of the results at the first step is to be shown to give the correct result at the first step. This point is not clarified at present.[20]

In small systems, which appear in aerosol science and microengineering, the deviation of the velocity distribution function from a uniform Maxwell distribution is important, because the Mach number of the flow and the relative temperature difference between boundaries are small in these systems. In such a case, straightforward application of the DSMC method described in this section is inefficient. In this method, the total distribution function consisting of the Maxwellian and its perturbation is obtained at a time. To obtain the perturbation (say, of a size 5%) accurately, for example within the error of 1%, we have to obtain the total distribution more accurately (up to 0.05%), which is very difficult. In finite-difference computation for small perturbation problems, the equation for the perturbation is used. The corresponding method should be devised.

[20] There is obviously no problem for the step (i) in Section B.1.3, but the step (iii), which is a nonlinear effect, has a problem generally. In fact, Babovsky [1992] reported a negative result for the corresponding problem in his simulation system for a one-dimensional discrete Boltzmann equation.

A similar difficulty is encountered in the computation for small Knudsen numbers. For small Knudsen numbers, the velocity distribution function is close to a local Maxwellian. Thus, the local Maxwellian contribution is cancelled out in the collision integral. The remaining part is amplified by the inverse of the Knudsen number and determine the (temporal and spatial) variation of the distribution function. Therefore, we have to compute the velocity distribution function accurately up to the perturbation (or the order of the Knudsen number). This requires a very large computation, and some technique should be introduced also in this case. Pareschi & Caflisch [1999] is an example.

B.1.6 Example

We will examine the bifurcation problem of an axially symmetric and uniform gas flow between two rotating coaxial circular cylinders made of the condensed phase of the gas by the DSMC method. The problem is discussed in Section 8.4.2, analytically by asymptotic analysis for small Knudsen numbers and numerically by a finite-difference method. The present study is a simplified version of the DSMC computation in Section 8.4.3 with additional condition of axial uniformity. However, owing to this simplicity, we can make more detailed examination, which is too large to be done without this assumption, and see two aspects, successful and non, of the method for describing the qualitative feature of the solution.

The problem considered in Section 8.4 is as follows: Take a gas between two coaxial circular cylinders made of the condensed phase of the gas. Let the radius, temperature, and circumferential velocity (on the surface) of the inner cylinder be, respectively, L_A, T_A, and $V_{\theta A}$, and let the corresponding quantities of the outer cylinder be L_B, T_B, and $V_{\theta B}$, where T_A, $V_{\theta A}$, T_B, and $V_{\theta B}$ are uniform on each cylinder; the saturated gas pressure at temperature T_A is denoted by p_A and that at T_B by p_B (see Fig. 8.19). Here, limiting to the axially symmetric and uniform case, where the radial coordinate r is the only nontrivial space variable, we will try to obtain the time-independent solution from the long-time behavior of the solution of the initial and boundary-value problem for various values of $V_{\theta A}$. The boundary condition on the cylinders is the complete-condensation condition. As the initial condition, two kinds of conditions are considered. That is, ICa: the Maxwell distribution with uniform pressure p_A and uniform temperature T_A and without gas motion and ICb: the Maxwell distribution making rigid body rotation at angular velocity $V_{\theta A}/L_A$ with uniform temperature T_A and with p_A as the average pressure.[21] The other parameters are chosen as $V_{\theta B} = 0$, $p_B/p_A = 1.2$, $T_B/T_A = 1$, $L_B/L_A = 2$, and Kn$= 0.01$. Here, in conformity with Section 8.4, the Knudsen number Kn is defined by Kn $= \ell_A/L_A$, where ℓ_A is the mean free path of the gas in the equilibrium state at rest with temperature T_A and pressure p_A.

The computation is carried out with four kinds of systems of numerical computation: Let N_c and N_p be, respectively, the number of cells into which the

[21] The pressure distribution is given by $P_0 \exp[(V_{\theta A}^2/2RT_A)(r/L_A)^2]$, where $P_0 = p_A[(L_B/L_A)^2 - 1](V_{\theta A}^2/2RT_A)\{\exp[(V_{\theta A}^2/2RT_A)(L_B/L_A)^2] - \exp[(V_{\theta A}^2/2RT_A)]\}^{-1}$.

range of r between the two cylinders is divided uniformly and the number of particles put in the domain initially (thus, N_p/N_c particles in a cell on average), and let $\Delta\hat{t}$ be the nondimensional time step $\Delta\hat{t} = \Delta t/L_A(2RT_A)^{-1/2}$ of computation; System A: $(N_c, N_p/N_c, \Delta\hat{t}) = (100, 25, 0.001)$, System B: $(100, 50, 0.001)$, System C: $(100, 100, 0.001)$, and System D: $(500, 100, 0.0005)$. The time-local quantities are the average of 10^5 time steps.

Let J be the mass flow per unit time from the inner cylinder to the outer per unit length of the cylinders. The time evolution of the nondimensional mass-flow rate $\hat{J}$ $[= J/2\sqrt{2}\pi L_A p_A(RT_A)^{-1/2}]$ computed on System D is shown for various values of $|V_{\theta A}|/(2RT_A)^{1/2}$ in Fig. B.2. The following discussion is based on the examination carried out at each step of 0.005 of $|V_{\theta A}|/(2RT_A)^{1/2}$. The solution with negative mass-flow rate (the lower branch) exists for $0 \leq |V_{\theta A}|/(2RT_A)^{1/2} \leq 0.695$, and the solution with positive mass-flow rate (the upper branch) exists for $0.675 \leq |V_{\theta A}|/(2RT_A)^{1/2}$. The fluctuations are small except in the solution with positive mass-flow rate at $|V_{\theta A}|/(2RT_A)^{1/2} = 0.675$. This solution on the upper branch at $|V_{\theta A}|/(2RT_A)^{1/2} = 0.675$ is difficult to be judged, only with the present data, whether it is time-independent or really fluctuating, but in the rest of the ranges, the solution can be considered time-independent. For $|V_{\theta A}|/(2RT_A)^{1/2} \leq 0.67$, the solutions from the two initial conditions ICa and ICb converge to a common time-independent solution with negative mass-flow rate, and for $|V_{\theta A}|/(2RT_A)^{1/2} \geq 0.7$, the two solutions converge to a common solution with positive mass-flow rate. In the range $0.675 \leq |V_{\theta A}|/(2RT_A)^{1/2} \leq 0.695$, the solution from ICa converges to that on the lower branch and the solution from ICb converges to that on the upper branch. The average of $\hat{J}$ over 10^7 time steps from $t/L_A(2RT_A)^{-1/2} = 5000$ are shown as the time-independent solutions, for convenience's sake, by long dashed lines in Fig. B.2 and the following Figs. B.3 and B.4.

On Systems A, B, and C, the fluctuations of solutions are larger. The time evolution of the (nondimensional) mass-flow rates $\hat{J}$ on Systems A, B, and C is shown for various $|V_{\theta A}|/(2RT_A)^{1/2}$ in Figs. B.3 and B.4. The fluctuations are larger for smaller systems. The fluctuations are largest around $|V_{\theta A}|/(2RT_A)^{1/2} = 0.675$ and show tendency to vanish away from there. When the fluctuations are large, the mass-flow rate ranges between the two branches of solutions on System D. With decrease of fluctuations, the solution fluctuates with one of the branches or only one branch existing as roughly one of the bounds, but the fluctuations are still large and the solution cannot be considered time-independent. For small or large $|V_{\theta A}|/(2RT_A)^{1/2}$, the solution approaches a unique solution with sufficiently small fluctuations. [See, for example, the case at $|V_{\theta A}|/(2RT_A)^{1/2} = 0.3$; the fluctuations are similarly small at $|V_{\theta A}|/(2RT_A)^{1/2} = 1.2$.] There are some gray zones of $|V_{\theta A}|/(2RT_A)^{1/2}$ where the decision of "time-independent" or "oscillatory" is difficult. The gray zone is inevitable in DSMC computation (see Aoki, Sone & Yoshimoto [1999] for another example). We could not find the values of $|V_{\theta A}|/(2RT_A)^{1/2}$ at which there are two time-independent solutions.

As has been seen, the mass-flow rates, for example, at $|V_{\theta A}|/(2RT_A)^{1/2} = 0.675$ on Systems A, B, and C vary oscillatorily and irregularly some time

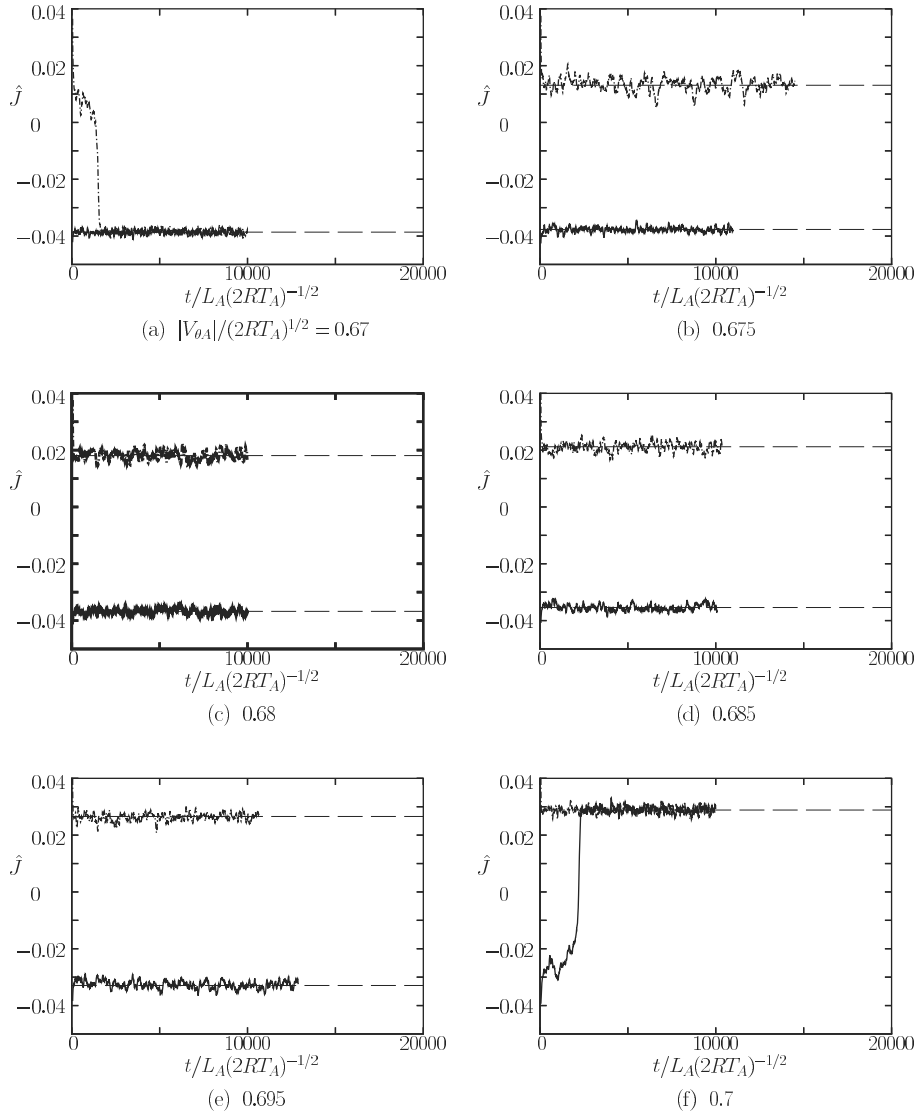

Figure B.2. Time evolution of the nondimensional mass-flow rate $\hat{J}$ [$= J/2\sqrt{2}\pi L_A p_A (RT_A)^{-1/2}$] in the axially uniform problem on System D for various $|V_{\theta A}|/(2RT_A)^{1/2}$ (Kn$= 0.01$, $L_B/L_A = 2$, $V_{\theta B} = 0$, $p_B/p_A = 1.2$, $T_B/T_A = 1$). (a) $|V_{\theta A}|/(2RT_A)^{1/2} = 0.67$, (b) 0.675, (c) 0.68, (d) 0.685, (e) 0.695, and (f) 0.7. The solid lines —— indicate the solutions from the initial condition ICa, the dot-dash lines –·– : the solutions from ICb, and the long dashed lines — — — : the time-independent solutions on System D.

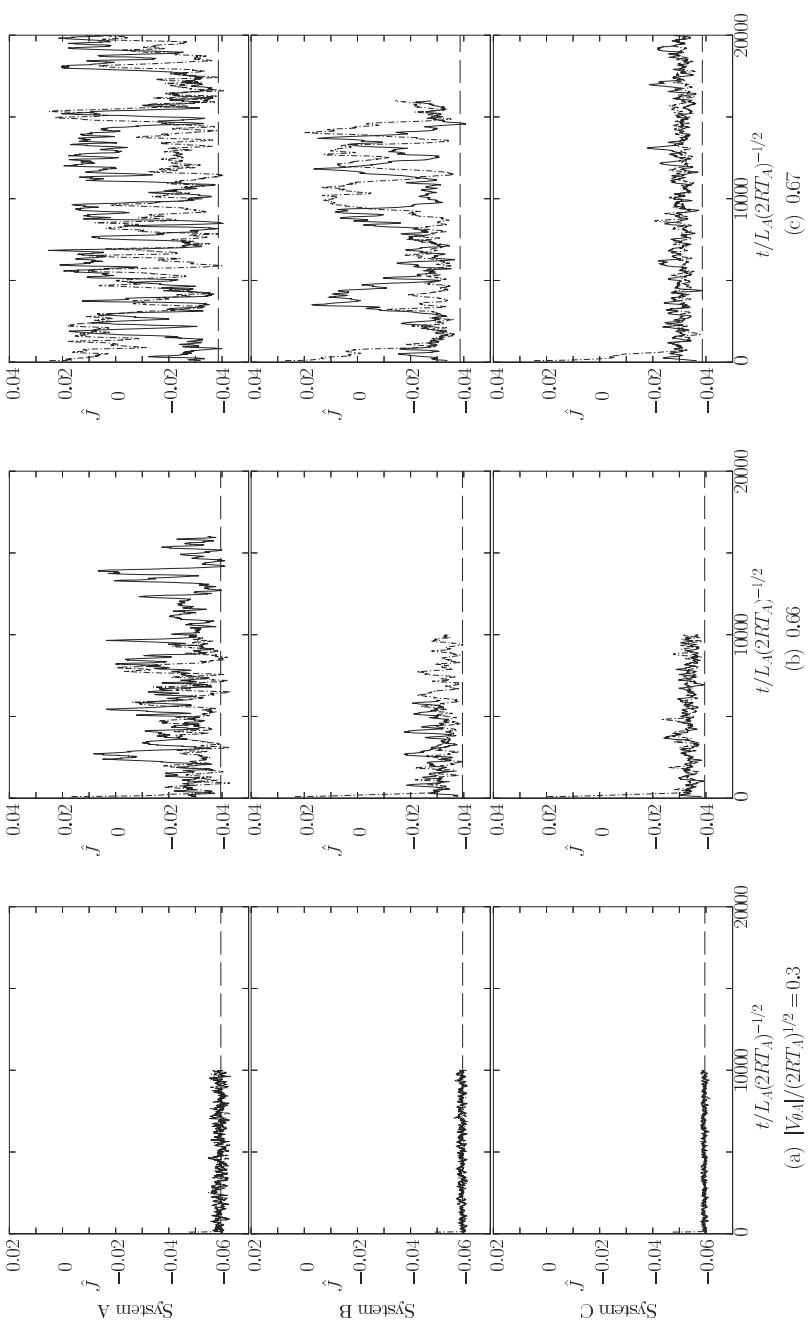

Figure B.3. Time evolution of the nondimensional mass-flow rate $\hat{J}$ in the axially uniform problem on Systems A, B, and C for various $|V_{\theta A}|/(2RT_A)^{1/2}$ (Kn = 0.01, $L_B/L_A = 2$, $V_{\theta B} = 0$, $p_B/p_A = 1.2$, $T_B/T_A = 1$). I. (a) $|V_{\theta A}|/(2RT_A)^{1/2} = 0.3$, (b) 0.66, and (c) 0.67. The solid lines: the solutions from the initial condition ICa, the dot-dash lines: the solutions from ICb, and the long dashed lines: the time-independent solutions on D.

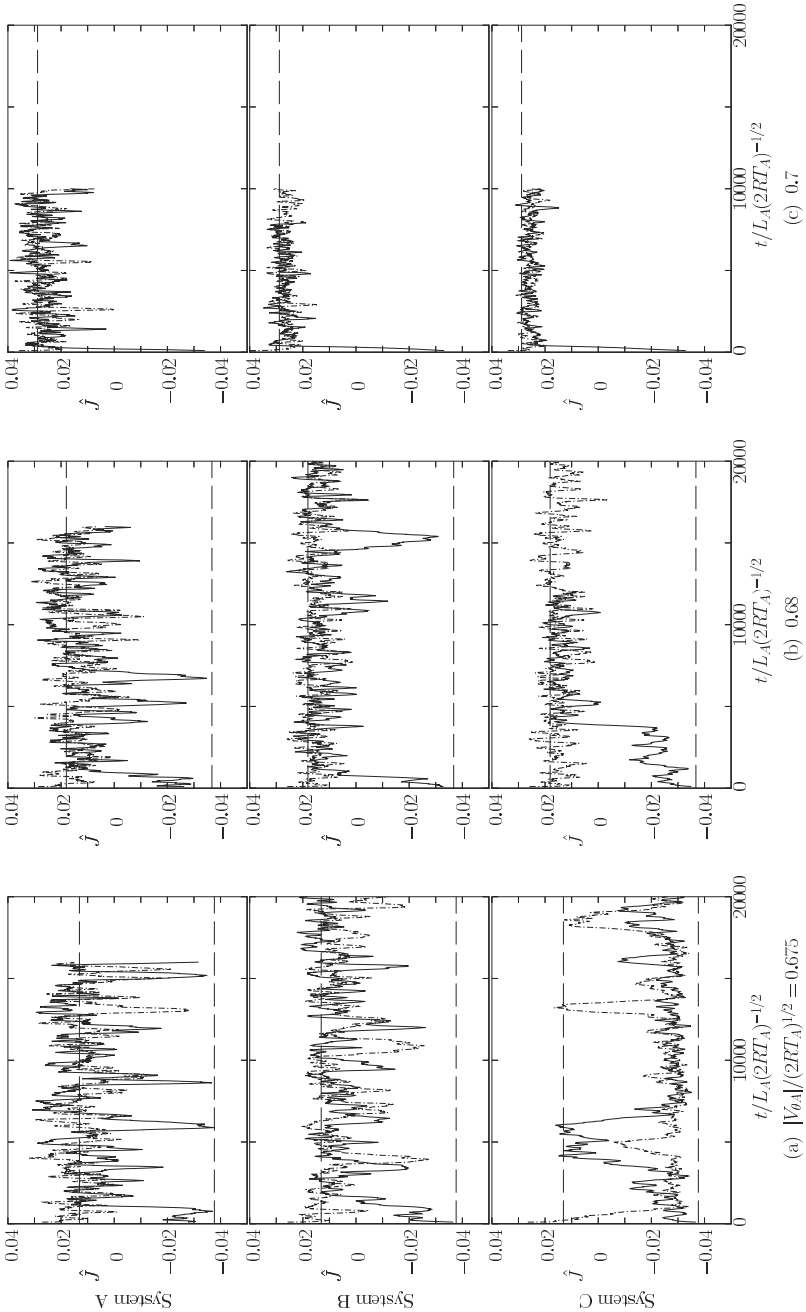

Figure B.4. Time evolution of the nondimensional mass-flow rate $\hat{J}$ in the axially uniform problem on Systems A, B, and C for various $|V_{\theta A}|/(2RT_A)^{1/2}$ (Kn = 0.01, $L_B/L_A = 2$, $V_{\theta B} = 0$, $p_B/p_A = 1.2$, $T_B/T_A = 1$). II. (a) $|V_{\theta A}|/(2RT_A)^{1/2} = 0.675$, (b) 0.68, and (c) 0.7. The solid lines: the solutions from the initial condition ICa, the dot-dash lines: the solutions from ICb, and the long dashed lines: the time-independent solutions on D.

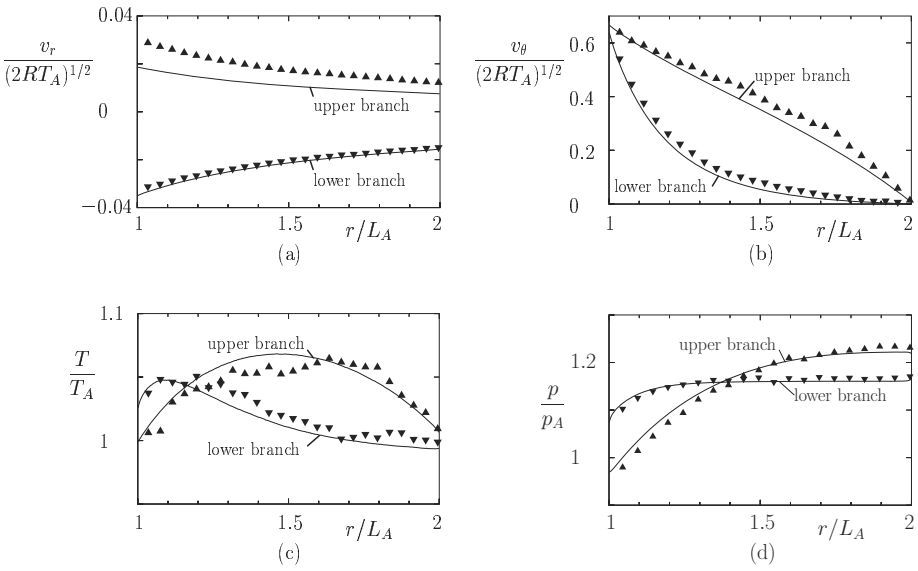

Figure B.5. The time-local profiles of flow velocity (v_r, v_θ), temperature (T), and pressure (p) of the oscillatory solution, starting from the initial condition ICa, on System A at the instants when the mass-flow rate is maximum and minimum $[|V_{\theta A}|/(2RT_A)^{1/2} = 0.68$ and Kn$= 0.01]$. (a) $v_r/(2RT_A)^{1/2}$, (b) $v_\theta/(2RT_A)^{1/2}$, (c) T/T_A, and (d) p/p_A. The symbol ▲ indicates the data at the maximum mass-flow rate, and ▼ at the minimum mass-flow rate. The time-independent solutions on System D are shown by solid lines —— for comparison.

near the upper branch and some time near the lower branch, and they remain roughly between them. This behavior also applies to their local variables. In Fig. B.5, the profiles of flow velocity, temperature, and pressure of the solution at $|V_{\theta A}|/(2RT_A)^{1/2} = 0.68$, starting from the initial condition ICa on System A, at the instants when the mass-flow rate is maximum and minimum are compared with the long-time averages over 10^7 time steps from $t/L_A(2RT_A)^{-1/2} = 5000$ of the solutions on System D (the time-independent solutions, for short). The profiles for the two extremum instants are similar to those of the two time-independent solutions on the upper and lower branches. Fluctuations of a considerable amplitude inevitably enter in DSMC computations, and thus this behavior of solution, shifting from one solution to the other, is easily conceivable.

There are definitely oscillatory solutions on Systems A, B, and C. With some instantaneous data of the oscillatory solutions as initial conditions, their time evolutions are computed on System D. They converge to the corresponding time-independent solutions on either of the two branches. Thus, the oscillatory solutions obtained on Systems A, B, and C are false.

No bifurcation was found in the solutions on Systems A, B, and C. Further, the computation on these systems gave false oscillatory solutions. The sizes of Systems A, B, and C were not large enough to analyze the stability and

bifurcation of a flow even for the present simple problem. Their sizes are not smaller (or even rather larger) than the size (or the number of cells and that of particles in a cell) of computations widely carried out. Thus, careful examination is required to confirm the real existence of an oscillatory solution by a DSMC computation. Presentation of oscillatory and irregular examples by a DSMC computation as turbulence should be accompanied by detailed examinations.

For problems where the feature of solution is known beforehand, the reasonable quantitative data can be obtained rather easily by the DSMC method of computation, but for problems where the qualitative feature of solution is unknown, it is very difficult to obtain a satisfactory or clear-cut solution by the method.

B.2 Moment method

B.2.1 Basic idea

Moment methods are used in obtaining an approximate solution of the Boltzmann equation, especially very often when the computer size was not so large. The idea of the *moment method* is simple. To examine a function $f(x)$ to be zero, we may confirm all the Fourier coefficients (generalized Fourier coefficients) to be zero instead of examining the value of f to be zero at all the points of the interval under consideration:

$$\int \varphi_n(x) f(x) \mathrm{d}x = 0 \quad (n = 0, 1, 2, ...),$$

where the system of test functions $\varphi_n(x)$ $(n = 0, 1, 2, 3, \ldots)$ is a complete system of functions[22] [e.g., $\cos n\pi x$, $\sin n\pi x$ $(n = 0, 1, 2, \ldots)$]. This is applied to functional equations to solve them. That is, let the functional equation for a function $f(x)$ be

$$F[f(x)] = 0. \tag{B.66}$$

This equation can be replaced by

$$\int \varphi_n(x) F[f(x)] \mathrm{d}x = 0 \quad (n = 0, 1, 2, \ldots). \tag{B.67}$$

[22]Let $f(\boldsymbol{x})$ be a function of $\boldsymbol{x}$ of a class (e.g., a continuous function, a piecewise continuous function) in the domain D of $\boldsymbol{x}$ under consideration. The system of functions $\varphi_n(\boldsymbol{x})$ $(n = 0, 1, 2, \ldots)$ is called *complete* if every function $f(\boldsymbol{x})$ in the class is approximated arbitrarily closely by a linear combination of $\varphi_n(\boldsymbol{x})$ in some sense, that is, the series

$$\sum_{n=0} c_n \varphi_n(\boldsymbol{x}) \ \text{ converges to } f(\boldsymbol{x}) \text{ in some sense (e.g., pointwise, in the mean),}$$

where the pointwise convergence and the convergence in the mean are defined by

$$\text{pointwise: } f(\boldsymbol{x}) = \sum_{n=0}^{\infty} c_n \varphi_n(\boldsymbol{x}); \ \text{ in the mean: } \lim_{m\to\infty} \int_D \left(f - \sum_{n=0}^{m} c_n \varphi_n \right)^2 \mathbf{d}\boldsymbol{x} = 0,$$

(see, e.g., Courant & Hilbert [1953], Bronshtein & Semendyayev [1997]).

The procedure of, what is called, the moment method of solution of the functional equation (B.67) is as follows: Choose a function $f^{(N)}(x)$ containing N parameters (say, $a_1, \ldots, a_N$) as $f(x)$, and construct N moment equations (B.67) by appropriate choice of N test functions. The moment equations are N equations for N parameters $a_1, \ldots, a_N$. Solving them, we can obtain an approximate solution $f^{(N)}(x)$. One has to examine the tendency of convergence by taking many values of N for confirming that the solution obtained is a good approximation. Wise choice of the form of $f^{(N)}(x)$ is essential to obtain a good approximate solution effectively.

In the Boltzmann equation, the independent variables are the time t, the space variable X_i, and the molecular velocity ξ_i. The above idea is applied to the variable ξ_i in many cases. Choose a complete system of test functions $\Psi^{(n)}(\xi_i)$ of ξ_i. Multiply the Boltzmann equation by $\Psi^{(n)}$ and integrate them over the whole space of ξ_i. Then an infinite number of equations, where the independent variables are t and X_i, are obtained. This set of infinite equations, which does not contain the variable ξ_i, is equivalent to the original Boltzmann equation. The moment method is a method to solve this system approximately.

Taking into account the character of the distribution function f, which is inferred from physical consideration, we choose an approximate solution and test functions: the approximate solution contains N unknown functions (say, g_m; $m = 1, 2, ..., N$) of t and X_i, and its functional form of ξ_i is explicit, and N test functions are chosen from a complete system of functions $\Psi^{(n)}$ (let them be the first N functions of the set for the simplicity of the following explanation). In the above choice of the approximate solution, we also take the boundary condition into account. Then, the first N equations of the infinite equations mentioned above are reduced to N equations for the N unknown functions g_m. Solving g_m, we obtain an approximate solution of the Boltzmann equation.

How accurately the approximate solution approximates the exact solution of the original equation is not known beforehand. Moreover, there is no evidence that N approximate equations reflect even the qualitative feature of the original infinite number of equations. Thus the approximate solution may differ qualitatively from the correct solution. Therefore, careful examination of the approximate solution is required. A set of functions that includes 1, ξ_i, and ξ_i^2 is generally chosen as the test functions $\Psi^{(n)}$, because the collision term of the Boltzmann equation vanishes on integration with respect to ξ_i and the equations obtained are the conservation equations (continuity, momentum, and energy equations), with the form of the stress tensor and heat-flow vector unspecified, of the classical fluid dynamics. Unfortunately, in many attempts, only small value of N is taken and the examination of convergence is not performed.

When one uses the moment method, one should know the qualitative feature of the solution. Otherwise one may make a serious error, as we see in some papers.

B.2.2 Examples

The Mott-Smith analysis of a plane shock wave

Mott-Smith [1951] studied the structure of a plane shock wave by a moment method. The plane shock wave is a time-independent one-dimensional flow in an infinite expanse of a gas with uniform states at upstream and downstream infinities (Section 4.7). Let the density, flow velocity, pressure, and temperature at upstream infinity (say, $X_1 \to -\infty$) be, respectively, $\rho_{-\infty}$, $[v_{1-\infty}(>0), 0, 0]$, $p_{-\infty}$, and $T_{-\infty}$ ($p_{-\infty} = R\rho_{-\infty}T_{-\infty}$), and those at downstream infinity ($X_1 \to \infty$) be ρ_∞, $[v_{1\infty}(>0), 0, 0]$, p_∞, and T_∞ ($p_\infty = R\rho_\infty T_\infty$). Choose the approximate solution in the form

$$f = \frac{a_1(X_1)\rho_{-\infty}}{[2\pi R b_1(X_1)T_{-\infty}]^{3/2}} \exp\left(-\frac{(\xi_1 - v_{1-\infty})^2 + \xi_2^2 + \xi_3^2}{2Rb_1(X_1)T_{-\infty}}\right) + \frac{a_2(X_1)\rho_\infty}{[2\pi R b_2(X_1)T_\infty]^{3/2}} \exp\left(-\frac{(\xi_1 - v_{1\infty})^2 + \xi_2^2 + \xi_3^2}{2Rb_2(X_1)T_\infty}\right), \tag{B.68}$$

where $a_1(X_1)$, $a_2(X_1)$, $b_1(X_1)$, and $b_2(X_1)$ are unknown functions, and the four test functions

$$\Psi^{(1)} = 1, \quad \Psi^{(2)} = \xi_1, \ \Psi^{(3)} = \xi_i^2, \ \Psi^{(4)} = \xi_1^2. \tag{B.69}$$

The moment equations of the Boltzmann equation with the first three test functions are the conservation equations of mass, momentum, and energy, i.e., the time-independent one-dimensional version of Eqs. (1.12)–(1.14) with $F_i = 0$. These equations can be integrated. Substituting Eq. (B.68) into the integrated form of the conservation equations, we have

$$a_1\rho_{-\infty}v_{1-\infty} + a_2\rho_\infty v_{1\infty} = M, \tag{B.70a}$$

$$a_1\rho_{-\infty}v_{1-\infty}^2 + a_1R\rho_{-\infty}b_1T_{-\infty} + a_2\rho_\infty v_{1\infty}^2 + a_2R\rho_\infty b_2T_\infty = P, \tag{B.70b}$$

$$a_1\rho_{-\infty}v_{1-\infty}\left(\frac{1}{2}v_{1-\infty}^2 + \frac{5}{2}Rb_1T_{-\infty}\right) + a_2\rho_\infty v_{1\infty}\left(\frac{1}{2}v_{1\infty}^2 + \frac{5}{2}Rb_2T_\infty\right) = E, \tag{B.70c}$$

where M, P, and E are integration constants, which are related to the conditions at infinities as

$$M = \rho_{-\infty}v_{1-\infty} = \rho_\infty v_{1\infty}, \tag{B.71a}$$

$$P = \rho_{-\infty}v_{1-\infty}^2 + R\rho_{-\infty}T_{-\infty} = \rho_\infty v_{1\infty}^2 + R\rho_\infty T_\infty, \tag{B.71b}$$

$$E = \rho_{-\infty}v_{1-\infty}\left(\frac{1}{2}v_{1-\infty}^2 + \frac{5}{2}RT_{-\infty}\right) = \rho_\infty v_{1\infty}\left(\frac{1}{2}v_{1\infty}^2 + \frac{5}{2}RT_\infty\right). \tag{B.71c}$$

Thus, the downstream state is determined by the upstream state, and their relations are called the shock conditions or Rankine–Hugoniot relation (Liepmann & Roshko [1957]). From Eqs. (B.70a) and (B.71a),

$$a_1(X_1) + a_2(X_1) = 1.$$

With this result in the conservation equations (B.70b) and (B.70c), the unknown functions $b_1(X_1)$ and $b_2(X_1)$ are determined as

$$b_1(X_1) = b_2(X_1) = 1.$$

Now, the approximate solution (B.68) contains only one unknown function $a_1(X_1)$. The moment equation made by the test function $\Psi^{(4)}$ gives the equation for $a_1(X_1)$ in the form

$$MR(T_\infty - T_{-\infty})\frac{\mathrm{d}a_1(X_1)}{\mathrm{d}X_1} = a_1(X_1)[1 - a_1(X_1)] \int_{\text{all } \boldsymbol{\xi}} \xi_1^2 J(f_{-\infty}, f_\infty)\mathbf{d}\boldsymbol{\xi}, \quad \text{(B.72)}$$

where $f_{-\infty}$ and f_∞ are, respectively, the velocity distribution functions of the state at upstream and downstream infinities, that is,

$$f_{-\infty} = \frac{\rho_{-\infty}}{(2\pi RT_{-\infty})^{3/2}} \exp\left(-\frac{(\xi_1 - v_{1-\infty})^2 + \xi_2^2 + \xi_3^2}{2RT_{-\infty}}\right),$$

$$f_\infty = \frac{\rho_\infty}{(2\pi RT_\infty)^{3/2}} \exp\left(-\frac{(\xi_1 - v_{1\infty})^2 + \xi_2^2 + \xi_3^2}{2RT_\infty}\right).$$

The boundary condition for $a_1(X_1)$ is

$$a_1(-\infty) = 1. \quad \text{(B.73)}$$

From Eqs. (B.72) and (B.73), the function $a_1(X_1)$ is determined. Whether this solution is a good approximate solution or not should be confirmed by increasing the numbers of the parameter functions in the solution and test functions. Naturally, the speed of convergence largely depends on the choice of the approximate solution and the test functions. Mott-Smith's description is a little different from the above one, but the content can be explained in the above way according to the general scheme of the moment method.

The Grad thirteen-moment method

In the *Grad thirteen-moment method* (Grad [1949]), the function with thirteen unknown functions ρ, v_i, $p_{ij}(= p_{ji})$, and q_i of t and X_i

$$f = f_e\left[1 + \frac{(\xi_i - v_i)(\xi_j - v_j)P_{ij}}{2pRT} + \frac{2q_i(\xi_i - v_i)}{5pRT}\left(\frac{(\xi_j - v_j)^2}{2RT} - \frac{5}{2}\right)\right], \quad \text{(B.74a)}$$

$$f_e = \frac{\rho}{(2\pi RT)^{3/2}} \exp\left(-\frac{(\xi_j - v_j)^2}{2RT}\right), \quad p = \frac{1}{3}p_{ii}, \quad RT = \frac{p}{\rho}, \quad P_{ij} = p_{ij} - p\delta_{ij}, \quad \text{(B.74b)}$$

where the parametric functions ρ, v_i, p_{ij}, and q_i are consistent with their definitions in Section 1.1, is chosen as the approximate solution, and the thirteen

functions

$$\left.\begin{aligned}
&\Psi^{(0)}=1,\ \ \Psi_i^{(1)}=\frac{\xi_i-v_i}{(2RT)^{1/2}},\ \ \Psi_{ij}^{(2)}=\frac{(\xi_i-v_i)(\xi_j-v_j)}{2RT}-\delta_{ij},\\
&\Psi_i^{(3)}=\frac{\xi_i-v_i}{(2RT)^{1/2}}\left(\frac{(\xi_j-v_j)^2}{2RT}-\frac{5}{2}\right)
\end{aligned}\right\} \tag{B.75}$$

are chosen as the test functions, where some modifications of super and subscripts are made. Putting Eq. (B.74a) into the Boltzmann equation and taking the thirteen moments with the test functions (B.75), we obtain thirteen equations for ρ, v_i, p_{ij}, and q_i. The product terms of P_{ij} and q_i in the collision integral being neglected in these equations, the Grad thirteen-moment equations (B.76a)–(B.76e) are derived:

$$\frac{\partial\rho}{\partial t}+\frac{\partial\rho v_i}{\partial X_i}=0, \tag{B.76a}$$

$$\frac{\partial v_i}{\partial t}+v_j\frac{\partial v_i}{\partial X_j}+\frac{1}{\rho}\frac{\partial p}{\partial X_i}+\frac{1}{\rho}\frac{\partial P_{ij}}{\partial X_j}=0, \tag{B.76b}$$

$$\frac{\partial p}{\partial t}+\frac{\partial pv_k}{\partial X_k}+\frac{2}{3}(p\delta_{ij}+P_{ij})\frac{\partial v_i}{\partial X_j}+\frac{2}{3}\frac{\partial q_j}{\partial X_j}=0, \tag{B.76c}$$

$$\begin{aligned}
&\frac{\partial P_{ij}}{\partial t}+\frac{\partial v_kP_{ij}}{\partial X_k}+\frac{2}{5}\left(\frac{\partial q_i}{\partial X_j}+\frac{\partial q_j}{\partial X_i}-\frac{2}{3}\frac{\partial q_k}{\partial X_k}\delta_{ij}\right)\\
&+P_{ik}\frac{\partial v_j}{\partial X_k}+P_{jk}\frac{\partial v_i}{\partial X_k}-\frac{2}{3}P_{kl}\frac{\partial v_k}{\partial X_l}\delta_{ij}\\
&+p\left(\frac{\partial v_i}{\partial X_j}+\frac{\partial v_j}{\partial X_i}-\frac{2}{3}\frac{\partial v_k}{\partial X_k}\delta_{ij}\right)+\frac{6}{m}B_1^{(2)}\rho P_{ij}=0,
\end{aligned} \tag{B.76d}$$

$$\begin{aligned}
&\frac{\partial q_i}{\partial t}+\frac{\partial v_kq_i}{\partial X_k}+\frac{7}{5}q_j\frac{\partial v_i}{\partial X_j}+\frac{2}{5}q_j\frac{\partial v_j}{\partial X_i}+\frac{2}{5}q_i\frac{\partial v_j}{\partial X_j}\\
&+RT\frac{\partial P_{ij}}{\partial X_j}+\frac{7}{2}P_{ij}\frac{\partial RT}{\partial X_j}-\frac{P_{ij}}{\rho}\frac{\partial p\delta_{jk}+P_{jk}}{\partial X_k}\\
&+\frac{5}{2}p\frac{\partial RT}{\partial X_i}+\frac{4}{m}B_1^{(2)}\rho q_i=0,
\end{aligned} \tag{B.76e}$$

where $B_1^{(2)}$ (the same notation as in Grad [1949]) is the function of RT determined by a molecular model, for example, for a hard-sphere gas,

$$B_1^{(2)}(RT)=\frac{8}{15}d_m^2(\pi RT)^{1/2}.$$

The approximate solution is an expansion in Hermite polynomials around local Maxwellian. The extension to higher orders is direct. Apparently, from this form of the solution, the thirteen-moment-type solution is difficult to describe the behavior of the Knudsen layer in a slightly rarefied gas flow and the

behavior of a gas with a finite Knudsen number. In a gas with a finite Knudsen number around a body or bodies, the velocity distribution function has discontinuities (see Sections 3.1.6, 4.8, 6.1– 6.4). Very large number of terms is required for the expansion as the thirteen-moment-type approximation to describe the discontinuity well. Nowadays, more systematic asymptotic theory is developed for small Knudsen numbers as shown in Chapter 3.

The Mott-Smith and Grad thirteen-moment works are pioneering and have historical meanings, but obviously from the above explanation, their results are temporal.

B.3 Modified Knudsen number expansion

In practical applications, we are often required a quick offer of the data of macroscopic variables for many arbitrary specified Knudsen numbers. Here, we introduce a method for this purpose and its application (Sone & Itakura [1990]). In this method, the solution is obtained by a series expansion in a function of the Knudsen number, and the coefficient functions of macroscopic variables in the expansion are stored. These data are summed up when the data are required. What should be noted is that the solution of the Boltzmann equation is singular at the two ends of the Knudsen number, $\mathrm{Kn} = 0$ and $\mathrm{Kn} = \infty$. Owing to the singularity at the origin, the range of convergence of the power series expansion of the solution in $\mathrm{Kn} - \mathrm{Kn}_0$ around some Knudsen number Kn_0 cannot be wider than $0 < \mathrm{Kn} < 2\mathrm{Kn}_0$, and therefore, some other form of function of Kn should be chosen.

We consider a time-independent boundary-value problem of the linearized Boltzmann equation

$$\zeta_i \frac{\partial \phi}{\partial x_i} = \frac{1}{k}\mathcal{L}(\phi) \tag{B.77}$$

under the boundary condition

$$\phi = b(\boldsymbol{\zeta}) + \mathcal{L}_B(\phi) \quad (\zeta_i n_i > 0). \tag{B.78}$$

Here, choosing some positive constant k_0, we introduce the new parameter ε defined by

$$\varepsilon = \frac{k - k_0}{k + k_0} = \frac{\mathrm{Kn} - \mathrm{Kn}_0}{\mathrm{Kn} + \mathrm{Kn}_0}, \qquad \mathrm{Kn}_0 = \frac{2}{\sqrt{\pi}} k_0, \tag{B.79}$$

and try to obtain the solution ϕ of the boundary-value problem, i.e., Eqs. (B.77) and (B.78), in a power series of ε, that is,

$$\phi(\boldsymbol{x}, \boldsymbol{\zeta}; k) = \sum_{n=0}^{\infty} \phi_n(\boldsymbol{x}, \boldsymbol{\zeta}; k_0)\varepsilon^n. \tag{B.80}$$

The parameter ε given by Eq. (B.79) is chosen in such a way that the range $0 < k \leq k_0$ corresponds to $-1 < \varepsilon \leq 0$ and $k_0 \leq k < \infty$ to $0 \leq \varepsilon < 1$. Thus

there is no singularity for $|\varepsilon| < 1$ and k in the range $0 < k < \infty$ is in $|\varepsilon| < 1$.[23] Substituting the series (B.80) into Eqs. (B.77) and (B.78), and arranging the same-order terms in ε, we obtain the equation for ϕ_n as

$$\zeta_i \frac{\partial \phi_n}{\partial x_i} = \frac{1}{k_0}\mathcal{L}(\phi_n) - \frac{2}{k_0} g_n \qquad (n \geq 0), \tag{B.81}$$

where

$$g_0 = 0, \qquad g_n = \mathcal{L}(\phi_{n-1}) - g_{n-1} \qquad (n \geq 1), \tag{B.82}$$

and the boundary condition for ϕ_n as

$$\phi_0 = b(\boldsymbol{\zeta}) + \mathcal{L}_B(\phi_0), \quad \phi_n = \mathcal{L}_B(\phi_n) \quad (n \geq 1) \quad (\zeta_i n_i > 0). \tag{B.83}$$

This is a boundary-value problem of inhomogeneous linearized Boltzmann equations at $k = k_0$.

The boundary-value problem is solved successively from the lowest order ($n = 0$), from which the coefficient functions of the expansion in ε of macroscopic variables are computed. The data of the coefficient functions are stored, and the program is prepared so as to sum up the coefficient functions providing the macroscopic variables. Thus, we can obtain the macroscopic variables for an arbitrary Knudsen number immediately only by inputting the Knudsen number.

The method is applied to the BKW equation for the analysis of the Poiseuille flow and thermal transpiration between parallel plane walls and through a circular pipe. A software for a personal computer giving the flow velocity profile and mass-flow rate in a figure and in a table immediately after inputting desired Knudsen numbers is prepared by Sone, Handa & Itakura. The software for a Windows PC can be downloaded from http://fd.kuaero.kyoto-u.ac.jp/members/sone or http://www.users.kudpc.kyoto-u.ac.jp/~a51424/Sone/database-e.html. The data of the software are prepared by the series with 80 terms for two k_0's, $k_0 = 1$ and $k_0 = 50$, and are supplemented with the data by the asymptotic theory for small k in Section 3.1 and the analytic works for large k in Ferziger [1967], Sone & Yamamoto [1968], and Niimi [1971].

B.4 Chapman–Enskog expansion

The *Chapman–Enskog expansion* (Chapman [1916], Enskog [1917]) is very well referred to when one mentions the relation of kinetic theory and fluid dynamics, although its discussion is done on the basis of the Hilbert expansion in the present book. The structure of the Chapman–Enskog expansion is briefly and clearly explained in Grad [1958]. Here, we explain the Chapman–Enskog expansion on the basis of Grad's procedure.

[23] The solution is implicitly assumed to be analytic not only for $0 < k < \infty$ but also for complex k that satisfies $|\varepsilon| < 1$.

Take the Boltzmann equation (1.47a) with (1.47b) in the absence of an external force ($\hat{F}_i = 0$) in a nondimensional form, that is,

$$\mathrm{Sh}\frac{\partial \hat{f}}{\partial \hat{t}} + \zeta_i \frac{\partial \hat{f}}{\partial x_i} = \frac{1}{k}\hat{J}(\hat{f}, \hat{f}), \tag{B.84a}$$

$$\hat{J}(\hat{f}, \hat{g}) = \frac{1}{2}\int (\hat{f}'\hat{g}'_* + \hat{f}'_*\hat{g}' - \hat{f}\hat{g}_* - \hat{f}_*\hat{g})\widehat{B}\,\mathrm{d}\Omega(\boldsymbol{\alpha})\,\mathbf{d}\boldsymbol{\zeta}_*. \tag{B.84b}$$

We introduce the variables $\hat{\rho}_r$ $(r = 0, 1, 2, 3, 4)$ defined by

$$\hat{\rho}_r = \int \psi_r \hat{f}\mathbf{d}\boldsymbol{\zeta}, \tag{B.85a}$$

where

$$\psi_0 = 1, \quad \psi_i = \zeta_i, \quad \psi_4 = \zeta_i^2 \qquad (i = 1, 2, 3).$$

The variables $\hat{\rho}_0$, $\hat{\rho}_i$, and $\hat{\rho}_4$ are related to the macroscopic variables $\hat{\rho}$, $\hat{v}_i$, and $\hat{T}$ [see Eqs. (1.54a)–(1.54c)] as

$$\hat{\rho}_0 = \hat{\rho}, \quad \hat{\rho}_i = \hat{\rho}\hat{v}_i, \quad \hat{\rho}_4 = \hat{\rho}(3\hat{T}/2 + \hat{v}_i^2), \tag{B.86}$$

but are introduced here for the brevity of expressions in the following discussion.

We consider the solution of Eq. (B.84a) whose time scale of variation corresponds to $\mathrm{Sh} = 1$ and that is expressed in the form

$$\hat{f} = \hat{f}(\hat{\rho}_r, \nabla\hat{\rho}_r, \boldsymbol{\zeta}, k), \tag{B.87}$$

where $\nabla\hat{\rho}_r$ represents partial derivatives with respect to x_i of arbitrary orders, as well as of the first order. As a solution of the Boltzmann equation (B.84a), $\hat{f}$ is a function of x_i, ζ_i, and $\hat{t}$ containing the parameter k, i.e., $\hat{f}(x_i, \hat{t}, k)$, and thus, $\hat{\rho}_r$ is a function of x_i and $\hat{t}$ containing the parameter k, i.e., $\hat{\rho}_r(x_i, \hat{t}, k)$. However, for the class of $\hat{f}$ in the form (B.87), the space and time variables x_i and $\hat{t}$ enter $\hat{f}$ only through $\hat{\rho}_r$ and $\nabla\hat{\rho}_r$. Then, from Eq. (B.84a), the time variation of $\hat{\rho}_r$ is given by the equation in the form

$$\frac{\partial \hat{\rho}_r}{\partial \hat{t}} + F_r(\hat{\rho}_s, \nabla\hat{\rho}_s, k) = 0. \tag{B.88}$$

We further limit the solution to the class that can be expressed in the form

$$\hat{f} = \sum_{n=0}^{\infty} k^n \hat{f}^{(n)}(\hat{\rho}_s, \nabla\hat{\rho}_s, \boldsymbol{\zeta}). \tag{B.89}$$

For this $\hat{f}$, Eq. (B.88) is reduced to

$$\frac{\partial \hat{\rho}_r}{\partial \hat{t}} + \sum_{n=0}^{\infty} k^n F_r^{(n)}(\hat{\rho}_s, \nabla\hat{\rho}_s) = 0. \tag{B.90}$$

On the other hand, from Eq. (B.87)

$$\frac{\partial \hat{f}}{\partial \hat{t}} = \sum_{r=0}^{4} \frac{\partial \hat{f}}{\partial \hat{\rho}_r} \frac{\partial \hat{\rho}_r}{\partial \hat{t}} + \sum_{*} \frac{\partial \hat{f}}{\partial \nabla \hat{\rho}_r} \frac{\partial \nabla \hat{\rho}_r}{\partial \hat{t}}, \tag{B.91}$$

where $*$ indicates the summation for all possible $\nabla\hat{\rho}_r$. Substituting Eqs. (B.89) and (B.90) into Eq. (B.91), we have $\partial\hat{f}/\partial\hat{t}$ for $\hat{f}$ given by Eq. (B.89) in the form

$$\frac{\partial \hat{f}}{\partial \hat{t}} = -\sum_{n=0}^{\infty} k^n \sum_{m=0}^{n} \left(\sum_{r=0}^{4} \frac{\partial \hat{f}^{(n-m)}}{\partial \hat{\rho}_r} F_r^{(m)} + \sum_{*} \frac{\partial \hat{f}^{(n-m)}}{\partial \nabla \hat{\rho}_r} \nabla F_r^{(m)} \right). \tag{B.92}$$

Now we try to construct the above-mentioned class of solution of the Boltzmann equation. Inserting Eqs. (B.89) and (B.92) into the Boltzmann equation (B.84a) with (B.84b), and arranging the same-order terms in k, we obtain the series of integral equations for $\hat{f}^{(n)}$ $(n = 0, 1, 2, \ldots)$, i.e.,

$$\hat{J}(\hat{f}^{(0)}, \hat{f}^{(0)}) = 0, \tag{B.93a}$$

$$\begin{aligned} 2\hat{J}(\hat{f}^{(0)}, \hat{f}^{(n)}) = &- \sum_{m=0}^{n-1} \left(\sum_{r=0}^{4} \frac{\partial \hat{f}^{(n-1-m)}}{\partial \hat{\rho}_r} F_r^{(m)} + \sum_{*} \frac{\partial \hat{f}^{(n-1-m)}}{\partial \nabla \hat{\rho}_r} \nabla F_r^{(m)} \right) \\ &+ \zeta_i \frac{\partial \hat{f}^{(n-1)}}{\partial x_i} - \sum_{m=1}^{n-1} \hat{J}(\hat{f}^{(n-m)}, \hat{f}^{(m)}) \qquad (n \geq 1), \end{aligned} \tag{B.93b}$$

in the second of which the last term is absent when $n = 1$.

The solution of Eq. (B.93a) is Maxwellian (see Section A.7.1), i.e.,

$$\ln \hat{f}^{(0)} = \Upsilon_0^{(0)} + \Upsilon_i^{(0)} \zeta_i + \Upsilon_4^{(0)} \zeta_i^2,$$

where $\Upsilon_0^{(0)}$, $\Upsilon_i^{(0)}$, and $\Upsilon_4^{(0)}$ are undetermined functions of x_i and $\hat{t}$. The linear integral equation (B.93b) for $\hat{f}^{(n)}$ has a solution only when the condition

$$\begin{aligned} &\int \psi_r \left[\sum_{m=0}^{n-1} \left(\sum_{s=0}^{4} \frac{\partial \hat{f}^{(n-1-m)}}{\partial \hat{\rho}_s} F_s^{(m)} + \sum_{*} \frac{\partial \hat{f}^{(n-1-m)}}{\partial \nabla \hat{\rho}_s} \nabla F_s^{(m)} \right) - \zeta_i \frac{\partial \hat{f}^{(n-1)}}{\partial x_i} \right] \mathbf{d}\boldsymbol{\zeta} \\ &= 0 \quad (n \geq 1) \end{aligned} \tag{B.94}$$

is satisfied, because, as shown in Section A.2.2,

$$\int \psi_r \hat{J}(\hat{f}, \hat{g}) \mathbf{d}\boldsymbol{\zeta} = 0,$$

for arbitrary $\hat{f}$ and $\hat{g}$. The corresponding homogeneous equation to Eq. (B.93b), i.e., $2\hat{J}(\hat{f}^{(0)}, \hat{f}^{(n)}) = 0$, has five independent nontrivial solutions $\hat{f}^{(0)}\psi_r$. Thus, the solution has a freedom in adding an arbitrary linear combination of these

solutions. With this freedom, we look for the solution that satisfies the following conditions:[24]

$$\int \psi_r \hat{f}^{(0)} \mathbf{d}\boldsymbol{\zeta} = \hat{\rho}_r, \qquad \int \psi_r \hat{f}^{(n)} \mathbf{d}\boldsymbol{\zeta} = 0 \quad (n \geq 1). \tag{B.95}$$

With this choice, $\hat{f}^{(0)}$ is expressed as

$$\hat{f}^{(0)} = \frac{\hat{\rho}}{(\pi \hat{T})^{3/2}} \exp\left(-\frac{(\zeta_i - \hat{v}_i)^2}{\hat{T}} \right). \tag{B.96}$$

The solvability condition (B.94) can be simplified owing to the relation (B.95). From Eqs. (B.95) and (B.96), we have

$$\int \psi_r \frac{\partial \hat{f}^{(0)}}{\partial \hat{\rho}_s} \mathbf{d}\boldsymbol{\zeta} = \frac{\partial \hat{\rho}_r}{\partial \hat{\rho}_s} = \delta_{rs}, \quad \int \psi_r \frac{\partial \hat{f}^{(n)}}{\partial \hat{\rho}_s} \mathbf{d}\boldsymbol{\zeta} = 0 \quad (n \geq 1),$$
$$\int \psi_r \frac{\partial \hat{f}^{(n)}}{\partial \nabla \hat{\rho}_s} \mathbf{d}\boldsymbol{\zeta} = 0.$$

With the aid of these relations, Eq. (B.94) is reduced to

$$F_r^{(n-1)} - \frac{\partial}{\partial x_j} \int \psi_r \zeta_j \hat{f}^{(n-1)} \mathbf{d}\boldsymbol{\zeta} = 0 \quad (n \geq 1). \tag{B.97}$$

When $n = 1$, from Eqs. (B.97) and (B.96),

$$F_0^{(0)} = \frac{\partial \hat{\rho} \hat{v}_i}{\partial x_i}, \quad F_i^{(0)} = \frac{1}{2} \frac{\partial \hat{p}}{\partial x_i} + \frac{\partial \hat{\rho} \hat{v}_i \hat{v}_j}{\partial x_j}, \quad F_4^{(0)} = \frac{\partial}{\partial x_i} \left[\hat{\rho} \hat{v}_i \left(\frac{5}{2} \hat{T} + \hat{v}_j^2 \right) \right], \tag{B.98}$$

where $i, j = 1, 2, 3$ (note $\hat{p} = \hat{\rho}\hat{T}$). The equation (B.93b) for $\hat{f}^{(1)}$ is reduced to

$$\begin{aligned} 2\hat{J}(\hat{f}^{(0)}, \hat{f}^{(1)}) &= -\sum_{r=0}^{4} \frac{\partial \hat{f}^{(0)}}{\partial \hat{\rho}_r} F_r^{(0)} + \zeta_i \frac{\partial \hat{f}^{(0)}}{\partial x_i} \\ &= \frac{(\zeta_i - \hat{v}_i)(\zeta_j - \hat{v}_j)}{\hat{T}} \left(\frac{\partial \hat{v}_i}{\partial x_j} + \frac{\partial \hat{v}_j}{\partial x_i} - \frac{2}{3} \frac{\partial \hat{v}_k}{\partial x_k} \delta_{ij} \right) \hat{f}^{(0)} \\ &\quad + \left(\frac{(\zeta_j - \hat{v}_j)^2}{\hat{T}} - \frac{5}{2} \right) \frac{\zeta_i - \hat{v}_i}{\hat{T}} \frac{\partial \hat{T}}{\partial x_i} \hat{f}^{(0)}. \end{aligned} \tag{B.99}$$

Introducing the new variable $\mathcal{C}_i = (\zeta_i - \hat{v}_i)/\hat{T}^{1/2}$ and expressing $\hat{f}^{(1)}$ in the form $\hat{f}^{(1)} = \hat{f}^{(0)} \Psi(\boldsymbol{\mathcal{C}})$, we obtain the equation for $\Psi(\boldsymbol{\mathcal{C}})$ in the form

$$\mathcal{L}_{\hat{T}}(\Psi) = \frac{1}{\hat{\rho}\hat{T}^{1/2}} \left(\mathcal{C}_i \mathcal{C}_j - \frac{1}{3} \mathcal{C}^2 \delta_{ij} \right) \left(\frac{\partial \hat{v}_i}{\partial x_j} + \frac{\partial \hat{v}_j}{\partial x_i} \right) + \frac{1}{\hat{\rho}\hat{T}} \mathcal{C}_i \left(\mathcal{C}^2 - \frac{5}{2} \right) \frac{\partial \hat{T}}{\partial x_i}, \tag{B.100}$$

[24]The condition (B.95) does not mean that $\Upsilon_r^{(0)}$ is independent of k when it is considered as a function of x_i and $\hat{t}$. Owing to the application of the condition (B.95), the component function $\hat{f}^{(n)}$ of the expansion (B.89) is not independent of k if it is considered as a function of x_i and $\hat{t}$. In the Hilbert expansion, including its variation in the present book, the component functions of the expansion are independent of k.

where $\mathcal{L}_{\hat{T}}$ is the linearized collision operator defined by Eq. (A.111) in Section A.2.8 and $\mathcal{C} = |\boldsymbol{\mathcal{C}}|$. The solution of this integral equation satisfying the second relation in Eq. (B.95) is expressed using the functions $\mathcal{A}(\mathcal{C},\hat{T})$ and $\mathcal{B}^{(0)}(\mathcal{C},\hat{T})$ defined, respectively, by Eqs. (A.123) and (A.124) with (A.128a) in Section A.2.9 in the following form:

$$\Psi = -\frac{1}{2\hat{\rho}\hat{T}^{1/2}}\left(\mathcal{C}_i\mathcal{C}_j - \frac{1}{3}\mathcal{C}^2\delta_{ij}\right)\mathcal{B}^{(0)}(\mathcal{C},\hat{T})\left(\frac{\partial \hat{v}_i}{\partial x_j} + \frac{\partial \hat{v}_j}{\partial x_i}\right) - \frac{1}{\hat{\rho}\hat{T}}\mathcal{C}_i\mathcal{A}(\mathcal{C},\hat{T})\frac{\partial \hat{T}}{\partial x_i}. \tag{B.101}$$

With this Ψ, $F_r^{(1)}$ is expressed as

$$F_r^{(1)} = \frac{\partial}{\partial x_j}\left(\hat{\rho}\int(\hat{T}^{1/2}\mathcal{C}_j + \hat{v}_j)\psi_r\Psi E(\mathcal{C})\mathrm{d}\boldsymbol{\mathcal{C}}\right),$$

where ψ_r is expressed as 1, $\hat{T}^{1/2}\mathcal{C}_i + \hat{v}_i$, or $(\hat{T}^{1/2}\mathcal{C}_i + \hat{v}_i)^2$ in terms of $\mathcal{C}_i$ and $E(\mathcal{C}) = \pi^{-3/2}\exp(-\mathcal{C}^2)$. After some manipulation, noting that

$$\begin{aligned}&\left[\int \mathcal{C}_i\mathcal{C}_j\left(\mathcal{C}_k\mathcal{C}_l - \frac{1}{3}\mathcal{C}^2\delta_{kl}\right)\mathcal{B}^{(0)}(\mathcal{C},\hat{T})E(\mathcal{C})\mathrm{d}\boldsymbol{\mathcal{C}}\right]\left(\frac{\partial \hat{v}_k}{\partial x_l} + \frac{\partial \hat{v}_l}{\partial x_k}\right)\\ &\qquad = \left(\frac{8\pi}{15}\int_0^\infty \mathcal{C}^6\mathcal{B}^{(0)}(\mathcal{C},\hat{T})E(\mathcal{C})\mathrm{d}\mathcal{C}\right)\left(\frac{\partial \hat{v}_i}{\partial x_j} + \frac{\partial \hat{v}_j}{\partial x_i} - \frac{2}{3}\frac{\partial \hat{v}_k}{\partial x_k}\delta_{ij}\right),\end{aligned}$$

and

$$\left(\int \mathcal{C}_i\mathcal{C}_j\mathcal{C}^2\mathcal{A}(\mathcal{C},\hat{T})E(\mathcal{C})\mathrm{d}\boldsymbol{\mathcal{C}}\right)\frac{\partial \hat{T}}{\partial x_j} = \left(\frac{4\pi}{3}\int_0^\infty \mathcal{C}^6\mathcal{A}(\mathcal{C},\hat{T})E(\mathcal{C})\mathrm{d}\mathcal{C}\right)\frac{\partial \hat{T}}{\partial x_i},$$

we have

$$F_0^{(1)} = 0, \tag{B.102a}$$

$$F_i^{(1)} = -\frac{1}{2}\frac{\partial}{\partial x_j}\left[\Gamma_1(\hat{T})\left(\frac{\partial \hat{v}_i}{\partial x_j} + \frac{\partial \hat{v}_j}{\partial x_i} - \frac{2}{3}\frac{\partial \hat{v}_k}{\partial x_k}\delta_{ij}\right)\right], \tag{B.102b}$$

$$\begin{aligned}F_4^{(1)} = &-\frac{5}{4}\frac{\partial}{\partial x_j}\left(\Gamma_2(\hat{T})\frac{\partial \hat{T}}{\partial x_j}\right)\\ &- \frac{\partial}{\partial x_j}\left[\Gamma_1(\hat{T})\left(\frac{\partial \hat{v}_i}{\partial x_j} + \frac{\partial \hat{v}_j}{\partial x_i} - \frac{2}{3}\frac{\partial \hat{v}_k}{\partial x_k}\delta_{ij}\right)\hat{v}_i\right],\end{aligned} \tag{B.102c}$$

where i, $j = 1, 2, 3$ and

$$\Gamma_1(\hat{T})\hat{T}^{-1/2} = \frac{8\pi}{15}\int_0^\infty \mathcal{C}^6\mathcal{B}^{(0)}(\mathcal{C},\hat{T})E(\mathcal{C})\mathrm{d}\mathcal{C},$$

$$\Gamma_2(\hat{T})\hat{T}^{-1/2} = \frac{16\pi}{15}\int_0^\infty \mathcal{C}^6\mathcal{A}(\mathcal{C},\hat{T})E(\mathcal{C})\mathrm{d}\mathcal{C},$$

as defined by Eq. (A.131) in Section A.2.9.

Noting the relations

$$\frac{\partial\hat{\rho}_0}{\partial\hat{t}}=\frac{\partial\hat{\rho}}{\partial\hat{t}},\qquad \frac{\partial\hat{\rho}_i}{\partial\hat{t}}=\frac{\partial\hat{\rho}\hat{v}_i}{\partial\hat{t}},\qquad \frac{\partial\hat{\rho}_4}{\partial\hat{t}}=\frac{\partial}{\partial\hat{t}}\left[\hat{\rho}\left(\frac{3}{2}\hat{T}+\hat{v}_i^2\right)\right],$$

[see Eq. (B.86)] and the results (B.98) and (B.102a)–(B.102c), we find that Eq. (B.90) is reduced to the Euler set of equations when only the terms with $n=0$ are retained and to the Navier–Stokes set when the terms with $n=0$ and 1 are retained. That is,

$$\frac{\partial\hat{\rho}}{\partial\hat{t}}+\frac{\partial\hat{\rho}\hat{v}_i}{\partial x_i}=0, \tag{B.103a}$$

$$\frac{\partial\hat{\rho}\hat{v}_i}{\partial\hat{t}}+\frac{\partial\hat{\rho}\hat{v}_i\hat{v}_j}{\partial x_j}=-\frac{1}{2}\frac{\partial\hat{p}}{\partial x_i}, \tag{B.103b}$$

$$\frac{\partial}{\partial\hat{t}}\left[\hat{\rho}\left(\frac{3}{2}\hat{T}+\hat{v}_i^2\right)\right]+\frac{\partial}{\partial x_i}\left[\hat{\rho}\hat{v}_i\left(\frac{5}{2}\hat{T}+\hat{v}_j^2\right)\right]=0, \tag{B.103c}$$

and

$$\frac{\partial\hat{\rho}}{\partial\hat{t}}+\frac{\partial\hat{\rho}\hat{v}_i}{\partial x_i}=0, \tag{B.104a}$$

$$\frac{\partial\hat{\rho}\hat{v}_i}{\partial\hat{t}}+\frac{\partial\hat{\rho}\hat{v}_i\hat{v}_j}{\partial x_j}=-\frac{1}{2}\frac{\partial\hat{p}}{\partial x_i}+\frac{k}{2}\frac{\partial}{\partial x_j}\left[\Gamma_1(\hat{T})\left(\frac{\partial\hat{v}_i}{\partial x_j}+\frac{\partial\hat{v}_j}{\partial x_i}-\frac{2}{3}\frac{\partial\hat{v}_k}{\partial x_k}\delta_{ij}\right)\right], \tag{B.104b}$$

$$\frac{\partial}{\partial\hat{t}}\left[\hat{\rho}\left(\frac{3}{2}\hat{T}+\hat{v}_i^2\right)\right]+\frac{\partial}{\partial x_i}\left[\hat{\rho}\hat{v}_i\left(\frac{5}{2}\hat{T}+\hat{v}_j^2\right)\right]=\frac{5k}{4}\frac{\partial}{\partial x_j}\left(\Gamma_2(\hat{T})\frac{\partial\hat{T}}{\partial x_j}\right)+k\frac{\partial}{\partial x_j}\left[\Gamma_1(\hat{T})\left(\frac{\partial\hat{v}_i}{\partial x_j}+\frac{\partial\hat{v}_j}{\partial x_i}-\frac{2}{3}\frac{\partial\hat{v}_k}{\partial x_k}\delta_{ij}\right)\hat{v}_i\right]. \tag{B.104c}$$

Incidentally, the equations derived at the next stage are called the *Burnett equations*. Obviously from the derivation, the order of the differential system increases by one if we advance the analysis to the next stage. An ill-posed set of equations is derived in the expansion (Sone [1968, 1984b]).[25]

Finally, it may be noted that it is inappropriate or incorrect to discuss the asymptotic behavior of the gas for small Knudsen numbers with the series of equations derived by the Chapman–Enskog expansion by simply relating the order at which a set of equations appears to the order that the set describes the asymptotic behavior, as we have seen in Chapter 3.

B.5 Hypersonic approximation

In order to study an expanding flow into a vacuum, Hamel & Willis [1966] and Edwards & Cheng [1966] introduced a method called *hypersonic approximation*.

[25] See Footnote 52 in Section 3.2.6.

In a hypersonic region, where Mach number is very large (Ma $\gg 1$), the width of the velocity distribution function is much smaller than the flow speed. Thus, some simplification can be possible. Here, we will explain the method for a spherically expanding flow with a hypersonic speed in a slightly different way from the original works.

As we have seen in various examples in an infinite domain (e.g., Sections 6.2.3 and 6.4.2), we consider the case where the length scale of variation is of the order of the distance $\hat{r}$ from the center of expansion, i.e.,

$$\frac{\partial(*)}{\partial \hat{r}} = O\left(\frac{*}{\hat{r}}\right). \tag{B.105}$$

In a hypersonic state [$v_r/(2RT)^{1/2} \gg 1$ or $\hat{v}_r/\hat{T}^{1/2} \gg 1$], the velocity distribution function $\hat{f}$ is appreciable only in the region where $|\zeta_r - \hat{v}_r| = O(\hat{T}^{1/2}) \ll \hat{v}_r$, $|\zeta_\theta| = O(\hat{T}^{1/2}) \ll \hat{v}_r$, and $|\zeta_\varphi| = O(\hat{T}^{1/2}) \ll \hat{v}_r$. Thus, $\hat{p}_{rr}$, $\hat{p}_{\theta\theta}$, $\hat{p}_{\varphi\varphi} = O(\hat{\rho}\hat{T}) \ll \hat{\rho}\hat{v}_r^2$ and $|\hat{q}_r| = O(\hat{\rho}\hat{T}^{3/2}) \ll \hat{\rho}\hat{T}\hat{v}_r$. The above two kinds of conditions, the slowly varying and the size of the variables, are the basic assumptions of the hypersonic approximation.

Under these two conditions, consider the Boltzmann equation in a time-independent state in the spherical coordinate system [Eq. (A.162) in Section A.3]

$$D_{sps}\hat{f} = \frac{1}{k}\hat{J}(\hat{f}, \hat{f}), \tag{B.106}$$

with

$$D_{sps} = \zeta_r \frac{\partial}{\partial \hat{r}} + \frac{\zeta_\theta^2 + \zeta_\varphi^2}{\hat{r}} \frac{\partial}{\partial \zeta_r} - \frac{\zeta_r \zeta_\theta}{\hat{r}} \frac{\partial}{\partial \zeta_\theta} - \frac{\zeta_r \zeta_\varphi}{\hat{r}} \frac{\partial}{\partial \zeta_\varphi}, \tag{B.107}$$

where the spherical symmetry is assumed and the external force is absent.[26] Here, we have the conservation equation

$$\int \begin{bmatrix} 1 \\ \zeta_r \\ \zeta^2 \end{bmatrix} D_{sps}\hat{f} \mathbf{d\zeta} = \frac{1}{k} \int \begin{bmatrix} 1 \\ \zeta_r \\ \zeta^2 \end{bmatrix} \hat{J}(\hat{f}, \hat{f}) \mathbf{d\zeta} = 0. \tag{B.108}$$

These equations are expressed as

$$\frac{\mathrm{d}\hat{\rho}\hat{v}_r\hat{r}^2}{\mathrm{d}\hat{r}} = 0, \tag{B.109a}$$

$$\frac{\mathrm{d}}{\mathrm{d}\hat{r}}\left[\left(\hat{\rho}\hat{v}_r^2 + \frac{1}{2}\hat{p}_{rr}\right)\hat{r}^2\right] = \frac{1}{2}(\hat{p}_{\theta\theta} + \hat{p}_{\varphi\varphi})\hat{r}, \tag{B.109b}$$

$$\frac{3}{2}\hat{\rho}\hat{v}_r\frac{\mathrm{d}\hat{T}}{\mathrm{d}\hat{r}} + \hat{p}_{rr}\frac{\mathrm{d}\hat{v}_r}{\mathrm{d}\hat{r}} + \frac{1}{\hat{r}^2}\frac{\mathrm{d}\hat{q}_r\hat{r}^2}{\mathrm{d}\hat{r}} = -\frac{(\hat{p}_{\theta\theta} + \hat{p}_{\varphi\varphi})\hat{v}_r}{\hat{r}}. \tag{B.109c}$$

The third equation is obtained with the combination of the three relations in Eq. (B.108). These relations are rigorous.

[26] As explained in Footnote 19 in Section 6.4.1, $\hat{f}$ is a function of $\hat{r}$, ζ_r, and $\zeta_\theta^2 + \zeta_\varphi^2$. Thus, the terms containing $\cot\theta$ in Eq. (A.165) cancel out each other.

Here, we introduce the hypersonic approximation, where $\hat{\rho}\hat{v}_r^2 \gg \hat{p}_{rr}$, $\hat{\rho}\hat{v}_r^2 \gg \hat{p}_{\theta\theta}$, $\hat{\rho}\hat{v}_r^2 \gg \hat{p}_{\varphi\varphi}$, $\hat{\rho}\hat{T}\hat{v}_r \gg |\hat{q}_r|$, and $\mathrm{d}(*)/\mathrm{d}\hat{r} \sim (*/\hat{r})$. Leaving the leading-order terms in Eq. (B.109b) and applying Eq. (B.109a) to the result, we have

$$\frac{\mathrm{d}\hat{v}_r}{\mathrm{d}\hat{r}} = 0, \quad \text{i.e.,} \quad \hat{v}_r = c_1, \tag{B.110}$$

where c_1 is a constant, and with this relation in Eq. (B.109a),

$$\hat{\rho} = c_0 \hat{r}^{-2}, \tag{B.111}$$

where c_0 is a constant. Equation (B.109c) is simplified as

$$\frac{3}{2}\hat{\rho}\hat{v}_r \frac{\mathrm{d}\hat{T}}{\mathrm{d}\hat{r}} + \hat{p}_{rr}\frac{\mathrm{d}\hat{v}_r}{\mathrm{d}\hat{r}} = -\frac{(\hat{p}_{\theta\theta} + \hat{p}_{\varphi\varphi})\hat{v}_r}{\hat{r}}, \tag{B.112}$$

because $|\hat{q}_r| \ll \hat{\rho}\hat{T}\hat{v}_r$, and further, with the aid of Eqs. (B.110) and (B.111),

$$\frac{3c_0}{2\hat{r}}\frac{\mathrm{d}\hat{T}}{\mathrm{d}\hat{r}} = -(\hat{p}_{\theta\theta} + \hat{p}_{\varphi\varphi}). \tag{B.113}$$

The equation contains $\hat{p}_{\theta\theta} + \hat{p}_{\varphi\varphi}$, which will be written as $2\hat{p}_\perp$ for short, in addition to $\hat{T}$.

Here, we will try to derive the equation for $\hat{p}_\perp$ under the hypersonic approximation on the basis of the BKW equation

$$D_{sps}\hat{f} = \frac{\hat{\rho}}{k}(\hat{f}_e - \hat{f}), \tag{B.114}$$

where

$$\hat{f}_e = \frac{\hat{\rho}}{(\pi\hat{T})^{3/2}} \exp\left(-\frac{(\zeta_r - \hat{v}_r)^2 + \zeta_\theta^2 + \zeta_\varphi^2}{\hat{T}}\right).$$

In a hypersonic region, the dominant terms in $D_{sps}\hat{f}$ are, obviously,

$$\begin{aligned} D_{sps}\hat{f} &= \zeta_r \frac{\partial \hat{f}}{\partial \hat{r}} - \frac{\zeta_r\zeta_\theta}{\hat{r}}\frac{\partial \hat{f}}{\partial \zeta_\theta} - \frac{\zeta_r\zeta_\varphi}{\hat{r}}\frac{\partial \hat{f}}{\partial \zeta_\varphi} \\ &= \hat{v}_r\left(\frac{\partial \hat{f}}{\partial \hat{r}} - \frac{\zeta_\theta}{\hat{r}}\frac{\partial \hat{f}}{\partial \zeta_\theta} - \frac{\zeta_\varphi}{\hat{r}}\frac{\partial \hat{f}}{\partial \zeta_\varphi}\right), \end{aligned} \tag{B.115}$$

because $\hat{f}$ is appreciable only for $|\zeta_r - \hat{v}_r|/\hat{v}_r \ll 1$. Then, the BKW equation (B.114) is simplified as

$$\frac{\partial \hat{f}}{\partial \hat{r}} - \frac{\zeta_\theta}{\hat{r}}\frac{\partial \hat{f}}{\partial \zeta_\theta} - \frac{\zeta_\varphi}{\hat{r}}\frac{\partial \hat{f}}{\partial \zeta_\varphi} = \frac{\hat{\rho}}{k\hat{v}_r}(\hat{f}_e - \hat{f}). \tag{B.116}$$

Multiplying Eq. (B.116) by $\zeta_\theta^2 + \zeta_\varphi^2$ and integrating it over the whole space of $\boldsymbol{\zeta}$, we obtain

$$\frac{\mathrm{d}\hat{p}_\perp}{\mathrm{d}\hat{r}} + \frac{4}{\hat{r}}\hat{p}_\perp = \frac{\hat{\rho}}{k\hat{v}_r}(\hat{\rho}\hat{T} - \hat{p}_\perp), \tag{B.117}$$

or

$$\frac{\mathrm{d}\hat{p}_\perp}{\mathrm{d}\hat{r}} + \frac{4}{\hat{r}}\hat{p}_\perp = \frac{c_0}{kc_1\hat{r}^2}\left(\frac{c_0}{\hat{r}^2}\hat{T} - \hat{p}_\perp\right). \tag{B.118}$$

This is the equation for $\hat{p}_\perp$, where only $\hat{T}$ is contained.[27] This simplification comes from the process that ζ_r in the operator D_{sps} is replaced by $\hat{v}_r$ by the hypersonic approximation. Eliminating $\hat{p}_\perp$ from Eqs. (B.113) and (B.118), we obtain the equation for $\hat{T}$ as

$$\frac{\mathrm{d}^2\hat{T}}{\mathrm{d}\hat{r}^2} + \left(\frac{3}{\hat{r}} + \frac{c_0}{c_1k\hat{r}^2}\right)\frac{\mathrm{d}\hat{T}}{\mathrm{d}\hat{r}} + \frac{4c_0}{3c_1k\hat{r}^3}\hat{T} = 0. \tag{B.119}$$

The solution of this equation is expressed by the confluent hypergeometric function as

$$\hat{T} = \frac{1}{\hat{r}^2}\left[c_2U\left(\frac{2}{3}, 3, \frac{c_0}{c_1k\hat{r}}\right) + c_3M\left(\frac{2}{3}, 3, \frac{c_0}{c_1k\hat{r}}\right)\right], \tag{B.120}$$

where $U(a, b, c)$ and $M(a, b, c)$ are the Kummer's functions (Abramowitz & Stegun [1972]) and c_2 and c_3 are constants.

Obviously, the hypersonic approximation is applicable irrespective of the value of k. This solution is used in Section 6.4.2 to express the far field in an evaporating flow from a sphere into vacuum, where the solution is joined to the isentropic flow for small k.

[27] The left-hand side is of the same form independently of the molecular model, but the right-hand side or the collision term takes such a simple form for the BKW equation.

Appendix C

Some Data

C.1 Some integrals

Here, some integrals that are often encountered in the analysis of the Boltzmann equation are listed. In the following formulas, n is a non-negative integer, and β is a positive constant. The first three are one-dimensional integrals:

$$\int_0^\infty \exp(-\beta\zeta^2)\mathrm{d}\zeta = \frac{1}{2}\sqrt{\frac{\pi}{\beta}}, \tag{C.1a}$$

$$\int_0^\infty \zeta^{2n}\exp(-\beta\zeta^2)\mathrm{d}\zeta = \frac{(2n-1)(2n-3)\cdots 1}{2^{n+1}\beta^n}\sqrt{\frac{\pi}{\beta}}, \tag{C.1b}$$

$$\int_0^\infty \zeta^{2n+1}\exp(-\beta\zeta^2)\mathrm{d}\zeta = \frac{n!}{2\beta^{n+1}} \qquad (0! = 1). \tag{C.1c}$$

The following are three-dimensional integrals:

$$\int_{\text{all }\boldsymbol{\zeta}} \zeta^{2n}\exp(-\beta\zeta^2)\mathbf{d}\boldsymbol{\zeta} = \frac{(2n+1)(2n-1)\cdots 1}{2^n\beta^n}\left(\frac{\pi}{\beta}\right)^{3/2}, \tag{C.2a}$$

$$\int_{\text{all }\boldsymbol{\zeta}} \zeta^{2n+1}\exp(-\beta\zeta^2)\mathbf{d}\boldsymbol{\zeta} = \frac{2(n+1)!}{\beta^{n+2}}\pi, \tag{C.2b}$$

where

$$\zeta = (\zeta_i^2)^{1/2}.$$

The generalization of Eq. (C.2a) is discussed in Sone [2002]. That is,

$$\int_{\text{all }\boldsymbol{\zeta}} \zeta_{i_1}\cdots\zeta_{i_{2S}}\exp(-\zeta^2)\mathbf{d}\boldsymbol{\zeta} = \frac{\pi^{3/2}}{2^S}\sum_{k=1}^{N_S}\prod_{\text{all the pairs }(i_t,i_u)\text{ in }C_k(S)}\delta_{i_t i_u}, \tag{C.3}$$

where some explanation of notation is required. Consider a sequence $(i_1, \ldots, i_{2S})$ of $2S$ indices. Let us compose a set of S pairs of indices [say $C_k(S)$], for example,

$$C_1(S) : \{\underbrace{(i_1, i_2), (i_3, i_4), \ldots, (i_{2S-3}, i_{2S-2}), (i_{2S-1}, i_{2S})}_{S}\},$$

where no distinction is made between the pairs (i, j) and (j, i), and the order of the pairs in the brackets $\{\ldots\}$ is indifferent. Let IP be the ensemble consisting of $C_k(S)$, and N_S be the number of the elements of the ensemble IP. That is,

$$IP = \{C_k(S) \quad (k = 1, 2, \ldots, N_S)\}. \tag{C.4}$$

Then, N_S is given by

$$N_S = \frac{\binom{2S}{2}\binom{2S-2}{2} \cdots \binom{4}{2}\binom{2}{2}}{S!} = \frac{(2S)!}{2^S S!}. \tag{C.5}$$

The formula (C.3) indicates first to compute the product

$$\prod_{\text{all the pairs } (i_t, i_u) \text{ in } C_k(S)} \delta_{i_t i_u}$$

for a $C_k(S)$ and then to sum up the results for all $C_k(S)$ in IP.

C.2 Some numerical data

Some numerical data are listed here to help to grasp the physical image. The data in this section, which are not aimed to be very accurate, are based on NIST Chemistry Webbook, http://www.nist.gov. or Mohr & Taylor [2005] unless otherwise stated.

The Boltzmann constant k_B, the Avogadro constant N_{Av} defined by the number of molecules per mol, and the gas constant R_{mol} ($= N_{\mathrm{Av}} k_B$) per mol are

$$\begin{aligned} k_B &= 1.3806505 \times 10^{-23} \text{ J/K}, \\ N_{\mathrm{Av}} &= 6.0221415 \times 10^{23} \text{ mol}^{-1}, \\ R_{\mathrm{mol}} &= 8.314472 \text{ J/mol K}. \end{aligned}$$

The specific gas constant R is the ratio of R_{mol} to the molar mass (say, m_{mol}) of a gas, i.e., $R = R_{\mathrm{mol}}/m_{\mathrm{mol}}$. Incidentally the *molar mass* m_{mol} is given by (the molecular weight) $\times 10^{-3}$ kg/mol. Some examples of molecular weight and specific gas constant are given in Table C.1.

At the *standard state*, the state of gas at 0 °C (273.15 K) and 1 atm (101 325 Pa), the number density n of molecules is

$$n = 2.6867773 \times 10^{25} \text{ m}^{-3}.$$

Table C.1. The molecular weight, the specific gas constant R, and some properties of gases at the standard state [0 °C (273.15 K) and 1 atm (101 325 Pa)]. The ρ is the density, μ is the viscosity, λ is the thermal conductivity, c is the speed of sound, ℓ is the mean free path, and d_m is the diameter of a molecule. The units are shown in the parentheses, where Pa (pascal) = kg/m s^2 and W (watt) = kg m^2/s^3.

	He	Ne	Ar	N_2	O_2	Air
molecular weight	4.003	20.18	39.95	28.02	32.00	28.96
R (10^2 m^2/s^2 K)	20.77	4.120	2.081	2.967	2.598	2.871
ρ (kg/m^3)	0.1785	0.8999	1.784	1.250	1.429	1.293
μ (10^{-5}Pa s)	1.870	2.939	2.096	1.664	1.906	1.71
λ (10^{-2}W/m K)	14.62	4.541	1.637	2.403	2.449	2.41
c (m/s)	973	433	308	337	315	331
ℓ (μm)	0.175	0.122	0.062	0.059	0.063	0.059
d_m (nm)	0.219	0.262	0.368	0.378	0.365	0.375

Table C.2. Saturated gas pressure p (torr) vs temperature T (°C) (Margrave [1967], Honing & Kramer [1969]). The superscript $*$ indicates that the correponding condensed phase is liquid. Note: 1 torr = 133.322 Pa.

As		Hg*		Mg		S		N_2^*	
T	p	T	10^2p	T	10^4p	T	10^6p	T	p
277	0.01	7	0.01	246	0.01	−10	0.01	−209.7	100
372	1	46	1	327	1	17	1	−195.8	760
518	100	125	100	439	100	55	100	−169.8	7600

The volume V_{mol} of a perfect gas per mol at the standard state is

$$V_{\mathrm{mol}} = 2.2413996 \times 10^{-2}\ \mathrm{m}^3 \cdot \mathrm{mol}^{-1}.$$

The density ρ, the viscosity μ, the thermal conductivity λ, the speed of sound c, the mean free path ℓ, and the diameter d_m of a molecule for several gases at standard state are tabulated in Table C.1. The mean free path ℓ and the diameter d_m of a molecule are rough estimated data by the formulas (1.22) and (3.70) on the basis of the data of viscosity using γ_1 for a hard-sphere gas to grasp the order of the quantities. It may be noted that the viscosity, the thermal conductivity, and the speed of sound are almost independent of the pressure of gas.

Examples of the saturated gas pressure vs the temperature of gas are tabulated in Table C.2.

Bibliography

[1] Abramowitz, M. and I. Stegun (1972), *Handbook of Mathematical Functions with Formulas, Graphs, and Mathematical Tables* (Dover, New York), 1001–1003.

[2] Aoki, K., C. Bardos, F. Golse, M. N. Kogan, and Y. Sone (1993), Steady flows of a rarefied gas around arbitrary obstacle distributions, *Eur. J. Mech. B/Fluids* **12**, 565–577.

[3] Aoki, K. and C. Cercignani (1983), Evaporation and condensation on two parallel plates at finite Reynolds numbers, *Phys. Fluids* **26**, 1163–1164.

[4] Aoki, K., T. Inamuro, and Y. Onishi (1979), Slightly rarefied gas flow over a body with small accommodation coefficient, *J. Phys. Soc. Jpn* **47**, 663–671.

[5] Aoki, K. and N. Masukawa (1994), Gas flows caused by evaporation and condensation on two parallel condensed phases and the negative temperature gradient: Numerical analysis by using a nonlinear kinetic equation, *Phys. Fluids* **6,** 1379–1395.

[6] Aoki, K., K. Nishino, Y. Sone, and H. Sugimoto (1991), Numerical analysis of steady flows of a gas condensing on or evaporating from its plane condensed phase on the basis of kinetic theory: Effect of gas motion along the condensed phase, *Phys. Fluids A* **3**, 2260–2275.

[7] Aoki, K. and Y. Sone (1991), Gas flows around the condensed phase with strong evaporation or condensation: Fluid dynamic equation and its boundary condition on the interface and their application, in: R. Gatignol and Soubbaramayer, eds., *Advances in Kinetic Theory and Continuum Mechanics* (Springer-Verlag, Berlin), 43–54.

[8] Aoki, K., Y. Sone, and N. Masukawa (1995), A rarefied gas flow induced by a temperature field, in: J. Harvey and G. Lord, eds., *Rarefied Gas Dynamics* (Oxford University Press, Oxford), 35–41.

[9] Aoki, K., Y. Sone, K. Nishino, and H. Sugimoto (1991), Numerical analysis of unsteady motion of a rarefied gas caused by sudden changes of wall

temperature with special interest in the propagation of a discontinuity in the velocity distribution function, in: A. E. Beylich, ed., *Rarefied Gas Dynamics* (VCH, Weinheim), 222–231.

[10] Aoki, K., Y. Sone, and T. Ohwada (1986), Forces on heated circular cylinders in a highly rarefied gas, in: V. Boffi and C. Cercignani, eds., *Rarefied Gas Dynamics* (Teubner, Stuttgart), Vol. I, 236–244.

[11] Aoki, K., Y. Sone, S. Takata, K. Takahashi, and G. A. Bird (2001), One-way flow of a rarefied gas induced in a circular pipe with a periodic temperature distribution, in: T. J. Bartel and M. A. Gallis, eds., *Rarefied Gas Dynamics* (AIP, New York), 940–947.

[12] Aoki, K., Y. Sone, and Y. Waniguchi (1998), A rarefied gas flow induced by a temperature field: Numerical analysis of the flow between two coaxial elliptic cylinders with different uniform temperatures, *Computers Math. Applic.* **35**, 15–28.

[13] Aoki, K., Y. Sone, and T. Yamada (1990), Numerical analysis of gas flows condensing on its plane condensed phase on the basis of kinetic theory, *Phys. Fluids A* **2**, 1867–1878.

[14] Aoki, K., Y. Sone, and T. Yano (1989), Numerical analysis of a flow induced in a rarefied gas between noncoaxial circular cylinders with different temperatures for the entire range of the Knudsen number, *Phys. Fluids A* **1**, 409–419.

[15] Aoki, K., Y. Sone, and M. Yoshimoto (1999), Numerical analysis of the Taylor-Couette problem for a rarefied gas by the direct simulation Monte Carlo method, in: R. Brun, R. Campargue, R. Gatignol, and J.-C. Lengrand, eds., *Rarefied Gas Dynamics* (CÉPADUÈS, Toulouse), Vol. 2, 109–116.

[16] Aoki, K., S. Takata, H. Aikawa, and F. Golse (2001), A rarefied gas flow caused by a discontinuous wall temperature, *Phys. Fluids* **13**, 2645–2661.

[17] Arkeryd, L. (1972), On the Boltzmann equation Part II: The full initial value problem, *Arch. Rational Mech. Anal.* **45**, 17–34.

[18] Arkeryd, L. and A. Nouri (2005), The stationary nonlinear Boltzmann equation in a Couette setting with multiple, isolated L_q-solutions and hydrodynamic limits, *J. Stat. Phys.* **118**, 849–881.

[19] Arkeryd, L. and A. Nouri (2006), On a Taylor–Couette type bifurcation for a stationary nonlinear Boltzmann equation, *J. Stat. Phys.* **119**, (to be published).

[20] Babovsky, H. (1986), On a simulation scheme for the Boltzmann equation, *Math. Mech. Appl. Sci.* **8**, 223–233.

[21] Babovsky, H. (1992), Time averages of simulation schemes as approximation to stationary kinetic equations, *Eur. J. Mech. B/Fluids* **11**, 199–212.

[22] Baganoff, D. and J. D. McDonald (1990), A collision-selection rule for a particle simulation method suited to vector computers, *Phys. Fluids A* **2**, 1248–1259.

[23] Bakanov, S. P. (1991), Thermophoresis in gases at small Knudsen numbers, *Aeros. Sci. Tech.* **15**, 77–92.

[24] Bakanov, S. P. and B. V. Deryaguin (1959), On the theory of thermal precipitation of highly disperse aerosol systems, *Kolloidnyi Z.* **21**, 377–384.

[25] Bakanov, S. P., V. V. Vysotskij, B. V. Deryaguin, and V. I. Roldughin (1983), Thermal polarization of bodies in the rarefied gas flow, *J. NonEquilib. Thermodyn.* **8**, 75–83.

[26] Bardos, C., R. E. Caflisch, and B. Nicolaenko (1986), The Milne and Kramers problems for the Boltzmann equation of a hard sphere gas, *Commun. Pure Appl. Math.* **39**, 323–352.

[27] Bardos, C., F. Golse, and D. Levermore (1998), Acoustic and Stokes limits for the Boltzmann equation, *C. R. Acad. Sci.* **327**, Serie I, 323–328.

[28] Bardos, C., F. Golse, and D. Levermore (2000), Acoustic limit for the Boltzmann equation, *Arch. Rational Mech. Anal.* **153**, Serie I, 177–204.

[29] Bardos, C., F. Golse, and Y. Sone (2006), Half-space problems for the Boltzmann equation: A survey, *J. Stat. Phys.* **119**, (to be published).

[30] Bedeaux, D., L. J. F. Hermans, and T. Ytrehus (1990), Slow evaporation and condensation, *Physica A* **169**, 263–280.

[31] Bénard, H. (1901), Les tourbillons cellulaires dans une nappe liquide transportant de la chaleur par convection en régime permanent, *Ann. Chim. (Phys.)* **23**, 62–144.

[32] Beresnev, S. A., and V. G. Chernyak (1985), Thermophoresis of a spherical particle at arbitrary Knudsen numbers, *Sov. Phys. Dokl.* **30**, 1055–1057.

[33] Bhatnagar, P. L., E. P. Gross, and M. Krook (1954), A model for collision processes in gases. I. Small amplitude processes in charged and neutral one-component systems, *Phys. Rev.* **94**, 511–525.

[34] Bird, G. A. (1963), Approach to translational equilibrium in a rigid sphere gas, *Phys. Fluids* **6**, 1518–1519.

[35] Bird, G. A. (1965), Shock wave structure in a rigid sphere gas, in: J. H. de Leeuw, ed., *Rarefied Gas Dynamics* (Academic, New York), 216–222.

[36] Bird, G. A. (1967), The velocity distribution function within a shock wave, *J. Fluid Mech.* **30**, 479–487.

[37] Bird, G. A. (1976), *Molecular Gas Dynamics* (Oxford University Press, Oxford).

[38] Bird, G. A. (1989), Perception of numerical methods in rarefied gas-dynamics, in: E. P. Munts, D. P. Weaver, and D. H. Campbell, eds., *Rarefied Gas Dynamics: Theoretical and Computational Technique* (AIAA, Washington, DC), 211–226.

[39] Bird, G. A. (1994), *Molecular Gas Dynamics and the Direct Simulation of Gas Flows* (Oxford University Press, Oxford).

[40] Bobylev, A. V., R. Grzhibovskis, and A. Heintz (2001), Entropy inequalities for evaporation / condensation problem in rarefied gas, *J. Stat. Phys.* **102**, 1156–1176.

[41] Bobylev, A. V., S. Østmo, and T. Ytrehus (1996), Qualitative analysis of the Navier-Stokes equations for evaporation-condensation problems, *Phys. Fluids* **8**, 1764–1773.

[42] Bodenschatz, E., W. Pesch, and G. Ahlers (2000), Recent developments in Rayleigh-Bénard convection, *Annu. Rev. Fluid Mech.* **32**, 709–778.

[43] Boltzmann, L. (1872), Weitere Studien über das Wärmelgeichgewicht unter Gasmolekülen, *Sitzungsberichte Akad. Wiss., Vienna, part II* **66**, 275–370 [English translation in: S. G. Brush, ed., *Kinetic Theory, Vol. 2, Irreversivle Processes* (Pergamon, Oxford, 1966), 88–175].

[44] Boltzmann, L. (1896, 98), *Vorlesungen über Gastheorie*, 2 Vols., (Barth, Leipzig) [English translation by S. G. Brush: (1964), *Lectures on Gas Theory* (University of California Press, Berkeley, CA)].

[45] Bouchut, F., F. Golse, and M. Pulvirenti (2000), *Kinetic Equation and Asymptotic Theory* (Gauthier-Villars, Paris).

[46] Brock, J. K. (1962), On the theory of thermal forces acting on aerosol particles, *J. Collid. Sci.* **17**, 768–780.

[47] Bronshtein, I. N. and K. A. Semendyayev (1997), *Handbook of Mathematics* (Springer-Verlag, Berlin).

[48] Buck, C. R. (1965), *Advanced Calculus, Second Edition* (McGraw-Hill, New York).

[49] Caflisch, R. E. (1985), The half-space problem for the Boltzmann equation at zero temperature, *Commun. Pure Appl. Math.* **38**, 529–547.

[50] Caflisch, R. E. and B. Nicolaenko (1982), Shock profiles solutions of the Boltzmann equation, *Commun. Math. Phys.* **86**, 161–194.

[51] Cartan, É. (1946), Géometrie des espaces de Riemann (Gauthier-Villars, Paris); Rémpression (Édition Jacques Gabay, Paris, 1988).

[52] Cercignani, C. (1988), *The Boltzmann Equation and Its Applications* (Springer-Verlag, Berlin).

[53] Cercignani, C. and A. Daneri (1963), Flow of a rarefied gas between two parallel plates, *J. Appl. Phys.* **34**, 3509–3513.

[54] Cercignani, C., A. Frezzotti, and P. Grosfils (1999), The structure of an infinitely strong shock wave, *Phys. Fluids* **11**, 2757–2764.

[55] Cercignani, C., R. Illner, and M. Pulvirenti (1994), *The Mathematical Theory of Dilute Gases* (Springer-Verlag, Berlin).

[56] Chandrasekhar, S. (1961), *Hydrodynamic and Hydromagnetic Stability* (Oxford University Press, London).

[57] Chapman, S. (1916), On the law of distribution of molecular velocities, and on the theory viscosity and thermal conduction, in a non-uniform simple monoatomic gas, *Philos. Trans. R. Soc. London* **216**, 279–348.

[58] Chapman, S. and T. G. Cowling (1952), *The Mathematical Theory of Non-uniform Gases* (Cambridge University Press, Cambridge, UK).

[59] Chen, C.-C., I.-K. Chen, T.-P. Liu, and Y. Sone (2006), Thermal transpiration for linearized Boltzmann equation, *Commun. Pure Appl. Math.* **59**, (to be published).

[60] Chorin, A. J. and J. Marsden (1997), *A Mathematical Introduction to Fluid Mechanics, Third Edition* (Springer-Verlag, New York).

[61] Chossat, P. and G. Iooss (1993), *The Couette–Taylor Problem* (Springer-Verlag, New York).

[62] Chu, C. K. (1965), Kinetic-theoretic description of the formation of a shock wave, *Phys. Fluids* **8**, 12–22.

[63] Coddington, E. A. and N. Levinson (1955), *Theory of Ordinary Differential Equations* (McGraw-Hill, New York).

[64] Cole, J. D. (1968), *Perturbation Methods in Applied Mathematics* (Blaisdell, Boston).

[65] Coron, F., F. Golse, and C. Sulem (1988), A classification of well-posed kinetic layer problems, *Commun. Pure Appl. Math.* **41**, 409–435.

[66] Courant, R. and K. O. Friedrichs (1948), *Supersonic Flow and Shock Waves* (Wiley-Interscience, New York).

[67] Courant, R. and D. Hilbert (1953), *Methods of Mathematical Physics* Vol. I (Wilely, New York).

[68] Courant, R. and D. Hilbert (1961), *Methods of Mathematical Physics* Vol. II (Wilely, New York).

[69] Darrozes, J. S. (1969), Approximate solutions of the Boltzmann equation for flows past bodies of moderate curvature, in: L. Trilling and H. Y. Wachman, eds., *Rarefied Gas Dynamics* (Academic Press, New York), Vol. I, 111–120.

[70] Darrozes, J. S. and J. P. Guiraud (1966), Généralisation formelle du théorème H en présence de parois. Application, *C. R. Acad. Sci. Paris A* **262**, 1368–1371.

[71] Derjaguin, B. V., A. I. Storozhilova, and Ya. I. Rabinovich (1966), Experimental verification of the theory of thermophoresis of aerosol particles, *J. Colliod Interface Sci.* **21**, 35–58.

[72] Diu, B., C. Guthmann, D. Lederer, and B. Roulet (1989), *Éléments de Physique Statistique* (Hermann, Paris).

[73] Edwards, R. H. and H. K. Cheng (1966), Steady expansion of a gas into a vacuum, *AIAA J.* **4**, 558–561.

[74] Elliot, J. P. and D. Baganoff (1974), Solution of the Boltzmann equation at the upstream and downstream singular points in a shock wave, *J. Fluid Mech.* **65**, 603–624.

[75] Enskog, D. (1917), *Kinetische Theorie der Vorgänge in mässig verdünnten Gasen, I. Allegemeiner Teil, Inaugural Dissertation* (Almqvist & Wiksell, Uppsala); see also Die numerische Berechnung der Vorgänge in massig verdünnten Gasen, *Arkiv. Mat. Astr. Fys.* **16**, No 16, 1–60 (1922).

[76] Epstein, P. S. (1929), Zur Theorie des Radiometer, *Z. Phys.* **54**, 537–563.

[77] Erwin, D. A., G. C. Pham-Van-Diep, and E. P. Muntz (1991), Nonequilibrium gas flows. I: A detailed validiation of Monte Carlo direct simulation for monatomic gases, *Phys. Fluids A* **3**, 697–705.

[78] Feller, W. (1968), *An Introduction to Probability Theory and Its Applications* Vol. I, *Third Edition* (Wiley, New York).

[79] Ferziger, J. H. (1967), Flow of a rarefied gas through a cylindrical tube, *Phys. Fluids* **10**, 1448–1453.

[80] Feynman, R. P., R. B. Leighton, and M. L. Sands (1963), *The Feynman Lectures on Physics* Vol. I (Addison-Wesley, Reading, MA).

[81] Garabedian, P. R. (1964), *Partial Differential Equations* (Wiley, New York).

[82] Garcia, A. L. and C. Penland (1991), Fluctuating hydrodynamics and principal oscillation pattern analysis, *J. Stat. Phys.* **64**, 1121–1132.

[83] Garzó, V. and A. Santos (2003), *Kinetic Theory of Gases in Shear Flows* (Kluwer Academic Publishers, Dordrecht).

[84] Goldstein, H. (1950), *Classical Mechanics* (Addison-Wesley, Reading, MA).

[85] Golse F. and F. Poupaud (1989), Stationary solutions of the linearized Boltzmann equation in a half-space, *Math. Methods Appl. Sci.* **11**, 483–502.

[86] Golse F. and L. Saint-Raymond (2004), The Navier–Stokes limit of the Boltzmann equation for bounded collision kernels, *Invent. Math.* **155**, 81–161.

[87] Grad, H. (1949), On the kinetic theory of rarefied gases, *Commun. Pure Appl. Math.* **2**, 331–407.

[88] Grad, H. (1958), Principles of the kinetic theory of gases, in: S. Flügge, ed., *Handbuch der Physik* (Springer-Verlag, Berlin), Band XII, 205–294.

[89] Grad, H. (1963a), Asymptotic theory of the Boltzmann equation, *Phys. Fluids* **6**, 147–181.

[90] Grad, H. (1963b), Asymptotic theory of the Boltzmann equation II, in: J. A. Laurmann, ed., *Rarefied Gas Dynamics* (Academic Press, New York), 26–59.

[91] Grad, H. (1969), Singular and nonuniform limits of solutions of the Boltzmann equation, in: R. Bellman, G. Birkhoff, and I. Abu-Shumays, eds., *Transport Theory* (American Mathematical Society, Providence), 269–308.

[92] Greengard, C. and L. G. Reyna (1992), Conservation of expected momentum and energy in Monte Carlo particle simulation, *Phys. Fluids A* **4**, 849–852.

[93] Ha, S.-Y., T.-P. Liu, and S.-H. Yu (2006), Interaction of shock and initial layers to the one-dimensional Boltzmann equation, (private communication).

[94] Hamel, B. B. and D. R. Willis (1966), Kinetic theory of source flow expansion with application to free jet, *Phys. Fluids* **9**, 829–841.

[95] Handa, M. and T. Doi (2004), Effect of a temperature difference between the cylinders on the Taylor–Couette bifurcation in a gas, *Phys. Fluids* **16**, 3557–3565.

[96] Hasegawa, M. and Y. Sone (1988), Poiseuille and thermal transpiration flows of a rarefied gas for various pipes, *J. Vac. Soc. Jpn* **31**, 416–419. (in Japanese)

[97] Hasegawa, M. and Y. Sone (1991a), Rarefied gas flow through a slit, *Phys. Fluids* A **3**, 466–477.

[98] Hasegawa, M. and Y. Sone (1991b), Rarefied gas flow through a slit II: Flow induced by a temperature difference, *J. Vac. Soc. Jpn* **34**, 390–393. (in Japanese)

[99] Hermans, L. J. F. and J. J. M. Beenakker (1986), The temperature paradox in the kinetic theory of evaporation, *Phys. Fluids* **29**, 4231–4232.

[100] Hilbert, D. (1912), G*rundzüge einer Allgemeinen Theorie der Linearen Integralgleichungen* (Teubner, Leipzig).

[101] Hill, T. L. (1987), *Statistical Mechanics, Principles and Selected Applications* (Dover, New York).

[102] Holway Jr., L. H. (1965), Kinetic theory of shock structure using an ellipsoidal distribution function, in: J. H. de Leeuw, ed., *Rarefied Gas Dynamics* (Academic, New York), Vol. 1, 193–215.

[103] Honing, R. E. and D. A. Kramer (eds.) (1969), Vapor pressure data for the solid and liquid elements, *RCA Review* **30**, 285–305

[104] Huber, C. A. (1995), Nanowire array composite, *Science* **263**, 800–802.

[105] Hudson, M. L. and T. J. Bartel (1999), DSMC simulation of thermal transpiration and accommodation pumps, in: R. Brun, R. Campargue, R. Gatignol, and J.-C. Lengrand, eds., *Rarefied Gas Dynamics* (CÉPADUÈS, Toulouse), Vol. 1, 719–726.

[106] Inamuro, T. (1989), Numerical studies on evaporation and deposition of a rarefied gas in a closed chamber, in: E. P. Muntz, D. P. Weaver, and D. H. Campbell, eds., *Rarefied Gas Dynamics: Physical Phenomena* (AIAA, Washington, DC), 418–433.

[107] Ivanov, M. S., G. N. Markelov, A. N. Kudryavtev, and S. F. Gimelshein (1998), Numerical analysis of shock wave reflection transition in steady flows, *AIAA J.* **36**, 2079–2086.

[108] Ivanov, M. S., S. V. Rogasinsky, and V. Ya. Rudyak (1989), Direct simulation method and master kinetic equation, in: E. P. Muntz, D. P. Weaver, and D. H. Campbell, eds., *Rarefied Gas Dynamics: Theoretical and Computational Technique* (AIAA, Washington), 171–181.

[109] Jacobsen, S. and J. R. Brock (1965), Thermal force on spherical sodium chloride aerosols *J. Colloid Sci*, **20**, 544–554.

[110] Jensen, J. L. W. V. (1906), Sur les fonctions convexes et les inégalités entre les valeurs moyennes, Acta Math. **30**, 175–193.

[111] Jeffreys, H. (1965), *Cartesian Tensors* (Cambridge University Press, Cambridge, UK).

[112] Jeffreys, H. and B. Jeffreys (1946), *Methods of Mathematical Physics* (Cambridge University Press, Cambridge, UK).

[113] Karniadakis, G. E., A. Beskok, and N. Aluru (2005), *Microflows and Nanoflows: Fundametals and Simulation* (Springer-Verlag, New York).

[114] Kato, T. (1976), *Perturbation Theory for Linear Operators*, *Second Edition* (Springer-Verlag, Berlin).

[115] Kennard, E. H. (1938), *Kinetic Theory of Gases* (McGraw-Hill, New York).

[116] Knudsen, M. (1910a), Eine Revision der Gleichgewichtsbedingung der Gase. Thermische Molekularströmung, *Ann. Phys.* (Leipzig) **31**, 205–229.

[117] Knudsen, M. (1910b), Thermischer Molekulardruck der Gase in Röhren, *Ann. Phys.* (Leipzig) **33**, 1435–1448.

[118] Kogan, M. N. (1958), On the equations of motion of a rarefied gas, *Appl. Math. Mech.* **22**, 597–607.

[119] Kogan, M. N. (1969), *Rarefied Gas Dynamics* (Plenum, New York).

[120] Kogan, M. N., V. S. Galkin, and O. G. Fridlender (1976), Stresses produced in gases by temperature and concentration inhomogeneities. New type of free convection, *Sov. Phys. Usp.* **19**, 420–438.

[121] Kogan, M. N. (1992), Kinetic theory in aerothermodynamics, *Prog. Aerosp. Sci.* **29**, 271–354.

[122] Koffman, L. D., M. S. Plesset, and L. Lees (1984), Theory of evaporation and condensation, *Phys. Fluids* **27**, 876–880.

[123] Koschmieder, E. L. (1993), *Bénard Cells and Taylor Vortices* (Cambridge University Press, Cambridge, UK).

[124] Koura, K. (1986), Null-collision technique in the direct-simulation Monte Carlo method, *Phys. Fluids* **29**, 3509–3511.

[125] Landau, L. D. and E. M. Lifshitz (1960), *Course of Theoretical Physics Vol. 1: Mechanics* (Pergamon Press, London).

[126] Landau, L. D. and E. M. Lifshitz (1963), *Course of Theoretical Physics Vol. 5: Statistical Physics* (Pergamon Press, London), Section 82.

[127] Lanford III, O. (1975), The evolution of large classical system, in: J. Moser, ed., *Lecture Notes in Physics* (Springer-Verlag, Heidelberg), 1–111.

[128] Lax, P. D. (1957), Hyperbolic systems of conservation laws II, *Commun. Pure Appl. Math.* **10**, 537–566.

[129] Lieb, E. H. and M. Loss (2001), *Analysis*, *Second edition*, (AMS, Providence).

[130] Liepmann, H. W., R. Narashimha, and M. T. Chahine (1962), Structure of a plane shock layer, *Phys. Fluids* **5**, 1313–1324.

[131] Liepmann, H. W. and A. Roshko (1957), *Elements of Gasdynamics* (Wiley, New York).

[132] Liu, T.-P. (1975), Riemann problem for general systems of conservation laws, *J. Diff. Equations* **18**, 218–234.

[133] Liu, T.-P., T. Yang, and S.-H. Yu (2003), Energy method for Boltzmann equation, *Physica D* **188**, 178–192.

[134] Liu, T.-P. and S.-H. Yu (2004a), Boltzmann equation: Micro-macro decompositions and positivity of shock profile, *Commun. Math. Phys.* **246**, 133–179.

[135] Liu, T.-P. and S.-H. Yu (2004b), The Green's function and large-time behavior of solutions for the one-dimensional Boltzmann equation, *Commun. Pure Appl. Math.* **57**, 1543–1608.

[136] Liu, T.-P. and S.-H. Yu (2006a), Green function of Boltzmann equation, 3-D waves, *Bulletin of Institute of Mathematics, Academia Sinica* **1**, 1–78.

[137] Liu, T.-P. and S.-H. Yu (2006b), Initial-boundary value problem for Boltzmann equation, planer waves, *Commun. Pure Appl. Math.* **59**, (to be published).

[138] Loeb, L. (1961), *Kinetic Theory of Gases* (Dover, New York).

[139] Loyalka, S. K. and K. A. Hickey (1989), Velocity slip and defect: Hard sphere gas, *Phys. Fluids A* **1**, 612–614.

[140] Mager R., G. Adomeit, and G. Wortberg (1989), Theoretical and experimental investigation of the strong evaporation of solids, in: D. P. Weaver, E. P. Muntz, and D. H. Campbell, eds., *Rarefied Gas Dynamics: Physical Phenomena* (AIAA, Washington, DC), 460–469.

[141] Margrave, J. L. (ed.) (1967), *The Characterization of High-temperature Vapors* (Wiley, New York).

[142] Matsushita, T. (1976), Kinetic analysis of the problem of evaporation and condensation, *Phys. Fluids* **19**, 1712–1715.

[143] Maxwell, J. C. (1867), On the dynamical theory of gases, *Philos. Trans. R. Soc.* **157**, 49–88 [Reprint in: S. G. Brush, ed., *Kinetic Theory, Vol. 2, Irreversivle Processes* (Pergamon, Oxford, 1966), 23–87].

[144] Maxwell, J. C. (1879), On stresses in rarefied gases arising from inequalities of temperature, *Philos. Trans. R. Soc.* **170**, 231–256.

[145] Mohr, P. J. and B. N. Taylor (2005), CODATA recommended values of the fundamental physical constants: 2002, *Reviews of Modern Physics* **77**, 1–107.

[146] Mott-Smith, H. M. (1951), The solution of the Boltzmann equation for a shock wave, *Phys. Rev. 2nd Ser.* **82**, 885–892.

[147] Niimi, H. (1971), Thermal creep flow of rarefied gas between two parallel plates, *J. Phys. Soc. Jpn* **30**, 572–574.

[148] Ohwada, T. (1993), Structure of normal shock waves: Direct numerical analysis of the Boltzmann equation for hard-sphere molecules, *Phys. Fluids A* **5**, 217–234.

[149] Ohwada, T., K. Aoki, and Y. Sone (1989), Heat transfer and temperature distribution in a rarefied gas between two parallel plates with different temperatures: Numerical analysis of the Boltzmann equation for a hard sphere molecule, in: E. P. Muntz, D. P. Weaver, and D. H. Campbell, eds., *Rarefied Gas Dynamics*: *Theoretical and Computational Techniques* (AIAA, Washington, DC), 70–81.

[150] Ohwada, T. and Y. Sone (1992), Analysis of thermal stress slip flow and negative thermophoresis using the Boltzmann equation for hard-sphere molecules, *Eur. J. Mech. B/Fluids* **11,** 389–414.

[151] Ohwada, T., Y. Sone, and K. Aoki (1989a), Numerical analysis of the shear and thermal creep flows of a rarefied gas over a plane wall on the basis of the linearized Boltzmann equation for hard-sphere molecules, *Phys. Fluids A* **1**, 1588–1599.

[152] Ohwada, T., Y. Sone, and K. Aoki (1989b), Numerical analysis of the Poiseuille and thermal transpiration flows between two parallel plates on the basis of the Boltzmann equation for hard-sphere molecules, *Phys. Fluids A* **1**, 2042–2049.

[153] Onishi, Y. and Y. Sone (1979), Kinetic theory of slightly strong evaporation and condensation: Hydrodynamic equation and slip boundary condition for finite Reynolds number, *J. Phys. Soc. Jpn* **47**, 1676–1685.

[154] Onishi, Y. and Y. Sone (1983), Kinetic theory of evaporation and condensation for a cylindrical condensed phase, *Phys. Fluids* **26**, 659–664.

[155] Oswatitsch, K. (1956), *Gasdynamics* (Academic Press, New York).

[156] Pao, Y. P. (1971), Application of kinetic theory to the problem of evaporation and condensation, *Phys. Fluids* **14**, 306–312.

[157] Pareschi, L. and R. E. Caflisch (1999), An implicit Monte Carlo method for rarefied gas dynamics, *J. Comput. Phys.* **154**, 90–116.

[158] Parzen, E. (1960), *Modern Probability Theory and Its Applications* (Wiley, New York).

[159] Pekeris, C. L. and Z. Alterman (1957), Solution of the Boltzmann-Hilbert integral equation II. the coefficients of viscosity and heat conduction, *Proceedings of the National Academy of Sciences of the U. S. A.* **43**, 998–1007.

[160] Pham-Van-Diep, G., P. Keeley, E. P. Muntz, and D. P. Weaver (1995), A micromechanical Knudsen compressor, in: J. Harvey and G. Lord, eds., *Rarefied Gas Dynamics* (Oxford University Press, London), Vol. I, 715–721.

[161] Phillips, W. F. (1975), Motion of aerosol particles in a temperature gradient, *Phys. Fluids* **18**, 144–147.

[162] Planck, M. (1945), *Treatise on Thermodynamics* (Dover, New York).

[163] Prandtl, L. (1952), *Essentials of Fluid Dynamics* (Blackie, London).

[164] Prodi, F., G. Santachiara, and V. Prodi (1979), Measurement of thermophoretic velocities of aerosol particles in the transition region, *J. Aerosol. Sci.* **10**, 421–425.

[165] Rayleigh, Lord (1916), On convection currents in a horizontal layer of fluid when the higher temperature is on the under side, *Scientific Papers* **6**, 432–446.

[166] Reid, W. T. (1971), *Ordinary Differential Equations* (Wiley, New York).

[167] Reif, F. (1965), *Fundamentals of Statistical and Thermal Physics* (McGraw-Hill, New York).

[168] Rényi, A. (1966), *Calcul des Probabilités* (Dunod, Paris).

[169] Riesz, F. and B. Sz.-Nagy (1990), *Functional Analysis* (Dover, New York).

[170] Romanov, V. A. (1973), Stability of plane-parallel Couette flow, *Functional Anal. and its Applics.* **7**, 137–146.

[171] Rudin, W. (1976), *Principles of Mathematical Analysis, Third Edition* (McGraw-Hill, New York).

[172] Rudin, W. (1987), *Real and Complex Analysis, Third Edition* (McGraw-Hill, New York).

[173] Salwen, H., C. E. Grosch, and S. Ziering (1964), Extension of the Mott–Smith method for a one-dimensional shock wave, *Phys. Fluids* **7**, 180–189.

[174] Schadt, C. F. and R. D. Cadle (1961), Thermal forces on aerosol particles, *J. Phys. Chem.* **65**, 1689–1694.

[175] Schlichting, H. (1979), *Boundary-Layer Theory* (McGraw-Hill, New York).

[176] Schmitt, K. H. (1959), Untersuchungen an Schwebstoffteilichen im Temperaturfeld, *Z. Naturforsch.* **14a**, 870–881.

[177] Shankar, P. N. and M. D. Deshpande (1990), On the temperature distribution in liquid-vapor phase change between plane liquid surfaces, *Phys. Fluids A* **2**, 1030–1038.

[178] Sharipov, F. (1994a), Onsager–Casimir reciprocity relations for open gaseous systems at arbitrary rarefaction I. General theory for single gas, *Physica A* **203**, 437–456.

[179] Sharipov, F. (1994b), Onsager–Casimir reciprocity relations for open gaseous systems at arbitrary rarefaction II. Application of the theory for single gas, *Physica A* **203**, 457–485.

[180] Smoller, J. (1983), *Shock Waves and Reaction Diffusion Equations* (Springer-Verlag, Berlin).

[181] Sommerfeld, A. (1964), *Mechanics of Deformable Bodies, Lectures on Theoretical Physics, Vol. II* (Academic Press, New York).

[182] Sommerfeld, A. (1964), *Thermodynamics and Statistical Mechanics, Lectures on Theoretical Physics, Vol. V* (Academic Press, New York).

[183] Sone, Y. (1964), Kinetic theory analysis of linearized Rayleigh problem, *J. Phys. Soc. Jpn* **19**, 1463–1473.

[184] Sone, Y. (1965), Effect of sudden change of wall temperature in a rarefied gas, *J. Phys. Soc. Jpn* **20**, 222–229.

[185] Sone, Y. (1966a), Some compressibility effects on rarefied gas flow in Rayleigh problem, *J. Phys. Soc. Jpn* **21**, 1593–1596.

[186] Sone, Y. (1966b), Thermal creep in rarefied gas, *J. Phys. Soc. Jpn* **21**, 1836–1837.

[187] Sone, Y. (1968), Asymptotic behavior of diffusion of tangential velocity discontinuity in rarefied gas, *Phys. Fluids* **11**, 1935–1937.

[188] Sone, Y. (1969), Asymptotic theory of flow of rarefied gas over a smooth boundary I, in: L. Trilling and H. Y. Wachman, eds., *Rarefied Gas Dynamics* (Academic Press, New York), Vol. I, 243–253.

[189] Sone, Y. (1970), A note on thermal creep in rarefied gas, *J. Phys. Soc. Jpn* **29**, 1655.

[190] Sone, Y. (1971), Asymptotic theory of flow of rarefied gas over a smooth boundary II, in: D. Dini, ed., *Rarefied Gas Dynamics* (Editrice Tecnico Scientifica, Pisa), Vol. II, 737–749.

[191] Sone, Y. (1972), Flow induced by thermal stress in rarefied gas, *Phys. Fluids* **15**, 1418–1423.

[192] Sone, Y. (1973), New kind of boundary layer over a convex solid boundary in a rarefied gas, *Phys. Fluids* **16**, 1422–1424.

[193] Sone, Y. (1974), Rarefied gas flow induced between non-parallel plane walls with different temperatures, in: M. Becker and M. Fiebig, eds., *Rarefied Gas Dynamics* (DFVLR Press, Porz-Wahn), Vol. 2, D. 23.

[194] Sone, Y. (1978a), On the equilibrium solution of the Boltzmann equation, *Phys. Fluids* **21**, 294–295.

[195] Sone, Y. (1978b), Kinetic theory of evaporation and condensation: Linear and nonlinear problems, *J. Phys. Soc. Jpn* **45**, 315–320.

[196] Sone, Y. (1984a), Highly rarefied gas around a group of bodies with various temperature distributions I: Small temperature variation, *J. de Mécanique Théorique et Appliquée* **3,** 315–328.

[197] Sone, Y. (1984b), Analytical studies in rarefied gas dynamics, in: H. Oguchi, ed., *Rarefied Gas Dynamics* (University of Tokyo Press, Tokyo), Vol. I, 71–87.

[198] Sone, Y. (1984c), Force, its moment, and energy transfer on a closed body in a slightly rarefied gas, in: H. Oguchi, ed., *Rarefied Gas Dynamics* (University of Tokyo Press, Tokyo), Vol. I, 117–126.

[199] Sone, Y. (1985), Highly rarefied gas around a group of bodies with various temperature distributions II: Arbitrary temperature variation, *J. de Mécanique Théorique et Appliquée* **4,** 1–14.

[200] Sone, Y. (1987), Flows with shock waves and contact discontinuities and weak solutions of Euler's equations, *Nagare* **6**, 182–186. (in Japanese)

[201] Sone, Y. (1991a), Asymptotic theory of a steady flow of a rarefied gas past bodies for small Knudsen numbers, in: R. Gatignol and Soubbaramayer, eds., *Advances in Kinetic Theory and Continuum Mechanics* (Springer-Verlag, Berlin), 19–31.

[202] Sone, Y. (1991b), A simple demonstration of a rarefied gas flow induced over a plane wall with a temperature gradient, *Phys. Fluids A* **3**, 997–998.

[203] Sone, Y. (1991c), Analytical and numerical studies of rarefied gas flows on the basis of the Boltzmann equation for hard-sphere molecules, in: A. E. Beylich, ed., *Rarefied Gas Dynamics* (VCH, Weinheim), 489–504.

[204] Sone, Y. (1997), Continuum gas dynamics in the light of kinetic theory and new features of rarefied gas flows, in: Ching Shen, ed., *Rarefied Gas Dynamics* (Peking University Press, Beijing), 3–24.

[205] Sone, Y. (2000a), Flows induced by temperature fields in a rarefied gas and their ghost effect on the behavior of a gas in the continuum limit, *Annu. Rev. Fluid Mech.* **32**, 779–811.

[206] Sone, Y. (2000b), Kinetic theoretical studies of the half-space problem of evaporation and condensation, *Transp. Theory Stat. Phys.* **29**, 227–260.

[207] Sone, Y. (2002), *Kinetic Theory and Fluid Dynamics* (Birkhäuser, Boston).

[208] Sone, Y. and K. Aoki (1977a), Slightly rarefied gas flow over a specularly reflecting body, *Phys. Fluids* **20**, 571–576.

[209] Sone, Y. and K. Aoki (1977b), Forces on a spherical particle in a slightly rarefied gas, in: J. L. Potter, ed., *Rarefied Gas Dynamics* (AIAA, New York), 417–433.

[210] Sone, Y. and K. Aoki (1979), Thermal force and drag on a volatile particle in a slightly rarefied gas, in: R. Campargue, ed., *Rarefied Gas Dynamics* (Commissariat a l'energie atomique, Paris), 1207–1218.

[211] Sone, Y. and K. Aoki (1981), Negative thermophoresis: Thermal stress slip flow around a spherical particle in a rarefied gas, in: S. S. Fisher, ed., *Rarefied Gas Dynamics* (AIAA, New York), 489–503.

[212] Sone, Y. and K. Aoki (1983), A similarity solution of the linearized Boltzmann equation with application to thermophoresis of a spherical particle, *J. de Mécanique Théorique et Appliquée* **2**, 3–12.

[213] Sone, Y. and K. Aoki (1987), Steady gas flows past bodies at small Knudsen numbers–Boltzmann and hydrodynamic systems, *Transp. Theory Stat. Phys.* **16**, 189–199.

[214] Sone, Y. and K. Aoki (1994), *Molecular Gas Dynamics* (Asakura, Tokyo). (in Japanese)

[215] Sone, Y., K. Aoki, and T. Doi (1992), Kinetic theory analysis of gas flows condensing on a plane condensed phase: Case of a mixture of a vapor and a noncondensable gas, *Transp. Theory Stat. Phys.* **21**, 297–328.

[216] Sone, Y., K. Aoki, and Y. Onishi (1977), Imperfect accommodation effects on the flow induced by thermal stresses in a rarefied gas, *Heat Transfer Japanese Research* **6**, 1–12.

[217] Sone, Y., K. Aoki, and H. Sugimoto (1997), The Bénard problem for a rarefied gas: Formation of steady flow patterns and stability of array of rolls, *Phys. Fluids* **9**, 3898–3914.

[218] Sone, Y., K. Aoki, and H. Sugimoto (1999), Stability of Bénard multi-rolls in a rarefied gas, in: R. Brun, R. Campargue, R. Gatignol, and J.-C. Lengrand, eds., *Rarefied Gas Dynamics* (CÉPADUÈS, Toulouse), Vol. 1, 695–702.

[219] Sone, Y., K. Aoki, H. Sugimoto, and H. Motohashi (1995), The Bénard problem of rarefied gas dynamics, in: J. Harvey and G. Lord, eds., *Rarefied Gas Dynamics* (Oxford University Press, Oxford), 135–141.

[220] Sone, Y., K. Aoki, H. Sugimoto, and T. Yamada (1988), Steady evaporation and condensation on a plane condensed phase, *Theoretical and Applied Mechanics* (Bulgarian Academy of Sciences), Year XIX, No. 3, 89–93.

[221] Sone, Y., K. Aoki, S. Takata, H. Sugimoto, and A. V. Bobylev (1996), Inappropriateness of the heat-conduction equation for description of a temperature field of a stationary gas in the continuum limit: examination by asymptotic analysis and numerical computation of the Boltzmann equation, *Phys. Fluids* **8**, 628–638; (1996), Erratum, *ibid.* **8**, 841.

[222] Sone, Y., K. Aoki, and I. Yamashita (1986), A study of unsteady strong condensation on a plane condensed phase with special interest in formation of steady profile, in: V. Boffi and C. Cercignani, eds., *Rarefied Gas Dynamics* (Teubner, Stuttgart), Vol. II, 323–333.

[223] Sone, Y., C. Bardos, F. Golse, and H. Sugimoto (2000), Asymptotic theory of the Boltzmann system for a steady flow of a slightly rarefied gas with a finite Mach number: General theory, *Eur. J. Mech. B/Fluids* **19**, 325–360.

[224] Sone, Y. and T. Doi (2000), Analytical study of bifurcation of a flow of a gas between coaxial circular cylinders with evaporation and condensation, *Phys. Fluids* **12**, 2639–2660.

[225] Sone, Y. and T. Doi (2003a), Bifurcation of and ghost effect on the temperature field in the Bénard problem of a gas in the continuum limit, *Phys. Fluids* **15**, 1405–1423.

[226] Sone, Y. and T. Doi (2003b), Bifurcation of a flow of a gas between rotating coaxial circular cylinders with evaporation and condensation, in: A. Ketsdever and E. P. Muntz, eds., *Rarefied Gas Dynamics* (AIP, New York), 646–653.

[227] Sone, Y. and T. Doi (2004), Ghost effect of infinitesimal curvature in the plane Couette flow of a gas in the continuum limit, *Phys. Fluids* **16**, 952–971.

[228] Sone, Y. and T. Doi (2005), Instability of the plane Couette flow by the ghost effect of infinitesimal curvature, in: M. Capitelli, ed., *Rarefied Gas Dynamics* (AIP, Melville, NY), 258–263.

[229] Sone, Y., T. Fukuda, T. Hokazono, and H. Sugimoto (2001), Experiment on a one-way flow of a rarefied gas through a straight pipe without average temperature and pressure gradients, in: T. J. Bartel and M. A. Gallis, eds., *Rarefied Gas Dynamics* (AIP, New York), 948–955.

[230] Sone, Y., F. Golse, T. Ohwada, and T. Doi (1998), Analytical study of transonic flows of a gas condensing onto its plane condensed phase on the basis of kinetic theory, *Eur. J. Mech. B/Fluids* **17**, 277–306.

[231] Sone, Y., M. Handa, and T. Doi (2003), Ghost effect and bifurcation in a gas between coaxial circular cylinders with different temperatures, *Phys. Fluids* **15**, 2903–2915.

[232] Sone, Y., M. Handa, and H. Sugimoto (2002), Bifurcation studies of flows of a gas between rotating coaxial circular cylinders with evaporation and condensation by the Boltzmann system, *Transp. Theory Stat. Phys.* **31**, 299–332.

[233] Sone, Y. and M. Hasegawa (1987), Poiseuille and thermal transpiration flows of a rarefied gas through a rectangular pipe, *J. Vac. Soc. Jpn.* **30**, 425–428. (in Japanese)

[234] Sone, Y. and E. Itakura (1990), Analysis of Poiseuille and thermal transpiration flows for arbitrary Knudsen numbers by a modified Knudsen number expansion method and their database, *J. Vac. Soc. Jpn* **33**, 92–94. (in Japanese)

[235] Sone, Y., T. Kataoka, T. Ohwada, H. Sugimoto, and K. Aoki (1994), Numerical examination of applicability of the linearized Boltzmann equation, *Eur. J. Mech. B/Fluids* **13**, 573–589.

[236] Sone, Y., T. Ohwada, and K. Aoki (1989a), Temperature jump and Knudsen layer in a rarefied gas over a plane wall: Numerical analysis of the linearized Boltzmann equation for hard-sphere molecules, *Phys. Fluids A* **1**, 363–370.

[237] Sone, Y., T. Ohwada, and K. Aoki (1989b), Evaporation and condensation on a plane condensed phase: Numerical analysis of the linearized Boltzmann equation for hard-sphere molecules, *Phys. Fluids A* **1**, 1398–1405.

[238] Sone, Y., T. Ohwada, and K. Aoki (1991), Evaporation and condensation of a rarefied gas between its two parallel plane condensed phases with different temperatures and negative temperature-gradient phenomenon: Numerical analysis of the Boltzmann equation for hard-sphere molecules, in: G. Toscani, V. Boffi, and S. Rionero, eds., *Mathematical Aspects of Fluid and Plasma Dynamics, Lecture Notes in Mathematics 1460* (Springer-Verlag, Berlin), 186–202.

[239] Sone, Y., T. Ohwada, and Y. Makihara (1999), Bifurcation in cylindrical Couette flow with evaporation and condensation: Effect of initial condition, in: R. Brun, R. Campargue, R. Gatignol, and J.-C. Lengrand, eds., *Rarefied Gas Dynamics* (CÉPADUÈS, Toulouse), Vol. 1, 511–518.

[240] Sone, Y. and Y. Onishi (1978), Kinetic theory of evaporation and condensation: Hydrodynamic equation and slip boundary condition, *J. Phys. Soc. Jpn* **44**, 1981–1994.

[241] Sone, Y. and K. Sato (2000), Demonstration of a one-way flow of a rarefied gas induced through a pipe without average pressure and temperature gradients, *Phys. Fluids* **12**, 1864–1868.

[242] Sone, Y., K. Sawada, and H. Hirano (1994), A simple experiment on the strength of thermal creep flow of a rarefied gas over a flat wall, *Eur. J. Mech. B/Fluids* **13**, 299–303.

[243] Sone, Y. and M. Shibata (1965), Kinetic theory analysis of diffusion of discontinuity plane of flow velocity, *AIAA J.* **3**, 1763–1764.

[244] Sone, Y. and H. Sugimoto (1990), Strong evaporation from a plane condensed phase, in: G. E. A. Meier and P. A. Thompson, eds., *Adiabatic Waves in Liquid-Vapor Systems* (Springer-Verlag, Berlin), 293–304.

[245] Sone, Y. and H. Sugimoto (1993), Kinetic theory analysis of steady evaporating flows from a spherical condensed phase into a vacuum, *Phys. Fluids A* **5**, 1491–1511.

[246] Sone, Y. and H. Sugimoto (1994), Steady evaporating flows from a spherical condensed phase into a vacuum, in: R. Brun and A. A. Chikhaoui, eds., *Aerothermocheministry of Spacecraft and Associated Hypersonic Flows*, Proceedings of the IUTAM Symposium Marseille 1992 (Jouve, Paris), 67–72.

[247] Sone, Y. and H. Sugimoto (1995), Evaporation of a rarefied gas from a cylindrical condensed phase into a vacuum, *Phys. Fluids* **7**, 2072–2085.

[248] Sone, Y. and H. Sugimoto (2002), Knudsen compressor, *J. Vac. Soc. Jpn* **45**, 138–141.

[249] Sone, Y. and H. Sugimoto (2003), Vacuum pump without a moving part and its performance, in: A. Ketsdever and E. P. Muntz, eds., *Rarefied Gas Dynamics* (AIP, New York), 1041–1048.

[250] Sone, Y., H. Sugimoto, and K. Aoki (1999), Cylindrical Couette flows of a rarefied gas with evaporation and condensation: Reversal and bifurcation of flows, *Phys. Fluids* **11**, 476–490.

[251] Sone, Y. and S. Takata (1992), Discontinuity of the velocity distribution function in a rarefied gas around a convex body and the S layer at the bottom of the Knudsen layer, *Transp. Theory Stat. Phys.* **21**, 501–530.

[252] Sone, Y., S. Takata, and F. Golse (2001), Notes on the boundary conditions for fluid-dynamic equations on the interface of a gas and its condensed phase, *Phys. Fluids* **13**, 324–334.

[253] Sone, Y., S. Takata, and T. Ohwada (1990), Numerical analysis of the plane Couette flow of a rarefied gas on the basis of the linearized Boltzmann equation for hard-shpere molecules, *Eur. J. Mech. B/Fluids* **9**, 273–288.

[254] Sone, Y., S. Takata, and H. Sugimoto (1996), The behavior of a gas in the continuum limit in the light of kinetic theory: The case of cylindrical Couette flows with evaporation and condensation, *Phys. Fluids* **8**, 3403–3413; (1998), Erratum, *ibid.* **10**, 1239.

[255] Sone, Y., S. Takata, and M. Wakabayashi (1994), Numerical analysis of a rarefied gas flow past a volatile particle using the Boltzmann equation for hard-sphere molecules, *Phys. Fluids* **6**, 1914–1928.

[256] Sone, Y. and S. Tanaka (1980), Thermal stress slip flow induced in rarefied gas between noncoaxial circular cylinders, in: F. P. J. Rimrott and B. Tabarrok, eds., *Theoretical and Applied Mechanics* (North-Holland, Amsterdam), 405–416.

[257] Sone, Y. and S. Tanaka (1986), Force and its moment on a heated inclined plate in a semi-infinite expanse of a highly rarefied gas bounded by a plane wall, in: V. Boffi and C. Cercignani, eds., *Rarefied Gas Dynamics* (Teubner, Stuttgart), Vol. I, 194–203.

[258] Sone, Y. and M. Wakabayashi (1988), Flow induced by nonlinear thermal stress in a rarefied gas, Preprint of Symposium on Flight Mechanics and Astrodynamics (Institute of Space and Aeronautical Science, Tokyo) (in Japanese). The content is available in a more easily accessible textbook by Sone & Aoki [1994].

[259] Sone, Y., Y. Waniguchi, and K. Aoki (1996), One-way flow of a rarefied gas induced in a channel with a periodic temperature distribution, *Phys. Fluids* **8**, 2227–2235.

[260] Sone, Y. and K. Yamamoto (1968), Flow of rarefied gas through a circular pipe, *Phys. Fluids* **11**, 1672–1678; (1970) erratum *ibid.* **13**, 1651.

[261] Sone, Y. and K. Yamamoto (1970), Flow of rarefied gas over plane wall, *J. Phys. Soc. Jpn* **29**, 495–508; Sone, Y. and Y. Onishi (1979), Flow of rarefied gs over plane wall, *J. Phys. Soc. Jpn* **47**, 672.

[262] Sone, Y. and M. Yoshimoto (1997), Demonstration of a rarefied gas flow induced near the edge of a uniformly heated plate, *Phys. Fluids* **9**, 3530–3534.

[263] Spohn, H. (1991), *Large Scale Dynamics of Interacting Particles* (Springer-Verlag, Berlin).

[264] Stefanov, S. and C. Cercignani (1992), Monte Carlo simulation of Bénard's instability in a rarefied gas, *Eur. J. Mech. B/Fluids* **11**, 543–553.

[265] Sugimoto, H. and Y. Sone (1992), Numerical analysis of steady flows of a gas evaporating from its cylindrical condensed phase on the basis of kinetic theory, *Phys. Fluids A* **4**, 419–440.

[266] Sugimoto, H. and Y. Sone (2005), Vacuum pump without a moving part driven by thermal edge flow, in: M. Capitelli, ed., *Rarefied Gas Dynamics* (AIP, Melville, NY), 168–173.

[267] Takagi, T. (1961), *Kaisekigairon* (*Introduction to Analysis*), *Third Edition* (Iwanami, Tokyo). (in Japanese)

[268] Takata, S., K. Aoki, and C. Cercignani (2000), The velocity distribution function in an infinitely strong shock wave, *Phys. Fluids* **12**, 2116–2127.

[269] Takata, S., K. Aoki, and Y. Sone (1994), Thermophoresis of a sphere with a uniform temperature: Numerical analysis of the Boltzmann equation for hard-sphere molecules, in: B. D. Shizgal and D. P. Weaver, eds., *Rarefied Gas Dynamics: Theory and Simulations* (AIAA, Washington, DC), 626–639.

[270] Takata, S. and Y. Sone (1995), Flow induced around a sphere with a non-uniform temperature in a rarefied gas, with application to the drag and thermal force problems of a spherical particle with an arbitrary thermal conductivity, *Eur. J. Mech. B/Fluids* **14**, 487–518.

[271] Takata, S., Y. Sone, and K. Aoki (1993), Numerical analysis of a uniform flow of a rarefied gas past a sphere on the basis of the Boltzmann equation for hard-sphere molecules, *Phys. Fluids A* **5**, 716–737.

[272] Takata, S., Y. Sone, D. Lhuillier, and M. Wakabayashi (1998), Evaporation from or condensation onto a sphere: Numerical analysis of the Boltzmann equation for hard-sphere molecules, *Computers Math. Applic.* **35**, 193–214.

[273] Takens, W. B., W. Mischke, J. Korving, and J. J. M. Beenakker (1984), A spectroscopic study of free evaporation of sodium, in: H. Oguchi, ed., *Rarefied Gas Dynamics* (Univ. of Tokyo Press, Tokyo), Vol. II, 967–974.

[274] Tamada, K. and Y. Sone (1966), Some studies on rarefied gas flows, *J. Phys. Soc. Jpn* **21**, 1439–1445.

[275] Tanaka, S. and Y. Sone (1987), Force acting on a heated nonconvex body in a highly rarefied gas, The 18th Annual Meeting of Japan Society of Aeronautical and Space Sciences (Japan Society of Aeronautical and Space Sciences, Tokyo), 165–166. (in Japanese)

[276] Taylor, G. I. (1923), Stability of a viscous liquid contained between two rotating cylinders, *Philos. Trans. R. Soc. London, Ser.* A. **223**, 289–343.

[277] Temam, R. (1984), *Navier–Stokes Equations* (Elsevier, New York).

[278] Tietjens, O. G. (1957), *Applied Hydro- and Aeromechanics Based on Lectures of L. Prandtl* (Dover, New York).

[279] Tolman, R. C. (1979), *Principles of Statistical Mechanics* (Dover, New York).

[280] Ukai, S., T. Yang, and S.-H. Yu (2003), Nonlinear boundary layers of the Boltzmann equation I. Existence, *Commun. Math. Phys.* **236**, 373–393.

[281] Ukai, S., T. Yang, and S.-H. Yu (2004), Nonlinear stability of boundary layers of the Boltzmann equation I. The case $M < 1$, *Commun. Math. Phys.* **244**, 99–109.

[282] Van Dyke, M. (1964), *Perturbation Methods in Fluid Mechanics* (Academic, New York).

[283] Vargo, S. and E. P. Muntz (1997), An evaluation of a multiple-stage micromechanical Knudsen compressor and vacuum pump, in: Ching Shen, ed., *Rarefied Gas Dynamics* (Peking University Press, Beijing), 995–1000.

[284] Vincenti, W. G. and C. H. Kruger Jr. (1965), *Introduction to Physical Gas Dynamics* (John Wiley and Sons, New York).

[285] Von Clausing, P. (1932), Über die Strömung sehr verdünnte Gase durch Röhren von beliebiger Länge, *Ann. Phys.* **12**, 961–989.

[286] von Karman, T. (1963), *From Low-speed Aerodynamics to Astronautics* (Pergamon Press, Oxford).

[287] Wagner, W. (1992), A convergence proof for Bird's direct simulation Monte Carlo method for the Boltzmann equation, *J. Stat. Phys.* **66**, 1011–1044.

[288] Wakabayashi, M., T. Ohwada, and F. Golse (1996), Numerical analysis of the shear and thermal creep flows of a rarefied gas over the plane wall of a Maxwell-type boundary condition on the basis of the linearized Boltzmann equation for hard-sphere molecules, *Eur. J. Mech. B/Fluids* **15,** 175–201.

[289] Waldmann, L. (1959), Über die Kraft eines inhomogenen Gases auf kleine suspendierte Kugeln, *Z. Naturforsch.* **14a**, 589–599.

[290] Welander, P. (1954), On the temperature jump in a rarefied gas, *Ark. Fys.* **7**, 507–553.

[291] Wennberg, B. (1992), On an entropy dissipation inequality for the Boltzmann equation, *Comptes Rundues Acad. Sci. Paris* **315**, 1441–1446.

[292] Young, M., Y. L. Han, E. P. Muntz, G. Shiflett, A. Ketsdever, and A. Green (2003), Thermal transpiration in microsphere membranes, in: A. Ketsdever and E. P. Muntz, eds., *Rarefied Gas Dynamics* (AIP, New York), 743–751.

[293] Ytrehus, T. (1996), Molecular-flow effects in evaporation and condensation at interfaces, *Multiphase Science and Technology* **9**, 205–327.

[294] Ytrehus, T. and T. Aukrust (1986), Mott-Smith solution for weak condensation, in: V. Boffi and C. Cercignani, eds., *Rarefied Gas Dynamics* (Teubner, Stuttgart), Vol. II, 271–280.

[295] Yu, S.-H. (2005), Hydrodynamic limits with shock waves of the Boltzmann equation, *Commun. Pure Appl. Math.* **58**, 397–431.

[296] Zachmanoglou, E. C. and D. W. Thoe (1986), *Introduction to Partial Differential Equations with Applications* (Dover, New York).

[297] Zeytounian, R. Kh. (2002), *Theory and Applications of Nonviscous Fluid Flows* (Springer-Verlag, Berlin).

[298] Zeytounian, R. Kh. (2003), *Theory and Applications of Viscous Fluid Flows* (Springer-Verlag, Berlin).

List of Symbols

The symbols used globally or generally are listed here. The bare number refers to the page where the symbol is defined, the number in the square brackets refers to the section number, the number in the parentheses refers to the number of the equation by which it is defined or where it appears and is defined in the following (or preceding) sentences, and the number that follows F refers to the number of the footnote with the number of its chapter before a hyphen.

There are many symbols that are not listed here; they are used locally or semi-locally. In the text, we don't hesitate to repeat the explanation of the notation for easier reading. Some symbols are used in two or more ways, including those listed here, e.g., F_i is used for various kind of forces and c is used for a constant, but they appear in different places and are explained in each place. No confusion will be induced. However, the "(other use)" is put for the case when it may be better to note that there is other use or uses to avoid misunderstanding.

Roman symbols

Greek symbols

α

α (1.23a), (1.28a)
α_c (1.28a)
α_i, $\boldsymbol{\alpha}$ (1.7)

γ

Γ_1, $\Gamma_1(*)$, etc. (A.131)
$\bar{\Gamma}_7$, $\bar{\Gamma}_7(*)$ (A.131)
γ (3.72)
γ (other use)
γ_1, γ_2 , γ_3, γ_6 (3.24)
γ_4, γ_5 (3.98)

δ

Δ 572
$\Delta\tau_w$, etc. (various uses)[1]
δ (various uses)[2]
$\delta(*)$ 9
δ_{ij} (1.16)

ϵ

ε (various uses)[3]
ϵ_{ijk} F3-30

ζ

ζ (1.44)
ζ_i, $\boldsymbol{\zeta}$ (1.43)
ζ_{i*}, $\boldsymbol{\zeta}_*$ (1.48f)
ζ_i', $\boldsymbol{\zeta}'$ (1.48f)
ζ_{i*}', $\boldsymbol{\zeta}_*'$ (1.48f)
$|\zeta_i|$ (1.44)
$|\boldsymbol{\zeta}|$ (1.44)
$(\zeta_r, \zeta_\theta, \zeta_z)$ [A.3]
$(\zeta_r, \zeta_\theta, \zeta_\varphi)$ [A.3]
ζ_ρ (A.203)
ζ_ρ in $(\zeta_\rho, \theta_\zeta)$ (6.10)

η

η in (η, χ_1, χ_2) (3.31)

θ

θ in (r, θ, z) (A.152)
θ in (r, θ, φ) (A.154)
θ in $(\hat{r}, \theta, \hat{z})$ (A.156)
θ in $(\hat{r}, \theta, \varphi)$ (A.161)
θ_ζ in $(\zeta, \theta_\zeta, \psi)$ F4-22
θ_ζ in $(\zeta_\rho, \theta_\zeta)$ (6.10)

κ

κ_1, κ_2 (3.44)
κ_{ij} (3.44)
$\bar{\kappa}$ (3.44)

λ

λ (1.16)

μ

μ (1.16)

ν

ν_c (1.18)
ν_L (A.139c)
$\bar{\nu}_c$ (1.19)
$\hat{\nu}_c$ (1.51b)

ξ

ξ 7
ξ_i, $\boldsymbol{\xi}$ 1
ξ_{i*}, $\boldsymbol{\xi}_*$ (1.7)
ξ_i', $\boldsymbol{\xi}'$ (1.7)
ξ_{i*}', $\boldsymbol{\xi}_*'$ (1.7)
$\bar{\xi}$ 7
$|\xi_i|$ 7
$(\xi_r, \xi_\theta, \xi_z)$ [A.3]
$(\xi_r, \xi_\theta, \xi_\varphi)$ [A.3]

ρ

ρ (1.2a)
ρ_0 (1.42)
ρ_w (1.28a)
$\hat{\rho}$ (1.43)
$\hat{\rho}_w$ (1.43)

σ

σ_w (1.23b)
$\hat{\sigma}_w$ (1.62b)
$\check{\sigma}_w$ (1.92b)

τ

τ (1.74)
τ_c 7
τ_w (1.74)
$\bar{\tau}_c$ 7

ϕ

ϕ (1.74)
ϕ_e (1.85)
φ in (r, θ, φ) (A.154)
φ in $(\hat{r}, \theta, \varphi)$ (A.161)
φ (other use)[4]

χ

χ_1, χ_2 (3.31)

ψ

ψ in $(\zeta, \theta_\zeta, \psi)$ F4-22
ψ (other use)[5]

ω

Ω as $\mathrm{d}\Omega(*)$ (1.6), (2.23)
ω (1.74)
ω_w (1.74)

Subscripts

C (4.3)
C (6.64)
G (3.3)
G (6.64)
H (4.3)
H (3.213), (8.68e)
h (3.168)
K (3.29), (3.59), (3.137), (3.184), (3.213), (9.25)[6]
S (3.77)
$\mathfrak{S}$ (9.12)
SB (3.138)
V (3.176)

[1]The Δ is used in combination with other symbols, e.g., u, τ, P_w.
[2]It is often used to express a small parameter.
[3]It is often used to express a small parameter.
[4]It is often used to indicate a function of $\boldsymbol{\xi}$ or $\boldsymbol{\zeta}$.
[5]It is often used to indicate a function of $\boldsymbol{\zeta}$.
[6]The subscript indicates the Knudsen-layer correction.

Other symbols and notes

- a/bc : $a/bc = a/(bc)$.
- $a_i b_i$: Summation convention in Cartesian-tensor notation, i.e., $a_i b_i = a_1 b_1 + a_2 b_2 + a_3 b_3$. Note that $a_i^2 = a_i a_i$ and that $\partial^2/\partial x_i^2 = \partial^2/\partial x_1^2 + \partial^2/\partial x_2^2 + \partial^2/\partial x_3^2$, where $\partial^2/\partial x_i^2$ is a conventional symbol for $(\partial/\partial x_i)(\partial/\partial x_i)$.
- $\boldsymbol{a}^2$: $\boldsymbol{a}^2 = a_i a_i$.
- $|\quad|$: the absolute value of its argument. When the argument is a vector, say, a_i, $|a_i| = (a_i^2)^{1/2}$.
- $\binom{N}{r}$: the binomial function, i.e., $\binom{N}{r} = \dfrac{N!}{r!(N-r)!}$ for $0 \le r \le N$ ($N \ge r$: integers).
- $O(*)$: a quantity of the order of $*$ (or smaller). The condition in the parentheses is sometimes excluded.
- $o(*)$: a quantity much smaller than the order of $*$.
- The prime $'$ or the subscript asterisk $*$ on a function of $\boldsymbol{\xi}$, e.g., f', f_*, f'_* : The rule in Eq. (1.7) applies to any function.
- The prime $'$ or the subscript asterisk $*$ on a function of $\boldsymbol{\zeta}$, e.g., $\hat{f}'$, $\hat{f}_*$, $\hat{f}'_*$: The rule in Eq. (1.48f) applies to any function.
- $\int(*)\mathbf{d}\boldsymbol{\xi}$ or $\int(*)\mathbf{d}\boldsymbol{\zeta}$, an integral with respect to $\boldsymbol{\xi}$ or $\boldsymbol{\zeta}$ without the range of integration indicated: The range is the whole space of $\boldsymbol{\xi}$ or $\boldsymbol{\zeta}$.
- The argument or arguments of a function are not always shown when no fear of confusion or misunderstanding is expected. This rule is applied to a special argument or arguments. For example, E and f or $f(\boldsymbol{\xi})$ instead of $E(\zeta)$ and $f(\boldsymbol{X}, \boldsymbol{\xi}, t)$.

Other information

The software mentioned in the text and other information, e.g., misprints, are found at

http://fd.kuaero.kyoto-u.ac.jp/members/sone

Index